

**Dissertation zur Erlangung des Doktorgrades
der Fakultät für Chemie und Pharmazie
der Ludwig-Maximilians-Universität München**

**Biomimetic Synthesis of Polyketides:
Dibefurin and Epicolactone**

and

Synthetic Studies Toward Gracilin Terpenoids

von

Pascal Ellerbrock

aus

Wuppertal, Deutschland

2015

Erklärung

Diese Dissertation wurde im Sinne von § 7 der Promotionsordnung vom 28. November 2011 von Herrn Prof. Dr. Dirk Trauner betreut.

Eidesstattliche Versicherung

Diese Dissertation wurde eigenständig und ohne unerlaubte Hilfe erarbeitet.

München, den 29.01.2015

.....
Pascal Ellerbrock

Dissertation eingereicht am: 29.01.2015

1. Gutachter: Prof. Dr. Dirk Trauner

2. Gutachter: Prof. Dr. Paul Knochel

Mündliche Prüfung am: 02.03.2015

- *Meinen Eltern* -

Parts of this work have been published in peer-reviewed journals.

‘Biomimetic Synthesis of the Calcineurin Phosphatase Inhibitor Dibefurin’, P. Ellerbrock, N. Armanino, and D. Trauner, *Angew. Chem. Int. Ed.* **2014**, 53, 13414–13418.

Parts of this work have been presented on scientific conferences.

‘Biomimetic Synthesis of Fungal Polyketides’ (poster), Syngenta Workshop for Talented PhD Chemistry Students, Stein (Switzerland), 29.09.–30.09.2014

‘Biomimetic Synthesis of Polyketides: Dibefurin and Epicolactone’ (oral communication), 127th BASF International Summer Course, Ludwigshafen (Germany), 03.08.–09.08.2014

‘Biomimetic Synthesis of Fungal Polyketides’ (poster), Gordon Research Conference: Heterocyclic Compounds, Newport (RI, USA), 15.06.–20.06.2014

‘Toward the Biomimetic Synthesis of Epicolactone’ (poster), CIPS^M conference, Wildbad Kreuth (Germany), 03.06.–06.06.2014

‘Employing Rhodium Carbenoids in Complex Settings: Toward the Total Synthesis of Gracilin Natural Products’ (poster), 14th Tetrahedron Symposium, Vienna (Austria), 25.06.–28.06.2014

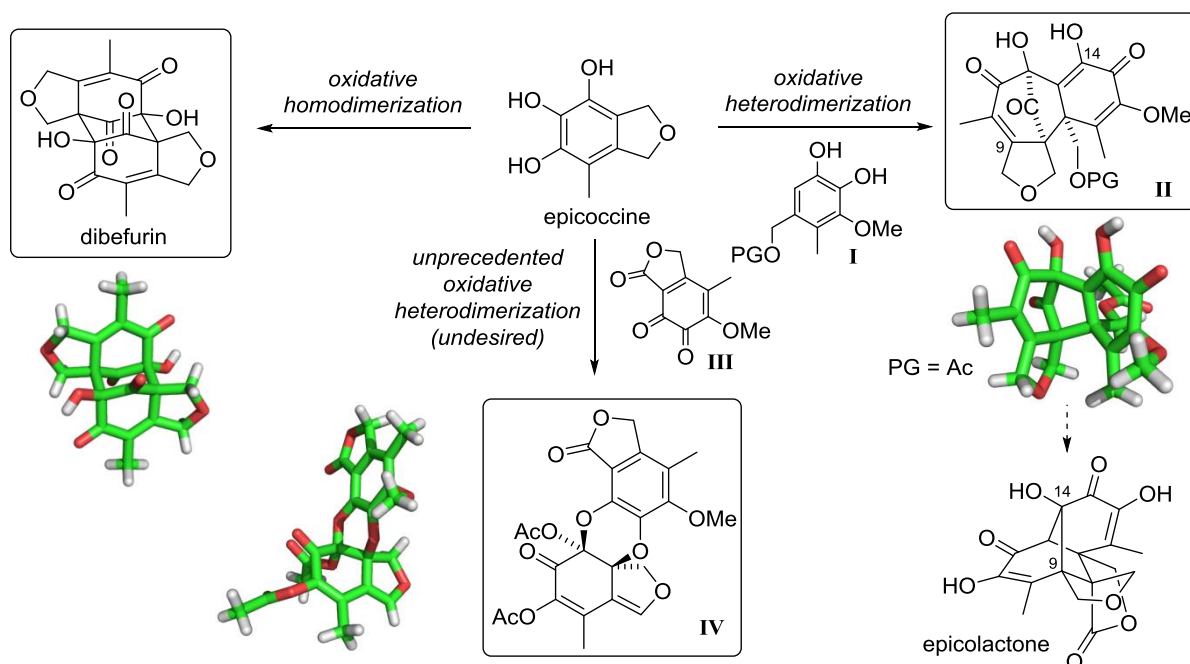
Parts of this work are in preparation for publication in peer-reviewed journals.

‘Biomimetic Synthesis of Epicolactone’, P. Ellerbrock*, N. Armanino*, R. Webster, M. K. Ilg, and D. Trauner, *manuscript in preparation*.

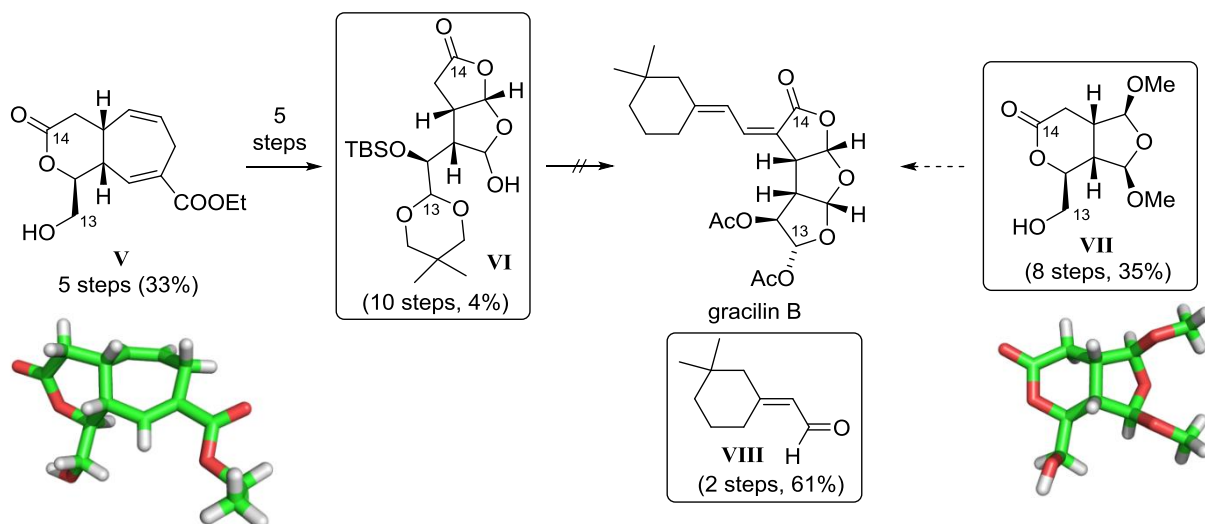
‘Synthetic Studies Toward Gracilin Natural Products’, P. Ellerbrock, M. Olbrich, and D. Trauner, *manuscript in preparation*.

ABSTRACT

This thesis describes the biomimetic synthesis of dibefurin as well as synthetic studies toward the polyketide epicolactone and the gracilin norditerpenoids. Following the biosynthesis proposed in this thesis, the C_1 -symmetric fungal metabolite dibefurin was synthesized by oxidative homodimerization of the natural product epicoccine. *En route* to epicolactone, an oxidative heterodimerization of epicoccine with different pyrogallol derivatives **I** was developed. This key step gave rise to tetracycles **II** featuring three tetrasubstituted carbon atoms with correct diastereoselectivity. During the investigation of this key step, a novel hetero-Diels–ALDER coupling of pyrogallols was identified.



In the second project, three strategies toward the gracilin natural products were tested. A Rh-catalyzed cyclopropanation/COPE rearrangement furnished cyclic diene **V**. Hemiacetal **VI**, synthesized *via* double oxidative cleavage, could not be converted to the target natural products. An alternative route involving a formal (3+2)-cycloaddition and desymmetrization of a *meso*-substrate efficiently afforded alcohol **VII**, providing an excellent basis for the completion of the total synthesis.



ACKNOWLEDGMENTS

First and foremost I would like to thank my supervisor Prof. Dr. Dirk Trauner for his support in the course of my PhD thesis. I am very grateful for my innovative and challenging projects and the freedom that I was granted while working on them. His confidence in the success of these endeavors and his ability to think outside the box were truly inspiring. I further thank him for his trust to let me present our work at several stimulating conferences and industry workshops. All in all, I was given extraordinary possibilities to improve as a chemist that have made the past years an exciting PhD experience.

I thank Prof. Dr. Knochel for agreeing to be the second reviewer of this PhD thesis. Moreover, I am grateful for the suggestions and comments of Prof. Dr. Bracher, Prof. Dr. Karaghiosoff, Prof. Dr. Heuschmann and especially Prof. Dr. Steglich regarding this thesis.

I want to thank Martin Olbrich, Nicolas Armanino and Laura Salonen for thoroughly proofreading this thesis and improving its quality with their excellent advice.

The generous support of this PhD thesis by the Chemical Industry Fund of the German Chemical Industry Association in form of a Kekulé Mobility Fellowship is gratefully acknowledged.

Moreover, I am very thankful to Nicolas Armanino for the great collaboration on the dibefurin and epicolactone project and to Robert Webster and Marina Ilg for their prior work on epicolactone. I also thank Martin Olbrich for his support in the gracilin natural product synthesis.

I further thank my students Komei Sakata, Masahiro Kojima and Henning Lumpe for their excellent work on either total synthesis or chemical biology projects.

I am thankful to Heike Traub and Aleksandra Sarman Grilc for their kind help with documents, recommendation letters and other organizational issues, to Martin Sumser for materials and reliable book ordering, to Carrie Louis for maintenance of the NMR, LC/MS and HPLC machines, to Peter Mayer for timely and skillful determination of X-ray single crystal structures, to Heidi Buchholz and Michael Gayer for their nice help with chemicals and especially Luis de la Osa de la Rosa for his assistance with materials and chemicals.

During my time in the Trauner research group, I was fortunate to work next to or close to several people. I thank Albert Schröckeneder, Alwin Reiter, Florian Löbermann, Irina Albrecht, Marina Ilg, Eddie Myers, Daniel Terwilliger, David Konrad, Felix Hartrampf, Nicolas Guimond, Oliver Thorn-Seshold, Martin Reynders, Raphael Wildermuth and Nicolas Armanino for a nice working

environment. Furthermore, the past years would not have been nearly as funny and nice without my friends Shu-An Liu, Katharina Hüll, Julien Lefranc, Olga Schöne, Nicolas Armanino, David Barber, Luis de la Osa de la Rosa, Benjamin Williams, Daniel Hog, Michael Pangerl, Dominik Hager, Anastasia Hager, Daniel Terwilliger, Nils Winter and James Frank. Thank you for the many laughs and interesting conversations!

Moreover, I could rely on the valuable friendship of the following people to share the good times and receive support when things did not work out as planned. Many thanks go to Giulio Volpin for the uncountable dinner evenings, to Nicolas Guimond for his inspiring positive attitude, to Ion Lazar for taking my mind off work and to Elena Herrero-Gómez and Laura M. Salonen, in true lack of words simply for all the great times we spent together.

Dank für seine Freundschaft und Hilfsbereitschaft gilt vor allem Martin Olbrich. Viele der schönen Momente während meiner Doktorarbeit habe ich ihm zu verdanken. Martin und Sophie Olbrich möchte ich für ihr Vertrauen danken, mich als Patenonkel von Lara und Tom Olbrich zu wählen. Die gemeinsame Zeit in den letzten Jahren hat mich sehr glücklich gemacht und bedeutet mir sehr viel.

Meinen Großeltern danke ich für ihre stete Ermunterung und dafür, dass sie meine Freude stets teilen können.

Meinem Bruder Marcel möchte ich dafür danken, dass er immer an meiner Seite steht und ich stets auf ihn zählen kann.

Der größte Dank gebührt meinen Eltern. Durch eure Liebe und bedingungslose Unterstützung habt ihr mir die Möglichkeit gegeben, das zu erreichen, was ich mir gewünscht habe. Danke, dass ihr immer für mich da seid!

LIST OF ABBREVIATIONS

Å	angstrom	DMSO	dimethyl sulfoxide
Ac	acetyl	dr	diastereomeric ratio
Ar	undefined aryl substituent	<i>E</i>	opposite (<i>trans</i>)
ATR	attenuated total reflection (IR)	EDA	ethyl diazoacetate
BAIB	(diacetoxyiodo)benzene	ee	enantiomeric excess
BDE	bond dissociation energy	EI	electron ionization (MS)
BHT	butylated hydroxyl toluene	eq.	equivalent(s)
BOM	benzyloxymethyl	ESI	electrospray ionization (MS)
Bn	benzyl	Et	ethyl
br	broad	EWG	electron-withdrawing group
Bu	butyl	g	gram(s)
Bz	benzoyl	h	hour(s)
calcd.	calculated	HMBC	heteronuclear multiple-bond correlation spectroscopy
CAN	ceric ammonium nitrate (NH ₄) ₂ [Ce(NO ₃) ₆]	HMDS	hexamethyldisilazane
CCDC	Cambridge Crystallographic Data Center	HMPA	hexamethylphosphoramide
COSY	correlation spectroscopy (NMR)	HPLC	high pressure liquid chromatography
Cp	cyclopentadienyl	HRMS	high resolution mass spectrometry
CSA	camphorsulfonic acid	HSQC	heteronuclear single-quantum correlation spectroscopy
d	day(s)	HV	high vacuum
d	dublet (NMR)	Hz	Hertz
δ	chemical shift (NMR)	<i>i</i>	iso (isomer)
DBU	1,8-diazabicycloundec-7-ene	IBX	2-iodoxybenzoic acid
DCE	1,2-dichloroethane	im.	imidazole
DDQ	2,3-Dichloro-5,6-dicyano-1,4-benzoquinone	IR	infrared
DIBAL	diisobutylaluminum hydride	IUPAC	International Union of Pure and Applied Chemistry
DIPA	diisopropylamine	<i>J</i>	coupling constant (NMR)
DIPT	di- <i>iso</i> -propyl tartrate	k	kilo (10 ³)
DMAD	dimethyl acetylenedicarboxylate	l	liter
DMAP	4-(dimethylamino)pyridine	LDA	lithium diisopropylamide
DMDO	dimethyldioxirane	LG	leaving group
DMF	dimethylformamide	LLS	longest linear sequence
DMP	DESS–MARTIN periodinane		
DMPU	<i>N,N'</i> -dimethylpropyleneurea		

m	medium (IR)	R _t	retention time
<i>m</i>	meta	RCM	ring-closing metathesis
m	milli (10 ⁻³)	R _f	retention factor
m	multiplet (NMR)	ROS	reactive oxygen species
M	molar	R _t	retention time
<i>m</i> -CPBA	<i>m</i> -chloroperoxybenzoic acid	rt	room temperature (<i>T</i> = 22 °C)
Me	methyl	s	singlet
min	minute(s)	s	strong (IR)
MOM	methyloxymethyl	SEM	[2-(trimethylsilyl)ethoxy]methyl
mol	mole(s)	s.m.	starting material
mp	melting point	t	triplet
MS	mass spectrometry, molecular sieves	<i>tert</i> or <i>t</i> -	tertiary (isomer)
Ms	methanesulfonyl	T	temperature
<i>n</i>	normal (isomer)	TBAF	tetra- <i>n</i> -butylammonium fluoride
NBS	<i>N</i> -bromosuccinimide	TBAI	tetrabutylammonium iodide
NCS	<i>N</i> -chlorosuccinimide	TBDPS	<i>tert</i> -Butyldiphenylsilyl
NMO	<i>N</i> -methylmorpholine <i>N</i> -oxide	TBS	<i>tert</i> -butyldimethylsilyl
NMR	nuclear magnetic resonance	TES	triethylsilyl
NOESY	nuclear Overhauser effect spectroscopy	Tf	trifluoromethanesulfonyl
<i>o</i>	ortho	TFA	trifluoroacetic acid
Oct	octanoate	THF	tetrahydrofuran
<i>p</i>	para	TIPS	tri- <i>iso</i> -propylsilyl
<i>p</i>	pressure	TLC	thin layer chromatography
PCC	pyridinium chlorochromate	TMEDA	tetramethylethylenediamine
PG	protecting group	TMS	trimethylsilyl
Ph	phenyl	TMP	2,2,6,6-tetramethylpiperidine
PIFA	(bis(trifluoroacetoxy)iodo)benzene	Tol	<i>p</i> -tolyl
ppm	parts per million (NMR)	TPAP	tetra- <i>n</i> -propylammonium perruthenate
PPTS	pyridinium <i>para</i> -toluenesulfonate	TPP	5,10,15,20-tetraphenylporphyrine
<i>p</i> -TsOH	<i>para</i> -toluenesulfonic acid	Ts	toluenesulfonyl
py	pyridine	UV	ultraviolet
q	quartet	v	very (IR)
R	undefined substituent	w	weak (IR)
R _f	retardation factor	W	watt(s)
		wt-%	weight percent
		Z	together (<i>cis</i>)

TABLE OF CONTENTS

Abstract	I
Acknowledgments.....	II
List of Abbreviations.....	IV
Table of Contents.....	VI
Theoretical Part.....	1
1 General Introduction	1
1.1 Symmetry	1
1.2 History of Natural Product Synthesis	2
1.3 Symmetry in Natural Product Synthesis	5
2 PART I: Biomimetic Synthesis of Dibefurin and Epicolactone	9
2.1 Introduction.....	9
2.1.1 Biomimetic Synthesis	9
2.1.2 Oxidative Dearomatization of Hydroxylated Arenes in Total Synthesis	10
2.1.2.1 Dearomatization of Phenols.....	11
2.1.2.2 Oxidation of Catechols: Reactivity of <i>ortho</i> -Quinones and Derivatives	14
2.1.2.3 Oxidation of Hydroquinones: Reactivity of <i>para</i> -Quinones and Derivatives	19
2.1.2.4 Oxidation of Resorcinols	21
2.1.2.5 Dearomatization of Phloroglucinols	22
2.1.2.6 Oxidation of Hydroxyquinols: Reactivity of Related Quinones and Quinols	23
2.1.2.7 Oxidation of Protected Pyrogallols.....	24
2.1.3 Oxidation of Unprotected Pyrogallols.....	27
2.1.3.1 Purpurogallin Formation Reaction	27
2.1.3.2 Formation of the PERKIN Dimer	32
2.1.3.3 Hetero-DIELS–ALDER Dimerization of Pyrogallols	33
2.1.3.4 Conceptualization of Substrate-Dependent Reactivity Trends	33
2.1.4 Natural Products from <i>Epicoccum</i> species	36
2.1.4.1 Overview	36

2.1.4.2	Dibefurin.....	38
2.1.4.3	Epicolactone – Origin, Structure and Bioactivity	40
2.2	Project Outline	41
2.2.1	General Biosynthetic Proposal.....	41
2.2.2	Aim of the Project	43
2.2.3	Initial Work	44
2.3	Results and Discussion.....	47
2.3.1	Synthesis of Epicoccine.....	47
2.3.1.1	Optimization Studies on Previous Route	47
2.3.1.2	Second Generation Synthesis of Epicoccine	48
2.3.2	Synthesis of Dibefurin.....	50
2.3.2.1	Potential Challenges	50
2.3.2.2	Oxidation of Epicoccine and Dibefurin Formation	51
2.3.2.3	Purification of the Natural Product Dibefurin	54
2.3.2.4	Supramolecular Interactions in Solid State.....	55
2.3.2.5	Mechanistic Proposal for the Formation of Dibefurin.....	56
2.3.2.6	Biological Activity of Dibefurin.....	58
2.3.2.7	Natural Occurrence of Dibefurin in <i>Epicoccum</i> sp.	59
2.3.3	Synthesis of Epicoccone B	61
2.3.3.1	Cycloaddition Approaches.....	61
2.3.3.2	Synthesis of Epicoccone B from Pyrogallol Derivative	64
2.3.4	Synthesis of Epicolactone	72
2.3.4.1	Heterodimerization of Epicoccine with Epicoccone B.....	72
2.3.4.2	Heterodimerization with Epicoccone B Methyl Ether.....	74
2.3.4.3	Heterodimerization <i>via</i> Methylated Epicoccine	83
2.3.4.4	Heterodimerization <i>via</i> Inverted Reactivity.....	85
2.3.4.5	Heterodimerization with Pentasubstituted Epicoccone B Derivatives	88
2.4	Conclusion and Outlook	107
3.	PART II: Synthetic Studies Toward Gracilin Terpenoids	114
3.1	Introduction.....	114
3.1.1	Strategies in the Synthesis of Cage-Shaped Compounds	114
3.1.2	Gracilin Natural Products.....	115
3.1.2.1	The Gracilin Family – Isolation and Structure	115

3.1.2.2	Biosynthesis of the Gracilin Natural Products	118
3.1.2.3	Bioactivity of the Gracilin Natural Products	119
3.1.2.4	COREY Synthesis of Gracilin B and C	120
3.2	Project Outline	123
3.3	Synthesis of the Side Chain of Gracilin B and C	125
3.4	First Strategy: Torquoselective 6π-electrocyclization	126
3.4.1	Retrosynthetic Analysis	126
3.4.2	Introduction to 4 π - and 6 π -Electrocyclization	127
3.4.3	Results and Discussion.....	131
3.4.3.1	Preparation of Achiral Coupling Partner	131
3.4.3.2	Preparation of Chiral Coupling Partner	131
3.4.3.3	Building Block Coupling and 6 π -Electrocyclization.....	132
3.5	Second Strategy: Rhodium-Catalyzed Formal (4+3)-Cycloaddition.....	136
3.5.1	Retrosynthesis	136
3.5.2	Introduction to Rhodium-Catalyzed Formal (4+3)-Cycloaddition	138
3.5.2.1	Synthesis of Vinyl Diazoacetates	138
3.5.2.2	Rhodium Carbenoid Formation	139
3.5.2.3	Intermolecular Cyclopropanation with Rhodium Carbenoids	140
3.5.2.4	Divinylcyclopropane Rearrangement	142
3.5.2.5	Application of the Cyclopropanation/COPE rearrangement Cascade	143
3.5.3	Results and Discussion.....	144
3.5.3.1	Preparation of Diene	144
3.5.3.2	Asymmetric Formal (4+3)-Cycloaddition with Achiral Substrates.....	144
3.5.3.3	Vinyl Diazoacetates with Olefin as C13 Aldehyde Equivalent	148
3.5.3.4	Vinyl Diazoacetates with Alcohols as C13 Aldehyde Equivalent.....	149
3.5.3.5	Initial Oxidative Cleavage Attempts by Ozonolysis.....	156
3.5.3.6	Synthesis of Bicyclic Substrate for Oxidative Cleavage	158
3.5.3.7	Oxidative Cleavage of Bicyclic Substrates.....	161
3.5.3.8	Synthesis and Oxidative Cleavage of C13 Oxidized Substrates.....	163
3.5.3.9	Oxidative Cleavage of Substrates with C14 Carboxylic Acid.....	168
3.5.3.10	Stepwise Oxidative Cleavage	172
3.5.3.11	Conclusion	175
3.6	Third Strategy: Formal (3+2) Cycloaddition and Desymmetrization.....	176
3.6.1	Retrosynthetic Analysis	176
3.6.2	Results and Discussion.....	177

3.6.2.1	Synthesis of <i>meso</i> -Ketone.....	177
3.6.2.2	Desymmetrization <i>via</i> Enolate Alkylation.....	179
3.6.2.3	Conversion of Desymmetrized Ketone to General Gracilin Precursor.....	181
3.7	Conclusion and Outlook	184
4.	Summary.....	185
Experimental Part		192
5.	General Procedures.....	194
6.	Experimental Procedures	198
6.1	Part I: Biomimetic Synthesis of Dibefurin and Epicolactone	198
6.1.1	Synthesis of Epicoccine.....	198
6.1.2	Synthesis of Dibefurin.....	203
6.1.3	Synthesis of Epicoccone B	208
6.1.4	Synthesis of Epicolactone	216
6.2	Part II: Total Synthesis of Gracilin Natural Products	252
6.2.1	Synthesis of Side Chain	252
6.2.2	First Strategy: Torquoselective 6 π -Electrocyclization	255
6.2.3	Second Strategy: Rhodium-Catalyzed Formal (4+3)-Cycloaddition.....	264
6.2.4	Third Strategy: Formal (3+2) Cycloaddition and Desymmetrization.....	306
Appendix		316
7.	NMR Spectra	318
7.1	PART I: Biomimetic Synthesis of Dibefurin and Epicolactone.....	318
7.2	PART II: Total Synthesis of Gracilin Natural Products	384
8.	Chrystallographic Data.....	446
9.	References	488

THEORETICAL PART

1 GENERAL INTRODUCTION

1.1 Symmetry

Symmetry (from Greek *symmetria*, “agreement in dimensions”) is mathematically defined as the invariance of an object to a transformation. Highly symmetric objects are exceptionally appealing and aesthetically pleasing to human beings and have therefore found frequent use in art and architecture. Among the myriad applications of symmetry considerations in science, the WOODWARD–HOFFMANN rules concerning the conservation of orbital symmetry in pericyclic reactions have had a profound impact on this thesis and organic chemistry in general.^[1–3]

The symmetry of an object can be described with the help of symmetry operations, operations that transform the object into a state indistinguishable of the starting state (Table 1).

Table 1. Symmetry operations.

category	symbol	description	special cases
proper rotation operation	C_n	rotation by $360/n^\circ$	identity I or E ; C_1
improper rotation operation	S_n	rotation by $360/n^\circ$ followed by reflection in plane perpendicular to rotation axis	inversion: S_1 (σ) reflection: S_2 (i)

Based on its symmetry operations, a molecule in a given conformation can be categorized in point groups (Table 2). In this context, symmetry elements such as rotation axis, mirror planes or inversion centers are the points of references, about which the symmetry operation in question can take place.

Table 2. Selection of molecular point groups (SCHOENFLIES notation).

point group	selection of symmetry elements
C_n	n -fold rotation axis
C_s	mirror plane
C_i	inversion center
C_{nv}	n -fold rotation axis, n vertical mirror planes
C_{nh}	n -fold rotation axis, horizontal mirror plane
D_n	n -fold rotation axis, n perpendicular two-fold rotation axes
D_{nh}	n -fold rotation axis n vertical mirror planes perpendicular two-fold rotation axis
T_d	tetrahedral symmetry (three-fold rotation axis)
O_h	octahedral symmetry (four-fold and three-fold rotation axes)
I_h	icosahedral symmetry (five-fold rotation axis)

In organic chemistry, inversion centers, mirror planes and two-fold rotation axes are of particular importance. Common point groups of organic molecules therefore include C_1 , C_s , C_i , C_2 , C_{2v} and C_{2h} (Figure 1).

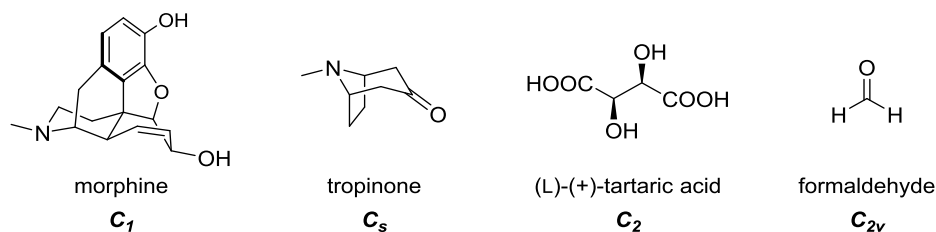


Figure 1. Examples of organic molecules with different point groups.

The point group of molecules determines whether they are chiral or achiral. Derived from the Greek word for “hand”, chirality is defined by the lack of improper rotation axes S_1 (i) and S_2 (σ). A molecule with this feature cannot be superimposed with its mirror image by rotation alone. In addition to the fact that many natural products are chiral, they mostly also only exist as one of the enantiomers in Nature. Since the biology activity of molecules depends on their absolute configuration, their total synthesis is required to discriminate between different enantiomers. To this end, topicity considerations are crucial. The term topicity defines the stereochemical relationship of objects, *e.g.* substituents or faces. The objects are homotopic if they can be transformed into each other by rotation and enantiotopic, if a superimposition with itself is only possible by a mirror plane. In all other cases, they are diastereotopic. Whereas homotopic substituents or faces react in the same way under all conditions and afford the same product, diastereotopic groups undergo transformations at different rates. Every enantioselective methodology relies on the fact that enantiotopic substituents behave like diastereotopic groups in a chiral environment.

1.2 History of Natural Product Synthesis

The history of natural product synthesis dates back almost 150 years to efforts of BAEYER, LADENBURG and WILLSTÄTTER (Figure 2).^[4] Major aim of these early investigations was to provide proof that natural products can indeed be accessed in laboratories. Already in 1870, BAEYER disclosed the first synthesis of the dye indigo from isatin.^[5] His report was followed by LADENBURG’s racemic route to the known alkaloid coniine from α -picoline in 1886.^[6] A breakthrough as a tool for structural elucidation of natural products was achieved by WILLSTÄTTER in his studies on the tropane alkaloid cocaine, which was ultimately accessed from cycloheptanone *via* tropinone.^[7,8] Due to the intricate structure and societal impact of the important antimalarial drug quinine, its successful total synthesis in 1944 by WOODWARD and DOERING based on previous work by RABE and KINDLER constitutes a milestone in the development of this field.^[9–11]

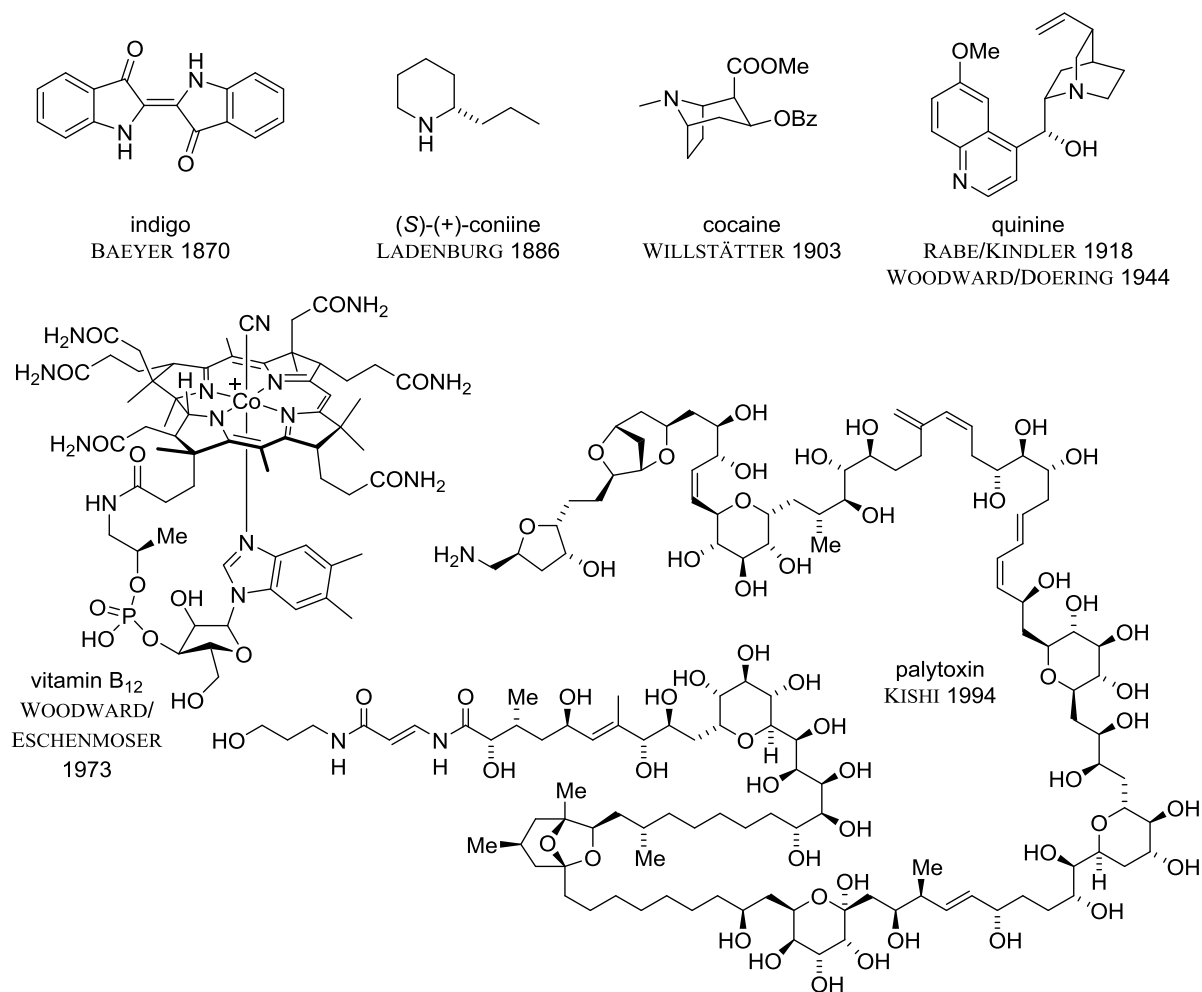


Figure 2. History of natural product synthesis.

Over the following decades, synthetic endeavours increasingly served the purpose of showcasing the power of total synthesis rather than obtaining structural proof. Many molecules such as vitamin B₁₂ or palytoxin that were previously deemed impossible to access succumbed to total synthesis.^[12–14] These efforts were the main driving force in the development of novel synthetic methodology (Figure 3). The significant progress ranges from the first application of Cu-mediated couplings to form trisubstituted olefins (COREY synthesis of juvenile hormone I) over studies on novel synthetic routes towards guanidines (KISHI synthesis of tetrodotoxin) to investigations on macrolactonization and glycosylation reactions for macrolide antibiotics (WOODWARD synthesis of erythromycin A).^[15–17] With the demonstration that highly complex natural products can indeed be accessed synthetically, the field of total synthesis slowly underwent a paradigm shift.

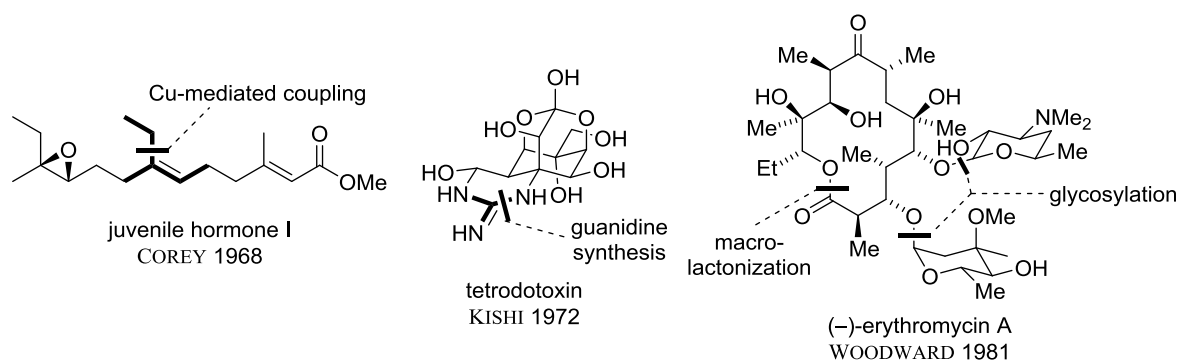


Figure 3. Development and application of new synthetic methodology in natural product synthesis.

Subsequently, the focus was put more on the general efficiency of the synthetic route rather than the mere accomplishment of the synthesis.^[18] Different criteria than structural complexity such as the potential benefit to society gained importance in the choice of targets. The pursuit to arrive at the right enantiomer of the bioactive natural product stimulated substantial research activity in the stereoselective preparation of molecules.

The developments in natural product synthesis have markedly broadened the portfolio of efficient and selective methods to access organic molecules in general. In turn, this field still serves as a valuable testing ground to assess the robustness and generality of new synthetic methodology.^[19–21] Based on these significant improvements in the synthesis of natural products over the past decades, sufficient quantities of highly bioactive, natural or non-natural molecules can now be provided in flexible routes that easily allow for the derivatization of the final structure. Prominent examples include the MYERS synthesis of tetracyclin antibiotic doxycycline and the fully synthetic production of the anti-cancer drug eribulin mesylate (Halaven®) on multi-gram scale (Figure 4).^[22,23] However, even in a time of advanced spectroscopic methods, total synthesis is still helpful in the structural elucidation of natural products.^[24]

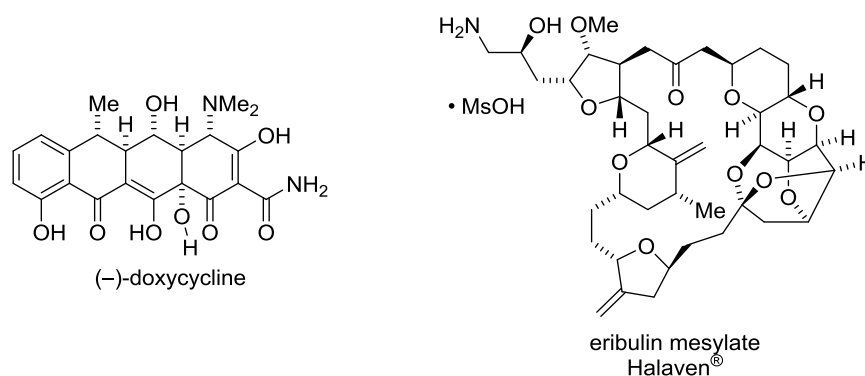
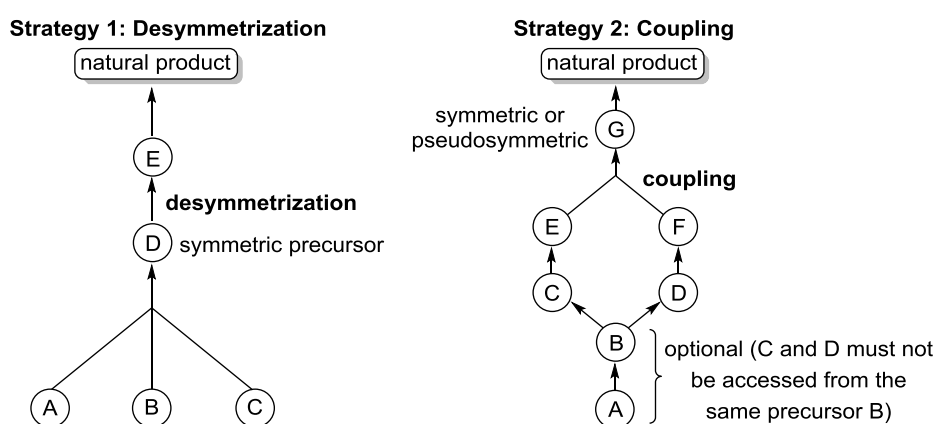


Figure 4. Highly bioactive molecules accessed by organic synthesis.

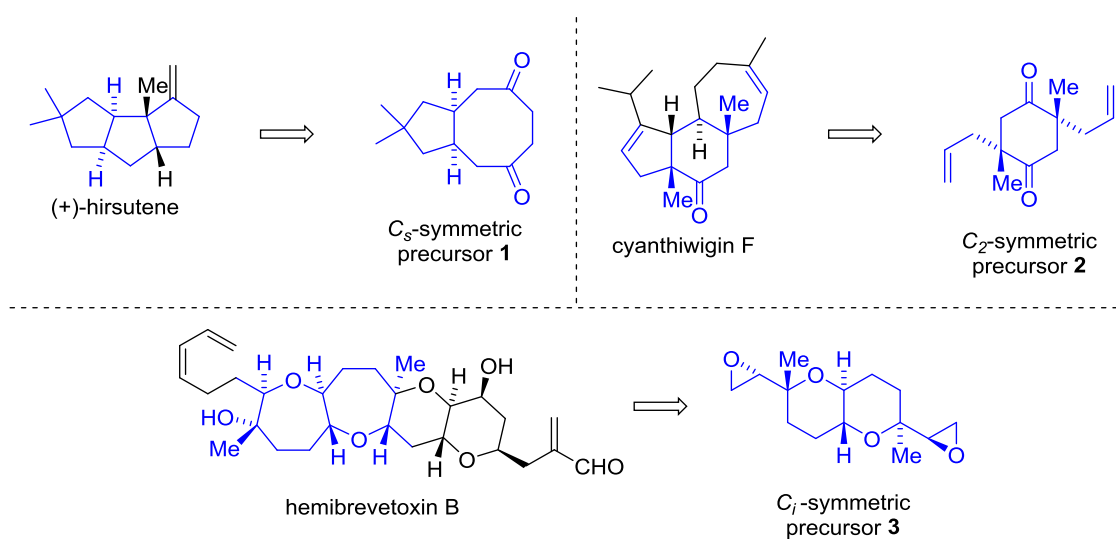
1.3 Symmetry in Natural Product Synthesis

The exploitation of the symmetry¹ of natural products in their total synthesis is considered very rewarding in terms of general efficiency. Besides a decrease in the number of steps, the stereoselective installation of substituents can be simplified. Depending on the molecule and the strategy, two main scenarios are possible (Scheme 1). In one case, the bidirectional synthesis, a target molecule can be traced back to one symmetric precursor by a desymmetrization reaction (strategy 1). In the other, the (pseudo-)symmetry of the natural product allows for a coupling reaction between two or more structurally related building blocks (strategy 2). Most frequently, strategy 2 involves a homo- ($E = F$) or a heterodimerization ($E \neq F$). Both strategies require thorough retrosynthetic planning since the identification of symmetry elements in the natural product can be challenging.



Scheme 1. Potential strategies for the exploitation of symmetry in total synthesis.

Approaches along the lines of strategy 1 can be subdivided according to the point group of the molecule that is projected to undergo the desymmetrization (Scheme 2).

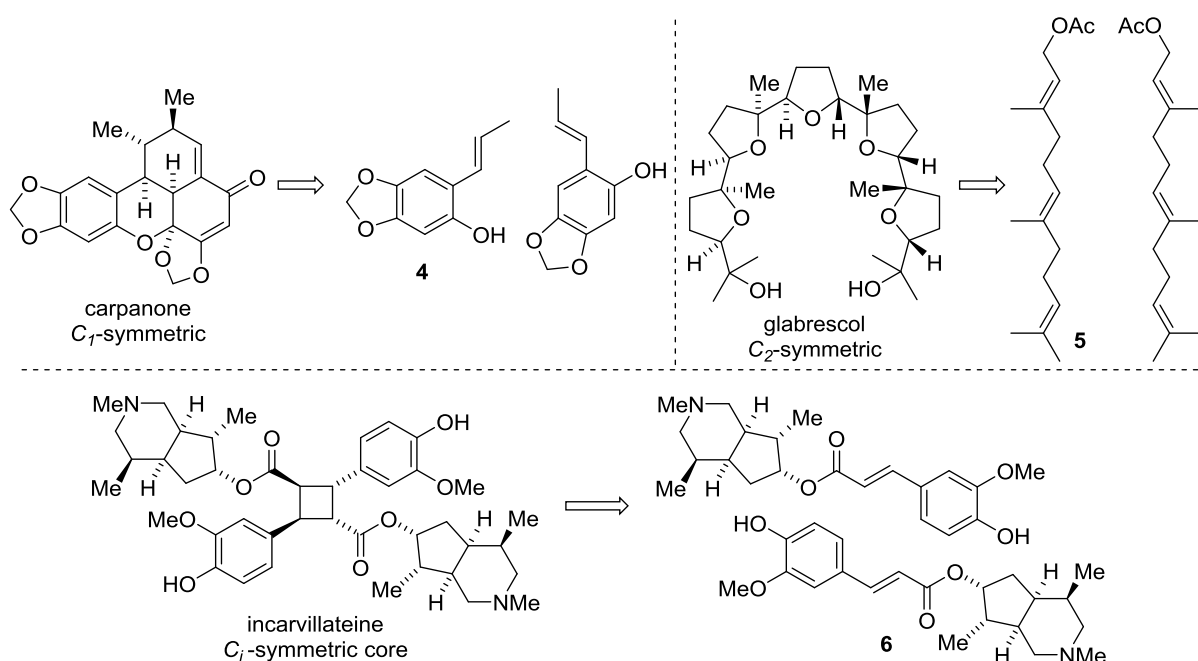


Scheme 2. Desymmetrization strategies in total synthesis.

¹ In the following, the term ‘symmetry’ with respect to molecules excludes C_1 symmetry unless explicitly stated.

Elegant examples with C_s - or C_i -symmetric compounds **1** and **2** have been disclosed by LIST and co-workers in their synthesis of hirsutene and the NELSON group in their studies on hemibrevetoxin B.^[25,26] Both desymmetrizations require asymmetric methodology due to the achirality of the starting material. In contrast to this, STOLTZ and co-workers accessed cyanthiwigin F by a desymmetrization of an already chiral C_2 -symmetric molecule **3**, which needed to be prepared by enantioselective decarboxylative allylation.^[27]

The coupling of building blocks according to strategy 2 constitutes one of the most frequently applied approaches to (pseudo-)symmetric multimeric molecules. Since Nature often follows a similar concept, biosynthetic considerations can be decisive in the identification of suitable coupling partners. Depending on the specific conditions, dimerizations can yield products with different symmetry elements (Scheme 3). The control over the selectivity in these reactions is crucial for the success of this strategy.



Scheme 3. Dimerization strategies in total synthesis.

Prominent examples of strategy 2 are illustrated in Scheme 3 with the CHAPMAN carpanone synthesis from phenol **4**, COREY's glabrescol synthesis from terpenoid **5** and KOBAYASHI's studies of the head-to-tail dimerization of ester **6** toward the C_i -symmetric core of incarvillateine.^[28–30]

Within this thesis, both strategies were applied in the course of the biomimetic synthesis of polyketides dibefurin and epicolactone and the total synthesis of gracilin terpenoids.

PART I:

**Biomimetic Synthesis of
Dibefurin and Epicolactone**

2 PART I: BIOMIMETIC SYNTHESIS OF DIBEFURIN AND EPICOLACTONE

2.1 Introduction

2.1.1 Biomimetic Synthesis

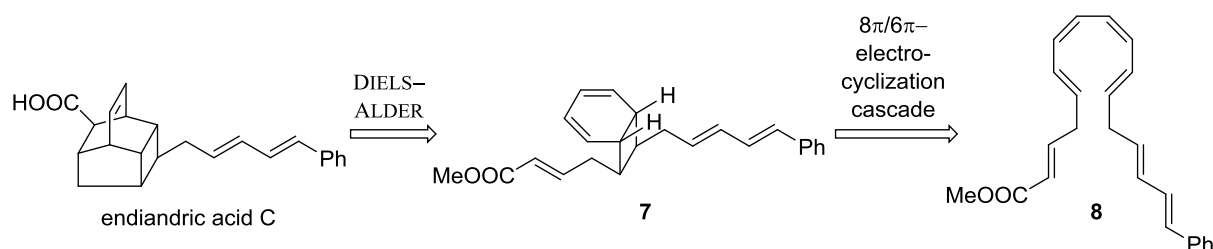
Biomimetic synthesis is defined as a transformation or a sequence of reactions that mimics the proposed biosynthesis of a natural product.^[31] As such, it can differ from a biogenetic route which strictly follows the biosynthetic pathway.

The first biomimetic synthesis was undertaken in 1917 by ROBINSON, who showed that the C_5 -symmetric natural product tropinone could be accessed from the simple components acetone dicarboxylic acid, succinic aldehyde and methyl amine by a sequence of MANNICH reactions.^[32] Ever since, the study of biosynthetic pathways and the synthesis of natural products along these lines have largely benefitted from each other. Some of the most recognized syntheses, such as the JOHNSON progesterone synthesis, the HEATHCOCK access to daphniphyllum alkaloids or the preparation of FR182877 by SORENSEN and co-workers, have been inspired by Nature.^[33–35] In turn, the WOODWARD/ESCHENMOSER total synthesis of vitamin B₁₂ or the DE BRABANDER synthesis of berkelic acid have prompted novel biosynthetic hypotheses.^[36,37]

Over the course of millenia, Nature has invented and optimized the synthesis of complex molecules from common precursors. Herein, cascade reactions, *i.e.* sequences where the product of one reaction is at the same time the starting material of a subsequent transformation, often form a crucial part and rapidly increase molecular complexity.^[38] The major advantage of a biomimetic strategy is therefore the possibility to employ these efficient cascade processes for a step-economic synthesis from readily available starting materials. In favorable cases, cascade processes can avoid stereoselectivity problems by affording the desired diastereomer based on previously present stereocenters. If a common biosynthetic precursor can be identified, biomimetic syntheses can also provide a general entry to a family of natural products, *e.g.* to the lycopodium alkaloids.^[39] Furthermore, HERTWECK's and TRAUNER's report on orinocin revealed that even new natural products can be found.^[40] Successful mimicry of the natural pathways can also enrich the synthetic methodology as evidenced by polyene cyclizations or biomimetic electrocyclizations.^[41,42]

The benefits of biomimetic syntheses are accompanied by significant challenges that need to be overcome.^[31] First, realistic proposals of biosyntheses require experience and oftentimes an in-depth analysis of co-isolated natural products.^[43] In this context, genome-based elucidation of biosynthetic pathways has recently emerged as a powerful tool and can provide valuable insights.^[44] Second, the experimental realization of biomimetic syntheses can be demanding. Nature has optimized biosyntheses through the development of complex enzyme machineries that are able to structurally pre-organize substrates, catalyze reactions, stabilize reactive intermediates and control the stereoselectivity. The absence of some of these factors in the laboratory can lead to the failure of

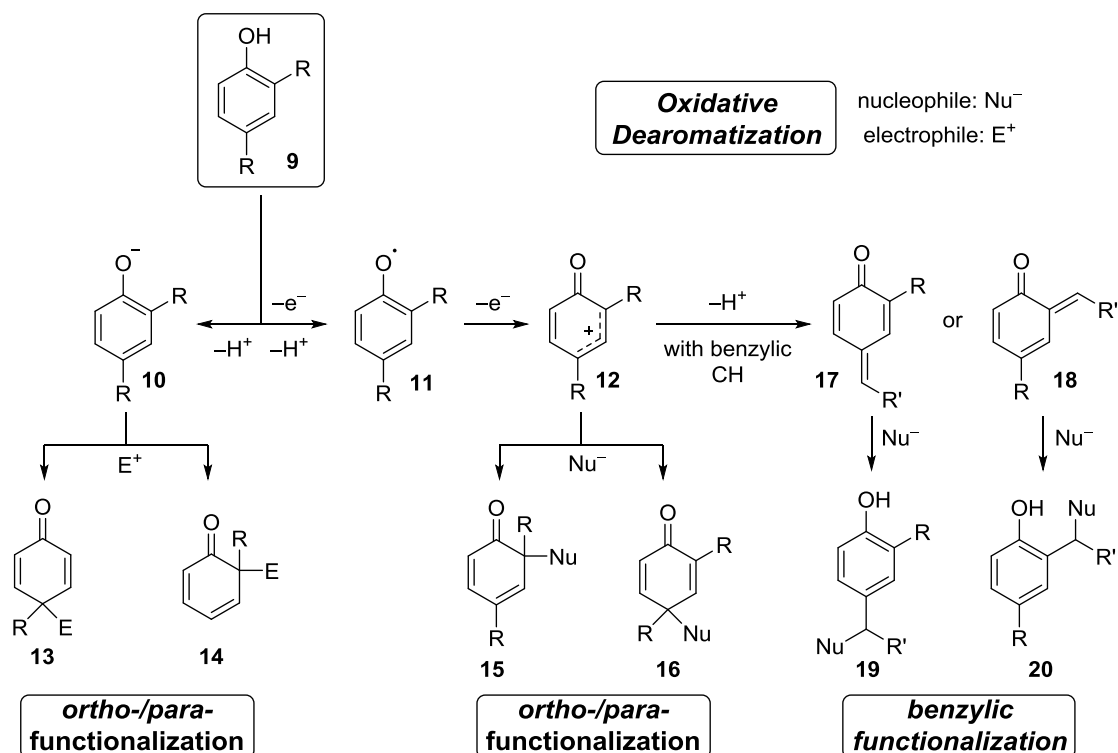
biomimetic strategies.^[45,46] Although by far not exclusively, biomimetic syntheses have therefore often been successful for racemic natural products that are anticipated to be formed by spontaneous processes without enzyme involvement. BLACK's biosynthetic proposal of the racemic endiandric acid natural products represents one example of such a transformation (Scheme 4).^[47] For instance, endiandric acid C as one member of this family was envisioned to stem from cyclohexadiene **7** by a DIELS–ALDER reaction, which in turn would be formed from polyene **8** through an $8\pi/6\pi$ -electrocyclization cascade. This hypothesis was supported by NICOLAOU's successful synthesis along these lines, which still is a testimony to the power of biomimetic strategies.^[48–51] As in many other cases, the actual precursor **8** to the biomimetic cascade was accessed by conventional, non-biomimetic methods.



Scheme 4. Biomimetic endiandric acid cascade.^[47–51]

2.1.2 Oxidative Dearomatization of Hydroxylated Arenes in Total Synthesis

The marked difference in reactivity between hydroxylated benzenes like **9** and their non-oxidized counterparts has frequently been exploited for the synthesis of functionalized cyclohexane skeletons (Scheme 5).^[52] Phenols can be viewed as stable enol tautomers with increased nucleophilicity in the *ortho*- and *para*-position, especially when deprotonated (**10**). In addition, other reaction pathways are also facilitated compared to arenes. Effective *Umpolung* of phenols by the abstraction of one (**11**) or two electrons (**12**) can render the resulting arene susceptible to nucleophilic attack.



Scheme 5. Dearomatization strategies in total synthesis.

Both processes, with phenol as nucleophile or electrophile, result in dearomatized cyclohexadienones such as **13**, **14**, **15** or **16** in case no tautomerization to the corresponding enol can occur ($R \neq H$). These products represent valuable synthetic intermediates due to their tendency to undergo pericyclic reactions or to engage in various ionic processes such as 1,2- or 1,4-additions. In the presence of benzylic hydrogen atoms, the phenonium ion **12** can also be deprotonated to yield *para*-quinone methides **17**. Mostly if *para*-quinone methides cannot form, the deprotonation gives rise to *ortho*-quinone methides **18**. These quinone methides are prone to react in cycloadditions, but can also rearomatize by benzylic nucleophilic attack to give phenols **19** and **20**.

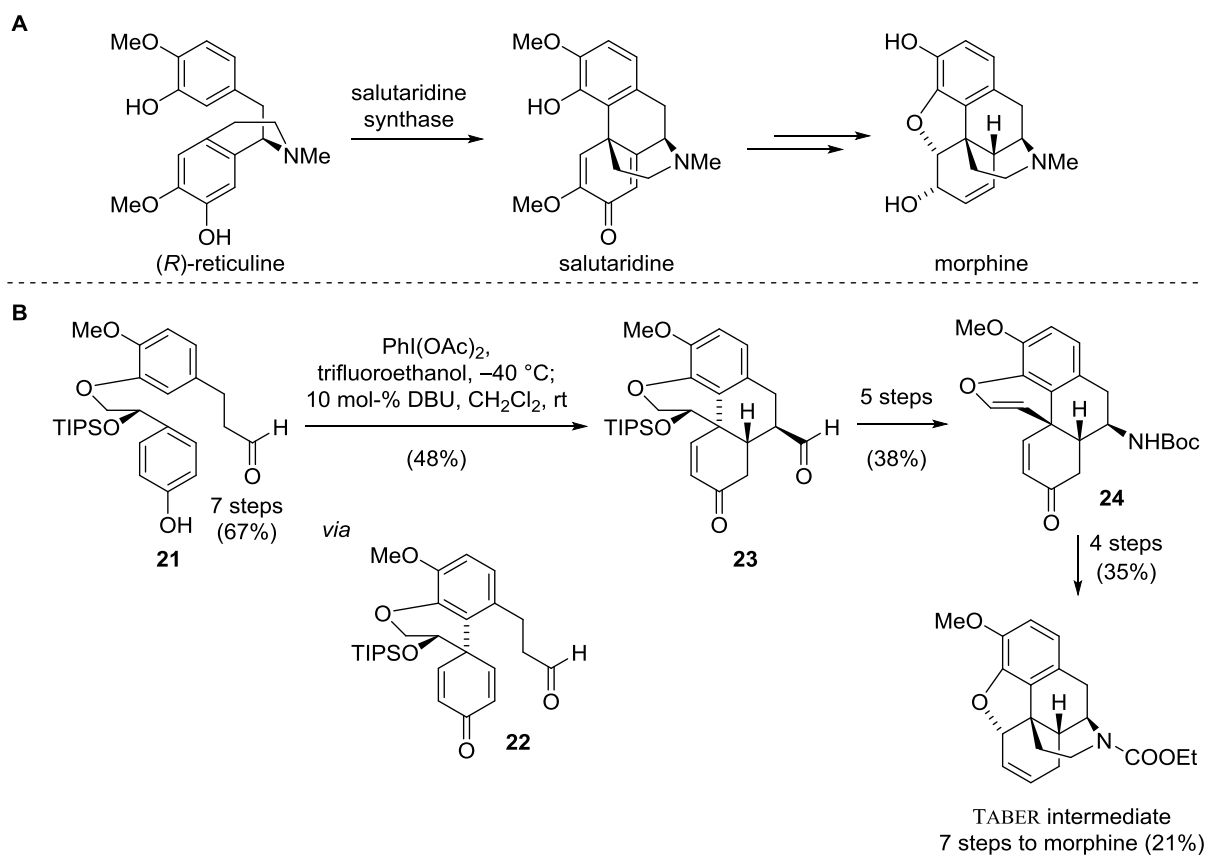
In the following, recent applications of oxidative dearomatization strategies in total synthesis will be highlighted. This will only include examples, where the dearomatization was triggered by an oxidant and no rearomatization occurred. Alkylative processes *via* phenolates, pericyclic reactions such as CLAISEN rearrangements or BUCHNER reactions, dearomatizations *via* BIRCH reductions or enzymatic oxidations as well as benzylic functionalizations will not form part of this overview.^[53–56]

2.1.2.1 Dearomatization of Phenols

Oxidation of phenols opens the path to nucleophilic attack on the aromatic core. The overall transformation thus represents a valuable entry into substituted six-membered ring systems. Among other factors, the regioselectivity is hereby either governed by the rate of ring size formation in intramolecular cases or by the substituents. If a substituent can effectively stabilize the developing positive charge in the arene, attack will mainly occur on the site of this substituent. In this context,

oxygen-based nucleophiles lead to the formation of quinones, quinols or quinone monoketals. The reactivity of these compounds will be described in the following chapter, because it largely resembles the reactivity of oxidized catechols. The main disadvantage of the generation of quinones from phenols can be the lack of regioselectivity.

An elegant application of the oxidative dearomatization of phenols was reported by GAUNT and co-workers in their synthesis of the alkaloid morphine.^[57] Their work is based on a bioinspired intramolecular *ortho-para*-coupling of two arenes that is reminiscent of the conversion of (*R*)-reticuline to salutaridine in the morphine biosynthesis (Scheme 6). Biomimetic approaches along these lines had thus far suffered from poor yields, *e.g.* 0.012% (BARTON)^[58] or 23% (SCHWARTZ).^[59] The GAUNT group therefore chose a different geometric setup in bicycle **21** for the projected I^{III} -mediated key step. The oxidative dearomatization triggered a *para*-selective attack of the pendant arene yielding cyclohexadienone **22** and was followed by a desymmetrizing MICHAEL addition to tetracycle **23**. A similar desymmetrization had previously been disclosed by the MAGNUS group.^[60] Remarkably, the one chiral center in phenol **21** set by asymmetric NOYORI transfer reduction induced the installation of three more stereocenters with the desired configuration.

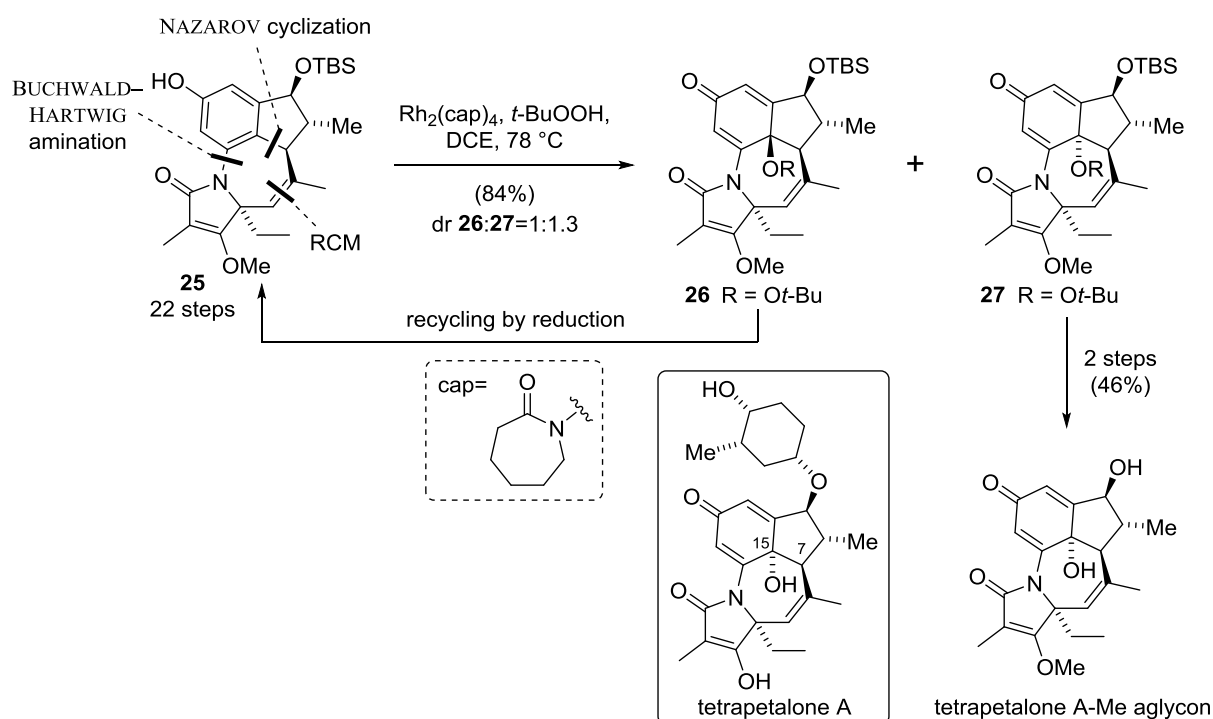


Scheme 6 A. Biosynthesis of Morphine. B. Morphine synthesis by GAUNT and co-workers.^[57]

The secondary alcohol in cyclohexenone **23** not only ensured the stereoselective synthesis of morphine, but was also used to convert the adjacent carbon atom to the aldehyde oxidation state in enol ether **24**. Further transformations of enol ether **24** led to TABER's intermediate, which can be

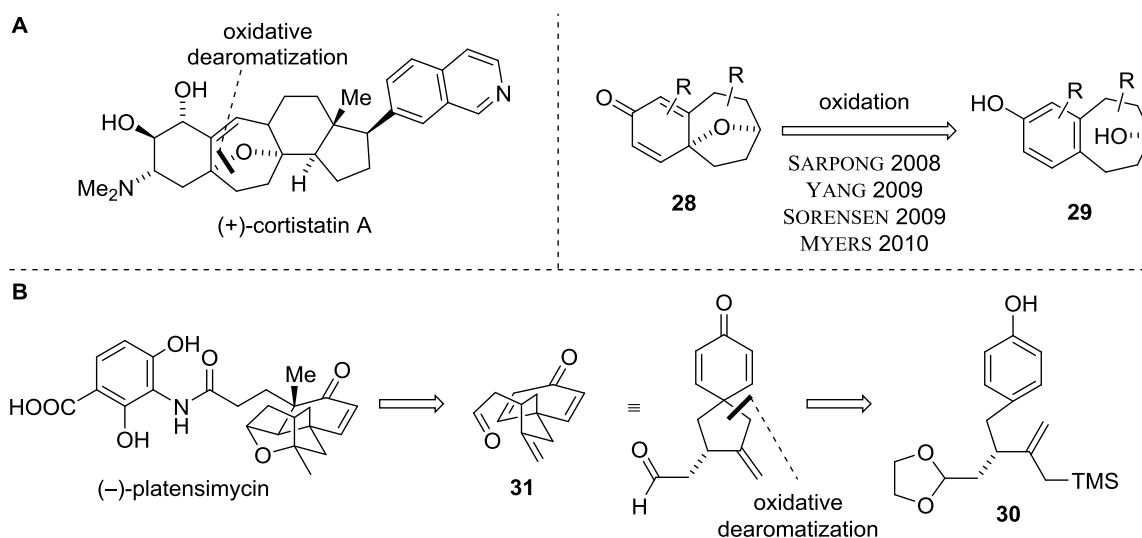
converted to morphine in 7 steps.^[61] The synthesis shows an efficient example of the installation of a quaternary carbon center by *para*-arylation upon dearomatization.

In their racemic synthesis of tetrapetalone A-Me aglycon, the FRONTIER group together with HOVEYDA and co-workers reported a late-stage oxidation of a phenol to a *para*-quinol (Scheme 7).^[62] Phenol **25** was accessed in a highly optimized route by NAZAROV cyclization, BUCHWALD-HARTWIG amination and a challenging ring-closing metathesis (RCM). Under a variety of conditions, the envisioned oxidation to *para*-quinol **27** resulted in the undesired oxidation at C7, probably *via* nucleophilic attack on the corresponding *para*-quinone methide. Suitable conditions were identified in a procedure published by DOYLE and co-workers using a Rh^{II} catalyst in combination with *tert*-butyl hydroperoxide and gave peroxides **26** and **27** as a diastereomeric mixture.^[63] The undesired isomer **26** could be recycled *via* reduction to phenol **25**. However, the desired isomer **27** could only be advanced to the target molecule through the reduction by a Cd/Pb couple since other conditions also resulted in the formation of phenol **25**. Consequently, the first synthesis of tetrapetalone A-Me aglycon was realized in 25 steps.



Scheme 7. Tetrapetalone A-Me aglycon synthesis by the FRONTIER and HOVEYDA group.^[62]

The potential of oxidative dearomatizations for the construction of highly functionalized cyclohexane rings was further showcased in a number of other total syntheses (Scheme 8). In studies on cortistatin A, several groups have closed the tetrahydrofuran ring in cyclohexadienone **28** *via* oxidative dearomatization of intermediates such as **29**.^[64–67] Furthermore, NICOLAOU and co-workers have employed this key step in the synthesis of platensimycin, a natural product with antibacterial properties.^[68] The phenonium ion derived from phenol **30** was efficiently trapped in a SAKURAI-type allylation to furnish spirocycle **31**.



Scheme 8 A. Studies on the synthesis of (+)-cortistatin A.^[64–67]
B. (–)-Platensimycin synthesis of NICOLAOU and co-workers.^[68]

2.1.2.2 Oxidation of Catechols: Reactivity of *ortho*-Quinones and Derivatives

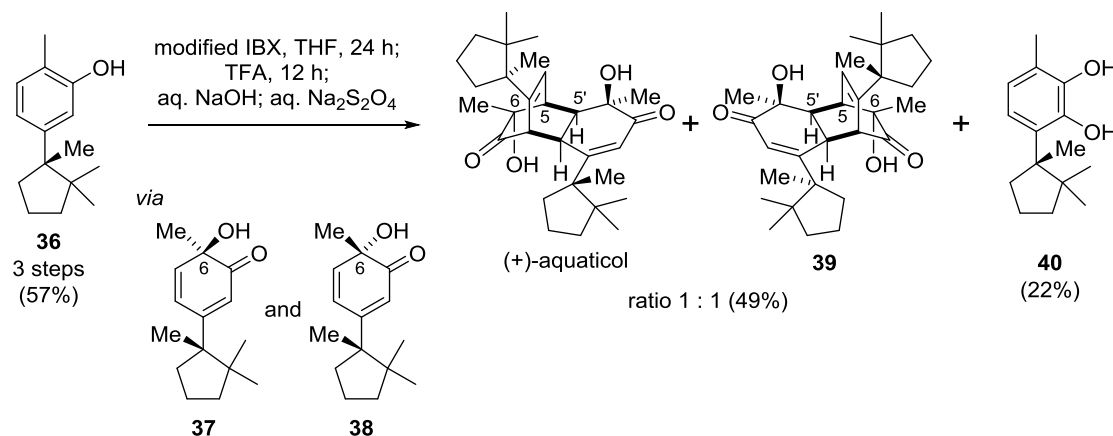
Upon oxidation, catechols can form *ortho*-quinones **32** or *ortho*-quinone monoketals **33** as well as quinone methides **34** depending on the substituents and reaction conditions (Figure 5). Major advantage of this *ortho*-quinone generation method compared to the oxidation of phenols is the excellent regiocontrol. In total synthesis, the more stable *ortho*-quinone monoketals derived from the oxidation of catechol monoethers are more frequently employed than their *ortho*-quinone counterparts. As mentioned previously, *ortho*-quinols **35** possess similar reactivity to *ortho*-quinone monoketals and will hence be described here.

<i>ortho</i> -quinones				
	32			34
<i>ortho</i> -quinone monoketals				
	33 R ≠ H		R ≠ H	
<i>ortho</i> -quinols				
	35 R ≠ H R' ≠ heteroatom, H		R ≠ H R' ≠ heteroatom, H	
feature:	electron-poor cyclic diene	hetero diene	enone	<i>para</i> -quinone methide
reaction:	inverse-demand Diels–Alder	hetero-Diels–Alder	1,2-additions 1,4-additions cycloadditions	rearomatization (benzylic functionalization)

Figure 5. Reactivity pattern of *ortho*-quinones, -quinone monoketals and -quinols.

Due to their electron-poor cyclic diene system, *ortho*-quinones and *ortho*-quinone monoketals can engage in inverse-demand DIELS–ALDER reactions. The fact that one of the most powerful reactions in synthetic chemistry can be employed after dearomatization of hydroxylated arenes represents one of the main reasons for their use in the total synthesis of structurally challenging natural products. In addition, *ortho*-quinones possess a second 4π -system, which can undergo hetero-DIELS–ALDER cycloaddition with electron-rich alkenes. Apart from the diene motifs, building blocks **32**, **33** and **35** feature several 2π -systems (alkene, carbonyl), which can react in ionic, radical and pericyclic processes. Comparable to phenols, the oxidation of catechols can afford quinone methides by tautomerization of benzylic hydrogen atoms in the *para*- or *ortho*-position. This lowers the dipole repulsion of the two carbonyls and can be thermodynamically favored. Apart from rearomatization by nucleophilic attack at the former benzylic position, the olefins could engage in concerted cycloadditions as a 2π -component (dienophile).

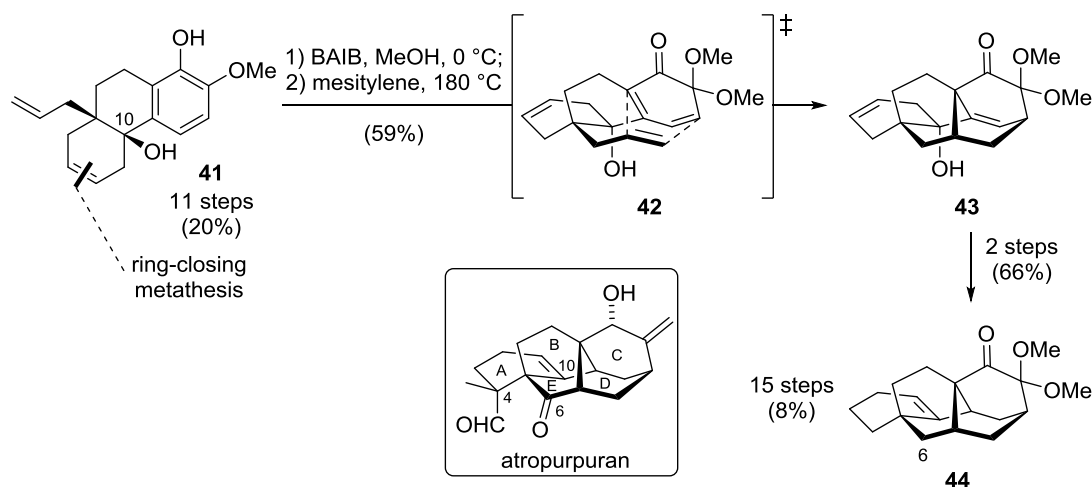
The cyclohexadienes **32**, **33** and **35** are known to undergo rapid homodimerization, which needs to be taken into account when applied in a total synthesis.^[69] In many examples, intramolecular processes were therefore envisioned to capture the resulting reactive intermediates and outcompete the intermolecular dimerization. However, precisely due to this high tendency, several natural products are derived from the homodimerization of *ortho*-quinones or -quinols. An example of their high reactivity in DIELS–ALDER reactions was provided by QUIDEAU and co-workers in their synthesis of (+)-aquaticol (Scheme 9).^[70]



Scheme 9. QUIDEAU synthesis of (+)-aquaticol (formed bonds are highlighted in bold).^[70]

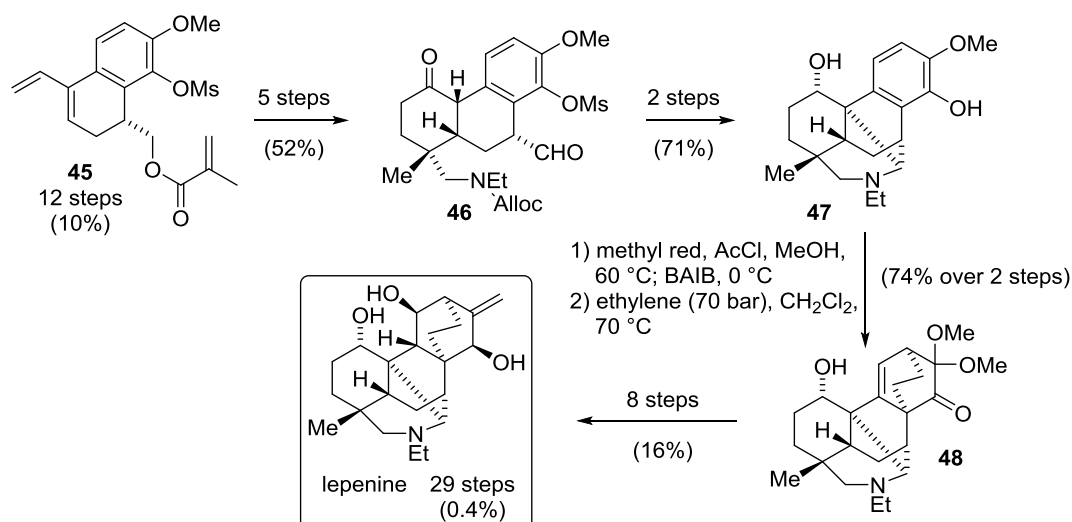
Phenol **36** was accessed in three steps from commercially available racemic cuparene and purified by chiral HPLC. No diastereoselection was observed in the following oxidation to quinols **37** and **38**. Remarkably, only the quinols with the same configuration at C6 combined to afford (+)-aquaticol and its diastereomer **39**. The observed recognition between the quinols was rationalized with CIEPLAK–FALLIS interactions, a hyperconjugative stabilization between the C6–Me bonding σ -orbital and the antibonding σ^* -orbital of the C5–C5' bond. Side product of the key step was catechol **40**, resulting from a regioisomer of the initial oxidation.

Several total syntheses have profited from the implementation of a catechol dearomatization to install additional rings on a cyclohexane skeleton by cycloaddition. In their study on atropurpuran, KOBAYASHI and co-workers accessed tricycle **41** in 11 steps (Scheme 10).^[71] Remarkably, the dearomatization and subsequent high-temperature intramolecular DIELS–ALDER cycloaddition of catechol **41** *via* transition state **42** delivered the *anti*-BREDT olefin **43**. The substituent at C10 was found to exert a major influence on the intramolecular cycloaddition since a substrate with a carbonyl functionality did not provide the desired cyclization product. Instead, this substrate homodimerized in a DIELS–ALDER reaction and could not be transformed into the desired product even at higher temperatures. Despite the lack of suitable handles to install the missing substituents on C6 and C4, pentacycle **43** was advanced to ketone **44**, providing the first synthesis of this rare skeleton.



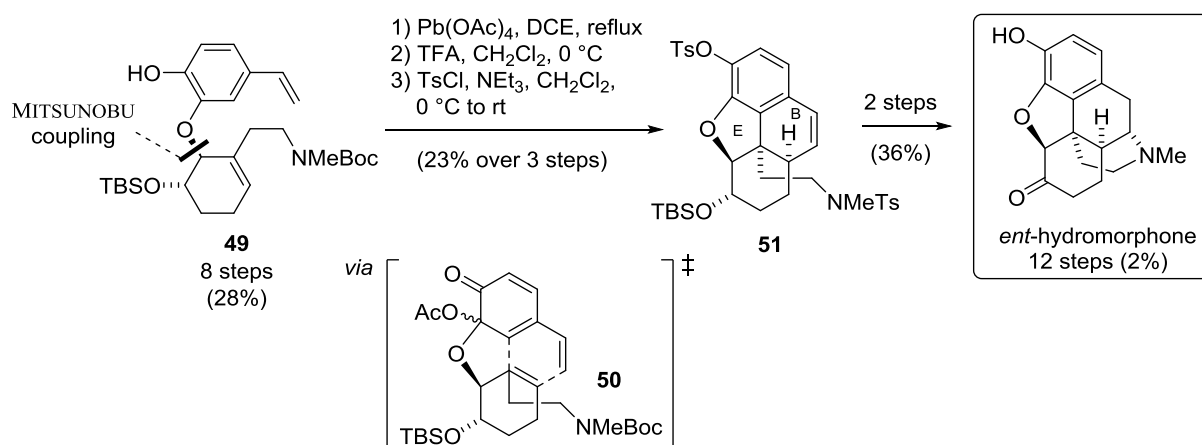
Scheme 10. Studies toward the synthesis of atropurpuran by KOBAYASHI and co-workers.^[71]

Lepenine belongs to the denudatine-type alkaloids and features a tetradecahydrophenanthrene skeleton with an additional *N*-containing ring and a bicyclo[2.2.2]octane. The FUKUYAMA group has reported the first successful synthesis of this natural product starting from acrylic ester **45**, which was accessed in 12 steps (Scheme 11).^[72] Subsequent intramolecular DIELS–ALDER reaction and functional group interconversions afforded ketone **46**, the substrate for the key MANNICH reaction. The latter proceeded smoothly to give phenol **47** after an additional step. Remarkably, the key oxidative dearomatization/DIELS–ALDER sequence was successfully carried out with ethylene as the dienophile under increased pressure to afford the desired bicyclo[2.2.2]octane **48**. The amine functionality had to be protected as an ammonium salt to prevent decomposition of the molecule resulting from its undesired oxidation. Lepenine was hence prepared in 29 steps as the first member of this class to be accessed by total synthesis.



Scheme 11. Lepenine synthesis by FUKUYAMA and co-workers.^[72]

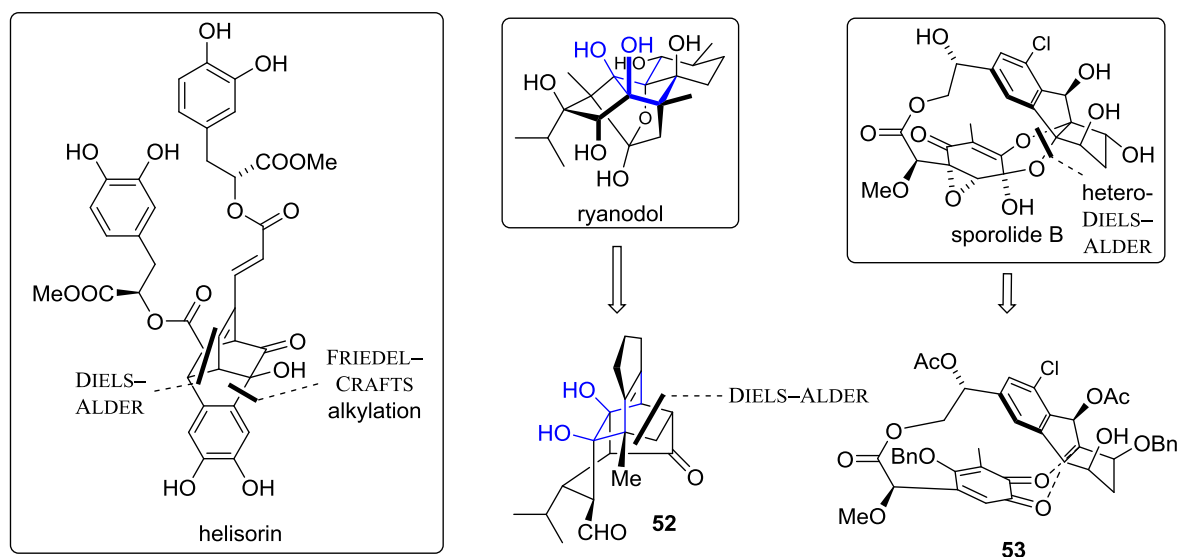
A rare reactivity mode in oxidative dearomatizations was observed by HUDLICKY and co-workers in their synthesis of *ent*-hydromorphone (Scheme 12).^[73] Ether **49** was accessed from a toluene derivative by enzymatic dihydroxylation and subsequent MITSUNOBU reaction. Oxidation with lead tetraacetate gave rise to an *ortho*-quinone monoketal, which underwent a DIELS–ALDER reaction *via* transition state **50**. The authors reason that, despite the reactivity of the cyclic diene, the diene involving the terminal olefin is sterically more accessible and therefore engages preferentially in the cycloaddition to afford tetracycle **51**. This key step affords the B and E ring of the desired product simultaneously. Radical cyclization to effect closure of the piperidine ring and oxidation yielded *ent*-hydromorphone.



Scheme 12. *ent*-Hydromorphone synthesis by HUDLICKY and co-workers.^[73]

Several other well-known syntheses have benefitted from the potential of *ortho*-quinone-type structures to engage in complex cycloadditions (Scheme 13). In their helisorin synthesis, SNYDER and co-workers initially attempted a fully biomimetic oxidative dimerization of the natural compound rosmarinic acid to the target molecule.^[74] However, this step afforded the kinetic product, *i.e.* a

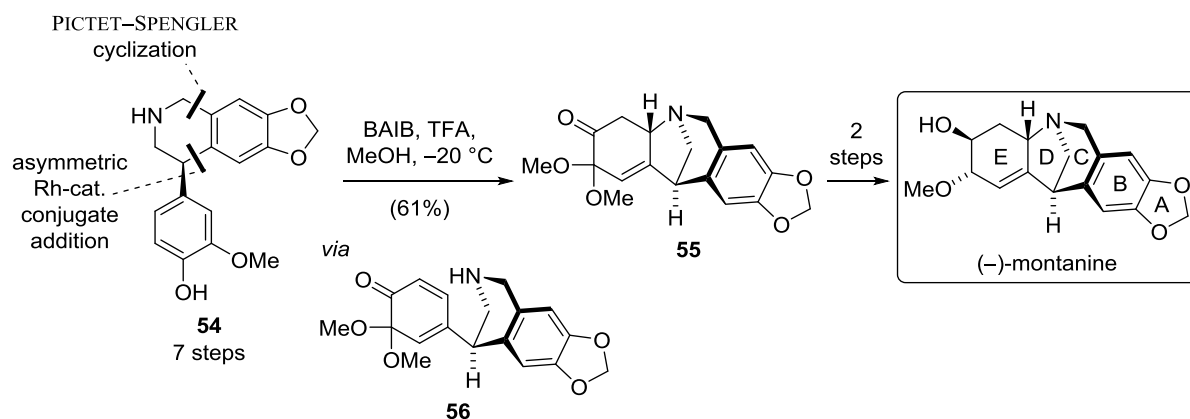
dimerization of both arene rings in a DIELS–ALDER reaction. The lack of regiocontrol in the laboratory was rationalized with the hypothesis that enzymes control the regioselectivity of the dimerization in Nature. It was argued that the thermodynamic product would be the natural product. Heating the initial kinetic dimer in the presence of a dienophile afforded the desired dimerization product that was converted to helisorin. In their landmark discovery of a synthetic route toward ryanodol, DESLONGCHAMPS and co-workers also employed an *ortho*-quinone DIELS–ALDER reaction to access pentacycle **52**.^[75]



Scheme 13. Further syntheses with *ortho*-quinone Diels–Alder reactions.^[74–76]

An example of the hetero-DIELS–ALDER reactivity of *ortho*-quinones was provided by NICOLAOU and co-workers in their synthesis of sporolide B (Scheme 13).^[76] A macrocycle was closed in this key step *via ortho*-quinone **53**, which required thorough investigation of the coupling partners to achieve the desired regioselectivity.

Apart from DIELS–ALDER reactions, the potential of catechol oxidation in combination with a subsequent 1,4-addition has also been exploited as demonstrated in the bioinspired synthesis of five members of the montanine-type *Amaryllidaceae* alkaloids by the FAN group (Scheme 14).^[77] Tetrahydroisoquinoline **54** was accessed in seven steps by an asymmetric conjugate addition of an arylboronic acid to a nitroalkene. Subsequently, the *N*-containing ring was closed using a regioselective PICTET–SPENGLER cyclization. Due to the inherent lower nucleophilicity of methylenedioxy-substituted ring B, an electron-withdrawing phenol protecting group on ring E had to be employed to arrive at the desired product **54**. The key oxidative dearomatization with subsequent aza-MICHAEL addition proceeded with excellent diastereoselectivity to give pentacycle **55** *via ortho*-quinone monoketal **56**.



Scheme 14. Montanine-type alkaloid synthesis by FAN and co-workers.^[77]

The intermediate **55** served as a common precursor to the montanine-type alkaloids by different transformations on ring E. Among others, the authors synthesized (–)-montanine by this novel bioinspired route.

2.1.2.3 Oxidation of Hydroquinones: Reactivity of *para*-Quinones and Derivatives

para-Hydroquinones and phenols, depending on the substrate and the conditions, can be oxidized to *para*-quinones **57**, -quinols **58** or -quinone monoketals **59** (Figure 6). Whereas the former are more reactive due to the presence of two LUMO-lowering carbonyl groups, the latter can undergo diastereoselective transformations without additives due to their tetrahedral carbon atom.

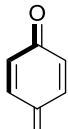
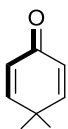
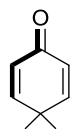
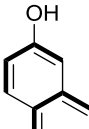
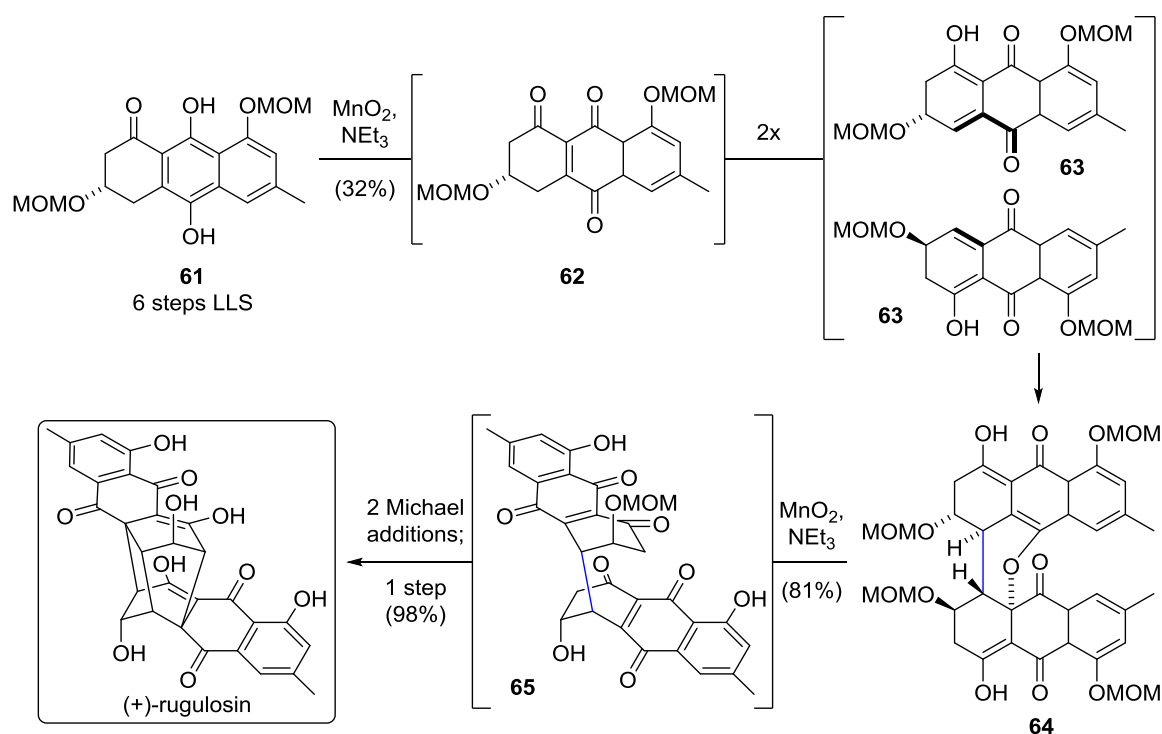
 57 <i>para</i> -quinones	 58 <i>para</i> -quinols $R \neq H$ $R' \neq \text{heteroatom, H}$	 59 <i>para</i> -quinone monoketals $R \neq H$	 60 <i>ortho</i> -quinone methide
reaction: 1,2-additions 1,4-additions cycloadditions	1,2-additions 1,4-additions cycloadditions	1,2-additions 1,4-additions cycloadditions	1,2-additions 1,4-additions cycloadditions (as dienophile and diene)
advantage: high reactivity	diastereoselectivity possible	enantioselectivity possible (chiral OR)	

Figure 6. Reactivity of *para*-quinones, -quinols, -quinone monoketals and *ortho*-quinone methides.

Since the 4π -systems of the above mentioned quinone-type structures are all locked in the *s-trans* configuration, they cannot undergo concerted cycloadditions. However, the alkene part of the respective enone moieties can engage in 1,2- or 1,4-additions of nucleophiles or react as a dienophile.

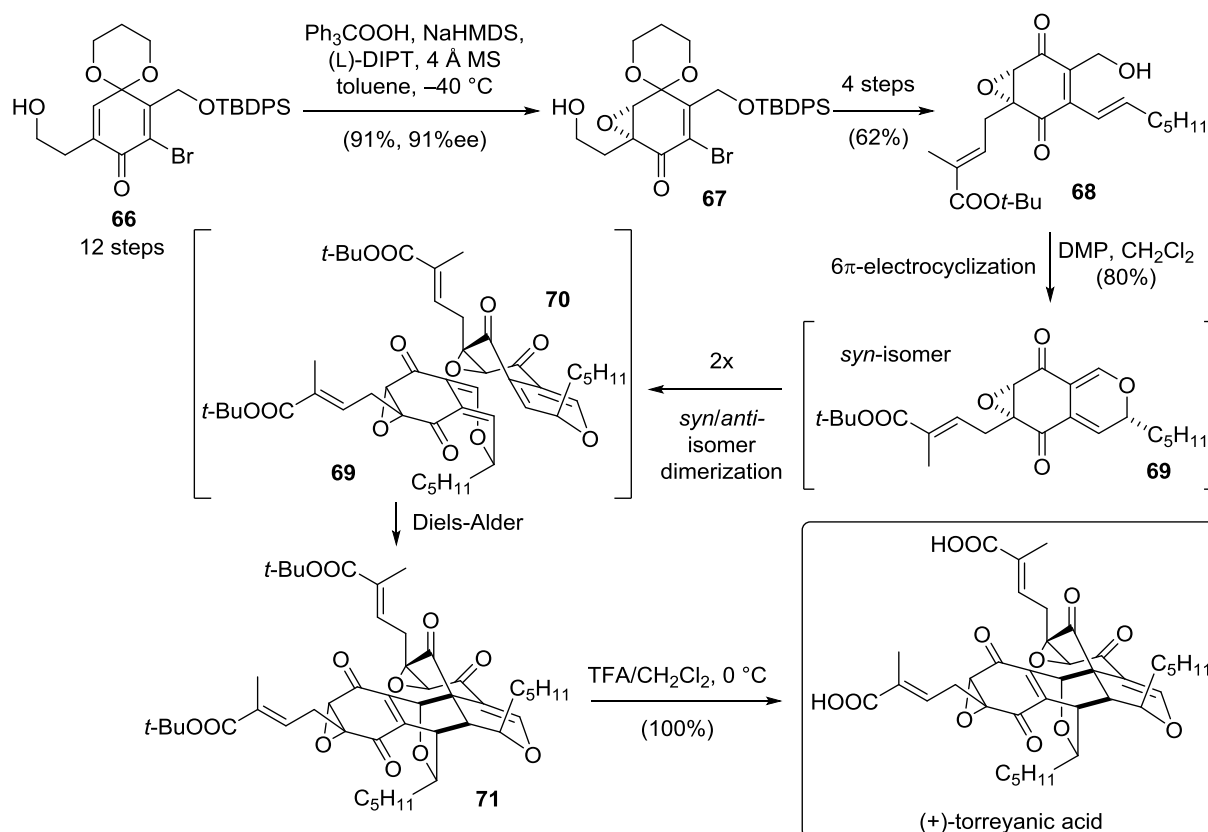
In case benzylic hydrogen atoms are present, the corresponding *ortho*-quinone methide **60** can be formed by tautomerization.^[78] Besides rearomatization by nucleophilic attack on the former benzylic position, they can undergo cycloadditions as a 4π -component *via* the cyclic all-carbon diene or *via* the exocyclic hetero diene. Several 2π -systems can furthermore engage in pericyclic reactions. In contrast to *ortho*-quinones, the dipole moments of *para*-quinones oppose each other, which renders them more stable. Numerous natural products containing *para*-quinones have been isolated.^[79]

The participation of *para*-quinones as dienophiles in DIELS–ALDER reactions has been reviewed very recently.^[80] Therefore, other applications of this structural motif in total synthesis will be highlighted. In 2005, the NICOLAOU group disclosed a biomimetic synthesis of (+)-rugulosin, which features several key aspects of the reactivity of *para*-quinones (Scheme 15).^[81] Oxidation of hydroquinone **61**, which was accessed in 6 steps, yielded quinone **62**. After tautomerization to quinone methide **63**, two molecules underwent a hetero-DIELS–ALDER homodimerization to pyran **64**. Further oxidation to hexaketone **65** resulted in a double MICHAEL addition cascade, furnishing (+)-rugulosin after global deprotection.



Scheme 15. (+)-Rugulosin synthesis by NICOLAOU and co-workers.^[81]

The potential of *para*-quinones was also exploited in the asymmetric and biomimetic synthesis of the dimeric epoxyquinone natural product (+)-torreyanic acid by PORCO and co-workers in 2003 (Scheme 16).^[82]

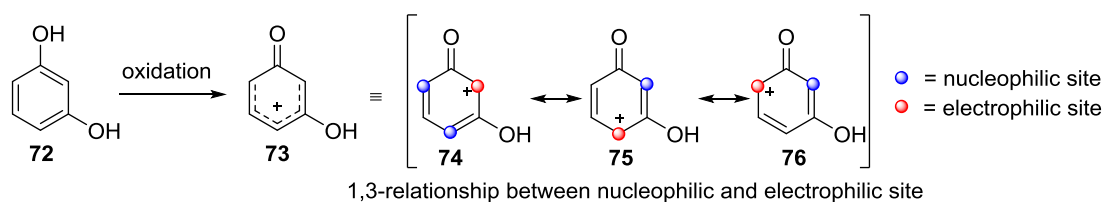


Scheme 16. (+)-Torreyanic acid synthesis by PORCO and co-workers.^[82]

Quinone monoketal **66** was synthesized in 12 steps involving an oxidation of a monoprotected hydroquinone by I^{III} . Asymmetric nucleophilic SCHEFFER–WEITZ-type epoxidation afforded enantioenriched epoxide **67**, which was converted to alcohol **68**. Upon oxidation, the resulting aldehyde underwent spontaneous electrocyclization to cyclic diene **69**. The latter can cyclize in a [4+2]-cycloaddition with its *anti*-isomer **70** to yield torreyanic acid precursor **71**. Deprotection furnished (+)-torreyanic acid. The synthesis demonstrates the versatility of quinones in the synthesis of functionalized cyclohexane rings. It provides an example of the influence of the *para*-quinone π -system on the reaction of neighboring olefins.

2.1.2.4 Oxidation of Resorcinols

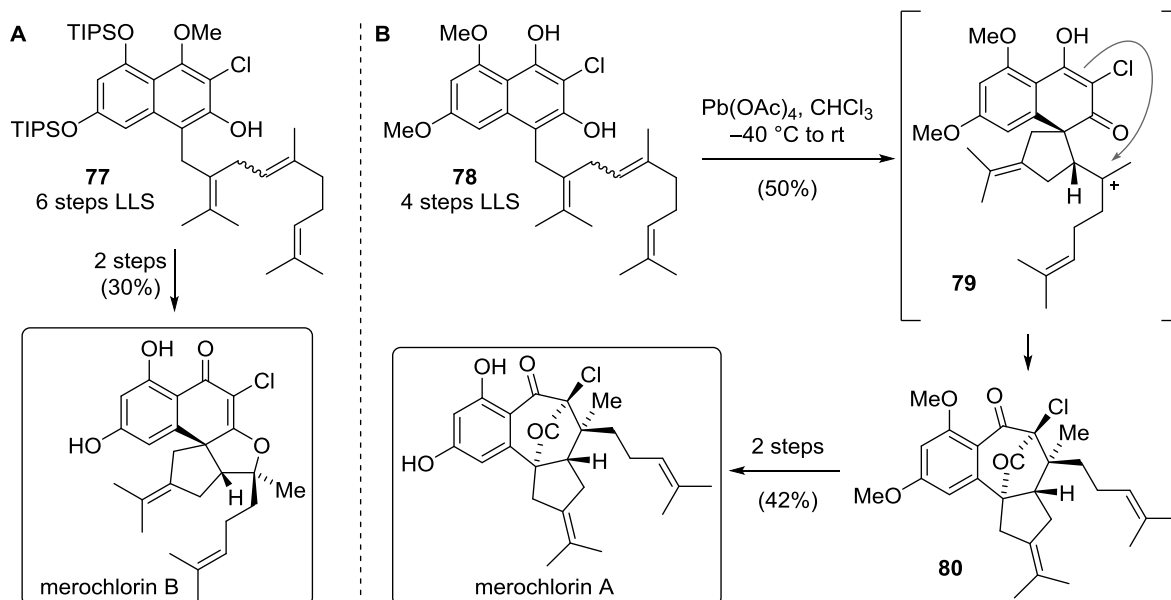
Resorcinols (**72**) cannot be oxidized to an isolable quinone structure since the OH in *meta*-position does not effectively stabilize the positive charge in the ring (Scheme 17).



Scheme 17. Resorcinol oxidation.

As a result, the reactivity of resorcinols upon oxidation (**73**) resembles more a 1,3-dipole since they possess nucleophilic and electrophilic sites in a 1,3-relationship in the mesomeric structure **74**, **75** or **76**. In addition to the displayed sites on carbon atoms, the oxygen atom can also act as a nucleophile.

The reactivity pattern of oxidized resorcinols was exploited in two publications on the synthesis of members of the merochlorin family by the TRAUNER and the GEORGE group (Scheme 18).^[83,84]

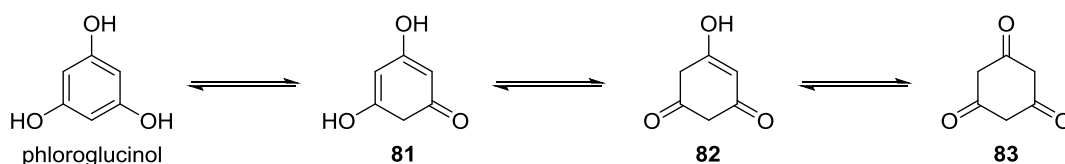


Scheme 18 A. Merochlorin B synthesis by TRAUNER and co-workers.^[83] **B.** Merochlorin A synthesis by GEORGE and co-workers.^[84]

Whereas TRAUNER and co-workers accomplished the synthesis of merochlorin B from naphthol **77** in a (3+2) cycloaddition involving the oxygen atom, GEORGE reported the intramolecular (5+2) cycloaddition of the related naphthalenediol **78** *via* intermediate **79**. Global deprotection of dimethyl ether **80** afforded merochlorin A. Both syntheses highlight the potential of resorcinols to engage in cascade additions of nucleophiles and electrophiles upon oxidation. Importantly, the reactivity of resorcinols can be channeled into the one of phenols if one of the resorcinol OH groups is protected with a suitable protecting group that is inert to the oxidation conditions.

2.1.2.5 Dearomatization of Phloroglucinols

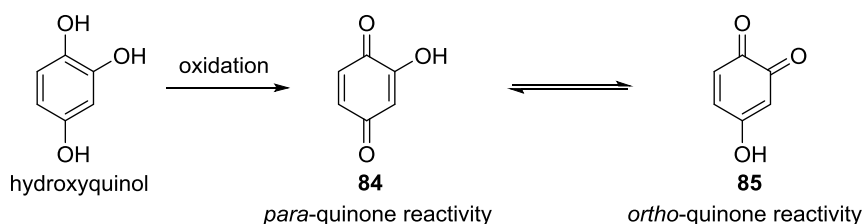
Numerous natural products contain the phloroglucinol subunit.^[85] Especially at higher pH, phloroglucinol can form substantial quantities of its keto-tautomers **81**, **82** or **83**.^[86] Therefore, phloroglucinols can be seen as partially intrinsically dearomatized (Scheme 19). Syntheses of related natural products therefore rely mostly on alkylative dearomatizations by α -functionalization of the respective ketones.



Scheme 19. Tautomerization between phloroglucinols and triketones.

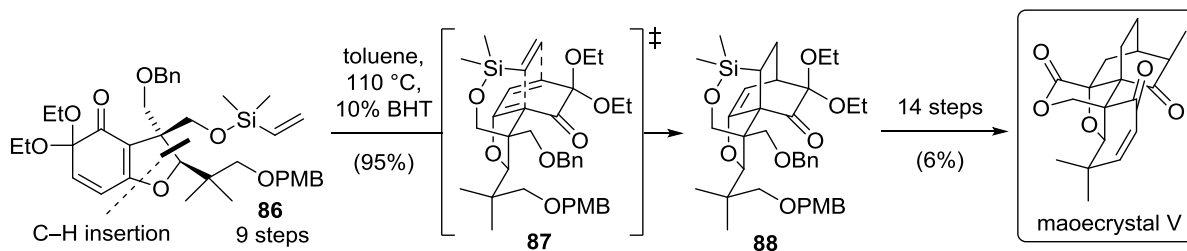
2.1.2.6 Oxidation of Hydroxyquinols: Reactivity of Related Quinones and Quinols

Hydroxyquinols are the second of three possible constitutional isomers of benzene triols. Their reactivity upon oxidation resembles either *para*- or *ortho*-quinones **84** or **85** depending on the substitution pattern of the substrate (Scheme 20). This also applies to related ketals or quinol-type systems. In this context, a control over the outcome of the oxidation is usually achieved by suitably protecting one or more of the hydroxyl groups. The protected hydroxyl group can then be seen as a spectator and the reactivity profile is mostly dictated by the remaining OH substituents. As such, protected hydroxyquinols can react like more electron-rich variants of either hydroquinones, resorcinols or catechols.



Scheme 20. Oxidation products of hydroxyquinol.

An elegant example of their reactivity as *ortho*-quinones was provided by ZAKARIAN and co-workers in their racemic synthesis of maoecrystal V, a cytotoxic *ent*-kauranoid with an unusual structure (Scheme 21).^[87] Silyl ether **86** was accessed in 9 steps from sesamol by MITSUNOBU reaction, C–H insertion and oxidation with PIFA.

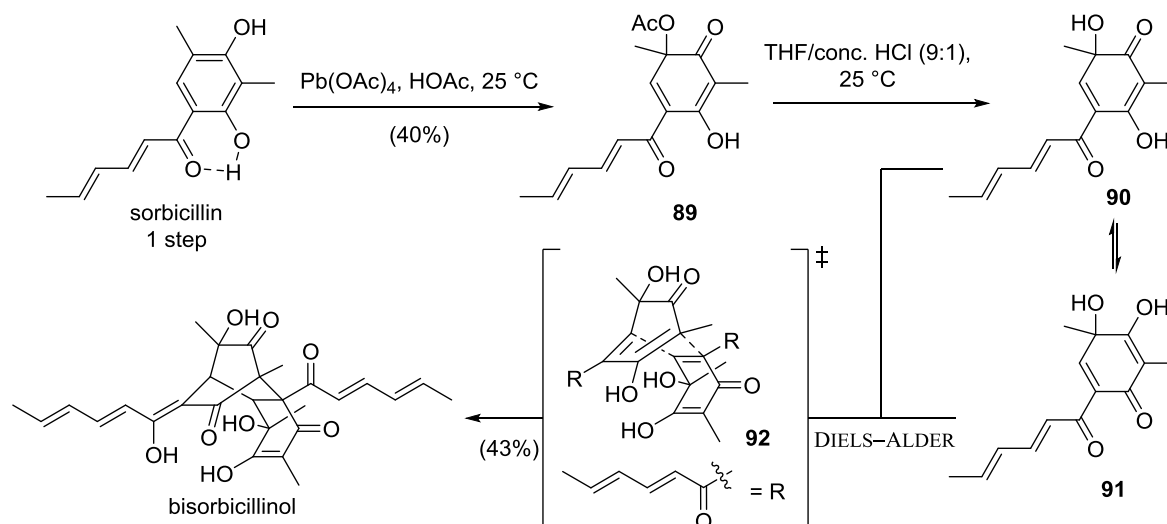


Scheme 21. Maoecrystal V synthesis by ZAKARIAN and co-workers.^[87]

The following intramolecular DIELS–ALDER reaction with a silyl tether proceeded smoothly *via* **87** to furnish tetracycle **88** in 95% yield. Removal of the silyl tether, subsequent carbonyl radical cyclization and a ring closing metathesis allowed for the successful synthesis of the challenging

natural product maoecrystal V. Later on, the ZAKARIAN group also reported an asymmetric version of this synthesis.^[88]

Similar to *ortho*-quinones, oxidized hydroxyquinols can homodimerize in a DIELS-ALDER cycloaddition. The biomimetic synthesis of bisorbicillinol by the NICOLAOU group took advantage of this key reactivity feature (Scheme 22).^[89]

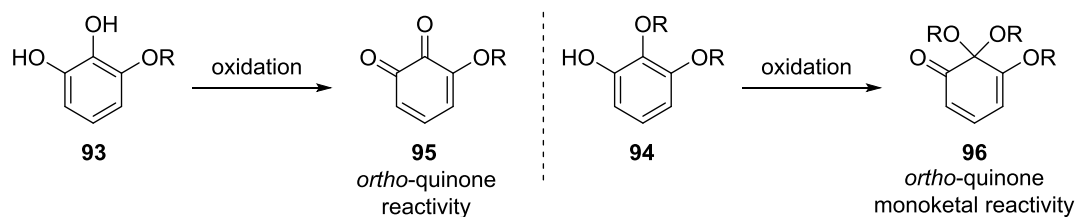


Scheme 22. Racemic bisorbicillinol synthesis by NICOLAOU and co-workers.^[89]

Oxidation of sorbicillin with lead tetraacetate allowed for the preparation of quinol precursor **89** in a controlled fashion in contrast to attempts of direct oxidation to quinol **90**. Furthermore, regioisomers could be removed by column chromatography. Acidic hydrolysis of the acetate protecting group afforded quinol **90**, which can react as a diene. Tautomerization gave rise to *para*-quinone-type quinol **91**. Both tautomers then engaged in a DIELS-ALDER dimerization *via* **92** to furnish the natural product bisorbicillinol in 43% yield. A homodimerization of quinol **90** followed by tautomerization would provide the same result.

2.1.2.7 Oxidation of Protected Pyrogallols

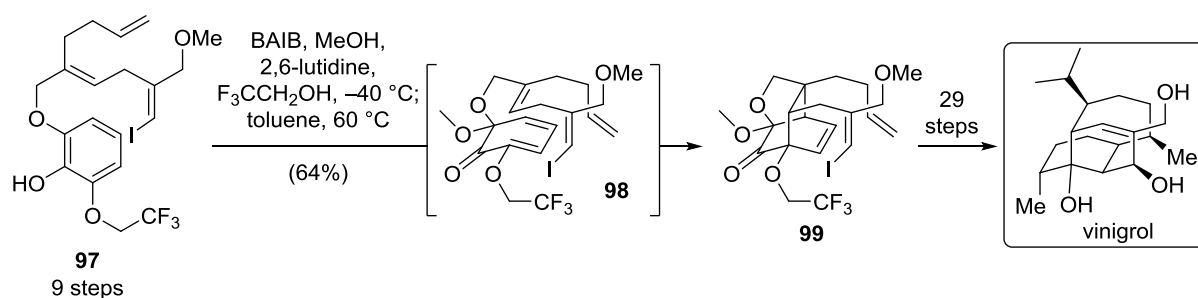
The oxidation of protected pyrogallols **93** or **94** gives quinones **95** or **96** that possess a similar reactivity to the already described *ortho*-quinones or their monoketals (Scheme 23). It is worth noting in this context that the reactivity of the oxidized unprotected pyrogallols can be very different from their protected analogs. As mentioned previously, the reactivity of hydroxylated arenes is mainly governed by the position and number of unprotected OH-groups.



Scheme 23. Oxidation of protected pyrogallols.

Since their reactivity profile is similar to *ortho*-quinones, the oxidation products of protected pyrogallols have mainly been employed in total syntheses for target molecules with higher degrees of oxidation or when the strategy required additional functionalization. The installation of hydroxyl-groups after the key step can thus be avoided.

The diterpenoid vinigrol was isolated in 1987 and attracted significant interest from the synthetic community over the years due to its unprecedented structure.^[90] Only in 2009, the BARAN group reported the first total synthesis of this tricyclic natural product, which features a diaxial butano-bridge over a *cis*-decalin core.^[91] The NJARDARSON group has recently accomplished a racemic synthesis of vinigrol by implementing an intramolecular DIELS–ALDER cycloaddition upon oxidative dearomatization of a pyrogallol derivative (Scheme 24).^[92] A protected pyrogallol rather than a catechol was necessary in this case to allow for further functionalization of the skeleton later on.



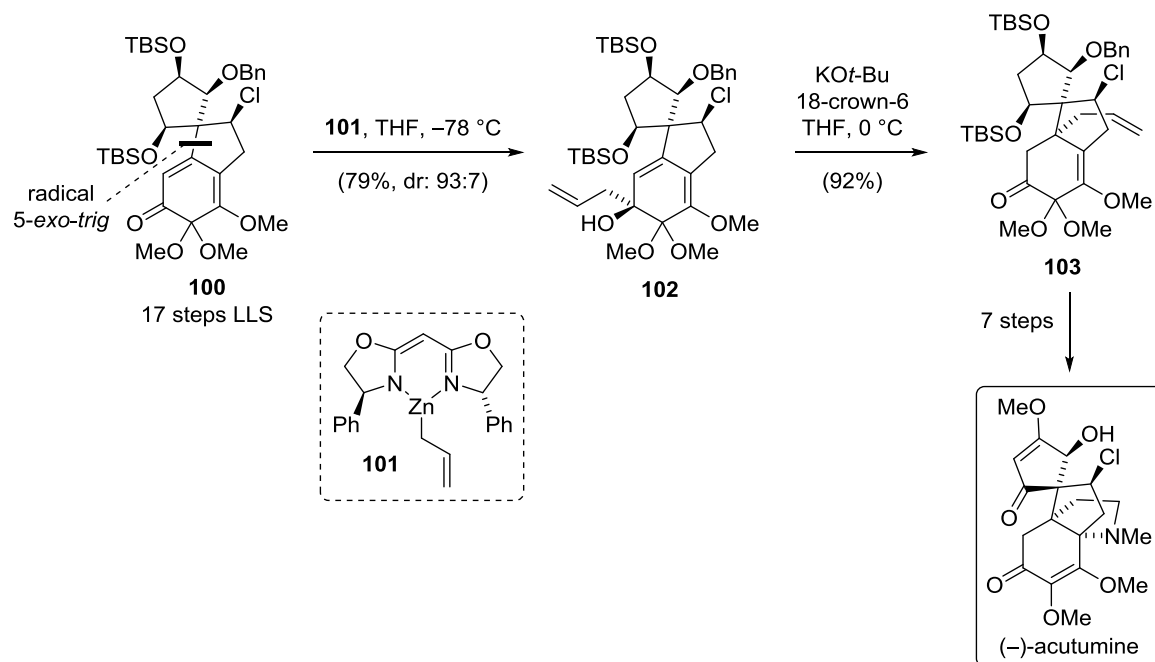
Scheme 24. Racemic synthesis of vinigrol by NJARDARSON and co-workers.

The starting material **97**, prepared in 9 steps, was oxidized by an I^{III} reagent to the corresponding quinone monoketal **98**. The electron-withdrawing trifluoroethyl group ensured the desired regioselectivity of the oxidation. Heating of the reaction mixture to $T = 60\text{ } ^\circ\text{C}$ allowed for the desired cycloaddition to occur, yielding tricycle **99**. The total synthesis of vinigrol was completed after 29 further steps, a testimony to its challenging structure.

In their acutumine synthesis, CASTLE and co-workers employ an elegant way for the installation of a quaternary center profiting from the enone functionality of a quinone.^[93] In this case, the natural product features a high oxidation degree so that the use of a protected pyrogallol obviates the need for additional installation of oxygen atoms after the key step.

Quinone monoketal **100** was prepared in 17 steps by a radical cyclization and oxidation with I^{III} . An asymmetric carbonyl allylation following NAKAMURA's methodology with chiral reagent **101** allowed for the synthesis of tertiary alcohol **102**, which underwent a subsequent anionic COPE

rearrangement to give rise to ketone **103** with two adjacent quaternary centers.^[94] Acutumine was accessed in seven additional steps from this advanced intermediate.



Scheme 25. (-)-Acutumine synthesis of CASTLE and co-workers.^[93]

In summary, the vast potential of oxidative dearomatizations can facilitate the construction and functionalization of six-membered rings and allow for the synthesis of carbon skeletons that are otherwise difficult to access.

2.1.3 Oxidation of Unprotected Pyrogallols

Intriguingly, the oxidation of unprotected pyrogallols gives rise to molecules containing an electrophilic and a nucleophilic site (Figure 7). In general, this reactivity pattern is observed when the oxidation of hydroxylated benzenes leads to compounds, where one of the former OH groups is still present in its enol form (in a non-zwitterionic structure, see for instance chapter 2.1.2.4 Oxidation of Resorcinols). This fact represents the main reason for the different reactivity of oxidized pyrogallols compared to oxidized catechols.

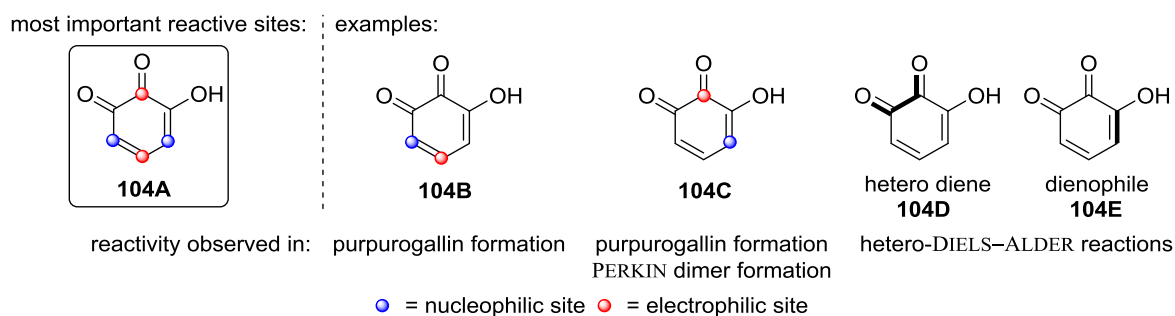


Figure 7. Reactivity analysis of oxidized pyrogallols.

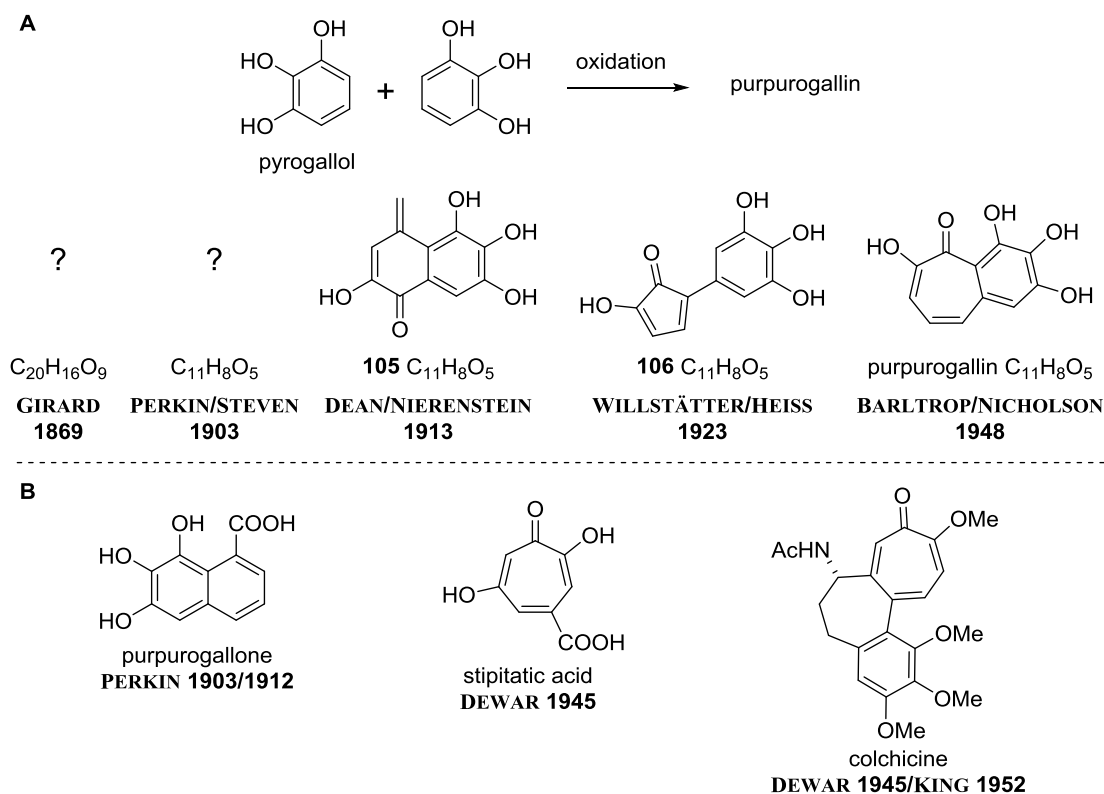
Depending on the conditions and the substrate, oxidized pyrogallols can react in several ways. Hydroxyquinone **104A** shows their most important nucleophilic and electrophilic sites. For instance, hydroxyquinone **104B** can engage in pericyclic reactions as a 2π -system or in ionic reaction cascades such as 1,4-additions with subsequent enol/enolate α -functionalization. An example is provided in the purpurogallin formation (see 2.1.3.1 Purpurogallin Formation Reaction). A nucleophilic attack on the most electrophilic carbonyl function and a reaction of the enol (**104C**) can also be observed in the purpurogallin formation and is of central importance to the formation of the PERKIN dimer (see 2.1.3.2

Formation of the PERKIN Dimer). Furthermore, like *ortho*-quinones, oxidized pyrogallols can undergo inverse-demand hetero-DIELS–ALDER reactions with the hetero-diene motif highlighted in structure **104D**. Importantly, due to the presence of a nucleophilic enol, they can also react as a dienophile (**104E**). Literature precedence will be reviewed in the following chapters to establish guidelines for the substrate dependence of these reactivity trends. Reactions according to the purpurogallin and PERKIN dimer formation as well as the hetero-DIELS–ALDER dimerization were observed in the course of this thesis.

2.1.3.1 Purpurogallin Formation Reaction

2.1.3.1.1 Historical Perspective

In 1869, GIRARD oxidized pyrogallol with silver nitrate or potassium permanganate and sulfuric acid to an unknown compound, which he named purpurogallin.^[95] His finding marked the beginning of decades of investigation concerning its constitution and structure (Scheme 26).

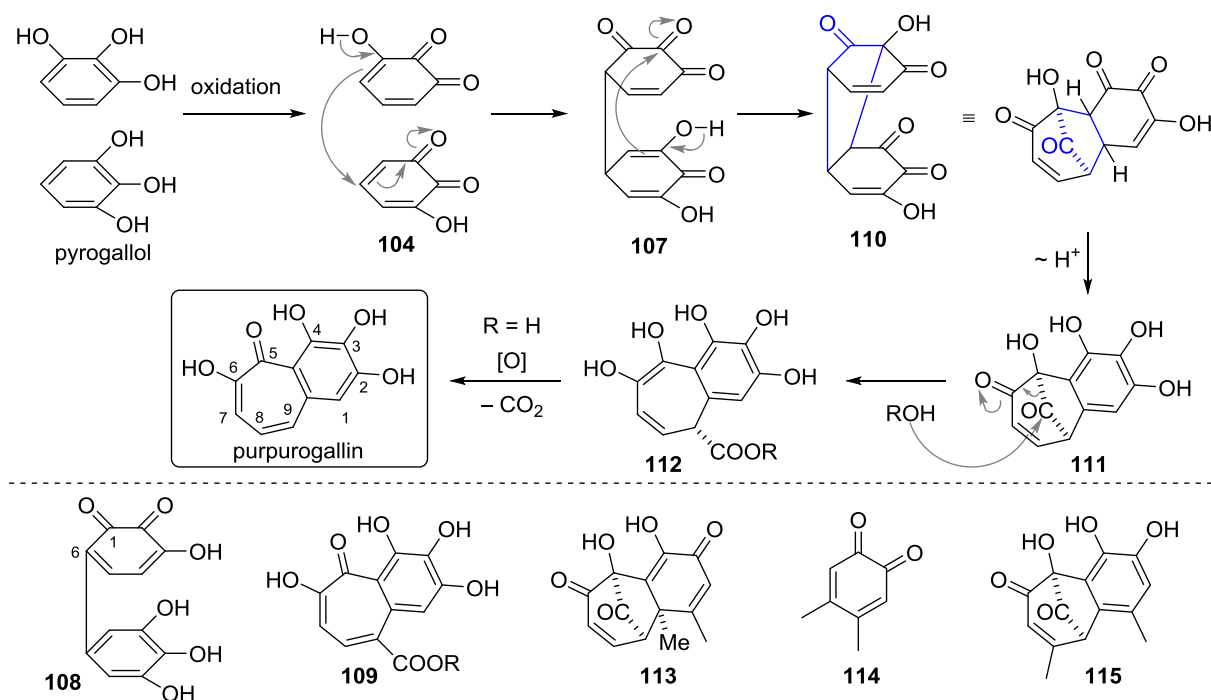


Scheme 26 A. Proposed constitution and structure of purpurogallin in history.^[95–99]
B. Additional structures of interest.^[96,100,101]

The originally proposed molecular formula $C_{20}H_{16}O_9$ by GIRARD was falsified early on, but it was only in 1903 that it could be adjusted to the correct $C_{11}H_8O_5$ by PERKIN and STEVEN.^[96] Both scientists also put forward a naphthalene structure for purpurogallone, one of the alkaline degradation products of purpurogallin. In 1913, DEAN and NIERENSTEIN suggested *para*-quinone methide **105** for purpurogallin, which in the following was highly disputed since experimental evidence clearly disproved this assignment.^[97] Unaware of its instability, WILLSTÄTTER and HEISS proposed the antiaromatic cyclopentadienone **106** in 1923.^[98] However, the considerations that led to this proposal were ingenious at the time. It was hypothesized that two molecules of pyrogallol dimerize after initial oxidation to the corresponding hydroxy *ortho*-quinone. The quinone part of the resulting dimer would undergo benzilic acid rearrangement and subsequent decarboxylation to give rise to pyrogallol **106**. After DEWAR's groundbreaking assignment of stipitatic acid and colchicine as cycloheptatrienones,² which he named tropolones, the similarity in chemical behaviour between these compounds provided evidence for the benzotropolone structure of purpurogallin (BARLTROP/NICHOLSON, 1948).^[99–101] Strong support for this proposal was offered by CRITCHLOW, HAWORTH and co-workers, who in a series of publications disclosed their studies on the reactivity and degradation of purpurogallin as well as its synthesis from different starting materials.^[102–104]

² The tropolone structure of colchicine was first proposed by DEWAR in 1945. In 1952, KING *et al.* assigned the correct regioisomer by X-ray single crystal structure analysis: M. V. King, J. L. De Vries, R. Pepinsky, *Acta Crystallogr. Sect. B* **1952**, 5, 437–440.

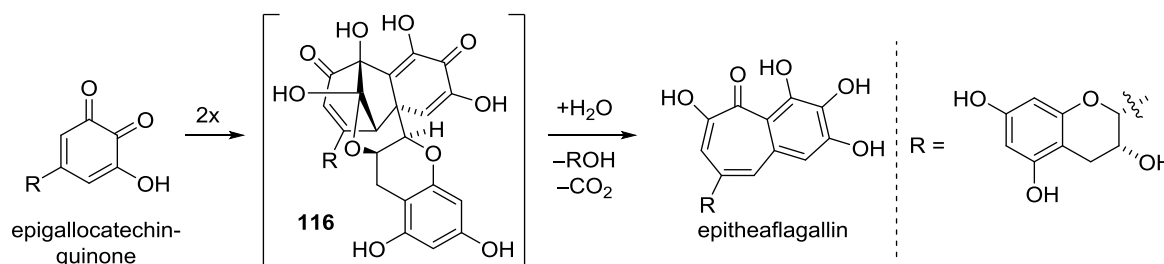
With the correct structure identified also by X-ray crystallography in 1952, a new search began toward the elucidation of the cascade mechanism.^[105] WILLSTÄTTER and HEISS had already suggested the oxidation of pyrogallol to its hydroxy *ortho*-quinone **104** and subsequent dimerization to tetraketone **107** by 1,4-addition (Scheme 27).^[98] In their mechanistic hypothesis, this compound would undergo tautomerization to pyrogallol **108**. It was long uncertain how this dimer could yield purpurogallin. Cleavage of the C1–C6 bond by hydrolysis, FRIEDEL-CRAFTS-type alkylation and loss of formic acid was envisioned by CRITCHLOW, HAWORTH and others.^[106]



Scheme 27. Mechanism of purpurogallin formation by SALFELD.^[107]

The isolation of a carboxylic ester **109** of purpurogallin from oxidation in alcoholic solvents led SALFELD to reconsider the mechanism (Scheme 27).^[107] According to him, the triketone moiety in tetraketone **107** would suffer from intramolecular attack of the nearby enol onto the most electrophilic, central carbonyl to form tricycle **110**. After tautomerization to pyrogallol **111**, the carbonyl bridge would be opened by water (R=H), or in alcoholic solvents the respective alcohol, to furnish bicycle **112**. For esters, further oxidation and tautomerization would give rise to purpurogallin ester **109**. In case of carboxylic acids, a decarboxylation is triggered by oxidation to afford purpurogallin. SALFELD's assumption of the ester at C9 was proven by HORNER and DÜRKHEIMER two years later, who also managed to trap the intermediate hydroxy quinones.^[108–110] Remarkably, in 1985, DÜRKHEIMER and PAULUS isolated and obtained X-ray single crystal structure proof of tricycle **113** from treatment of pyrogallol with *ortho*-quinone **114**.^[111] The similarity between the characterized compound and presumed intermediate **110** of the purpurogallin cascade was striking and led to the general acceptance of the mechanism depicted in Scheme 27. Further evidence of the formation of tricycle **111** was offered by studies of NAKATSUKA and co-workers in 2005, who were able to fully

characterize catechol **115** from oxidation of 5-methyl pyrogallol with 4-methyl *ortho*-quinone.^[112] Upon addition of water, extrusion of CO₂ and conversion to a benzotropolone was observed, supporting the proposed transformation of tricycle **111** to bicycle **112**. In addition, the mechanism in Scheme 27 was underlined by TANAKA and co-workers with the isolation and identification of hemiacetal **116**. The latter compound was formed by enzymatic oxidation of epigallocatechin and subsequent dimerization of its quinone. Hemiacetal **116** converted to epitheaflagallin by hydrolysis and decarboxylation (Scheme 28).^[113]



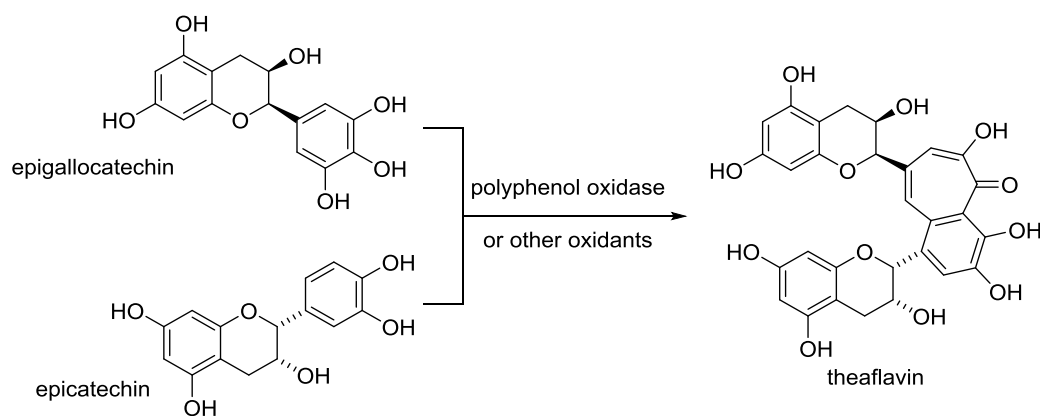
Scheme 28. Intercepted purpurogallin cascade by TANAKA and co-workers.^[113]

However, the details of the early stages of the purpurogallin cascade to intermediate **110** still remain subject of speculation. It is still unknown, if two *ortho*-quinones dimerize or one *ortho*-quinone suffers from 1,4-addition of an unoxidized pyrogallol followed by oxidation of the dimer.

2.1.3.1.2 Use in Total Synthesis

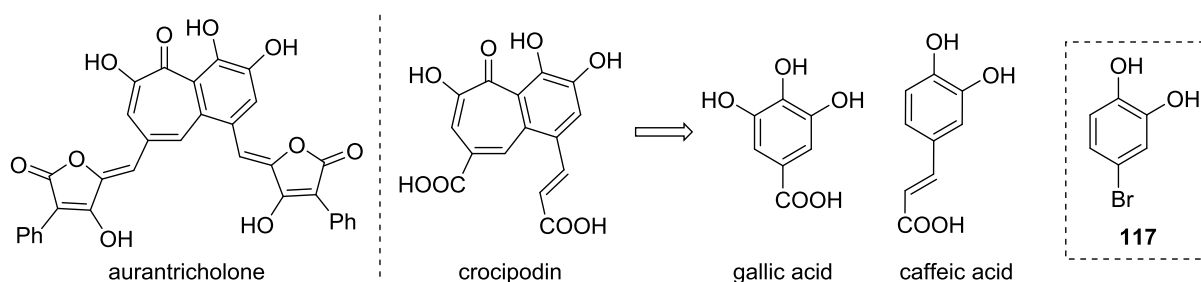
Purpurogallin itself can be found in some oak bars and possesses antioxidant bioactivity.^[114] In Nature, it stems from gallic acid and is therefore a shikimic acid derivative. The purpurogallin reaction is widely found in Nature as the biosynthetic pathway toward benzotropolones.^[115,116] Due to this fact, it has been mostly applied in biomimetic total syntheses toward this class of natural products.

During the fermentation of tea leaves to produce black tea, the naturally occurring catechins are oxidatively dimerized to benzotropolones, so-called theaflavins that are among others responsible for the characteristic color of black tea.^[117] Due to the beneficial antioxidant properties of tea, many research groups have investigated this cascade process.^[113] TAKINO *et al.* achieved the first biomimetic synthesis of these compounds using an oxidative dimerization of epigallocatechin with epicatechin with oxidases or inorganic oxidants in 1964 (Scheme 29).^[117] Since then, many more biomimetic syntheses of tea ingredients have been disclosed, all following the same principle.^[118,119]



Scheme 29. Theaflavin synthesis by TAKINO *et al.*^[117]

The purpurogallin cascade is also involved in the biosynthesis of benzotropolone pigments such as aurantricholone or crocipodin that were isolated from fungi.^[120,121] The latter was synthesized employing an enzymatic oxidation of gallic acid and bromo catechol **117** (Scheme 30).^[121] A fully biomimetic approach involving gallic acid and caffeic acid failed, potentially because the more electron-poor caffeic acid was not readily oxidized.



Scheme 30. Purpurogallin derivatives of fungal origin.^[120,121]

Purpurogallin derivatives have also attracted attention in medicinal chemistry as potential anti-parasitics (**118**) or as a molecular probe for the investigation of ligand interactions (**119**, Figure 8).^[122–124] Furthermore, purpurogallin was often employed as a starting material for the total synthesis of colchicine.^[125]

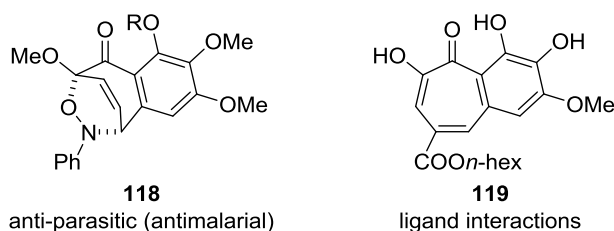
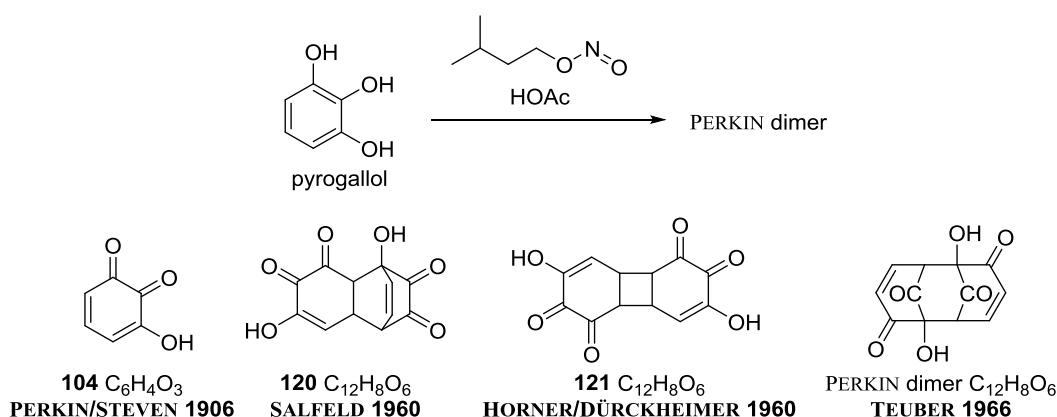


Figure 8. Use of purpurogallin in medicinal chemistry.^[122–124]

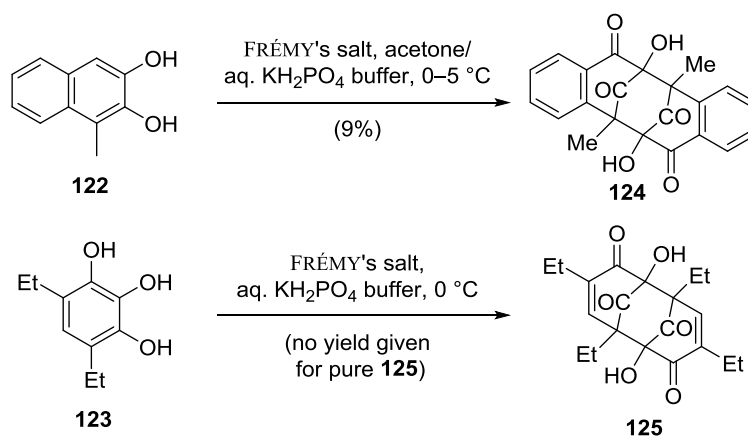
2.1.3.2 Formation of the PERKIN Dimer

The structural elucidation of another dimer of oxidized pyrogallols is closely linked to the history of purpurogallin. In 1906, PERKIN and STEVEN made the peculiar observation that treatment of pyrogallol with acetic acid and isoamyl nitrite did not afford purpurogallin, but an almost colorless crystalline solid (Scheme 31).^[126] The compound with the formula $(C_6H_4O_3)_n$, later referred to as the PERKIN dimer, reverted back to pyrogallol under reducing conditions, but most intriguingly formed purpurogallin upon boiling in water. In lack of a better solution and despite its colorless nature, PERKIN and STEVEN suggested hydroxy quinone **104** as the structure of the obtained product (Scheme 31).

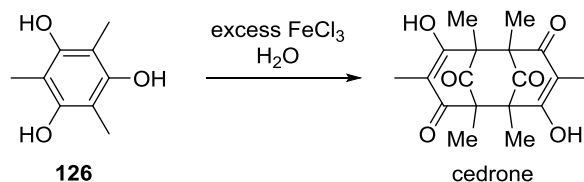


Scheme 31. Formation of the PERKIN dimer and structural elucidation.^[98,126–130]

WILLSTÄTTER and HEISS recognized the dimeric nature of this compound in 1923,^[98] and subsequently molecular structures were proposed by SALFELD (**120**) and HORNER and DÜCKHEIMER (**121**).^[127,128] Since none of these structures accounted for the lack of color, TEUBER and co-workers assigned and later proved that the PERKIN dimer in fact possesses a tricyclo[5.3.1.1^{2,6}]dodecane skeleton.^[129,130] Previously, the same group had accessed related dimers by FRÉMY's salt (= potassium nitroso disulfonate) oxidation of 2,3-dihydroxynaphthalene **122** and 4,6-diethyl pyrogallol **123** to dimers **124** and **125** respectively (Scheme 32).^[129–131]



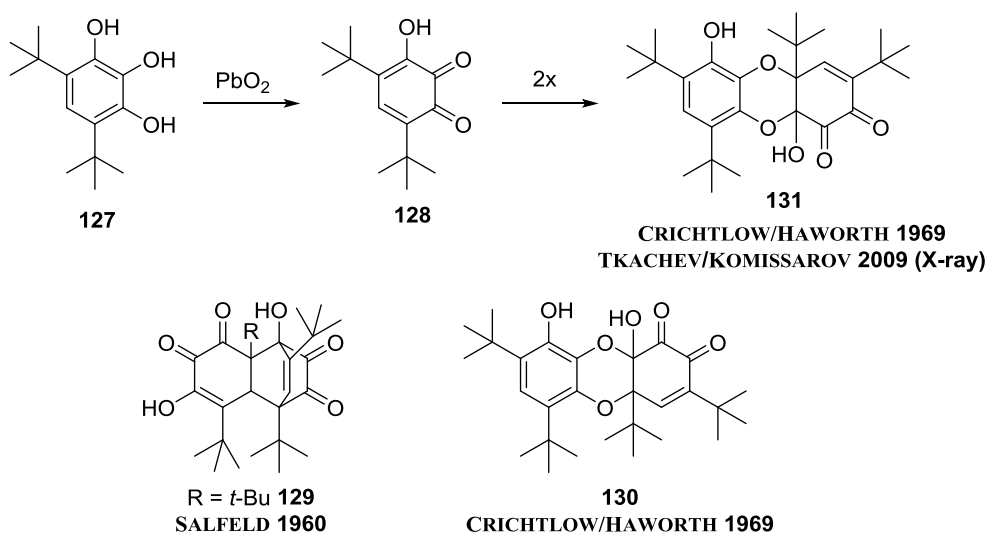
It should be mentioned that related dimers have also been reported for phloroglucinols like **126** which was oxidatively coupled by ČEČELSKY in 1899 to a tricycle he named cedrone.^[132] Its structure was successfully elucidated by ERDTMAN and FALES in 1969 and 1971 respectively (Scheme 33).^[133,134]



Scheme 33. Synthesis of cedrone.^[132]

2.1.3.3 Hetero-DIELS–ALDER Dimerization of Pyrogallols

The extensive investigations on pyrogallol oxidation also resulted in the identification of a third reactivity trend. In 1955, FLAIG *et al.* oxidized pyrogallol **127** and upon heating observed the dimerization of its *ortho*-quinone **128**.^[135] SALFELD first misassigned the product, based on analogy to the corresponding *ortho*-quinone dimers, as tricycle **129**.^[128] CRITCHLOW *et al.* later recognized, based on NMR and IR-spectroscopy, that only two carbonyls were present in the structure and assigned it to dioxines **130** or **131**.^[136] In 2009, it became evident that dioxine **131** is the correct isomer based on single crystal X-ray analysis.^[137] Dimers of type **131** have been found to decompose easily into the monomeric species.



Scheme 34. Dimerization of sterically hindered oxidized pyrogallols.^[128,135–137]

2.1.3.4 Conceptualization of Substrate-Dependent Reactivity Trends

The literature analysis of known pyrogallol oxidations reveals that the assignment of products resulting from this reaction has been challenging. Despite this fact, guidelines for the reactivity trends of hydroxy *ortho*-quinones can be proposed. The purpurogallin cascade reaction is usually undergone

by substrates which are ultimately able to aromatize to benzotropolones like **132**. This in general involves 4-substituted pyrogallols **133**, but can be extended to any pyrogallol if the substituent(s) can be cleaved under the reactions conditions, *e.g.* decarboxylation of carboxylic acids. Even if PERKIN-type dimer products are observed, these can be channeled into the purpurogallin cascade due to the ultimate rearomatization as a thermodynamic driving force.

It appears that the competing pathway of the oxidative pyrogallol dimerization, the formation of PERKIN-type dimer tricyclic systems **134**, is mainly operational with substrates that cannot form aromatic benzotropolones (such as **135** or **136**). However, substrates that are too sterically congested and cannot give aromatic purpurogallin derivatives (**137**) tend to dimerize *via* their hetero-diene in a hetero-DIELS–ALDER reaction (**138**). Driving force of this reaction is mostly the rearomatization of one of the hydroxy *ortho*-quinone partners. This cycloaddition places the substituents on each ring further away from each other than in the other reaction modes due to the formation of C–O instead of C–C bonds.

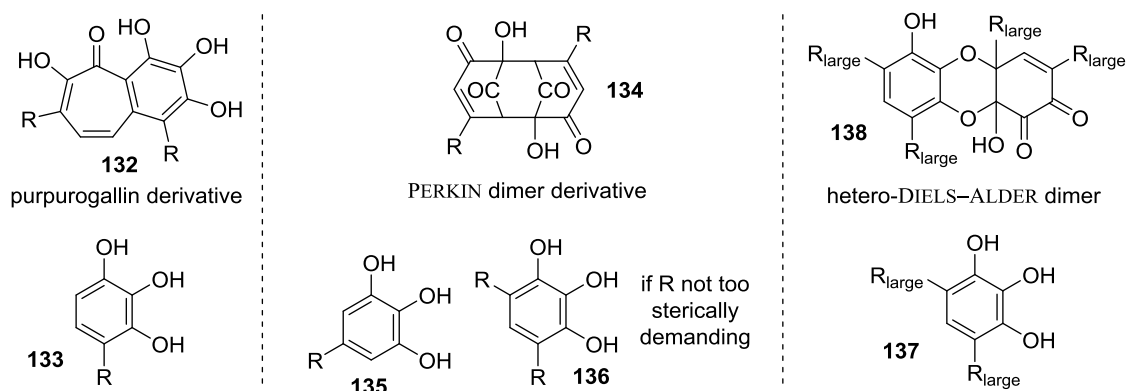


Figure 9. Substrate substitution pattern for different reaction modes in oxidative dimerizations of pyrogallols.

In particular, the investigation of the purpurogallin cascade has demonstrated that slight modifications of the substrate can lead to the desired reactivity. For instance, the purpurogallin cascade to molecules of type **139** in principle only requires one of the coupling partners to be a hydroxy *ortho*-quinone **104** with the crucial combination of nucleophilic and electrophilic site (Figure 10). The other component (**140**) reacts in a 1,4-addition with subsequent enol alkylation, a characteristic reaction of any *ortho*-quinone (1,2-relation between nucleophilic and electrophilic site).

In contrast to this, the PERKIN dimer can only form between two benzene triols, *e.g.* two molecules of hydroxy *ortho*-quinone **104**, because both coupling partners need to possess a 1,3-relationship between nucleophilic and electrophilic site. Thus, in order to avoid competitive or exclusive PERKIN dimer formation and achieve a purpurogallin cascade even with substrates that do not lead to aromatic benzotropolones, a hydroxy quinone should be combined with an *ortho*-quinone. Following this guideline, DÜRCKHEIMER and PAULUS were able to access tricycle **113** (Scheme 27).^[111]

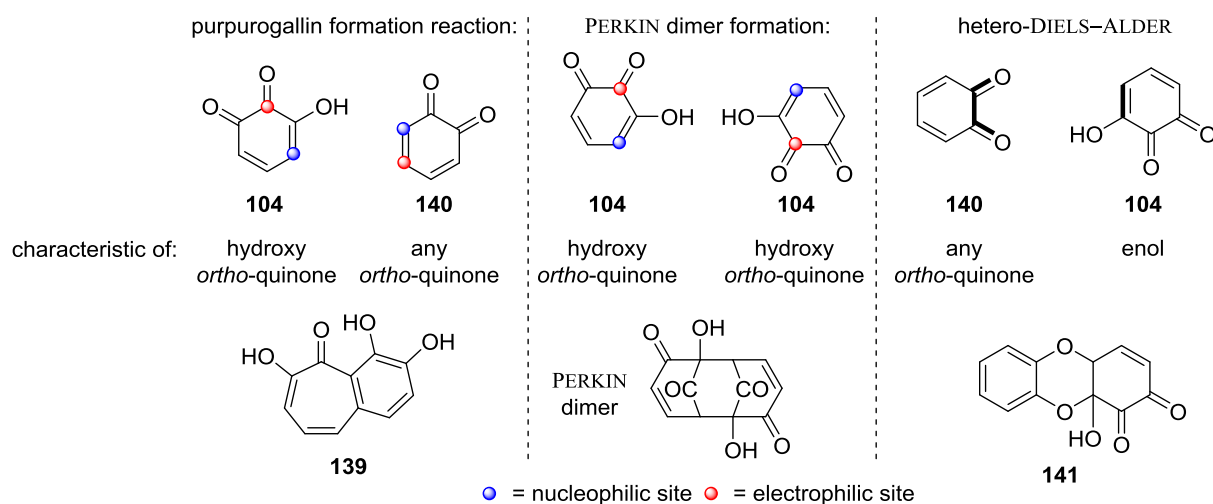


Figure 10. Minimal reactivity profiles for oxidative dimerization of pyrogallols.

Furthermore, hetero-DIELS–ALDER reactions to dimers of type **141** could in principle be achieved between any *ortho*-quinones **140** and any oxidized hydroxylated benzene that still contains an enol, *e.g.* enol **104**.

This chapter included the most important reactivity profiles that were exploited or observed in this thesis. Therefore, other important reactions of hydroxylated benzenes like biaryl couplings upon oxidation were not mentioned. A differentiation between one- and two-electron oxidations of phenolic compounds will be discussed in 2.3.2 Synthesis of Dibefurin.

2.1.4 Natural Products from *Epicoccum* species

2.1.4.1 Overview

Epicoccum nigrum is an endophytic fungus of the phylum Ascomycota, which is distributed worldwide in soils and plants.^[138] It is mostly recognized for its activity against pathogens and production of pigments.^[139] Numerous secondary metabolites with various properties such as the fluorescent dye epicocconone, the thiodiketopiperazine epicoccin J and the antibiotic flavipin have been isolated from this fungus (Figure 11).^[140–142]

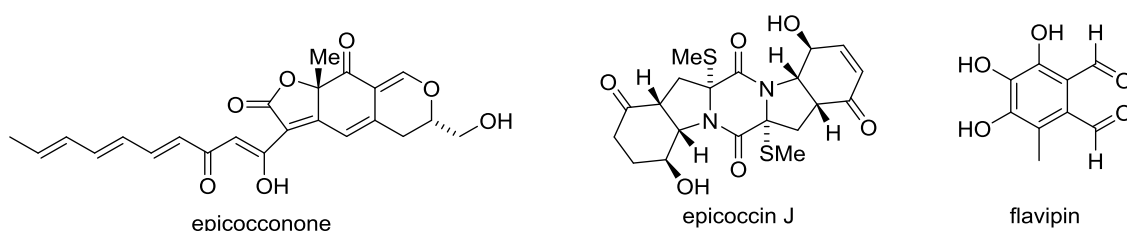
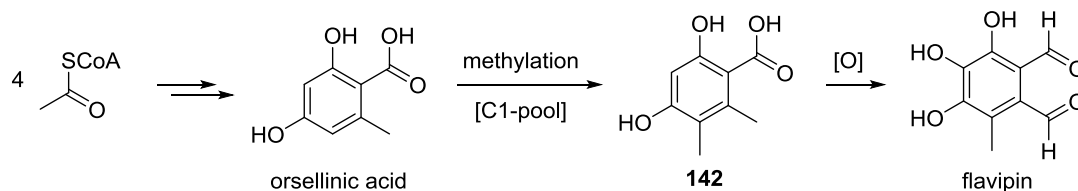


Figure 11. Secondary metabolites isolated from *Epicoccum nigrum*.^[140–142]

Flavipin is of particular interest to this thesis since both targeted natural products dibefurin and epicolactone are proposed to be derivatives of this dialdehyde. Biosynthetically, flavipin stems from orsellinic acid and is therefore of polyketidic origin (Scheme 35).^[143]



Scheme 35. Biosynthesis of flavipin *via* orsellinic acid.^[143]

The isolation of orsellinic acid and carboxylic acid **142** before the observation of flavipin production led to the proposal that flavipin can be biosynthetically traced back to these acids.^[143] Indeed, it appears that the aromatic methyl group in flavipin is introduced into orsellinic acid since labelling of (L)-methionine as ¹⁴C-(L)-methionine resulted in the incorporation of radioactivity into acid **142**. Furthermore, the biosynthetic pathway outlined in Scheme 35 was supported by experiments, in which radioactive orsellinic acid as well as radioactive acid **142** were shown to lead to radioactive flavipin.

Numerous flavipin-derived antioxidant natural products were isolated from *Epicoccum* species (Figure 12). The structural variety ranges from the reduced cyclic derivatives epicoccine and epicoccine methyl ether **143** over redox-isomerized cyclic congeners epicoccone A and B to the dimeric epicocconigrone and epicoccolides.^[144–149]

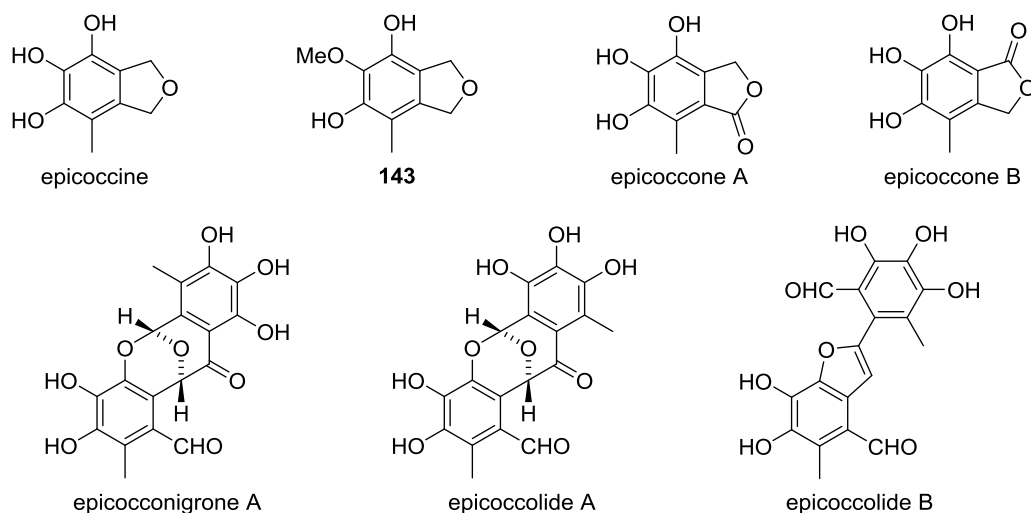
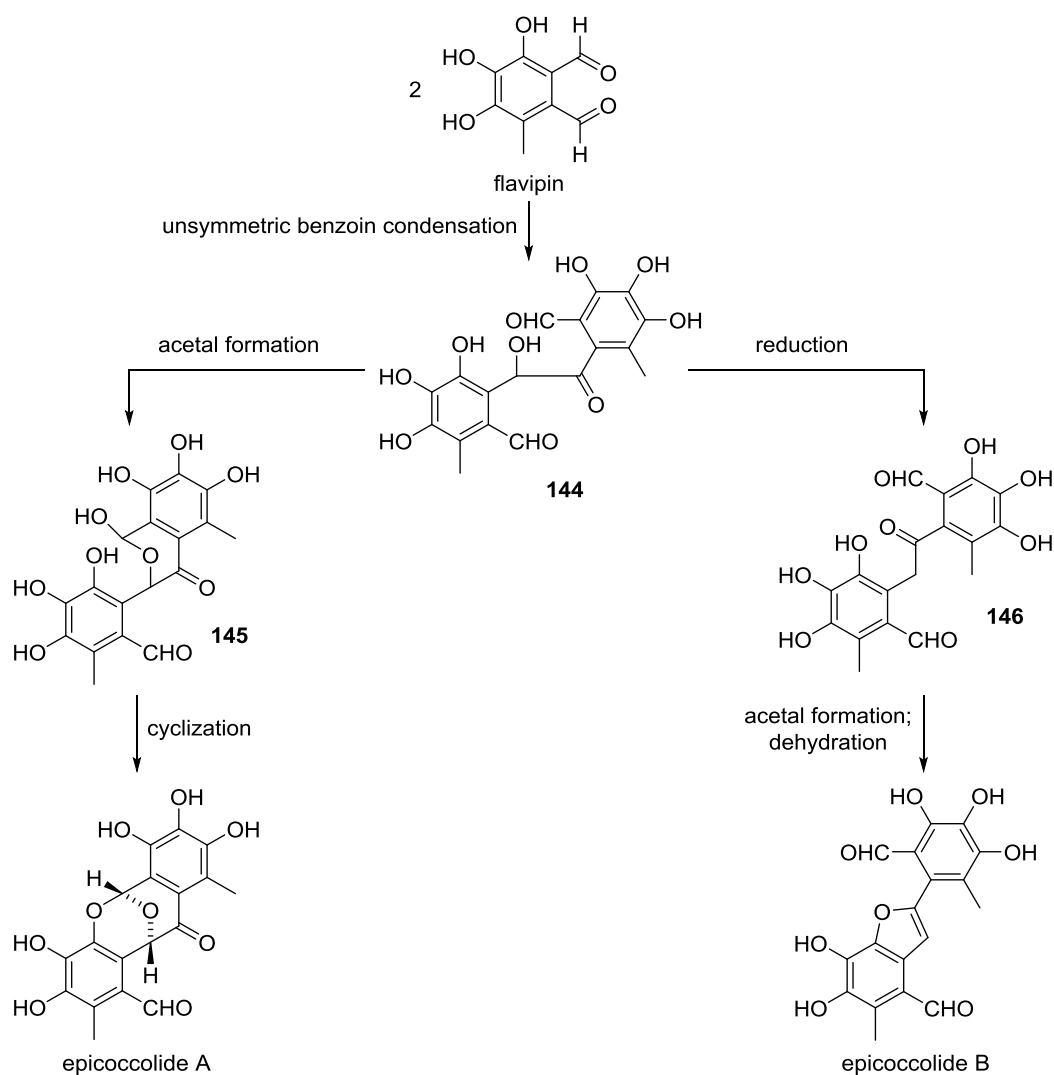


Figure 12. Flavipin-derived natural products from *Epicoccum* species.^[144–149]

LAATSCH and co-workers have suggested a biosynthetic pathway from flavipin to the dimeric epicoccolides A and B (Scheme 36).^[148]



Scheme 36. Proposed biosynthetic relationship between flavipin and epicoccolides A and B.^[148]

According to the hypothesis, two molecules of flavipin would undergo an unsymmetric benzoin condensation catalyzed by thiamine to give rise to hydroxy ketone **144**. The latter could cyclize *via* hemiacetal **145** to epicoccolide A. Alternatively, hydroxy ketone **144** could be reduced to ketone **146** and subsequently cyclize to afford benzofuran epicoccolide B. Epicocconigrone A results from a regioisomer of the initial benzoin condensation of two flavipin molecules.

2.1.4.2 Dibefurin

2.1.4.2.1 Origin and Structure

Dibefurin was isolated³ from the fungal culture AB 1650I-759 at Abbott Laboratories (now AbbVie) following a bioactivity-directed search for novel immunosuppressants.^[150] In the course of this thesis, the fungus got identified as a fungus of phylum Basidiomycota, different from the ascomycete *Epicoccum*.⁴ The structure of dibefurin was elucidated with NMR spectroscopy, mass spectrometry and X-ray single crystal analysis. Crystallographic data revealed the centrosymmetric triclinic space group ($P\bar{1}$).

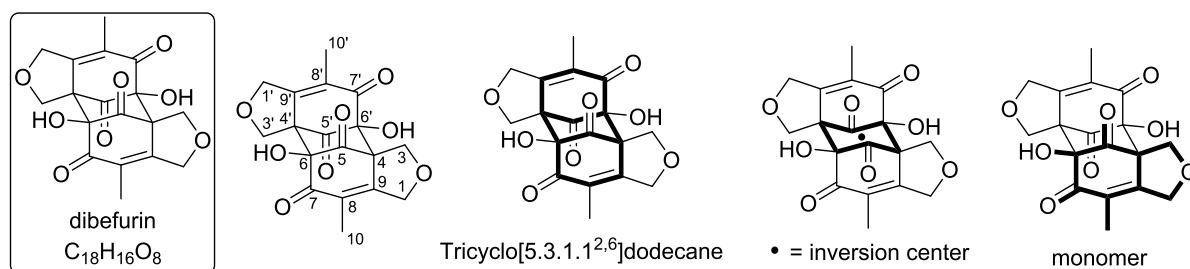


Figure 13. Dibefurin, a fungal metabolite from a basidiomycete.^[150]

Dibefurin is a pentacycle with the molecular formula $C_{18}H_{16}O_8$ and was suggested to be biosynthetically related to the polyketide flavipin (Figure 13).^[150] A central cyclohexane ring features two 1,3-diaxial connections by a three-carbon atom bridge giving rise to a tricyclo[5.3.1.1^{2,6}]dodecane skeleton, which is decorated with two tetrahydrofuran rings. The natural product thus has four tetrasubstituted centers that are adjacent in pairs. Remarkably, dibefurin possesses an inversion center, which, due to the absence of other symmetry elements (apart from the identity), makes it C_i -symmetric and therefore achiral. This feature is very rare among natural products (*vide infra*). The unusual symmetry can be explained by the dimeric nature of dibefurin, with the monomer unit highlighted in Figure 13.

³ The natural product was obtained from the EtOAc extract after purification by countercurrent, reverse phase and gel filtration chromatography. The natural product was crystallized from MeOH.

⁴ Personal communication with Dr. George S. Sheppard (AbbVie, Wilmette, Illinois, USA).

2.1.4.2.2 Bioactivity

Since dibefurin was isolated in a bioactivity-guided search for novel potential immunosuppressants, it was proposed to possess interesting bioactivity.^[150] Dibefurin was found to directly inhibit calcineurin phosphatase, an enzyme which is critically involved in the immune response.^[150] Indirect calcineurin phosphatase inhibitors such as cyclosporin A or FK-506 (tacrolimus) have a significant impact on society due to their use as an immunosuppressant to prevent organ rejection after transplantation (Figure 14).^[151]

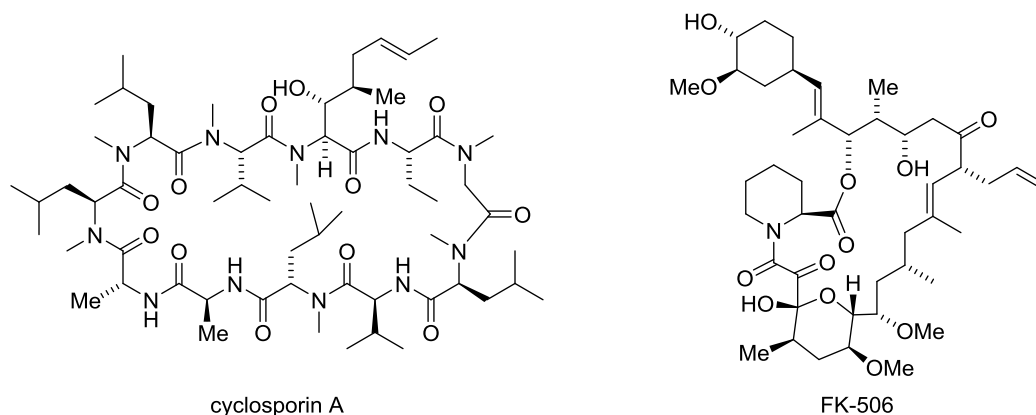


Figure 14. Indirect calcineurin phosphatase inhibitors.^[151]

These drugs act upon forming a complex with immunophilin proteins, which can then inhibit the calcineurin phosphatase.^[152] Thus, the cytosolic component of NFAT (nuclear factor of activated T cells) does not get dephosphorylated so that the production of interleukin-2 and other cytokines responsible for the growth and differentiation of T cells is not activated. Direct inhibition of calcineurin phosphatase is yet highly desirable, since it would obviate the need for other proteins and thus not inhibit their usual cytosolic function. Dibefurin showed a moderate direct calcineurin phosphatase inhibition with a half-maximal inhibitory concentration of $IC_{50} = 44 \mu M$.^[153]

2.1.4.2.3 C_i -symmetric natural products

As mentioned above, C_i -symmetric natural products are rare and usually form upon head-to-tail dimerization of two C_s -symmetric molecules. A privileged reaction in this context appears to be the [2+2]-photocycloaddition of olefins.^[154–157] Hence, the main representatives of C_i -symmetric natural products are head-to-tail dimers of cinnamic acid, so called truxillic acid derivatives, such as α -diplicatin B or piplartine dimer (Figure 15).

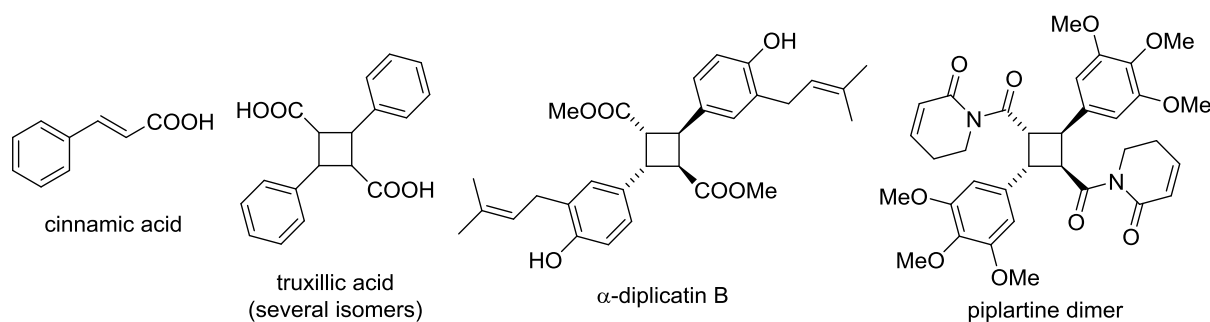


Figure 15. Truxillic acid derivatives as example of C_2 -symmetric natural products.^[154–157]

Achieving the desired selectivity of these dimerizations in a biomimetic synthesis can be challenging. Thus, the BARAN group for instance has reported the successful synthesis of piperarborenines, chiral natural products similar to piplartine dimer, based on a non-biomimetic approach.^[158] However, selectivity can be achieved by preorganization of the substrates or based on the thermodynamic stability of the products. In their synthesis of incarvillateine, shown in chapter 1.3

Symmetry in Natural Product Synthesis, the KOBAYASHI group has crystallized the monomer so that both monomer units were oriented in a head-to-tail arrangement.^[30] Based on the resulting inflexibility of the starting material in the solid state, the following [2+2] photocycloaddition could then only proceed with the desired regioselectivity.

2.1.4.3 Epicolactone – Origin, Structure and Bioactivity

Epicolactone was isolated⁵ from the endophytic fungus *Epicoccum nigrum* in sugarcane and *Epicoccum* sp. CAFTBO in *Theobroma cacao*, the cocoa tree, as a white crystalline solid.^[148,159] Its structure was elucidated with NMR spectroscopy, mass spectrometry as well as X-ray single crystal analysis. Epicolactone attracted much attention due to its unprecedented structure which also does not belong to any known family of natural products (Figure 16). Remarkably, epicolactone is a racemic natural product because it crystallized in a centrosymmetric space group ($P\bar{1}$).

⁵ The isolation procedure separated cyclohexane-soluble fractions from the EtOAc extract of the culture. The crude mixture was purified by silica gel and Sephadex LH-20 chromatography to yield $m = 1.8$ mg of epicolactone from $m = 39.2$ g of crude extract.^[148]

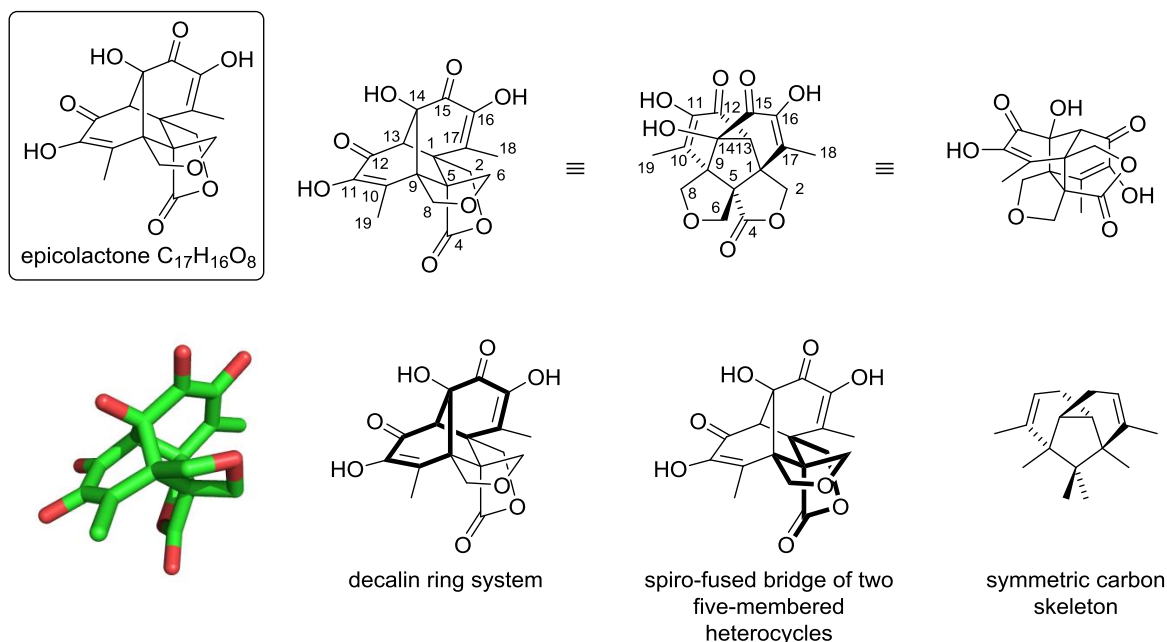


Figure 16. Epicolactone, a secondary metabolite from *Epicoccum*;^[148,159] CCDC: 865386, 788534; H-atoms omitted for clarity. Color code: green = carbon, red = oxygen.

The secondary metabolite with the molecular formula $C_{17}H_{16}O_8$ is a pentacycle presumably of polyketide origin. The basis of epicolactone is a decalin ring system, which is bridged by the spiro carbon center $C5$. Since each bond of the one carbon bridge ($C1-C5$; $C5-C9$) is part of a five-membered heterocycle, epicolactone possesses three neighboring spiro centers ($C1$, $C5$, $C9$). One of the heterocycles is a lactone ($C1$ to $C5$), the other a tetrahydrofuran ($C5$ to $C9$). This molecular architecture inevitably results in a central five-membered carbocycle. It features five stereogenic centers that are all adjacent to each other, three of which are contiguous quaternary carbon atoms ($C1$, $C5$, $C9$). Alternatively, a heterotriquinane skeleton can be identified in epicolactone, which is bridged by two carbon bridges consisting of three carbon atoms each.

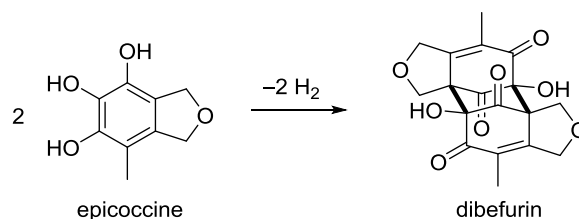
Despite the overall C_1 -symmetry of epicolactone, the carbon skeleton is symmetric. Oxidation at carbon atoms $C4$ and $C14$ result in the lowering of the overall symmetry. The crystal structure of epicolactone reveals that the $C9-C14$ bond is slightly elongated to $d = 1.58 \text{ \AA}$ and therefore potentially the weakest C–C bond.

Epicolactone was found to possess antimicrobial and antifungal activity and LAATSCH and co-workers suggested that it might be responsible of protecting the host plant from devastating pathogens.^[148]

2.2 Project Outline

2.2.1 General Biosynthetic Proposal

Dibefurin and epicolactone are both pentacyclic polyketides of fungal origin. It was noticed that both natural products could stem from epicoccine, a natural product that was co-isolated with epicolactone. Although dibefurin was identified in a different fungus, a head-to-tail homodimerization of epicoccine was envisioned to be involved in its biosynthesis (Scheme 37). Hypothetically, its formation could occur spontaneously upon oxidation of epicoccine without enzymatic assistance.



Scheme 37. Proposed biosynthesis of dibefurin.

In contrast to dibefurin, the epicoccine moiety in epicolactone is more complicated to identify as it seems to have undergone further metabolic processing (Figure 17). The aromatic core seems to have been oxidized and fragmented and more substituents were introduced on carbon atoms C5 and C9 of the tetrahydrofuran ring. Due to the pseudosymmetry of epicolactone, its racemic nature and its high oxidation degree, it was assumed that a coupling of two distinct hydroxylated arenes occurs upon their oxidation without the involvement of enzymes. The molecular formula of epicolactone with 17 carbon atoms suggested that either a building block with uneven carbon atom number could combine with one of even number or two molecules with uneven numbers could be coupled and subsequently lose a carbon atom.

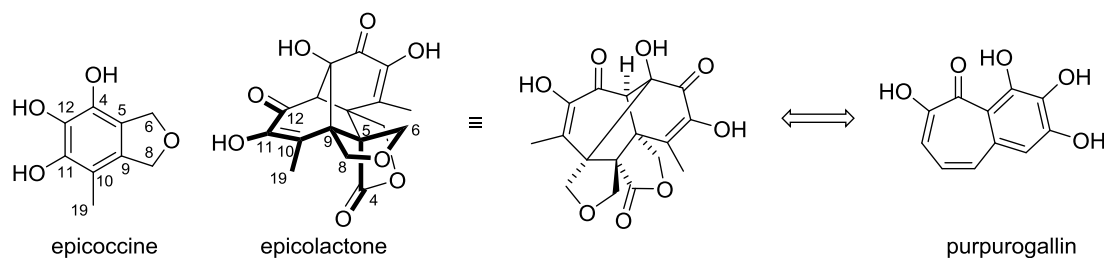
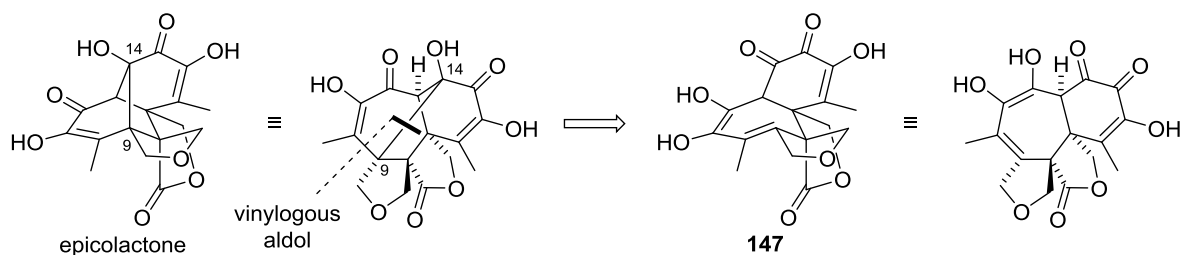


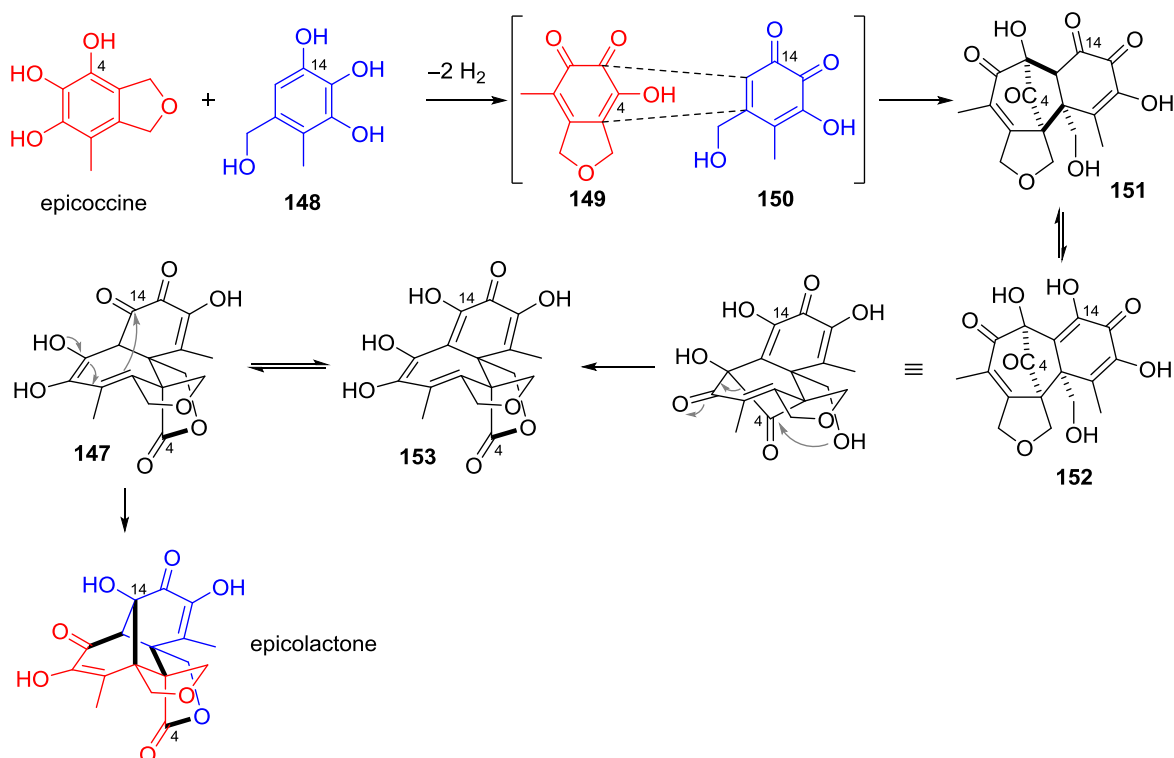
Figure 17. Analysis of biosynthetic origin of epicolactone; epicoccine part shown in bold.

It was recognized that epicolactone featured a 7/6-ring system that closely resembles the one of purpurogallin (Figure 17). Epicolactone was therefore initially traced back to precursor **147** by a vinylogous aldol reaction to form the C9–C14 bond. This bond was found to be slightly elongated^[148,159] with $d = 1.58 \text{ \AA}$ and hence represents a likely first retrosynthetic simplification in the potential biosynthesis (Scheme 38).



Scheme 38. Vinylogous aldol reaction in the hypothetical epicolactone biosynthesis.

Ene diol **147** is structurally similar to intermediates in the purpurogallin cascade. With suitable substituents, these intermediates would not be able to aromatize to a benzotropolone. The proposed biosynthesis that formed the basis of this project is depicted in Scheme 39.

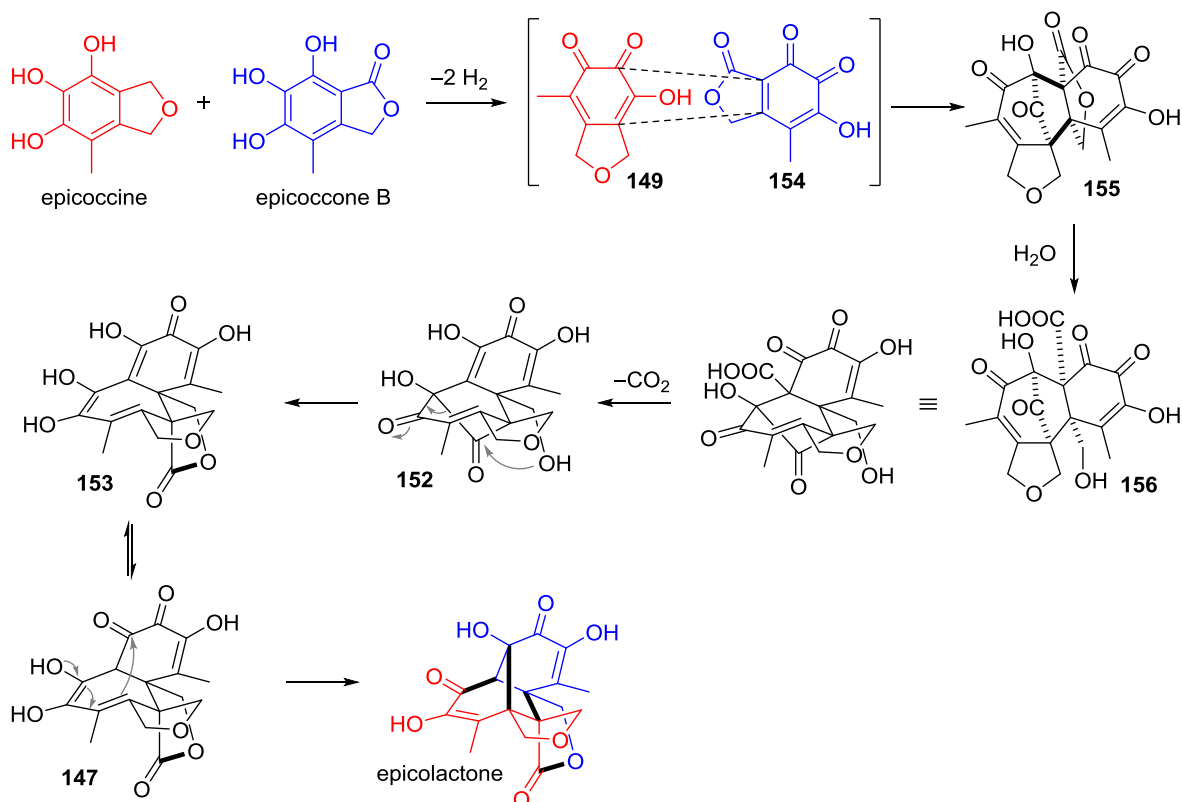


Scheme 39. Biosynthetic proposal for epicolactone with benzyl alcohol **148**.

Epicoccine and benzyl alcohol **148** would be oxidized to their corresponding *ortho*-quinones **149** and **150** that could subsequently combine in a formal (5+2)-cycloaddition to give tetracycle **151** (alternative nomenclature: (3+2)-cycloaddition). This step also occurs accordingly in the purpurogallin cascade. Tautomerization of the diketone to the more stable enone **152** would be followed by an intramolecular attack of the primary alcohol onto the bridge carbonyl at C4 instead of an intermolecular attack of water as in the biosynthesis of benzotropolone natural products. A hemiacetal derived from such an attack was characterized in 2009 in studies on black tea and supports the feasibility of this biosynthetic proposal.^[113] The resulting hemiacetal derived from **152** could collapse in a retro-DIECKMANN-type reaction to afford tetracycle **153** in a net transacylation from carbon to

oxygen. The latter compound could undergo the final vinylogous aldol reaction after tautomerization to diketone **147** to furnish epicolactone.

The required benzyl alcohol **148** was not yet identified in Nature, but closely resembles epicoccone B and could be derived from it by hydrolysis and decarboxylation. Epicoccone B as a congener of epicolactone also represents a possible partner for the oxidative heterodimerization with epicoccine to epicolactone. Since epicoccone B possesses one extra carbon atom, which would need to be lost in a valid biosynthetic proposal, a decarboxylation was envisioned to occur during the biosynthesis (Scheme 40).



Scheme 40. Biosynthetic proposal for epicolactone with epicoccone B.

Both epicoccine and epicoccone B would again combine as their *ortho*-quinones **149** and **154** to afford the sterically encumbered pentacycle **155** according to the purpurogallin formation reaction. The latter would be opened by water to afford β -keto carboxylic acid **156**, which would rapidly decarboxylate to give rise to the same tetracycle **152** as in the above-mentioned biosynthetic proposal (Scheme 39). However, it is also possible to switch the order of events of alcohol attack on bridged carbonyl and decarboxylation.

2.2.2 Aim of the Project

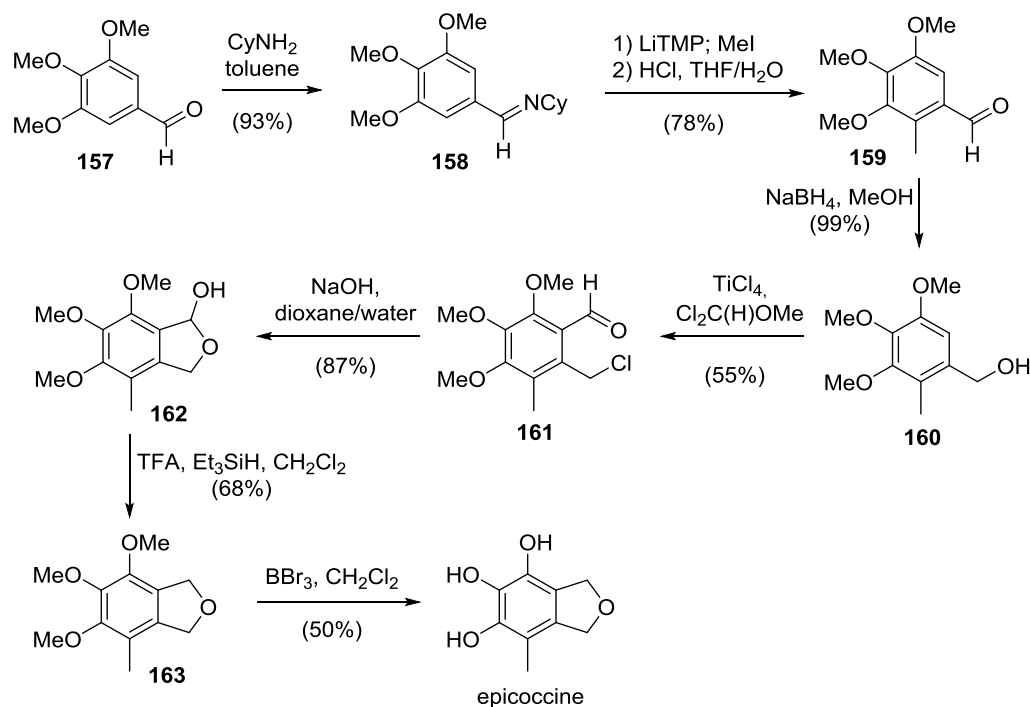
The project aimed at a biomimetic synthesis of dibefurin and epicolactone following the biosynthetic hypotheses outlined in Scheme 37, Scheme 39 and Scheme 40. Since epicoccone B had

already been isolated from Nature, it was first focused on evaluating its potential in the biomimetic synthesis of epicolactone rather than the supposedly labile benzylic alcohol **148**. The project therefore involved a step-economic preparation of the natural products epicoccine and epicoccone B. Control over the reaction outcome of their oxidation was expected to require the introduction of suitable protecting groups to tame the reactive nature of free hydroxy *ortho*-quinones.

In a broader sense, the project was intended to study the behavior of pyrogallols under oxidative conditions and to provide evidence for potential biosynthetic pathways. Part of this work was to conceptualize and generalize the reactions that can occur upon oxidation of different pyrogallols, which formed the basis of the introductory chapter of this thesis. The purpurogallin cascade or the PERKIN dimer formation have neither been identified nor applied in the synthesis of natural products that are as structurally complex as epicolactone or dibefurin. Proving that they might take place spontaneously in Nature might help to understand their involvement in the biogenesis of other natural products. Furthermore, the identification of suitable conditions to effect these cascade reactions would offer a valuable methodology tool for the rapid increase in structural complexity starting from planar building blocks. This might be beneficial for the total synthesis of other intricate molecules in general. It was therefore envisioned to test the power and limits of biomimetic synthesis in the preparation of the complex targets dibefurin and epicolactone.

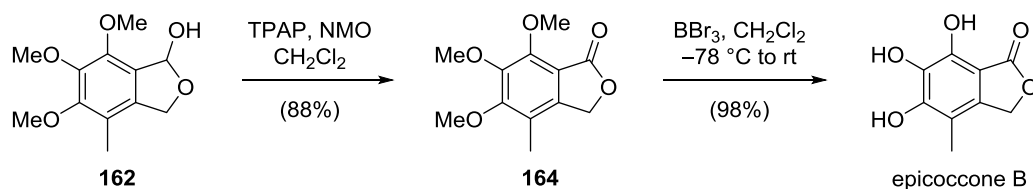
2.2.3 Initial Work

Before the contributions described in this thesis, Dr. Robert Webster as a postdoctoral scholar in the TRAUNER group devised a synthetic route toward epicoccine and a protected derivative of the benzylic alcohol **148**. After optimization studies by Marina K. Ilg in her Master Thesis, epicoccine was synthesized in 8 steps and 12% overall yield (Scheme 41).^[160]

Scheme 41: Previous epicoccine synthesis.^[160]

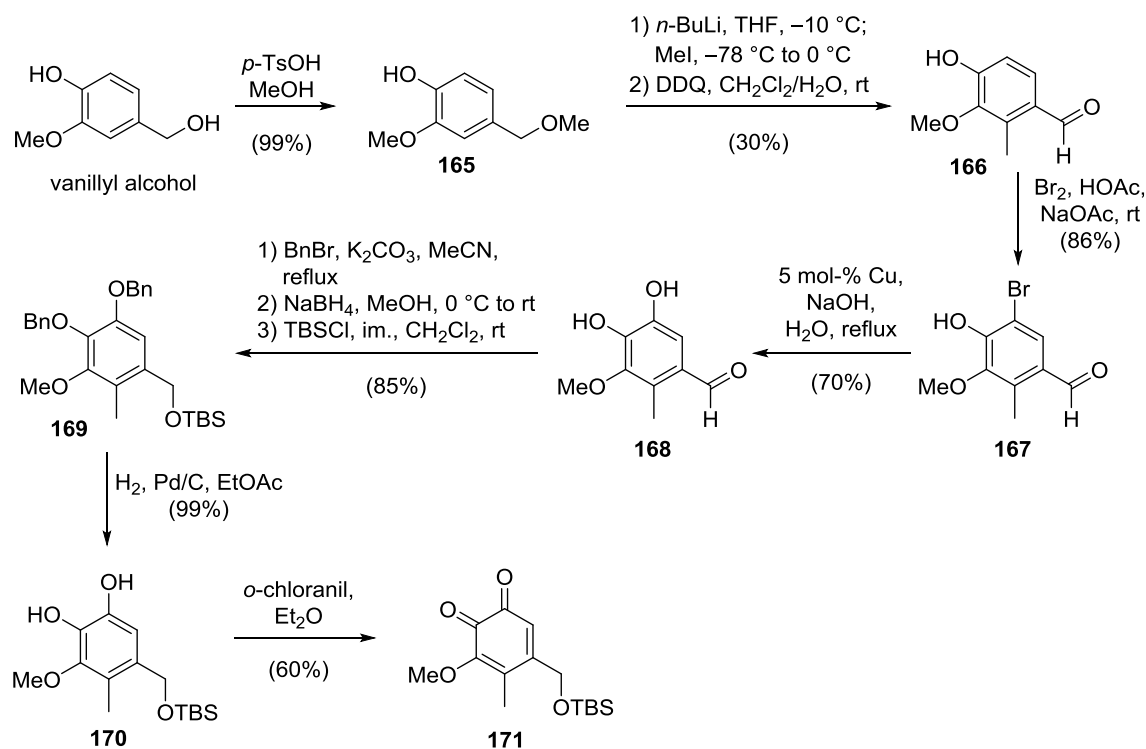
Benzaldehyde **157** was chosen as a starting material and converted to imine **158** under dehydration conditions. The latter proved to be a better directing group on scale for the following *ortho*-metalation by deprotonation with LiTMP. Subsequent methylation and hydrolysis afforded benzaldehyde **159**. Reduction with NaBH₄ to alcohol **160** and RIECHE formylation installed the last substituent of the benzene core in moderate yield. Benzylic chloride **161** was treated with NaOH to effect ring closure to dihydrofuran **162**, the hemiacetal of which was reduced with triethylsilane and TFA to trimethylated epicoccine derivative **163**. Final deprotection with BBr₃ gave the natural product in a best yield of 50%. However, this reaction proved to be capricious and could only be conducted on *m* = 200 mg scale with varying yields from 10–50%.

Using this route, Marina K. Ilg also synthesized epicoccone B in 8 steps and 30% yield (Scheme 42).^[160] The hemiacetal **162** was converted to lactone **164** in a LEY oxidation and subsequently deprotected with BBr₃. The final product was not purified due to the lability of the natural product, but B NMR showed no boron impurities.

Scheme 42. Synthesis of epicoccone B.^[160]

An already oxidized and protected analog of benzylic alcohol **148** was synthesized from vanillyl alcohol in 10 steps and 9% overall yield (Scheme 43). Displacement of the benzylic alcohol by MeOH

yielded methyl ether **165**, which was lithiated, methylated and oxidized in the benzylic position with DDQ to give aldehyde **166** in modest yield. Electrophilic bromination to pentasubstituted benzene **167** and following heterogeneous Cu-catalyzed phenol synthesis afforded catechol **168** in good yield. Selective protection of the benzylic alcohol was achieved by benzylation of the catechol, reduction of the benzaldehyde and subsequent protection to silyl ether **169**. Hydrogenolysis of the benzyl groups to catechol **170** and its subsequent oxidation furnished *ortho*-quinone **171**. This sequence was suitable for gram-scale synthesis.



Scheme 43. Synthesis of quinone **171**, an oxidized analog of benzylic alcohol **148**.

Although with poor yields, both building blocks could be successfully combined to a purpurogallin cascade intermediate by Marina K. Ilg. To increase comprehensiveness in the following chapters, this result will be discussed in more detail when applicable.

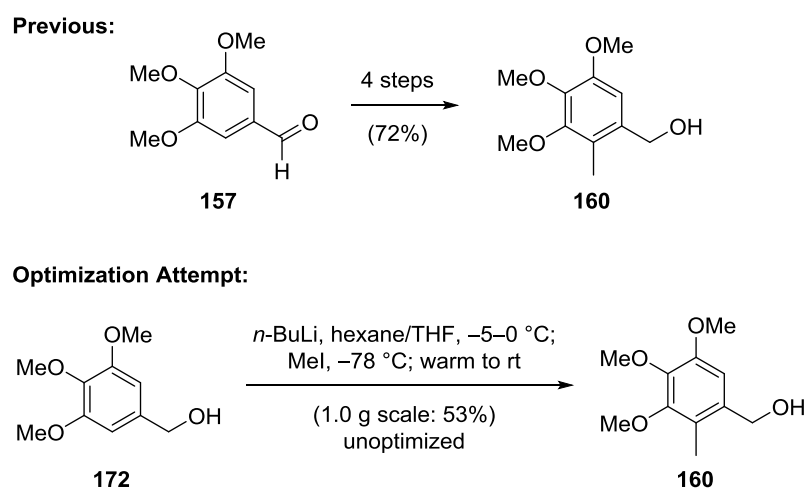
2.3 Results and Discussion⁶

2.3.1 Synthesis of Epicoccine

2.3.1.1 Optimization Studies on Previous Route

The studies toward the synthesis of dibefurin and epicolactone both required a scalable synthetic route toward the natural product epicoccine. In the first generation synthesis (Scheme 41), epicoccine was prepared in 12% yield over 8 steps. The main purpose of this route had been to provide material for proof-of-principle studies on the biomimetic cascade toward epicolactone. However, with the additional target molecule dibefurin, a more time-economic route with less steps and higher yields was required. Especially better scalability was necessary since the last global deprotection step of the previous synthesis proved to be very unreliable even on smaller scale.

First, the four-step procedure from aldehyde **157** to alcohol **160** could be shortened to provide a more rapid access (Scheme 44). According to a literature-known procedure, benzylic alkoxides can serve as *ortho*-directing groups for metalations.^[161] Although unknown for pyrogallol derivatives, the method was adapted to the current system.



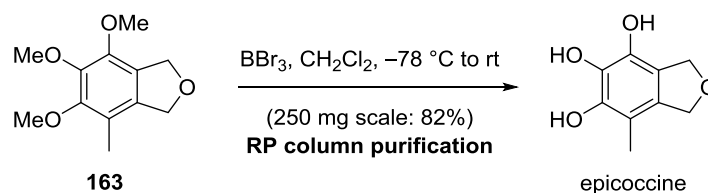
Scheme 44. Optimization attempt at synthesis of benzylic alcohol **160**.

Commercially available benzylic alcohol **172** was deprotonated twice and subsequently methylated to afford benzylic alcohol **160** in one step and an unoptimized yield of 53%. Remarkably, no methyl ether formation was observed. Potentially, the methyl ether could be hydrolyzed during workup since the aromatic ring is fairly electron-rich and could accelerate S_N2-type displacements. Despite the success of the first attempt, this initial result could not be reliably reproduced since varying amounts of starting material were formed alongside the desired product. Due to the

⁶ The synthesis of dibefurin and epicolactone was a joint project together with Dr. Nicolas Armanino, postdoctoral scholar in the TRAUNER group.

identification of a more efficient route in the meantime, it remained undetermined if the deprotonation was unsuccessful or a subsequent protic quench by aqueous impurities in MeI occurred.

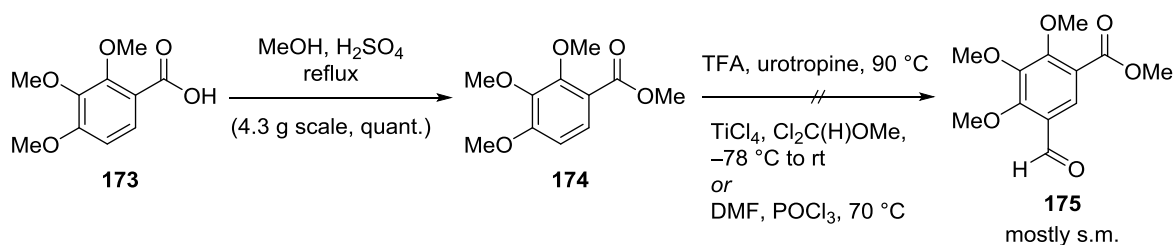
The most significant drawback of the previous route however was the unreliable final deprotection step. Herein, it was assumed that the reaction proceeds smoothly, but that epicoccine decomposes upon workup and purification by flash column chromatography on silica gel. Indeed, changes in workup protocols and purification with reverse phase silica significantly improved yield, reliability and scalability of the reaction. Among others, this observation proved to be the key to the successful purification of multiple compounds involved in this thesis.



Scheme 45. Optimization of final deprotection step with key observation for this thesis.

2.3.1.2 Second Generation Synthesis of Epicoccine

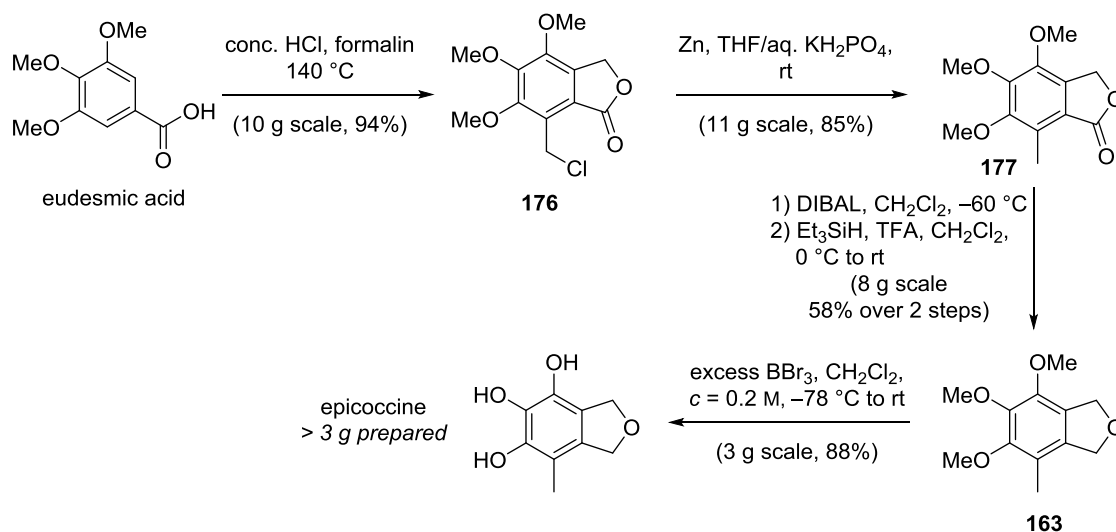
Epicoccine represents a challenging natural product due to its electron-rich hexasubstituted benzene nucleus. The resulting steric encumbrance and lability to oxidizing conditions and even spontaneous air oxidation, though desired for the biomimetic cascade, can complicate its synthesis. It was speculated that the inherent electron-richness and nucleophilicity can be turned to an advantage by exploiting electrophilic aromatic substitution reactions rather than metalation pathways. Initial trials focused on commercially available trihydroxylated benzoic acid derivatives such as acid **173**. The introduction of the methyl group was envisioned by formylation and subsequent reduction (Scheme 46). Acid **173** was converted to methyl ester **174** by FISCHER esterification to avoid undesired directing group effects of the carboxylic acid. However, the following formylation to aldehyde **175** was not met with success under a variety of conditions involving DUFF, RIECHE or VILSMEIER–HAACK formylation.



Scheme 46. Attempts at epicoccine synthesis with electrophilic aromatic substitution reactions.

An isomeric benzoic acid precursor would potentially avoid regioselectivity problems if both available sites on the aromatic ring are homotopic. Thus, harsher functionalization procedures could be

employed. Epicoccine was therefore traced back to eudesmic acid, a gallic acid derivative (Scheme 47).



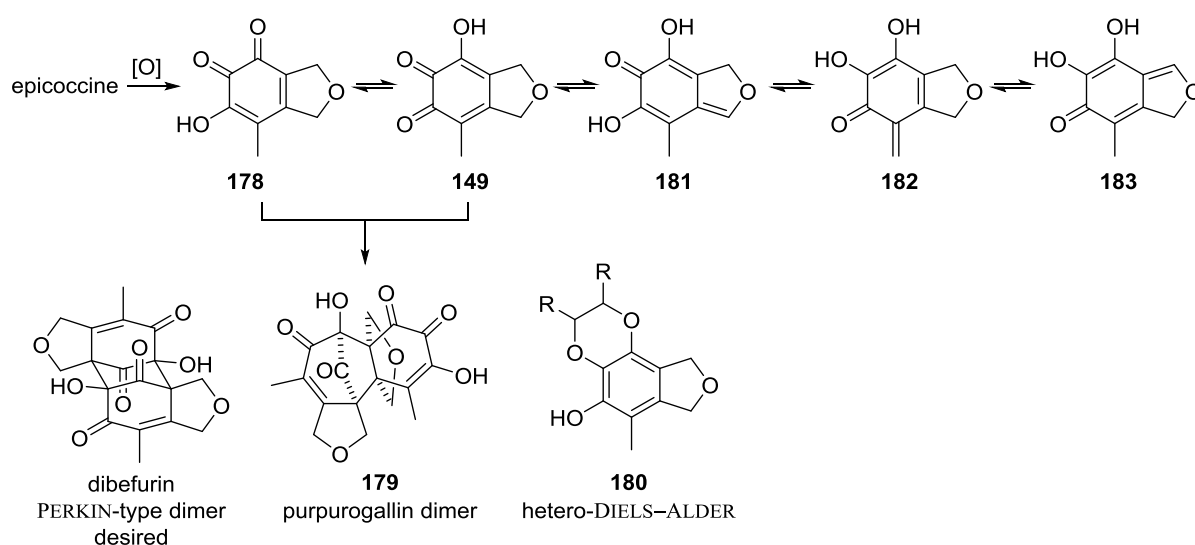
Scheme 47. Second generation synthesis of epicoccine.

In a procedure first described by KING and KING in 1942,^[162] eudesmic acid was converted to phthalide **176** by reaction with formaldehyde as a small electrophile to enable the introduction of six substituents on the benzene core. This procedure exploits that the initial bischloride from the chloromethylation possesses homotopic benzylic positions that the carboxylic acid can cyclize onto. In one step, all carbon atoms of epicoccine are installed. Oxidation state adjustment was carried out in a stepwise fashion by first removing the benzylic chloride with elemental Zn in slightly acidic medium to afford lactone **177**. It was then crucial to avoid the formation of a diol by single-step reduction of lactone **177** since Dr. Robert Webster had previously encountered difficulties in its dehydration to the required tetrahydrofuran. Therefore, a two-step reduction of lactone **177** was implemented by conversion to a labile hemiacetal, which was subsequently reduced with triethylsilane in TFA to give trimethyl ether **163** in good yield over two steps. The previously identified procedure (Scheme 45) was further optimized especially concerning the reaction concentration for the demethylation of intermediate **163** to furnish epicoccine on multi-gram scale within three days of work for the entire sequence. The route required only two column chromatographic purifications and provided sufficient quantities of epicoccine to study the proposed biomimetic cascades.

2.3.2 Synthesis of Dibefurin

2.3.2.1 Potential Challenges

As outlined in Scheme 37, dibefurin was envisioned to be synthesized from oxidative dimerization of epicoccine. Several challenges can arise from a direct oxidation of this pyrogallol derivative. In general, hydroxy *ortho*-quinones like **149** or **178** can possess various reactivities as described in 2.1.3 Oxidation of Unprotected Pyrogallols. Beside purpurogallin-type dimers **179**, PERKIN dimer formation, hetero-DIELS–ALDER reactions to dioxines **180** and decomposition by other pathways could be observed (Scheme 48). Furthermore, the hydroxy quinone could tautomerize involving the benzylic hydrogen atoms to furnish quinone methides **181**, **182** or **183**.



Scheme 48. Different reactivities upon oxidation of epicoccine.

The literature survey and concepts drawn from this (2.1.3.4 Conceptualization of Substrate-Dependent Reactivity Trends) suggested that the PERKIN dimer formation would be feasible. Both reaction partners are unprotected oxidized pyrogallols that cannot aromatize upon purpurogallin formation. Although the reaction partners are sterically hindered, which could favor hetero-DIELS–ALDER reaction, the steric encumbrance was not considered comparable to quinones of type **128** (Scheme 34).

If epicoccine primarily formed PERKIN-type dimers upon oxidation, three products would be possible (Figure 18). Dibefurin as the desired product could be accompanied by another C_i -symmetric dimer **184** and a racemic C_1 -symmetric dimer **185**. The required nucleophilic and electrophilic sites are depicted for one of the possible hydroxy *ortho*-quinones.

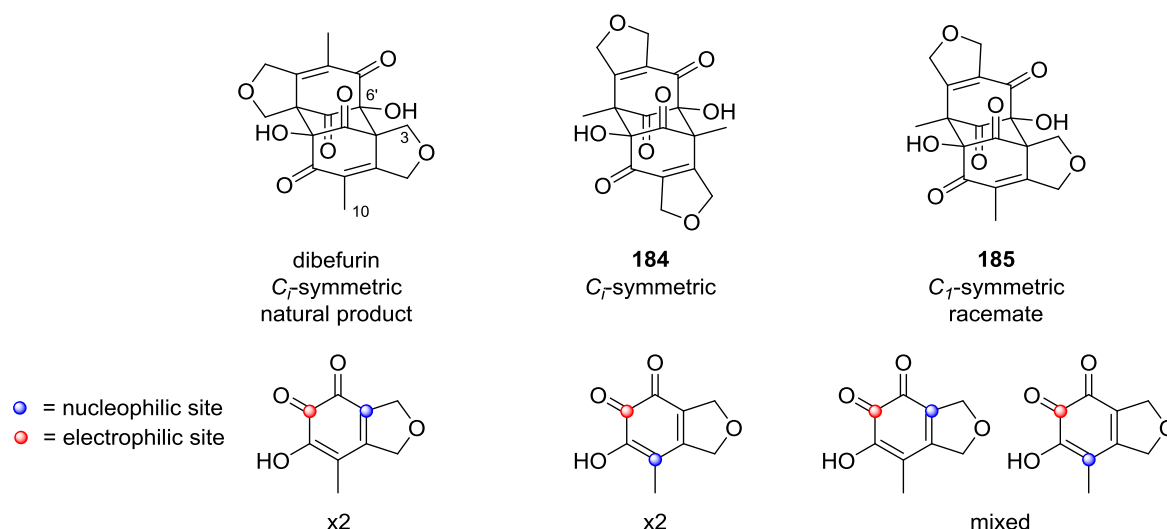


Figure 18. Potential PERKIN-type dimers from oxidation of epicoccine.

It was reasoned that dibefurin could be the most stable and kinetically accessible dimer of the three, because the methylene group (C3), tied back in the tetrahydrofuran ring, was considered less sterically demanding than the freely rotating methyl group (C10). Therefore, steric repulsion with the neighboring substituents on the tetrasubstituted carbon atom C6' would be reduced. As the retrosynthetic plan is based on the potential biosynthesis, it was assumed that despite the plethora of possibilities, dibefurin would form as one of the major products.

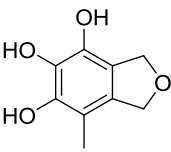
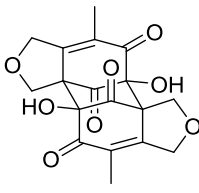
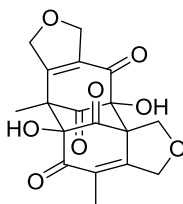
2.3.2.2 Oxidation of Epicoccine and Dibefurin Formation

The trials toward the formation of dibefurin commenced with attempts involving organic oxidants such as *ortho*-chloranil or DDQ (entries 1, 2). Both oxidants failed to provide the desired product. It was reasoned that they could prevent the dimerization by forming stable π -complexes with the substrate. Chloranil and DDQ are known to form charge-transfer complexes, which would be supported by the observed intense color change upon mixing of the reagents.^[163,164] Furthermore, since the mechanism of formation was unknown, it was speculated if the dimerization could occur through radical intermediates. Frémy's salt as an organic single-electron oxidant was therefore employed and indeed furnished dibefurin in modest yield as a 1:1 mixture with the chiral dimer **185** (entry 3). This result encouraged a screen of more oxidants that are less expensive and easier to handle, also to achieve a better yield and selectivity. Inorganic oxidants like Mn^{IV} , Ag^{II} and Ce^{IV} failed to deliver dibefurin (entries 4, 6, 7), but Ag^I and I^{III} both effected the oxidation and dimerization, albeit in worse yield and comparable selectivity (entries 5, 8). Decomposition reactions could arise from quinone methide species formed in the reaction mixture. Copper-based oxidants were supposedly too weak to oxidize epicoccine (entry 9).

Next, epicoccine was treated with Fe^{III} oxidants such as $FeCl_3$ or ferrocenium^{III} that did not afford isolable amounts of the natural product (entries 10, 11). While ferrocenium^{III} might not be able to

oxidize epicoccine efficiently,^[165] the rapid formation of a dark blue solution with FeCl₃ suggested that epicoccine forms catechol or *ortho*-quinone complexes with Fe^{III} or Fe^{II} respectively.^[166] The dimerization might therefore be impossible in the ligand sphere of the iron–substrate complex. In addition, the acidic iron trichloride might change the pH dramatically. An excess of base was therefore premixed with the substrate, but only formation of insoluble iron oxides was observed upon FeCl₃ addition.

Table 3. Selected conditions of the oxidation of epicoccine and formation of dibefurin.

<div style="display: flex; align-items: center; justify-content: center;"> <div style="text-align: center;">  <p>epicoccine</p> </div> <div style="margin: 0 20px;"> <p>conditions</p> <p>→</p> </div> <div style="text-align: center;">  <p>dibefurin</p> </div> <div style="margin: 0 20px;">+</div> <div style="text-align: center;">  <p>185</p> </div> </div>						
entry	oxidant ^[a]	additive (eq.)	solvent (ratio)	T [°C]	NMR yield dibefurin (isolated) [%] ^[b]	NMR yield 185 [%]
1	o-chloranil	-	dioxane	rt	decomp.	decomp.
2	DDQ	-	MeCN	0	-	-
3	FRÉMY's salt ^[c]	-	pH 5 phosphate buffer	0	42 (25)	38
4	MnO₂ ^[d]	-	dioxane	rt	decomp.	decomp.
5	Ag₂O	-	dioxane	rt	30	n.d. ^[e]
6	AgO	aq. HNO ₃	acetone	rt	decomp.	decomp.
7	CAN	-	MeCN	rt	decomp.	decomp.
8	PIFA	-	MeOH	0	43	38
9	CuSO₄·5 H₂O	NaHCO ₃ (6.0)	MeCN/H ₂ O (1:3)	0	-	-
10	FeCl₃·6 H₂O	NaHCO ₃ (2.0)	MeCN/H ₂ O (1:2)	0	-	-
11	[Fe(cp)₂]PF₆	NaHCO ₃ (2.0)	MeCN	rt	-	-
12	K₃Fe(CN)₆	NaHCO₃ (2.0)	MeCN/H₂O (1:2)	0	62 (49)	36
13	K ₃ Fe(CN) ₆	NaHCO ₃ (2.0)	dioxane/water	0	n.d. ^[f]	n.d. ^[f]
14	K ₃ Fe(CN) ₆	NaHCO ₃ (2.0)	MeCN/MeOH/H₂O (1:1:1)	-40	45	26
15	K ₃ Fe(CN) ₆	imidazole	MeCN/H ₂ O (1:2)	0	36	28
16	K ₃ Fe(CN) ₆	-	MeCN/H ₂ O (1:2)	0	-	-
17	air	M(II) salts (cat.) ^[g]	H ₂ O	rt	-	-
18	air	FeSO₄·7H₂O (0.1)	MeCN/H ₂ O (2:1)	rt	29	22
19	O₂ (balloon)	FeSO ₄ ·7H ₂ O (0.1)	MeCN/H ₂ O (1:2)	rt	31 (23)	22
20	O ₂ (balloon)	Fe(TPP)Cl (0.05)	MeCN/H ₂ O (1:1)	rt	24	8

a. 2 eq. of oxidant used (if applicable); b. NMR yield was determined by addition of 1,3,5-trimethoxybenzene to the crude sample; c. 4.0 eq. used; d. 5.0 eq. used; e. Crude NMR contains other signals that overlap with the isomer; f. isomer ratio remained unchanged (dibefurin:**185** = 1.8:1) g. Cat. CuSO₄·5 H₂O, cat. ZnSO₄·7 H₂O, cat. MnSO₄·H₂O; changes in condition are highlighted in bold.

In order to use iron oxidants in basic media and avoid potential coordination to the substrate, potassium ferricyanide as a known outer-sphere oxidant was employed.^[167] This oxidant possesses strong ligands that do not dissociate in basic medium to allow the substrate to coordinate. Indeed,

these conditions yielded dibefurin in good yield as the major isomer (entry 12). The oxidation proved to be almost quantitative with dibefurin and isomer **185** precipitating from the reaction mixture (more on isolation, see chapter 2.3.2.3 Purification of the Natural Product Dibefurin). Although potassium ferricyanide is not a strong oxidant, the possibility to conduct this reaction in aqueous medium might help to provide additional driving force for the synthesis of dibefurin. As opposed to the reaction with ferrocenium in acetonitrile, the equilibrium portion of oxidized epicoccine could be withdrawn through dimerization and rapid precipitation in aqueous solution.

Since the solvent and temperature might have a significant effect on yield and selectivity, further conditions were tested. Changing the solvent (entry 13) or temperature (entry 14) however did not improve the result of entry 12. Alternative counterions by use of Li_2CO_3 , Na_2CO_3 or Cs_2CO_3 showed comparable results to NaHCO_3 . The reaction was less efficient with weaker bases (entries 15) and was completely inhibited when no base was employed (entry 16), which in accordance with literature precedence implies that the actual oxidation occurs with the phenolate ion rather than with neutral epicoccine.^[167] Due to the fact that no improvement could be achieved in this screening, it was tested whether dibefurin and isomer **185** can rapidly equilibrate to form a thermodynamic mixture in DMSO solution. No rapid conversion of the two compounds was observed.

In order to further support the biosynthetic proposal, it was studied whether dibefurin could form spontaneously on air. Since only air as an oxidant did not lead to dibefurin, known catalysts for the autoxidation of phenols such as Cu^{II} , Zn^{II} or Mn^{II} were employed (entry 17).^[168] Gratifyingly, Fe^{II} as an additive yielded noticeable amounts of dibefurin (entry 18). This result clearly shows that dibefurin can be formed in Nature spontaneously without the help of enzymes. Attempts at increasing the yield of this transformation by oxidation with pure oxygen in the presence of Fe^{II} were unfruitful (entry 19). Since the substrate can potentially also coordinate to Fe^{II} , an Fe–porphyrin catalyst was chosen that could act as a biomimetic catalyst for the desired oxidation (entry 20). No performance enhancement could be achieved though. Potentially, the reaction largely depends on the contact between gas and liquid phase and is therefore less suitable than the homogeneous reaction under conditions of entry 12.

Intriguingly, it was noticed that the minor impurities in the NMR spectra of natural dibefurin could be assigned to isomer **185** (see 6.1 Part I: Biomimetic Synthesis of Dibefurin and Epicolactone for more information). It is likely that isomer **185** also forms upon oxidation of epicoccine in Nature and yet remains to be isolated from natural sources. The experimental details provided in this thesis might therefore help to identify this potential natural product in complex mixtures. However, since the amount of this isomer in the spectrum of natural dibefurin is small, it cannot be excluded that it formed through decomposition of dibefurin to its *ortho*-quinones and recombination.

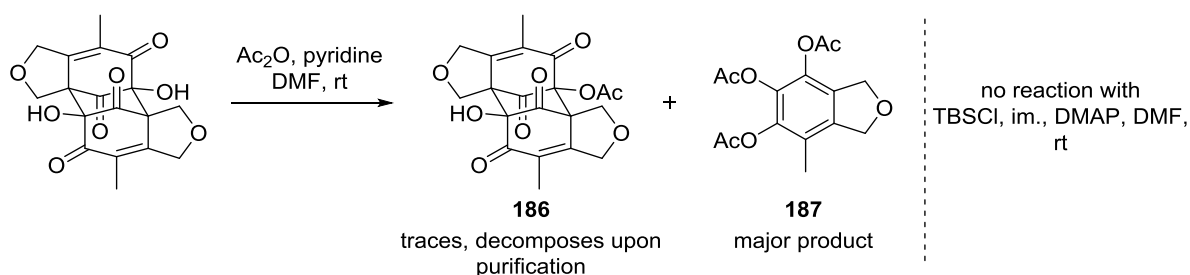
The conditions in entry 12 were found to be most efficient in the biomimetic synthesis of dibefurin from epicoccine. Analytical data of dibefurin was consistent in all aspects to the natural sample.^[150] In a single step, four tetrasubstituted stereocenters, adjacent in pairs, are formed by the

action of the inexpensive outer-sphere oxidant potassium ferricyanide. The dimerization highlights the potential of biomimetic synthesis for the rapid generation of molecular complexity.

2.3.2.3 Purification of the Natural Product Dibefurin

Since dibefurin was found to be very poorly soluble in almost every organic solvent except DMSO and DMF and isomer **185** showed similar properties, the purification of the natural product presented a considerable challenge. Precipitation from the aqueous reaction medium and subsequent centrifugation was identified to separate inorganic impurities. Initial attempts at recrystallization from refluxing dioxane were found to slightly increase the purity of the natural product, but also resulted in significantly lower yields. Presumably, the natural product decomposes to the monomers at higher temperatures. Ambient-temperature recrystallizations from DMSO revealed that dibefurin also decomposes in polar solvents. Eventually, epicoccine could be identified as the ultimate product of the decomposition in DMSO. The nature of the reductant could not be identified, but *ortho*-quinones **149** and **178** could be sufficient oxidants for DMSO. The poor solubility of dibefurin prevented any flash column chromatographic purification, and even HPLC purification on reverse phase silica gel was not able to separate the two dimers. Furthermore, size-exclusion chromatography also failed to increase the purity of the natural product.

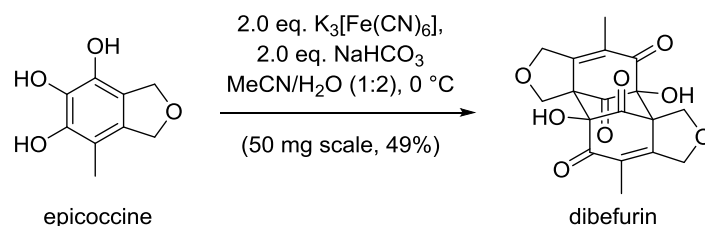
In an attempt to increase the solubility of dibefurin and then purify it by conventional methods, efforts were undertaken to derivatize the natural product with protecting groups that could be removed cleanly (Scheme 49). Dibefurin proved to be labile under mild acetylation conditions, affording traces of monoacetylated product **186** and mainly triacetoxyated epicoccine **187**. The potential redox partner of this reaction could be pyridine. NMR experiments of dibefurin in pyridine were unable to support this conclusion due to the poor solubility of dibefurin. No conversion was observed in a similar reaction toward TBS protection, probably due to the steric hindrance of the tertiary alcohols.



Scheme 49. Derivatization attempts of dibefurin.

Since the products showed moderate solubility in DMF, slow diffusion of water into a solution of dibefurin and isomer **185** gratifyingly afforded pure dibefurin in 40% isolated yield. Additionally, a solvent screen demonstrated that isomer **185** is slightly more soluble in THF than dibefurin, which resulted in an alternative purification protocol by repeated triturations with THF. This purification

protocol was not only more time-economic, but also afforded dibefurin in a higher yield of 49% (Scheme 50).



Scheme 50. Optimized synthesis of dibefurin.

2.3.2.4 Supramolecular Interactions in Solid State

The poor solubility of dibefurin and its instability in solution deserved further investigation. It was possible to obtain X-ray suitable crystals for structural confirmation and analysis of the supramolecular interactions (Figure 19). From MeCN, dibefurin crystallized in the centrosymmetric monoclinic space group $P2_1/c$, which differs from the sample of the isolation group.^[150] It was found that the longest and therefore weakest bond in dibefurin is the $C4-C6'$ bond with $d_{C-C} = 1.598$ Å. The tertiary alcohol possesses a slightly shortened $C-O$ bond of $d_{C-O} = 1.387$ Å. Together with a torsion angle φ ($O-C_6-C_4-C_5$) of $\varphi = 179.83^\circ$, the crystal structure points at a facile decomposition *via* retro-aldol reaction. The lone pair of the oxygen can be oriented in a way that it overlaps with the σ^* -antibonding orbital of the $C4-C6'$ bond, causing this bond to lengthen and simultaneously resulting in a shortening of the $C6'-O$ bond. In turn, the σ^* -antibonding orbital is correctly aligned with the π^* -orbital of the $C5=O$ double bond so that an enol can be directly formed in the retro-aldol reaction.

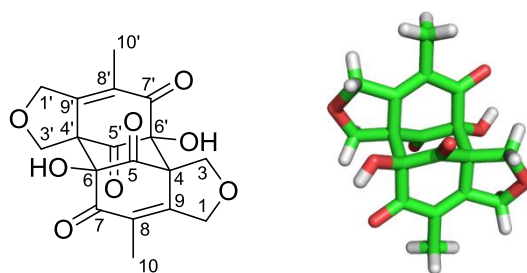


Figure 19. X-Ray single crystal structure of synthetic dibefurin, CCDC: 1022042.
Color code: green = carbon, red = oxygen, white = hydrogen.

The reason for the poor solubility of dibefurin became evident by a close analysis of the supramolecular contacts. Both $C6(-)OH$ groups act as a hydrogen-bond donors while the tetrahydrofuran oxygen atoms are the corresponding acceptors. The resulting hydrogen bond is characterized by the length of $d_{O-O} = 2.792$ Å. Accordingly, dibefurin forms one-dimensional rods of hydrogen-bonded molecules along the c -axis (Figure 20).

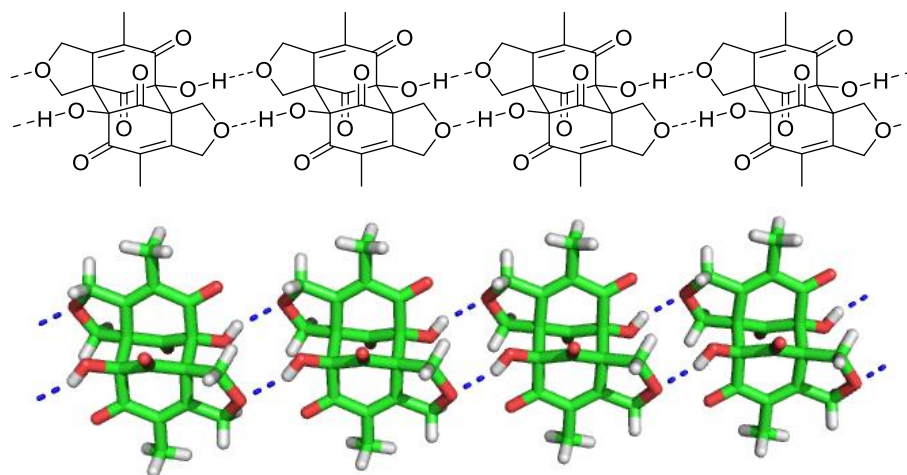


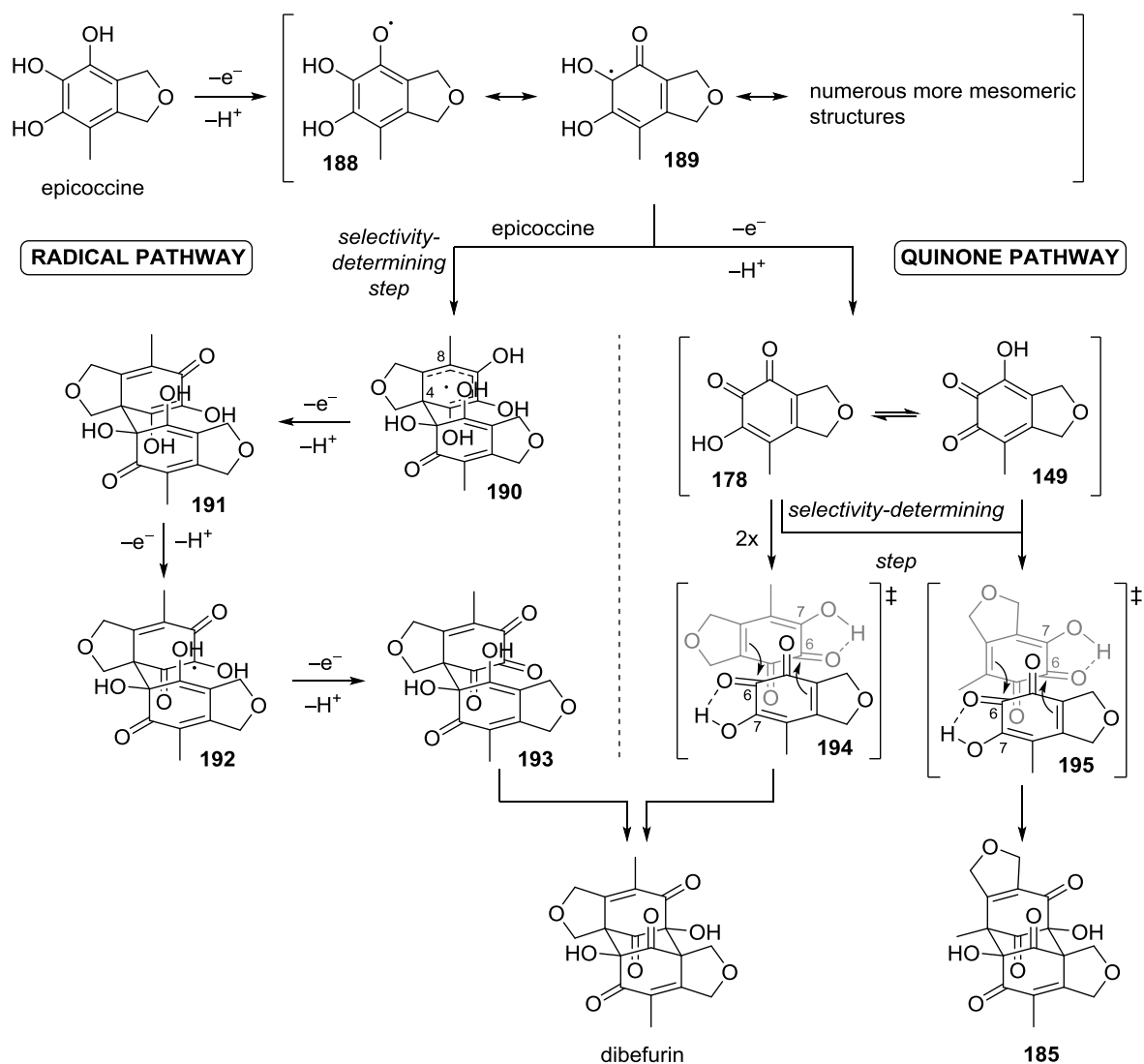
Figure 20. Hydrogen-bond network in solid dibefurin.
Color code: green = carbon, red = oxygen, white = hydrogen.

These rods assemble through hydrophobic interactions to extended sheets, which stack in the solid state structure. Especially the network of 4 hydrogen bonds per molecule of dibefurin should be responsible for the poor solubility in most solvents.

2.3.2.5 Mechanistic Proposal for the Formation of Dibefurin

Mechanistically, the formation of dibefurin is not yet fully elucidated and part of an ongoing project involving, among others, computational methods.⁷ It is uncertain whether the dimerization occurs on the oxidation state of an *ortho*-quinone or through radical intermediates. Due to the presence of a single-electron oxidant, it can be safely assumed that the first step involves oxidation to a semiquinone radical with mesomeric structures **188**, **189** and others (Scheme 51). Only one of the possible tautomers is depicted.

⁷ with Martin Maier, graduate student in the TRAUNER group.



Scheme 51. Possible mechanistic pathways in the formation of dibefurin.

Simple phenol radicals are known to undergo radical coupling processes in the *ortho*- and *para*-position, *e.g.* to PUMMERER's ketone.^[169,170] However, polyhydroxylated arenes can be easily oxidized further. Several pathways can therefore be proposed.

The first pathway, the “radical pathway”, would involve attack of a neutral or deprotonated epicoccine molecule onto the semiquinone radical to form dimer **190**. This step determines the selectivity of the overall coupling since epicoccine can either attack with *C4* or *C8*. Another oxidation would lead to ene diol **191**, from which another electron can be abstracted to yield radical **192**. The final cyclization could occur next, but the formed radical would be potentially less stable. Thus, it is suggested that first triketone **193** is accessed by yet another oxidation before the last bond is forged, leading to dibefurin. The latter is withdrawn from the reaction mixture by precipitation, which might constitute a major driving force of its formation.

Alternatively, the semiquinone radical could be oxidized further to quinones **149** or **178** and undergo dimerization either by a concerted pathway *via* transition states **194** and **195** or with stepwise

formation of the resulting bonds. Intriguingly, the hydrogen bond between C6-ketone and C7–OH in the transition states not only activates the ketone as an electrophile, but also simultaneously increases the nucleophilicity of the dienol.

A potential radical combination of two semiquinones is not depicted since the oxidant is introduced slowly into the reaction mixture. Due to the resulting low concentration of radicals, it seems kinetically unlikely that two radicals collide. Side reactions arising from quinone methide species are also not included since they were not observed.

The presence of iron complexes prevents NMR spectroscopic investigation of the reaction mechanism. To gain mechanistic insights, it could be envisioned to perform selective trapping experiments for radicals or quinones and attempts at identifying potential radical intermediates could be made by ESR spectroscopy. Furthermore, the selectivity-determining steps could be calculated and the energy differences compared to the experimentally observed isomer ratio. The overall success of single-electron oxidants tempts one to consider radical pathways more likely, however the two-electron oxidants employed all had the potential to coordinate quinones or pyrogallols, which might be the real reason for their failure.

2.3.2.6 Biological Activity of Dibefurin⁸

In an interleukin-2 reporter gene assay monitoring the expression of β -galactosidase,^[171] dibefurin was previously found to inhibit calcineurin phosphatase activity with an $IC_{50} = 44 \mu M$.^[150] However, the unusual linear dose–response curve and the observed instability of dibefurin toward decay into the monomer quinones and their redox activity demanded further studies concerning its bioactivity. Quinones are known for their off-target effects either by covalently binding to proteins, complexing metals or producing hydrogen peroxide in cells.^[172] The compounds depicted in Figure 21 were therefore sent to Novartis Pharma AG in Basel for testing of their ability to act as an immunosuppressant. An interleukin-2 reporter gene assay in jurkat cells monitoring the expression of luciferase with AEB071 as a control substance was employed.^[173,174] All compounds, dibefurin, epicoccine, its trimethylether **163**, epicoccone B and its methyl ether **196** were found to be inactive. The initial test results of dibefurin could therefore be based on non-specific effects rather than selective binding to calcineurin phosphatase.

⁸ We are grateful to Dr. Klemens Hoegenauer, Adeline Unterreiner and Dr. Frederic Bornancin at Novartis Pharma AG, Basel for the results of the biological tests of dibefurin and related compounds presented in this chapter.

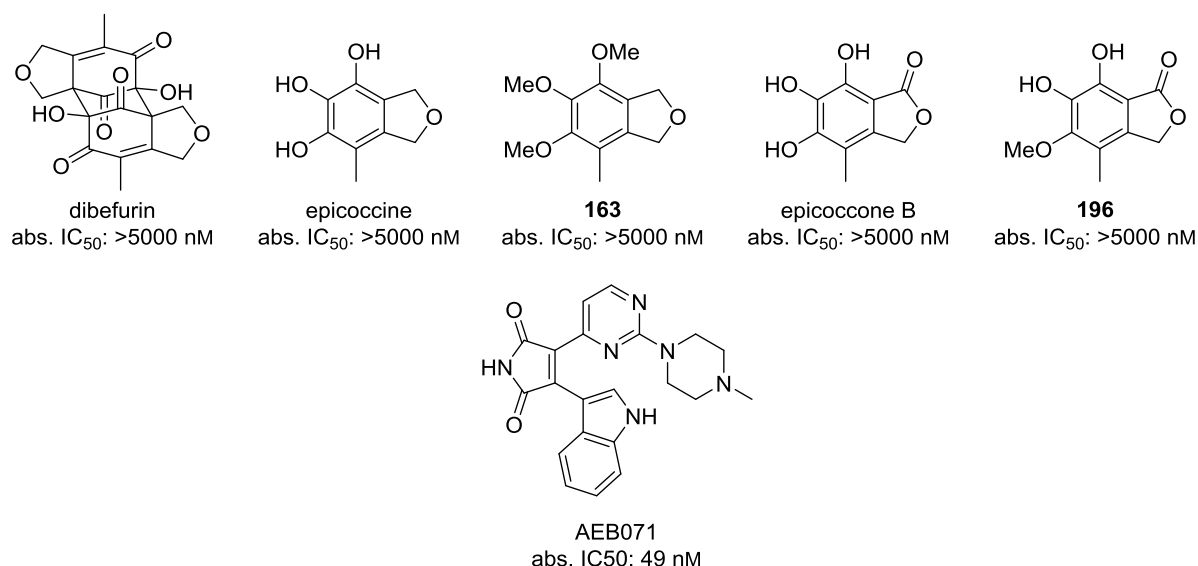
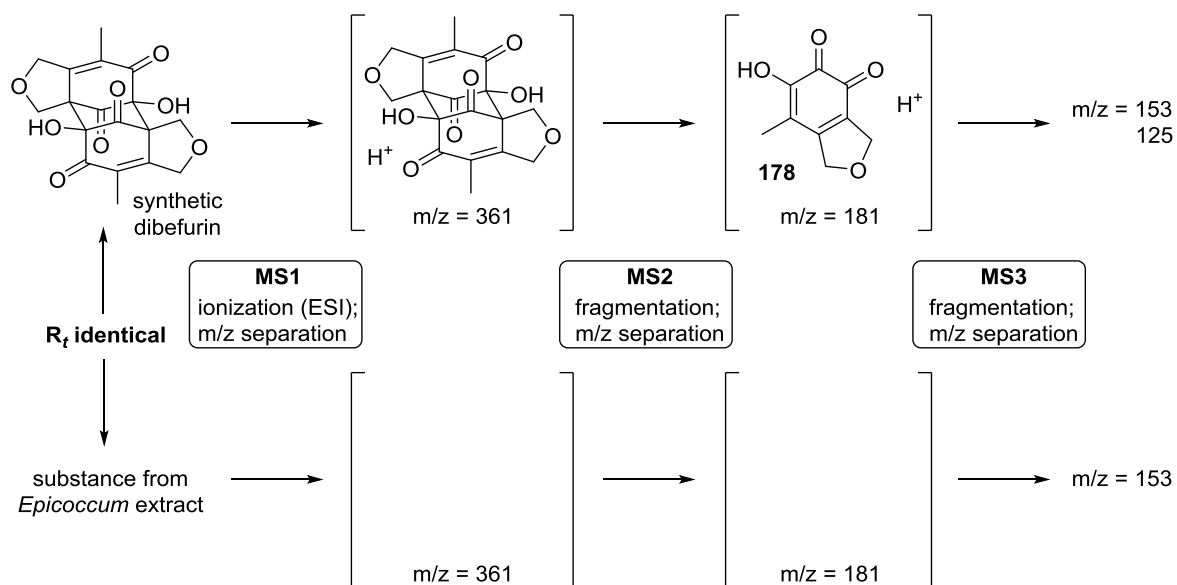


Figure 21. Biological test results of dibefurin and related compounds.

2.3.2.7 Natural Occurrence of Dibefurin in *Epicoccum* sp.⁹

As mentioned above, dibefurin was not isolated from an *Epicoccum* species, but from a fungus of different phylum. It was therefore of interest to investigate, whether dibefurin also occurs in the same species as epicolactone, epicoccine and related natural products. A sample of dibefurin was sent to Prof. Dr. Laatsch (Georg August University of Göttingen) and Prof. Dr. Dr. h.c. Spiteller (TU Dortmund) for comparison with the culture extract. Strong support was provided to our biosynthetic hypothesis and the proposal that dibefurin should also be found in *Epicoccum* sp. when a compound with the same retention time (LC/MS) as dibefurin was identified in the *Epicoccum* extract (Scheme 52). The substance was purified and showed matching MS1, MS2 and MS3 spectra to the ones of dibefurin. Although this compound will have to be isolated to provide final proof of the existence of dibefurin in *Epicoccum*, these results strongly suggest its occurrence also in fungi of phylum Ascomycota.

⁹ We thank Prof. Dr. Laatsch and Prof. Dr. Dr. Spiteller for help in generating the results presented in this chapter.



Scheme 52. Comparison of MS spectra of dibefurin with MS spectra of a compound in the *Epicoccum* extract.

2.3.3 Synthesis of Epicoccone B

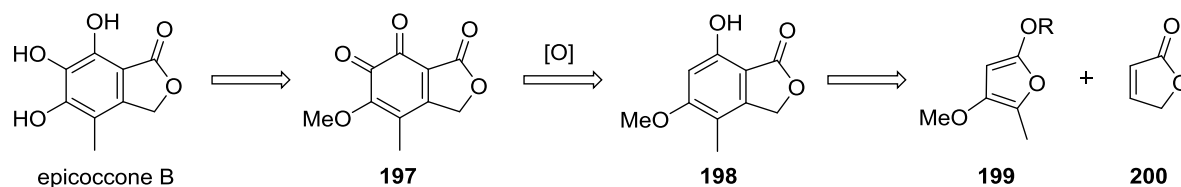
Despite the high-yielding previous synthesis of epicoccone B, it was necessary to invent a new route that is amenable to selective protection of the different phenolic OH groups. The first generation synthesis involved a non-discriminating global deprotection of the phenolic methyl ethers in the final step.

2.3.3.1 Cycloaddition Approaches

The introduction of OH groups on aromatic systems is still more challenging than the installation of other heteroatoms.^[175] The reason for this is the lack of mild electrophilic oxygen sources, which is why oxygen atoms are either introduced by nucleophilic aromatic substitution ArS_{N} on electron-poor arenes,^[176] indirectly through manipulation of carbonyl groups (DAKIN oxidation),^[177] boronates,^[178] silanes^[179] or halides (ULLMANN reaction, BUCHWALD–HARTWIG phenol synthesis)^[180] or through directed C–H activation.^[181]

It was therefore envisioned to access the trihydroxylated benzene derivative epicoccone B by cycloaddition in a *de novo*-arene synthesis. Following this protocol, a high substitution degree of the arene can be achieved and the required oxygen atoms can be included in the diene. For reasons outlined in 2.3.4 Synthesis of Epicolactone, it was focused on a route that would also allow for the preparation of C5 mono methyl ether of epicoccone B. Since many retrosynthetic alternatives existed and were tried in parallel, attempts were discarded rather than optimized when problems concerning reactivity, scalability or selectivity became evident early on.

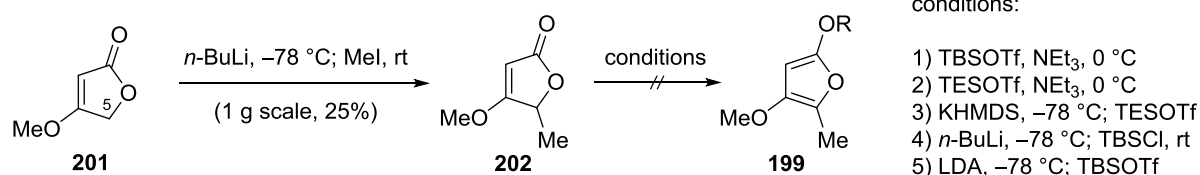
Furans and especially tetronic acid derivatives have proven to be excellent dienes for the synthesis of hydroxylated arenes.^[182] The first retrosynthesis was based on the strategic introduction of the last oxygen atom by oxidation to an *ortho*-quinone with FRÉMY's salt (Scheme 53). Epicoccone B was therefore traced back to quinone **197**, which would arise from resorcinol derivative **198**. The latter would be accessed through a [4+2]-cycloaddition of furan **199** and butenolide **200**.



Scheme 53. Retrosynthesis of epicoccone B involving cycloaddition of a tetronic acid derivative.

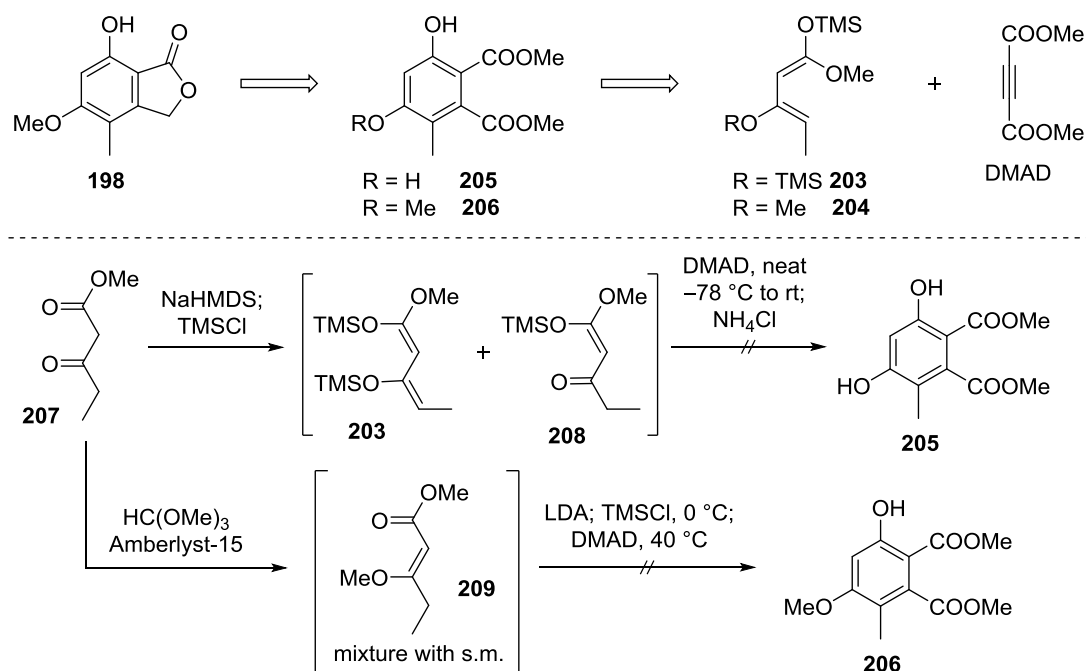
Commercially available tetronic acid derivative **201** was deprotonated and C5 methylated in an unoptimized procedure to give methyl tetronate **202** in poor yield (Scheme 54). Further deprotonation and *O*-silylation was attempted under a variety of conditions, but failed to provide the desired furan derivative **199**. Since in conditions 1 and 2, only starting material was recovered, amine bases seemed too weak or too sterically hindered to deprotonate the C5 position. Problematic *O*-silylations with

similar derivatives have been reported.^[183] However, stronger bases like KHMDS or *n*-BuLi in combination with TBSCl delivered the same result (conditions 3, 4).^[184] Deprotonation with LDA and trapping with TBSOTf resulted in the formation of dimeric species and hence failed to provide a robust route to furan **199**. Due to the difficulties encountered already at an early stage of the synthesis and a variety of possible alternatives, the route was discontinued. However, tetronate **202** was identified as another challenging member of this class that fails to undergo efficient *O*-silylation.^[185]



Scheme 54. Attempts at preparation of tetronic acid derivatives.

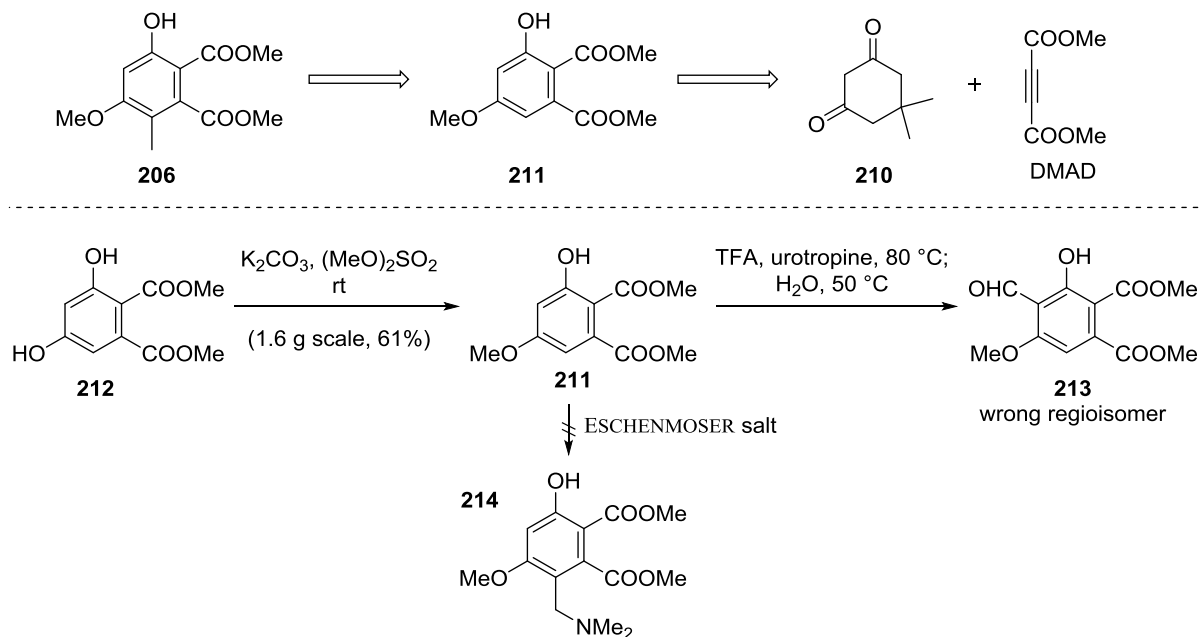
The next retrosynthesis was again based on a cycloaddition approach, but involved the use of non-cyclic diene partners such as **203** or **204** and more activated dienophiles like DMAD for the preparation of resorcinol **198** (Scheme 55). The resorcinol **198** should therefore stem from diester **205** or **206** by cyclization to the corresponding anhydride and selective reduction according to literature precedence.^[186,187] A cycloaddition between dienes **203** or **204** and DMAD was expected to furnish this building block.^[188]



Scheme 55. Alternative access to resorcinol **198** by cycloaddition with open diene.

The preparation of the required dienes proved less efficient and more sensitive than anticipated. Double deprotonation of keto ester **207** and following *O*-silylation to bis silylether **203** either did not proceed with full consumption of the starting material or reverted back to monosilyl ether **208** by

hydrolysis.^[189] The key cycloaddition was nonetheless attempted with this mixture, but did not occur despite promising literature precedence.^[190] Only hydrolyzed starting material was recovered from the reaction mixture. The same sequence was tested with a different diene prepared from enol ether **209**, but analogously failed to give product **206** even at slightly elevated temperatures.^[191] Due to the lability of the open dienes and the identification of a better strategy, this route was abandoned and no further attempts were undertaken to optimize the required cycloaddition at higher temperatures.



Scheme 56. Alternative preparation of resorcinol **206** by ALDER-RICKERT cycloaddition.

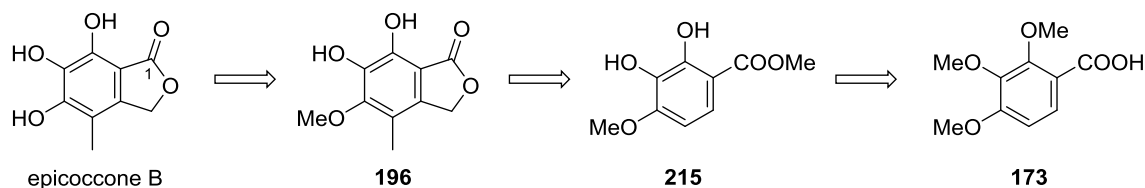
The ALDER-RICKERT cycloaddition is a well-precedented way to synthesize resorcinols from cyclohexadiones like **210**.^[192] A DIELS-ALDER cycloaddition gives rise to a bicycle that subsequently undergoes retro-DIELS-ALDER reaction to release isobutylene and afford an aromatic system. In an alternative approach to resorcinol **206**, it was hence traced back to its demethylated analog **211**, which would be synthesized from a [4+2]-cycloaddition of diketone **210** with DMAD (Scheme 56).¹⁰

Resorcinol **212** was selectively methylated to phenol **211** at the more acidic OH group due to the stronger electron-withdrawing effect of the *para*-positioned ester (as opposed to *ortho*-). As evident from the analysis of the crude reaction mixture, the subsequent DUFF formylation to introduce the methyl-carbon atom proceeded with the wrong regioselectivity to aldehyde **213**. The reagent was potentially directed by the free hydroxyl group. An aminomethylation to diester **214** with ESCHENMOSER's salt led to no conversion.^[193] Whereas a DAKIN oxidation could have converted resorcinol **213** to a pyrogallol that could undergo the desired methylation, a more step- and time-economic route was identified in the meantime.

¹⁰ Resorcinol **212** was kindly provided by M. Sc. Klaus Speck, graduate student in the MAGAUER group (LMU Munich).

2.3.3.2 Synthesis of Epicoccone B from Pyrogallol Derivative

The multitude of inexpensive commercially available pyrogallol starting materials and the challenges encountered in the cycloaddition approaches to epicoccone B led to the reconsideration of the strategy. It was therefore proposed to commence the synthesis with a pyrogallol that features the correct oxidation state at carbon atom C1. The subsequent carbon atoms would need to be introduced successively by electrophilic aromatic substitution reactions, which should readily proceed with the electron-rich arene (Scheme 57).

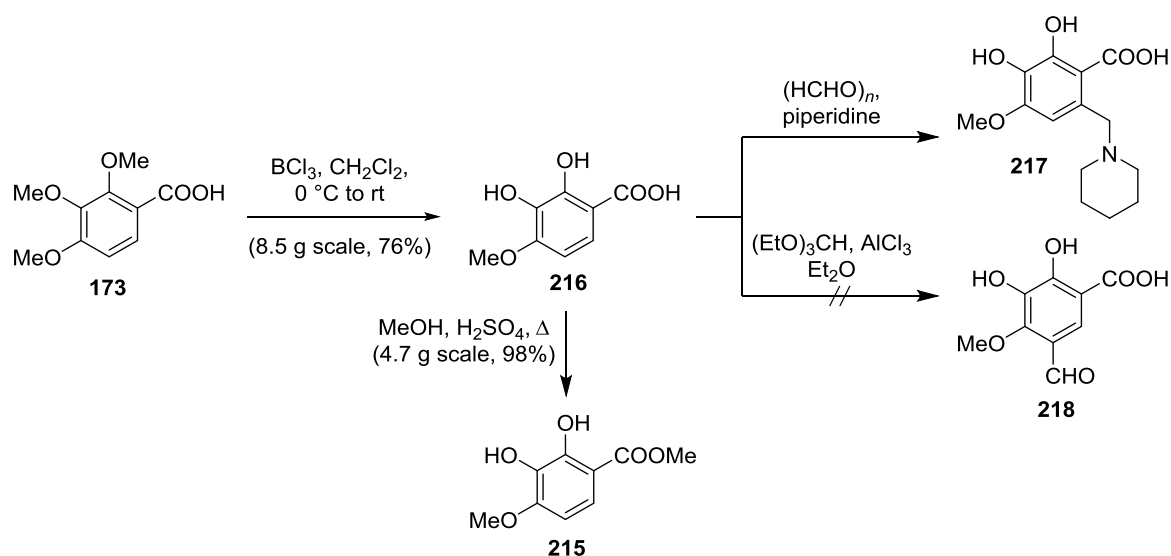


Scheme 57. Retrosynthesis of epicoccone B by electrophilic aromatic substitutions.

The retrosynthetic plan involved a deprotection of the last remaining methyl ether **196** as the final step of the synthesis. This methyl ether **196** was to be accessed by introduction of the lactone and arene methylation of catechol **215**. Selective deprotection of aryl methyl ethers in **173** should give rise to this catechol.

2.3.3.2.1 Synthesis of Catechol 215

The selective deprotection of acid **173** was literature-known and proceeded smoothly on multi-gram scale in good yield (Scheme 58).^[194]



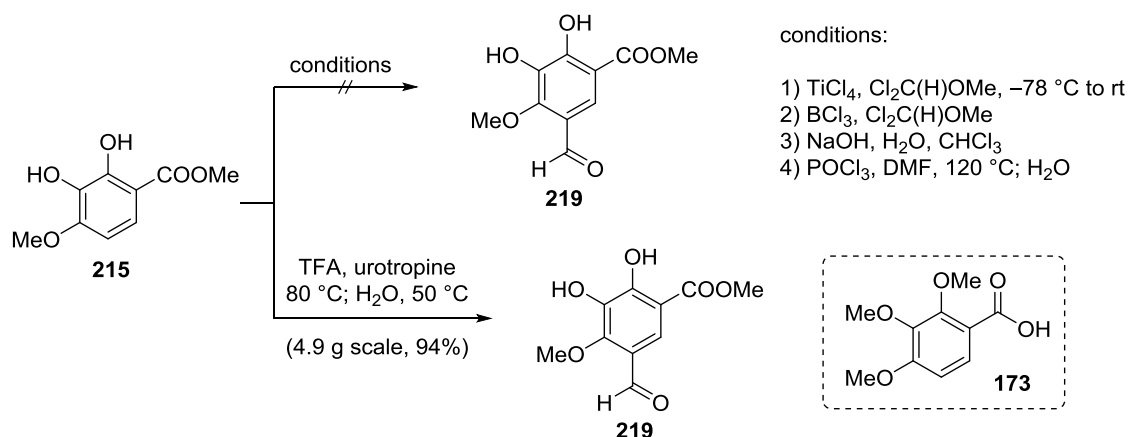
Scheme 58. Synthesis of methyl ester **215**.

Although the resulting acid **216** showed poor solubility in most organic solvents, it was tested whether the methyl group of epicoccone B could be introduced. MANNICH-type reaction with

piperidine and formaldehyde was stopped at partial conversion to assess the regioselectivity of the aminomethylation, which proved to exclusively afford the wrong regioisomer **217**. Apparently, the carboxylic acid directs the reagent to the *ortho*-position. A LEWIS acid mediated formylation with triethyl orthoformate to aldehyde **218** did not show any conversion. To be able to test further formylation methods and to increase the solubility and practicability of the route, acid **216** was subjected to a FISCHER esterification to afford methyl ester **215** in almost quantitative yield.

2.3.3.2.2 Introduction of the Methyl Group in Epicoccone B

A two-step procedure of formylation and reduction constitutes an efficient way to introduce a methyl group on arenes.^[195–197] Alternatives would be deprotonation and treatment with a methylating agent like MeI or dimethyl sulfate or NEGISHI coupling reactions with ZnMe₂. Since catechol **215** seemed very activated to electrophilic aromatic substitution reactions, the latter procedure was chosen. After the isolation of catechol **215** in the previous step, it became evident that any process involving this compound or further catechols would need to furnish a clean product without conventional purification since it decomposed on regular silica gel. For time and cost reasons, flash column chromatography on reverse phase silica was to be avoided to ensure a scalable and efficient route. Unexpectedly, initial formylation trials to aldehyde **219** were not met with success (Scheme 59).

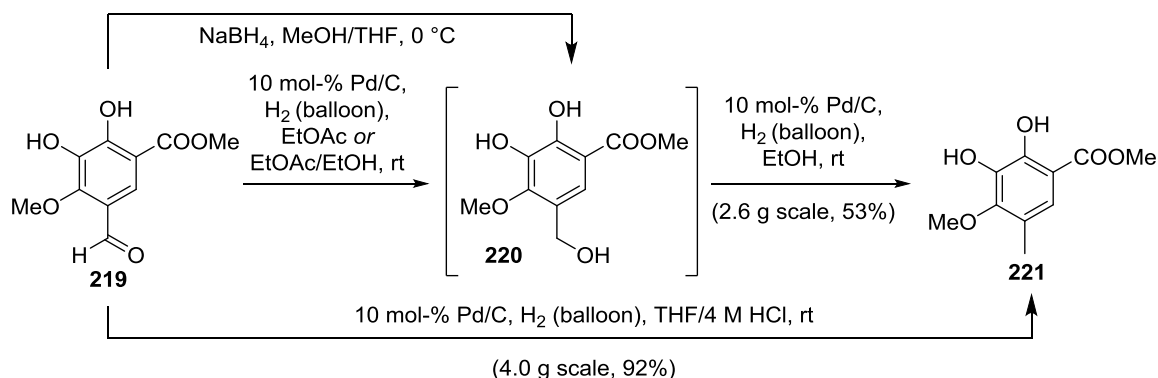


Scheme 59. Formylation of catechol **215**.

While the RIECHE formylation either only led to recovery of starting material (conditions 1)^[198] or partial *O*-demethylation (condition 2),^[199] the REIMER–TIEMANN reaction resulted in complete decomposition of the starting material (condition 3). In general, it was observed that catechols like **215** were sensitive to basic conditions, potentially due to the more facile oxidation to very reactive *ortho*-quinones. Only ester hydrolysis was detected using VILSMEIER–HAACK formylation conditions, which probably occurred during workup (condition 4). It was argued that the reactions failed because the catechol coordinates to metal ions or undergoes phosphorylation, which largely decreases the nucleophilicity of the aromatic system. Therefore, a DUFF formylation was employed, which is free of coordinating metal ions, and proved to be the only successful formylation method. Benzaldehyde **219**

was synthesized almost quantitatively on multi-gram scale in a facile procedure. Intriguingly, in an attempt to access an alternative precursor to epicoccone B, acid **173** failed to undergo any reaction under these conditions.

The reduction of benzaldehydes like **219** to toluene derivatives is described in the literature mostly by using heterogeneous hydrogenation.^[196,197] Attempts to remove the oxygen atom by hydrogenation with catalytic Pd on activated charcoal in EtOAc first only resulted in the formation of the labile benzyl alcohol **220** (Scheme 60).



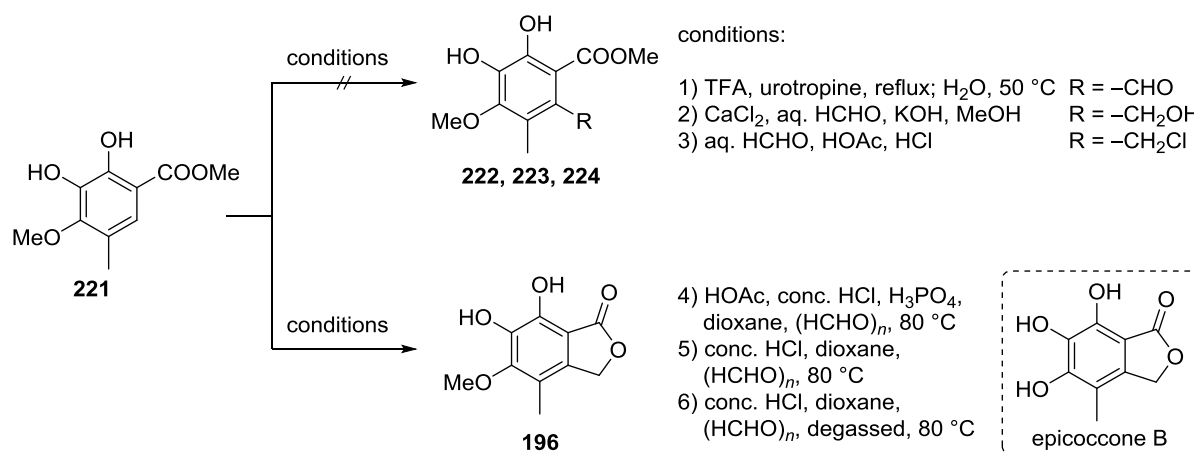
Scheme 60. Reduction of aldehyde to methyl group.

Immediate resubjection to the heterogeneous hydrogenation in EtOH gave rise to the desired toluene derivative **221**. It was reasoned that the poor solubility of intermediate benzyl alcohol **220** in EtOAc hinders the second reduction to take place, but conducting the reaction with aldehyde **219** in a solvent mixture of EtOAc/EtOH also only furnished benzyl alcohol **220**. Using ethanol as the exclusive solvent for the two-step process was not possible since the starting benzaldehyde was insoluble. As the first reduction could be achieved more cost-efficiently, benzaldehyde was reduced with sodium borohydride to benzyl alcohol **220**. The latter readily decomposed upon isolation attempts or even under low pressure, presumably by dehydration and generation of the reactive *para*-quinone methide. Further investigation of the hydrogenolysis revealed that the outcome is dependent on the batch of Pd/C employed, the size of the reaction vessel and the quality of the starting material. Aldehydes that had been filtered over a reverse-phase silica plug performed worse than crude aldehydes. A probable rationale for the inconsistent results of this reaction was the varying acid content of the Pd/C batch and the starting material. Ultimately, the reaction was performed on multi-gram scale in excellent yield in large reaction vessels to ensure maximum solvent exposure to the hydrogen atmosphere in strongly acidic media to facilitate hydrogenolysis of the intermediate benzyl alcohol to catechol **221**. The reaction probably benefits from protonation of the benzyl alcohol and subsequent hydrogenolysis to directly furnish water.

2.3.3.2.3 Introduction of the Sixth Substituent

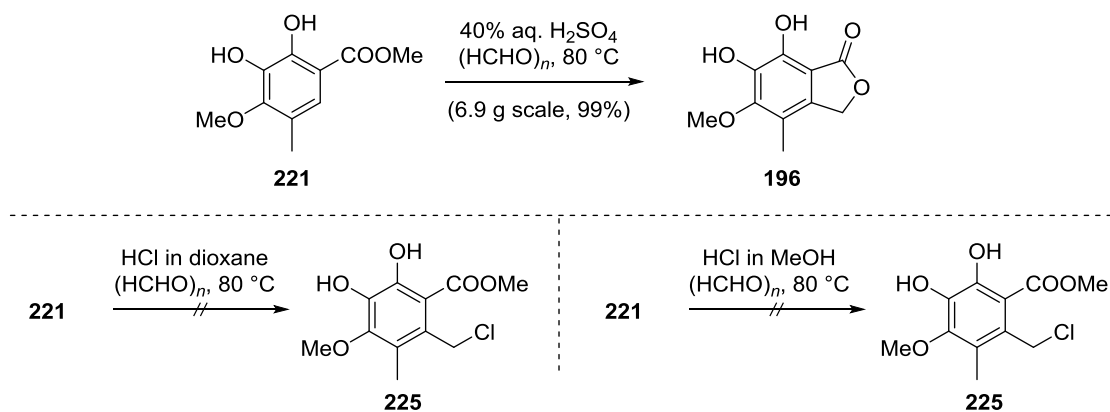
The remaining task was to introduce the sixth substituent on the aromatic ring of ester **221**. Due to the steric challenge of this endeavor, the transformation was mainly tried with small electrophiles,

benefitting from the electron-richness of the benzene ring (Scheme 61). Since several other formylation methods had failed previously, only the DUFF formylation to aldehyde **222** was tried (condition 1). However, starting material was recovered. Since hydroxy- or chloromethylations would be more step- and redox-economic and would involve the use of the small reagent formaldehyde, it was next focused on these transformations to access esters **223** or **224**. Functionalization attempts proved unfruitful with decomposition under basic conditions (condition 2)^[200] and no reaction under acidic conditions at ambient temperature (condition 3).^[201] It was reasoned that acidic conditions were more likely to provide the product if temperatures were to be increased. Indeed, chloromethylation conditions adapted from the literature with a mix of acids and paraformaldehyde at elevated temperatures provided the already cyclized product **196** with an unknown side product (condition 4).^[202] As mentioned above, purification of the catechol products presented a challenge and further reaction conditions were therefore screened.



Scheme 61. Attempts at introduction of last substituent toward epicoccone B.

The conditions were found equally effective if acetic and phosphoric acid were omitted, but the side product remained. It was observed that its quantity increased with longer reaction times. Potentially, the side product could arise from concomitant oxidation of the catechol moiety and subsequent decomposition, which would explain the dark brown color of the reaction mixture. Yet, conducting the reaction under strict exclusion of oxygen with deaerated solvents did not change the result. The side product was eventually identified as epicoccone B, resulting from demethylation with a nucleophile. As the nucleophile could only arise from hydrochloric acid, a change to the non-nucleophilic sulfuric acid allowed for the optimal hydroxymethylation conditions to introduce the last epicoccone B substituent (Scheme 62). This reaction could be successfully applied on multi-gram scale in quantitative yield and did not require purification of the product **196**.



Scheme 62. Optimal hydroxymethylation conditions for the synthesis of epicoccone B precursor.

Mechanistically, ester **221** first has to hydrolyze to the corresponding acid to undergo functionalization. Prior to the completion of the reaction, this acid could be identified by LC/MS. Non-aqueous conditions with paraformaldehyde and HCl in dioxane or in MeOH did not afford appreciable amounts of the chloromethylation product **225**. It appears that the related carboxylic acid can direct the reagent to the *ortho*-position, which enables the installation of the last substituent. Lactone **196** was crystallized to obtain unambiguous confirmation of its structure (Figure 22). The structure reveals that the methyl group of the ether is twisted out of the arene plane, which facilitates a demethylation by nucleophilic attack on the methyl group due to less steric hindrance.

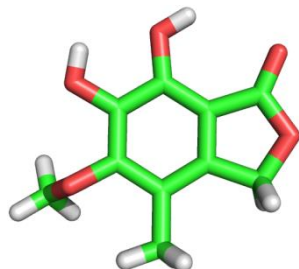
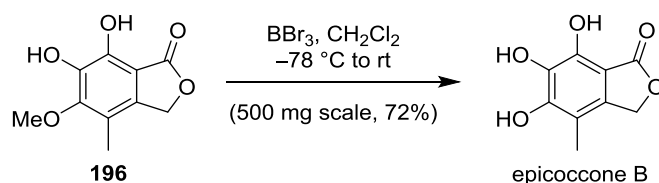


Figure 22. X-Ray single crystal structure of lactone **196**; CCDC: 1022041.
Color code: green = carbon, red = oxygen, white = hydrogen.

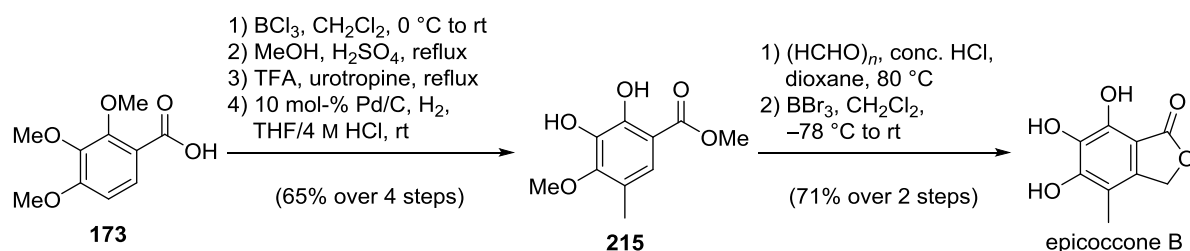
2.3.3.2.4 Completion of the Synthesis of Epicoccone B

The previous reaction had demonstrated that demethylation of the last remaining methyl ether is feasible. Isolation of epicoccone B from this reaction mixture proved to be difficult though. Therefore, a standard procedure involving BBr_3 was applied, with which epicoccone B was synthesized in good yield (Scheme 63).



Scheme 63. Final demethylation in the synthesis of epicoccone B.

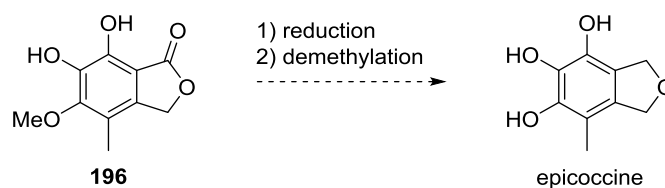
In summary, epicoccone B was synthesized in 6 steps and 46% overall yield in a sequence depicted in Scheme 64. This route allows for the preparation of the natural product without flash column chromatographic purification of the intermediates with similar results.



Scheme 64. Completed synthesis of epicoccone B.

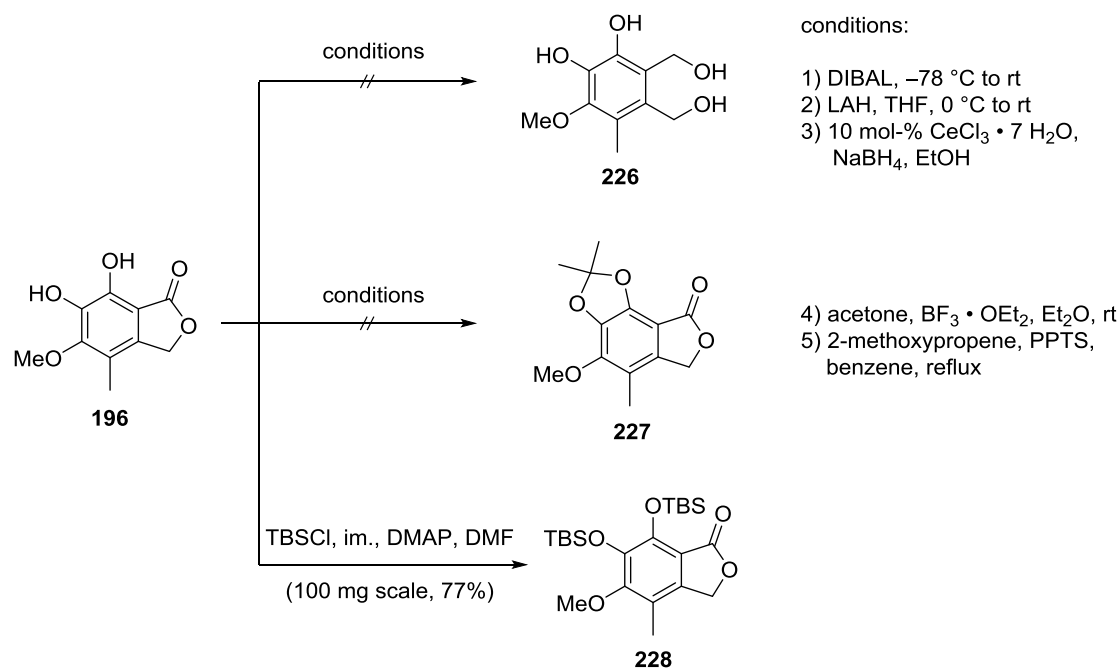
2.3.3.2.5 Combination of Epicoccine and Epicoccone B Synthesis

Due to the structural similarity of epicoccine and epicoccone B and the excellent scalability of the epicoccone B synthesis, it was attempted to prepare epicoccine by a similar route. The potential branching point of the route was identified in catechol **196**. A reduction and subsequent demethylation would yield epicoccine (Scheme 65).



Scheme 65. Potential synthesis of epicoccine from epicoccone B intermediate.

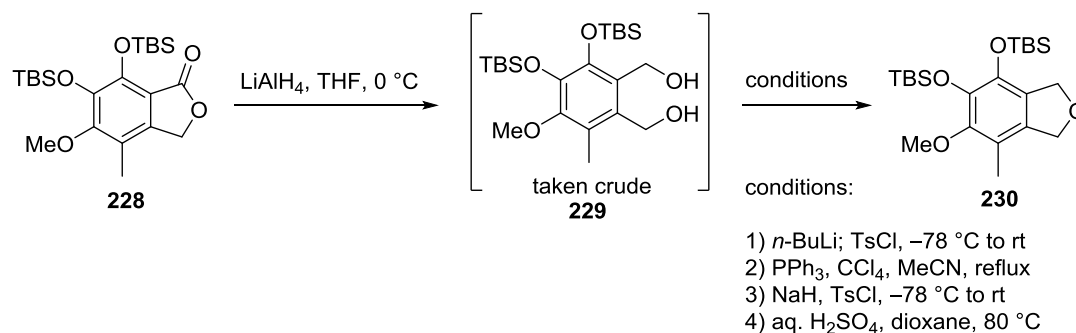
The previous studies had exposed the base sensitivity of the catechols as well as their ability to coordinate to metal ions, which is why a reduction was not expected to be facile. Treatment of lactone **196** under various conditions with DIBAL (only one shown, condition 1) or LAH (condition 2) or attempted LUCHE reduction to yield diol **226** exclusively led to decomposition (Scheme 66).^[203]



Scheme 66. Attempts at reduction or protection of catechol **196**.

It was observed that a diol of type **226** formed rather than the desired hemiacetal, but the diol resisted isolation. It was reasoned that a benzylic alcohol next to a phenol is very prone to elimination under generation of the reactive *ortho*-quinone methide. Therefore, protection of the catechol became necessary. After unsuccessful trials to protect the catechol as dioxolane **227** (conditions 4, 5), TBS protection proceeded smoothly to yield bis-silyl ether **228**. It was crucial to conduct this reaction at concentrations c as high as $c = 1.6\text{ M}$ to obtain the product.

The protected catechol **228** underwent reduction with LAH to afford crude diol **229**, which due to the danger of silyl migration was not purified (Scheme 67). Although the steric bulk of the TBS groups could favor cyclization to tetrahydrofuran **230**, no product was observed under the conditions tested. Whereas tosylation or substitution by chloride was successful, no cyclization was observed in conditions 1 and 2. Condition 3 led to a multitude of silyl migration products. Cyclization and parallel TBS deprotection was further attempted with aq. sulfuric acid (condition 4), but no product was detected.



Scheme 67. Attempt at reduction of lactone **228**.

The unfruitful attempts at converting epicoccone B intermediate **196** to epicoccine showed that a resulting route to epicoccine would not be as efficient as the already established one. Efforts toward this goal were therefore abandoned and focused on the synthesis of epicolactone.

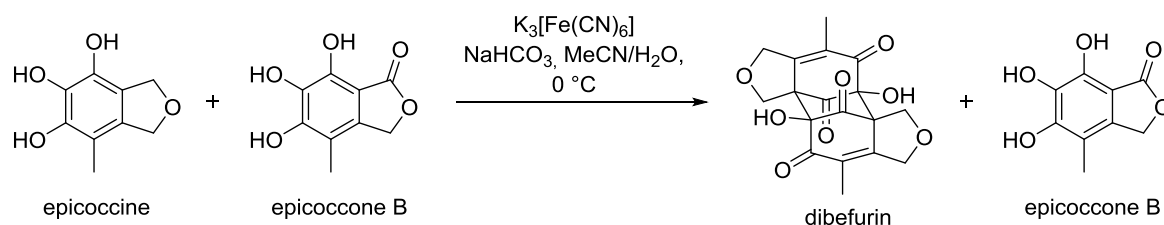
2.3.4 Synthesis of Epicolactone

The envisioned synthesis of epicolactone involved a heterodimerization of two pyrogallol building blocks as the key step and subsequent skeletal rearrangement. In general, the challenge of a heterocoupling is always the competing homocoupling of either compound. It is therefore crucial to provide a driving force for the heterocoupling by substrate manipulation or the reaction setup. Since epicolactone was isolated alongside other natural products and evidence was found in this thesis that dibefurin is one of these, it was expected that an attempted heterodimerization might generate dibefurin as a side product. Furthermore, potential side reactions arising from quinone methides described in 2.3.2.1 Potential Challenges would have to be suppressed.

2.3.4.1 Heterodimerization of Epicoccine with Epicoccone B

The envisioned heterodimerization was first attempted with epicoccone B as one of the potential biomimetic coupling partner. Epicoccone B was already isolated from the same fungus that also produces epicolactone and therefore represented a viable choice.^[147]

The optimized conditions for the synthesis of dibefurin were applied to an equimolar mixture of epicoccine and epicoccone B (Scheme 68). However, only the formation of dibefurin was observed and epicoccone B was isolated as unreacted starting material. Even with a ten-fold excess of epicoccone B compared to epicoccine, no heterodimerization product was obtained. Instead, only a small quantity of dibefurin was formed and both starting natural products were reisolated.

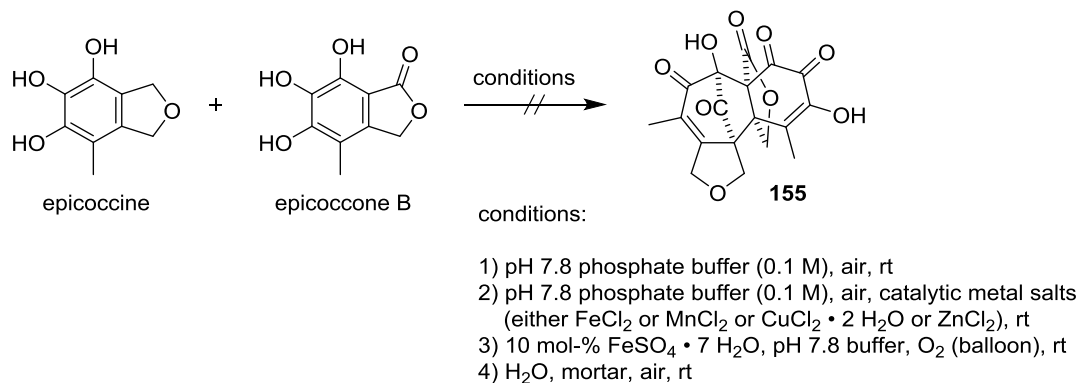


Scheme 68. Heterodimerization attempt of epicoccine and epicoccone B.

This result can be rationalized with the more facile oxidation of epicoccine compared to epicoccone B. Due to the additional carbonyl as an electron-withdrawing group, epicoccone B is more electron-deficient than epicoccine. The oxidant therefore preferentially abstracts electrons from epicoccine, which activates this natural product for coupling reactions. If the dimerization proceeds *via ortho*-quinone dimerizations, dibefurin will be the only feasible product. In case that a nucleophilic attack occurs on an epicoccine semiquinone radical, it will also again be the more electron-rich and more nucleophilic epicoccine that preferentially intercepts this reactive intermediate. Both scenarios result in a favored homodimerization. However, the fact that no trace of heterodimerization product was detected could point toward a potential instability of the corresponding product or toward the fact that potassium ferricyanide is not capable of efficiently oxidizing epicoccone B. A control experiment

under the same conditions with only epicoccone B showed unreacted epicoccone B and oxidation of the lactone ring in the benzylic position. Regardless of whether the oxidation arose from an *ortho*-quinone tautomerization or by direct benzylic oxidation, the fact that mostly starting material was recovered proved that potassium ferricyanide cannot quantitatively oxidize epicoccone B.

It was reasoned that a more basic medium would facilitate the oxidation of epicoccone B since epicoccone B was assumed to be the more acidic pyrogallol derivative of the two starting materials. To this end, the fermentation conditions with a basic pH were mimicked with and without metal salt additives (Scheme 69).

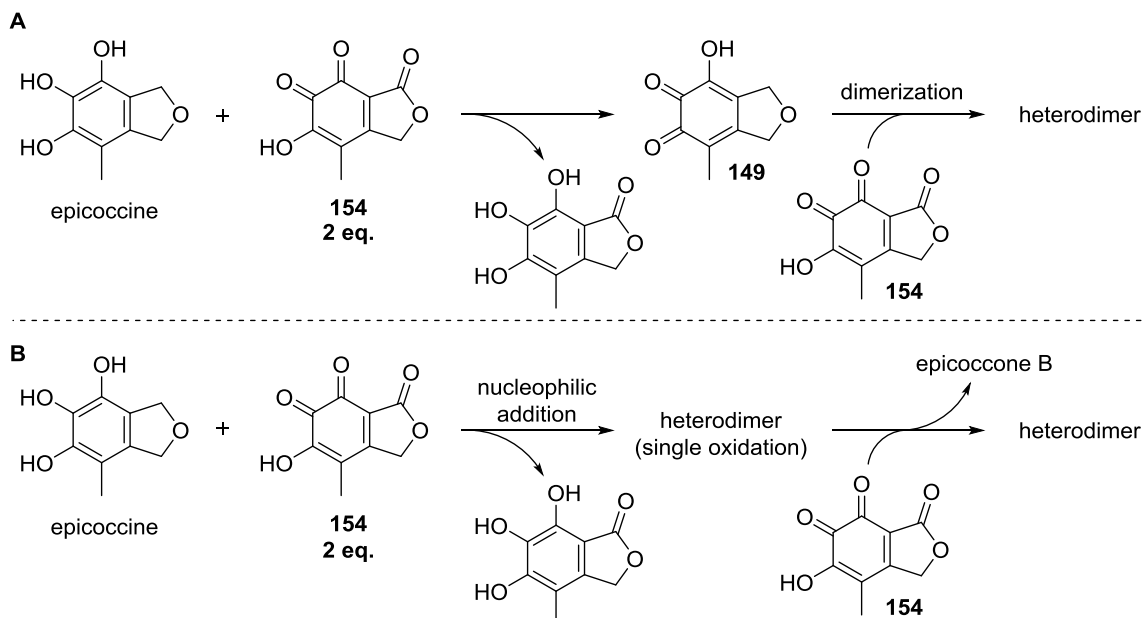


Scheme 69. Attempts at biomimetic heterodimerization in basic media or solid state.

Both pyrogallols, insoluble in neutral water, readily dissolved in the phosphate buffer exposed to air (condition 1). The mass of a heterodimer that had undergone a single oxidation was identified after days. Since the structure of the desired heterodimer can only stem from double oxidation, the observed heterodimer potentially is an ether adduct resulting from nucleophilic attack of a phenol onto an *ortho*-quinone. Its lability during isolation attempts and even under acetylation trials with acetic anhydride and pyridine would be in line with this conclusion. In order to effect the necessary second oxidation, known autoxidation catalysts such as Fe^{II} , Mn^{II} , Cu^{II} and Zn^{II} salts were added, only leading to the decay of the initial heterodimer (condition 2).^[168] The catalytic conditions under oxygen atmosphere with Fe^{II} salts that had previously proven to afford dibefurin were also tested but only gave rise to dibefurin (condition 3). In an effort to increase the proximity between the reaction partners and thus enable heterodimerization, both were intimately mixed in a mortar, moisturized with water and left standing on air for the duration of 1 month. Only unreacted starting material was recovered.

It appeared as if any dimerization attempt between epicoccine and epicoccone B with *in situ* oxidation would always preferentially lead to dibefurin for the reasons outlined above. Therefore, preoxidized epicoccone B was envisioned to be treated with epicoccine (Scheme 70). In scenario A, epicoccine would first be oxidized by *ortho*-quinone **154** obtained from epicoccone B to furnish epicoccine *ortho*-quinone **149**. This could now dimerize with a second equivalent of quinone **154** to afford a heterodimer. Likewise, in scenario B the heterodimerization would occur first by nucleophilic attack of epicoccine onto quinone **154** and then undergo oxidation by the second equivalent of quinone

154. Independent of the actual dimerization mode (scenario A or B), epicoccone B quinone **154** would always be present in higher amounts than epicoccine quinone **149**. Therefore, the homodimerization should be largely suppressed and the desired heterodimerization should be favored. If successful, the role of epicoccone B as a sacrificial oxidant could also be taken over by conventional reagents.



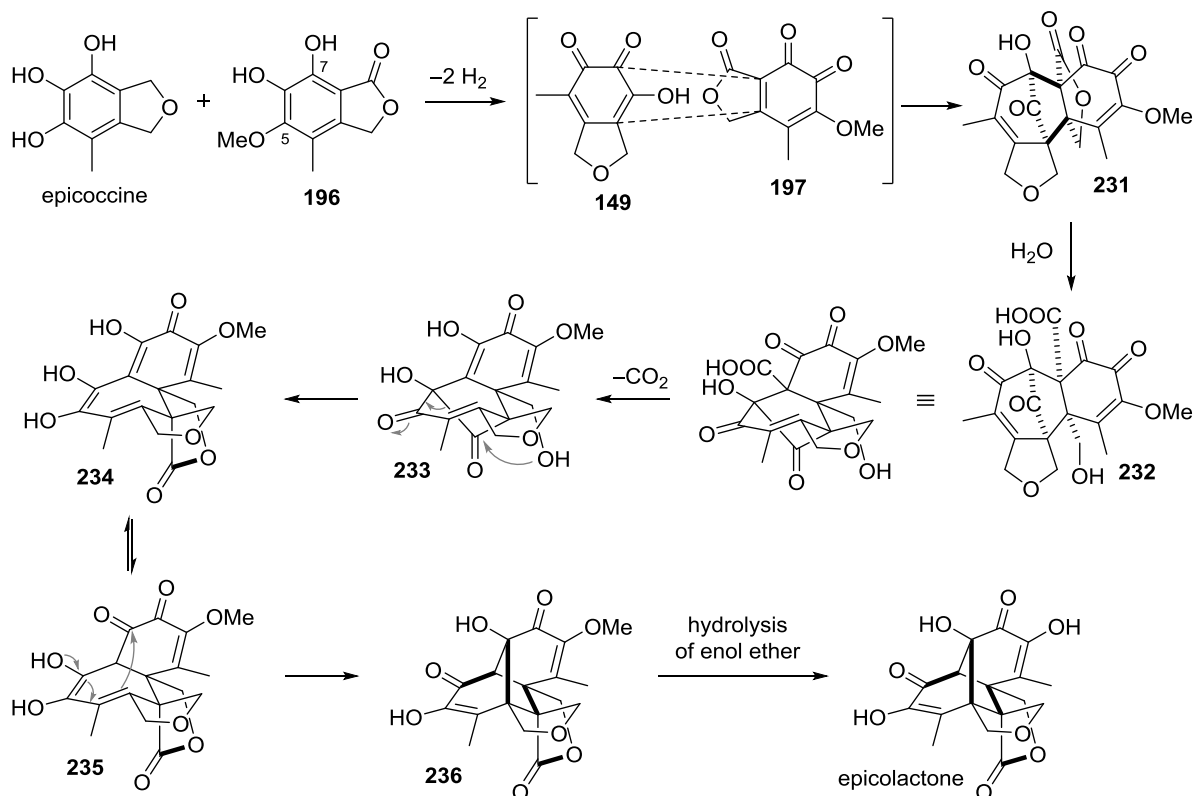
Scheme 70. Rationale behind preoxidation of epicoccone B.

Preoxidation of epicoccone B proved to be challenging since quinone **154**, probably as a mixture with its tautomers, resisted isolation and characterization. Hence, epicoccone B was presumably oxidized with *ortho*-chloranil yielding a dark burgundy precipitate that was insoluble in ether at $T = -78\text{ }^{\circ}\text{C}$. As the reagent and its reduction product are both soluble in ether, the precipitate was assumed to be quinone **154** or its tautomers. Treating epicoccine resulted in the formation of dibefurin, epicoccone B and a heterodimer with covalently bound water by mass analysis. The structure of the heterodimer could not be elucidated at the time (for hypothesis on its structure, see chapter 2.3.4.2.2 Preformation of *ortho*-Quinone).

2.3.4.2 Heterodimerization with Epicoccone B Methyl Ether

The inability to analyze the *ortho*-quinone of epicoccone B led to the conclusion that the synthesis of a suitably protected analog was required. As known from the concepts of pyrogallol dimerization (see 2.1.3.4 Conceptualization of Substrate-Dependent Reactivity Trends), the oxidized epicoccone B only has to react as an enone for a successful purpurogallin-type dimerization. Thus, one of the phenol groups was to be protected by conversion to methyl ether **196**, which still allowed for oxidation to a quinone (Scheme 71). Blocking the C7–OH rather than the C5–OH could also be feasible, but quinone **197** was reasoned to be the most activated for the cascade reaction. The alteration of the synthetic plan is depicted in Scheme 71 and reveals that the overall cascade process should not be affected. After

oxidation to quinones **149** and **197**, both should still dimerize in a formal (5+2)-cycloaddition to adduct **231**, which upon hydrolysis would yield acid **232**. Decarboxylation to alcohol **233**, skeletal rearrangement to tetracycle **234** and final bond formation from diketone **235** to methyl ether **236** should furnish epicolactone after additional hydrolysis of the enol ether.



Scheme 71. Alternative synthetic plan with methyl ether **196**.

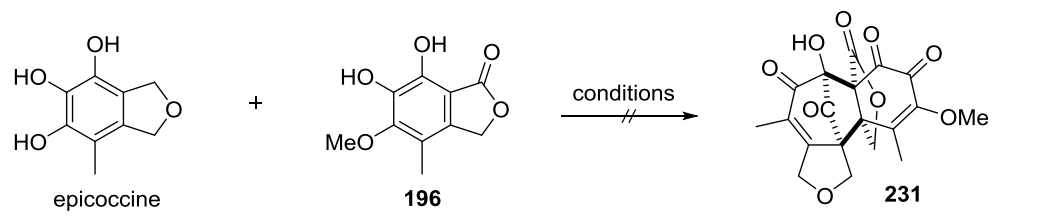
The advantage of the altered strategy was that quinone **197** could be synthesized and isolated in contrast to the oxidation product of epicoccone B. If similar challenges arose in the oxidation of the epicoccine/**196** mixtures, it would be possible to test heterodimerizations between quinone **197** and epicoccine.

2.3.4.2.1 Dimerization upon Oxidation with External Oxidants

Despite the unsuccessful dimerization trials upon oxidation of epicoccine and epicoccone B mixtures by external oxidants, this strategy was first attempted with the new epicoccone B methyl ether **196**. Due to the electron-donating effect of the additional alkyl substituent in ether **196**, the redox potential might have changed and could allow for the competitive oxidation of ether **196** in the presence of epicoccine. A selection of attempted conditions is provided in Table 4. Since the products were not isolated or purified, the table only contains qualitative information by LC/MS analysis. Oxidation with *ortho*-chloranil (entry 1) indeed afforded a hydrated heterodimer and, surprisingly, dibefurin. Since *ortho*-chloranil was unable to convert epicoccine to dibefurin, it was speculated whether the initially formed quinone **197** could effect this transformation or if the heterodimer

decomposes to give rise to dibefurin. However, the formation of a hydrated heterodimer was encouraging, although side products were observed.

Table 4. Selection of external oxidants for oxidation and dimerization of epicoccine and ether **196**.

					
entry	oxidant	additive	solvent (ratio)	T [°C]	result
1	<i>o</i> -chloranil	-	Et ₂ O	0	dibefurin + heterodimer
2	MnO ₂	-	CH ₂ Cl ₂	rt	no reaction
3	CAN	-	MeCN/H ₂ O	0 to rt	decomposition
4	Ag ₂ O	-	Et ₂ O	0 to rt	decomposition
5	PIFA	-	MeCN/H ₂ O	0 to rt	decomposition
6	K ₃ Fe(CN) ₆	NaHCO ₃	MeCN/H ₂ O	0	dibefurin + heterodimer
7	horseradish peroxidase	H ₂ O ₂	acetone/pH 5 buffer	rt	dibefurin + heterodimer
8	mushroom tyrosinase	O ₂ (stream)	acetone/pH 6.4 buffer	rt	decomposition

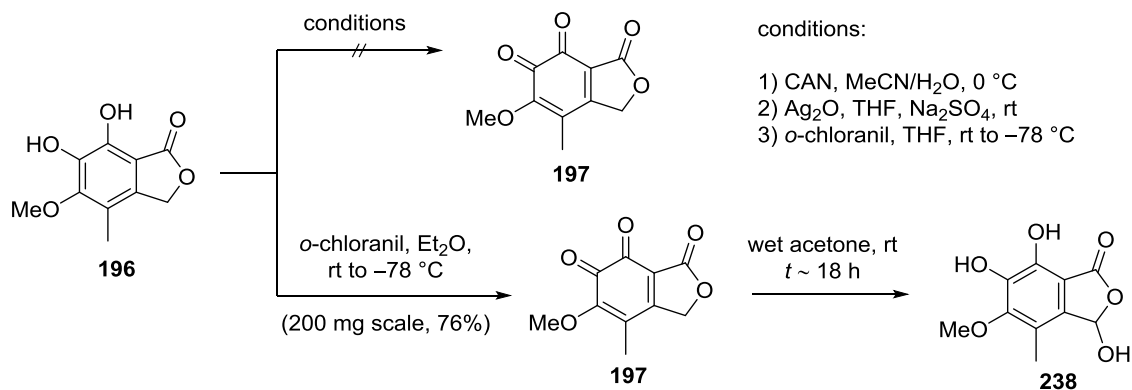
Inorganic external oxidants such as Mn^{IV}, Ce^{IV}, Ag^I or I^{III} failed to provide the heterodimer (entries 2–5). Decomposition reactions are likely to involve quinone methides or uncontrolled reactions of the quinones with nucleophilic solvent molecules such as water. Adaptation of the optimal conditions in the dibefurin synthesis revealed that the heterodimerization can indeed be competitive to the dibefurin formation (entry 6). Interestingly, enzymatic approaches were successful in the case of horseradish peroxidase, a 44 kDa glycoprotein with the cofactor heme, whereas they failed with mushroom tyrosinase, a copper-containing enzyme.^[204,205] However, these approaches were not further investigated due to the multiple side products and decomposition of the heterodimer under the reaction conditions.

Product isolation by chromatography on reverse phase silica was not possible due to the numerous side products and unreacted starting material. Efforts were therefore directed at the optimization of the reaction conditions to enable isolation and characterization of the heterodimer.

2.3.4.2.2 Preformation of *ortho*-Quinone

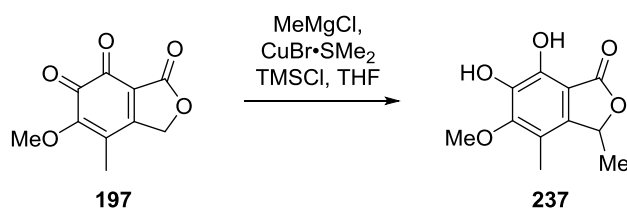
As mentioned in chapter 2.3.4.1 Heterodimerization of Epicoccine with Epicoccone B, heterodimerization could be favored by preformation of the respective *ortho*-quinone (Scheme 72). Hence, ether **196** was subjected to oxidation by Ce^{IV} (condition 1), Ag^I (condition 2) or *ortho*-chloranil in THF (condition 3). None of the conditions led to the formation of the desired *ortho*-quinone. It was reasoned that its high reactivity was the source of this complication and that the desired *ortho*-quinone would have to precipitate from solution immediately after its formation to avoid side reactions. Hence,

quinone **197** was successfully synthesized at room temperature with *ortho*-chloranil as the oxidant in ether and precipitated at $T = -78\text{ }^{\circ}\text{C}$ (Scheme 72). It proved to have limited stability and decomposed under oxidation of the benzylic position, presumably *via* nucleophilic attack of water on the *para*-quinone methide tautomer.



Scheme 72. Preformation of *ortho*-quinone **197**.

The potential tautomerization to the *para*-quinone methide was of concern, because it would hinder the desired reaction of quinone **197** as an *ortho*-quinone. It was therefore tested whether a potential 1,4-addition of nucleophiles onto quinone **197** was feasible (Scheme 73). A cuprate was generated *in situ* and allowed to react with quinone **197** to give rise to lactone **237**, which was identified by mass and NMR. This reaction underlined the potential of quinone **197** to undergo benzylic functionalization and shows the marked tendency toward rearomatization. However, the reaction conditions and partners largely differ from the intended biomimetic cascade and therefore only serve as a warning of potential side reactions.



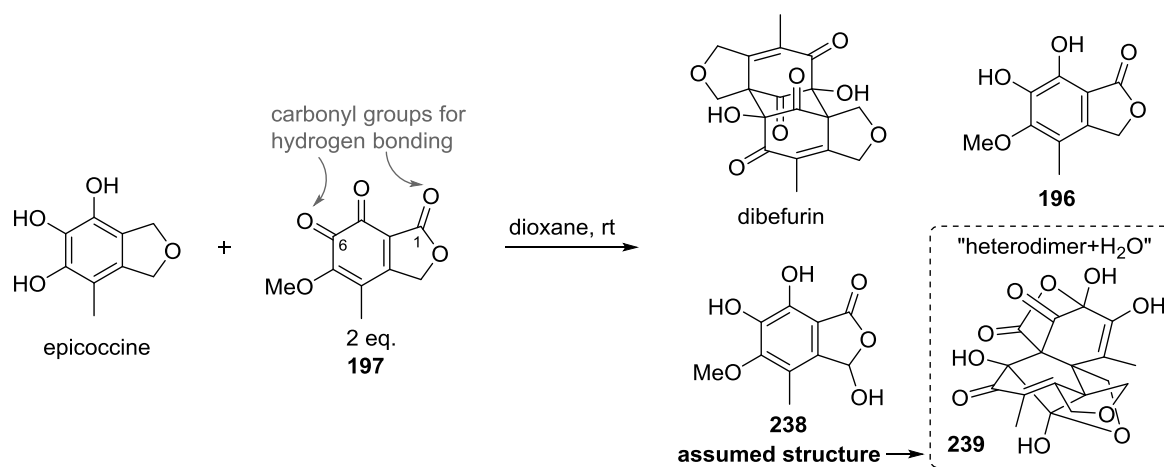
Scheme 73. Cuprate addition to *ortho*-quinone **197**.

When quinone **197** and epicoccine were combined in dioxane at room temperature, multiple products were observed (Table 5). Some of the products were identified by LC/MS as dibefurin, methyl ether **196**, decomposition product **238** and two hydrated heterodimers. While formation of dibefurin and ether **196** as the reduction product from the use of one equivalent of quinone **197** was expected, the observed larger quantities of hemiacetal **238** were not predicted. The fact that the reaction mixture contained two heterodimers could have arisen from poor diastereoselectivity of the cascade reaction. In the standard purpurogallin cascade, the face-selective approach of the coupling partner could result from hydrogen bonding to the *ortho*-quinone (here C6). Since quinone **197**

possesses two carbonyl groups (*C6/C1*) that are geometrically capable of hydrogen bonding in the transition state, the approach of the dimerization partner could be less selective.

The addition of water to the heterodimer was rationalized with lactone ring-opening and cyclization to a stable hemiacetal **239**, as previously observed.^[113] The structure **239** was assigned to the product as a working hypothesis, since only HRMS proof could be obtained. Attempts to isolate and characterize the structure were thwarted by its instability, low yield and the existence of multiple byproducts. In a qualitative attempt to raise the amount of heterodimers, several reaction conditions were tried but none could improve the initial result (Table 5).

Table 5. Combination of epicoccine and quinone **197** and resulting products.

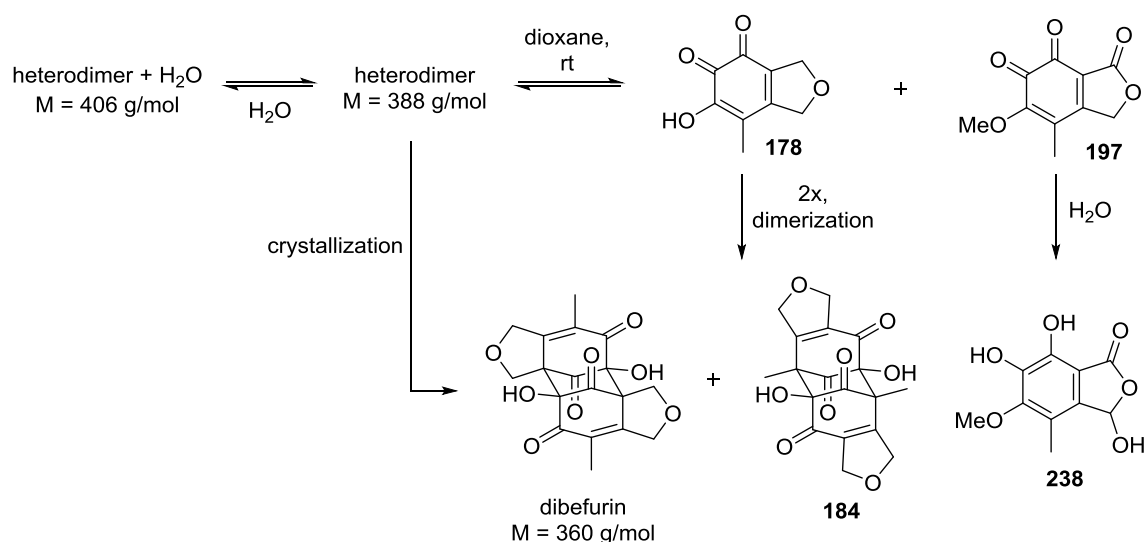


entry	reaction conditions	heterodimer formation	comment
1	open to air	yes	no difference observed
2	lower concentration	no	no product formation
3	excess of 197	yes	more 238 , otherwise no difference
4	solvent: THF	yes	no difference observed
5	solvent: CH ₂ Cl ₂	yes	epicoccine insoluble
6	solvent: MeCN	no	epicoccine almost insoluble
7	solvent: HFIP	no	more 238 , otherwise no difference
8	aq. pH 4.5 buffer	yes	preference for one heterodimer observed over time
9	MgSO ₄ as additive	yes	less 238 , otherwise no difference
10	4 Å molecular sieves	yes	less 238 , otherwise no difference
11	Schreiner's thiourea catalyst	no	no product formation

It was found that the reaction could be conducted under air with the same result (entry 1), but lowering the concentration inhibited the heterodimer formation completely (entry 2). Surprisingly, larger-scale reactions with the same concentration as the small-scale reactions also failed. Product was only obtained if as little amount of solvent was used as necessary to dissolve the components. An excess of *ortho*-quinone to favor heterodimerization did not lead to more heterodimer (entry 3) and a solvent screen showed that only polar solvents could be used because the coupling partners needed to be fully dissolved (entries 4–7). Acidic aqueous media to effect cleavage of the presumed hemiacetal

239 and trigger the desired retro-DIECKMANN reaction revealed that the two heterodimers seemed to be able to convert into each other or that one of them decomposes more readily (entry 8). As the latter appeared to occur, these conditions also did not provide more of the desired heterodimer. Drying agents such as MgSO_4 or molecular sieves partially prevented the decomposition of the *ortho*-quinone during the reaction, but did not favor heterodimer formation (entries 9, 10). An attempt at hydrogen-bond catalysis was not met with success (entry 11). The best conditions (dioxane, rt) were scaled to $m = 340$ mg (**197**), the product purified as much as possible by chromatography on reverse phase silica and extensive NMR analysis undertaken. However, 2D NMR spectra did not reveal many cross peaks and the molecule decomposed during prolonged INADEQUATE studies.

As the lability of the compound and the number of side products did not allow efficient purification, a sample enriched in the hydrated heterodimer was set up for crystallization. Numerous attempts failed, but crystallization from DMSO/ H_2O in a hanging-drop setup afforded X-ray suitable crystals. X-Ray single crystal structure analysis revealed that the structure was dibefurin, a compound with a different mass and retention time than the hydrated heterodimer. Therefore, it was reasoned that the heterodimer is in equilibrium with its monomeric *ortho*-quinones **178** and **197** (Scheme 74). Both can undergo irreversible reactions and would therefore be withdrawn from the equilibrium. A reformation of the heterodimer would then be impossible. Upon crystallization, additional driving force is offered for quinone **178** or its tautomer to engage in a homodimerization to the insoluble dibefurin. Furthermore, in contact with water, quinone **197** could irreversibly convert to hemiacetal **238**.



Scheme 74. Dibefurin as the result of crystallization attempts of the hydrated heterodimer.

Intriguingly, the dibefurin X-ray single crystal structure revealed the presence of the so far unobserved isomer **184** (Figure 23). Dibefurin and isomer **184** were mixed in the crystal with an occupation ratio of 9:1, but the space group remained centrosymmetric ($P2_1/n$). Therefore, the presence of the C_2 -symmetric **185** can be excluded. The observation that different products were

obtained in this experiment might hint at a different mechanism of formation. In the previous Fe-mediated oxidation, radicals or *ortho*-quinones could have combined to yield dibefurin. However, the decomposition of the heterodimer can only yield *ortho*-quinones. This result of this experiment therefore supports the hypothesis of a radical-type mechanism in the dibefurin formation upon oxidation with potassium ferricyanide.

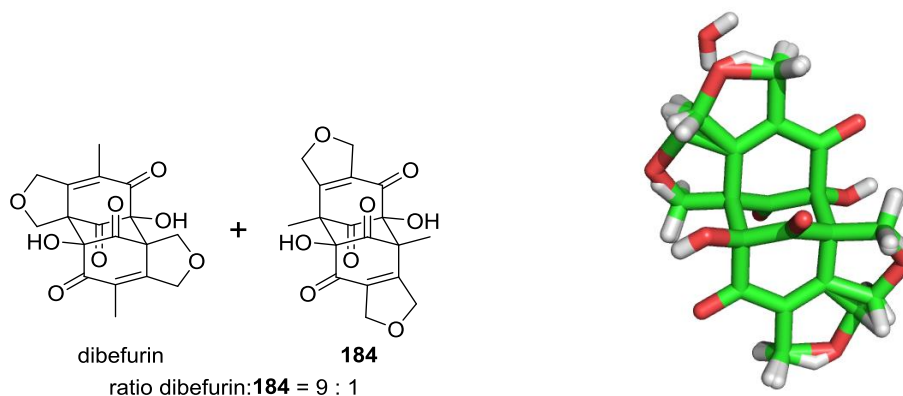


Figure 23. X-Ray single crystal structure of dibefurin and isomer **184** with H₂O; CCDC 1022043. Color code: green = carbon, red = oxygen, white = hydrogen.

Given its instability, it became necessary to protect crucial functionalities in the heterodimer to ensure its stability and prevent it from reverting back to the starting materials. Free hydroxyl groups were thought to be the main reason for potential decomposition.

Since hemiacetal carbon atoms were identified in the hydrated heterodimer during NMR studies, it was attempted to convert the hemiacetal to a full acetal with various alcohols. Full acetals were detected by LC/MS after reaction with aliphatic alcohols under acid catalysis, but the acetal was cleaved upon purification attempts.

Furthermore, hydroxyl groups were acyl protected by treatment with acetic anhydride or benzoyl chloride. Both reactions showed double incorporation of the respective acyl group under loss of water. This result was not compatible with the structure proposal **239** of the hydrated heterodimer. Remarkably, the acetylated heterodimer proved to be a solid and stable to conventional purification methods, as intended. However, NMR spectroscopic analysis only showed two diastereotopic methylene groups, another hint that the proposed structure **239** was incorrect.

Since the molecule first did not form suitable crystals for X-ray single crystal structure analysis, a recently reported procedure by FUJITA and co-workers was applied.^[206,207] The procedure involves the growth of molecular-organic framework (MOF) crystals that can host organic molecules. If the lattice is saturated with the organic molecule in question, the structure of the guest can be determined by X-ray structure analysis due to the crystallinity of the host even though the guest molecule itself did not crystallize. Host crystals with the formula (Zn₃C₃₆H₂₄I₆N₁₂ · C₆H₁₂)_n were grown according to literature procedures,^[207] but the inclusion of the hydrated heterodimer led to a structure that was too

complicated to be elucidated. It appears that the occupation of the host cavities was insufficient. The obtained crystal structure of the host is shown in Figure 24.

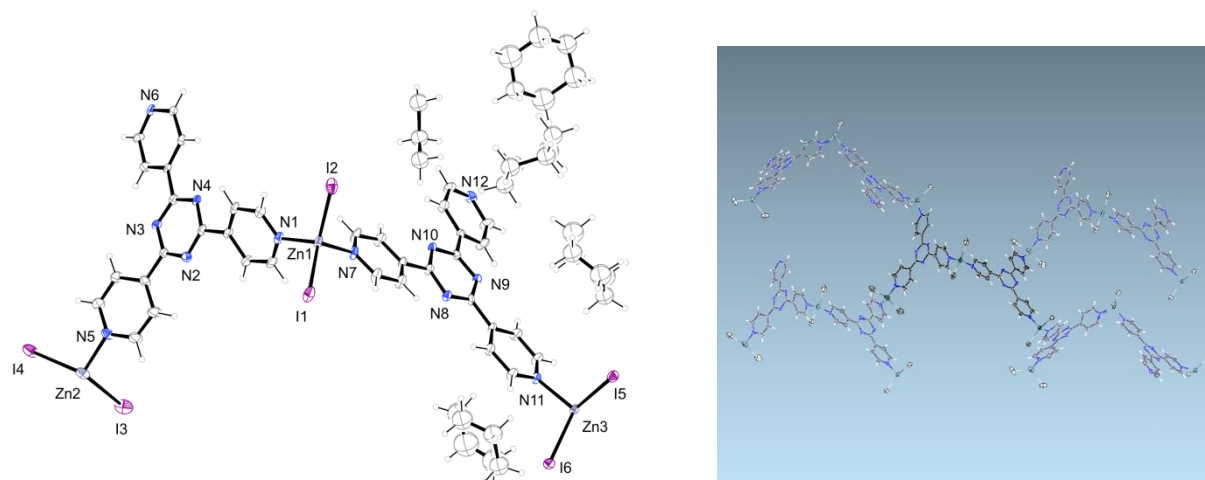


Figure 24. X-Ray structure of host ($\text{Zn}_3\text{C}_{36}\text{H}_{24}\text{I}_6\text{N}_{12} \cdot \text{C}_6\text{H}_{12}$)_n
Color code: white (large ellipsoids) = carbon, blue = nitrogen, violet = iodine, white (small ellipsoids) = hydrogen, grey = zinc.

Eventually, crystallization from DMSO/H₂O in a hanging drop setup resulted in X-ray suitable crystals that led to the structural elucidation of the heterodimer as a hetero-Diels–ALDER adduct **240** (Figure 25).

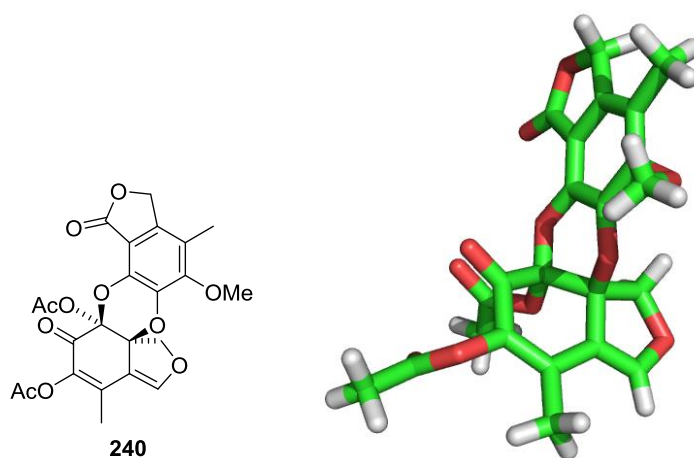
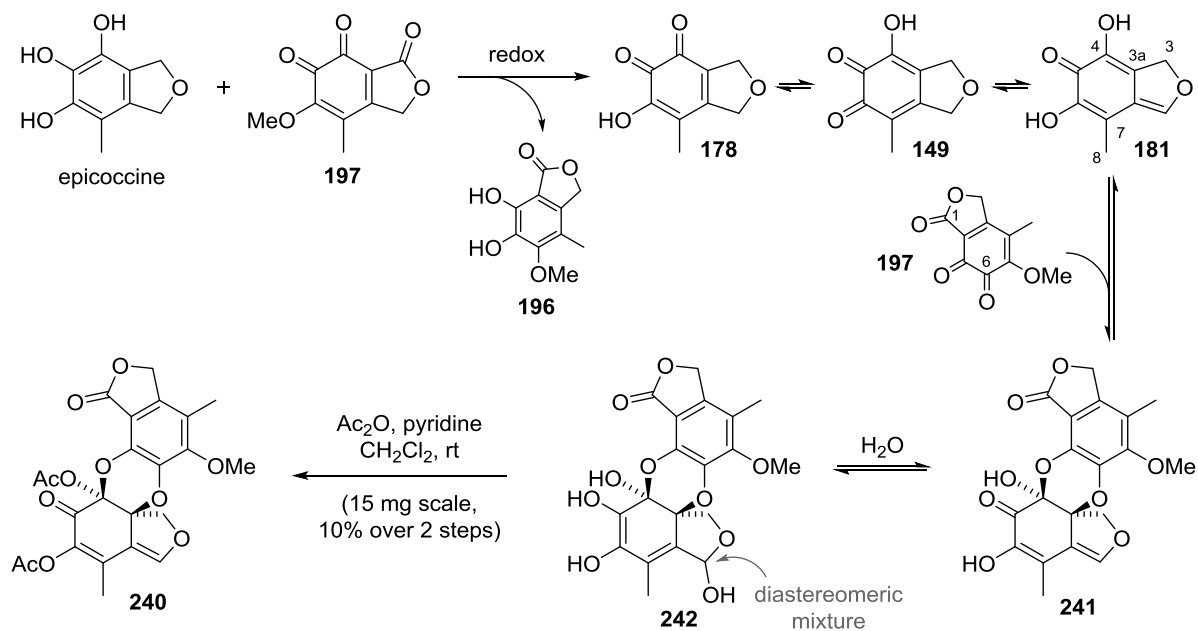


Figure 25. X-Ray crystal structure of acetylated heterodimer; CCDC: 1022044.
Color code: green = carbon, red = oxygen, white = hydrogen.

Mechanistically, the generation of this heterodimer can be rationalized as depicted in Scheme 75. Epicoccine undergoes oxidation by quinone **197** as intended to furnish *ortho*-quinone **178** or tautomer **149**. This step explains the previously observed formation of dibefurin in the attempted heterodimerization, because these quinones can also undergo homocoupling. However, under the reaction conditions, they also isomerize to the supposedly more stable *para*-quinone methide **181** under release of dipole repulsion of the carbonyl groups. Other quinone methides are omitted for clarity and only the one with the most nucleophilic double bond, an enol, is presented. Quinone methide **181** engages in an inverse electron-demand hetero-Diels–ALDER reaction to dioxine **241**

with the second equivalent of quinone **197**. Due to the reversibility of this process and the fact that structural proof was only acquired after one additional step, it cannot be excluded that other regioisomers than **241** form. However, this regioselectivity of the cycloaddition could be rationalized based on steric and electronic effects. Quinone methide **181** possesses two major nucleophilic sites, *C3a* and *C7*. The *C7* methyl group can rotate freely as opposed to the stiff, tied-back *C3* methylene unit and could therefore render the *C7* position less accessible. Concerning *ortho*-quinone **197**, the *C6* oxygen atom is the most electrophilic because it is in full conjugation with the *C1* carbonyl group. Therefore, a bond is forged between *C3a* and *O=C6*.



Scheme 75. Hetero-DIELS–ALDER heterodimerization.

The initial heterodimer could get attacked by water to form the observed hydrated heterodimer **242** as a diastereomeric mixture. This would explain the detection of two hydrated heterodimers. Acetylation of hemiacetal **242** would yield pentacycle **240** by dehydration and double acetate group introduction to prevent the retro-cycloaddition.

Low concentration would greatly disfavor heterodimerization and rather lead to dibefurin formation or decomposition of quinone and quinone methide species, which would provide a rationale for the observed concentration dependence. The apparent instability of compound **242** is also easily explained since the dimerization process until hemiacetal **242** is reversible. Once the monomers are present during workup or purification, they can irreversibly rearomatize by addition of nucleophiles, thus decreasing the amount of the original heterodimer. During the attempts to couple epicoccine with quinone **197**, it was also observed that residual *ortho*-chloranil completely inhibits the formation of the heterodimer. This could be rationalized by the fact that *ortho*-chloranil is a much more electrophilic hetero diene for the inverse demand hetero-DIELS–ALDER reaction and thus more readily engages in the cycloaddition than quinone **197**.

Dioxine **242** constitutes the first hetero-DIELS–ALDER adduct of two different pyrogallols. In general, this type of dimerization is not preceded with pyrogallols that are structurally as complex as epicoccine and epicoccone B derivative **196**. It is reasonable to assume that the heterodimer obtained in chapter 2.3.4.1 Heterodimerization of Epicoccine with Epicoccone B also dimerized in a hetero-cycloaddition.

In Nature, some triterpenoid catechols have been shown to be able to form homodimers after oxidation to quinones.^[208–212] The biomimetic synthesis of dibefurin provides strong support to the hypothesis that pyrogallol oxidation can occur in fungi of species *Epicoccum*. Combined with the fact that quinone dimerization to dioxines has been observed in Nature with catechols, heterodimers of type **240** might well be present in *Epicoccum* sp. and were thus far not isolated due to their instability.

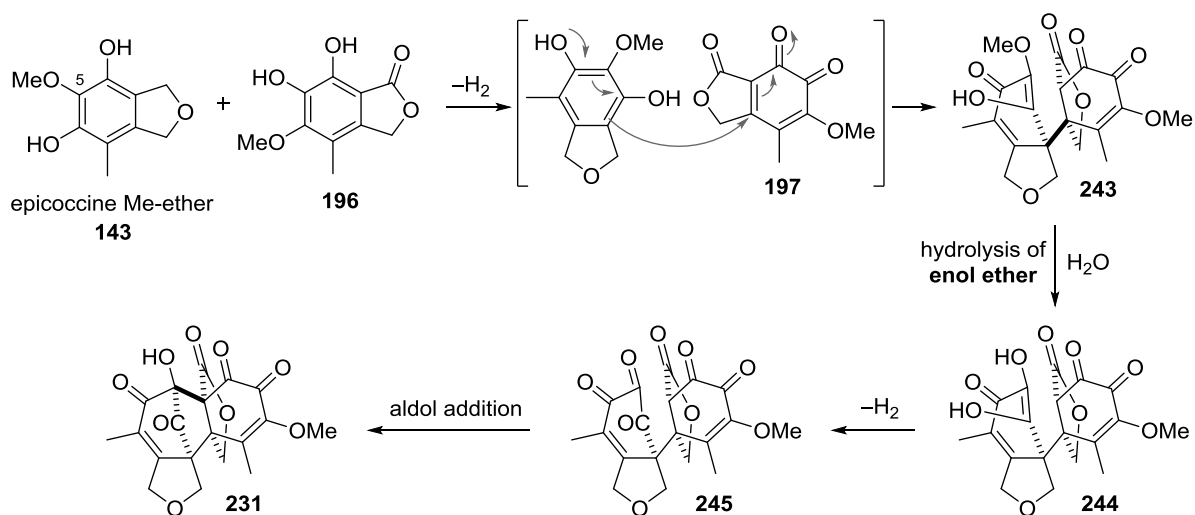
The fact that an undesired heterodimer was obtained *via* a DIELS–ALDER cycloaddition can be rationalized by the high steric congestion of both hexasubstituted arenes. In order to avoid unfavorable steric interactions, the heterodimerization occurs *via* the oxygen atoms rather than the carbon atoms to ensure maximum distance between the substituents. The results obtained in this thesis seem to disprove one of the biosynthetic hypotheses for epicolactone presented in 2.2.1 General Biosynthetic Proposal. Epicoccone B appears to be an unlikely heterodimerization partner to engage in a purpurogallin cascade, at least if both pyrogallols dimerize on the oxidation state of an *ortho*-quinone. However, the fact that a biosynthesis cannot be mimicked in the laboratory does not prove its impossibility.

In the following, strategies will be presented that aim at achieving the desired heterodimerization.

2.3.4.3 Heterodimerization *via* Methylated Epicoccine

Two major reasons for the challenges encountered in the heterodimerization, concomitant homodimerization and formation of a DIELS–ALDER dimer, can be traced back to the initial oxidation of epicoccine. The existence of an *ortho*-quinone of epicoccine gives rise to dibefurin and the *para*-quinone methide that engages in the cycloaddition. It was argued that if epicoccone B were to be the correct coupling partner in the biomimetic cascade, initial oxidation of epicoccine would have to be avoided. Mechanistically, this proposal follows the hypothesis that the purpurogallin cascade is not a dimerization of two quinones but rather the union of one pyrogallol with one quinone (see 2.1.3.1.1 Historical Perspective).

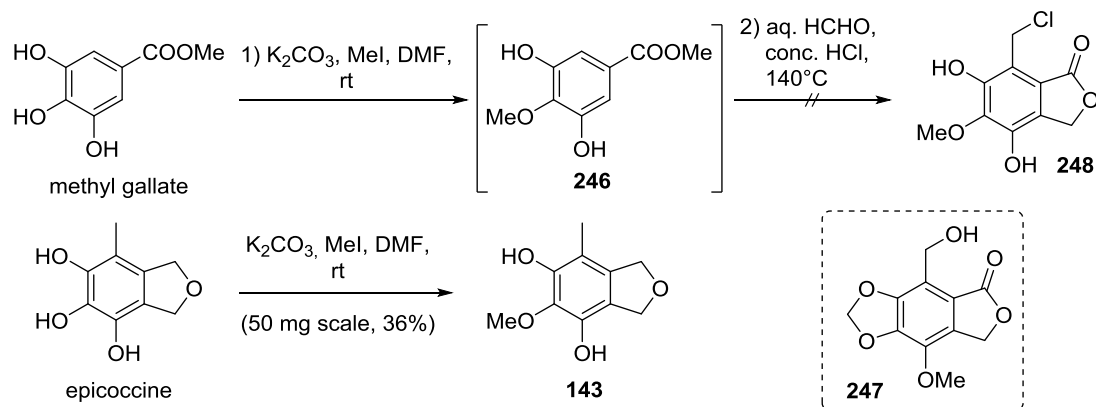
Therefore, the use of epicoccine methyl ether **143** was envisioned, which would be unable to undergo oxidation to an *ortho*-quinone if the methyl group was a stable protecting group under the reaction conditions (Scheme 76). Intriguingly, the new biomimetic strategy was supported by the fact that methyl ether **143** was isolated as a natural product from *Epicoccum* species as well.^[145]



Scheme 76. Epicoccine methyl ether as epicoccine substitute in the synthesis of epicolactone.

The new biomimetic strategy would involve initial oxidation of epicoccone B derivative **196**, which as quinone **197** would subsequently suffer from nucleophilic attack of ether **143** to yield adduct **243**. Since the methyl ether in adduct **243** is now an enol ether, a subsequent hydrolysis could convert it to ene diol **244**. Intriguingly, the initial oxidation could therefore be circumvented, but adduct **244** could be channeled into the originally envisioned biomimetic cascade after further oxidation to triketone **245** and subsequent aldol addition to already proposed cascade intermediate **231**.

Epicoccine methyl ether (**143**) synthesis was first attempted from methyl gallate *via* the known route to epicoccine (Scheme 77).

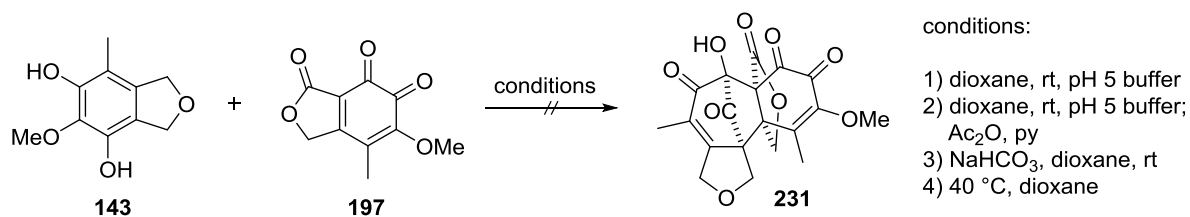


Scheme 77. Epicoccine methyl ether (**143**) synthesis.

Selective methylation of the most acidic phenol group due to its conjugation to the *para*-carboxylic ester group according to a literature procedure proceeded smoothly to provide pyrogallol derivative **246**.^[213] However, the subsequent double functionalization according to KING and KING led to the migration of the methyl ether under formation of dioxolane **247**.^[162] No product **248** was observed. Potentially due to the least steric hindrance of the central hydroxyl group,

epicoccine itself could be selectively methylated to furnish the target natural product **143**, accompanied by dimethylated side products.

Next, the dimerization with known quinone **197** was tested (Scheme 78). It was focused on conditions that would allow for dimerization and hydrolysis of the intermediate enol ether **243**. No trace of dimerization product was detected in dioxane and acidic aqueous buffer solution (condition 1) or with subsequent acetylation in case the initial heterodimer was too unstable for isolation (condition 2). The only identified product was the hemiacetal **238** from the decomposition of quinone **197**.



Scheme 78. Dimerization trials with methylated epicoccine.

It was tried to achieve the initial attack to adduct **243** under inert conditions and then introduce water for the required hydrolysis, albeit without success. Neither attempted deprotonation to increase the nucleophilicity of ether **143** nor thermal activation were met with success (conditions 3, 4).

As it appeared that the required intermediate hydrolysis from enol ether **243** to ene diol **244** would be incompatible with the instability of quinone **197** under aqueous conditions, alternative routes were pursued.

2.3.4.4 Heterodimerization *via* Inverted Reactivity

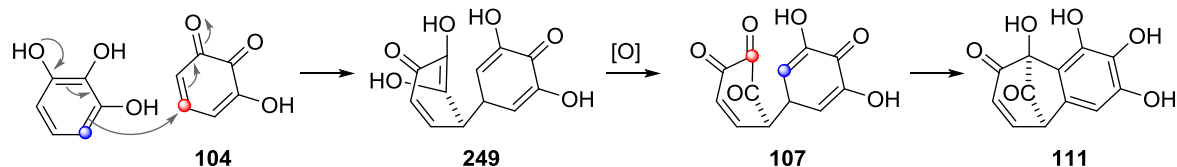
Since epicoccine and epicoccone B were still believed to be the biosynthetic precursors to epicolactone was still high, given their isolation from the same fungus and the oxidative metabolism within the fungus, it was suggested that the cascade reaction to epicolactone could proceed differently than originally envisioned.

It had been shown that the dimerization of two pyrogallols as their *ortho*-quinones leads to a DIELS–ALDER dimer (see 2.3.4.2.2 Preformation of *ortho*-Quinone). Trials to dimerize one pyrogallol with one *ortho*-quinone by blocking the oxidation of epicoccine had completely inhibited the coupling (see 2.3.4.3 Heterodimerization *via* Methylated Epicoccine). Furthermore, it had also become evident that epicoccine is more readily oxidized than epicoccone B (see 2.3.4.1 Heterodimerization of Epicoccine with Epicoccone B). It was therefore reasoned that the preformation of an epicoccine *ortho*-quinone in combination with epicoccone B as the unoxidized pyrogallol component could result in the desired heterodimerization. This proposal constitutes a novel mechanistic idea for the purpurogallin cascade that had not yet been considered (Scheme 79).¹¹ As mentioned in chapter 2.1.3.1.1 Historical Perspective, the exact mechanism of the dimerization of pyrogallols is yet

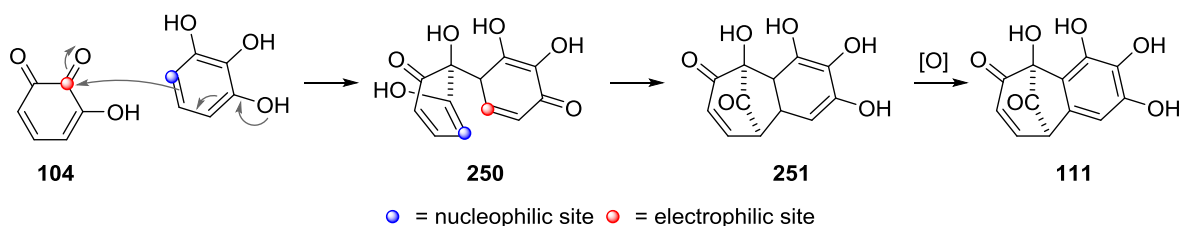
¹¹ to the best of our knowledge

unknown. Dimerization of two *ortho*-quinones as well as coupling of one unoxidized pyrogallol with one *ortho*-quinone have been proposed.^[107,113] In the latter case, the pyrogallol always attacks the *ortho*-quinone **104** in a 1,4-addition. The resulting ene diol **249** is oxidized and a final aldol reaction gives rise to pyrogallol **111** after tautomerization.

previous proposal:



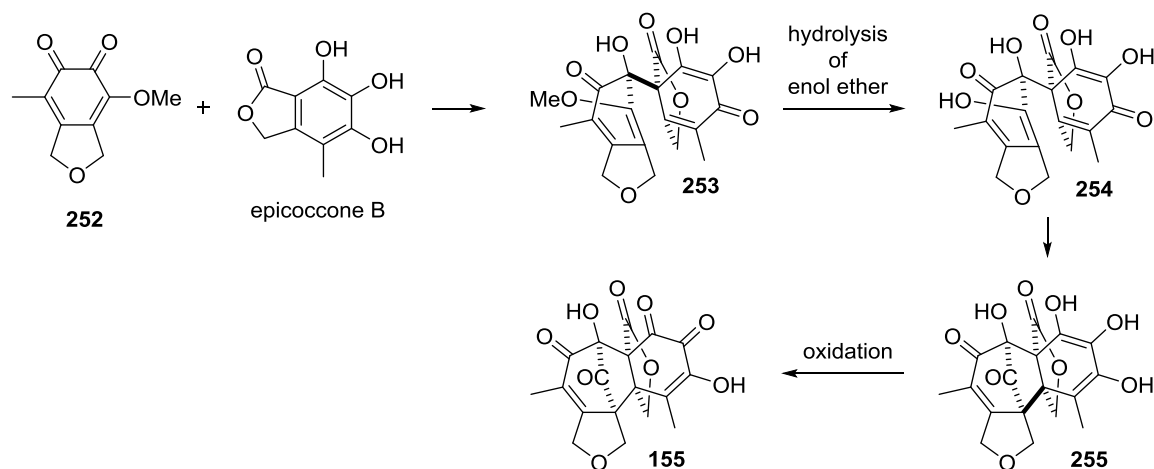
alternative proposal:



Scheme 79. Alternative mechanistic proposal for the purpurogallin cascade.

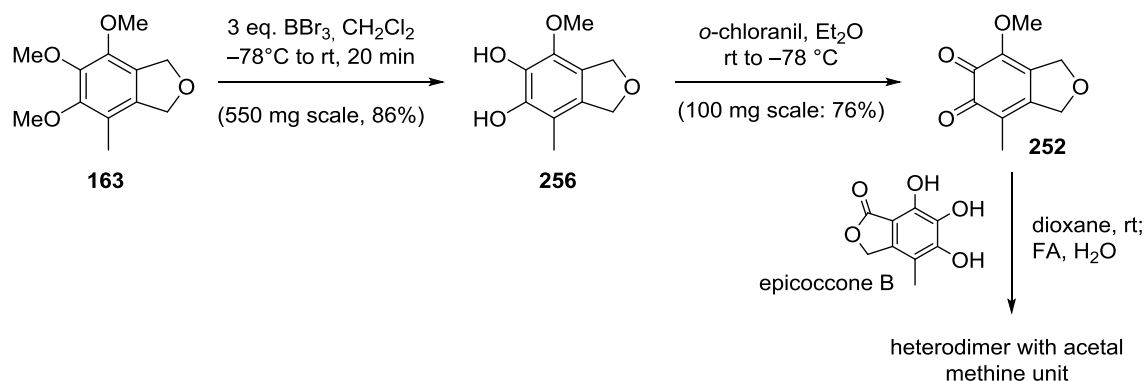
An alternative is proposed herein, according to which the initial bond formation occurs between the pyrogallol and the carbonyl group of the *ortho*-quinone **104** to give rise to ene diol **250**, which could immediately undergo a 1,4-addition to furnish cyclohexadiene **251**. A final oxidation would then lead to known intermediate **111**.

The realization that the purpurogallin cascade might also occur by a different mechanism had an important impact on the retrosynthetic planning. Instead of changing the strategy to a preoxidized epicoccone B coupling partner, a preoxidized epicoccine derivative might lead to a successful heterodimerization (Scheme 80).



Scheme 80. Proposed heterodimerization with methylated epicoccine derivative **252**.

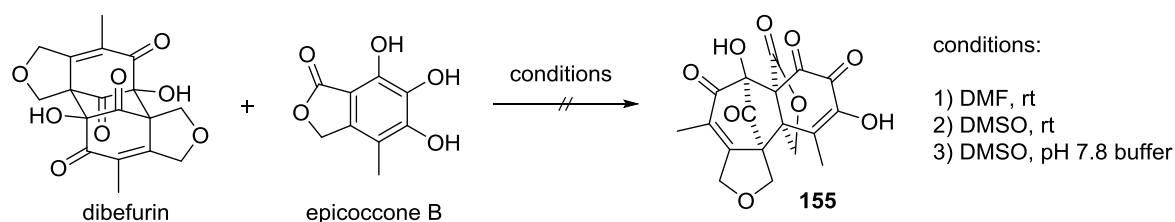
The *ortho*-quinone of epicoccine, **252**, could get attacked by epicoccone B to form adduct **253**, which would need to undergo hydrolysis to enol **254** to engage in a 1,4-addition without prior oxidation. Cyclohexadiene **255** could then either be a stable adduct or get further oxidized to already proposed intermediate **155**. The regioisomeric *ortho*-quinone of **252** would also be possible, but access to quinone **252** was more facile (Scheme 81).



Scheme 81. Cascade attempts with oxidized epicoccine.

Trimethyl ether **163** was selectively demethylated with BBr_3 and the position of the remaining OMe-group determined by nOe experiments. Catechol **256** was next oxidized to quinone **252** under the conditions that had proven successful in the synthesis of other *ortho*-quinones. When epicoccone B was treated with quinone **252** and subsequently subjected to hydrolysis conditions, a heterodimer was identified that showed an acetal methine by NMR spectra analysis. Since this carbon atom could only be formed by DIELS–ALDER dimerization involving *para*-quinone methides, no further experiments with quinone **252** were conducted.

Next, it was attempted to access the *ortho*-quinone of epicoccine without protecting groups and combine it with epicoccone B. Oxidation of epicoccine inevitably forms dibefurin, but it was known that dibefurin can decompose to its monomers in solution and especially when treated with base. Hence, the natural product dibefurin was employed as a protected version of the required *ortho*-quinone **149** or **178**. Treatment with epicoccone B under conditions that had previously been identified to decompose dibefurin did not lead to detectable amounts of heterodimers (conditions 1–3, Scheme 82). Presumably, the decomposition of dibefurin only gives rise to small equilibrium amounts of the required epicoccine *ortho*-quinones **149** or **178** that decompose by other pathways involving the solvent, *e.g.* redox processes as previously observed. An efficient dimerization with epicoccone B can therefore not be achieved since epicoccone B is present in lower concentration than the solvent.



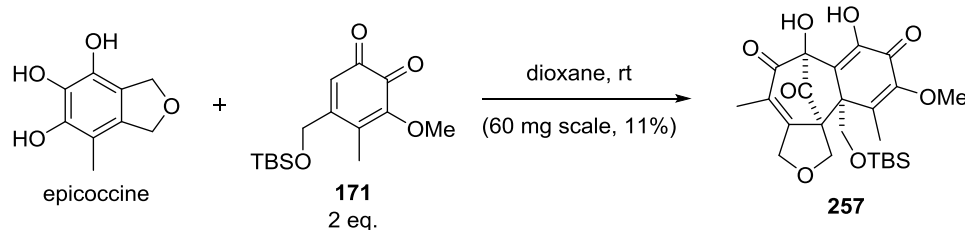
Scheme 82. Heterodimerization attempts with dibefurin as protected *ortho*-quinone precursor.

2.3.4.5 Heterodimerization with Pentasubstituted Epicoccone B Derivatives

The results obtained from the heterodimerization attempts of epicoccine and epicoccone B and their derivatives did not support the initial biosynthetic hypotheses. It appeared as if epicoccone B as a surrogate for benzyl alcohol **148** is too sterically encumbered to allow for a purpurogallin-type coupling, rather undergoing DIELS–ALDER-type dimerizations. In addition, the diketone moiety in intermediate **155** cannot stabilize itself by tautomerization as opposed to intermediate **152**. Therefore, it was considered more likely that a pentasubstituted pyrogallol would engage in the desired heterocoupling (for biosynthetic hypothesis, see Scheme 39).

The originally proposed benzyl alcohol could form in Nature prior to reaction with epicoccine and would be much less sterically hindered. It is possible that its potential instability has thus far prevented isolation. The initial heterodimer based on benzyl alcohol **148** would not contain four contiguous tetrasubstituted stereocenters, the steric strain of which probably prevented the successful synthesis of dimer **155**. However, oxidation of alcohol **148** seemed challenging since the benzylic position is more prone to oxidation, be it *via* a direct pathway or *via* the quinone to quinone methide tautomerization. Furthermore, it was considered important to eliminate possible side reactions such as PERKIN dimer formation by suitable protection of one of the phenolic hydroxyl groups.

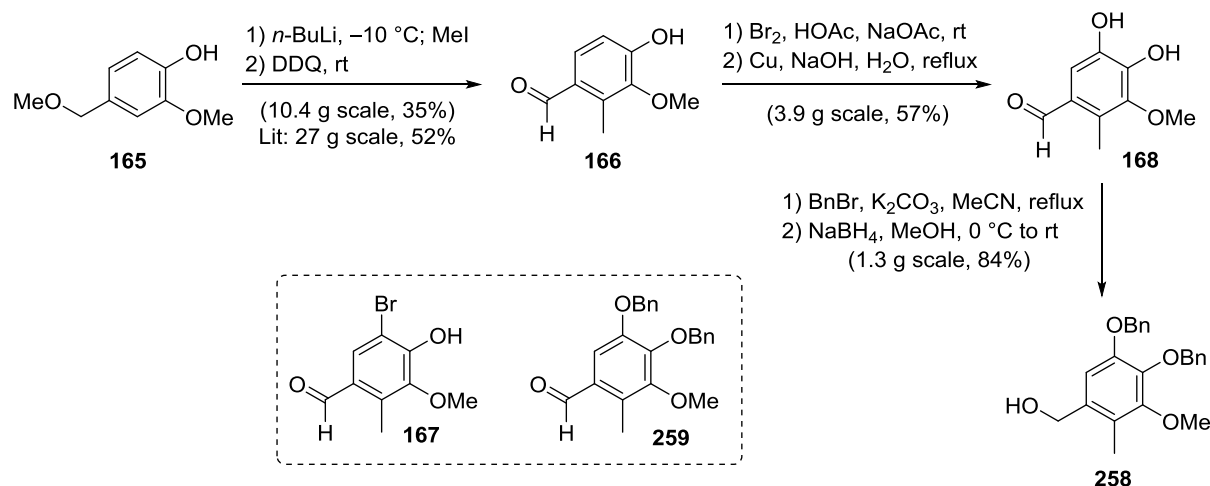
Prior to this thesis, the quinone **171** had been accessed and employed with two equivalents in a purpurogallin formation reaction (Scheme 83).^[160] The structure of dimer **257** was elucidated by NMR and MS, but no crystal structure proof was obtained, which prevented definitive assignment of the relative stereochemistry. Moreover, the yield of the transformation was poor and dimer **257** required HPLC purification on reverse phase silica.



Scheme 83. Successful heterodimerization of quinone **171** with epicoccine.

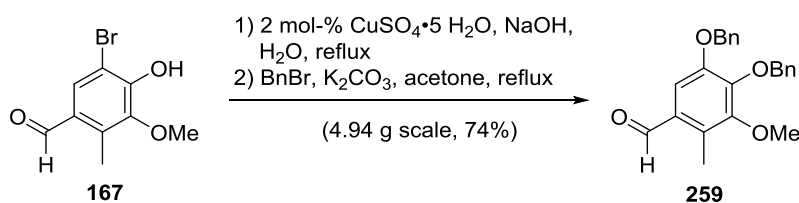
2.3.4.5.1 Synthesis of Benzyl Alcohol Derivatives

In this thesis, the synthesis toward *ortho*-quinone **171** was conducted on multi-gram scale to benzylic alcohol **258** with comparable yields to the route identified by Dr. Robert A. Webster (Scheme 43, Scheme 84). A description of the route is offered in 2.2.3 Initial Work.



Scheme 84. Synthesis of benzylic alcohol **258**.

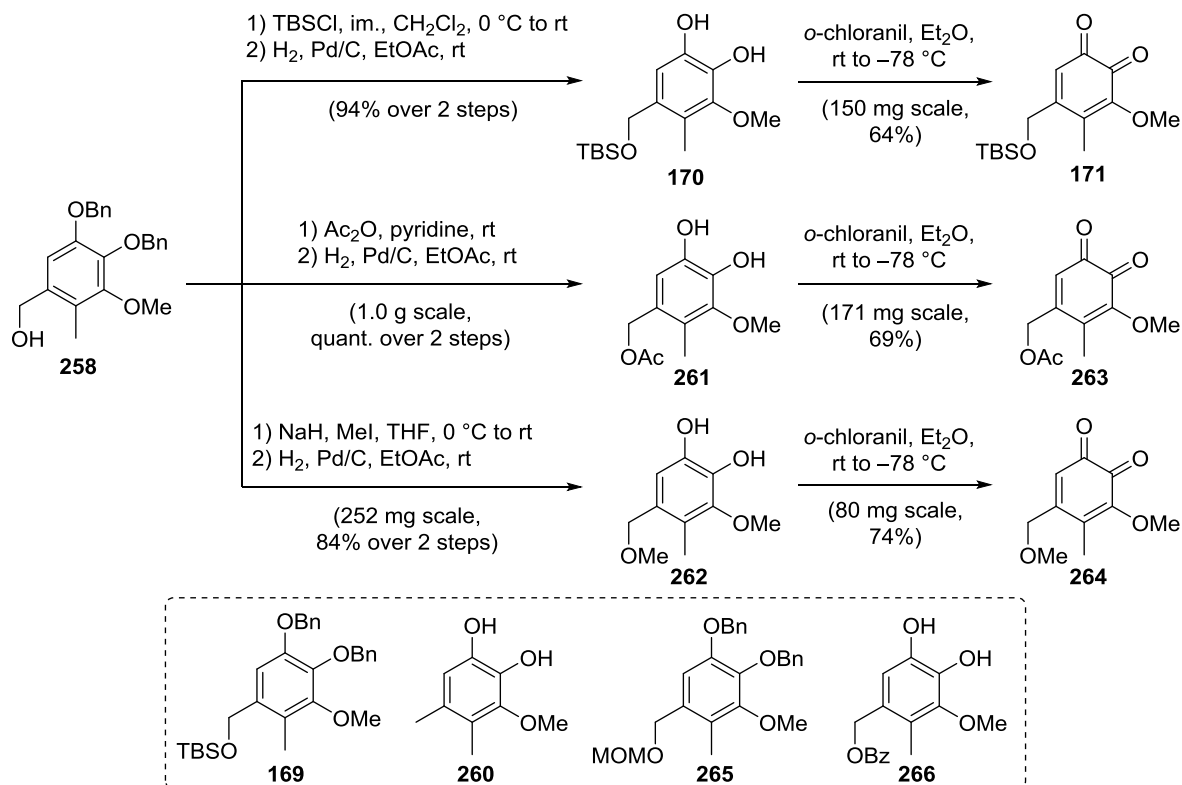
The crucial Cu-catalyzed step for the installation of a hydroxyl group in exchange for an aryl bromide was optimized in collaboration with Dr. Nicolas Armanino, because the heterogeneous reaction proved to be unreliable on larger scales (Scheme 85). It seemed as if efficient contact of the Cu metal surface with the solution could not be accomplished on larger scale due to insufficient mixing. Upon switching to a homogeneous Cu catalyst, the reaction proved to be scalable and afforded the aldehyde **259** in very good yield after dibenylation (Scheme 85).



Scheme 85. Optimization of Cu-catalyzed introduction of hydroxyl group.

Other *ortho*-quinones were synthesized from benzylic alcohol **258** in a three-step sequence (Scheme 86). TBS protection of alcohol **258** to ether **169** followed by hydrogenolysis afforded catechol **170**, which upon oxidation gave the known quinone **171** in good yield. Prolonged reaction times during the deprotection of the benzyl groups exclusively led to toluene derivative **260** so that careful monitoring of this reaction was required. In analogy, acetylation or methylation of alcohol **258** yielded catechols **261** and **262**, which were oxidized to *ortho*-quinones **263** and **264** as substrates for the desired heterodimerization. The requirement of a methyl ether as an alcohol equivalent will be explained in 2.3.4.5.4 Final Studies Toward the Synthesis of Epicolactone. In contrast, MOM

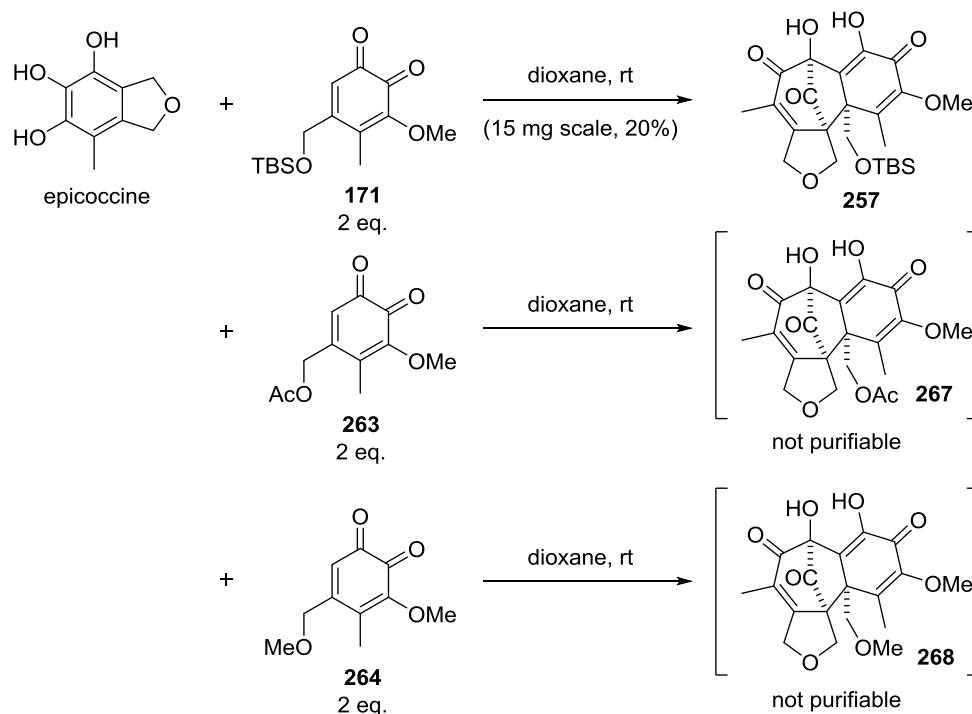
protection of alcohol **258** to give compound **265** was inefficient and therefore not pursued. Acyl groups that form better leaving groups than acetate could not be implemented since catechols like **266** were found to be labile and not purifiable. Presumably, *para*-quinone methides are formed from elimination of the acyl group and result in decomposition.



Scheme 86. Synthesis of other *ortho*-quinones for heterodimerization.

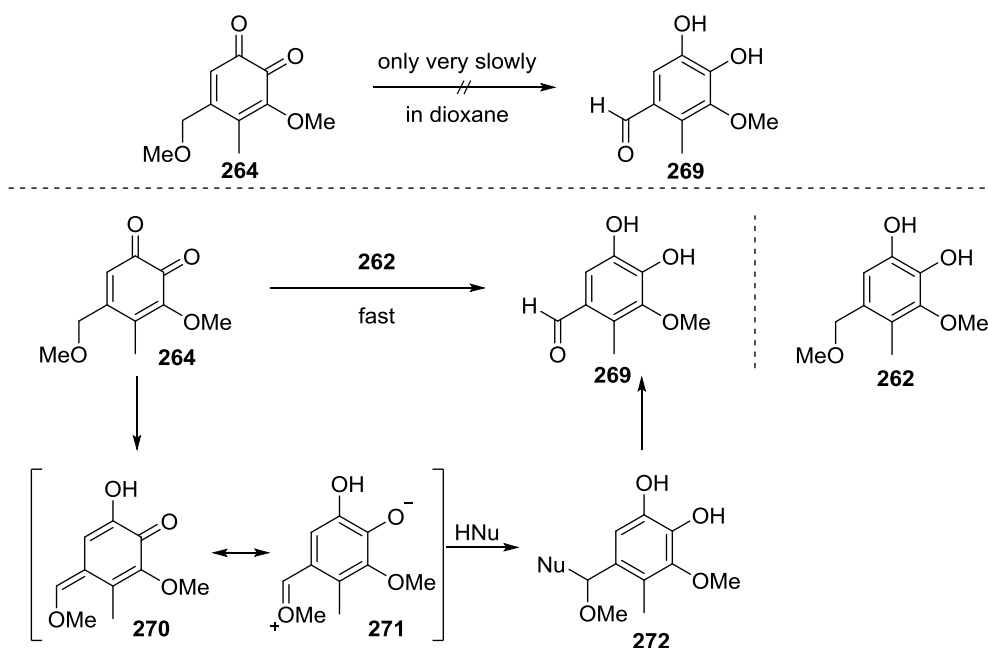
2.3.4.5.2 Heterodimerization with Benzyl Alcohol Derivatives

In order to access heterodimers with different protecting groups for maximum flexibility, the accessed *ortho*-quinones were employed in the coupling. The TBS dimer was synthesized according to the previous procedure and LC/MS analysis also revealed a successful synthesis of heterodimers **267** and **268** by combination of epicoccine and quinone **263** or **264** in dioxane at room temperature (Scheme 87).



Scheme 87. Heterodimerization with different pentasubstituted *ortho*-quinones.

Common side product in all reactions was dibefurin. In contrast to the TBS dimer **257**, the other dimers **267** and **268** were not purifiable since they were copolar with the respective reduced form of quinones **263** or **264** that inevitably exist due to their use as sacrificial oxidant. Other purification methods such as size-exclusion chromatography or crystallization failed. However, analysis of the crude reaction mixture allowed for the observation of an important trend concerning the stability of the employed *ortho*-quinone. When employing *ortho*-quinone **264** as a heterodimerization partner, the crude reaction mixture showed substantial amounts of aldehyde **269** (Scheme 88). However, in a separate experiment it was shown that the *ortho*-quinone **264** itself does not decompose under the reaction conditions, but mixtures of catechol **262** and quinone **264** did. Mixtures of quinone **264** and protected catechols such as **265** with Me instead of MOM did not lead to aldehyde **269**. It appeared as if the benzylic C–H bond in quinone **264** was exceptionally prone to tautomerization to enol ether **270**. The mesomeric structure **271** is thereby more stable than with other benzylic alcohol protecting groups. Attack of a nucleophile would yield acetale **272**. In this mechanism, the catechol **262** could act as a potential BRØNSTEDT acid catalyst.



Scheme 88. Decomposition of *ortho*-quinone in autocatalysis with catechol **262**.

This process affects the heterodimerization attempt since it provides another pathway by which the valuable *ortho*-quinone **264** can be consumed. As the catechol will inevitably form during the reaction, this process can best be avoided by different protecting groups. Indeed, no aldehydes according to **269** were detected in the case of quinones **171** or **263**. Whereas it is likely that the electron-withdrawing acetate group prevents the formation of methides **270/271**, an intermediate of type **270** would probably be unstable in the case of TBS protected alcohols since the bulky OTBS group would be forced into the plane of the arene, suffering from steric repulsion.

The analysis of the stability of *ortho*-quinones under the reaction conditions had important implications for strategic considerations. It was focused on protected benzylic alcohols rather than the potential biosynthetic benzylic alcohol **148** because the oxidation of the latter would probably lead to rapid benzylic oxidation. Furthermore, only bulky or electron-withdrawing protecting groups were to be considered to avoid the use of additional equivalents of valuable *ortho*-quinone.

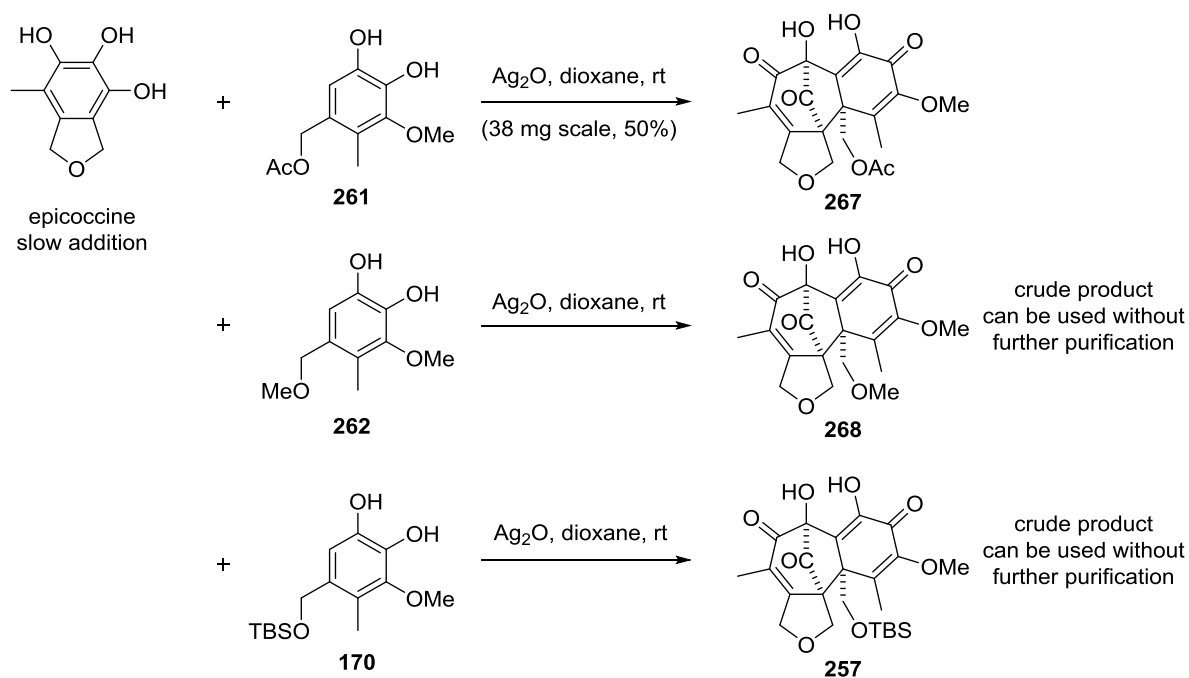
It became apparent that the synthesis of heterodimer analogs of dimers **257** according to this protocol would be complicated by the use of coupling partners like **171** or **263** as a sacrificial oxidant. The use of an excess of these valuable *ortho*-quinones was not only wasteful, but also resulted in time-extensive and cumbersome purification, which even failed for important dimers such as **267**.

2.3.4.5.3 Optimization of Purpurogallin-type Cascade

It was desirable to develop a protocol for this reaction that would provide access to larger quantities of the purpurogallin cascade intermediates for further investigation. This would include higher yields, more facile purification and a stoichiometric dimerization with the use of only one equivalent of both coupling partners. Ideally, both pyrogallols would be mixed and oxidized *in situ* to

trigger the dimerization. The viability of this approach had already been established in this thesis as described in 2.3.4.2.1 Dimerization upon Oxidation with External Oxidants. Main challenge of such an endeavor is the competitive formation of dibefurin, which could previously not be solved by slow addition of epicoccine to a mixture of oxidant and pyrogallol **196** due to the instability of the corresponding quinone **197**. However, the pentasubstituted quinones **171** and **263** had shown no sign of decomposition in solution.

Therefore, efforts for the optimization of the cascade reaction were directed at the use of external oxidants in collaboration with Dr. Armanino. It was focused on inorganic oxidants that could easily be removed from the reaction mixture by filtration. By use of an excess Ag^{I} oxide premixed with catechol **170** or **261** in dioxane and slow addition of epicoccine, a protocol was identified that afforded the corresponding heterodimers in excellent yield without the need for purification (Scheme 89). Purification of the crude product by flash chromatography on reverse-phase silica gel can provide analytically pure products, but was also found to partially decompose the dimers. Therefore, purification of dimers **257** and **268** was not performed and the products were used directly in the next steps.



Scheme 89. Optimized protocols for the heterodimerization toward epicolactone.

This cascade reaction forms three stereocenters simultaneously, two of which are neighboring quaternary centers, by the equimolar coupling of two aromatic compounds in excellent yield.

Due to the higher purity of the product, X-ray-suitable crystals of acetate **267** could be obtained. Its structure was unambiguously assigned by X-ray single crystal structure analysis as the desired heterodimer formed through C–C bond coupling (Figure 26). Remarkably, the correct diastereomer is exclusively formed in the heterodimerization, a fact that is currently under mechanistic investigation by computational methods.

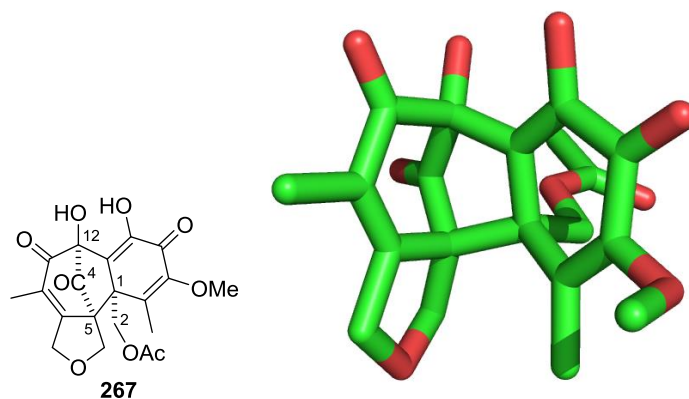


Figure 26. X-Ray single crystal structure of acetate **267**; H atoms omitted for clarity.
Color code: green = carbon, red = oxygen.

Several aspects of the structure **267** in the solid state deserve to be discussed. In agreement with the experimental observation (see 2.3.4.5.4 Final Studies Toward the Synthesis of Epicolactone), the weakest bond in the molecule appears to be the slightly elongated C1–C5 with a distance d of $d = 1.579 \text{ \AA}$. Interestingly, the distance d between the C2 oxygen atom and the C4 ketone of $d = 2.567 \text{ \AA}$ is significantly below the sum of their VAN DER WAALS radii of $d = 3.22 \text{ \AA}$. A nucleophilic attack on the C4 carbonyl could therefore be feasible. Despite the close contact, the C4 ketone is only slightly pyramidalized, with an angle χ of the C5–C4–C12 plane and the C4–O vector of $\chi = 4.74^\circ$. Significant distortion would show interaction of the oxygen atom lone pairs with the π^* -orbital of the C4 carbonyl.

The acetate **267** crystallized more easily than the corresponding TBS ether **257** since a relatively unhindered hydrogen-bond network could be formed. The bulky TBS group probably prevents closer interactions due to steric repulsion. The tertiary C12 alcohol acts as a hydrogen-bond donor and acceptor at the same time (Figure 27). The corresponding acceptor is the C15 ketone with $d_{\text{C12O-C15O}} = 2.777 \text{ \AA}$ and the donor the C14 enol OH of another molecule with $d_{\text{C12O-C14O}} = 2.703 \text{ \AA}$. Thus, each molecule **267** binds to one other molecule *via* the C12–OH and yet another *via* the C14 enol/C15 ketone, forming chains of hydrogen-bonded molecules in one dimension. These chains stack in the other dimensions *via* VAN DER WAALS interactions.

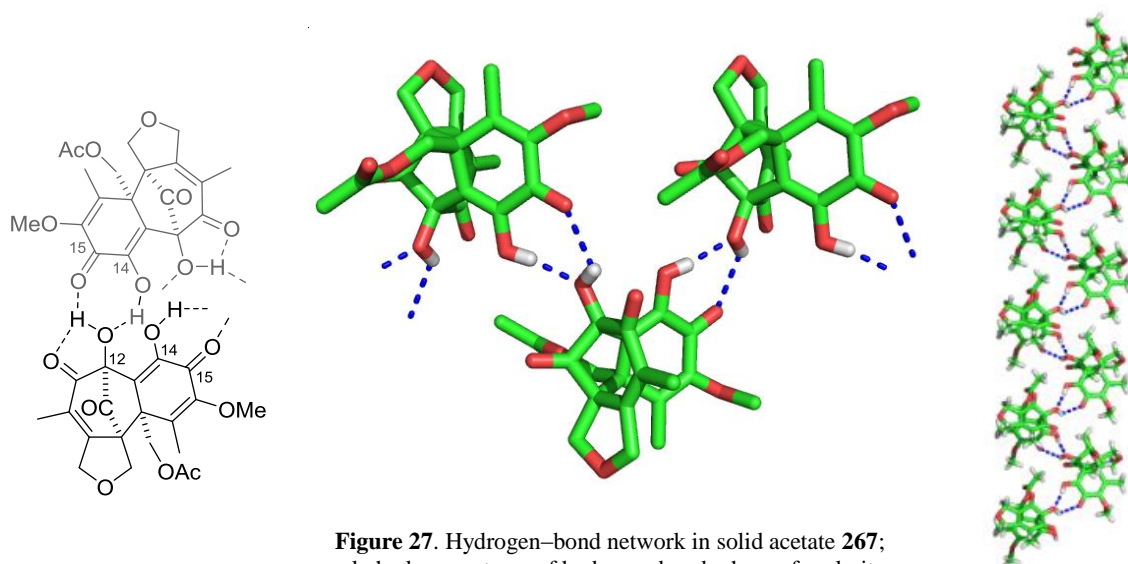


Figure 27. Hydrogen-bond network in solid acetate **267**; only hydrogen atoms of hydrogen bonds shown for clarity. Color code: green = carbon, red = oxygen, white = hydrogen.

2.3.4.5.4 Final Studies Toward the Synthesis of Epicolactone

With the purpurogallin cascade intermediates **267** and **257** accessed, their conversion to epicolactone was attempted. According to the biosynthetic hypothesis, deprotection of the primary alcohol protecting group would give intermediate **152** that would trigger skeletal rearrangement to epicolactone.

First, deprotection of the TBS protected alcohol **257** was tried with monitoring by NMR spectroscopy and LC/MS (Table 6). Stirring in slightly acidic medium or addition of formic acid did not lead to any conversion (entries 1, 2). However, addition of CSA as a stronger acid with MeOD as the nucleophile resulted in very slow deprotection and formation of a new compound (entry 3). The latter could be obtained very rapidly by addition of TFA and was identified as compound **273** by NMR spectroscopy and HRMS (entry 4). It appeared that a deprotection of the primary alcohol effects the loss of formaldehyde under rearomatization (*vide infra*). Since this reaction should have a positive reaction entropy, it was tested whether lower temperatures could prevent the extrusion of formaldehyde. No reaction was observed at $T = -80\text{ }^{\circ}\text{C}$, but warming to $T = -40\text{ }^{\circ}\text{C}$ triggered the undesired rearomatization, which was completed in $t = 30\text{ min}$ (entry 5). It appeared as if this undesired transformation could not be avoided under these conditions. Therefore, alternatives were screened to test if the projected alcohol addition to the bridged carbonyl group (C4) might occur. However, several fluoride-mediated deprotections with TBAF, HF complexes, CsF or the very mild silicate TASF either resulted in unidentified decomposition products or pyrogallol **273** (entries 6–10).

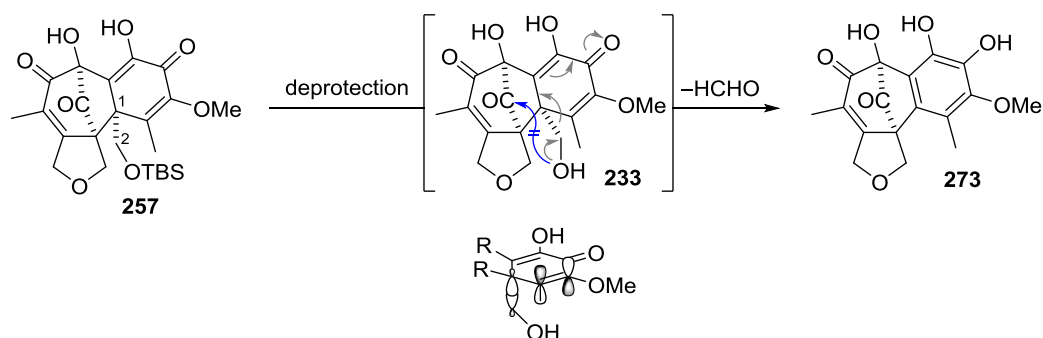
Table 6. Deprotection studies of cascade intermediate.

$\text{R} = \text{H}$ epicolactone **231**
 $\text{R} = \text{Me}$ **273**

entry	reagent	solvent (ratio)	T [°C]	t	comment
1	-	HOAc/THF/H ₂ O (3:3:1)	rt	28 h	s.m. recovered
2	formic acid	THF-d ₈ / D ₂ O	rt	6 h	no reaction
3	CSA	CD ₂ Cl ₂ /MeOD (5:1)	rt	54 h	slow deprotection; 273 formation
4	TFA-d ₁	CD ₂ Cl ₂	rt	10 min	273 formation
5	TFA-d ₁	CD ₂ Cl ₂	-80 to -40	30 min	273 formation
6	TBAF	THF	rt	10 min	decomposition
7	Et ₃ N • 3HF	MeCN	rt	19 h	273 formation
8	HF • pyridine	THF	rt	23 h	273 formation
9	CsF	THF	0 to rt	22 h	decomposition
10	TASF	DMF	0	2 h	hint at formation of 273
11	-	benzene	reflux	1 h	s.m. recovered
12	-	toluene	reflux	5 h	mostly s.m. and decomposition

The arene **273** proved to be labile, probably because the loss of the shielding OTBS group opens up the trajectory to attack the bridged carbonyl group (C4). The X-ray single crystal structure of acetate **267** suggested that the primary protected alcohol (C2) would be perfectly aligned to attack the carbonyl (C4) in the BÜRGI–DUNITZ trajectory. Therefore, simple thermal cyclization was tried with traces of water to remove the silyl protecting group from a putative oxonium ion formed by attack of the OTBS ether onto the carbonyl. These attempts were not met with success (entries 11, 12).

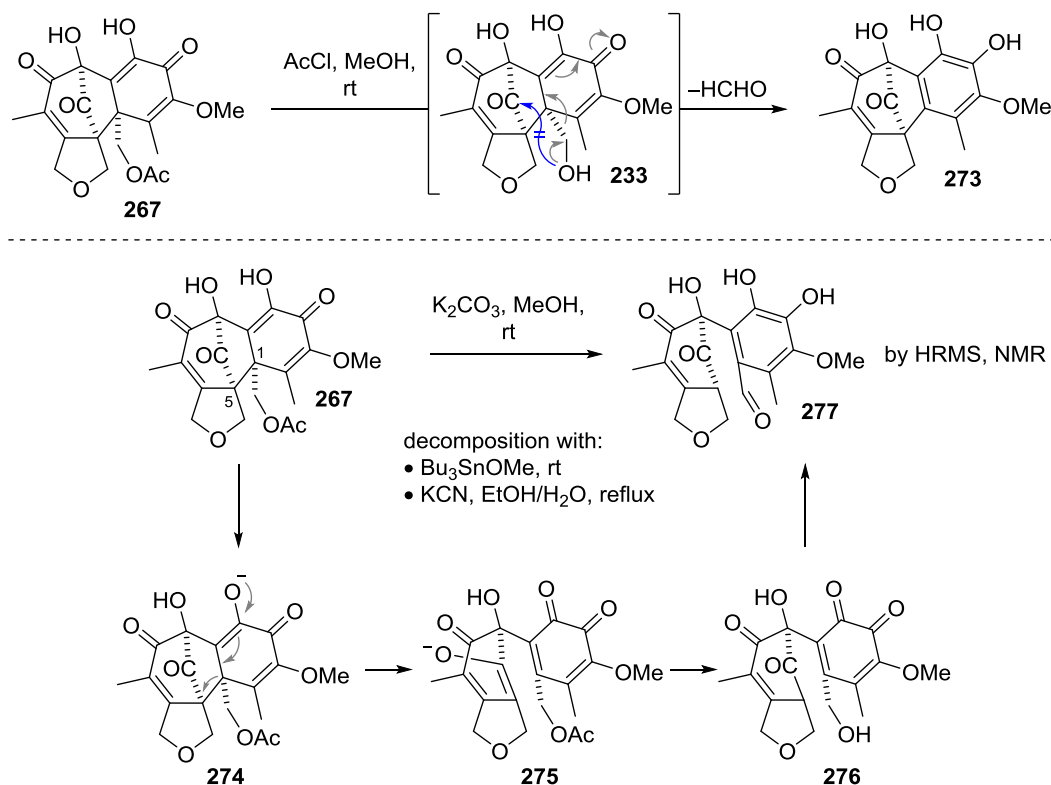
The undesired rearomatization under removal of formaldehyde can be rationalized by a retro-aldol type mechanism (Scheme 90). The σ -bonding orbital of the C1–C2 bond is already aligned with the π^* -antibonding orbital of the neighboring olefins. In essence, the C1–C2 σ -bond forms a part of the delocalized dienone system (see also Figure 26). It therefore appears to be enthalpically and entropically favorable to undergo rearomatization by extrusion of formaldehyde.



Scheme 90. Rationalization of the rearomatization of TBS protected alcohol **257**.

Potentially, the tetrahedral intermediate during acetate hydrolysis could deliver the $C2$ oxygen atom directly to the bridged carbonyl group in a net transacylation.

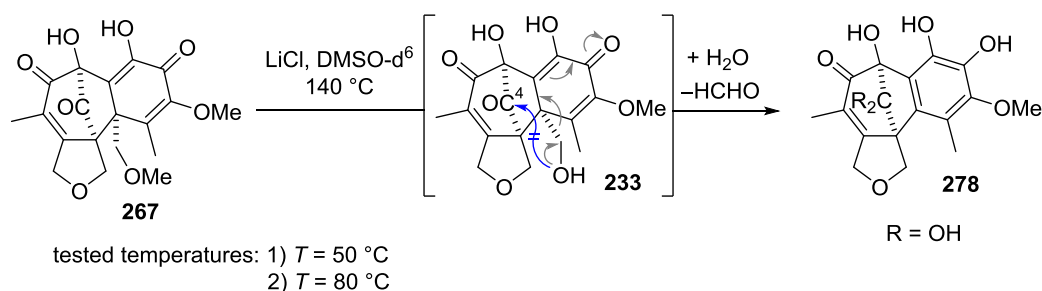
Acidic hydrolysis only delivered pyrogallol **273** under rearomatization as previously observed (Scheme 91). During basic hydrolysis, a product could be identified by NMR and HRMS that probably resulted from decomposition of the dimer prior to acetate hydrolysis. This crucial insight revealed the lability of the $C1$ – $C5$ bond in the dimer especially under basic conditions that easily convert the enol moiety into an enolate **274**, giving rise to enolate **275** in a retro-MICHAEL reaction. After hydrolysis to alcohol **276**, the known redox isomerization occurs to afford the product **277**.



Scheme 91. Attempted conversion of acetylated dimer **257** to epicolactone.

Hydrolysis attempts under neutral conditions, namely Bu_3SnOMe or potassium cyanide, both led to decomposition of the starting material.^[214]

Since deprotection and then cyclization was not with success, it was attempted to reverse the order of these events. To this end, a nucleophilic oxygen atom would be needed that can cyclize onto C4 ketone to yield an oxonium ion. The latter would be neutralized by cleavage of the protecting group. It was known that OMe ethers could undergo this type of reaction.^[215–217] Therefore, dimer **268** was heated with LiCl in DMSO and the reaction was monitored by ¹H NMR (Scheme 92). At temperatures of $T = 50\text{ }^{\circ}\text{C}$, no reaction was observed. At $T = 80\text{ }^{\circ}\text{C}$, formation of epicoccine was detected. This observation was rationalized with a decomposition of the dimer into its monomers and subsequent redox reaction with DMSO as previously observed (see 2.3.2.3 Purification of the Natural Product Dibefurin). It was reasoned that higher temperatures could help to overcome the activation barrier for oxonium ion formation. Heating to $T = 140\text{ }^{\circ}\text{C}$ did provide a new compound, but it became evident by crude NMR analysis that a methylene group was lost during the reaction. Eventually, it appeared as if the methyl ether had been cleaved without cyclization, triggering the same process *via* alcohol **233** as observed with the other protecting groups. Water impurities in DMSO then reacted with C4 ketone to form hydrate **278**.



Scheme 92. Cyclization and deprotection attempts with dimer **268**.

The observation of the rearomatization had important consequences for the biosynthetic hypothesis. It seems unlikely that the biosynthesis would proceed through an intermediate such as alcohol **152**, because rearomatization could occur. Although enzymes could potentially stabilize the presumed intermediate, the racemic nature of epicolactone hints at a spontaneous dimerization without enzymatic assistance. Therefore, intermediates such as acid **156** would seem more likely since the quaternization of C13 would decrease the driving force for immediate aromatization by formaldehyde extrusion (Figure 28).

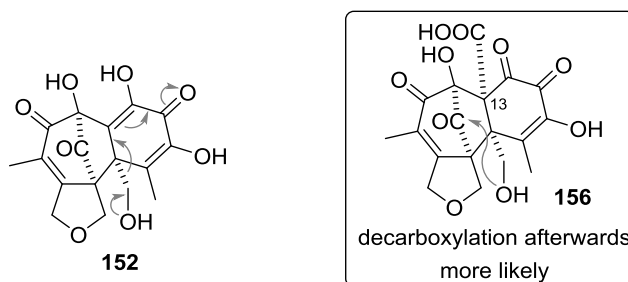


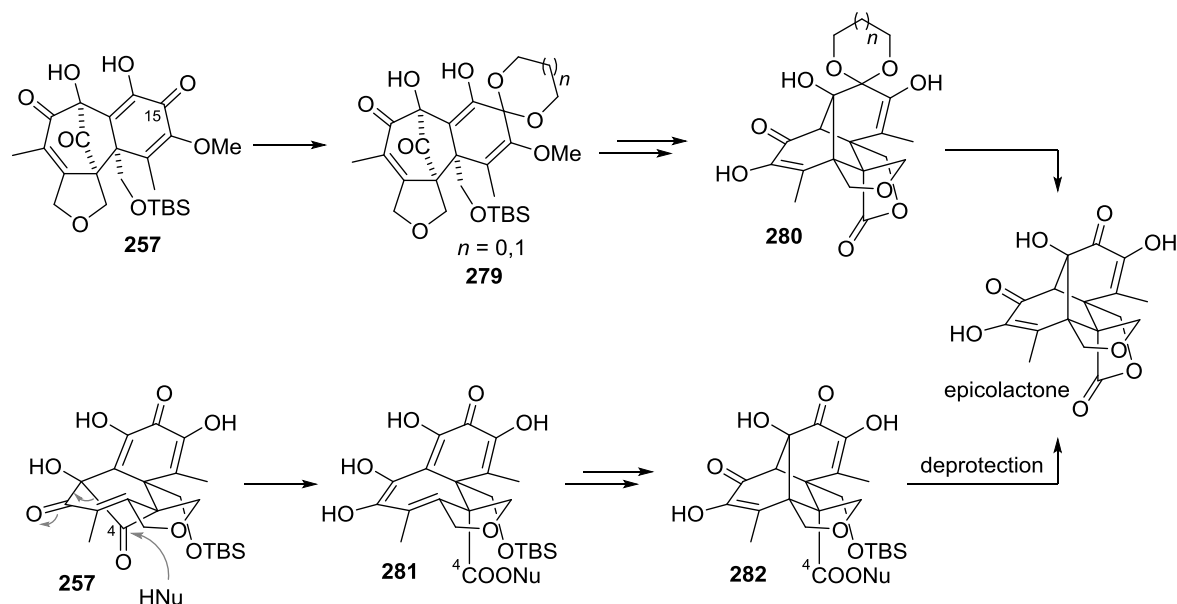
Figure 28. Reevaluation of biosynthetic precursors.

Independent of the way that Nature avoids the observed rearomatization, strategies became necessary to prevent this process in the laboratory, which will be presented in the following chapters. It was envisioned to quaternize one center in the carbocycle that is prone to rearomatization or to attack the bridged carbonyl (C4) with an external nucleophile (see 2.3.4.5.5 Strategies to Prevent Rearomatization of Advanced Intermediate). Furthermore, an advanced model of the biosynthetic hypothesis was proposed (see 2.4 Conclusion and Outlook).

2.3.4.5.5 Strategies to Prevent Rearomatization of Advanced Intermediate

In order to convert the promising advanced intermediates to epicolactone, two strategies were envisioned (Scheme 93). The first involved the transformation of one of the carbon atoms of the cyclohexadiene ring that is prone to rearomatization into a tetrasubstituted carbon atom. This operation would need to be reversible and the installed group removable under mild conditions due to the intricate structure of the molecule. It was therefore planned to manipulate the C15 ketone to ketal **279**, preferably a cyclic one so the risk of elimination would be reduced. The latter could undergo the same cascade sequence as envisioned in the biosynthesis to arrive at protected epicolactone **280** that would be deprotected to epicolactone itself in the final step.

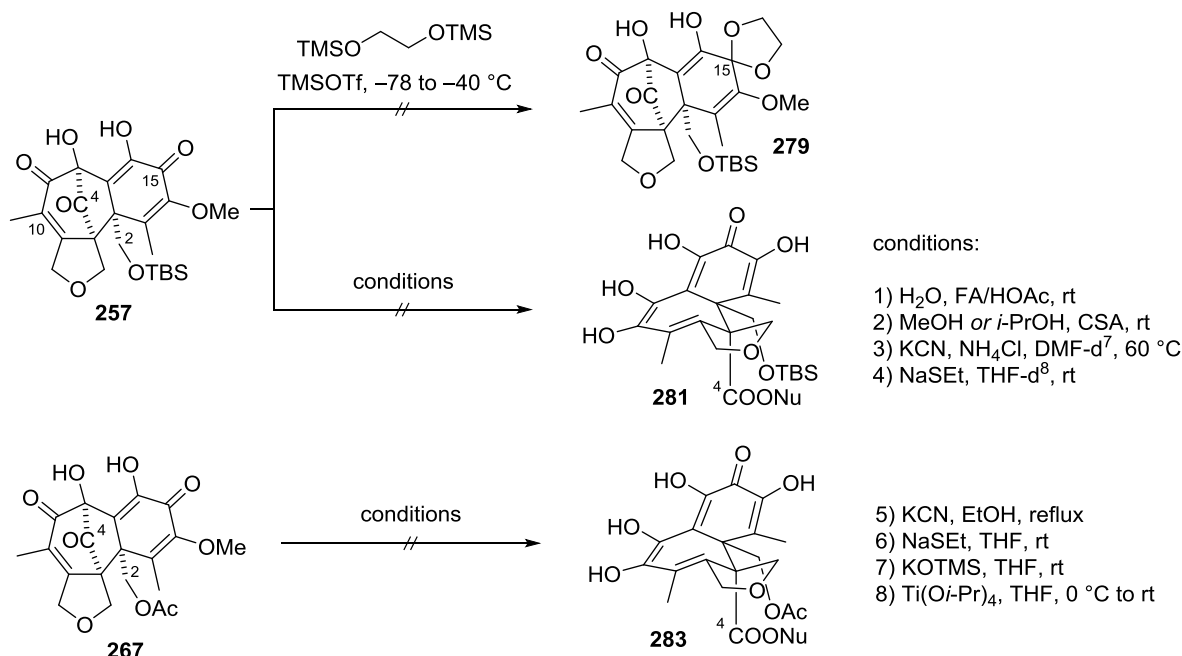
Second, the intermolecular attack of a nucleophile onto the bridged carbonyl (C4) in dimer **257** could yield dienol **281**. In analogy to the biosynthesis, this intermediate could furnish TBS ether **282** that upon deprotection would close the lactone ring to give epicolactone.



Scheme 93. Attempts to convert advanced intermediates to epicolactone without rearomatization.

Initial experiments were performed along the lines of these two strategies, but were so far unfruitful (Scheme 94). A NOYORI ketalization strategy was followed to access dioxolane **279** from TBS ether **257**, but the conditions only led to decomposition. Mild attempts to attack the ketone at C4 with water or methanol for the synthesis of products like **281** did not show any conversion (Scheme

94, conditions 1, 2). It was thus focused on good but non-basic nucleophiles. Treatment with potassium cyanide at elevated temperatures led to the formation of achiral substrates, which were assumed to result from decomposition of the substrate (condition 3). Thiolate as a nucleophile only gave rise to decomposition (condition 4). It was reasoned that the BÜRGI–DUNITZ trajectory of the C4 ketone could be blocked from both faces by either the $-\text{CH}_2\text{OTBS}$ group or the C10–Me group. Hence, external nucleophilic attack was attempted with the less sterically demanding acetate protecting group for the C2 primary alcohol to arrive at products like **283** (Scheme 94). Both KCN and ethylthiolate led to intractable mixtures, probably due to cleavage of the acetate group (conditions 5, 6). No conversion was observed with KOTMS as a mild reagent, because it might have been too bulky to attack the sterically congested C4 ketone (condition 7). LEWIS-acidic attempts with Ti^{IV} only gave intractable decomposition. Substrate **267** possesses multiple coordination sites that could coordinate to Ti^{IV} and give rise to decomposition products.



Scheme 94. Initial attempts to convert intermediates to epicolactone without rearomatization.

As it appeared that it would be difficult to attack the C4 ketone with nucleophiles due to steric reasons and since substrates such as **257** and **267** proved to be sensitive, this strategy was not further pursued.

Strategically, an attack of the C2 oxygen atom on the C4 ketone would be the most straightforward solution. Therefore, an alternative strategy was proposed which would directly give rise to precursors such as **279** that would be less prone to rearomatization. Instead of *ortho*-quinones, the related quinone monoketal could potentially also engage in purpurogallin-type dimerizations because the crucial enone moiety would remain intact. Therefore, four different monoketals **284–287** were prepared. Although the *ortho*-quinone analog of **284** had given the undesired hetero-DIELS–ALDER dimerization, its monoketal cannot engage in this reaction.

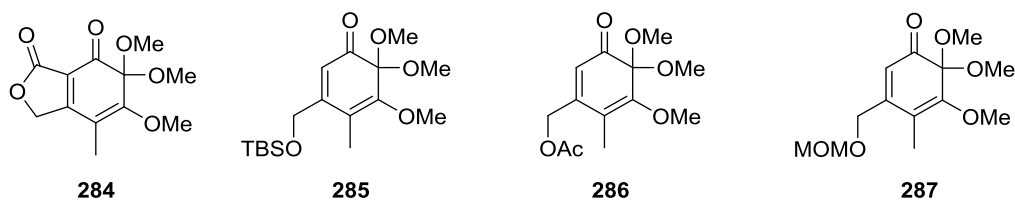
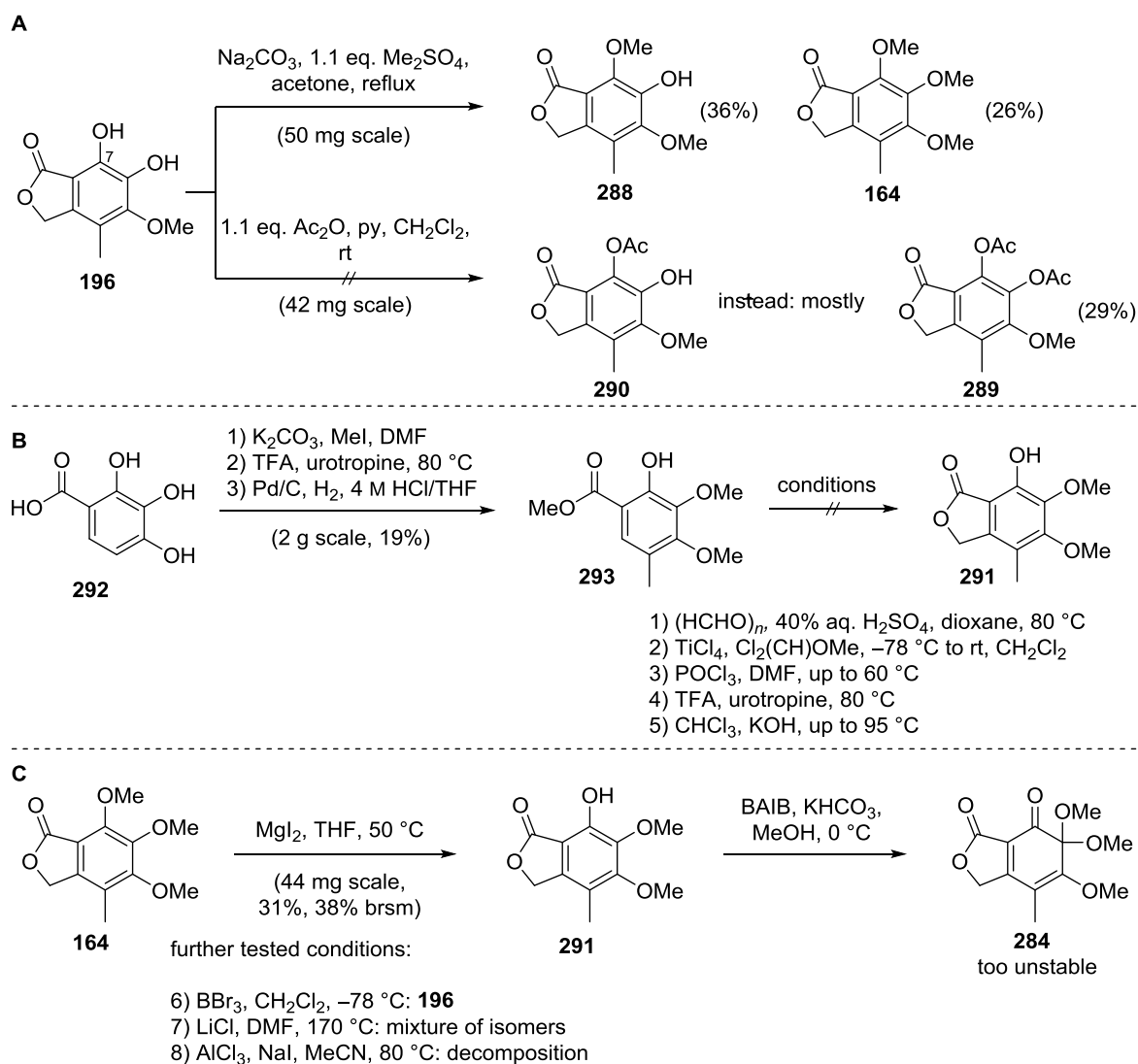


Figure 29. Targeted monoketals to prevent rearomatization of advanced intermediates.

The most time-economic way to synthesize ketal **284** would be from intermediates of the epicocone B synthesis (Scheme 95). Hence, monomethylated epicocone B **196** was submitted to methylation conditions and yielded a mixture of undesired isomer **288** and trimethylated epicocone B **164**. Selective protection of the *C7* phenol by acetylation or benzylation also suffered from the significant overreaction, affording mostly bisacetate **289** instead of phenol **290** (Scheme 95).



Scheme 95 A. Selective protection of epicocone B intermediate. **B.** Novel synthetic route to dimethylated epicocone B derivative. **C.** Successful synthesis of epicocone B derivative by selective demethylation.

It was therefore tested if the dimethylated epicoccone B **291** could be accessed in an analogous synthesis to epicoccone B (Scheme 95). Pyrogallol **292** was trimethylated with relatively poor selectivity, but the desired isomer could be separated and smoothly underwent formylation and reduction to give phenol **293**. Under a variety of conditions, the compound resisted introduction of the sixth benzene substituent, proving that the C6 free phenol is crucial for the successful epicoccone B synthesis. Only hydrolysis of the ester was detected under the previously identified conditions (condition 1). No reaction was observed in the RIECHE, VILSMEIER–HAACK or DUFF formylation (conditions 2–4). Furthermore, the REIMER–TIEMANN reaction also only resulted in hydrolysis of the ester.

Since trimethylated pyrogallol **164** could be obtained by methylation of intermediate **196**, a selective demethylation was tried rather than the selective methylation. After screening of conditions with BBr_3 (overreaction), LiCl (unselective) and AlCl_3 (decomposition), selective demethylation could be effected by MgI_2 in THF to afford **291** in moderate yield. The structure of phenol **291** was unambiguously proven by X-ray single crystal structure (Figure 30). In the solid state, the molecules engage in aromatic π – π interactions with parallel-displaced geometry and a distance d of the two arene planes of $d = 3.468 \text{ \AA}$.^[218]

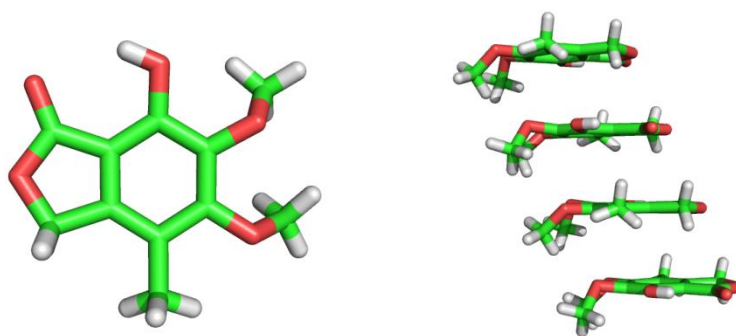
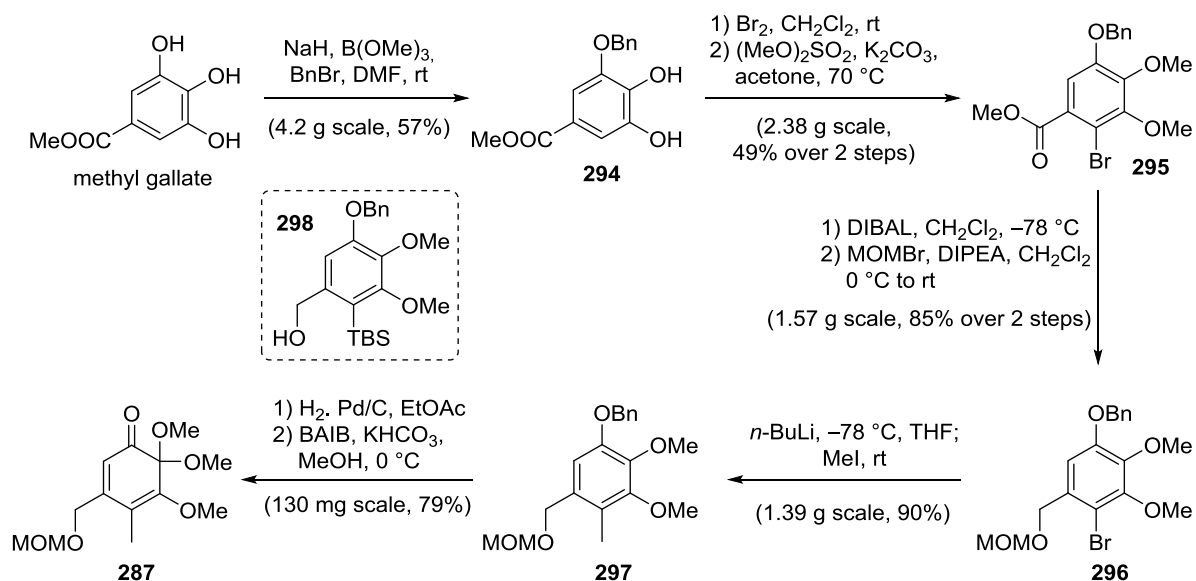


Figure 30. X-Ray single crystal structure of phenol **291** and supramolecular aromatic π – π interactions.
Color code: green = carbon, red = oxygen, white = hydrogen.

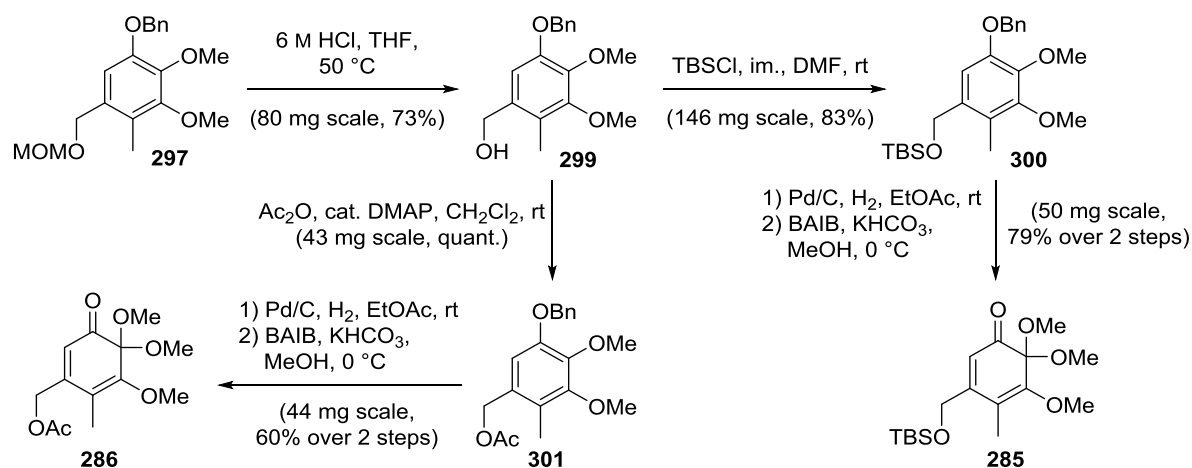
However, the oxidation product **284** proved to be too unstable for isolation. Oxidation of a mixture of epicoccine and phenol **291** was complicated by competitive homodimerization to dibefurin. Due to the low stability of the quinone monoketal **284** and its high substitution degree, which had previously led to an undesired dimerization mode, it was focused on pentasubstituted benzene derivatives.

With the aim of a divergent synthesis of the three pentasubstituted pyrogallol derivatives **285–287**, the route depicted in Scheme 96 was developed.

Scheme 96. Synthesis of quinone monoketal building block **287**.

Methyl gallate was selectively benzylated to catechol **294** by intermediate formation of a catechol borate in good yield.^[219] Sterically controlled regioselective bromination and methylation of the catechol yielded bromide **295**, which after reduction of the ester and MOM-protection delivered pentasubstituted benzene **296**. The MOM protecting group had to be chosen since other protecting groups were incompatible with the following methylation to pyrogallol **297** via metalation with *n*-BuLi. The OTBS analog underwent a 1,3-retro-BROOK rearrangement under these conditions, yielding silylated benzene **298**. An alternative NEGISHI cross coupling showed inferior results. Debenzylation and oxidation afforded quinone monoketal **287**.

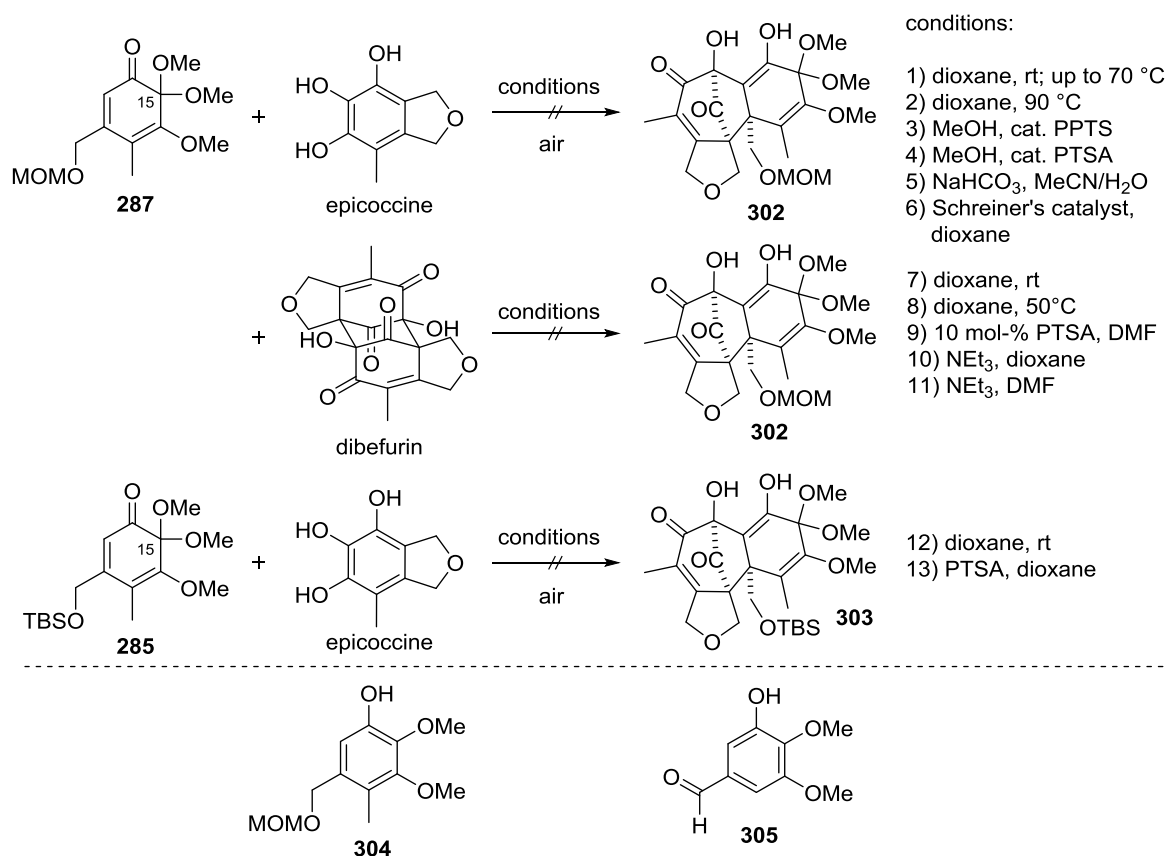
Acidic deprotection of MOM ether **297** had to be implemented to access benzylic alcohol **299** (Scheme 97). The latter served as the precursor to the other two quinone monoketals **285** and **286**.

Scheme 97. Synthesis of further *ortho*-quinone monoketals.

TBS protection or acetylation respectively gave rise to protected benzyl alcohols **300** and **301**. Debenzylation and oxidation furnished two further *ortho*-quinone monoketals **285** and **286**.

The quinone monoketals were next tested in the dimerization with epicoccine to tetracycles of type **302** or **303** (Scheme 98). It was expected that epicoccine would attack the enone moiety of the quinone ketals **285**–**287** in a 1,4-fashion to give rise to an ene diol of type **244**. The latter would need to get oxidized before the cascade would proceed, which is why the reactions were left open to air. Use of other oxidants was ruled out due to the danger of competitive dibefurin formation.

Nucleophilic attack of epicoccine on quinone ketal **287** did not occur in dioxane up to $T = 70\text{ }^{\circ}\text{C}$ (condition 1). At higher temperatures, the reduced form **304** was identified and epicoccine seemed to have decomposed (condition 2). Presumably, epicoccine was oxidized by a putative quinone methide intermediate resulting from thermal elimination of MeOH from quinone monoketal **287**.



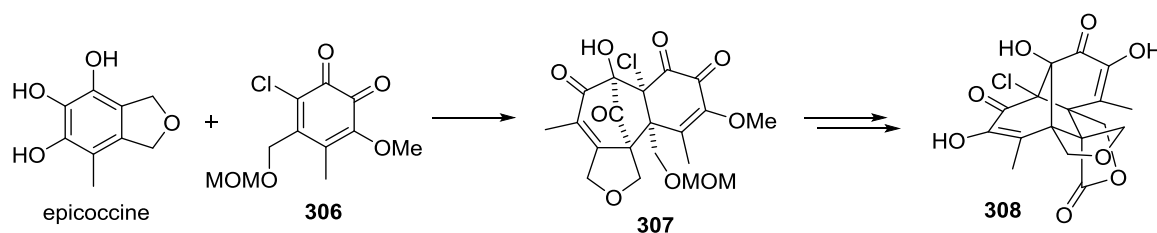
Scheme 98. Dimerization attempts with quinone monoketal building blocks.

No dimerization was observed upon electrophilic activation of the quinone monoketal or increasing the nucleophilicity of epicoccine in basic medium (conditions 3–5). Thiourea catalysts slowly led to decomposition over several weeks, but no product was detected (condition 6). Since air might not be sufficient to oxidize intermediates, dibefurin as a preoxidized epicoccine was employed. Neither thermal nor acid-promoted conditions led to any conversion (condition 7–9). Although dibefurin decomposition was efficient with triethylamine, no product was observed (condition 10). While stirring with triethylamine in DMF, the quinone monoketal decomposed to aldehyde **305**, potentially *via* the previously observed pathways (condition 11). These results were discouraging for trials with the other building blocks since the challenges did not arise from the protecting group, but

rather from a general lack of reactivity. Similar conditions with ketal **285** therefore were also unsuccessful, with aldehyde **305** formed in condition 13 (conditions 12, 13).

Quinone monoketals are stabilized *ortho*-quinones that for instance lack the large dipole repulsion between the carbonyl groups. They are therefore also less reactive than *ortho*-quinones. The fact that no dimerization was observed under a variety of conditions could be attributed to the higher stability of these ketals. Additionally, it could be reasoned that the approach of epicoccine is hindered by the substituents on the C15 carbon atom. The former flat reaction partner was transformed into a three-dimensional molecule by breaking the conjugation of the π -system, which could severely interfere with π -stacking of the reaction partners prior to C–C bond formation.

Another alternative to install a quaternary center in intermediates such as **257** would be the use of C13-halogenated building blocks (Scheme 99). The halogen blocking group could later be removed by radical defunctionalization. Despite the fact that hexasubstituted pyrogallol derivatives appear to engage in hetero-DIELS–ALDER dimerizations, the additional halogen might increase the π -stacking ability of this coupling partner and therefore potentially facilitate C–C bond formation due to a proximity effect. By coupling of epicoccine with chloroarene **306**, intermediate **307** could be accessed and converted to chloro epicolactone **308**.

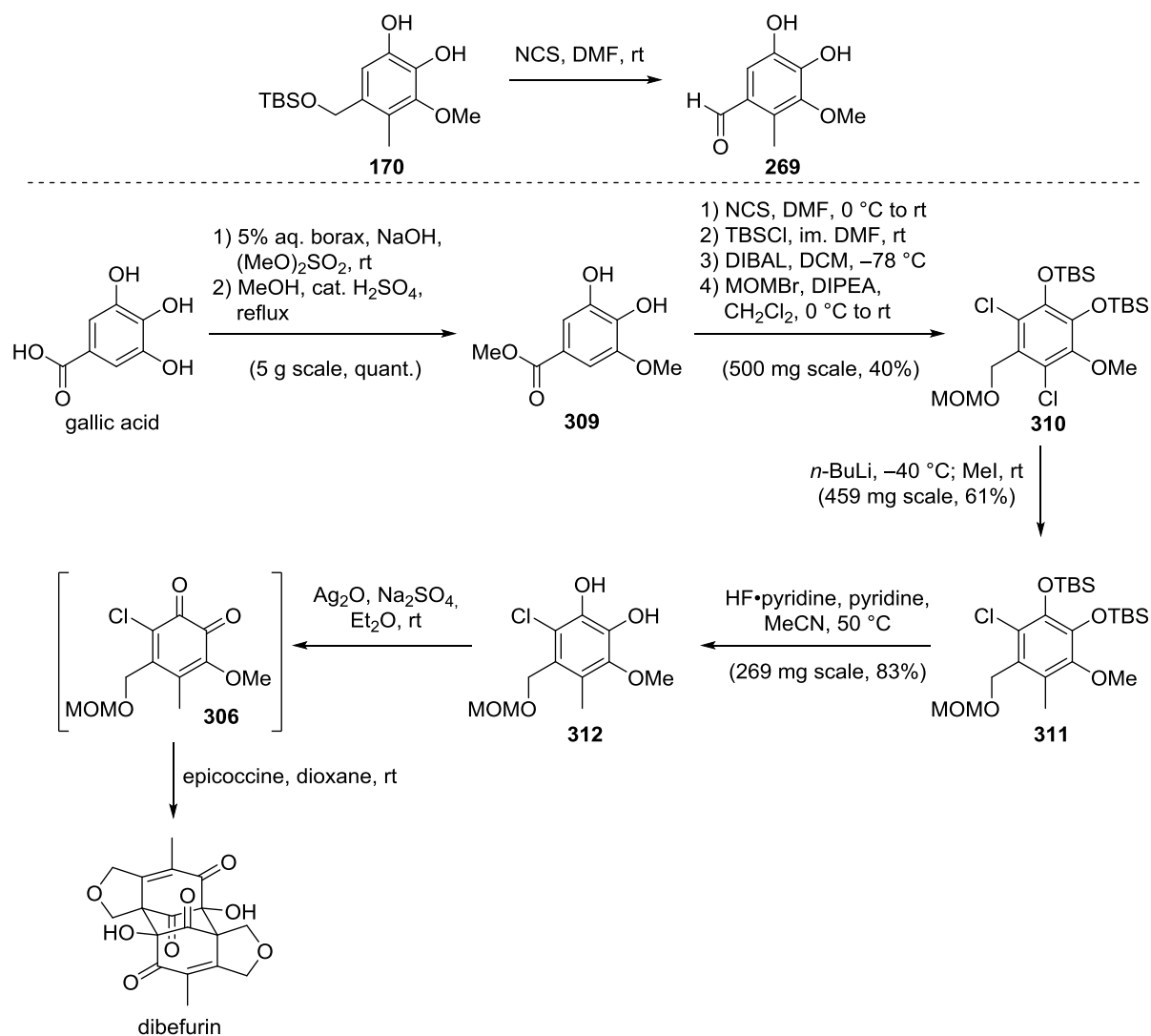


Scheme 99. Quaternization of carbon atom in cascade intermediate to prevent rearomatization.

In order to access these intermediates, it was first envisioned to chlorinate advanced intermediates of the synthesis of pentasubstituted pyrogallols such as **170**. This route was not met with success since only benzylic oxidation occurred to aldehyde **269** (Scheme 100). This could either occur by a direct benzylic chlorination or by initial *O*-chlorination and subsequent formation of *ortho*-quinones, which give rise to the product by TBS deprotection and redox-isomerization.

A novel route was therefore developed starting from gallic acid, which was selectively methylated by intermediate formation of a catechol borate and then esterified to provide ester **309**. Against expectation, the following chlorination always afforded mixtures of mono- and double chlorination. Therefore, catechol **309** was double chlorinated with NCS, the catechol was TBS protected, the ester reduced and the resulting benzylic alcohol protected with a MOM group to afford hexasubstituted benzene **310**. Generation of a monoanionic species by bromine/lithium exchange and following methylation gave rise to toluene derivative **311**, which could be deprotected with HF in pyridine to afford catechol **312**. The optimized oxidation procedure with *ortho*-chloranil was ineffective because

the *ortho*-quinone **306** did not precipitate from the reaction mixture. An alternative procedure with Ag₂O gave the desired quinone **306**, to which epicoccine was immediately added. However, only dibefurin and catechol **312** were identified in the reaction mixture.



Scheme 100. Synthesis of chlorinated building block for heterodimerization.

In addition to other hexasubstituted building blocks, also quinone **306** was considered to be unsuitable for the synthesis of picolactone precursors.

2.4 Conclusion and Outlook

In this thesis, the three fungal metabolites epicoccine, epicoccone B and dibefurin were efficiently synthesized. The biosynthetic hypothesis of dibefurin involving a spontaneous dimerization of epicoccine upon oxidation was largely supported by the preparation of dibefurin along these lines. The reason for its insolubility was unraveled by the identification of a hydrogen–bond network in the solid state. A proposal for the interesting mechanism of the oxidative dimerization has been put forward that is currently under investigation by computational methods. Further studies on this intriguing C_i -symmetric natural product reinforced the hypothesis that dibefurin is also produced by *Epicoccum* species.

Several different routes toward the pseudosymmetric and racemic epicolactone were tested employing the heterodimerization of two different pyrogallols. The required monomers were all efficiently prepared by relying on the potential of electrophilic aromatic substitution reactions involving the electron-rich benzene core of pyrogallol derivatives. It is worth noting that the synthetic routes presented herein can be applied to the preparation of various pyrogallol natural products. It was found that hexasubstituted pyrogallol derivatives were unsuitable for the desired heterodimerization toward epicolactone, which was attributed to increased steric hindrance and inability of the initial product to avoid an energetically unfavorable diketone. During these studies, an unprecedented hetero-DIELS–ALDER heterodimerization of a quinone methide with an *ortho*-quinone was identified, which constituted an undesired reaction mode.

In accordance with the concepts of pyrogallol dimerization that were put forward in this thesis, it was established that the epicoccine part requires all free hydroxyl groups for a successful heterodimerization. The use of pentasubstituted and suitably protected pyrogallol derivatives allowed for the successful preparation of heterodimers with the desired connectivity and diastereoselectivity. This reaction leads to the formation of three tetrasubstituted carbon atoms in one reaction and constitutes the first application of the purpurogallin cascade for the synthesis of non-benzotropolone natural products. Its success and especially the correct simple diastereoselectivity provide valuable support to the presented biosynthetic hypothesis and certainly underline the power of biomimetic synthesis. The completed targets and the remaining challenge toward epicolactone are summarized in Figure 31.

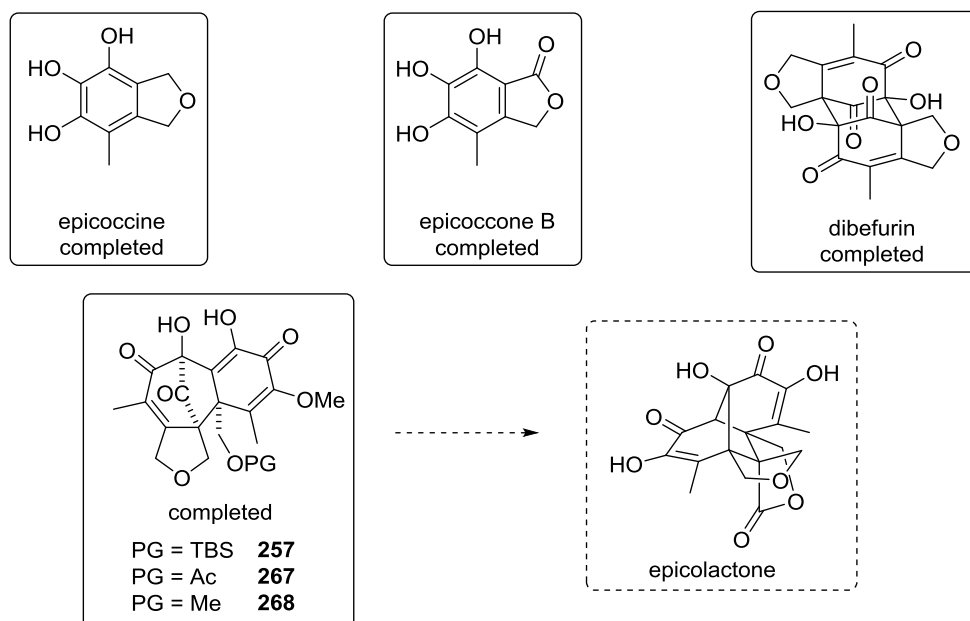


Figure 31. Completed targets of this thesis and one remaining challenge.

The transformation of the advanced intermediates **257**, **267** or **268** into epicolactone proved challenging due to unwanted side reactions of the sensitive heterodimers. Several strategies were envisioned to overcome these challenges.

First, already attempted strategies will have to be investigated in more detail. The installation of protecting groups for C15 ketone, *e.g.* dioxolanes, dioxanes or dithianes, will need to be revisited with more stable protecting groups on the primary alcohol at C2 (Figure 32). Once protected, the driving force for rearomatization will be greatly reduced.

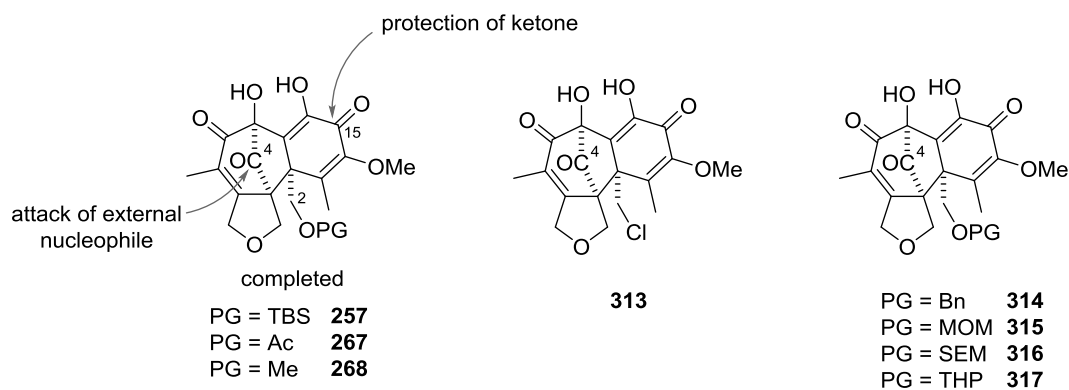


Figure 32. Future directions in the biomimetic synthesis of epicolactone.

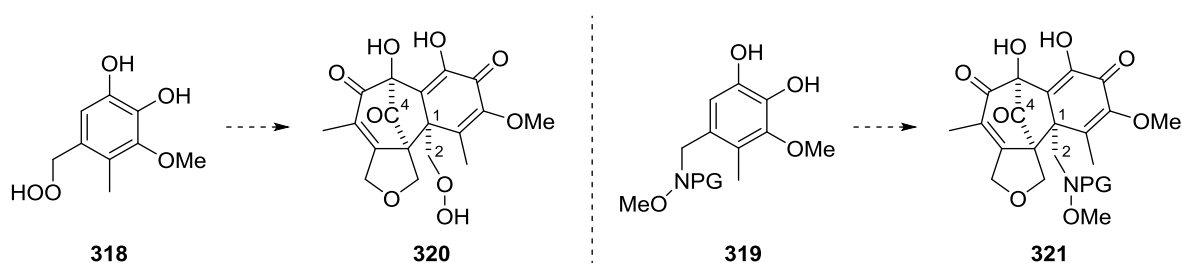
Furthermore, attack of external nucleophiles should be attempted with C2 alcohol protecting groups that are small enough not to block the BÜRGI–DUNITZ trajectory and yet stable to the reaction conditions. As a proof of principle, dimer **268** should be subjected to cyanide, azide or thiolate anions to assess whether external nucleophiles are able to attack the sterically shielded C4 ketone. These experiments would also reveal if the second part of the cascade toward epicolactone *via* retro-DIECKMANN-type reaction and vinylogous aldol addition is feasible. If successful, even a chloride

substituent could be chosen at C2 as in substrate **313** to enable facile lactone formation after external nucleophilic attack on the C4 ketone.

In addition to these experiments, each deprotection step should be tested under high pressure to disfavor the cleavage of formaldehyde.

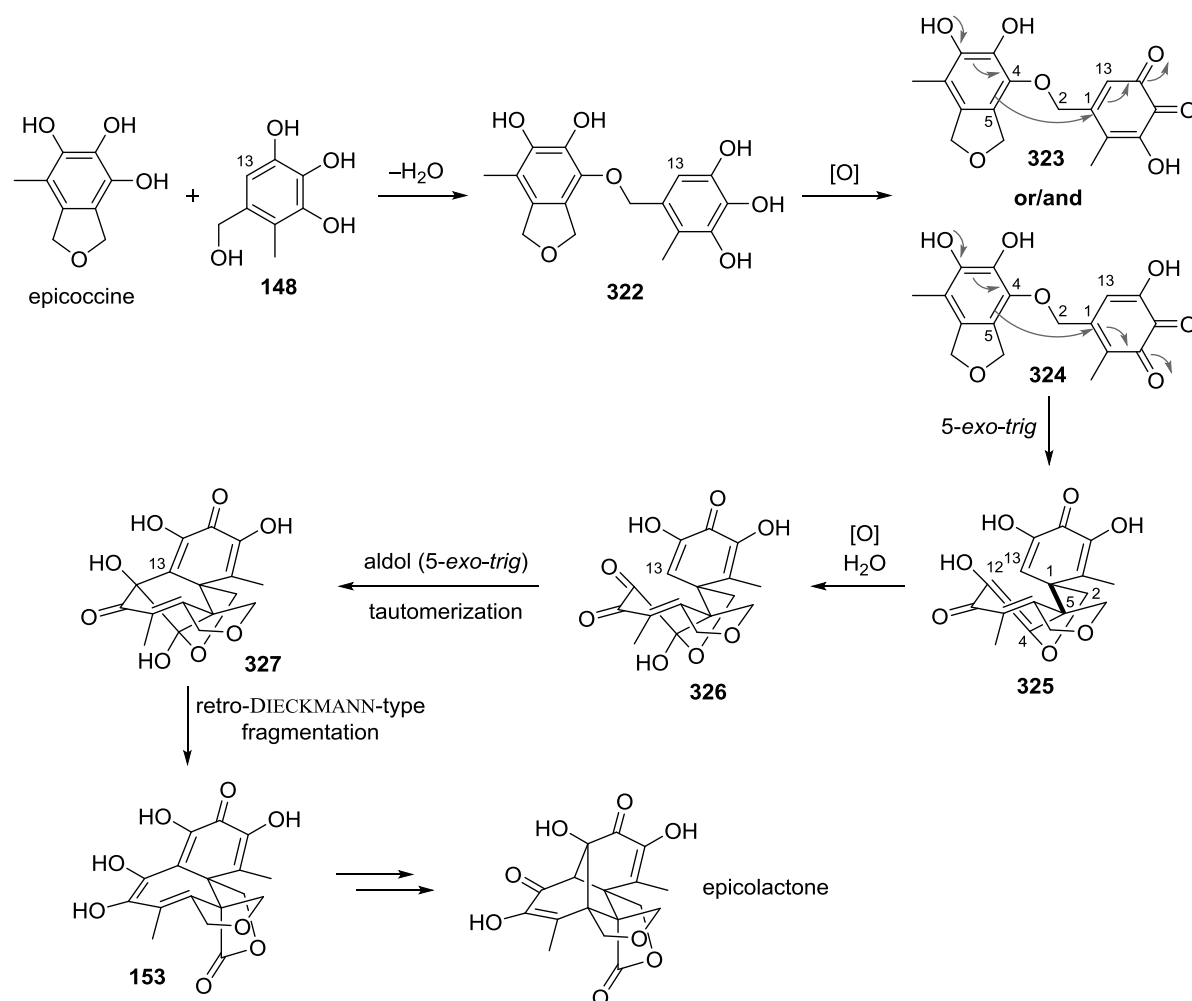
Since the protocol toward heterodimers appears to be robust, a variety of different C2 alcohol protecting groups should be employed (Figure 32). Special focus should be on protecting groups with the ability to cyclize onto the carbonyl group at C4 followed by deprotection of the resulting oxonium ion. In this context, the use of benzyl ethers (**314**) or acetals such as MOM (**315**), SEM (**316**) or THP (**317**) protecting groups should be considered. Silyl protecting groups, potentially with less steric bulk than TBS, could also be reinvestigated concerning their ability to attack the C4 ketone in the presence of halides or other nucleophiles. A different type of deprotection under metal catalysis could be offered by C2 allylic ethers that might not proceed *via* the free alcohol **233**.

Another potential alternative would be the use of heteroatoms on the C2 oxygen atom that would not only increase its nucleophilicity, but also reduce the tendency to cleave the C1–C2 bond. Since sulfur would be readily oxidized under the dimerization conditions, possible heteroatoms would include oxygen or nitrogen if protected with EWGs as in monomers **318** and **319**. The corresponding dimers **320** and **321** are shown in Scheme 101. Substrate **320** could either form a five- or six-membered lactone. The latter could be contracted to a five-membered ring under reducing conditions. Upon *N*-deprotection and cyclization onto the C4 ketone, substrate **321** would yield a WEINREB amide, which would be activated toward subsequent hydrolysis.



Scheme 101. Potential alternative substrates to avoid cleavage of the C1–C2 bond.

In conclusion, an advanced model of the potential biosynthesis can be proposed, which is based on the experimental results obtained in this thesis (Scheme 102). It was argued that alcohol **148** was not yet isolated from *Epicoccum* species due to its potential instability, although it might form in Nature by hydrolysis and decarboxylation of epicoccone B. Alcohol **148** would be very prone to S_N2 reaction in the benzylic position, so that it might occur that the phenol of epicoccine condenses to form benzylic ether **322**. Other regioisomers could result from this condensation, but would probably not lead to epicolactone.



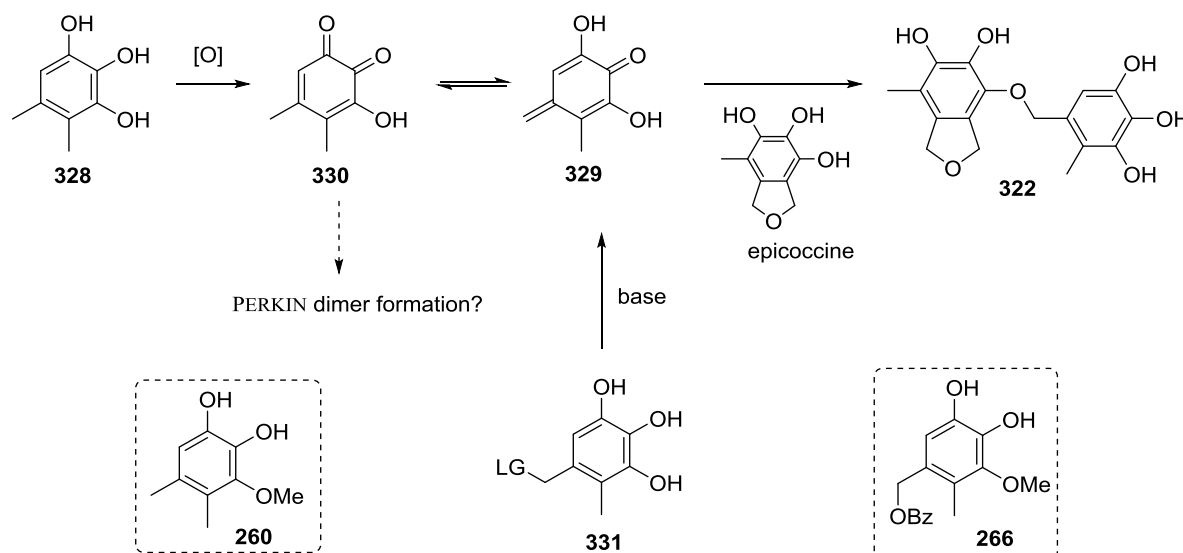
Scheme 102. Alternative biosynthetic hypothesis based on intramolecular dimerization.

The resulting benzyl ether **322** could be oxidized to *ortho*-quinones **323** or **324** since the unprotected pyrogallol moiety should be more electron-rich especially in slightly basic media. Intriguingly, both quinones would yield the same product if the epicoccine portion underwent dearomatization to attack the quinone in a 1,4-fashion. The C1–C5 bond would be forged in this step in a 5-exo-trig cyclization, yielding bisdienone **325**. The ene diol portion (C4/C12) could then be oxidized in the presence of water to afford diketone **326**, which could be captured by the pendant enol to give **327** after tautomerization. A retro-DIECKMANN-type fragmentation would afford proposed intermediate **153** that would yield epicolactone according to the steps shown in Scheme 39.

Several aspects of this biosynthetic proposal are worth mentioning. First, a synthesis of epicolactone along these lines would prevent a competing oxidative homodimerization of epicoccine since the coupling partners would be tethered prior to oxidation. Second, other cyclization modes such as the PERKIN dimer formation or hetero-DIELS–ALDER cycloaddition would be suppressed due to ring formation constraints. Third, the problematic loss of the C2 substituent would be suppressed because the C2 alcohol would be present as an enol ether (**325**) or involved in a hemiacetal (**326**). Fourth, for the same reason of ring formation considerations, the correct diastereoselectivity would be obtained in

325 with a *cis*-orientation of the C1–C2 and C4–C5 bond. Fifth, all rings up to ene diol **153** are forged through 5-*exo-trig* cyclizations, which are favored according to the BALDWIN rules.^[220] Sixth, the biosynthesis could analogously be envisioned with epicoccone B if a –COOH was attached to the C13 position. Seventh, suitable conditions for this transformation could be adapted from the dibefurin synthesis since the biosynthesis would also require an oxidant in aqueous medium.

Whereas the synthesis of benzyl ether **322** could be difficult, several possibilities exist to form the required ether linkage *in situ* (Scheme 103). A dimethyl pyrogallol derivative **328** could be oxidized, forming equilibrium amounts of *para*-quinone methide **329** via quinone **330**. The quinone methide could be nucleophilically attacked by epicoccine in the benzylic position to furnish the desired ether **322**. Potential drawbacks of this strategy would be competitive PERKIN dimer formation of quinone **330**, potential purpurogallin-type dimerization between quinone **330** and epicoccine and regioselectivity problems concerning the hydroxyl groups of epicoccine. The competitive PERKIN dimer formation could be suppressed by synthesizing quinone **329** from pyrogallols of type **331** *via* elimination. In addition, selectively protected analogs of the pyrogallol substrates **328** and **331** could be employed, *e.g.* arene **260** or **266**.



Scheme 103. Possible methods to form benzyl ether bond *in situ* prior to oxidation.

Although a biomimetic synthesis along the lines of this alternative biosynthesis could be accompanied by various side reactions, it would solve many challenges that had previously been observed.

PART II:

**Synthetic Studies Toward
Gracilin Terpenoids**

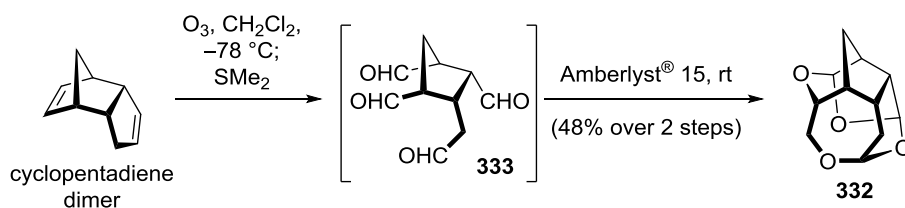
3. PART II: SYNTHETIC STUDIES TOWARD GRACILIN TERPENOIDS

3.1 Introduction

3.1.1 Strategies in the Synthesis of Cage-Shaped Compounds

The challenge in the synthesis of cage-shaped compounds, be it natural products, hydrocarbons or ligands, is the high steric hindrance associated with their structure. During the synthesis of these compounds, the stereoselective installation of substituents that are located on the concave side of the molecule will be complicated by the fact that the convex face is more accessible.

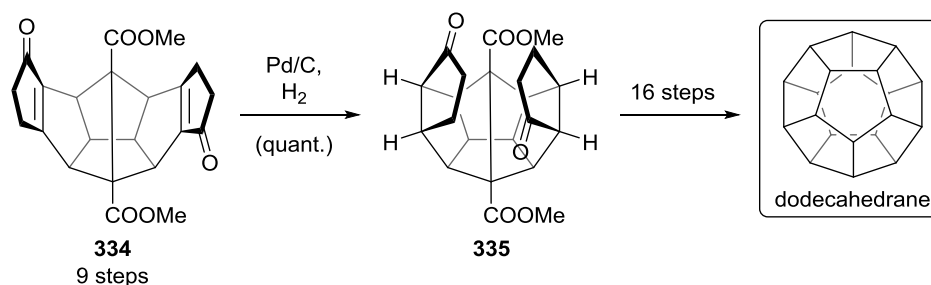
One strategy to overcome this challenge is to enforce a puckered conformation in polycyclic systems. So-called oxa-cages, cage-like compounds including oxygen atoms, have been studied due to their potential application in selective metal-ion complexation and the interest in discovering novel transannular interactions. MEHTA and VIDYA have accessed polyacetal **332** by ozonolysis and cyclization of the cyclopentadiene dimer (a tricyclo[5.2.1.0^{2,6}]decane), which enforces the proximity of the olefins by the one-carbon bridge (Scheme 104).^[221] After ozonolysis, all carbonyl functionalities in tetraaldehyde **333** thus point to the same side of the molecule to form the caged-shaped compound by acetalization.



Scheme 104. Synthesis of oxa-cages by enforcing the conformation in a bicycle.^[221]

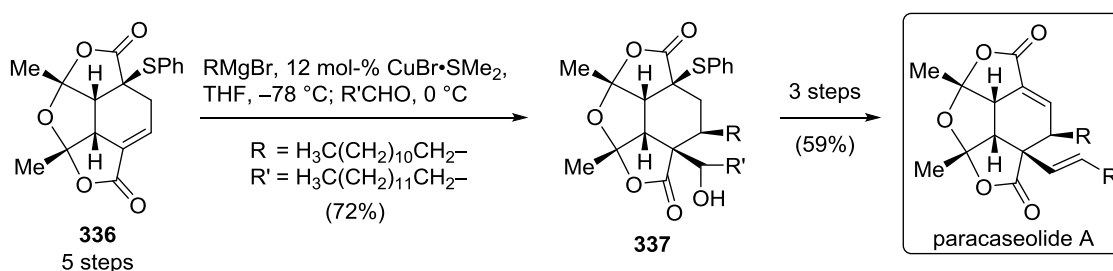
In order to take advantage of this strategy, the respective bridge would either have to be incorporated into the natural product or be removable in the course of the synthesis. Hence, this approach is either limited to certain target molecules or decreases the overall efficiency of the synthesis due to additional steps required for the removal of the bridge.

Another prominent strategy for the synthesis of cage-shaped compounds is the addition of substituents from the convex, less sterically encumbered face to increase the curvature of the molecule. In the most frequently applied scenario, this would involve the reduction of an olefin with H₂ from the convex face. PAQUETTE and co-workers employed this strategy in the synthesis of dodecahedrane (Scheme 105).^[222,223] The starting material **334** was accessed in 9 steps employing *e.g.* a double DIELS–ALDER reaction. The ensuing face-selective heterogeneous hydrogenation to bisketone **335** occurred from the convex side of the molecule and forced the cyclopentanone ring further onto the concave side. Dodecahedrane was successfully synthesized in additional 16 steps.



Scheme 105. Hydrogenation strategy to increase curvature in the PAQUETTE synthesis of dodecahedrane.^[222,223]

Another example of this general strategy, closely related to the synthesis of the gracilin natural products discussed in 3.1.2 Gracilin Natural Products, was reported by KRAUS and GUNEY in their route toward paracaseolide A (Scheme 106).^[224]



Scheme 106. Paracaseolide A synthesis by KRAUS and GUNEY.^[224]

Bent tetracycle **336** was synthesized in five steps and was diastereoselectively converted to alcohol **337** by a sequential conjugate cuprate addition and enolate alkylation. Both reactions occurred from the convex side of the molecule and increased the curvature of the already bent tetracycle even further. The natural product paracaseolide A was accessed in three additional steps. The general strategy of adding substituents from the convex side to increase the curvature of the molecule will also be employed in the synthesis of the gracilin natural products (see 3.6 Third Strategy: Formal (3+2) Cycloaddition and Desymmetrization).

3.1.2 Gracilin Natural Products

3.1.2.1 The Gracilin Family – Isolation and Structure

The gracilin family of natural products is considered to belong to the large class of spongian diterpenoids.^[225] The general skeleton is shown in Figure 33.

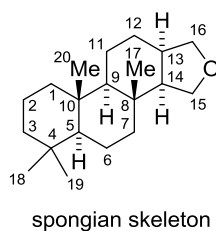


Figure 33. Spongian diterpenoid skeleton.^[225]

The first member of the gracilin family, the norditerpenoid gracilin A, was isolated from the Mediterranean sponge *Spongionella gracilis* (order: Dictyoceratida; family: Dysideidae) in 1985 by SICA and co-workers (Figure 34).^[226] In the same year, this research group also reported the isolation¹² and structural elucidation of the first bisnorditerpenoid ever found in marine sponges, gracilin B.^[227] Further investigation of the sponge led to the identification of gracilins C, D, E and F.^[228,229] Almost twenty years later, the novel members gracilin G, H and I were discovered in *Spongionella pulchella* and additional members gracilin J, K and L from a *Spongionella* species were added in 2009.^[230,231] Structurally, the norditerpenoids of the gracilin family differ significantly from the bis- and trisnorditerpenoid members.

¹² The natural product was obtained from a MeOH/CHCl₃ extract after several flash column chromatographies on silica gel.

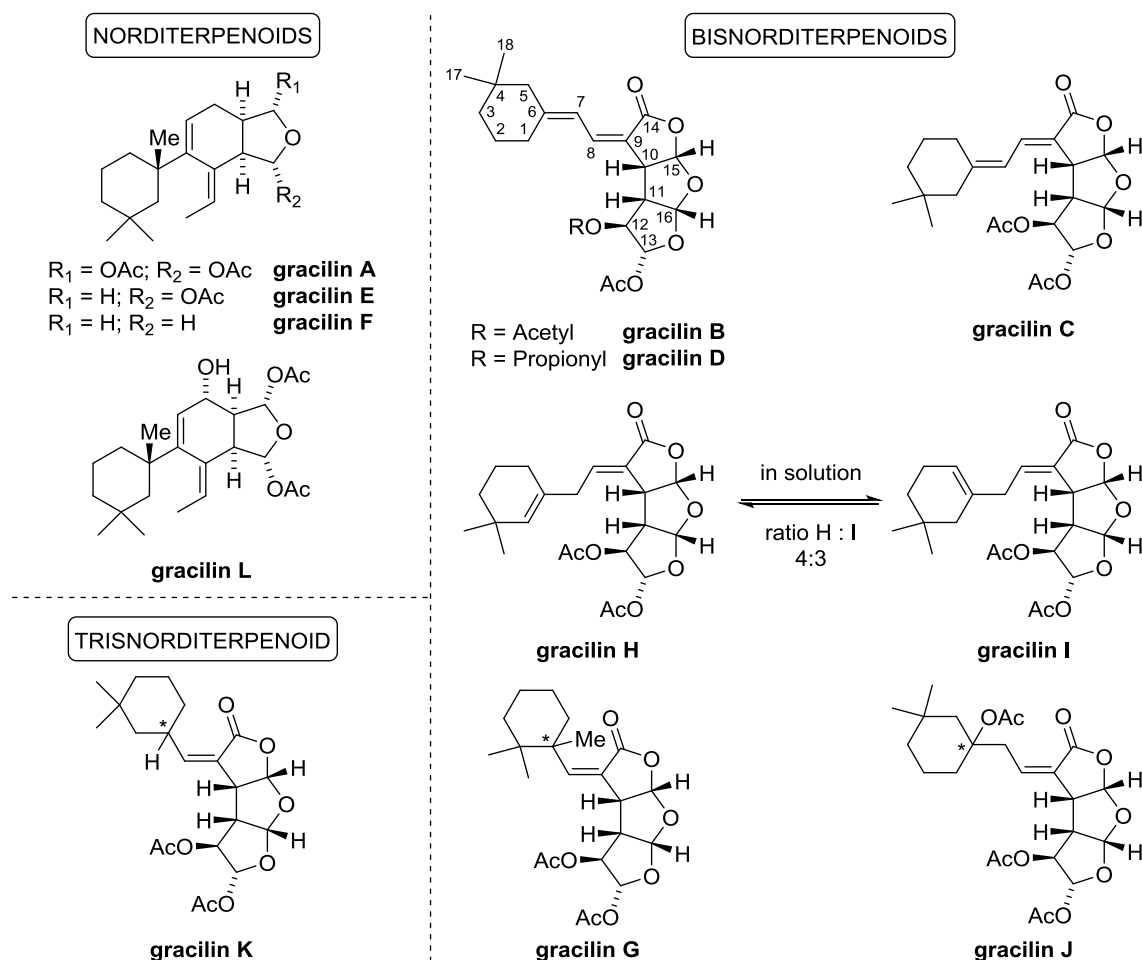


Figure 34. Members of the gracilin family of natural products.^[226–231]

This thesis focuses on the synthesis of the bis- and trisnorditerpenoids of this family, thus their structure will be described in more detail. The core of these natural products is characterized by a rare linear heterotriquinane skeleton, which can be classified as a hexahydrodifurofuranone. In essence, the core is the cyclic form of a trialdehyde carboxylic acid with additional oxidation at C12. The three furan-based heterocycles are all *cis*-fused, so that the molecule adopts the shape of an arc as can be seen in the X-ray single crystal structure of gracilin H (Figure 35).

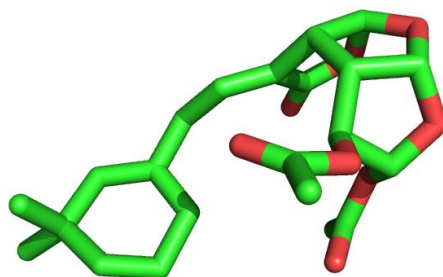


Figure 35. X-Ray single crystal structure of gracilin H; H atoms omitted for clarity; CCDC: 702621.
Color code: green = carbon, red = oxygen.

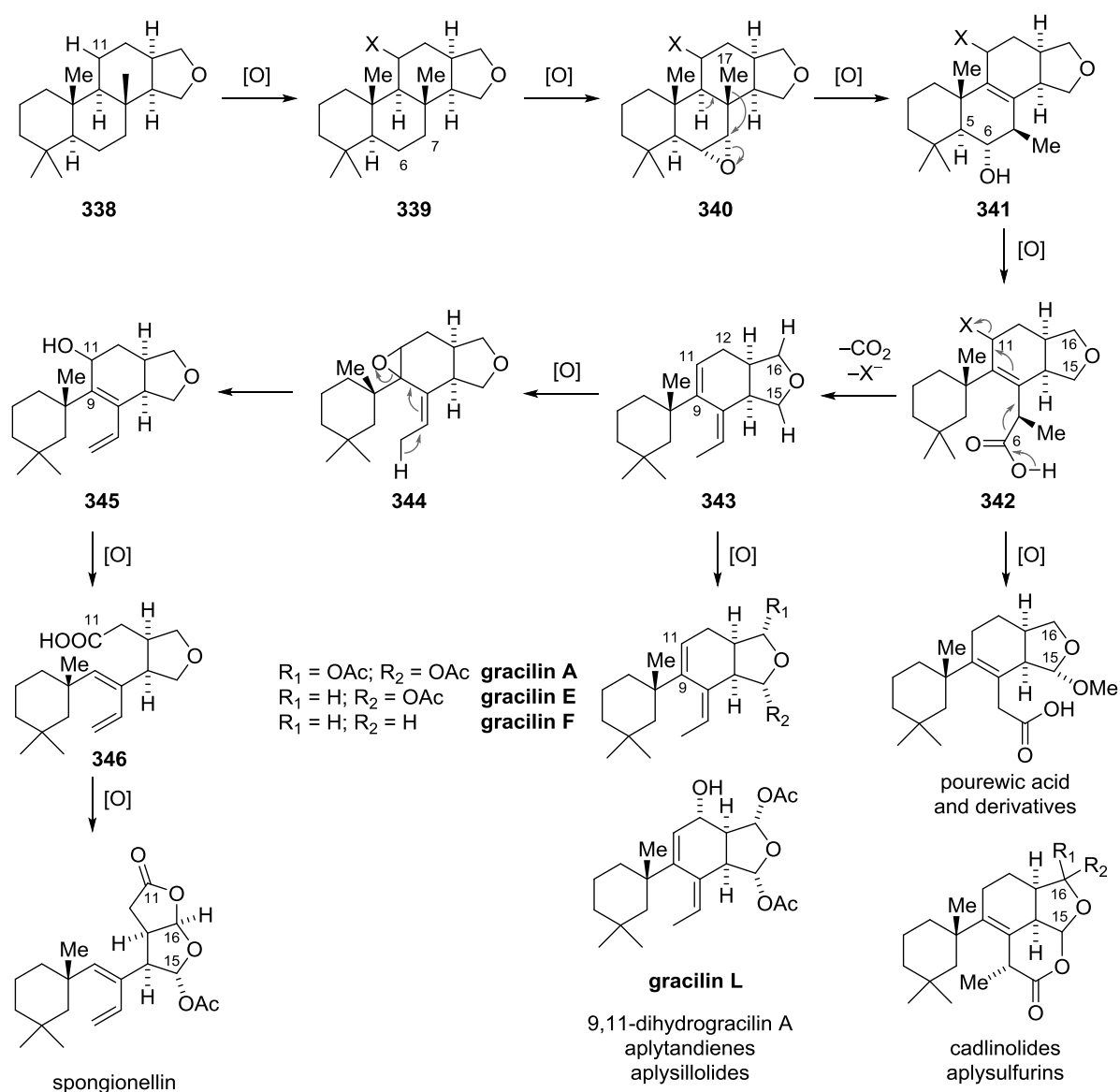
The acetate group at C12 points to the convex face whereas the one at C13 is situated on the concave side of the molecule. Overall, the core of this family of natural products features six stereogenic centers that are all adjacent to each other. The only structural difference within the bis- and trisnorditerpenoid members, apart from gracilin D possessing a propionate instead of an acetate group at C12, is the α -substituent of the lactone. In all structures, the substituent features a six-membered ring containing a *gem*-dimethyl group that is attached to the heterotriquinane by a linear carbon chain. The linker length varies from one to two carbon atoms and can have different degrees of unsaturation. The olefins can either possess (*Z*)- or (*E*)-configuration. Diene systems are either skipped or conjugated. The side chain attached to the α -position of the lactone can contain another stereocenter, the relative configuration of which is still unknown.

3.1.2.2 Biosynthesis of the Gracilin Natural Products

Many members of the spongian diterpenoids are oxidatively metabolized to other natural products.^[225] A comparison of the norditerpenoid and especially the bis- and trisnorditerpenoid members of the gracilin family with the spongian skeleton reveals that these natural products must also have undergone extensive metabolic processing. A biosynthetic route from the spongian skeleton to the gracilane one, the skeleton of gracilin A, E, F and L, was proposed, whereas the biogenesis of the other members still remains unclear (Scheme 107).^[225]

According to the proposal, starting from the spongian skeleton **338**, the C11 position is oxidized (**339**) and an epoxidation occurs at C6/C7 to afford epoxide **340**. This undergoes a WAGNER–MEERWEIN rearrangement of the C17–Me group to furnish secondary alcohol **341**, which provides a handle for oxidative C5–C6-bond cleavage to carboxylic acid **342**. The diterpenoid loses carbon atom C6 by a subsequent GROB-type decarboxylation that expels the leaving group at C11 to yield norditerpenoid **343**. The gracilin natural products can be accessed from there by further cyclic ether oxidation at C15/C16 for gracilin A, E and F and additionally at C12 for gracilin L. In addition, related metabolites with this skeleton such as the aplytandienes and aplysillolides are accessible *via* this pathway.^[232]

The biosynthetic hypothesis was supported by the fact that the existence of several other spongian-derived diterpenoids could be explained by this pathway. Prevention of the decarboxylation of carboxylic acid **342** and further oxidation of the cyclic ether at C15 or C16 can either yield the pourewic acid derivatives or the cadlinolide and aplysulfurin skeletons, all diterpenoid natural products. Furthermore, oxidation of norditerpenoid **343** at C9/C11 to epoxide **344** could trigger another elimination reaction to give rise to diene **345**, which after oxidative fissure of the C9–C11 bond to carboxylic acid **346** could afford spongionellin, a congener of the gracilin natural products, after another oxidation step.

Scheme 107. Biosynthesis of spongian diterpenoid derivatives.^[225]

3.1.2.3 Bioactivity of the Gracilin Natural Products

The gracilin natural products were identified as antioxidants, which might feature neuroprotective properties.^[233] Neurons have a higher energy demand compared to other cells, the supply of which is ensured by the increased production of ATP molecules in mitochondria.^[234] Therefore, these cells require a high amount of the total oxygen in the human body. The reduction of oxygen by electrons from the electron transport chain can lead to reactive oxygen species (ROS), which are detrimental to the cell.^[235] Several intracellular enzymatic and non-enzymatic defense mechanisms are then activated.^[233] However, the outperformance of these mechanisms by the ROS production, a situation called oxidative stress, ultimately results in apoptosis. The death of neuron cells is of central importance in many neurodegenerative diseases such as ALZHEIMER's or PARKINSON's disease. Gracilin J showed neuroprotective properties in cells under oxidative stress induced by H_2O_2 .^[233] In a

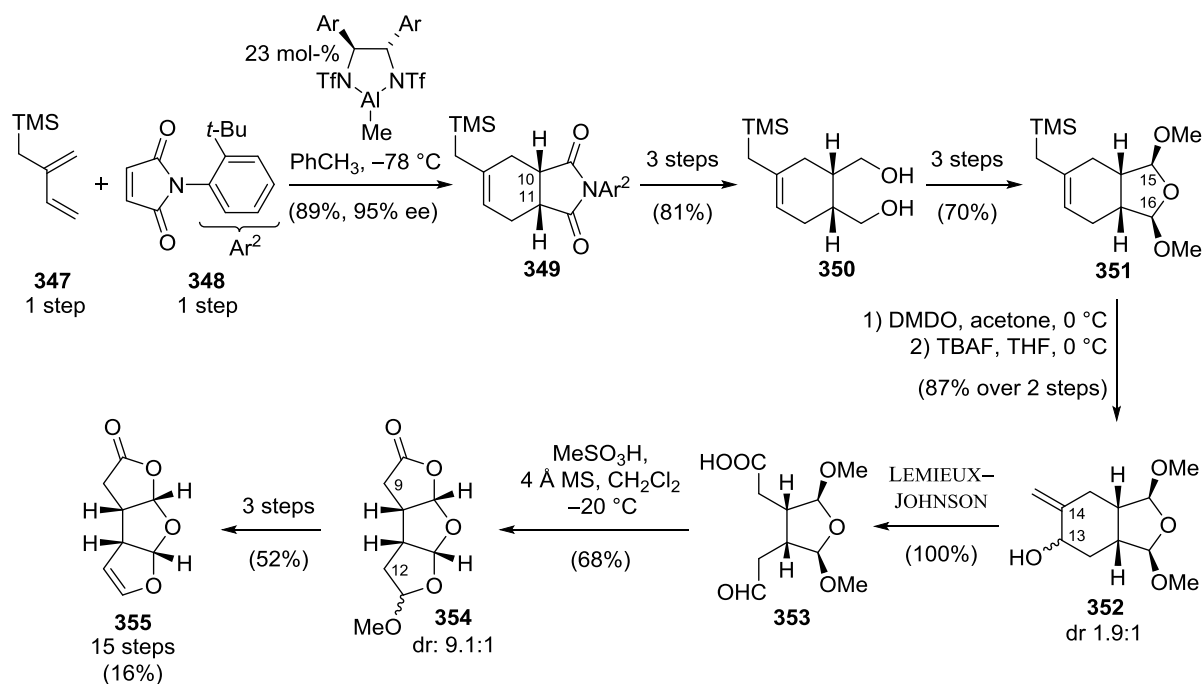
control experiment without gracilin J, the viability decrease d of cells from the primary cortical neurons of mice incubated with $c = 200 \mu\text{M}$ H_2O_2 was $d = 28.7\% \pm 1.1\%$, meaning almost 30% of the cells underwent apoptosis. However, co-incubation of H_2O_2 and gracilin J at $c = 0.1 \mu\text{M}$ protected the cells, showing a total viability $v = 92.0\% \pm 5.6\%$. Thus only around 8% of the cells underwent apoptosis. The action of gracilin J could not be elucidated on a mechanistic level.

Gracilin G, H and I were found to be cytotoxic against a range of human cancer cells.^[230] The values of the concentration of 50% maximal inhibition of cell proliferation (GI_{50}) were moderate in the μM -range. In cytotoxicity tests against leukemia, gracilin H, I, J and K were also found to be cytotoxic with IC_{50} in the μM -range, but the selectivity over healthy cells was poor. Gracilin B was found to inhibit the cell adhesion of tumor cells to extracellular matrix proteins.^[230] As such, it could disrupt the tumor-cell communication with the extracellular space and therefore potentially arrest tumor growth.

3.1.2.4 COREY Synthesis of Gracilin B and C

Due to their unusual tricyclic heterotriquinane skeleton, the gracilin molecules have attracted attention as synthetic targets. In 1995, COREY and LETAVIC reported the first and thus far only successful total synthesis of gracilin B and C in 20 and 21 steps with an overall yield of 6% and 8% respectively.^[236,237] The overall yield corresponds to an average yield of 87% (gracilin B) and 89% (gracilin C) per step. Strategically, their synthesis relied on the stereoselective installation of the *cis*-relation at C10/C11 by a concerted [4+2]-cycloaddition. Oxidative cleavage of the bicyclic ring should then afford the gracilin tricycle, which would require further manipulations to give rise to the natural products. Rather late installation of the lactone α -substituent was envisioned to provide a synthetic route toward gracilin B and C.

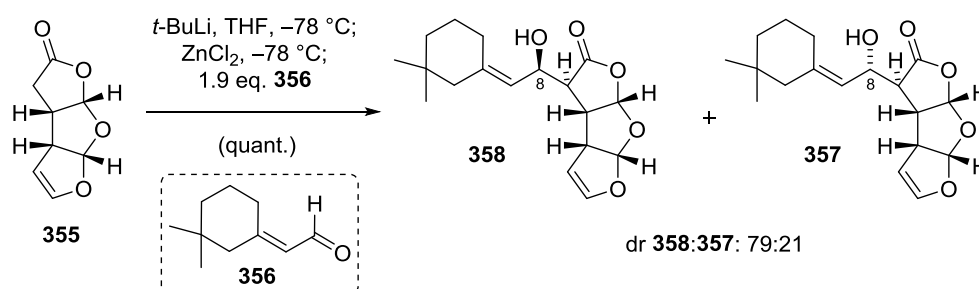
The synthesis commenced with an asymmetric LEWIS acid-catalyzed DIELS–ALDER reaction developed in the COREY laboratory between diene **347** and maleimide **348** to furnish *cis*-bicycle **349** in excellent yield and enantiomeric excess (Scheme 108).^[238] Thus, the first step already set the stereocenters that provide the stereocontrol in the following steps. Conversion of the succinimide moiety in **349** to diol **350** was accomplished by stepwise reduction. The desired 1,4-dialdehyde motif at C15/C16 was introduced by subsequent double SWERN oxidation and protection to yield tetrahydrofuran **351**.



Scheme 108. Asymmetric DIELS–ALDER reaction in the first part of COREY's gracilin synthesis.^[236,237]

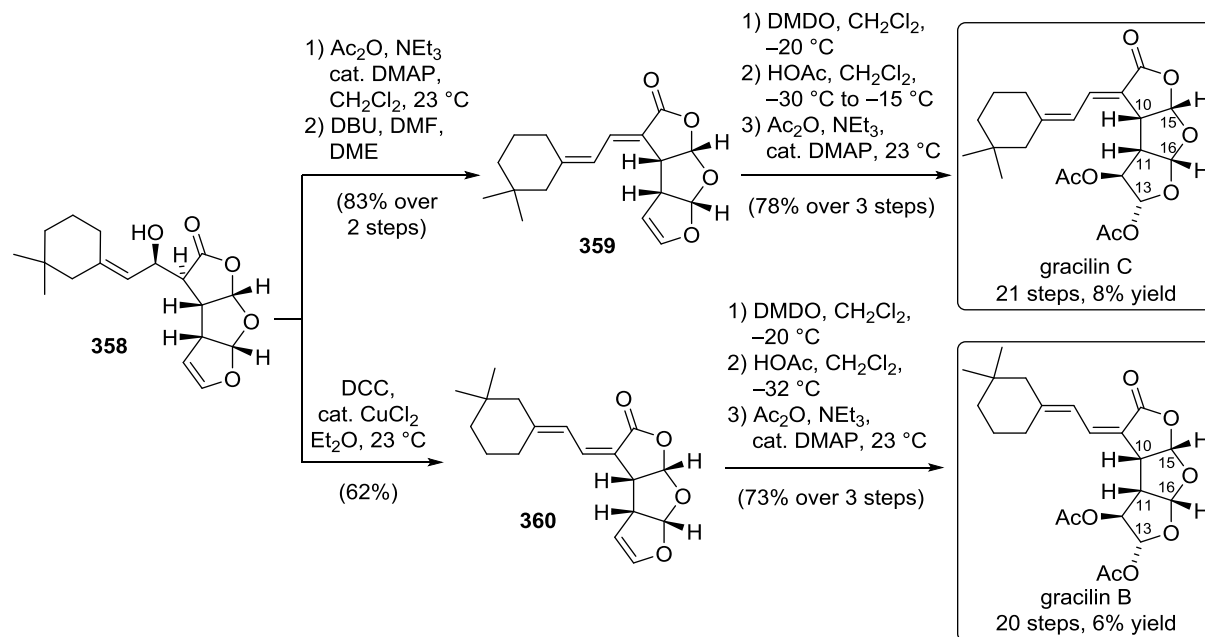
In preparation of the oxidative cleavage of the cyclohexene part, the *C*13/*C*14 olefin was epoxidized and the epoxide opened by generation of a neighboring silicate anion to yield exocyclic methylene **352** as an inconsequential mixture of diastereomers. The following LEMIEUX–JOHNSON oxidation allowed for the generation of the correct oxidation states at *C*13 and *C*14 with concomitant ring opening to labile aldehyde acid **353**. Acid-mediated acetalization resulted in the formation of the desired tricycle **354**, still lacking oxidation at *C*12 and a substituent at *C*9. Elimination of MeOH to dihydrofuran **355** was realized in three steps *via* replacement by a thiol and subsequent sulfoxide elimination.

COREY and LETAVIC then first installed the diene side chain in quantitative yield by aldol addition of the zinc-enolate of lactone **355** to an excess of unsaturated aldehyde **356**, which selectively approached from the convex face (Scheme 109). The resulting 4:1 mixture of diastereomers at *C*8 could be separated. Whereas minor alcohol **357** could also be used for the synthesis of gracilin C, it was demonstrated that the major diastereomer **358** can be taken forward to gracilin B and C.



Scheme 109. Face-selective aldol addition for the installation of the side chain.^[236,237]

The completion of the aldol condensation could either be achieved *via* elimination of an acetate to yield (*E*)/(*E*)-diene **359** or replacement of the secondary alcohol with a chloride and subsequent elimination to give (*Z*)/(*E*)-diene **360** (Scheme 110). Selective epoxidation of the dihydrofuran part afforded an epoxide, which was opened in acetic acid and the resulting alcohol acetylated to complete the synthesis of either gracilin B or C. The epoxide opening occurred selectively from the concave side of the molecule, which installed the correct stereochemistry at C13.

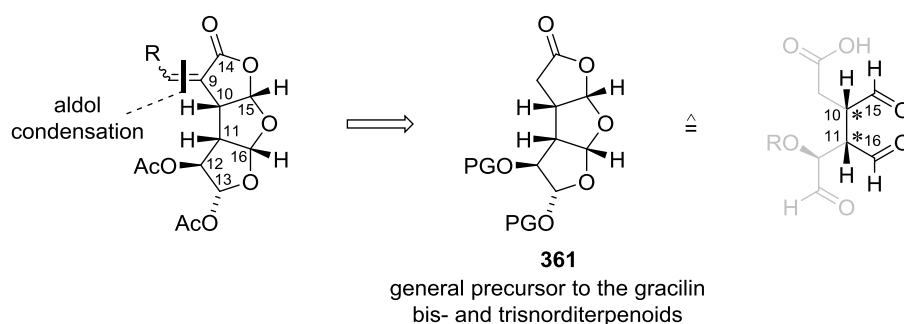


Scheme 110. Completion of the synthesis of gracilin B and C.^[236,237]

The COREY synthesis rapidly and efficiently sets the desired configurations at C10 and C11, but requires several redox manipulations to obtain the correct oxidation state at C15 and C16. The common tricyclic precursor **355** allows for the preparation of both natural products, but access to dihydrofuran was only possible after a three-step sequence to effect the elimination of MeOH from acetal **354**. However, the *endo*-substituent at C13 was effectively introduced by stereoselective epoxide opening.

3.2 Project Outline

The project focused on the identification of a step-economic and general access to the structurally unusual gracilin natural products. Recently, interest in gracilin and more general spongian-derived natural products has increased due to their intriguing biological activity.^[239] However, an efficient synthesis that rivals the isolation from Nature is yet to be established for further detailed investigations. Novel members of the gracilin family have neither been stereochemically assigned nor prepared. To provide a general entry to the bis- and trisnorditerpenoid gracilin natural products, a late-stage aldol condensation inspired by the work of COREY and LETAVIC was envisioned (Scheme 111).^[236] A precursor such as tricycle **361** would feature the correct oxidation states for all carbon atoms, a major advantage over the COREY synthesis.



Scheme 111. General retrosynthesis of gracilin natural products with late-stage aldol condensation.

The retrosynthetic strategies toward the unusual skeleton **361** of the gracilin bis- and trisnorditerpenoids were to take advantage of powerful pericyclic or metal-catalyzed reactions and will be discussed in due course. Special attention was given to the synthesis of the central 1,4-dialdehyde motif with trisubstituted stereocenters in the α -positions (C10 and C11). Although this motif is often synthesized *via* the potent DIELS–ALDER reaction, alternatives are sought-after and would greatly enrich the synthetic methodology.^[236,240,241]

In addition, it was unknown whether the substituent at C13 points to the concave side for thermodynamic or kinetic reasons or both (Figure 36). Although the steric hindrance on the concave side should be sizeable, the C13 substituent could also try to avoid steric repulsion and parallel dipole moments with the C12 acetate group (**A**). In addition, an anomeric effect, depicted as **B**, could potentially favor the *anti*-relationship between the two. However, this *trans*-arrangement could also represent the result of a neighboring group effect from the C12 acetate during the biosynthesis of the gracilin natural products (**C**).

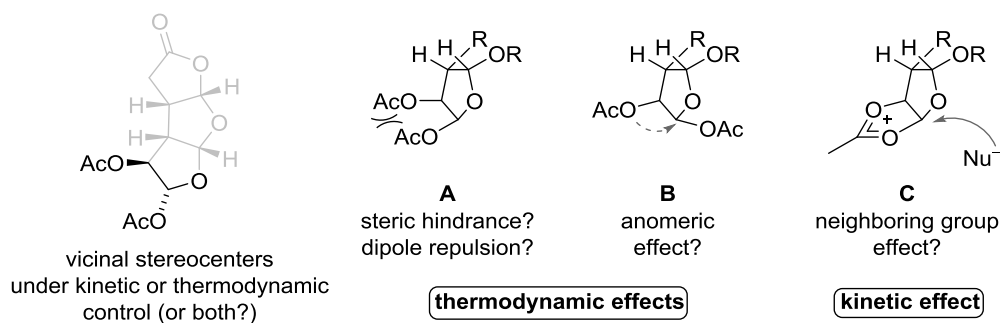


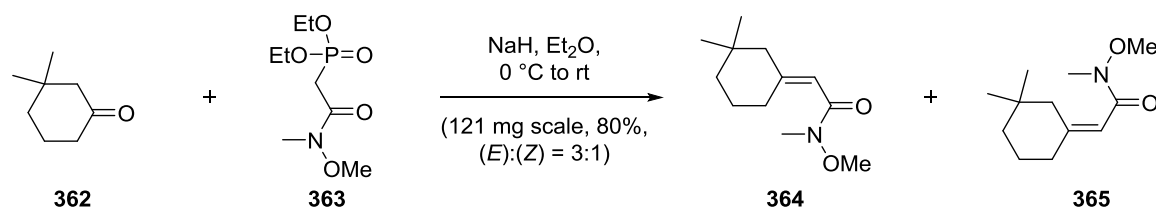
Figure 36. Stereochemical control in gracilin natural products either through thermodynamic or kinetic effects.

Since precursor **361** would not possess acyl protecting groups such as acetate due to their incompatibility with the following aldol condensation, it would become apparent whether the *anti*-relationship of the C12 and C13 substituents results from a thermodynamic or kinetic effect. If the concave side is thermodynamically disfavored for the C13 substituent, the precursor **361** without acyl protecting groups could preferentially show a *cis*-relationship between the C12 and C13 residues.

Different retrosynthetic strategies toward tricycle **361** were pursued and the results will be presented in the following chapters. Each retrosynthesis will also contain a part in which its potential benefit to total synthesis or methodology will be highlighted.

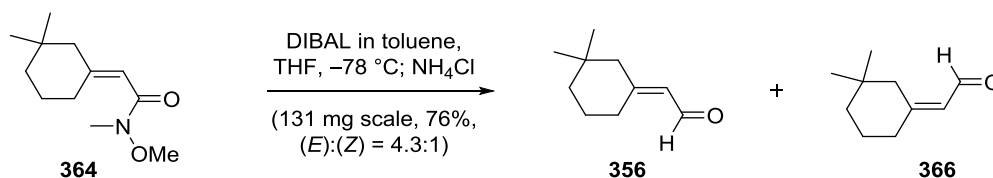
3.3 Synthesis of the Side Chain of Gracilin B and C

The initial objective of the project was to synthesize gracilin B and C, which had already been prepared by COREY and LETAVIC, and then access further members of the gracilin family. To this end, the aldehyde for the final aldol condensation was synthesized from commercially available starting materials in a two-step procedure. A HORNER–WADSWORTH–EMMONS olefin synthesis involving ketone **362** and phosphonate **363** provided WEINREB amides **364** and **365** in very good yield as a 3:1 mixture of diastereomers in favor of the desired one **364** (Scheme 112).



Scheme 112. HORNER–WADSWORTH–EMMONS olefination to unsaturated WEINREB amides **364** and **365**.

The isomers were readily separated by flash column chromatography and WEINREB amide **364** was subjected to reduction (Scheme 113). Treatment with DIBAL at low temperatures resulted in the formation of a mixture of aldehydes **356** and **366** in good yield after purification. Mechanistically, the aldehyde can isomerize *via* tautomerization to a dienol. Due to this tendency, it will therefore be necessary to effect this transformation and the purification under milder conditions to avoid the undesired formation of isomer **366**. Nevertheless, the required aldehyde **356** for gracilin B and C was successfully prepared.

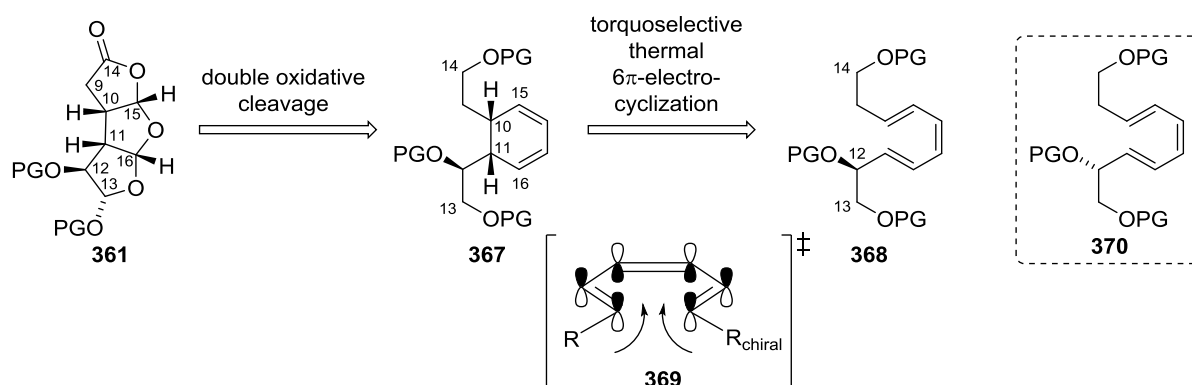


Scheme 113. Reduction of WEINREB amide **364** to mixture of aldehydes.

3.4 First Strategy: Torquoselective 6π -electrocyclization

3.4.1 Retrosynthetic Analysis

In the first synthetic strategy, it was intended to prepare the central 1,4-dialdehyde motif in tricycle **361** by a double oxidative cleavage of a cyclic diene like **367** (Scheme 114). The resulting C15 and C16 aldehydes would be converted to tricycle **361** under suitable cyclization conditions. It was expected that this alternative synthesis of 1,4-dialdehydes by ozonolysis or LEMIEUX–JOHNSON oxidation would largely avoid reactive intermediates and enable a novel access to this sensitive functionality. Diene **367** was planned to arise from a torquoselective thermal 6π -electrocyclization of (*E*)/(*Z*)/(*E*)-triene **368**. This key step was chosen since only a disrotatory pericyclic reaction would ensure the *cis*-relationship between the C10/C11 substituents if the more practical *trans*-olefins were to be employed. Any oxidation state at carbon atoms C13 and C14 would be possible.

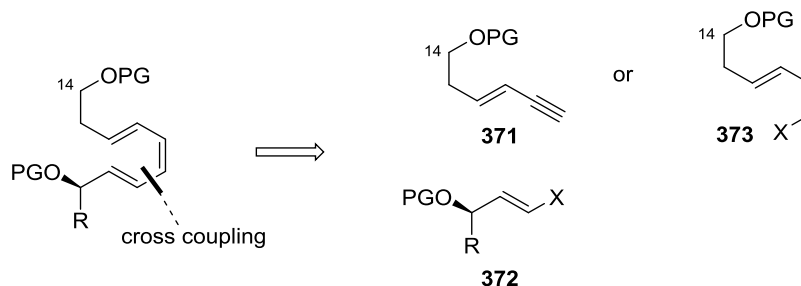


Scheme 114. Retrosynthesis plan involving a torquoselective thermal 6π -electrocyclization.

It was planned to control the absolute configuration of the two new stereocenters by an already existing one at C12 in close proximity to the triene. Despite the required high temperatures, thermal 6π -electrocyclizations have previously been shown to be able to proceed in a highly torquoselective fashion with cyclic substituents on the triene.^[242] In part, this strategy was aimed at establishing diastereoselective electrocyclizations as a more broadly applicable synthetic method and to provide mechanistic rationales and guidelines for the torquoselectivity. Since it was difficult to predict the extent and direction of the stereochemical influence of the existing stereocenter in transition state **369**, it was expected that several substrates with protecting groups of different electronic and steric properties would need to be prepared. Furthermore, if necessary, it was considered to invert the absolute configuration of the C12 stereocenter in triene **370** and later correct the stereochemistry by a MITSUNOBU inversion. A potentially more atom-economic strategy *via* the oxidative cleavage of a cyclobutene by photochemical 4π -electrocyclization was discarded because satisfactory results can only be achieved in polycyclic systems.

The required triene was to be synthesized by cross-coupling methodology in a convergent way (Scheme 115). Thus, the triene was traced back to equally complex building blocks, enyne **371** and

vinyl halide **372**, that could be coupled in a SONOGASHIRA reaction with subsequent alkyne reduction. Enyne **371** could feature any oxidation state from alcohol to carboxylic acid at carbon atom C14 and the residue R in vinyl halide **372** would need to be a synthetic equivalent of an aldehyde. The use of alkenes, epoxides and primary alcohols was envisioned. Alternatively, the cross coupling could be realized in a STILLE or SUZUKI reaction with a diene coupling partner like **373**, where either of the components **372** or **373** could be the organometallic species.



Scheme 115. Retrosynthesis of triene by cross-coupling methodology.

Since the major aim was to test the electrocyclization key step, it was focused on a rapid access to trienes of type **368**.

3.4.2 Introduction to 4π - and 6π -Electrocyclization

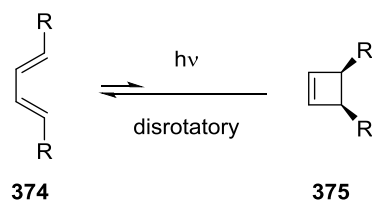
Electrocyclizations are pericyclic reactions in which one σ -bond is formed at the expense of one π -bond ($\Delta\sigma = 1$). As such, they differ from cycloadditions ($\Delta\sigma = 2$) and sigmatropic rearrangements ($\Delta\sigma = 0$), but are also concerted and therefore subject to the WOODWARD–HOFFMANN rules.^[2] The stereochemical outcome of electrocyclizations depends on whether they were triggered by thermal energy or by irradiation (Table 7). Whether an electrocyclization proceeds in a conrotatory or disrotatory fashion also depends on the number of electrons involved.

Table 7. Stereochemical requirements of thermal and photochemical electrocyclizations; $n = \mathbb{N}$.

number of electrons	thermal	photochemical
$4n$	conrotatory	disrotatory
$4n + 2$	disrotatory	conrotatory

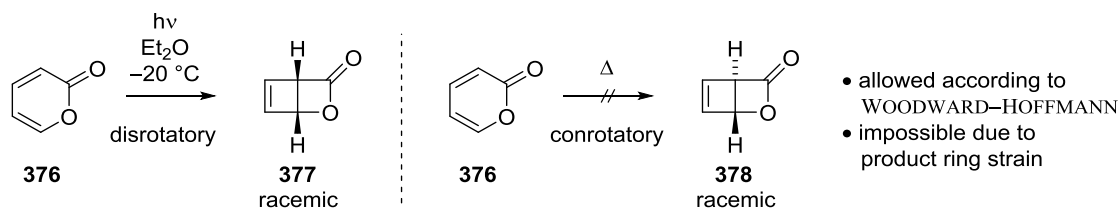
Herein, only thermal 6π - and photochemical 4π -electrocyclizations, both disrotatory, will be covered due to their relevance to this thesis. Therefore, typical reaction conditions and challenges as well as torquoselectivity will be discussed. Other types of this pericyclic reaction have been reviewed in the context of biomimetic syntheses.^[42]

Thermodynamically, 4π -electrocyclizations usually proceed in direction of the open diene **374** rather than the strained cyclobutene **375** (Scheme 116).



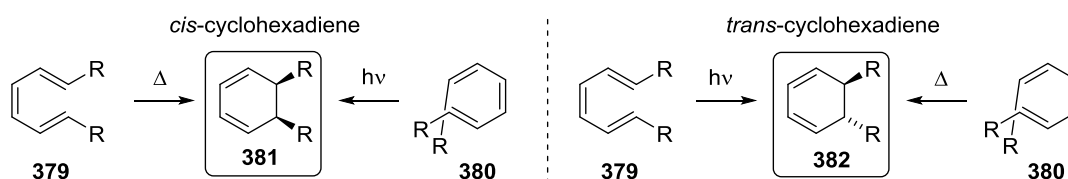
Scheme 116. Disrotatory photochemical 4π -electrocyclization.

Although a σ -bond is formed at the expense of a π -bond, which is a general thermodynamic driving force of electrocyclizations, the formation of cyclobutene is disfavored due to its immense ring strain and negative reaction entropy. However, if the conformation of the starting material is constrained in a cycle or a polycycle, cyclobutenes will form from dienes under irradiation with UV light. COREY and STREITH have taken advantage of this feature in their efforts toward cyclobutadiene (Scheme 117).^[243] The starting 2-pyrone (**376**) was successfully converted to bicycle **377** in a disrotatory 4π -electrocyclization. Although both photochemical and thermal electrocyclizations are allowed in a given conjugated polyene according to the WOODWARD–HOFFMANN rules, the stability of the product has to be considered. For instance, the electrocyclization of pyrone **376** would never occur thermally since these reactions could only proceed in a conrotatory fashion to yield *trans*-bicycle **378** with a preventively high ring strain.



Scheme 117. Electrocyclizations of 2-pyrone triggered by light or thermal energy.^[243]

6π -electrocyclizations transform a triene such as **379** or **380** into a 1,3-cyclohexadiene like **381** or **382** and *vice versa*.^[244] Both *cis*- and *trans*-substitution of the cyclohexadiene can hereby be achieved either by switching the activation mode from thermal to photochemical or by changing the configuration of one olefin (Scheme 118). However, although symmetry-allowed, these electrocyclizations usually possess considerable activation barriers due to the required highly-ordered transition state.^[245]

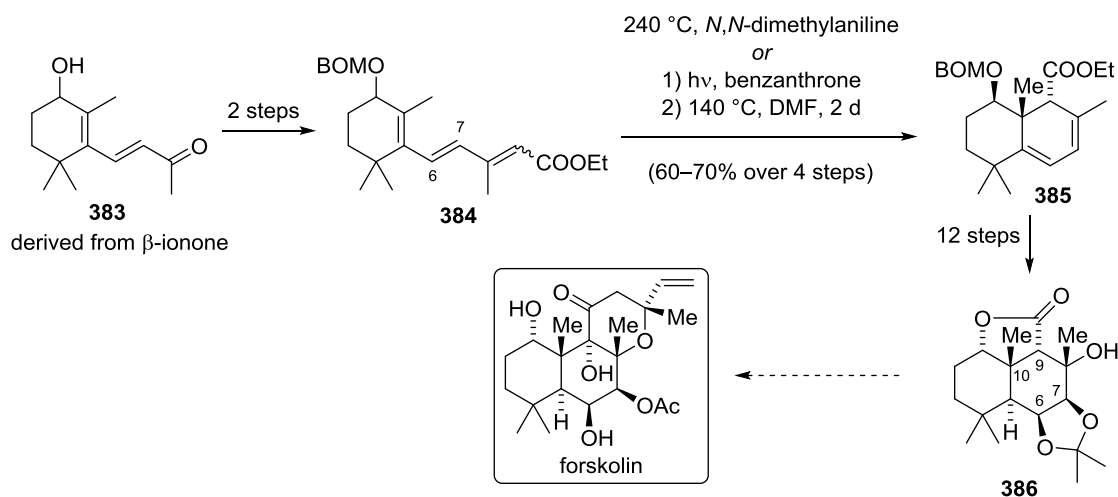


Scheme 118. Stereochemistry of 6π -electrocyclizations.^[244]

Due to certain drawbacks, thermal 6π -electrocyclizations have not been frequently used in total syntheses.^[42] Whereas light can provide the required activation energy more easily, these

electrocyclizations can be difficult to effect thermally since temperatures of $T \geq 150\text{ }^{\circ}\text{C}$ are often necessary.^[246] Furthermore, the preparation of the central (*Z*)-configured olefin can be challenging and the olefin differentiation in the resulting cyclohexadiene problematic. Achieving absolute stereocontrol of the newly formed stereocenters is also not considered straightforward. However, the application of these electrocyclizations can be highly beneficial for cascade reactions since cyclohexadienes can be employed in *e.g.* DIELS–ALDER reactions.

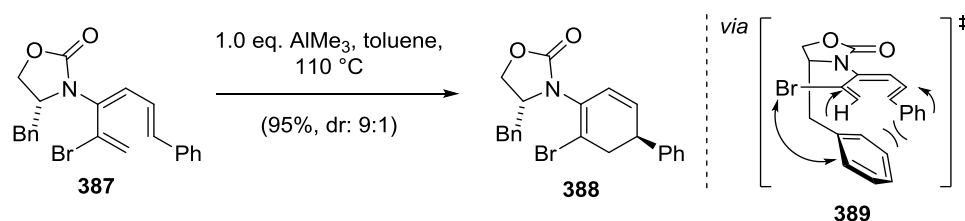
In the following, selected examples of thermal 6π -electrocyclizations in total synthesis will be highlighted. In their efforts toward the oxygenated diterpenoid forskolin, the CHA group made use of a thermal 6π -electrocyclization for forging the C9–C10 bond (Scheme 119).^[247] Starting material **383** was converted to triene **384** in two steps. The authors envisioned first the isomerization of the C6/C7 olefin to the required (*Z*)-configuration and a subsequent electrocyclic ring closure. Both transformations were either realized by heating to $T = 240\text{ }^{\circ}\text{C}$ or by isomerization of the olefin with light followed by a milder thermal disrotatory electrocyclozation at $T = 140\text{ }^{\circ}\text{C}$ to yield diene **385**.



Scheme 119. Synthetic efforts toward forskolin by the CHA group.^[247]

To their benefit, triene **384** and diene **385** were not sensitive to the harsh reaction conditions that the pericyclic reaction required. A similar transformation under related conditions was also employed by JUNG and MIN in the synthesis of arisugacin A.^[248] The resulting cyclohexadiene **385** was taken forward to lactone **386**, which was envisioned as an intermediate in the synthesis of forskolin.

HSUNG and co-workers were able to demonstrate a 1,6-induction of an attached auxiliary in LEWIS acid-accelerated thermal electrocyclizations (Scheme 120).^[249] This methodology was later used in synthetic efforts toward atropurpuran.^[250]



Scheme 120. Diastereoselective thermal 6π -electrocyclization.^[249]

Starting material **387** containing an EVANS auxiliary was cyclized in the presence of AlMe_3 to accelerate the ring closure, decrease the necessary temperature and therefore accomplish higher diastereomeric ratios. Cyclohexadiene **388** was obtained in excellent yield and good diastereomeric ratio *via* transition state **389**. The arrangement in the latter was rationalized by a preferential rotation of the Ph-ring away from the Bn substituent of the chiral auxiliary, which in turn avoids steric clash with the halogen atom. Such preferential rotation of substituents in electrocyclizations is named a torquoselectivity. Depending on the substrate, the authors also observed aromatization of the cyclohexadiene product under the reaction conditions, a common side reaction. Addition of radical inhibitors or milder reaction conditions through catalysis, as shown by the TRAUNER group, can help to decrease these undesired byproducts.^[251] However, catalysis by LEWIS acids will only be feasible if suitable LEWIS bases are attached to the triene (*e.g.* oxazolidones, esters, ...).

In 2006, YU *et al.* disclosed their computational results of substituent effects on thermal 6π -electrocyclization.^[246] They were able to validate previous reports that a C1 substituent in a triene usually slightly decelerates the reaction due to steric hindrance. Monosubstitution at C2 and C3 however is beneficial for the rate due to ground-state destabilization and conformational restriction.^[252] The authors were able to identify that disubstitution of trienes with an electron-donating and -withdrawing group in suitable positions can render an electrocyclization very facile through captodative effects (Figure 37). However, 1,6-disubstitution as presented in this thesis was considered disfavored due to the increased steric hindrance of both substituents.

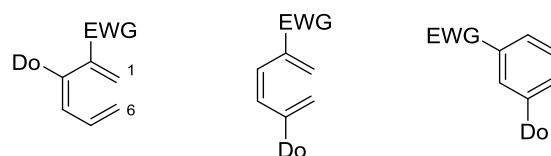
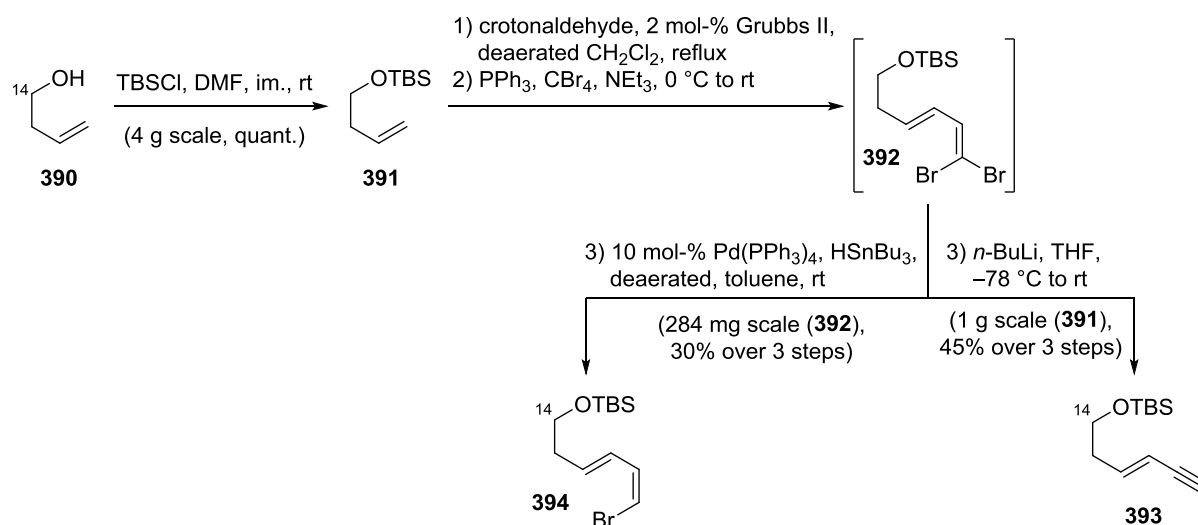


Figure 37. Substrates with very facile electrocyclization.^[246]

3.4.3 Results and Discussion

3.4.3.1 Preparation of Achiral Coupling Partner

The achiral coupling partner of type **371** or **373** was planned to feature the alcohol oxidation state at carbon atom C14 due to the ease of its synthesis (Scheme 121). Commercially available alcohol **390** was quantitatively protected as silyl ether **391**, which was subjected to a cross metathesis with crotonaldehyde. The resulting aldehyde proved to be volatile and was immediately subjected to a RAMIREZ olefination, furnishing dibromo alkene **392**.



Scheme 121. Synthesis of achiral coupling partners, enyne **393** and bromo alkene **394**.

In order to complete the COREY–FUCHS alkyne synthesis, dibromo alkene **392** was treated with *n*-BuLi triggering the desired FRITSCH–BUTTENBERG–WIECHELL rearrangement to alkyne **393** in good yield over three steps. Alternative alkyne syntheses from the intermediate aldehyde such as the SHIOIRI reaction or the SEYFERTH–GILBERT homologation with the OHIRA–BESTMANN reagent did not lead to the desired product **393**.

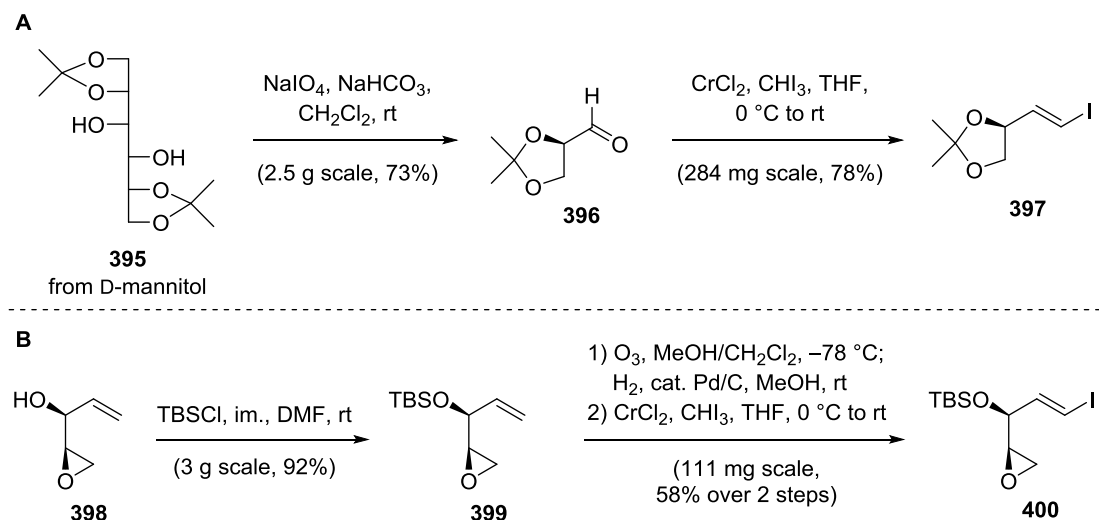
In order to increase the flexibility of the envisioned cross coupling, dibromo alkene **392** was also selectively reduced under Pd catalysis to afford (*Z*)-bromo alkene **394** in moderate yield over three steps.^[253] However, bromo alkene **394** proved to be unstable to light and noticeably isomerized to the (*E*)-isomer at room temperature. It was thus focused on enyne **393**.

3.4.3.2 Preparation of Chiral Coupling Partner

The coupling partner of type **372** contained a stereocenter, which either required chiral pool starting materials or asymmetric methodology. Concerning the aldehyde equivalent R, a primary alcohol and an epoxide were chosen that both can be oxidatively converted to an aldehyde.^[254] As

enyne **393** constituted the nucleophilic cross coupling partner in the envisioned SONOGASHIRA coupling, it was necessary to synthesize a suitable electrophile.

The first coupling partner was accessed from chiral pool starting materials (Scheme 122). Mannitol derivative **395** was oxidatively cleaved to aldehyde **396** according to a literature procedure.^[255] The following TAKAI olefination proceeded smoothly to give vinyl iodide **397**.



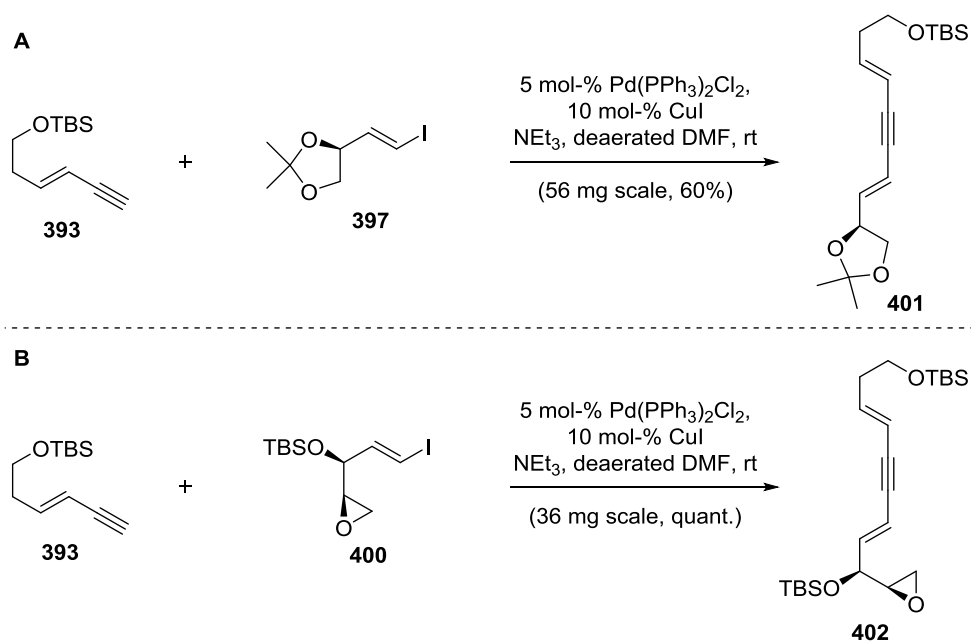
Scheme 122. A. Synthesis of dioxolane **397**. **B.** Synthesis of epoxide **400**.

In order to test an alternative building block, epoxy alcohol **398**, available by SHARPLESS asymmetric epoxidation of divinyl carbinol,¹³ was subsequently protected to yield silyl ether **399** (Scheme 122). Ozonolysis followed by reductive workup through catalytic hydrogenation gave a labile aldehyde, which was immediately converted to vinyl iodide **400** in a TAKAI olefination.

3.4.3.3 Building Block Coupling and 6π -Electrocyclization

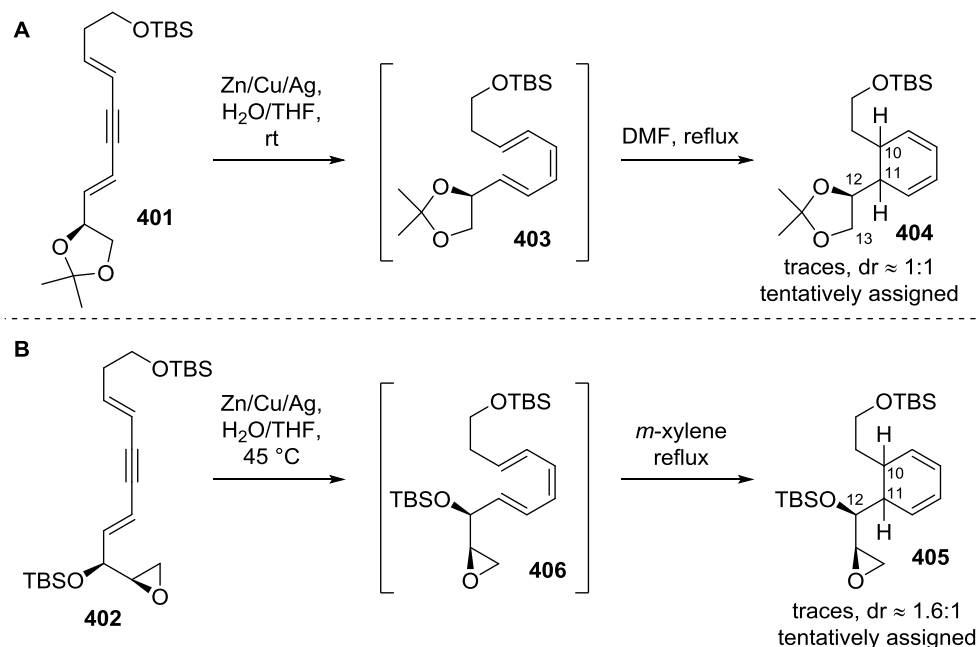
The Pd- and Cu-catalyzed coupling of enyne **393** with the respective vinyl iodides **397** and **400** in a SONOGASHIRA reaction proceeded smoothly to afford the dienyne **401** and **402** in good yield (Scheme 123).

¹³ Crude epoxy alcohol **398** was present in the TRAUNER research group. Purification by high-vacuum Kugelrohr distillation gave the pure starting material for this synthesis.



Scheme 123. Coupling of building blocks in SONOGASHIRA reaction.

Whereas alkynes with neighboring olefins can usually be selectively reduced to polyenes in LINDLAR hydrogenations,^[48–51] problems concerning overreduction have frequently been reported.^[256] It was thus focused on a heterogeneous reduction method involving activated Zn in a Zn/Cu/Ag couple (Scheme 124).^[257]



Scheme 124. A. Electrocyclization attempt with dioxolane **401**. B. Electrocyclization attempt with epoxide **402**.

The alkyne in **401** was readily reduced to give crude triene **403**, which was directly subjected to thermal electrocyclicization conditions. It was reasoned that the torquoselectivity would be under kinetic control, hence higher diastereomeric ratios were expected at lower temperatures. As mentioned in

chapter 3.4.2 Introduction to 4π - and 6π -Electrocyclization, electrocyclizations usually require higher temperatures than the refluxing temperature of DMF. Although the electrocyclization would probably not be complete under the employed conditions, valuable insight could be obtained concerning the degree of torquoselectivity. Indeed, a cyclohexadiene **404** was identified in the reaction mixture by NMR and HRMS, but only a 1:1 mixture of diastereomers was detected. Given that electrocyclizations are stereospecific, it was concluded that the chiral center at C12 was incapable of efficient stereoinduction. Epimerization of the newly formed stereocenters C10 and C11 by a radical mechanism is unlikely under these conditions since a strong C–H bond would have to be cleaved. Furthermore, loss of stereoinformation would then occur on both stereocenters, leading to more diastereomers. The reason for the low diastereoselection is probably the similar size of the oxygen atom of the dioxolane moiety and the C13 methylene.

Therefore, the electrocyclization to cyclohexadiene **405** was attempted with a sterically demanding TBS protecting group on the allylic alcohol of enyne **402** (Scheme 124). Analogous heterogeneous reduction to triene **406** set the stage for the subsequent electrocyclization. Xylene was chosen as the solvent since it does not decompose at refluxing temperatures in contrast to DMF. A cyclohexadiene was identified in the reaction mixture based on NMR and HRMS analysis and showed a poor diastereomeric ratio of 1.6:1. The product decomposed upon purification attempts.

Based on the observed low diastereomeric ratios even at comparably low temperatures, it did not seem promising to continue this synthetic strategy especially because the required trienes of type **403** or **406** do not possess suitable handles to catalyze the key electrocyclization by LEWIS acid coordination. It was reasoned that milder reaction conditions could result in higher diastereomeric ratios. The activation entropy of trienes **403** or **406** was considered immense, given that the most stable triene conformation would resemble the one shown in Figure 38 with *s-trans* configured bonds between the olefins. A possibility to reduce the activation entropy would be the installation of a cyclic substituent, *e.g.* as in triene **407**. The additional ring would lock the conformation of the triene in the *s-cis* configuration and thus favor the electrocyclization at lower temperatures. However, this strategy would significantly decrease the atom economy of the gracilin synthesis because the whole cyclic substituent would be removed in the subsequent ozonolysis or LEMIEUX–JOHNSON oxidation.

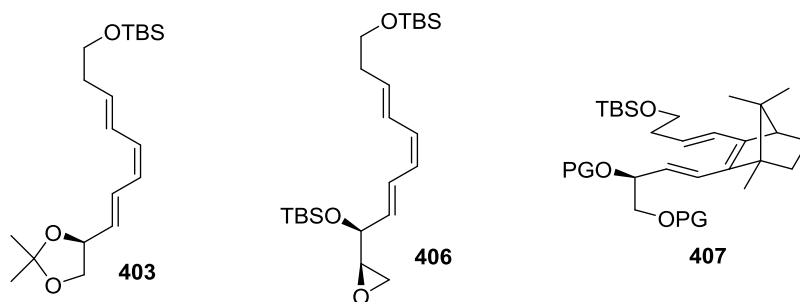


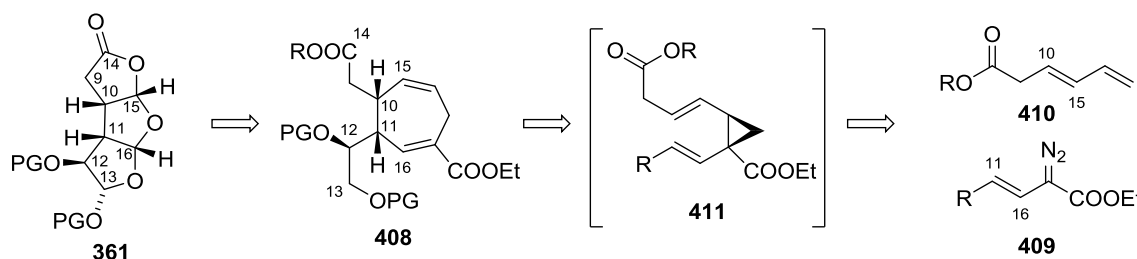
Figure 38. Stable conformation of trienes **403** and **406** and alternative substrate to reduce the temperature of the key electrocyclization.

Since in the meantime, an efficient, more step-economic strategy to another cyclic diene had been developed, the electrocyclization approach was discontinued. Although efficient torquoselectivity in thermal 6π -electrocyclizations could not be achieved, the results presented in this chapter have highlighted the efficiency of SONOGASHIRA couplings in complex settings and the alternative use of activated zinc for the selective reduction of alkynes flanked by olefins. The investigation of this route has led to a new versatile building block, vinyl iodide **400** that can find application in future total syntheses.

3.5 Second Strategy: Rhodium-Catalyzed Formal (4+3)-Cycloaddition

3.5.1 Retrosynthesis

As an alternative to the disrotatory 6π -electrocyclization for the synthesis of the required cyclic dienes, a Rh-catalyzed formal (4+3)-cycloaddition was envisioned (Scheme 125). Precursor **361** could be accessed by oxidative cleavage of cycloheptadiene **408**, which would stem from vinyl diazoacetate **409** and diene **410** *via* divinylcyclopropane **411** under Rh catalysis. Cycloheptadiene **408** could feature various oxidation states at carbon atoms C12, C13 and C14. The residue R in vinyl diazoacetate **409** should allow conversion to the C12/C13 substitution pattern in cycloheptadiene **408**.



Scheme 125. Rh-catalyzed formal (4+3) cycloaddition in the retrosynthetic strategy of gracilin natural products.

As discussed in 3.5.2.3 Intermolecular Cyclopropanation with Rhodium Carbenoids, Rh-catalyzed decomposition of vinyl diazoacetate **409** would result in *cis*-selective cyclopropanation of the terminal olefin of diene **410**, which would give rise to divinylcyclopropane **411**. A spontaneous, strain-releasing COPE rearrangement would then lead to the desired cycloheptadiene **408**. Since the COPE rearrangement proceeds stereoselectively, the success of the formal (4+3)-cycloaddition hinges on the diastereoselectivity of the initial *cis*-cyclopropanation. *trans*-Divinylcyclopropanes usually do not rearrange under the employed conditions so that low diastereoselectivities of the initial cyclopropanation will be reflected in lower yields of the cycloheptadiene product rather than its isolation as a diastereomeric mixture. Parallel oxidative cleavage of both olefins would furnish C15 and C16 aldehydes, which would be converted to tricycle **361**. However, the two olefins of skipped diene **408** are electronically and sterically distinct, which could be taken advantage of in a stepwise oxidative cleavage procedure.

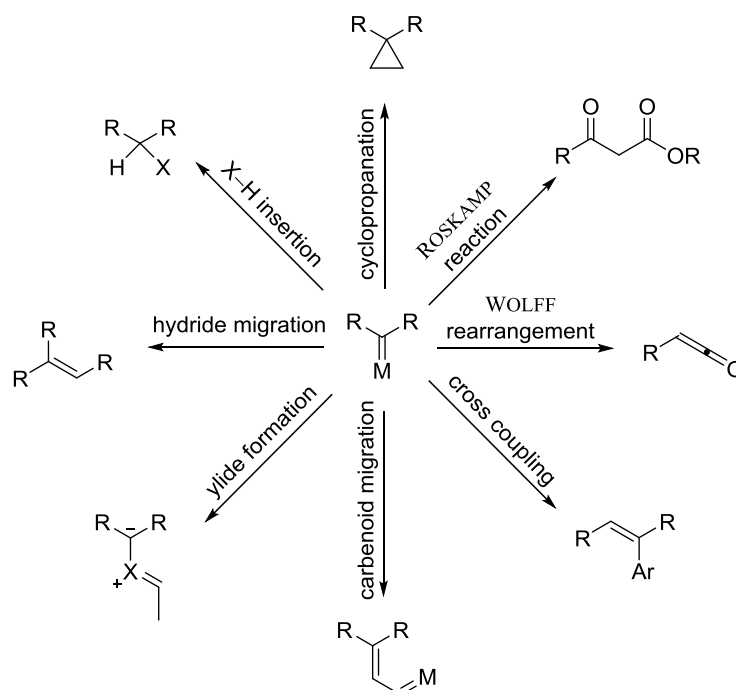
The success of the proposed retrosynthesis would expand the utility of the formal (4+3) cycloaddition methodology.^[258] Strategies involving this key step, mostly advanced by DAVIES and co-workers, have largely been employed for the synthesis of functionalized seven-membered rings.^[258] Therefore, the investigation of oxidative cleavage reactions with cycloheptadienes like **408** could render this methodology useful to the stereoselective preparation of a variety of other highly oxidized natural products beyond those featuring carbocyclic seven-membered rings. Furthermore, mostly electron-rich dienes with alkyl- or heteroatom substituents have thus far been employed.^[258–260] The envisaged diene **410** is not as electron-rich as previously employed dienes and the identification of

suitable reaction conditions for its conversion to cycloheptadiene **408** could be beneficial for future applications of the formal (4+3)-cycloaddition.^[261] Thus far, it has also not been studied whether an allylic stereocenter in vinyl diazoacetate **409** can control the stereoselectivity of the initial cyclopropanation and thus the diastereoselective installation of two further stereocenters. Diastereoselectivity was observed to be moderate when stereocenters were present in the diene reaction partner.^[262] Apart from this, only chiral auxiliaries attached to the ester moiety of the vinyl diazoacetates were used in this methodology.^[263–266]

As an advantage over the synthetic route presented in 3.4.1, the cycloheptadiene products **408** are not prone to aromatization and would also be formed under milder reaction conditions as compared to cyclohexadienes **367**. Most importantly, in case substrate control fails or favors the undesired diastereomer, the use of literature-precedent chiral Rh catalysts would enable a reagent-controlled stereoselective synthesis of the cyclic diene **408**. These advantages were thought to outcompete the slightly worse atom economy of this synthetic route.

3.5.2 Introduction to Rhodium-Catalyzed Formal (4+3)-Cycloaddition

The discovery of metal carbenoids as synthetic equivalents of very reactive carbenes has opened intriguing opportunities for their application in selective transformations and complex total syntheses.^[267] The metal stabilizes the electron-deficient carbene-like carbon center by forming a σ - and a π -bond in a resulting metal-carbene complex. As such, metal carbenoids engage in a variety of reactions such as cyclopropanation, X–H bond insertion (X = C, N, O, S, ...), hydride migration, ylide formation, carbenoid migration or metal-catalyzed coupling reactions.^[267–271] The investigation of carbenoids and carbenoid precursors has led to the development of named reactions like the WOLFF rearrangement, ARNDT–EISTERT homologation or the ROSKAMP reaction (Scheme 126).^[272–274]



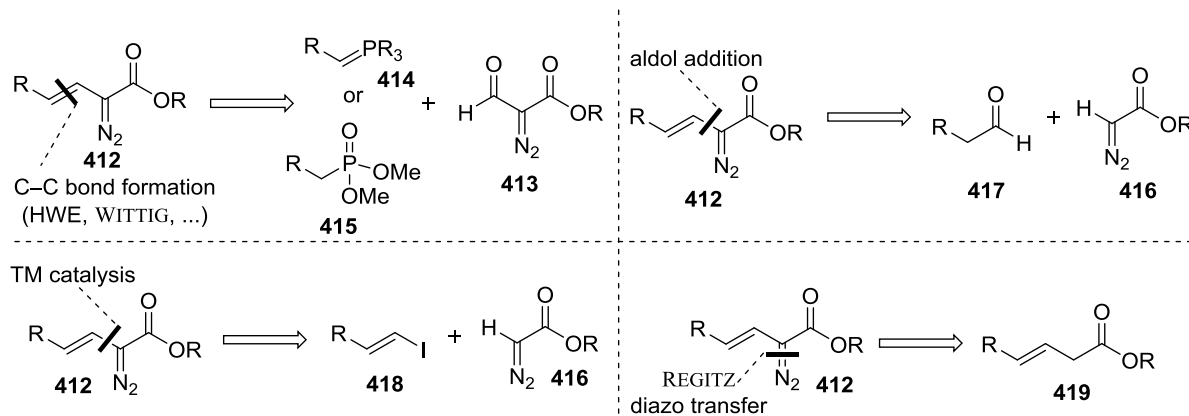
Scheme 126. Possible reactions of metal carbenoids. M = metal; R = generic substituent.^[267–274]

In this thesis, a Rh-catalyzed formal (4+3)-cycloaddition of a vinyl diazoester and a diene was employed for the stereoselective synthesis of a cycloheptadiene. Hence, only the relevant literature to this specific topic will be discussed focusing on the synthetic application rather than the physicochemical aspects of carbenoid chemistry.

3.5.2.1 Synthesis of Vinyl Diazoacetates

Substrates containing a diazo group have been preferentially employed in the preparation of Rh-carbenoids due to their facile synthesis or even commercial availability.^[275] DAVIES and co-workers noticed that the use of carbenoids derived from donor-/acceptor-substituted diazo compounds allowed for an increase in selectivity of typical reactions like cyclopropanation and C–H insertions.^[258] This was rationalized by the attenuation of reactivity through increased stabilization of

the electrophilic carbenoid through electron donation. Of particular importance to this thesis was the synthetic access to vinyl diazoacetates as one type of donor-/acceptor-substituted diazo compounds for the synthesis of seven-membered rings in a formal (4+3)-cycloaddition. Four main pathways have been identified for the synthesis of vinyl diazoacetates (Scheme 127).



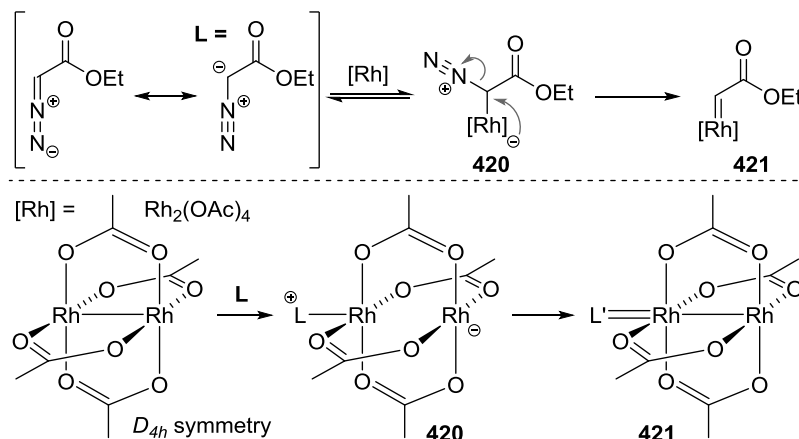
Scheme 127. Synthesis of vinyl diazoacetates.^[276–281]

Vinyl diazoacetates like **412** can be formed by mild C–C bond-forming olefin syntheses like the HORNER–WADSWORTH–EMMONS reaction under the MASAMUNE–ROUSH conditions or WITTIG olefinations.^[276,277] The required α -formyl diazo compounds **413** were shown to be accessible in one step from commercially available reagents and can then be coupled with ylens **414** or phosphonates **415**.^[278] Alternatively, diazoacetates **416** can be employed in aldol reactions with aldehydes **417**. The resulting β -hydroxy- α -diazoester is dehydrated to yield the desired vinyl diazoacetate **412**.^[279] Diazoacetates were also shown to engage in Pd-catalyzed cross-coupling reactions with vinyl iodides **418**.^[280] The REGITZ diazotransfer provides another possibility for the synthesis of vinyl diazoacetates **412** by formally adding a diazo group to enolates of esters **419** using sulfonil azides.^[281]

3.5.2.2 Rhodium Carbenoid Formation

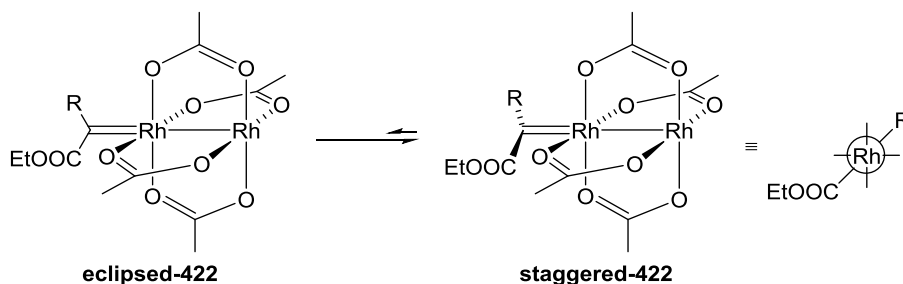
As mentioned above, rhodium carbenoids are mostly formed from diazo compounds, although the use of triazoles is increasing.^[282] Mechanistically, the rhodium carbenoid formation is believed to involve two separate steps (Scheme 128).^[283] The α -carbon atom in α -diazoesters like ethyl diazoacetate (EDA, **L**) displays nucleophilic character and is able to reversibly coordinate to the free axial coordination site of D_{4h} -symmetric Rh complexes such as $\text{Rh}_2(\text{OAc})_4$ (paddlewheel complex, “Chinese lantern” complex).^[284] The second Rh atom thereby acts as an electron sink in complex **420**, which however could also be depicted with an intact Rh–Rh bond and negative charge on the ligated Rh atom. Detailed investigation has revealed that the nitrogen extrusion from complex **420** is the rate-limiting step.^[285] Herein, electrons flow from the ligands and from the other Rh atom to the ligated Rh metal to form a double bond between Rh and the carbene-like carbon atom (**421**). Simultaneously, the C–N bond is broken and molecular nitrogen is released. This mechanism is

supported by HAMMETT values of the carboxylate ligands, a large normal ^{15}N -kinetic isotope effect and the observation of saturation kinetics in cyclopropanation reactions.^[285–287]



Scheme 128. Mechanism of rhodium carbenoid formation.^[283–287]

The carbene complex exists in a staggered conformation between the carbenoid carbon and Rh substituents as shown with the more general carbenoid complex **422** (Scheme 129).^[288] Intuitively, steric arguments would be in favor of this arrangement. However, a π -backbonding of the Rh complex (d_{xz} or d_{yz}) into the p -orbital of the carbene is only possible in this conformation.



Scheme 129. Most stable conformation of Rh carbenoids.^[288]

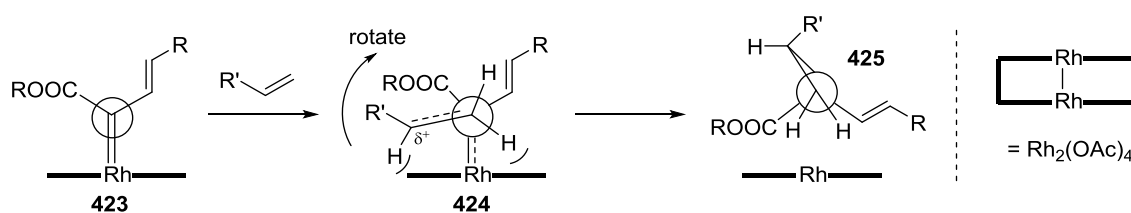
The formation of carbenoids is greatly facilitated by the presence of the second Rh atom and its role as a stabilizing electron sink in the first step and as an electron-releasing group during nitrogen extrusion.^[289] Rhodium carbenoids play an important role in synthesis due to their facile tunability, the air stability of the precatalysts and the associated mild reaction conditions.^[258] DAVIES, BERRY and co-workers recently managed to structurally characterize a Rh-carbene complex similar to complex **421** and prove its effectiveness as a catalyst.^[290]

3.5.2.3 Intermolecular Cyclopropanation with Rhodium Carbenoids

Rhodium carbenoids from donor-/acceptor-substituted diazo compounds such as vinyl diazoacetate are stable enough to undergo intermolecular reactions. They display electrophilic character at the carbenoid carbon atom. However, these rhodium carbenoids are sensitive to steric bulk

and can therefore be employed in selective cyclopropanations of terminal alkenes or *cis*-disubstituted olefins.^[288,291]

The transition state of these cyclopropanations involves a concerted bond formation between the carbenoid carbon atom and the olefin, which results in the conservation of configuration of the alkene (Scheme 130).^[292] Similar to the JACOBSEN–KATSUKI epoxidation, the alkene is believed to approach the carbenoid in a side-on fashion because no reaction was observed with *trans*-olefins and Rh carbenoids of type **423**.^[293] However, the extent to which the two bonds of the final cyclopropane are being built is different.^[288] The more nucleophilic olefin carbon atom is already closer to the carbenoid carbon, which results in a non-synchronous transition state **424** and charge development with the negative charge residing on the former carbenoid carbon and the positive on the other olefin carbon atom.



Scheme 130. Mechanism of the diastereoselective cyclopropanation with Rh carbenoids.^[292]

The olefin presumably orients itself so that the ester group, or more general the EWG, can stabilize the positive charge build-up on the other olefin carbon atom.^[288] Furthermore, the olefin substituent avoids unfavorable steric interactions with the bulky Rh catalyst. This arrangement is responsible for the high diastereoselectivity of these cyclopropanations. Replacement of either of the carbenoid carbon substituents would result in a less defined trajectory of the alkene approach. In addition, the transition state model **424** explains why *trans*-olefins are unreactive: one of their residues would always collide with the bulky Rh catalyst. Rotation of the olefin substituent and resulting bond formation yields cyclopropane **425** with former olefin substituent R' and the olefin of the vinyl diazoacetate on the same side.^[288]

Although the rhodium complexes were initially thought to provide poor enantioselectivities since two sites of coordination exist and the carboxylate substituents all point away from them, several chiral Rh complexes have been developed that show extraordinarily high levels of enantiocontrol.^[294] Some of the chiral Rh complexes are depicted in Figure 39.^[295]

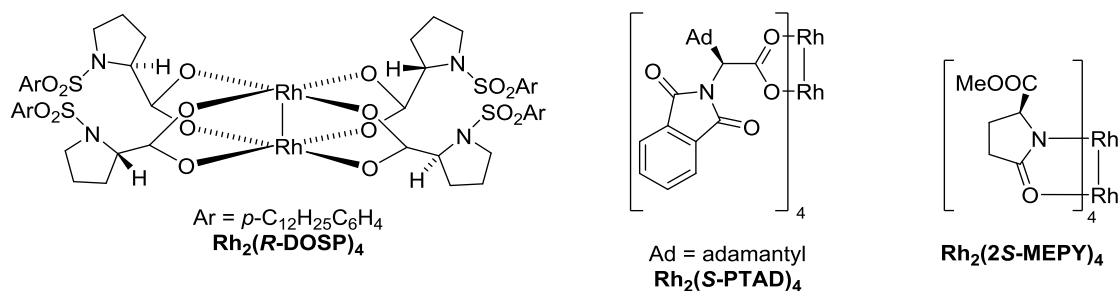
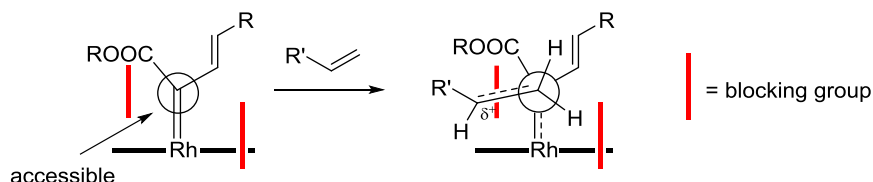


Figure 39. Selection of chiral Rh(II) catalysts.^[295]

For high enantioselectivities, the alkene approach has to occur preferentially from one side. Based on empiric results, the chiral catalyst structure of the Rh₂(DOSP)₄ was proposed to be *D*₂-symmetric, in which both Rh atoms are equivalent.^[291] A corresponding carbenoid can then be approached from a less sterically hindered face, whereas the opposite face is blocked by the proline substituent (Scheme 131).

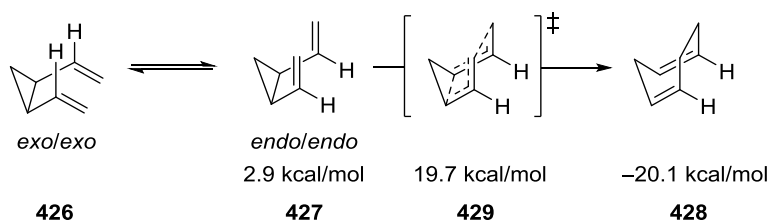


Scheme 131. Asymmetric cyclopropanation with chiral Rh catalyst.^[291]

This transition state is in accordance with experimental observations. For instance, the fact that hydrocarbon solvents lead to higher enantioselectivities was rationalized by a tighter transition state that decreases unfavorable charge separation.

3.5.2.4 Divinylcyclopropane Rearrangement

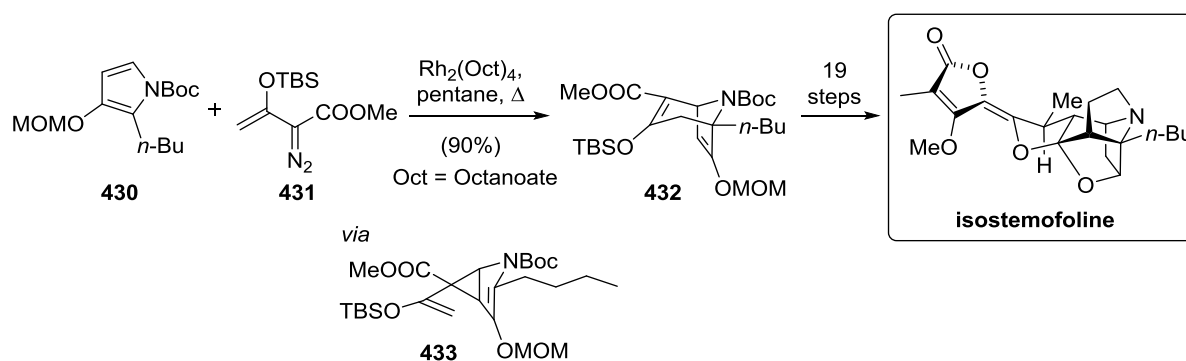
COPE rearrangements are [3,3]-sigmatropic rearrangements of 1,5-dienes and therefore belong to the class of pericyclic reactions.^[296] Both 1,5-dienes are in equilibrium and a certain driving force has to be incorporated to obtain preference for one side of the equilibrium. One strategy in this context has been the divinylcyclopropane rearrangement, in which a cyclopropane ring is irreversibly opened during the COPE rearrangement to afford 1,4-cycloheptadienes.^[297] The driving force results from the release of the inherent large ring strain of cyclopropanes. Whereas the preferred conformation of the divinylcyclopropane is *exo/exo* **426**, the *endo/endo* isomer **427** is thermally accessible ($\Delta E = 2.9$ kcal/mol). Only this conformer can rearrange to afford *cis/cis*-cycloheptadienes **428**, while the others would deliver very strained seven-membered rings with at least one *trans*-olefin. Remarkably, the transition state of the rearrangement **429** displays a boat conformation as opposed to the standard COPE reaction, which possesses a large preference for the chair-type transition state (Scheme 132).^[297]



Scheme 132. Boat-type transition state of divinylcyclopropane rearrangement.^[297]

3.5.2.5 Application of the Cyclopropanation/COPE rearrangement Cascade

Both powerful transformations, asymmetric, regio- and diastereoselective cyclopropanation and divinylcyclopropane rearrangement, can be efficiently combined for the enantioselective synthesis of seven-membered rings. Their potential to rapidly increase molecular complexity in this formal (4+3)-cycloaddition has been exploited in total synthesis especially when the target molecule featured this motif.^[258] In 1999, KENDE and co-workers employed this transformation to elegantly construct the tropane skeleton in isostemofoline (Scheme 133).^[260]



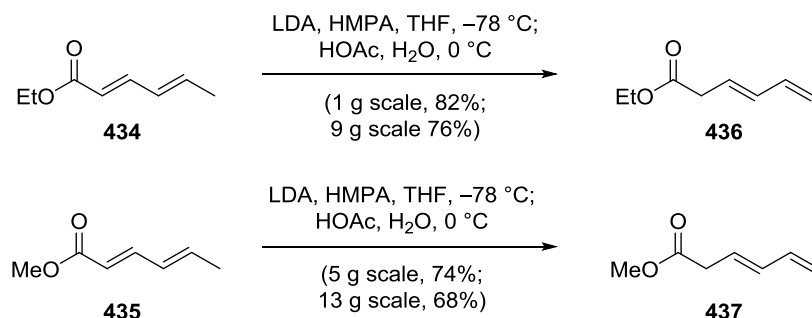
Scheme 133. Construction of the tropane skeleton by cyclopropanation/COPE rearrangement cascade.^[260]

The starting pyrrole **430** was allowed to react with vinyl diazoacetate **431** in the presence of an achiral Rh catalyst to afford the bicycle **432** in excellent yield. As described above, the reaction proceeded *via* a diastereoselective cyclopropanation to furnish cyclopropane **433**, which subsequently underwent the desired COPE rearrangement. In 19 further steps, tropane **432** was converted to isostemofoline, completing the first synthesis of this challenging polycyclic natural product.

3.5.3 Results and Discussion

3.5.3.1 Preparation of Diene

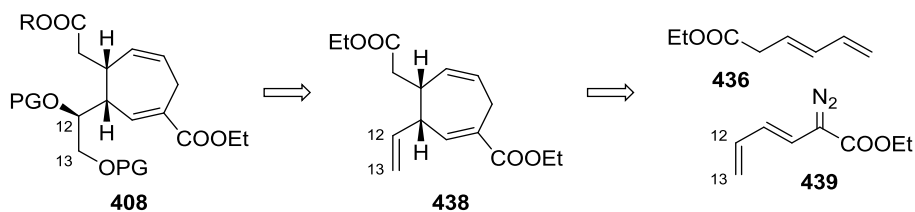
The required dienes of type **410** were prepared in a literature-known procedure from inexpensive sorbic acid esters by deprotonation and kinetic reprotonation.^[298,299] Ethyl ester **434** and methyl ester **435** were treated with LDA and HMPA as additive and then reprotonated with an acetic acid/water mixture to afford deconjugated esters **436** and **437** in good yield.



Scheme 134. Preparation of dienes **436** and **437** by deprotonation/reprotonation.

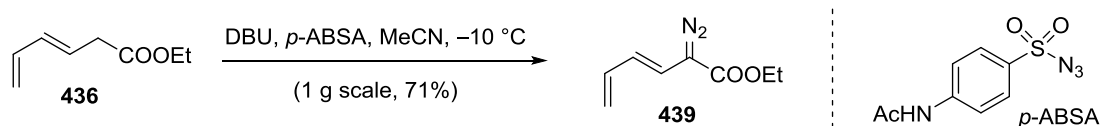
3.5.3.2 Asymmetric Formal (4+3)-Cycloaddition with Achiral Substrates

The key cycloheptadiene **408** could potentially be accessed from a triene such as **438** by selective dihydroxylation of the monosubstituted olefin (Scheme 135). Despite the challenge of this chemo- and stereoselective dihydroxylation, the strategy was attractive since triene **438** could stem from dienes **436** and **439** in an enantioselective cyclopropanation/COPE rearrangement cascade. Both are available from inexpensive sorbic acid esters.^[291,298,299] In case the dihydroxylation would afford a diastereomeric mixture, reagent control could be used to overcome the substrate preference. As an additional advantage, the C14 acid could be used to correct the C12 stereochemistry by an intramolecular MITSUNOBU lactonization.



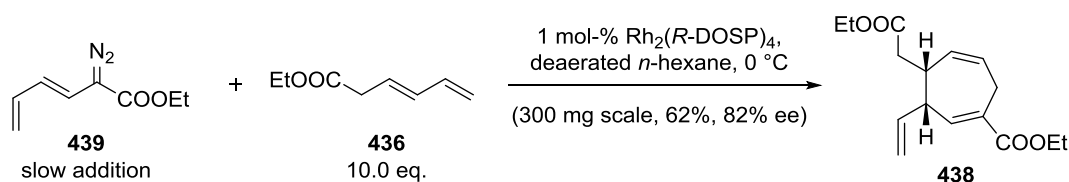
Scheme 135. Convergent retrosynthesis with achiral substrates for formal (4+3)-cycloaddition.

The required vinyl diazoacetate **439** was synthesized in a REGITZ diazo transfer reaction from diene **436** (Scheme 136).^[291] Related one-pot protocols, in which ethyl sorbate was deprotonated and then treated with diazo transfer reagent *para*-ABSA (*para*-acetamidobenzenesulfonyl azide) failed. The resulting vinyl diazoacetate **439** proved to be prone to polymerization at room temperature and had to be handled carefully in the dark.



Scheme 136. Synthesis of required vinyl diazoacetate **439**.

Initial experiments to combine both building blocks in a Rh-catalyzed cyclopropanation/COPE rearrangement cascade at various temperatures below $T = -30\text{ }^{\circ}\text{C}$ failed and were only accompanied by the precipitation of a colorless solid, which seemed to result from decomposition of vinyl diazoacetate **439**. It was reasoned that diene **436** is too electron-poor to engage in a cyclopropanation at low temperatures due to the electron-withdrawing effect of the ester group. This might explain the observation that only the diazo compound decomposed in the presence of the Rh catalyst, despite the excess of diene **436**. In order to investigate whether both building blocks would be able to combine at all, the reaction was conducted at $T = 0\text{ }^{\circ}\text{C}$ although this might be detrimental to the enantiomeric excess (Scheme 137).



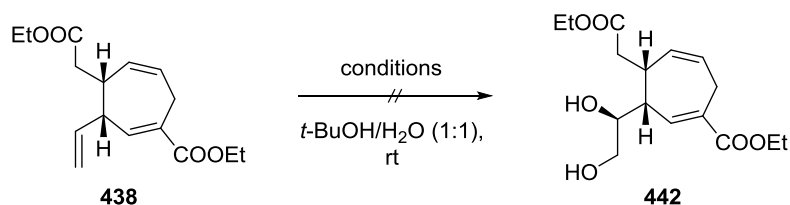
Scheme 137. Successful asymmetric cyclopropanation/COPE rearrangement.

Remarkably, upon slow addition of vinyl diazoacetate **439** to an excess of diene **436** and catalytic amounts of a chiral dimeric Rh catalyst in deaerated *n*-hexane, triene **438** formed in good yield and enantiomeric excess. Despite the numerous reactions that diazo compounds can undergo, the instability of diazo compound **439** and the multitude of olefins that could engage in a cyclopropanation, both building blocks combined in a regio- and even stereoselective fashion, a testimony to the power of the methodology developed by DAVIES and co-workers. The enantiomeric excess of triene **438** was determined by chiral HPLC in comparison to a sample prepared with catalytic amounts of $\text{Rh}_2(\text{OAc})_4$ in CH_2Cl_2 and the absolute configuration was assigned based on literature similarity.^[291] Although triene **438** contains two skipped diene moieties, no sign of olefin migration was observed. The reaction was not further optimized since the following crucial selective dihydroxylation had to be explored first.

Selective dihydroxylations of terminal olefins in the presence of more highly substituted ones are challenging because the electrophilic dihydroxylation reagent usually reacts with the more electron-rich olefin.^[300–302] Nevertheless, selectivity for terminal olefins has been achieved, especially with bulky reagents that are sensitive to steric hindrance.^[303–307] It was first attempted to dihydroxylate triene **438** under UPJOHN conditions (Table 8, entry 1), but apart from starting material, only diol **440** was identified. This outcome was not unexpected since the disubstituted olefin is considered more

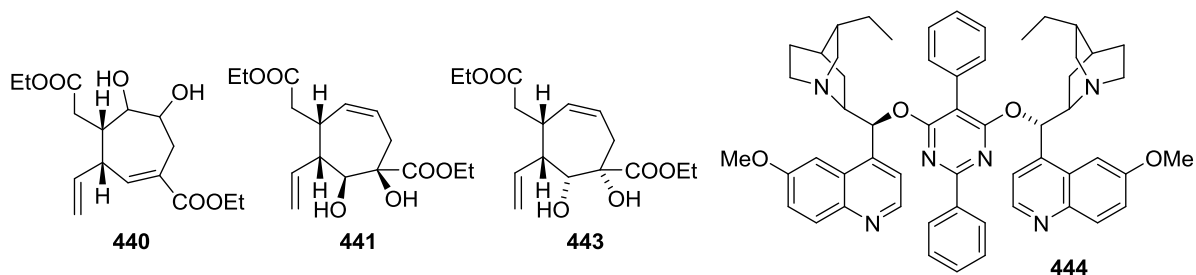
electron-rich and therefore more reactive. Furthermore, the *cis*-olefin is inherently more strained due to its incorporation in a carbocycle.

Table 8. Selective dihydroxylation trials for triene **438**.



entry	reagent (eq.)	oxidant (eq.)	additive (eq.)	product
1	OsO ₄ (0.032) ^[a]	NMO (1.02)	none	rec. s.m. + 440 ^[b]
2	AD-mix α (2.0)	-	MeSO ₂ NH ₂ (1.0)	rec. s.m. + 441 ^[c]
3	AD-mix α (1.0)	-	MeSO ₂ NH ₂ (1.0)	rec. s.m. + 441 ^[c]
4	AD-mix α ^[d]	K ₃ [Fe(CN) ₆] (3.0)	none	rec. s.m. + 441 ^[c]
5	AD-mix β ^[d]	K ₃ [Fe(CN) ₆] (3.0)	none	rec. s.m. + 443 ^[c]
6	AD-mix with 444 ^[d]	K ₃ [Fe(CN) ₆] (3.0)	none	rec. s.m. + 440 ^[e] + 441

a. solvent *t*-BuOH/H₂O/THF (10:3:1); b. diastereomers not assigned, dr = 3:1; c. single diastereomer; d. K₂CO₃ (3.0 eq.), K₃[Fe(CN)₆] (3.0 eq.), chiral ligand (0.012 eq., **442** 0.024 eq.) and substrate were mixed in solvent prior to addition of OsO₄ (0.02 eq.) in *t*-BuOH; e. corresponds to minor diastereomer in entry 1.

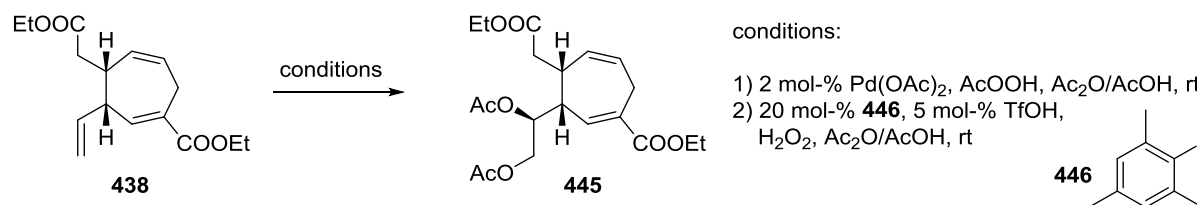


Subsequent trials therefore focused on an olefin differentiation based on steric grounds. As previously reported, the bulky ligands of the active reagent in an asymmetric SHARPLESS dihydroxylation could be able to lead to the desired product by favoring the sterically more accessible terminal olefin.^[305] Dihydroxylation with different numbers of equivalents were not met with success, unexpectantly affording the diol **441** (entries 2, 3). The corresponding olefin as a trisubstituted alkene with electron-withdrawing substituents was considered to be the least reactive under the employed conditions, but seems to fit best into the chiral binding pocket of the reagent. Since previous reports had established that methanesulfonamide as an additive only accelerates the dihydroxylation of nonterminal olefins, this additive was omitted to effect preferential dihydroxylation of the terminal olefin, without success (entry 4).^[308] Furthermore, fresh preparation of the AD-mix instead of commercially available batches did not affect the outcome of the reaction. Since triene **438** is a chiral substrate, it might be that the AD-mix α leads to a mismatched case and therefore does not yield the desired dihydroxylation product **442**. However, a change to the pseudo-enantiomeric AD-mix β only led to diastereomer **443** without change in regioselectivity. A complete change in the ligand platform to ligand **444**, which was reported to increase the enantiomeric excess especially for terminal olefins,

afforded a mixture of diols **440** and **441**, but no formation of the desired product was observed (entry 6).^[309]

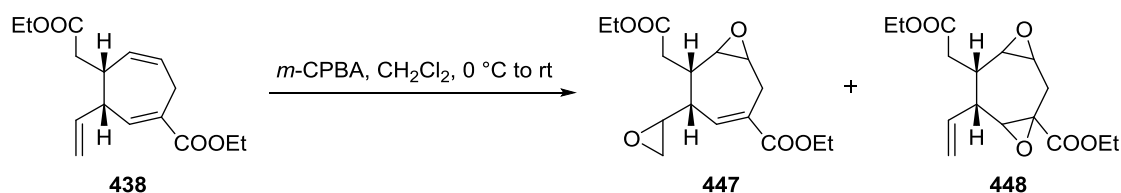
It appeared as if the terminal olefin was the least sterically accessible of the three olefins despite the fact that it only possesses one substituent. One of its faces might be blocked by the *cis*-substituent at C10. As no selective dihydroxylation seemed possible with osmium-based reagents, alternative methods were investigated.

Recently, Pd-catalyzed or organocatalytic diacetoxylation of alkenes has emerged as a promising alternative to osmium-catalyzed dihydroxylation (Scheme 138).^[310] It was hence attempted to effect the desired transformation to diacetate **445** either under Pd- (condition 1) or organocatalysis with iodide **446** (condition 2).^[311,312] Neither starting material nor product was isolated from the reaction mixture, which can be rationalized by the highly acidic medium that might have resulted in olefin migration. It is possible that a cycloheptatriene was formed, that then underwent decomposition reactions.



Scheme 138. Alternative olefin difunctionalization methods.

In order to verify if the terminal olefin would undergo reactions with electrophilic reagents, the sterically undemanding epoxidation reagent *m*-CPBA was employed (Scheme 139). It was expected that concomitant epoxidation of the more reactive *cis*-disubstituted olefin would occur. When triene **438** was subjected to these reaction conditions, two bisepoxides **447** and **448** were identified. Whereas it was proven that the terminal olefin can be functionalized, it also became evident that the *cis*-olefin is epoxidized first and can then react further in a rather unselective fashion.

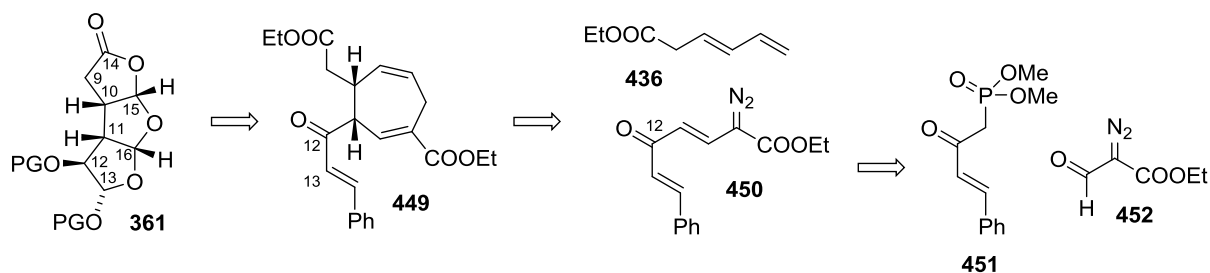


Scheme 139. Epoxidation attempts with triene **438**.

The results presented in this chapter discouraged further attempts toward the selective functionalization of triene **438**. Since more promising results were obtained with chiral vinyl diazoacetates (see 3.5.3.4 Vinyl Diazoacetates with Alcohols as C13 Aldehyde), which led to the efficient synthesis of derivatives of diol **442** or diacetate **445**, further methods such as the dihydroxylation *via* diborylation by MORKEN and co-workers were not investigated.^[313]

3.5.3.3 Vinyl Diazoacetates with Olefin as C13 Aldehyde Equivalent

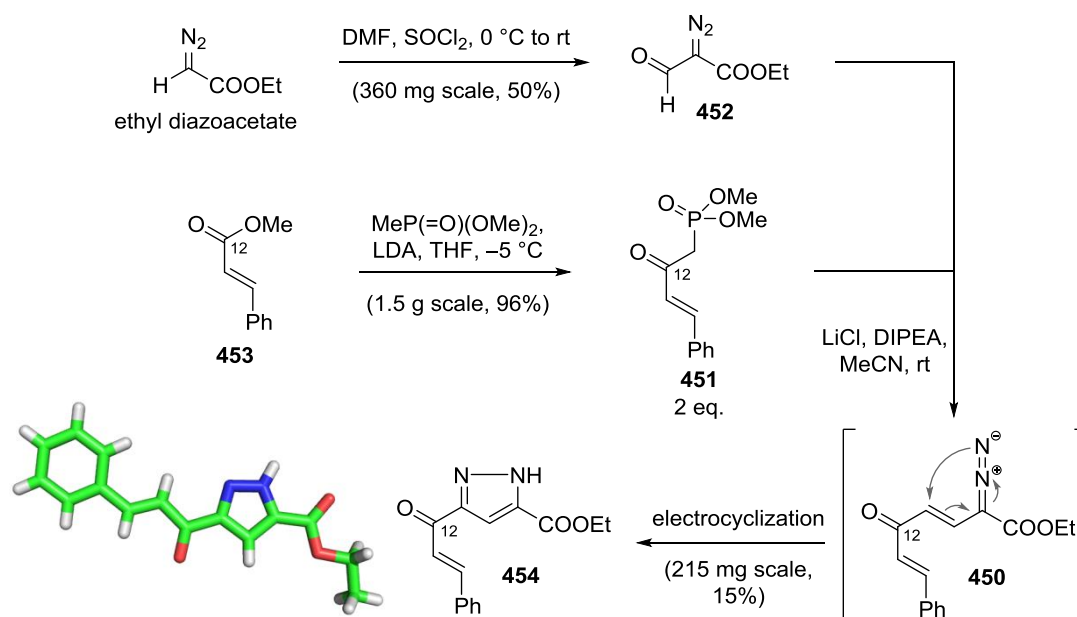
The unsuccessful attempts to functionalize triene **438** led to the reconsideration that prefunctionalized vinyl diazoacetates should be employed in the key cyclopropanation/COPE rearrangement. Due to the accomplishment of an asymmetric version of this reaction, it was first focused on further achiral diazo compounds. Thus, gracilin precursor **361** was traced back to triene **449**, which features a ketone oxidation state at carbon atom C12 and an olefin as an aldehyde precursor (Scheme 140). It was envisioned to cleave the three olefins by ozonolysis, which would result in spontaneous cyclization to the tricyclic core. C12 ketone would then be reduced from the convex face and the stereochemistry corrected by MITSUNOBU inversion to yield precursor **361**.



Scheme 140. Retrosynthesis involving an olefin as C13 aldehyde precursor.

The prerequisite triene **449** would be accessed by asymmetric formal (4+3)-cycloaddition of diazo compound **450** and diene **436**. The former would stem from a HORNER–WADSWORTH–EMMONS olefination of literature known phosphonate **451** and aldehyde **452**.^[278,314]

The synthesis commenced with the formylation of ethyl diazoacetate in a procedure similar to the VILSMEIER–HAACK formylation, giving aldehyde **452** in moderate yield (Scheme 141).^[278] A CLAISEN-type condensation of ester **453** gave rise to phosphonate **451**, which was coupled in a HORNER–WADSWORTH–EMMONS reaction under MASAMUNE–ROUSH conditions, presumably to diazoester **450**.^[276] However, the latter spontaneously underwent a 6π -electrocyclization to pyrazole **454**, which was isolated in poor yield. The structure of pyrazole **454** was unambiguously proven by X-ray single crystal structure analysis.

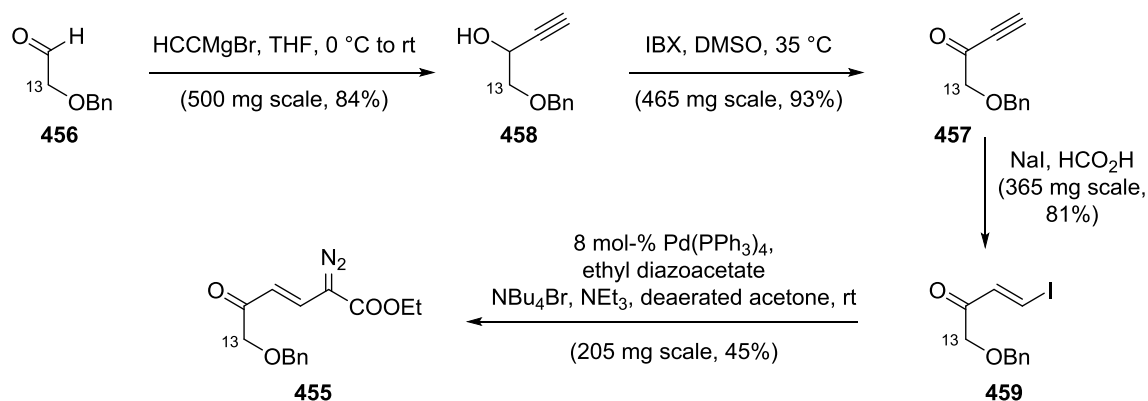


Scheme 141. Electrocyclization to pyrazole **454** and its X-ray single crystal structure.

Spontaneous pyrazole formation is a known unimolecular reaction of vinyl diazoesters that is significantly accelerated by conjugation.^[315] As a potential reason, it was proposed that a different degree of bond formation in the transition state can lead to charge separation, which would be stabilized by additional conjugation.^[315] It seemed unlikely that this unwanted side reaction could be suppressed with vinyl diazoesters of type **450** with olefins as the aldehyde precursor. Furthermore, reduction of the C12 ketone in order to break the conjugation would yield a divinylcarbinol that would be prone to decomposition. Thus, it was focused on the synthesis of different vinyl diazoesters.

3.5.3.4 Vinyl Diazoacetates with Alcohols as C13 Aldehyde Equivalent

Following the general retrosynthetic analysis shown in chapter 3.5.1 Retrosynthesis, vinyl diazoacetates such as **409** with alcohols as the C13 aldehyde precursor were chosen as substrates. In order to still be able to use the asymmetric cyclopropanation/COPE rearrangement cascade with achiral substrates, ketone **455** was to be prepared (Scheme 142).

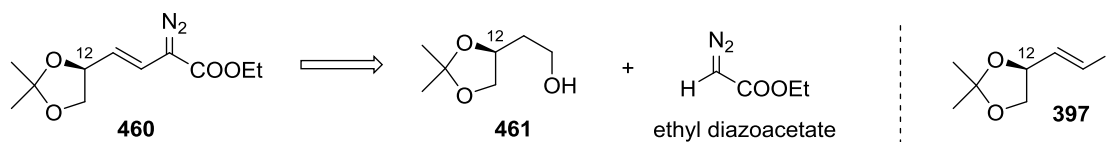


Scheme 142. Synthesis of achiral vinyl diazoacetate **455** with alcohol as C13 aldehyde precursor.

Commercially available aldehyde **456** was converted to alkynoate **457** via propargylic alcohol **458** in a literature-known sequence of GRIGNARD addition and reoxidation (Scheme 142).^[316] Conjugate addition of sodium iodide, inspired by reports of NIPHAKIS *et al.*, afforded vinyl iodide **459**.^[317] The stage was now set for a Pd-catalyzed coupling of ethyl diazoacetate with this vinyl iodide according to a procedure developed by the WANG group. The coupling furnished the desired vinyl diazoacetate **455** only in moderate yield.^[280] The synthesis of this precursor proved to be less efficient and more cumbersome than the one of chiral vinyl diazoacetates from chiral pool starting materials, which had been completed in parallel. Vinyl diazoacetate **455** was therefore not further tested in the gracilin synthesis.

As an alternative to the discussed vinyl diazoacetates, the synthesis of cycloheptadiene **408** seemed to be more redox-economic if a C12 alcohol was incorporated from the beginning. This would require setting the C12 stereocenter in the vinyl diazoacetate coupling partner prior to the key step. In this case, a potentially diastereoselective cyclopropanation/COPE rearrangement key step with achiral Rh catalysts could be tested with this strategy.

The prerequisite vinyl diazoacetate **460** was to be prepared from commercially available malic acid derivative **461** and ethyl diazoacetate by aldol addition and elimination (Scheme 143). An analogous Pd-catalyzed coupling of already prepared vinyl iodide **397** and ethyl diazoacetate failed, in accordance with literature precedence.^[280]

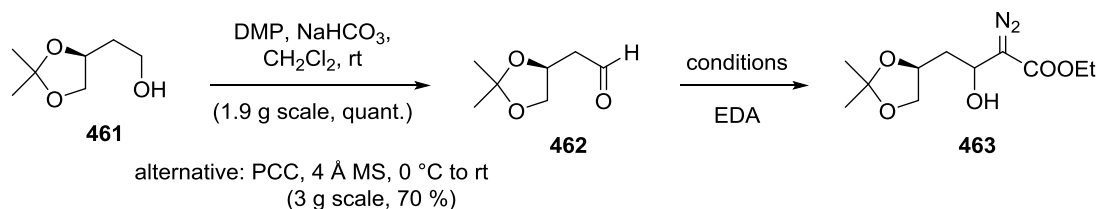


Scheme 143. Retrosynthesis of desired vinyl diazoacetate **460**.

Oxidation of alcohol **461** to commercially available aldehyde **462** proceeded uneventfully (Table 9).^[318] Unexpectantly, the subsequent aldol addition to β -hydroxy- α -diazoester **463** proved to be challenging. In a routine procedure, aldehyde **462** was treated with ethyl diazoacetate and catalytic

amounts of DBU, but the desired product was only isolated in modest yield as an inconsequential mixture of diastereomers (entry 1).^[279]

Table 9. Aldol addition of ethyl diazoacetate to aldehyde **462**.



entry	reagent	equiv.	solvent	T [°C]	yield [%]
1	DBU	0.2	MeCN	rt	41
2	DBU	0.2	MeCN	0	46
3	DBU	0.2	MeCN	−20	48
4	DBU	0.2	THF	−78 to 0 to rt	-
5	NBu₄OH in MeOH	0.32	DMSO	rt	25
6	LiHMDS	1.05	THF	−78	49
7	NaHMDS	1.1	THF	−78	56
8	NaHMDS	1.05	THF	−78	33
9	NaH	1.1	THF	0	39
10	LDA	1.1	THF	−78	51
11	ZnEt₂	1.5	CH ₂ Cl ₂	−78 to −50 to rt	55
12	PhCO₂H	0.5	neat	rt	66

Subsequent trials at lower temperatures only slightly increased the yield of the transformation (entries 2, 3). The reaction failed completely in THF as the solvent at dry ice temperature, which might be attributed to a rapid aldehyde decomposition that still occurred at low temperatures where the desired aldol addition was too slow. Presumably, aldehyde **462** is more susceptible to base-catalyzed enol formation under the reaction conditions since the respective enol can form a hydrogen bond to the dioxolane protecting group. Alternatively, the α -protons of aldehyde **462** might be sufficiently acidified for the generation of enolates owing to the inductive effect of the dioxolane moiety. Thus, alongside the enolate formation of EDA, also the very reactive enol or enolate of the aldehyde forms and decomposes by dimerization. It has to be mentioned though that a corresponding decomposition product could not be isolated from the reaction mixture.

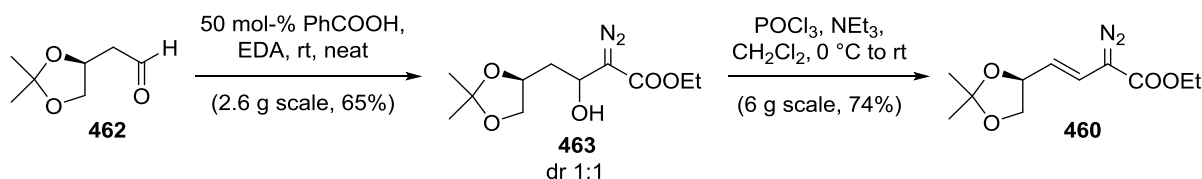
Preformation of the EDA enolate to avoid competing deprotonation of the aldehyde failed with LDA, but was successful with Bu₄NOH in MeOH (entry 5).^[319] A substoichiometric amount of base was used to ensure a low equilibrium amount of a β -alkoxy- α -diazoester compared to the corresponding β -hydroxy- α -diazoester. The β -alkoxy- α -diazoester was suspected to be cause side reactions with unconsumed aldehyde **462**. However, the yield decreased significantly. It seemed as if a free hydroxide or methoxide base was still present in the reaction mixture that led to the decomposition of aldehyde **462**.

No better yield compared to the initial result was obtained by treatment of an EDA/aldehyde mixture with LiHMDS (entry 6). To verify if aldehyde deprotonation was a problem, the reaction was conducted in the presence of TMSCl. The recovery of unreacted aldehyde supported this hypothesis, because it likely stemmed from the TMS enol ether of aldehyde **462**. A retro-aldol reaction upon workup seemed improbable since changes in the workup procedure did not affect the yield.

Trials with less coordinating counter cations surprisingly seemed to give slightly better results (entry 7), but a slow addition of NaHMDS was detrimental to the yield. The intermediate β -alkoxy- α -diazoester was assumed to be able to react with the remaining aldehyde by deprotonation or acetal formation, making it unavailable for the envisioned aldol condensation. To exclude that the HMDS base condenses with the aldehyde, NaH was employed as a base (entry 9).^[320] The resulting comparable yield suggested that HMDS condensation was not problematic. Furthermore, LDA as an alternative base with a Li counterion was used, but gave equally modest yields (entry 10).^[321]

It was concluded that the reactivity of the intermediate alkoxide would have to be reduced by coordination to higher valent cations and that the competing deprotonation of the aldehyde would have to be suppressed. Thus, ZnEt₂ was employed as a base to preform the EDA Zn-enolate, which would then react with the added aldehyde (entry 11).^[322] As Zn cations are strongly chelating, the nucleophilicity of the intermediate β -alkoxy- α -diazoester would be decreased and retro-aldol reactions inhibited. Nonetheless, the yield of the transformation did not exceed moderate values. In a paradigm shift, it was tested whether acidic conditions could avoid the above-mentioned problems of aldehyde decomposition from deprotonation or reaction with the intermediate β -alkoxy- α -diazoester. Indeed, substoichiometric amounts of benzoic acid did lead to a yield improvement and a significantly easier reaction setup.^[323] It was assumed that the benzoic acid concertedly protonates the aldehyde while deprotonating EDA in a chelating fashion. Other mechanisms would not be able to explain the high yield for the desired product without observation of DARZENS epoxide formations or the ROSKAMP reaction.

With the prerequisite β -hydroxy- α -diazoester **463** as an inconsequential mixture of diastereomers in hand, dehydration proceeded smoothly with POCl₃ (Scheme 144).^[324] Alternative methods with MsCl were found less efficient. The desired diazo compound **460** was prepared on multi-gram scale, but required careful handling and had to be stored in a benzene matrix at $T = -78\text{ }^{\circ}\text{C}$. The compound decomposes in solution to a colorless solid at room temperature over the course of one day.

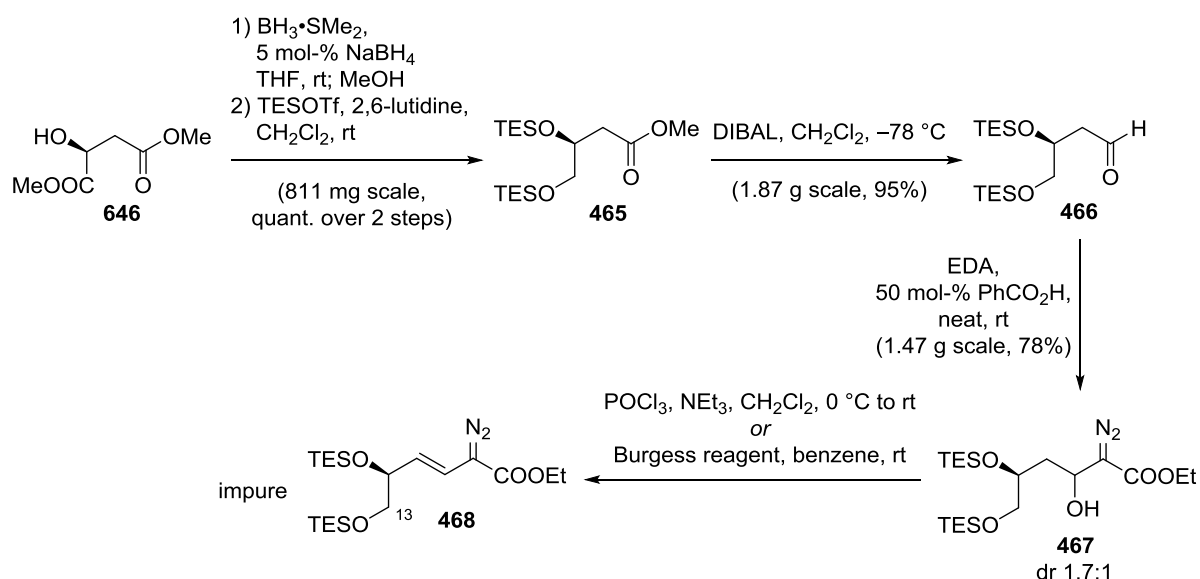


Scheme 144. Optimized synthesis of vinyl diazoacetate **460**.

As observed previously (see 3.4.3.3 Building Block Coupling and 6π -Electrocyclization), the dioxolane moiety might not provide high stereocontrol in the following key step. Therefore,

alternative related vinyl diazoacetates were planned to be accessed, ideally with a TES protecting group for the C12 and C13 alcohol. Primary TES ethers are known for their potential to be oxidized to aldehydes under SWERN conditions, whereas secondary TES ethers remain untouched.^[325] This potential could be used to differentiate the C12/C13 diol after the key cyclopropanation/COPE rearrangement.

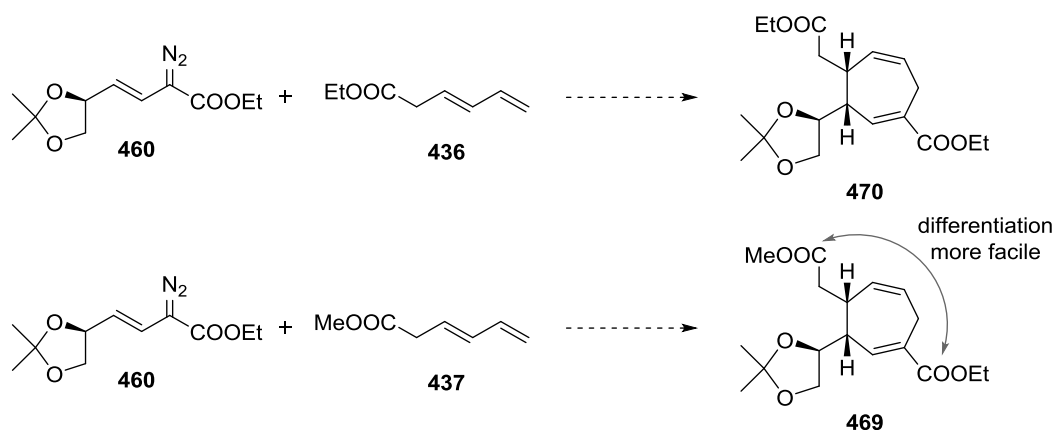
The ester moiety adjacent to the secondary alcohol of malic acid derivative **464** was selectively reduced by borane and the resulting diol TES protected to ester **465**. The latter was reduced to yield aldehyde **466** (Scheme 145).^[326] The previously optimized aldol addition was conducted on gram-scale and furnished hydroxy diazoester **467** as a mixture of diastereomers in good yield using EDA and substoichiometric amounts of benzoic acid. The subsequent dehydration with POCl₃ proved to be problematic and only gave traces of the desired product **468**. Purification by flash column chromatography on silica gel was impossible due to decomposition of the molecule. Aluminum oxide (grade II) as a solid phase allowed for the separation of most side products from vinyl diazoacetate **468**. Milder dehydration conditions with BURGESS reagent did not give better results.



Scheme 145. Synthesis of alternative vinyl diazoacetate **468**.

A possible explanation of these results would be that silyl protecting group shifts are operative in the reaction mixture, which could then lead to a mixture of different dehydration products. Since the reaction was low-yielding and the purification cumbersome, which would render larger-scale reactions challenging, it was decided not to pursue this building block.

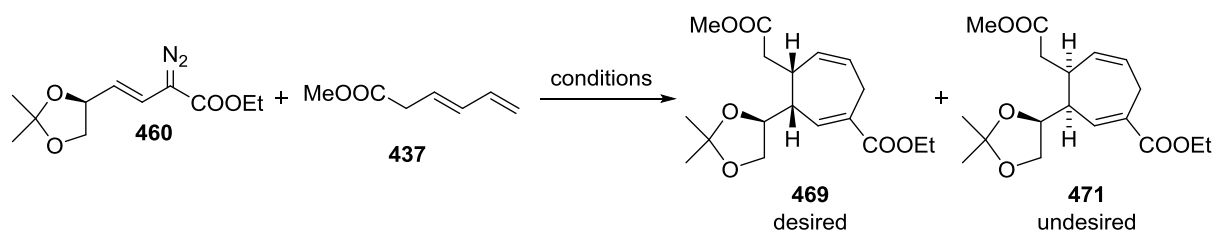
Due to the chirality of vinyl diazoacetate **460**, diastereoselective cyclopropanation/COPE rearrangements based on substrate control were tried first. Both ethyl ester **436** and methyl ester **437** were employed in the key cascade reaction (Scheme 146). However, it seemed advisable to continue the synthesis with product **469** rather than cycloheptadiene **470** because a differentiation of the two ester functionalities in the product would be more facile. Only the optimization with methyl ester **437** toward cycloheptadiene **469** will be described, but ethyl ester **470** was prepared analogously.



Scheme 146. Different products of the key cyclopropanation/COPE rearrangement and advantage of diester **469**.

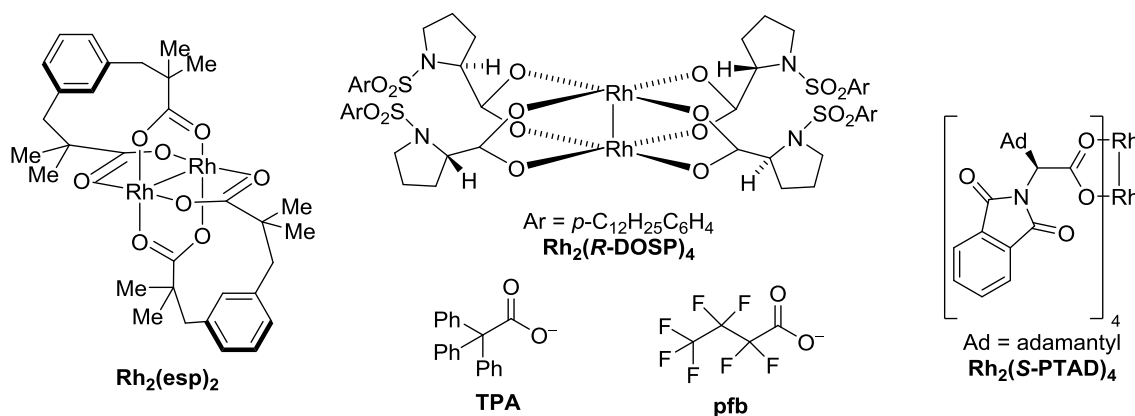
Upon slow addition of diazo compound **460** to a solution of diene **437**, present in excess, and the respective Rh catalyst, a mixture of both possible stereoisomers was obtained with a *trans*-cyclopropane as side product (Table 10, also see page 282). For convenience, the catalyst screening was mostly conducted at room temperature and suitable catalysts were then chosen for optimization. The standard $\text{Rh}_2(\text{OAc})_4$ catalyst provided slightly more of the desired (**469**) than of the undesired isomer **471** (entry 1). It was expected that bulkier, electron-donating ligands such as pivalate, esp or TPA would increase the long-range steric sensitivity of the catalyst while also attenuating its reactivity, which both could lead to higher diastereoselectivities. However, these ligands all favored the formation of cycloheptadiene **471** (entries 2–4). It was thus tested whether more electrophilic and therefore more reactive catalysts would be in favor of the desired cycloheptadiene. Indeed, TFA as a ligand gave a diastereomeric ratio of almost dr (**469**:**471**) = 2:1, while the more electron-withdrawing pfb ligand did not follow this trend (entries 5, 6). As it was known that the solvent polarity plays a crucial role in the ordered arrangement of the transition state (see 3.5.2.3

Intermolecular Cyclopropanation with Rhodium Carbenoids), less polar solvents were to be used. However, most Rh dimers are not soluble in these solvents. It was therefore switched to chiral Rh dimers that could also lead to higher diastereoselectivities by reagent control. Encouragingly, the chiral (*R*)-PTAD ligand exclusively afforded the undesired isomer **471**, which showed that reagent control can overrule substrate control (entry 7). In contrast to this, the enantiomeric ligand (*S*)-PTAD was unable to discriminate between both isomers, proving that the former case represented a matched scenario (entry 8). In this mismatched case, substrate control competes with the reagent preference. It was tested if a different chiral scaffold would result in better selectivities by using the (*S*)-DOSP ligand in deaerated *n*-hexane. The employed catalyst system favored formation of the undesired isomer **471** (entry 9). However, its enantiomer (*R*)-DOSP gave the best values thus far with a diastereomeric ratio dr (**469**:**471**) = 2.5:1 at room temperature (entry 10).

Table 10. Optimization of diastereoselective cyclopropanation/COPE rearrangement.

entry	Rh-catalyst	solvent	eq. (437)	T [°C] ^[a]	469:471 ^[b]	yield [%]
1	Rh₂(OAc)₄	CH ₂ Cl ₂	10	0	1.5:1	n.d.
2	Rh₂(OPiv)₄	CH ₂ Cl ₂	2	0 to rt	1:1.2	n.d.
3	Rh₂(esp)₂	CH ₂ Cl ₂	2	rt	1:1.2	n.d.
4	Rh₂(TPA)₄	CH ₂ Cl ₂	10	rt	1:3.3	n.d.
5	Rh₂(TFA)₄	CH ₂ Cl ₂	10	rt	1.9:1	n.d.
6	Rh₂(pfb)₄	CH ₂ Cl ₂	10	rt	1.5:1	n.d.
7	Rh₂(R-PTAD)₄	toluene	10	rt	0:1	n.d.
8	Rh₂(S-PTAD)₄	toluene	10	rt	1:1.3	n.d.
9	Rh₂(S-DOSP)₄	deaerated <i>n</i> -hexane	10	rt	1:5	n.d.
10	Rh₂(R-DOSP)₄	deaerated <i>n</i> -hexane	10	rt	2.5:1	80
11	Rh₂(R-DOSP)₄	deaerated <i>n</i> -hexane	2	rt	2.7:1	60
12	Rh₂(R-DOSP)₄	deaerated <i>n</i> -hexane	2	0 to rt	4.4:1	n.d.
13	Rh₂(R-DOSP)₄	deaerated <i>n</i> -hexane	2	−40/−30 to rt	5.4:1	82
14	Rh₂(R-DOSP)₄	deaerated <i>n</i> -hexane	2	−78 to rt	4.5:1	n.d.

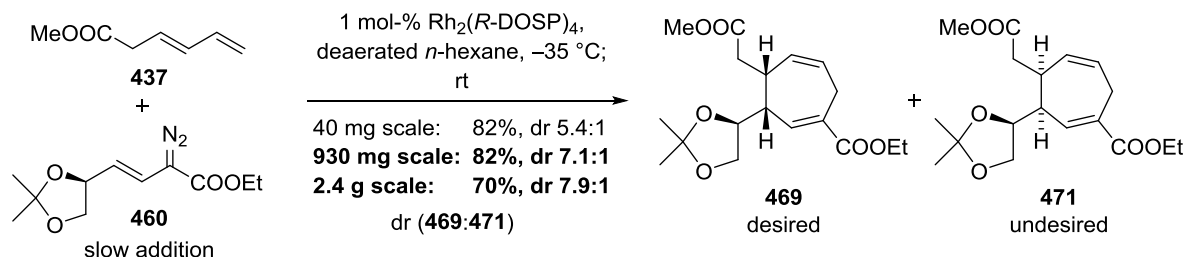
a. addition done at first indicated temperature, then left in cold bath to warm up over indicated time; b. based on crude NMR analysis of $\text{RCH}=\text{C}(\text{R}')\text{COOEt}$ in C_6D_6 .



Although diene **437** was readily available, it was highly desirable to lower its equivalents because its excess significantly complicated workup and purification. A slight decrease in yield, but the same diastereoselectivity was observed when lowering the equivalents of diene **437** from 10 to two (entry 11). The Rh dimer with the (*R*)-DOSP ligand was thus chosen for further optimization, which mainly focused on the temperature. The diastereomeric ratio was increased to useful values by lowering the temperature to $T = 0^\circ\text{C}$ or $T = -30/40^\circ\text{C}$ (range, entries 12, 13). After complete addition, the reaction mixture was allowed to warm to room temperature very slowly. As previously observed, no reaction occurred at lower temperatures due to the lack of reactivity of diene **437** compared to more electron-rich olefins. The conditions in entry 14 only furnished the product, because the reaction mixture was

allowed to warm to room temperature. The lower diastereomeric ratio shows that the reaction started once $T = -30\text{ }^{\circ}\text{C}$ was reached. As the temperature increased, the cyclopropanation presumably got less selective, leading to a worse overall dr.

The conditions of entry 13 were chosen for future experiments and the synthesis of cycloheptadiene **469** was successfully realized on scale (Scheme 147). Vinyl diazoacetate was unstable in solution even at $T = -78\text{ }^{\circ}\text{C}$, which demanded a thoroughly optimized setup procedure because of its slow addition. The diastereomeric ratio on scale was even improved and the undesired cycloheptadiene **471** was readily separated by flash column chromatography.



Scheme 147. Optimized Rh-catalyzed formal (4+3)-cycloaddition.

It was crucial to obtain unambiguous proof of the relative stereochemistry of the desired isomer **469**, which could not be crystallized because it was a liquid. However, the undesired isomer **471** proved to be a solid and X-ray single crystal structure was obtained, providing indirect evidence of structure **469** (Figure 40).

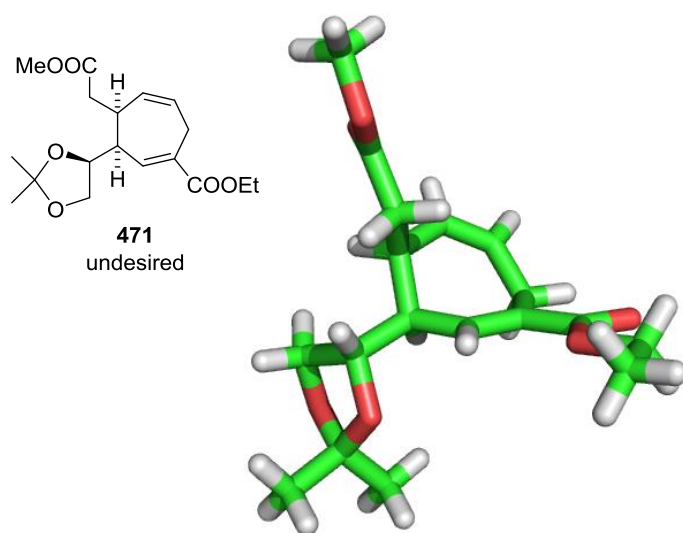


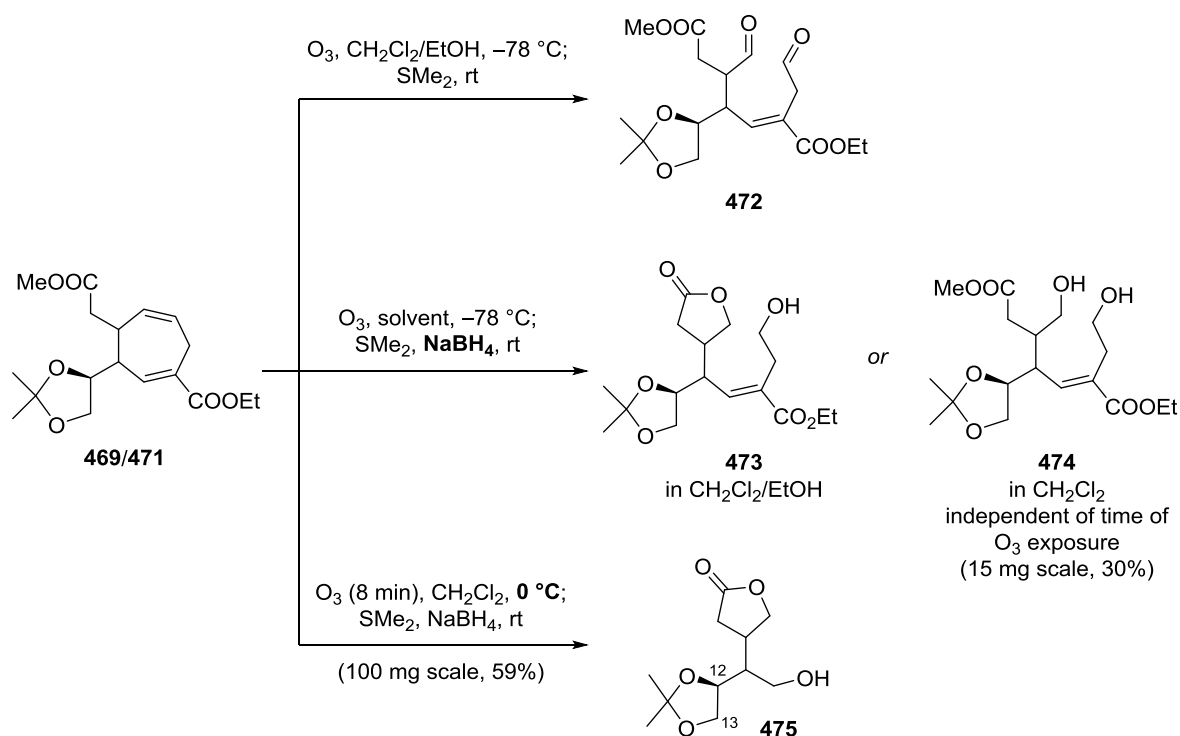
Figure 40. X-Ray single crystal structure of undesired isomer **471**. Color code: green = carbon, red = oxygen, white = hydrogen.

3.5.3.5 Initial Oxidative Cleavage Attempts by Ozonolysis

In general, the envisioned oxidative cleavage reactions proved to be very challenging especially in attempts to yield dialdehydes. Numerous attempts were thwarted by decomposition either during the

reaction, upon workup or especially upon purification attempts. Multiple side products, poor reproducibility or the polarity of the highly oxidized product and its subsequent loss in the aqueous phase further complicated these attempts. From a practical viewpoint, the reactions were challenging to analyze because oftentimes, formation of numerous products was observed simply due to partial lactonization or acetalization. In the following, only the experiments that provided clear results or insights will be summarized.

With cycloheptadiene **469** in hand, the the feasibility of the oxidative cleavage was first investigated. The feasibility of this reaction had been previously reported, albeit in low yield.^[327] As it was expected that the ozonolysis would show similar rates of olefin cleavage for both diastereomers **469** and **471**, these investigations were initially carried out with diastereomeric mixtures enriched in isomer **469** (entry 1, Table 10). Exposure of dioxolanes **469/471** to ozone at low temperatures followed by reductive workup with dimethyl sulfide gave dialdehyde **472** as indicated by crude NMR analysis (Scheme 148). The compound was not stable to purification or derivatization. In order to obtain structural confirmation, sodium borohydride was added to the reductive workup, which led to either lactone **473** in the presence of alcoholic co-solvents or to diol **474** without alcohol additives. These results were obtained even under long exposure times to ozone, implying that the olefin conjugated to the ethyl ester could be inert to oxidative cleavage under these conditions.



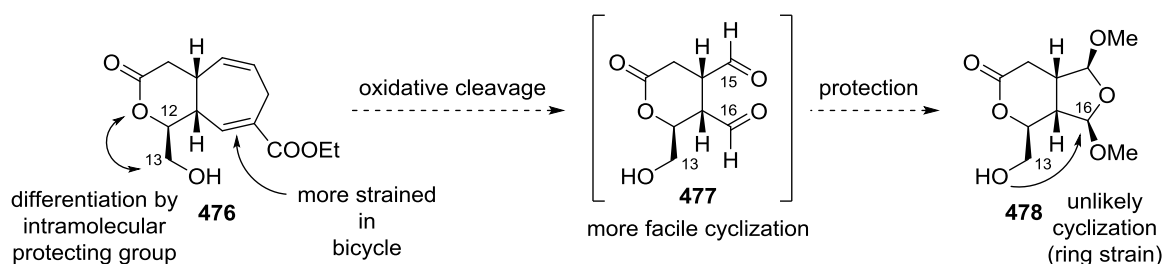
Scheme 148. Ozonolysis studies with dioxolane **469/471**.

In an attempt to also cleave the electron-poor olefin, the ozonolysis was conducted under harsh conditions at $T = 0\text{ }^\circ\text{C}$ (Scheme 148). Remarkably, lactone **475** was isolated in good yield after reductive workup. This result encouraged further effort concerning the oxidative cleavage with more

elaborate substrates that would easily allow for differentiation between the multiple sites of oxidation. Lactone **475** features several carbon atoms on the alcohol oxidation state that would probably require multi-step differentiation in the following steps.

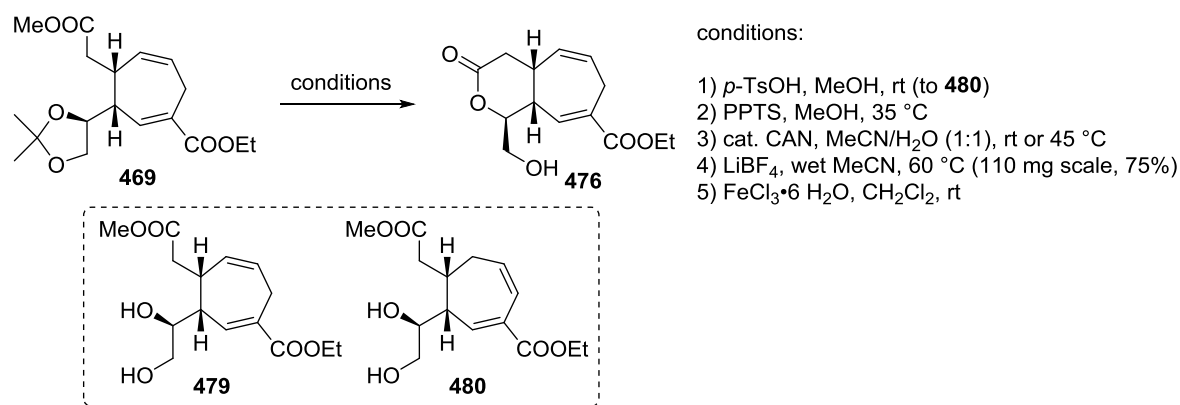
3.5.3.6 Synthesis of Bicyclic Substrate for Oxidative Cleavage

With good support of the feasibility of the envisioned key oxidative cleavage, substrates were to be prepared that would allow for a more facile conversion to the gracilin natural products. Therefore, it was envisioned that the formation of a lactone could efficiently differentiate the C12 and the C13 alcohol functionality based on ring size considerations (Scheme 149). A bicyclic molecule could also undergo oxidative cleavage under milder conditions because the cyclic olefins would be more strained and hence more reactive. Strategically, it seemed very effective to use the lactone in **476** as an intramolecular protecting group that also would allow for a more facile cyclization of the sensitive intermediate C15/C16 dialdehyde **477** to bisacetal **478**. The oxidation state of carbon atom C13 could be adjusted prior or after the key oxidative cleavage. In either case, a cyclization of the C13 oxygen atom on C16 was considered unlikely because it would form a rather strained *trans*-hydrindane-type skeleton.



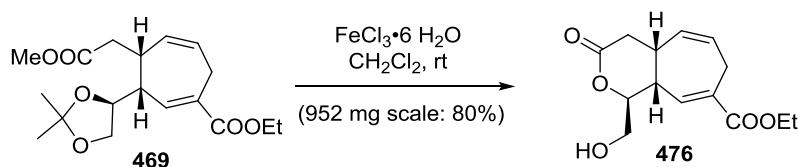
Scheme 149. Alternative substrate **476** for oxidative cleavage and its advantages *en route* to gracilin natural products.

Initial attempts focused on the deprotection of the dioxolane moiety in cycloheptadiene **469** with the final aim to convert the intermediate diol **479** to lactone **476** in one overall step (Scheme 150). Standard acidic conditions for the deprotection were found to be unsuitable due to olefin migration into conjugation to yield diene **480** (condition 1). The olefin migration was suppressed with weaker acids and the dioxolane was effectively deprotected to diol **479**, but cyclization to lactone **476** was very slow (condition 2).



Scheme 150. Deprotection studies of dioxolane **469** to lactone **476**.

Both reactions could be realized by LEWIS rather than BRØNSTEDT acids. Consequently, a literature-inspired deprotection with CAN was attempted.^[328] No side reactions were observed under these conditions and deprotection of the dioxolane was rapid, but cyclization to lactone **476** was only quantitative after several days even at elevated temperatures (condition 3). An alternative procedure based on the intermediate formation of HF from LiBF₄ and wet MeCN was attempted and afforded the product cleanly in good yield at higher temperature (condition 4).^[329] To shorten the reaction time further, an iron-based deprotection was tested (condition 5).^[330] These conditions proved to be most efficient for the deprotection and cyclization to lactone **476** and were used on gram scale in very good yield (Scheme 151). The use of additives to increase the rate of lactonization was found to be ineffective (4 Å MS) or inhibited the dioxolane deprotection (K₂CO₃ or DBU). This is in accordance with the assumption in the literature that this dioxolane cleavage is not merely a LEWIS acid-based process, but also involves protonation.



Scheme 151. Optimized procedure for the deprotection of dioxolane **469** and cyclization to lactone **476**.

At this point, the structure of lactone **476** resulting from diastereomer **469** was unambiguously proven by X-ray single crystal structure analysis (Figure 41).

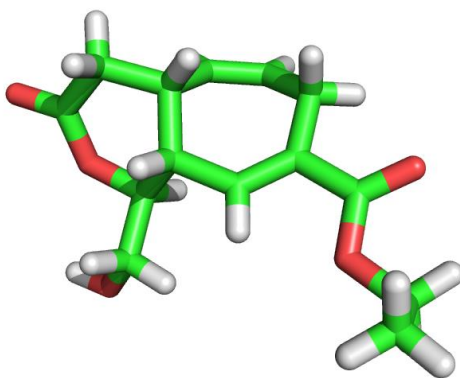
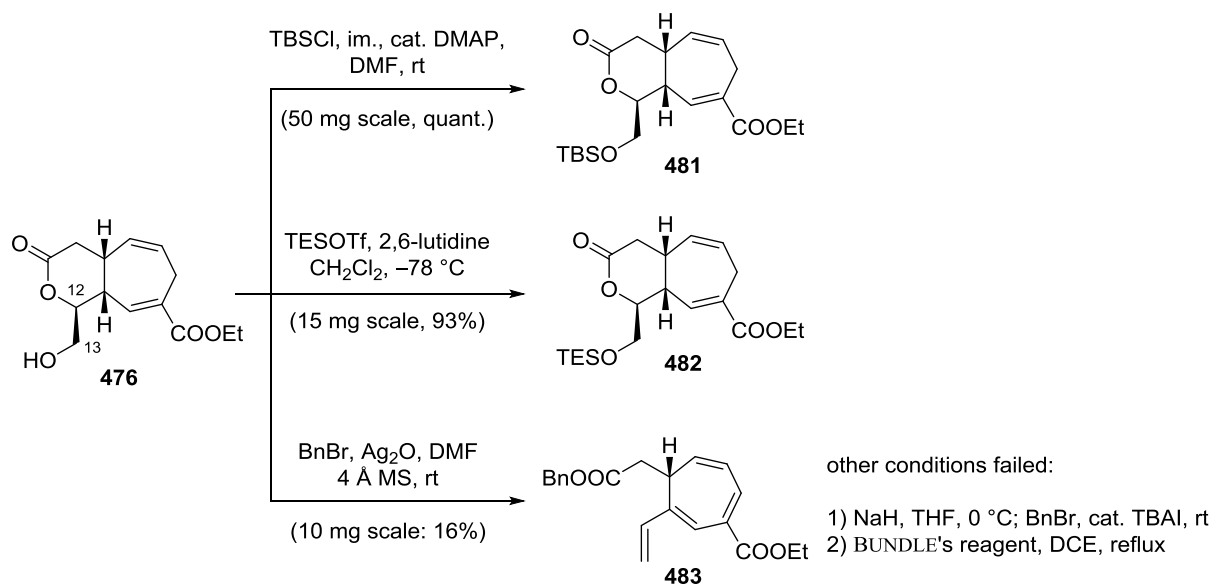


Figure 41. X-Ray single crystal structure of lactone **476**.
Color code: green = carbon, red = oxygen, white = hydrogen.

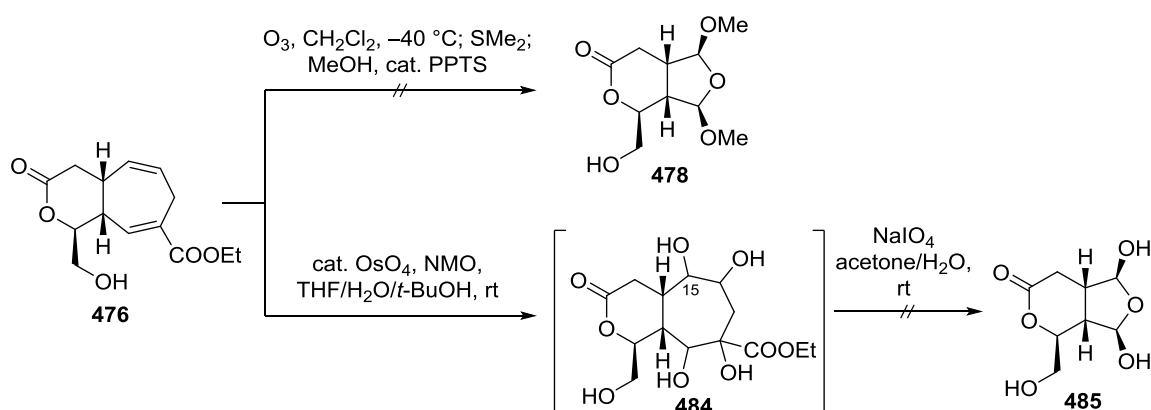
In order to decrease the polarity of alcohol **476** to avoid potentially cumbersome workup after the oxidative cleavage, the alcohol functionality was protected (Scheme 152). Both TBS and TES protection were successful under standard conditions to afford silyl ethers **481** and **482**. However, benzyl protection again highlighted the sensitivity of cycloheptadienes such as **476** under certain conditions. Both oxygen functionalities (C12/C13) were successively eliminated under the reaction conditions, with intermediate migration of the olefin into conjugation. Since C13 alcohol was probably eliminated after benzyl ether formation, the resulting BnOH could be acylated to eventually afford benzyl ester **483**. Alternative benzylation methods either led to reisolation of starting material alongside with ester hydrolysis (condition 1), potentially upon workup, or decomposition (condition 2).



Scheme 152. Protection of alcohol **476** to decrease polarity.

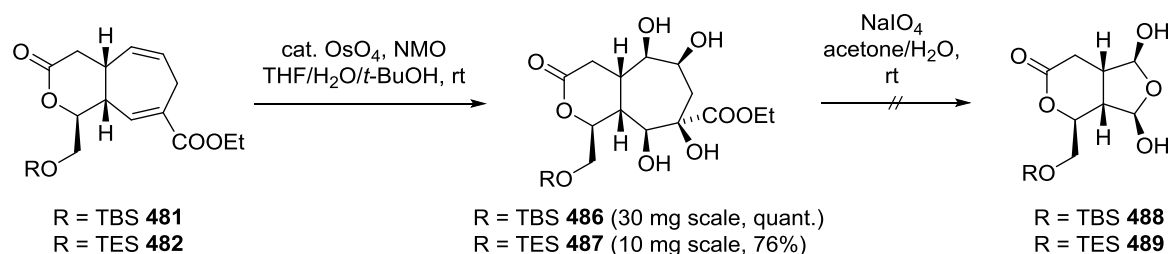
3.5.3.7 Oxidative Cleavage of Bicyclic Substrates

With a route to the required lactone **476** secured, its oxidative cleavage was studied. Three key experiments are shown in Scheme 153. It had been identified that ozonolysis at $T = -40\text{ }^{\circ}\text{C}$ was able to cleave both cyclic olefins. Despite the previous success of this transformation with dioxolane **469**, the application of these conditions only afforded multiple intractable products. When subsequent cyclization to bisacetal **478** was attempted, a furan was identified by crude NMR and HRMS. It appeared as if the intermediate dialdehyde would need to be handled carefully, because dehydrative aromatization could otherwise occur.



Scheme 153. Oxidative cleavage trials by ozonolysis of lactone **476**.

An alternative two-step LEMIEUX–JOHNSON procedure delivered pentaol **484** as judged by LC/MS, which was immediately subjected to NaIO_4 -mediated cleavage to give product **485** (Scheme 153). However, only monocleavage to the C15 aldehyde was observed. In order to decrease the polarity of the products, the protected analogs **481** and **482** were tetrahydroxylated to tetraol **486** and **487** respectively (Scheme 154). The relative stereochemistry was not proven and assumed based on the higher probability of the functionalization from the convex face. A different diastereomer was not detected.

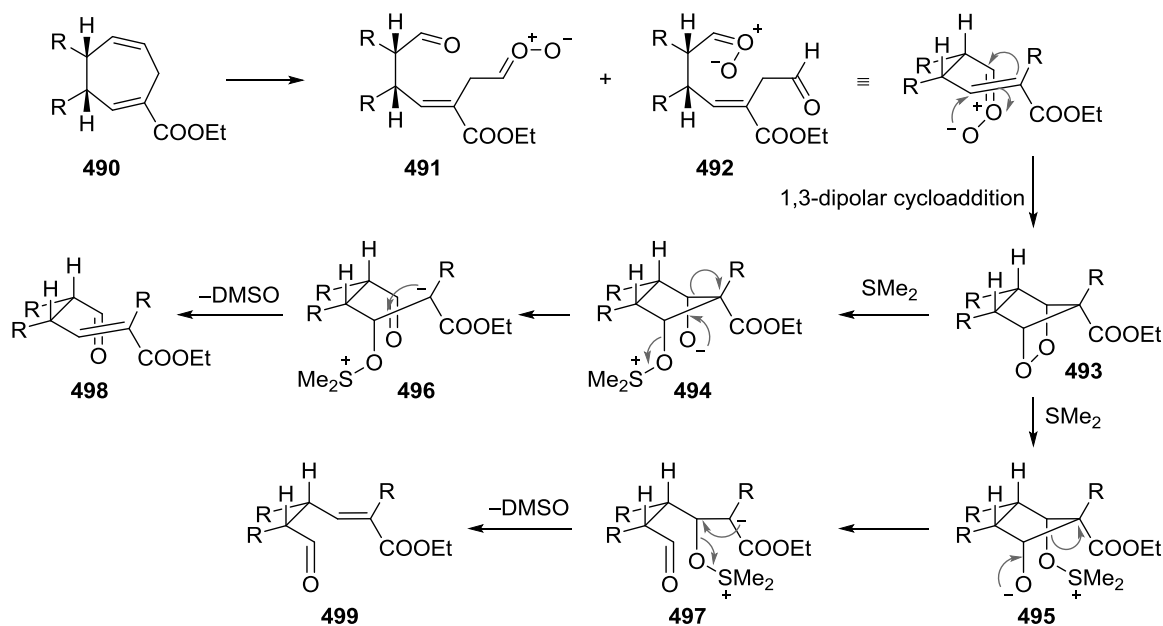


Scheme 154. Tetrahydroxylation of protected alcohol derivatives.

Subjection to LEMIEUX–JOHNSON oxidation conditions led to exclusive monocleavage of tetraol **486** regardless of the oxidation agent. No bisacetal **488** was detected. The TES protecting group in tetraol **487** was unstable to the cleavage conditions and the resulting product, either monocleavage or bisacetal **489**, therefore became too polar for isolation. The results of the LEMIEUX–JOHNSON cleavage

were obtained in parallel with results presented in 3.5.3.8 Synthesis and Oxidative Cleavage of C13 Oxidized Substrates and will be discussed in detail there.

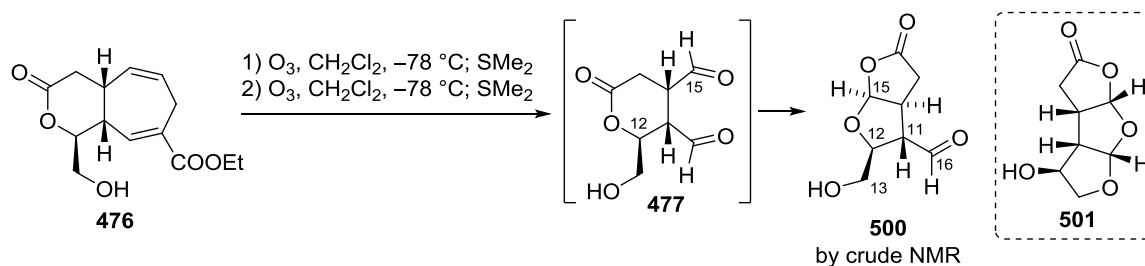
Unexpectedly, the ozonolysis reactions with lactone **476** often generated complex reaction mixtures, from which some components could be identified. In some cases, enones were recovered after ozonolysis at $T = -78\text{ }^{\circ}\text{C}$, which was first attributed to the low reactivity of the electron-poor olefin. In another hypothesis, the recovery of enones was credited to the possibility that the conjugated olefin might get masked during the reaction and is reinstalled during workup. A detailed analysis of the reaction mechanism suggested that the intermediate carbonyl oxide most likely underwent a 1,3-dipolar cycloaddition with the conjugated olefin (Scheme 155). Thus, initial cleavage of the more reactive bond in general substrate **490** could yield carbonyl oxide **491** or **492**. The former could lead to the desired product, whereas the latter is also able to undergo intramolecular (3+2)-cycloaddition to furnish peroxide **493**. Upon workup, dimethyl sulfide could cleave the labile O–O bond in two distinct ways. Both would initially yield an alkoxide **494/495** that would engage in a retro-aldol reaction to furnish enolate **496/497**. The latter would expel DMSO and give rise to unsaturated ester **498/499**.



Scheme 155. Hypothesis for recovery of unsaturated esters **498** and **499** from ozonolysis.

The hypothesis was in line with previously obtained results. The complete ozonolysis of dioxolane **469** to lactone **475** would presumably suffer less from this undesired cycloaddition, because the conformation of the substrate is more flexible and disfavors rapid cyclization. In contrast, bicyclic substrates were designed to undergo fast cyclization, *e.g.* of dialdehyde **477** to bisacetal **478**. The restriction of the substrate conformation would also accelerate other cyclization processes, which would increase the amount of undesired side products **498** and **499**. Conducting the reaction in alcoholic solvent might help to trap the carbonyl oxide **492**, but the resulting hydroperoxide is still predestined to engage in an oxa-MICHAEL reaction with the conjugated olefin.

As a potential solution, the ozonolysis could be conducted twice because product **498/499** cannot undergo the same masking process again. Indeed, when alcohol **476** was subjected to two consecutive ozonolyses, double oxidative cleavage occurred more cleanly. Alcohol **500** was observed by crude NMR as the major product (Scheme 156). The relative stereochemistry was not proven, but was assigned based on the assumption that no epimerization occurred.



Scheme 156. Double ozonolysis of cycloheptadiene **476** to aldehyde **500**.

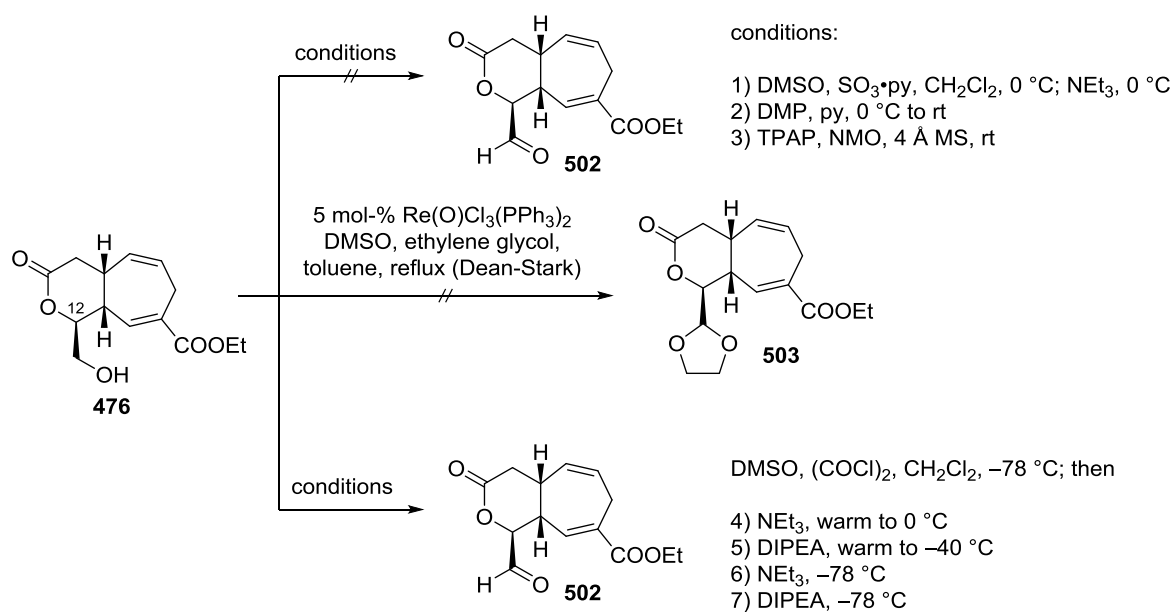
Under the reaction conditions, the initial dialdehyde **477** was able to rearrange to aldehyde **500**. It had not been expected that aldehyde **500** would form preferentially over tricycle **501**, but this result was observed often in this thesis with unprotected C12 secondary alcohols, even under thermodynamic conditions. Aldehyde **500** was found to be unstable to purification. Therefore, it seemed unlikely that the aldehyde moiety would survive conditions that could convert undesired bicycle **500** to desired tricycles of type **501**. Especially the C11 stereocenter would be very prone to epimerization so that the C13 alcohol could cyclize on the C16 aldehyde.

Concerning the envisioned total synthesis, the different cyclization mode was problematic since it inhibited the synthesis of the desired tricycle **501** when the C12 alcohol was unprotected. A possible way to enforce the formation of the desired tricycle **501** might be the oxidation of the C13 position to an aldehyde. Due to its lability, it was not possible to test this hypothesis with alcohol **500**. It was rather decided to oxidize the C13 position prior to oxidative cleavage.

3.5.3.8 Synthesis and Oxidative Cleavage of C13 Oxidized Substrates

The alcohol **476** was subjected to known oxidation protocols that are mild enough to avoid epimerization of the sensitive oxygenated α -stereocenter at C12. This oxidation would deliver a molecule with the correct oxidation states of all atoms except C15 and C16 for gracilin precursor **361**. After olefin cleavage, this molecule was expected to directly cyclize to the desired tricycle.

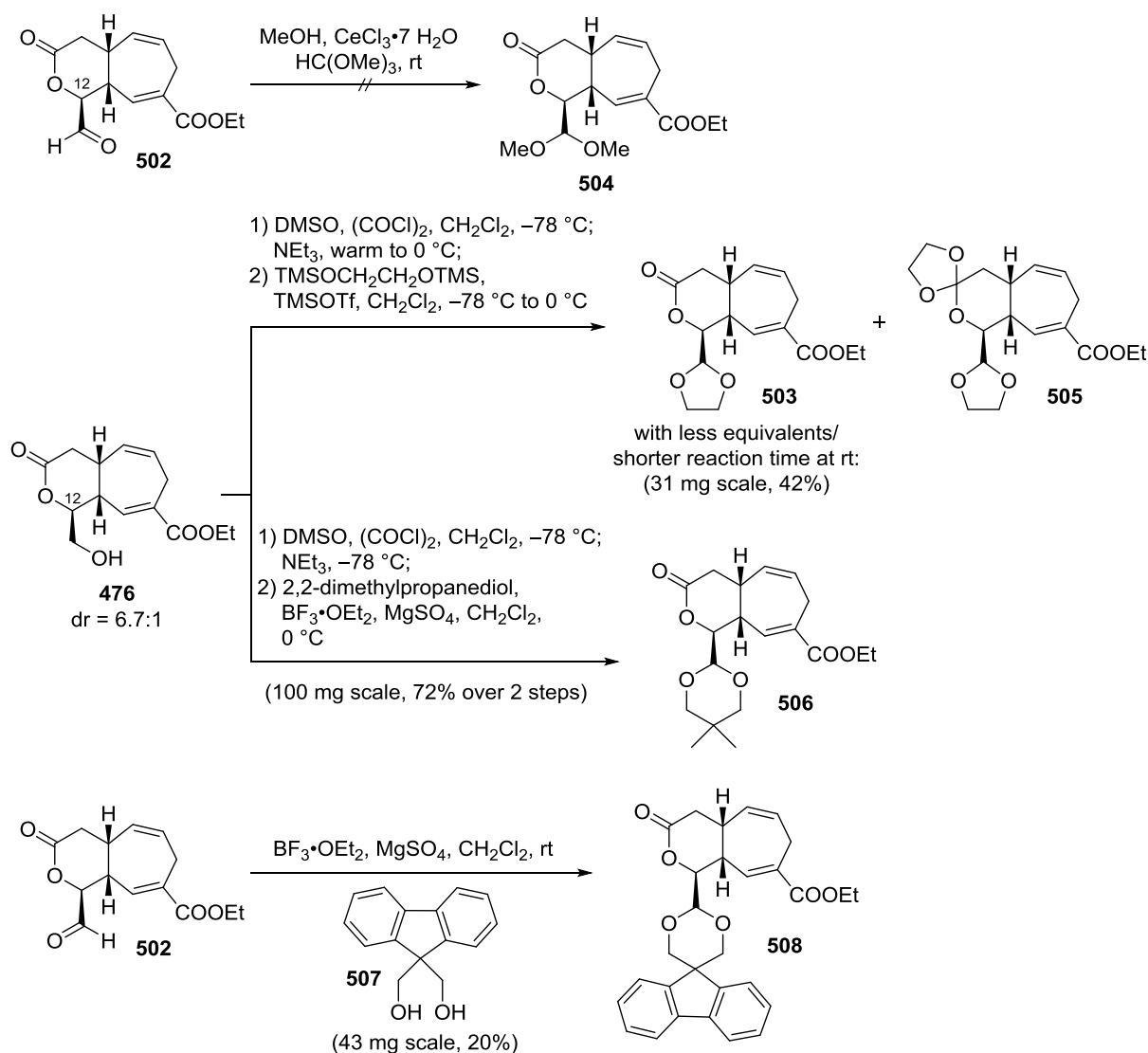
Neither PARIKH–DOERING nor DESS–MARTIN nor LEY oxidation gave aldehyde **502** and the starting material was recovered (Scheme 157, conditions 1–3). A protocol described by ARTERBURN and PERRY was tested, wherein alcohol **476** would be directly converted to dioxolane **503**, albeit without success. Starting material was reisolated (condition 3).^[331]



Scheme 157. Oxidation of lactone **476** to aldehyde **502**.

A standard SWERN oxidation protocol gave rise to the desired aldehyde **502** that could not be purified due to its lability (condition 4). Gratifyingly, the α -stereocenter of crude aldehyde **502** in benzene solution did not show signs of epimerization. The presence of base at higher temperatures seemed to lead to partial decomposition, which was rationalized with side reactions arising from aldehyde enolization. Thus, DIPEA as a more bulky base that would not readily deprotonate aldehyde **502** was employed. A corresponding SWERN oxidation furnished the latter very cleanly at temperatures as low as $T = -40\text{ }^\circ\text{C}$ (judged by crude NMR analysis, condition 5). As an alternative, triethylamine at $T = -78\text{ }^\circ\text{C}$ could also be used whereas DIPEA was not an effective base at this temperature (conditions 6, 7).

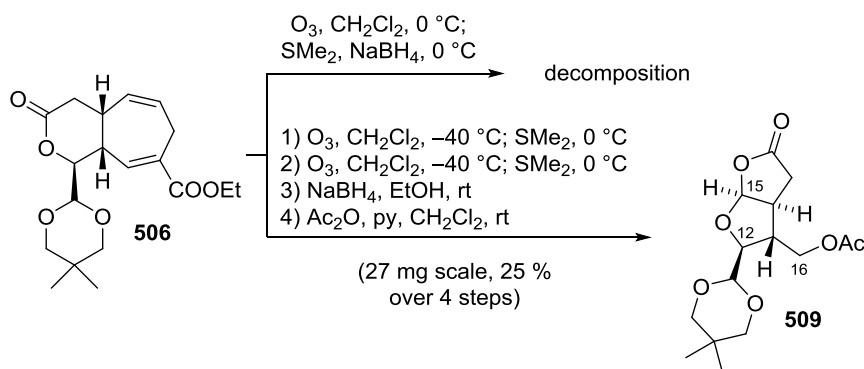
As evident from the lability of aldehyde **502**, its protection was crucial for further transformations. Initial efforts to convert aldehyde **502** to dimethoxyacetal **504**, which could be easily deprotected, proved to be unfruitful with MeOH and Ce^{III} (Scheme 158).^[332] Starting material was reisolated and epimerization was observed at carbon atom C12.

Scheme 158. Protection of aldehyde **502** as an acetal.

It was attempted to protect the labile aldehyde **502** as a cyclic acetal, which forms more readily and is usually more stable.^[333] NOYORI ketalization conditions provided the desired dioxolane **503** along with overprotected orthoester **505** if an excess of the ethane diol derivative was employed and reaction times were long. The formation of the side product was suppressed at shorter reaction times with only slight excess of the protection reagent, but the yield was still moderate. It was hypothesized that the strongly LEWIS-basic conditions could lead to the formation of an enol, which could decompose by dimerization or other reactions. Thus, a diol was chosen that cyclizes more rapidly due to the THORPE–INGOLD effect. Exposure of the labile aldehyde to strong LEWIS acids would thus be limited. Acetalization with BF_3 as a LEWIS acid activator and MgSO_4 as drying agent successfully gave dioxane **506** in good yield over two steps.^[334] Several reproducibility problems had to be addressed in this two-step procedure. Thorough drying of aldehyde **502** by coevaporation with benzene, pre-drying of MgSO_4 at $T = 650^\circ\text{C}$ on high vacuum as well as careful temperature control in the protection step were crucial. CuSO_4 as drying agent was equally effective, but less practical to dry.

Incorporation of a UV-active protecting group to facilitate monitoring of the oxidative cleavage by reaction with diol **507** in an analogous procedure was possible, but the yield of dioxane **508** was low and not synthetically useful. Presumably, the protection is too slow to prevent decomposition of the aldehyde under these conditions.

Dioxane **506** was subjected to the previously effective ozonolysis conditions, but only unidentified decomposition products were observed (Scheme 159). The comparably high temperature of $T = 0\text{ }^{\circ}\text{C}$ was probably too harsh for the more elaborate substrate **506**. Especially the oxidative cleavage of aldehyde acetals by ozone had been reported in the literature and probably constitutes one of the main decomposition pathways.^[335] Following a previously successful protocol, the ozonolysis was conducted at lower temperature twice but no product could be isolated at this stage. Thus, it became necessary to reduce the intermediate product with NaBH_4 and even acetylation was required to be able to identify products from this reaction.

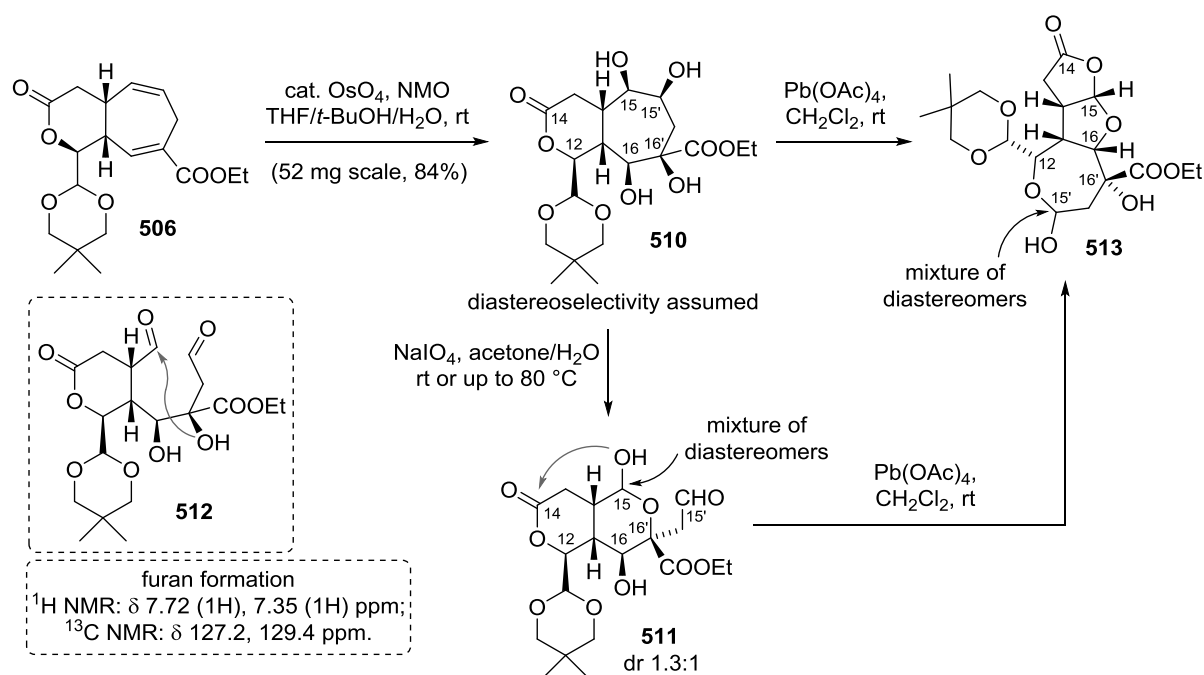


Scheme 159. Ozonolysis attempts with dioxane **506**.

The dioxane **509** was obtained from the reaction mixture in good yield over four steps (71% per step). However, since reduction and protection are usually high-yielding, the low overall yield probably reflects the formation of several byproducts in the ozonolysis step. According to earlier observations, it became apparent that the undesired cyclization mode was also operative in this substrate. The stability of the double ozonolysis product did not allow for their isolation so that reduction became necessary. Therefore, acidic deprotection to C13 aldehyde with parallel skeletal rearrangement to tricycles of type **501** as originally planned could not be tested.

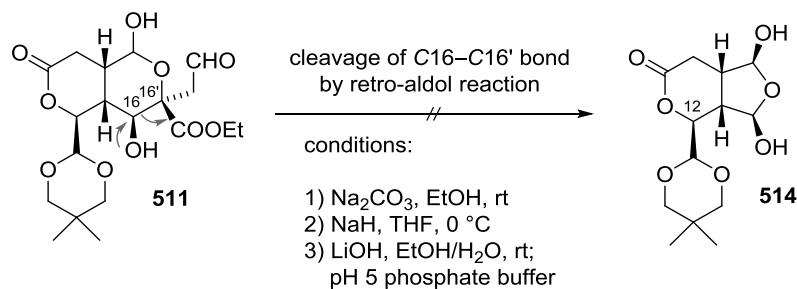
As a consequence, alternatives of the ozonolysis for the synthesis of the gracilin natural products were to be tested. Despite the initial success of the double ozonolytic cleavage, the reactions were problematic to monitor and product mixtures were often generated with more elaborate structures. A more controlled and stepwise approach to the oxidative cleavage of dioxane **506** could be pursued with a two-step LEMIEUX–JOHNSON oxidation. One-pot protocols had also afforded intractable product mixtures.

To this end, dioxane **506** was tetrahydroxylated to tetraol **510** using catalytic amounts of OsO_4 and an excess NMO (Scheme 160). The resulting tetraol **510** was used without purification.

Scheme 160. LEMIEUX–JOHNSON cleavage of dioxane **506**.

Diol cleavage was attempted with $\text{PhI}(\text{OAc})_2$,^[336] but it became evident that a suitable analysis of the products would only be possible with inorganic oxidants that would remain in the aqueous workup phase. Cleavage with NaIO_4 at room temperature or up to $T = 80\text{ }^\circ\text{C}$ resulted in the formation of the monocleavage product **511** as a mixture of diastereomers (dr = 1.2:1), probably *via* dialdehyde **512**. Not unexpectedly, the cleavage of the less sterically encumbered diol (C15/C15') occurred first. The remaining diol probably cyclizes onto the newly formed C15-aldehyde, which is encouraged by the preorganization induced by the lactone ring. The resulting hemiacetal proved to be stable up to $T = 95\text{ }^\circ\text{C}$, where the sterically hindered dialdehyde **512** could be cleaved. However, the resulting C15/C16-dialdehyde underwent dehydrative aromatization to a furan under these conditions as judged by crude NMR analysis, potentially again supported by the structural preorganization. It was hypothesized that the use of stronger oxidants with LEWIS-acidic properties would facilitate the cleavage of the second diol motif in hemiacetal **511**. Upon treatment with Pb^{IV} , a structural reorganization was detected, but no cleavage occurred. The same product was observed when tetraol **510** was directly treated with lead tetraacetate and could be assigned as hemiacetal **513**, again as a mixture of diastereomers. Unambiguous determination of the diastereomeric ratio was not possible based on crude NMR analysis. Upon LEWIS acid activation, the C15 hemiacetal apparently formed an isomeric hemiacetal with the C16 alcohol. One of the diastereomers of this new hemiacetal might cyclize onto lactone (C14), liberating the C12 secondary alcohol. Potentially again under LEWIS acid catalysis, the latter can attack the C15' aldehyde to furnish hemiacetal **513**. The cyclization of C16 alcohol onto C15 aldehyde probably is as unselective as the cyclization of C16' alcohol to hemiacetal **511**, but one of the diastereomers is removed from the equilibrium by cyclization onto C14 lactone. Hence, product **513** only exists as a mixture of two diastereomers based on the C15' stereocenter.

An alternative cleavage method of the C16–C16' bond in hemiacetal **511** to bisacetal **514** was attempted by a retro-aldol reaction (Scheme 161). Whereas treatment with carbonate base in alcohol solvents did not lead to the desired bond fragmentation (condition 1), NaH in THF converted the lactone **511** to hemiacetal **513** (condition 2). Hydroxide base was found efficient to cleave the desired C16–C16' bond, but also led to the formation of the previously observed furan (condition 3, see Scheme 160 for comparison).



Scheme 161. Retro-aldol attempts at cleavage of C16–C16' bond.

The LEMIEUX–JOHNSON oxidation was found much more straight-forward and easier to analyze than related ozonolyses. The results obtained showed that double oxidative cleavage is possible, but milder conditions would be needed to avoid cyclization to a furan.

3.5.3.9 Oxidative Cleavage of Substrates with C14 Carboxylic Acid

The crucial challenge of the successful double oxidative cleavage would be to avoid premature cyclization of the remaining diol onto the formed C15 aldehyde. One possibility would include a competing cyclization of a C14 acid such as **515** that would in any case ensure a higher equilibrium content of the free C16/C16' diol (Figure 42). Furthermore, the problem of C12 alcohol cyclization on C15 to afford undesired bicycles such as **500** could be avoided by installation of suitable protecting groups after lactone hydrolysis.

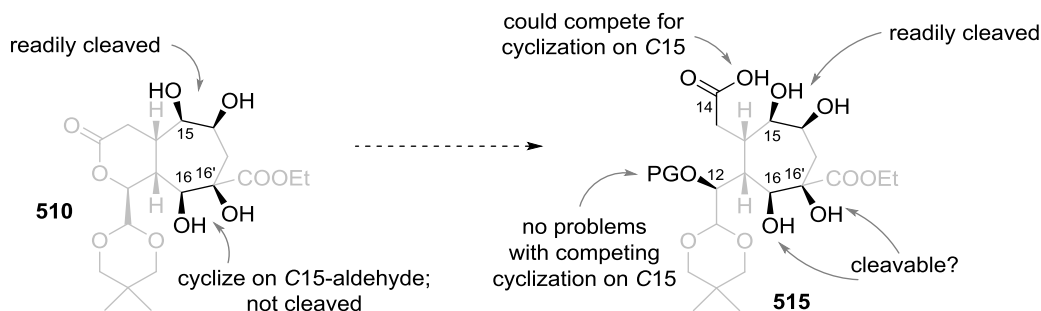
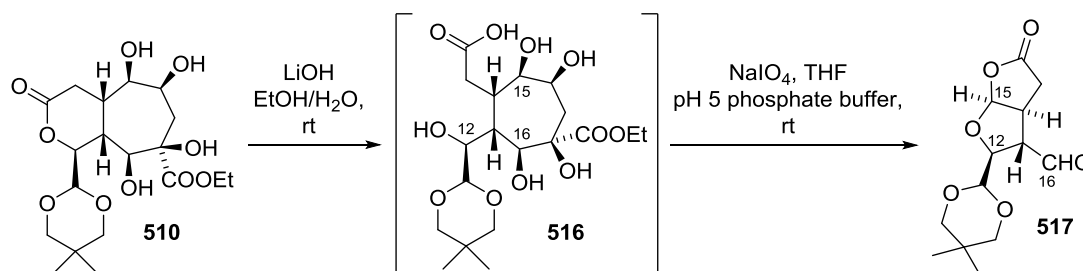


Figure 42. Rationale behind synthesis of acid precursor **515**.

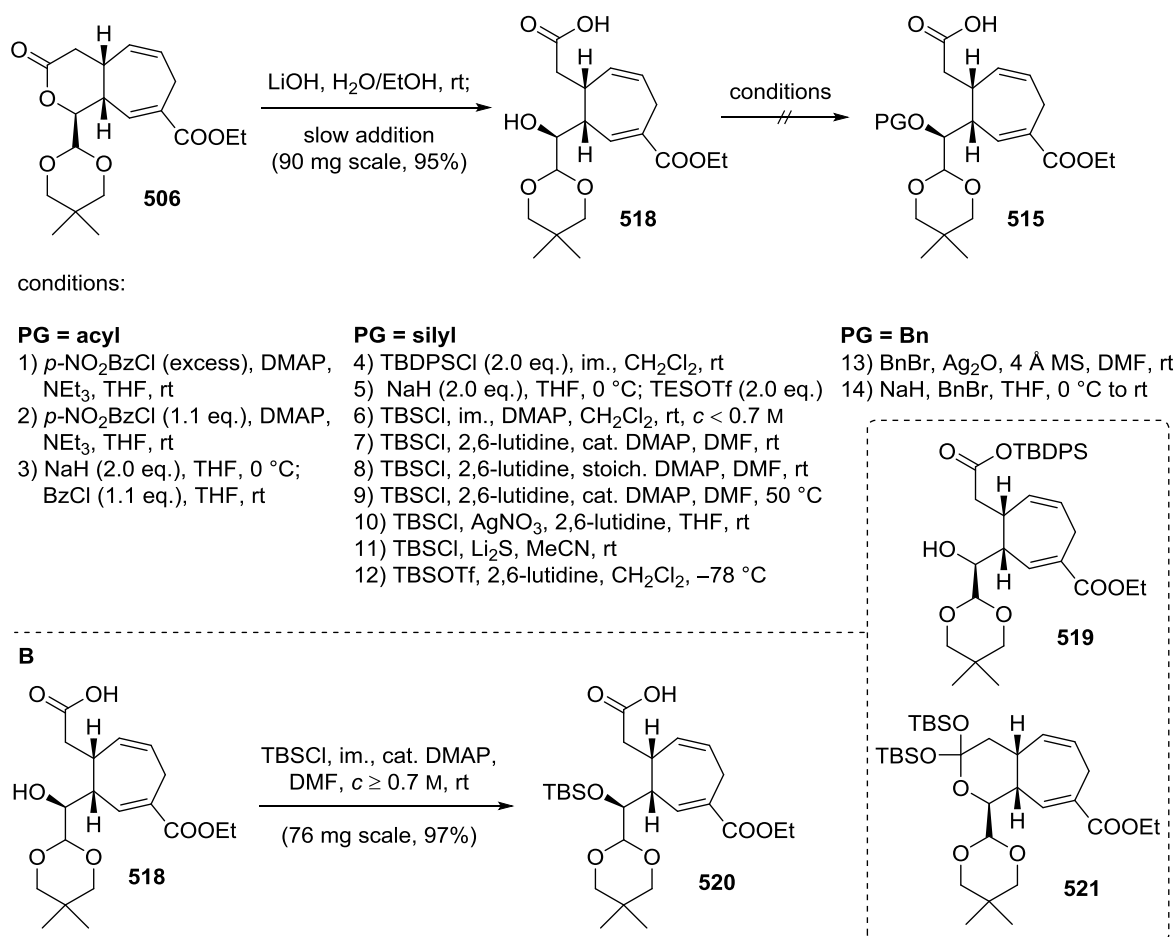
As a proof of principle, the intermediate tetraol **510** was treated with base to effect the hydrolysis of the lactone (Scheme 162). The resulting pentaol **516** was immediately subjected to NaIO₄ in slightly

acidic solution in the same reaction vessel. Indeed, the olefin diol cleavage went to completion and furnished aldehyde **517** as evident from LC/MS and crude NMR analysis.



Scheme 162. Proof of principle of milder reaction conditions to complete diol cleavage.

Lactone **506** was selectively hydrolyzed to acid **518** with a stoichiometric amount of LiOH, which had to be introduced slowly to ensure that the conjugated ester remained untouched (Scheme 163). The subsequent protection of the secondary alcohol to products of type **515** proved to be very challenging due to its low reactivity, probably resulting from steric encumbrance. Furthermore, some conditions activated the acid so that lactone **506** was formed again.

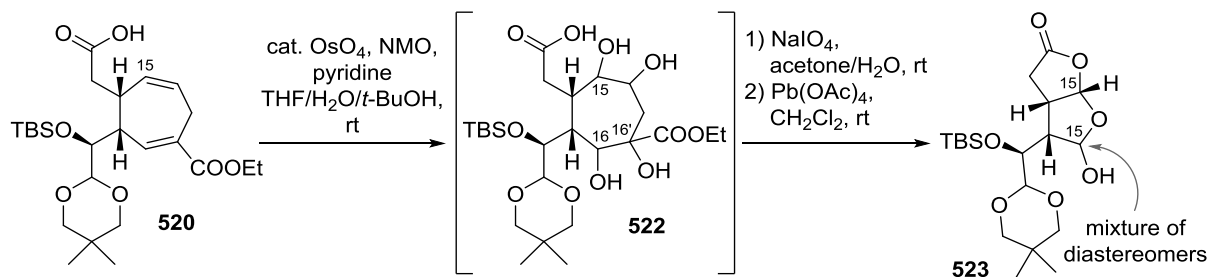


Scheme 163 A. Hydrolysis and protecting studies of lactone **506**. **B.** Optimized protection conditions.

Acyl protecting groups could not be introduced since they first reacted with the carboxylic acid and then underwent lactonization to dioxane **506** (conditions 1, 2). Even deprotonation of both

functionalities and treatment with one equivalent of BzCl afforded lactone **506**. Despite the higher nucleophilicity of an alkoxide compared to the carboxylate, the steric hindrance of the secondary alcohol apparently prevented its functionalization. It was thus switched to silyl protecting groups, which were supposed not to activate the acid functionality. Concomitant silyl protection of the acid was expected, but the silyl ester would be hydrolyzed upon workup. The bulky TBDPS group could not be installed on the secondary alcohol, but silyl ester **519** was isolated since it resisted hydrolysis (condition 4). Only starting material was isolated when acid **518** was completely deprotonated with NaH and treated with TESOTf (condition 5). TBS protection was not met with success under a variety of conditions involving 2,6-lutidine as the base, even at elevated temperatures (conditions 6–9). Activation of TBSCl with AgNO₃ or Li₂S was not effective (conditions 10, 11).^[337,338] Formation of product **520** was observed when acid **518** was treated with TBSOTf (condition 12, 10 mg scale, 25%). However, the side product of this reaction proved to be orthoester **521**, which was assigned by crude NMR analysis since it was not stable during purification. Mild benzyl protection with Ag₂O and BnBr lead to Bn incorporation under closure of the lactone (condition 13). Presumably, the α -position of lactone **506** was functionalized, but no further analyses were performed. Benzyl protection by WILLIAMSON ether synthesis only gave unreacted starting material (condition 14). It appeared as if the secondary alcohol was very reluctant to react as a nucleophile due to steric hindrance. Using a procedure that was found optimal for the TBS protection of phenols (see *e.g.* 2.3.3.2.5 Combination of Epicoccine and Epicoccone B Synthesis), it was possible to protect the secondary alcohol as TBS silyl ether **520** in excellent yield. The installed TBS group did not represent a desirable protecting group since it was suspected that it might not be compatible with ensuing transformations. Nevertheless, it was more important to have the secondary alcohol protected to prevent formation of undesired bicycles such as **500**. Purification of this product was complicated by recyclization to lactone **506** upon contact with silica gel.

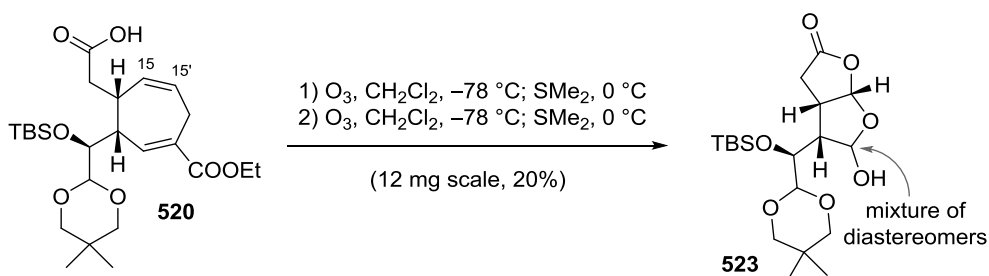
With the required acid **520** in hand, the two-step LEMIEUX–JOHNSON oxidation was attempted (Scheme 164). Tetrahydroxylation to tetraol **522** proved to be more complicated than with previous substrates, requiring more equivalents of OsO₄ and longer reaction times. In addition, on larger scales, the reaction was found to be capricious with only partial conversion after long reaction times. On small scale, tetraol **522** was accessed as a mixture of diastereomers resulting from its more conformationally flexible skeleton compared to cycloheptadiene **506**.



Scheme 164. Oxidative cleavage of acid **520**.

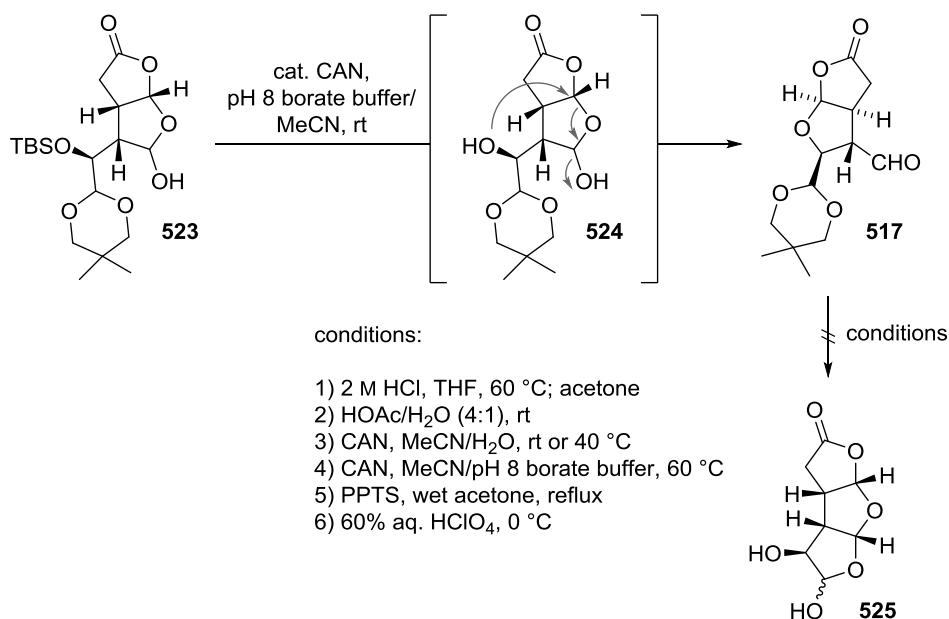
The tetraol **522** was isolable, but could not be purified and was therefore immediately subjected to oxidative cleavage with NaIO_4 . Only monocleavage was observed, but treatment of the intermediate product with $\text{Pb}(\text{OAc})_4$ afforded crude hemiacetal **523** as a mixture of diastereomers. The accomplishment of the synthesis of hemiacetal **523** was encouraging for the synthetic efforts toward the gracilin natural products. However, the tetrahydroxylation was not reproducible on larger scale. Repetition of the synthesis of the initially obtained compound, supposedly tetraol **522**, was not achieved. Instead, an isomeric tetraol was obtained in all following experiments, which upon subjection to the same oxidation conditions only yielded monocleavage products as judged by LC/MS. It was speculated that the longer exposure to the reaction conditions on larger scale might eventually lead to lactone formation with the free acid, most likely involving the C15-OH . Oxidative cleavage would thus only occur once with the C16/C16' diol.

Due to these reproducibility problems, an ozonolysis strategy was revisited that could potentially profit from the fact that an intermediate carbonyl oxide would be captured by the pendant acid moiety. It was reasoned that associated side reactions such as intramolecular 1,3-dipolar cycloadditions could be suppressed. Indeed, ozonolysis of acid **520** gave the hemiacetal **523** in modest yield next to C15/C15' monocleavage product even after a second ozonolysis (Scheme 165). It appeared as if the conjugated olefin needed higher temperatures for an efficient cleavage.



Scheme 165. Double ozonolysis toward hemiacetal **523**.

Prior to optimization studies of this reaction, it was attempted to convert hemiacetal **523** to the desired tricyclic precursor of type **361** by deprotection of the dioxane protecting group (Scheme 166).



Scheme 166. Deprotection attempts of dioxane **523** to acetal **525**.

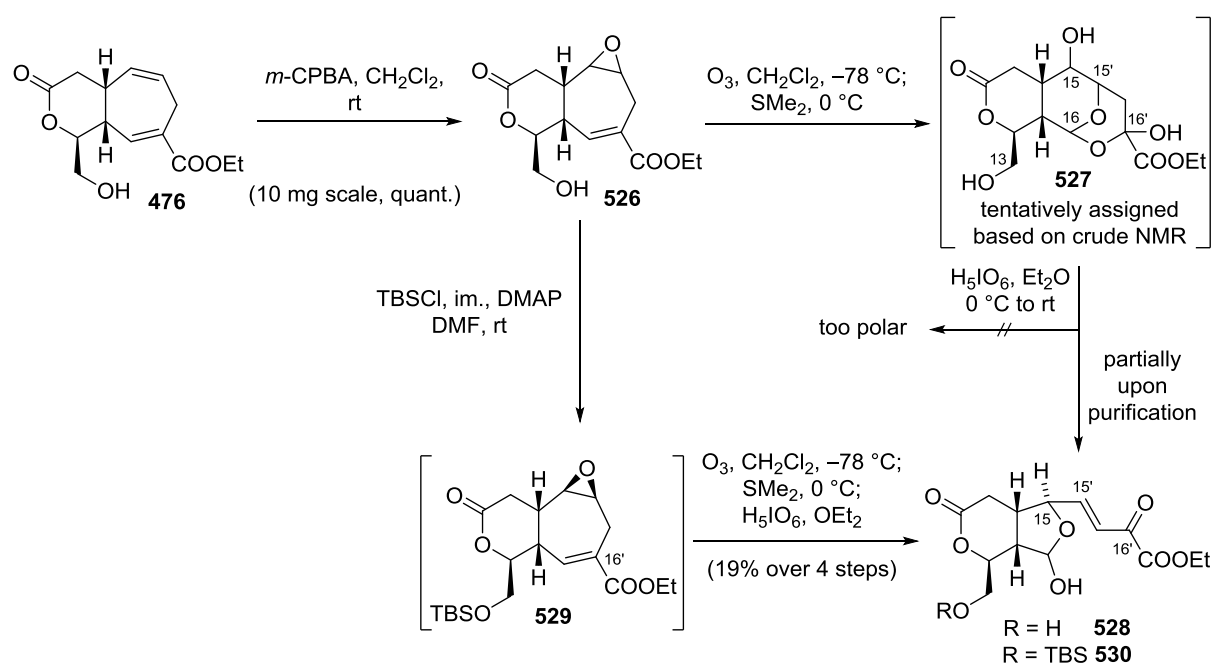
Previously successful acetal deprotection conditions with CAN at basic pH were tested first, but only resulted in the formation of undesired bicycle **517** by TBS deprotection *via* alcohol **524**.^[328] As a consequence, it was tried to cleave the dioxane protecting group in aldehyde **517** to identify suitable conditions for future experiments. In order to arrive at tricycle **525**, it was focused on aqueous conditions that could mediate the transacetalization. Under a variety of conditions, only starting material was reisolated. Neither aqueous hydrochloric acid nor acetic acid provided the product (Scheme 166, conditions 1, 2). Decomposition was observed when acetone was added, which could result from nucleophilic attack of the acetone enol on the free aldehyde in substrate **517**. Ce^{IV} as an oxidant and LEWIS acid was employed at neutral and basic pH, but no reaction was observed (conditions 3, 4). Transacetalization to acetone was attempted with the weaker acid PPTS, without success (condition 5). Even HClO₄ was not able to cleave the dioxane protecting group (condition 6). As previously expected, it seemed as if the TBS protecting group would not be stable under harsh conditions to cleave the dioxane moiety. However, formation of a TBS silyl ether had been identified as the only successful conditions for the protection of the C12 alcohol. This route was therefore discontinued since it did not seem possible to prevent cyclization to the undesired bicycle **517**.

3.5.3.10 Stepwise Oxidative Cleavage

The main challenge of the envisioned double oxidative cleavage was the presence of another olefin or diol that can undergo subsequent reactions to prevent completion of the procedure. In the case of the ozonolysis, it appeared as if the unsaturated ester engaged in a 1,3-dipolar cycloaddition (see 3.5.3.7 Oxidative Cleavage of Bicyclic Substrates), whereas in the case of the LEMIEUX–JOHNSON oxidation, the other diol prematurely cyclized on the formed aldehyde (see 3.5.3.8

Synthesis and Oxidative Cleavage of C13 Oxidized Substrates). As a potential solution, it was planned to functionalize one of the olefins prior to oxidative cleavage.

First, the *cis*-disubstituted olefin in cycloheptadiene **476** was targeted. Selective epoxidation was possible using *m*-CPBA to afford epoxide **526** as an inconsequential mixture of diastereomers (Scheme 167). Support of the hypothesis presented in Scheme 155 was offered by the fact that ozonolysis of this substrate was straight-forward, yielding hemiacetal **527** as the major oxidative cleavage product. The carbon skeleton and the oxidation states of the carbon atoms were reliably assigned by crude NMR analysis, but the acetal connections are speculative. It could only be secured that C15'-O must be bound to C16 based on 2D NMR spectra. The hemiacetal **527** partially decomposed to give olefin **528** upon purification attempts by retro-oxa-MICHAEL reaction. Therefore, crude **527** was subjected to oxidative cleavage conditions that could also convert epoxides in case they were present in the crude mixture as a minor component.^[254] The resulting products were too polar for isolation. It was hence attempted to decrease the polarity by incorporation of a TBS protecting group. Since TBS ether **481** was found to be unstable during purification, it was argued that the TBS protecting group would be cleaved under the epoxidation conditions. Thus, the order of steps was inverted and the TBS group installed in epoxide **526**.

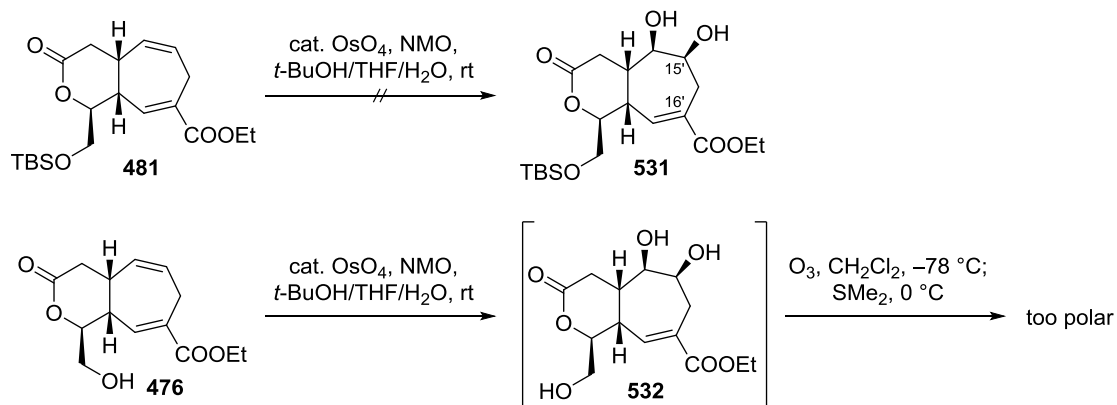


Scheme 167. Selective epoxidation of *cis*-disubstituted olefin in cycloheptadiene **476** and its oxidative cleavage.

The resulting epoxide **529** was taken forward to the ozonolysis with ensuing oxidative cleavage by I^{VII}. Hemiacetal **530** was identified the major product based on crude NMR analysis. Considering that both ozonolysis products were prone to a retro-oxa-MICHAEL type reaction once C16' ketone had formed during ozonolysis, further attempts involving epoxides **526** or **529** were not undertaken. The C16' ketone will always be likely to enolize due to its nature as an α -keto ester, which will lead to the

observed decomposition and significantly complicate the desired oxidative cleavage of the C15–C15' bond.

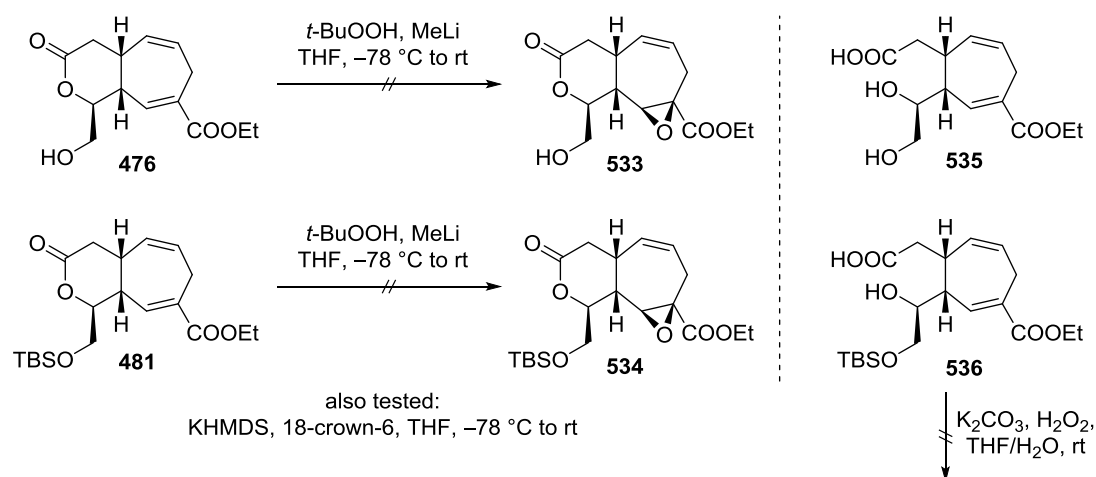
In addition to epoxidation, a selective dihydroxylation was attempted. Although a diol would also be prone to undergo β -elimination of the C15'–OH once the C16' ketone was formed, it would lack the driving force of the epoxide opening.



Scheme 168. Stepwise oxidative cleavage attempts via selective dihydroxylation.

TBS ether **481** was therefore subjected to dihydroxylation conditions, but only very poor selectivity between diol **531** and tetraol **486** was obtained based on LC/MS. An analogous reaction involving alcohol **476** showed the same lack of selectivity, but the corresponding tetraol **484** remained in the aqueous phase upon workup. As expected, the ozonolysis of triol **532** proceeded but the products were too polar for isolation.

Since masking of the *cis*-disubstituted olefin had only led to undesired side reactions, it was attempted to transform the conjugated trisubstituted olefin *via* nucleophilic SCHEFFER–WEITZ-type epoxidation. However, the olefin in alcohol **476** or silyl ether **481** resisted functionalization to epoxides **533** or **534** even under forcing conditions and only lactone hydrolysis to acids **535/536** occurred (Scheme 169). The hydrolysis probably resulted from peroxide attack on the lactone and cleavage of the labile O–O bond during reductive workup. Hydrogen peroxide as a less sterically demanding reagent to overcome the apparent high steric hindrance was equally ineffective in a related nucleophilic epoxidation of acid **536**.



Scheme 169. SCHEFFER–WEITZ epoxidation attempts.

3.5.3.11 Conclusion

This chapter has described the use of DAVIES' Rh-catalyzed formal (4+3)-cycloaddition in the context of the synthesis of the gracilin natural products. The methodology could be successfully extended to less electron-rich dienes and afforded cyclic dienes for the envisioned double oxidative cleavage. The latter proved to be complicated by the fact that initial oxidation products could engage in side reactions with the remaining olefin. After a solution had been identified, the oxidative cleavage of conformationally restricted substrates led to partial furan formation by dehydrative aromatization of the intermediate 1,4-dialdehyde. Reduction of the conformational restriction and implementation of an acid that could stabilize the intermediate dialdehydes resulted in successful double oxidative cleavage reactions. However, limited protecting group options in previous steps prevented the application of this methodology to the synthesis of gracilin natural products.

3.6 Third Strategy: Formal (3+2) Cycloaddition and Desymmetrization

3.6.1 Retrosynthetic Analysis

Due to the difficulties to either access the required cyclic diene (see 3.4 First Strategy: Torquoselective 6π -electrocyclization) or effect the double oxidative cleavage while preventing furan formation (see 3.5 Second Strategy: Rhodium-Catalyzed Formal (4+3)-Cycloaddition), an alternative, more atom-economic retrosynthesis was envisioned. It was realized that the gracilin natural products are pseudosymmetric to some extent (Figure 43). The symmetry-breaking elements are a substituent at C9, oxidation at C12 and reduction at C13. All of these features could be installed in *meso*-bislactones like **537**. However, the necessary deprotonation of one of the lactones could lead to an attack onto the other lactone functionality, which is the reason why this approach was not prioritized.

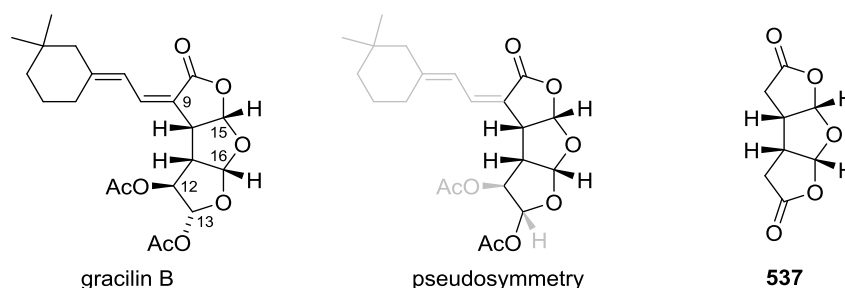
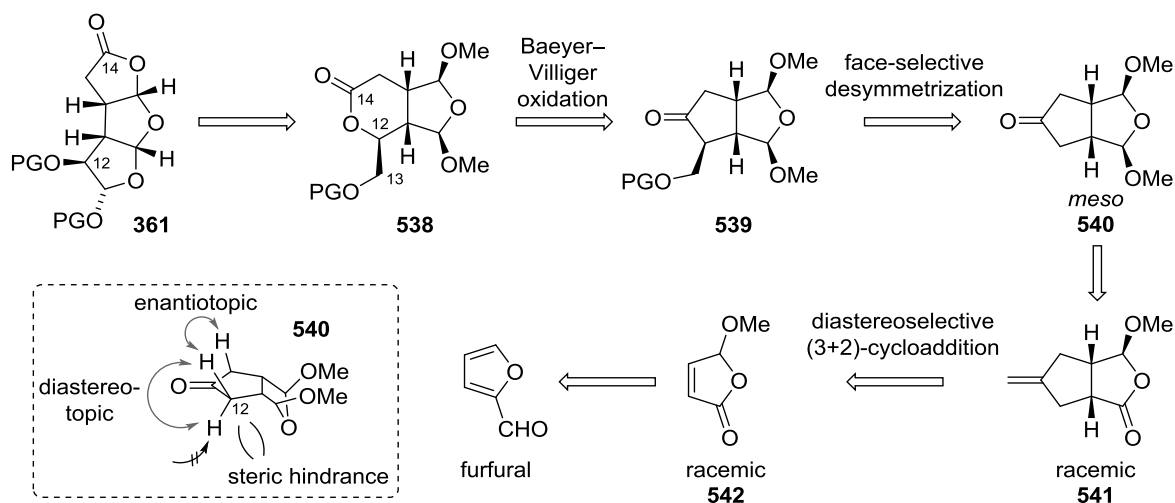


Figure 43. Pseudosymmetry in gracilin natural products.

It was envisioned that the crucial central 1,4-dialdehyde (C15/C16) would ultimately result from a furan. Furthermore, in contrast to COREY's synthesis, a *meso*-substrate was to be accessed that would undergo desymmetrization (strategy 1, 1.3 Symmetry in Natural Product Synthesis). The synthesis would therefore not need to be asymmetric until this point, which would greatly facilitate each transformation and reduce the step count. The planned retrosynthesis is depicted in Scheme 170.



Scheme 170. Retrosynthesis of gracilin natural products.

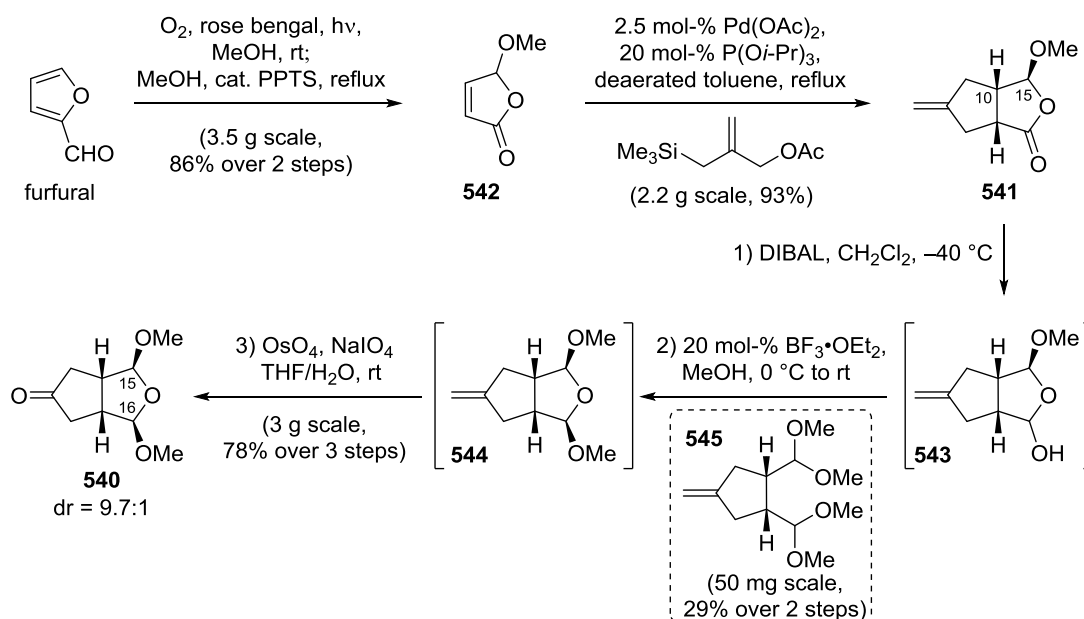
The general precursor **361** would be traced back to chiral lactone **538** by selective oxidation of the C13 alcohol, lactone opening and cyclization. The lactone itself would stem from a chiral bicyclic ketone **539** by regioselective BAEYER–VILLIGER oxidation. It is well preceded that a preferential migration of the more highly-substituted carbon atom occurs.^[339] The key step of this synthesis would be the face-selective desymmetrizing α -alkylation of *meso*-ketone **540** to ketone **539**. The diastereoselectivity of the enolate alkylation would be governed by the bicyclic structure of the substrate since the convex face is much more sterically accessible than the concave face. The desymmetrization would be ensured by a selective deprotonation of one of the enantiotopic protons by a chiral base. The corresponding set of diastereotopic protons is inaccessible due to the steric repulsion with the tetrahydrofuran ring. An asymmetric deprotonation/alkylation sequence was already successfully applied in related diquinane systems.^[340–343] The prerequisite diketone **540** could be synthesized from racemic olefin **541** that would be derived from lactone **542** through diastereoselective trimethylene methane (TMM) cycloaddition inspired by reports by TROST and CRAWLEY.^[241] This lactone is literature-known and stems from furfural by singlet oxygen DIELS–ALDER cycloaddition in MeOH.

This new retrosynthetic strategy would install the crucial 1,4-dialdehyde early on in a protected form so that aromatization to a furan will become less likely. The success of this strategy would stress the importance of symmetry considerations in retrosynthetic planning and establish the potential of lactone **542** as a dialdehyde precursor.

3.6.2 Results and Discussion

3.6.2.1 Synthesis of *meso*-Ketone

Furfural was oxidized to lactone **542** by singlet oxygen DIELS–ALDER reaction and subsequent completion of the acetalization under PPTS catalysis (Scheme 171).^[344]

Scheme 171. Synthesis of *meso*-ketone **540**.

The subsequent TMM cycloaddition proceeded smoothly even on multi-gram scale to afford olefin **541** in excellent yield. The reaction was *cis*-selective with respect to carbon atoms C10 and C11. The inconsequential diastereoselectivity based on carbon atoms C10 and C15 was not determined by crude NMR analysis, but product **541** after purification was exclusively the *trans*-isomer. It was found that the subsequent conversion to ketone **540** was best conducted in the presented order without intermediate purification due to the volatility of the intermediates. DIBAL reduction gave the best results in methylene chloride as a solvent at low temperatures, cleanly furnishing hemiacetal **543**. The latter was acetalized to bisacetal **544** under LEWIS acid catalysis since BRØNSTEDT acids led to olefin migration. With added HC(OMe)₃ as a drying agent, the formation of bisacetal **545** was observed. Olefin cleavage using a LEMIEUX–JOHNSON oxidation gave rise to the desired ketone **540** in very good yield over three steps. The structure of *C_s*-symmetric ketone **540** was unambiguously proven by X-ray single crystal structure analysis (Figure 44).

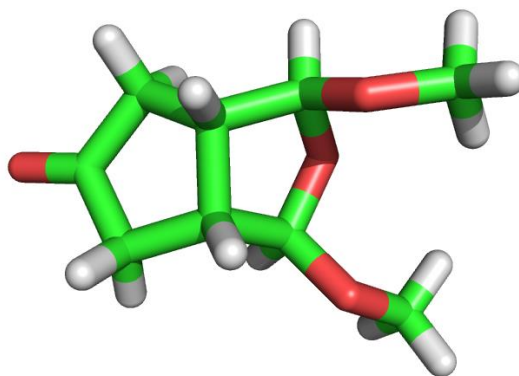


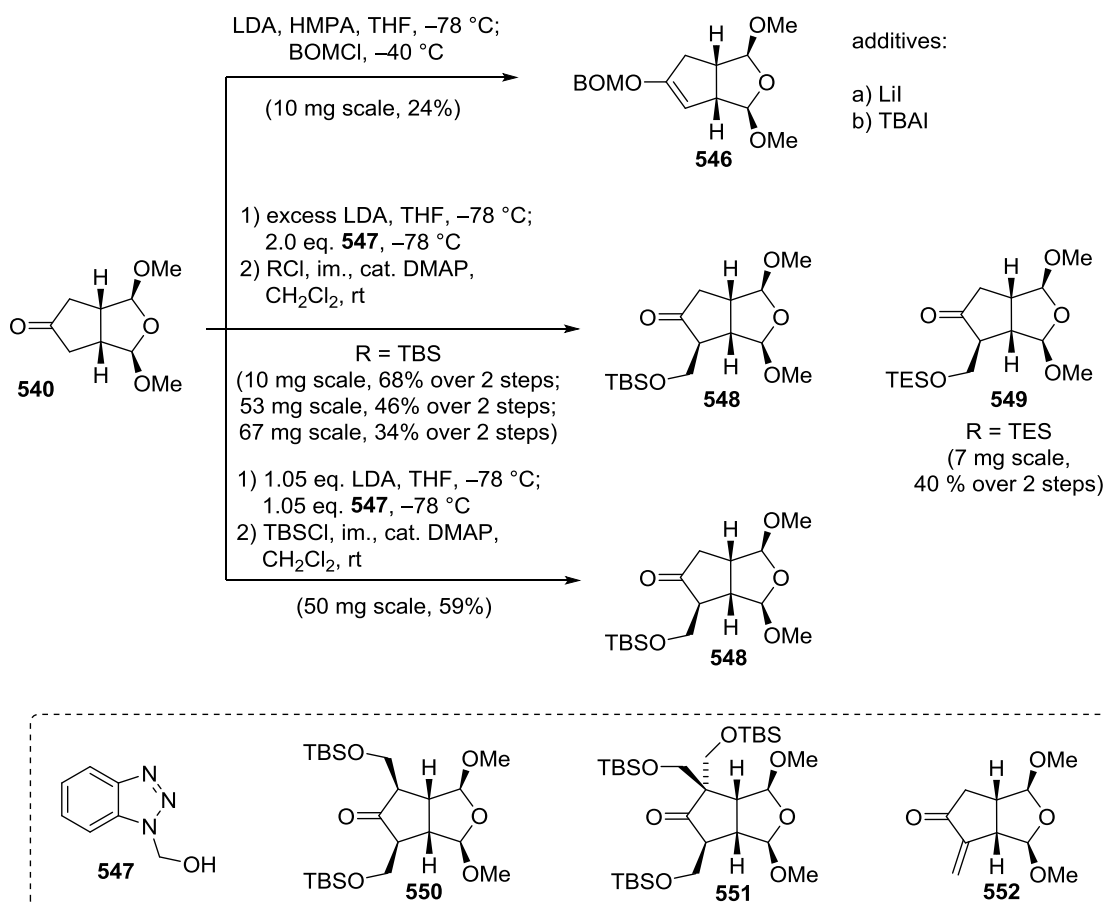
Figure 44. X-Ray single crystal structure of ketone **540**.
 Color code: green = carbon, red = oxygen, white = hydrogen.

In the crystal structure, each molecule is frozen in a C_1 -symmetric conformation. However, in solution on the NMR spectroscopy timescale, the structure proved to be C_s -symmetric with only one set of symmetry-equivalent signals.

3.6.2.2 Desymmetrization *via* Enolate Alkylation

The desymmetrization by alkylation was initially tested without chiral bases for practical reasons. However, the employed procedures were chosen according to the potential of their realization with chiral bases.

Introduction of a $-\text{CH}_2\text{OBn}$ group with a robust alcohol protecting group by deprotonation of ketone **540** with LDA and subsequent treatment with BOMCl only led to functionalization when HMPA was employed as a cosolvent (Scheme 172). However, the intermediate enolate was *O*-alkylated to give enol ether **546** in low yield due to its instability during purification. Softening of the electrophile and therefore increasing the tendency toward *C*-alkylation by addition of LiI or TBAI was unsuccessful. Using benzotriazole **547** as a *C1* source allowed for the preparation of the desired hydroxymethylated ketone, which proved to be unstable and had to be immediately protected.^[345] Silylated derivatives **548** and **549** were accessed in moderate yield over two steps. Upon conducting the reaction on larger scale, it became evident that the major byproducts of the alkylation resulted from overreaction due to the excess of base and reagent **547**. Difunctionalized **550** as well as trifunctionalized ketone **551** were identified in the reaction mixture. Reduction of the equivalents and slow addition of reagent **547** was found effective to prevent the formation of these products. TBS ether **548** was therefore prepared in good yield as a single diastereomer.

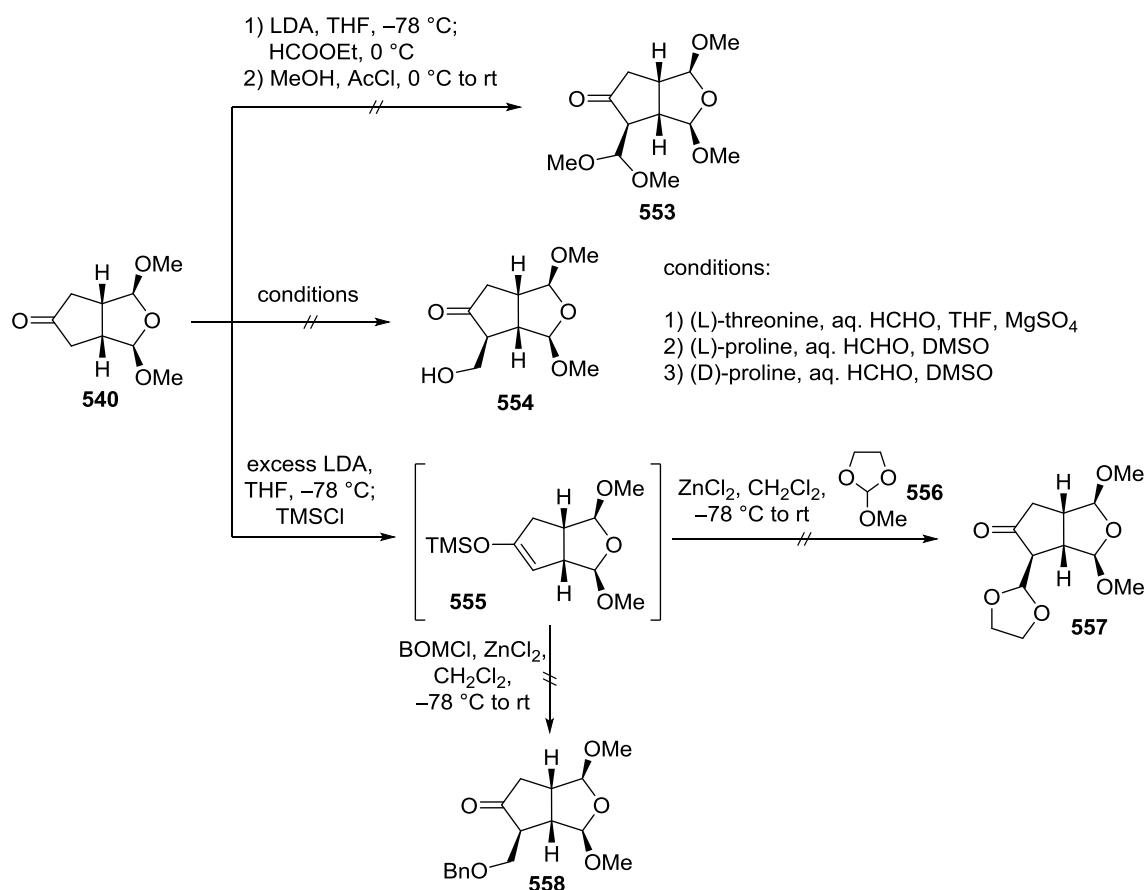


Scheme 172. Desymmetrizing alkylation attempts with nitrogen bases.

The installation of acyl protecting groups was attempted by treatment with *p*-BrBzCl, but only gave the corresponding elimination product **552** as judged by crude NMR analysis. It was concluded that the alcohol should not be protected with electron-withdrawing groups that increase the leaving group quality.

Alternatives to the above-mentioned hydroxymethylation were tried with the direct installation of an aldehyde (Scheme 173). Treatment of the ketone-enolate with ethyl formate yielded the corresponding α -formyl ketone, which was present as its enol tautomer. However, protection of this intermediate with MeOH and *in situ*-generated HCl *en route* to acetal **553** only resulted in decomposition, which was attributed to the sensitive bisacetal in ketone **540**. Organocatalytic methods, which could potentially lead to an asymmetric α -functionalization, either resulted in self-condensation of ketone **540** (condition 1) or no conversion (conditions 2, 3).^[346,347] Alcohol **554** was not detected in the reaction mixtures.

In order to increase the *C*-nucleophilicity of ketone **540**, it was tried to synthesize silyl enol ether **555**. Its preparation succeeded by treatment of the corresponding enolate of ketone **540** with TMSCl.



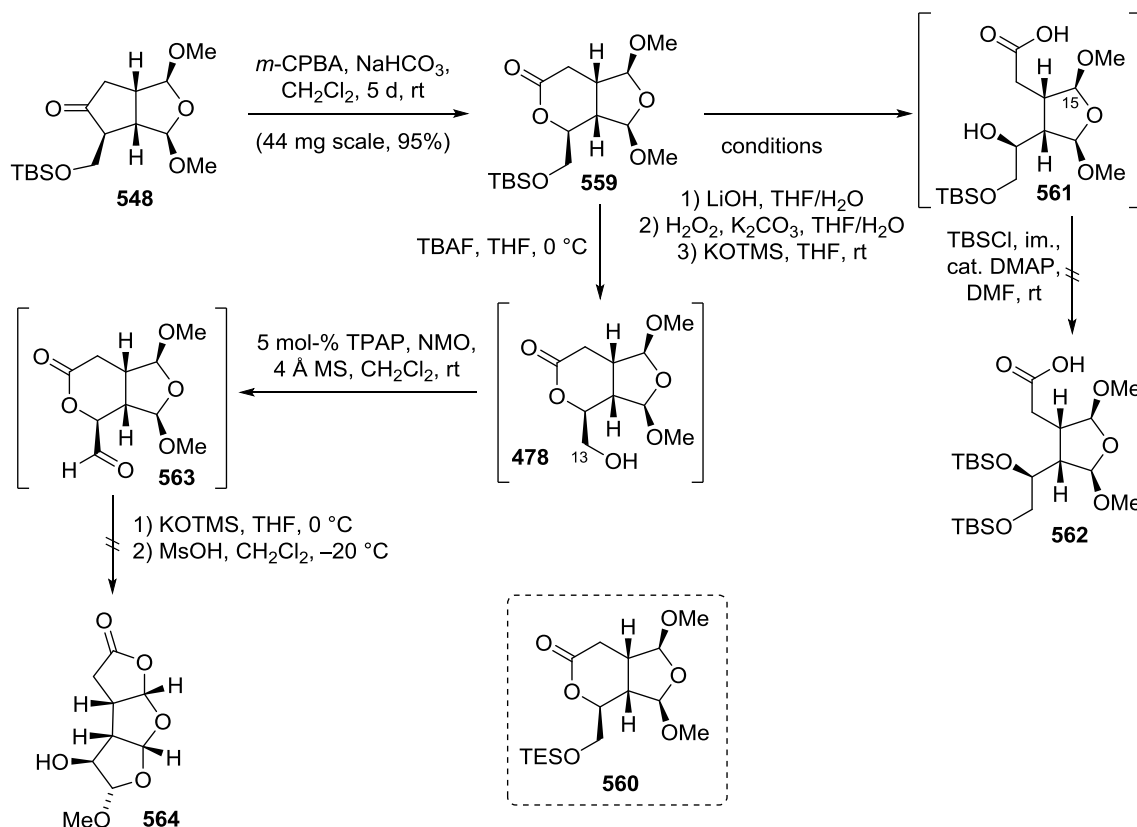
Scheme 173. Alternative desymmetrization approaches.

The silyl enol ether was employed in LEWIS acid-catalyzed functionalization attempts with BOMCl or aldehyde equivalent **556**. Both reactions to yield either dioxolane **557** or benzyl ether **558** were not met with success and only ketone **540** was recovered. Since ketone **548** was a suitable precursor to the gracilin natural products, other silyl enol ethers were not attempted.

3.6.2.3 Conversion of Desymmetrized Ketone to General Gracilin Precursor

With the desired desymmetrized ketone **548** in hand, it was tried to advance this substance to the general gracilin precursor **361**. BAEYER–VILLIGER oxidation proved to be very efficient in accessing lactone **559**, although the reaction times were long (Scheme 174). The regioisomeric oxidation product was not detected and lactone **559** was isolated in excellent yield. Attempted acceleration of the reaction by use of KHCO_3 and 18-crown-6 inhibited the oxidation. The alternative TES protected alcohol **560** was isolated in low yields next to alcohol **476**, also in low yields. It was argued that the TES protecting group is labile under the reaction conditions. Cleavage of the TES group would afford labile alcohol **554**, which is prone to decomposition.

Subsequent lactone hydrolysis of lactone **559** was complicated by the lability of the primary TBS protecting group, which was cleaved when LiOH was employed. Hydrogen peroxide afforded the product, but the method was inferior to a mild hydrolysis protocol using KOTMS.

Scheme 174. Transformations of ketone **548**.

Acid **561** could not be purified, but the crude product was sufficiently pure for further transformations. Protection of the secondary alcohol to bisilyl ether **562** was impossible and only afforded complex mixtures. A potential reason for this observation might be that the acid moiety partially cyclizes onto C15 and therefore epimerizes this center. Furthermore, the acidity of carboxylic acid **561** might lead to deprotection of the TBS groups, which was not noticed in the hydrolysis step since the acid was protected as a silyl ester until workup. An immediate cyclization of acid **561** could not be allowed because it would yield the undesired bicyclic product of type **500**. Hence, it was attempted to first oxidize the C13 position prior to lactone hydrolysis. Deprotection of TBS ether **559** with HF in pyridine was ineffective, but TBAF in THF afforded the desired alcohol **478**. Its structure was unambiguously proven by X-ray single crystal structure analysis (Figure 45). The C13 alcohol forms hydrogen bonds to the C14 lactone with a distance of $d_{O-O} = 2.722 \text{ \AA}$, which thus connect to one-dimensional chains of hydrogen-bonded molecules.

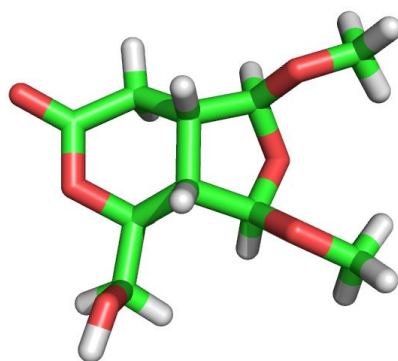
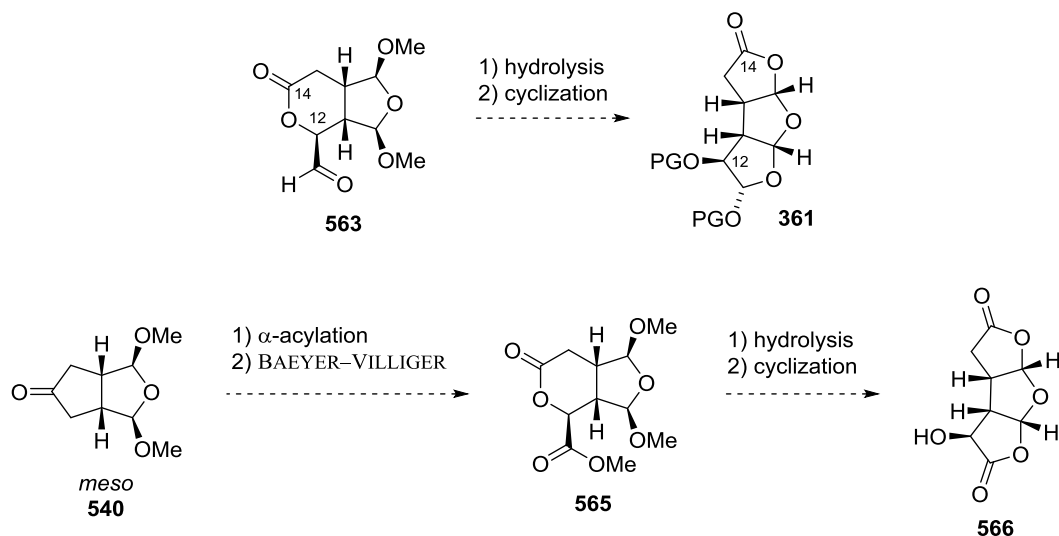


Figure 45. X-Ray single crystal structure of alcohol **478**. Color code: green = carbon, red = oxygen, white = hydrogen.

SWERN oxidation was found to decompose alcohol **478**, but mild LEY oxidation afforded the desired aldehyde **563**. The labile aldehyde was hydrolyzed with KOTMS and subsequently subjected to cyclization conditions adapted from COREY's synthesis of gracilin B and C. However, no formation of product **564** was observed and the substrate decomposed under the reaction conditions.

3.7 Conclusion and Outlook

In PART II of this thesis, synthetic studies toward the gracilin natural products were described. In attempts to implement a double oxidative cleavage for the synthesis of 1,4-dialdehydes, cyclic dienes were to be prepared. Whereas the stereoselective preparation of cyclohexadienes by electrocyclization proved unsatisfactory, cycloheptadienes were efficiently accessed using DAVIES' Rh-catalyzed formal (4+3)-cycloaddition. The success of the ensuing oxidative cleavage was dependent on the choice of substrates. Eventually suitable conditions were identified, but could not be applied to the synthesis of the gracilin natural products due to incompatibility problems of the different protecting groups. In a third strategy, the aldehyde **563**, containing all carbon atoms of general gracilin precursor **361** at the correct oxidation state, was accessed in a short and efficient sequence. The conversion of this aldehyde to the gracilin natural products by hydrolysis and cyclization will be subject to future studies toward these marine natural products (Scheme 175). An alternative synthesis could take advantage of ketone **540** in an α -acylation and following BAEYER–VILLIGER oxidation to furnish bicycle **565** that would be more stable than aldehyde **563**. Hydrolysis of both esters and cyclization might give rise to bislactone **566**, which could be selectively reduced to afford the general precursor **361**. Once successful, the synthesis would need to be conducted asymmetrically with the help of chiral bases in the ketone functionalization step.



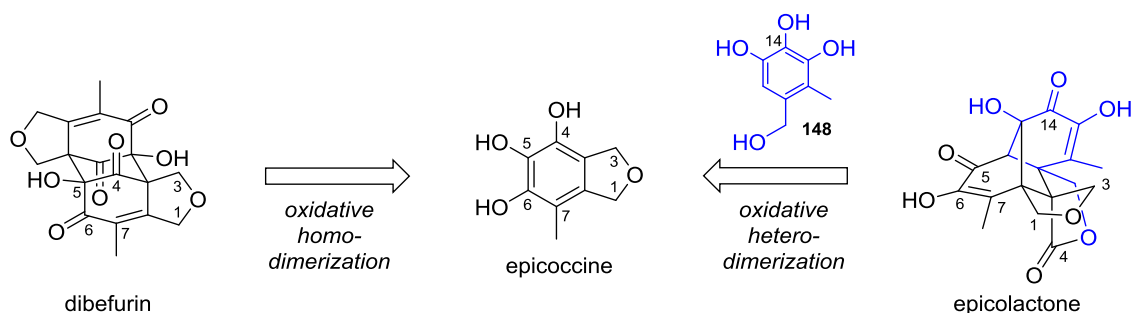
Scheme 175. Future directions toward the synthesis of gracilin natural products.

4. SUMMARY

This thesis dealt with the biomimetic synthesis of the polyketide dibefurin and synthetic studies toward epicolactone (PART I) and the gracilin terpenoids (PART II).

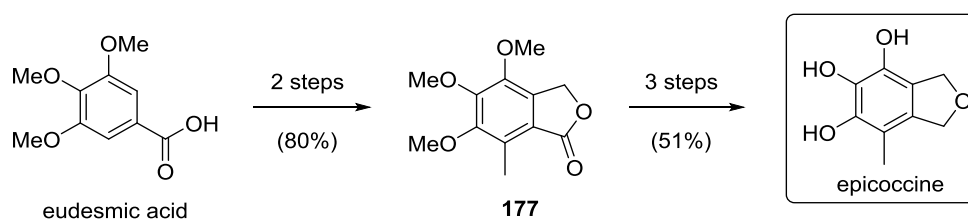
PART I: Biomimetic Synthesis of Dibefurin and Epicolactone

In PART I, the oxidative dimerization modes of pyrogallols were reviewed and conceptualized to establish guidelines for future synthetic endeavours in this area. A biosynthetic hypothesis for the C_2 -symmetric polyketide dibefurin and the pseudosymmetric racemic polyketide epicolactone was proposed that served as the basis of their biomimetic synthesis (Scheme 176).



Scheme 176. Biosynthetic hypothesis of dibefurin and epicolactone.

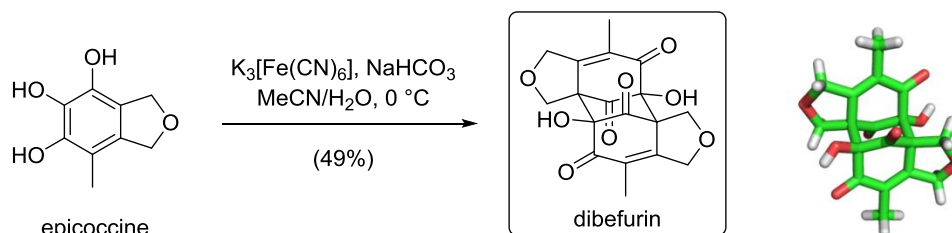
First, the natural product epicoccine, a hexasubstituted and electron-rich benzene derivative isolated from *Epicoccum* species, was synthesized on multi-gram scale in five steps and 41% overall yield from inexpensive eudesmic acid. The sequence only required two column chromatographic purifications and relied on the power of classic electrophilic aromatic substitution reactions with formaldehyde (Scheme 177).



Scheme 177. Total synthesis of epicoccine from eudesmic acid and formaldehyde.

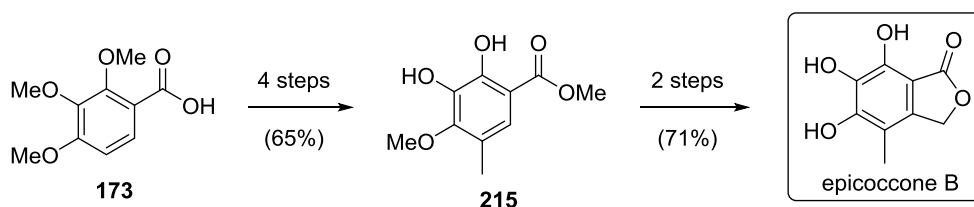
Epicoccine was successfully homodimerized in good yield upon oxidation with the outer-sphere single-electron oxidant potassium ferricyanide (Scheme 178). In this head-to-tail dimerization, four challenging tetrasubstituted centers were formed that are adjacent in pairs. Suitable crystals for X-ray single crystal structure analysis were obtained and a hydrogen-bond network in the solid state was identified as the source of the insolubility of dibefurin. Data were presented that support the alleged presence of dibefurin also in *Epicoccum* species. The accomplishment of the synthesis of dibefurin by

oxidative dearomatization of epicoccine constitutes the first application of the PERKIN dimer formation in natural product synthesis and supports the validity of the proposed biosynthetic pathway.



Scheme 178. Successful oxidative dimerization of epicoccine to dibefurin; CCDC: 1022042.
Color code: green = carbon, red = oxygen, white = hydrogen.

In order to study the oxidative heterodimerization toward epicolactone, epicoccone B, another natural product from *Epicoccum* sp., was accessed on multi-gram scale in six steps and 46% overall yield. The sequence only required one column chromatographic purification.



Scheme 179. Successful synthesis of natural product epicoccone B.

In attempts to synthesize epicolactone through oxidation of epicoccine and epicoccone B as an equivalent of alcohol **148**, a high driving force of the dibefurin formation was identified and rationalized with thermodynamic and kinetic factors. The dominating homodimerization of epicoccine was largely reduced by preoxidation of the dimerization partner and optimized setup procedures.

It was found that hexasubstituted pyrogallol derivatives were unreactive in the desired heterodimerization, because epicoccone B analog **197** or chloro arene **306** gave dibefurin either next to other products (**197**) or exclusively (**306**). This tendency was explained by the immense steric repulsion between four contiguous tetrasubstituted carbon atoms (*C*5/*C*1/*C*13/*C*12) in the corresponding dimers **155** or **307**. Furthermore, the *C*14 ketone is unable to tautomerize to the more stable enol form, leaving an energetically unfavorable diketone.

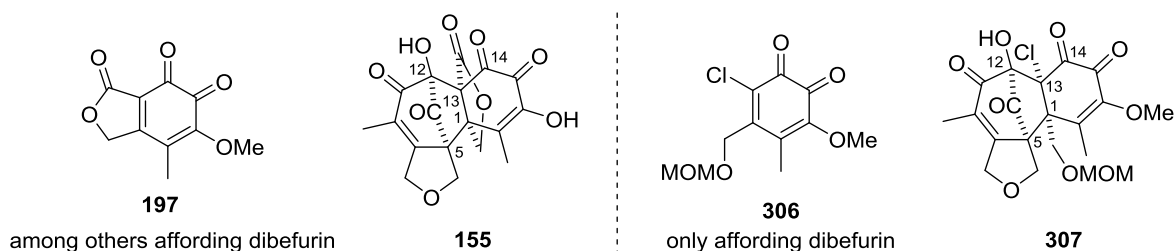
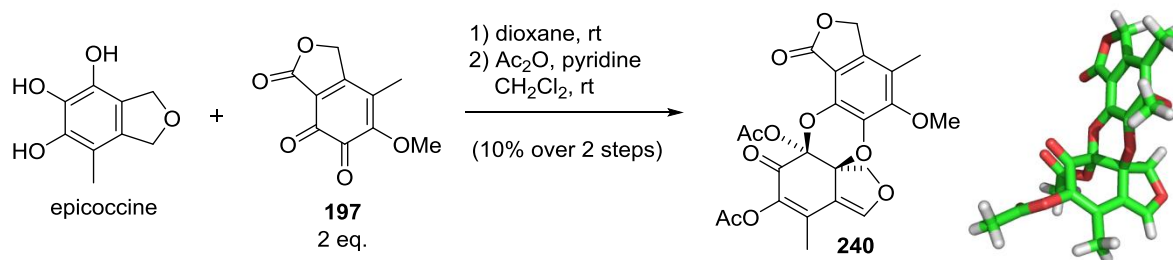


Figure 46. Heterodimerization partners in epicolactone synthesis that result in dibefurin formation.

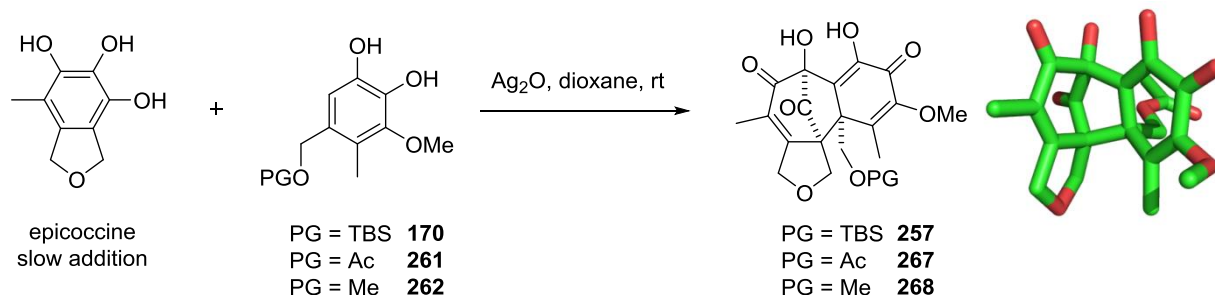
During the studies with quinone **197**, an unprecedented pyrogallol oxidative dimerization *via* a hetero-Diels–ALDER reaction of a *para*-quinone methide with *ortho*-quinone **197** was identified (Scheme 180). Isolation and characterization proved to be challenging due to the sensitivity of the heterodimer, but X-ray single crystal structure proof was nonetheless obtained. Identification of dimers of type **240** in Nature might have been complicated by their instability. It was proposed that this dimerization between epicoccine B and epicoccine might well occur in Nature so that the isolation protocol presented in this thesis could help to identify this compound in natural sources.



Scheme 180. Hetero-Diels–ALDER heterodimerization of epicoccine and epicoccone B derivative **197**; CCDC: 1022044. Color code: green = carbon, red = oxygen, white = hydrogen.

Subsequent alternations of the epicoccine structure led to the conclusion that all three hydroxyl groups of epicoccine need to be unprotected for a successful dimerization to occur.

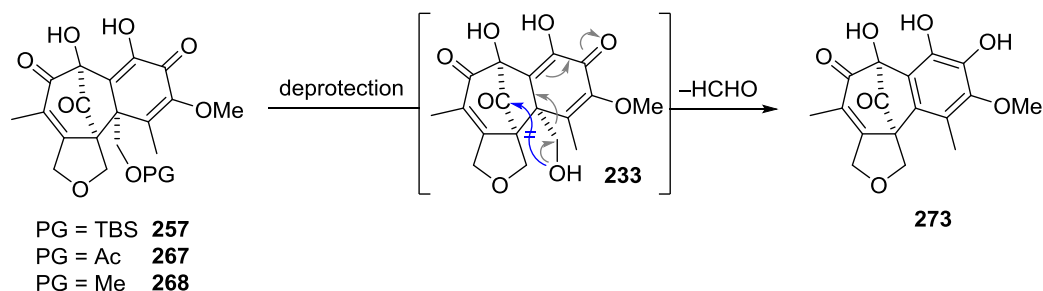
Following the initial biosynthetic hypothesis involving pentasubstituted benzene derivatives such as **170**, **261** or **262**, it was possible to effect the desired oxidative heterodimerization with various protecting groups on the primary alcohol (Scheme 181). The resulting heterodimers were the major product by crude NMR analysis and pure enough for further transformations. Suitable crystals for X-ray single crystal structure analysis were obtained of acetate **267** that provided unambiguous evidence of its structure. In this key step, two aromatic pyrogallol derivatives are oxidatively coupled with exclusive regio- and diastereoselectivity, setting three tetrasubstituted stereocenters in a single step. The reaction constitutes the first example of the purpurogallin formation reaction in the synthesis of non-benzotropolone natural products and could find broader application as a tool for rapid increase in molecular complexity.



Scheme 181. Successful heterodimerization of pentasubstituted pyrogallol derivatives with epicoccine. X-Ray single crystal structure of acetate **267**; H atoms omitted for clarity. Color code: green = carbon, red = oxygen.

The obtained heterodimers were sensitive to a variety of reaction conditions and preferably underwent rearomatization (Scheme 182). This experimental result implies that Nature might have

found a way to inhibit the undesired fragmentation of tetracycles such as **233** in the biosynthesis of epicolactone.



Scheme 182. Rearomatization of desired heterodimer.

Strategies to prevent the rearomatization were not met with success either because of the sensitivity of the heterodimers or because the desired heterodimers could not be synthesized (Figure 47).

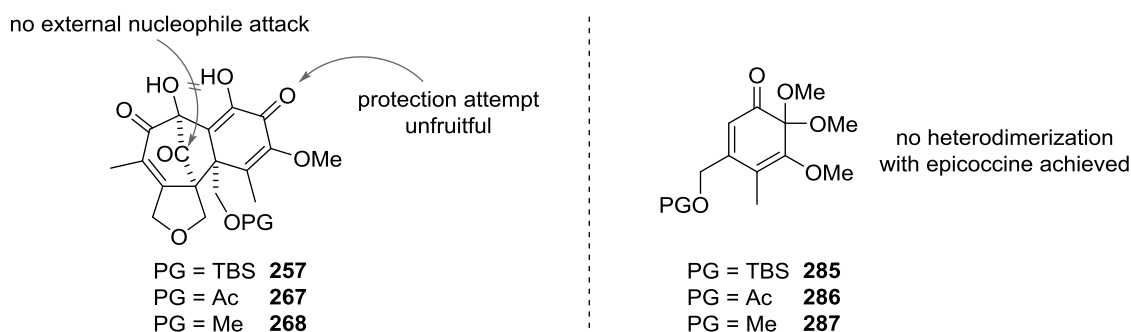


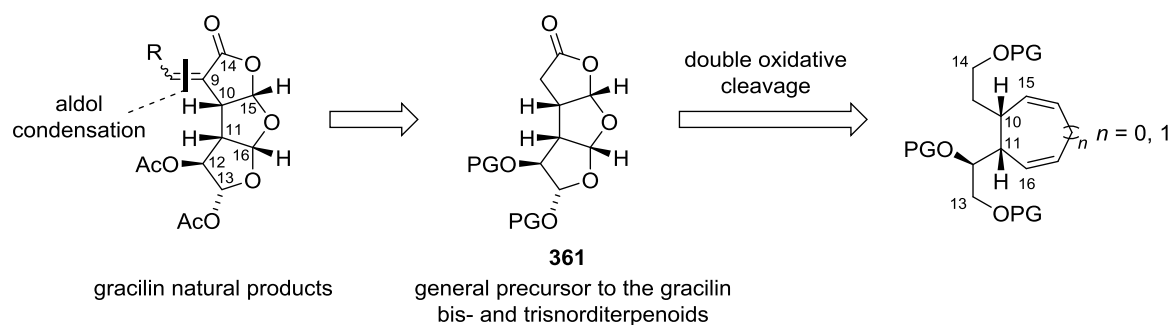
Figure 47. Unsuccessful attempts to prevent rearomatization of heterodimers.

An alternative biosynthetic proposal was developed based on the experimental results. Several strategies to enable the transformation of heterodimers of type **257** into the fungal metabolite epicolactone have been suggested for future experiments.

PART I presented the total synthesis of the three natural products epicoccine, dibefurin and epicoccone B and the successful heterodimerization of epicoccine with a pentasubstituted benzene derivative to give rise to a tetracycle featuring all carbon atoms of the natural product epicolactone. The obtained results showcase the vast potential of biomimetic synthesis in the preparation of intricate molecules.

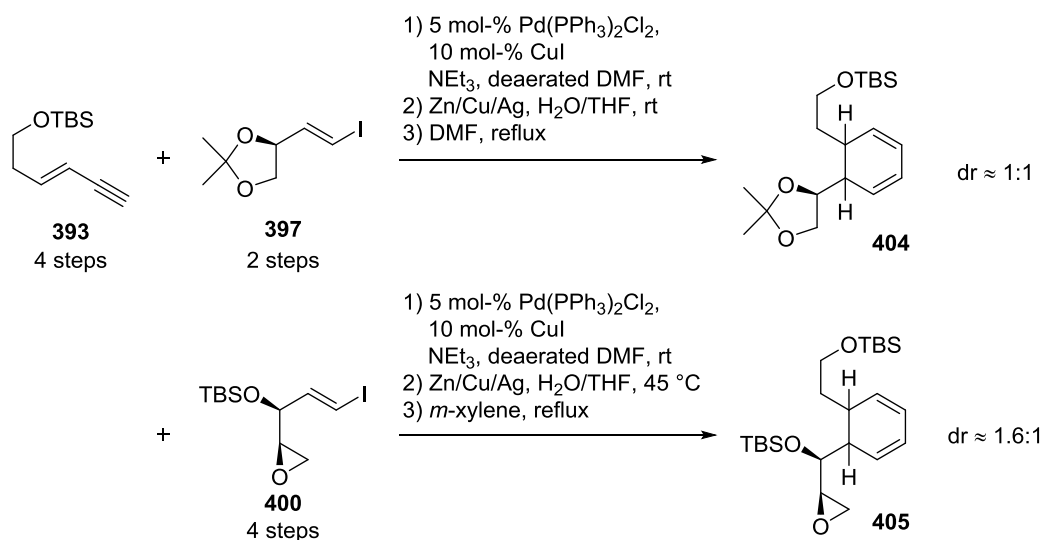
PART II: Total Synthesis of Gracilin Terpenoids

PART II of this thesis presented three different synthetic studies toward the gracilin natural products. The first two approaches focused on accessing a potential common precursor **361** to these marine secondary metabolites by double oxidative cleavage of a cyclic diene (Scheme 183).



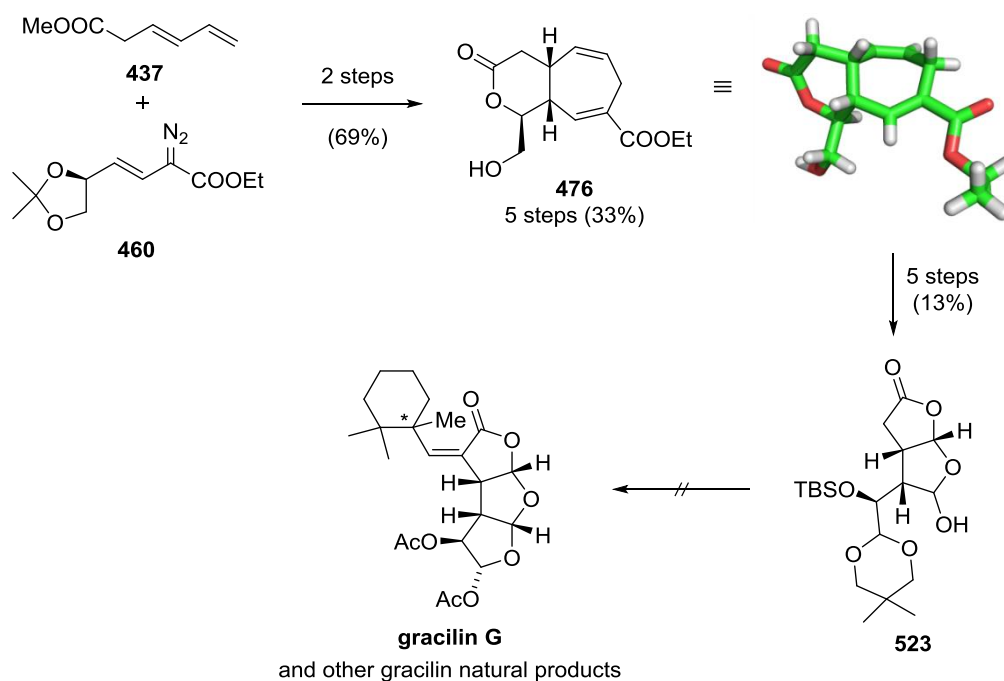
Scheme 183. Retrosynthetic analysis for the first two approaches to gracilin natural products.

An efficient synthesis of trienes **404** and **405** was developed (Scheme 184). The following torquoselective 6π -electrocyclization did not proceed with diastereoselectivities that would allow for an efficient synthesis of the gracilin natural products. Therefore, this approach was discontinued in favor of another strategy.



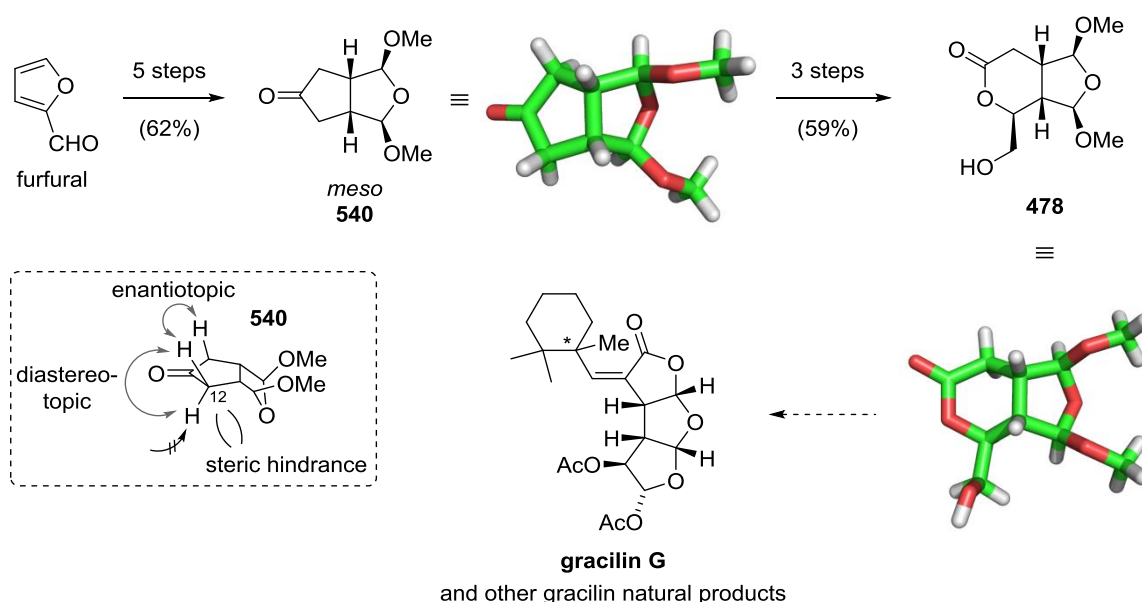
Scheme 184. First strategy toward gracilin natural products by 6π -electrocyclization.

A Rh-catalyzed formal (4+3)-cycloaddition *via* a cyclopropanation/COPE rearrangement cascade was employed to furnish cycloheptadienes such as **476** as precursors to 1,4-dialdehydes (Scheme 185). For the first time, stereochemical induction of the allylic stereocenter in vinyl diazoacetates like **460** was observed in this formal (4+3)-cycloaddition. After thorough optimization of conditions and the substrate, the envisioned double oxidative cleavage was successfully applied to furnish hemiacetal **523**, which in turn could not be converted into the gracilin natural products.



Scheme 185. Synthesis of lactone **476** and advanced intermediate **523** toward gracilin natural products.
Color code: green = carbon, red = oxygen, white = hydrogen.

In a third attempt, the use of furan as a 1,4-dialdehyde precursor was highlighted by accessing *meso*-ketone **540** through Pd-catalyzed formal (3+2)-cycloaddition (Scheme 186). Efficient desymmetrization of this substrate and subsequent transformations afforded alcohol **478**, which was shown to undergo oxidation to the corresponding aldehyde. Future studies will focus on the conversion of this building block to the gracilin natural products.



Scheme 186. Third strategy toward gracilin natural products by desymmetrization of *meso*-intermediate **540**.

In short, an efficient synthetic route was identified toward the gracilin norditerpenoids that could be applied as a general entry to these marine natural products.

EXPERIMENTAL PART

5. GENERAL PROCEDURES

Air and/or moisture sensitive reactions were conducted under inert gas atmosphere (nitrogen). Glassware was stored in an oven (130 °C) and heat-gun dried (650 °C) under high-vacuum prior to use (three times, in between filled with nitrogen). Liquids and solutions were transferred via three times nitrogen-flushed syringes with oven-dried stainless steel cannulas (130 °C). Solids were added under counter flow of nitrogen (Schlenk technique). Reaction temperatures refer to the external oil or cooling bath temperature. Large scale reactions (reaction vessel ≥ 1 l) were conducted by monitoring the temperature of the reaction mixture with an internal thermometer. Drying over Na₂SO₄ involved stirring the organic solvent over the anhydrous salt and subsequent separation of the solids by filtration. The filter cake was rinsed multiple times with the respective extraction solvent. Solutions were concentrated under reduced pressure by rotary evaporation at 30 °C with *Heidolph* Laborota 4000 efficient employing a *vacuubrand* PC 3001 pump.

- membrane pump for rotary evaporation (VACUUBRAND): 4 mbar
- oil pump for high-vacuum: 0.006 mbar

Yields, unless noted otherwise, are isolated yields. All reactions were magnetically stirred and monitored either by LC/MS or TLC (*vide infra*).

5.1 Solvents and Reagents

Commercial reagents and dry solvents over molecular sieves were used as purchased from Acros Organics with the following exceptions. Tetrahydrofuran (THF) and diethylether (Et₂O) were pre-dried over CaCl₂ and distilled over sodium and benzophenone under a nitrogen atmosphere before use. Triethylamine (NEt₃), diisopropylamine (DIPA) and diisopropylethylamine (DIPEA) were distilled over CaH₂ under a nitrogen atmosphere prior to use. Solvents were stored under nitrogen. Deaeration of solvents was performed by passing a stream of nitrogen through the solvent for $t \geq 15$ min for solvents such as water, DMSO, DMF or toluene. For lower-melting solvents, the freeze-pump-thaw (FPT) method was applied. Solvents were placed in a vessel under nitrogen atmosphere, frozen at $T = -196$ °C with an external liquid nitrogen bath and the vessel evacuated. The frozen solvent was allowed to melt under high vacuum and the vessel placed under nitrogen atmosphere again.

5.2 Chromatography

Thin-Layer Chromatography (TLC): TLC plates (silica gel 60) on glass with fluorescence indicator F-254 (MERCK KGAA) were used for monitoring of reactions, analysis of column chromatography fractions (unless C18 silica was employed, *vide infra*) and determination of R_f values. Eluents were of HPLC grade. TLCs were analyzed by UV light ($\lambda = 254$ nm), if applicable, or immersing in staining solutions. After staining, TLC plates were heated with a heat-gun at 300 °C until dry.

Staining solutions:

- KMnO_4 -solution: 3 g KMnO_4 , 20 g K_2CO_3 , 5 ml 5% NaOH (aq), 300 ml dist. H_2O
- CAN-solution: 6.25 g molybdophosphoric acid, 2.50 g $\text{Ce}(\text{SO}_4)_2 \cdot 4\text{H}_2\text{O}$ and 15 ml sulfuric acid (97%) in 230 ml dist. H_2O

Flash Column Chromatography: Purification by flash column chromatography was achieved using Geduran[®] Si60 silica gel (40–63 μm , MERCK KGAA) with HPLC grade solvents. The volume of silica gel used is provided in (height x diameter column). The compounds were loaded in the respective eluent (if soluble), CH_2Cl_2 (if soluble) or EtOAc. If insoluble in either of these solvents, compounds were dissolved in an appropriate solvent (acetone or MeOH), silica gel was added and the solvent evaporated under reduced pressure. The remaining solid was loaded on the column (dry load). For purification with C18 silica gel flash column chromatography, silica gel (preparative C18, 125 Å, 55–105 μm , Waters Corp.) was suspended in HPLC grade MeCN, the column packed and the silica gel washed twice with the starting eluent. The volume of silica gel used is provided in (height x diameter column). The compounds were loaded in dioxane or THF and fractions analyzed by LC/MS (*vide infra*). The combined fractions were extracted with EtOAc three times, the combined organic phases dried over Na_2SO_4 and concentrated under reduced pressure.

High performance liquid chromatography (HPLC): HPLC was performed on C18 silica with HPLC grade solvents and deionized water purified by a TKA MICROPURE water purification system. All solvents were deaerated with helium gas prior to use. HPLC purification was carried out at room temperature with the specified column. Analytical HPLC traces were recorded on an ultra high performance liquid chromatography (UHPLC) system from AGILENT 1260 Infinity series (1260 degasser, 1260 binary pump VL, 1260 ALS auto sampler, 1260 TCC thermostatted column compartment, 1260 DAD diode array detector), which was computer-controlled by AGILENT ChemStation software. Preparative HPLC was performed on a computer-operated VARIAN system (Galaxie Chromatography Software, two PrepStar pumps Model SD-1, manual injection, ProStar 335 Photo Diode Array Detector, 380-LC Evaporative Light Scattering Detector).

5.3 NMR Spectroscopy

All nuclear magnetic resonance spectra were recorded either on VARIAN VNMRs 300, VNMRs 400, INOVA 400, VNMRs 600 or a BRUKER AVANCE III HD 400 spectrometer. NMR spectra were referenced to the undeuterated solvent signal relative to SiMe_4 :

- CDCl_3 : ^1H NMR δ 7.26 ppm, ^{13}C NMR δ 77.16 (t) ppm
- CD_2Cl_2 : ^1H NMR δ 5.32 (t) ppm, ^{13}C NMR δ 53.84 (quint) ppm
- C_6D_6 : ^1H NMR δ 7.16 ppm, ^{13}C NMR δ 128.06 (t) ppm
- $(\text{D}_3\text{C})_2\text{CO}$: ^1H NMR δ 2.05 (quint) ppm, ^{13}C NMR δ 29.84 (sept) ppm
- $\text{DMSO}-d_6$: ^1H NMR δ 2.50 (quint) ppm, ^{13}C NMR δ 39.52 (sept) ppm

- MeOD: ^1H NMR δ 3.31 (quint) ppm, ^{13}C NMR δ 49.00 (sept) ppm
- THF- d^8 : ^1H NMR δ 1.72 (m) ppm, ^{13}C NMR δ 25.31 (quint) ppm
- DMF- d^7 : ^1H NMR δ 2.75 (quint) ppm, ^{13}C NMR δ 29.76 (sept) ppm

Spectral data is provided in ppm from downfield to upfield. The following abbreviations are utilized in the analysis of NMR spectra: s = singlet, d = doublet, t = triplet, q = quartet, quint = quintet, sept = septet, m = multiplet, brs = broad singlet. Combination of these abbreviations is applied whenever more than one coupling is observed. Data is provided in the following order: chemical shift in ppm (multiplicity, coupling constant J in Hz, signal integration, assignment to molecule). Unless noted differently, coupling constants are $^3J_{\text{H,H}}$ in ^1H NMR. The assignment to the molecule refers to the numbered atoms of title compound as shown in the respective scheme and is denoted as C_xH_y , with x = carbon atom number and y = number of hydrogen atoms attached to this carbon atom. Diastereotopic methylene protons were denoted with $y = 1$. The carbon atom numbering of the title compound and its nomenclature do not necessarily follow IUPAC conventions.

NMR spectra were recorded at $T = 27^\circ\text{C}$. Analysis of all spectra was performed with MestReNova version 8.1 by MESTREC LABORATORIES.

5.4 Mass Spectrometry

High resolution (HRMS) and low resolution (MS) mass spectra were recorded on a FINNIGAN MAT 95 (GC/EI or DEP/EI) or a THERMO FINNIGAN MAT 95 (ESI), JEOL JMS-700 (CI) instrument. Ionization of the samples was achieved using electrospray ionization (ESI) or electron ionization (EI).

5.5 Melting Points

Melting points were measured on a B-540 meltin point apparatus from BÜCHI LABORTECHNIK AG and are uncorrected.

5.6 Infrared Spectroscopy (IR)

Infrared (IR) spectra were recorded on a PERKIN ELMER Spectrum BX II FT-IR instrument with a SMITHS DETECTION DuraSampl IR II Diamond ATR sensor for detection in the range from $\tilde{\nu} = 4500\text{ cm}^{-1}$ to $\tilde{\nu} = 600\text{ cm}^{-1}$. Samples were prepared as a film for liquid or neat for solid substances and directly applied on the ATR unit. The wavenumbers are followed by intensities in brackets and intensities are given with vw (very weak, 1–20%), w (weak, 20–40%), m (medium, 40–60%), s (strong, 60–80%) and vs (very strong, 80–100%) referring to the most intense peak (100%). The abbreviation br was used for broad absorption bands.

5.7 LC/MS

LC/MS data was obtained on Agilent Technologies 1260 Infinity with C18 silica gel columns and Agilent 1100 Series LC/MSD mass detector. As eluent, a mixture of MeCN (HPLC grade) with H₂O (Milli-Q Integral Water Purification System) and 0.1 vol-% formic acid as additive was employed.

5.8 Optical Rotation

Optical rotation values were recorded on a PERKINELMER 241 polarimeter. The sodium D line ($\lambda = 589 \text{ nm}$) was used as the standard wavelength. For different temperatures T , the specific rotation is denoted as $[\alpha]_{\text{D}}^T$ (D = sodium D line). The specific rotation values are reported in units of $^{\circ} \text{ ml g}^{-1} \text{ dm}^{-1}$ followed by the concentration of the solution in mg ml^{-1} and the respective solvent.

5.9 Ozonolysis

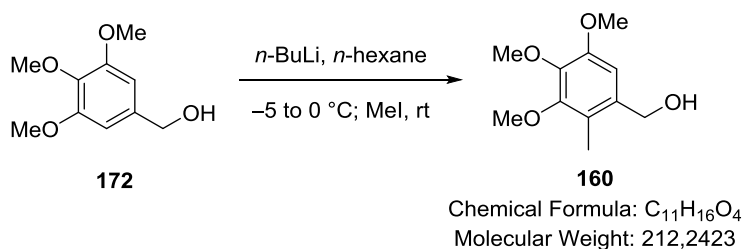
All ozonolyses were carried out with a DÉGREMONT TECHNOLOGIES ozone generator on level 2 oxygen flow with power level 11 of ozone production.

6. EXPERIMENTAL PROCEDURES

6.1 Part I: Biomimetic Synthesis of Dibefurin and Epicolactone

6.1.1 Synthesis of Epicoccine

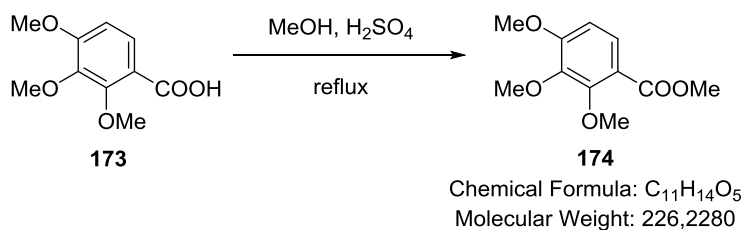
(3,4,5-trimethoxy-2-methylphenyl)methanol (**160**)



Benzyl alcohol **172** (1.0 ml, 1.2 g, 6.2 mmol) was suspended in *n*-hexane (13 ml) and *n*-BuLi in *n*-hexane (*c* = 2.5 M, 5.2 ml, 13 mmol, 2.1 eq.) was added slowly at $-5\text{ }^\circ\text{C}$. After stirring for 10 h at $0\text{ }^\circ\text{C}$, the reaction mixture was treated with MeI (1.2 ml, 2.7 g, 19 mmol, 3.0 eq.) stirred at rt for 13 h. The reaction mixture was diluted with EtOAc (20 ml) and the organic phases washed with aq. sat. NaHCO₃ solution (3x20 ml). The organic phase was concentrated under reduced pressure and the residue purified by flash column chromatography (13x2.5 cm, 30–40% EtOAc/hexanes) to yield the title compound as a yellowish oil (705 mg, 53%).

The analytical data was in agreement with literature precedence.^[195]

TLC	$R_f = 0.20$ (30% EtOAc/hexanes).
¹H NMR	(600 MHz, CDCl ₃): δ 6.76 (s, 1H), 5.29 (s, 2H), 3.86 (s, 3H), 3.85 (s, 3H), 3.83 (s, 3H), 2.18 (s, 3H) ppm.
¹³C NMR	(150 MHz, CDCl ₃): δ 152.2, 151.3, 141.9, 134.4, 122.1, 107.4, 63.6, 61.0, 60.8, 56.2, 10.8 ppm.
MS	(EI, %): 212.10 (100, M ⁺), 194.09 (27), 141.09 (20), 77.04 (7).
HRMS	(EI, m/z): calc. [M ⁺]: 212.1049; found: 212.1041 [M ⁺].
IR	$\tilde{\nu}$ = 3417 (vw), 2935 (w), 2834 (vw), 1602 (vw), 1583 (vw), 1491 (m), 1458 (m), 1432 (w), 1405 (m), 1325 (s), 1281 (vw), 1238 (w), 1194 (m), 1167 (vs), 1048 (s), 1007 (m), 975 (m), 914 (m), 840 (w), 779 (vw), 713 (w), 671 (vw) cm ⁻¹ .

methyl 2,3,4-trimethoxybenzoate (174)

Acid **173** (4.00 g, 0.0189 mol) was dissolved in MeOH (32 ml) and conc. H₂SO₄ was added (1.15 ml, 2.12 g, 0.0216 mol, 1.14 eq). The reaction mixture was heated to reflux for 26 h. Sat. aq. NaHCO₃ (100 ml) was added and the aqueous phase was extracted with CH₂Cl₂ (3x150 ml). The combined organic phases were washed with brine (150 ml), dried over Na₂SO₄ and concentrated under reduced pressure to afford the title compound as a yellow oil (4.28 g, quant.) that was taken forward without further purification.

Analytical data was in agreement with literature precedence.^[194]

TLC $R_f = 0.39$ (20% EtOAc/hexanes).

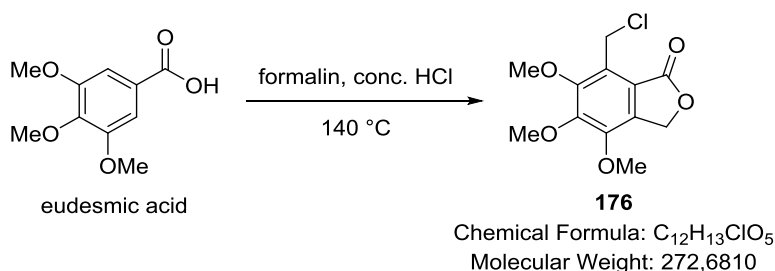
¹H NMR (400 MHz, CDCl₃): δ 7.59 (d, $J = 8.9$ Hz, 1H), 6.69 (d, $J = 8.9$ Hz, 1H), 3.92 (s, 3H), 3.89 (s, 3H), 3.87 (s, 3H), 3.86 (s, 3H) ppm.

¹³C NMR (100 MHz, CDCl₃): δ 166.2, 157.3, 154.8, 143.0, 127.1, 117.9, 107.0, 61.9, 61.1, 56.2, 52.1 ppm.

MS (EI, %): 226.06 (100, M⁺), 195.04 (100), 193.03 (62), 179.01 (34), 153.01 (28), 137.00 (20), 109.00 (12).

HRMS (EI, m/z): calc. [M⁺]: 226.0841; found: 226.0832 [M⁺].

IR $\tilde{\nu} = 2992$ (vw), 2945 (vw), 2841 (vw), 1722 (s), 1593 (s), 1494 (m), 1464 (s), 1430 (m), 1411 (s), 1288 (vs), 1270 (vs), 1237 (w), 1216 (vs), 1188 (w), 1137 (m), 1095 (vs), 1033 (s), 1015 (m), 982 (w), 923 (vw), 872 (vw), 820 (vw), 799 (w), 790 (w), 750 (w), 695 (w) cm⁻¹.

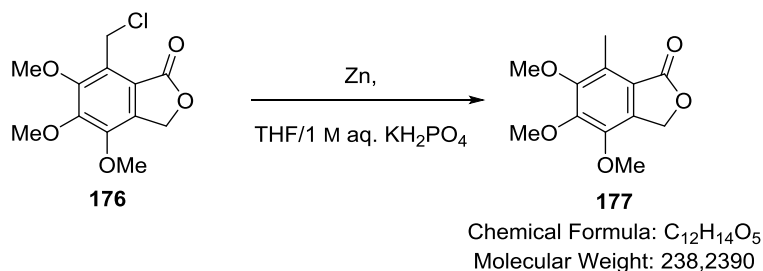
7-(chloromethyl)-4,5,6-trimethoxyisobenzofuran-1(3H)-one (176)

Eudesmic acid (10.0 g, 47.1 mmol) was dissolved in formalin (25 ml) and conc. HCl solution (40 ml) and the reaction mixture was heated to 140 °C in a preheated oil bath for 20 min. The oil bath was removed and the suspension was allowed to cool for 5 min before H₂O (50 ml) was added. The title compound was precipitated upon cooling to 0 °C with an ice bath. The precipitate was filtered off and dried under HV to afford the title compound **176** (12.1 g, 94%) as a colorless solid. The title compound could be taken forward to the next step without need for purification.

Analytical data was in agreement with literature precedence.^[162]

TLC	R _f = 0.19 (20% EtOAc/hexanes).
¹H NMR	(400 MHz, CDCl ₃): δ 5.24 (s, 2H), 5.06 (s, 2H), 4.00 (s, 3H), 3.99 (s, 3H), 3.96 (s, 3H) ppm.
¹³C NMR	(100 MHz, CDCl ₃): δ 169.6, 154.4, 150.2, 148.1, 134.4, 126.2, 118.6, 67.2, 62.0, 61.2, 60.5, 34.1 ppm.
HRMS	(EI, m/z): calc. [M ⁺]: 272.0452; found: 272.0439 [M ⁺].
IR	$\tilde{\nu}$ = 2976 (vw), 2944 (vw), 2834 (vw), 1755 (vs), 1610 (vw), 1485 (m), 1460 (m), 1433 (w), 1414 (w), 1343 (vs), 1294 (w), 1266 (vw), 1192 (w), 1128 (s), 1066 (m), 1032 (m), 1001 (vs), 958 (m), 936 (w), 899 (vw), 853 (vw), 771 (vw), 721 (vw), 667 (w) cm ⁻¹ .

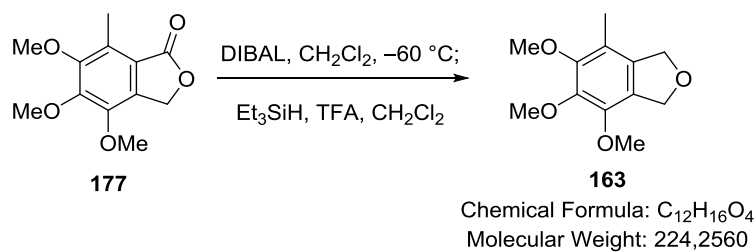
4,5,6-trimethoxy-7-methylisobenzofuran-1(3H)-one (**177**)



Benzyl chloride **176** (11.25 g, 41.26 mmol) was dissolved in THF (150 ml) and aq. KH₂PO₄ solution (*c* = 1 M, 72 ml) and zinc powder (27.0 g, 0.412 mol, 10 eq.) were added. The resulting suspension was stirred for 1 h, filtered over Celite and the filter cake was washed with EtOAc. Sat. aq. NaHCO₃ solution (150 ml) was added to the filtrate and the resulting mixture was extracted with EtOAc (2x150 ml). The combined organic phases were dried over Na₂SO₄ and concentrated under reduced pressure. The crude product was purified by flash column chromatography (15x7 cm, 25% EtOAc/hexanes) to afford the title compound **177** (8.37 g, 85%) as a colorless solid. The crude product could also be carried forward in the following steps without purification affording comparable overall yield.

TLC	$R_f = 0.49$ (33% EtOAc/hexanes)
m.p.:	90–91 °C
^1H NMR	(400 MHz, CDCl_3): δ 5.19 (s, 2H), 3.97 (s, 3H), 3.94 (s, 3H), 3.83 (s, 3H), 2.52 (s, 3H) ppm.
^{13}C NMR	(100 MHz, CDCl_3): δ 170.8, 153.5, 150.5, 145.3, 134.3, 128.4, 118.7, 66.8, 61.2, 60.9, 60.6, 10.1 ppm.
HRMS	(EI, m/z): calc. $[\text{M}^+]$: 238.0841; found: $[\text{M}^+]$ 238.0839
IR	$\tilde{\nu} = 2976$ (vw), 2940 (vw), 2838 (vw), 1743 (vs), 1608 (vw), 1589 (vw), 1485 (m), 1455 (s), 1427 (m), 1406, 1364 (m), 1341 (vs), 1298 (w), 1281 (w), 1191 (w), 1154 (w), 1124 (vs), 1083 (s), 1034 (vs), 1011 (vs), 997 (vs), 961 (s), 889 (m), 854 (m), 783 (m), 767 (m), 756 (w), 709 (w), 667 (w) cm^{-1}

4,5,6-trimethoxy-7-methyl-1,3-dihydroisobenzofuran (**163**)

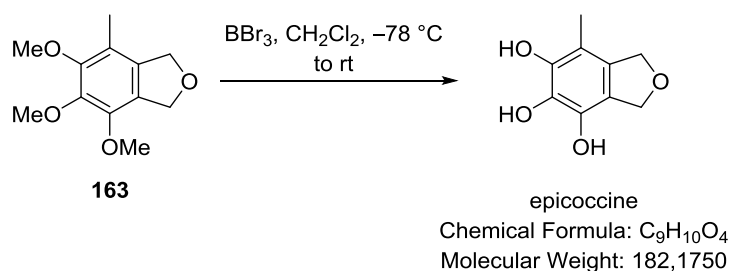


Lactone **177** (8.00 g, 33.6 mmol) was dissolved in CH_2Cl_2 (500 ml) and cooled to -60°C . DIBAL ($c = 1.2$ M in toluene, 64.3 ml, 77.2 mmol, 2.3 eq.) was added in a slow stream and the reaction mixture was stirred for 2 h. MeOH (20 ml) and water (20 ml) were added carefully and the reaction mixture was allowed to warm to rt. Sat. aq. Rochelle salt solution (200 ml) was added and the aqueous phase was extracted with CH_2Cl_2 (4x150 ml). The combined organic phases were washed with brine (200 ml), dried over Na_2SO_4 and concentrated under reduced pressure. The crude product was dried on HV before it was redissolved in CH_2Cl_2 (170 ml) and cooled to 0°C . Triethylsilane (53.7 ml, 39.1 g, 0.336 mol, 10 eq.) and TFA (2.57 ml, 3.83 g, 33.6 mmol, 1.0 eq.) were added and the reaction mixture was allowed to warm to rt. After 2 h, aq. pH 7.2 phosphate buffer ($c = 1.0$ M, 150 ml) was added and the aqueous phase was extracted with EtOAc (3x100 ml). The combined organic phases were dried over Na_2SO_4 and concentrated under reduced pressure. The crude product was purified by flash column chromatography (22x7 cm, 8% EtOAc/hexanes) to afford the title compound **163** as a colorless solid (4.34 g, 58% over 2 steps).

TLC	$R_f = 0.71$ (33% EtOAc/hexanes).
m.p.:	43°C .
^1H NMR	(400 MHz, CDCl_3): δ 5.16 (t, $J = 2.1$ Hz, 2H), 5.00 (t, $J = 2.1$ Hz, 2H), 3.88 (s, 3H), 3.86 (s, 3H), 3.83 (s, 3H), 2.08 (s, 3H) ppm.

^{13}C NMR	(100 MHz, CDCl_3): δ 152.0, 145.8, 144.8, 134.2, 125.2, 119.5, 73.4, 72.7, 61.2, 60.9, 60.3, 12.5 ppm.
HRMS	(EI, m/z): calc. $[\text{M}^+]$: 224.1049; found: $[\text{M}^+]$ 224.1036.
IR	$\tilde{\nu}$ = 2935 (w), 1478 (s), 1422 (m), 1363 (s), 1349 (vs), 1195 (w), 1114 (s), 1059 (s), 1015 (m), 976 (m), 904 (w) cm^{-1} .

7-methyl-1,3-dihydroisobenzofuran-4,5,6-triol (epicoccine)

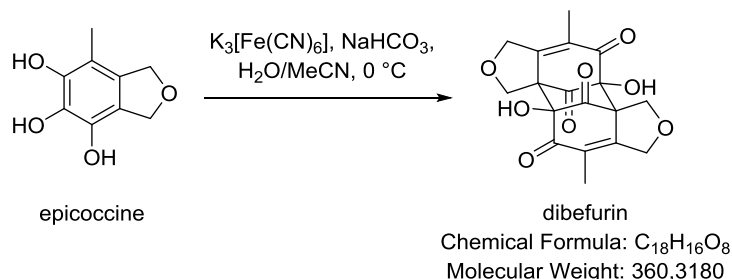


Trimethylether **163** (3.00 g, 13.4 mmol) was dissolved in CH_2Cl_2 (50 ml) and the solution was cooled to $-78\text{ }^\circ\text{C}$. Neat BBr_3 (5.71 ml, 60.2 mmol, 4.5 eq.) was added dropwise, the reaction was allowed to warm to rt and stirred for 14 h. The reaction mixture was slowly poured onto aq. pH 4.5 phosphate buffer ($c = 1\text{ M}$, 100 ml) cooled to $0\text{ }^\circ\text{C}$ and the aqueous layer was extracted with EtOAc (3x150 ml). The combined organic phases were dried over Na_2SO_4 and concentrated under reduced pressure. The residue was filtered over a C18 silica plug (10% MeCN/ H_2O + 1% FA) and the filtrate was extracted with EtOAc (3x50 ml). The combined organic phases were dried over Na_2SO_4 and concentrated under reduced pressure to afford epicoccine as a colorless solid (1.95 g, 80%).

TLC	$R_f = 0.12$ (33% EtOAc/hexanes) – unstable on silica
m.p.:	$> 200\text{ }^\circ\text{C}$ (gradual decomp.).
^1H NMR	(400 MHz, $(\text{D}_3\text{C})_2\text{CO}$): δ 7.19 (brs, 3H), 4.96 (t, $J = 2.1\text{ Hz}$, 2H), 4.90 (t, $J = 2.1\text{ Hz}$, 2H), 2.01 (s, 3H) ppm.
^{13}C NMR	(100 MHz, $(\text{D}_3\text{C})_2\text{CO}$): δ 144.7, 138.4, 133.1, 130.6, 117.1, 109.6, 73.6, 72.6, 12.2 ppm.
HRMS	(EI, m/z): calc. $[\text{M}^+]$: 182.0579; found: $[\text{M}^+]$: 182.0574
IR	$\tilde{\nu}$ = 3428 (w), 3182 (br, w), 2916 (vw), 2876 (vw), 1625 (vw), 1505 (m), 1477 (m), 1382 (m), 1306 (vs), 1259 (s), 1111 (s), 1099 (s), 1049 (m), 1015 (m), 952 (m), 883 (vs), 867 (vs), 767 (s), 723 (w) cm^{-1}

6.1.2 Synthesis of Dibefurin

(3a*R*,4*S*,9a*S*,10*R*)-4,10-dihydroxy-6,12-dimethyl-1*H*,3*H*,4*H*,9*H*-3a,10:4,9a-dimethanocyclodeca[1,2-*c*:6,7-*c'*]difuran-5,11,13,14(7*H*,10*H*)-tetraone (dibefurin)



Epicoccine (50 mg, 0.27 mmol) was suspended in MeCN (2.0 ml) and cooled to 0 °C. A solution of K₃[Fe(CN)₆] (181 mg, 0.550 mmol, 2.0 eq.) and NaHCO₃ (46 mg, 0.55 mmol, 2.0 eq.) in H₂O (4.0 ml) was added dropwise. The reaction mixture was stirred for 30 min at 0 °C and the precipitate was separated by centrifugation (4000 rpm, 15 min, 10 °C). The aqueous phase was decanted off, crude dibefurin triturated with THF (1 ml) and the suspension centrifuged (11000 rpm, 5 min). The trituration was repeated twice to afford dibefurin as a colorless solid. The combined THF phases were concentrated under reduced pressure and the remaining solid was again triturated according to the above procedure to afford a second batch of dibefurin as a colorless solid (combined yield: 24 mg, 49%). Alternatively, crude dibefurin can be crystallized from DMF by slow diffusion of water at rt to afford the title compound as a colorless solid (20 mg, 40%). X-Ray suitable crystals were obtained by crystallization from MeCN.

Formation of a major byproduct, regioisomer **185**, was observed under the dimerization conditions (*vide infra*).

The natural product decomposes in DMSO at rt. The ¹³C NMR spectrum was hence recorded in DMF-d⁷ in addition to DMSO-d⁶.

The analytical data was in agreement with literature precedence.^[150]

LC/MS	2.58 min (10–40% MeCN/H ₂ O, 5 min, 2 ml/min).
m.p.:	204–205 °C (decomposition).
¹H NMR	(400 MHz, DMSO-d⁶): δ 7.21 (s, 2H), 4.63 (d, <i>J</i> = 15.5 Hz, 2H), 4.57 (d, <i>J</i> = 15.5 Hz, 2H), 4.35 (d, <i>J</i> = 9.4 Hz, 2H), 4.23 (d, <i>J</i> = 9.4 Hz, 2H), 1.70 (s, 6H) ppm.
¹³C NMR	(100 MHz, DMSO-d⁶): δ 196.0, 192.3, 158.0, 128.1, 88.7, 69.9, 65.9, 64.3, 12.4 ppm.
¹³C NMR	(100 MHz, DMF-d⁷): δ 197.2, 193.7, 159.6, 129.6, 90.3, 71.3, 67.6, 65.8, 13.0 ppm.
HRMS	(EI, m/z): calc. [M ⁺]: 360.0845; found: 360.0835 [M ⁺].

IR $\tilde{\nu}$ = 3294 (br, w), 2970 (vw), 2907 (vw), 2849 (vw), 1752 (vs), 1668 (s), 1648 (vs), 1536 (vw), 1509 (vw), 1480 (vw), 1444 (vw), 1381 (vw), 1344 (m), 1314 (w), 1238 (vs), 1172 (m), 1063 (s), 1025 (s), 924 (m), 883 (vs), 749 (w), 700 (vw) cm^{-1} .

^1H NMR (DMSO- d^6):

chemical shift δ/ppm (natural sample)	chemical shift δ/ppm (synthetic sample)	$\Delta\delta/\text{ppm}$
7.16 (s, 2H)	7.21 (s, 2H)	+0.05
4.63 (d, J = 15 Hz, 2H)	4.63 (d, J = 15.5 Hz, 2H)	0.00
4.58 (d, J = 15 Hz, 2H)	4.57 (d, J = 15.5 Hz, 2H)	−0.01
4.36 (d, J = 9.3 Hz, 2H)	4.35 (d, J = 9.4 Hz, 2H)	−0.01
4.24 (d, J = 9.3 Hz, 2H)	4.23 (d, J = 9.4 Hz, 2H)	−0.01
1.70 (s, 6H)	1.70 (s, 6H)	0.00

^{13}C NMR (DMSO- d^6):

chemical shift δ/ppm (natural sample)	chemical shift δ/ppm (synthetic sample)	$\Delta\delta/\text{ppm}$
195.8	196.0	+0.2
192.2	192.3	+0.1
157.9	158.0	+0.1
128.0	128.1	+0.1
88.6	88.7	+0.1
69.8	69.9	+0.1
65.9	65.9	0.0
64.3	64.3	0.0
12.3	12.4	+0.1

Successful procedures from Table 3.

NMR yields were determined from the crude sample by addition of internal standard 1,3,5-trimethoxybenzene to solution of crude dibefurin in DMSO- d^6 .

Entry 3:

Epicoccine (40 mg, 0.22 mmol) was dissolved in pH 5 phosphate buffer (c = 1 M, 2 ml) and MeCN (2 ml) and cooled to 0 °C. A solution of Frémy salt (247 mg, 0.92 mmol, 4.2 eq.) in water (2

ml) was added dropwise and the solution was allowed to slowly warm to rt overnight. The resulting suspension was centrifuged (11000 rpm, 15 min) and the obtained crude dibefurin triturated with THF (0.7 ml) and the suspension centrifuged (11000 rpm, 5 min). The trituration was repeated to afford dibefurin as a colorless solid (10 mg, 25%).

Entry 5:

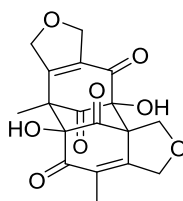
Epicoccine (11 mg, 0.060 mmol) was dissolved in dioxane (1 ml) and treated with Ag₂O (124 mg, 0.54 mmol, 9.0 eq.). After 3 h, the solution was concentrated under reduced pressure to afford crude dibefurin (NMR yield: 30%). Purification by trituration was not applicable due to the presence of inorganic solids.

Entry 18:

Epicoccine (30 mg, 0.16 mmol) was dissolved in MeCN/H₂O (3 ml, 2:1) and FeSO₄·7H₂O (5 mg, 0.02 mmol, 0.1 eq.) was added. The solution was stirred for 20 h and the resulting suspension was centrifuged to give crude dibefurin (NMR yield: 29%).

Entry 19:

Epicoccine (45 mg, 0.25 mmol) was dissolved in MeCN/H₂O (1.3 ml, 1:2) and FeSO₄·7H₂O (7 mg, 0.03 mmol, 0.1 eq.) was added. Oxygen was passed through the solution for 5 min. The solution was stirred under oxygen pressure (balloon) for 62 h before a sat. aq. Na₂H₂EDTA solution (0.5 ml) was added. The suspension was centrifuged (11000 rpm, 10 min), crude dibefurin triturated with THF (0.5 ml) and the suspension centrifuged (11000 rpm, 5 min). The trituration was repeated two times to afford dibefurin as a colorless solid (10 mg, 23%).

Dibefurin Isomer (185)**185**

Chemical Formula: C₁₈H₁₆O₈
Molecular Weight: 360,3180

Regioisomer **185** was observed as a side product of the oxidative dimerization of epicoccine. It can be removed from the crude reaction mixture by successive washings with THF, which yields pure

dibefurin (see procedure above). Concentration of these combined washings gives a sample that is enriched in isomer **185**, but still contains dibefurin. From this sample, the spectroscopic data for isomer **185** can be tabulated.

NMR spectroscopic data for dibefurin isomer **185**:

- ¹H NMR** (400 MHz, DMSO-**d**⁶): δ 7.25 (s, 1H), 7.19 (s, 1H), 4.92 (dd, *J* = 16.9, 3.9 Hz, 1H), 4.81 (d, *J* = 16.9, 4.1 Hz, 1H), 4.75–4.65 (m, 2H), 4.64–4.50 (m, 2H), 4.29 (d, *J* = 9.4 Hz, 1H), 4.19 (d, *J* = 9.4 Hz, 1H), 1.70 (s, 3H), 1.23 (s, 3H) ppm. NMR data was assigned based on analysis of an enriched mixture of dibefurin and isomer **185** (1:3.5).
- ¹³C NMR** (100 MHz, DMSO-**d**⁶): δ 199.3, 196.4, 191.9, 186.8, 161.0, 157.5, 133.4, 128.7, 89.8, 89.6, 76.0, 72.0, 70.0, 65.8, 64.5, 57.8, 12.6, 10.0 ppm. NMR data was assigned based on analysis of an enriched mixture of dibefurin and isomer **185** (1:3.5).
- ¹H NMR** (400 MHz, THF-**d**⁸): δ 6.47 (s, 1H), 6.34 (s, 1H), 5.05 (ddd, *J* = 16.3, 5.5, 3.5 Hz, 1H), 4.75 (ddd, *J* = 16.3, 5.7, 3.4 Hz, 1H), 4.73–4.63 (m, 2H), 4.65–4.55 (m, 2H), 4.36 (d, *J* = 9.3 Hz, 1H), 4.26 (d, *J* = 9.3 Hz, 1H), 1.75 (s, 3H), 1.29 (s, 3H) ppm. NMR data was assigned based on analysis of an enriched mixture of dibefurin and isomer **185** (1:5).
- ¹³C NMR** (100 MHz, THF-**d**⁸): δ 199.1, 196.6, 192.6, 187.8, 162.3, 159.1, 134.9, 129.6, 91.1, 91.0, 77.1, 73.2, 71.0, 67.0, 65.8, 59.1, 12.6, 10.5 ppm. NMR data was assigned based on analysis of an enriched mixture of dibefurin and isomer **185** (1:5).

The natural dibefurin spectrum shown in Figure 48 and Figure 49 was kindly provided by Dr. George S. Sheppard (AbbVie, Wilmette, Illinois, USA). Especially the singlet at δ 1.24 ppm could correspond to isomer **185** (Figure 48). Furthermore, Figure 49 shows the appearance of dublets that could be assigned to isomer **185**.

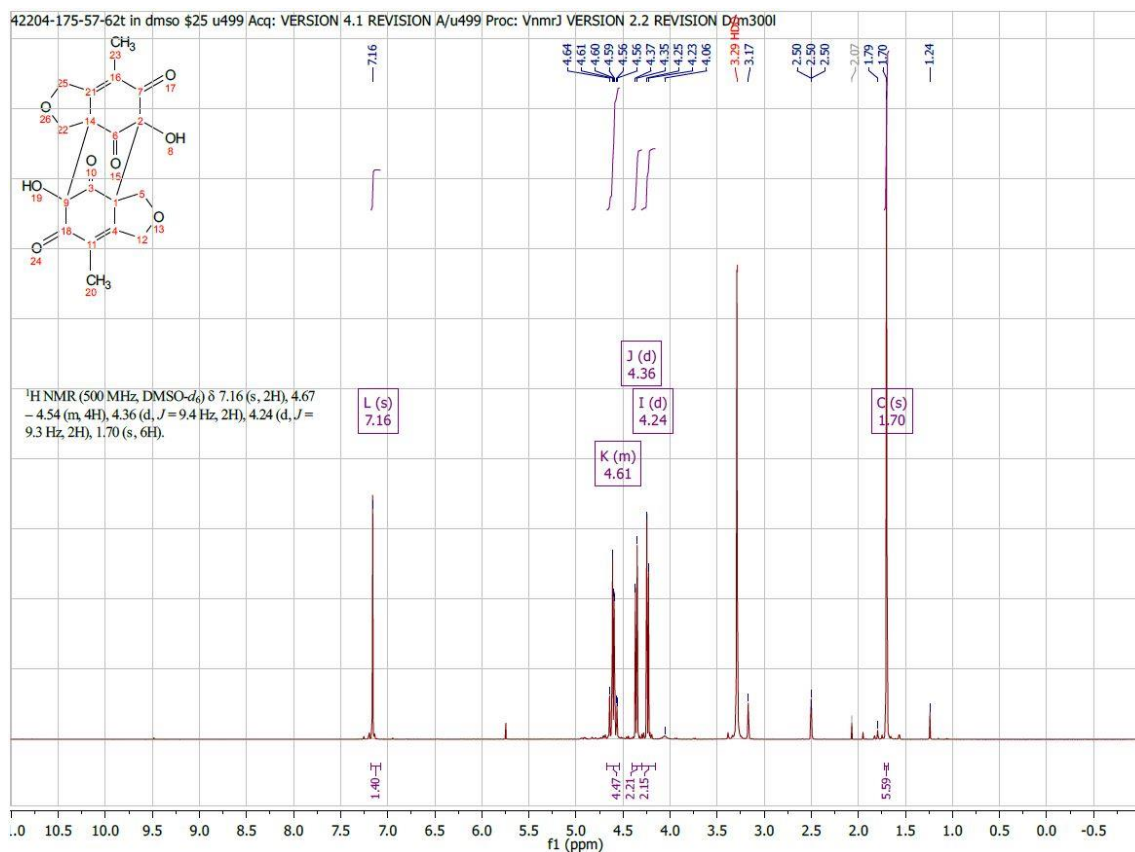


Figure 48. ¹H NMR spectrum of natural dibefurin with potential isomer 185.

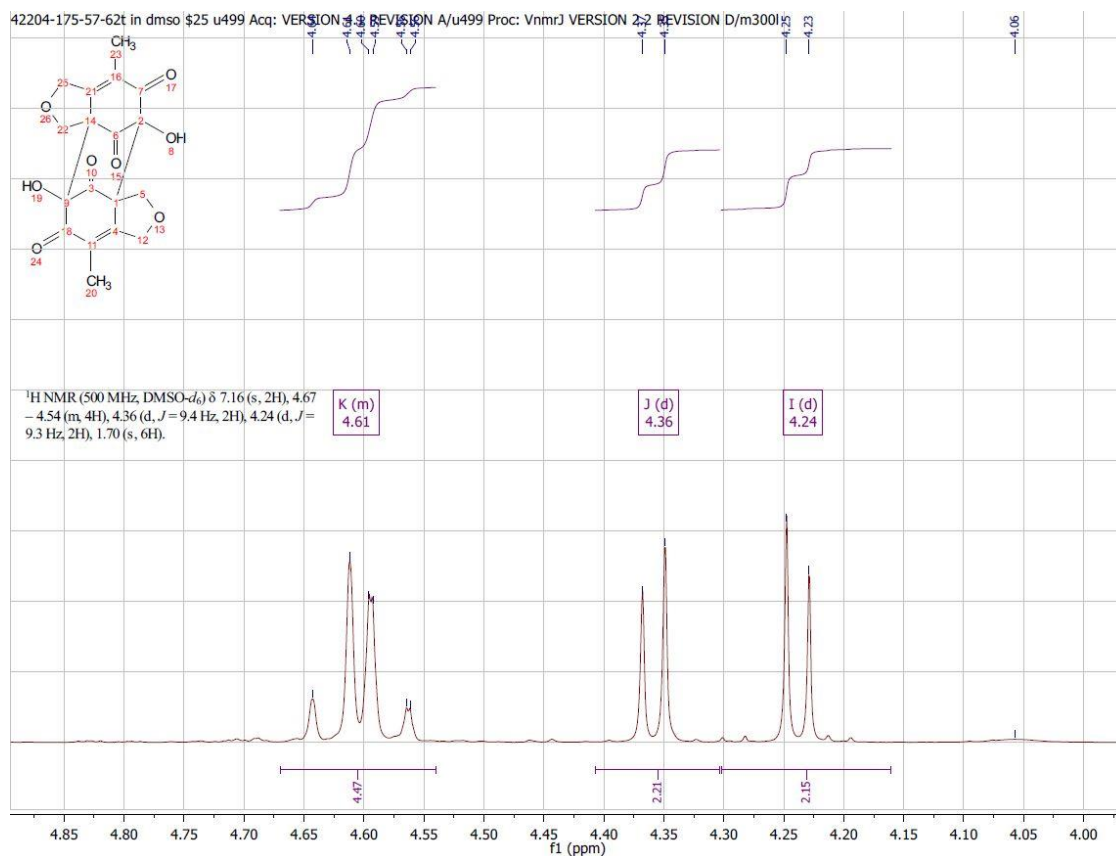
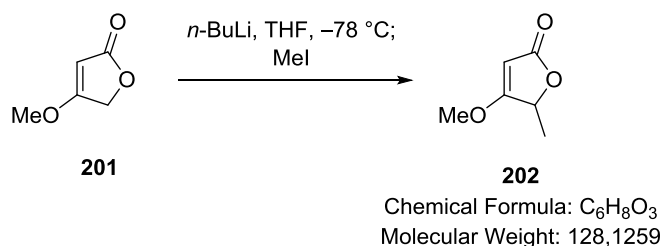


Figure 49. Expansion of a selected area of ¹H NMR spectrum of natural dibefurin.

6.1.3 Synthesis of Epicoccone B

4-methoxy-5-methylfuran-2(5H)-one (202)

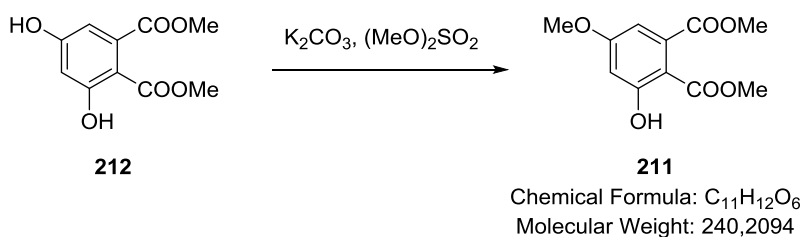


Furanone **201** (1.0 g, 8.8 mmol) in THF (9 ml) was added dropwise to a solution of *n*-BuLi (2.8 M in *n*-hexane, 3.3 ml, 9.2 mmol, 1.05 eq.) in THF (24 ml) at $-78\text{ }^{\circ}\text{C}$. The reaction mixture was stirred for 1 h before MeI (0.82 ml, 1.9 g, 13 mmol, 1.5 eq.) was added and the solution was allowed to warm to rt overnight. After 12 h, the reaction mixture was treated with aq. sat. NaHCO₃ solution (50 ml). The aqueous phase was extracted with CH₂Cl₂ (2x75 ml), EtOAc (1x75 ml), the combined organic phases washed with brine, dried over Na₂SO₄ and concentrated under reduced pressure. The crude product was purified by flash column chromatography (13x3.5 cm, 20–30–35–40% EtOAc/hexanes) to afford the title compound as a colorless oil (277 mg, 25%).

The title compound seems to decompose under flash column chromatography conditions.

TLC	R _f = 0.24 (40% EtOAc/hexanes).
¹H NMR	(300 MHz, CDCl₃): δ 5.03 (brs, 1H), 4.81 (qd, <i>J</i> = 6.7, 0.9 Hz, 1H), 3.87 (s, 3H), 1.44 (d, <i>J</i> = 6.7 Hz, 3H) ppm.
¹³C NMR	(75 MHz, CDCl₃): δ 183.6, 172.5, 88.1, 75.4, 59.6, 17.9 ppm.
MS	(EI, %): 128.02 (49, M ⁺), 113.00 (62), 85.02 (100), 69.00 (40).
HRMS	(EI, m/z): calc. [M ⁺]: 128.0473; found: 128.0469 [M ⁺].
IR	$\tilde{\nu}$ = 3490 (br, vw), 3107 (vw), 2988 (vw), 2945 (vw), 1842 (vw), 1744 (vs), 1625 (vs), 1452 (w), 1379 (w), 1365 (s), 1296 (s), 1244 (s), 1159 (s), 1109 (vw), 1085 (m), 1057 (w), 982 (m), 943 (s), 897 (w), 830 (m), 804 (m), 703 (w), 654 (w) cm ⁻¹ .

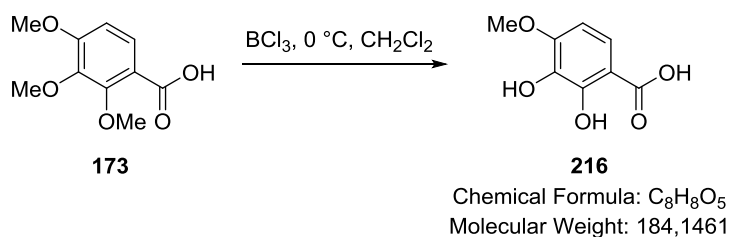
dimethyl 3-hydroxy-5-methoxyphthalate (211)



Resorcinol **212** (1.61 g, 7.11 mmol) was dissolved in acetone (32 ml) and K_2CO_3 (1.47 g, 10.7 mmol, 1.5 eq.) and dimethyl sulfate (0.67 ml, 0.89 g, 7.1 mmol, 1.0 eq.) were added. The reaction mixture was stirred for 4 h, filtered over Celite and concentrated under reduced pressure. The crude product was purified by flash column chromatography (13x4.5 cm, 15–20% EtOAc/hexanes) to afford the title compound as a colorless solid (1.03 g, 61%).

TLC	$R_f = 0.29$ (20% EtOAc/hexanes).
m.p.:	71–73 °C.
1H NMR	(400 MHz, $CDCl_3$): δ 11.00 (s, 1H), 6.48 (s, 1H), 6.45 (s, 1H), 3.85 (s, 6H), 3.79 (s, 3H) ppm.
^{13}C NMR	(100 MHz, $CDCl_3$): δ 169.4, 169.3, 164.5, 163.9, 137.2, 107.8, 102.7, 102.2, 55.8, 52.7, 52.7 ppm.
MS	(EI, %): 240.03 (26, M^+), 208.00 (40), 150.01 (100), 83.96 (17), 48.91 (19).
HRMS	(EI, m/z): calc. [M^+]: 240.0634; found: 240.0630 [M^+].
IR	$\tilde{\nu} = 3145$ (br, vw), 3088 (vw), 3006 (vw), 2954 (vw), 2850 (vw), 1737 (s), 1669 (vs), 1617 (s), 1583 (m), 1501 (vw), 1435 (s), 1372 (w), 1344 (s), 1311 (m), 1268 (vs), 1237 (s), 1200 (vs), 1152 (vs), 1115 (w), 1039 (m), 1024 (m), 971 (vw), 955 (vw), 899 (vw), 850 (w), 803 (w), 783 (w), 762 (w), 707 (vw) cm^{-1} .

2,3-dihydroxy-4-methoxybenzoic acid (**216**)



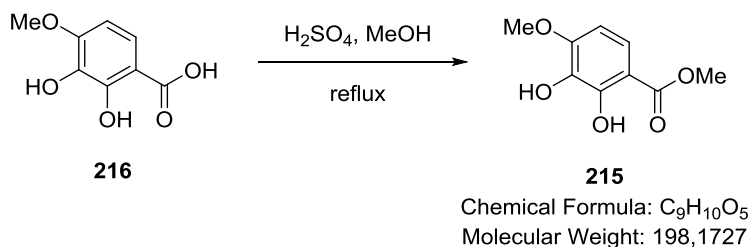
Benzoic acid **173** (8.49 g, 40.0 mmol) was dissolved in CH_2Cl_2 (30 ml) and the resulting solution was treated with BCl_3 ($c = 1$ M in CH_2Cl_2 , 40.0 ml, 40.0 mmol, 1.0 eq.) at 0 °C. The reaction mixture was warmed to rt and stirred for 1.5 h. BCl_3 ($c = 1$ M in CH_2Cl_2 , 60.0 ml, 60.0 mmol, 1.5 eq.) was added over 40 min to the reaction mixture and stirring was continued at rt for 12 h. The reaction mixture was poured onto an ice/water mixture (100 ml), treated with EtOAc (100 ml) and neutralized with aq. NaOH solution (2 M) and sat. aq. $NaHCO_3$ solution. The organic layer was discarded and the aqueous phase acidified to pH 1 with aq. HCl solution ($c = 6$ M). The aqueous phase was extracted with EtOAc (3x100 ml), the combined organic phases were dried over Na_2SO_4 and concentrated under reduced pressure. Boron impurities were removed by addition of MeOH (20 ml) and heating to reflux for 45 min. The crude mixture was cooled to 0 °C and the precipitate was filtered off to afford the title compound **216** as a colorless solid (3.78 g). The mother liquor was concentrated under reduced pressure, the residue taken up in MeOH, cooled to 0 °C and filtered to furnish an additional crop of the

title compound as a colorless solid (691 mg). Repetition of this procedure afforded a third batch of the title compound (198 mg). The mother liquor was concentrated under reduced pressure and the residue recrystallized from H₂O (70 ml) to afford the title compound as a colorless solid (966 mg, combined yield: 76%).

The analytical data was in agreement with literature precedence.^[194]

TLC	$R_f = 0.12$ (20% MeOH/CH ₂ Cl ₂).
m.p.:	233–235 °C.
¹H NMR	(400 MHz, CD ₃ OD): δ 7.41 (d, $J = 8.9$ Hz, 1H), 6.58 (d, $J = 8.9$ Hz, 1H), 3.90 (s, 3H) ppm.
¹³C NMR	(100 MHz, CD ₃ OD): δ 173.7, 153.9, 151.8, 134.9, 122.6, 108.0, 104.0, 56.5 ppm.
NOESY	(400 MHz, CD ₃ OD): δ 6.58 (Ar- <i>H</i>) \leftrightarrow 3.90 (–OCH ₃) ppm.
HRMS	(EI, <i>m/z</i>): calc. [<i>M</i> ⁺]: 184.0372; found: 184.0372 [<i>M</i> ⁺].
IR	$\tilde{\nu} = 3349$ (w), 3187 (w), 2954 (w), 2850 (w), 2628 (w), 2549 (w), 1650 (vs), 1618 (s), 1507 (s), 1485 (m), 1459 (m), 1438 (s), 1391 (s), 1327 (m), 1275 (vs), 1231 (vs), 1182 (m), 1162 (w), 1088 (vs), 1046 (w), 973 (vw), 933 (w), 920 (m), 897 (m), 812 (vw), 770 (vs), 727 (s), 715 (w), 682 (m) cm ^{–1} .

methyl 2,3-dihydroxy-4-methoxybenzoate (**215**)

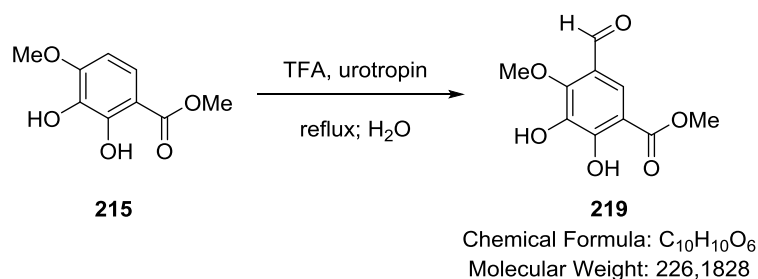


Catechol **216** (4.65 g, 25.3 mmol) was heated to reflux in MeOH (42 ml) and conc. H₂SO₄ (1.5 ml) for 18 h. The reaction mixture was concentrated under reduced pressure and washed with water (50 ml). The aqueous phase was extracted with EtOAc (2x75 ml), the combined organic phases were dried over Na₂SO₄ and concentrated under reduced pressure. The residue was filtered over a short plug of silica with 70% EtOAc/hexanes and the solvent was removed under reduced pressure to afford the title compound **215** as a colorless solid (4.88 g, 98%). The filtration over a silica gel plug was not required and the crude sample could be used in the following steps with comparable yields.

TLC	$R_f = 0.38$ (30% EtOAc/hexanes).
m.p.:	84–86 °C.
¹H NMR	(600 MHz, CDCl ₃): δ 10.83 (s, 1H), 7.41 (d, $J = 8.9$ Hz, 1H), 6.50 (d, $J = 8.9$ Hz, 1H), 5.45 (s, 1H), 3.94 (s, 3H), 3.93 (s, 3H) ppm.

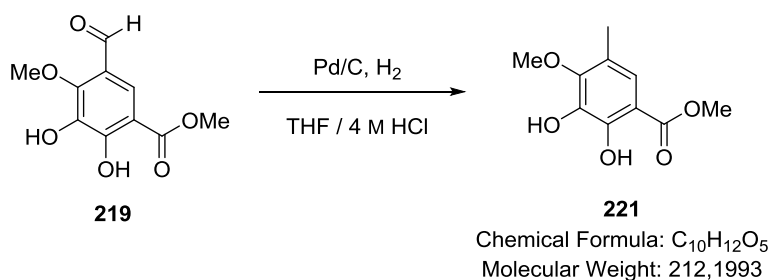
¹³C NMR	(150 MHz, CDCl ₃): δ 170.6, 151.7, 149.4, 133.5, 121.5, 106.8, 103.1, 56.3, 52.3 ppm.
HRMS	(EI, m/z): calc. [M ⁺]: 198.0528; found: 198.0520 [M ⁺].
IR	$\tilde{\nu}$ = 3467 (br, w), 3164 (br, vw), 3008 (vw), 2956 (vw), 2844 (vw), 1666 (s), 1622 (w), 1589 (vw), 1512 (m), 1456 (m), 1438 (s), 1392 (vw), 1369 (w), 1315 (m), 1288 (vs), 1229 (s), 1192 (m), 1154 (m), 1082 (s), 1013 (m), 942 (vw), 901 (vw), 813 (vw), 801 (vw), 771 (m), 730 (w), 714 (vw), 690 (vw) cm ⁻¹ .

methyl 5-formyl-2,3-dihydroxy-4-methoxybenzoate (**219**)



Catechol **215** (4.88 g, 24.6 mmol) was heated to reflux in TFA (100 ml) with urotropine (6.90 g, 49.2 mmol, 2.0 eq.). After 13 h, the reaction mixture was cooled to 50 °C, treated with water (425 ml) and stirred for 2 h at 50 °C. The suspension was cooled to rt and the aqueous phase was extracted with EtOAc (3x350 ml). The combined organic phases were washed with aq. pH 7.2 phosphate buffer (*c* = 1 M, 3x200 ml), dried over Na₂SO₄ and concentrated under reduced pressure to afford the title compound **219** as a colorless solid (5.20 g, 94%).

TLC	R _f = 0.26 (40% EtOAc/hexanes).
m.p.:	180–183 °C.
¹H NMR	(400 MHz, CDCl ₃): δ 11.51 (s, 1H), 10.24 (s, 1H), 8.01 (s, 1H), 4.16 (s, 3H), 3.97 (s, 3H) ppm. 1 –OH missing.
¹³C NMR	(75 MHz, CDCl ₃): δ 188.5, 170.4, 154.8, 153.4, 136.8, 122.3, 121.6, 108.3, 61.9, 52.9 ppm.
NOESY	(400 MHz, CDCl ₃): δ 3.97 (–COOCH ₃) ↔ 8.01 (Ar–H); 10.24 (–CHO) ↔ 8.01 (Ar–H), 4.16 (–OCH ₃) ppm.
HRMS	(EI, m/z): calc. [M ⁺]: 226.0477; found: 226.0468 [M ⁺].
IR	$\tilde{\nu}$ = 3150 (br, w), 2953 (w), 2925 (w), 2851 (w), 1665 (vs), 1593 (m), 1490 (w), 1462 (m), 1442 (s), 1382 (w), 1316 (vs), 1289 (s), 1267 (m), 1233 (m), 1188 (m), 1091 (s), 1033 (w), 1014 (vw), 994 (w), 941 (w), 898 (vw), 792 (m), 731 (m), 705 (w), 658 (vw) cm ⁻¹ .

methyl 2,3-dihydroxy-4-methoxy-5-methylbenzoate (221)

Aldehyde **219** (3.99 g, 17.6 mmol) was dissolved in THF / aq. HCl ($c = 4$ M, 200 ml, 1:1) and Pd/C (10 wt-%, 3.76 g, 3.52 mmol, 0.20 eq.) was added. The reaction mixture was purged with hydrogen gas and stirred for 45 h at room temperature under hydrogen atmosphere. The reaction mixture was filtered over Celite and the filter cake was washed with EtOAc. The biphasic mixture was extracted with EtOAc (3x250 ml), the combined organic phases were dried over Na₂SO₄ and concentrated to give the title compound **221** as a colorless solid (3.43 g, 92%) after purification by filtration over a silica gel plug with CH₂Cl₂. The filtration over a silica gel plug was not required and the crude sample could be used in the following steps with comparable yields.

TLC $R_f = 0.26$ (10% EtOAc/hexanes).

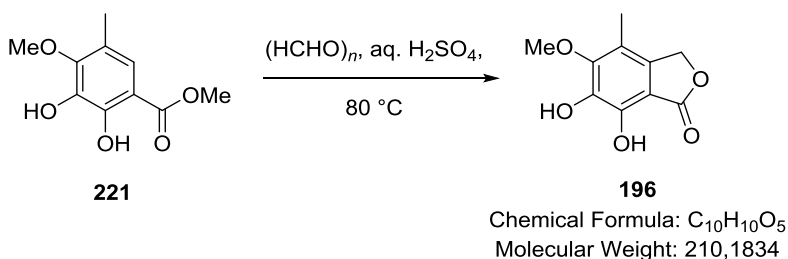
m.p.: 77–79 °C.

¹H NMR (400 MHz, CDCl₃): δ 10.74 (s, 1H), 7.18 (s, 1H), 5.55 (s, 1H), 3.95 (s, 3H), 3.92 (s, 3H), 2.19 (s, 3H) ppm.

¹³C NMR (100 MHz, CDCl₃): δ 170.6, 150.3, 148.7, 137.2, 122.4, 121.2, 107.5, 60.3, 52.3, 15.8 ppm.

HRMS (EI, m/z): calc. [M^+]: 212.0685; found: 212.0681 [M^+].

IR $\tilde{\nu} = 3444$ (br, vw), 3162 (br, vw), 2954 (w), 2855 (vw), 1667 (s), 1621 (w), 1496 (w), 1465 (m), 1440 (vs), 1382 (w), 1353 (m), 1304 (vs), 1246 (vs), 1205 (vs), 1173 (s), 1090 (s), 1044 (vs), 1000 (s), 943 (s), 876 (m), 789 (s), 764 (m), 704 (m), 661 (w) cm⁻¹.

6,7-dihydroxy-5-methoxy-4-methylisobenzofuran-1(3H)-one (196)

Catechol **221** (6.90 g, 32.5 mmol) was dissolved in aq. H₂SO₄ (40%, 260 ml) and dioxane (70 ml). Paraformaldehyde (2.44 g, 81.3 mmol, 2.5 eq.) was added and the reaction mixture was heated to 80 °C for 12 h. The reaction mixture was cooled to 0 °C and neutralized by dropwise addition of aq. NaOH soln. (120 g in 250 ml). The mixture was then treated with water (250 ml) and extracted with EtOAc (5x250 ml). The combined organic phases were washed with water (2x250 ml), dried over Na₂SO₄ and concentrated under reduced pressure. The residue was taken up in Et₂O and concentrated under reduced pressure. The co-evaporation procedure was repeated three more times to afford the title compound **12** as a brown solid (6.83 g, 99%).

The title compound decomposes on silica gel but could be purified by filtration through a plug of C18 silica gel (20% MeCN/H₂O + 1% FA).

Strong acids HX with X⁻ being nucleophilic led to partial demethylation and subsequent decomposition of the unprotected pyrogallol derivative under the reaction conditions.

Single crystals for X-ray analysis were obtained by recrystallization from hot benzene.

TLC R_f = 0.36 (5% MeOH/CH₂Cl₂).

m.p.: 113–115 °C.

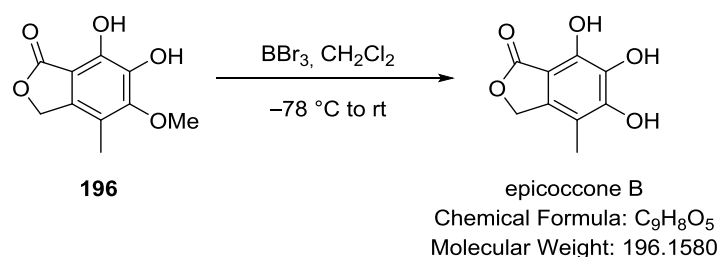
¹H NMR (400 MHz, (CD₃)₂CO): δ 7.71 (brs, 2H), 5.18 (s, 2H), 3.87 (s, 3H), 2.11 (s, 3H) ppm.

¹³C NMR (100 MHz, (CD₃)₂CO): δ 171.5, 153.2, 143.8, 138.8, 137.4, 117.1, 107.5, 69.6, 60.7, 11.1 ppm.

HRMS (EI, m/z): calc. [M⁺]: 210.0528; found: 210.0525 [M⁺].

IR $\tilde{\nu}$ = 3426 (br, m), 2939 (w), 2865 (vw), 1732 (vs), 1626 (w), 1505 (m), 1456 (m), 1382 (m), 1311 (s), 1220 (s), 1137 (m), 1083 (m), 1037 (s), 970 (m), 858 (w), 786 (w) cm⁻¹.

5,6,7-trihydroxy-4-methylisobenzofuran-1(3H)-one (epicoccone B)

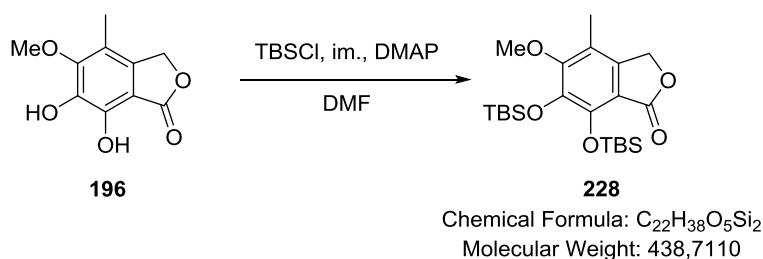


Methyl ether **196** (500 mg, 2.38 mmol) was dissolved in CH₂Cl₂ (1.7 ml) and cooled to -78 °C. BBr₃ (c = 1 M in CH₂Cl₂, 9.5 ml, 9.5 mmol, 4.0 eq.) was added dropwise and the reaction mixture was allowed to stir for 12 h while slowly warming to rt. The reaction mixture was cooled to 0 °C and quenched by dropwise addition of aq. pH 7 phosphate buffer (c = 1 M, 5 ml) followed by 5% aq. H₂SO₄ (10 ml). The mixture was extracted with EtOAc (3x50 ml) and the combined organic phases dried over Na₂SO₄ and concentrated under reduced pressure. The title compound decomposes on silica

gel but could be purified by filtration through a plug of C18 silica gel (10% MeCN/H₂O + 0.3% FA) to afford the title compound epicoccocone B as a colorless solid (338 mg, 72%).

LC/MS	2.01 min (10–90% MeCN/H ₂ O, 6 min, 2ml/min).
m.p.:	233–240 °C (gradual decomp.).
¹H NMR	(400 MHz, DMSO- <i>d</i> ⁶): δ 9.37 (brs, 1H), 9.27 (brs, 1H), 8.74 (brs, 1H), 5.10 (s, 2H), 1.97 (s, 3H) ppm.
¹³C NMR	(100 MHz, DMSO- <i>d</i> ⁶): δ 169.9, 151.2, 143.1, 138.1, 132.9, 109.1, 102.8, 67.8, 10.8 ppm.
HRMS	((–)-ESI, <i>m/z</i>): calc. [M–H [–]]: 195.0299; found: 195.0296 [M–H [–]].
IR	$\tilde{\nu}$ = 3511 (w), 3438 (w), 3335 (w), 1741 (s), 1634 (w), 1519 (s), 1483 (w), 1455 (m), 1404 (vw), 1382 (m), 1346 (vw), 1327 (vw), 1265 (vs), 1223 (s), 1188 (m), 1121 (w), 1102 (m), 1068 (m), 1021 (vs), 990 (vs), 943 (s), 873 (s), 774 (vs), 742 (m), 736 (w), 713 (m) cm ^{–1} .

6,7-bis((*tert*-butyldimethylsilyl)oxy)-5-methoxy-4-methylisobenzofuran-1(3*H*)-one (228)



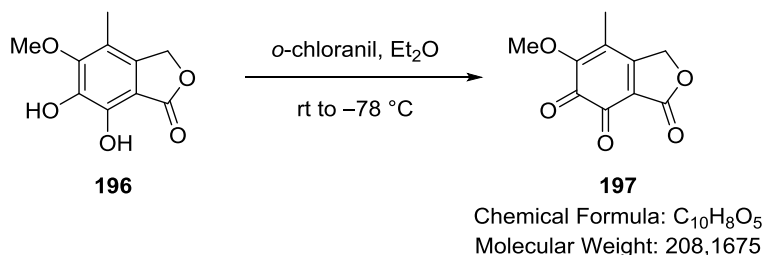
Catechol **196** (102 mg, 0.485 mmol) was dissolved in DMF (0.3 ml) and TBSCl (176 mg, 1.16 mmol, 2.4 eq.), imidazole (159 mg, 2.33 mmol, 4.8 eq.) and DMAP (12 mg, 0.097 mmol, 0.2 eq.) were added. After 22 h, pH 4.5 phosphate buffer (*c* = 0.1 M, 3 ml) was added and the aqueous phase was extracted with Et₂O (3x10 ml). The combined organic phases were dried over Na₂SO₄ and concentrated under reduced pressure. The residue was purified by flash column chromatography (12x2 cm, 5–10% EtOAc/hexanes + 1% NEt₃) to afford the title compound as a yellowish oil (163 mg, 77%).

TLC	R _f = 0.20 (5% EtOAc/hexanes).
m.p.:	90–92 °C.
¹H NMR	(400 MHz, CD ₂ Cl ₂): δ 5.04 (s, 2H), 3.74 (s, 3H), 2.12 (s, 3H), 1.05 (s, 9H), 1.01 (s, 9H), 0.14 (s, 6H), 0.14 (s, 6H) ppm.
¹³C NMR	(100 MHz, CD ₂ Cl ₂): δ 169.6, 157.3, 145.8, 141.9, 140.1, 119.1, 113.2, 68.0, 60.6, 26.4, 26.3, 18.8, 18.7, 11.3, –3.9, –3.9 ppm.
HRMS	((+)-ESI, <i>m/z</i>): calc. [M+H ⁺]: 439.2331; found: 439.2331 [M+H ⁺]

IR $\tilde{\nu}$ = 2950 (w), 2929 (m), 2887 (w), 2858 (w), 1769 (vs), 1606 (vw), 1591 (vw), 1472 (s), 1449 (m), 1408 (w), 1356 (vs), 1282 (w), 1250 (m), 1193 (vw), 1138 (m), 1037 (s), 1018 (w), 983 (s), 961 (w), 885 (s), 837 (vs), 825 (s), 813 (s), 797 (w), 781 (s), 677 (vw) cm^{-1} .

6.1.4 Synthesis of Epicolactone

5-methoxy-4-methylisobenzofuran-1,6,7(3*H*)-trione (**197**)



To catechol **196** (100 mg, 0.476 mmol) was added Et₂O (20 ml) and the suspension was stirred until most of catechol **196** was dissolved. *o*-Chloranil (123 mg, 0.500 mmol, 1.05 eq.) was added and the solution was cooled to $-78\text{ }^{\circ}\text{C}$ after 30 sec. The reaction mixture was stirred at this temperature for 1 h and the solvent was quickly removed under reduced pressure at below $0\text{ }^{\circ}\text{C}$ (ca. 100–125 mbar). The residue was washed with $-78\text{ }^{\circ}\text{C}$ cold Et₂O until the ethereal phase was only pale yellow (5x1.5 ml). The title compound **197** was obtained as a red-brown solid (76 mg, 77%) with traces of tetrachlorocatechol and starting material as minor impurity.

The title compound fully decomposes overnight in solution. It is stable as a solid at $-30\text{ }^{\circ}\text{C}$ for more than three months.

m.p.: 179–182 $^{\circ}\text{C}$ (decomposition).

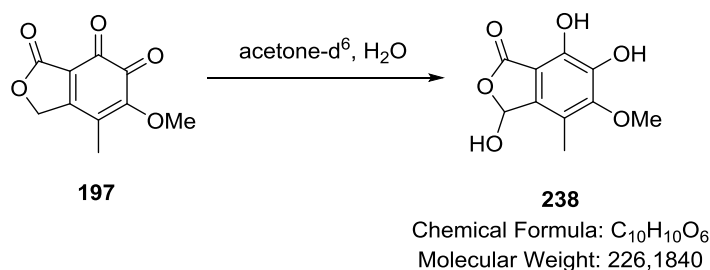
¹H NMR (400 MHz, (D₃C)₂CO): δ 5.53 (s, 2H), 4.03 (s, 3H), 2.08 (s, 3H) ppm.

¹³C NMR (100 MHz, (D₃C)₂CO): δ 177.1, 176.4, 172.3, 166.7, 155.4, 125.6, 118.5, 69.5, 61.0, 10.8 ppm.

HRMS ((+)-ESI, *m/z*): calc. [M+H⁺]: 209.0444; found: 209.0444 [M+H⁺].

IR $\tilde{\nu}$ = 3341 (br, vw), 2950 (vw), 2919 (vw), 2849 (vw), 1760 (vs), 1743 (m), 1678 (vs), 1653 (w), 1578 (m), 1450 (w), 1440 (w), 1407 (w), 1385 (w), 1346 (m), 1295 (m), 1278 (m), 1182 (vw), 1102 (s), 1024 (vs), 955 (w), 938 (s), 873 (w), 827 (vw), 807 (vw), 747 (w), 729 (vw) cm⁻¹.

3,6,7-trihydroxy-5-methoxy-4-methylisobenzofuran-1(3*H*)-one (**238**)

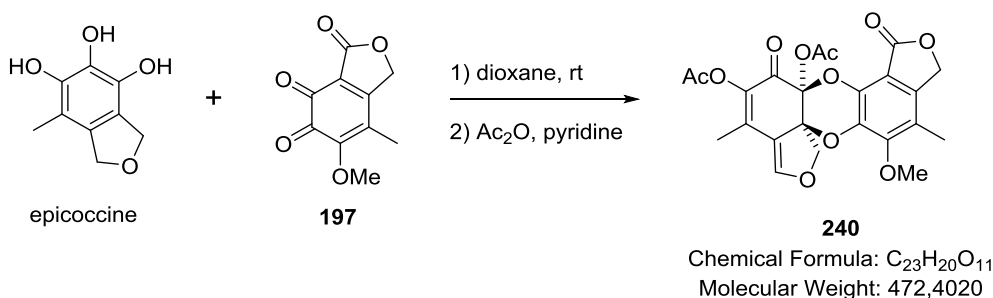


o-Quinone **197** was dissolved in acetone- d^6 (0.7 ml) and its decomposition was monitored by ^1H NMR. After 18 h, the *o*-quinone **197** was fully converted into hydroxyisobenzofuranone **238**.

^1H NMR (400 MHz, $(\text{D}_3\text{C})_2\text{CO}$): δ 6.57 (s, 1H), 3.87 (s, 3H), 2.23 (s, 3H) ppm.

HRMS ((-)-ESI, m/z): calc. $[\text{M}-\text{H}]^-$: 225.0399; found: 225.0404 $[\text{M}-\text{H}]^-$.

***rac*-(6*aR*,12*aR*)-5-methoxy-4,10-dimethyl-1,12-dioxo-1,3-dihydro-7*H*-[1,4]dioxino[2,3-*d*:3,2-*d'*:6,5-*e''*]trienobenzofuran-11,12*a*(12*H*)-diyl diacetate (**240**)**



Epicoccine (15 mg, 0.082 mmol) and *o*-quinone **197** (34 mg, 0.16 mmol, 2.0 eq.) were suspended in dioxane (0.1 ml) and the resulting mixture stirred at rt for 12 h. CH_2Cl_2 (0.5 ml) was added, followed by Ac_2O (0.2 ml) and pyridine (0.2 ml) and the resulting mixture stirred for 2 h at rt. The reaction mixture was diluted with EtOAc (20 ml) and washed with aq. pH 5 phosphate buffer ($c = 1$ M, 10 ml), dried over Na_2SO_4 and concentrated under reduced pressure. The crude mixture was purified by preparative TLC (70% EtOAc in hexanes) to give the title compound as a pale yellow film (4.0 mg, 10%). Single crystals for X-ray analysis were obtained by slow diffusion of water into a DMSO solution of the compound in a hanging-drop setup.

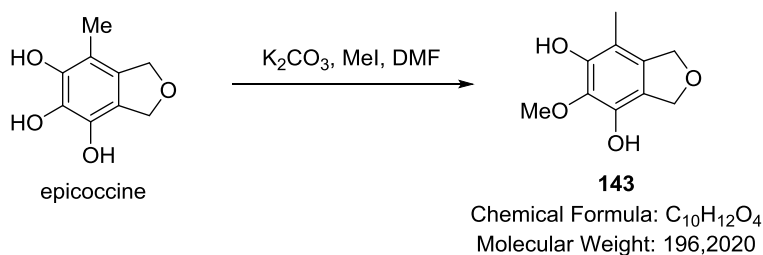
TLC $R_f = 0.32$ (70% EtOAc/hexanes).

^1H NMR (400 MHz, CDCl_3): δ 7.10 (s, 1H), 5.09 (s, 2H), 4.71 (d, $J = 11.5$ Hz, 1H), 4.36 (d, $J = 11.5$ Hz, 1H), 3.81 (s, 3H), 2.21 (s, 3H), 2.21 (s, 3H), 2.08 (s, 3H), 2.02 (s, 3H) ppm.

^{13}C NMR (100 MHz, CDCl_3): δ 180.6, 168.3, 167.8, 166.1, 153.3, 151.3, 141.2, 138.9, 135.2, 133.5, 132.9, 119.0, 113.0, 108.1, 92.7, 84.7, 74.7, 68.4, 61.2, 21.2, 20.3, 13.3, 11.1 ppm.

HRMS ((+)-ESI, m/z): calc. $[\text{M}+\text{Na}^+]$: 495.0898; found: 495.0896 $[\text{M}+\text{Na}^+]$.

IR $\tilde{\nu} = 1765$ (s), 1708 (w), 1622 (m), 1600 (s), 1562 (m), 1556 (m), 1510 (w), 1502 (m), 1483 (m), 1463 (s), 1364 (s), 1344 (m), 1326 (w), 1280 (w), 1253 (w), 1192 (s), 1124 (vs), 1085 (s), 1059 (s), 1032 (vs), 1006 (m), 970 (w), 782 (m) cm^{-1} .

5-methoxy-7-methyl-1,3-dihydroisobenzofuran-4,6-diol (143)

Epicoccine (49 mg, 0.27 mmol) was dissolved in DMF (1.0 ml) and K₂CO₃ (38 mg, 0.27 mmol, 1.0 eq.) and MeI (17 μ l, 38 mg, 0.27 mmol, 1.0 eq.) were added. The reaction mixture was stirred for 12 h and pH 7.2 buffer ($c = 1$ M, 10 ml) was added. The aqueous phase was extracted with EtOAc (3x10 ml), the combined organic phases were washed with brine (2x15 ml), dried over Na₂SO₄ and concentrated under reduced pressure. The residue was subjected to flash column chromatography (16x2.5 cm, 25–35–45% EtOAc/hexanes) to afford the title compound as a colorless solid (19 mg, 36%).

TLC $R_f = 0.48$ (50% EtOAc/hexanes).

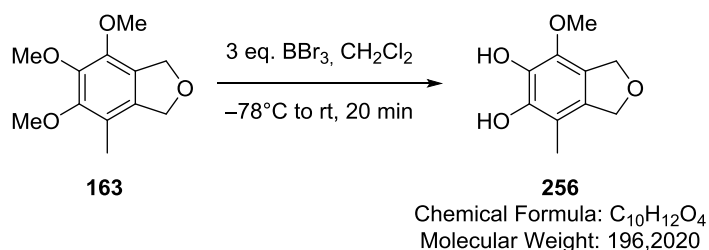
m.p.: 157–160 °C.

¹H NMR (400 MHz, (D₃C)₂CO): δ 7.85 (s, 1H), 7.58 (s, 1H), 4.96 (t, $J = 2.0$ Hz, 2H), 4.91 (t, $J = 2.0$ Hz, 2H), 3.74 (s, 3H), 2.00 (s, 3H) ppm.

¹³C NMR (100 MHz, (D₃C)₂CO): δ 148.7, 142.7, 135.7, 135.2, 116.8, 109.4, 73.7, 72.5, 61.0, 12.0 ppm.

HRMS ((–)-ESI, m/z): calc. [M–H][–]: 195.0657; found: 195.0660 [M–H][–].

IR $\tilde{\nu} = 3360$ (br, m), 2915 (w), 2853 (w), 1615 (w), 1494 (m), 1463 (m), 1455 (m), 1435 (w), 1375 (vs), 1337 (m), 1321 (s), 1272 (m), 1229 (m), 1114 (vs), 1054 (s), 985 (s), 935 (w), 896 (s), 878 (s), 765 (m), 726 (w) cm^{–1}.

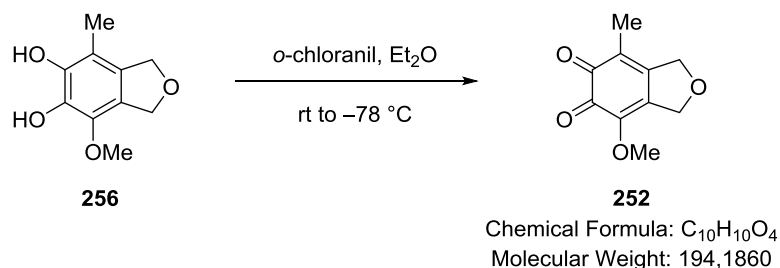
4-methoxy-7-methyl-1,3-dihydroisobenzofuran-5,6-diol (256)

Trimethyl ether **163** (100 mg, 0.446 mmol) was dissolved in CH₂Cl₂ (4.5 ml) and the solution was cooled to –78 °C. A solution of BBr₃ in CH₂Cl₂ ($c = 1$ M, 1.3 ml, 1.3 mmol, 3 eq.) was introduced dropwise and the reaction mixture allowed to warm to rt. After stirring for 20 min at rt, the reaction

mixture was cooled to $-78\text{ }^{\circ}\text{C}$ and pH 5 buffer ($c = 1\text{ M}$, 5 ml) and brine (10 ml) were added. The aqueous phase was extracted with EtOAc (4x10 ml). The combined organic phases were dried over Na_2SO_4 and concentrated under reduced pressure. The crude product was purified by flash column chromatography (12x2.5 cm, 33% EtOAc/hexanes) to afford the title compound as a colorless solid (72 mg, 83%).

TLC	$R_f = 0.51$ (33% EtOAc/hexanes).
m.p.:	139–141 $^{\circ}\text{C}$.
^1H NMR	(400 MHz, $(\text{D}_3\text{C})_2\text{CO}$): δ 7.67 (brs, 1H), 7.20 (brs, 1H), 5.09 (s, 2H), 4.90 (s, 2H), 3.75 (s, 3H), 2.03 (s, 3H) ppm.
^{13}C NMR	(100 MHz, $(\text{D}_3\text{C})_2\text{CO}$): δ 144.6, 140.9, 136.1, 130.6, 119.8, 112.7, 73.2, 72.6, 59.8, 12.2 ppm.
MS	(EI, %): 196.08 (100, M^+), 195.07 (93), 167.06 (64), 152.04 (19), 77.00 (15).
HRMS	(EI, m/z): calc. $[\text{M}^+]$: 196.0736; found: 196.0733 $[\text{M}^+]$.
IR	$\tilde{\nu} = 3342$ (m), 2855 (w), 1627 (w), 1501 (vs), 1472 (s), 1368 (s), 1327 (s), 1290 (vs), 1271 (vs), 1193 (m), 1111 (vs), 1053 (s), 1003 (m), 903 (s), 766 (w), 725 (w), 668 (w) cm^{-1} .

4-methoxy-7-methylisobenzofuran-5,6(1*H*,3*H*)-dione (**252**)

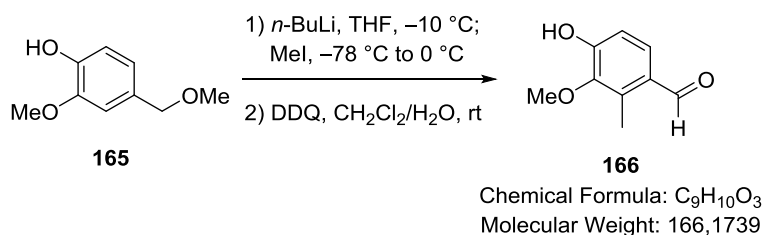


Catechol **256** (100 mg, 0.510 mmol) was dissolved in Et_2O (20 ml) and *o*-chloranil (132 mg, 0.537 mmol, 1.05 eq.) was added. The reaction mixture was stirred for 1 min at rt and then cooled to $-78\text{ }^{\circ}\text{C}$. After additional stirring for 1 h at $-78\text{ }^{\circ}\text{C}$, the suspension was filtered at $-78\text{ }^{\circ}\text{C}$ with precooled glassware. The filter cake was washed with $-78\text{ }^{\circ}\text{C}$ cold Et_2O and the title compound was obtained as a dark red solid (75 mg, 76%).

m.p.:	130–131 $^{\circ}\text{C}$ (decomposition).
^1H NMR	(400 MHz, $(\text{D}_3\text{C})_2\text{CO}$): δ 4.84 (s, 2H), 4.74 (s, 2H), 3.90 (s, 3H), 1.79 (s, 3H) ppm.
^{13}C NMR	(100 MHz, $(\text{D}_3\text{C})_2\text{CO}$): δ 178.5, 176.5, 153.3, 145.0, 135.4, 125.1, 70.9, 69.8, 59.7, 11.7 ppm.
MS	(EI, %): 195.04 (4, M^+), 167.03 (3), 57.99 (43), 42.97 (100).
HRMS	(EI, m/z): calc. $[\text{M}^+]$: 194.0579; found: 194.0587 $[\text{M}^+]$.

IR $\tilde{\nu}$ = 3013 (vw), 2953 (vw), 2891 (vw), 2848 (vw), 1688 (s), 1664 (s), 1651 (s), 1621 (vw), 1600 (s), 1455 (w), 1443 (m), 1383 (w), 1359 (w), 1338 (w), 1324 (s), 1284 (s), 1247 (w), 1227 (w), 1200 (w), 1186 (w), 1119 (m), 1094 (vs), 1057 (s), 1005 (m), 978 (m), 933 (m), 922 (s), 885 (w), 811 (vw), 750 (vw), 726 (m), 667 (vw) cm^{-1} .

4-hydroxy-3-methoxy-2-methylbenzaldehyde (**166**)



A solution of *n*-BuLi in hexanes ($c = 2.5$ M, 74.0 ml, 185 mmol, 3.0 eq.) was added dropwise to a solution of phenol **165** (10.35 g, 61.51 mmol) in THF (100 ml) at -10 °C. The resulting mixture was stirred at -5 °C for 5 h and then cooled to -78 °C. MeI (13.4 ml, 30.6 g, 215 mmol, 3.5 eq.) was subsequently added very slowly and the resulting reaction mixture was allowed to warm to 0 °C. Stirring was continued for 30 min before H_2O (100 ml) and CH_2Cl_2 (300 ml) were added. The organic phase was washed with sat. aq. NaHCO_3 (3x150 ml) and brine (200 ml) and concentrated under reduced pressure.

The crude product was dissolved in $\text{CH}_2\text{Cl}_2/\text{H}_2\text{O}$ (95:5, 385 ml) and DDQ (14.1 g, 62.1 mmol, 1.01 eq.) was added in 2 portions in a water bath. The water bath was removed and the reaction mixture stirred for 5 h before concentration under reduced pressure. The suspension was filtered over a silica plug (3x6.5 cm, CH_2Cl_2) and the crude product was purified by flash column chromatography (16x10 cm, 20–30–40–50% Et_2O /hexanes). The resulting mixed fractions were again subjected to flash column chromatography to afford the title compound as a colorless solid (3.60 g, 35%).

TLC $R_f = 0.24$ (15% EtOAc /hexanes).

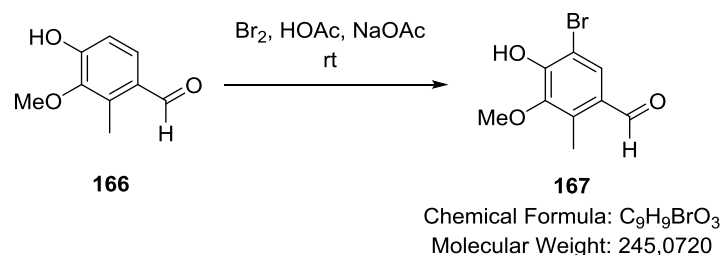
^1H NMR (300 MHz, CDCl_3): δ 10.05 (s, 1H), 7.54 (d, $J = 8.4$ Hz, 1H), 6.95 (d, $J = 8.4$ Hz, 1H), 6.24 (s, 1H), 3.81 (s, 3H), 2.61 (s, 3H) ppm.

^{13}C NMR (75 MHz, CDCl_3): δ 191.6, 154.1, 146.0, 134.3, 131.4, 128.6, 113.2, 61.4, 12.1 ppm.

MS (EI, %): 166.01 (100, M^+), 151.00 (57), 123.01 (36), 77.02 (20).

HRMS (EI, m/z): calc. [M^+]: 166.0630; found: 166.0621 [M^+].

IR $\tilde{\nu}$ = 3239 (br, w), 2996 (vw), 2976 (vw), 2948 (vw), 2866 (vw), 2833 (vw), 2766 (vw), 1669 (s), 1585 (vs), 1491 (w), 1458 (vs), 1438 (w), 1410 (m), 1378 (vw), 1351 (vw), 1310 (vs), 1264 (w), 1212 (m), 1173 (vs), 1155 (vs), 1093 (m), 1031 (vw), 986 (m), 955 (vw), 879 (vw), 835 (vw), 821 (w), 783 (m), 764 (vw), 700 (vw), 664 (m) cm^{-1} .

5-bromo-4-hydroxy-3-methoxy-2-methylbenzaldehyde (167)

Bromine (1.5 ml, 4.5 g, 28 mmol, 1.2 eq.) was added to a solution of aldehyde **166** (3.91 g, 23.5 mmol) and NaOAc (2.32 g, 28.3 mmol, 1.2 eq.) in HOAc (66 ml) in a water bath. The water bath was removed and the resulting solution was stirred at rt for 8.5 h. The reaction mixture was poured onto ice water (290 ml) and subsequently filtered at 0 °C (Büchner funnel sintered glass por. 4) to obtain the title compound as a colorless solid (5.59 g, 97%) after drying under HV.

TLC $R_f = 0.24$ (20% EtOAc/hexanes).

m.p.: 157–160 °C.

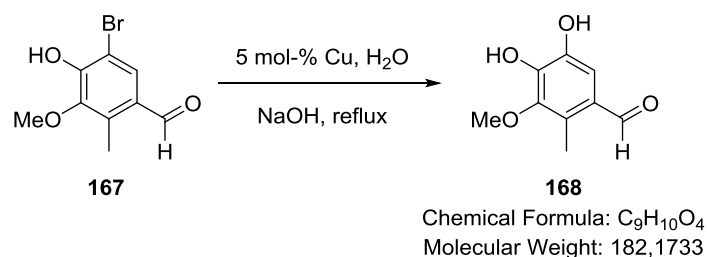
^1H NMR (600 MHz, CDCl_3): δ 10.04 (s, 1H), 7.76 (s, 1H), 6.36 (s, 1H), 3.84 (s, 3H), 2.57 (s, 3H) ppm.

^{13}C NMR (150 MHz, CDCl_3): δ 190.2, 151.4, 146.5, 133.9, 132.9, 129.0, 107.0, 61.3, 11.8 ppm.

MS (EI, %): 243.93 (100, M^+), 228.90 (64), 200.90 (32), 94.01 (22), 65.00 (35) Mass data only given for ^{79}Br containing compound.

HRMS (EI, m/z): calc. $[\text{M}^+]$: 243.9735; found: 243.9731 $[\text{M}^+]$.

IR $\tilde{\nu} = 3131$ (br, w), 3067 (w), 2992 (w), 2944 (w), 2881 (vw), 2794 (vw), 2639 (vw), 1657 (s), 1561 (s), 1505 (vw), 1456 (m), 1418 (s), 1377 (vw), 1300 (vs), 1248 (m), 1203 (vs), 1164 (vs), 1076 (m), 989 (vs), 894 (m), 827 (s), 781 (vw), 737 (w), 703 (m), 688 (w) cm^{-1} .

4,5-dihydroxy-3-methoxy-2-methylbenzaldehyde (168)

Bromide **167** (310 mg, 1.26 mmol) and NaOH (506 mg, 12.6 mmol, 10.0 eq.) were dissolved in H_2O (6.5 ml) and Cu powder (particle size 45 μm , 4 mg, 0.06 mmol, 0.05 eq.) was added. The resulting suspension was heated to reflux for 17 h, filtered and the pH of the resulting solution was

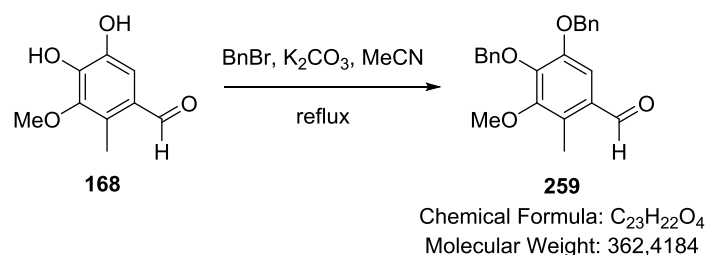
adjusted to pH = 7 with an aq. HCl solution (2 M). The aqueous phase was extracted with EtOAc (3x15 ml), the combined organic phases washed with aq. sat. Na₂H₂EDTA solution (50 ml), dried over Na₂SO₄ and concentrated under reduced pressure. The crude product was purified by flash column chromatography (12x2.5 cm, 50% EtOAc/hexanes) to afford the title compound as a brownish solid (173 mg, 75%).

The purity of the starting material proved to be crucial for the success of this reaction. Traces of residual bromine led to failure presumably due to oxidation of the copper catalyst. Larger scale reactions were conducted under inert gas atmosphere with deaerated water (nitrogen bubbling through H₂O for 20 min), higher catalyst loading (10 mol-%) and reflux for 47 h (58% product + 16% hydrodebrominated side product).

TLC	R _f = 0.21 (40% EtOAc/hexanes).
m.p.:	148–150 °C.
¹H NMR	(400 MHz, D ₃ COD): δ 10.01 (s, 1H), 7.09 (s, 1H), 3.76 (s, 3H), 2.48 (s, 3H) ppm.
¹³C NMR	(100 MHz, D ₃ COD): δ 192.9, 147.9, 146.5, 145.5, 128.3, 127.2, 114.7, 60.8, 10.7 ppm.
MS	(EI, %): 182.96 (100, M ⁺), 167.95 (31), 139.98 (36), 65.00 (30).
HRMS	(EI, m/z): calc. [M ⁺]: 182.0579; found: 182.0573 [M ⁺].
IR	$\tilde{\nu}$ = 3308 (br, m), 2940 (w), 2849 (vw), 2730 (vw), 1665 (s), 1587 (s), 1495 (m), 1465 (s), 1429 (w), 1411 (w), 1374 (m), 1366 (m), 1315 (vs), 1226 (s), 1194 (m), 1105 (vs), 1017 (w), 946 (w), 874 (vw), 761 (vw), 731 (w), 705 (w) cm ⁻¹ .

An alternative procedure was identified using a homogeneous Cu catalyst:

CuSO₄·5 H₂O (100 mg, 0.400 mmol, 0.02 eq.) was added to a solution of NaOH (8.06 g, 202 mmol, 10.0 eq.) in deaerated H₂O (81 ml) and the mixture was deaerated by passing a nitrogen stream through the solution for 30 min. The solution was gently heated to dissolve the copper salt and then cannulated onto bromide **167** (4.94 g, 20.2 mmol). The reaction mixture was heated to reflux for 16 h. After cooling to rt, the suspension was filtered and acidified with aq. HCl solution (*c* = 6 M). The aqueous phase was extracted with EtOAc (3x200 ml). The combined organic phases were dried over Na₂SO₄ and concentrated under reduced pressure. The crude product was dissolved in acetone (100 ml) and K₂CO₃ (5.86 g, 42.4 mmol, 2.1 eq.) and BnBr (5.03 ml, 7.25 g, 42.4 mmol, 2.1 eq.) were added. The reaction mixture was heated to reflux for 15 h and then cooled to rt. NEt₃ (1.0 ml) was added and the reaction mixture concentrated under reduced pressure. The residue was dissolved in EtOAc (100 ml), washed with aq. HCl solution (*c* = 1 M, 2x100 ml), dried over Na₂SO₄ and concentrated under reduced pressure. Purification of the crude product by flash column chromatography (5–9% EtOAc/hexanes) to afford the compound **259** as a colorless oil (5.41 g, 74%). For analytical data, see compound **259**.

4,5-bis(benzyloxy)-3-methoxy-2-methylbenzaldehyde (259)

Catechol **168** (1.32 g, 7.23 mmol) was dissolved in MeCN (36 ml) and BnBr (2.60 g, 1.49 ml, 15.2 mmol, 2.1 eq.) and K_2CO_3 (2.19 g, 15.9 mmol, 2.2 eq.) were subsequently added. The reaction mixture was heated to 85 °C for 16 h, filtered and concentrated under reduced pressure. The crude product could be used in the next step without further purification. An analytical sample was obtained after flash column chromatography (5–7–10% EtOAc/hexanes) as a yellow oil.

TLC R_f = 0.31 (10% EtOAc/hexanes).

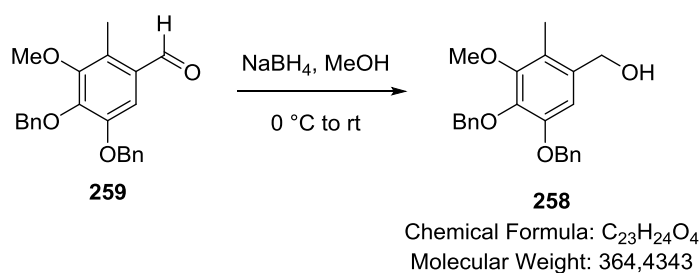
1H NMR (300 MHz, $CDCl_3$): δ 10.24 (s, 1H), 7.47–7.29 (m, 11H), 5.15 (s, 2H), 5.13 (s, 2H), 3.86 (s, 3H), 2.54 (s, 3H) ppm.

^{13}C NMR (75 MHz, $CDCl_3$): δ 190.9, 152.9, 151.1, 147.3, 137.4, 136.6, 129.9, 129.1, 128.7, 128.5, 128.5, 128.2, 127.7, 110.4, 75.4, 71.2, 61.1, 10.4 ppm. 1 aromatic C missing (overlapping)

MS (EI, %): 362.21 (2, M^+), 271.12 (8), 181.09 (12), 91.04 (100), 65.02 (6).

HRMS (EI, m/z): calc. [M^+]: 362.1518; found: 365.1518 [M^+].

IR $\tilde{\nu}$ = 3091 (vw), 3063 (vw), 3030 (vw), 2934 (vw), 2873 (vw), 2726 (vw), 1740 (vw), 1680 (s), 1589 (m), 1568 (w), 1497 (w), 1481 (m), 1452 (s), 1412 (w), 1376 (m), 1326 (vs), 1282 (s), 1240 (w), 1219 (w), 1199 (w), 1188 (w), 1118 (vs), 1079 (m), 1040 (s), 1028 (s), 1001 (m), 973 (m), 933 (w), 910 (w), 852 (w), 839 (w), 775 (w), 736 (s), 695 (vs) cm^{-1} .

(4,5-bis(benzyloxy)-3-methoxy-2-methylphenyl)methanol (258)

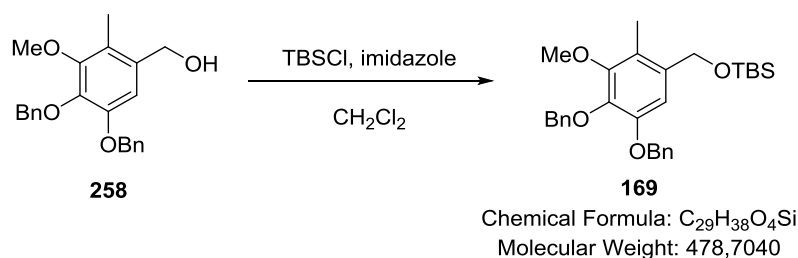
Benzaldehyde **259** (5.41 g, 14.9 mmol) was dissolved in EtOH (80 ml) and the solution cooled to 0 °C. $NaBH_4$ (845 mg, 22.4 mmol, 1.5 eq.) was introduced in 3 portions and the reaction mixture was

stirred at 0 °C for 2 h. The reaction mixture was treated with aq. phosphate buffer ($c = 1$ M, pH 5, 150 ml) and the aqueous phase was extracted with EtOAc (2x200 ml). The combined organic phases were washed with H₂O (200 ml) and brine (400 ml), dried over Na₂SO₄ and concentrated under reduced pressure. The product can be taken forward without further purification.

The crude product can be purified by flash column chromatography (12x4.5 cm, 1–1.5% MeOH/CH₂Cl₂) on 10.4 mmol scale to yield the title compound as a pale yellow solid (3.19 g, 84% over 2 steps from **168**).

TLC	$R_f = 0.11$ (20% EtOAc/hexanes).
m.p.:	50–52 °C.
¹H NMR	(600 MHz, CDCl₃): δ 7.48–7.45 (m, 2H), 7.45–7.42 (m, 2H), 7.39–7.35 (m, 2H), 7.35–7.29 (m, 4H), 5.09 (s, 2H), 5.04 (s, 2H), 4.64 (s, 2H), 3.86 (s, 3H), 2.21 (s, 3H), 1.56 (brs, 1H) ppm.
¹³C NMR	(150 MHz, CDCl₃): δ 152.7, 150.8, 141.6, 138.0, 137.3, 134.6, 128.6, 128.5, 128.4, 128.0, 127.6, 122.7, 109.5, 75.5, 71.3, 63.7, 61.0, 11.0 ppm. 1 aromatic C missing (overlapping).
MS	(EI, %): 364.15 (3, M ⁺), 273.08 (8), 227.06 (3), 195.04 (3), 91.03 (100).
HRMS	(EI, m/z): calc. [M ⁺]: 364.1675; found: 364.1673 [M ⁺].
IR	$\tilde{\nu} = 3396$ (br, vw), 3089 (vw), 3063 (vw), 3031 (vw), 2921 (w), 2850 (w), 1658 (vw), 1594 (vw), 1497 (w), 1487 (m), 1452 (s), 1411 (m), 1372 (m), 1324 (s), 1278 (w), 1223 (w), 1187 (w), 1113 (vs), 1079 (m), 1035 (s), 1027 (s), 1002 (s), 974 (s), 929 (w), 910 (w), 880 (w), 840 (w), 773 (vw), 734 (s), 694 (vs), 592 (w) cm ⁻¹ .

((4,5-bis(benzyloxy)-3-methoxy-2-methylbenzyl)oxy)(*tert*-butyl)dimethylsilane (169**)**

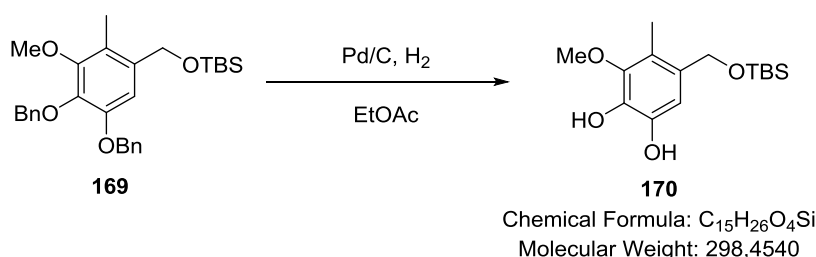


Benzyl alcohol **258** (431 mg, 1.18 mmol) was dissolved in CH₂Cl₂ (2.1 ml) and the solution was cooled to 0 °C. Imidazole (121 mg, 1.77 mmol, 1.5 eq.) and TBSCl (232 mg, 1.54 mmol, 1.3 eq.) were added and the reaction mixture was stirred for 2 h. H₂O (10 ml) was added and the aqueous phase was extracted with CH₂Cl₂ (3x20 ml). The combined organic phases were washed with brine, dried over Na₂SO₄ and concentrated under reduced pressure. The crude product was used directly in the following deprotection to catechol **170**.

An analytical sample was purified by flash column chromatography (5% EtOAc/hexanes) to afford the title compound as a colorless oil.

TLC	$R_f = 0.69$ (10% EtOAc/hexanes).
^1H NMR	(400 MHz, CD_2Cl_2): δ 7.49–7.27 (m, 10H), 6.91 (s, 1H), 5.10 (s, 2H), 5.02 (s, 2H), 4.63 (s, 2H), 3.82 (s, 3H), 2.10 (s, 3H), 0.95 (s, 9H), 0.10 (s, 6H) ppm. The compound shows rotamers in the ^1H NMR spectrum.
^{13}C NMR	(100 MHz, CD_2Cl_2): δ 152.6, 150.7, 140.9, 138.6, 137.9, 135.6, 128.8, 128.7, 128.6, 128.2, 128.1, 127.9, 121.7, 108.4, 75.5, 71.2, 63.5, 61.1, 26.1, 18.7, 10.6, –5.2 ppm.
HRMS	((+)-ESI, m/z): calc. $[\text{M}+\text{Na}^+]$: 501.2432; found: 501.2427 $[\text{M}+\text{Na}^+]$.
IR	$\tilde{\nu} = 3065$ (vw), 3031 (vw), 2952 (w), 2927 (w), 2881 (vw), 2855 (w), 1600 (vw), 1585 (vw), 1497 (w), 1486 (w), 1471 (w), 1452 (m), 1413 (w), 1371 (m), 1326 (m), 1252 (m), 1223 (w), 1188 (vw), 1116 (vs), 1055 (s), 1027 (s), 1004 (m), 937 (w), 910 (w), 834 (vs), 814 (m), 774 (vs), 732 (s), 694 (vs), 677 (m) cm^{-1} .

5-(((*tert*-butyldimethylsilyl)oxy)methyl)-3-methoxy-4-methylbenzene-1,2-diol (**170**)

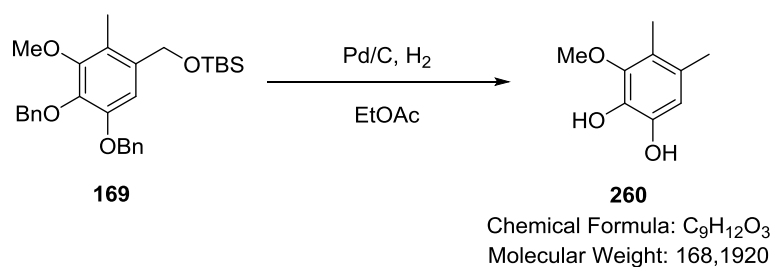


Crude TBS ether **169** was dissolved in EtOAc (9.5 ml) and Pd/C (10 wt-%, 63 mg, 0.059 mmol, 0.05 eq.) was added. The reaction vessel was evacuated and filled with hydrogen gas three times repetitively and stirred for 1.5 h. The reaction mixture was filtered over silica, the filter cake washed with EtOAc and the organic phase concentrated. Purification of the residue by flash column chromatography (12x2.5 cm, 20% EtOAc/hexanes) afforded the title compound as a colorless solid (333 mg, 94% over 2 steps).

TLC	$R_f = 0.22$ (20% EtOAc/hexanes).
m.p.:	117–118 °C.
^1H NMR	(400 MHz, $(\text{D}_3\text{C})_2\text{CO}$): δ 7.52 (brs, 1H), 7.44 (brs, 1H), 6.71 (s, 1H), 4.60 (s, 2H), 3.71 (s, 3H), 2.09 (s, 3H), 0.91 (s, 9H), 0.08 (s, 6H) ppm.
^{13}C NMR	(100 MHz, $(\text{D}_3\text{C})_2\text{CO}$): δ 147.3, 144.2, 137.7, 131.1, 120.1, 111.1, 64.1, 60.4, 26.3, 18.9, 10.8, –5.1 ppm.
HRMS	((–)-ESI, m/z): calc. $[\text{M}-\text{H}^-]$: 297.1522; found: 297.1524 $[\text{M}-\text{H}^-]$.

IR $\tilde{\nu}$ = 3458 (br, m), 3235 (br, m), 2950 (m), 2927 (m), 2876 (w), 2850 (m), 1605 (m), 1494 (s), 1470 (m), 1459 (m), 1383 (w), 1365 (w), 1309 (s), 1251 (m), 1217 (s), 1171 (s), 1129 (s), 1106 (s), 1056 (m), 1009 (m), 937 (m), 866 (s), 850 (s), 837 (vs), 778 (s) cm^{-1} .

3-methoxy-4,5-dimethylbenzene-1,2-diol (**260**)



TBS ether **169** (623 mg, 1.30 mmol) was dissolved in EtOAc (10.5 ml) and Pd/C (10 wt-%, 69 mg, 0.065 mmol, 0.05 eq.) was added. The reaction vessel was evacuated and filled with hydrogen gas four times repetitively and stirred for 15 h. The reaction mixture was filtered over Celite, the filter cake washed with EtOAc and the organic phase concentrated. Purification of the residue by flash column chromatography (dry load from acetone, 10x2.5 cm, 20% EtOAc/hexanes) afforded the title compound as a colorless solid (216 mg, 99%).

TLC R_f = 0.27 (20% EtOAc/hexanes).

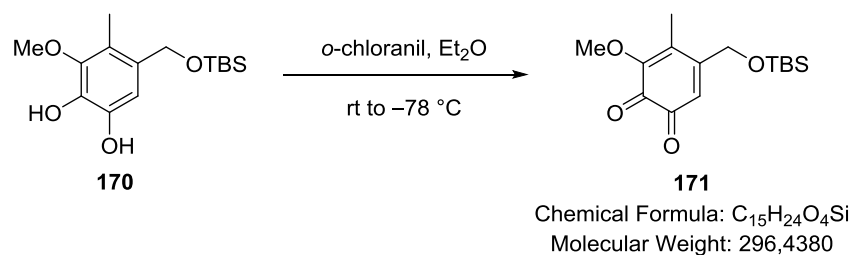
m.p.: 136–137 °C.

^1H NMR (400 MHz, CDCl_3): δ 6.55 (s, 1H), 5.35 (s, 1H), 5.11 (s, 1H), 3.77 (s, 3H), 2.16 (s, 3H), 2.12 (s, 3H) ppm.

^{13}C NMR (100 MHz, CDCl_3): δ 145.7, 141.8, 134.1, 128.9, 120.7, 112.7, 61.0, 19.6, 12.0 ppm.

HRMS ((–)-ESI, m/z): calc. $[\text{M}-\text{H}]^-$: 167.0708; found: 167.0711 $[\text{M}-\text{H}]^-$.

IR $\tilde{\nu}$ = 3453 (s), 3254 (br, m), 3010 (vw), 2967 (w), 2938 (vw), 1624 (vw), 1602 (w), 1498 (vs), 1470 (s), 1448 (m), 1426 (w), 1367 (s), 1301 (vs), 1243 (w), 1225 (w), 1194 (s), 1177 (s), 1099 (vs), 1087 (s), 1009 (vs), 933 (m), 874 (m), 868 (m), 778 (vw), 717 (w), 668 (vw) cm^{-1} .

5-(((*tert*-butyldimethylsilyl)oxy)methyl)-3-methoxy-4-methylcyclohexa-3,5-diene-1,2-dione (171)

Catechol **170** (150 mg, 0.503 mmol) was dissolved in Et₂O (9.5 ml) and *o*-chloranil (148 mg, 0.602 mmol, 1.2 eq.) was added. The reaction mixture was stirred for 1 min at rt and then cooled to -78°C . After stirring for 1 h, the suspension was filtered at -78°C with precooled glassware and the filter cake was washed with -78°C cold Et₂O to afford the product as a bronze solid (96 mg, 64%).

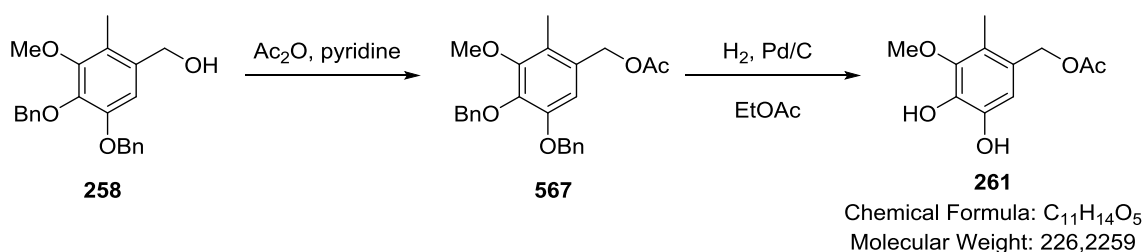
m.p.: 98–100 $^{\circ}\text{C}$

¹H NMR (400 MHz, (D₃C)₂CO): δ 6.32 (t, $J = 2.1$ Hz, 1H), 4.67 (d, $J = 2.1$ Hz, 2H), 3.81 (s, 3H), 2.03 (s, 3H), 0.96 (s, 9H), 0.16 (s, 6H) ppm.

¹³C NMR (100 MHz, (D₃C)₂CO): δ 179.9, 177.4, 157.9, 151.3, 134.1, 121.1, 63.1, 60.4, 26.2, 18.8, 10.7, -5.3 ppm.

HRMS ((+)-ESI, m/z): calc. [M+Na⁺]: 319.1336; found: 319.1335 [M+Na⁺]

IR $\tilde{\nu} = 2948$ (vw), 2926 (w), 2892 (vw), 2853 (w), 1675 (w), 1659 (m), 1621 (vw), 1603 (vw), 1563 (w), 1472 (w), 1460 (w), 1441 (w), 1396 (w), 1371 (vw), 1360 (vw), 1328 (m), 1299 (w), 1252 (m), 1227 (w), 1196 (w), 1177 (w), 1128 (m), 1049 (s), 1004 (m), 935 (w), 874 (m), 835 (vs), 816 (s), 792 (m), 776 (vs), 704 (w), 676 (w) cm⁻¹

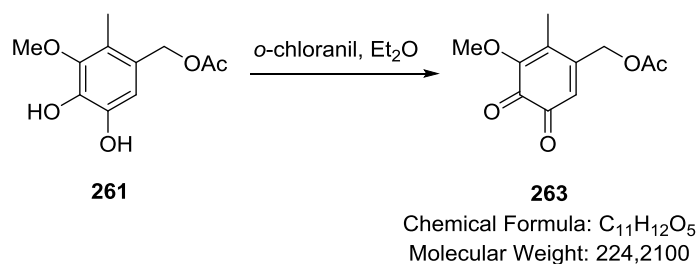
4,5-dihydroxy-3-methoxy-2-methylbenzyl acetate (261)

Benzyl alcohol **258** (1.0 g, 2.7 mmol) was dissolved in pyridine (14 ml) and Ac₂O (0.34 μl , 0.37 g, 3.6 mmol, 1.3 eq.) was added. The reaction mixture was stirred at rt for 25 h before aq. HCl solution (2 M, 30 ml) was added. The aqueous phase was extracted with EtOAc (2x100 ml), the combined organic phases were washed with aq. HCl solution (2 M, 2x100 ml), dried over Na₂SO₄ and concentrated under reduced pressure. The crude product **567** could be used without further purification.

TLC	$R_f = 0.56$ (20% EtOAc/hexanes)
^1H NMR	(400 MHz, CDCl_3): δ 7.48–7.30 (m, 10H), 6.78 (s, 1H), 5.08 (s, 2H), 5.04 (s, 2H), 5.04 (s, 2H), 3.86 (s, 3H), 2.21 (s, 3H), 2.10 (s, 3H) ppm.
^{13}C NMR	(100 MHz, CDCl_3): δ 171.1, 152.7, 150.7, 142.3, 137.9, 137.1, 129.6, 128.6, 128.5, 128.4, 128.0, 127.6, 124.2, 111.3, 75.4, 71.3, 65.0, 61.0, 21.2, 11.3 ppm. One C missing (overlapping).
MS	(EI, %): 406.14 (4, M^+), 315.06 (4), 245.05 (7), 181.04 (2), 91.02 (100), 65.01 (4).
HRMS	(EI, m/z): calc. [M^+]: 406.1780; found: 406.1778 [M^+].
IR	$\tilde{\nu} = 3031$ (vw), 2933 (vw), 2865 (vw), 1735 (s), 1599 (vw), 1583 (vw), 1490 (m), 1453 (m), 1414 (w), 1372 (m), 1359 (m), 1328 (s), 1226 (vs), 1115 (vs), 1079 (w), 1027 (s), 957 (m), 930 (w), 911 (w), 879 (vw), 834 (w), 735 (s), 695 (vs) cm^{-1} .

The crude product was dissolved in EtOAc (22 ml) and Pd/C (10 wt-%, 146 mg, 0.137 mmol, 0.05 eq.) was added. The reaction vessel was evacuated and filled with hydrogen gas for four times and the reaction mixture was stirred under hydrogen gas atmosphere for 3.5 h at rt. The reaction mixture was filtered over celite with EtOAc and the organic phase was concentrated under reduced pressure to afford the title compound as a pale green solid (623 mg, 100% over 2 steps).

TLC	$R_f = 0.63$ (60% EtOAc/hexanes).
m.p.:	98–100 °C.
^1H NMR	(400 MHz, THF-d_8): δ 7.73 (brs, 2H), 6.52 (s, 1H), 4.91 (s, 2H), 3.70 (s, 3H), 2.12 (s, 3H), 1.95 (s, 3H) ppm.
^{13}C NMR	(100 MHz, THF-d_8): δ 170.4, 147.6, 144.9, 139.2, 125.9, 121.6, 113.6, 65.2, 60.1, 20.6, 11.1 ppm.
MS	(EI, %): 226.03 (14, M^+), 167.02 (36), 166.01 (100), 151.00 (28), 123.01 (26), 42.90 (40).
HRMS	(EI, m/z): calc. [M^+]: 226.0841; found: 226.0826 [M^+].
IR	$\tilde{\nu} = 3390$ (br, w), 2940 (vw), 2839 (vw), 1709 (s), 1606 (w), 1501 (m), 1466 (m), 1432 (w), 1363 (s), 1299 (s), 1217 (vs), 1090 (vs), 1018 (vs), 941 (m), 859 (w), 677 (w) cm^{-1} .

(5-methoxy-6-methyl-3,4-dioxocyclohexa-1,5-dien-1-yl)methyl acetate (263)

Catechol **261** (171 mg, 0.756 mmol) was dissolved in Et₂O (14 ml) and *o*-chloranil (195 mg, 0.793 mmol, 1.05 eq.) was added. After 1 min, the reaction mixture was cooled to -78°C and stirred for 1 h. The reaction mixture was subsequently filtered (por 4 frit) at -78°C and the filter cake washed with -78°C cold Et₂O (2 ml) to afford the title compound as a red solid (117 mg, 69 %).

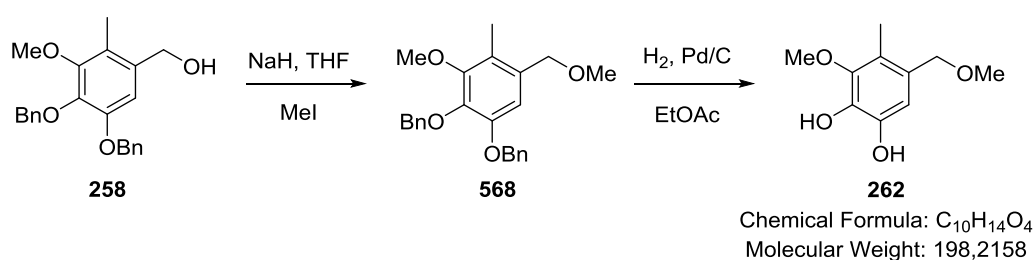
m.p.: 83–85 $^{\circ}\text{C}$.

¹H NMR (600 MHz, CDCl₃): δ 6.26 (s, 1H), 4.90 (s, 2H), 3.91 (s, 3H), 2.18 (s, 3H), 2.04 (s, 3H) ppm.

¹³C NMR (150 MHz, CDCl₃): δ 179.1, 176.2, 170.1, 151.4, 151.1, 132.6, 121.9, 62.6, 60.7, 20.9, 11.7 ppm.

HRMS (EI, *m/z*): calc. [M⁺]: 224.0685; found: 224.0661 [M⁺].

IR $\tilde{\nu}$ = 3636 (vw), 3460 (vw), 3326 (vw), 3004 (vw), 2941 (vw), 2847 (vw), 1745 (vs), 1683 (m), 1665 (vs), 1629 (vw), 1564 (w), 1442 (w), 1397 (w), 1370 (w), 1328 (m), 1304 (m), 1222 (vs), 1204 (s), 1137 (vw), 1113 (vw), 1095 (w), 1039 (vs), 1021 (m), 935 (w), 864 (vw), 793 (vw) cm⁻¹.

3-methoxy-5-(methoxymethyl)-4-methylbenzene-1,2-diol (262)

Alcohol **258** (252 mg, 0.692 mmol) was dissolved in THF (0.7 ml) and cooled to 0 $^{\circ}\text{C}$. NaH (60% dispersion in mineral oil, 42 mg, 1.0 mmol, 1.5 eq.) was subsequently added and the resulting suspension was stirred at rt for 30 min. The suspension was treated with MeI (65 μl , 150 mg, 1.0 mmol, 1.5 eq.) and stirred for 2 h before sat. aq. NH₄Cl solution (5 ml) was added. The aqueous phase was extracted with EtOAc (3x10 ml) and the combined organic phases were dried over Na₂SO₄ and

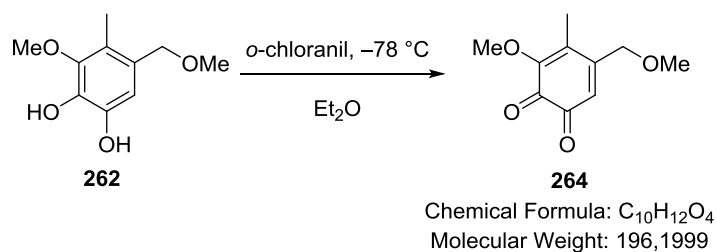
concentrated under reduced pressure. The crude product could be used in the next step without further purification.

TLC	$R_f = 0.34$ (10% EtOAc/hexanes).
^1H NMR	(600 MHz, CDCl_3): δ 7.48–7.45 (m, 2H), 7.45–7.42 (m, 2H), 7.39–7.35 (m, 2H), 7.34–7.29 (m, 4H), 6.81 (s, 1H) ppm.
^{13}C NMR	(150 MHz, CDCl_3): δ 152.6, 150.6, 141.6, 138.0, 137.3, 132.1, 128.6, 128.5, 128.4, 128.0, 127.7, 123.3, 110.4, 75.4, 73.1, 71.3, 61.0, 58.5, 11.0 ppm. One aromatic carbon missing (overlapping)
MS	(EI, %): 378.21 (4), 287.12 (9), 259.12 (4), 227.09 (6), 195.06 (3), 91.04 (100).
HRMS	(EI, m/z): calc. $[\text{M}^+]$: 378.1831; found: 378.1819 $[\text{M}^+]$.
IR	$\tilde{\nu} = 3092$ (vw), 3063 (vw), 3031 (vw), 2925 (w), 2870 (w), 2820 (vw), 1599 (w), 1584 (vw), 1497 (m), 1488 (m), 1452 (s), 1412 (w), 1373 (m), 1327 (s), 1237 (w), 1227 (w), 1188 (w), 1115 (vs), 1078 (s), 1041 (m), 1028 (m), 1008 (m), 977 (w), 930 (w), 910 (w), 841 (w), 735 (m), 696 (s) cm^{-1} .

The crude product was dissolved in EtOAc (5.3 ml) and Pd/C (10 wt-%, 37 mg, 0.035 mmol, 0.05 eq.) was added. The reaction vessel was evacuated and filled with hydrogen gas three times and the suspension was stirred under hydrogen atmosphere for 6.5 h. The reaction mixture was filtered over celite with EtOAc and the filtrate was concentrated under reduced pressure. The crude product was purified by flash column chromatography (11x2.5 cm, 30–40% EtOAc/hexanes) to afford the title compound as a pale brown solid (115 mg, 84%).

The product slowly oxidizes to the corresponding *o*-quinone in solution under air. The *o*-quinone then redoxisomerizes to a catechol with benzaldehyde functionality presumably with air moisture or wet solvents.

TLC	$R_f = 0.18$ (30% EtOAc/hexanes).
m.p.:	81–83 °C.
^1H NMR	(300 MHz, CDCl_3): δ 6.70 (s, 1H), 5.49 (s, 1H), 5.20 (s, 1H), 4.33 (s, 2H), 3.78 (s, 3H), 3.37 (s, 3H), 2.20 (s, 3H) ppm.
^{13}C NMR	(150 MHz, CDCl_3): δ 146.0, 141.9, 136.0, 128.5, 121.6, 112.7, 73.1, 61.0, 58.1, 11.2 ppm.
MS	(EI, %): 198.07 (62, M^+), 167.05 (76), 166.04 (100), 151.03 (34), 123.03 (27).
HRMS	(EI, m/z): calc. $[\text{M}^+]$: 198.0892; found: 198.0876 $[\text{M}^+]$.
IR	$\tilde{\nu} = 3345$ (br, w), 2922 (m), 2850 (w), 1605 (w), 1500 (m), 1464 (m), 1376 (m), 1362 (m), 1303 (s), 1219 (s), 1190 (m), 1091 (vs), 1066 (vs), 1016 (m), 900 (w), 882 (w), 855 (w), 759 (vw), 729 (w), 688 (w) cm^{-1} .

3-methoxy-5-(methoxymethyl)-4-methylcyclohexa-3,5-diene-1,2-dione (264)

Catechol **262** (110 mg, 0.555 mmol) was dissolved in Et₂O (10 ml) and *o*-chloranil (136 mg, 0.555 mmol, 1.0 eq.) was added at room temperature. The reaction was stirred for 1 h at $-78\text{ }^\circ\text{C}$ and subsequently filtered with the help of a Buchner funnel at $-78\text{ }^\circ\text{C}$. The remaining solid was washed with $-78\text{ }^\circ\text{C}$ cold Et₂O (4 ml) and the title compound was obtained as a bronze solid (80 mg, 74%).

TLC $R_f = 0.18$ (20% EtOAc/hexanes).

m.p.: $98\text{--}100\text{ }^\circ\text{C}$ (decomposition).

¹H NMR (600 MHz, CDCl₃): δ 6.34 (s, 1H), 4.21 (d, $J = 1.9\text{ Hz}$, 2H), 3.88 (s, 3H), 3.46 (s, 3H), 2.01 (s, 3H) ppm.

¹³C NMR (150 MHz, CDCl₃): δ 179.5, 176.5, 153.6, 150.9, 133.7, 122.3, 71.8, 60.6, 59.1, 11.4 ppm.

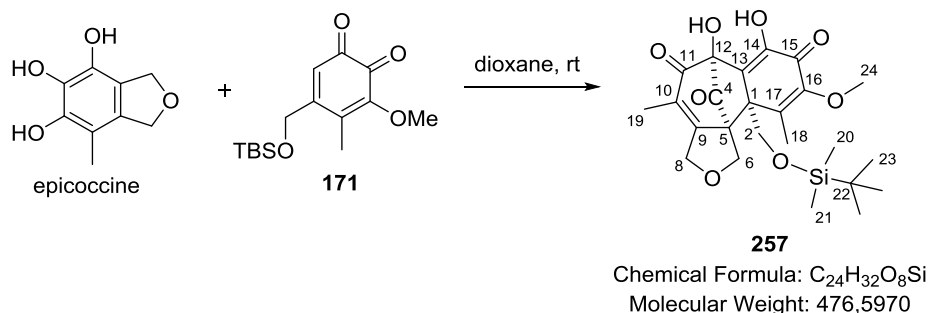
The sample proved to be unstable in solution, possibly undergoing decomposition pathways via its *p*-quinone methide.

MS (EI, %): 196.05 (20, M⁺), 166.04 (20), 149.02 (22), 125.08 (18), 97.08 (30), 84.99 (68), 82.98 (100), 71.08 (42), 57.01 (69), 43.88 (86).

HRMS (EI, m/z): calc. [M⁺]: 196.0736; found: 196.0729 [M⁺].

IR $\tilde{\nu} = 3001$ (br, vw), 3001 (vw), 2945 (vw), 2916 (w), 2848 (vw), 1738 (vw), 1681 (m), 1659 (vs), 1624 (vw), 1561 (w), 1470 (w), 1434 (w), 1403 (w), 1385 (vw), 1333 (s), 1304 (w), 1240 (vw), 1200 (w), 1133 (w), 1112 (vw), 1069 (s), 1017 (w), 980 (vw), 932 (w), 871 (vw), 856 (w), 810 (vw), 793 (vw), 755 (vw), 719 (vw), 673 (vw) cm⁻¹.

***rac*-(6*S*,10*aS*,10*bR*)-10*a*-(((*tert*-butyldimethylsilyl)oxy)methyl)-6,7-dihydroxy-9-methoxy-4,10-dimethyl-1*H*,3*H*-6,10*b*-methanobenzo[3,4]cyclohepta[1,2-*c*]furan-5,8,11(6*H*,10*aH*)-trione (257)**



Quinone **171** (49 mg, 0.17 mmol, 2.0 eq.) was dissolved in dioxane (0.1 ml) and epicoccine (15 mg, 0.083 mmol) in dioxane (0.1 ml) was added at rt. The reaction mixture was stirred for 12 h and then concentrated under reduced pressure. The crude product was purified by HPLC (40–90% MeCN/H₂O + 0.15% FA, 45 min, 20ml/min, *R*_t = 25.7 min) to afford the title compound as a waxy solid (8 mg, 19%).

The title compound can also be synthesized using a procedure described for the preparation of acetate **267**. The crude product can then be used without further purification.

TLC *R*_f = 0.34 (5% MeOH/CH₂Cl₂).

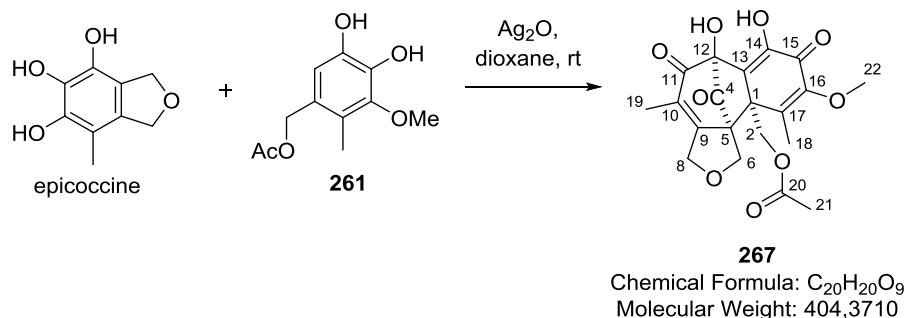
¹H NMR (600 MHz, CDCl₃): δ 6.45 (brs, 1H, C₁₄OH), 4.69 (dd, *J* = 17.3, 1.5 Hz, 1H, C₈H), 4.61 (dd, *J* = 17.3, 1.5 Hz, 1H, C₈H), 4.58 (d, *J* = 10.7 Hz, 1H, C₆H), 4.51 (d, *J* = 10.7 Hz, 1H, C₆H), 4.35 (brs, 1H, C₁₂OH), 3.87 (d, *J* = 9.6 Hz, 1H, C₂H), 3.75 (s, 3H, C₂₄H₃), 3.68 (d, *J* = 9.6 Hz, 1H, C₂H), 2.18 (s, 3H, C₈H₃), 1.76 (s, 3H, C₁₉H₃), 0.83 (s, 9H, 3×C₂₃H₃), 0.04 (s, 3H, C₂₀H₃ or C₂₁H₃), 0.01 (s, 3H, C₂₀H₃ or C₂₁H₃) ppm.

¹³C NMR (150 MHz, CDCl₃): δ 195.0 (C4), 188.5 (C11), 177.3 (C15), 159.9 (C9), 151.8 (C16), 146.8 (C14), 143.7 (C17), 128.0 (C10), 124.3 (C13), 88.8 (C12), 71.0 (C2), 69.6 (C8), 66.7 (C6), 64.1 (C5), 60.2 (C24), 56.8 (C1), 25.9 (3×C₂₃), 18.5 (C22), 12.7 (C19), 12.4 (C18), −5.7 (C20/C21), −5.8 (C20/C21) ppm.

HRMS ((+)-ESI, *m/z*): calc. [M+Na⁺]: 499.1759; found: 499.1764 [M+Na⁺].

IR $\tilde{\nu}$ = 3410 (w), 2927 (s), 2856 (m), 1782 (s), 1738 (w), 1691 (s), 1644 (s), 1548 (vw), 1463 (w), 1452 (w), 1376 (w), 1290 (m), 1251 (s), 1154 (m), 1101 (vs), 1006 (w), 940 (w), 838 (vs), 782 (w), 699 (w) cm^{−1}.

***rac*-((6*S*,10*aS*,10*bR*)-6,7-dihydroxy-9-methoxy-4,10-dimethyl-5,8,11-trioxo-3,5,6,8-tetrahydro-1*H*,10*aH*-6,10*b*-methanobenzo[3,4]cyclohepta[1,2-*c*]furan-10*a*-yl)methyl acetate (**267**)**

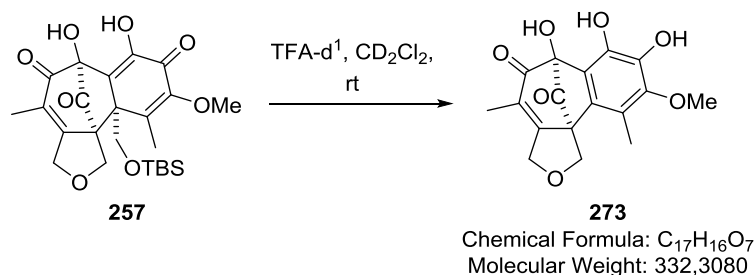


Catechol **261** (38 mg, 0.17 mmol) was dissolved in dioxane (0.5 ml) and epicoccine (31 mg, 0.17 mmol, 1.0 eq.) was added in small portions over 3.5 h. The crude product was purified by flash column chromatography on reverse-phase silica (10–20–30–40% MeCN/H₂O + 0.1% FA). The product-containing fractions were extracted with EtOAc (2x) and the combined organic phases were washed with brine and concentrated under reduced pressure to afford the title compound as a colorless solid (34 mg, 50%). X-Ray suitable crystals were obtained by slow diffusion of hexanes into a solution of the title compound in EtOAc.

The crude product can also be taken forward without further purification.

LC/MS	$R_t = 2.738$ min (10–90% MeCN/H ₂ O + 0.1% FA, 7 min, 2 ml/min).
m.p.:	205–215 °C (gradual decomposition).
¹H NMR	(800 MHz, (D₃C)₂CO): δ 8.28 (s, 1H, OH, C ₁₄ OH), 5.24 (s, 1H, OH, C ₁₂ OH), 4.88 (d, $J = 17.5$ Hz, 1H, C ₈ H), 4.73–4.69 (m, 2H, C ₆ H, C ₈ H), 4.42 (d, $J = 11.0$ Hz, 1H, C ₆ H), 4.39 (d, $J = 11.1$ Hz, 1H, C ₂ H), 4.36 (d, $J = 11.1$ Hz, 1H, C ₂ H), 3.68 (s, 3H, C ₂₂ H ₃), 2.21 (s, 3H, C ₁₈ H ₃), 1.92 (s, 3H, C ₂₁ H ₃), 1.73 (s, 3H, C ₁₉ H ₃) ppm.
¹³C NMR	(200 MHz, (D₃C)₂CO): δ 197.0 (C4), 189.3 (C11), 178.1 (C15), 169.8 (C20), 159.6 (C9), 153.1 (C16), 149.1 (C14), 142.2 (C17), 129.2 (C10), 123.7 (C13), 89.9 (C12), 69.9 (C8), 68.1 (C2), 66.8 (C6), 65.4 (C5), 60.0 (C22), 55.0 (C1), 20.5 (C21), 12.3 (C19), 12.1 (C18) ppm.
MS	(EI, %): 404.08 (6, M ⁺), 334.11 (14), 275.13 (32), 193.12 (26), 181.09 (32), 153.13 (42), 123.14 (20), 69.12 (28), 60.13 (42), 45.12 (51), 43.14 (100).
HRMS	(EI, m/z): calc. [M ⁺]: 404.1107; found: 404.1101 [M ⁺]
IR	$\tilde{\nu} = 3369$ (w), 2926 (w), 2849 (vw), 1782 (s), 1739 (s), 1694 (vs), 1652 (vs), 1604 (w), 1455 (w), 1378 (m), 1291 (s), 1224 (vs), 1149 (m), 1100 (vs), 1049 (s), 1002 (m), 961 (w), 942 (w), 909 (m), 879 (w), 802 (vw), 767 (vw), 729 (m), 687 (vw) cm ⁻¹ .

***rac*-(6*S*,10*bS*)-6,7,8-trihydroxy-9-methoxy-4,10-dimethyl-1*H*,3*H*-6,10*b*-methanobenzo[3,4]cyclohepta[1,2-*c*]furan-5,11(6*H*)-dione (**273**)**

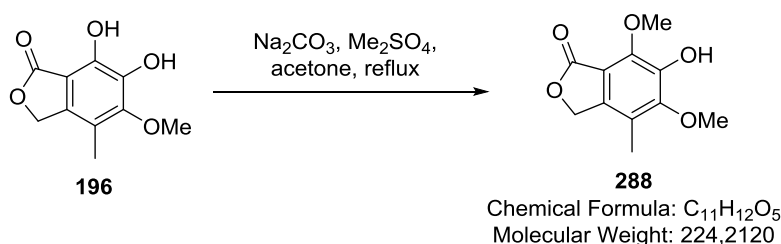


TBS ether **257** was dissolved in CD_2Cl_2 (0.6 ml) and the solution treated with TFA-d^1 (3 drops). The product formed instantaneously as judged by NMR analysis.

^1H NMR (600 MHz, CD_2Cl_2): δ 5.03 (dq, $J = 17.5, 1.4$ Hz, 1H), 4.82 (d, $J = 10.6$ Hz, 1H), 4.79 (dq, $J = 17.5, 1.5$ Hz, 1H), 4.69 (d, $J = 10.6$ Hz, 1H), 3.85 (s, 3H), 2.34 (s, 3H), 1.76 (s, 3H) ppm.

HRMS ((+)-ESI, m/z): calc. $[\text{M}+\text{Na}^+]$: 355.0788; found: 355.0794 $[\text{M}+\text{Na}^+]$.

6-hydroxy-5,7-dimethoxy-4-methylisobenzofuran-1(3*H*)-one (288**)**



Catechol **196** (50 mg, 0.24 mmol) was dissolved in acetone (1.0 ml) and Na_2CO_3 (31 mg, 0.29 mmol, 1.2 eq.) and Me_2SO_4 (25 μl , 33 mg, 0.26 mmol, 1.1 eq.) were added. The suspension was heated to 60 $^\circ\text{C}$ and stirred for 5 h. After stirring at rt overnight, the reaction mixture was diluted with EtOAc and washed with aq. HCl solution ($c = 1$ M). The organic phase was dried over Na_2SO_4 and concentrated under reduced pressure. The crude product was purified by flash column chromatography (25–29% EtOAc/hexanes) to afford the title compound as a colorless solid.

TLC $R_f = 0.12$ (25% EtOAc/hexanes).

m.p.: 119–120 $^\circ\text{C}$.

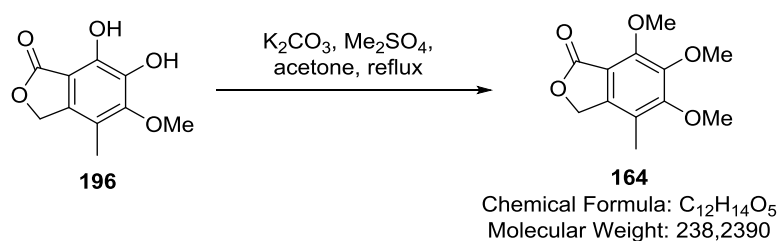
^1H NMR (300 MHz, CDCl_3): δ 5.96 (s, 1H), 5.10 (s, 2H), 4.17 (s, 3H), 3.95 (s, 3H), 2.14 (s, 3H) ppm.

^{13}C NMR (75 MHz, CDCl_3): δ 169.1, 151.3, 144.2, 141.9, 138.2, 119.9, 111.2, 68.6, 63.0, 60.7, 11.3 ppm.

HRMS (EI, m/z): calc. $[\text{M}^+]$: 225.0757; found: 225.0756 $[\text{M}^+]$.

IR $\tilde{\nu}$ = 3390 (br, w), 2941 (vw), 2840 (vw), 1737 (vs), 1614 (w), 1486 (s), 1454 (m), 1435 (m), 1362 (m), 1318 (vs), 1233 (s), 1195 (m), 1136 (s), 1115 (m), 1083 (w), 1033 (vs), 1015 (s), 995 (s), 962 (s), 930 (m), 844 (w), 789 (vw), 756 (vw), 737 (vw), 717 (vw) cm^{-1} .

5,6,7-trimethoxy-4-methylisobenzofuran-1(3H)-one (164)



Catechol **196** (195 mg, 0.928 mmol) was dissolved in acetone (5.0 ml) and K_2CO_3 (450 mg, 3.26 mmol, 3.5 eq.) and Me_2SO_4 (0.26 ml, 0.35 g, 2.8 mmol, 3.0 eq.) were added. The reaction mixture was heated to reflux for 2 h, before H_2O (15 ml) was added. The aqueous phase was extracted with EtOAc (3x20 ml). The combined organic phases were dried over Na_2SO_4 and concentrated under reduced pressure. The crude product was purified by flash column chromatography (9–25% EtOAc/hexanes) to afford the title compound as a colorless solid (175 mg, 79%).

TLC R_f = 0.24 (25% EtOAc/hexanes).

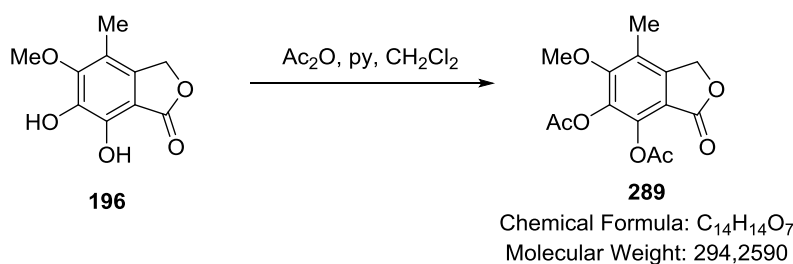
m.p.: 48–50 °C.

^1H NMR (300 MHz, CDCl_3): δ 5.09 (s, 2H), 4.10 (s, 3H), 3.95 (s, 3H), 3.89 (s, 3H), 2.12 (s, 3H) ppm.

^{13}C NMR (75 MHz, CDCl_3): δ 169.0, 157.8, 151.5, 146.1, 142.2, 120.2, 112.5, 68.2, 62.6, 61.5, 61.0, 11.3 ppm.

HRMS ((+)-ESI, m/z): calc. 239.0914 $[\text{M}+\text{H}^+]$; ; found: 239.0913 $[\text{M}+\text{H}^+]$.

IR $\tilde{\nu}$ = 2942 (vw), 1754 (vs), 1597 (w), 1481 (m), 1455 (m), 1423 (m), 1400 (w), 1355 (s), 1336 (vs), 1284 (m), 1199 (w), 1135 (s), 1115 (w), 1087 (vw), 1043 (s), 1028 (s), 1002 (w), 977 (m), 962 (m), 907 (vw), 851 (vw), 796 (vw), 764 (vw), 734 (vw), 715 (vw) cm^{-1} .

6-methoxy-7-methyl-3-oxo-1,3-dihydroisobenzofuran-4,5-diyl diacetate (289)

The aim of the experiment was to achieve selective monoacetylation.

Catechol **196** (42 mg, 0.20 mmol) was dissolved in CH₂Cl₂ (1.0 ml) and pyridine (32 µl, 32 mg, 0.40 mmol, 2.0 eq.) and acetic anhydride (21 µl, 22 mg, 0.22 mmol, 1.1 eq.) were added. The reaction mixture was stirred for 15 h before pH 7.2 aq. phosphate buffer (*c* = 1 M, 5 ml) was introduced. The aqueous phase was extracted with EtOAc (3x10 ml). The combined organic phases were dried over Na₂SO₄ and concentrated under reduced pressure. Purification by preparative TLC (40% EtOAc/hexanes) afforded the title compound as a colorless solid (17 mg, 29%) next to monoacetylated starting material.

TLC R_f = 0.37 (40% EtOAc/hexanes).

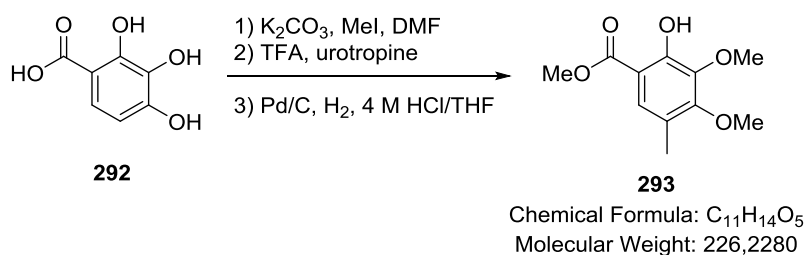
m.p.: 192–194 °C.

¹H NMR (400 MHz, CDCl₃): δ 5.16 (s, 2H), 3.87 (s, 3H), 2.39 (s, 3H), 2.37 (s, 3H), 2.21 (s, 3H) ppm.

¹³C NMR (100 MHz, CDCl₃): δ 168.1, 168.0, 167.8, 156.5, 144.7, 139.8, 137.1, 123.9, 113.9, 68.5, 61.4, 20.5, 20.5, 11.7 ppm.

HRMS (EI, *m/z*): calc. [M⁺]: 294.0740; found: 294.0742 [M⁺].

IR ν̃ = 2987 (vw), 2940 (vw), 2858 (vw), 1767 (vs), 1616 (vw), 1483 (w), 1454 (w), 1363 (m), 1337 (m), 1196 (vs), 1177 (vs), 1139 (w), 1103 (w), 1083 (w), 1036 (m), 1017 (w), 968 (m), 950 (w), 893 (w), 846 (vw), 787 (vw), 760 (vw) cm⁻¹.

methyl 2-hydroxy-3,4-dimethoxy-5-methylbenzoate (293)

To a suspension of acid **292** (1.99 g, 11.7 mmol) and K₂CO₃ (6.49 g, 47.0 mmol, 4.0 eq.) in DMF (45 mL) was added methyl iodide (4.40 mL, 70.7 mmol, 6.0 eq.). The resulting mixture was stirred at

room temperature for 24 hours. The reaction mixture was adjusted to pH 3 with aq. HCl ($c = 1$ M). After extraction with EtOAc (2x200 mL), the organic layer was dried over Na₂SO₄, filtered and concentrated under reduced pressure to afford the crude title compound. The crude product could be purified by flash column chromatography (17% EtOAc:petroleum ether) to give a mixture of trimethyl and tetramethylated starting material. An analytical sample was obtained by preparative TLC (15% EtOAc/hexanes).

TLC	$R_f = 0.26$ (10% EtOAc/hexanes).
¹H NMR	(400 MHz, CDCl₃): δ 10.91 (s, 1H), 7.60 (d, $J = 9.0$ Hz, 1H), 6.49 (d, $J = 9.0$ Hz, 1H), 3.93 (s, 3H), 3.92 (s, 3H), 3.89 (s, 3H) ppm.
¹³C NMR	(100 MHz, CDCl₃): δ 170.6, 158.2, 156.1, 136.6, 125.9, 107.2, 103.3, 60.9, 56.2, 52.3 ppm.
MS	(EI, %): 212.15 (71, M ⁺), 180.13 (100), 152.14 (96), 137.13 (50), 120.13 (29), 109.14 (20), 69.15 (22).
HRMS	(EI, m/z): calc. [M ⁺]: 212.0685; found: 212.0676 [M ⁺].
IR	$\tilde{\nu} = 3092$ (vw), 2992 (vw), 2942 (vw), 2841 (vw), 1721 (m), 1704 (w), 1672 (m), 1615 (vw), 1592 (m), 1505 (w), 1494 (w), 1462 (m), 1431 (m), 1410 (m), 1331 (w), 1278 (vs), 1238 (m), 1215 (s), 1190 (m), 1147 (m), 1137 (m), 1092 (vs), 1031 (vs), 1013 (s), 983 (m), 948 (w), 922 (w), 871 (w), 819 (vw), 796 (m), 785 (s), 747 (s), 703 (w) cm ⁻¹ .

A mixture of tetra- and trimethylated acid **292** (1.05 g, max. 4.94 mmol of desired trimethylated acid **292**) was dissolved in TFA (19.8 ml) and urotropine (1.39 g, 9.88 mmol, 2.0 eq.) was added. The solution was heated to 80 °C for 15 h before water (75 ml) was added. The suspension was stirred for 1.5 h at 50 °C before the precipitate was separated by centrifugation (10000 rpm, 10 min). The solid was washed with sat. aq. NaHCO₃ solution (20 ml) and centrifuged off (11000 rpm, 15 min). The combined aqueous phases were extracted with CH₂Cl₂ (2x150 ml) and the combined organic phases were washed with sat. aq. NaHCO₃ solution (200 ml). The organic phase was dried over Na₂SO₄ and concentrated under reduced pressure to afford a crude product that was used in the next step. An analytical sample was obtained by preparative TLC (40% EtOAc/hexanes).

TLC	$R_f = 0.50$ (20% EtOAc/hexanes).
¹H NMR	(400 MHz, CDCl₃): δ 11.53 (s, 1H), 10.23 (s, 1H), 8.19 (s, 1H), 4.16 (s, 3H), 3.97 (s, 3H), 3.93 (s, 3H) ppm.
¹³C NMR	(100 MHz, CDCl₃): δ 188.3, 170.4, 161.8, 160.4, 140.0, 126.2, 121.4, 109.1, 62.2, 61.1, 52.8 ppm.
MS	(EI, %): 240.17 (75, M ⁺), 208.13 (99), 180.12 (100), 165.08 (41), 150.09 (29), 69.02 (15).
HRMS	(EI, m/z): calc. [M ⁺]: 240.0634; found: 240.0639 [M ⁺].

IR $\tilde{\nu}$ = 3071 (vw), 3002 (vw), 2941 (vw), 2881 (vw), 2844 (vw), 1671 (vs), 1602 (w), 1578 (m), 1558 (vw), 1506 (vw), 1481 (w), 1447 (m), 1424 (m), 1352 (s), 1304 (m), 1272 (w), 1231 (m), 1212 (m), 1197 (w), 1174 (w), 1094 (s), 1055 (m), 1000 (m), 959 (w), 917 (w), 890 (vw), 798 (w), 774 (w), 749 (vw), 727 (w) cm^{-1} .

The crude product was dissolved in THF (29 ml) and aq. HCl solution ($c = 4 \text{ M}$, 22 ml). Palladium on activated charcoal (10 wt-%, 502 mg, 0.471 mmol, 0.1 eq.) was added and the reaction vessel was purged with hydrogen gas by successive evacuation and filling with hydrogen. The reaction mixture was stirred for 14 h and more Pd/C (200 mg, 0.19 mmol, 0.04 eq.) was added after the reaction vessel had been flushed with nitrogen gas. The reaction mixture was purged with hydrogen gas according to the above procedure and stirred for 6 h. Filtration over a silica gel plug with 30% EtOAc/hexanes, extraction of the aqueous layer with EtOAc (2x100 ml), drying of the combined organic phases over Na_2SO_4 and concentration under reduced pressure gave a residue that was purified by column chromatography (12x4.5 cm, 10% EtOAc/hexanes) to afford the title compound as a colorless oil (500 mg, 19% over 3 steps).

TLC $R_f = 0.77$ (20% EtOAc/hexanes).

^1H NMR (400 MHz, CDCl_3): δ 10.79 (s, 1H), 7.39 (s, 1H), 3.96 (s, 1H), 3.92 (s, 1H), 3.89 (s, 3H), 2.16 (s, 3H) ppm.

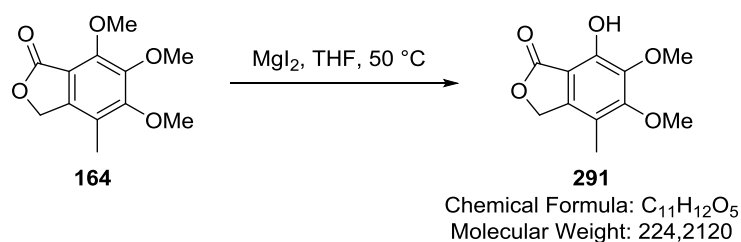
^{13}C NMR (100 MHz, CDCl_3): δ 170.7, 157.1, 155.2, 140.6, 125.5, 122.2, 108.1, 60.9, 60.7, 52.3, 15.9 ppm.

MS (EI, %): 226.19 (89, M^+), 194.15 (100), 166.13 (84), 151.10 (43), 136.10 (36), 123.08 (11), 69.02 (15).

HRMS (EI, m/z): calc. [M^+]: 226.0841; found: 226.0840 [M^+].

IR $\tilde{\nu}$ = 3129 (vw), 2992 (vw), 2952 (vw), 2952 (vw), 2844 (vw), 1699 (w), 1669 (s), 1652 (w), 1616 (w), 1558 (w), 1539 (w), 1506 (w), 1486 (w), 1471 (w), 1456 (m), 1441 (m), 1418 (w), 1345 (vs), 1273 (m), 1239 (m), 1212 (s), 1172 (w), 1100 (w), 1067 (m), 1003 (w), 966 (w), 927 (vw), 797 (w), 763 (vw), 725 (vw), 667 (vw) cm^{-1} .

7-hydroxy-5,6-dimethoxy-4-methylisobenzofuran-1(3H)-one (**291**)



Lactone **164** (44 mg, 0.18 mmol) was dissolved in THF (1.8 ml) and MgI_2 (77 mg, 0.27 mmol, 1.5 eq.) was added. The reaction mixture was heated to 50 °C and stirred for 1 h. An aq. HCl solution

($c = 2$ M, 2 ml) and an aq. sat. $\text{Na}_2\text{S}_2\text{O}_3$ solution (5 ml) were added and the aqueous phase extracted with EtOAc (3x 10 ml). The combined organic phases were dried over Na_2SO_4 and concentrated under reduced pressure. Purification by flash column chromatography (9–17–33% EtOAc/hexanes) afforded the title compound as a yellow solid (13 mg, 31%) next to unreacted starting material (8 mg). X-Ray suitable crystals were obtained by crystallization from EtOAc.

TLC $R_f = 0.60$ (50% EtOAc/hexanes).

m.p.: 122–124 °C.

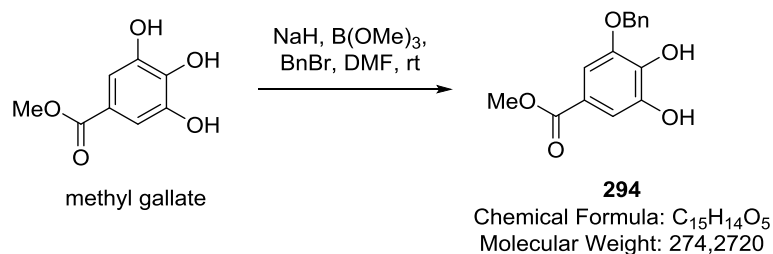
^1H NMR (400 MHz, CDCl_3): δ 7.39 (s, 1H), 5.18 (s, 2H), 3.95 (s, 3H), 3.93 (s, 3H), 2.10 (s, 3H) ppm.

^{13}C NMR (100 MHz, CDCl_3): δ 172.5, 158.2, 148.2, 140.4, 140.0, 117.2, 106.6, 69.9, 61.1, 61.1, 11.5 ppm.

HRMS ((–)-ESI, m/z): calc. $[\text{M} - \text{H}]^-$: 223.0612; found: 223.0610 $[\text{M} - \text{H}]^-$.

IR $\tilde{\nu} = 3401$ (br, w), 2958 (vw), 2865 (vw), 1757 (vs), 1615 (w), 1485 (w), 1470 (w), 1456 (w), 1436 (w), 1371 (s), 1314 (vw), 1287 (s), 1233 (w), 1196 (vw), 1131 (m), 1084 (vw), 1040 (m), 1012 (w), 995 (w), 958 (w), 932 (w), 836 (vw), 790 (vw), 762 (vw), 718 (vw) cm^{-1} .

methyl 3-(benzyloxy)-4,5-dihydroxybenzoate (**294**)



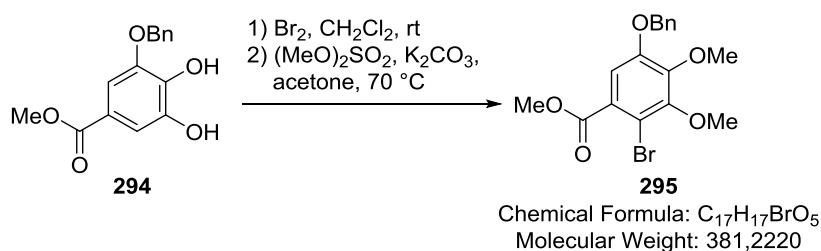
Methyl gallate (5.00 g, 27.2 mmol) was dissolved in DMF (150 ml) and the solution cooled to 10 °C. NaH (2.17 g, 54.4 mmol, 2.0 eq.) was added in portions and the reaction mixture was allowed to warm to rt. B(OMe)_3 (3.03 ml, 2.82 g, 27.2 mmol, 1.0 eq.) was added and the solution treated with a solution of BnBr (3.23 ml, 4.64 g, 27.2 mmol, 1.0 eq.) in DMF (50 ml) over the course of 1 h. The reaction mixture was stirred for 12 h and poured onto ice and aq. HCl solution ($c = 1$ M, 100 ml) and then extracted with EtOAc (3x200 ml). The combined organic phases were washed with brine (3x50 ml), dried over Na_2SO_4 and concentrated under reduced pressure. The residue was dissolved in EtOAc (200 ml) and again washed with brine (5x50 ml), then dried over Na_2SO_4 and concentrated under reduced pressure. The crude product was purified by recrystallization from toluene and afterwards recrystallization from benzene to afford the title compound as a colorless solid (4.26 g, 57%).

The compound is literature-known.^[219]

¹H NMR (400 MHz, (D₃C)₂CO): δ 8.50–7.94 (brm, 2H), 7.54–7.49 (m, 2H), 7.43–7.31 (m, 3H), 7.28–7.20 (m, 2H), 5.18 (s, 2H), 3.80 (s, 3H) ppm.

¹³C NMR (100 MHz, (D₃C)₂CO): δ 166.5, 151.9, 151.6, 146.8, 136.2, 128.8, 128.4, 127.6, 127.5, 112.2, 110.1, 71.4, 61.4, 61.2, 52.7 ppm.

methyl 5-(benzyloxy)-2-bromo-3,4-dimethoxybenzoate (295)



Catechol **294** (2.38 g, 8.66 mmol) was dissolved in CH₂Cl₂ (30 ml) and cooled to 0 °C. Bromine (0.49 ml, 1.5 g, 9.5 mmol, 1.1 eq.) was added and the reaction allowed to warm to rt. After stirring for 3 h, pH 7.2 aq. phosphate buffer (*c* = 1 M, 10 ml) and sat. aq. NaHCO₃, aq. sat. Na₂S₂O₃ and aq. sat. Na₂CO₃ solution (5:1:1, 70 ml) were added. The aqueous phase was extracted with CH₂Cl₂ (5x50 ml). The combined organic phases were dried over Na₂SO₄ and concentrated under reduced pressure. The crude product was dissolved in acetone (30 ml) and K₂CO₃ (4.32 g, 31.3 mmol, 3.5 eq.) and Me₂SO₄ (2.5 ml, 3.3 g, 26 mmol, 3.0 eq.) were introduced. The reaction mixture was heated to reflux for 40 min, before NEt₃ and H₂O (1:1, 40 ml) were added. The aqueous phase was extracted with EtOAc (3x50 ml). The combined organic phases were dried over Na₂SO₄ and concentrated under reduced pressure. Purification of the residue by flash column chromatography (2–4% EtOAc/hexanes) afforded the title compound as a colorless oil (1.62 g, 49% over 2 steps).

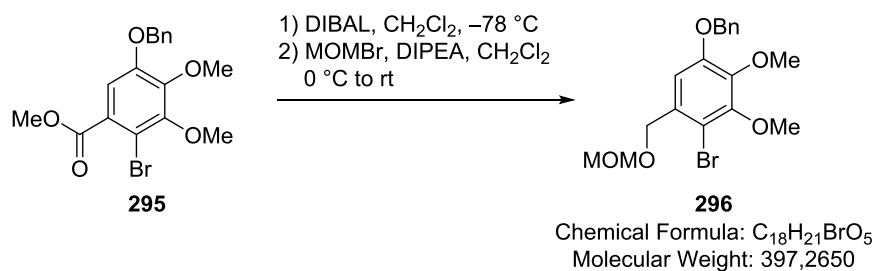
TLC R_f = 0.50 (17% EtOAc/hexanes).

¹H NMR (400 MHz, CDCl₃): δ 7.35–7.45 (m, 5H), 7.25 (s, 1H), 5.12 (s, 2H), 3.94 (s, 3H), 3.91 (s, 3H), 3.90 (s, 3H) ppm.

¹³C NMR (100 MHz, CDCl₃): δ 166.5, 151.9, 151.6, 146.8, 136.2, 128.8, 128.4, 127.6, 127.5, 112.2, 110.1, 71.4, 61.4, 61.2, 52.7 ppm.

HRMS ((+)-ESI, *m/z*): calc. [M+H⁺]: 381.0332; found: 381.0329 [M+H⁺].

IR $\tilde{\nu}$ = 3036 (vw), 3004 (vw), 2940 (vw), 1857 (vw), 1732 (s), 1570 (vw), 1550 (vw), 1498 (vw), 1482 (m), 1451 (w), 1428 (m), 1385 (s), 1338 (vs), 1260 (w), 1218 (s), 1190 (w), 1173 (w), 1159 (w), 1097 (s), 1028 (w), 1006 (m), 947 (vw), 904 (vw), 848 (vw), 819 (vw), 778 (vw), 741 (w), 698 (w) cm⁻¹.

1-(benzyloxy)-4-bromo-2,3-dimethoxy-5-((methoxymethoxy)methyl)benzene (296)

Bromide **295** (1.57 g, 4.12 mmol) was dissolved in CH₂Cl₂ (20 ml) and cooled to -78 °C. The solution was treated with a solution of DIBAL in toluene (*c* = 1 M, 10 ml, 10 mmol, 2.4 eq.) and the reaction stirred for 25 min. EtOAc (1 ml) was introduced slowly before an aq. sat. Rochelle salt solution was added. The aqueous phase was extracted with EtOAc (3x30 ml) and the combined organic phases were dried over Na₂SO₄. Concentration under reduced pressure gave the crude product, which was pure enough for further transformations. An analytical sample was obtained by flash column chromatographic purification (5–9–17% EtOAc/hexanes).

TLC R_f = 0.20 (17% EtOAc/hexanes).

¹H NMR (400 MHz, CDCl₃): δ 7.45–7.31 (m, 5H), 6.95 (s, 1H), 5.13 (s, 2H), 4.68 (d, *J* = 8.0 Hz, 2H), 3.91 (s, 3H), 3.90 (s, 3H), 1.97 (t, *J* = 8.0 Hz, 1H) ppm.

¹³C NMR (100 MHz, CDCl₃): δ 152.2, 151.2, 143.1, 136.7, 135.4, 129.2, 128.8, 128.4, 128.2, 127.5, 109.7, 109.0, 71.2, 65.3, 61.3, 61.3 ppm.

HRMS ((-)-ESI, *m/z*): calc. [M+HCOO⁻]: 397.0292; found: 397.0292 [M+HCOO⁻].

IR $\tilde{\nu}$ = 3412 (br, w), 2937 (w), 1569 (w), 1498 (w), 1481 (s), 1449 (m), 1429 (m), 1400 (vs), 1356 (w), 1330 (vs), 1242 (w), 1189 (w), 1163 (m), 1099 (vs), 1075 (s), 1009 (vs), 928 (w), 843 (w), 810 (w), 738 (w), 698 (m) cm⁻¹.

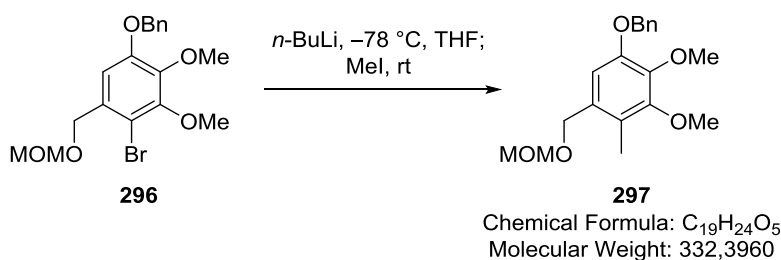
The crude product was dissolved in CH₂Cl₂ (8.0 ml) and MOMBr (0.50 ml, 0.79 g, 6.2 mmol, 1.5 eq.) and DIPEA (2.2 ml, 1.6 g, 12 mmol, 3.0 eq.) were added at 0 °C. The reaction mixture was allowed to warm to rt and stirred for 18 h. H₂O (15 ml) was introduced and the aqueous phase extracted with CH₂Cl₂ (3x20 ml). The combined organic phases were dried over Na₂SO₄ and concentrated under reduced pressure. Purification of the crude product by flash column chromatography (2–5% EtOAc/hexanes) yielded the title compound as a colorless oil (1.39 g, 85% over 2 steps).

TLC R_f = 0.50 (17% EtOAc/hexanes).

¹H NMR (400 MHz, CDCl₃): δ 7.31–7.45 (m, 5H), 6.94 (s, 1H), 5.13 (s, 2H), 4.72 (s, 2H), 4.60 (s, 2H), 3.91 (s, 3H), 3.90 (s, 3H), 3.40 (s, 3H) ppm.

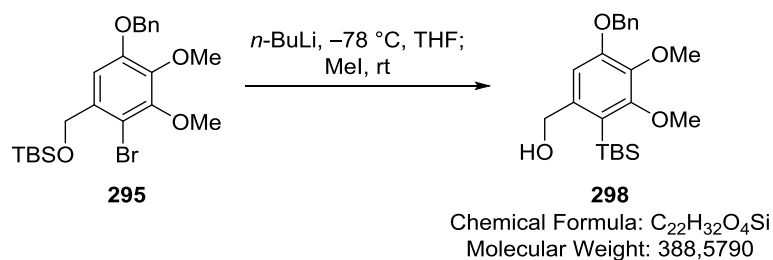
^{13}C NMR	(100 MHz, CDCl_3): δ 152.0, 151.2, 143.1, 136.8, 133.0, 128.7, 128.2, 127.5, 110.1, 109.5, 96.2, 71.2, 69.0, 61.3, 61.2, 55.7 ppm.
HRMS	((+)-ESI, m/z): calc. $[\text{M}-\text{MOMO}^+]$: 335.0277; found: 335.0275 $[\text{M}-\text{MOMO}^+]$.
IR	$\tilde{\nu}$ = 2936 (w), 2885 (w), 2824 (vw), 1570 (w), 1498 (w), 1482 (m), 1453 (w), 1430 (w), 1397 (m), 1375 (m), 1333 (m), 1242 (w), 1212 (w), 1190 (w), 1165 (m), 1150 (s), 1101 (vs), 1063 (s), 1034 (s), 1010 (s), 924 (w), 841 (vw), 814 (vw), 739 (w), 699 (w) cm^{-1} .

1-(benzyloxy)-2,3-dimethoxy-5-((methoxymethoxy)methyl)-4-methylbenzene (297)



Bromide **296** (1.39 g, 3.50 mmol) was dissolved in THF (7.0 ml) and the solution cooled to -78°C . A solution of *n*-BuLi in hexanes ($c = 2.4$ M, 1.6 ml, 3.85 mmol, 1.1 eq.) was added and the reaction mixture stirred for 40 min. MeI (1.10 ml, 2.51 g, 17.7 mmol, 5.0 eq.) was introduced and the reaction mixture was allowed to warm to rt. After 30 min, aq. sat. NH_4Cl solution (5 ml) was added and the aqueous phase was extracted with EtOAc (3x30 ml). The combined organic phases were dried over Na_2SO_4 and concentrated under reduced pressure. Purification of the crude product by flash column chromatography (2–5% EtOAc/hexanes) afforded the title compound as a colorless oil (1.05 g, 90%).

TLC	$R_f = 0.50$ (17% EtOAc/hexanes).
^1H NMR	(400 MHz, CDCl_3): δ 7.52–7.29 (m, 5H), 6.79 (s, 1H), 5.11 (s, 2H), 4.69 (s, 2H), 4.50 (s, 2H), 3.89 (s, 3H), 3.85 (s, 3H), 3.40 (s, 3H), 2.18 (s, 3H) ppm.
^{13}C NMR	(100 MHz, CDCl_3): δ 152.3, 150.4, 142.7, 137.3, 131.4, 128.7, 128.0, 127.5, 123.5, 110.7, 96.0, 71.2, 67.7, 61.1, 60.9, 55.6, 11.1 ppm.
HRMS	((+)-ESI, m/z): calc. $[\text{M}-\text{MOMO}^+]$: 271.1329; found: 271.1326 $[\text{M}-\text{MOMO}^+]$.
IR	$\tilde{\nu}$ = 2937 (w), 2885 (w), 1601 (vw), 1492 (m), 1454 (m), 1410 (w), 1377 (w), 1329 (m), 1242 (w), 1191 (vw), 1149 (m), 1121 (vs), 1041 (vs), 921 (w), 839 (w), 839 (vw), 737 (w), 698 (w) cm^{-1} .

(5-(benzyloxy)-2-(*tert*-butyldimethylsilyl)-3,4-dimethoxyphenyl)methanol (298**)**

Bromide **295** (34 mg, 0.073 mmol) was dissolved in THF (0.7 ml) and the solution cooled to -78°C . A solution of *n*-BuLi in hexanes ($c = 2.4\text{ M}$, 35 μl , 0.081 mmol, 1.1 eq.) was added and the reaction mixture stirred for 1 h. MeI (40 μl , 89 mg, 0.63 mmol, 8.6 eq.) was introduced and the reaction mixture was allowed to warm to rt. After 20 min, aq. sat. NH_4Cl solution (5 ml) was added and the aqueous phase was extracted with EtOAc (3x10 ml). The combined organic phases were dried over Na_2SO_4 and concentrated under reduced pressure. Purification of the crude product by flash column chromatography (2–5–9% EtOAc/hexanes) afforded the title compound as a colorless oil (19 mg, 66%).

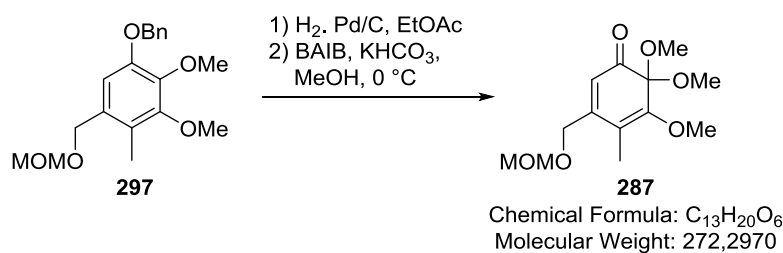
TLC $R_f = 0.30$ (17% EtOAc/hexanes).

^1H NMR (400 MHz, CDCl_3): δ 7.49–7.30 (m, 5H), 6.98 (s, 1H), 5.14 (s, 2H), 4.64 (s, 2H), 3.87 (s, 3H), 3.83 (s, 3H), 0.90 (s, 9H), 0.36 (s, 6H) ppm.

^{13}C NMR (100 MHz, CDCl_3): δ 159.4, 154.0, 143.1, 140.8, 137.1, 128.7, 128.1, 127.5, 120.1, 109.0, 70.7, 65.7, 60.8, 60.5, 27.4, 18.5, 0.1 ppm.

HRMS ((+)-ESI, m/z): calc. $[\text{M}+\text{H}^+]$: 389.2143; found: 389.2140 $[\text{M}+\text{H}^+]$.

IR $\tilde{\nu} = 3416$ (br, vw), 2951 (m), 2930 (m), 2884 (w), 2855 (m), 1583 (m), 1561 (w), 1498 (vw), 1471 (m), 1463 (m), 1431 (w), 1386 (m), 1371 (m), 1310 (s), 1258 (w), 1249 (w), 1189 (w), 1164 (w), 1101 (vs), 1073 (m), 1021 (m), 925 (vw), 842 (m), 827 (s), 803 (m), 779 (w), 738 (w), 697 (m), 676 (w) cm^{-1} .

5,6,6-trimethoxy-3-((methoxymethoxy)methyl)-4-methylcyclohexa-2,4-dien-1-one (287**)**

Benzyl ether **297** (129 mg, 0.387 mmol) was dissolved in EtOAc (4.0 ml) and Pd on activated charcoal (10 wt-%, 13 mg, 0.012 mmol, 3 mol-%) was added. The vessel was purged 3x with

hydrogen gas and stirred for 1 h. A stream of nitrogen was passed through the solution. Since the starting material was not entirely consumed, more Pd on activated charcoal (10 wt-%, 26 mg, 0.024 mmol, 6 mol-%) was added and the vessel purged with hydrogen gas (3x). After stirring for an additional 1 h, the suspension was filtered over celite and the organic phase concentrated under reduced pressure.

The crude product was dissolved in MeOH (2 ml) and the solution cooled to 0 °C. KHCO_3 (102 mg, 1.02 mmol, 2.6 eq.) and $\text{PhI}(\text{OAc})_2$ (137 mg, 0.425 mmol, 1.1 eq.) were added and the reaction mixture stirred for 20 min. Sat. aq. NaHCO_3 solution (7 ml) was introduced and the aqueous phase extracted with EtOAc (3x10 ml). The combined organic phases were dried over Na_2SO_4 and concentrated under reduced pressure. Purification by flash column chromatography (2–5–9% EtOAc/hexanes) afforded the title compound as a yellow oil (83 mg, 79% over 2 steps).

TLC $R_f = 0.35$ (17% EtOAc/hexanes).

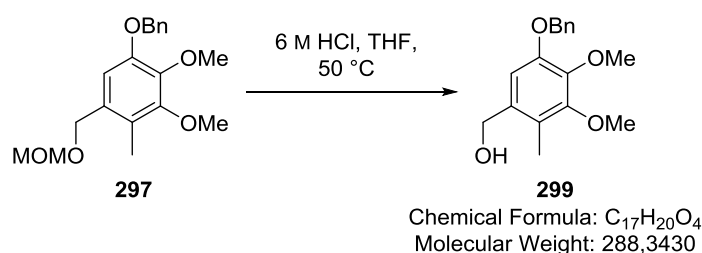
^1H NMR (400 MHz, CDCl_3): δ 6.08 (s, 1H), 4.71 (s, 2H), 4.32 (s, 2H), 3.96 (s, 3H), 3.39 (s, 3H), 3.28 (s, 6H), 1.82 (s, 3H) ppm.

^{13}C NMR (100 MHz, CDCl_3): δ 194.1, 156.6, 155.4, 116.6, 115.5, 96.3, 94.6, 66.6, 59.8, 59.7, 55.8, 51.0, 9.9 ppm.

HRMS ((+)-ESI, m/z): calc. $[\text{M}+\text{Na}^+]$: 295.1152; found: 295.1149 $[\text{M}+\text{Na}^+]$.

IR $\tilde{\nu} = 2992$ (vw), 2947 (w), 2897 (vw), 2834 (vw), 1673 (m), 1649 (w), 1566 (w), 1463 (vw), 1450 (vw), 1408 (vw), 1381 (vw), 1335 (vw), 1290 (w), 1265 (vw), 1206 (w), 1151 (m), 1079 (s), 1043 (vs), 995 (w), 985 (w), 920 (vw), 849 (vw), 704 (vw) cm^{-1} .

(5-(benzyloxy)-3,4-dimethoxy-2-methylphenyl)methanol (**299**)

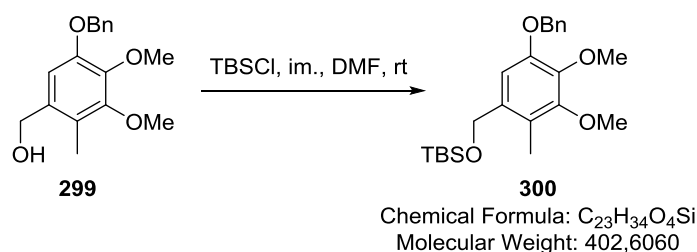


MOM ether **297** (349 mg, 0.879 mmol) was dissolved in THF (3.0 ml) and conc. HCl (0.1 ml) was added. The solution was heated to 50 °C and stirred for 50 min. pH 7.2 Phosphate buffer ($c = 1\text{ M}$, 2 ml) and H_2O (5 ml) was added and the aqueous phase extracted with EtOAc (3x10 ml). The combined organic phases were dried over Na_2SO_4 and concentrated under reduced pressure. Purification by flash column chromatography (9–25% EtOAc/hexanes) afforded the title compound as a colorless oil (148 mg, 58%).

TLC $R_f = 0.25$ (20% EtOAc/hexanes).

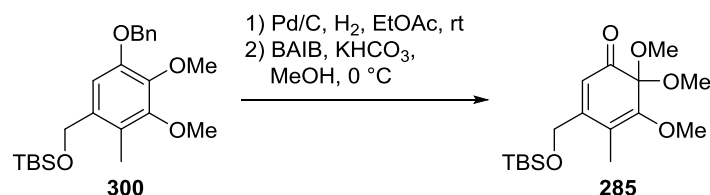
¹H NMR	(400 MHz, CDCl₃): δ 7.47–7.30 (m, 5H), 6.82 (s, 1H), 5.12 (s, 2H), 4.62 (s, 2H), 3.90 (s, 3H), 3.85 (s, 3H), 2.19 (s, 3H) ppm.
¹³C NMR	(100 MHz, CDCl₃): δ 152.4, 150.5, 142.6, 137.3, 134.3, 128.7, 128.0, 127.5, 122.7, 109.6, 71.2, 63.7, 61.1, 60.9, 10.9 ppm.
HRMS	((+)-ESI, m/z): calc. [M–HO ⁺]: 271.1329; found: 271.1327 [M–HO ⁺]
IR	$\tilde{\nu}$ = 3412 (vw), 2934 (w), 2860 (w), 1603 (vw), 1583 (vw), 1490 (m), 1454 (m), 1408 (m), 1377 (w), 1327 (s), 1280 (vw), 1241 (w), 1191 (w), 1115 (vs), 1048 (s), 1030 (m), 1006 (m), 982 (w), 926 (vw), 908 (vw), 837 (w), 808 (vw), 777 (vw), 737 (w), 698 (w) cm ^{–1} .

((5-(benzyloxy)-3,4-dimethoxy-2-methylbenzyl)oxy)(*tert*-butyl)dimethylsilane (300)



Alcohol **299** (146 mg, 0.508 mmol) was dissolved in DMF (2.5 ml) and imidazole (76 mg, 1.1 mmol, 2.2 eq.) and TBSCl (84 mg, 0.56 mmol, 1.1 eq.) were added. The reaction mixture was stirred for 30 min, before H₂O (10 ml) was introduced. The aqueous phase was extracted with EtOAc (2x10 ml). The combined organic phases were dried over Na₂SO₄ and concentrated under reduced pressure. Purification by flash column chromatography (1% EtOAc/hexanes) afforded the title compound as a colorless oil (170 mg, 83%).

TLC	R _f = 0.90 (20% EtOAc/hexanes).
¹H NMR	(400 MHz, CDCl₃): δ 7.46–7.30 (m, 5H), 6.89 (s, 1H), 5.12 (s, 2H), 4.60 (s, 2H), 3.89 (s, 3H), 3.84 (s, 3H), 2.08 (s, 3H), 0.93 (s, 9H), 0.07 (s, 6H) ppm.
¹³C NMR	(100 MHz, CDCl₃): δ 151.9, 150.3, 141.6, 137.5, 134.9, 128.6, 127.9, 127.3, 121.1, 108.1, 71.0, 63.1, 61.1, 61.0, 26.1, 18.5, 10.5, –5.2 ppm.
HRMS	((+)-ESI, m/z): calc. [M+Na ⁺]: 425.2119; found: 425.2121 [M+Na ⁺].
IR	$\tilde{\nu}$ = 2950 (m), 2932 (m), 2881 (w), 2857 (w), 1602 (vw), 1583 (vw), 1490 (m), 1455 (m), 1409 (w), 1374 (w), 1328 (m), 1255 (w), 1190 (vw), 1119 (vs), 1060 (s), 1030 (w), 1003 (w), 937 (vw), 927 (vw), 838 (s), 813 (vw), 777 (m), 735 (w), 696 (w) cm ^{–1} .

3-(((*tert*-butyldimethylsilyl)oxy)methyl)-5,6,6-trimethoxy-4-methylcyclohexa-2,4-dien-1-one (285)


Benzyl ether **300** (50 mg, 0.124 mmol) was dissolved in EtOAc (1.0 ml) and Pd on activated charcoal (10 wt-%, 5 mg, 0.005 mmol, 4 mol-%) was added. The vessel was purged 3x with hydrogen gas and stirred for 3 h. The suspension was filtered over celite and the organic phase concentrated under reduced pressure.

TLC $R_f = 0.70$ (20% EtOAc/hexanes).

¹H NMR (400 MHz, CDCl₃): δ 6.84 (s, 1H), 5.54 (s, 1H), 4.59 (s, 2H), 3.90 (s, 3H), 3.80 (s, 3H), 2.08 (s, 3H), 0.94 (s, 9H), 0.10 (s, 6H) ppm.

¹³C NMR (100 MHz, CDCl₃): δ 150.7, 147.0, 138.6, 135.8, 120.1, 109.0, 63.2, 61.0, 60.4, 26.1, 18.6, 10.4, -5.2 ppm.

HRMS ((-)-ESI, *m/z*): calc. [M+HCOO⁻]: 357.1739; found: 357.1734 [M+HCOO⁻].

IR $\tilde{\nu} = 3418$ (br, vw), 2955 (m), 2931 (m), 2892 (w), 2857 (w), 1591 (w), 1488 (m), 1470 (m), 1464 (m), 1375 (w), 1348 (w), 1307 (w), 1256 (m), 1217 (w), 1188 (w), 1168 (w), 1106 (vs), 1058 (s), 1022 (m), 1003 (w), 944 (w), 850 (s), 837 (vs), 813 (w), 776 (m), 674 (vw) cm⁻¹.

The crude product was dissolved in MeOH (0.6 ml) and the solution cooled to 0 °C. KHCO₃ (37 mg, 0.37 mmol, 3.0 eq.) and PhI(OAc)₂ (44 mg, 0.14 mmol, 1.1 eq.) were added and the reaction mixture stirred for 30 min. Sat. aq. NaHCO₃ solution (4 ml) was introduced and the aqueous phase extracted with EtOAc (3x10 ml). The combined organic phases were dried over Na₂SO₄ and concentrated under reduced pressure. Purification by flash column chromatography (1–3% EtOAc/hexanes) afforded the title compound as a yellow oil (83 mg, 79% over 2 steps).

TLC $R_f = 0.60$ (20% EtOAc/hexanes).

¹H NMR (400 MHz, CDCl₃): δ 6.13 (s, 1H), 4.42 (s, 2H), 3.96 (s, 3H), 3.28 (s, 6H), 1.79 (s, 3H), 0.93 (s, 9H), 0.10 (s, 6H) ppm.

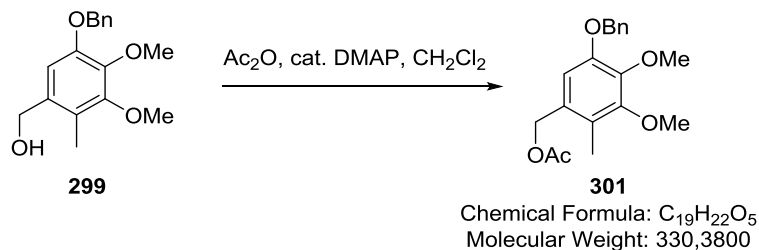
¹³C NMR (100 MHz, CDCl₃): δ 194.1, 159.9, 155.1, 115.9, 115.3, 94.7, 62.8, 59.8, 51.0, 26.0, 18.5, 9.5, -5.3 ppm.

HRMS ((+)-ESI, *m/z*): calc. [M+Na⁺]: 365.1755; found: 365.1754 [M+Na⁺].

IR $\tilde{\nu} = 2950$ (w), 2932 (w), 2857 (w), 1742 (vw), 1673 (m), 1569 (w), 1463 (w), 1446 (vw), 1388 (vw), 1359 (vw), 1328 (vw), 1290 (w), 1258 (w), 1203 (w), 1180 (w),

1154 (w), 1135 (w), 1077 (s), 1056 (vs), 1006 (w), 982 (vw), 840 (s), 813 (vw), 779 (m), 692 (vw) cm^{-1} .

5-(benzyloxy)-3,4-dimethoxy-2-methylbenzyl acetate (**301**)



Alcohol **299** (43 mg, 0.15 mmol) was dissolved in CH_2Cl_2 (1.5 ml) and acetic anhydride (20 μl , 22 mg, 0.21 mmol, 1.5 eq.) and DMAP (2 mg, 0.02 mmol, 0.1 eq.) were added. After stirring for 15 min, the reaction mixture was concentrated under reduced pressure. Purification by flash column chromatography (33% EtOAc/hexanes) afforded the title compound as colorless oil (48 mg, quant.).

TLC $R_f = 0.70$ (20% EtOAc/hexanes).

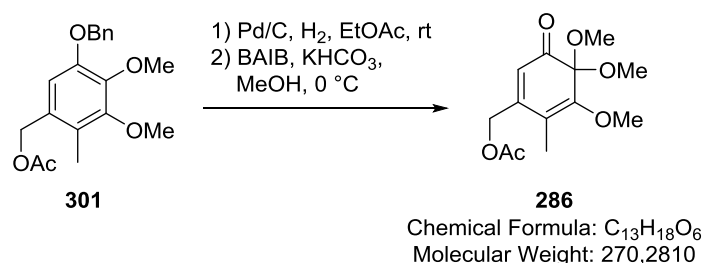
^1H NMR (400 MHz, CDCl_3): δ 7.46–7.30 (m, 5H), 6.74 (s, 1H), 5.10 (s, 2H), 5.02 (s, 2H), 3.90 (s, 3H), 3.85 (s, 3H), 2.18 (s, 3H), 2.08 (s, 3H) ppm.

^{13}C NMR (100 MHz, CDCl_3): δ 171.1, 152.4, 150.4, 143.2, 137.2, 129.3, 128.7, 128.0, 127.5, 124.2, 111.4, 71.3, 65.0, 61.1, 60.9, 21.1, 11.3 ppm.

HRMS ((+)-ESI, m/z): calc. $[\text{M}+\text{Na}^+]$: 353.1359; found: 353.1359 $[\text{M}+\text{Na}^+]$.

IR $\tilde{\nu} = 3066$ (vw), 3029 (vw), 2936 (vw), 2865 (vw), 2828 (vw), 1738 (vs), 1585 (vw), 1493 (m), 1454 (m), 1410 (w), 1373 (w), 1361 (w), 1329 (m), 1234 (vs), 1191 (w), 1116 (vs), 1047 (m), 1027 (m), 982 (w), 952 (w), 927 (vw), 739 (w), 698 (w) cm^{-1} .

(4,4,5-trimethoxy-6-methyl-3-oxocyclohexa-1,5-dien-1-yl)methyl acetate (**286**)



Benzyl ether **301** (44 mg, 0.14 mmol) was dissolved in EtOAc (1.3 ml) and Pd on activated charcoal (10 wt-%, 5 mg, 0.005 mmol, 4 mol-%) was added. The vessel was purged 3x with hydrogen gas and stirred for 30 min. The reaction mixture was filtered over celite and concentrated under reduced pressure.

The crude product was dissolved in MeOH (1.3 ml) and the solution cooled to 0 °C. KHCO_3 (34 mg, 0.37 mmol, 2.5 eq.) and $\text{PhI}(\text{OAc})_2$ (47 mg, 0.14 mmol, 1.1 eq.) were added and the reaction mixture stirred for 15 min. H_2O (5 ml) was introduced and the aqueous phase extracted with EtOAc (3x10 ml). The combined organic phases were dried over Na_2SO_4 and concentrated under reduced pressure. Purification by flash column chromatography (9–17% EtOAc/hexanes) afforded the title compound as a yellow oil (22 mg, 60% over 2 steps).

TLC $R_f = 0.50$ (20% EtOAc/hexanes).

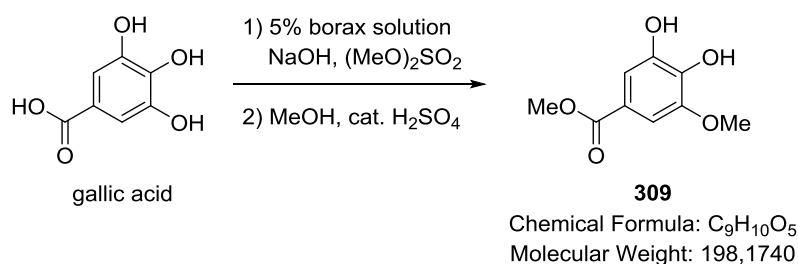
^1H NMR (400 MHz, CDCl_3): δ 5.91 (s, 1H), 4.86 (s, 2H), 3.98 (s, 3H), 3.28 (s, 6H), 2.15 (s, 3H), 1.85 (s, 3H) ppm.

^{13}C NMR (100 MHz, CDCl_3): δ 193.9, 170.3, 155.8, 154.3, 116.4, 114.7, 94.5, 63.0, 59.8, 51.0, 20.9, 10.1 ppm.

HRMS (EI, m/z): calc. $[\text{M}^+]$: 270.1103; found: 270.1083 $[\text{M}+\text{Na}^+]$.

IR $\tilde{\nu} = 2992$ (vw), 2948 (w), 2834 (vw), 1748 (vs), 1675 (s), 1647 (w), 1566 (w), 1449 (w), 1404 (vw), 1372 (w), 1328 (vw), 1292 (m), 1262 (m), 1227 (vs), 1211 (vs), 1151 (w), 1080 (vs), 1042 (vs), 982 (w), 932 (vw), 850 (vw) cm^{-1} .

methyl 3,4-dihydroxy-5-methoxybenzoate (309)

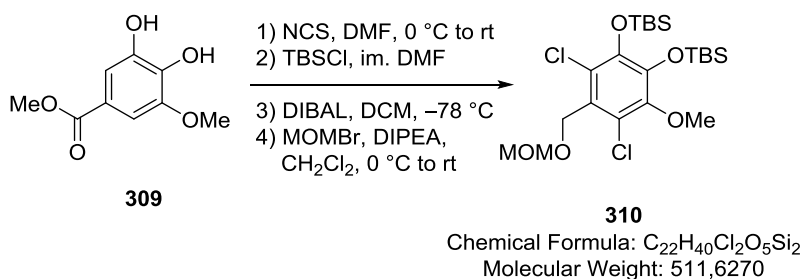


Gallic acid (5.00 g, 29.4 mmol) was dissolved in 5% aq. borax solution (400 ml) and aq. NaOH solution (26%, 25 ml) and dimethyl sulfate (20.0 g, 15.0 ml, 158 mmol, 5.4 eq.) were added simultaneously in a slow stream. The reaction mixture was stirred for 4 h and then acidified with aq. H_2SO_4 (1 M) to pH 1. The aqueous phase was extracted with EtOAc (2x60 ml) and the combined organic phases were washed with brine, dried over Na_2SO_4 and concentrated under reduced pressure. The residue was dissolved in MeOH (25 ml) and conc. H_2SO_4 (1.0 ml) was added. The reaction mixture was heated to reflux for 3 h and then cooled to rt. pH 7.2 buffer ($c = 1$ M, 50 ml) was added and the aqueous phase extracted with EtOAc (3x50 ml). The combined organic phases were dried over Na_2SO_4 and concentrated under reduced pressure to afford the title compound as a brownish oil (5.84 g, 100%). The title compound could be taken forward without further purification.

TLC $R_f = 0.33$ (40% EtOAc/hexanes).

¹H NMR	(400 MHz, (D₃C)₂CO): δ 8.23 (s, 1H), 8.01 (s, 1H), 7.22 (d, <i>J</i> = 1.9 Hz, 1H), 7.16 (d, <i>J</i> = 1.9 Hz, 1H), 3.87 (s, 3H), 3.81 (s, 3H) ppm.
¹³C NMR	(100 MHz, (D₃C)₂CO): δ 167.1, 148.5, 145.9, 139.7, 121.6, 111.6, 105.6, 56.5, 52.0 ppm.
HRMS	((-)-ESI, <i>m/z</i>): calc. [M-H ⁻]: 197.0450; found: 197.0453 [M-H ⁻].
IR	$\tilde{\nu}$ = 3373 (m), 3007 (vw), 2954 (w), 2848 (vw), 1695 (s), 1610 (s), 1518 (m), 1457 (m), 1436 (s), 1340 (vs), 1317 (vs), 1229 (vs), 1203 (vs), 1181 (s), 1104 (s), 1089 (vs), 1006 (m), 959 (vw), 904 (vw), 872 (vw), 807 (vw), 767 (m), 751 (w) cm ⁻¹ .

((3,5-dichloro-6-methoxy-4-((methoxymethoxy)methyl)-1,2-phenylene)bis(oxy))bis(*tert*-butyldimethylsilane) (310)



Catechol **309** (503 mg, 2.54 mmol) was dissolved DMF (25 ml) and cooled to 0 °C. NCS (746 mg, 5.59 mmol, 2.2 eq.) was added in portions. Upon completed addition, the reaction mixture was allowed to stir at rt for 16 h. The solution was poured onto aq. Na₂S₂O₃ solution (*c* = 1 M, 50 ml) and aq. HCl solution (*c* = 1 M, 100 ml) and the aqueous phase was extracted with EtOAc (3x150 ml). The combined organic phases were dried over Na₂SO₄ and concentrated under reduced pressure.

The crude product, imidazole (817 mg, 12.0 mmol, 4.8 eq.) and DMAP (61 mg, 0.50 mmol, 0.2 eq.) were dissolved in DMF (0.3 ml). TBSCl (904 mg, 6.00 mmol) was added and the mixture was stirred for 19 h. H₂O (100 ml) was added and the aqueous phase was extracted with EtOAc (3x100 ml). The combined organic phases were dried over Na₂SO₄ and concentrated under reduced pressure.

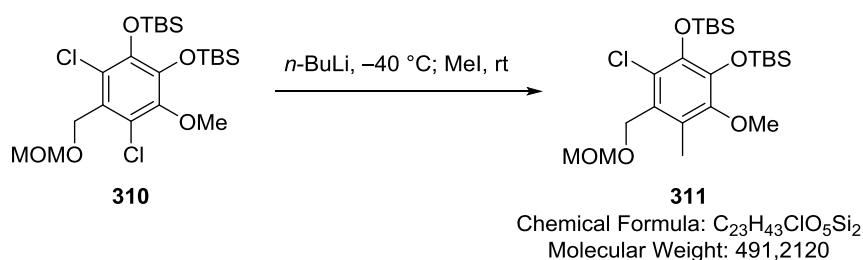
The crude product was dissolved in CH₂Cl₂ (10 ml) and cooled to -78 °C. DIBAL (25 wt-% in toluene, 4.2 ml, 6.3 mmol, 2.5 eq.) was added dropwise and the reaction mixture was stirred for 40 min. EtOAc (30 ml) and sat. aq. Rochelle salt solution (30 ml) were added successively, and the mixture was stirred for 1 h. The water phase was extracted with EtOAc (3x30 ml) and the combined organic layer was dried with Na₂SO₄ and concentrated under reduced pressure.

The crude product and DIPEA (1.8 ml, 10 mmol, 3.0 eq.) were dissolved in CH₂Cl₂ (5 ml) and cooled to 0 °C. MOMBr (0.69 ml, 8.8 mmol, 1.5 eq.) was added dropwise and the mixture was warmed to rt. After 4 h, pH 7.2 aq. phosphate buffer (*c* = 1 M, 5 ml) was added and the aqueous phase was extracted with CH₂Cl₂ (3x15 ml). The combined organic layers were dried over Na₂SO₄ and concentrated under reduced pressure. Purification of the crude product by flash column

chromatography (2.5% EtOAc/hexanes) afforded the title compound (526 mg, 40% over 4 steps) as colorless oil.

TLC	$R_f = 0.48$ (9% EtOAc/hexanes).
^1H NMR	(400 MHz, CDCl_3): δ 4.83 (s, 2H), 4.76 (s, 2H), 3.75 (s, 3H), 3.45 (s, 3H), 1.04 (s, 9H), 1.00 (s, 9H), 0.17 (s, 6H), 0.14 (s, 6H) ppm.
^{13}C NMR	(100 MHz, CDCl_3): δ 148.1, 144.3, 143.2, 126.7, 125.2, 123.6, 96.5, 65.0, 60.8, 55.6, 26.4, 26.2, 18.9, 18.6, -3.2 , -3.8 ppm.
HRMS	($(-)$ -ESI, m/z): calc. $[\text{M}-\text{TBS}]^-$: 395.0854; found: 395.0859 $[\text{M}-\text{TBS}]^-$.
IR	$\tilde{\nu} = 2948$ (w), 2932 (w), 2899 (w), 2890 (w), 2860 (w), 1462 (s), 1448 (m), 1439 (w), 1402 (s), 1341 (w), 1255 (m), 1232 (vw), 1151 (w), 1100 (m), 1076 (w), 1039 (m), 978 (m), 933 (m), 838 (vs), 786 (m), 722 (w) cm^{-1} .

((3-chloro-6-methoxy-4-((methoxymethoxy)methyl)-5-methyl-1,2-phenylene)bis(oxy))bis(*tert*-butyldimethylsilane) (311)

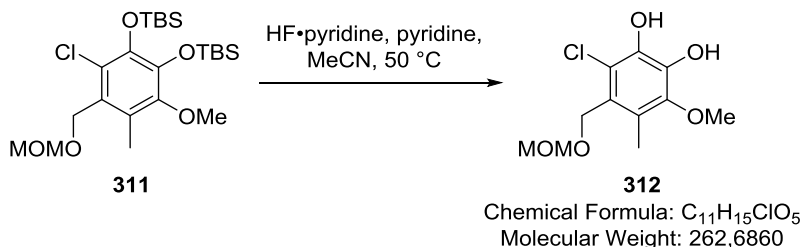


MOM ether **310** (459 mg, 0.897 mmol) was dissolved in THF (41 ml) and a solution of *n*-BuLi in hexanes ($c = 2.35$ M, 1.0 ml, 2.4 mmol, 10.0 eq.) was added at -40°C and stirred for 1 h. MeI (2.8 ml, 6.4 g, 45 mmol, 50 eq.) was added and the solution was slowly warmed to room temperature. After 41 h, sat. aq. NH_4Cl solution (30 ml) was added and the aqueous phase extracted with EtOAc (3x50 ml). The combined organic layers were dried with Na_2SO_4 and concentrated under reduced pressure. Purification of the crude product by flash column chromatography (2.5% EtOAc/hexanes) gave the title compound as a colorless oil (269 mg, 61%).

TLC	$R_f = 0.43$ (9% EtOAc/hexanes).
^1H NMR	(400 MHz, CDCl_3): δ 4.72 (s, 2H), 4.72 (s, 2H), 3.64 (s, 3H), 3.44 (s, 3H), 2.29 (s, 3H), 1.03 (s, 9H), 1.00 (s, 9H), 0.16 (s, 6H), 0.11 (s, 6H) ppm.
^{13}C NMR	(100 MHz, CDCl_3): δ 149.9, 142.9, 142.0, 127.0, 126.1, 124.4, 96.3, 64.7, 60.3, 55.6, 26.4, 26.3, 18.9, 18.6, 12.1, -3.2 , -3.8 ppm.
HRMS	(EI, m/z): calc. $[\text{M}-\text{CH}_3]^+$: 475.2103; found: 475.2103 $[\text{M}-\text{CH}_3]^+$.
IR	$\tilde{\nu} = 2952$ (w), 2930 (m), 2894 (w), 2858 (w), 2858 (w), 1461 (s), 1411 (w), 1390 (w), 1379 (w), 1362 (w), 1341 (w), 1252 (m), 1211 (vw), 1190 (vw), 1150 (w), 1115 (s),

1103 (m), 1031 (s), 1014 (m), 980 (m), 940 (w), 923 (w), 857 (s), 839 (vs), 810 (m), 779 (s), 732 (vw) cm^{-1} .

3-chloro-6-methoxy-4-((methoxymethoxy)methyl)-5-methylbenzene-1,2-diol (312)



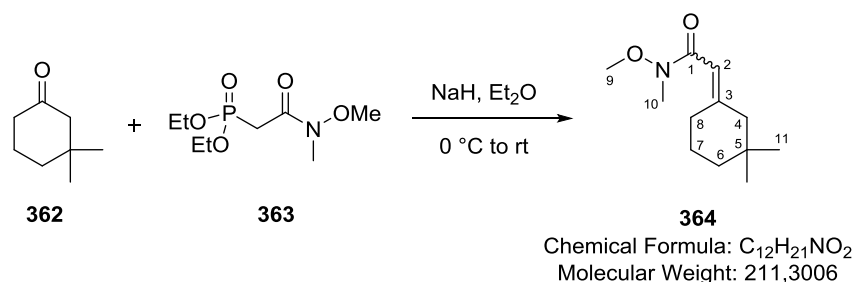
Chloro arene **311** (269 mg, 0.547 mmol) was dissolved in MeCN (15.6 ml) and cooled to 0 °C. A solution of HF·pyridine (70 wt-% HF, 0.17 ml, 6.6 mmol, 12 eq.) and pyridine (0.71 ml) were added and the reaction mixture was heated to 50 °C. After 14 h, pH 5 aq. phosphate buffer ($c = 1 \text{ M}$, 15 ml) and H_2O (10 ml) were added and the aqueous phase was extracted with EtOAc (4x20 ml). The combined organic layers were dried over Na_2SO_4 and concentrated under reduced pressure. Purification of the crude product by flash column chromatography (3% MeOH/ CH_2Cl_2) afforded the title compound as a brownish oil (119 mg, 83%).

TLC	$R_f = 0.25$ (5% MeOH/ CH_2Cl_2)
^1H NMR	(400 MHz, CDCl_3): δ 5.56 (brs, 1H), 5.49 (brs, 1H), 4.71 (s, 2H), 4.70 (s, 2H), 3.80 (s, 3H), 3.44 (s, 3H), 2.31 (s, 3H) ppm.
^{13}C NMR	(100 MHz, CDCl_3): δ 144.7, 138.4, 137.6, 124.9, 124.5, 117.5, 96.2, 64.0, 61.0, 55.7, 11.9 ppm.
MS	(EI, %): 262.20 (30, M^+), 257.18 (17), 200.14 (100), 185.11 (30), 167.16 (22).
HRMS	(EI, m/z): calc. [M^+]: 262.0608; found: 262.0602 [M^+].
IR	$\tilde{\nu} = 3355$ (br, w), 2938 (w), 2892 (w), 1597 (vw), 1478 (m), 1458 (m), 1382 (m), 1344 (w), 1298 (m), 1247 (w), 1224 (m), 1212 (w), 1148 (m), 1097 (vs), 1033 (vs), 964 (w), 934 (w), 903 (w), 816 (m) cm^{-1} .

6.2 Part II: Total Synthesis of Gracilin Natural Products

6.2.1 Synthesis of Side Chain

2-(3,3-dimethylcyclohexylidene)-*N*-methoxy-*N*-methylacetamide (**364**)^[348]



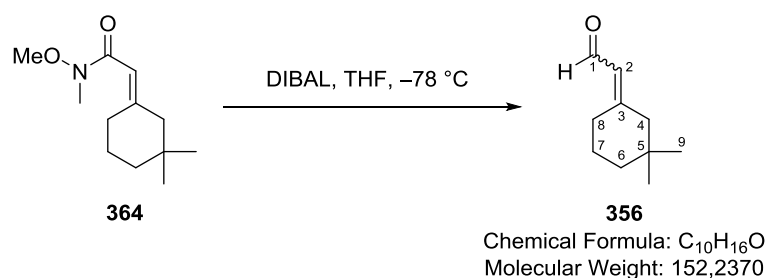
To a solution of phosphonate **363** (0.40 ml, 0.46 g, 1.9 mmol, 2.0 eq.) in Et₂O (2.4 ml) was added NaH (60% dispersion in mineral oil, 73 mg, 1.8 mmol, 1.9 eq.) at 0 °C and the reaction mixture was stirred for 10 min. A solution of ketone **362** (0.13 ml, 0.12 g, 0.91 mmol) in Et₂O (0.9 ml) was added and the reaction mixture was allowed to warm to rt. After stirring for 17 h, sat. aq. NaHCO₃ (5 ml) was added and the aqueous phase was extracted with EtOAc (3x15 ml). The combined organic phases were dried over Na₂SO₄ and concentrated under reduced pressure. Crude ¹H NMR analysis revealed a diastereomeric ratio (*E*):(*Z*) of 4:1 based on the olefinic proton. The crude product was purified by flash column chromatography (21x2.5 cm, 15–20% EtOAc/hexanes) to afford pure (*E*)- and (*Z*)-title compound as colorless oils (118 mg, 58%; 44 mg, 22 %).

(**364**) Major (*E*)

TLC	R _f = 0.25 (15% EtOAc/hexanes).
¹H NMR	(600 MHz, CDCl₃): δ 5.99 (s, 1H, C ₂ H), 3.68 (s, 3H, C ₉ H ₃), 3.21 (s, 3H, C ₁₀ H ₃), 2.70 (t, <i>J</i> = 6.0 Hz, 2H, C ₈ H ₂), 1.99 (s, 2H, C ₄ H ₂), 1.64–1.58 (m, 2H, C ₇ H ₂), 1.40 (t, <i>J</i> = 6.4 Hz, 2H, C ₆ H ₂), 0.91 (s, 6H, 2xC ₁₁ H ₃) ppm.
¹³C NMR	(150 MHz, CDCl₃): δ 168.1 (C1), 158.3 (C3), 113.2 (C2), 61.5 (C9), 51.5 (C4), 39.3 (C6), 34.4 (C5), 32.3 (br, C10), 29.6 (C8), 28.6 (C11), 23.6 (C7) ppm.
MS	(EI, %): 211.05 (1, M ⁺), 152.04 (11), 151.04 (100), 123.07 (14), 81.05 (20), 69.06 (16).
HRMS	(EI, m/z): calc. [M ⁺]: 211.1572; found: 211.1588 [M ⁺].
IR	$\tilde{\nu}$ = 2928 (m), 2866 (w), 2843 (w), 1652 (vs), 1632 (vs), 1460 (m), 1438 (m), 1410 (m), 1385 (m), 1364 (w), 1345 (m), 1322 (m), 1299 (w), 1242 (vw), 1177 (w), 1150 (w), 1100 (w), 1048 (vw), 1018 (w), 1002 (s), 975 (vw), 960 (w), 916 (vw), 889 (vw), 878 (vw), 863 (w), 841 (w), 823 (w), 799 (vw), 727 (vw), 707 (vw) cm ⁻¹ .

(365) Minor (*Z*)

TLC	$R_f = 0.31$ (15% EtOAc/hexanes).
^1H NMR	(600 MHz, CDCl_3): δ 6.12 (s, 1H, C_2H), 3.68 (s, 3H, C_9H_3), 3.20 (s, 3H, C_{10}H_3), 2.58 (s, 2H, C_4H_2), 2.16 (t, $J = 6.3$ Hz, 2H, C_8H_2), 1.68–1.63 (m, 2H, C_7H_2), 1.40 (t, $J = 6.2$ Hz, 2H, C_6H_2), 0.93 (s, 6H, $2\times\text{C}_{11}\text{H}_3$) ppm.
^{13}C NMR	(150 MHz, CDCl_3): δ 168.1 (C1), 158.5 (C3), 113.4 (C2), 61.5 (C9), 42.7 (C4), 39.5 (C6), 37.9 (C8), 34.2 (C5), 32.4 (C10), 28.5 (C11), 24.4 (C7) ppm.
MS	(EI, %): 211.04 (1, M^+), 196.03 (3), 151.04 (100), 123.07 (14), 81.05 (17), 69.06 (18).
HRMS	(EI, m/z): calc. [M^+]: 211.1572; found: 211.1552 [M^+].
IR	$\tilde{\nu} = 2932$ (m), 2864 (w), 2841 (w), 1651 (vs), 1632 (vs), 1456 (m), 1436 (m), 1409 (m), 1384 (s), 1364 (m), 1347 (w), 1339 (m), 1325 (m), 1298 (w), 1263 (vw), 1234 (vw), 1176 (m), 1163 (w), 1150 (w), 1103 (m), 1091 (m), 1047 (w), 1016 (w), 1001 (vs), 977 (w), 958 (m), 932 (vw), 872 (m), 847 (m), 828 (w), 804 (m), 730 (vw), 707 (w) cm^{-1} .

2-(3,3-dimethylcyclohexylidene)acetaldehyde (356**)^[348]**

A solution of Weinreb amide **364** (0.13 g, 0.62 mmol) in THF (3 ml) was cooled to $-78\text{ }^\circ\text{C}$ and treated with a solution of DIBAL in toluene ($c = 1.2\text{ M}$, 1.0 ml, 1.2 mmol, 2.0 eq.). The reaction mixture was stirred for 1.25 h before a sat. aq. NH_4Cl solution (1.5 ml) was carefully added. The mixture was allowed to warm to $0\text{ }^\circ\text{C}$ and was stirred for additional 2 h. Aq. HCl solution (1 M) was then added to adjust the pH to 4–5. The aqueous phase was extracted with CH_2Cl_2 (2x10 ml), the combined organic phases were dried over Na_2SO_4 and concentrated under reduced pressure. The crude product was purified by flash column chromatography (5% EtOAc/hexanes) to afford a diastereomeric mixture of the title compound as a colorless oil (72 mg, 76%, (*E*):(*Z*) = 4:1).

(356) Major (*E*)

TLC	$R_f = 0.39$ (10% EtOAc/hexanes).
------------	-----------------------------------

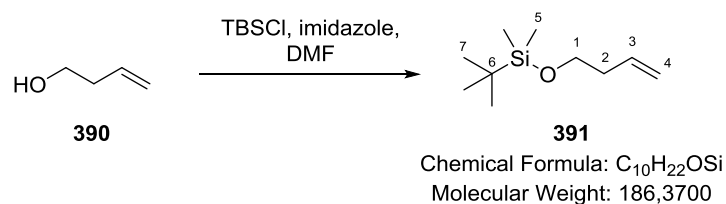
¹H NMR	(600 MHz, CDCl ₃): δ 10.01 (d, <i>J</i> = 8.3 Hz, 1H, C ₁ H), 5.80–5.78 (m, 1H, C ₂ H), 2.64 (td, <i>J</i> = 6.3, 0.9 Hz, 2H, C ₈ H ₂), 2.08 (s, 2H, C ₄ H ₂), 1.74–1.69 (m, 2H, C ₇ H ₂), 1.48–1.44 (m, 2H, C ₆ H ₂), 0.93 (s, 6H, 2xC ₁₁ H ₃) ppm.
¹³C NMR	(150 MHz, CDCl ₃): δ 190.6 (C1), 166.7 (C3), 126.9 (C2), 51.3 (C4), 39.0 (C6), 34.9 (C5), 29.2 (C8), 28.6 (C9), 23.9 (C7) ppm.
MS	(EI, %): 152.12 (83, M ⁺), 137.10 (45), 109.02 (100), 96.02 (23), 69.07 (48)
HRMS	(EI, m/z): calc. [M ⁺]: 152.1201; found: 152.1180 [M ⁺].
IR	$\tilde{\nu}$ = 2948 (w), 2866 (w), 2845 (w), 2770 (vw), 2740 (vw), 1668 (vs), 1629 (m), 1456 (w), 1445 (w), 1401 (vw), 1386 (vw), 1365 (w), 1346 (vw), 1323 (vw), 1299 (vw), 1264 (vw), 1240 (vw), 1198 (w), 1165 (m), 1115 (m), 1088 (vw), 1049 (vw), 1013 (vw), 993 (vw), 975 (vw), 947 (vw), 919 (vw), 889 (vw), 873 (vw), 861 (vw), 841 (vw), 803 (vw), 763 (vw), 723 (vw), 673 (vw) cm ⁻¹ .

(366) Minor (Z)

TLC	R _f = 0.42 (10% EtOAc/hexanes).
¹H NMR	(600 MHz, CDCl ₃): δ 9.97 (d, <i>J</i> = 8.3 Hz, 1H, C ₁ H), 5.94–5.92 (m, 1H, C ₂ H), 2.47 (s, 2H, C ₄ H ₂), 2.23 (td, <i>J</i> = 6.2, 0.9 Hz, 2H, C ₈ H ₂), 1.74–1.69 (m, 2H, C ₇ H ₂), 1.48–1.44 (m, 2H, C ₆ H ₂), 0.96 (s, 6H, 2xC ₉ H ₃) ppm.
¹³C NMR	(150 MHz, CDCl ₃): δ 190.7 (C1), 166.8 (C3), 127.2 (C2), 42.8 (C4), 39.1 (C6), 37.8 (C8), 34.8 (C5), 28.6 (C9), 24.2 (C7) ppm.

6.2.2 First Strategy: Torquoselective 6 π -Electrocyclization

(but-3-en-1-yloxy)(*tert*-butyl)dimethylsilane (**391**)^[349]



Alcohol **390** (4.8 ml, 4.0 g, 50 mmol, 1 eq.) in DMF (60 ml) was treated with TBSCl (10.0 g, 67.0 mmol, 1.2 eq.) and imidazole (7.50 g, 110 mmol, 2.0 eq.) at 0 °C. The ice bath was removed and the reaction mixture stirred for 30 min. H₂O (100 ml) was added and the aqueous phase was extracted with *n*-pentane (3x25 ml). The combined organic phases were dried over Na₂SO₄ and concentrated under reduced pressure. The crude product was filtered over a small silica plug with *n*-pentane (350 ml) and could be used without further purification (10.2 g, 110% due to TBSOTBS impurities).

TLC R_f = 0.17 (100% *n*-pentane).

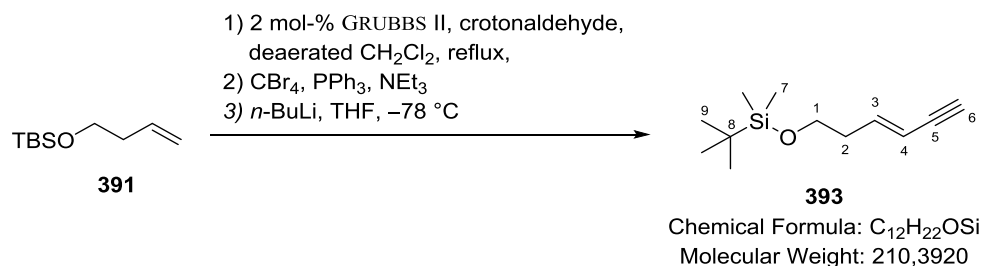
¹H NMR (300 MHz, CDCl₃): δ 5.89–5.75 (m, 1H, C₃H), 5.11–4.99 (m, 2H, *cis*-C₄H, *trans*-C₄H), 3.66 (t, J = 6.8 Hz, 2H, C₁H₂), 2.27 (tddd, J = 6.8, 6.8, 1.3, 1.3 Hz, 2H, C₂H₂), 0.89 (s, 9H, 3xC₇H₃), 0.06 (s, 6H, 2xC₅H₃) ppm.

¹³C NMR (75 MHz, CDCl₃): δ 135.6 (C3), 116.4 (C4), 63.0 (C1), 37.6 (C2), 26.1 (C7), 18.5 (C6), –5.1 (C5) ppm.

MS (CI, %): 187.1 (MH⁺, 94), 145.1 (22), 129.1 (24).

IR $\tilde{\nu}$ = 3081 (vw), 2955 (w), 2930 (w), 2896 (vw), 2858 (w), 1642 (vw), 1472 (w), 1464 (vw), 1432 (vw), 1387 (vw), 1362 (vw), 1254 (m), 1096 (vs), 1006 (w), 986 (w), 938 (vw), 910 (m), 833 (vs), 811 (m), 774 (vs), 734 (w), 665 (w), 626 (vw) cm^{–1}.

(*E*)-*tert*-butyl(hex-3-en-5-yn-1-yloxy)dimethylsilane (**393**)



A mixture of TBS ether **391** (985 mg, 5.29 mmol), crotonaldehyde (1.11 g, 15.9 mmol, 3.0 eq.) and Grubbs II catalyst (90 mg, 0.11 mmol, 0.02 eq.) in deaerated CH₂Cl₂ (21 ml) was heated to reflux

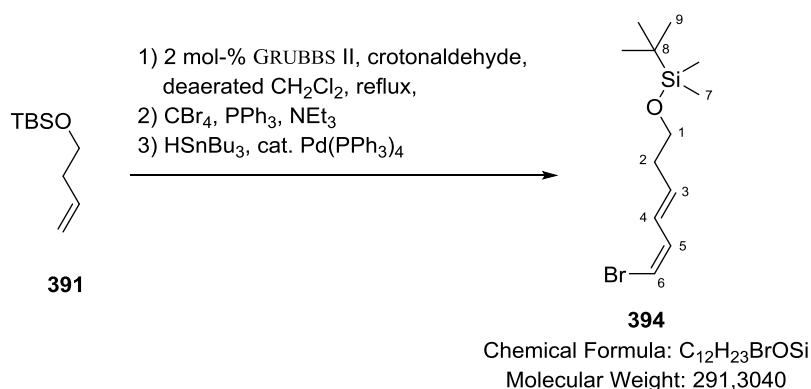
for 3 h. The reaction mixture was filtered over a short silica plug with CH₂Cl₂ (100 ml) and Et₂O (50 ml) and the organic phase was concentrated in vacuo.

CBr₄ (4.39 g, 13.2 mmol, 2.5 eq.) in CH₂Cl₂ (70 ml) was added dropwise to a solution of PPh₃ (6.94 g, 26.5 mmol, 5.0 eq.) in CH₂Cl₂ (75 ml) at 0 °C. This mixture was treated with NEt₃ (1.7 ml, 1.2 g, 13 mmol, 2.3 eq.) and stirred for 30 min. The crude aldehyde in CH₂Cl₂ (20 ml) was added dropwise over 10 min and the ice bath was removed upon completed addition. After 17 h, the reaction mixture was diluted with hexanes (200 ml) and the resulting precipitate filtered off. The organic phase was concentrated in vacuo. The suspension was again filtered after addition of hexanes (100 ml) and the remaining organic phase concentrated under reduced pressure.

The crude intermediate was dissolved in THF (50 ml) and cooled to –78 °C. A solution of *n*-BuLi in *n*-hexane (2.5 M, 9.1 ml, 23 mmol, 4.3 eq.) was added dropwise. The reaction mixture was stirred for 1 h at –78 °C and then allowed to warm to rt. Water (75 ml) was added and the aqueous phase was extracted with CH₂Cl₂ (3x100 ml). The combined organic phases were washed with brine (200 ml), dried over Na₂SO₄ and concentrated under reduced pressure. The crude product was purified by flash column chromatography (5–15% CH₂Cl₂/hexanes) to afford the title compound as a yellowish oil (425 mg). The mixed fractions were resubjected to flash column chromatography (5–10% CH₂Cl₂/hexanes) to furnish the title compound as a yellowish oil (79 mg, combined yield over 3 steps 45%).

TLC	R _f = 0.34 (2% Et ₂ O/ <i>n</i> -pentane).
¹H NMR	(300 MHz, CDCl ₃): δ 6.25 (dt, <i>J</i> = 16.1, 7.2 Hz, 1H, C ₃ H), 5.52 (ddd, <i>J</i> = 16.1, 2.2, 1.6, 1H, C ₄ H), 3.66 (t, <i>J</i> = 6.6 Hz, 2H, C ₁ H ₂), 2.80–2.78 (m, 1H, C ₆ H), 2.37–2.28 (m, 2H, C ₂ H ₂), 0.89 (s, 9H, 3xC ₉ H ₃), 0.06 (s, 6H, 2xC ₇ H ₃) ppm.
¹³C NMR	(75 MHz, CDCl ₃): δ 143.4 (C3), 110.5 (C4), 82.5 (C5), 76.1 (C6), 62.2 (C1), 36.7 (C2), 26.1 (C9), 18.5 (C8), –5.2 (C7) ppm.
MS	(EI, %): 212.21 (18), 153.11 (100), 123.08 (52), 75.04 (73).
HRMS	(EI, <i>m/z</i>): [M–CH ₃ ⁺] calc.: 195.1205; found: 195.1216 (M–CH ₃ ⁺).
IR	$\tilde{\nu}$ = 3314 (vw), 2954 (w), 2928 (w), 2897 (vw), 2856 (w), 1472 (w), 1463 (w), 1389 (vw), 1361 (vw), 1252 (m), 1094 (vs), 1043 (vw), 1006 (w), 957 (m), 938 (w), 833 (vs), 812 (m), 774 (vs), 721 (w), 670 (w), 660 (w), 634 (m) cm ^{–1} .

(((3*E*,5*Z*)-6-bromohexa-3,5-dien-1-yl)oxy)(*tert*-butyl)dimethylsilane (394)



A mixture of TBS ether **391** (314 mg, 1.68 mmol), crotonaldehyde (354 mg, 5.05 mmol, 3.0 eq.) and GRUBBS II catalyst (71 mg, 0.084 mmol, 0.05 eq.) in deaerated CH₂Cl₂ (7 ml) was heated to reflux for 4 h. The reaction mixture was filtered over a short silica plug with CH₂Cl₂ (80 ml) and the organic phase was concentrated under reduced pressure.

CBr₄ (1.68 g, 5.05 mmol, 3.0 eq.) in CH₂Cl₂ (20 ml) was treated dropwise with a solution of PPh₃ (2.65 g, 10.1 mmol, 6.0 eq.) in CH₂Cl₂ (15 ml) at 0 °C. This mixture was subjected to NEt₃ (2.4 ml). The crude aldehyde in CH₂Cl₂ (6 ml) was added dropwise over 10 min and the ice bath was removed upon completed addition. After 1.5 h, the reaction mixture was quenched with sat. NH₄Cl (30 ml), the aqueous phase extracted with CH₂Cl₂ (3x75 ml), dried over Na₂SO₄ and concentrated under reduced pressure. The crude product was purified by column chromatography (5% EtOAc/hexanes) to afford the dibromoolefin as a yellow oil (284 mg, 45% over 2 steps).

The latter was dissolved in toluene (2.5 ml) and Pd(PPh₃)₄ (89 mg, 0.077 mmol, 0.1 eq.) and HSnBu₃ (0.23 ml, 0.26 g, 0.87 mmol, 1.14 eq.) were added subsequently. The reaction mixture was stirred for 1 h before it was filtered over a silica plug with CH₂Cl₂ (350 ml) and hexanes (50 ml). The organic phase was concentrated under reduced pressure and the crude product was purified by column chromatography (10–15% CH₂Cl₂/hexanes) to afford the product as a colorless oil (150 mg, 67%). MS spectral analysis failed for this compound.

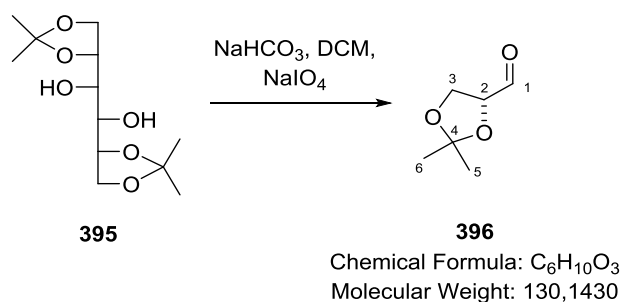
TLC R_f = 0.42 (1% EtOAc/hexanes).

¹H NMR (300 MHz, C₆D₆): δ 6.62–6.52 (m, 1H, C₄H), 6.24–6.14 (m, 1H, C₆H), 5.77–5.65 (m, 2H, C₃H, C₅H), 3.45 (t, J = 6.5 Hz, 2H, C₁H₂), 2.15–2.07 (m, 2H, C₂H₂), 0.96 (s, 9H, 3xC₉H₃), 0.02 (s, 3H, 2xC₇H₃) ppm.

¹³C NMR (75 MHz, C₆D₆): δ 136.1 (C3), 132.9 (C6), 106.3 (C5), 62.5 (C1), 36.7 (C2), 26.1 (C9), 18.5 (C8), –5.2 (C7) ppm. C4 hidden by solvent signal.

IR $\tilde{\nu}$ = 2953 (w), 2927 (w), 2883 (vw), 2856 (w), 1725 (vw), 1698 (vw), 1619 (vw), 1471 (w), 1462 (w), 1388 (vw), 1361 (w), 1330 (vw), 1252 (m), 1095 (s), 1005 (w), 971 (w), 938 (w), 834 (vs), 812 (s), 775 (vs), 724 (w), 665 (m) cm^{–1}.

(*R*)-2,2-dimethyl-1,3-dioxolane-4-carbaldehyde (396)^[255]



Diol **395** (2.50 g, 9.50 mmol) in CH₂Cl₂ (23 ml) was treated with sat. aq. NaHCO₃ (1 ml) and NaIO₄ (4.10 g, 19.1 mmol, 2.0 eq.) and stirred for 1.5 h. The solid phase was filtered off and washed with CH₂Cl₂ (4x10 ml) and the organic phase was concentrated in vacuo. The crude product was purified by distillation (b.p.: 50 °C, *p* = 30 mbar) to afford the title compound as a colorless oil (1.77 g, 73%).

TLC *R*_f = 0.20 (30% EtOAc/hexanes).

b.p.: 50 °C (*p* = 30 mbar).

¹H NMR (**300 MHz**, CDCl₃): δ 9.72 (d, *J* = 2.0 Hz, 1H, C₁H), 4.38 (ddd, *J* = 7.0, 4.8, 2.0 Hz, 1H, C₂H), 4.17 (dd, *J* = 8.8, 7.0 Hz, 1H, C₃H), 4.10 (dd, *J* = 8.8, 4.8 Hz, 1H, C₃H), 1.49 (s, 3H, C₅H₃), 1.42 (s, 3H, C₆H₃) ppm.

¹³C NMR (**75 MHz**, CDCl₃): δ 201.9 (C1), 111.4 (C4), 80.0 (C2), 65.7 (C3), 26.4 (C5), 25.3 (C6) ppm.

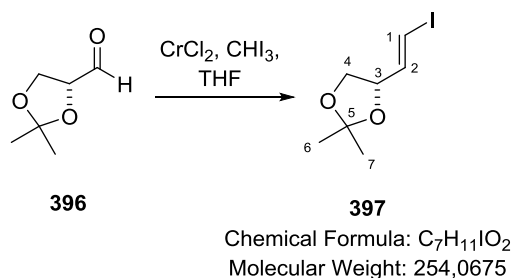
MS (**EI**, %): 131.12 (14), 115.09 (63), 101.11 (100), 85.06 (17), 43.00 (79).

HRMS (**EI**, *m/z*): calc: 131.0663 [MH⁺]; found: 131.0695 (MH⁺).

IR $\tilde{\nu}$ = 3450 (vw), 2990 (vw), 2938 (vw), 2892 (vw), 2820 (vw), 1734 (s), 1456 (vw), 1374 (m), 1253 (m), 1214 (m), 1149 (m), 1067 (vs), 964 (w), 917 (w), 839 (vs), 791 (vw), 733 (m), 648 (vw) cm⁻¹.

OR $[\alpha]_D^{22} = +81.0^\circ$ (12 mg/ml, CHCl₃).

(*S,E*)-4-(2-iodovinyl)-2,2-dimethyl-1,3-dioxolane (**397**)

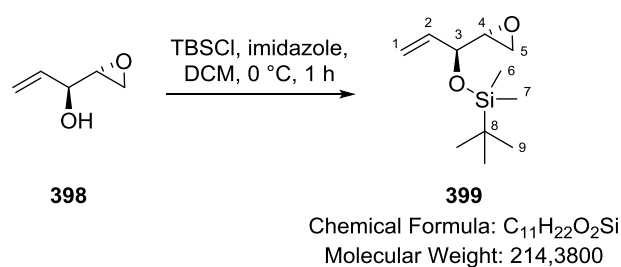


A suspension of CrCl₂ (1.34 g, 10.9 mmol, 5.0 eq.) in THF (50 ml) was treated with a solution of CHI₃ (1.07 g, 2.73 mmol, 1.25 eq.) and aldehyde **396** (284 mg, 2.18 mmol) in THF (10 ml) at 0 °C. The ice bath was removed and the reaction mixture stirred for 22 h. After addition of H₂O (30 ml), the

aqueous phase was extracted with Et₂O (3x250 ml) and the combined organic phases were dried over Na₂SO₄ and concentrated in vacuo. The crude product was purified by column chromatography (0.5–1–2–5% EtOAc/hexanes) to afford the title compound as a colorless oil (430 mg, 78%, *E*:*Z* 15:1).

TLC	$R_f = 0.26$ (1% EtOAc/hexanes).
¹H NMR	(400 MHz, C₆D₆): δ 6.24 (dd, $J = 14.5, 6.7$ Hz, 1H, C ₂ H), 6.06 (dd, $J = 14.5, 1.0$ Hz, 1H, C ₁ H), 3.96–3.90 (m, 1H, C ₃ H), 3.54 (dd, $J = 8.3, 6.3$ Hz, 1H, C ₄ H), 3.16 (dd, $J = 8.3, 7.1$ Hz, 1H, C ₄ H), 1.26 (s, 3H, C ₆ H ₃), 1.24 (s, 3H, C ₇ H ₃) ppm.
¹³C NMR	(100 MHz, C₆D₆): δ 144.2 (C2), 109.6 (C5), 79.2 (C1), 78.2 (C3), 68.4 (C4), 26.7 (C6), 26.0 (C7) ppm. Unknown impurity at δ 2.7 ppm.
MS	(EI, %): 253.98 (2, M ⁺), 238.95 (48), 126.92 (8), 97.04 (24).
HRMS	(EI, m/z): [M ⁺] calc.: 253.9804; found: 253.9800 [M ⁺].
IR	$\tilde{\nu} = 3405$ (vw), 3051 (vw), 2985 (w), 2935 (vw), 2874 (vw), 1610 (w), 1455 (vw), 1380 (w) 1371 (m), 1248 (m), 1216 (s), 1179 (m), 1152 (s), 1112 (w), 1057 (vs), 1028 (m), 943 (s), 914 (w), 851 (s), 793 (w), 765 (w), 732 (w), 645 (vw) cm ⁻¹ .
OR	$[\alpha]_D^{21} = +23.1^\circ$ (27 mg/ml, CHCl ₃).

***tert*-butyldimethyl(((*S*)-1-((*R*)-oxiran-2-yl)allyl)oxy)silane (**399**)**^[350]

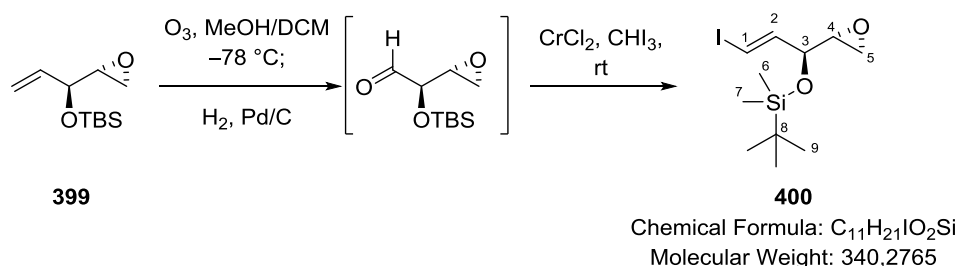


A solution of epoxyalcohol **398** (1.99 g, 16.0 mmol) in CH₂Cl₂ (31 ml) was cooled to 0 °C and TBSCl (2.97 g, 19.7 mmol, 1.2 eq.) and imidazole (1.63 g, 23.9 mmol, 1.5 eq.) were added. The reaction mixture was stirred for 1 h before the addition of H₂O (40 ml) and Et₂O (60 ml). The aqueous phase was extracted with Et₂O (3x20 ml) and the combined organic phases were washed with HCl (*c* = 0.1 M, 50 ml), brine, dried over Na₂SO₄ and concentrated under reduced pressure. The crude product was purified by flash column chromatography (2% Et₂O/*n*-pentane) to afford the title compound as a colorless oil (3.09 g, 14.4 mmol, 90%).

TLC	$R_f = 0.36$ (2% Et ₂ O/ <i>n</i> -pentane).
¹H NMR	(400 MHz, CD₂Cl₂): δ 5.88 (ddd, $J = 17.2, 10.5, 5.6$ Hz, 1H, C ₂ H), 5.31 (ddd, $J = 17.2, 1.6, 1.6$ Hz, 1H, <i>trans</i> -C ₁ H), 5.17 (ddd, $J = 10.5, 1.4, 1.4$ Hz, 1H, <i>cis</i> -C ₁ H), 4.14–4.10 (m, 1H, C ₃ H), 2.93–2.89 (m, 1H, C ₄ H), 2.68–2.63 (m, 2H, C ₅ H, C ₅ H), 0.90 (s, 9H, 3xC ₉ H ₃), 0.07 (s, 3H, C ₆ H ₃), 0.06 (s, 3H, C ₇ H ₃) ppm.

^{13}C NMR	(100 MHz, CD_2Cl_2): δ 137.9 (C2), 116.0 (C1), 73.0 (C3), 54.7 (C4), 44.4 (C5), 25.9 (C9), 18.5 (C8), -4.7 (C6/C7), -4.7 (C6/C7) ppm.
MS	(EI, %): 171.21 (6), 157.15 (13), 127.12 (100), 101.09 (13), 75.05 (24).
HRMS	(EI, m/z): $[\text{M}-\text{CH}_3]^+$ calc.: 199.1154; found: 199.1136 $[\text{M}-\text{CH}_3]^+$.
IR	$\tilde{\nu}$ = 2956 (w), 2930 (w), 2887 (vw), 2858 (w), 1646 (vw), 1472 (w), 1464 (vw), 1404 (vw), 1390 (vw), 1362 (vw), 1339 (vw), 1287 (vw), 1251 (m), 1170 (vw), 1158 (w), 1136 (w), 1119 (w), 1080 (m), 1033 (m), 1001 (m), 926 (m), 834 (vs), 801 (m), 775 (vs), 674 (m), 648 (vw) cm^{-1} .

***tert*-butyl(((*S,E*)-3-iodo-1-((*R*)-oxiran-2-yl)allyl)oxy)dimethylsilane (**400**)**



A stream of ozone/oxygen was bubbled through a solution of TBS ether **399** (111 mg, 0.520 mmol) in $\text{CH}_2\text{Cl}_2/\text{MeOH}$ (1:1, 2.6 ml) cooled to $-78\text{ }^\circ\text{C}$ until TLC analysis indicated full conversion (35 sec). The solution was purged with N_2 to remove excess ozone. Pd on charcoal (spatula tip) was added to the reaction mixture and a H_2 atmosphere was introduced. After 3 h, the suspension was filtered over Celite with Et_2O , the organic phase washed with water (10 ml), brine, dried over Na_2SO_4 and concentrated under reduced pressure ($p = 390$ mbar).

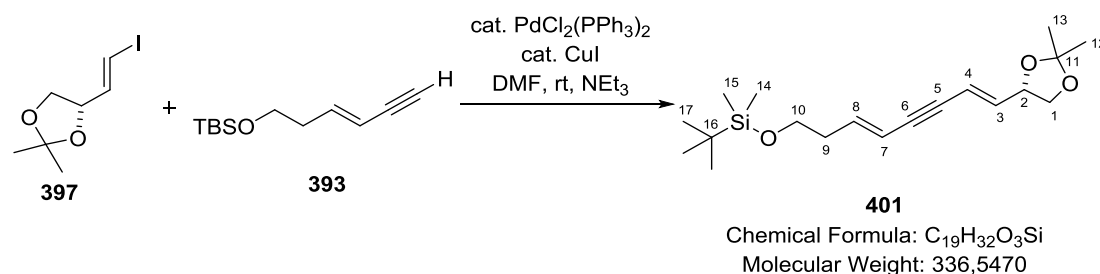
A suspension of CrCl_2 (447 mg, 3.64 mmol, 7.0 eq.) in THF (12 ml) was treated with a solution of CHI_3 (512 mg, 1.30 mmol, 2.5 eq.) in THF (1 ml) and the crude aldehyde in THF (1.5 ml) at $0\text{ }^\circ\text{C}$. The ice bath was removed and the reaction mixture stirred for 5 h. After dilution with Et_2O (10 ml), the organic phase was washed with half-saturated $\text{Na}_2\text{S}_2\text{O}_3$ solution (10 ml), washed with H_2O (2x10 ml), dried over Na_2SO_4 and concentrated in vacuo. The crude product was purified by flash column chromatography (1–2.5–5% $\text{Et}_2\text{O}/\text{hexanes}$) to afford the title compound as a colorless oil ((*E*):(*Z*) = 11:1, 103 mg, 58% over 2 steps). MS spectral analysis failed for this compound.

TLC	$R_f = 0.17$ (5% $\text{EtOAc}/\text{hexanes}$).
^1H NMR	(300 MHz, CDCl_3): δ 6.56 (dd, $J = 14.6, 6.9$ Hz, 1H, C_2H), 6.44 (dd, $J = 14.6, 0.7$ Hz, 1H, C_1H), 4.14 (ddd, $J = 6.9, 5.6, 0.7$ Hz, 1H, C_3H), 3.52 (ddd, $J = 5.6, 5.6, 5.6$ Hz, 1H, C_4H), 3.29–3.25 (m, 2H, $\text{C}_5\text{H}, \text{C}_5\text{H}$), 0.90 (s, 9H, $3\times\text{C}_9\text{H}_3$), 0.10 (s, 3H, C_6H_3), 0.07 (s, 3H, C_7H_3) ppm.
^{13}C NMR	(75 MHz, CDCl_3): δ 144.6 (C2), 79.7 (C1), 77.7 (C3), 73.7 (C4), 25.9 (C9), 18.2 (C8), 9.3 (C5), -4.2 (C6/C7), -4.7 (C6/C7) ppm.

IR $\tilde{\nu}$ = 3464 (vw), 2954 (m), 2929 (m), 2886 (w), 2857 (m), 1607 (vw), 1472 (w), 1362 (w), 1254 (m), 1090 (s), 1181 (w), 1090 (s), 948 (w), 867 (s), 837 (vs), 778 (vs), 680 (vw) cm^{-1} .

OR $[\alpha]_{\text{D}}^{21} = +3.0^{\circ}$ (17 mg/ml, CHCl_3).

***tert*-butyl(((3*E*,7*E*)-8-((*S*)-2,2-dimethyl-1,3-dioxolan-4-yl)octa-3,7-dien-5-yn-1-yl)oxy)dimethylsilane (**401**)**



Vinyl iodide **397** (71 mg, 0.28 mmol, 1.05 eq.) in DMF (1 ml) and NEt_3 (0.8 ml) was added to a solution of $\text{PdCl}_2(\text{PPh}_3)_2$ (9 mg, 0.01 mmol, 0.05 eq.) and CuI (5 mg, 0.03 mmol, 0.1 eq.) in DMF (1 ml) at room temperature and stirred for 10 min. The mixture was treated with alkyne **393** (56 mg, 0.27 mmol, 1.0 eq.) in DMF (1 ml) and stirred for 5 h before sat. aq. NH_4Cl solution (7 ml) was added. The aqueous phase was extracted with Et_2O (3x25 ml) and the combined organic phases were dried over Na_2SO_4 and concentrated under reduced pressure. The crude product was purified by column chromatography twice (1–3% Et_2O /hexanes; 3–5–7% EtOAc /hexanes) to afford the product as a colorless oil (57 mg, 60%).

TLC R_f = 0.31 (10% Et_2O /hexanes).

^1H NMR (300 MHz, CDCl_3): δ 6.15 (ddd, J = 16.0, 7.2, 7.2 Hz, 1H, C_8H), 6.04 (dd, J = 15.9, 6.8 Hz, 1H, C_3H), 5.92–5.84 (m, 1H, C_4H), 5.68–5.59 (m, 1H, C_7H), 4.53 (ddd, J = 6.9, 6.8, 6.5, 1H, C_2H), 4.11 (dd, J = 8.3, 6.5 Hz, 1H, C_1H), 3.68–3.58 (m, 3H, C_{10}H , C_{10}H , C_1H), 2.33 (dddd, J = 7.2, 7.2, 7.2, 1.5 Hz, 2H, C_9H , C_9H), 1.42 (s, 3H, C_{12}H_3), 1.39 (s, 3H, C_{13}H_3), 0.89 (s, 9H, $3\times\text{C}_{17}\text{H}_3$), 0.06 (s, 3H, C_{14}H_3), 0.06 (s, 3H, C_{15}H_3) ppm.

^{13}C NMR (75 MHz, CDCl_3): δ 141.8 (C8), 139.5 (C3), 113.0 (C4), 111.4 (C7), 109.9 (C11), 89.8 (C6), 86.0 (C5), 76.5 (C2), 69.4 (C1), 62.3 (C10), 36.9 (C9), 26.7 (C12), 26.1 (C17), 26.0 (C13), 18.5 (C16), –5.1 (C14, C15) ppm.

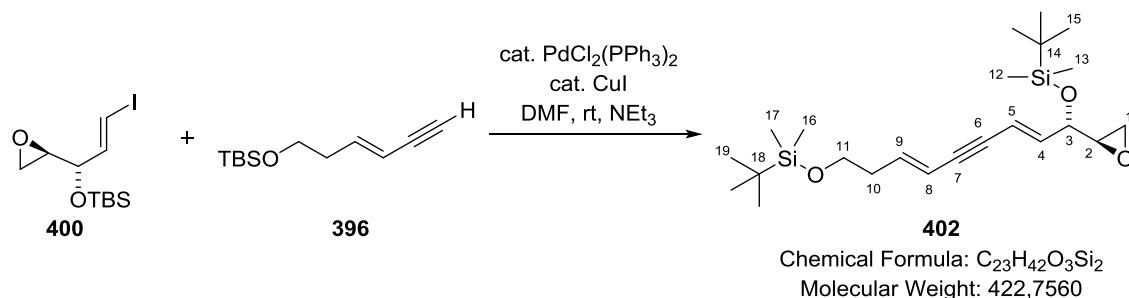
MS (EI, %): 321.26 (14), 279.23 (88), 147.15 (95), 115.12 (36), 89.07 (85), 75.05 (92), 73.07 (100).

HRMS (EI, m/z): $[\text{M}]^+$ calc.: 336.2121; found: 336.2116 $[\text{M}]^+$.

IR $\tilde{\nu}$ = 2986 (vw), 2955 (w), 2930 (w), 2858 (w), 1472 (w), 1464 (vw), 1380 (w), 1371 (w), 1290 (vw), 1252 (m), 1213 (w), 1155 (w), 1094 (s), 1060 (s), 1030 (w), 1006 (w), 952 (s), 834 (vs), 775 (vs), 721 (vw), 662 (w) cm^{-1} .

OR $[\alpha]_{\text{D}}^{21} = +28.0^{\circ}$ (7 mg/ml, CHCl_3).

(*S*,6*E*,10*E*)-2,2,3,3,15,15,16,16-octamethyl-5-((*R*)-oxiran-2-yl)-4,14-dioxa-3,15-disilaheptadeca-6,10-dien-8-yne (402**)**



Vinyl iodide **400** (62 mg, 0.18 mmol, 1.05 eq.) in DMF (0.7 ml) and NEt₃ (0.5 ml) was added to a solution of PdCl₂(PPh₃)₂ (6 mg, 0.01 mmol, 0.05 eq.) and CuI (3 mg, 0.02 mmol, 0.1 eq.) in DMF (0.7 ml) at room temperature and stirred for 10 min. The mixture was treated with alkyne **393** (36 mg, 0.17 mmol, 1.0 eq.) in DMF (0.7 ml) and stirred for 17 h before sat. aq. NH₄Cl solution (10 ml) was added. The aqueous phase was extracted with Et₂O (3x25 ml) and the combined organic phases were dried over Na₂SO₄ and concentrated under reduced pressure. The crude product was purified by column chromatography (3–5–7% Et₂O /hexanes) to afford the product as a colorless oil (89 mg, quant.).

TLC R_f = 0.61 (10% Et₂O/hexanes).

¹H NMR (**600 MHz**, CDCl₃): δ 6.18–6.12 (m, 2H, C₄H, C₉H), 5.89 (ddd, J = 15.9, 2.0, 2.0 Hz, 1H, C₅H), 5.68–5.62 (m, 1H, C₈H), 4.21–4.17 (m, 1H, C₃H), 3.66 (t, J = 6.7 Hz, 2H, C₁₁H, C₁₁H), 2.94–2.91 (m, 1H, C₂H), 2.71–2.68 (m, 2H, C₁H, C₁H), 2.37–2.31 (m, 2H, C₁₀H, C₁₀H), 0.89 (s, 18H, 3xC₁₅H₃, 3xC₁₉H₃), 0.06 (s, 3H, C₁₂H₃), 0.05 (s, 3H, C₁₃H₃), 0.05 (s, 6H, C₁₆H₃, C₁₇H₃) ppm.

¹³C NMR (**150 MHz**, CDCl₃): δ 141.5 (C₄/C₉), 141.3 (C₄/C₉), 111.5 (C₈), 111.1 (C₅), 89.5 (C₆/C₇), 86.4 (C₆/C₇), 71.6 (C₃), 62.4 (C₁₁), 54.4 (C₂), 44.4 (C₁), 36.9 (C₁₀), 26.1 (C₁₅/C₁₉), 25.9 (C₁₅/C₁₉), 18.5 (C₁₄/C₁₈), 18.4 (C₁₄/C₁₈), –4.7 (C₁₂, C₁₃), –5.1 (C₁₆, C₁₇) ppm.

MS (**EI**, %): 365.20 (25), 233.17 (25), 205.20 (10), 163.16 (8), 147.12 (18), 115.12 (25), 89.06 (75), 73.06 (100).

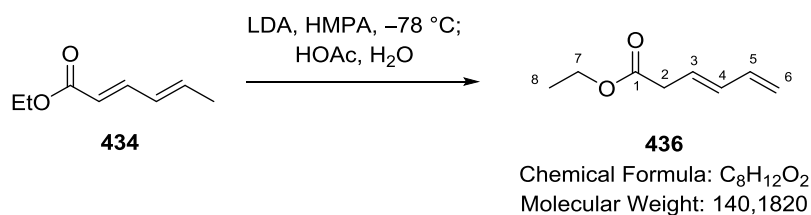
HRMS (**EI**, **m/z**): [M⁺] calc.: 422.2672; found: 422.2672 [M⁺].

IR $\tilde{\nu}$ = 2954 (w), 2929 (w), 2886 (vw), 2857 (w), 1613 (vw), 1472 (w), 1463 (w), 1389 (vw), 1361 (vw), 1284 (vw), 1252 (m), 1164 (vw), 1117 (m) 1095 (m), 1000 (m), 953 (m), 834 (vs), 813 (m), 775 (vs), 676 (w) cm^{–1}.

OR $[\alpha]_D^{24}$ = +23.4° (28 mg/ml, CHCl₃).

6.2.3 Second Strategy: Rhodium-Catalyzed Formal (4+3)-Cycloaddition

ethyl (*E*)-hexa-3,5-dienoate (**436**)^[299]



n-BuLi (*c* = 2.45 M, 29.4 ml, 72.0 mmol, 1.2 eq.) was added to DIPA (10.1 ml, 7.29 g, 72.0 mmol, 1.2 eq.) in THF (120 ml) cooled to $-78\text{ }^\circ\text{C}$. After 45 min, HMPA (13.6 ml, 14.0 g, 78.0 mmol, 1.3 eq.) was added slowly dropwise and stirring was continued for 1.5 h. After the addition of diene **434** (9.1 ml, 8.7 g, 60 mmol) was complete, the reaction mixture was stirred for an additional hour, before it was poured onto HOAc (10.3 ml, 10.8 g, 180 mmol, 3.0 eq.) in H₂O (210 ml) cooled to $0\text{ }^\circ\text{C}$ under vigorous stirring. The aqueous phase was extracted with hexanes (2x300 ml) and the combined organic phases were washed with H₂O, sat. aq. NaHCO₃, dried over Na₂SO₄ and concentrated under reduced pressure. The crude product was distilled under reduced pressure (20 ± 5 mbar) to afford the title compound as a colorless oil (6.39 g, 76%).

b.p.: $66\text{--}70\text{ }^\circ\text{C}$ ($p = 20$ mbar).

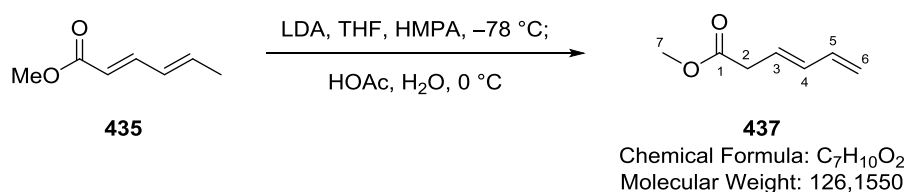
¹H NMR (**300 MHz**, CDCl₃): δ 6.34 (ddd, $J = 20.3, 10.4, 10.4$ Hz, 1H, C₅H), 6.20–6.08 (m, 1H, C₄H), 5.85–5.72 (m, 1H, C₃H), 5.16 (d, $J = 16.6$ Hz, 1H, *trans*-C₆H), 5.06 (d, $J = 10.4$ Hz, 1H, *cis*-C₆H), 4.15 (q, $J = 7.0$ Hz, 2H, C₇H₂), 3.11 (d, $J = 7.4$ Hz, 2H, C₂H₂), 1.26 (t, $J = 7.0$ Hz, 3H, C₈H₃) ppm.

¹³C NMR (**75 MHz**, CDCl₃): δ 171.6 (C1), 136.5 (C5), 134.4 (C4), 125.9 (C3), 117.0 (C6), 60.9 (C7), 38.2 (C2), 14.3 (C8) ppm.

MS (**EI**, %): 140.15 (33, M⁺), 97.11 (14), 85.13 (22), 67.14 (100).

HRMS (**EI**, **m/z**): calc. [M⁺]: 140.0837; found: 140.0827 [M⁺].

IR $\tilde{\nu} = 3089$ (vw), 2982 (vw), 2937 (vw), 1734 (vs), 1654 (vw), 1604 (vw), 1465 (vw), 1447 (vw), 1407 (vw), 1369 (w), 1337 (w), 1303 (w), 1244 (m), 1179 (s), 1140 (m), 1097 (vw), 1026 (m), 1004 (s), 953 (w), 904 (w), 858 (vw), 828 (vw) cm⁻¹.

methyl (*E*)-hexa-3,5-dienoate (437)

A solution of LDA in THF was prepared by adding a solution of *n*-BuLi in THF (2.4 M, 20.0 ml, 48.0 mmol, 1.2 eq.) to DIPA (6.7 ml, 4.8 g, 48 mmol, 1.2 eq.) in THF (80 ml) at $-78\text{ } ^\circ\text{C}$. This mixture was stirred for 25 min at the same temperature before it was treated with HMPA (9.1 ml, 9.3 g, 52 mmol, 1.3 eq.) *via* syringe pump (50 ml/hr). The resulting mixture was stirred for 35 min at $-78\text{ } ^\circ\text{C}$. Subsequently, diene **435** (5.3 ml, 5.0 g, 40 mmol) was slowly introduced to the reaction mixture *via* syringe pump (5 ml/hr). Upon completed addition, the orange solution was stirred for 1 h and then poured onto ice-cold acetic acid (6.9 ml, 7.2 g, 0.12 mol, 3.0 eq.) in H₂O (180 ml). The aqueous phase was extracted with hexanes (2x300 ml) and the combined organic phases were washed with H₂O (200 ml) and sat. aq. NaHCO₃ solution (150 ml), dried over Na₂SO₄ and concentrated under reduced pressure. The remaining residue was distilled under reduced pressure (22 ± 5 mbar) to afford the title compound as a colorless oil (3.73 g, 74%).

The title compound coevaporates with solvents such as THF, hexanes, *n*-hexane, CH₂Cl₂, CHCl₃ and EtOAc upon concentration under reduced pressure. Other solvents were not employed in combination with the title compound but are expected to show the same behavior.

b.p.: 61 °C ($p = 22$ mbar).

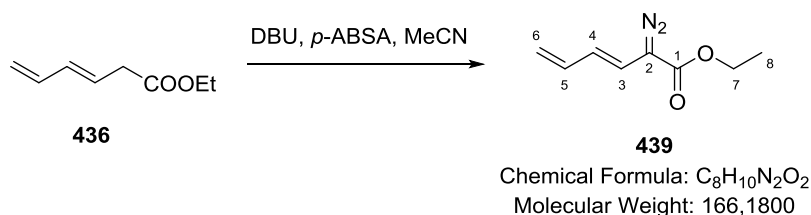
¹H NMR (300 MHz, CDCl₃): δ 6.34 (ddd, $J = 16.8, 10.2, 10.2$ Hz, 1H, C₅H), 6.20–6.08 (m, 1H, C₄H), 5.78 (dt, $J = 15.0, 7.2$ Hz, 1H, C₃H), 5.17 (dm, $J = 16.8$ Hz, 1H, *trans*-C₆H), 5.07 (dm, $J = 10.2$ Hz, 1H, *cis*-C₆H) 3.69 (s, 3H, C₇H₃), 3.13 (d, $J = 7.2$ Hz, 2H, C₂H₂) ppm.

¹³C NMR (75 MHz, CDCl₃): δ 172.0 (C1), 136.5 (C5), 134.6 (C4), 125.6 (C3), 117.2 (C6), 52.0 (C7), 37.9 (C2) ppm.

MS (EI, %): 126.18 (90, M⁺), 84.14 (100), 67.05 (96).

HRMS (EI, m/z): calc. [M⁺]: 126.0681; found: 126.0676 [M⁺].

IR $\tilde{\nu} = 3089$ (vw), 3002 (vw), 2954 (vw), 2845 (vw), 1737 (vs), 1654 (vw), 1604 (vw), 1436 (m), 1408 (vw), 1343 (w), 1306 (w), 1249 (m), 1192 (m), 1171 (s), 1065 (vw), 1003 (vs), 954 (m), 904 (m), 883 (w), 825 (w), 738 (vw), 708 (vw) cm⁻¹.

ethyl (*E*)-2-diazohepta-3,5-dienoate (**439**)

DBU (0.19 ml, 0.19 g, 1.3 mmol, 1.18 eq.) was added dropwise to a solution of compound **436** (160 μ l, 150 mg, 1.07 mmol) and *p*-ABSA (273 mg, 1.13 mmol, 1.06 eq.) in MeCN (2.3 ml) at -10°C . After 2 h, the reaction was treated with sat. aq. NH₄Cl (10 ml), extracted with Et₂O (2x40 ml), the combined organic phases washed with brine (25 ml) and dried over Na₂SO₄. The solvent was evaporated under reduced pressure and the crude product purified by column chromatography (18x2.5 cm, 2% Et₂O/hexanes, deactivated silica) to afford the title compound as a red oil (140 mg, 79%).

The title compound polymerizes at room temperature. It should therefore be stored frozen in benzene at -78°C .

TLC $R_f = 0.32$ (5% Et₂O/hexanes).

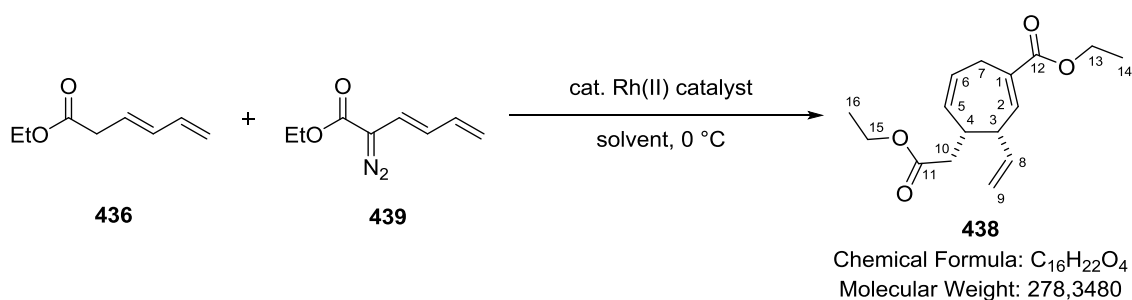
¹H NMR (600 MHz, CDCl₃): δ 6.46–6.39 (m, 1H, C₅H), 5.99–5.90 (m, 2H, C₃H, C₄H), 5.14–5.10 (m, 1H, *trans*-C₆H), 5.03–5.00 (m, 1H, *cis*-C₆H), 4.28 (q, $J = 7.2$ Hz, 2H, C₇H₂), 1.30 (t, $J = 7.2$ Hz, 3H, C₈H₃) ppm.

¹³C NMR (150 MHz, CDCl₃): δ 165.2 (C1), 136.3 (C5), 124.4 (C3/C4), 118.7 (C2), 115.3 (C3/C4), 115.3 (C6), 61.5 (C7), 14.6 (C8) ppm.

MS (EI, %): 166.17 (100), 121.15 (30), 92.15 (11), 64.12 (32).

HRMS (EI, m/z): calc. [M⁺]: 166.0742; found: 166.0743 [M⁺].

IR $\tilde{\nu} = 3089$ (vw), 2982 (vw), 2931 (vw), 2074 (vw), 2856 (vw), 2074 (vs), 1698 (vs), 1627 (m), 1597 (vw), 1478 (vw), 1465 (w), 1446 (w), 1421 (w), 1392 (w), 1369 (m), 1320 (vs), 1243 (vs), 1218 (w), 1167 (vs), 1123 (m), 1099 (vs), 996 (vs), 934 (m), 892 (m), 873 (m), 838 (w), 786 (w), 760 (w), 739 (s), 673 (w) cm⁻¹.

ethyl (3*R*,4*R*)-4-(2-ethoxy-2-oxoethyl)-3-vinylcyclohepta-1,5-diene-1-carboxylate (**438**)

Racemic procedure:

To a solution of diene **436** (5.7 ml, 5.4 g, 38 mmol, 8.0 eq.) and $\text{Rh}_2(\text{OAc})_4$ (21 mg, 0.048 mmol, 0.01 eq.) in CH_2Cl_2 (95 ml) was slowly added a solution of vinyl diazo compound **439** (793 mg, 1.56 mmol) in CH_2Cl_2 (55 ml) *via* syringe pump (18 ml/hr) at 0 °C. After stirring the reaction for 15 min after the addition was complete, the mixture concentrated under reduced pressure. The crude product was purified by flash column chromatography (13x7 cm, deactivated silica, 2–4–6–10% EtOAc/hexanes) and the mixed fraction resubjected to flash column chromatography (2–3–4% EtOAc/hexanes) to afford the title compound as a yellowish oil (668 mg, 50%).

Yield is given for product after 2 flash column chromatographies. Yet, mixed fractions still existed afterwards (not included).

Asymmetric procedure (absolute configuration not verified):

To a solution of diene **436** (2.4 ml, 2.2 g, 16 mmol, 10.0 eq.) and $\text{Rh}_2(R\text{-DOSP})_4$ (weighed out and stored in glove box, 30 mg, 0.016 mmol, 0.01 eq.) in deaerated *n*-hexane (31 ml, deaerated by 2xFPT) was slowly added a solution of vinyl diazo compound **439** (260 mg, 1.56 mmol) in deaerated *n*-hexane (31 ml) *via* syringe pump (12 ml/hr) at 0 °C. After stirring the reaction for 15 min after the addition was complete, the mixture was filtered over a silica plug (4x3.5 cm, deactivated silica, 5 % EtOAc/hexanes) and concentrated under reduced pressure. The crude product was purified by flash column chromatography (19x3.5 cm, deactivated silica, 2–3–4% EtOAc/hexanes) to afford the title compound as a yellowish oil (273 mg, 63%, 82% ee).

TLC $R_f = 0.49$ (10% EtOAc/hexanes).

^1H NMR (300 MHz, CDCl_3): δ 6.93 (dd, $J = 6.6, 1.9$ Hz, 1H, C_2H), 5.85–5.70 (m, 2H, C_4H , C_6H), 5.55 (ddd, $J = 11.2, 5.7, 2.4$ Hz, 1H, C_5H), 5.20–5.11 (m, 2H, *cis*- C_9H , *trans*- C_9H), 4.18 (q, $J = 7.2$ Hz, 2H, $2\times\text{C}_{13}\text{H}$), 4.12 (q, $J = 7.2$ Hz, 2H, $2\times\text{C}_{15}\text{H}$), 3.37–3.28 (m, 1H, C_3H), 3.25–3.19 (m, 2H, $2\times\text{C}_7\text{H}$), 3.18–3.09 (m, 1H, C_4H), 2.43 (dd, $J = 15.3, 6.3$ Hz, 1H, C_{10}H), 2.31 (dd, $J = 15.3, 8.9$ Hz, 1H, C_{10}H), 1.29 (t, $J = 7.0$ Hz, 3H, C_{14}H_3), 1.25 (t, $J = 7.2$ Hz, 3H, $3\times\text{C}_{16}\text{H}_3$) ppm.

^{13}C NMR (75 MHz, CDCl_3): δ 172.6 (C11), 167.7 (C12), 142.6 (C2), 136.6 (C8), 133.0 (C5), 131.3 (C1), 127.6 (C6), 117.7 (C9), 61.0 (C13), 60.6 (C15), 46.0 (C3), 37.7 (C10), 37.4 (C4), 26.9 (C7), 14.4 (C14), 14.4 (C16) ppm.

MS (EI, %): 278.22 (12, M^+), 249.19 (21), 232.18 (77), 191.17 (34), 158.14 (65), 131.14 (80), 117.11 (100), 91.09 (56).

HRMS (EI, m/z): calc. $[\text{M}^+]$: 278.1518; found: 178.1505 $[\text{M}^+]$.

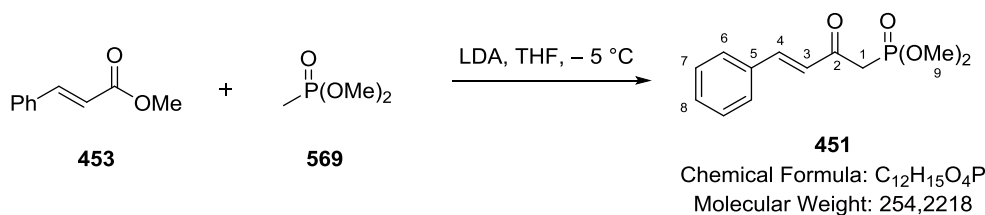
IR $\tilde{\nu} = 3079$ (vw), 2980 (w), 2928 (vw), 2854 (vw), 1732 (s), 1706 (vs), 1645 (vw), 1590 (vw), 1464 (w), 1446 (w), 1417 (vw), 1391 (w), 1370 (w), 1352 (vw), 1277 (m), 1237

(vs), 1197 (s), 1159 (s), 1095 (m), 1053 (m), 1029 (m), 996 (m), 920 (m), 861 (w), 827 (vw), 810 (w), 707 (w), 690 (w), 662 (w) cm^{-1} .

OR $[\alpha]_{\text{D}}^{21} = +78.9^\circ$ (11 mg/ml, CHCl_3) (82% ee).

Chiral HPLC $R_t = 18.59$ min (major); $R_t = 20.16$ (minor) (Nucleocel Delta S, 0.5% *i*-PrOH/*n*-hexane, $\lambda = 220\text{nm}$), 82% ee.

dimethyl (*E*)-(2-oxo-4-phenylbut-3-en-1-yl)phosphonate (451**)**^[314]



n-BuLi (2.45 M, 5.3 ml, 13 mmol, 2.1 eq.) was added dropwise to a solution of DIPA (1.82 ml, 1.31 g, 12.9 mmol, 2.1 eq.) in THF (7 ml) at -78°C and stirred for 20 min. The solution was warmed to 0°C and added to a solution of **453** (1.0 g, 6.2 mmol, 1 eq.) and phosphonate **569** (0.76 ml, 0.84 g, 6.8 mmol, 1.1 eq.) in THF (10 ml) at -5°C . After 45 min, the reaction was treated with aq. HCl solution ($c = 5$ M, 6 ml) to a pH of 4–5 and extracted with EtOAc (3x25 ml). The combined organic phases were washed with H_2O (50 ml) and brine (50 ml), dried over Na_2SO_4 and concentrated under reduced pressure. The crude product was purified by column chromatography (13x6.5 cm, 5% MeOH/ CH_2Cl_2) to afford the title compound as a yellow oil (1.50 g, 96%).

TLC $R_f = 0.29$ (5% MeOH/ CH_2Cl_2).

^1H NMR (**300 MHz**, CDCl_3): δ 7.64 (d, $J = 16.2$ Hz, 1H, C_4H), 7.60–7.55 (m, 2H, $\text{C}_{\text{Ar}}\text{H}$), 7.43–7.37 (m, 3H, $\text{C}_{\text{Ar}}\text{H}$), 6.87 (1H, $J = 16.2$ Hz, 1H, C_3H), 3.80 (d, $^3J_{\text{HP}} = 11.2$ Hz, 6H, $2\times\text{C}_9\text{H}_3$), 3.33 (d, $^2J_{\text{HP}} = 22.8$ Hz, 2H, C_1H_2) ppm.

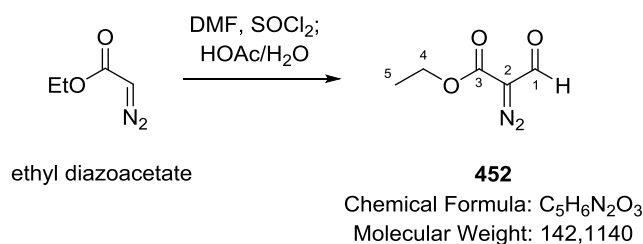
^{13}C NMR (**75 MHz**, CDCl_3): δ 191.0 (d, $^2J_{\text{C-P}} = 6.2$ Hz, C2), 145.2 (C4), 134.2, 131.1, 129.1, 128.8, 125.8 (d, $^3J_{\text{CP}} = 1.6$ Hz, C3), 53.3 (d, $^2J_{\text{CP}} = 6.5$ Hz, C9), 40.1 (d, $^1J_{\text{CP}} = 129.1$ Hz, C1) ppm.

^{31}P NMR (**162 MHz**, CDCl_3): δ 22.9 ppm.

MS (**EI**, %): 254.21 (12, M^+), 144.17 (100), 131.15 (60), 103.15 (24)

HRMS (**EI**, **m/z**): calc. $[\text{M}^+]$: 254.0708; found: 254.0708 $[\text{M}^+]$.

IR $\tilde{\nu} = 3468$ (br, vw), 3028 (vw), 2957 (vw), 2854 (vw), 1686 (v), 1654 (m), 1607 (m), 1576 (w), 1496 (vw), 1450 (w), 1404 (vw), 1333 (w), 1254 (m), 1208 (w), 1185 (w), 1029 (vs), 983 (w), 930 (vw), 881 (vw), 837 (w), 803 (w), 762 (vw), 735 (vw), 693 (w) cm^{-1} .

ethyl 2-diazo-3-oxopropanoate (452)^[351]

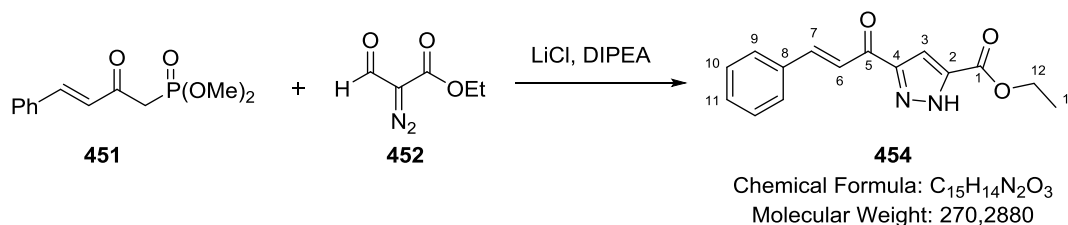
DMF (0.39 ml, 0.37 g, 5.0 mmol, 1.0 eq.) was treated with SOCl₂ (0.36 ml, 0.59 g, 5.0 mmol, 1.0 eq.) and the reaction mixture was heated to 40 °C. After 2 h, the solvent was removed under high vacuum and the remaining solid dissolved in CHCl₃ (2.2 ml). Ethyl diazoacetate (13 wt-% CH₂Cl₂, 1.2 ml, 1.3 g, 10 mmol, 2.0 eq.) was added dropwise at 0 °C and the reaction mixture was warmed to rt after the addition was complete. After 1 h, the solvent was removed under reduced pressure, the resulting precipitate washed with Et₂O (3 ml) and stirred in HOAc/H₂O (10%) for 14 h. The reaction mixture was extracted with Et₂O (3x10 ml), the combined organic phases washed with sat. aq. NaHCO₃ solution (10 ml), 10% aq. H₂SO₄ (10 ml), brine (10 ml) and dried over Na₂SO₄ to afford the title compound as a yellow oil (359 mg, 50%). MS spectral analysis failed for this compound.

TLC R_f = 0.48 (20% EtOAc/hexanes).

¹H NMR (300 MHz, CDCl₃): δ 9.70 (s, 1H, C₁H), 4.36 (q, J = 7.1 Hz, 2H, C₄H₂), 1.35 (t, J = 7.1 Hz, 3H, C₅H₃) ppm.

¹³C NMR (75 MHz, CDCl₃): δ 197.6 (C1), 181.5 (C3), 161.4 (C2), 62.1 (C4), 14.5 (C5) ppm.

IR $\tilde{\nu}$ = 2986 (vw), 2940 (vw), 2873 (vw), 2139 (s), 1707 (vs), 1660 (vs), 1467 (vw), 1448 (vw), 1401 (w), 1386 (w), 1369 (w), 1290 (vs), 1231 (vs), 1174 (w), 1113 (s), 1011 (m), 860 (w), 843 (w), 796 (m), 779 (m), 764 (m), 740 (s) cm⁻¹.

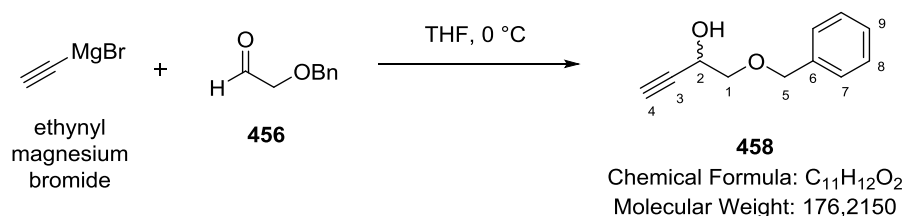
ethyl 3-cinnamoyl-1H-pyrazole-5-carboxylate (454)

LiCl (dried at 140 °C on HV overnight, stored in glove box, 121 mg, 2.85 mmol, 2.0 eq.), phosphonate **451** (738 mg, 2.90 mmol, 2.0 eq.) and diazo ester **452** (215 mg, 1.51 mmol) were dissolved in MeCN (10.4 ml) and DIPEA (0.51 ml, 0.38 g, 2.85 mmol, 2.0 eq.) was introduced. The resulting mixture was stirred for 18 h. H₂O (20 ml) was added and the aqueous layer was extracted with Et₂O (5x30 ml). The combined organic phases were washed with brine (100 ml), dried over

Na_2SO_4 and concentrated under reduced pressure. The residue was purified by flash column chromatography (16x3.5 cm, 30–50–60% EtOAc/hexanes) to afford the product as a yellow solid (61 mg, 15%). X-Ray suitable crystals were obtained by slow diffusion of hexanes into a solution of the title compound in EtOAc.

TLC	$R_f = 0.58$ (50% EtOAc/hexanes).
m.p.:	124–126 °C.
^1H NMR	(600 MHz, CDCl_3): δ 7.96 (d, $J = 15.9$ Hz, 1H, C_7H), 7.70–7.66 (m, 2H, $\text{C}_{\text{Ar}}\text{H}$), 7.64–7.55 (m, 1H, C_3H), 7.45 (d, $J = 15.9$ Hz, 1H, C_6H), 7.44–7.41 (m, 3H, $\text{C}_{\text{Ar}}\text{H}$), 4.45 (q, $J = 7.2$ Hz, 2H, C_{12}H_2), 1.43 (t, $J = 7.2$ Hz, 3H, C_{13}H_3) ppm.
^{13}C NMR	(150 MHz, CDCl_3): δ 181.8 (C5), 160.4 (C1), 145.5 (C7), 134.6 (C8), 131.2 (CAr), 129.2 (CAr), 128.9 (CAr), 121.5 (C3), 110.2 (C6), 61.9 (C12), 14.4 (C13) ppm. C2 and C4 missing.
MS	(EI, %): 270.21 (100, M^+), 269.21 (68), 224.16 (25), 195.15 (15), 103.10 (19).
HRMS	(EI, m/z): calc. $[\text{M}^+]$: 270.1004; found: 270.0999 $[\text{M}^+]$.
IR	$\tilde{\nu} = 3218$ (vw), 3145 (vw), 3083 (vw), 2981 (vw), 1721 (m), 1662 (m), 1595 (s), 1575 (m), 1495 (w), 1469 (m), 1448 (m), 1403 (w), 1385 (w), 1361 (w), 1330 (w), 1300 (m), 1281 (m), 1221 (s), 1204 (s), 1131 (m), 1095 (w), 1067 (w), 1039 (m), 1019 (m), 988 (s), 970 (s), 907 (m), 884 (m), 851 (m), 764 (vs), 725 (vs), 685 (vs) cm^{-1} .

1-(benzyloxy)but-3-yn-2-ol (**458**)^[316]

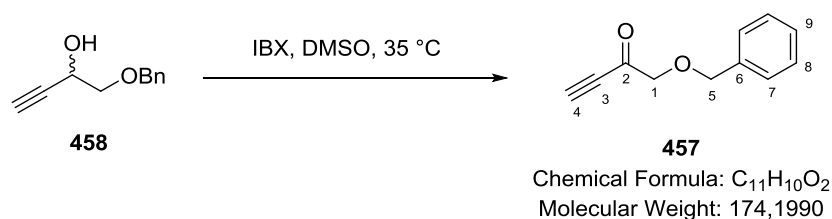


Ethynylmagnesium bromide ($c = 0.5$ M in THF, 7.3 ml, 3.7 ml, 1.1 eq.) was added fast dropwise to a solution of aldehyde **456** (0.47 ml, 0.50 g, 3.3 mmol) in THF (24 ml) at 0 °C. The reaction was warmed to rt and stirred for 2 h. After treatment with sat. aq. NH_4Cl solution (25 ml), the mixture was extracted with EtOAc (3x70 ml), the combined organic phases washed with brine (100 ml), dried over Na_2SO_4 and concentrated under reduced pressure. The crude product was purified by column chromatography (15x2.5 cm, 20–30% EtOAc/hexanes) to afford the title compound as a colorless oil (488 mg, 84%).

TLC	$R_f = 0.46$ (30% EtOAc/hexanes).
^1H NMR	(300 MHz, CDCl_3): δ 7.41–7.26 (m, 5H, $\text{C}_{\text{Ar}}\text{H}$), 4.65 (d, $J = 12.1$ Hz, 1H, C_5H), 4.60 (d, $J = 12.1$ Hz, 1H, C_5H), 4.56 (ddd, $J = 6.9, 3.7, 2.2$ Hz, 1H, C_2H), 3.67 (dd, $J = 9.7,$

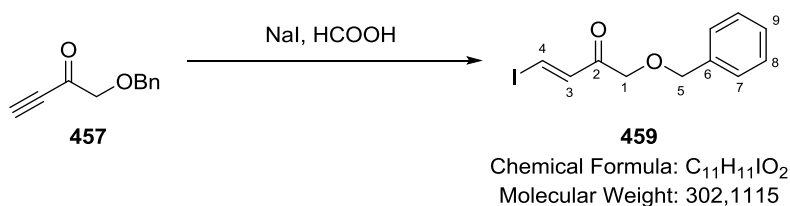
	3.7 Hz, 1H, C ₁ H), 3.59 (dd, <i>J</i> = 9.7, 7.1 Hz, 1H, C ₁ H), 2.65–2.14 (brs, 1H, C ₂ OH), 2.46 (d, <i>J</i> = 2.2 Hz, 1H, C ₄ H) ppm.
¹³C NMR	(75 MHz, CDCl₃): δ 137.6 (C6), 128.7 (CAr), 128.1 (CAr), 128.0 (CAr), 81.8 (C3), 73.7 (C4), 73.6 (C5), 73.5 (C1), 61.7 (C2) ppm.
MS	(EI, %): 176.06 (2), 146.15 (2), 117.12 (3), 91.09 (100).
HRMS	(EI, m/z): calc. [M ⁺]: 176.0837; found: 176.0842 [M ⁺].
IR	$\tilde{\nu}$ = 3403 (vw), 3287 (w), 3088 (vw), 3060 (vw), 3031 (vw), 2911 (vw), 2866 (vw), 2117 (vw), 1496 (vw), 1454 (w), 1391 (w), 1362 (w), 1313 (w), 1252 (w), 1206 (w), 1107 (s), 1072 (vs), 942 (w), 919 (w), 878 (w), 809 (w), 737 (vs), 697 (vs) cm ⁻¹ .

1-(benzyloxy)but-3-yn-2-one (**457**)^[316]



IBX (3.47 g, 12.4 mmol, 4.7 eq.) was suspended in DMSO (100 ml) and alcohol **458** (465 mg, 2.64 mmol) in DMSO (3 ml) was added. The reaction mixture was heated to 35 °C for 17 h and then treated with H₂O (12 ml). The mixture was cooled to 0 °C, H₂O (20 ml) was added and the resulting precipitate filtered off. The filtrate was extracted with Et₂O (2x125 ml), the combined organic phases washed with H₂O (3x100 ml), sat. aq. NaHCO₃ (100 ml), brine (100 ml) and dried over Na₂SO₄. After concentration under reduced pressure, the title compound was obtained as a colorless oil (427 mg, 93%) which was used without further purification.

TLC	R _f = 0.54 (20% EtOAc/hexanes).
¹H NMR	(300 MHz, CDCl₃): δ 7.41–7.27 (m, 5H, C _{Ar} H), 4.65 (s, 2H, C ₅ H ₂), 4.24 (s, 2H, C ₁ H), 3.31 (s, 1H, C ₄ H) ppm.
¹³C NMR	(75 MHz, CDCl₃): δ 184.6 (C2), 137.0 (C6), 128.7 (CAr), 128.3 (CAr), 128.2 (CAr), 81.4 (C4), 79.6 (C3), 75.9 (C1), 73.7 (C5) ppm.
MS	(EI, %): 143.10 (2), 116.10 (8), 107.08 (63), 91.08 (100), 65.04 (10).
HRMS	(EI, m/z): calc. [M ⁺]: 174.0681 ; found: 173.0597 [M–H ⁺].
IR	$\tilde{\nu}$ = 3261 (vw), 3090 (vw), 3064 (vw), 3033 (vw), 2926 (vw), 2869 (vw), 2092 (m), 1697 (s), 1683 (s), 1604 (vw), 1585 (vw), 1496 (vw), 1455 (w), 1417 (vw), 1389 (vw), 1359 (vw), 1338 (vw), 1314 (vw), 1260 (vw), 1243 (vw), 1205 (w), 1177 (w), 1155 (w), 1065 (vs), 1028 (m), 942 (w), 909 (w), 837 (vw), 824 (vw), 738 (vs), 697 (vs) cm ⁻¹ .

(*E*)-1-(benzyloxy)-4-iodobut-3-en-2-one (459)

NaI (0.94 g, 6.3 mmol, 3.0 eq.) was added to compound **457** (365 mg, 2.09 mmol) in formic acid (21 ml). After stirring for 2 h, the reaction was treated with H₂O (30 ml) and sat. aq. NaHCO₃ (25 ml) and poured onto sat. aq. NaHCO₃ (40 ml) at 0 °C. The mixture was extracted with EtOAc (2x100 ml), washed with sat. aq. NaHCO₃ (100 ml), brine (50 ml) and dried over Na₂SO₄. After concentration of the organic phase under reduced pressure, the residue was subjected to column chromatography (16x3.5 cm, 4–5 % EtOAc/hexanes) to afford the title compound as a yellow oil (502 mg, 81%).

TLC R_f = 0.17 (5% EtOAc/hexanes).

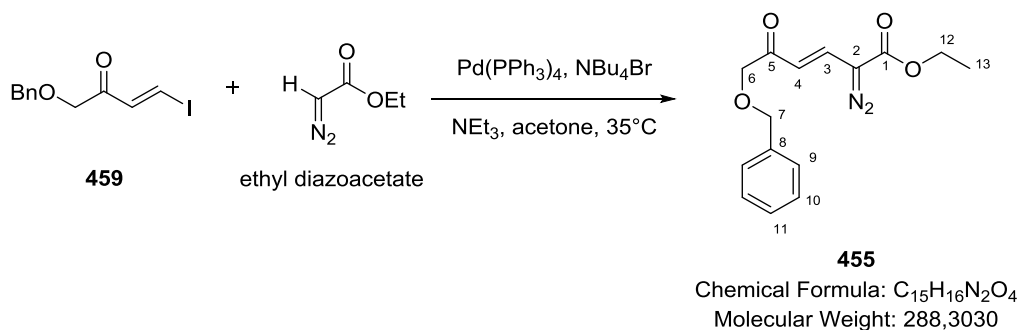
¹H NMR (300 MHz, CDCl₃): δ 8.00 (d, J = 15.0 Hz, 1H, C₄H), 7.42–7.28 (m, 6H, C₃H, C_{Ar}H), 4.60 (s, 2H, C₅H₂), 4.16 (s, 2H, C₁H₂) ppm.

¹³C NMR (75 MHz, CDCl₃): δ 194.5 (C2), 140.7 (C3), 137.0 (C6), 128.7 (CAr), 128.3 (CAr), 128.2 (CAr), 101.1 (C4), 73.9 (C1), 73.7 (C5) ppm.

MS (EI, %): 303.13 (1), 196.02 (44), 181.04 (100), 153.04 (14), 127.01 (6), 91.14 (31)

HRMS (EI, m/z): calc. [M⁺]: 301.9804; found: 301.9872 [M⁺].

IR $\tilde{\nu}$ = 3062 (vw), 3032 (vw), 2922 (w), 2855 (w), 1707 (m), 1691 (s), 1559 (vs), 1496 (w), 1454 (w), 1433 (vw), 1389 (vw), 1368 (vw), 1289 (m), 1202 (m), 1099 (s), 1053 (s), 1028 (m), 948 (vs), 907 (w), 868 (w), 820 (vw), 736 (vs), 697 (vs) cm⁻¹.

ethyl (*E*)-6-(benzyloxy)-2-diazo-5-oxohex-3-enoate (455)

Pd(PPh₃)₄ (39 mg, 0.034 mmol, 0.05 eq.) was added to a solution of compound **459** (205 mg, 0.679 mmol), NEt₃ (0.14 ml, 1.0 mmol, 1.5 eq.), NBu₄Br (0.22 g, 0.68 mmol, 1.0 eq.) and ethyl diazoacetate (13% CH₂Cl₂, 0.21 ml, 0.22 g, 1.7 mmol, 2.5 eq.) in deaerated acetone (3.4 ml) and heated to 35 °C for 30 min. CH₂Cl₂ (10 ml) was added the reaction mixture and the solvents were

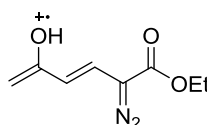
removed under reduced pressure. The crude product was purified by column chromatography (15x3.5 cm, 7–10–15% EtOAc/*n*-pentane, deactivated silica) to afford the title compound as an orange oil (88 mg, 45%).

TLC $R_f = 0.13$ (10% EtOAc/hexanes).

^1H NMR (300 MHz, CDCl_3): δ 7.45 (d, $J = 15.7$ Hz, 1H, C_3H), 7.39–7.27 (m, 5H, $\text{C}_{\text{Ar}}\text{H}$), 6.34 (d, $J = 15.7$ Hz, 1H, C_4H), 4.61 (s, 2H, C_7H_2), 4.32 (q, $J = 7.1$ Hz, 2H, C_{12}H_2), 4.18 (s, 2H, C_6H_2), 1.32 (t, $J = 7.1$ Hz, 3H, C_{13}H_3) ppm.

^{13}C NMR (75 MHz, CDCl_3): δ 195.3 (C5), 163.1 (C1), 137.3 (C8), 130.9 (C3), 128.7 (CAr), 128.2 (CAr), 128.1 (CAr), 115.4 (C4), 74.7 (C6), 73.6 (C7), 66.8 (C2), 62.2 (C12), 14.5 (C13) ppm.

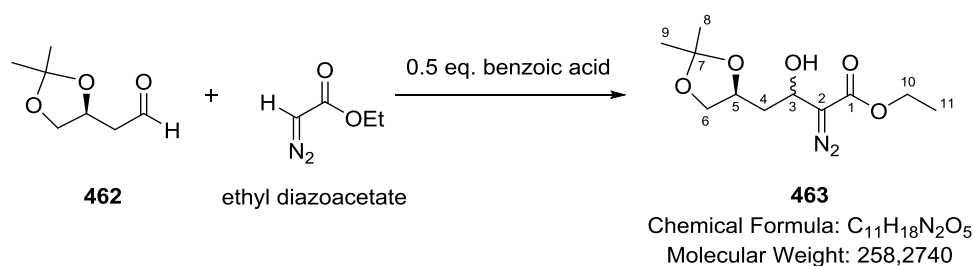
MS (EI, %): molecule not detected, instead McLafferty rearrangement: 182.17 (56), 154.19 (72), 91.17 (100).



Chemical Formula: $\text{C}_8\text{H}_{10}\text{N}_2\text{O}_3^{++}$
Molecular Weight: 182,1761

IR $\tilde{\nu} = 3032$ (vw), 2983 (vw), 2868 (vw), 2096 (s), 1703 (vs), 1574 (vs), 1497 (vw), 1454 (w), 1395 (w), 1373 (m), 1340 (w), 1287 (s), 1235 (vs), 1207 (s), 1190 (s), 1174 (s), 1102 (vs), 1061 (s), 1014 (s), 968 (m), 909 (m), 870 (w), 820 (w), 737 (vs), 698 (vs), 674 (w) cm^{-1} .

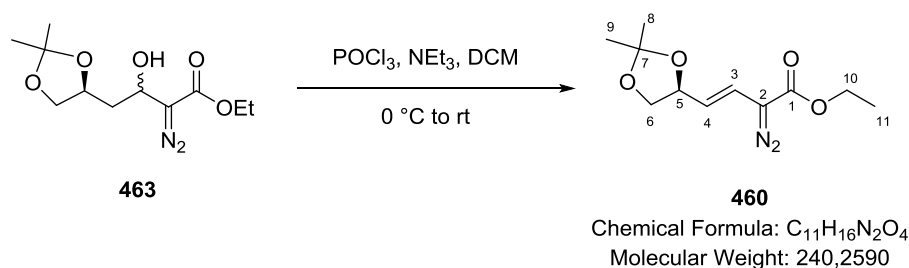
ethyl 2-diazo-4-((*S*)-2,2-dimethyl-1,3-dioxolan-4-yl)-3-hydroxybutanoate (**463**)



Benzoic acid (1.08 g, 8.84 mmol, 0.5 eq.) was added to a mixture of aldehyde **462** (2.55 g, 17.7 mmol) and ethyl diazoacetate (contains approx. 13–20% CH_2Cl_2 , 3.0 ml, 3.2 g, 19 mmol, 1.1 eq) in CH_2Cl_2 (1 ml) in a water bath. The water bath was removed after 5 min and the reaction mixture was allowed to stir for 13 h. The crude reaction mixture was directly purified by flash column chromatography (17x4.5 cm, deactivated silica, 20–25–30% EtOAc/hexanes) to afford the title compound as a yellow oil (2.97 g, dr 1:1, 65%).

TLC	$R_f = 0.15$ (20% EtOAc/hexanes).
^1H NMR	(600 MHz, CDCl_3): NMR data refers to both diastereoisomer δ 4.89 (dd, $J = 8.9, 3.5$ Hz, 1H, C_3H), 4.82 (dd, $J = 8.7, 4.4$ Hz, 1H, C_3H), 4.37–4.32 (m, 1H, C_5H), 4.32–4.27 (m, 1H, C_5H), 4.26–4.21 (m, 4H, $2\times\text{C}_{10}\text{H}$, $2\times\text{C}_{10}\text{H}$), 4.11 (dd, $J = 8.2, 6.1$ Hz, 1H, C_6H), 4.11 (dd, $J = 8.3, 6.1$ Hz, C_6H), 3.64–3.59 (m, 2H, C_6H , C_6H), 3.44 (brs, 1H, C_3OH), 3.04 (brs, 1H, C_3OH), 2.00–1.86 (m, 4H, $2\times\text{C}_4\text{H}$, $2\times\text{C}_4\text{H}$), 1.43 (s, 3H, C_8H_3), 1.42 (s, 3H, C_9H_3), 1.36 (s, 3H, C_8H_3), 1.36 (s, 3H, C_9H_3), 1.28 (t, $J = 7.2$ Hz, 3H, C_{11}H_3), 1.28 (t, $J = 7.2$ Hz, 3H, C_{11}H_3) ppm.
^{13}C NMR	(150 MHz, CDCl_3): δ 166.4 (C1), 166.1 (C1), 109.8 (C7), 109.3 (C7), 74.6 (C5), 73.2 (C5), 69.5 (C6), 69.5 (C6), 65.4 (C3), 64.1 (C3), 61.1 (C10), 61.1 (C10), 38.8 (C4), 38.0 (C4), 27.0 (C8/C9), 27.0 (C8/C9), 25.8 (C8/C9), 25.8 (C8/C9), 14.6 (C11), 14.6 (C11) ppm. C2 not detected.
MS	(EI, %): 215.14 (64 M- C_3H_6), 169.11 (35), 155.13 (100, M- $\text{C}_3\text{H}_6\text{N}_2$), 127.10 (37), 101.13 (44).
IR	$\tilde{\nu} = 3448$ (br, vw), 2986 (w), 2934 (w), 2875 (vw), 2092 (s), 1741 (w), 1687 (vs), 1456 (w), 1396 (w), 1371 (vs), 1291 (s), 1246 (s), 1217 (s), 1157 (s), 1109 (s), 1060 (vs), 1028 (s), 974 (w), 920 (w), 839 (m), 791 (w), 742 (m), 704 (vw) cm^{-1} .

ethyl (*S,E*)-2-diazo-4-(2,2-dimethyl-1,3-dioxolan-4-yl)but-3-enoate (460**)**

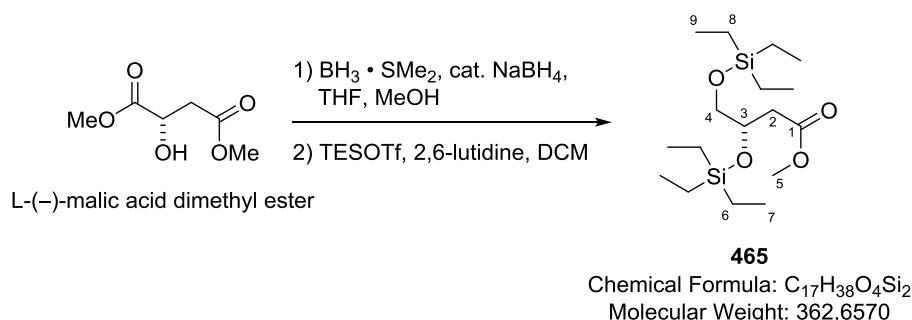


To a solution of alcohol **463** (5.93 g, 23.0 mmol) in CH_2Cl_2 (115 ml) was added NEt_3 (12.8 ml, 9.29 g, 9.18 mmol, 4.0 eq.) at 0 $^\circ\text{C}$. A solution of POCl_3 (3.2 ml, 5.3 g, 34 mmol, 1.5 eq.) in CH_2Cl_2 (75 ml) was slowly introduced *via* syringe pump over 3 h. The reaction mixture was subsequently warmed to rt, stirred for 12 h and then washed with H_2O (2x300 ml). The collected aqueous phase was extracted with CH_2Cl_2 (1x300 ml) and the combined organic phases washed with brine (500 ml), dried over Na_2SO_4 and concentrated under reduced pressure. The crude product was purified by flash column chromatography (15x6.5 cm, deactivated silica, 3–4–7–10–20–30–50% EtOAc/hexanes) to afford the title compound as a yellow oil (4.08 g, 74%).

The title compound is light sensitive and polymerizes at room temperature. Therefore, it was stored in frozen benzene at $-78\text{ }^\circ\text{C}$.

TLC	$R_f = 0.22$ (5% EtOAc/hexanes).
^1H NMR	(300 MHz, CDCl_3): δ 6.15 (dd, $J = 15.8, 0.8$ Hz, 1H, C_3H), 5.31 (dd, $J = 15.8, 7.8$ Hz, C_4H), 4.63 (dddd, $J = 7.8, 7.8, 6.1, 0.8$ Hz, 1H, C_5H), 4.27 (q, $J = 7.2$ Hz, 2H, $2\times\text{C}_{10}\text{H}$), 4.10 (dd, $J = 8.2, 6.1$ Hz, 1H, C_6H), 3.59 (dd, $J = 8.2, 7.8$ Hz, 1H, C_6H), 1.43 (s, 3H, C_9H_3), 1.39 (s, 3H, C_{10}H_3), 1.29 (t, $J = 7.2$ Hz, 3H, C_{11}H_3) ppm.
^{13}C NMR	(75 MHz, CDCl_3): δ 164.8, 120.6 (C4), 117.8 (C3), 109.5 (C7), 77.1 (C5), 69.7 (C6), 61.5 (C10), 26.9 (C9), 26.0 (C10), 14.6 (C11) ppm. C2 not detected.
MS	(EI, %): 240.23 (12, M^+), 197.19 (10), 125.15 (9), 109.13 (23), 81.13 (31), 53.10 (24), 43.10 (100).
HRMS	(EI, m/z): calc. $[\text{M}^+]$: 240.1110; found: 240.1102 $[\text{M}^+]$.
IR	$\tilde{\nu} = 2985$ (w), 2936 (vw), 2874 (vw), 2082 (vs), 1698 (vs), 1647 (w), 1456 (vw), 1396 (w), 1370 (s), 1306 (s), 1236 (vs), 1214 (s), 1148 (vs), 1099 (s), 1057 (vs), 1023 (s), 952 (m), 917 (vw), 862 (m), 812 (vw), 790 (w), 739 (m) cm^{-1} .
OR	$[\alpha]_{\text{D}}^{23} = +12.0^\circ$ (4 mg/ml, CHCl_3).

methyl (S)-3,4-bis((triethylsilyl)oxy)butanoate (**465**)

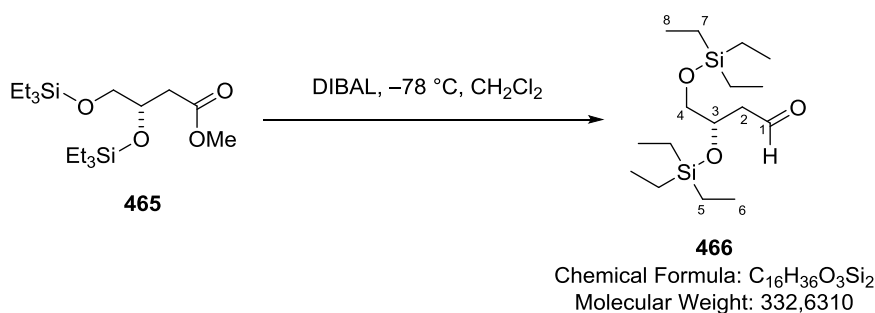


To a solution of L-(-)-malic acid dimethyl ester (**464**, 0.66 ml, 0.81 g, 5.0 mmol) in THF (5 ml) was added $\text{BH}_3\cdot\text{SMe}_2$ ($c = 2$ M in THF, 2.6 ml, 5.3 mmol, 1.05 eq.) at rt and the resulting solution was stirred for 1 h. Then, NaBH_4 (10 mg, 0.25 mmol, 0.05 eq.) was added and stirring was continued for 45 min. The reaction mixture was treated with MeOH (10 ml) and concentrated under reduced pressure. The crude product was purified by flash column chromatography (13x3.5 cm, 2–5–7% MeOH/ CH_2Cl_2) to afford a diol, which was dissolved in CH_2Cl_2 (20 ml). 2,6-lutidine (1.9 ml, 1.7 g, 16 mmol, 3.2 eq.) and TESOTf (2.5 ml, 2.9 g, 11 mmol, 2.2 eq.) were successively added to the solution and the reaction mixture was stirred for 16 h. The solution was then treated with aq. HCl (2 M, 2 ml) and H_2O (16 ml), the aqueous phase extracted with CH_2Cl_2 (2x30 ml), the combined organic phases dried over Na_2SO_4 and concentrated under reduced pressure. The crude product was purified by flash column chromatography (11x3.5 cm, 5% EtOAc/hexanes) to afford the title compound as a colorless oil (1.87 g, 103%).

TLC $R_f = 0.41$ (5% EtOAc/hexanes).

- ^1H NMR** (300 MHz, CDCl_3): δ 4.21–4.12 (m, 1H, C_3H), 3.67 (s, 3H, C_5H_3), 3.60 (dd, $J = 9.9$, 4.9 Hz, 1H, C_4H), 3.41 (dd, $J = 9.9$, 7.5 Hz, 1H, C_4H), 2.66 (dd, $J = 15.0$, 4.9 Hz, 1H, C_2H), 2.38 (dd, $J = 15.0$, 7.5 Hz, 1H, C_2H), 0.97–0.92 (m, 18H, $3\times\text{C}_7\text{H}_3$, $3\times\text{C}_9\text{H}_3$), 0.64–0.55 (m, 12H, $3\times\text{C}_6\text{H}_2$, $3\times\text{C}_8\text{H}_2$) ppm. Sample contains impurities of residual TESOTES.
- ^{13}C NMR** (75 MHz, CDCl_3): δ 172.5 (C1), 70.4 (C3), 66.8 (C4), 51.6 (C5), 40.3 (C2), 6.9 (C7), 6.9 (C9), 5.0 (C6/C8), 4.5 (C6/C8) ppm.
- HRMS** ((+)-ESI, m/z): calc. 385.2201 [$\text{M}+\text{Na}^+$]; found: 385.2198 [$\text{M}+\text{Na}^+$].
- IR** $\tilde{\nu} = 2953$ (w), 2911 (w), 2876 (w), 1741 (m), 1458 (w), 1436 (vw), 1414 (vw), 1378 (vw), 1310 (vw), 1238 (w), 1190 (w), 1170 (w), 1117 (m), 1077 (s), 1003 (s), 975 (w), 882 (vw), 811 (w), 724 (vs), 672 (w) cm^{-1} .
- OR** $[\alpha]_{\text{D}}^{25} = -19.9^\circ$ (6.5 mg/ml, CHCl_3).

(S)-3,4-bis((triethylsilyl)oxy)butanal (466)



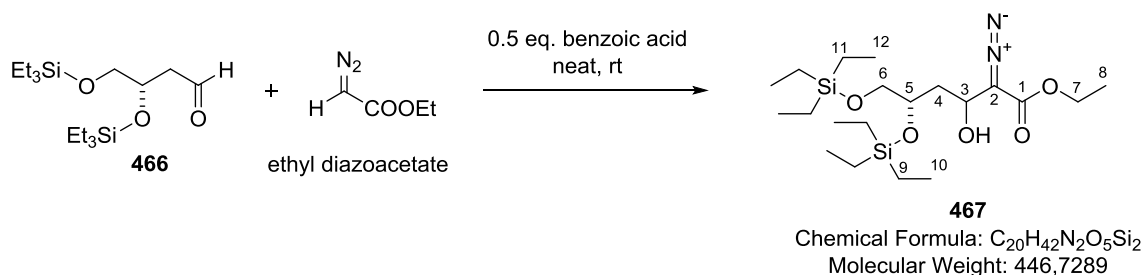
Methyl ester **465** (1.87 g, 5.16 mmol) was dissolved in CH_2Cl_2 (45 ml) and the solution was cooled to -78°C . A solution of DIBAL in toluene ($c = 1.0$ M in toluene, 5.7 ml, 5.7 mmol, 1.1 eq.) was added over 10 min and the reaction mixture was stirred for 1 h. MeOH (2.1 ml) and sat. aq. NH_4Cl solution (0.9 ml) were carefully added to the solution and the mixture was allowed to warm to rt. After 20 min, Et_2O (60 ml) was introduced and the organic phase dried over Na_2SO_4 , filtered and concentrated under reduced pressure. The crude product was purified by flash column chromatography (11x3.5 cm, deactivated silica, 2% EtOAc/hexanes) to afford the title compound as a colorless oil (1.64 g, 95%).

TLC $R_f = 0.45$ (5% EtOAc/hexanes).

^1H NMR (400 MHz, CDCl_3): δ 9.81 (dd, $J = 2.5$, 2.5 Hz, 1H, C_1H), 4.26–4.18 (m, 1H, C_3H), 3.65 (dd, $J = 9.9$, 5.1 Hz, 1H, C_4H), 3.45 (dd, $J = 9.7$, 7.0 Hz, 1H, C_4H), 2.66 (ddd, $J = 15.7$, 5.4, 2.5 Hz, 1H, C_2H), 2.51 (ddd, $J = 15.7$, 6.3, 2.5 Hz, 1H, C_2H), 0.98–0.92 (m, 18H, $3\times\text{C}_6\text{H}_3$, $3\times\text{C}_8\text{H}_3$), 0.65–0.55 (m, 12H, $3\times\text{C}_5\text{H}_2$, $3\times\text{C}_7\text{H}_2$) ppm.

- ^{13}C NMR** (100 MHz, CDCl_3): δ 201.8 (C1), 69.1 (C3), 66.9 (C4), 49.1 (C2), 6.9 (C6), 6.9 (C8), 5.0 (C5/C7), 4.4 (C5/C7) ppm.
- HRMS** ((+)-ESI, m/z): calc. $[\text{M}+\text{H}^+]$: 331.2125; found: 331.2119 $[\text{M}+\text{H}^+]$.
- IR** $\tilde{\nu}$ = 2953 (w), 2911 (w), 2876 (w), 1729 (w), 1457 (vw), 1413 (vw), 1379 (vw), 1321 (vw), 1238 (w), 1096 (m), 1002 (s), 972 (w), 811 (w), 781 (w), 724 (vs), 672 (m) cm^{-1} .
- OR** $[\alpha]_{\text{D}}^{25} = -13.57^\circ$ (7 mg/ml, CHCl_3).

(5S)-ethyl 2-diazo-3-hydroxy-5,6-bis((triethylsilyl)oxy)hexanoate (467)



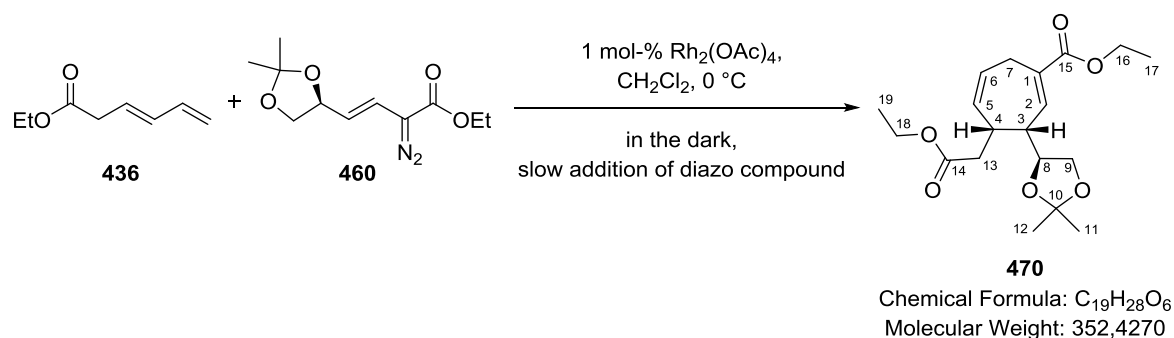
Benzoic acid (270 mg, 2.21 mmol, 0.5 eq.) was added to a mixture of aldehyde **466** (1.47 g, 4.43 mmol) and ethyl diazoacetate (contains 13–20 wt-% CH_2Cl_2 , 0.74 ml, 0.81 g, 4.87 mmol, 1.1 eq.) at rt. The reaction mixture was vigorously stirred for 21 h before pH 7.2 aq. phosphate buffer solution ($c = 1$ M, 5 ml) was added. The aqueous phase was extracted with CH_2Cl_2 (2x20 ml) and the combined organic phases were dried over Na_2SO_4 and concentrated under reduced pressure. The crude product was purified by flash column chromatography (15x3.5 cm, deactivated silica, 5–10% EtOAc/hexanes) to afford the title compound as yellow oil (1.55 g, 78%). The title compound was obtained as a mixture of diastereomers (dr 1.7:1).

NMR spectral data is provided for the major diastereomer.

- TLC** $R_f = 0.27$ (major) / 0.21 (5% EtOAc/hexanes).
- ^1H NMR** (600 MHz, CDCl_3): 4.90 (ddd, $J = 7.6, 4.4, 2.9$ Hz, 1H, C_3H), 4.24 (q, $J = 7.0$ Hz, 2H, $2\times\text{C}_7\text{H}$), 3.95–3.90 (m, 1H, C_5H), 3.70 (brs, 1H, OH), 3.61 (dd, $J = 10.1, 4.8$ Hz, 1H, C_6H), 3.47 (dd, $J = 10.1, 6.9$ Hz, 1H, C_6H), 2.00 (ddd, $J = 15.1, 4.4, 4.4$ Hz, 1H, C_4H), 1.84 (ddd, $J = 15.1, 7.6, 7.6$ Hz, 1H, C_4H), 1.28 (t, $J = 7.0$ Hz, 3H, C_8H_3), 0.98–0.93 (m, 18H, $3\times\text{C}_{10}\text{H}_3, 3\times\text{C}_{12}\text{H}_3$), 0.65–0.58 (m, 12H, $3\times\text{C}_9\text{H}_2, 3\times\text{C}_{11}\text{H}_2$) ppm.
- ^{13}C NMR** (150 MHz, CDCl_3): δ 166.2 (C1), 70.9 (C5), 66.4 (C6), 63.4 (C3), 60.8 (C7), 38.9 (C4), 14.5 (C8), 6.8 (C10/C12), 6.7 (C10/C12), 4.8 (C9/C11), 4.2 (C9/C11) ppm. C2 missing.
- HRMS** ((+)-ESI, m/z): calc. $[\text{M}+\text{Na}^+]$: 469.2530; found: 469.2520 $[\text{M}+\text{Na}^+]$.

IR $\tilde{\nu}$ = 3463 (vw), 2954 (w), 2911 (w), 2876 (w), 2092 (m), 1690 (m), 1458 (w), 1413 (w), 1372 (w), 1292 (m), 1238 (w), 1171 (vw), 1113 (m), 1079 (s), 1003 (s), 806 (w), 725 (vs), 672 (w) cm^{-1} .

ethyl (3*R*,4*R*)-3-((*S*)-2,2-dimethyl-1,3-dioxolan-4-yl)-4-(2-ethoxy-2-oxoethyl)cyclohepta-1,5-diene-1-carboxylate (470)



To a solution of diene **436** (0.17 ml, 0.16 g, 1.2 mmol, 10.0 eq.) and $\text{Rh}_2(\text{OAc})_4$ (1 mg, 0.002 mmol, 0.02 eq.) in CH_2Cl_2 (1.3 ml) was slowly added a solution of vinyl diazo compound **460** (28 mg, 0.12 mmol) in CH_2Cl_2 (1.2 ml) over 2 h *via* syringe pump at 0 °C. The reaction was stirred for 4 h, filtered through a silica plug (25% EtOAc/hexanes) and concentrated under reduced pressure. The crude product was purified by flash column chromatography (5–10–15–20% EtOAc/hexanes) to afford the title compound as a mixture of diastereomers as a colorless oil (21 mg, 50%, dr 2:1).

major diastereomer (470)

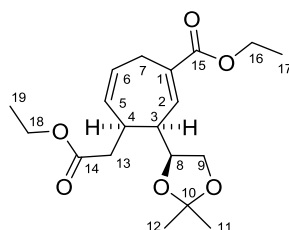
TLC R_f = 0.30 (15% EtOAc/hexanes).

^1H NMR (400 MHz, CDCl_3): δ 6.67 (dd, J = 6.7, 2.5 Hz, 1H, C_2H), 5.73 (ddd, J = 11.5, 5.7, 2.3 Hz, 1H, C_5H), 5.69–5.63 (m, 1H, C_6H), 4.18 (q, J = 7.2 Hz, 2H, $2\times\text{C}_{16}\text{H}$), 4.12 (q, J = 7.2 Hz, 2H, $2\times\text{C}_{18}\text{H}$), 4.20–4.17 (m, 1H, C_8H), 4.07 (dd, J = 8.1, 5.9 Hz, 1H, C_9H), 3.60 (dd, J = 8.1, 5.9 Hz, 1H, C_9H), 3.28 (dd, J = 16.4, 7.1 Hz, 1H, C_7H), 3.26–3.19 (m, 1H, C_4H), 3.21–3.16 (m, 1H, C_7H), 3.01–2.94 (m, 1H, C_3H), 2.56 (dd, J = 15.3, 5.1 Hz, 1H, C_{13}H), 2.32 (dd, J = 15.3, 10.1 Hz, 1H, C_{13}H), 1.41 (s, 3H, C_{11}H_3), 1.35 (s, 3H, C_{12}H_3), 1.29 (t, J = 7.2 Hz, 3H, C_{17}H_3), 1.25 (t, J = 7.2 Hz, 3H, C_{19}H_3) ppm.

^{13}C NMR (100 MHz, CDCl_3): δ 172.6 (C_{14}), 166.8 (C_{15}), 139.9 (C_2), 134.6 (C_1), 133.1 (C_5), 126.3 (C_6), 109.5 (C_{10}), 75.7 (C_8), 68.7 (C_9), 61.1 (C_{16}), 60.6 (C_{18}), 45.4 (C_3), 36.9 (C_{13}), 34.7 (C_4), 27.4 (C_7), 27.1 (C_{11}), 25.8 (C_{12}), 14.4 ($\text{C}_{17}/\text{C}_{19}$), 14.4 ($\text{C}_{17}/\text{C}_{19}$) ppm.

MS	(EI , %): 337.36 ($\text{M}-\text{CH}_3^+$, 4), 252.26 (10), 206.19 (12), 125.20 (16), 111.18 (28), 101.12 (100), 71.13 (56), 57.10 (80).
HRMS	(EI , m/z): calc. $[\text{M}^+]$: 352.1886; found: 352.1888 $[\text{M}^+]$.
IR	$\tilde{\nu}$ = 2982 (w), 2934 (vw), 1731 (s), 1707 (vs), 1652 (vw), 1447 (vw), 1369 (s), 1241 (vs), 1211 (vs), 1156 (vs), 1069 (vs), 1033 (vs), 963 (w), 920 (w), 896 (w), 882 (w), 855 (s), 827 (w), 792 (w), 701 (m) cm^{-1} .

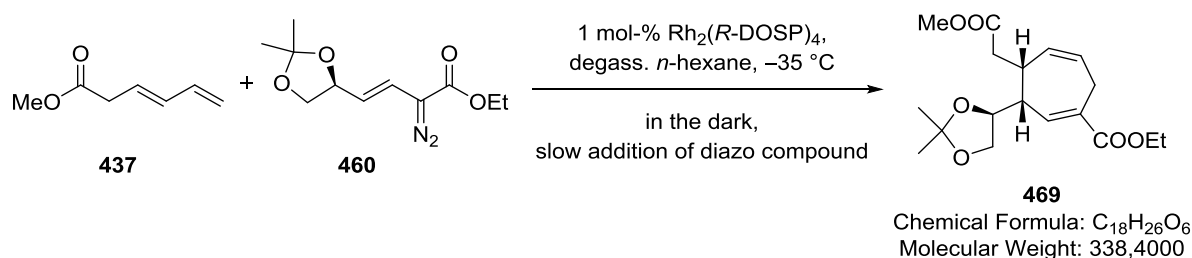
minor diastereomer (ethyl (3*S*,4*S*)-3-((*S*)-2,2-dimethyl-1,3-dioxolan-4-yl)-4-(2-ethoxy-2-oxoethyl)cyclohepta-1,5-diene-1-carboxylate (**564**))

**564**

Chemical Formula: $\text{C}_{19}\text{H}_{28}\text{O}_6$
Molecular Weight: 352,4270

^1H NMR	(400 MHz , CDCl_3): δ 7.11 (dd, J = 6.5, 2.8 Hz, 1H, C_2H), 5.71–5.66 (m, 1H, C_5H), 5.59 (dddd, J = 11.8, 7.4, 2.8, 1.1 Hz, 1H, C_6H), 4.23–4.04 (m, 6H, $2\times\text{C}_{16}\text{H}$, $2\times\text{C}_{18}\text{H}$, C_8H , C_9H), 3.58 (dd, J = 8.1, 7.8 Hz, 1H, C_9H), 3.33 (dd, J = 16.6, 7.4 Hz, 1H, C_7H), 3.15–3.11 (m, 1H, C_7H), 3.11–3.06 (m, 1H, C_3H), 2.83–2.74 (m, 1H, C_4H), 2.68 (dd, J = 16.1, 4.9 Hz, 1H, C_{13}H), 2.21 (dd, J = 16.1, 9.5 Hz, 1H, C_{13}H), 1.43 (s, 3H, C_{11}H_3), 1.36 (s, 3H, C_{12}H_3), 1.30 (t, J = 7.2 Hz, 3H, C_{17}H_3), 1.25 (t, J = 7.2 Hz, 3H, C_{19}H_3) ppm.
^{13}C NMR	(100 MHz , CDCl_3): δ 172.8 (C_{14}), 166.9 (C_{15}), 141.2 (C_2), 134.6 (C_1), 132.7 (C_5), 125.9 (C_6), 109.8 (C_{10}), 77.9 (C_8), 68.6 (C_9), 61.0 (C_{16}), 60.6 (C_{18}), 43.8 (C_3), 37.1 (C_4), 36.9 (C_{13}), 27.1 (C_7), 26.8 (C_{11}), 25.8 (C_{12}), 14.4 ($\text{C}_{17}/\text{C}_{19}$), 14.4 ($\text{C}_{17}/\text{C}_{19}$) ppm.

ethyl (3*R*,4*R*)-3-((*S*)-2,2-dimethyl-1,3-dioxolan-4-yl)-4-(2-methoxy-2-oxoethyl)cyclohepta-1,5-diene-1-carboxylate (**469**)

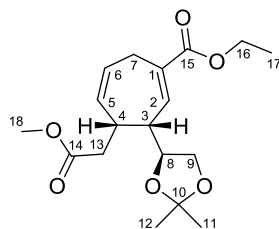


To a solution of diene **437** (0.98 ml, 0.93 g, 7.4 mmol, 2.0 eq.) and $\text{Rh}_2(\text{R-DOSP})_4$ (70 mg, 0.037 mmol, 0.01 eq.) in deaerated *n*-hexane (deaerated by 2xFPT, 74 ml) was slowly added a solution of vinyl diazo compound **460** (885 mg, 3.68 mmol) in deaerated *n*-hexane (deaerated by 2xFPT, 74) *via* syringe pump (6 ml/hr) in a 20 ml and a 50 ml portion at $-35\text{ }^\circ\text{C}$. The solution of vinyl diazo compound **460** in *n*-hexane was kept at $-78\text{ }^\circ\text{C}$ and the syringe was covered with dry ice. Upon complete addition, the reaction mixture was allowed to warm to rt over 7 h. The solution was concentrated under reduced pressure. The remaining residue was subjected to flash column chromatography (19x4.5 cm, 15–20% EtOAc/hexanes) and the resulting mixed fractions were purified again by flash column chromatography (19x2.5 cm, 15–20% EtOAc/hexanes) to afford the title compound as a colorless oil (1.02 g, 82%, dr = 7.1:1).

The excess equivalent of diene **437** can be recovered after the first flash column chromatography.

Vinyl diazo compound **460** proved to be unstable in *n*-hexane upon standing at $-78\text{ }^\circ\text{C}$ for longer time. During scale-up experiments, a stock solution of compound **460** in benzene was frozen at $-78\text{ }^\circ\text{C}$ over the course of the addition time. A part of this stock solution was taken when needed, concentrated under reduced pressure and HV, directly dissolved in *n*-hexane ($c = 0.05\text{ M}$) and added to the reaction mixture as described above.

(469) major diastereoisomer



469

Chemical Formula: $\text{C}_{18}\text{H}_{26}\text{O}_6$

Molecular Weight: 338,4000

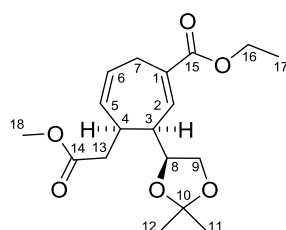
TLC $R_f = 0.25$ (15% EtOAc/hexanes).

^1H NMR (600 MHz, C_6D_6): δ 6.72 (dd, $J = 6.6, 2.6\text{ Hz}$, 1H, C_2H), 5.84–5.77 (m, 1H, C_5H), 5.44 (ddd, $J = 7.5, 3.0, 1.4\text{ Hz}$, 1H, C_6H), 3.98 (q, $J = 7.2\text{ Hz}$, 2H, $2\times\text{C}_{16}\text{H}$), 3.91–3.86 (m, 1H, C_8H), 3.71 (dd, $J = 8.2, 5.9\text{ Hz}$, 1H, C_9H), 3.45–3.40 (m, 1H, C_4H), 3.39 (dd, $J = 8.2, 6.5\text{ Hz}$, 1H, C_9H), 3.33 (dd, $J = 19.9, 7.5\text{ Hz}$, 1H, C_7H), 3.30 (s, 3H, C_{18}H_3), 3.02–2.96 (m, 1H, C_7H), 2.95–2.89 (m, 1H, C_3H), 2.51 (dd, $J = 15.5, 4.9\text{ Hz}$, 1H, C_{13}H), 2.32 (dd, $J = 15.5, 10.4\text{ Hz}$, 1H, C_{13}H), 1.33 (s, 3H, C_{11}H_3), 1.23 (s, 3H, C_{12}H_3), 0.96 (t, $J = 7.2\text{ Hz}$, 3H, C_{17}H_3) ppm.

^{13}C NMR (150 MHz, C_6D_6): δ 172.4 (C14), 166.4 (C15), 140.0 (C2), 135.0 (C1), 133.4 (C5), 126.4 (C6), 109.5 (C10), 75.8 (C8), 68.8 (C9), 60.8 (C16), 51.1 (C18), 45.6 (C3), 36.8 (C13), 35.0 (C4), 27.6 (C7), 27.1 (C11), 25.8 (C12), 14.3 (C17) ppm.

MS	(EI , %): 322.89 (4), 237.94 (9), 191.94 (8), 162.96 (6), 105.00 (6), 101.00 (100), 91.00 (9), 43.02 (25).
HRMS	(EI , m/z): calc. [M^+]: 338.1729; found: 338.1721 [M^+].
IR	$\tilde{\nu}$ = 2985 (w), 2953 (vw), 2876 (vw), 1736 (s), 1708 (vs), 1652 (vw), 1436 (w), 1380 (w), 1370 (m), 1331 (w), 1242 (vs), 1212 (vs), 1159 (vs), 1070 (vs), 922 (w), 884 (w), 856 (m), 793 (vw), 703 (w) cm^{-1} .
OR	$[\alpha]_D^{25} = -65.0^\circ$ (2 mg/ml, CHCl_3).

(471) minor diastereoisomer: **ethyl (3*S*,4*S*)-3-((*S*)-2,2-dimethyl-1,3-dioxolan-4-yl)-4-(2-methoxy-2-oxoethyl)cyclohepta-1,5-diene-1-carboxylate**

**471**Chemical Formula: $\text{C}_{18}\text{H}_{26}\text{O}_6$

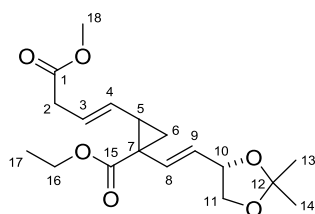
Molecular Weight: 338,4000

X-Ray suitable crystals were obtained by slow diffusion of hexanes into a solution of diastereomer **471** in EtOAc.

TLC	$R_f = 0.25$ (15% EtOAc/hexanes).
m.p.:	62–64 °C.
^1H NMR	(600 MHz , C_6D_6): δ 7.41–7.37 (m, 1H, C_2H), 5.73 (dddd, $J = 11.7, 6.0, 2.9, 0.9$ Hz, 1H, C_5H), 5.42 (dddd, $J = 11.7, 7.5, 2.8, 1.1$ Hz, 1H, C_6H), 3.96 (q, $J = 6.8$ Hz, 2H, $2 \times \text{C}_{16}\text{H}$), 3.92–3.88 (m, 1H, C_8H), 3.73 (dd, $J = 8.3, 6.3$ Hz, 1H, C_9H), 3.47 (dd, $J = 19.9, 7.7$ Hz, 1H, C_7H), 3.28 (s, 3H, C_{18}H_3), 2.99–2.93 (m, 1H, C_7H), 2.82–2.76 (m, 2H, C_3H , C_4H), 2.72 (dd, $J = 16.3, 4.7$ Hz, 1H, C_{13}H), 2.25 (dd, $J = 16.3, 9.2$ Hz, 1H, C_{13}H), 1.38 (s, 3H, C_{11}H_3), 1.24 (s, 3H, C_{12}H_3), 0.91 (t, $J = 7.1$ Hz, 3H, C_{17}H_3) ppm.
^{13}C NMR	(150 MHz , C_6D_6): δ 172.7 (C_{14}), 166.4 (C_{15}), 141.1 (C_2), 135.0 (C_1), 133.1 (C_5), 125.9 (C_6), 109.7 (C_{10}), 78.1 (C_8), 68.6 (C_9), 60.7 (C_{16}), 51.1 (C_{18}), 43.9 (C_3), 37.6 (C_4), 36.8 (C_{13}), 27.4 (C_7), 26.7 (C_{11}), 25.8 (C_{12}), 14.2 (C_{17}) ppm.
MS	(EI , %): 322.89 (4), 237.94 (10), 191.94 (9), 162.96 (6), 101.00 (100), 91.00 (6), 43.02 (23).
HRMS	(EI , m/z): calc. [M^+]: 338.1729; found: 338.1731 [M^+].

IR $\tilde{\nu}$ = 2985 (w), 2953 (vw), 2876 (vw), 1736 (s), 1708 (vs), 1652 (vw), 1436 (w), 1380 (w), 1370 (m), 1331 (w), 1242 (vs), 1212 (vs), 1159 (vs), 1070 (vs), 922 (w), 884 (w), 856 (m), 793 (vw), 703 (w) cm^{-1} .

ethyl 1-((*E*)-2-((*S*)-2,2-dimethyl-1,3-dioxolan-4-yl)vinyl)-2-((*E*)-4-methoxy-4-oxobut-1-en-1-yl)cyclopropane-1-carboxylate (570)

**570**

Chemical Formula: $\text{C}_{18}\text{H}_{26}\text{O}_6$
Molecular Weight: 338,4000

The title compound is a colorless oil that was identified in the formal (4+3)-cycloaddition of diene **437** with vinyl diazoacetate **460**.

TLC R_f = 0.19 (15% EtOAc/hexanes).

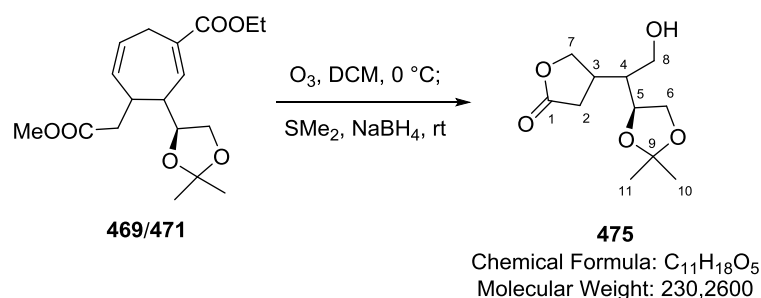
^1H NMR (**600 MHz**, C_6D_6): δ 6.34 (d, J = 15.6 Hz, 1H, C_8H), 5.65 (ddd, J = 15.4, 7.1, 7.1 Hz, 1H, C_3H), 5.38 (dd, J = 15.4, 9.0 Hz, 1H, C_4H), 5.20 (dd, J = 15.6, 7.9 Hz, 1H, C_9H), 4.40 (ddd, J = 8.1, 7.9, 6.1 Hz, 1H, C_{10}H), 4.06 (q, J = 7.1 Hz, 2H, $2\times\text{C}_{16}\text{H}$), 3.98 (dd, J = 8.1, 6.1 Hz, C_{11}H), 3.58 (s, 3H, C_{18}H_3), 3.45 (dd, J = 8.1, 8.1 Hz, 1H, C_{11}H), 2.96–2.93 (m, 2H, $2\times\text{C}_2\text{H}$), 1.85 (ddd, J = 9.0, 8.8, 7.5 Hz, 1H, C_5H), 1.66 (dd, J = 7.5, 5.1 Hz, 1H, C_6H), 1.39 (dd, J = 8.8, 5.1 Hz, 1H, C_6H), 1.32 (s, 3H, C_{13}H_3), 1.28 (s, 3H, C_{14}H_3), 1.16 (t, J = 7.1 Hz, 3H, C_{17}H_3) ppm.

^{13}C NMR (**150 MHz**, C_6D_6): δ 171.2 (C_1), 170.5 (C_{15}), 132.8 (C_8), 130.5 (C_4), 125.9 (C_9), 125.5 (C_3), 109.3 (C_{12}), 77.2 (C_{10}), 69.7 (C_{11}), 61.0 (C_{16}), 51.2 (C_{18}), 37.9 (C_2), 36.6 (C_5), 33.0 (C_7), 27.1 (C_{13}), 26.1 (C_{14}), 21.0 (C_6), 14.3 (C_{17}) ppm.

MS (**EI**, %): 338.17 (7, M^+), 217.09 (12), 190.07 (27), 145.07 (25), 117.07 (23), 105.07 (21), 101.06 (100), 91.05 (27), 84.08 (46), 72.06 (38), 42.97 (59).

HRMS (**EI**, m/z): calc. $[\text{M}^+]$: 338.1729; found: 338.1730 $[\text{M}^+]$.

IR $\tilde{\nu}$ = 2984 (w), 2934 (vw), 2874 (vw), 1720 (vs), 1635 (vw), 1437 (w), 1370 (m), 1305 (m), 1236 (s), 1214 (s), 1153 (vs), 1096 (w), 1057 (vs), 1026 (s), 968 (s), 938 (w), 917 (w), 862 (m), 797 (w), 746 (vw), 702 (vw) cm^{-1} .

4-(1-((S)-2,2-dimethyl-1,3-dioxolan-4-yl)-2-hydroxyethyl)dihydrofuran-2(3H)-one (475)

Ozone (O₂ flow level 1–2, generator level 11) was bubbled through a solution of cycloheptadiene **469/471** (103 mg, 0.304 mmol) in CH₂Cl₂ (6 ml) at 0 °C for 8 min. The solution was then purged with N₂ for 2 min and SMe₂ (0.4 ml) and NaBH₄ (100 mg) were subsequently added. The reaction mixture was stirred for 15 h before H₂O (4 ml) was added. The aqueous phase was extracted with CH₂Cl₂ (3x10 ml), the combined organic phases washed with brine, dried over Na₂SO₄ and concentrated under reduced pressure. The crude product was purified by flash column chromatography (17x2.5 cm, 1–3% MeOH/CH₂Cl₂) to afford the title compound as a colorless oil (41 mg, 59%).

When a starting material with a diastereomeric ratio dr (**469:471**) = 2.2:1 was employed, the product could be purified to yield a diastereomeric ratio dr = 6.7:1.

TLC R_f = 0.38 (5% MeOH/CH₂Cl₂).

¹H NMR (600 MHz, CDCl₃): δ 4.59 (dd, *J* = 9.6, 7.8 Hz, 1H, C₇H), 4.18–4.12 (m, 3H, C₅H, C₆H, C₇H), 3.72–3.66 (m, 3H, C₆H, C₈H, C₈H), 2.88–2.80 (m, 1H, C₃H), 2.64 (dd, *J* = 17.2, 8.3 Hz, 1H, C₂H), 2.43 (dd, *J* = 17.2, 10.8 Hz, 1H, C₂H), 1.78–1.72 (m, 1H, C₄H), 1.66 (brs, 1H, C₈OH), 1.39 (s, 3H, C₁₀H₃), 1.35 (s, 3H, C₁₁H₃) ppm.

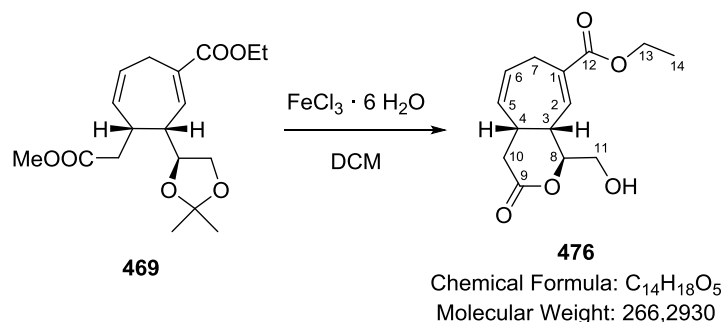
¹³C NMR (150 MHz, CDCl₃): δ 176.8, 109.1 (C₉), 76.9 (C₅), 73.1 (C₇), 68.6 (C₆), 62.2 (C₈), 47.1 (C₄), 36.9 (C₃), 33.2 (C₂), 26.7 (C₁₀), 25.6 (C₁₁) ppm.

MS (EI, %): 215.17 (78), 173.14 (26), 155.13 (45), 109.11 (32), 101.10 (60), 72.09 (44).

HRMS (EI, *m/z*): calc. [M⁺]: 231.1227; found: 231.1273 [M⁺].

IR $\tilde{\nu}$ = 3401 (w), 2985 (w), 2918 (w), 1765 (s), 1456 (vw), 1418 (vw), 1370 (m), 1246 (m), 1205 (s), 1161 (s), 1053 (vs), 1024 (vs), 1004 (vs), 935 (w), 856 (s), 794 (w), 763 (w), 688 (m) cm⁻¹.

ethyl (1*S*,4*aR*,9*aR*)-1-(hydroxymethyl)-3-oxo-1,3,4,4*a*,7,9*a*-hexahydrocyclohepta[*c*]pyran-8-carboxylate (476)



Dioxolane **469** (401 mg, dr 7.7:1, 1.19 mmol) was dissolved in CH₂Cl₂ (20 ml) and FeCl₃·6 H₂O was added. The suspension was stirred vigorously for 14 h before aq. sat. NaHCO₃ solution (25 ml) was added. The aqueous phase was extracted with CH₂Cl₂ (3x40 ml), the combined organic phases were washed with brine, dried over Na₂SO₄ and concentrated under reduced pressure. The crude product was purified by flash column chromatography (11x2 cm, 2.5% MeOH/CH₂Cl₂) to afford the title compound as a colorless solid (265 mg, dr 7.7:1, 84%). X-Ray suitable crystals were obtained by slow diffusion of hexanes into a solution of the title compound in EtOAc.

The reproducibility of this reaction was only assured when using heat-gun-dried glassware and dry solvent. Otherwise, the reaction times varied or the reaction did not reach full conversion.

NMR sample is a diastereomeric mixture (dr 7:1), NMR spectral data only provided for major isomer (title compound).

TLC $R_f = 0.36$ (5% MeOH/CH₂Cl₂).

m.p.: 113–115 °C (C₆D₆).

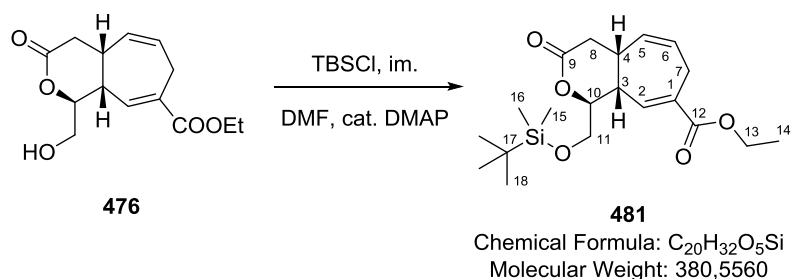
¹H NMR (600 MHz, C₆D₆): δ 6.94 (ddd, $J = 7.1, 1.9, 0.7$ Hz, 1H, C₂H), 5.38 (dddd, $J = 11.1, 6.7, 4.1, 2.5$ Hz, 1H, C₆H), 5.03 (ddd, $J = 11.1, 3.5, 3.5$ Hz, 1H, C₅H), 4.10 (ddd, $J = 9.0, 3.5, 3.0$ Hz, 1H, C₈H), 3.98 (q, $J = 7.1$ Hz, 2H, 2xC₁₃H), 3.53 (ddd, $J = 12.5, 6.0, 3.0$ Hz, 1H, C₁₁H), 3.32 (ddd, $J = 12.5, 7.3, 3.5$ Hz, 1H, C₁₁H), 3.10 (dd, $J = 20.5, 6.7$ Hz, 1H, C₇H), 3.01 (dm, $J = 20.5$ Hz, 1H, C₇H), 2.67–2.62 (m, 1H, C₃H), 2.48–2.44 (m, 1H, C₄H), 2.39–2.34 (brs, 1H, C₁₁OH), 2.19 (dd, $J = 17.6, 4.5$ Hz, 1H, C₁₀H), 2.09 (dd, $J = 17.6, 5.4$ Hz, 1H, C₁₀H), 0.95 (t, $J = 7.1$ Hz, 3H, C₁₄H₃) ppm. Shifts highly depend on *c*, pH and water content of the sample.

¹³C NMR (150 MHz, C₆D₆): δ 169.1 (C₉), 166.8 (C₁₂), 138.3 (C₂), 133.8 (C₁), 131.6 (C₅), 128.8 (C₆), 81.6 (C₈), 63.0 (C₁₁), 61.0 (C₁₃), 37.2 (C₃), 37.0 (C₁₀), 32.5 (C₄), 27.6 (C₇), 14.2 (C₁₄) ppm.

MS (EI, %): 266.25 (2, M⁺), 220.18 (14), 192.16 (10), 164.16 (38), 135.11 (100), 105.12 (24), 91.10 (78), 84.13 (22), 57.08 (14).

HRMS (EI, m/z): calc. $[M]^+$: 266.1154; found: 266.1162 $[M]^+$.
IR $\tilde{\nu}$ = 3371 (br, vw), 2964 (vw), 2932 (vw), 2878 (vw), 1710 (vs), 1652 (vw), 1368 (w), 1292 (w), 1250 (vs), 1170 (w), 1097 (m), 1064 (s), 884 (vw), 804 (vw), 709 (w) cm^{-1} .
OR $[\alpha]_{\text{D}}^{25} = +13.0^\circ$ (20 mg/ml, CH_2Cl_2).

ethyl (1*S*,4*aR*,9*aR*)-1-(((*tert*-butyldimethylsilyl)oxy)methyl)-3-oxo-1,3,4,4*a*,7,9*a*-hexahydro-cyclohepta[*c*]pyran-8-carboxylate (**481**)

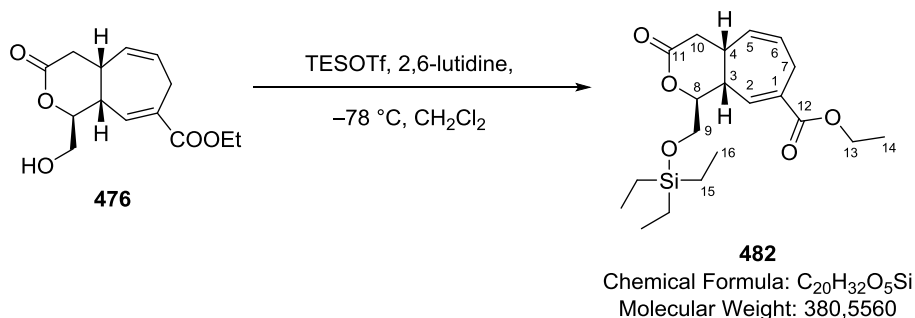


Alcohol **476** (50 mg, 0.19 mmol) was dissolved in DMF (0.5 ml) and imidazole (30 mg, 0.41 mmol, 2.4 eq.), TBSCl (32 mg, 0.21 mmol, 1.1 eq.) and DMAP (5 mg, 0.04 mmol, 0.2 eq.) were sequentially added. The reaction mixture was stirred for 14 h before pH 7.2 phosphate buffer ($c = 1$ M, 10 ml) was added. The aqueous phase was extracted with EtOAc (3x15 ml), the combined organic phases dried over Na_2SO_4 and concentrated under reduced pressure to afford the title compound as a colorless oil (75 mg, quant.).

The TBS group is partially deprotected during flash column chromatography. The title compound was thus taken forward without further purification.

TLC $R_f = 0.47$ (20% EtOAc/hexanes).
 ^1H NMR (400 MHz, $(\text{D}_3\text{C})_2\text{CO}$): δ 7.02 (d, $J = 6.3$ Hz, 1H, C_2H), 5.87–5.79 (m, 1H, C_6H), 5.61–5.54 (m, 1H, C_5H), 4.50 (ddd, $J = 7.0, 3.5, 3.1$ Hz, 1H, C_{10}H), 4.16 (q, $J = 7.2$ Hz, 2H, $2 \times \text{C}_{13}\text{H}$), 3.90 (dd, $J = 11.5, 3.5$ Hz, 1H, C_{11}H), 3.84 (dd, $J = 11.5, 3.1$ Hz, 1H, C_{11}H), 3.32–3.22 (m, 4H, $\text{C}_3\text{H}, \text{C}_4\text{H}, 2 \times \text{C}_{12}\text{H}$), 2.63 (dd, $J = 17.6, 5.2$ Hz, C_8H), 2.45 (dd, $J = 17.6, 5.3$ Hz, C_8H), 1.26 (t, $J = 7.2$ Hz, 3H, C_{14}H_3), 0.91 (s, 9H, C_{18}H_3), 0.12 (s, 3H, C_{15}H_3), 0.10 (s, 3H, C_{16}H_3) ppm.
 ^{13}C NMR (100 MHz, $(\text{D}_3\text{C})_2\text{CO}$): δ 169.3 (C9), 167.3 (C12), 139.8 (C2), 134.8 (C1), 132.4 (C5), 129.0 (C6), 81.8 (C10), 64.6 (C11), 61.4 (C13), 37.9 (C3), 37.1 (C8), 32.9 (C4), 27.7 (C7), 26.2 (C18), 18.8 (C17), 14.5 (C14), -5.3 (C15/C16), -5.4 (C15/C16) ppm.
HRMS ((+)-ESI, m/z): calc. $[\text{M}+\text{H}^+]$: 381.2097; found: 381.2089 $[\text{M}+\text{H}^+]$.
IR $\tilde{\nu}$ = 2950 (w), 2930 (w), 2855 (w), 1742 (s), 1711 (s), 1472 (w), 1462 (w), 1388 (vw), 1367 (w), 1341 (vw), 1244 (vs), 1201 (m), 1140 (m), 1125 (m), 1101 (w), 1069 (s), 1024 (vw), 1003 (w), 948 (vw), 837 (s), 811 (w), 780 (m), 711 (vw) cm^{-1} .
OR $[\alpha]_{\text{D}}^{22} = +53.0^\circ$ (2 mg/ml, CH_2Cl_2).

ethyl (1*S*,4*aR*,9*aR*)-3-oxo-1-(((triethylsilyl)oxy)methyl)-1,3,4,4*a*,7,9*a*-hexahydrocyclohepta[*c*]pyran-8-carboxylate (482)



2,6-Lutidine (13 μl , 12 mg, 0.11 mmol, 2.0 eq.) and TESOTf (15 μl , 18 mg, 0.068 mmol, 1.2 eq.) were successively added to a $-78\text{ }^{\circ}\text{C}$ cold solution of alcohol **476** (15 mg, 0.056 mmol) in CH_2Cl_2 (0.5 ml). After 3 h, 2,6-lutidine (13 μl , 12 mg, 0.11 mmol, 2.0 eq.) and TESOTf (15 μl , 18 mg, 0.068 mmol, 1.2 eq.) were added since the reaction was judged incomplete by TLC analysis. After stirring for 2 h, pH 5 phosphate buffer ($c = 1\text{ M}$, 3 ml) was added and the reaction mixture was allowed to warm to rt. The aqueous phase was extracted with EtOAc (3x5 ml) and the combined organic phases were dried over Na_2SO_4 and concentrated under reduced pressure. The crude product was purified by flash column chromatography (12x2.5 cm, 5–10–20% EtOAc/hexanes) to afford the product as a colorless oil (20 mg, 93%).

TLC $R_f = 0.26$ (20% EtOAc/hexanes).

$^1\text{H NMR}$ (**400 MHz**, **C_6D_6**): δ 7.01 (dd, $J = 6.9, 1.8\text{ Hz}$, 1H, C_2H), 5.42 (dddd, $J = 11.0, 6.8, 4.0, 2.4\text{ Hz}$, 1H, C_6H), 5.12–5.06 (m, 1H, C_5H), 4.16 (ddd, $J = 8.6, 3.6, 3.0\text{ Hz}$, 1H, C_8H), 3.98 (q, $J = 7.1\text{ Hz}$, 2H, $2\times\text{C}_{13}\text{H}$), 3.60 (dd, $J = 11.5, 3.6\text{ Hz}$, 1H, C_9H), 3.46 (dd, $J = 11.5, 3.0\text{ Hz}$, 1H, C_9H), 3.18 (dd, $J = 20.2, 6.8\text{ Hz}$, 1H, C_7H), 3.08–2.99 (m, 1H, C_7H), 2.87–2.81 (m, 1H, C_3H), 2.57–2.50 (m, 1H, C_4H), 2.23 (dd, $J = 17.6, 4.8\text{ Hz}$, 1H, C_{10}H), 2.10 (dd, $J = 17.6, 5.6\text{ Hz}$, 1H, C_{10}H), 1.00–0.93 (m, 12H, C_{14}H_3 , $3\times\text{C}_{16}\text{H}_3$), 0.62–0.54 (m, 6H, $3\times\text{C}_{15}\text{H}_2$) ppm.

$^{13}\text{C NMR}$ (**100 MHz**, **C_6D_6**): δ 168.0 (C11), 166.8 (C12), 138.8 (C2), 133.8 (C1), 131.8 (C5), 128.8 (C6), 80.9 (C8), 63.6 (C9), 61.0 (C13), 37.5 (C3), 37.0 (C10), 32.5 (C4), 27.5 (C7), 14.2 (C14), 7.0 (C16), 4.7 (C15) ppm.

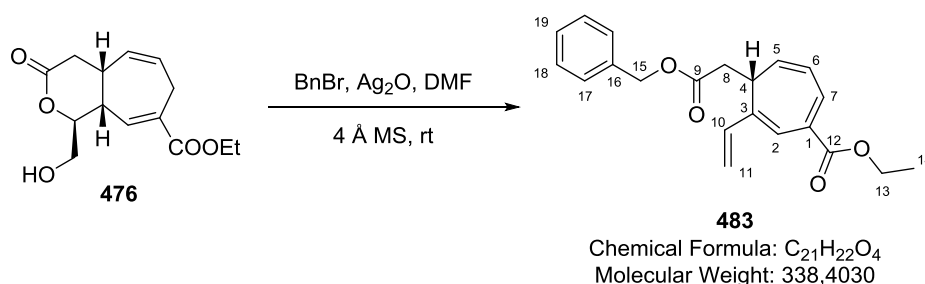
MS (**EI, %**): 351.11 (42), 307.10 (46), 145.02 (26), 131.04 (100), 117.01 (54), 91.02 (38)

HRMS (**EI, m/z**): calc. $[\text{M}^+]$: 380.2019; found: 380.2003 $[\text{M}^+]$.

IR $\tilde{\nu} = 2954\text{ (w)}$, 2936 (w) , 2912 (w) , 2875 (w) , 1740 (vs) , 1708 (vs) , 1653 (vw) , 1458 (w) , 1414 (w) , 1367 (w) , 1344 (vw) , 1274 (w) , 1239 (vs) , 1199 (s) , 1142 (m) , 1122 (m) , 1097 (m) , 1068 (vs) , 1003 (m) , 977 (w) , 950 (w) , 925 (vw) , 912 (vw) , 882 (vw) , 859 (vw) , 819 (w) , 787 (w) , 744 (s) , $730\text{ (s)}\text{ cm}^{-1}$.

OR $[\alpha]_{\text{D}}^{21} = +14.4^{\circ}$ (18 mg/ml, CH_2Cl_2).

ethyl (*R*)-5-(2-(benzyloxy)-2-oxoethyl)-6-vinylcyclohepta-1,3,6-triene-1-carboxylate (483)



Lactone **476** (10 mg, 0.038 mmol) was dissolved in DMF (0.4 ml) and 4 Å MS was added. Benzyl bromide (5 μl , 7 mg, 0.04 mmol, 1.05 eq.) and Ag_2O (10 mg, 0.041 mmol, 1.1 eq.) were successively introduced and the reaction mixture stirred for 58 h. In the meantime, BnBr (3 μl , 4 mg, 0.02 mmol, 0.5 eq.) had been added after 9 h and again benzyl bromide (5 μl , 7 mg, 0.04 mmol, 1.05 eq.) and Ag_2O (10 mg, 0.041 mmol, 1.1 eq.) after 25 h. Preparative TLC (15% EtOAc/hexanes) afforded the title compound as a colorless solid (2 mg, 16%).

TLC $R_f = 0.25$ (5% EtOAc/hexanes).

^1H NMR (400 MHz, $(\text{D}_3\text{C})_2\text{CO}$): δ 7.57 (d, $J = 6.6$ Hz, 1H, C_7H), 7.39–7.29 (m, 5H, ArH), 6.86 (s, 1H, C_2H), 6.56 (dd, $J = 17.4, 10.8$ Hz, 1H, C_{10}H), 6.42 (dd, $J = 9.9, 6.6$ Hz, 1H, C_6H), 5.98 (dd, $J = 9.2, 9.2$ Hz, 1H, C_5H), 5.63 (d, $J = 17.4$ Hz, 1H, *trans*- C_{11}H), 5.18 (d, $J = 10.7$ Hz, 1H, *cis*- C_{11}H), 5.09 (d, $J = 12.5$ Hz, 1H, C_{15}H), 5.04 (d, $J = 12.5$, 1H, C_{15}H), 4.25 (q, $J = 7.2$ Hz, 2H, $2\times\text{C}_{13}\text{H}$), 4.15–4.06 (m, 1H, C_4H), 2.28 (dd, $J = 15.8, 9.1$ Hz, 1H, C_8H), 2.14 (dd, $J = 15.8, 6.7$ Hz, 1H, C_8H), 1.31 (t, $J = 7.2$ Hz, 3H, C_{14}H) ppm.

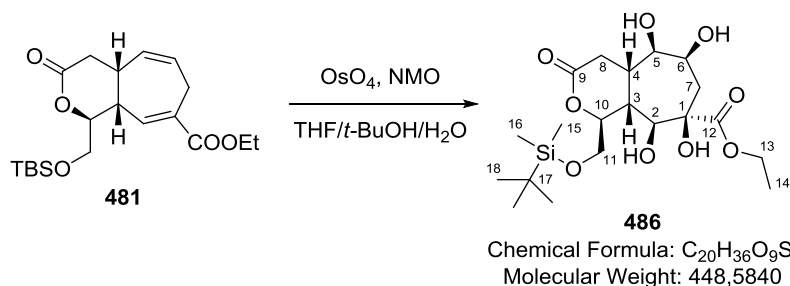
^{13}C NMR (100 MHz, $(\text{D}_3\text{C})_2\text{CO}$): δ 171.7 (C9), 167.3 (C12), 139.1 (C10), 137.4 (C16), 136.3 (C7), 135.9 (C3), 133.3 (C5), 132.3 (C1), 129.2 (C17/C18/C19), 128.9 (C17/C18/C19), 128.8 (C17/C18/C19), 126.9 (C6), 125.2 (C2), 115.8 (C11), 66.5 (C15), 61.6 (C13), 34.0 (C4), 33.0 (C8), 14.5 (C14) ppm.

HRMS ((+)-ESI, m/z): calc. $[\text{M}+\text{Na}^+]$: 361.1410; found: 361.1408 $[\text{M}+\text{Na}^+]$.

IR $\tilde{\nu} = 3029$ (vw), 2976 (vw), 2960 (vw), 2923 (w), 2851 (vw), 1728 (s), 1713 (vs), 1613 (vw), 1530 (vw), 1496 (vw), 1454 (w), 1415 (w), 1380 (w), 1367 (w), 1283 (m), 1257 (vs), 1219 (s), 1161 (s), 1111 (w), 1076 (w), 1022 (w), 992 (w), 908 (w), 866 (w), 733 (m), 698 (m) cm^{-1} .

OR $[\alpha]_{\text{D}}^{22} = -116^{\circ}$ (1 mg/ml, CH_2Cl_2).

ethyl (1*S*,4*aS*,5*R*,6*S*,8*R*,9*S*,9*aR*)-1-(((*tert*-butyldimethylsilyl)oxy)methyl)-5,6,8,9-tetrahydroxy-3-oxodecahydrocyclohepta[*c*]pyran-8-carboxylate (486)



Lactone **481** (30 mg, 0.079 mmol) was dissolved in THF/*t*-BuOH/H₂O (2:1:1, 1.2 ml) and OsO₄ (4 wt-% in H₂O, 50 μ l, 0.0079 mmol, 0.1 eq.) and NMO (28 mg, 0.24 mmol, 3.0 eq.) were added. The reaction mixture was stirred in the dark for 47 h, when OsO₄ (4 wt-% in H₂O, 100 μ l, 0.016 mmol, 0.2 eq) was introduced. After further stirring for 39 h, the reaction was judged complete and aq. sat. Na₂S₂O₃ (2 ml) and pH 5 buffer (*c* = 1 M, 3 ml) was added. The aqueous phase was saturated with NaCl and extracted with EtOAc (3x10 ml). The combined organic phases were dried over Na₂SO₄ and concentrated to afford the crude product (40 mg, >quant.), which could be used without further purification.

LC/MS R_t = 3.463 min (10–90% MeCN/H₂O + 0.1% FA, 7 min, 2 ml/min).

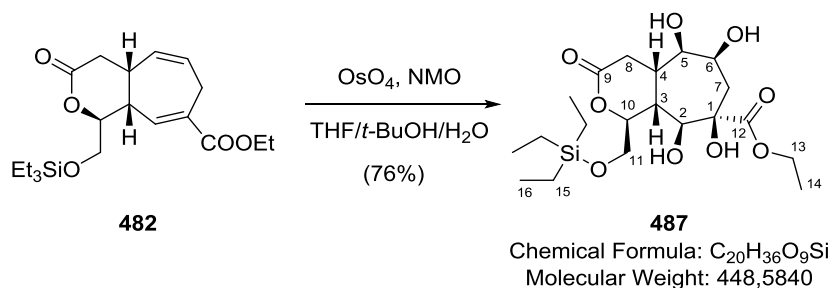
¹H NMR (400 MHz, (D₃C)₂CO): δ 4.71 (dd, *J* = 9.4, 4.7 Hz, 1H, C₁₀H), 4.47–4.33 (brs, 2H, 2xOH), 4.19 (q, *J* = 7.1 Hz, 2H, 2xC₁₃H), 4.13–4.06 (m, 1H, C₆H), 4.05–3.96 (m, 2H, C₂H, OH), 3.93 (dd, *J* = 11.0, 4.4 Hz, 1H, C₁₁H), 3.86 (dd, *J* = 11.0, 4.5 Hz, 1H, C₁₁H), 3.68–3.64 (m, 1H, C₅H), 2.93–2.81 (brs, 1H, OH), 2.71–2.61 (m, 2H, C₃H, C₄H), 2.60–2.54 (m, 2H, 2xC₈H), 2.21 (dd, *J* = 15.0, 8.8 Hz, 1H, C₇H), 2.03 (dd, *J* = 15.0, 2.9 Hz, 1H, C₇H), 1.26 (t, *J* = 7.1 Hz, 3H, C₁₃H₃), 0.90 (s, 9H, 3xC₁₈H₃), 0.10 (s, 3H, C₁₅H₃), 0.09 (s, 3H, C₁₆H₃) ppm.

¹³C NMR (100 MHz, (D₃C)₂CO): δ 175.9 (C₁₂), 170.9 (C₉), 81.1 (C₁₀), 79.7 (C₁), 74.9 (C₅), 72.3 (C₂), 70.1 (C₆), 66.4 (C₁₁), 62.1 (C₁₃), 39.3 (C₇), 37.0 (C₃), 35.3 (C₄), 32.6 (C₈), 26.2 (C₁₈), 18.8 (C₁₇), 14.4 (C₁₄), –5.2 (C₁₅/C₁₆), –5.3 (C₁₅/C₁₆) ppm.

HRMS ((+)-ESI, *m/z*): calc. [M+Na⁺]: 471.2021; found: 471.2030 [M+Na⁺].

IR $\tilde{\nu}$ = 3408 (w), 2955 (w), 2930 (w), 2886 (vw), 2857 (w), 1723 (s), 1472 (w), 1464 (w), 1445 (w), 1391 (w), 1362 (w), 1252 (s), 1195 (m), 1123 (s), 1089 (s), 1069 (s), 1024 (s), 935 (w), 908 (w), 836 (vs), 816 (w), 779 (s), 725 (w), 668 (w) cm^{–1}.

ethyl (1*S*,4*aS*,5*R*,6*S*,8*R*,9*S*,9*aR*)-5,6,8,9-tetrahydroxy-3-oxo-1-(((triethylsilyl)oxy)methyl)decahydrocyclohepta[*c*]pyran-8-carboxylate (487)



Cycloheptadiene **482** (10 mg, 0.026 mmol) was dissolved in THF/*t*-BuOH/H₂O (1.0 ml, 2:1:1) and OsO₄ (4 wt-% in H₂O, 17 µl, 17 mg, 0.0026 mmol, 0.1 eq.) and NMO (10 mg, 0.079 mmol, 3.0 eq.) were added. The reaction mixture was stirred in the dark for 41 h and OsO₄ (4 wt-% in H₂O, 17 µl, 17 mg, 0.0026 mmol, 0.1 eq.) and NMO (10 mg, 0.079 mmol, 3.0 eq.) were added. Further stirring for 53 h led to completion of the reaction as judged by LC/MS. Sat. aq. Na₂S₂O₃ (4 ml) and solid NaCl was added to the reaction mixture and the NaCl saturated aqueous solution was extracted with EtOAc (3x10ml). The combined organic phases were dried over Na₂SO₄ and concentrated under reduced pressure to afford the title compound as a colorless oil (9 mg, 76%). The product could be used without further purification.

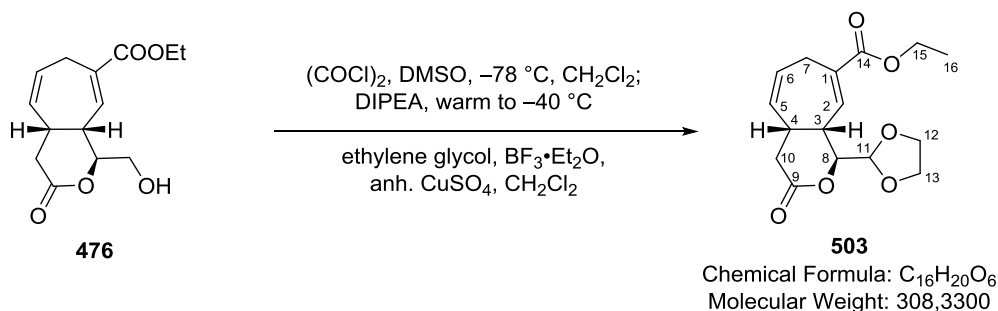
¹H NMR (400 MHz, (D₃C)₂CO): δ 4.70 (ddd, *J* = 4.8, 4.8, 4.4, 1H, C₁₀H), 4.20 (q, *J* = 7.1 Hz, 2H, 2xC₁₃H), 4.09 (ddd, *J* = 8.8, 2.8, 2.1 Hz, 1H, C₆H), 4.02 (d, *J* = 8.7 Hz, 1H, C₂H), 3.93 (dd, *J* = 11.0, 4.4 Hz, 1H, C₁₁H), 3.86 (dd, *J* = 11.0, 4.8 Hz, 1H, C₁₁H), 3.66 (dd, *J* = 6.6, 2.1 Hz, 1H, C₅H), 2.70–2.61 (m, 2H, C₃H, C₄H), 2.60–2.56 (m, 2H, 2xC₈H), 2.21 (dd, *J* = 14.9, 8.8 Hz, 1H, C₇H), 2.03 (dd, *J* = 14.9, 2.8 Hz, 1H, C₇H), 1.26 (t, *J* = 7.1 Hz, 3H, C₁₄H₃), 0.97 (t, *J* = 8.0 Hz, 9H, 3xC₁₆H₃), 0.64 (q, *J* = 8.0 Hz, 6H, 3xC₁₅H₂) ppm. Sample contains EtOAc and an unknown impurity.

¹³C NMR (100 MHz, (D₃C)₂CO): δ 175.9 (C₁₂), 170.9 (C₉), 81.2 (C₁₀), 79.6 (C₁), 74.8 (C₅), 72.2 (C₂), 70.1 (C₆), 66.2 (C₁₁), 62.1 (C₁₃), 39.3 (C₇), 37.0 (C₃), 35.4 (C₄), 32.6 (C₈), 14.4 (C₁₄), 7.0 (C₁₆, C₁₈, C₂₀), 4.9 (C₁₅, C₁₇, C₁₉) ppm. Sample contains EtOAc and an unknown impurity.

HRMS ((+)-ESI, *m/z*): calc. [M+Na⁺]: 471.2021; found: 471.2020 [M+Na⁺].

IR $\tilde{\nu}$ = 3409 (br, w), 2953 (m), 2921 (m), 2874 (m), 1725 (vs), 1457 (w), 1414 (w), 1392 (w), 1369 (w), 1238 (s), 1191 (m), 1114 (vs), 1088 (vs), 1066 (s), 1017 (vs), 864 (w), 822 (w), 743 (s), 667 (w) cm⁻¹.

ethyl (1*S*,4*aR*,9*aR*)-1-(1,3-dioxolan-2-yl)-3-oxo-1,3,4,4*a*,7,9*a*-hexahydrocyclohepta[*c*]pyran-8-carboxylate (503)



Oxalyl chloride (19 μ l, 28 mg, 0.22 mmol, 2.0 eq.) in CH₂Cl₂ (0.8 ml) was cooled to -78 °C and DMSO (31 μ l, 34 mg, 0.44 mmol, 4.0 eq.) was added slowly. This solution was treated with alcohol **476** (dr: 6.3:1, 29 mg, 0.11 mmol) in CH₂Cl₂ (0.9 ml) after 5 min and stirring was continued for 25 min. DIPEA (0.15 ml, 0.11 g, 0.87 mmol, 8.0 eq.) was introduced at -78 °C and after 1 h, the reaction mixture was allowed to warm to -40 °C over 30 min. Aq. phosphate buffer ($c = 0.15$ M, pH 7.2, 3 ml) was added, the aqueous phase was extracted with CH₂Cl₂ (3x10 ml) and the combined organic phases were dried over Na₂SO₄ and concentrated under reduced pressure. Half of the crude product was dissolved in CH₂Cl₂ (1.5 ml) and cooled to 0 °C. Ethylene glycol (9 μ l, 5 mg, 0.05 mmol, 3.0 eq.), anhydrous CuSO₄ (dried at 120 °C overnight on HV, 23 mg, 0.15 mmol, 2.7 eq.) and BF₃·OEt₂ (14 μ l, 16 mg, 0.12 mmol, 2.2 eq.) were successively added and the reaction mixture stirred at rt for 17 h. Aq. phosphate buffer ($c = 0.15$ M, pH 7.2, 4 ml) was added, the aqueous phase was extracted with CH₂Cl₂ (3x10 ml) and the combined organic phases were dried over Na₂SO₄ and concentrated under reduced pressure to afford the title compound as a colorless oil (23 mg, >100%). The product could be used without further purification. An analytical sample was obtained by flash column chromatography (15x1.5 cm, 25–30–35–60% EtOAc/hexanes).

This reaction only led to success when alcohol **476** was purified by flash column chromatography to remove traces of Fe^{III} salts from the previous step. Otherwise, the intermediate aldehyde proved unstable during concentration under reduced pressure.

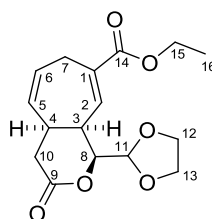
TLC $R_f = 0.29$ (40% EtOAc/hexanes).

¹H NMR (400 MHz, C₆D₆): δ 6.97 (dd, $J = 6.7, 2.2$ Hz, 1H, C₂H), 5.34 (dddd, $J = 11.3, 7.3, 3.6, 2.1$ Hz, 1H, C₆H), 4.95 (ddd, $J = 11.3, 4.5, 2.8$ Hz, 1H, C₅H), 4.77 (d, $J = 1.2$ Hz, 1H, C₁₁H), 4.32 (dd, $J = 5.6, 1.2$ Hz, 1H, C₈H), 3.98 (q, $J = 7.1$ Hz, 2H, 2x C₁₅H), 3.71–3.58 (m, 2H, C₁₂H, C₁₃H), 3.32–3.25 (m, 2H, C₁₂H, C₁₃H), 3.16 (dd, $J = 19.7, 7.3$ Hz, 1H, C₇H), 2.97–2.89 (m, 1H, C₇H), 2.71–2.63 (m, 2H, C₃H, C₄H), 2.19 (dd, $J = 17.6, 6.1$ Hz, 1H, C₁₀H), 2.13 (dd, $J = 17.6, 7.5$ Hz, 1H, C₁₀H), 0.95 (t, $J = 7.1$ Hz, 3H, C₁₆H₃) ppm.

¹³C NMR	(100 MHz, C₆D₆): δ 168.0 (C9), 166.4 (C14), 139.3 (C2), 135.5 (C1), 130.9 (C5), 127.4 (C6), 103.5 (C11), 81.6 (C8), 65.8 (C12/C13), 65.6 (C12/C13), 61.0 (C15), 37.1 (C3), 36.0 (C10), 32.2 (C4), 26.7 (C7), 14.2 (C16) ppm.
HRMS	((+)-ESI, m/z): calc. [M+Na ⁺]: 331.1152; found: 331.1152 [M+Na ⁺].
IR	$\tilde{\nu}$ = 3397 (vw), 2979 (vw), 2896 (vw), 1740 (vs), 1705 (vs), 1653 (vw), 1474 (vw), 1445 (vw), 1367 (w), 1278 (m), 1241 (vs), 1196 (s), 1151 (s), 1071 (vs), 1045 (m), 991 (w), 946 (m), 929 (w), 910 (w), 883 (w), 808 (vw), 770 (vw), 745 (vw), 706 (w) cm ⁻¹ .
OR	[α] _D ²³ = +5.2° (6.5 mg/ml, CHCl ₃).

Minor diastereomer (**571**): ethyl (1*S*,4*aS*,9*aS*)-1-(1,3-dioxolan-2-yl)-3-oxo-1,3,4,4*a*,7,9*a*-hexahydrocyclohepta[*c*]pyran-8-carboxylate

Since the intermediate aldehyde can also epimerize at C8, the isolated diastereomer can also be a C8-epimer of the major product of this reaction. Due to the irrelevance of the minor diastereomer to the overall total synthesis, the relative stereochemistry was not elucidated. It was assumed that the isolated diastereomer results from the minor diastereomer **571** of the starting material.

**571**

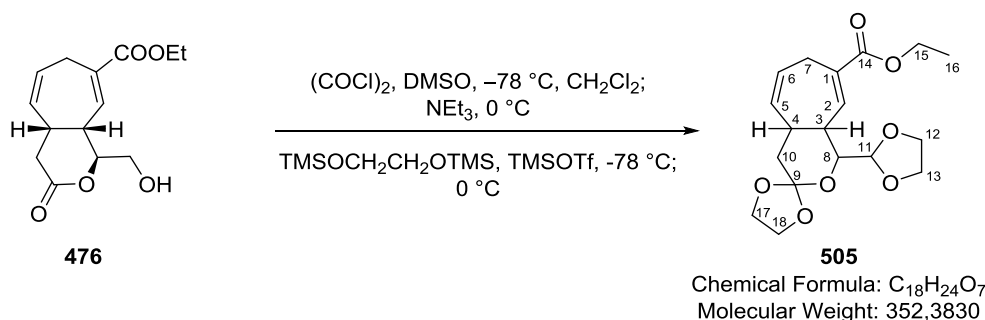
Chemical Formula: C₁₆H₂₀O₆
Molecular Weight: 308,3300

TLC	R _f = 0.23 (40% EtOAc/hexanes).
¹H NMR	(400 MHz, C₆D₆): δ 7.44 (ddd, <i>J</i> = 6.1, 1.4, 1.4 Hz, 1H, C ₂ H), 5.36 (dddd, <i>J</i> = 11.5, 8.5, 2.8, 1.7 Hz, 1H, C ₆ H), 4.90 (d, <i>J</i> = 4.7 Hz, 1H, C ₁₁ H), 4.82 (ddd, <i>J</i> = 11.5, 5.1, 3.0 Hz, 1H, C ₅ H), 3.95 (q, <i>J</i> = 7.2 Hz, 2H, 2xC ₁₅ H), 3.84 (dd, <i>J</i> = 4.7, 2.3 Hz, 1H, C ₈ H), 3.50 (ddd, <i>J</i> = 7.5, 6.4, 6.1 Hz, 1H, C ₁₂ H), 3.40 (ddd, <i>J</i> = 7.2, 6.4, 5.8 Hz, 1H, C ₁₃ H), 3.35 (ddd, <i>J</i> = 18.2, 8.5, 1.2 Hz, 1H, C ₇ H), 3.28 (ddd, <i>J</i> = 7.5, 6.8, 5.8 Hz, 1H, C ₁₂ H), 3.16 (ddd, <i>J</i> = 7.2, 6.8, 6.1 Hz, 1H, C ₁₃ H), 3.07–3.03 (m, 1H, C ₃ H), 2.88–2.80 (m, 1H, C ₇ H), 2.15–2.10 (m, 2H, 2xC ₁₀ H), 1.87–1.77 (m, 1H, C ₄ H), 0.90 (t, <i>J</i> = 7.2 Hz, 3H, C ₁₆ H ₃) ppm.
¹³C NMR	(100 MHz, C₆D₆): δ 167.3 (C9), 165.9 (C14), 138.0 (C1), 136.7 (C2), 130.4 (C5), 125.8 (C6), 102.7 (C8), 82.2 (C8), 65.5 (C12), 65.0 (C13), 61.0 (C15), 36.6 (C3), 35.8 (C4), 34.0 (C10), 25.4 (C7), 14.2 (C16) ppm.
HRMS	((+)-ESI, m/z): calc. [M+Na ⁺]: 331.1152; found: 331.1149 [M+Na ⁺].

IR $\tilde{\nu}$ = 3403 (vw), 2956 (w), 2923 (w), 2857 (vw), 1742 (vs), 1707 (vs), 1649 (vw), 1443 (vw), 1368 (w), 1294 (w), 1250 (vs), 1160 (m), 1079 (m), 1032 (m), 945 (w), 885 (vw), 817 (vw), 746 (vw), 712 (w) cm^{-1} .

OR $[\alpha]_{\text{D}}^{23} = -12.8^{\circ}$ (3 mg/ml, CHCl_3).

ethyl **1-(1,3-dioxolan-2-yl)-4,4a,7,9a-tetrahydro-1H-spiro[cyclohepta[c]pyran-3,2'-[1,3]dioxolane]-8-carboxylate (505)**



Oxalyl chloride (10 μl , 14 mg, 0.11 mmol, 2.0 eq.) in CH_2Cl_2 (1.0 ml) was cooled to -78°C and DMSO (16 μl , 18 mg, 0.23 mmol, 4.0 eq.) was added slowly. This solution was treated with alcohol **476** (15 mg, 0.06 mmol) in CH_2Cl_2 (0.6 ml) after 15 min and stirring was continued for 40 min. NEt_3 (0.06 ml, 0.04 g, 0.4 mmol, 7.5 eq.) was introduced at -78°C and the reaction mixture was allowed to warm to 0°C over 1.5 h. Sat. aq. NaHCO_3 solution (5 ml) was added, the aqueous phase was extracted with CH_2Cl_2 (3x10 ml) and the combined organic phases were dried over Na_2SO_4 and concentrated under reduced pressure. The crude product was redissolved in CH_2Cl_2 , cooled to -78°C and $\text{TMSOCH}_2\text{CH}_2\text{OTMS}$ (42 μl , 35 mg, 0.17 mmol, 3.0 eq.) was added. TMSOTf (10 μl , 12 mg, 1 eq.) was introduced and the reaction mixture was stirred at the same temperature for 3.5 h. The reaction mixture was then allowed to warm to 0°C , stirred for 2 h, then allowed to warm to rt overnight. Pyridine (2 ml) was added, the organic phase washed with sat. aq. NaHCO_3 solution and the aqueous phase extracted with CH_2Cl_2 (3x10 ml). The combined organic phases were dried over Na_2SO_4 and concentrated under reduced pressure. The crude product was purified by flash column chromatography (17x2.5 cm, 30–40% EtOAc/hexanes) to afford the product as a colorless oil (2 mg, 10%) next to monoprotected dioxolane **503** and a diastereomer of diprotected **505**.

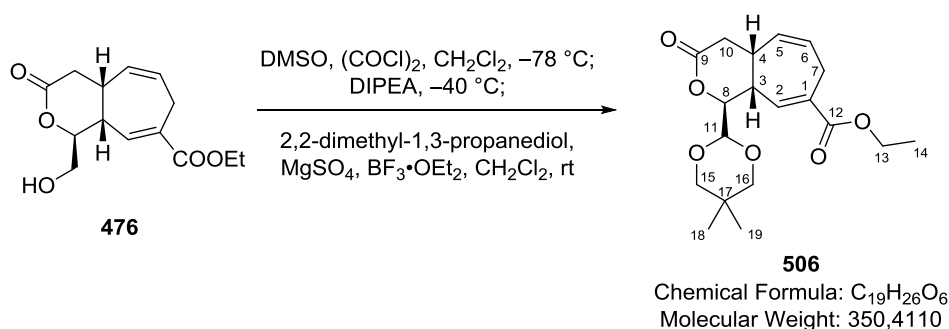
This reaction only led to success when alcohol **476** was purified by flash column chromatography to remove traces of Fe^{III} salts from the previous step. Otherwise, the intermediate aldehyde proved unstable during concentration under reduced pressure.

TLC R_f = 0.39 (40% EtOAc/hexanes).

^1H NMR (400 MHz, C_6D_6): δ 7.35 (dd, J = 6.5, 2.2 Hz, 1H, C_2H), 5.71 (ddd, J = 11.3, 4.6, 2.4 Hz, 1H, C_5H), 5.62 (dddd, J = 11.3, 7.4, 3.7, 2.2 Hz, 1H, C_6H), 5.39 (d, J = 4.5 Hz,

	1H, C ₁₁ H), 4.12 (dd, <i>J</i> = 6.1, 4.5 Hz, 1H, C ₈ H), 4.03–3.91 (m, 3H, 2xC ₁₅ H, C ₁₇ H), 3.87–3.82 (m, 1H, C ₁₈ H), 3.64–3.60 (m, 1H, C ₁₂ H), 3.59–3.55 (m, 1H, C ₁₃ H), 3.51–3.47 (m, 2H, C ₁₇ H, C ₁₈ H), 3.43–3.39 (m, 1H, C ₁₂ H), 3.39–3.35 (m, 1H, C ₁₃ H), 3.29 (dd, <i>J</i> = 19.1, 7.5 Hz, 1H, C ₇ H), 3.19–3.15 (m, 1H, C ₃ H), 3.12–3.06 (m, 1H, C ₇ H), 2.94–2.89 (m, 1H, C ₄ H), 2.03–2.97 (m, 2xC ₁₀ H), 0.92 (t, <i>J</i> = 7.2 Hz, 3H, C ₁₆ H ₃) ppm.
¹³ C NMR	(100 MHz, C ₆ D ₆): δ 167.0 (C14), 141.2 (C2), 134.4 (C1), 133.2 (C5), 127.1 (C6), 119.7 (C9), 103.3 (C11), 77.0 (C8), 65.5 (C13), 65.1 (C12), 64.1 (C18), 63.7 (C17), 60.7 (C15), 39.2 (C3), 36.3 (C10), 33.6 (C4), 26.3 (C7), 14.3 (C16) ppm.
HRMS	((+)-ESI, <i>m/z</i>): calc. [M+Na ⁺]: 375.1414; found: 331.1413 [M+Na ⁺].
IR	$\tilde{\nu}$ = 2963 (w), 2902 (w), 1706 (vs), 1653 (vw), 1438 (vw), 1374 (w), 1298 (w), 1281 (w), 1242 (vs), 1195 (m), 1167 (w), 1075 (vs), 1023 (s), 1004 (s), 950 (m), 869 (w), 803 (vw), 745 (vw), 702 (vw), 663 (vw) cm ⁻¹ .
OR	$[\alpha]_D^{23}$ = –30.0° (1 mg/ml, CHCl ₃).

ethyl (1*S*,4*aR*,9*aR*)-1-(5,5-dimethyl-1,3-dioxan-2-yl)-3-oxo-1,3,4,4*a*,7,9*a*-hexahydrocyclohepta[*c*]pyran-8-carboxylate (506)



Oxalyl chloride (97.0 µl, 143 mg, 1.13 mmol, 3.0 eq.) in CH₂Cl₂ (2.7 ml) was cooled to –78 °C and DMSO (160 µl, 176 mg, 2.25 mmol, 6.0 eq.) was added slowly. This solution was treated with alcohol **476** (100 mg, 0.38 mmol) in CH₂Cl₂ (3.0 ml) after 25 min and stirring was continued for 45 min. NEt₃ (0.42 ml, 0.30 g, 3.0 mmol, 8.0 eq.) was introduced at –78 °C and after 2 h, the reaction mixture was treated with aq. phosphate buffer (*c* = 1 M, pH 7.2, 10 ml). The aqueous phase was extracted with EtOAc (3x20 ml) and the combined organic phases were washed with an aq. sat. NH₄Cl solution (3x40 ml) and brine (50 ml), dried over Na₂SO₄ and concentrated under reduced pressure. The intermediate aldehyde was dried on HV for 5 min.

The crude product was dissolved in CH₂Cl₂ (5.5 ml) and 2,2-Dimethylpropanediol (79 mg, 0.76 mmol, 2.0 eq.) was added. Stirring was continued until the diol dissolved (15 min). The solution was cooled to 0 °C and treated with BF₃·OEt₂ (61 µl, 70 mg, 0.49 mmol, 1.3 eq.) and MgSO₄ (dried at 650 °C twice under HV, purged with nitrogen in between, 128 mg, 1.06 mmol, 2.8 eq.) and stirred at rt for 3 h. Additional BF₃·OEt₂ (30 µl, 35 mg, 0.24 mmol, 1.3 eq.) and MgSO₄ (dried at 650 °C twice under

HV, purged with nitrogen in between, 56 mg, 0.47 mmol, 1.2 eq.) were added and stirring continued for 1 h. Aq. phosphate buffer ($c = 1$ M, pH 7.2, 15 ml) was added, the aqueous phase was extracted with EtOAc (3x20 ml) and the combined organic phases were dried over Na_2SO_4 and concentrated under reduced pressure. The crude product was purified by flash column chromatography (17x2.5 cm, 20–25–30% EtOAc/hexanes) to afford the title compound as a colorless oil (95 mg, 72% over 2 steps).

This reaction only led to success when alcohol **476** was purified by flash column chromatography to remove traces of Fe^{III} salts from the previous step. Otherwise, the intermediate aldehyde proved unstable during concentration under reduced pressure. Additionally, exposure to amine bases has to be as short and mild as possible to obtain reproducible yields.

TLC $R_f = 0.21$ (20% EtOAc/hexanes).

^1H NMR (400 MHz, C_6D_6): δ 7.20 (dd, $J = 6.7, 2.2$ Hz, 1H, C_2H), 5.42 (dddd, $J = 11.2, 7.3, 3.7, 2.2$ Hz, 1H, C_6H), 5.07 (ddd, $J = 11.2, 4.7, 2.7$ Hz, 1H, C_5H), 4.44 (d, $J = 2.6$ Hz, 1H, C_{11}H), 4.41 (dd, $J = 6.4, 2.6$ Hz, 1H, C_8H), 4.00 (q, $J = 7.2$ Hz, 2H, $2 \times \text{C}_{13}\text{H}$), 3.36–3.18 (m, 4H, C_3H , C_7H , C_{15}H , C_{16}H), 3.05–2.96 (m, 1H, C_7H), 2.97–2.91 (m, 2H, C_{15}H , C_{16}H), 2.85–2.78 (m, 1H, C_4H), 2.24–2.16 (m, 2H, $2 \times \text{C}_{10}\text{H}$), 1.07 (s, 3H, C_{18}H_3), 0.97 (t, $J = 7.2$ Hz, 3H, C_{14}H_3), 0.21 (s, 3H, C_{19}H_3) ppm.

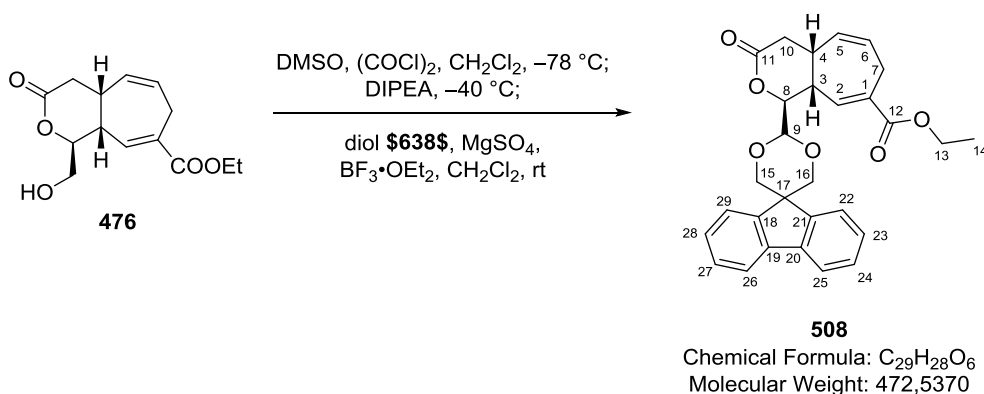
^{13}C NMR (100 MHz, C_6D_6): δ 167.8 (C9), 166.7 (12), 140.4 (C2), 134.3 (C1), 131.1 (C5), 128.2 (C6), 101.2 (C11), 81.2 (C8), 77.2 (C15/C16), 77.0 (C15/C16), 60.9 (C13), 36.2 (C10), 35.8 (C3), 32.7 (C4), 30.1 (C17), 26.7 (C7), 23.1 (C18), 21.3 (C19), 14.3 (C14) ppm.

HRMS ((+)-ESI, m/z): calc. $[\text{M} + \text{Na}^+]$: 373.1622; found: 373.1618 $[\text{M} + \text{Na}^+]$.

IR $\tilde{\nu} = 2957$ (w), 2928 (w), 2854 (w), 1744 (vs), 1707 (vs), 1653 (vw), 1471 (w), 1396 (w), 1366 (w), 1281 (m), 1243 (vs), 1200 (s), 1146 (s), 1083 (vs), 1032 (m), 1016 (m), 992 (m), 908 (vw), 872 (vw), 804 (vw), 744 (vw), 715 (vw), 689 (vw), 668 (vw) cm^{-1}

OR $[\alpha]_{\text{D}}^{25} = +10.2^\circ$ (6 mg/ml, CH_2Cl_2).

ethyl (1*S*,4*aR*,9*aR*)-3-oxo-1-(spiro[fluorene-9,5'-[1,3]dioxan]-2'-yl)-1,3,4,4*a*,7,9*a*-hexahydrocyclohepta[*c*]pyran-8-carboxylate (508)



Oxalyl chloride (27 μ l, 40 mg, 0.32 mmol, 2.0 eq.) in CH_2Cl_2 (1.2 ml) was cooled to -78°C and DMSO (45 μ l, 49 mg, 0.63 mmol, 4.0 eq.) was added slowly. This solution was treated with alcohol **476** (42 mg, 0.16 mmol) in CH_2Cl_2 (1.3 ml) after 15 min and stirring was continued for 15 min. DIPEA (0.22 ml, 0.16 g, 1.3 mmol, 8.0 eq.) was introduced at -78°C and after 1 h, the reaction mixture was allowed to warm to -40°C over 30 min. Aq. phosphate buffer ($c = 0.15\text{ M}$, pH 7.2, 10 ml) was added, the aqueous phase was extracted with CH_2Cl_2 (3x20 ml) and the combined organic phases were washed with brine (50 ml), dried over Na_2SO_4 and concentrated under reduced pressure.

The crude product was dissolved in CH_2Cl_2 (2.4 ml) and MgSO_4 (dried with heat gun three times under vacuum, purged with nitrogen in between, 53 mg, 0.44 mmol, 2.8 eq.) was added. Diol **507** (71 mg, 0.32 mmol, 2.0 eq.) was introduced. The suspension was treated with $\text{BF}_3\cdot\text{OEt}_2$ (25 μ l, 29 mg, 0.20 mmol, 1.3 eq.) and stirred at rt for 2.5 h. Aq. phosphate buffer ($c = 0.15\text{ M}$, pH 7.2, 10 ml) was added, the aqueous phase was extracted with CH_2Cl_2 (3x20 ml) and the combined organic phases were dried over Na_2SO_4 and concentrated under reduced pressure. The crude product was purified by flash column chromatography (14x2 cm, 10–20–30% EtOAc/hexanes) to afford the title compound as a colorless oil (15 mg, 20% over 2 steps).

This reaction did not go to full completion probably due to the low solubility of diol **507** in CH_2Cl_2 . Longer reaction times will be required.

This reaction only led to success when alcohol **476** was purified by flash column chromatography to remove traces of Fe^{III} salts from the previous step. Otherwise, the intermediate aldehyde proved unstable during concentration under reduced pressure.

TLC $R_f = 0.16$ (20% EtOAc/hexanes).

^1H NMR (400 MHz, C_6D_6): δ 8.60–8.56 (m, 1H, $\text{C}_{\text{Ar}}\text{H}$), 7.60–7.45 (m, 3H, $3\times\text{C}_{\text{Ar}}\text{H}$), 7.29–7.24 (m, 1H, $\text{C}_{\text{Ar}}\text{H}$), 7.23–7.17 (m, 2H, C_2H , $\text{C}_{\text{Ar}}\text{H}$), 7.12–7.06 (m, 1H, $\text{C}_{\text{Ar}}\text{H}$), 6.91–6.88 (m, 1H, $\text{C}_{\text{Ar}}\text{H}$), 5.48–5.40 (m, 1H, C_6H), 5.07 (ddd, $J = 11.4, 4.6, 2.7\text{ Hz}$, 1H, C_5H), 4.70 (d, $J = 2.3\text{ Hz}$, 1H, C_9H), 4.56 (dd, $J = 5.9, 2.3\text{ Hz}$, 1H, C_8H), 4.01 (q, $J = 7.1\text{ Hz}$, 2H, $2\times\text{C}_{13}\text{H}$), 3.86–3.76 (m, 2H, C_{15}H , C_{16}H), 3.52–3.46 (m, 2H, C_{15}H , C_{16}H), 3.30–3.26 (m, 1H, C_3H), 3.24 (dd, $J = 20.0, 7.2\text{ Hz}$, 1H, C_7H), 3.07–2.98 (m, 1H, C_7H), 2.93–2.86 (m, 1H, C_4H), 2.27 (dd, $J = 17.6, 7.4\text{ Hz}$, 1H, C_{10}H), 2.22 (dd, $J = 17.6, 5.7\text{ Hz}$, 1H, C_{10}H), 0.97 (t, $J = 7.1\text{ Hz}$, 3H, C_{14}H_3) ppm.

^{13}C NMR (100 MHz, C_6D_6): δ 167.8 (C11), 166.5 (C12), 149.4 (CqAr), 142.9 (CqAr), 142.1 (CqAr), 139.8 (C2), 139.8 (CqAr), 135.7 (C1), 130.9 (C5), 128.8 (CAr), 128.0 (CAr), 128.0 (CAr), 127.5 (C6), 127.2 (CAr), 127.2 (CAr), 123.8 (CAr), 120.6 (CAr), 120.0 (CAr), 100.8 (C9), 81.4 (C8), 73.9 (C15/C16), 73.8 (C15/C16), 61.1 (C13), 49.3 (C17), 36.1 (C3/C10), 36.0 (C3/C10), 32.6 (C4), 26.8 (C7), 14.3 (C14) ppm.

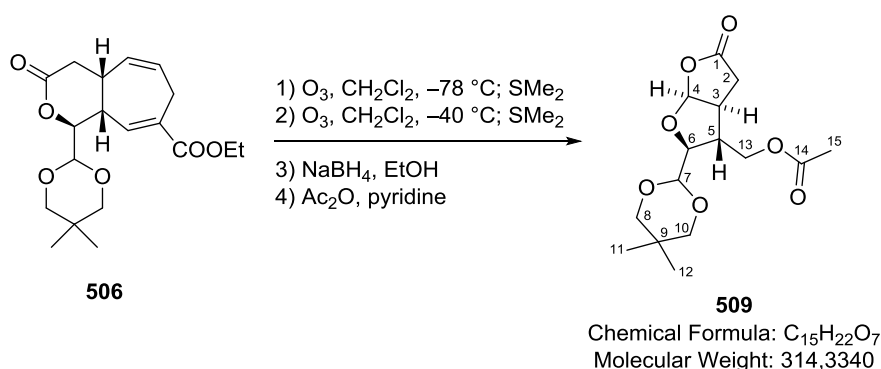
MS (EI, %): 471.96 (M^+ , 2), 238.00 (3), 191.00 (39), 178.00 (100), 83.94 (4).

HRMS (EI, m/z): calc. [M^+]: 472.1886; found: 472.1872 [M^+].

IR $\tilde{\nu}$ = 3396 (br, vw), 2976 (w), 2927 (vw), 2853 (vw), 1741 (vs), 1708 (vs), 1652 (vw), 1477 (w), 1448 (m), 1371 (w), 1280 (m), 1242 (vs), 1193 (m), 1142 (vs), 1090 (m), 1067 (vs), 1032 (m), 998 (m), 946 (w), 920 (w), 808 (vw), 763 (m), 735 (vs), 711 (w), 679 (w) cm^{-1} .

OR $[\alpha]_{\text{D}}^{25} = +57.1^{\circ}$ (8 mg/ml, CH_2Cl_2).

((2*S*,3*R*,3*aS*,6*aS*)-2-(5,5-dimethyl-1,3-dioxan-2-yl)-5-oxohexahydrofuro[2,3-*b*]furan-3-yl)methyl acetate (509**)**



Lactone **506** (27 mg, 0.077 mmol) was dissolved in CH_2Cl_2 (2.0 ml) and cooled to -78°C . Ozone was bubbled through the solution for 1 min and TLC analysis showed complete consumption of the starting material. Nitrogen was passed through the solution and dimethyl sulfide (0.2 ml) was added. The reaction mixture was allowed to warm to 0°C and stirred for 2 h. An aq. phosphate buffer solution (pH 7.2, $c = 1$ M, 10 ml) was added and the aqueous phase extracted with EtOAc (3x10 ml). The combined organic phases were dried over Na_2SO_4 and concentrated under reduced pressure.

The crude intermediate was dissolved in CH_2Cl_2 (2.0 ml) and cooled to -40°C . Ozone was bubbled through the solution for 30 s and excess ozone was removed by passing a nitrogen stream through. Dimethyl sulfide (0.2 ml) was added and the reaction mixture stirred for 1 h at 0°C . An aq. phosphate buffer solution (pH 7.2, $c = 1$ M, 10 ml) was added and the aqueous phase extracted with EtOAc (3x10 ml). The combined organic phases were dried over Na_2SO_4 and concentrated under reduced pressure.

The crude product was dissolved in EtOH (1.0 ml) and NaBH_4 (15 mg, 0.39 mmol, 5.0 eq.) was added. After stirring for 5 h at rt, an aq. phosphate buffer solution (pH 5, $c = 1$ M, 10 ml) was added and the aqueous phase extracted with EtOAc (3x10 ml). The combined organic phases were dried over Na_2SO_4 and concentrated under reduced pressure.

The crude product was dissolved in CH_2Cl_2 (1.0 ml) and acetic anhydride (0.3 ml) and pyridine (0.4 ml) were added. The reaction was stirred for 7 h at rt before an aq. phosphate buffer solution (pH 5, $c = 1$ M, 10 ml) was added and the aqueous phase extracted with EtOAc (3x10 ml). The combined organic phases were dried over Na_2SO_4 and concentrated under reduced pressure. The crude product

was purified by flash column chromatography (deactivated silica, 24x1 cm, 40–50–60% EtOAc/hexanes) to afford the title compound as a colorless oil (6 mg, 25% over 4 steps).

TLC $R_f = 0.21$ (40% EtOAc/hexanes).

^1H NMR (400 MHz, $(\text{D}_3\text{C})_2\text{CO}$): δ 6.03 (d, $J = 5.9$ Hz, 1H, C_4H), 4.52 (d, $J = 3.1$ Hz, 1H, C_7H), 4.17–4.07 (m, 2H, $2\times\text{C}_{13}\text{H}$), 4.05–4.01 (m, 1H, C_6H), 3.65–3.41 (m, 4H, $2\times\text{C}_8\text{H}$, $2\times\text{C}_{10}\text{H}$), 3.11–3.04 (m, 1H, C_5H), 2.83–2.78 (m, 1H, C_2H), 2.70–2.63 (m, 1H, C_3H), 2.54 (dd, $J = 18.0, 2.5$ Hz, 1H, C_2H), 2.02 (s, 3H, C_{15}H_3), 1.14 (s, 3H, C_{11}H_3), 0.73 (s, 3H, C_{12}H_3), 0.15 (s, 3H, C_{12}H_3) ppm.

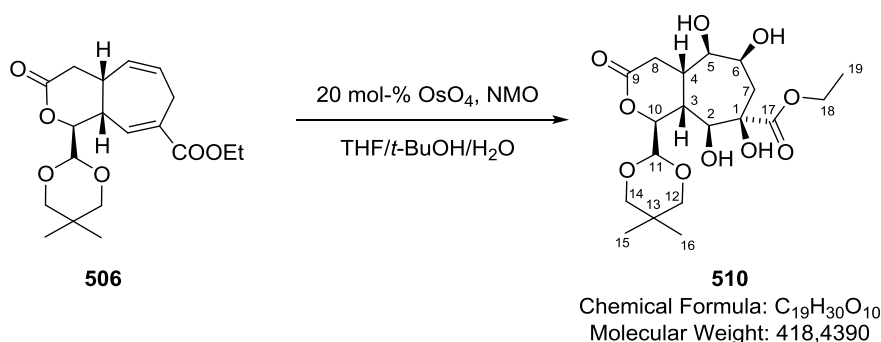
^{13}C NMR (100 MHz, $(\text{D}_3\text{C})_2\text{CO}$): δ 175.3 (C1), 171.0 (C14), 109.5 (C4), 101.5 (C9), 85.3 (C6), 77.3 (C8), 77.1 (C10), 65.9 (C13), 45.9 (C5), 43.4 (C3), 35.8 (C2), 30.7 (C9), 23.2 (C11), 21.7 (C12), 20.7 (C15) ppm.

HRMS (EI, m/z): calc. $[\text{M}-\text{H}^+]$: 313.1287; found: 313.1264 $[\text{M}-\text{H}^+]$.

IR $\tilde{\nu} = 2956$ (w), 2928 (w), 2852 (vw), 1783 (s), 1740 (vs), 1471 (vw), 1417 (vw), 1394 (w), 1366 (w), 1343 (vw), 1232 (vs), 1176 (w), 1148 (w), 1105 (m), 1029 (s), 1001 (m), 989 (w), 828 (vw), 792 (vw) cm^{-1} .

OR $[\alpha]_{\text{D}}^{21} = +12.0^\circ$ (1.5 mg/ml, EtOAc).

ethyl (1*S*,4*aS*,5*R*,6*S*,8*R*,9*S*,9*aR*)-1-(5,5-dimethyl-1,3-dioxan-2-yl)-5,6,8,9-tetrahydroxy-3-oxodecahydrocyclohepta[c]pyran-8-carboxylate (**510**)



Lactone **506** (52 mg, 0.15 mmol) was dissolved in THF/*t*-BuOH/ H_2O (2:1:1, 5.0 ml) and a solution of OsO_4 in *t*-BuOH (2.5 wt-%, 0.15 ml, 151 mg, 0.015 mmol, 0.1 eq.) and NMO (52 mg, 0.46 mmol, 3.0 eq.) were successively added. The reaction mixture was stirred for 47 h in the dark. A solution of OsO_4 in H_2O (4 wt-%, 0.094 ml, 94 mg, 0.015 mmol, 0.1 eq.) and NMO (52 mg, 0.46 mmol, 3.0 eq.) were successively added since the reaction was judged incomplete by LC/MS analysis and the reaction mixture was further stirred for 24 h in the dark. Sat. aq. $\text{Na}_2\text{S}_2\text{O}_3$ solution (7 ml) was added to the reaction mixture and the aqueous phase was saturated with NaCl and extracted with EtOAc (3x10 ml). The combined organic phases were dried over Na_2SO_4 and concentrated under

reduced pressure to afford the title compound as a colorless oil (52 mg, 84%). No further purification was needed.

Purification of the crude product can be performed by flash column chromatography on reverse phase silica (10–15–20% MeCN/H₂O + 0.5% FA). The fractions containing the product are extracted with EtOAc (2x), the organic phases dried over Na₂SO₄ and the solvents removed under reduced pressure to afford the title compound as a colorless oil. The sample after purification was less pure than the crude sample.

LC/MS $R_t = 2.770$ min (10–40% MeCN/H₂O + 0.1% FA, 5 min, 2 ml/min).

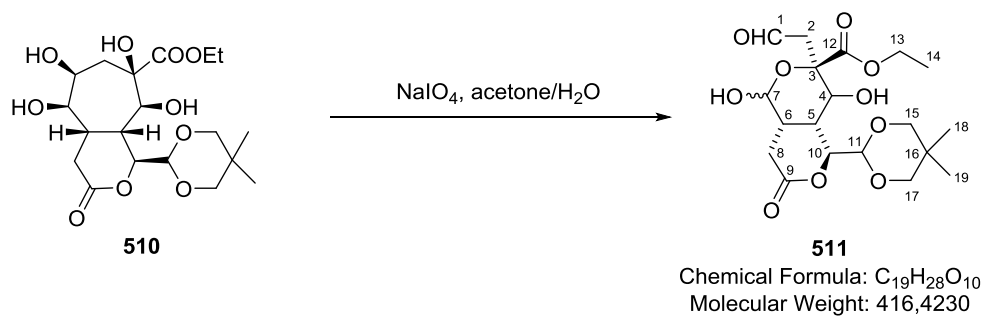
¹H NMR (400 MHz, (D₃C)₂CO): δ 4.77 (dd, $J = 3.6, 3.6$ Hz, 1H, C₁₀H), 4.71 (d, $J = 3.6$ Hz, 1H, C₁₁H), 4.20 (q, $J = 7.1$ Hz, 2H, 2xC₁₈H), 4.10 (ddd, $J = 8.9, 2.2, 2.2$ Hz, 1H, C₆H), 3.97 (d, $J = 9.0$ Hz, 1H, C₂H), 3.69–3.60 (m, 4H, C₅H, C₁₂H, C₁₄H, OH), 3.56–3.47 (m, 2H, C₁₂H, C₁₄H), 2.90–2.82 (m, 2H, C₃H, C₄H), 2.60 (dd, $J = 18.0, 6.4$ Hz, 1H, C₈H), 2.55–2.45 (m, 1H, C₈H), 2.29 (dd, $J = 15.0, 9.0$ Hz, 1H, C₇H), 2.02 (dd, $J = 15.0, 2.3$ Hz, 1H, C₇H), 1.26 (s, 3H, C₁₉H₃), 1.17 (s, 3H, C₁₅H₃), 0.73 (s, 3H, C₁₆H₃) ppm.

¹³C NMR (100 MHz, (D₃C)₂CO): δ 176.1 (C17), 170.4 (C9), 101.9 (C11), 80.1 (C10), 79.1 (C1), 77.6 (C12/C14), 77.5 (C12/C14), 75.7 (C5), 71.6 (C2), 69.6 (C6), 62.1 (C18), 39.0 (C7), 35.4 (C3/C4), 34.5 (C3/C4), 32.1 (C13), 30.9 (C8), 23.2 (C15), 21.7 (C16), 14.4 (C19) ppm.

HRMS ((+)-ESI, m/z): calc. [M+Na⁺]: 441.1731; found: 441.1730 [M+Na⁺].

IR $\tilde{\nu} = 3419$ (br, w), 2956 (w), 2929 (w), 2869 (vw), 1727 (s), 1471 (w), 1395 (w), 1370 (w), 1256 (m), 1242 (s), 1190 (m), 1141 (s), 1089 (vs), 1063 (s), 1026 (vs), 989 (s), 922 (w), 860 (w), 799 (w), 732 (m), 700 (w) cm⁻¹.

ethyl (3*R*,4*aR*,8*aS*)-5-(5,5-dimethyl-1,3-dioxan-2-yl)-1,4-dihydroxy-7-oxo-3-(2-oxoethyl)octahydropyrano[4,3-*c*]pyran-3-carboxylate (511)



Crude Tetraol **510** (35 mg, 0.084 mmol) was dissolved in acetone/H₂O (3:2, 1.0 ml) and NaIO₄ (50 mg, 0.23 mmol, 2.8 eq.) was added. The reaction mixture was stirred in the dark for 1 h. H₂O (5 ml) saturated with NaCl was added and the aqueous phase extracted with EtOAc (3x10 ml). The

combined organic phases were dried over Na_2SO_4 and concentrated under reduced pressure to afford the title compound (dr = 1.3:1, 26 mg, 75%) as a colorless oil.

The analysis is provided for the diastereomeric mixture of the crude product which was sufficiently pure to take forward to the next steps.

TLC R_f = 0.44 (5% MeOH/ CH_2Cl_2).

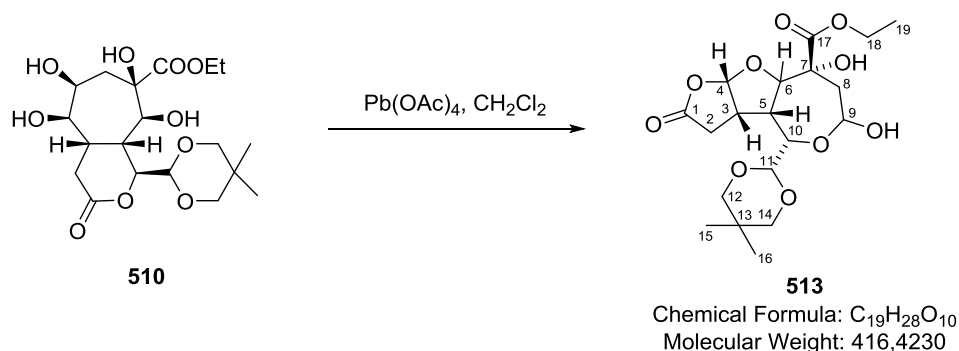
^1H NMR (400 MHz, $(\text{D}_3\text{C})_2\text{CO}$): δ 9.84 (dd, J = 3.0, 2.3 Hz, 1H, C_1H), 9.77 (dd, J = 2.6, 2.2 Hz, 1H, C_1H), 6.04 (d, J = 4.5 Hz, 1H, C_7OH), 5.97 (d, J = 5.0 Hz, 1H, C_7OH), 5.64–5.59 (m, 1H, C_7H), 4.93 (d, J = 4.5 Hz, 1H, C_7H), 4.86 (d, J = 3.3 Hz, 1H, C_{10}H), 4.77–4.75 (m, 2H, $2\times\text{C}_{11}\text{H}$), 4.71–4.66 (m, 1H, C_{10}H), 4.40 (d, J = 8.4 Hz, 1H, C_4OH), 4.34–4.19 (m, 4H, $2\times 2\times\text{C}_{13}\text{H}$), 3.91–3.78 (m, 2H, $2\times\text{C}_4\text{H}$), 3.72–3.45 (m, 8H, $2\times 2\times\text{C}_{15}\text{H}$, $2\times 2\times\text{C}_{17}\text{H}$), 3.10 (dd, J = 16.2, 2.7 Hz, 1H, C_2H), 3.06 (dd, J = 11.0, 6.1 Hz, 1H, C_5H), 2.98–2.91 (m, 2H, $2\times\text{C}_6\text{H}$), 2.91–2.88 (m, 2H, $2\times\text{C}_2\text{H}$), 2.85–2.83 (m, 1H, C_2H), 2.73 (dd, J = 11.5, 5.0 Hz, 1H, C_5H), 2.60 (dd, J = 18.7, 7.4 Hz, 1H, C_8H), 2.55–2.44 (m, 3H, $3\times\text{C}_8\text{H}$), 1.31–1.23 (m, 6H, $2\times\text{C}_{13}\text{H}_3$), 1.17 (s, 6H, $2\times\text{C}_{18}\text{H}_3$), 0.74 (s, 6H, $2\times\text{C}_{19}\text{H}_3$) ppm. C_4OH signal missing.

^{13}C NMR (100 MHz, $(\text{D}_3\text{C})_2\text{CO}$): δ 199.9 (C1), 199.3 (C1), 174.7 (C12), 172.0 (C12), 170.0 (C9), 169.3 (C9), 101.6 (C11), 101.6 (C11), 94.7 (C7), 93.1 (C7), 80.6 (C3), 78.1 (C10), 77.8 (C10), 77.6 (C15/C17), 77.6 (C15/C17), 77.5 (C15/C17), 77.4 (C15/C17), 75.9 (C3), 68.9 (C4), 67.8 (C4), 62.2 (C13), 62.0 (C13), 50.9 (C2), 50.9 (C2), 36.4 (C6), 35.1 (C6), 35.1 (C5), 31.3 (C5), 30.9 (C16), 30.9 (C16), 26.2 (C8), 23.2 (C18), 23.2 (C18), 21.6 (C19), 21.6 (C19), 14.3 (C14), 14.0 (C14) ppm. One carbon atom (C8) underneath solvent peak at δ 29.84 (sept) ppm.

HRMS ((+)-ESI, m/z): calc. $[\text{M}+\text{Na}^+]$: 439.1575; found: 439.1572 $[\text{M}^+]$.

IR $\tilde{\nu}$ = 3441 (br, w), 2958 (w), 2918 (w), 2854 (w), 1723 (vs), 1470 (w), 1394 (w), 1288 (w), 1259 (m), 1217 (m), 1140 (m), 1077 (vs), 1040 (s), 1013 (s), 792 (w) cm^{-1} .

ethyl (3a*S*,3b*R*,4*S*,8*R*,9a*S*)-4-(5,5-dimethyl-1,3-dioxan-2-yl)-6,8-dihydroxy-2-oxodecahydrofuro [3',2':4,5]furo[3,2-*c*]oxepine-8-carboxylate (513)



Tetraol **510** (8 mg, 0.02 mmol) was dissolved in CH_2Cl_2 (1.0 ml) and $\text{Pb}(\text{OAc})_4$ (24 mg, 0.54 mmol, 2.8 eq.) was added. The reaction mixture was stirred for 16 h. H_2O (5 ml) was sat. aq. $\text{Na}_2\text{S}_2\text{O}_3$ solution (5 ml) was added and the reaction mixture was extracted with CH_2Cl_2 (3x10 ml). The combined organic phases were dried over Na_2SO_4 and concentrated under reduced pressure to afford the crude title compound.

Purification by preparative TLC led to decomposition of the compound. Analytical data is thus provided for the crude product.

TLC $R_f = 0.48$ (5% $\text{MeOH}/\text{CH}_2\text{Cl}_2$).

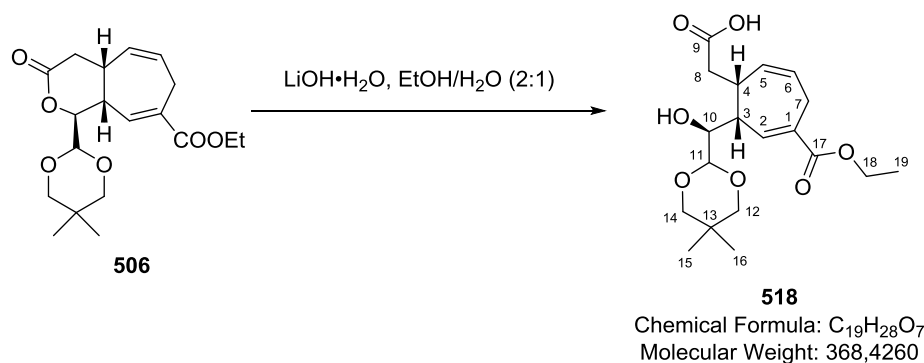
^1H NMR (400 MHz, $(\text{D}_3\text{C})_2\text{CO}$): δ 5.94 (d, $J = 6.5$ Hz, 1H, C_4H), 5.34–5.32 (m, 1H, C_9H), 4.56 (d, $J = 9.0$ Hz, 1H, C_6H), 4.44 (d, $J = 5.2$ Hz, 1H, C_{11}H), 4.35 (dd, $J = 5.2, 2.6$ Hz, 1H, C_{10}H), 4.28 (q, $J = 7.1$ Hz, 2H, $2\times\text{C}_{18}\text{H}$), 3.82 (dd, $J = 18.9, 5.8$ Hz, 1H, C_2H), 3.71–3.57 (m, 3H, C_{12}H , C_{14}H , C_7OH), 3.53–3.41 (m, 2H, C_{12}H , C_{14}H), 3.30–3.22 (m, 1H, C_3H), 2.97 (dd, $J = 9.0, 9.0, 2.6$ Hz, 1H, C_5H), 2.80 (brs, 1H, C_9OH), 2.34 (dd, $J = 18.9, 11.7$ Hz, 1H, C_2H), 2.07–2.03 (m, 2H, $2\times\text{C}_8\text{H}$), 1.29 (t, $J = 7.1$ Hz, 3H, C_{19}H_3), 1.18 (s, 3H, C_{15}H_3), 0.74 (s, 3H, C_{16}H_3) ppm.

^{13}C NMR (100 MHz, $(\text{D}_3\text{C})_2\text{CO}$): δ 178.0 (C1), 174.5 (C17), 108.2 (C4), 101.4 (C11), 92.3 (C9), 86.4 (C6), 77.3 (C12/C14), 77.0 (C12/C14), 74.6 (C7), 66.8 (C10), 63.1 (C18), 41.7 (C5), 39.5 (C3), 35.5 (C8), 30.3 (C13), 30.2 (C2), 22.8 (C15), 21.4 (C16), 13.9 (C19) ppm.

HRMS ((+)-ESI, m/z): calc. $[\text{M}+\text{Na}^+]$: 439.1575; found: 439.1576 $[\text{M}+\text{Na}^+]$.

IR $\tilde{\nu} = 3454$ (vw), 2957 (m), 2926 (m), 2855 (w), 1781 (m), 1727 (vs), 1463 (w), 1415 (vw), 1378 (w), 1260 (s), 1227 (m), 1111 (s), 1109 (vs), 1073 (s), 1038 (s), 984 (vs), 867 (vw), 791 (vw), 742 (w), 706 (vw) cm^{-1} .

2-((1*R*,7*R*)-7-((*S*)-(5,5-dimethyl-1,3-dioxan-2-yl)(hydroxy)methyl)-5-(ethoxycarbonyl)cyclohepta-2,5-dien-1-yl)acetic acid (518**)**



Lactone **506** (90 mg, 0.26 mmol) was dissolved in EtOH (2.0 ml) and a solution of $\text{LiOH}\cdot\text{OH}_2$ in H_2O ($c = 0.11$ M, 3 ml, 0.33 mmol, 1.3 eq.) was added over 3 h. After complete addition, the reaction

mixture was stirred for 15 min and then treated with aq. phosphate buffer (pH 5, $c = 1$ M, 10 ml). The aqueous phase was saturated with NaCl and extracted with EtOAc (3x20 ml). The combined organic phases were dried over Na₂SO₄ and concentrated under reduced pressure to afford the title compound as a colorless foam (90 mg, 95%), which could be used without further purification.

The title compound was not purified by flash column chromatography due to insufficient mass recovery after purification.

TLC $R_f = 0.29$ (5% MeOH/CH₂Cl₂).

¹H NMR (**400 MHz**, (D₃C)₂CO): δ 10.63 (brs, 1H, -COOH), 7.11 (dd, $J = 7.1, 1.8$ Hz, 1H, C₂H), 5.78 (ddd, $J = 11.6, 5.9, 2.7$ Hz, 1H, C₅H), 5.63–5.55 (m, 1H, C₆H), 4.52 (d, $J = 3.2$ Hz, 1H, C₁₁H), 4.15 (q, $J = 7.1$ Hz, 2H, 2xC₁₈H), 3.74 (dd, $J = 8.9, 3.2$ Hz, 1H, C₁₀H), 3.63–3.58 (m, 2H, C₁₂H, C₁₄H), 3.51–3.43 (m, 2H, C₁₂H, C₁₄H), 3.34–3.17 (m, 3H, C₃H, C₄H, C₇H), 3.15–3.06 (m, 1H, C₇H), 2.78 (dd, $J = 15.8, 3.9$ Hz, 1H, C₈H), 2.12 (dd, $J = 15.8, 11.0$ Hz, 1H, C₈H), 1.26 (t, $J = 7.1$ Hz, 3H, C₁₉H₃), 1.11 (s, 3H, C₁₅H₃), 0.71 (s, 3H, C₁₆H₃) ppm.

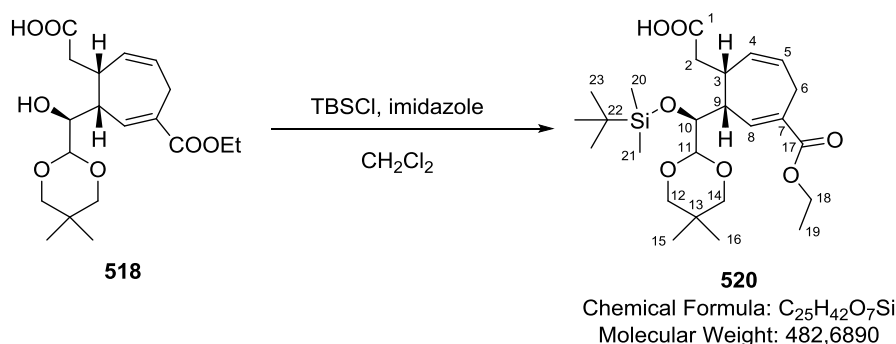
¹³C NMR (**100 MHz**, (D₃C)₂CO): δ 174.0 (C₉), 167.1 (C₁₇), 144.0 (C₂), 134.5 (C₅), 133.5 (C₁), 125.9 (C₆), 103.3 (C₁₁), 77.6 (C₁₂), 77.4 (C₁₄), 72.8 (C₁₀), 61.0 (C₁₈), 42.4 (C₃), 36.6 (C₈), 33.9 (C₄), 30.9 (C₁₃), 27.2 (C₇), 23.1 (C₁₅), 21.8 (C₁₆), 14.6 (C₁₉) ppm.

HRMS ((-)-ESI, m/z): calc. [M-H]⁻: 367.1757; found: 367.1764 [M-H]⁻.

IR $\tilde{\nu} = 3477$ (br, w), 2956 (w), 2908 (w), 2869 (w), 1734 (m), 1704 (vs), 1651 (w), 1471 (w), 1395 (w), 1371 (w), 1241 (vs), 1198 (m), 1151 (m), 1132 (m), 1087 (s), 1041 (m), 1028 (s), 989 (m), 925 (w), 884 (w), 794 (w), 750 (vw), 689 (w) cm⁻¹.

OR $[\alpha]_D^{21} = -81.0^\circ$ (2 mg/ml, EtOAc).

2-((1*R*,7*R*)-7-((*S*)-((*tert*-butyldimethylsilyl)oxy)(5,5-dimethyl-1,3-dioxan-2-yl)methyl)-5-(ethoxycarbonyl)cyclohepta-2,5-dien-1-yl)acetic acid (520**)**



Acid **518** (dr 7.1:1, 76 mg, 0.21 mmol) was dissolved in DMF (0.3 ml) and the solution cooled to 0 °C. Imidazole (67 mg, 1.0 mmol, 4.8 eq.), TBSCl (75 mg, 0.50 mmol, 2.4 eq.) and DMAP (5 mg,

0.04 mmol, 0.2 eq.) were added and the reaction mixture stirred for 7 h at rt. An aq. phosphate buffer solution (pH 5, $c = 1$ M, 5 ml) was added. The aqueous phase was extracted with EtOAc (3x10 ml). The combined organic phases were dried over Na_2SO_4 and concentrated under reduced pressure. The crude product was purified by column chromatography (15x2.5 cm, 10–15–20–30–40–50% EtOAc/hexanes) to afford the title compound as a colorless oil (dr 7.1:1, 96 mg, 97%).

TLC $R_f = 0.40$ (5% MeOH/ CH_2Cl_2).

^1H NMR (400 MHz, CD_2Cl_2): δ 7.12 (dd, $J = 6.8, 2.4$ Hz, 1H, C_8H), 5.77 (dddd, $J = 10.9, 6.1, 2.6, 0.9$ Hz, 1H, C_4H), 5.58 (dddd, $J = 10.9, 7.1, 3.0, 0.7$ Hz, 1H, C_5H), 4.46 (d, $J = 4.9$ Hz, 1H, C_{11}H), 4.14 (q, $J = 7.1$ Hz, 2H, $2\times\text{C}_{18}\text{H}$), 3.80 (dd, $J = 5.7, 4.9$ Hz, 1H, C_{10}H), 3.64–3.57 (m, 2H, C_{12}H , C_{14}H), 3.45–3.37 (m, 2H, C_{12}H , C_{14}H), 3.38–3.33 (m, 1H, C_9H), 3.26 (dd, $J = 19.5, 7.1$ Hz, 1H, C_6H), 3.16–3.07 (m, 1H, C_6H), 3.09–3.02 (m, 1H, C_3H), 2.99 (dd, $J = 15.9, 3.6$ Hz, 1H, C_2H), 2.20 (dd, $J = 15.9, 11.3$ Hz, 1H, C_2H), 1.27 (t, $J = 7.1$ Hz, 3H, C_{19}H_3), 1.11 (s, 3H, C_{15}H_3), 0.91 (s, 9H, C_{23}H_3), 0.71 (s, 3H, C_{16}H_3), 0.14 (s, 3H, C_{21}H_3), 0.11 (s, 3H, C_{20}H_3) ppm. $\text{C}_1(=\text{O})\text{OH}$ peak missing.

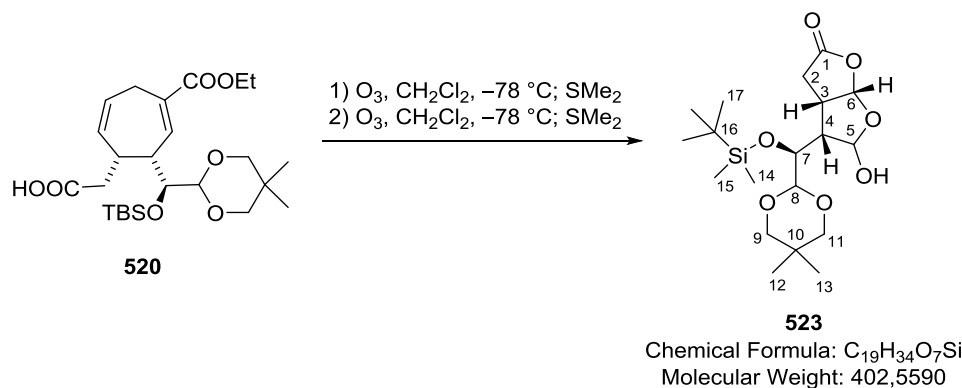
^{13}C NMR (100 MHz, CD_2Cl_2): δ 177.8 (C1), 167.2 (C17), 143.2 (C8), 133.2 (C4), 133.0 (C7), 125.9 (C5), 103.0 (C11), 77.6 (C12), 77.3 (C14), 75.3 (C10), 61.0 (C18), 41.9 (C9), 37.0 (C2), 33.4 (C9), 30.5 (C13), 27.2 (C6), 26.2 (C23), 23.1 (C15), 21.9 (C16), 18.7 (C22), 14.4 (C19), –3.8 (C20), –4.9 (C21) ppm.

HRMS ((+)-ESI, m/z): calc. $[\text{M}+\text{Na}^+]$: 505.2592; found: 505.2588 $[\text{M}+\text{Na}^+]$.

IR $\tilde{\nu} = 3023$ (vw), 2953 (m), 2927 (m), 2853 (w), 1706 (vs), 1650 (w), 1471 (w), 1464 (w), 1393 (w), 1362 (w), 1244 (vs), 1197 (m), 1141 (m), 1114 (s), 1092 (vs), 1031 (s), 1002 (m), 936 (w), 834 (vs), 814 (m), 777 (s), 687 (w), 669 (w) cm^{-1} .

OR $[\alpha]_{\text{D}}^{22} = -85.6^\circ$ (2.5 mg/ml, CH_2Cl_2).

(3a*S*,4*S*,6a*S*)-4-((*S*)-((*tert*-butyldimethylsilyl)oxy)(5,5-dimethyl-1,3-dioxan-2-yl)methyl)-5-hydroxytetrahydrofuro[2,3-*b*]furan-2(3*H*)-one (523)



Acid **520** (12 mg, 0.025 mmol) was dissolved in CH₂Cl₂ (2.0 ml) and the solution cooled to –78 °C. Ozone was passed through the solution (15 sec) and excess ozone was removed by bubbling nitrogen through the solution (1 min). Dimethylsulfide (0.2 ml) was added to the reaction mixture and the solution was allowed to warm to 0 °C. Stirring was continued at this temperature for 3 h. The solution was concentrated under reduced pressure and the residue in CH₂Cl₂ (2.0 ml). The solution was cooled to –78 °C. Ozone was passed through the solution (17 sec) and excess ozone was removed by bubbling nitrogen through the solution (1 min). Dimethylsulfide (0.2 ml) was added to the reaction mixture and the solution was allowed to warm to 0 °C. After stirring for 3 h, the reaction mixture was concentrated under reduced pressure. The crude product was purified by preparative TLC (40% EtOAc/hexanes) to afford the product as a colorless oil (2 mg, 20%).

TLC R_f = 0.38 (30% EtOAc/hexanes).

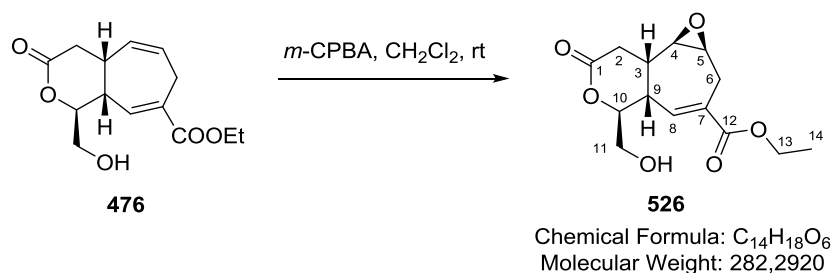
¹H NMR (400 MHz, (D₃C)₂CO): δ 6.04 (d, J = 6.0 Hz, 1H, C₆H), 5.76-5.74 (d, J = 3.7 Hz, 1H, OH), 5.51 (dd, J = 3.9, 3.7 Hz, 1H, C₅H), 4.56 (d, J = 3.0 Hz, 1H, C₈H), 4.03 (dd, J = 10.0, 3.0 Hz, 1H, C₇H), 3.69-3.60 (m, 2H, C₉H, C₁₁H), 3.54-3.44 (m, 2H, C₉H, C₁₁H), 3.36-3.26 (m, 1H, C₃H), 2.88-2.84 (m, 1H, C₂H), 2.61-2.53 (m, 2H, C₂H, C₄H), 1.17 (s, 3H, C₁₂H₃), 0.91 (s, 9H, 3xC₁₇H₃), 0.16 (s, 3H, C₁₄H₃), 0.14 (s, 3H, C₁₅H₃) ppm.

¹³C NMR (100 MHz, (D₃C)₂CO): δ 176.8 (C1), 107.9 (C6), 103.3 (C8), 98.8 (C7), 77.6 (C9/C11), 77.6 (C9/C11), 72.3 (C7), 49.2 (C4), 41.6 (C3), 31.5 (C2), 30.9 (C10), 26.5 (C17), 23.6 (C12/C13), 21.8 (C12/C13), 18.8 (C16), –3.0 (C14/C15), –4.8 (C14/C15) ppm.

HRMS ((+)-ESI, m/z): calc. [M+Na⁺]: 425.1966; found: 425.1963[M+Na⁺].

IR $\tilde{\nu}$ = 3444 (br, vw), 2954 (m), 2928 (m), 2856 (m), 1788 (s), 1472 (w), 1414 (vw), 1362 (w), 1314 (vw), 1251 (m), 1172 (m), 1145 (m), 1099 (vs), 1030 (s), 991 (s), 976 (s), 945 (m), 868 (w), 835 (vs), 810 (w), 778 (m), 665 (w) cm^{–1}.

ethyl (1a*S*,4a*S*,5*S*,8a*S*,8b*R*)-5-(hydroxymethyl)-7-oxo-1a,2,4a,5,7,8,8a,8b-octahydrooxireno [2',3':3,4]cyclohepta[1,2-*c*]pyran-3-carboxylate (526)



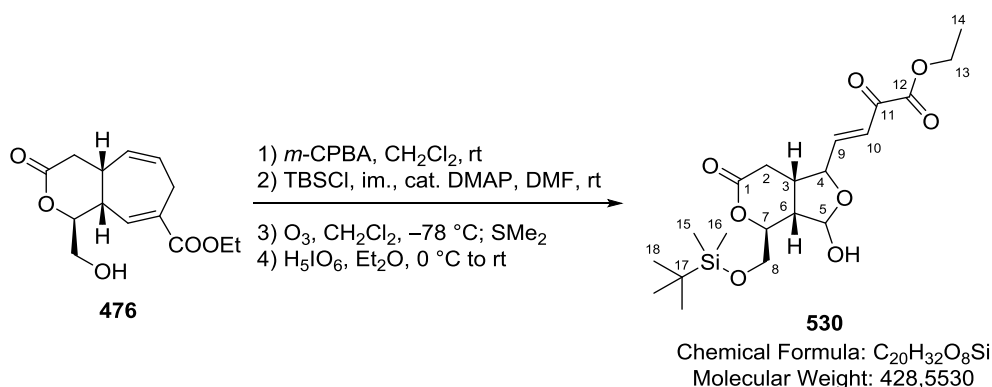
Lactone **476** (dr 6.7:1, 10 mg, 0.038 mmol) was dissolved in CH₂Cl₂ (0.6 ml) and *m*-CPBA ($\leq 77\%$ purity, 13 mg, 0.041 mmol, 1.5 eq.) was added. After stirring for 18 h, an aq. sat. NaHCO₃

solution (5 ml) was added and the aqueous phase extracted with EtOAc (3x10 ml). The combined organic phases were washed with NaHCO₃ solution (3x20 ml), dried over Na₂SO₄ and concentrated under reduced pressure to afford the title compound as a mixture of diastereomers (dr = 3.2:1). Purification by preparative TLC (5% MeOH/CH₂Cl₂) afforded the title compound as a colorless oil (8 mg, 75%) and its diastereomer (3 mg, 28%).

Analytical data is only provided for the major diastereomer.

TLC	R _f = 0.18 (5% MeOH/CH ₂ Cl ₂).
¹H NMR	(400 MHz , (D ₃ C) ₂ CO): δ 6.89 (dd, <i>J</i> = 5.6, 2.5 Hz, 1H, C ₈ H), 4.56–4.50 (m, 1H, OH), 4.40 (dd, <i>J</i> = 5.8, 5.8 Hz, 1H, C ₁₀ H), 4.18 (q, <i>J</i> = 7.1 Hz, 2H, 2xC ₁₃ H), 3.88–3.77 (m, 2H, 2xC ₁₁ H), 3.39–3.26 (m, 2H, C ₅ H, C ₆ H), 3.10–3.04 (m, 1H, C ₉ H), 2.99–2.90 (m, 2H, C ₃ H, C ₄ H), 2.72 (dd, <i>J</i> = 17.7, 5.1 Hz, 1H, C ₂ H), 2.58–2.48 (m, 2H, C ₂ H, C ₆ H), 1.26 (t, <i>J</i> = 7.1 Hz, 3H, C ₁₄ H ₃) ppm.
¹³C NMR	(100 MHz , (D ₃ C) ₂ CO): δ 168.8 (C1), 167.0 (C12), 140.6 (C8), 132.5 (C7), 83.0 (C10), 63.0 (C11), 61.6 (C13), 55.9 (C4), 54.1 (C5), 36.2 (C9), 33.3 (C2), 32.3 (C3), 27.5 (C6), 14.5 (C14) ppm.
HRMS	(EI, m/z): calc. [M ⁺]: 282.1103; found: 282.1096 [M ⁺].
IR	$\tilde{\nu}$ = 3451 (br, vw), 2982 (vw), 2932 (vw), 1733 (vs), 1708 (vs), 1651 (vw), 1448 (vw), 1419 (vw), 1370 (w), 1343 (vw), 1282 (m), 1251 (s), 1205 (m), 1173 (w), 1091 (w), 1062 (m), 1019 (w), 987 (vw), 947 (vw), 917 (vw), 864 (vw), 832 (vw), 793 (vw), 757 (vw), 716 (vw) cm ⁻¹ .
OR	[α] _D ²¹ = +9.3° (3 mg/ml, EtOAc).

ethyl (E)-4-((3a*S*,4*S*,7a*S*)-4-(((*tert*-butyldimethylsilyl)oxy)methyl)-3-hydroxy-6-oxohexahydro-3*H*-furo[3,4-*c*]pyran-1-yl)-2-oxobut-3-enoate (530)



Lactone **476** was dissolved in CH₂Cl₂ (0.9 ml) and cooled to 0 °C. *m*-CPBA (77 wt-%, 22 mg, 0.096 mmol, 1.7 eq.) was added and the reaction mixture stirred at rt. After 23 h, an aq. sat. Na₂S₂O₃ solution (5 ml) and an aq. sat. NaHCO₃ solution (4 ml) were added. The aqueous phase was extracted

with EtOAc (3x10 ml). The combined organic phases were washed with aq. sat. NaHCO_3 (2x15 ml), dried over Na_2SO_4 and concentrated under reduced pressure.

The crude product was dissolved in DMF (0.2 ml) and imidazole (9 mg, 0.1 mmol, 2.4 eq.), TBSCl (10 mg, 0.062 mmol, 1.1 eq.) and DMAP (1 mg, 0.01 mmol, 0.2 eq.) was added. The reaction mixture was stirred for 15 h, before an aq. phosphate buffer (pH 7, $c = 1$ M, 10 ml) was added. The aqueous phase was extracted with EtOAc (3x10 ml). The combined organic phases were dried over Na_2SO_4 and concentrated under reduced pressure.

The crude product was dissolved in CH_2Cl_2 (2.0 ml) and the solution was cooled to -78°C . Ozone was bubbled through the solution for 20 s and excess ozone was removed by passing a stream of nitrogen through the solution. Dimethyl sulfide (0.2 ml) was added and the reaction mixture stirred at 0°C for 6 h. Volatiles were removed under reduced pressure.

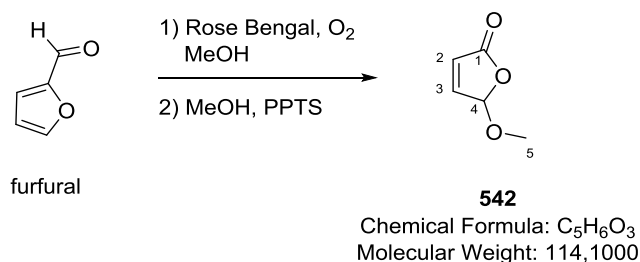
The crude product was dissolved in Et_2O (1.0 ml) and the solution cooled to 0°C . H_5IO_6 (17 mg, 0.11 mmol, 1.5 eq.) was added and the reaction mixtures stirred for 5 h at rt. An aq. sat. $\text{Na}_2\text{S}_2\text{O}_3$ solution (5 ml) was added and the aqueous phase was extracted with EtOAc (3x10 ml). The combined organic phases were dried over Na_2SO_4 and concentrated under reduced pressure. Purification of the crude product by preparative TLC (30% EtOAc/hexanes) afforded the title compound as a colorless oil (dr: 2.3:1, 4 mg, 17% over 4 steps).

Analytical data is only provided for the major diastereomer.

TLC	$R_f = 0.23$ (30% EtOAc/hexanes).
^1H NMR	(400 MHz, (D_3C)$_2\text{CO}$): δ 7.19 (dd, $J = 16.0, 3.7$ Hz, 1H, C_9H), 6.83 (d, $J = 16.0$ Hz, 1H, C_{10}H), 5.62 (d, $J = 4.0$ Hz, 1H, C_5OH), 5.49 (d, $J = 4.0$ Hz, 1H, C_5H), 5.21–5.16 (m, 1H, C_4H), 4.33 (q, $J = 7.2$ Hz, 2H, $2\times\text{C}_{13}\text{H}$), 4.28–4.23 (m, 1H, C_7H), 3.97–3.89 (m, 2H, $2\times\text{C}_8\text{H}$), 3.08–2.96 (m, 1H, C_3H), 2.79–2.73 (m, 1H, C_6H), 2.36 (dd, $J = 14.5, 14.2$ Hz, 1H, C_2H), 2.16 (dd, $J = 14.5, 5.3$ Hz, 1H, C_2H), 1.33 (t, $J = 7.2$ Hz, 3H, C_{14}H_3), 0.92 (s, 3H, C_{15}H_3), 0.12 (s, 3H, C_{16}H_3) ppm.
^{13}C NMR	(100 MHz, (D_3C)$_2\text{CO}$): δ 184.3 (C11), 172.1 (C1), 163.1 (C4), 148.5 (C9), 125.9 (C10), 100.6 (C5), 79.2 (C7), 78.1 (C4), 65.0 (C8), 62.8 (C13), 49.1 (C6), 39.4 (C3), 29.8 (C2), 26.2 (C18), 18.9 (C17), 14.3 (C14), -5.2 (C15/C16), -5.3 (C15/C16) ppm.
HRMS	((+)-ESI, m/z): calc. $[\text{M}+\text{NH}_4^+]$: 446.2205; found: 446.2203 $[\text{M}+\text{NH}_4^+]$.
IR	$\tilde{\nu} = 3438$ (br, vw), 2953 (w), 2929 (w), 2857 (w), 1731 (vs), 1704 (m), 1681 (w), 1631 (w), 1471 (w), 1464 (w), 1444 (vw), 1362 (w), 1303 (w), 1251 (vs), 1143 (s), 1107 (s), 1071 (s), 1045 (m), 1014 (s), 976 (m), 835 (vs), 814 (w), 779 (s), 665 (w) cm^{-1} .
OR	$[\alpha]_{\text{D}}^{21} = +3.0^\circ$ (2 mg/ml, EtOAc).

6.2.4 Third Strategy: Formal (3+2) Cycloaddition and Desymmetrization

5-methoxyfuran-2(5H)-one (542)



Furfural (4.0 ml, 3.5 g, 36 mmol) was dissolved in MeOH (33 ml) and Rose Bengal (sodium salt, 25 mg) was added. A stream of oxygen was passed through the solution while it was cooled with a water bath and irradiated with a sunlight lamp (150 W). Rose Bengal (20 mg, 30 mg respectively) was added after 6 h and 11 h of irradiation. After 24 h, the reaction was judged complete by ¹H NMR analysis of an aliquot. The solution was diluted with MeOH (17 ml), PPTS (10 mg) was added and the solution heated to reflux for 21 h. The solution was concentrated under reduced pressure and the crude product was purified by vacuum distillation ($p = 14$ mbar, bp: 80 °C) to afford the product as a colorless oil (3.53 g, 86% over 2 steps).

TLC $R_f = 0.11$ (10% EtOAc/hexanes).

b.p.: 80 °C ($p = 14$ mbar).

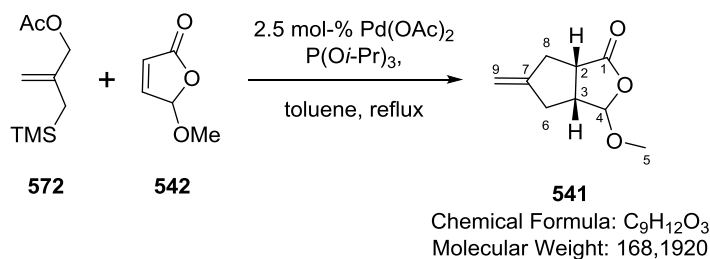
¹H NMR (400 MHz, CDCl₃): δ 7.20 (dd, $J = 5.7, 1.2$ Hz, 1H, C₃H), 6.22 (dd, $J = 5.7, 1.3$ Hz, 1H, C₂H), 5.85 (dd, $J = 1.3, 1.2$ Hz, 1H, C₄H), 3.56 (s, 3H, C₅H₃) ppm.

¹³C NMR (100 MHz, CDCl₃): δ 170.4, 150.2, 125.3, 104.2, 57.1 ppm.

HRMS (EI, m/z): calc. [M-H⁺]: 113.0239; found: 113.0235 [M-H⁺].

IR $\tilde{\nu} = 3102$ (vw), 2939 (vw), 2839 (vw), 1792 (s), 1758 (vs), 1448 (vw), 1371 (w), 1322 (w), 1206 (w), 1165 (m), 1125 (s), 1081 (m), 1011 (s), 988 (m), 932 (m), 892 (m), 821 (m), 791 (w), 694 (m) cm⁻¹.

rac-(3*aR*,6*aS*)-3-methoxy-5-methylenhexahydro-1*H*-cyclopenta[*c*]furan-1-one (541)



Furanone **542** (404 mg, 3.54 mmol), allyl acetate **572** (1.1 ml, 1.0 g, 5.3 mmol, 1.5 eq.) and Pd(OAc)₂ (20 mg, 0.0089 mmol, 2.5 mol-%) were dissolved in deaerated toluene (10 min nitrogen stream through solvent, 40 ml). Tri-*iso*-propylphosphite (175 μ l, 148 mg, 0.71 mmol, 0.2 eq.) was added and the solution heated to reflux for 12 h. The solution was cooled to rt and concentrated under reduced pressure. The crude product was purified by flash column chromatography (12x4.5 cm, 10–15–20% Et₂O/hexanes) to afford the product as a colorless oil (547 mg, 92%).

TLC R_f = 0.32 (10% EtOAc/hexanes).

¹H NMR (**400 MHz, CDCl₃**): δ 5.08 (s, 1H, C₄H), 4.91–4.88 (m, 2H, 2xC₉H), 3.48 (s, 3H, C₅H₃), 3.20–3.14 (m, 1H, C₂H), 2.84–2.78 (m, 1H, C₃H), 2.72–2.62 (m, 3H, C₆H, 2xC₈H), 2.22 (dd, J = 16.3, 5.9 Hz, 1H, C₆H) ppm.

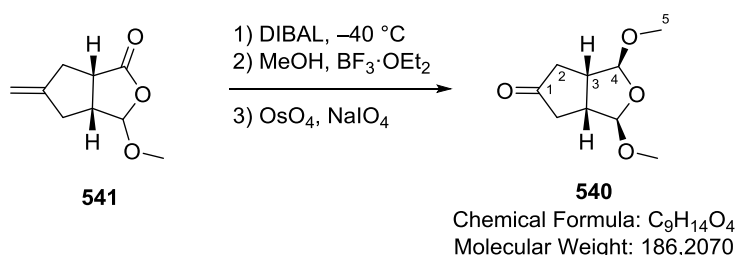
¹³C NMR (**100 MHz, CDCl₃**): δ 179.5 (C1), 147.3 (C7), 108.9 (C4), 108.5 (C9), 56.7 (C5), 45.8 (C3), 43.7 (C2), 36.3 (C6), 35.7 (C8) ppm.

MS (**EI, %**): 168.16 (4, M⁺), 137.13 (34), 109.12 (28), 92.09 (64), 80.08 (93), 79.07 (100), 77.05 (32).

HRMS (**EI, m/z**): calc. [M⁺]: 168.0786; found: 168.0777 [M⁺].

IR $\tilde{\nu}$ = 3077 (vw), 2939 (vw), 2843 (vw), 1771 (vs), 1659 (vw), 1467 (vw), 1443 (vw), 1431 (vw), 1378 (vw), 1353 (m), 1314 (vw), 1270 (vw), 1207 (w), 1160 (m), 1110 (vs), 1068 (w), 1046 (m), 983 (m), 954 (m), 915 (vs), 835 (vw), 784 (vw), 741 (vw), 690 (vw) cm⁻¹.

***rac*-(1*R*,3*S*,3*aS*,6*aR*)-1,3-dimethoxytetrahydro-1*H*-cyclopenta[*c*]furan-5(3*H*)-one (**540**)**

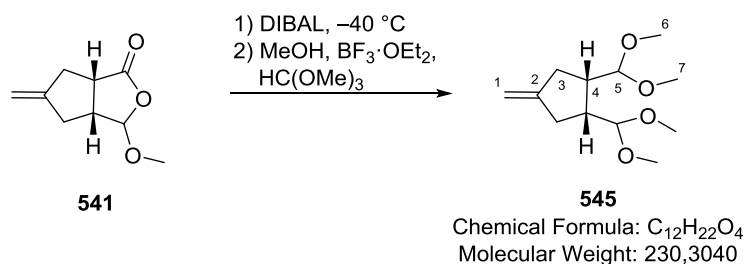


Olefin **541** (420 mg, 2.50 mmol) in CH₂Cl₂ (23 ml) was cooled to –40 °C and DIBAL (c = 1 M in CH₂Cl₂, 3.0 ml, 3.0 mmol, 1.2 eq.) was added slowly dropwise. The reaction mixture was stirred for 1.5 h at the same temperature before a sat. aq. Rochelle salt solution (50 ml) and pH 7.2 phosphate buffer (c = 1 M, 20 ml) were carefully added. The aqueous phase was extracted with Et₂O (3x100 ml), the combined organic phases dried over Na₂SO₄ and concentrated under reduced pressure. The crude product was dissolved in MeOH (8 ml) and the solution cooled to 0 °C. BF₃·OEt₂ (62 μ l, 71 mg, 0.50 mmol, 0.2 eq.) was added and the reaction mixture stirred at rt for 13 h. pH 7.2 Phosphate buffer (c = 1 M, 20 ml) was added and the aqueous phase was extracted with Et₂O (3x30 ml). The combined organic phases were dried over Na₂SO₄ and concentrated under reduced pressure. The crude product

was dissolved in THF (25 ml) and OsO_4 (4 wt-% in H_2O , 0.80 ml, 0.80 g, 0.13 mmol, 0.05 eq.) was added. A solution of NaIO_4 (1.60 g, 7.48 mmol, 3.0 eq.) in H_2O (25 ml) was introduced slowly and the reaction mixture stirred for 5.5 h. A sat. aq. $\text{Na}_2\text{S}_2\text{O}_3$ solution (50 ml) was added and the aqueous phase extracted with CH_2Cl_2 (3x70 ml). The combined organic phases were dried over Na_2SO_4 and concentrated under reduced pressure. The crude product was purified by flash column chromatography (12x4.5 cm, 1–1.5–2–3% acetone/ CH_2Cl_2) to afford the title compound as a colorless solid (dr 9.7:1, 293 mg, 63% over 3 steps). X-Ray suitable crystals were obtained by slow diffusion of hexanes into a solution of the title compound in EtOAc while allowing slow evaporation.

TLC	$R_f = 0.36$ (3% acetone/ CH_2Cl_2).
m.p.:	86–87 °C.
^1H NMR	(400 MHz, CD_2Cl_2): δ 4.87 (s, 2H, $2\times\text{C}_4\text{H}$), 3.39 (s, 6H, $2\times\text{C}_5\text{H}_3$), 3.00–2.93 (m, 2H, $2\times\text{C}_3\text{H}$), 2.54–2.44 (m, $2\times\text{C}_2\text{H}$), 2.25–2.17 (m, 2H, $2\times\text{C}_2\text{H}$) ppm.
^{13}C NMR	(100 MHz, CD_2Cl_2): δ 217.3 (C1), 112.0 (C4), 55.7 (C5), 46.1 (C3), 41.3 (C2) ppm.
MS	(EI, %): 185.13 (M–H, 5), 155.14 (56), 126.15 (100), 98.18 (42), 85.17 (45), 67.17 (44).
HRMS	(EI, m/z): calc. $[\text{M}-\text{H}^+]$: 185.0814; found: 185.0874 $[\text{M}-\text{H}^+]$.
IR	$\tilde{\nu} = 2955$ (vw), 2912 (w), 2834 (vw), 1741 (vs), 1470 (vw), 1446 (vw), 1381 (w), 1301 (vw), 1283 (vw), 1267 (vw), 1243 (vw), 1220 (w), 1188 (w), 1159 (w), 1107 (vs), 1085 (s), 1059 (w), 1040 (w), 971 (vs), 939 (vs), 811 (vw), 771 (vw) cm^{-1} .

***rac*-(1*R*,2*S*)-1,2-bis(dimethoxymethyl)-4-methylenecyclopentane (545)**



Olefin **541** (53 mg, 2.50 mmol) in CH_2Cl_2 (3 ml) was cooled to -40°C and DIBAL ($c = 1$ M in CH_2Cl_2 , 0.38 ml, 0.38 mmol, 1.2 eq.) was added slowly dropwise. The reaction mixture was stirred for 1 h at the same temperature before a sat. aq. Rochelle salt solution (10 ml) and pH 7.2 phosphate buffer ($c = 1$ M, 5 ml) were carefully added. The aqueous phase was extracted with CH_2Cl_2 (3x15 ml), the combined organic phases dried over Na_2SO_4 and concentrated under reduced pressure. The crude product was dissolved in MeOH (1.0 ml) and the solution cooled to 0°C . HC(OMe)_3 (0.10 ml, 0.10 g, 0.96 mmol, 3.0 eq.) and $\text{BF}_3\cdot\text{OEt}_2$ (8 μl , 9 mg, 0.06 mmol, 0.2 eq.) was added and the reaction mixture stirred at rt for 13 h. The reaction mixture was treated with pH 7.2 buffer ($c = 1$ M, 5 ml) and the aqueous phase was extracted with Et_2O (3x10 ml). The combined organic phases were dried over

Na_2SO_4 and concentrated under reduced pressure. The crude product was purified by flash column chromatography (14x2 cm, 5–7.5–10% Et_2O /hexanes) to afford the title compound as a colorless oil (21 mg, 29% over 2 steps).

TLC $R_f = 0.49$ (15% EtOAc /hexanes).

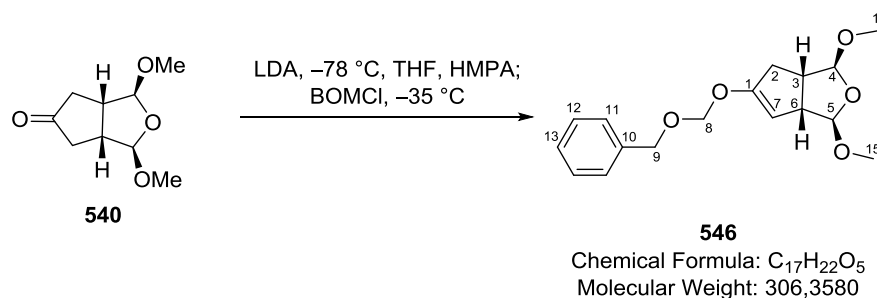
^1H NMR (400 MHz, CD_2Cl_2): δ 4.80–4.77 (m, 2H, $2\times\text{C}_1\text{H}$), 4.34–4.31 (m, 2H, $2\times\text{C}_5\text{H}$), 3.31 (s, 6H, $2\times\text{C}_6\text{H}_3$), 3.28 (s, 6H, $2\times\text{C}_7\text{H}_3$), 2.45–2.23 (m, 6H, $2\times\text{C}_4\text{H}$, $2\times\text{C}_3\text{H}_2$) ppm.

^{13}C NMR (100 MHz, CD_2Cl_2): δ 151.6 (C2), 105.5 (C5), 105.1 (C1), 54.1 (C6), 53.1 (C7), 43.1 (C4), 34.2 (C3) ppm.

HRMS (EI, m/z): calc. $[\text{M}-\text{OMe}^+]$: 199.1334; found: 199.1323 $[\text{M}-\text{OMe}^+]$.

IR $\tilde{\nu} = 3071$ (vw), 2982 (vw), 2934 (w), 2910 (w), 2829 (vw), 2660 (vw), 1465 (vw), 1444 (vw), 1392 (vw), 1367 (vw), 1312 (vw), 1282 (vw), 1248 (vw), 1217 (vw), 1189 (w), 1156 (w), 1137 (m), 1113 (s), 1055 (vs), 974 (m), 931 (w), 904 (w), 873 (m), 748 (vw) cm^{-1} .

***rac*-(1*R*,3*S*,3*aS*,6*aR*)-5-((benzyloxy)methoxy)-1,3-dimethoxy-3,3*a*,4,6*a*-tetrahydro-1*H*-cyclopenta[*c*]furan (546)**



DIPA (23 μl , 16 mg, 0.16 mmol, 3.0 eq.) in THF (0.55 ml) was treated with *n*-BuLi ($c = 2.35$ M in hexanes, 70 μl , 0.16 mmol, 3.0 eq.) at -78 °C and the resulting solution stirred for 30 min. Ketone **540** (10 mg, 0.054 mmol) and HMPA (0.2 ml) were added and stirring was continued for 25 min. BOMCl (30 μl , 34 mg, 0.21 mmol, 4.0 eq.) was introduced and the reaction mixture allowed to warm to -35 °C. After 1.5 h, pH 7.2 phosphate buffer ($c = 1$ M, 10 ml) was added and the aqueous phase extracted with CH_2Cl_2 (3x10 ml). The combined organic phases were dried over Na_2SO_4 and concentrated under reduced pressure. The crude product was purified by column chromatography (16x2 cm, 10–15–20% EtOAc /hexanes) to afford the title compound as a colorless oil (4 mg, 24%).

The product partially decomposes during the purification.

TLC $R_f = 0.47$ (20% EtOAc /hexanes).

^1H NMR (400 MHz, CDCl_3): δ 7.39–7.27 (m, 5H, $2\times\text{C}_{11}\text{H}$, $2\times\text{C}_{12}\text{H}$, C_{13}H), 5.04 (d, $J = 6.3$ Hz, 1H, C_8H), 5.02 (d, $J = 6.3$ Hz, 1H, C_8H), 4.92 (s, 1H, C_4H), 4.81 (s, 1H, C_5H), 4.68–

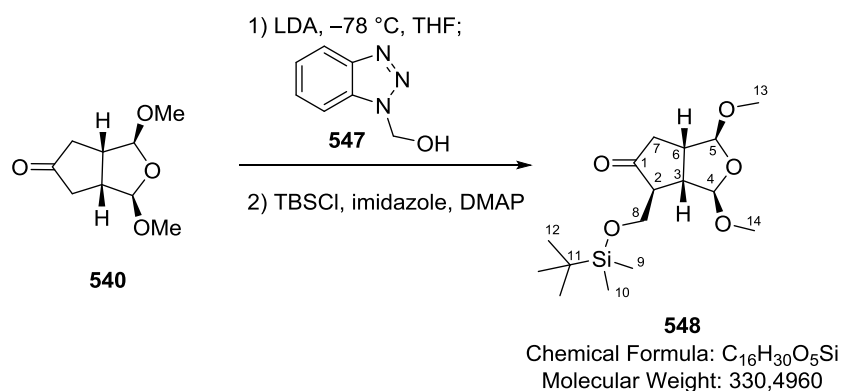
4.66 (m, 1H, C₇H), 4.66 (d, *J* = 11.9 Hz, 1H, C₉H), 4.62 (d, *J* = 11.9 Hz, 1H, C₉H), 3.44 (s, 3H, C₁₄H₃), 3.42 (s, 3H, C₁₅H₃), 3.42–3.36 (m, 1H, C₆H), 2.93–2.86 (m, 1H, C₃H), 2.78–2.69 (m, 1H, C₂H), 2.42–2.33 (m, 1H, C₂H) ppm.

¹³C NMR (100 MHz, CDCl₃): δ 157.0 (C1), 137.3 (C10), 128.6 (C11/C12/C13), 128.1 (C11/C12/C13), 128.0 (C11/C12/C13), 114.5 (C4), 110.6 (C5), 97.5 (C7), 93.1 (C8), 70.6 (C9), 55.7 (C14/C15), 55.4 (C14/C15), 54.7 (C6), 44.5 (C3), 36.8 (C2) ppm.

HRMS (EI, *m/z*): calc. [M–H⁺]: 305.1389; found: 305.1315 [M–H⁺].

IR $\tilde{\nu}$ = 3499 (br, vw), 2909 (w), 2831 (vw), 1744 (vw), 1651 (w), 1497 (vw), 1467 (vw), 1453 (vw), 1376 (w), 1343 (w), 1288 (vw), 1255 (vw), 1228 (m), 1199 (w), 1190 (vw), 1156 (w), 1100 (vs), 1082 (s), 1057 (m), 979 (vs), 816 (vw), 771 (vw), 739 (w), 698 (w) cm^{–1}.

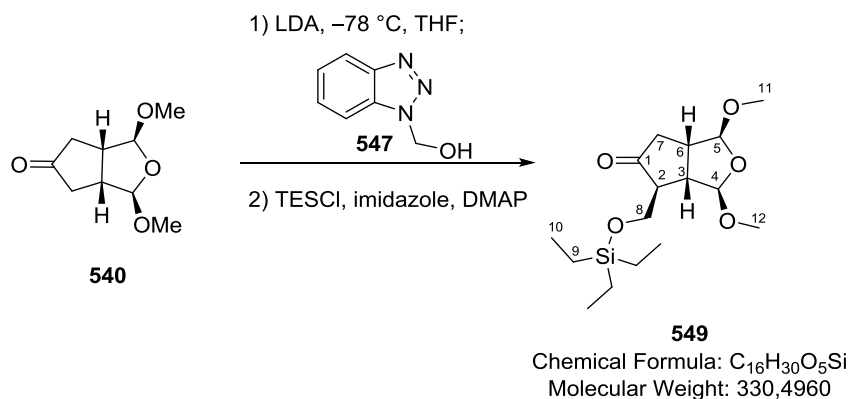
***rac*-(1*S*,3*R*,3*aS*,4*S*,6*aS*)-4-(((*tert*-butyldimethylsilyl)oxy)methyl)-1,3-dimethoxytetrahydro-1*H*-cyclopenta[*c*]furan-5(3*H*)-one (548)**



DIPA (42 µl, 30 mg, 0.29 mmol, 1.1 eq.) in THF (1.5 ml) was treated with *n*-BuLi (*c* = 2.35 M in hexanes, 123 µl, 0.28 mmol, 1.05 eq.) at –78 °C and the resulting solution stirred for 20 min. Ketone **540** (50 mg, 0.27 mmol) in THF (1.0 ml) was added and stirring was continued for 25 min at the same temperature. Triazole **547** (42 mg, 0.28 mmol, 1.05 eq.) dissolved in THF (1.0 ml) was added and the reaction mixture further stirred for 55 min. An aq. phosphate buffer (pH 7.2, *c* = 1 M, 10 ml) was added and the aqueous phase extracted with EtOAc (3x20 ml). The combined organic phases were dried over Na₂SO₄ and concentrated under reduced pressure. The crude product was dissolved in CH₂Cl₂ (3.0 ml) and imidazole (129 mg, 1.89 mmol, 7.0 eq.), TBSCl (163 mg, 1.08 mmol, 4.0 eq.) and DMAP (3 mg, 0.027 mmol, 0.1 eq.) were successively added. The reaction mixture was stirred for 17 h. An aq. phosphate buffer (pH 7.2, *c* = 1 M, 10 ml) was added and the aqueous phase extracted with EtOAc (3x20 ml). The combined organic phases were dried over Na₂SO₄ and concentrated under reduced pressure. The crude product was purified by flash column chromatography (14x2 cm, 5–10–15–20% EtOAc/hexanes) to afford the title compound as a colorless oil (52 mg, 59% over 2 steps).

TLC	$R_f = 0.51$ (30% EtOAc/hexanes).
^1H NMR	(400 MHz , CDCl_3): δ 4.97 (s, 1H, C_4H), 4.87 (s, 1H, C_5H), 3.87 (dd, $J = 9.7, 4.8$ Hz, 1H, C_8H), 3.79 (dd, $J = 9.7, 3.4$ Hz, 1H, C_8H), 3.45 (s, 3H, C_{13}H_3), 3.44 (s, 3H, C_{14}H_3), 3.05–2.97 (m, 2H, C_3H , C_6H), 2.56–2.44 (m, 1H, C_7H), 2.37–2.29 (m, 1H, C_7H), 2.28–2.22 (m, 1H, C_2H), 0.85 (s, 9H, $3 \times \text{C}_{12}\text{H}_3$), 0.03 (s, 3H, C_9H_3), 0.01 (s, 3H, C_{10}H_3) ppm.
^{13}C NMR	(100 MHz , CDCl_3): δ 218.0 (C1), 112.4 (C5), 111.3 (C4), 62.8 (C8), 55.8 (C13/C14), 55.4 (C13/C14), 53.7 (C2), 50.5 (C3), 44.2 (C6), 42.0 (C7), 25.8 (C12), 18.1 (C11), –5.6 (C9/C10), –5.7 (C9/C10) ppm.
MS	(EI , %): 299.26 ($\text{M}-\text{OMe}^+$, 6), 241.18 (60), 213.17 (50), 181.14 (100), 167.12 (19), 107.07 (19), 89.05 (36), 75.03 (82), 73.05 (28).
HRMS	(EI , m/z): calc. $[\text{M}-\text{OMe}^+]$: 299.1679; found: 299.1677 $[\text{M}-\text{OMe}^+]$.
IR	$\tilde{\nu} = 2954$ (w), 2929 (w), 2897 (w), 2857 (w), 1743 (s), 1471 (w), 1445 (vw), 1406 (vw), 1384 (w), 1361 (w), 1254 (w), 1223 (w), 1191 (vw), 1166 (vw), 1093 (vs), 1052 (w), 1037 (w), 990 (s), 961 (s), 836 (vs), 814 (w), 778 (m), 744 (vw), 666 (vw) cm^{-1} .

***rac*-(1*S*,3*R*,3*aS*,4*S*,6*aS*)-1,3-dimethoxy-4-(((triethylsilyl)oxy)methyl)tetrahydro-1*H*-cyclopenta[*c*]furan-5(3*H*)-one (**549**)**



DIPA (45 μl , 33 mg, 0.32 mmol, 3.0 eq.) in THF (1.1 ml) was treated with *n*-BuLi ($c = 2.35$ M in hexanes, 137 μl , 0.322 mmol, 3.0 eq.) at -78°C and the resulting solution stirred for 25 min. Ketone **540** (20 mg, 0.11 mmol) was added and stirring was continued for 25 min at the same temperature. Triazole **547** (32 mg, 0.21 mmol, 2.0 eq.) was added and the reaction mixture further stirred for 2.5 h. An aq. phosphate buffer (pH 7.2, $c = 1$ M, 10 ml) was added and the aqueous phase extracted with CH_2Cl_2 (3x10 ml). The combined organic phases were dried over Na_2SO_4 and concentrated under reduced pressure. The crude product was dissolved in CH_2Cl_2 (1.5 ml) and divided in three batches. One batch was treated with imidazole (7 mg, 0.11 mmol, 4.0 eq.), TESCl (18 μl , 16 mg, 0.11 mmol, 3.0 eq.) and a grain of DMAP successively. The reaction mixture was stirred for 13 h. An aq. phosphate buffer (pH 7.2, $c = 1$ M, 10 ml) was added and the aqueous phase extracted with CH_2Cl_2

(3x10 ml). The combined organic phases were dried over Na₂SO₄ and concentrated under reduced pressure. The crude product was purified by preparative TLC (20% EtOAc/hexanes) to afford the title compound as a colorless oil (5 mg, 40% over 2 steps).

TLC R_f = 0.29 (15% EtOAc/hexanes).

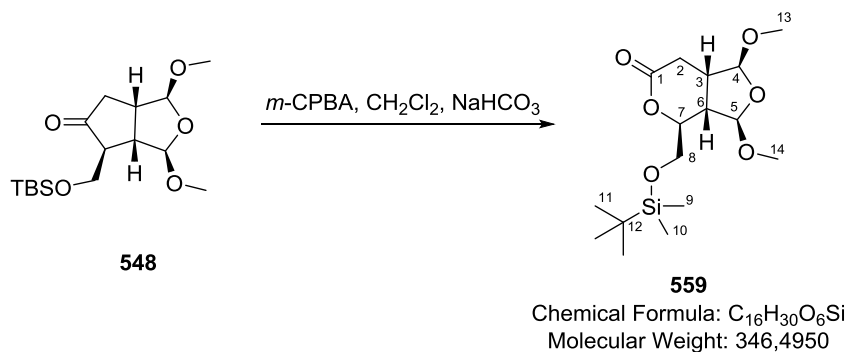
¹H NMR (400 MHz, CD₂Cl₂): δ 4.95 (s, 1H, C₄H), 4.85 (d, J = 2.1 Hz, 1H, C₅H), 3.85 (dd, J = 9.8, 5.0 Hz, 1H, C₈H), 3.78 (dd, J = 9.8, 3.7 Hz, 1H, C₈H), 3.41 (s, 3H, C₁₁H₃), 3.39 (s, 3H, C₁₂H₃), 2.97–2.89 (m, 2H, C₃H, C₆H), 2.50–2.41 (m, 1H, C₇H), 2.34–2.27 (m, 1H, C₇H), 2.24–2.19 (m, C₂H), 0.93 (t, J = 8.0 Hz, 9H, 3xC₁₀H₃), 0.58 (q, J = 8.0 Hz, 6H, 3xC₉H₂) ppm.

¹³C NMR (100 MHz, CD₂Cl₂): δ 217.8 (C1), 112.7 (C5), 111.4 (C4), 62.6 (C8), 55.9 (C11/C12), 55.4 (C11/C12), 54.0 (C2), 50.8 (C3/C6), 44.5 (C3/C6), 42.1 (C7), 6.8 (C10), 4.5 (C9) ppm.

HRMS (EI, m/z): calc. [M–OMe⁺]: 299.1679; found: 299.1677 [M–OMe⁺].

IR $\tilde{\nu}$ = 2954 (m), 2912 (m), 2877 (m), 2828 (vw), 1744 (s), 1459 (w), 1410 (vw), 1382 (w), 1293 (vw), 1224 (w), 1193 (w), 1166 (w), 1095 (vs), 1052 (w), 1037 (w), 1016 (m), 990 (s), 961 (s), 864 (vw), 817 (vw), 786 (w), 745 (m), 729 (m), 673 (vw) cm^{−1}.

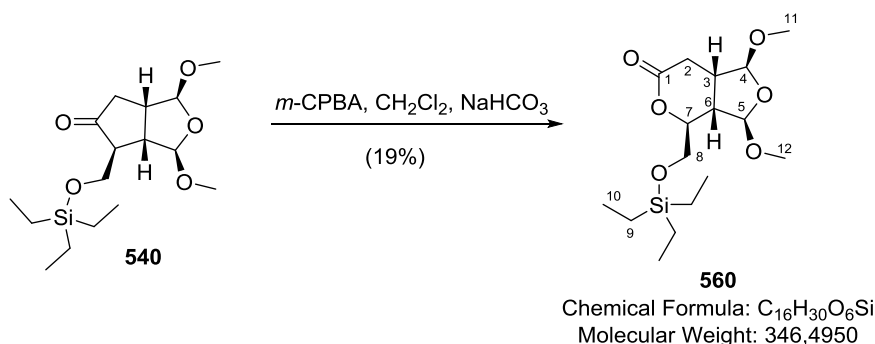
rac-(1*S*,3*R*,3*aS*,4*S*,7*aS*)-4-(((*tert*-butyldimethylsilyl)oxy)methyl)-1,3-dimethoxytetrahydro-3*H*-furo[3,4-*c*]pyran-6(1*H*)-one (559)



Ketone **548** (44 mg, 0.13 mmol) was dissolved in CH₂Cl₂ (2.0 ml) and NaHCO₃ (56 mg, 0.67 mmol, 5.0 eq.) and *m*-CPBA ($\leq 77\%$ purity, 51 mg, 0.23 mmol, 1.7 eq.) were added. The reaction mixture was stirred for 7 d before more *m*-CPBA ($\leq 77\%$ purity, 24 mg, 0.11 mmol, 0.8 eq.), NaHCO₃ (28 mg, 0.33 mmol, 2.5 eq.) and CH₂Cl₂ (0.5 ml) were added. After stirring for 18 h, an aq. sat. NaHCO₃ solution (5 ml) and an aq. sat. Na₂S₂O₃ solution (5 ml) were added. The aqueous phase was extracted with EtOAc (3x10 ml). The combined organic layers were washed with aq. sat. NaHCO₃ (3x20 ml), dried over Na₂SO₄ and concentrated under reduced pressure to afford the title compound as a colorless oil (45 mg, 98%).

TLC	$R_f = 0.33$ (30% EtOAc/hexanes).
^1H NMR	(400 MHz, CDCl_3): δ 5.02 (s, 1H, C_5H), 4.84 (s, 1H, C_4H), 4.16 (ddd, $J = 9.2, 4.4, 4.4$ Hz, 1H, C_7H), 3.87–3.84 (m, 2H, $2\times\text{C}_8\text{H}$), 3.44 (s, 3H, C_{14}H_3), 3.43 (s, 3H, C_{13}H_3), 2.85–2.67 (m, 3H, C_2H , C_3H , C_6H), 2.31 (dd, $J = 15.1, 11.5$ Hz, 1H, C_2H), 0.90 (s, 9H, $3\times\text{C}_{11}\text{H}_3$), 0.09 (s, 3H, C_9H_3), 0.09 (s, 3H, C_{10}H_3) ppm.
^{13}C NMR	(100 MHz, CDCl_3): δ 171.1 (C1), 111.0 (C4), 109.1 (C5), 78.7 (C7), 64.8 (C8), 56.1 (C14), 55.6 (C13), 46.1 (C6), 42.2 (C3), 31.2 (C2), 26.0 (C11), 18.5 (C12), –5.3 (C9/C10), –5.3 (C9/C10) ppm.
MS	(EI, %): 315.25 (1, $\text{M}-\text{OMe}^+$), 257.18 (20), 197.15 (22), 117.07 (90), 89.015 (28), 58.04 (27), 43.03 (100).
HRMS	(EI, m/z): calc. $[\text{M}-\text{OMe}^+]$: 315.1628; found: 315.1646 $[\text{M}-\text{OMe}^+]$.
IR	$\tilde{\nu} = 3460$ (br, vw), 2949 (m), 2928 (m), 2856 (w), 1751 (s), 1471 (w), 1443 (w), 1386 (w), 1359 (w), 1306 (w), 1253 (s), 1227 (m), 1196 (w), 1127 (s), 1096 (vs), 1065 (s), 1045 (s), 1008 (m), 985 (s), 947 (m), 921 (w), 887 (w), 836 (vs), 813 (w), 779 (s), 734 (w), 668 (w) cm^{-1} .

***rac*-(1*S*,3*R*,3*aS*,4*S*,7*aS*)-1,3-dimethoxy-4-(((triethylsilyl)oxy)methyl)tetrahydro-3*H*-furo[3,4-*c*]pyran-6(1*H*)-one (560)**

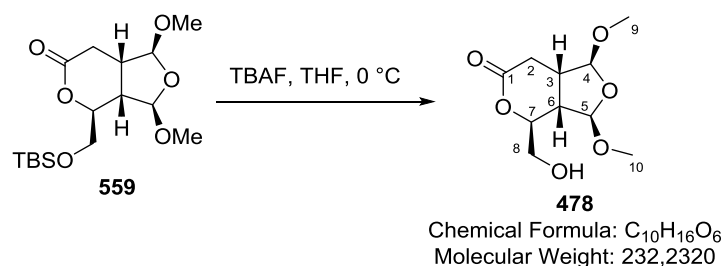


Ketone **540** (5 mg, 0.02 mmol) was dissolved in CH_2Cl_2 (0.5 ml) and NaHCO_3 (6 mg, 0.07 mmol, 5.0 eq.) and *m*-CPBA ($\leq 77\%$ purity, 5 mg, 0.02 mmol, 1.5 eq.) were added. The reaction mixture was stirred for 26 h and more NaHCO_3 (3 mg, 0.04 mmol, 2.5 eq.) and *m*-CPBA ($\leq 77\%$ purity, 3 mg, 0.01 mmol, 0.9 eq.) were added. The reaction mixture was stirred for further 21 h. Sat. aq. NaHCO_3 solution (5 ml) and sat. aq. $\text{Na}_2\text{S}_2\text{O}_3$ solution (5 ml) were introduced and the aqueous phase extracted with EtOAc (3x10 ml). The combined organic phases were washed with sat. aq. NaHCO_3 solution (2x20 ml) and dried over Na_2SO_4 and concentrated under reduced pressure. The crude product was purified by preparative TLC (40% EtOAc/hexanes) to afford the title compound (1 mg, 19%) as a colorless oil.

Major side product of this reaction was the alcohol from *in situ* TES deprotection of the title compound.

TLC	$R_f = 0.18$ (20% EtOAc/hexanes).
^1H NMR	(400 MHz, CDCl_3): δ 5.02 (d, $J = 1.5$ Hz, 1H, C_5H), 4.84 (s, 1H, C_4H), 4.17 (ddd, $J = 9.3, 4.5, 4.5$ Hz, 1H, C_7H), 3.87 (dd, $J = 11.1, 4.5$ Hz, 1H, C_8H), 3.83 (dd, $J = 11.1, 4.5$ Hz, 1H, C_8H), 3.44 (s, 3H, C_{12}H_3), 3.43 (s, 3H, C_{11}H_3), 2.85–2.67 (m, 3H, C_2H , C_3H , C_6H), 2.31 (dd, $J = 15.0, 11.8$ Hz, 1H, C_2H), 0.96 (t, $J = 8.0$ Hz, 9H, $3\times\text{C}_{10}\text{H}_3$), 0.63 (q, $J = 8.0$ Hz, 6H, $3\times\text{C}_9\text{H}_2$) ppm.
^{13}C NMR	(100 MHz, CDCl_3): δ 171.1 (C1), 111.0 (C4), 109.3 (C5), 78.7 (C7), 64.5 (C8), 56.1 (C12), 55.6 (C11), 46.2 (C6), 42.3 (C3), 31.3 (C2), 6.8 (C10), 4.3 (C9) ppm.
MS	(EI, %): 317.22 (2, $\text{M}-\text{Et}^+$), 285.21 (27), 197.17 (28), 145.13 (100), 117.09 (42), 83.98 (26), 43.03 (58).
HRMS	(EI, m/z): calc. $[\text{M}-\text{Et}^+]$: 317.1420; found: 317.1418 $[\text{M}-\text{Et}^+]$.
IR	$\tilde{\nu} = 2955$ (m), 2907 (m), 2875 (m), 1753 (s), 1459 (vw), 1443 (vw), 1414 (vw), 1381 (vw), 1309 (vw), 1253 (m), 1245 (m), 1140 (m), 1127 (m), 1097 (vs), 1063 (m), 1046 (s), 1003 (s), 985 (vs), 947 (m), 804 (w), 789 (w), 746 (m) cm^{-1} .

***rac*-(1*S*,3*R*,3*aS*,4*S*,7*aS*)-4-(hydroxymethyl)-1,3-dimethoxytetrahydro-3*H*-furo[3,4-*c*]pyran-6(1*H*)-one (478)**



Lactone **559** (29 mg, 0.084 mmol) was dissolved in THF (0.7 ml) and the solution cooled to 0 °C. A solution of TBAF in THF ($c = 1$ M, 0.17 ml, 0.17 mmol, 2.0 eq.) was stirred at 0 °C for 25 min. An aq. phosphate buffer (pH 5, $c = 1$ M, 10 ml) was added and the aqueous phase extracted with EtOAc (3x10 ml). The combined organic phases were dried over Na_2SO_4 and concentrated under reduced pressure. Purification by preparative TLC (5% MeOH/ CH_2Cl_2) gave the title compound as a colorless solid (4 mg, 21%). X-Ray suitable crystals were obtained by slow diffusion of hexanes into a solution of the title compound in EtOAc while allowing slow evaporation.

The crude product is sufficiently pure for further transformations. Purification on silica gel should be avoided since it leads to the decomposition of the product.

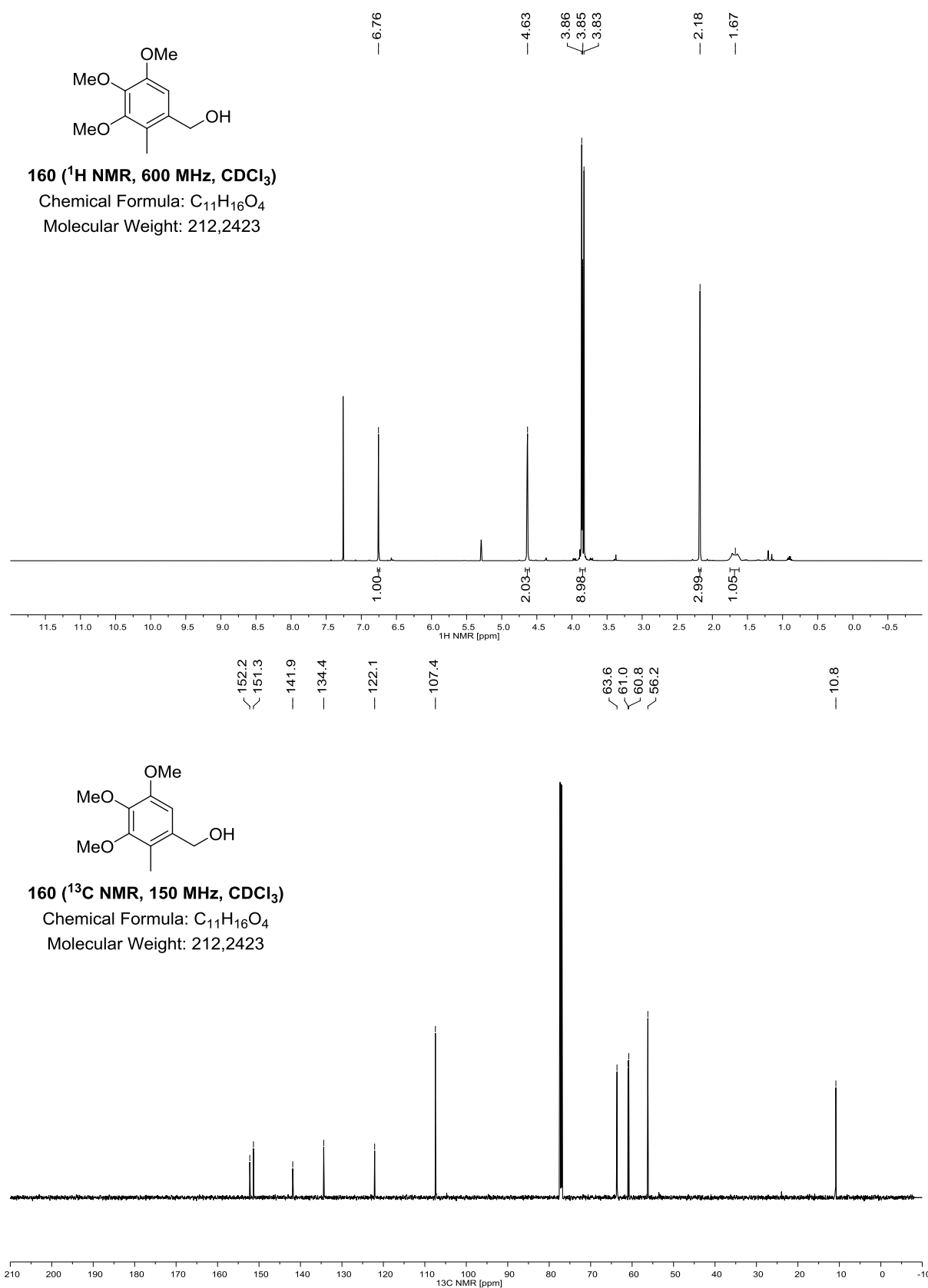
TLC	$R_f = 0.15$ (50% EtOAc/hexanes).
m.p.:	159–160 °C.

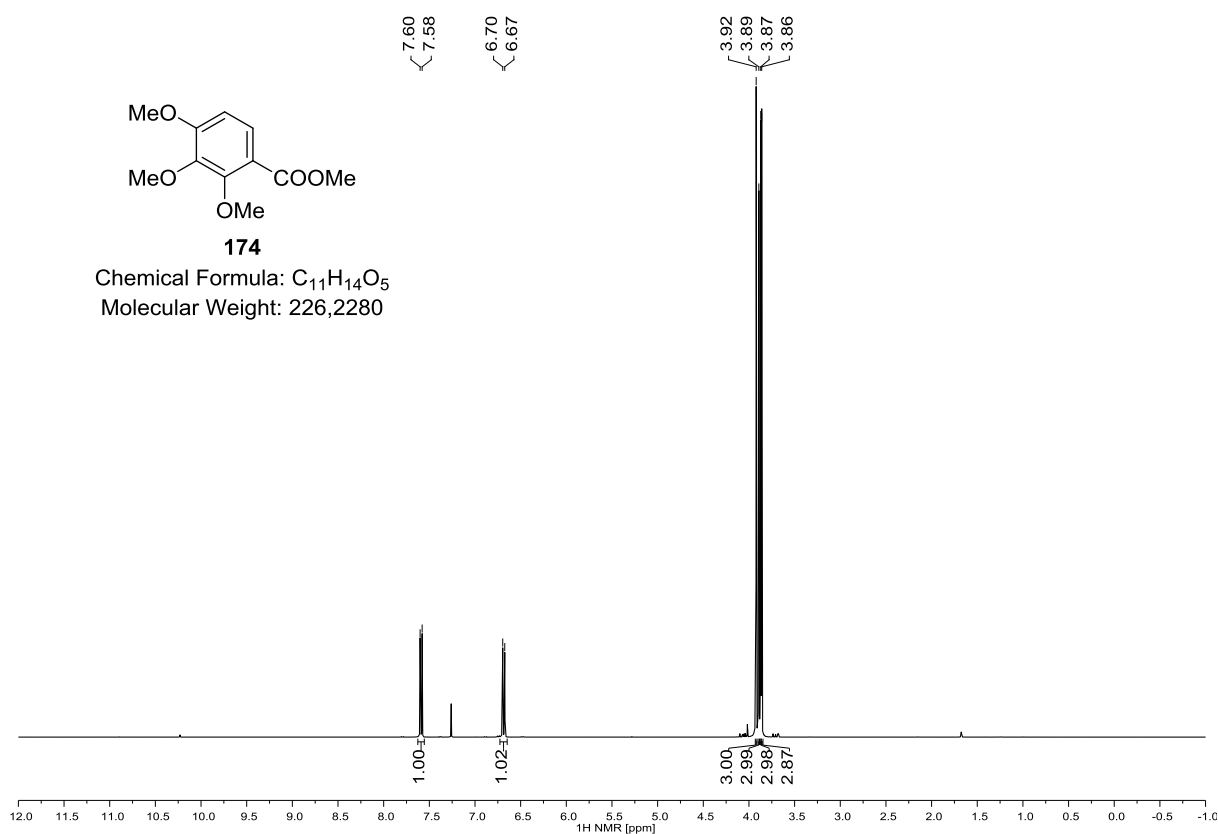
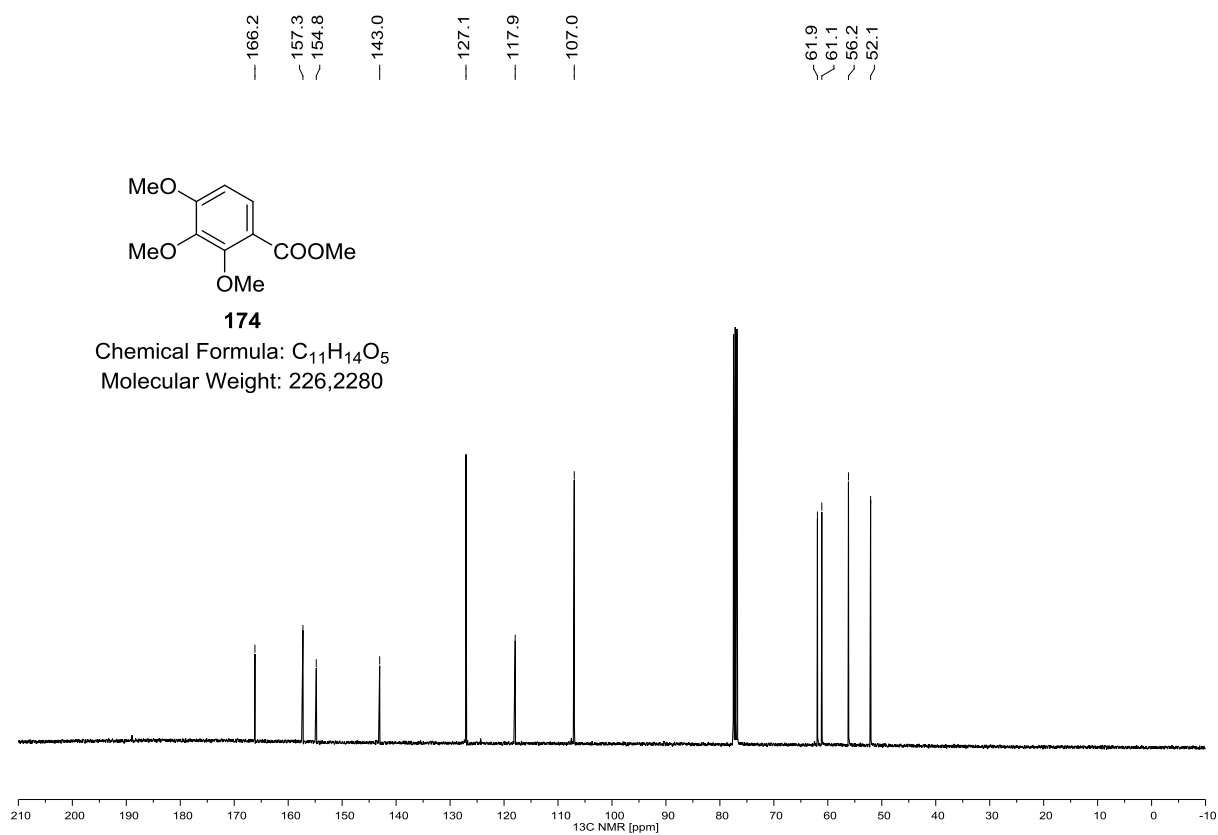
¹H NMR	(400 MHz, (D₃C)₂CO): δ 5.03 (s, 1H, C ₅ H), 4.89 (s, 1H, C ₄ H), 4.30–4.23 (m, 1H, C ₇ H), 4.19 (dd, <i>J</i> = 6.1 Hz, 1H, C ₈ OH), 3.82–3.68 (m, 2H, 2xC ₈ H), 3.37 (s, 3H, C ₁₀ H ₃), 3.33 (s, 3H, C ₉ H ₃), 2.71–2.45 (m, 4H, 2xC ₂ H, C ₃ H, C ₆ H) ppm.
¹³C NMR	(100 MHz, (D₃C)₂CO): δ 171.6 (C1), 111.6 (C4), 110.1 (C5), 79.8 (C7), 63.5 (C8), 55.7 (C10), 55.1 (C9), 46.0 (C6), 43.2 (C3), 31.6 (C2) ppm.
MS	(EI, %): 201.17 (30, M–OMe ⁺), 153.16 (36), 141.18 (94), 109.16 (47), 84.20 (100), 81.18 (75), 69.19 (36), 55.18 (27).
HRMS	(EI, m/z): calc. [M–OMe ⁺]: 201.0763; found: 201.0769 [M–OMe ⁺].
IR	$\tilde{\nu}$ = 3359 (br, w), 2992 (vw), 2948 (w), 2917 (w), 2849 (vw), 1744 (s), 1717 (s), 1464 (vw), 1446 (w), 1376 (w), 1367 (w), 1315 (w), 1292 (w), 1270 (m), 1253 (s), 1197 (w), 1145 (w), 1092 (vs), 1060 (s), 1042 (s), 981 (vs), 961 (s), 941 (s), 915 (w), 885 (vw), 847 (vw), 792 (vw), 765 (vw), 699 (vw) cm ^{−1} .

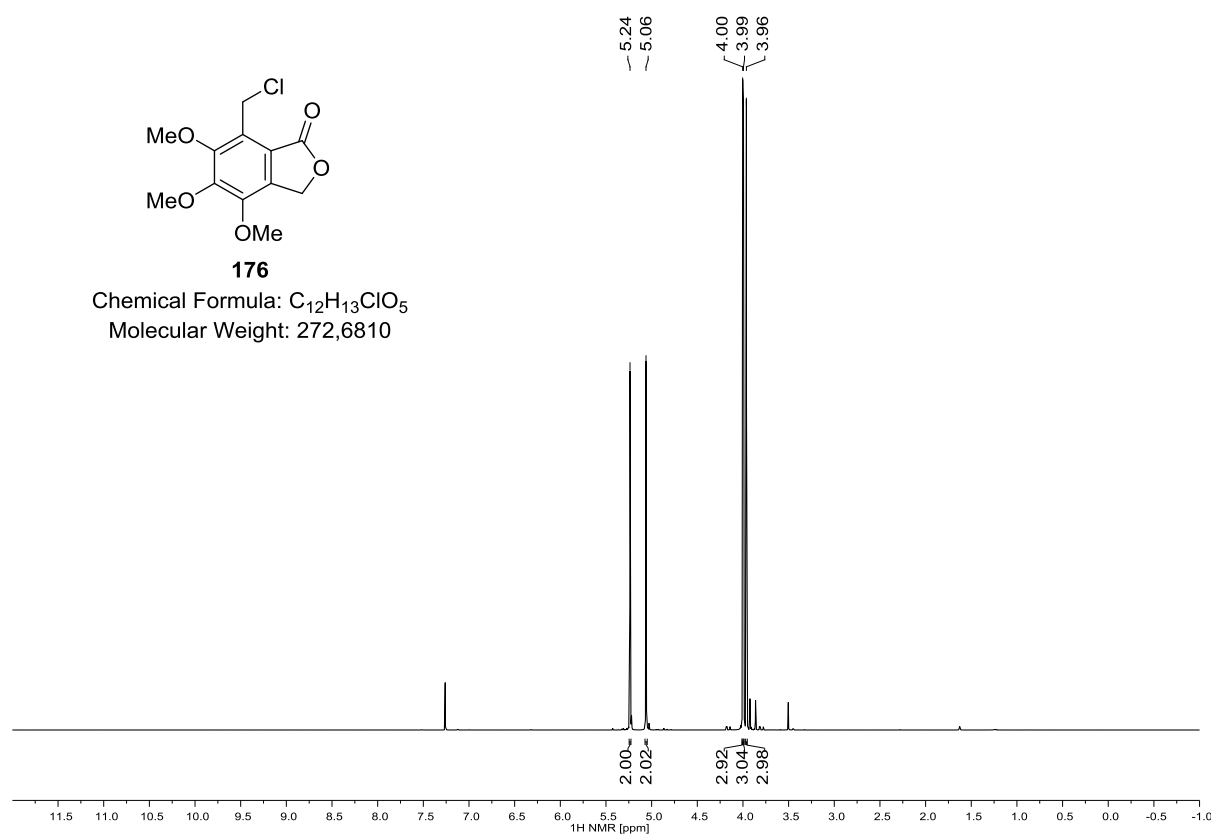
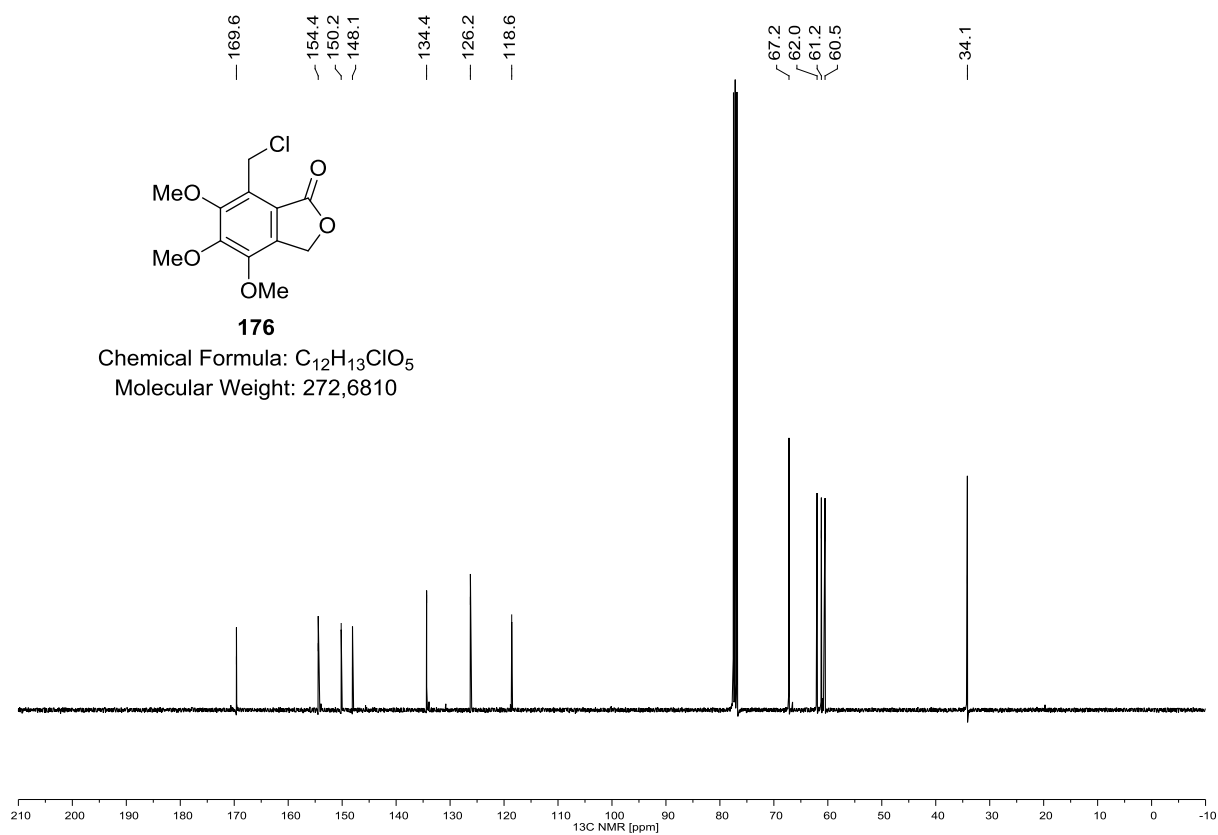
APPENDIX

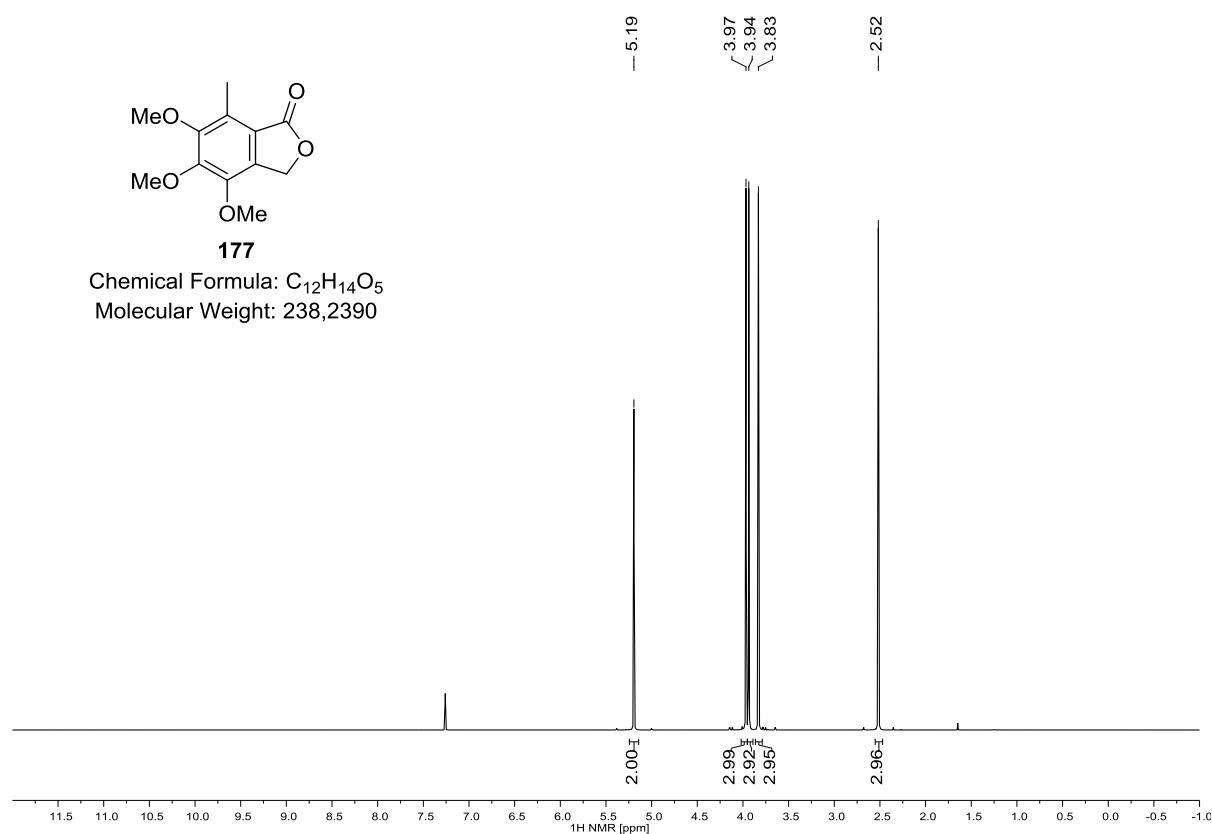
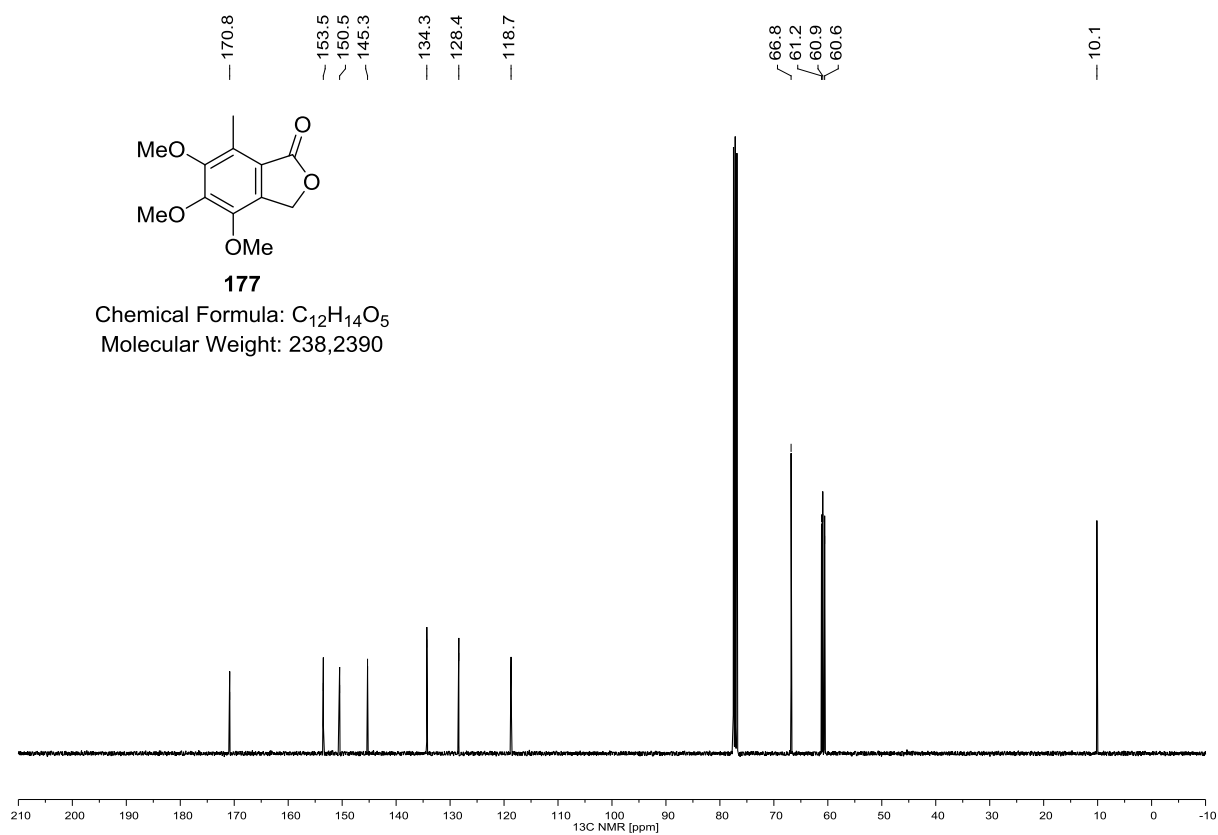
7. NMR SPECTRA

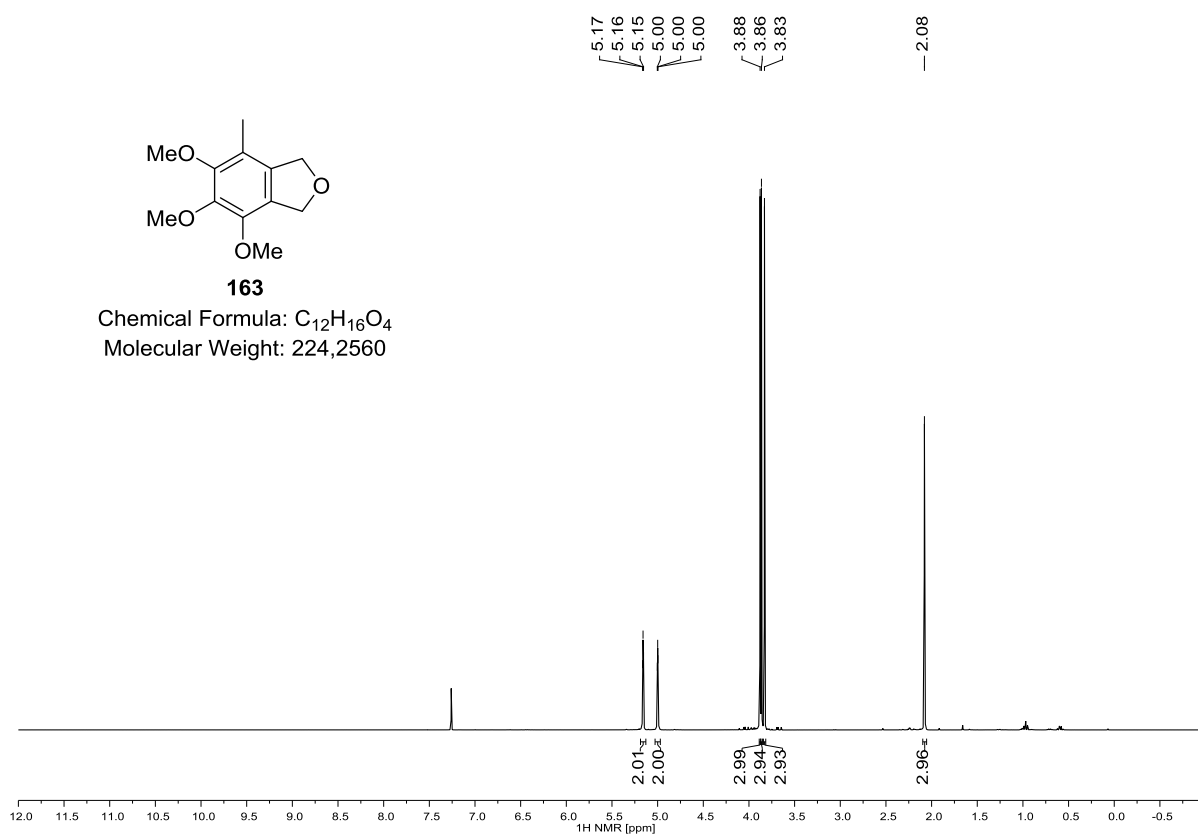
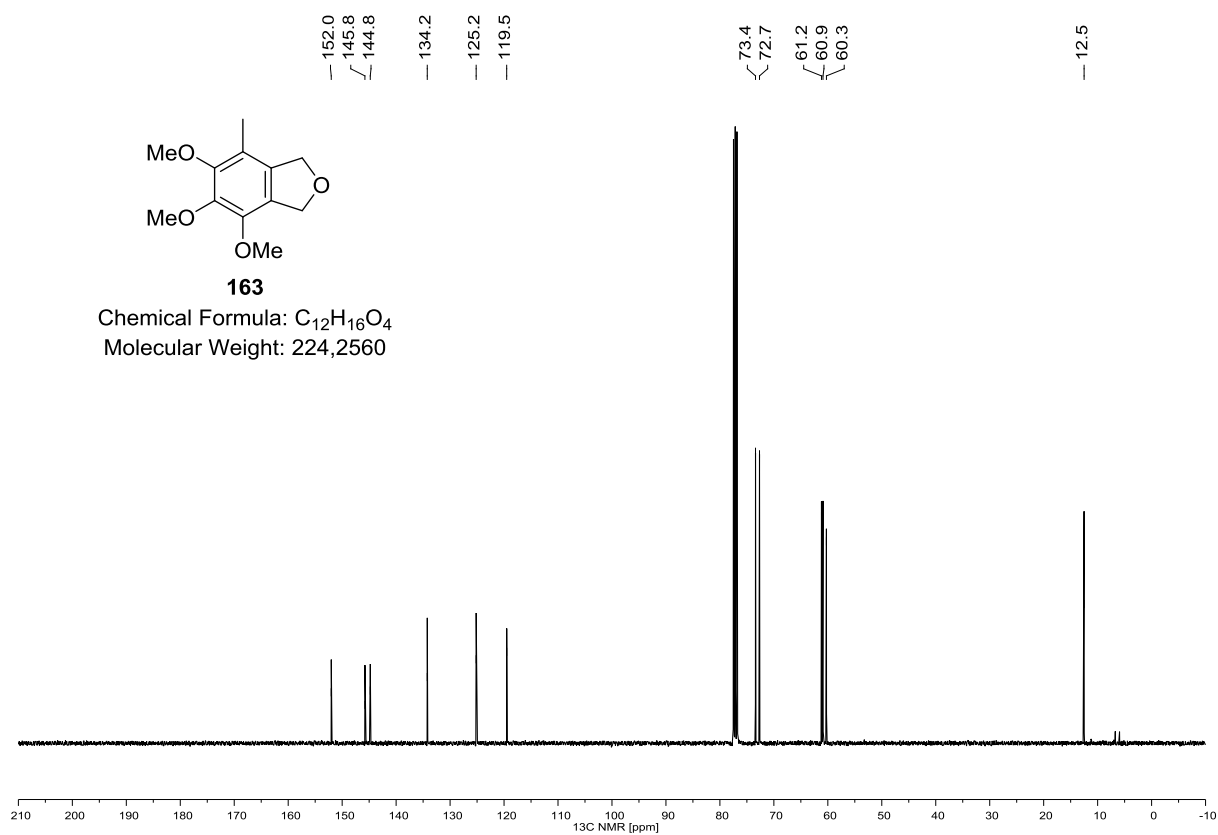
7.1 PART I: Biomimetic Synthesis of Dibefurin and Epicolactone

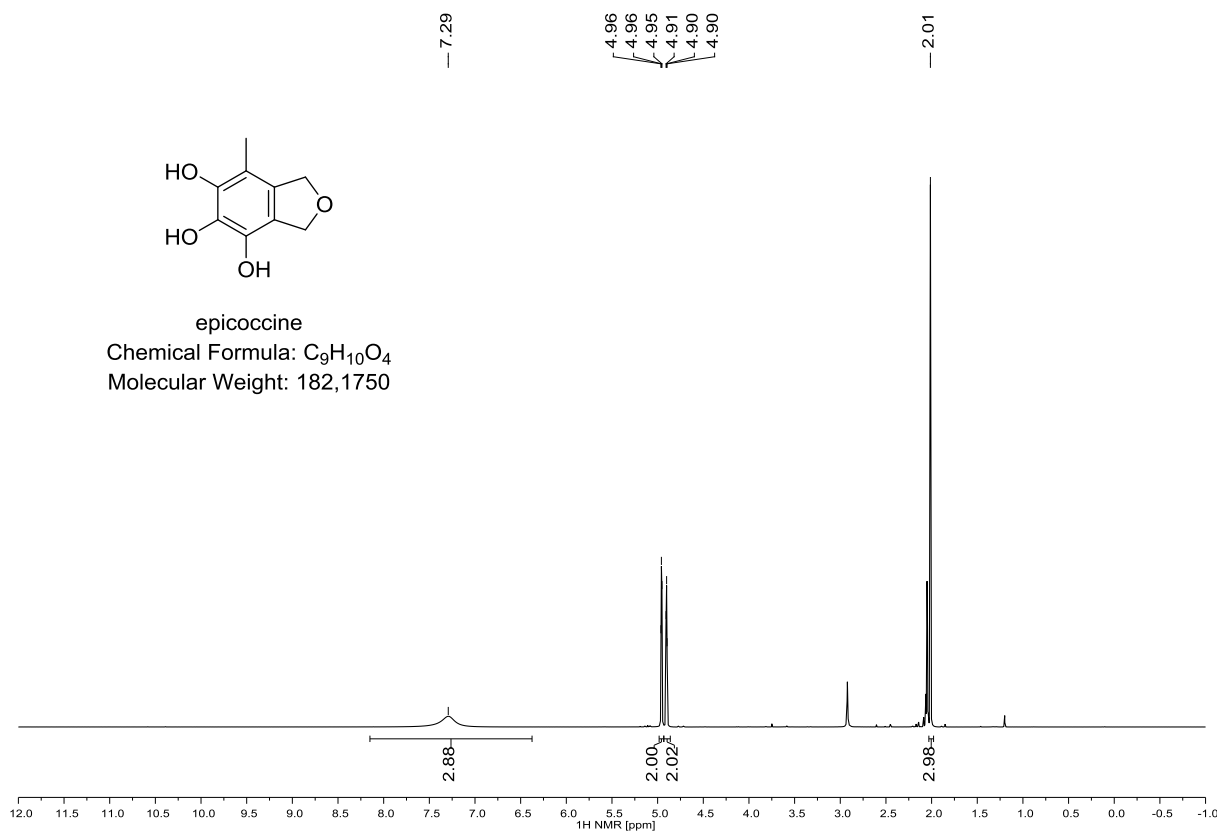
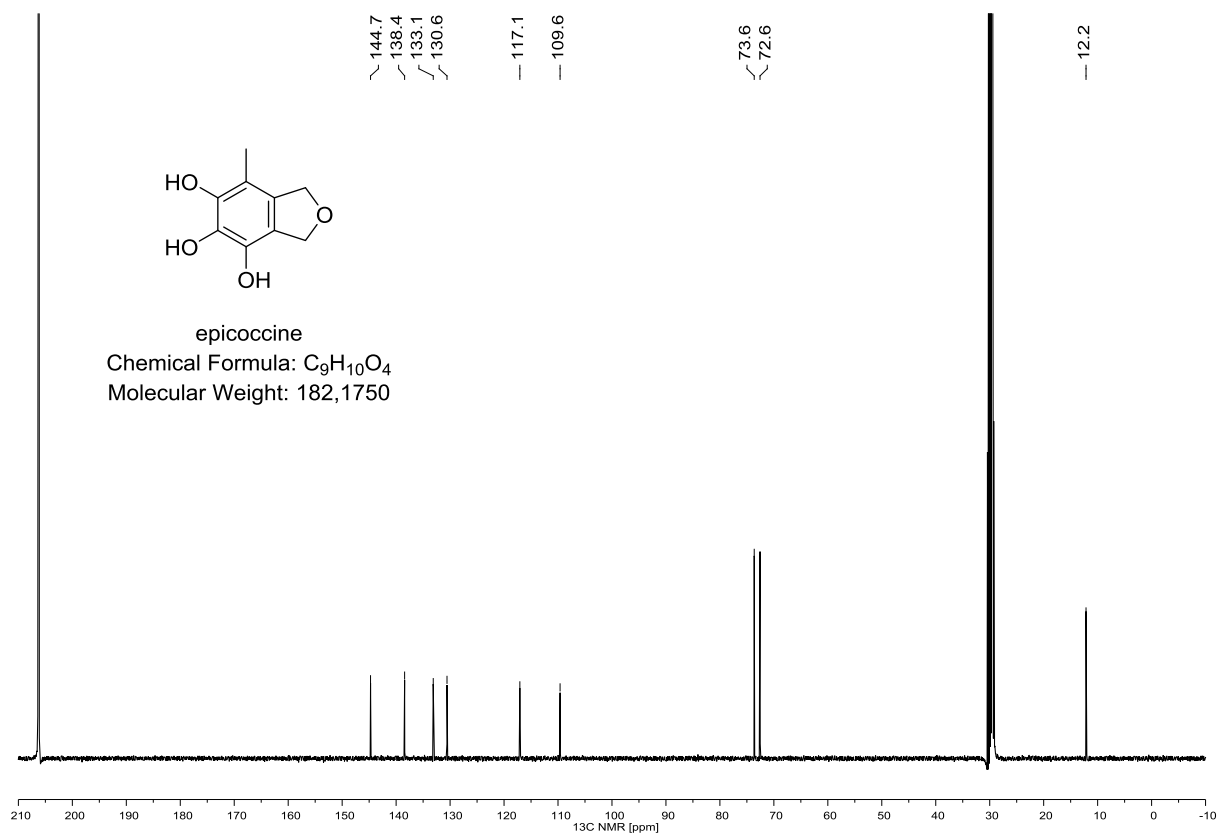


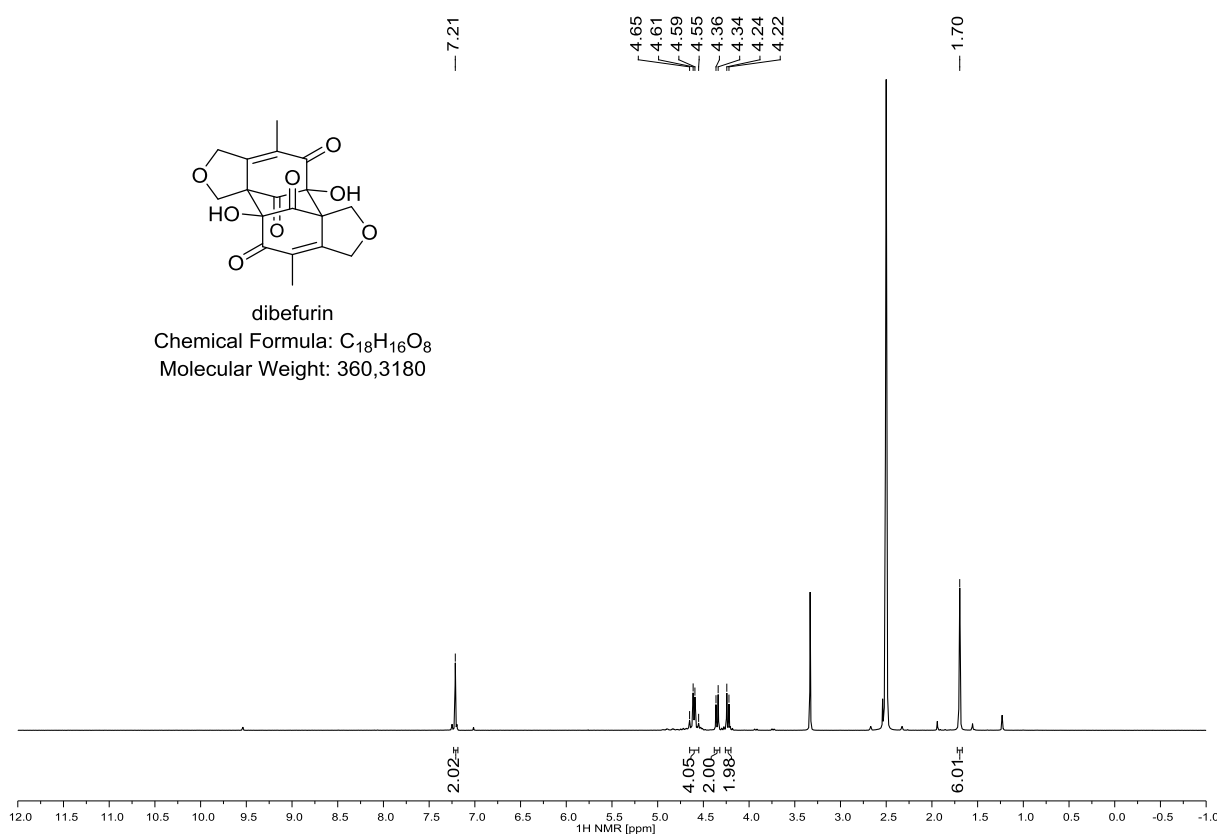
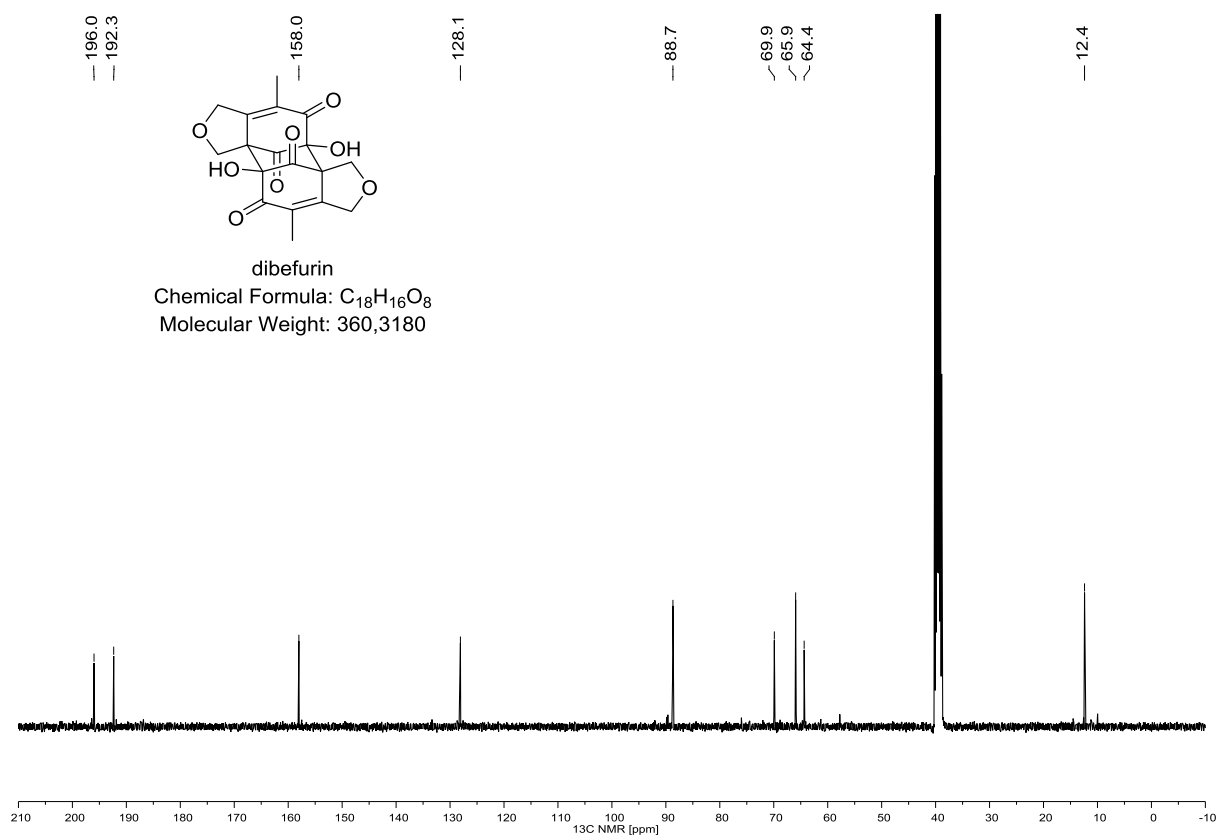
174 (^1H NMR, 400 MHz, CDCl_3)**174 (^{13}C NMR, 100 MHz, CDCl_3)**

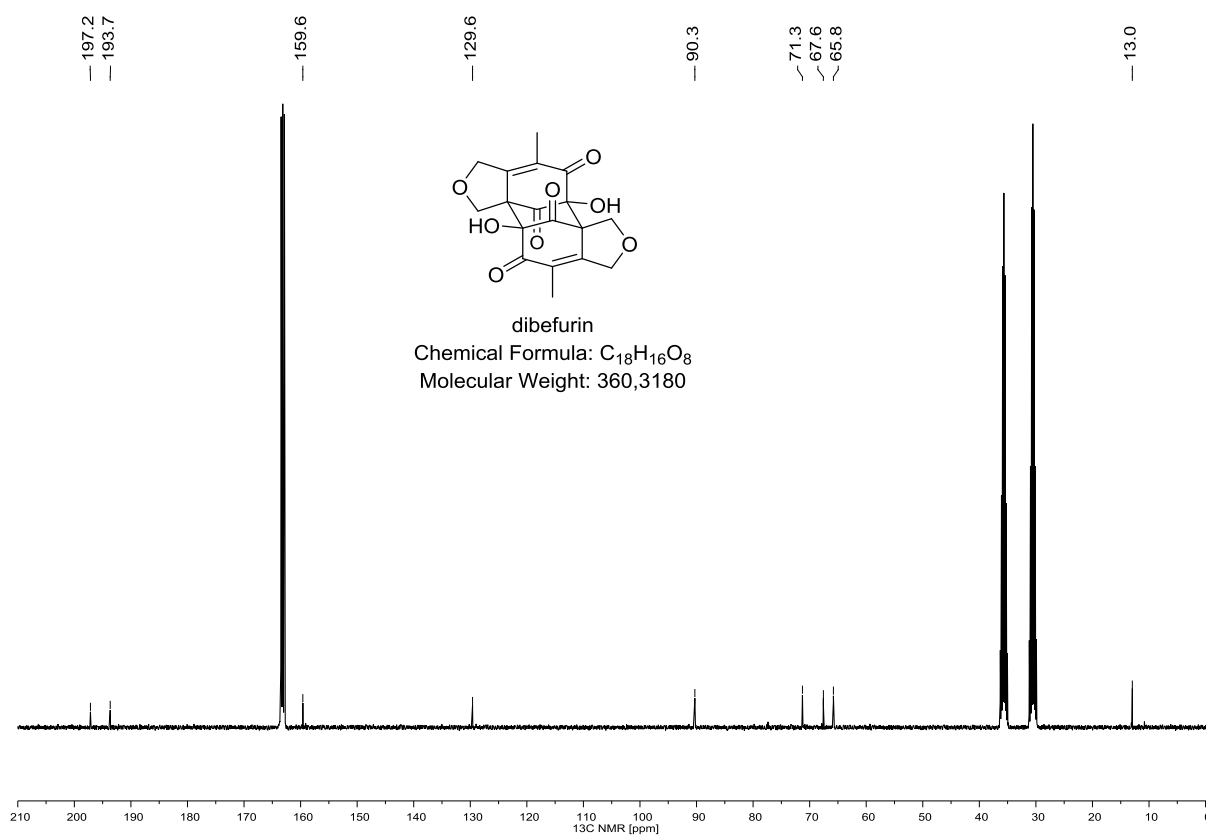
176 (^1H NMR, 400 MHz, CDCl_3)**176 (^{13}C NMR, 100 MHz, CDCl_3)**

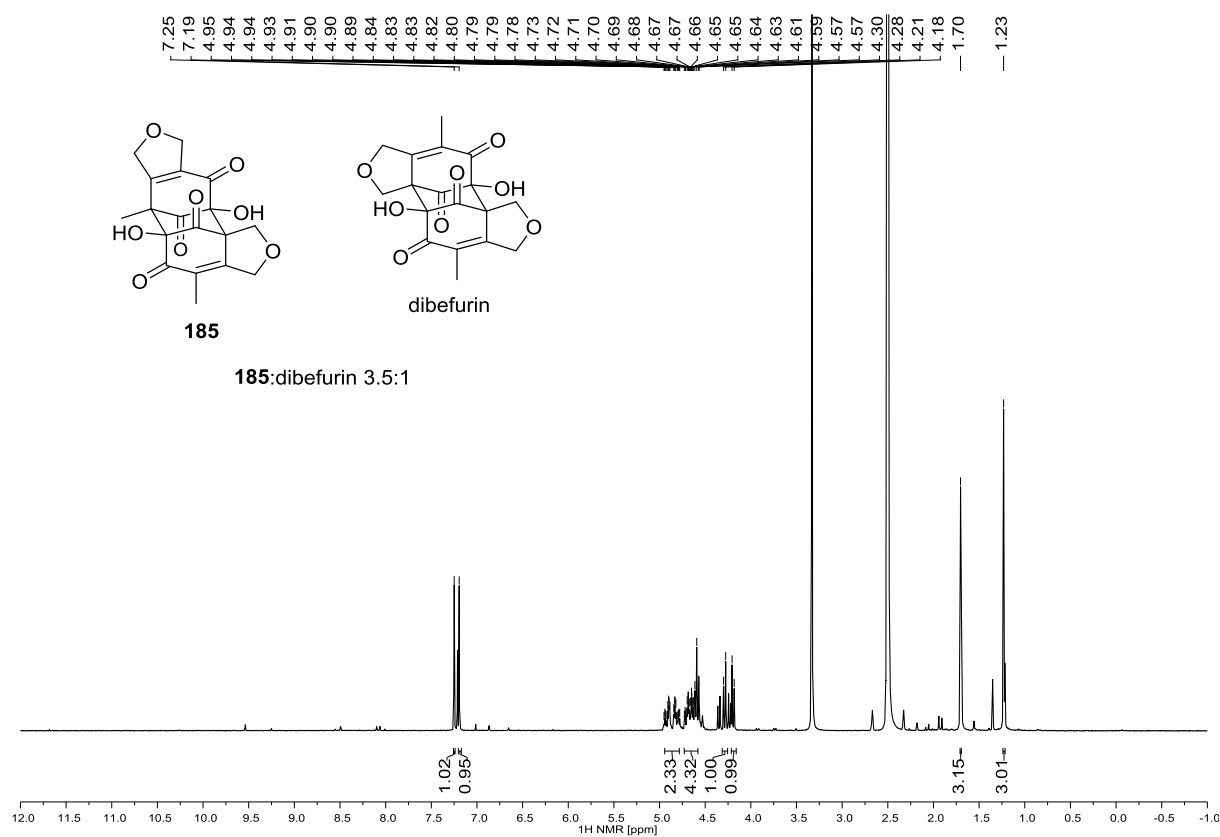
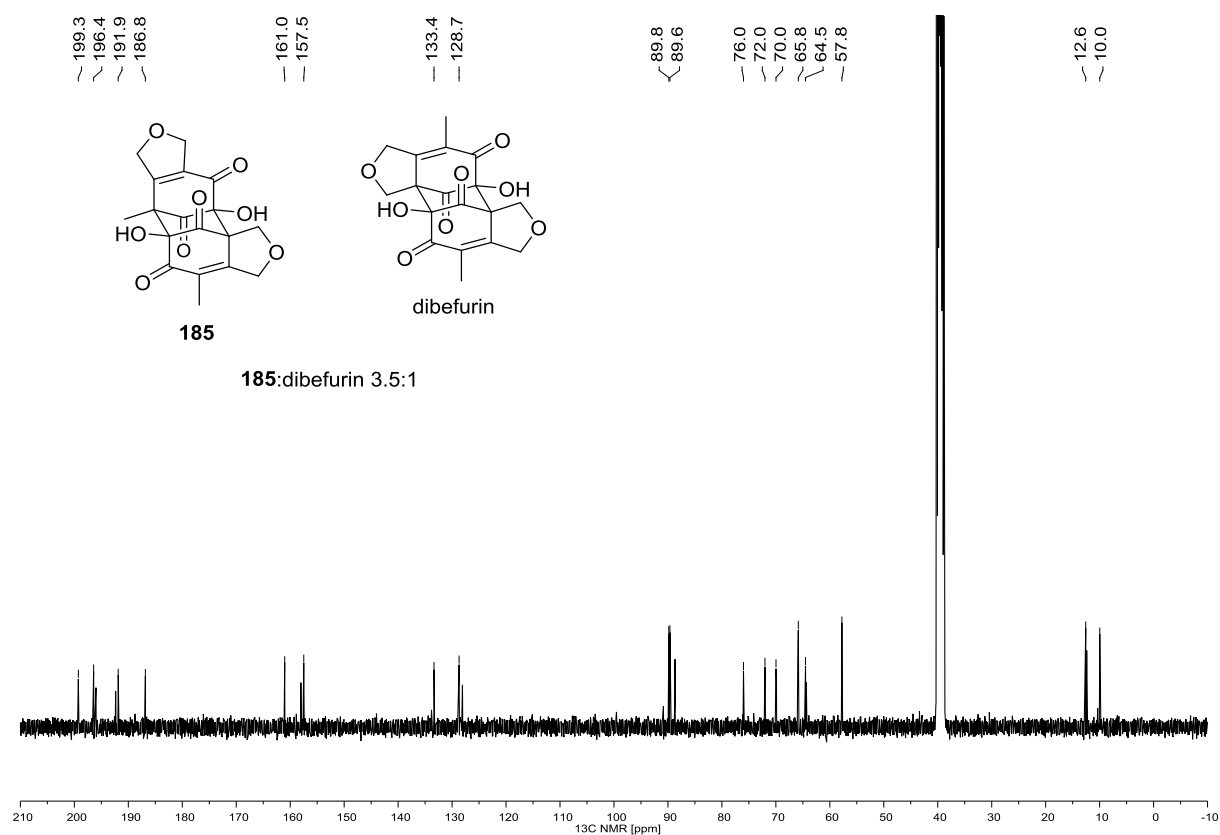
177 (^1H NMR, 400 MHz, CDCl_3)**177 (^{13}C NMR, 100 MHz, CDCl_3)**

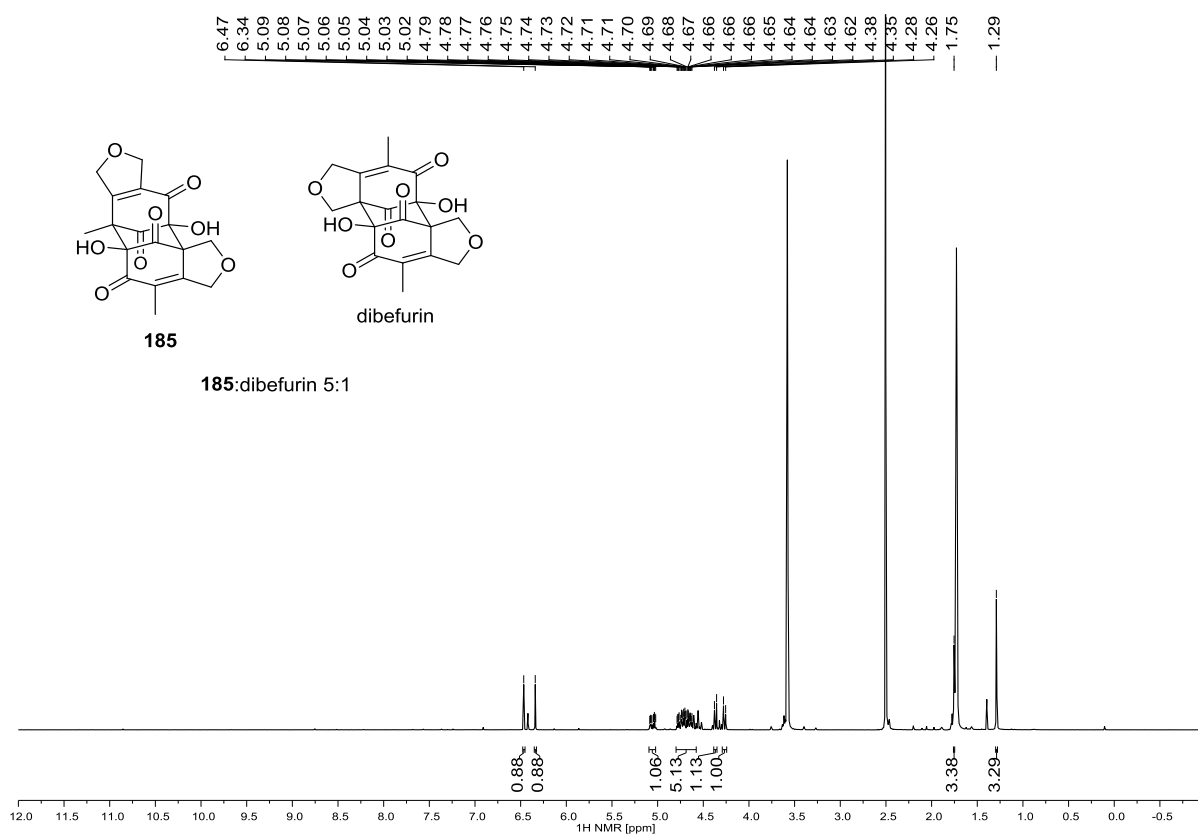
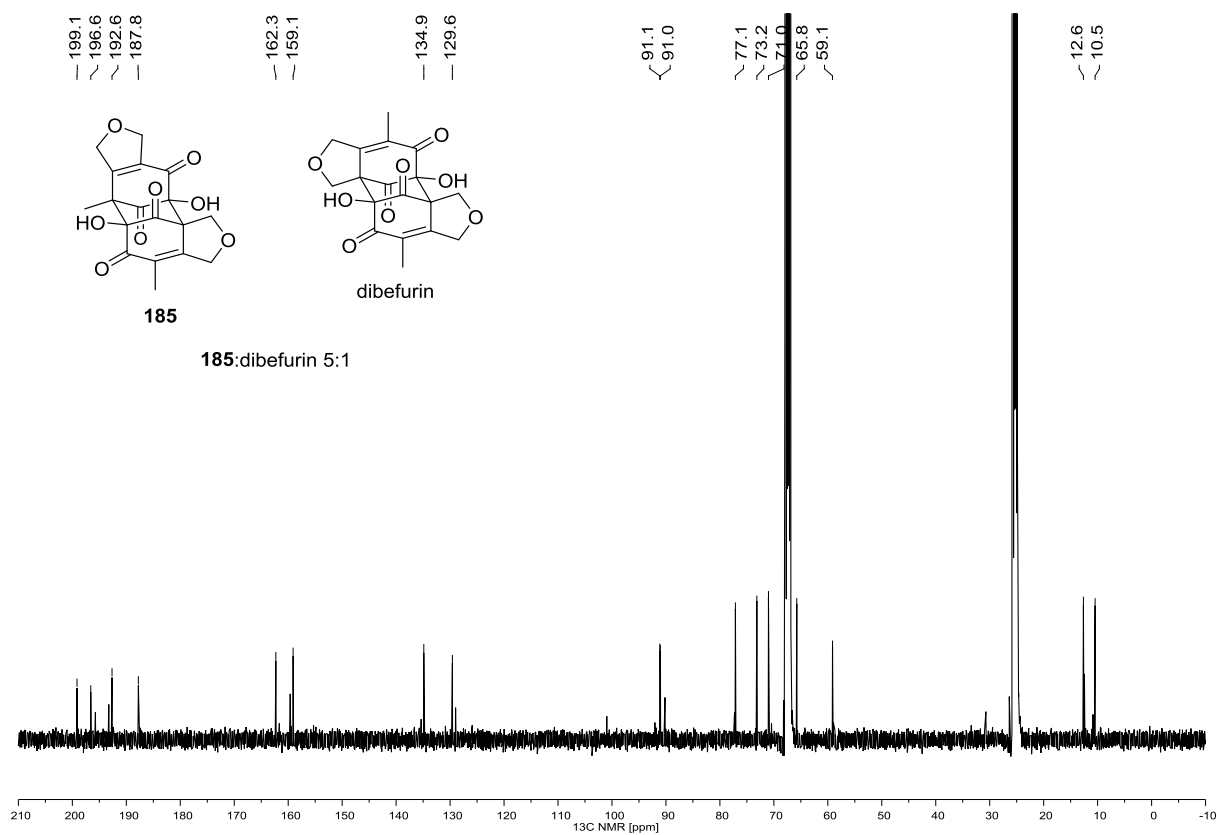
163 (^1H NMR, 400 MHz, CDCl_3)**163 (^{13}C NMR, 100 MHz, CDCl_3)**

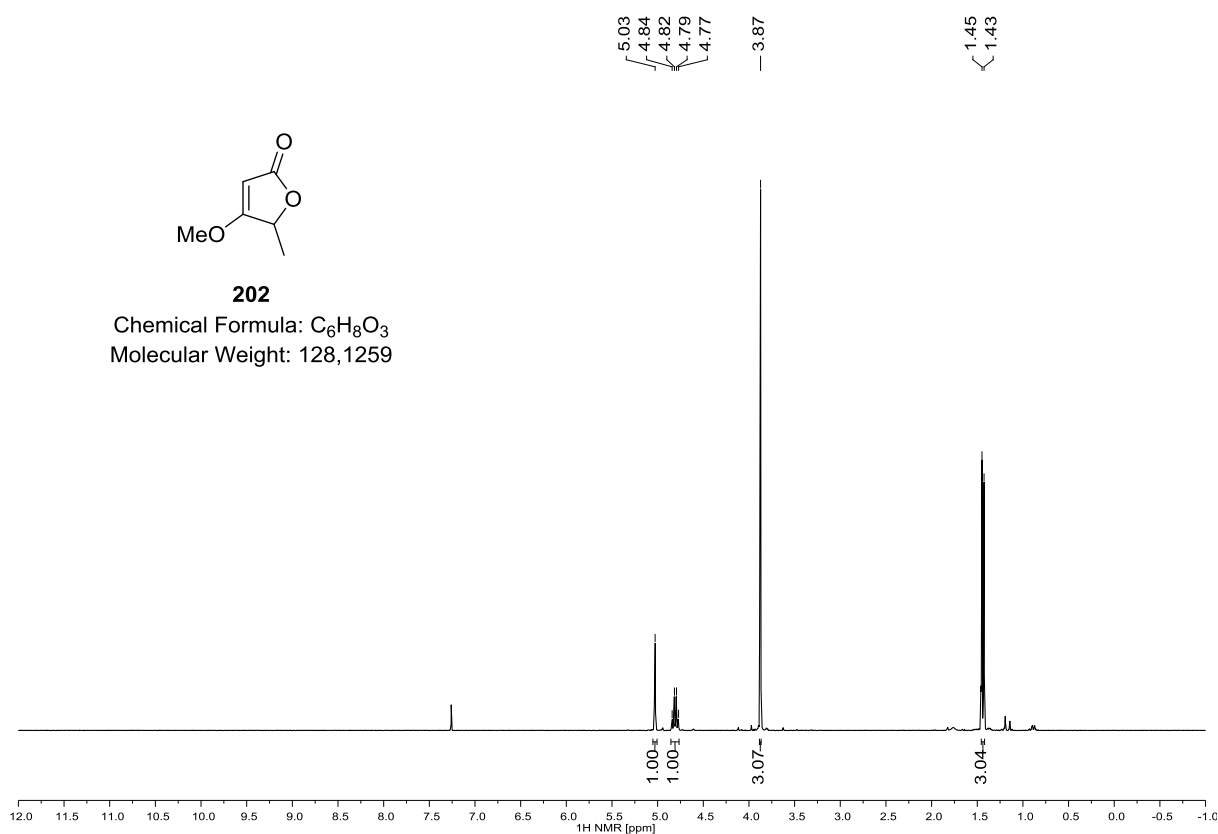
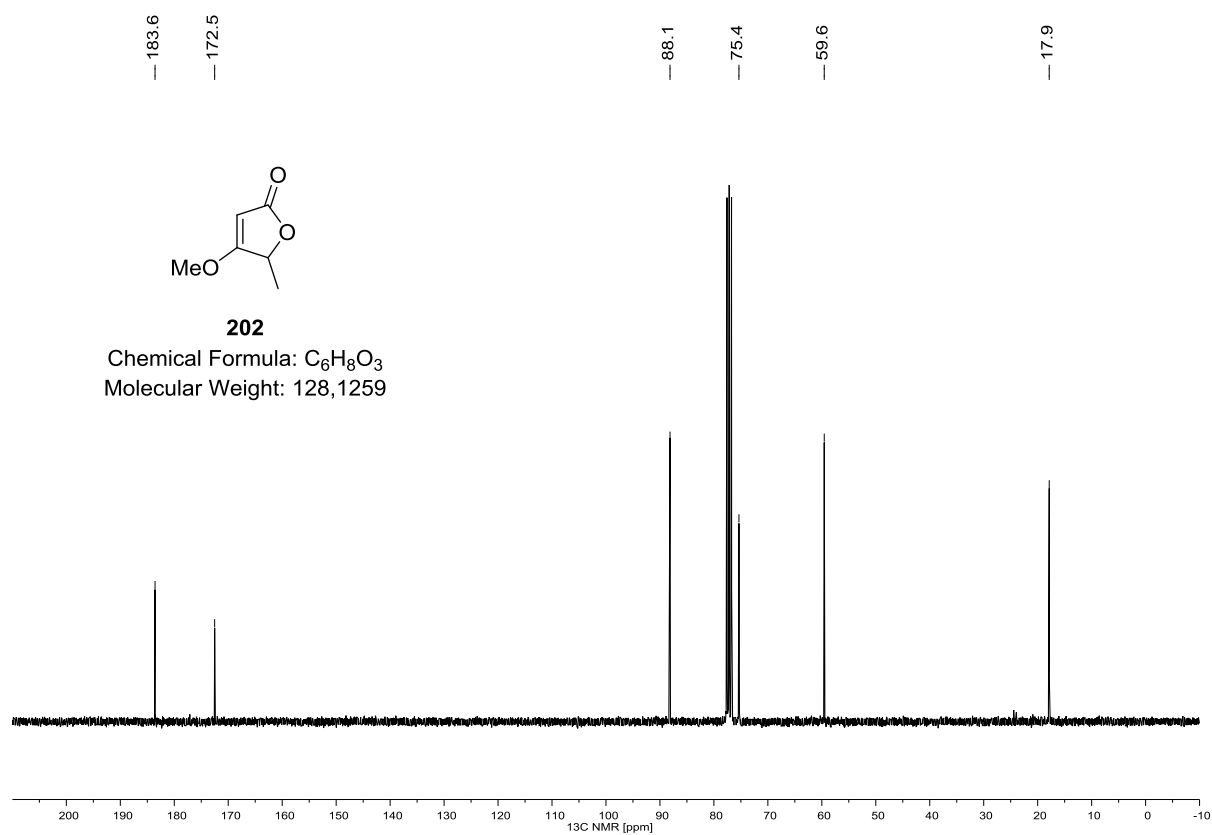
Epicoccine (^1H NMR, 400 MHz, $(\text{D}_3\text{C})_2\text{CO}$)**Epicoccine (^{13}C NMR, 100 MHz, $(\text{D}_3\text{C})_2\text{CO}$)**

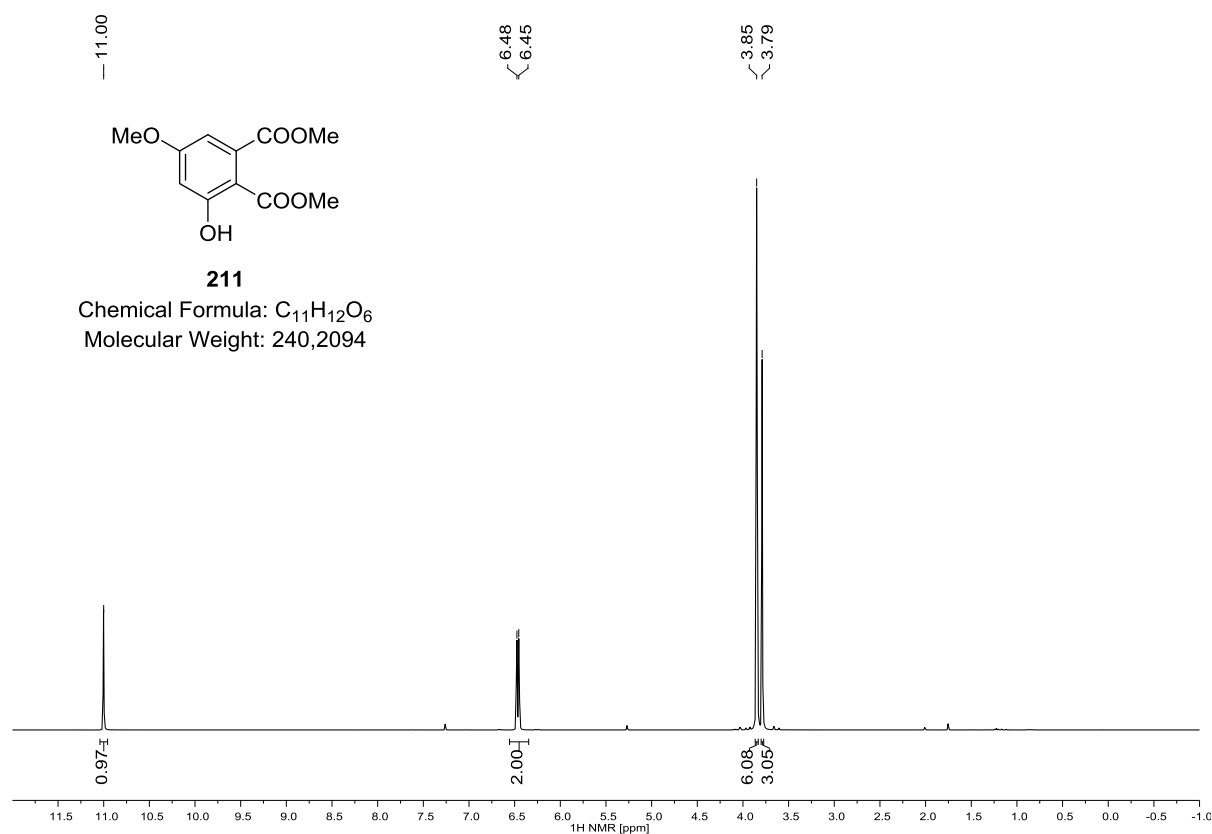
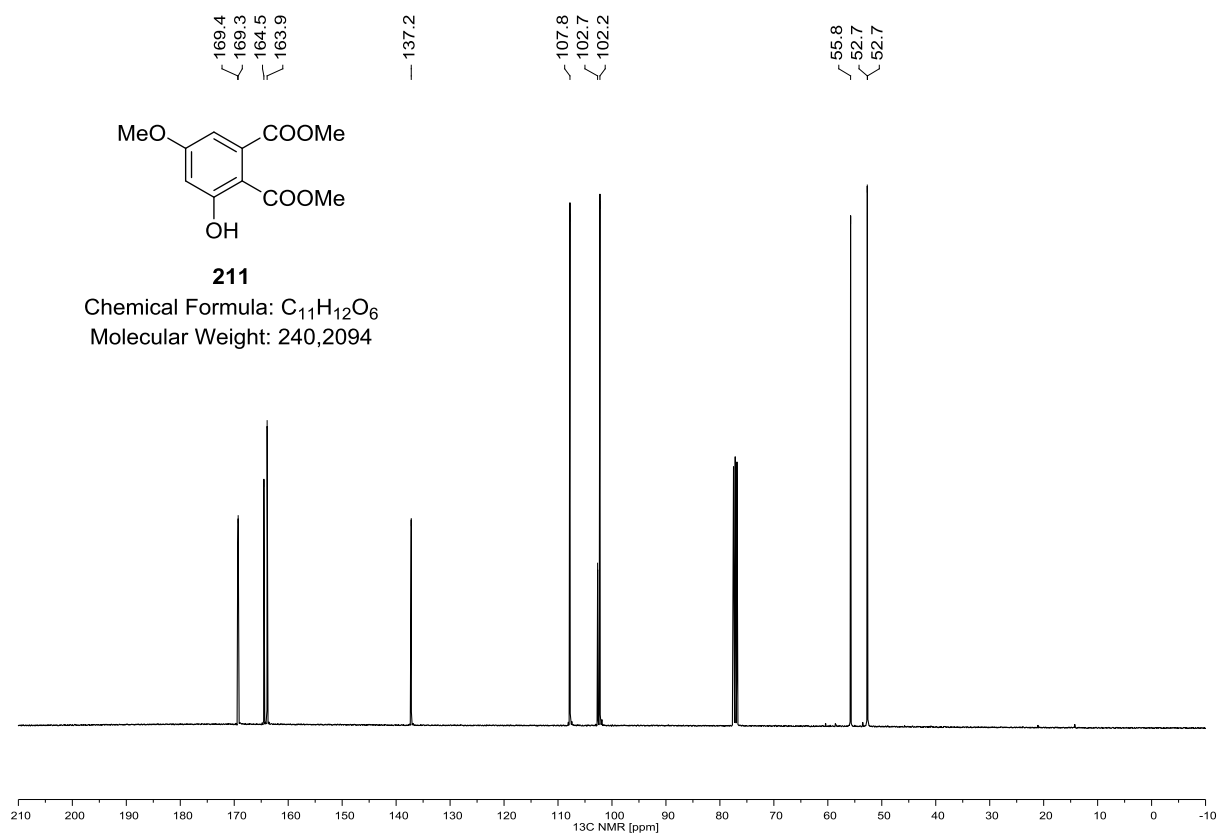
Dibefurin (^1H NMR, 400 MHz, DMSO-d^6)**Dibefurin (^{13}C NMR, 100 MHz, DMSO-d^6)**

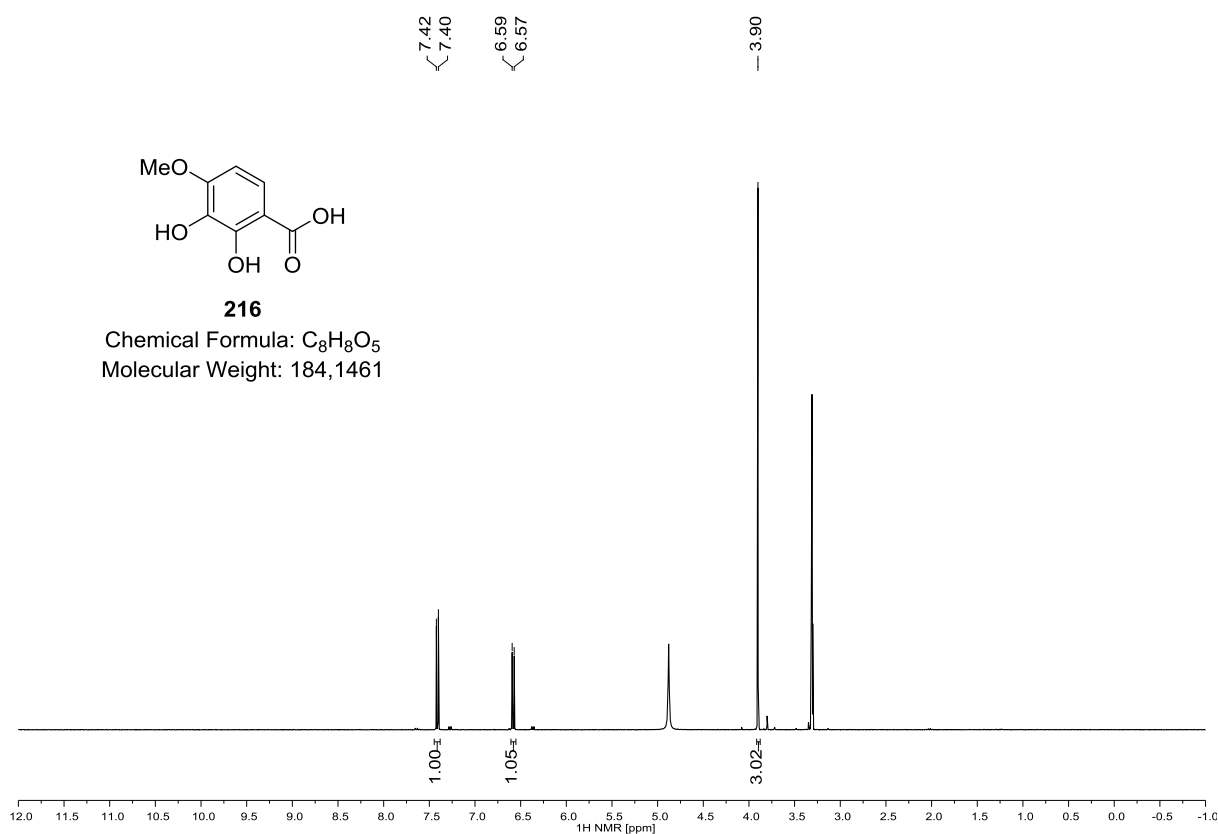
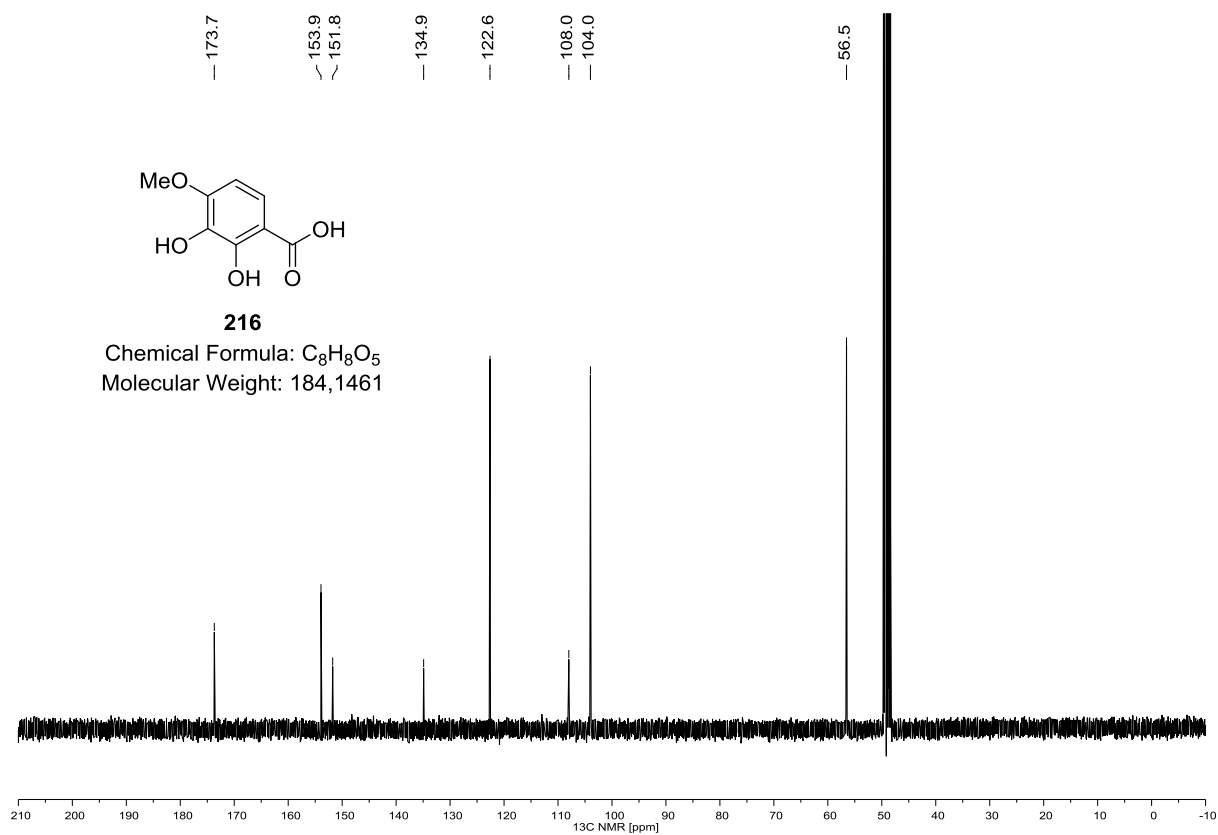
Dibefurin (^{13}C NMR, 100 MHz, DMF- d^7)

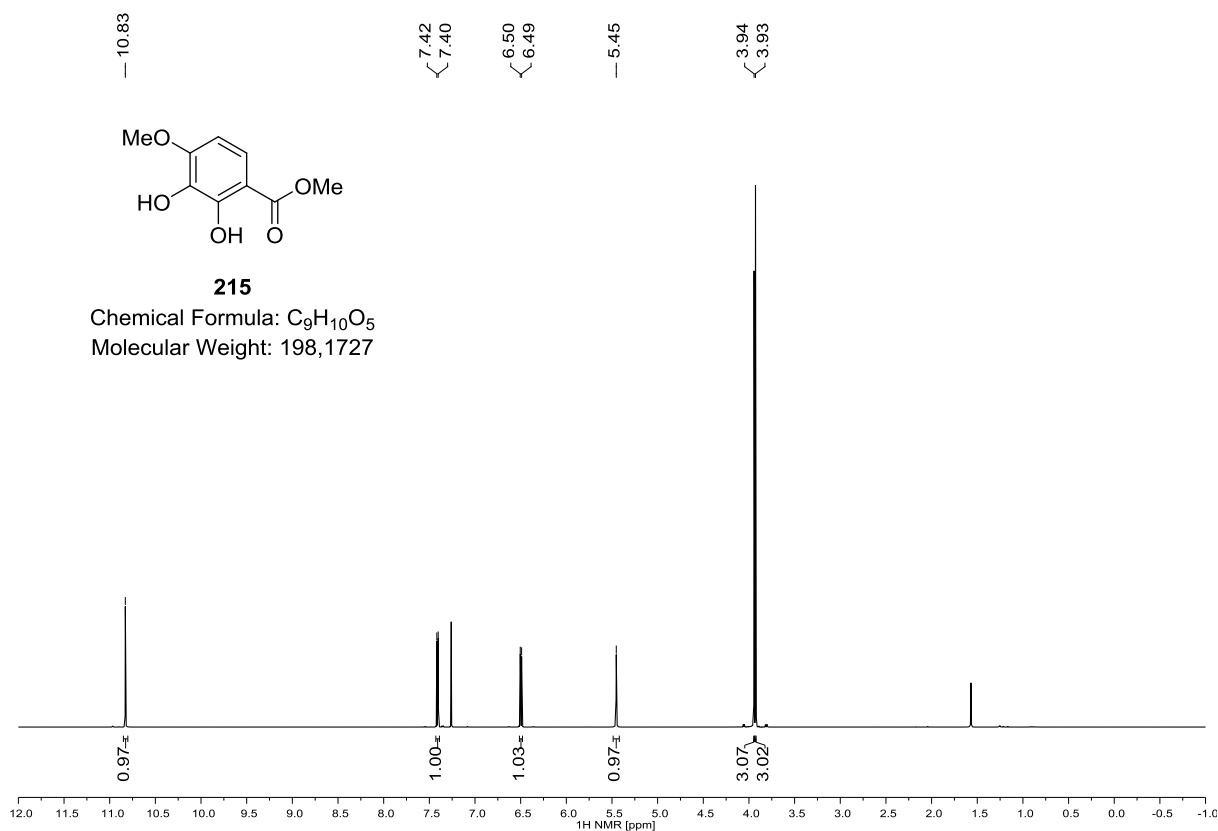
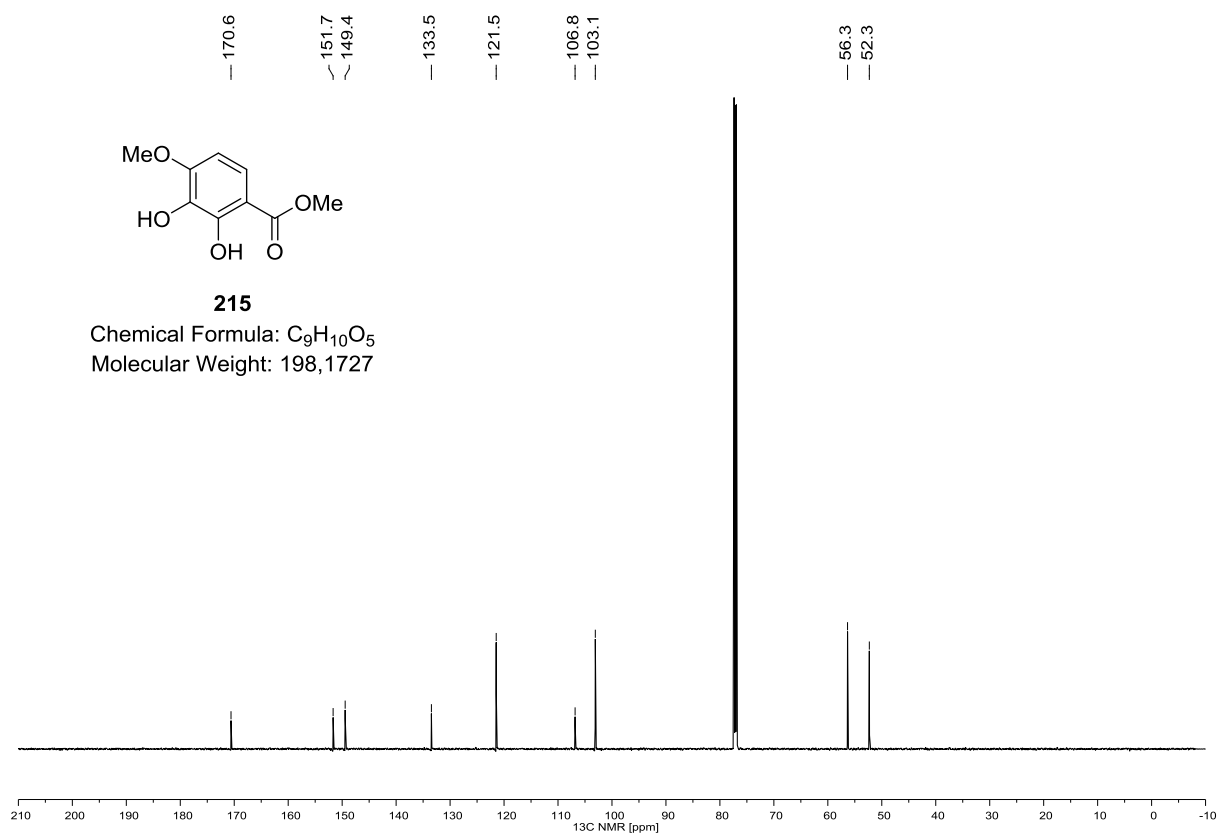
185 (^1H NMR, 400 MHz, DMSO-d_6)**185 (^{13}C NMR (100 MHz, DMSO-d_6))**

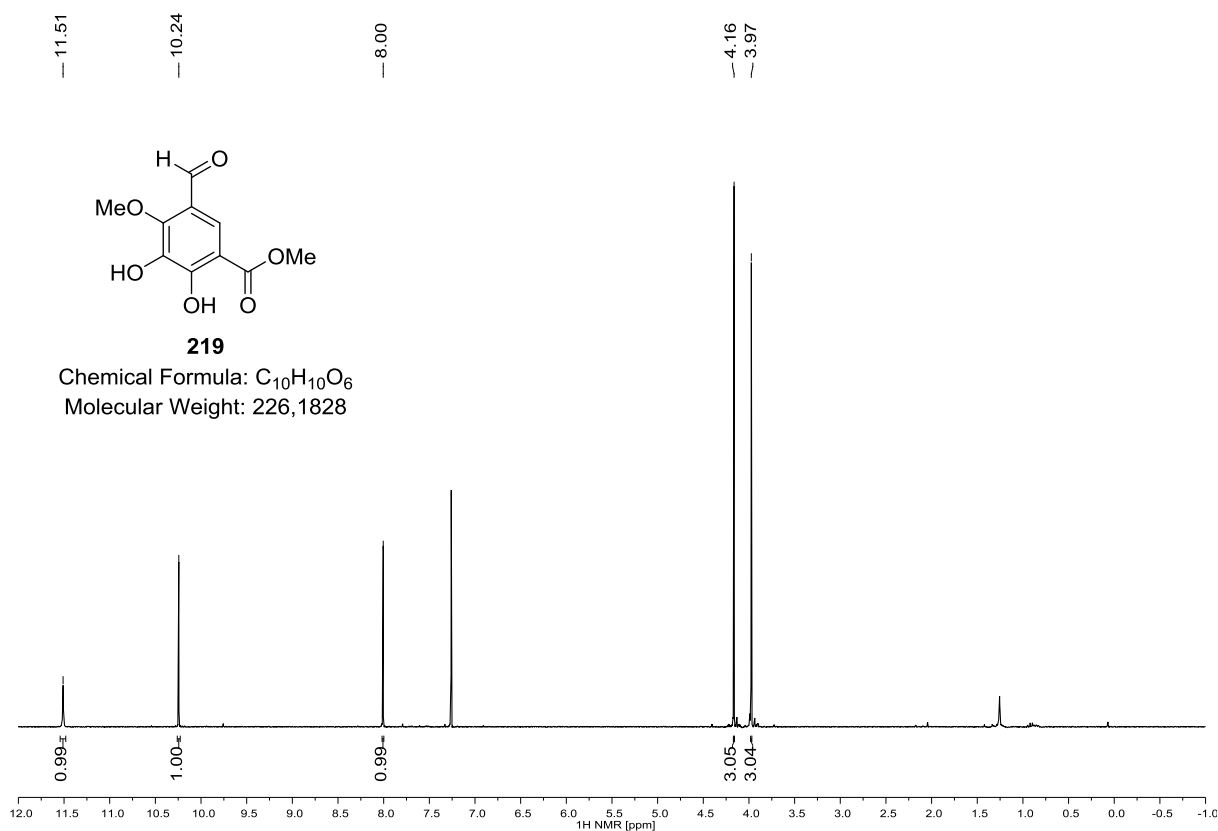
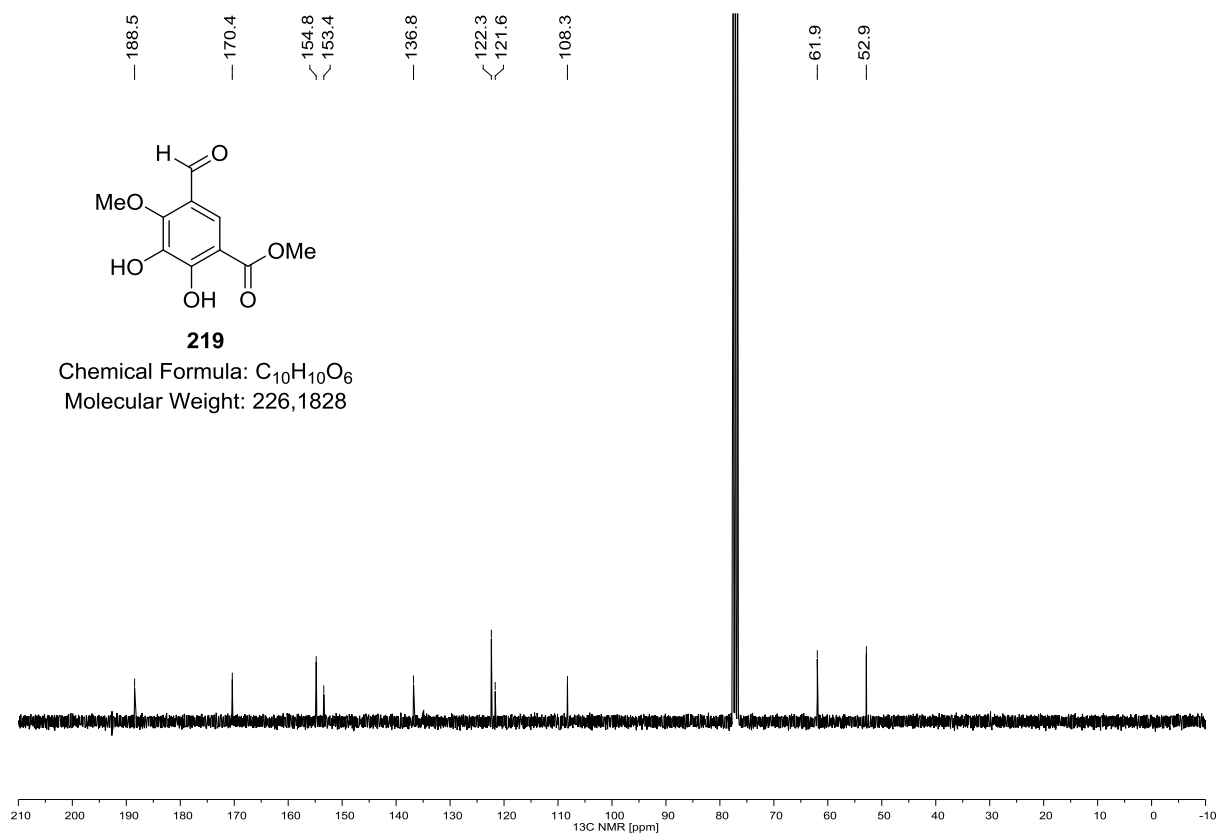
185 (^1H NMR, 400 MHz, THF-d^8)**185 (^{13}C NMR, 100 MHz, THF-d^8)**

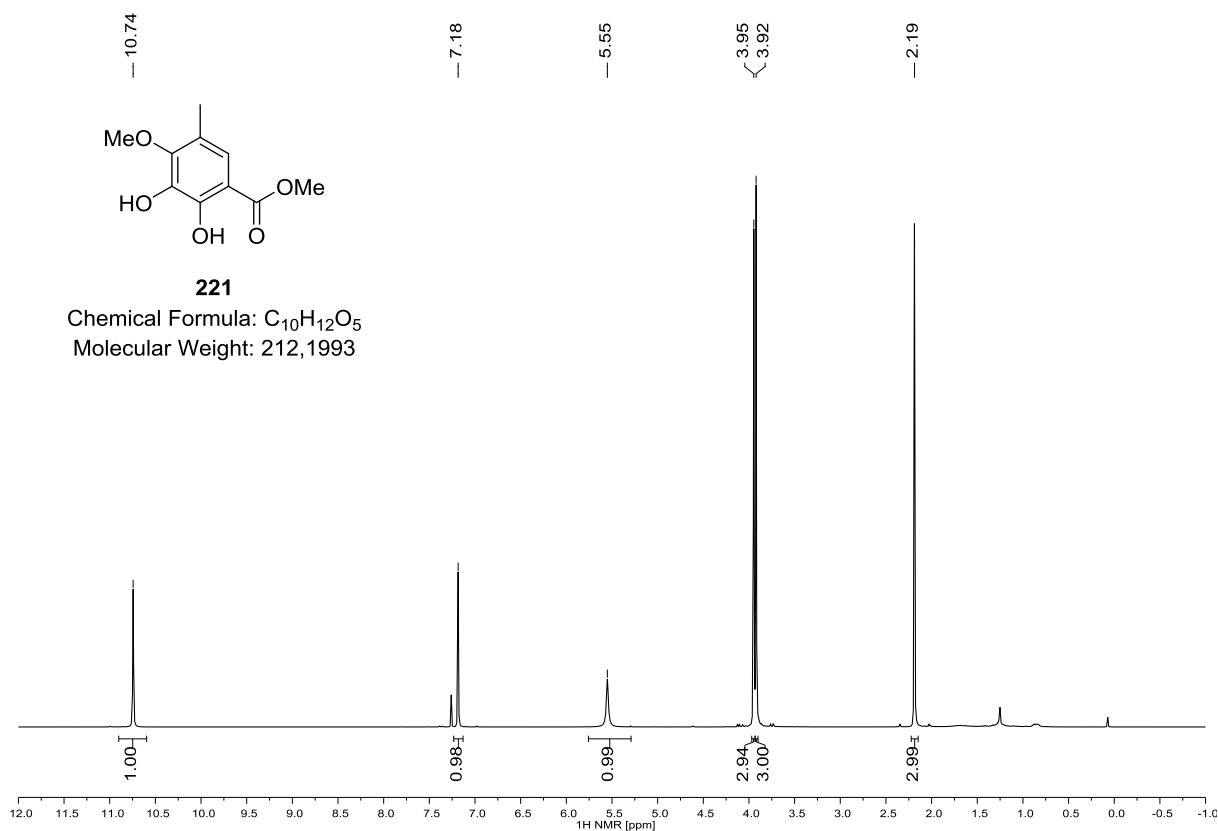
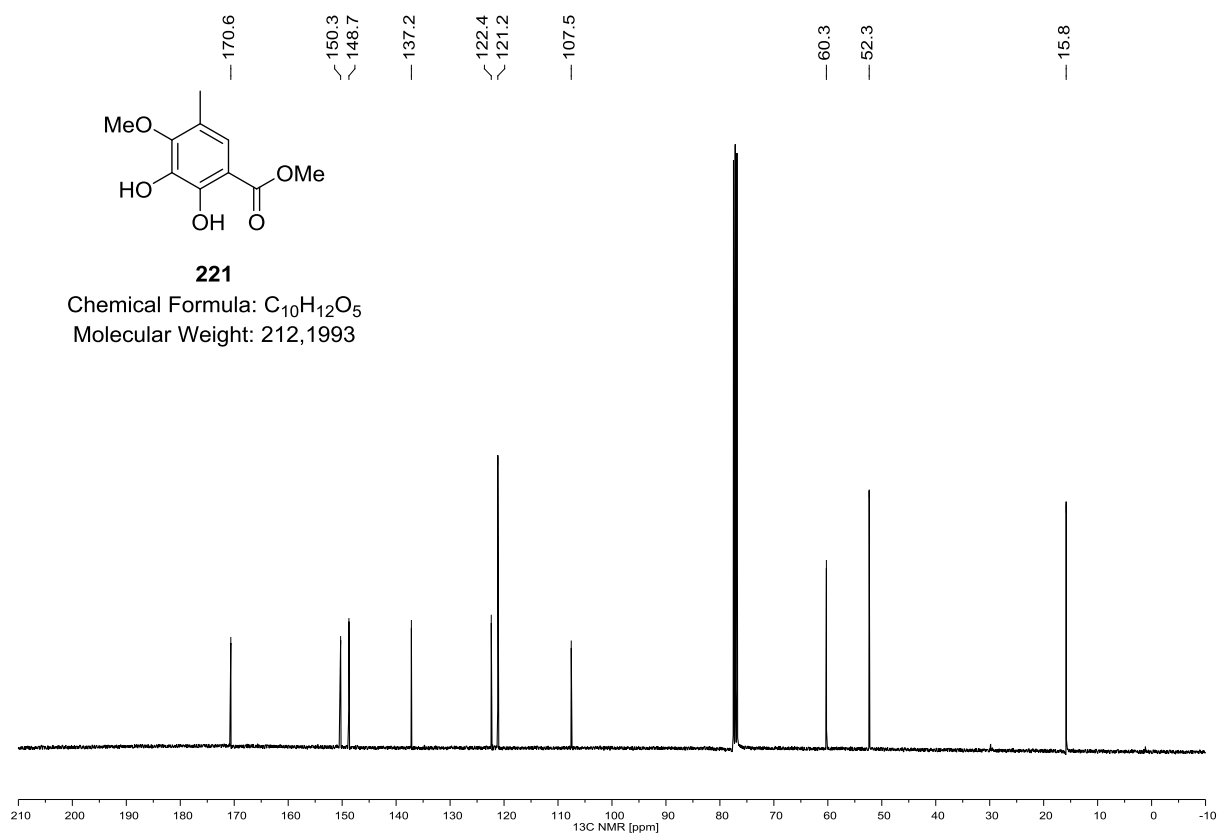
202 (^1H NMR, 300 MHz, CDCl_3)**202 (^{13}C NMR, 75 MHz, CDCl_3)**

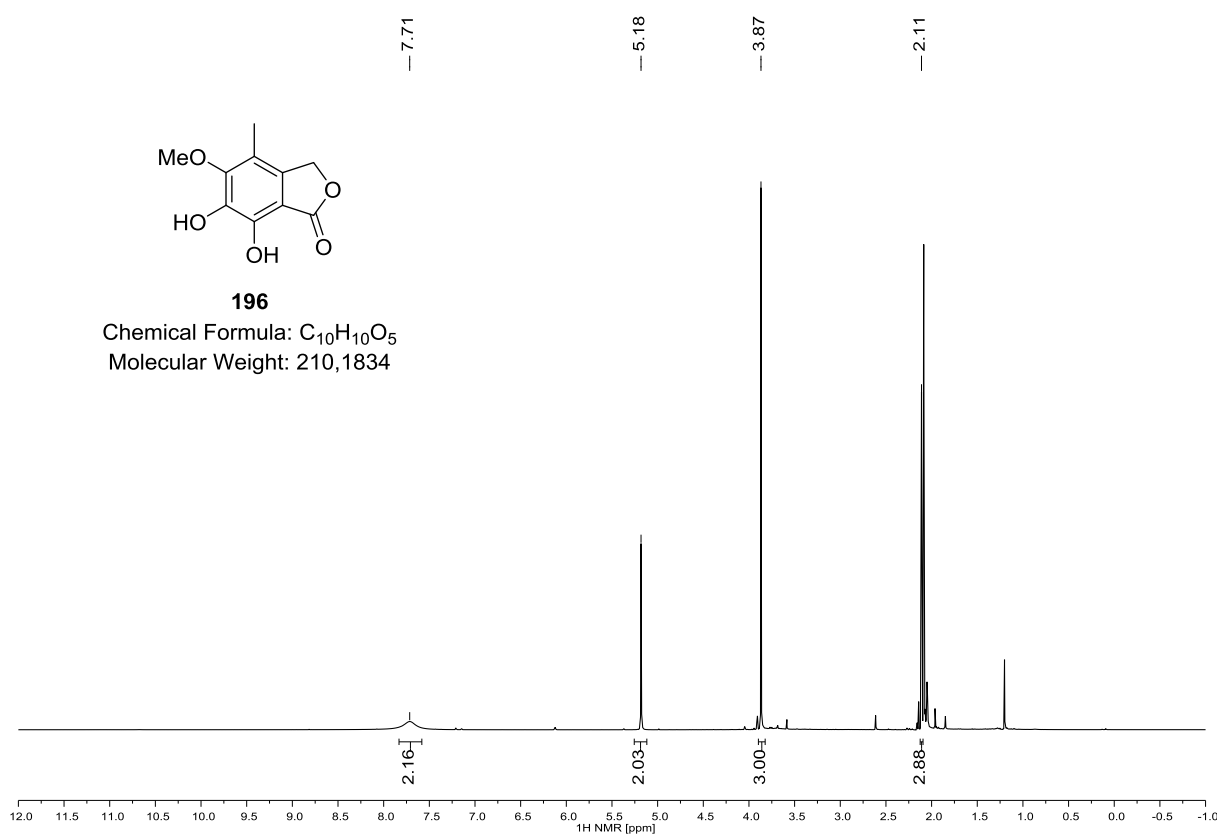
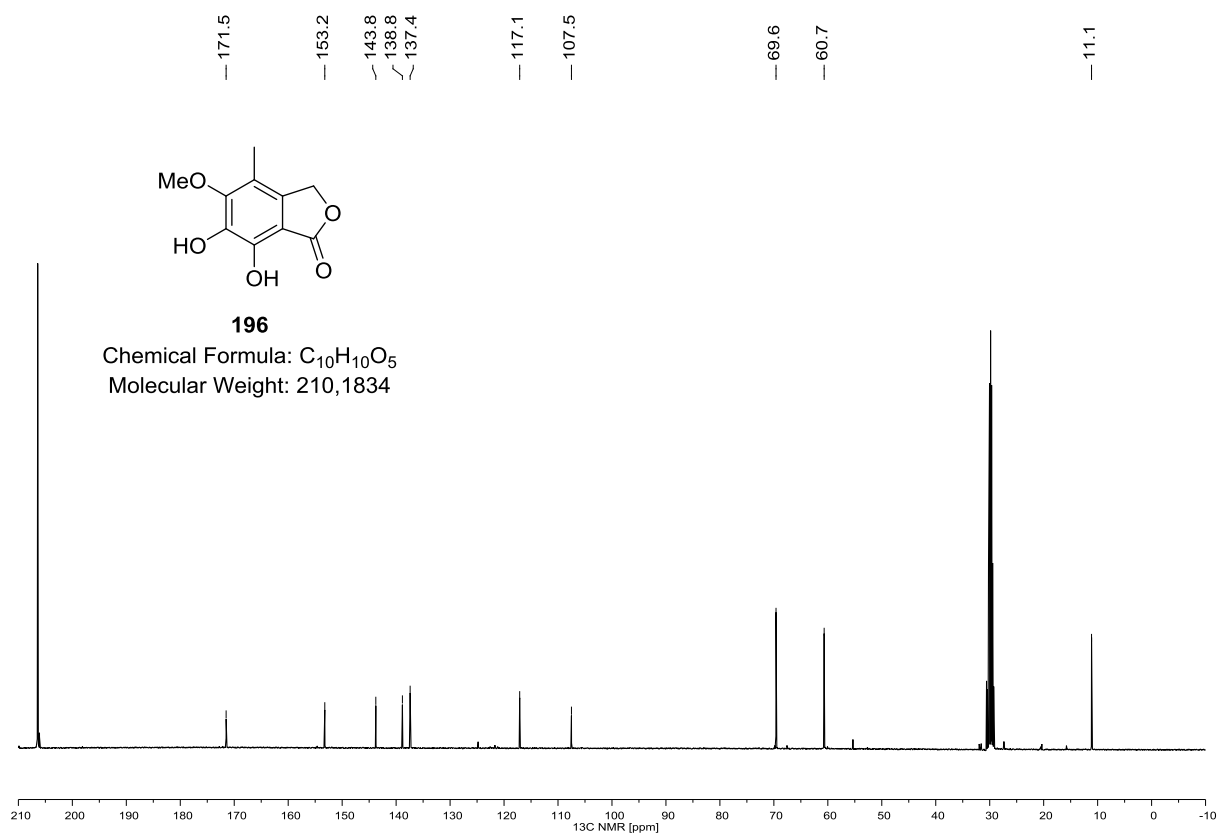
211 (^1H NMR, 400 MHz, CDCl_3)**211 (^{13}C NMR, 100 MHz, CDCl_3)**

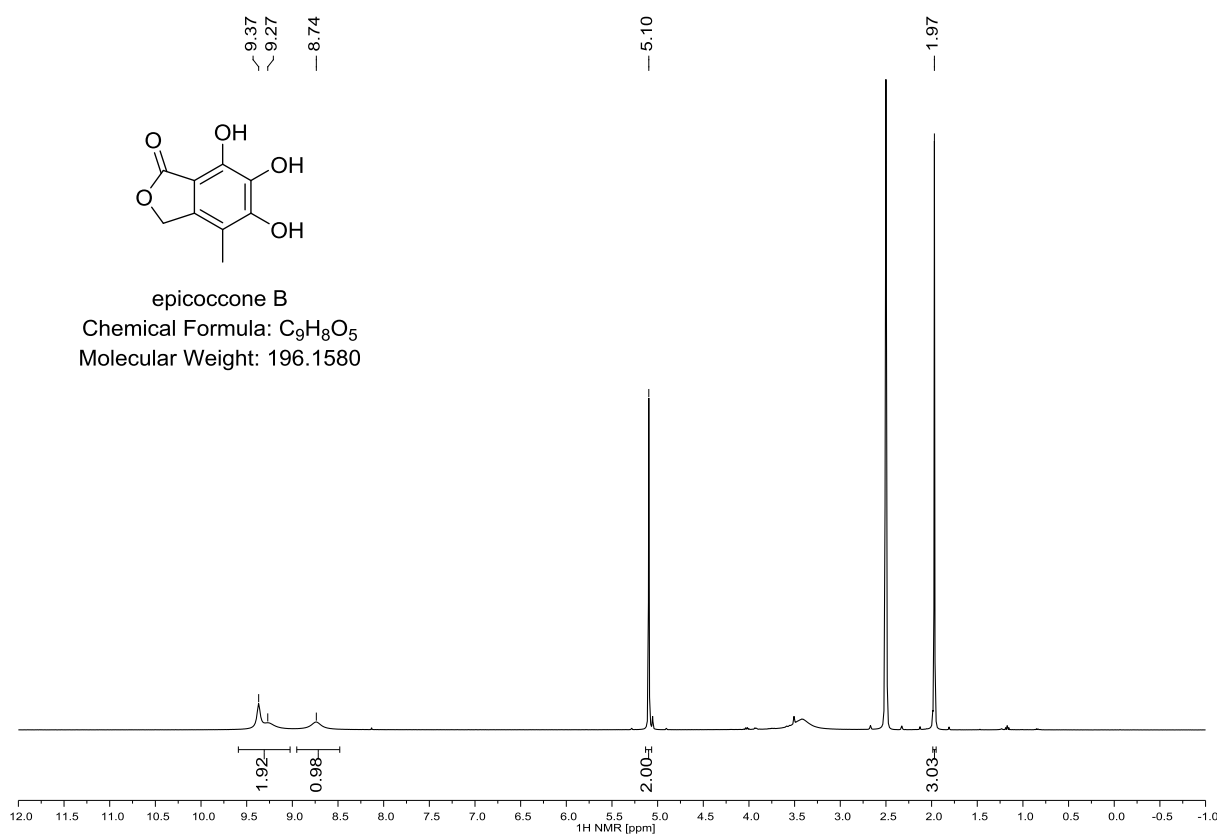
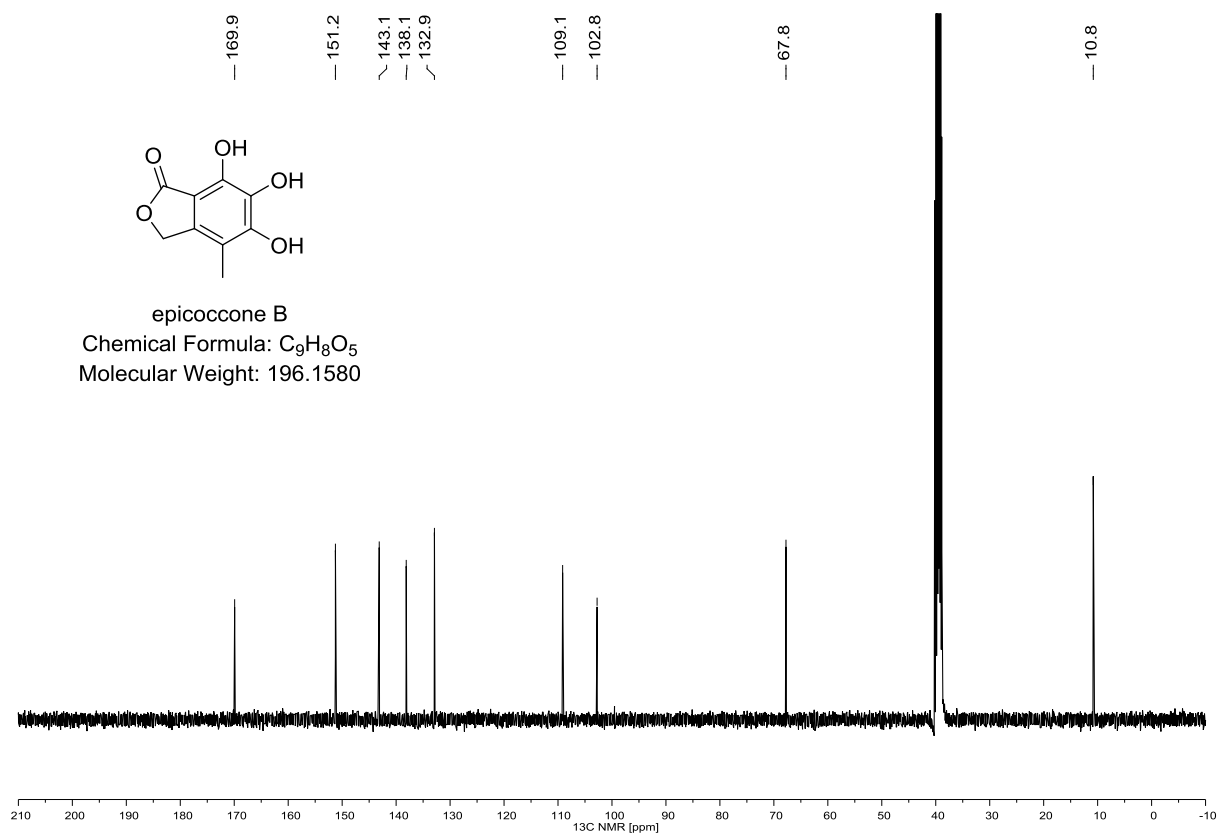
216 (^1H NMR, 400 MHz, CD_3OD)**216 (^{13}C NMR, 100 MHz, CD_3OD)**

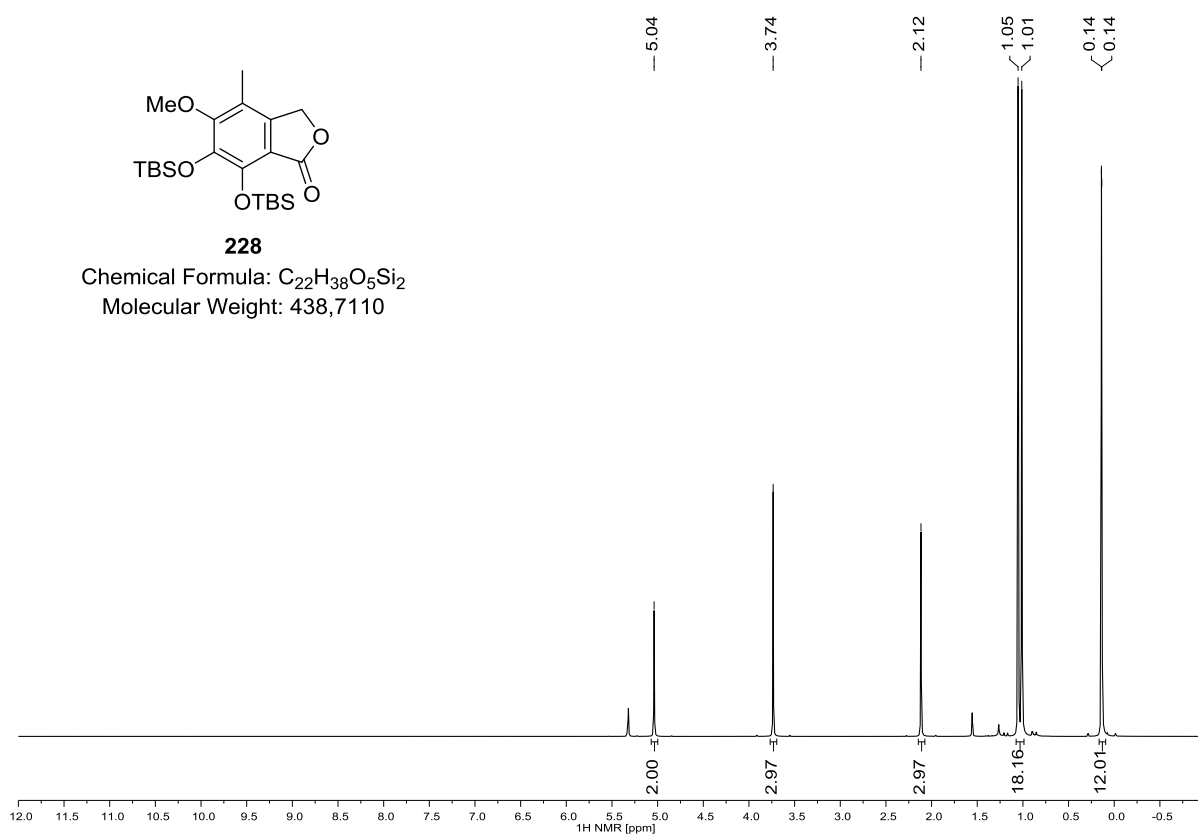
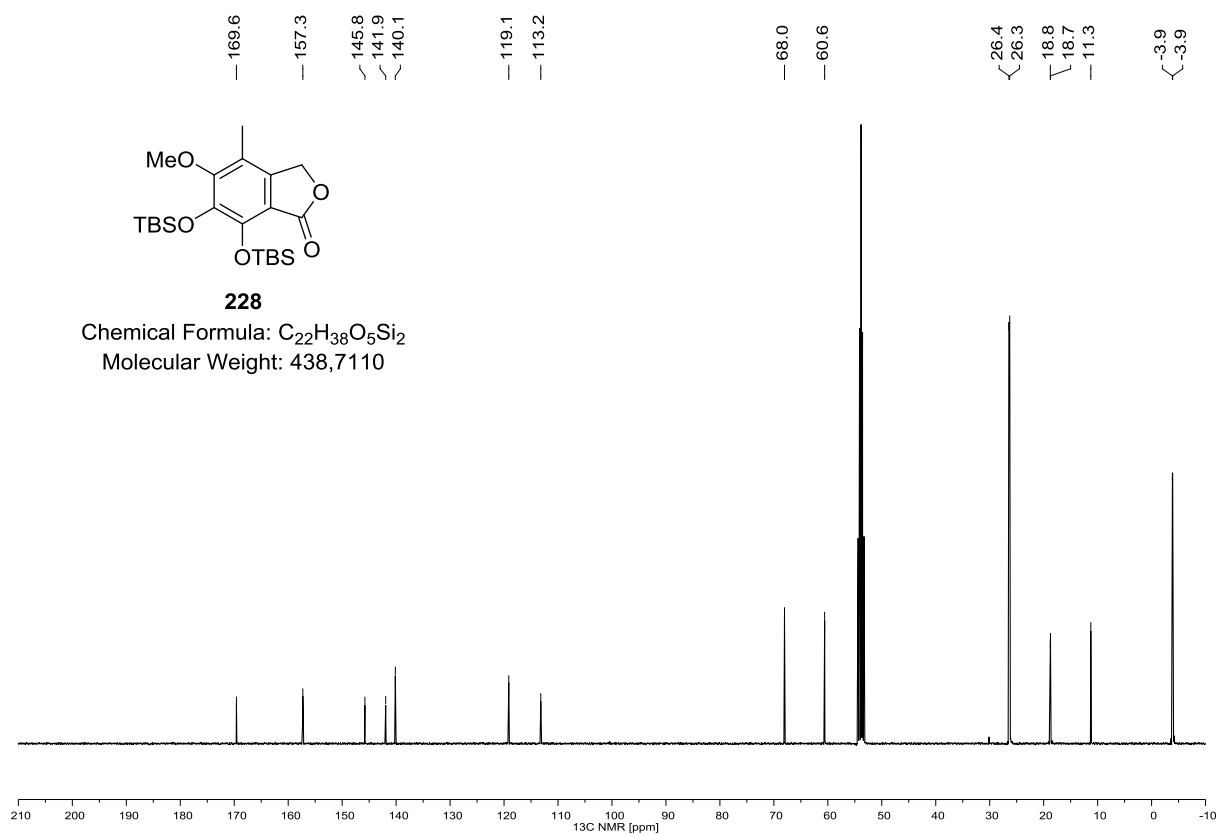
215 (^1H NMR, 600 MHz, CDCl_3)**215 (^{13}C NMR, 150 MHz, CDCl_3)**

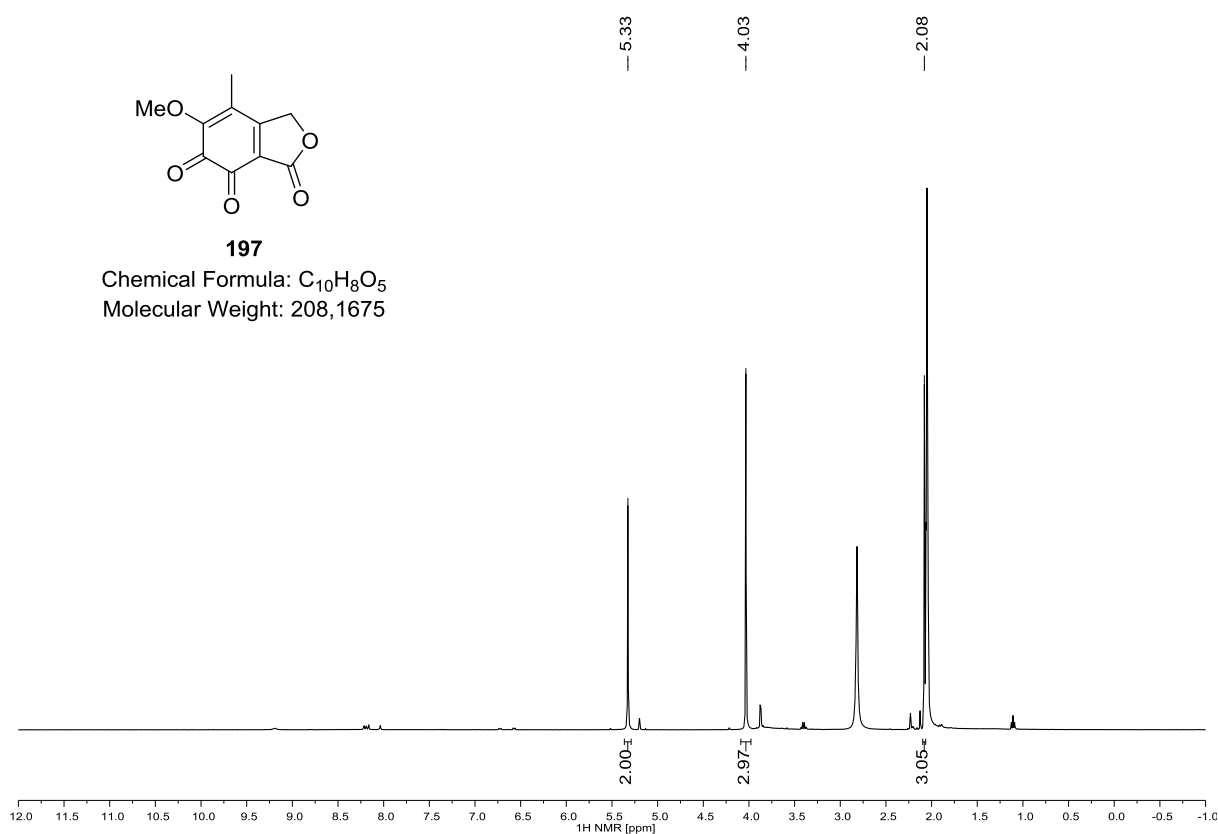
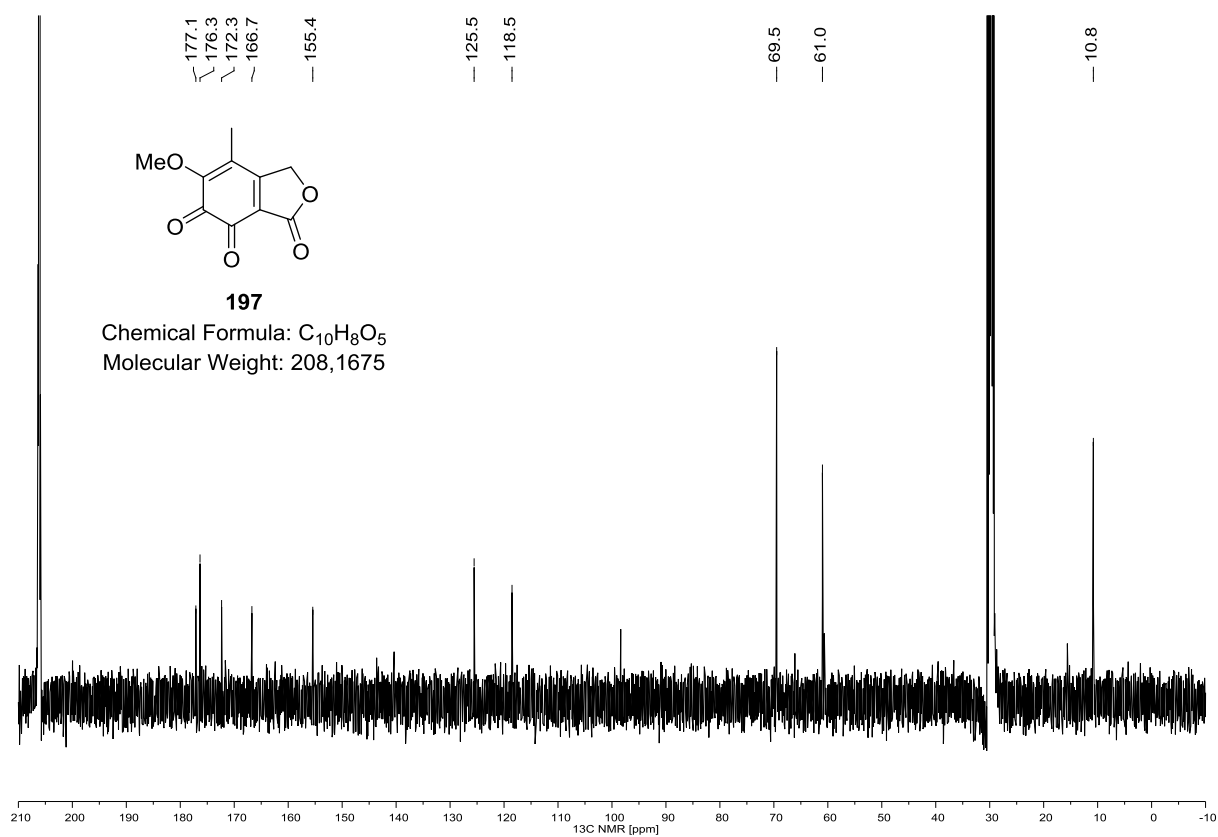
219 (^1H NMR, 400 MHz, CDCl_3)**219 (^{13}C NMR, 100 MHz, CDCl_3)**

221 (^1H NMR, 400 MHz, CDCl_3)**221 (^{13}C NMR, 100 MHz, CDCl_3)**

196 (^1H NMR, 400 MHz, $(\text{CD}_3)_2\text{CO}$)**196 (^{13}C NMR, 100 MHz, $(\text{CD}_3)_2\text{CO}$)**

Epicoccone B (^1H NMR, 400 MHz, DMSO-d_6)**Epicoccone B (^{13}C NMR, 100 MHz, DMSO-d_6)**

228 (^1H NMR, 400 MHz, CD_2Cl_2)**228 (^{13}C NMR, 100 MHz, CD_2Cl_2)**

197 (^1H NMR, 400 MHz, $(\text{CD}_3)_2\text{CO}$)**197 (^{13}C NMR, 100 MHz, $(\text{CD}_3)_2\text{CO}$)**

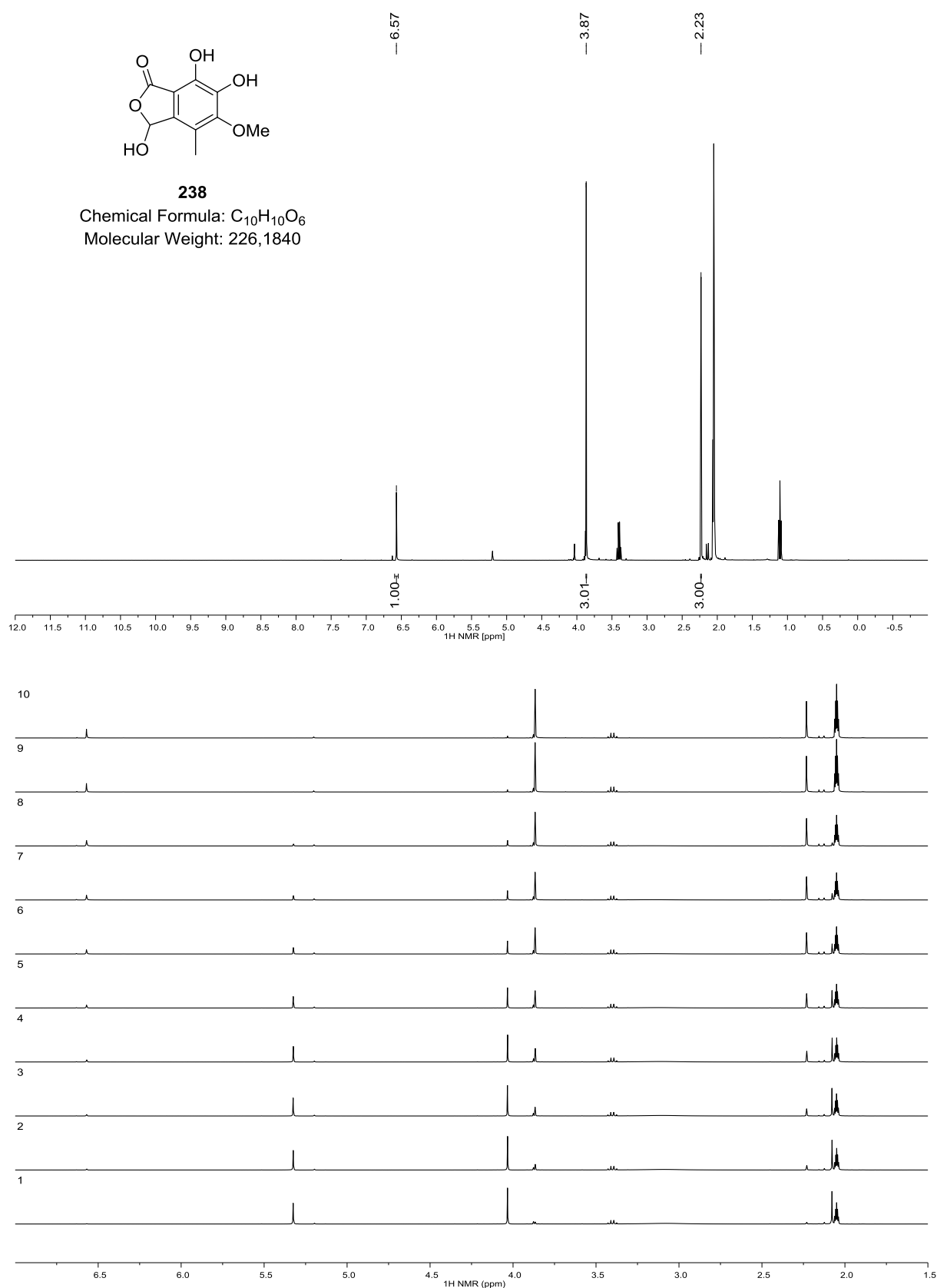
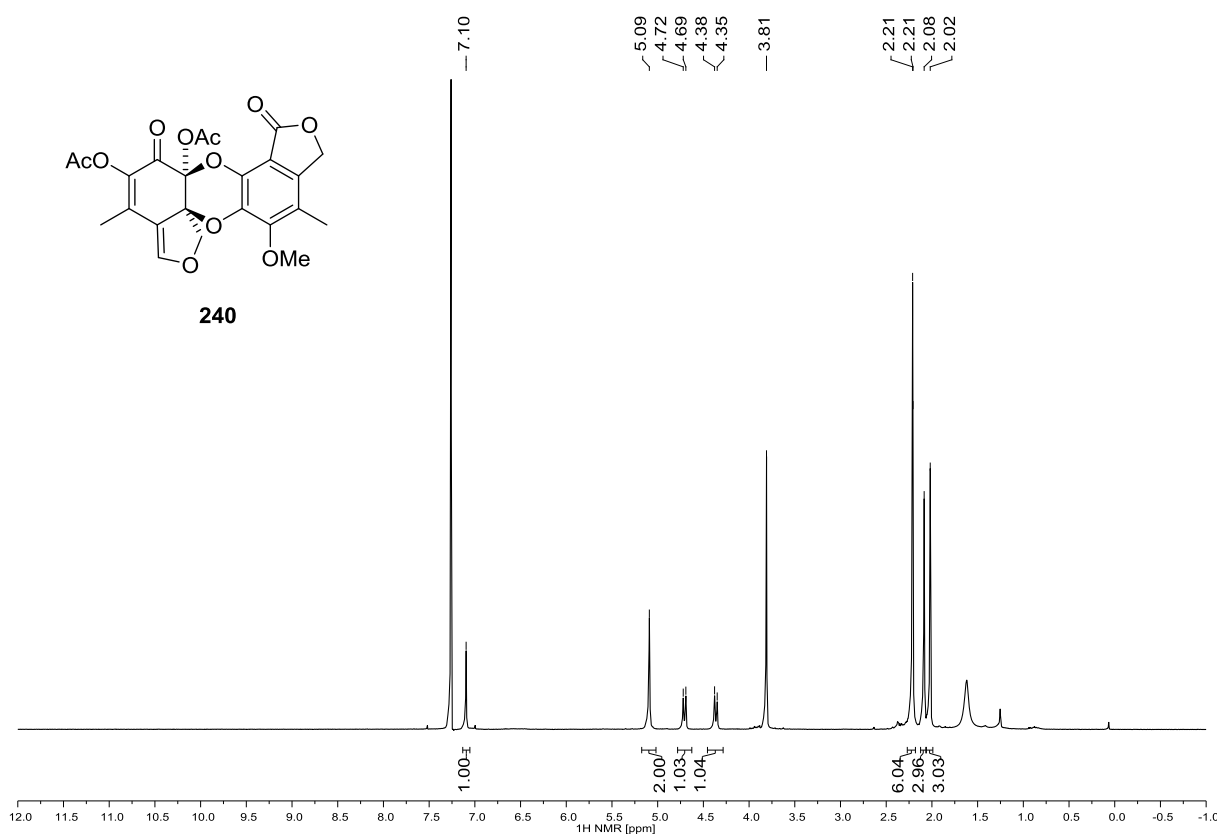
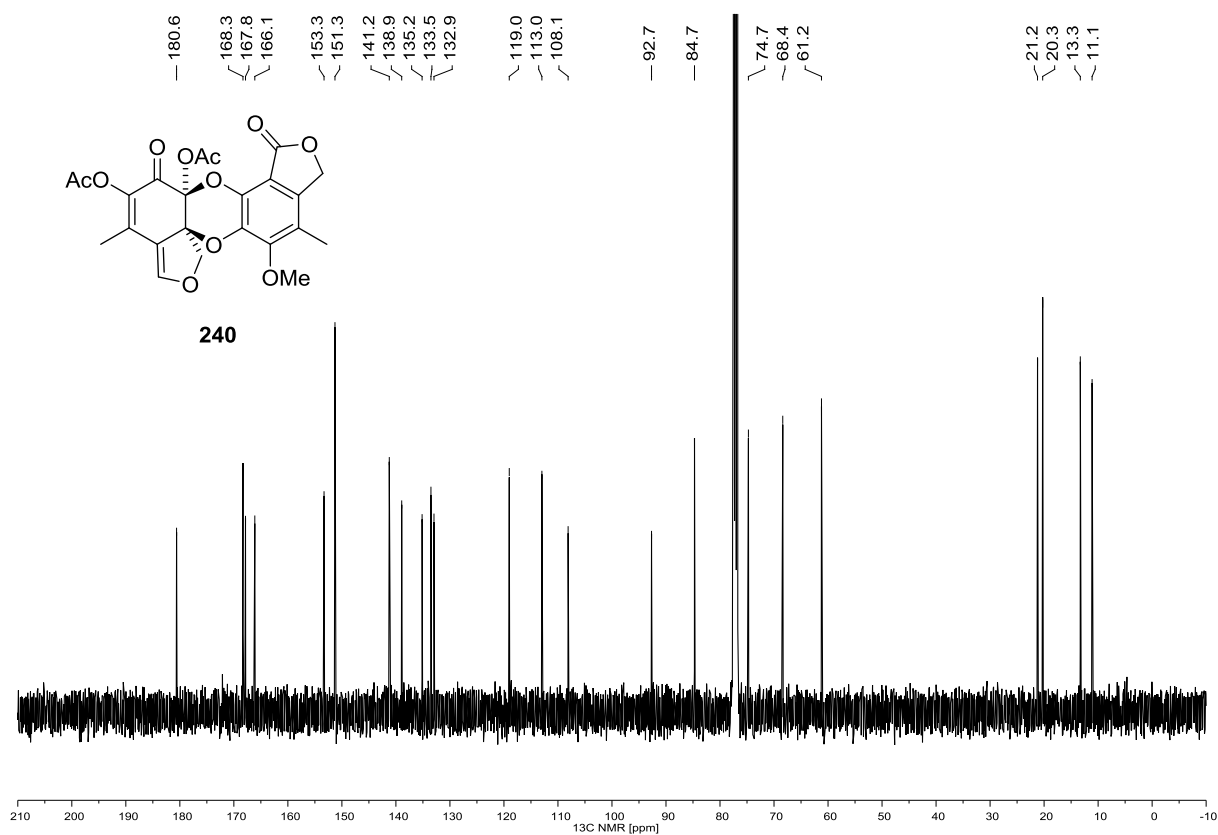
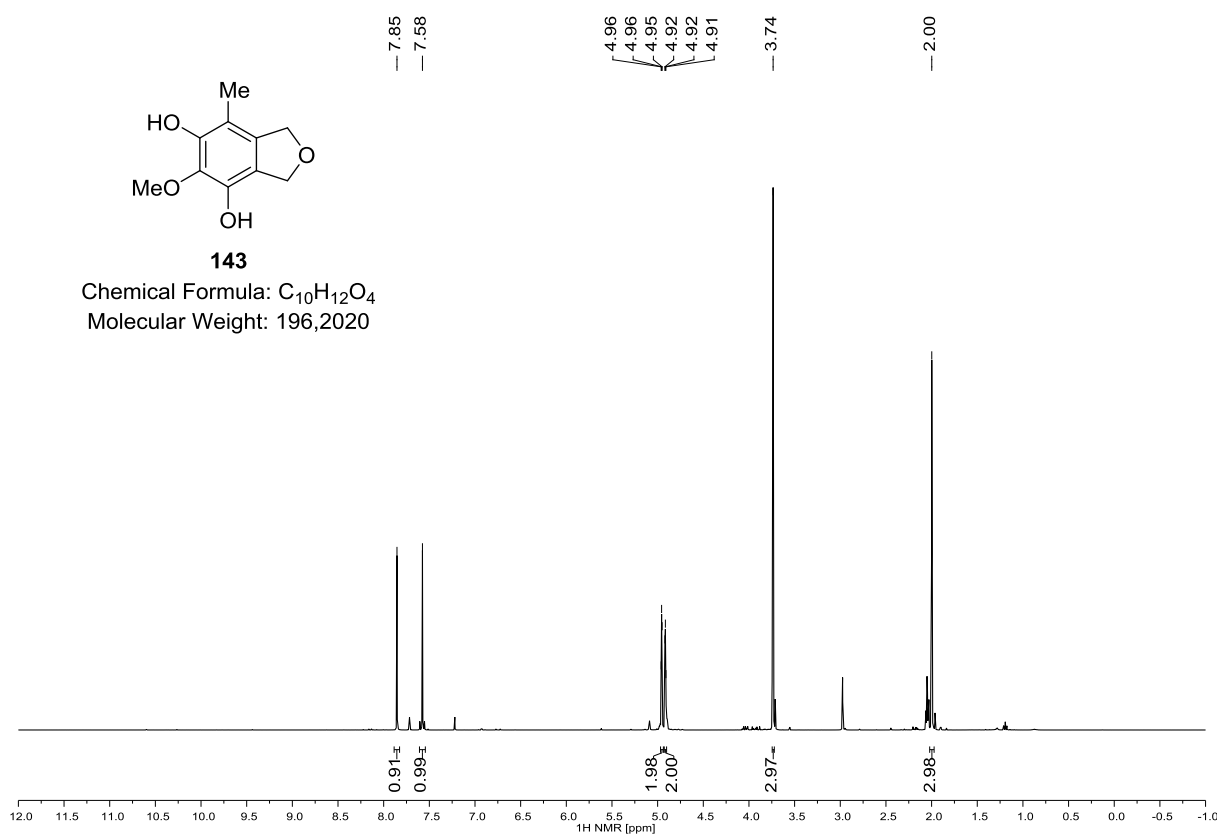
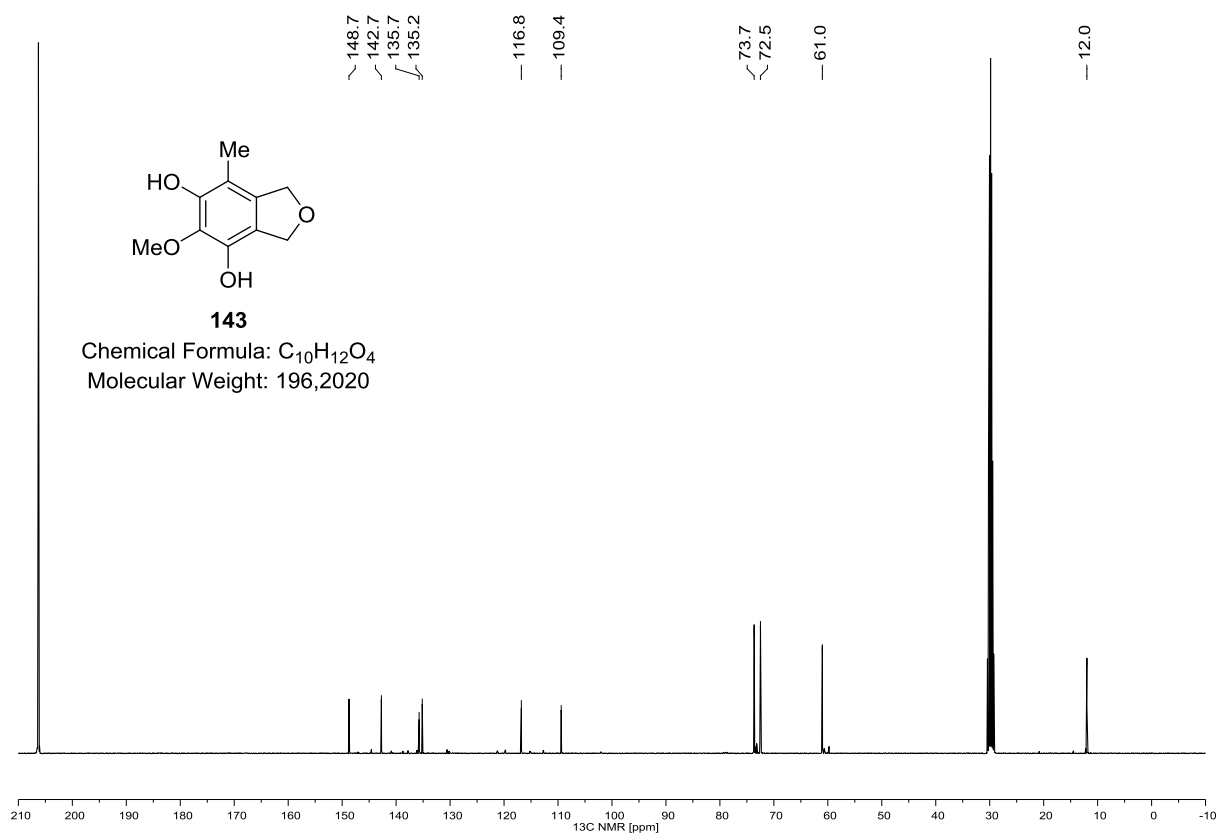
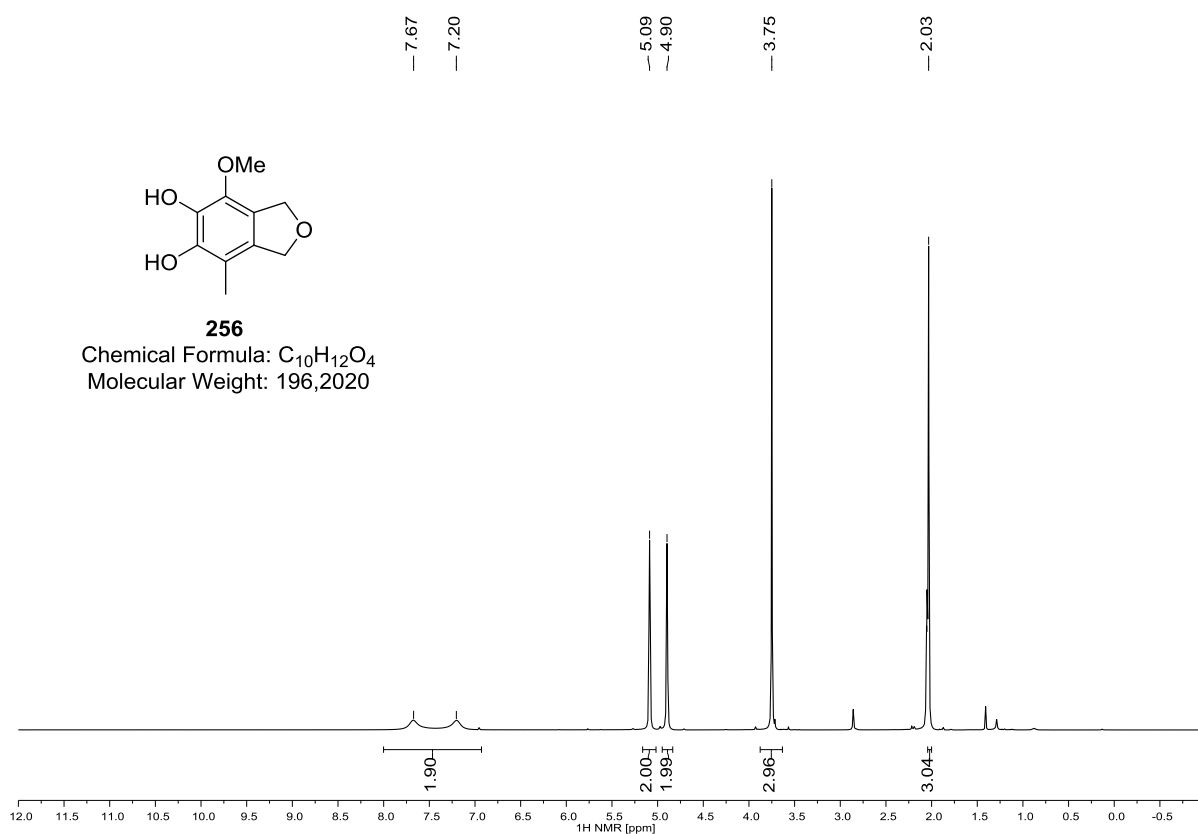
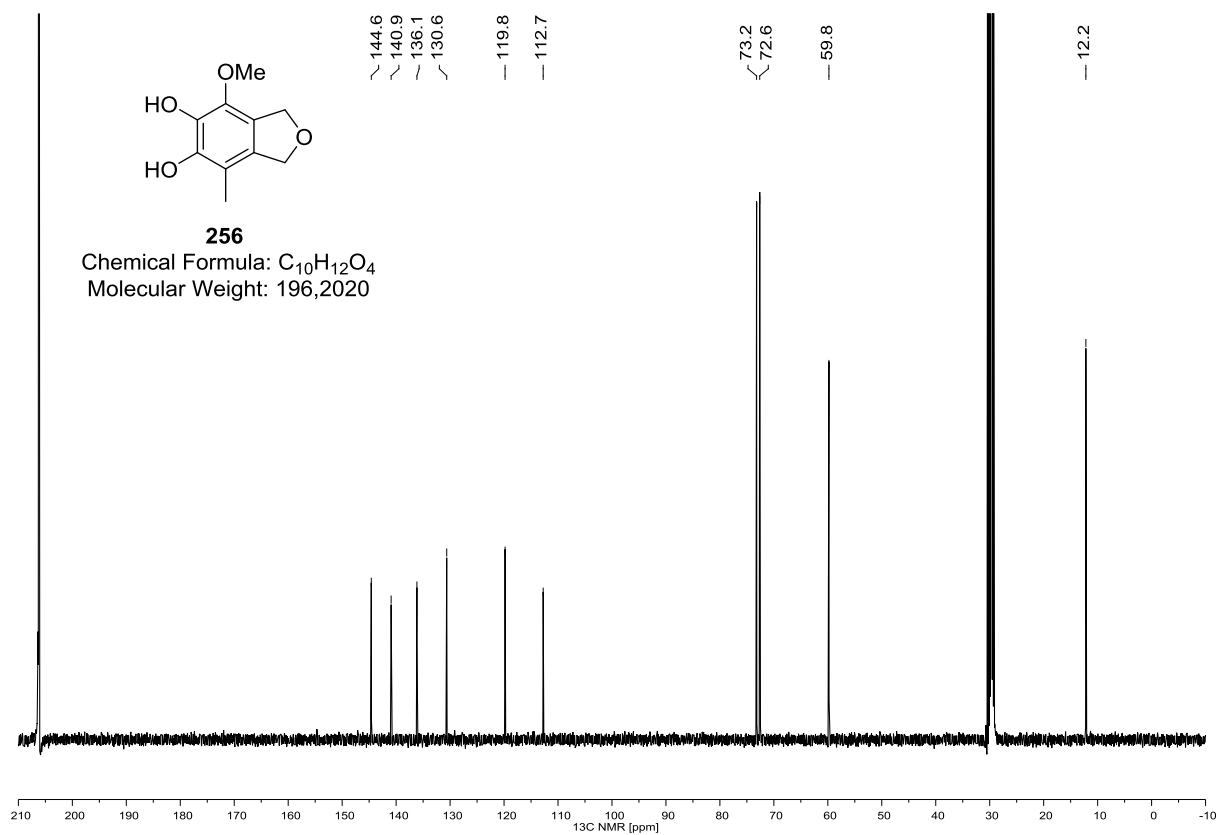
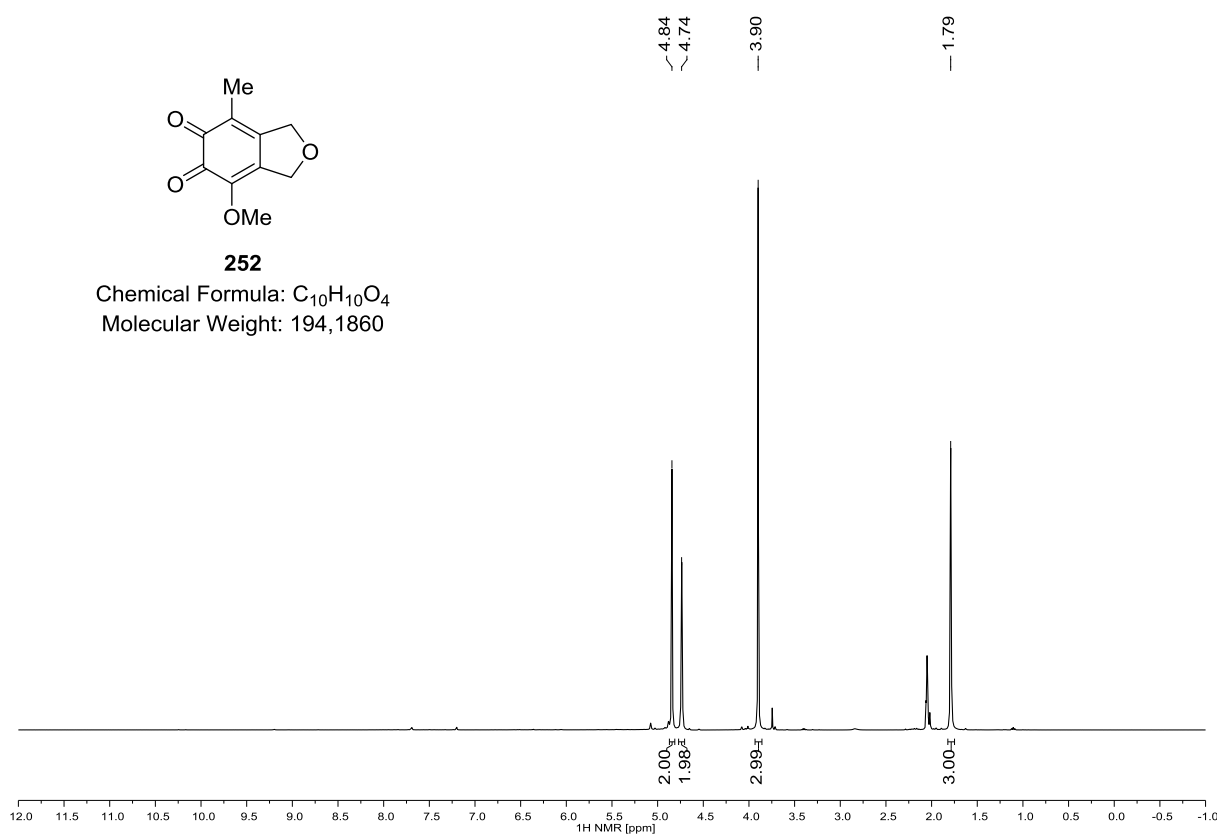
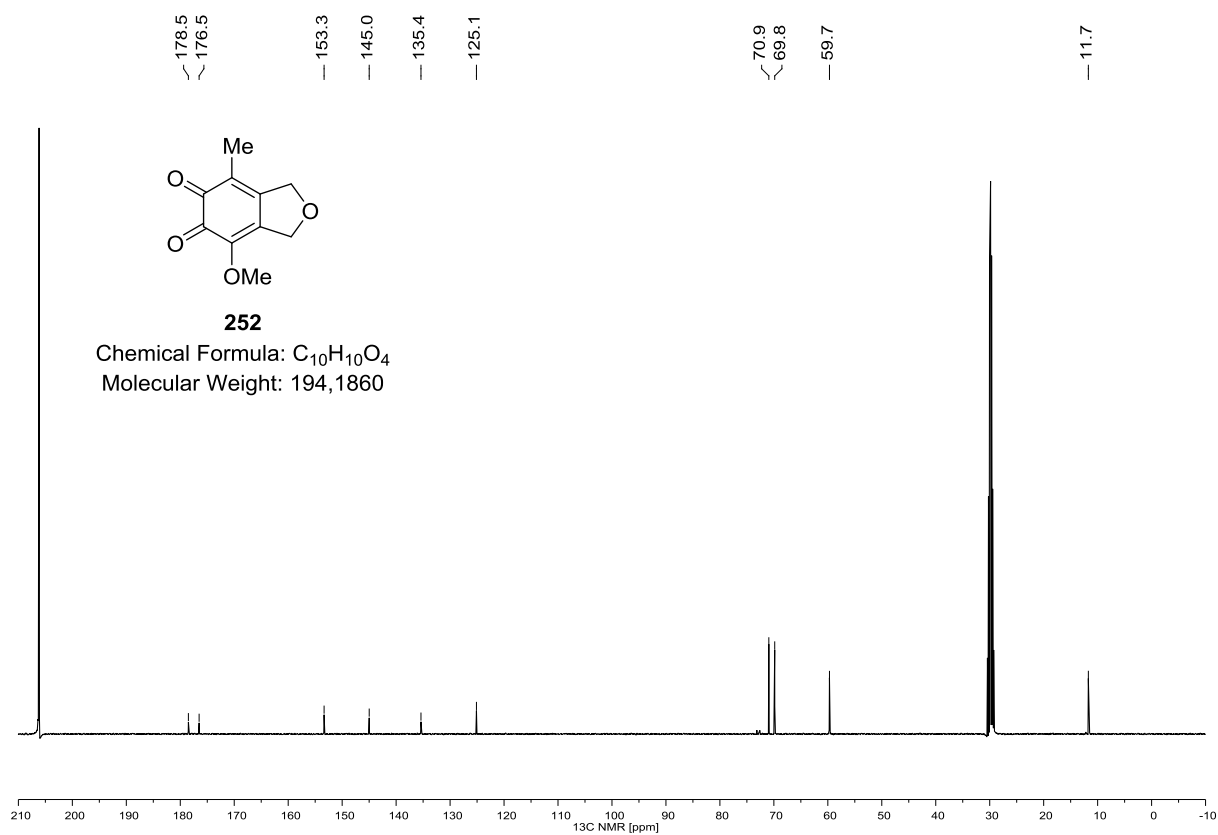
238 (^1H NMR, 400 MHz, $(\text{D}_3\text{C})_2\text{CO}$)

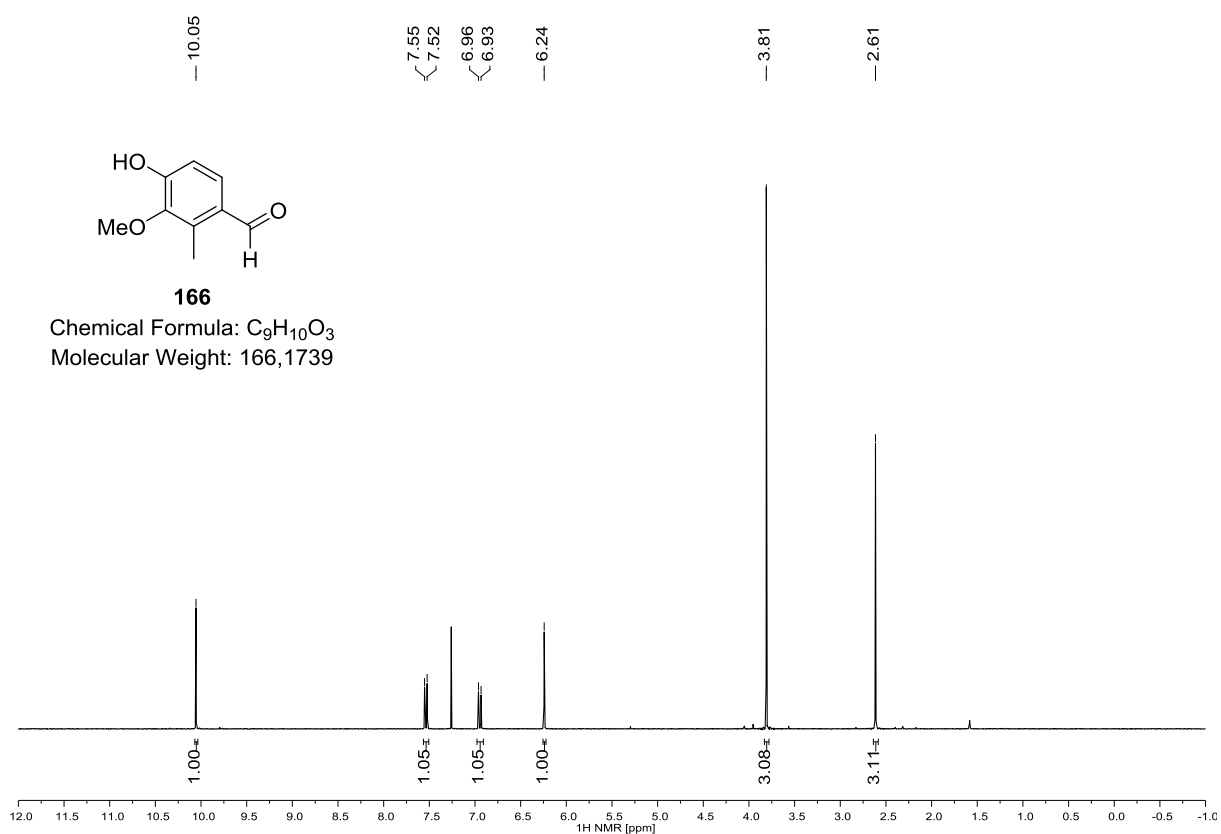
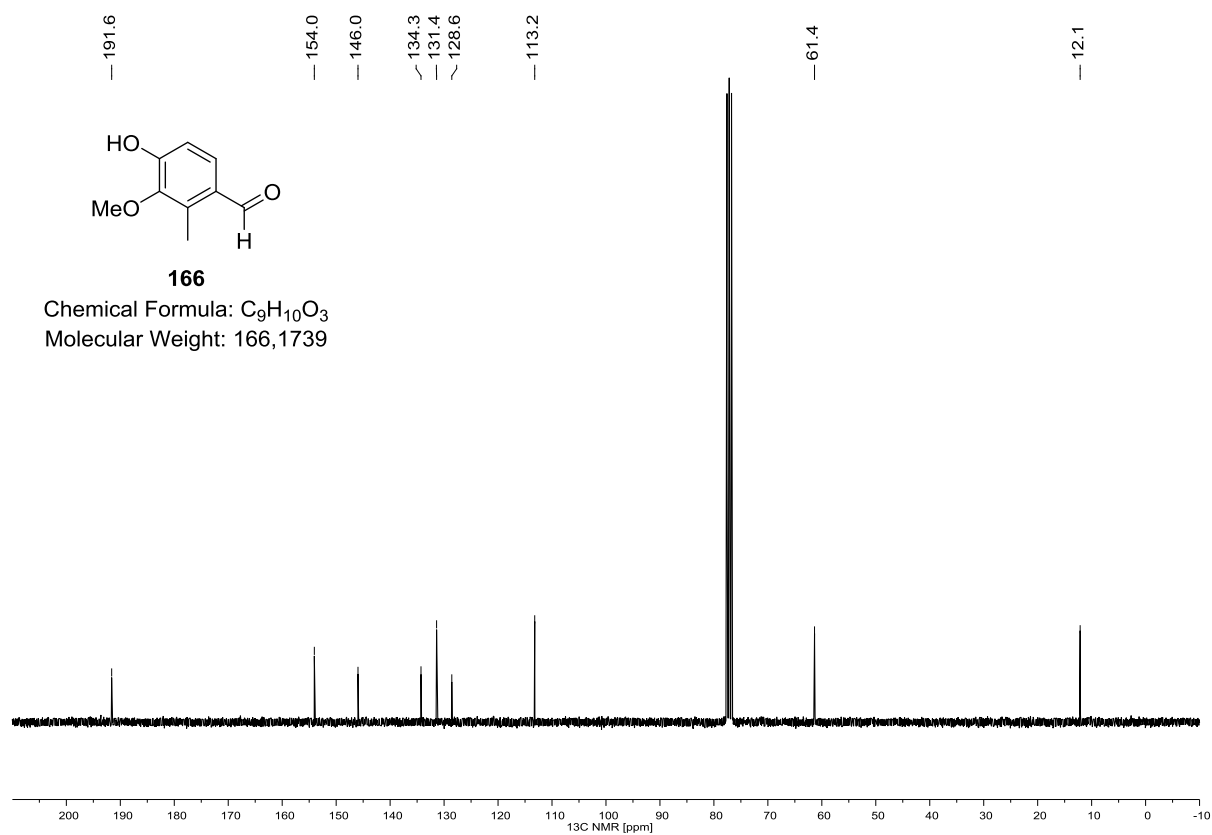
Figure 50. Decomposition study with quinone **197** in acetone- d_6 at rt. (^1H NMR spectrum 1: quinone **197**, spectrum 10: hemiacetal **238**, timeframe spectrum 1 to 10: 18 h)

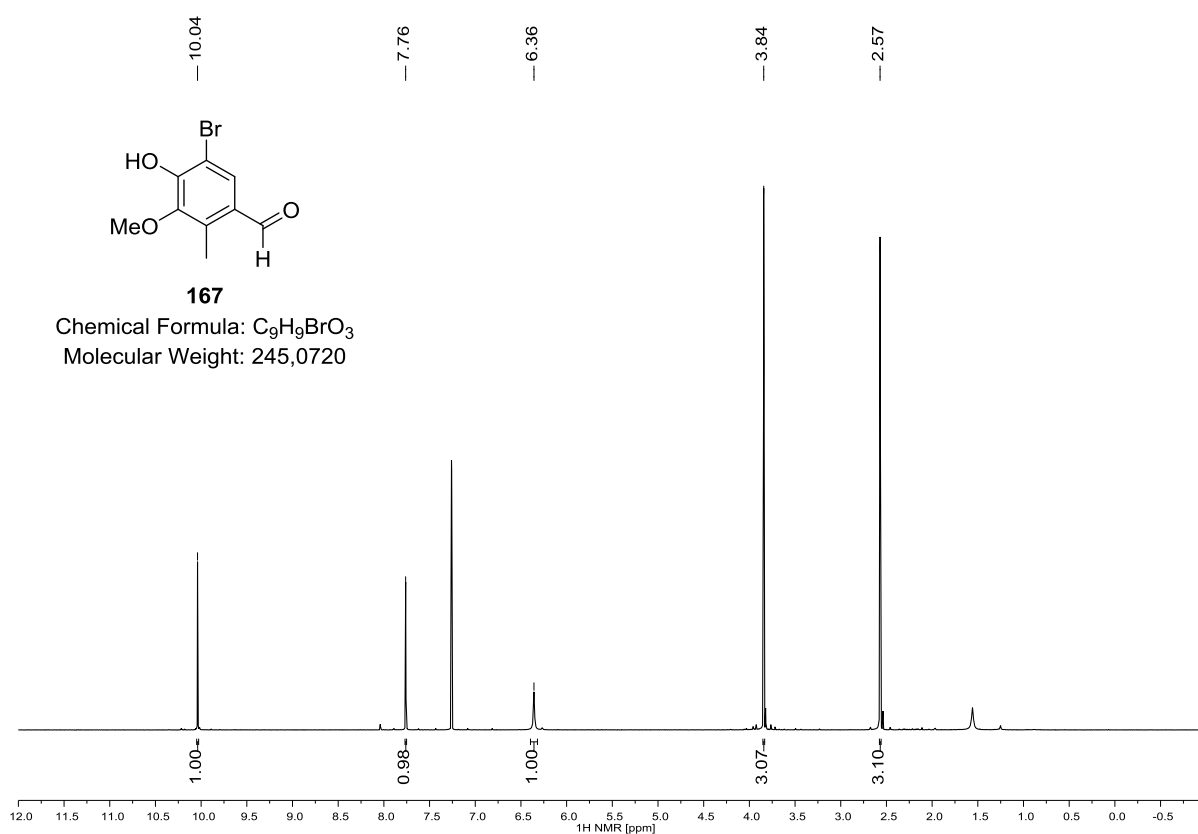
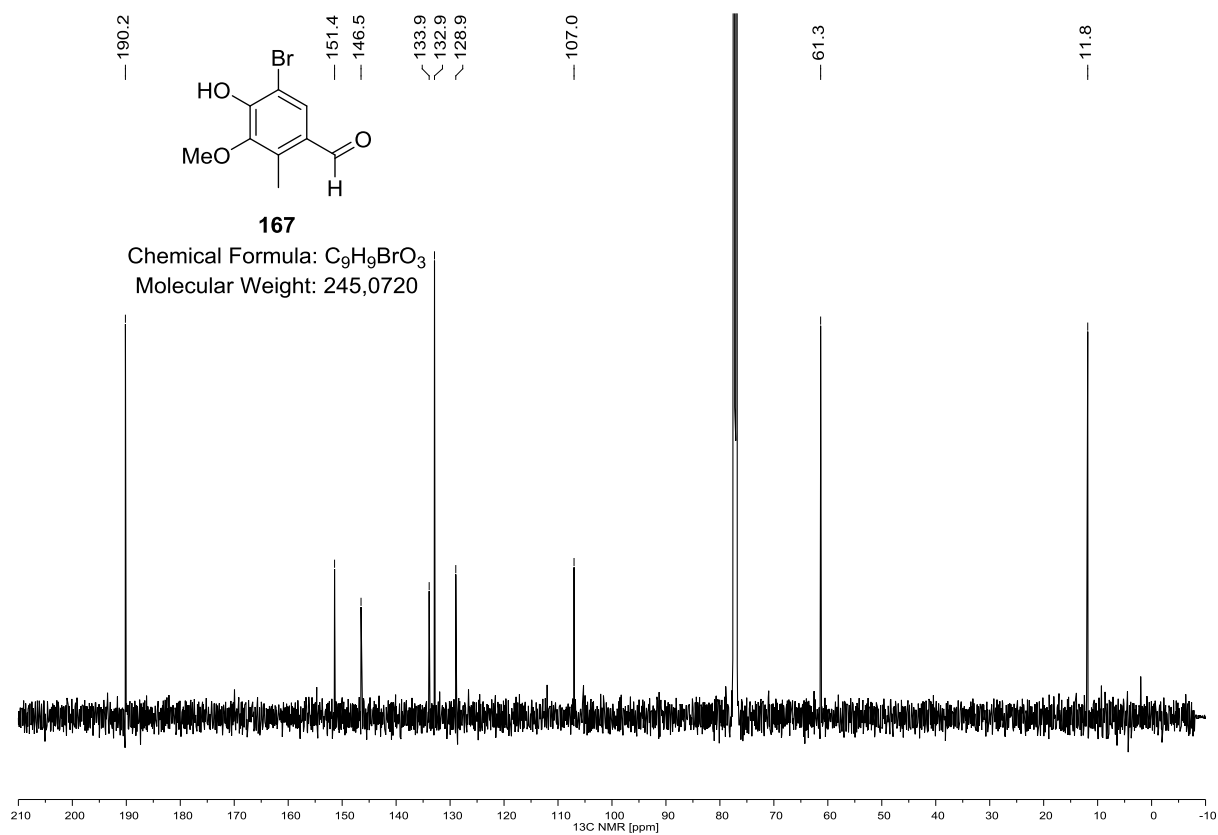
240 (^1H NMR, 400 MHz, CDCl_3)**240 (^{13}C NMR, 100 MHz, CDCl_3)**

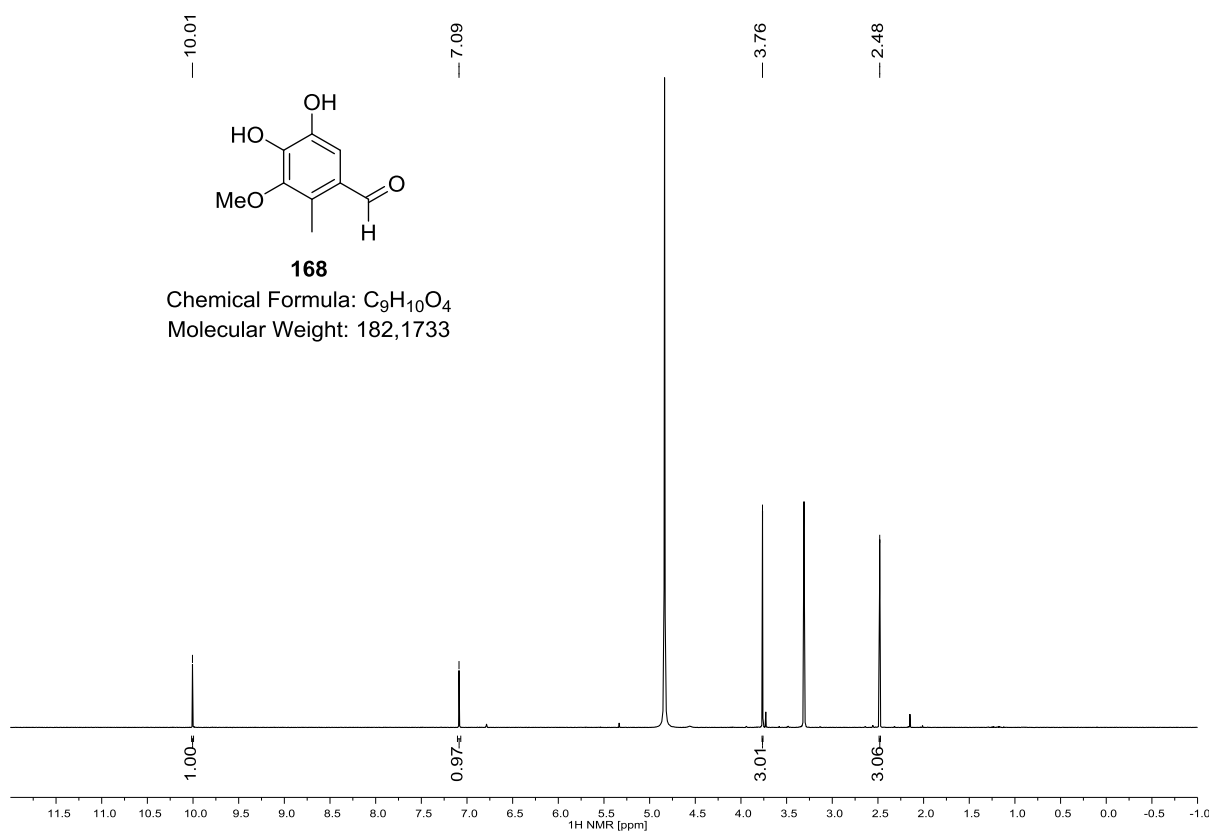
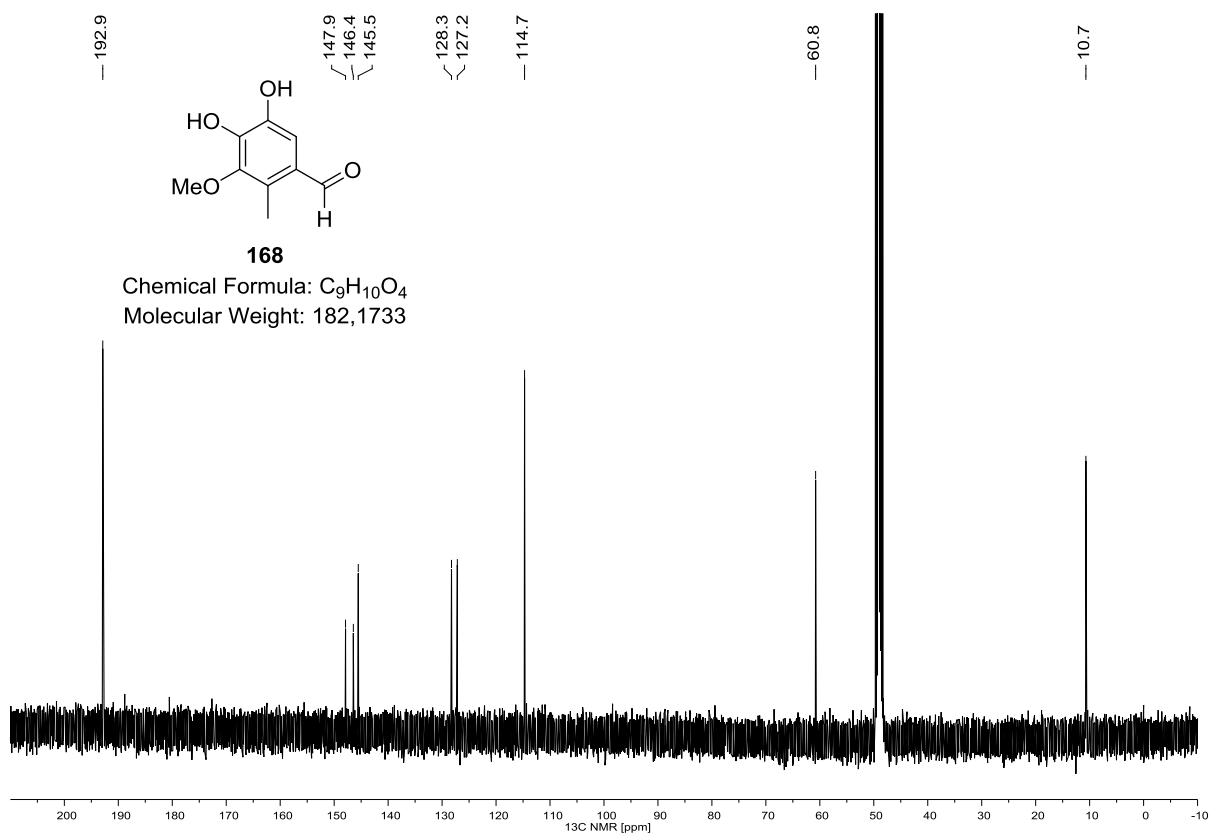
143 (^1H NMR, 400 MHz, $(\text{D}_3\text{C})_2\text{CO}$)**143 (^{13}C NMR, 100 MHz, $(\text{D}_3\text{C})_2\text{CO}$)**

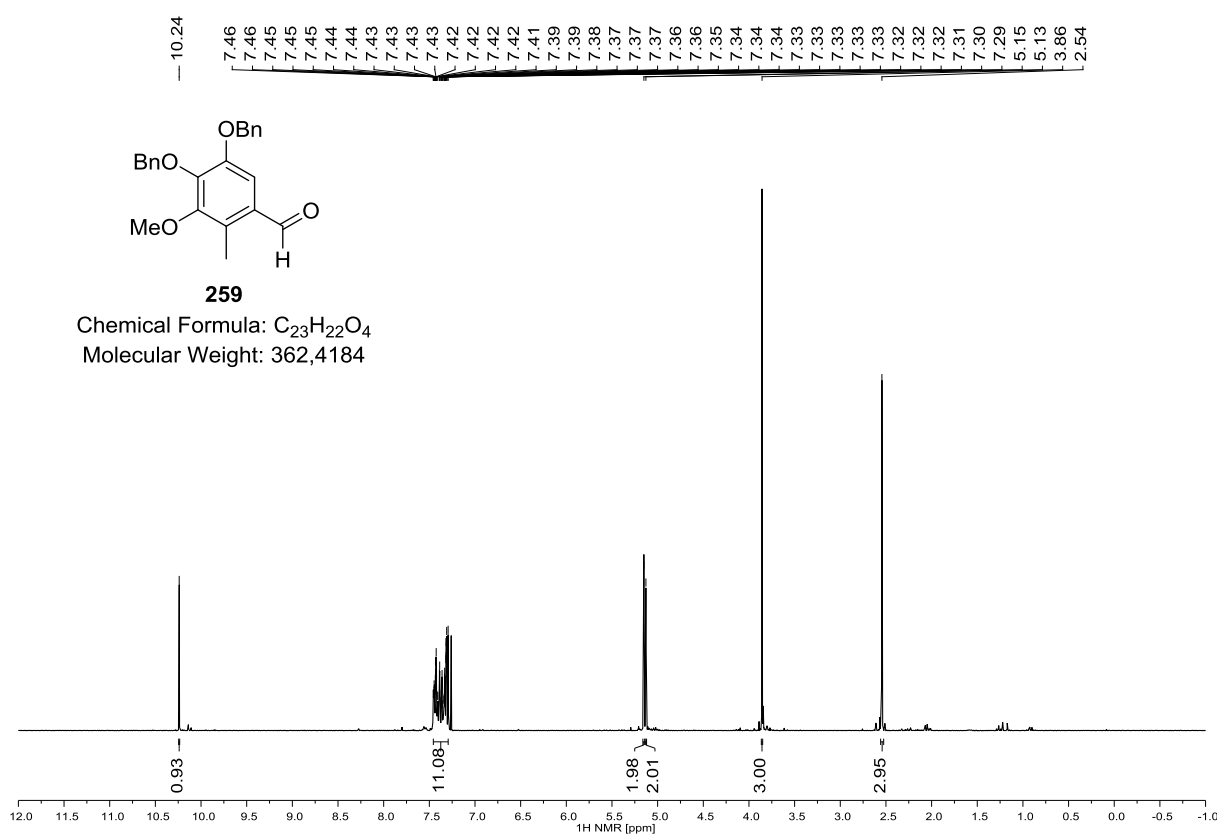
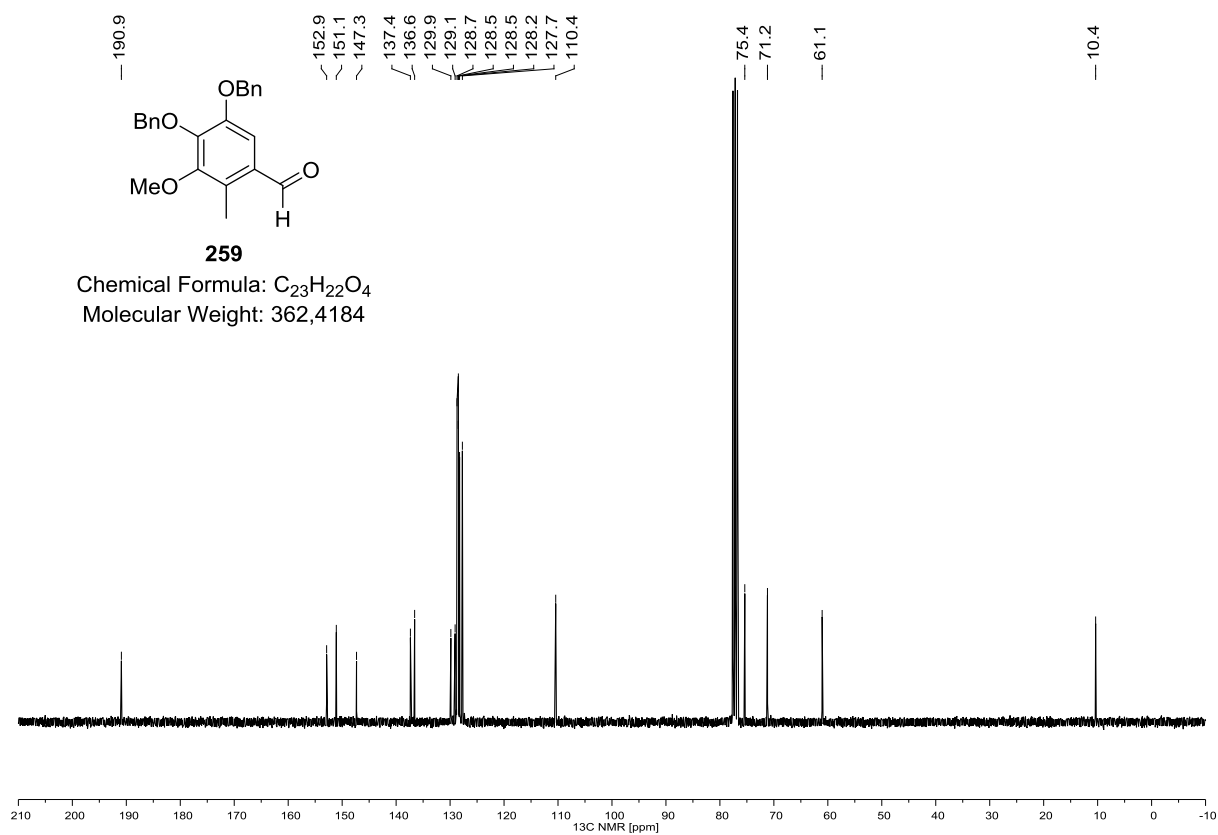
256 (^1H NMR, 400 MHz, $(\text{D}_3\text{C})_2\text{CO}$)**256 (^{13}C NMR, 100 MHz, $(\text{D}_3\text{C})_2\text{CO}$)**

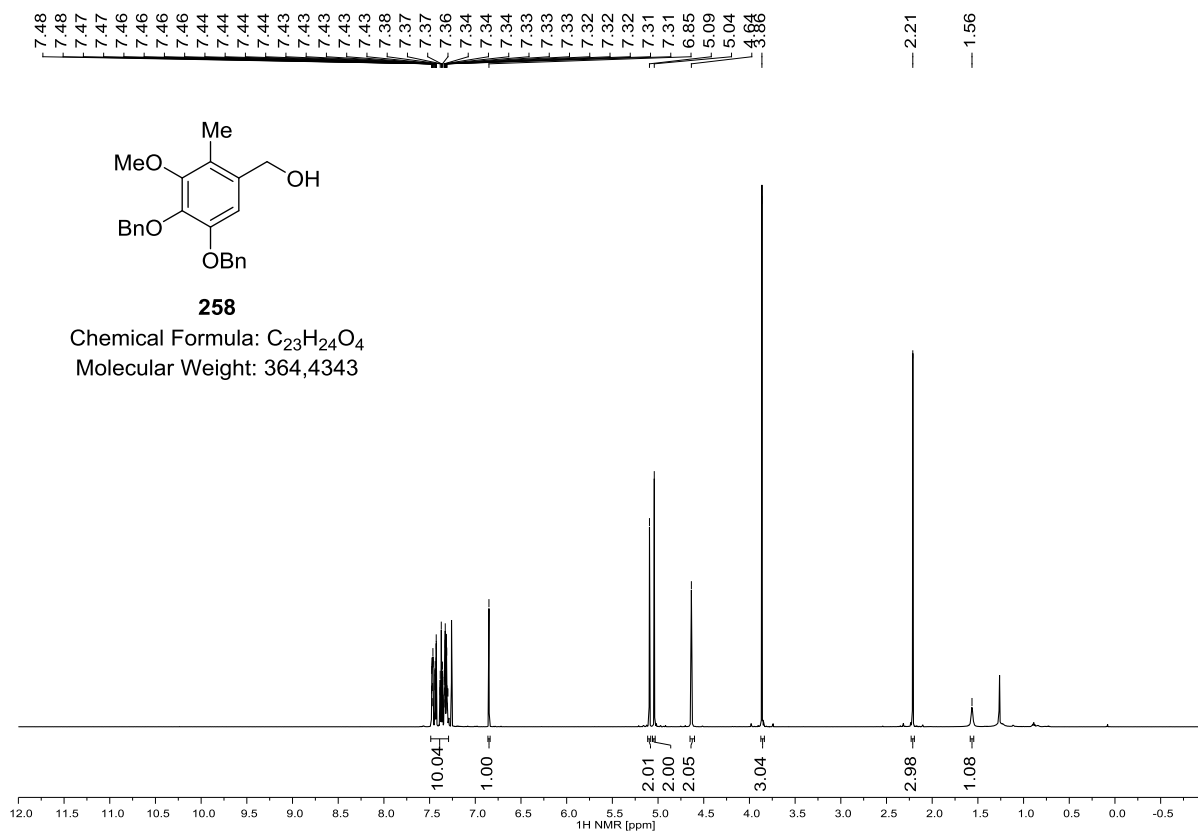
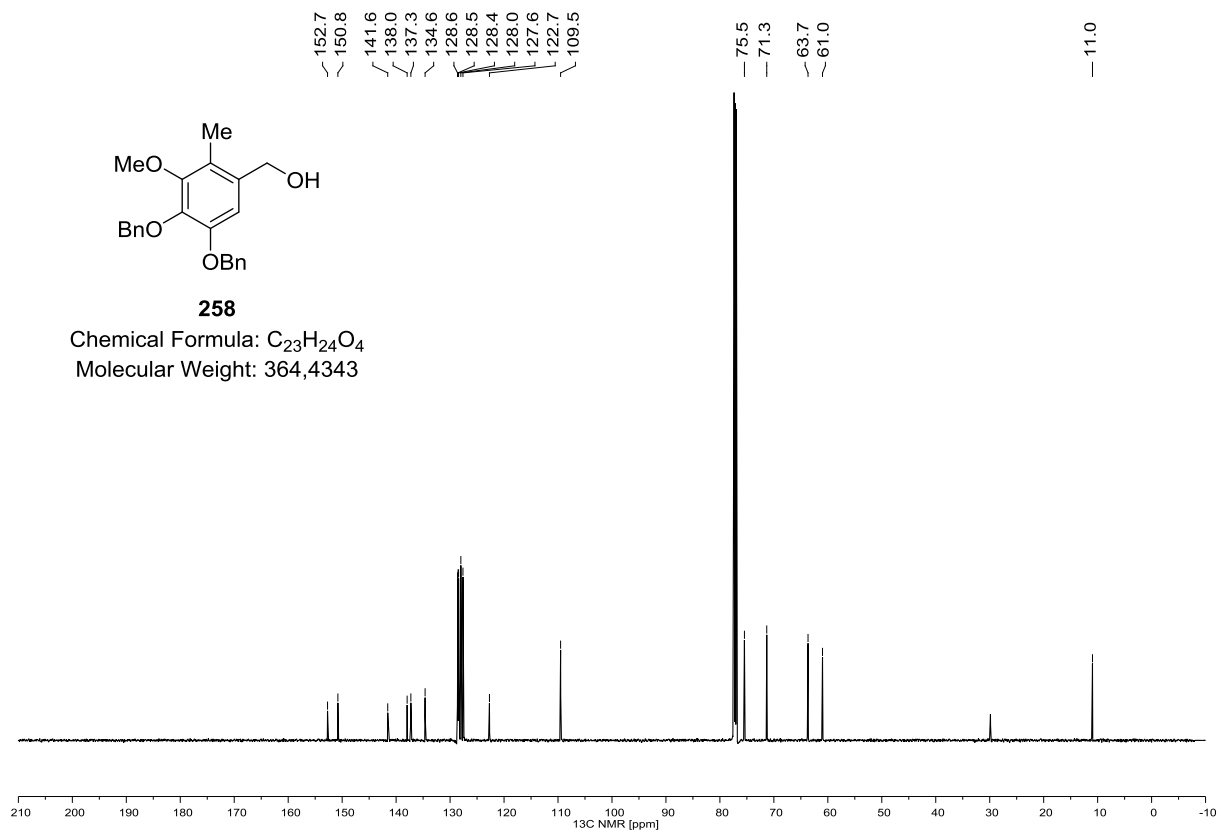
252 (^1H NMR, 400 MHz, $(\text{D}_3\text{C})_2\text{CO}$)**252 (^{13}C NMR, 100 MHz, $(\text{D}_3\text{C})_2\text{CO}$)**

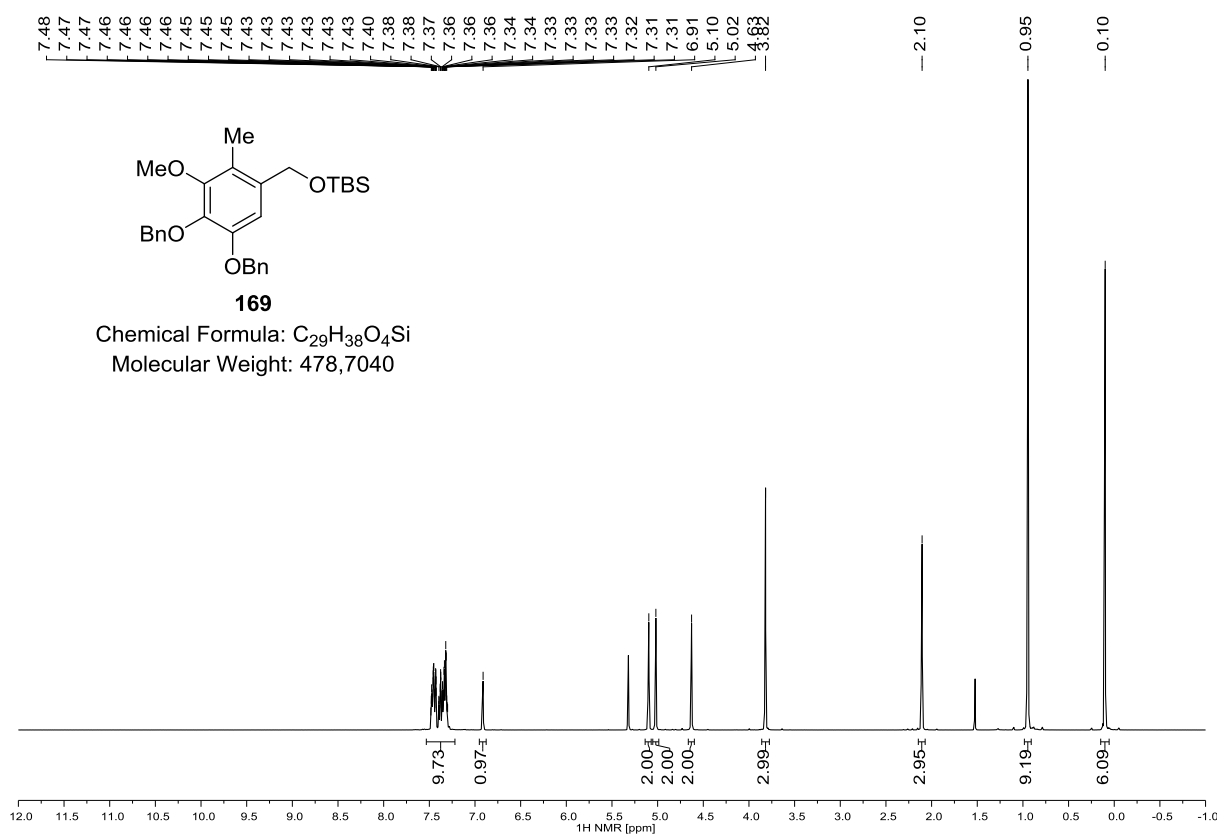
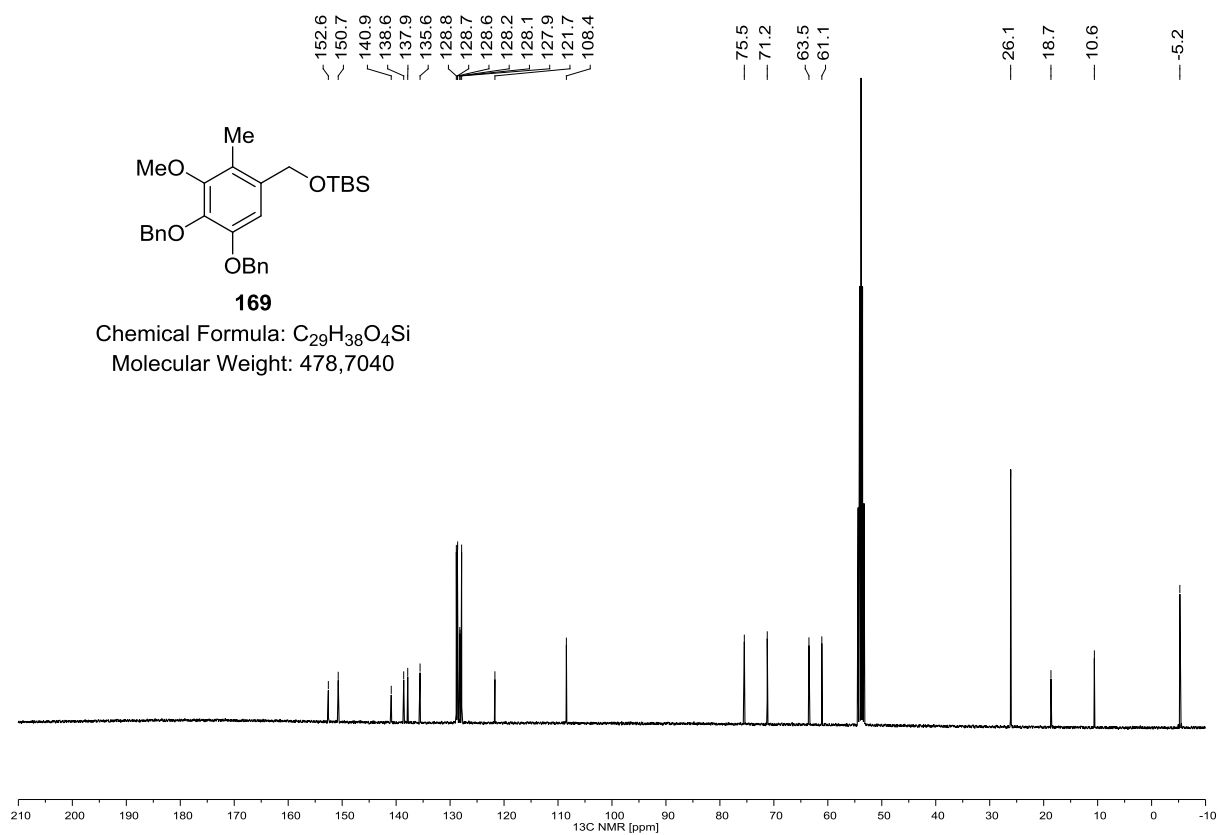
166 (^1H NMR, 300 MHz, CDCl_3)**166 (^{13}C NMR, 75 MHz, CDCl_3)**

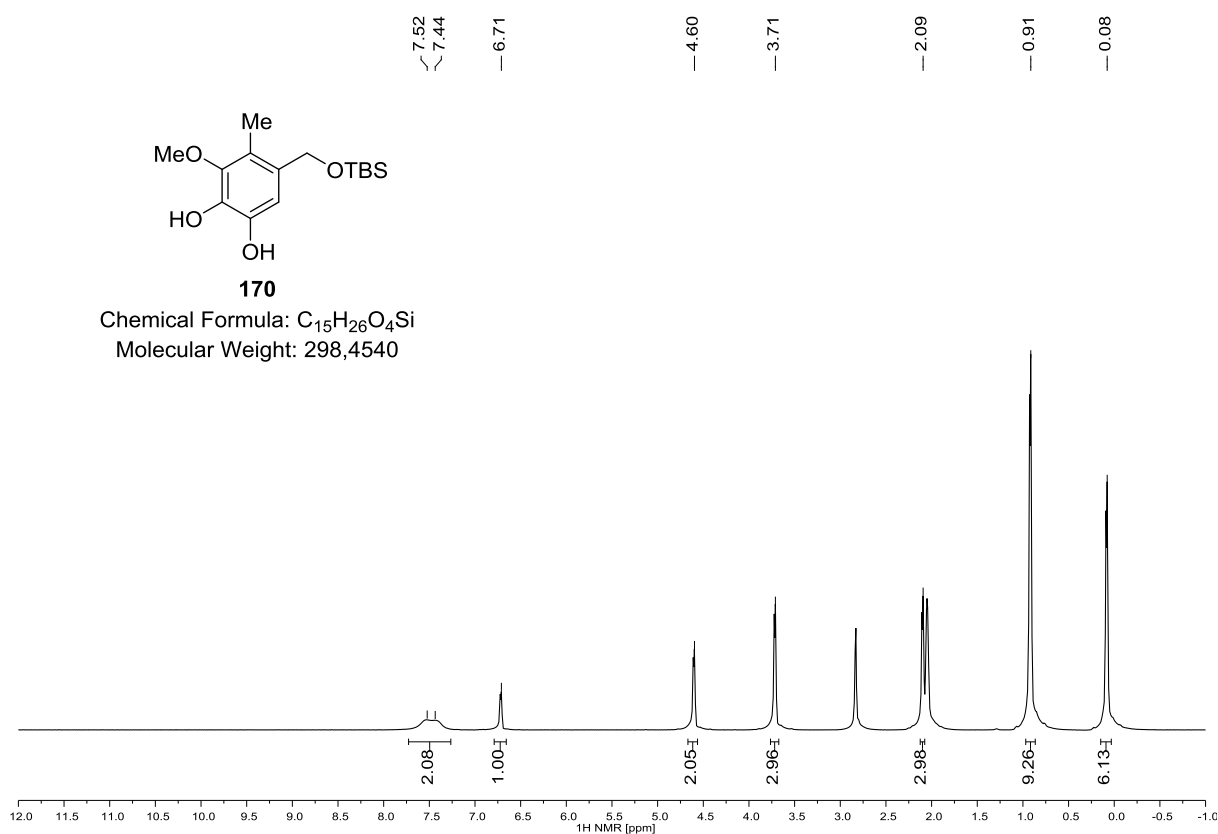
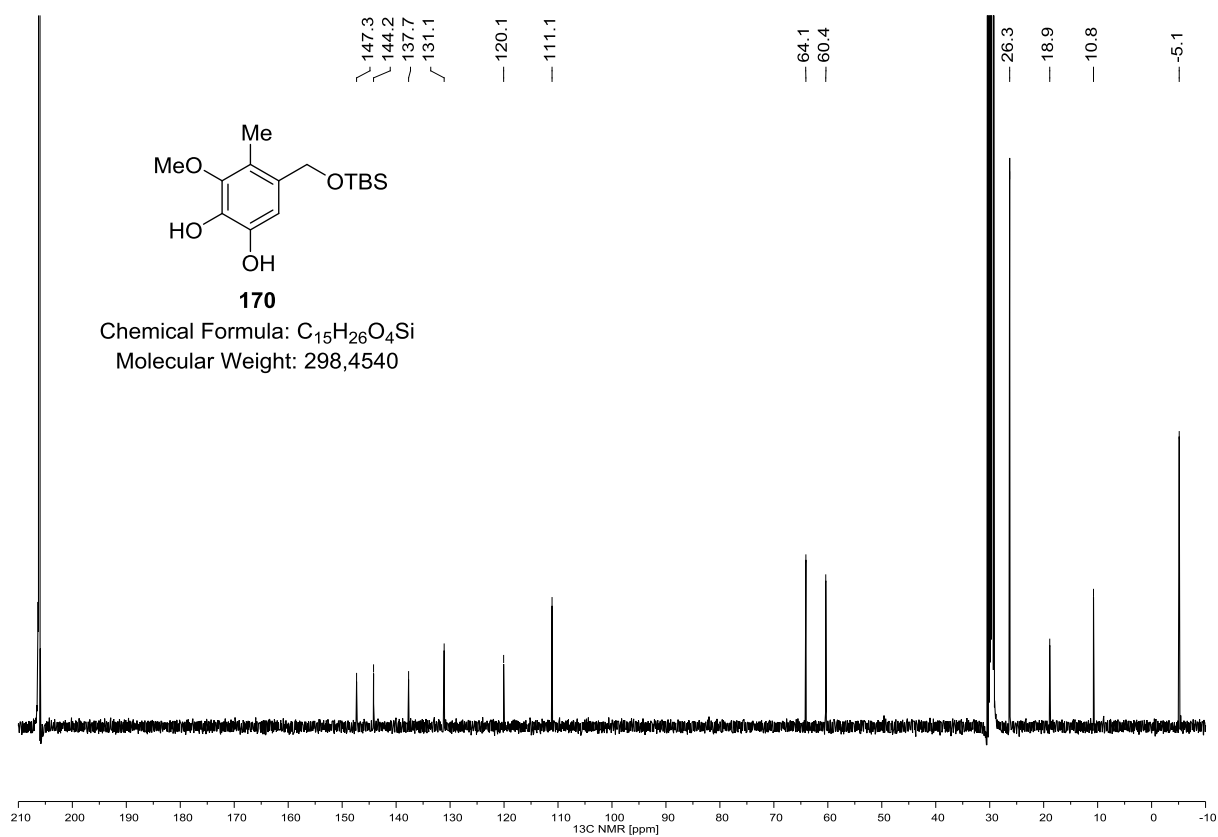
167 (^1H NMR, 600 MHz, CDCl_3)**167 (^{13}C NMR, 150 MHz, CDCl_3)**

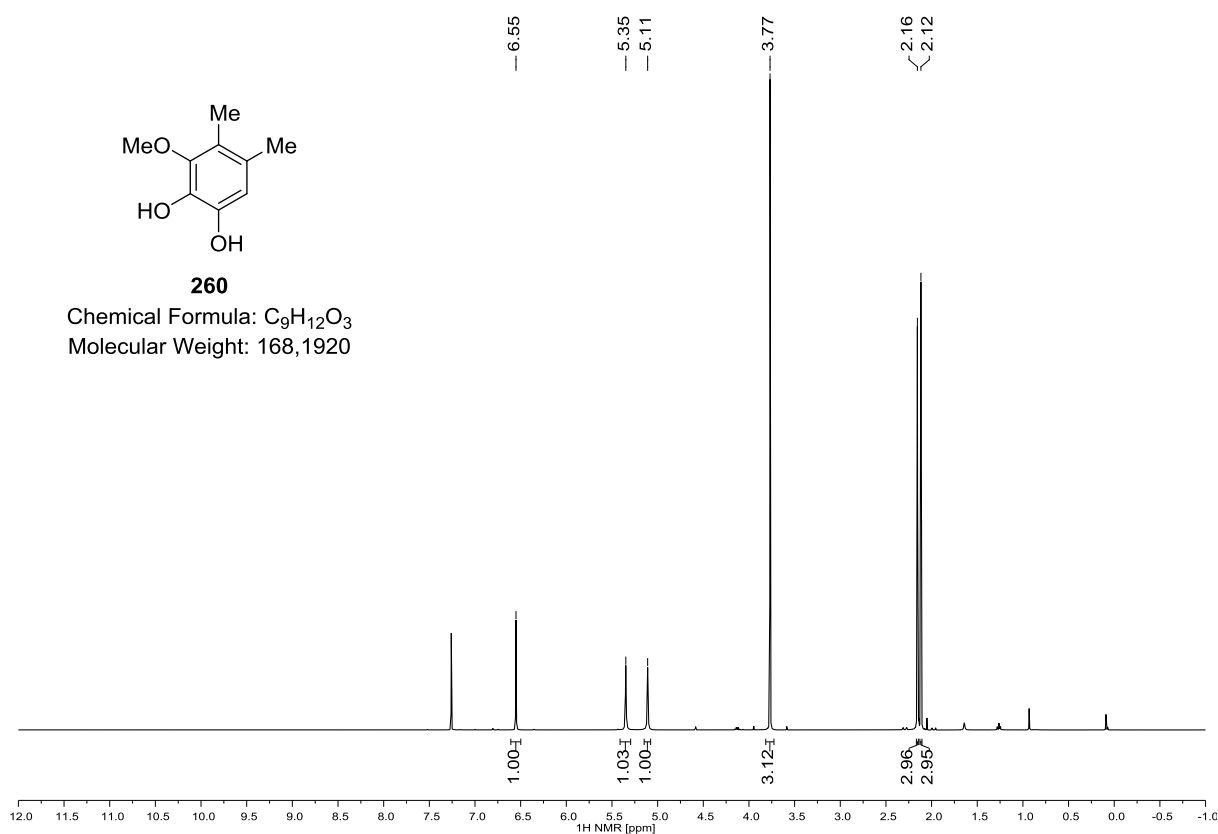
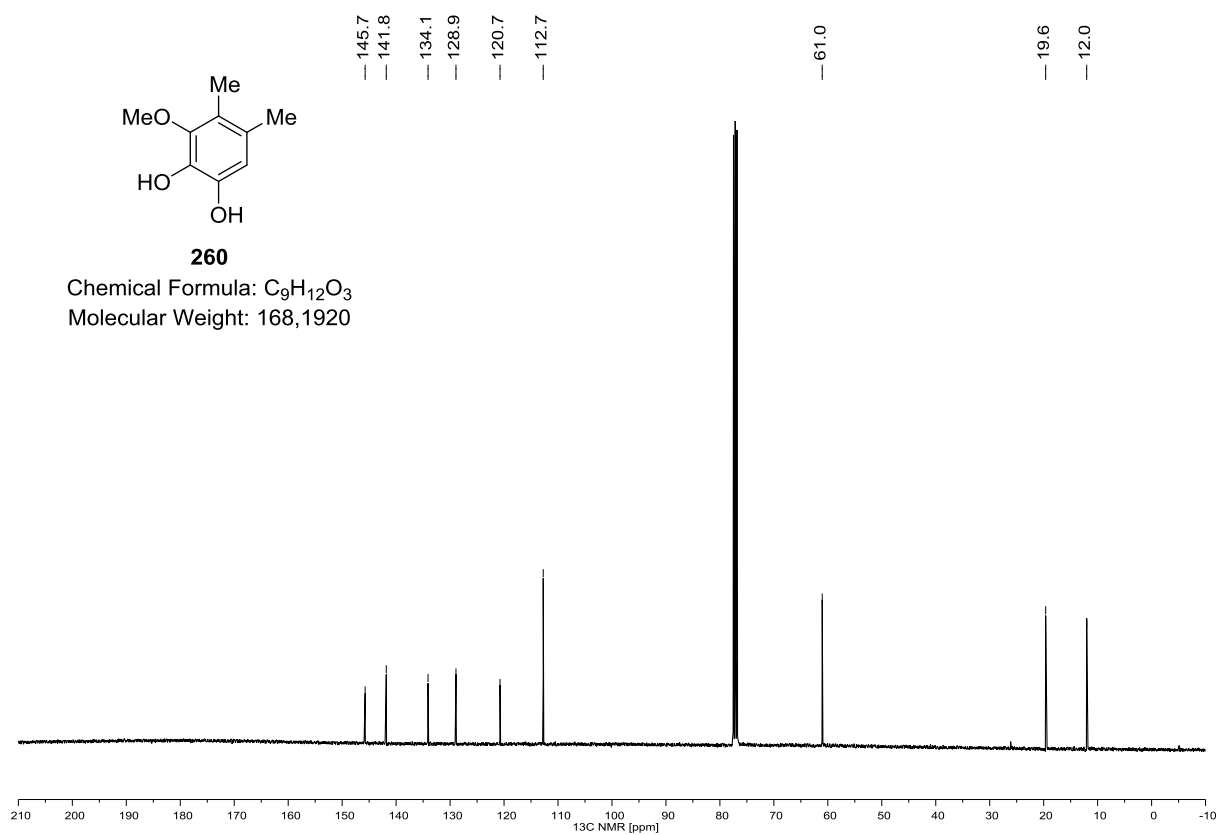
168 (^1H NMR, 400 MHz, D_3COD)**168 (^{13}C NMR, 100 MHz, D_3COD)**

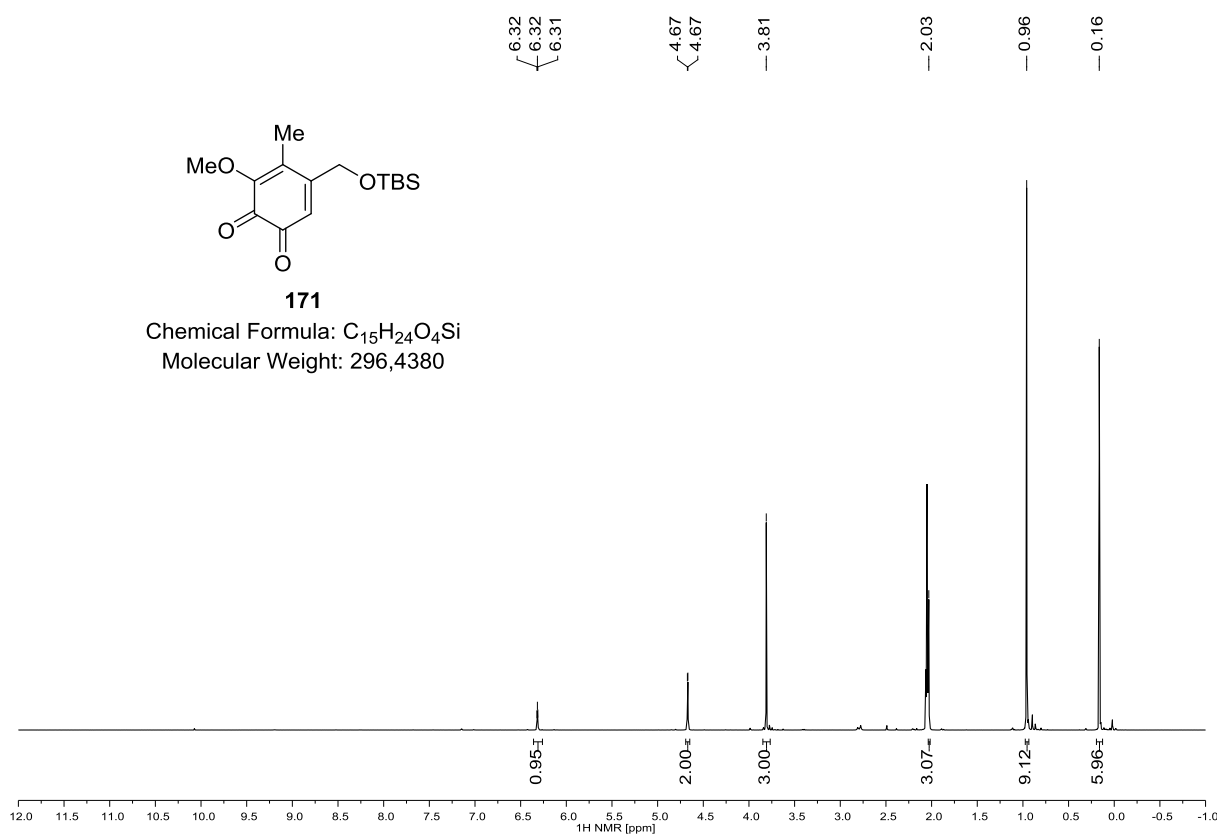
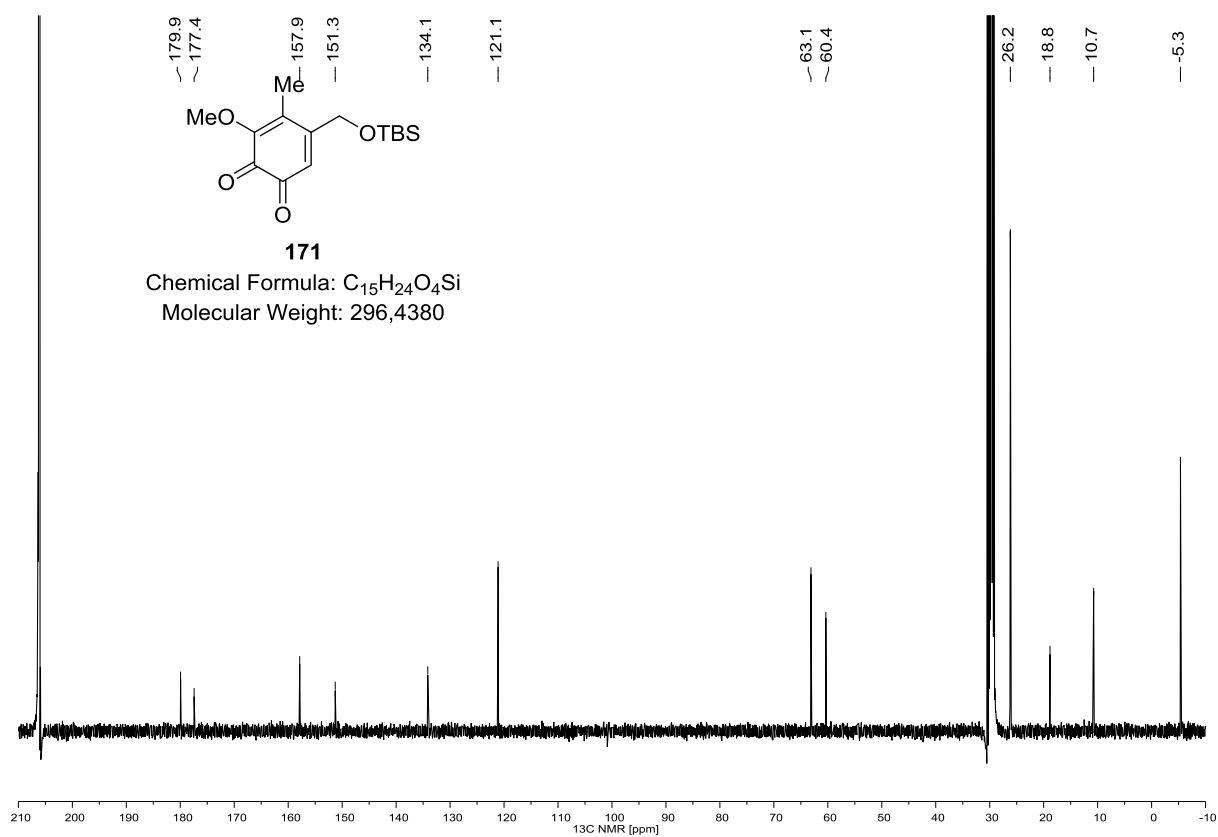
259 (^1H NMR, 300 MHz, CDCl_3)**259 (^{13}C NMR, 75 MHz, CDCl_3)**

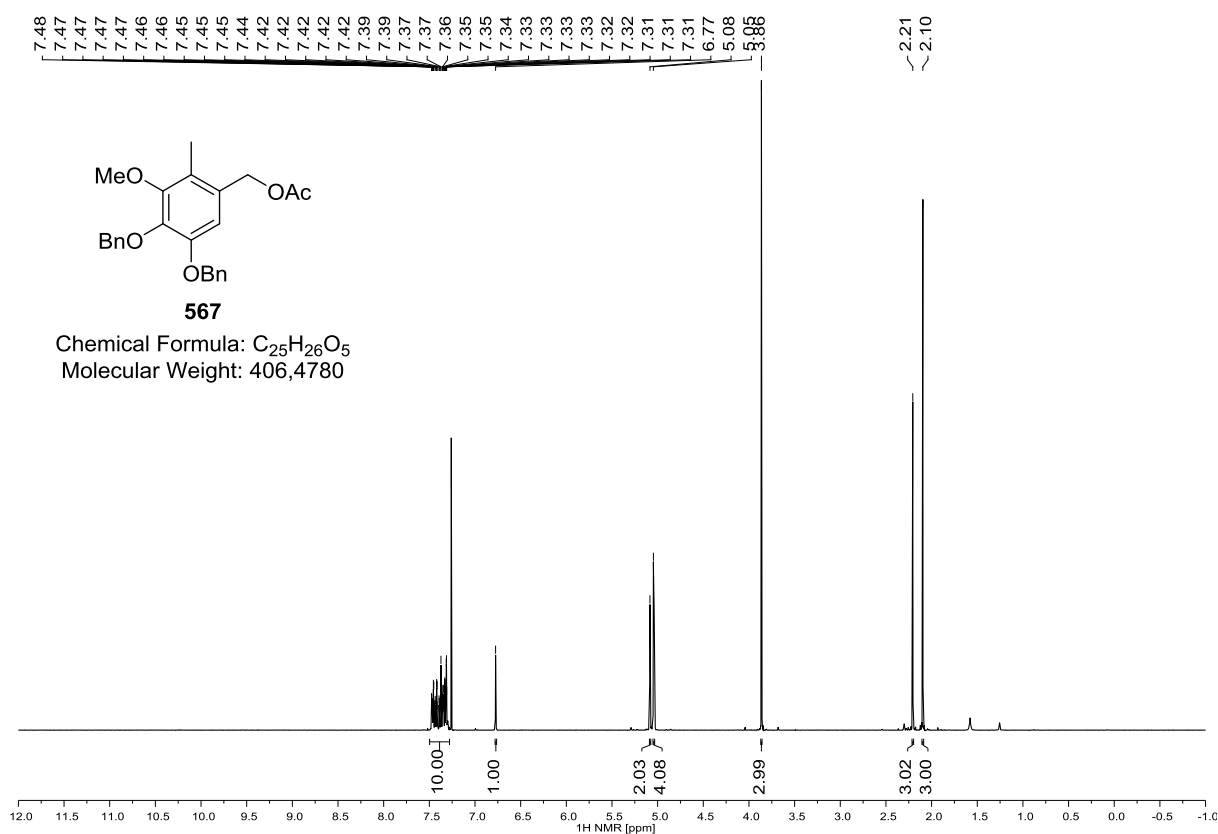
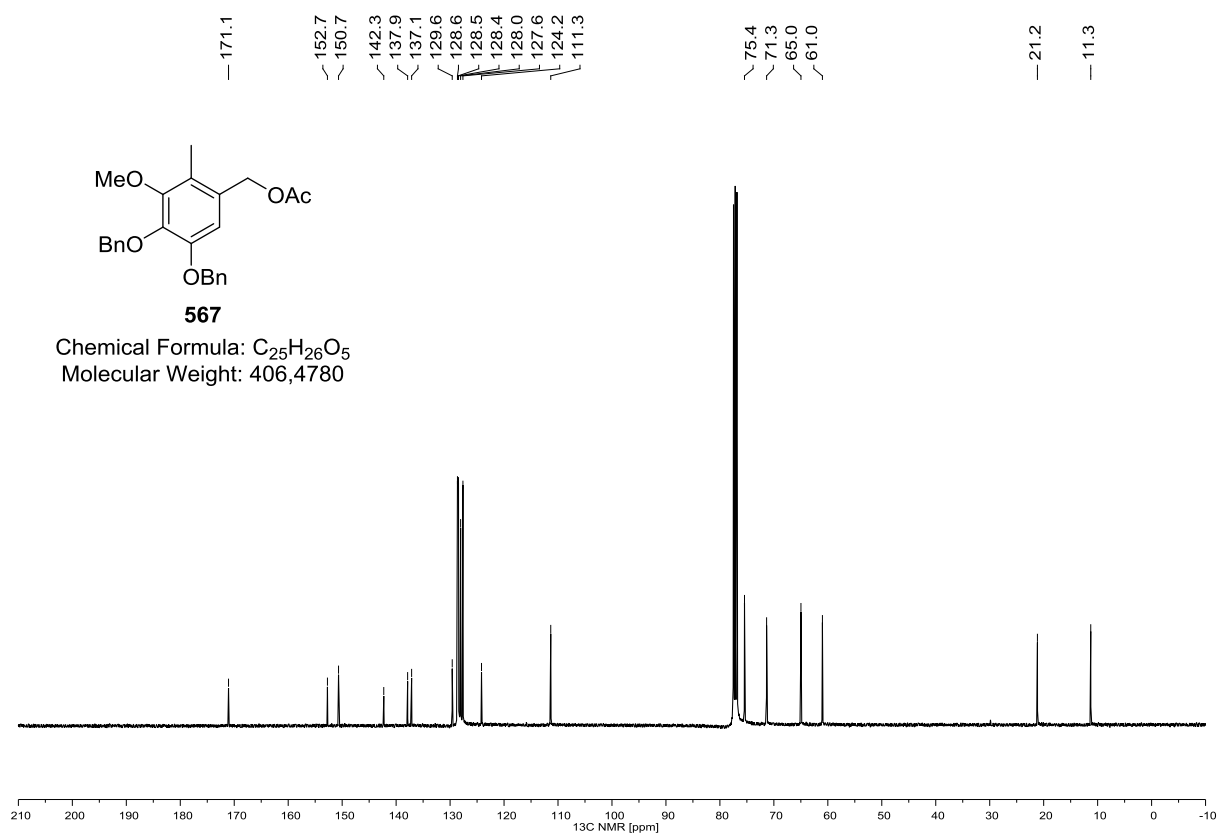
258 (^1H NMR, 600 MHz, CDCl_3)**258 (^{13}C NMR, 150 MHz, CDCl_3)**

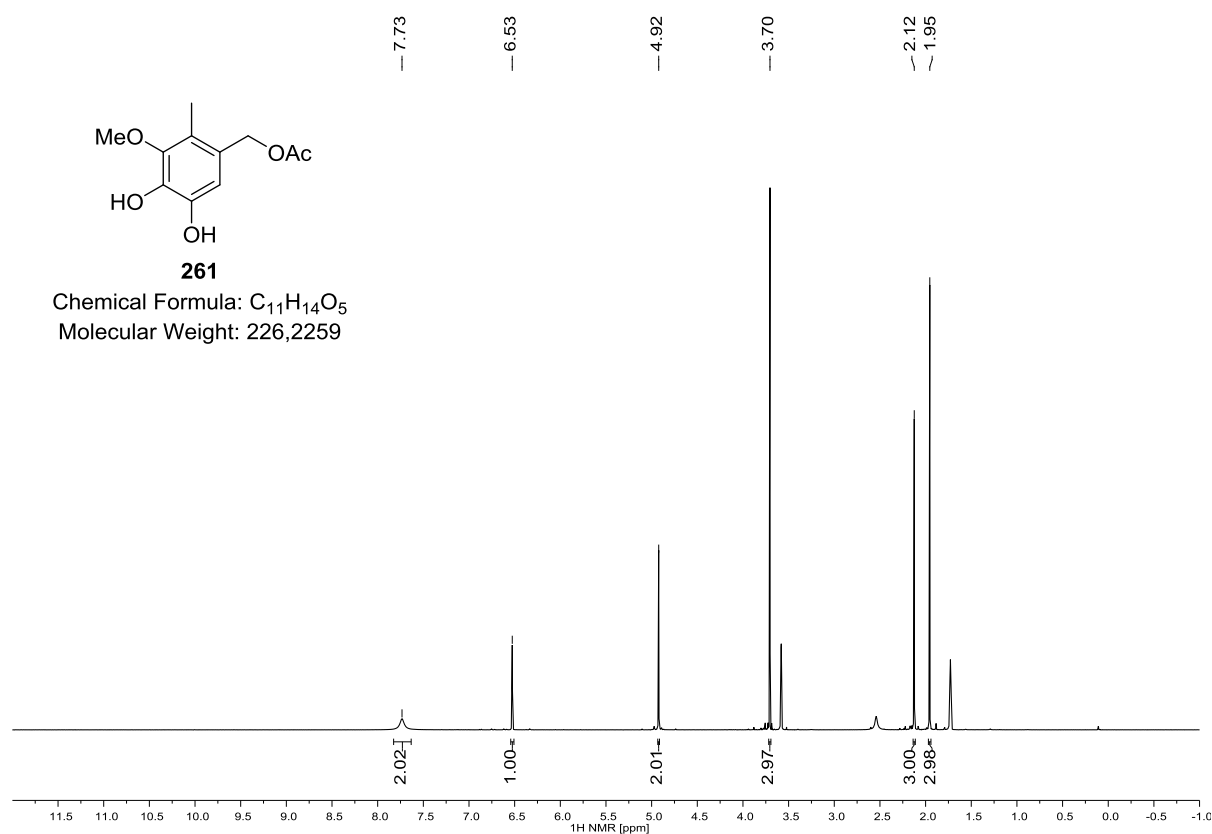
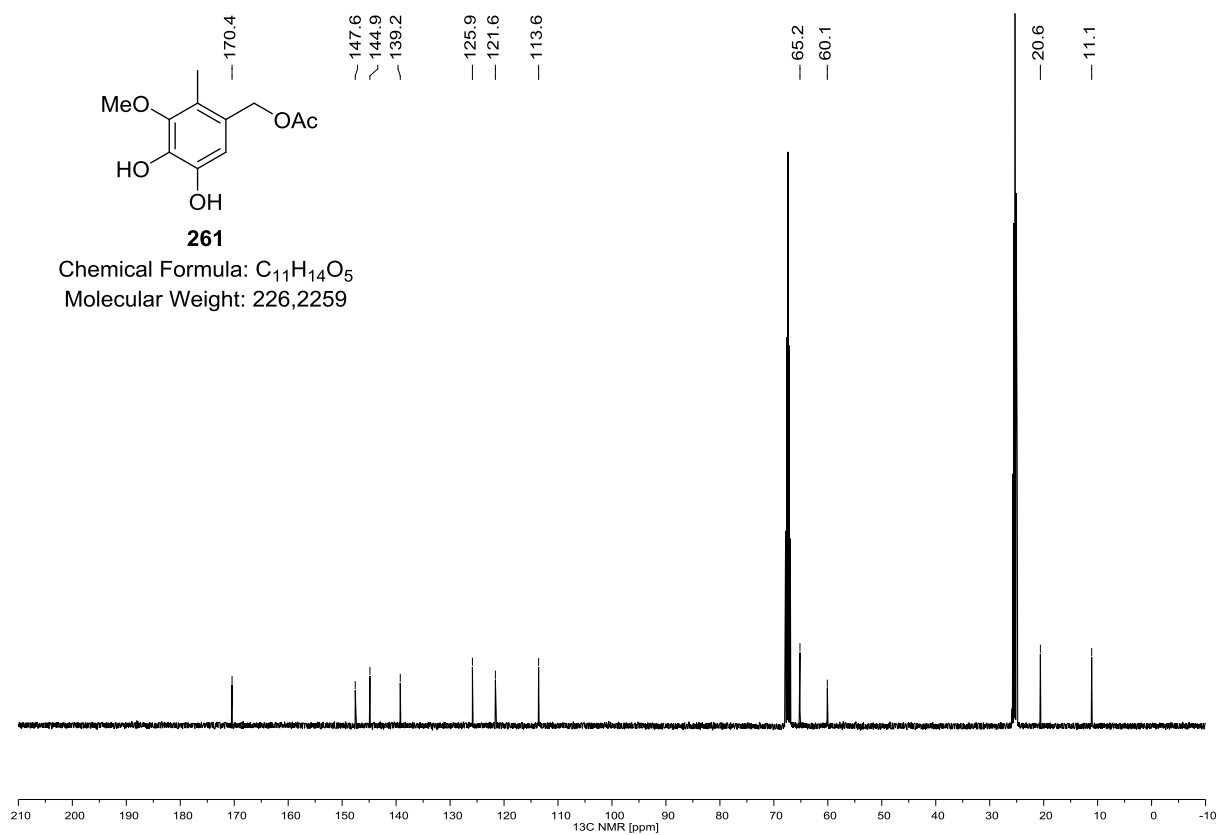
169 (¹H NMR, 400 MHz, CD₂Cl₂)**169 (¹³C NMR, 100 MHz, CD₂Cl₂)**

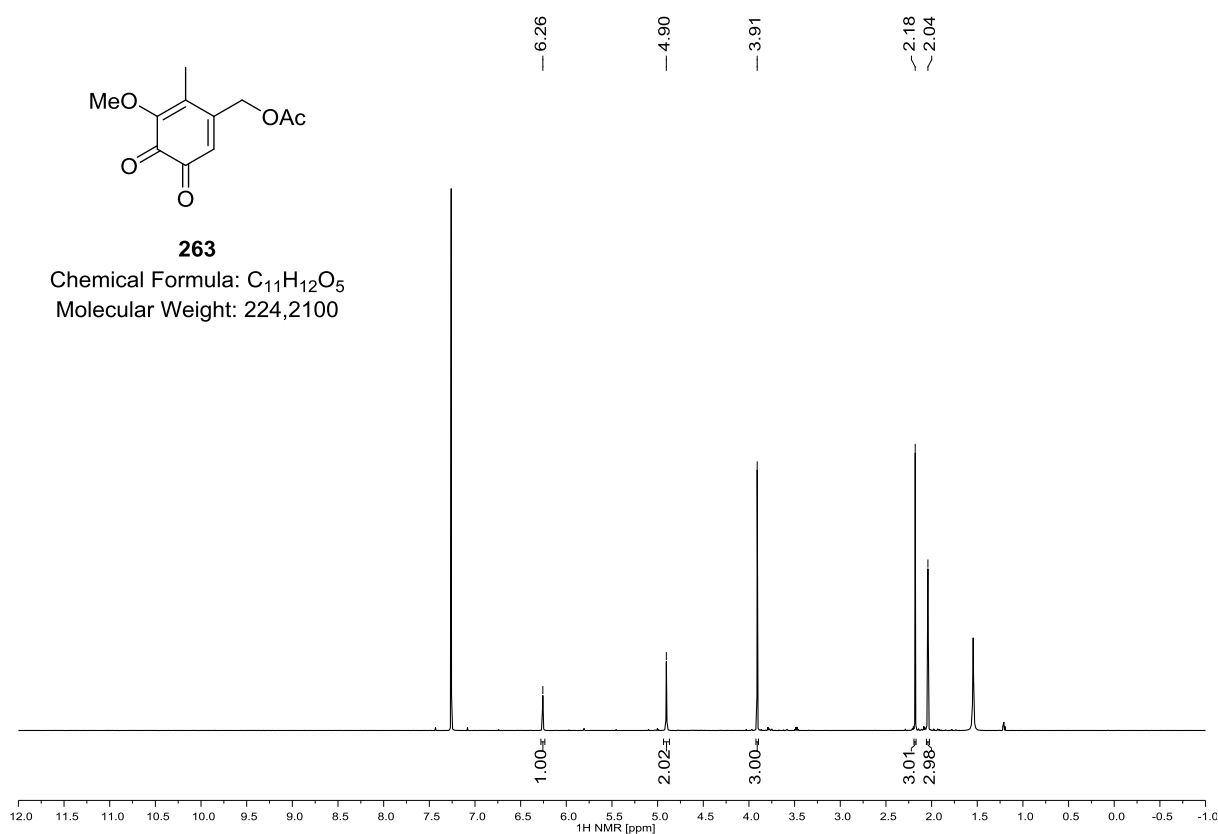
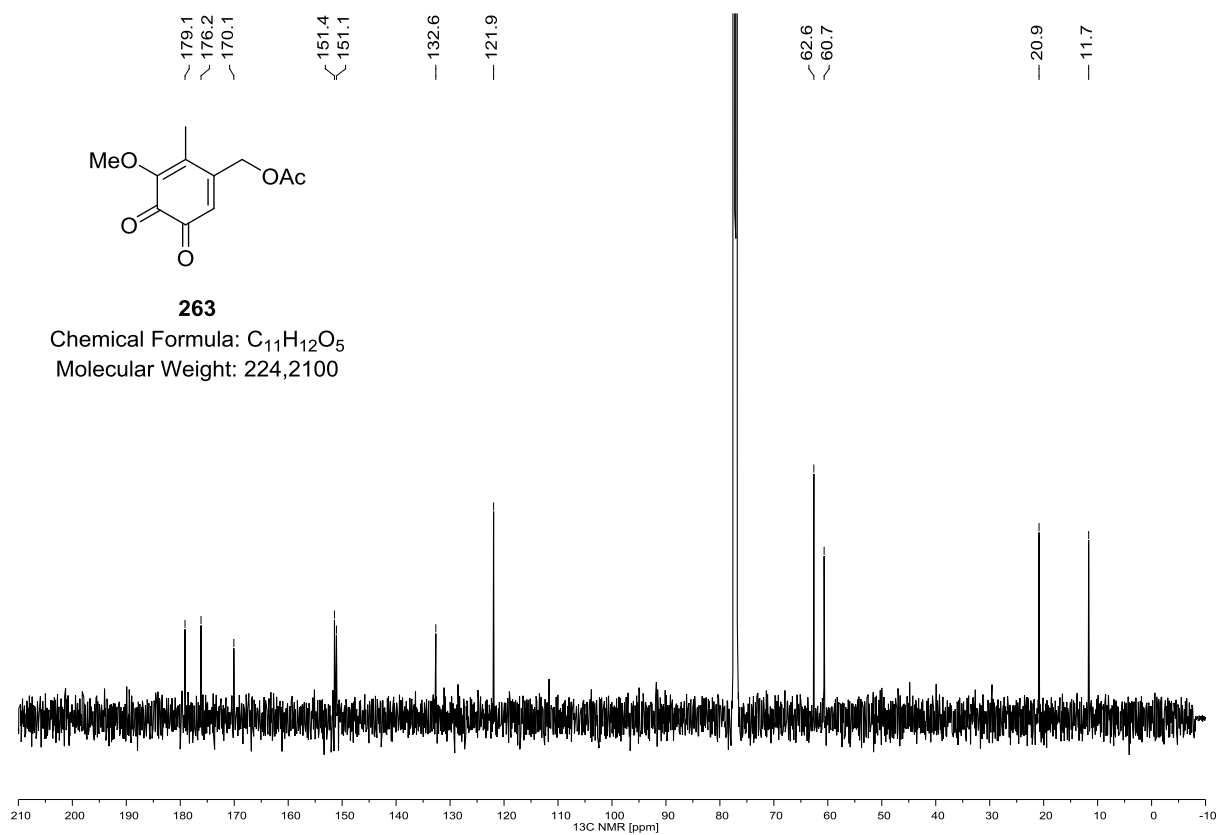
170 (^1H NMR, 400 MHz, $(\text{D}_3\text{C})_2\text{CO}$)**170 (^{13}C NMR, 100 MHz, $(\text{D}_3\text{C})_2\text{CO}$)**

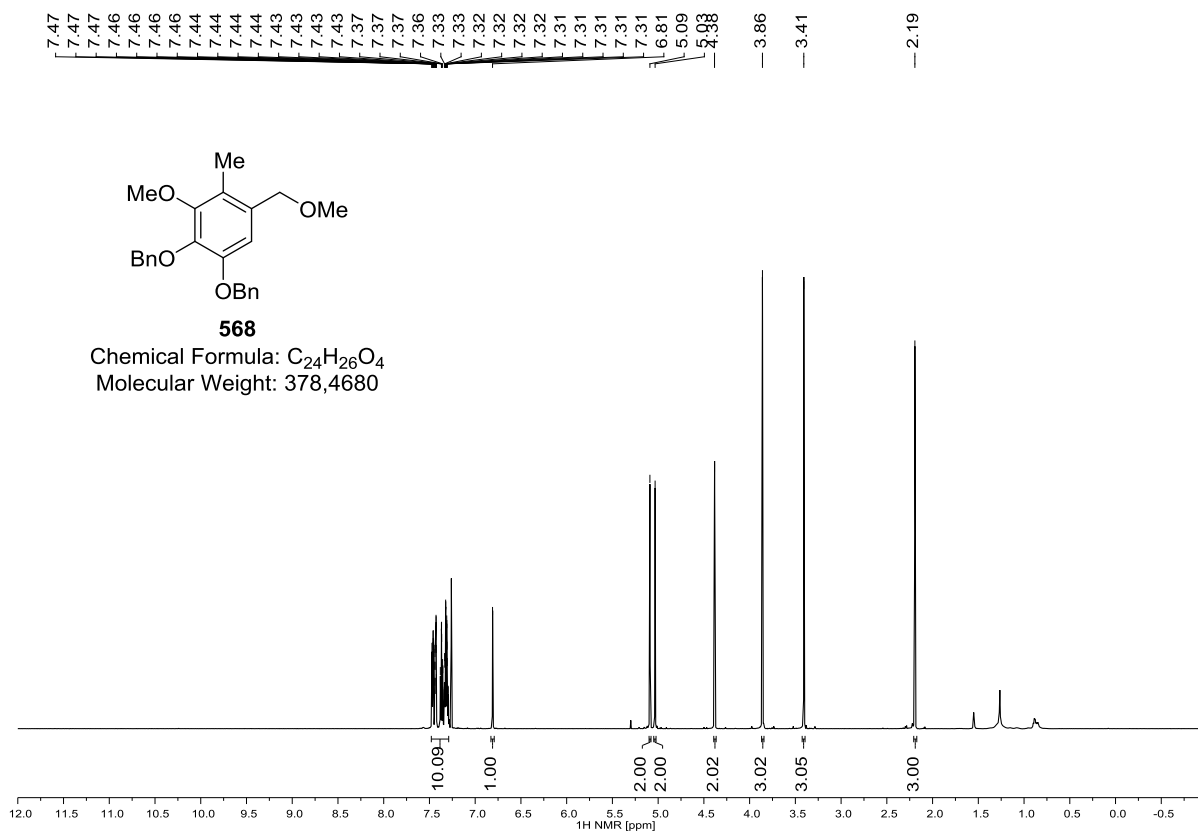
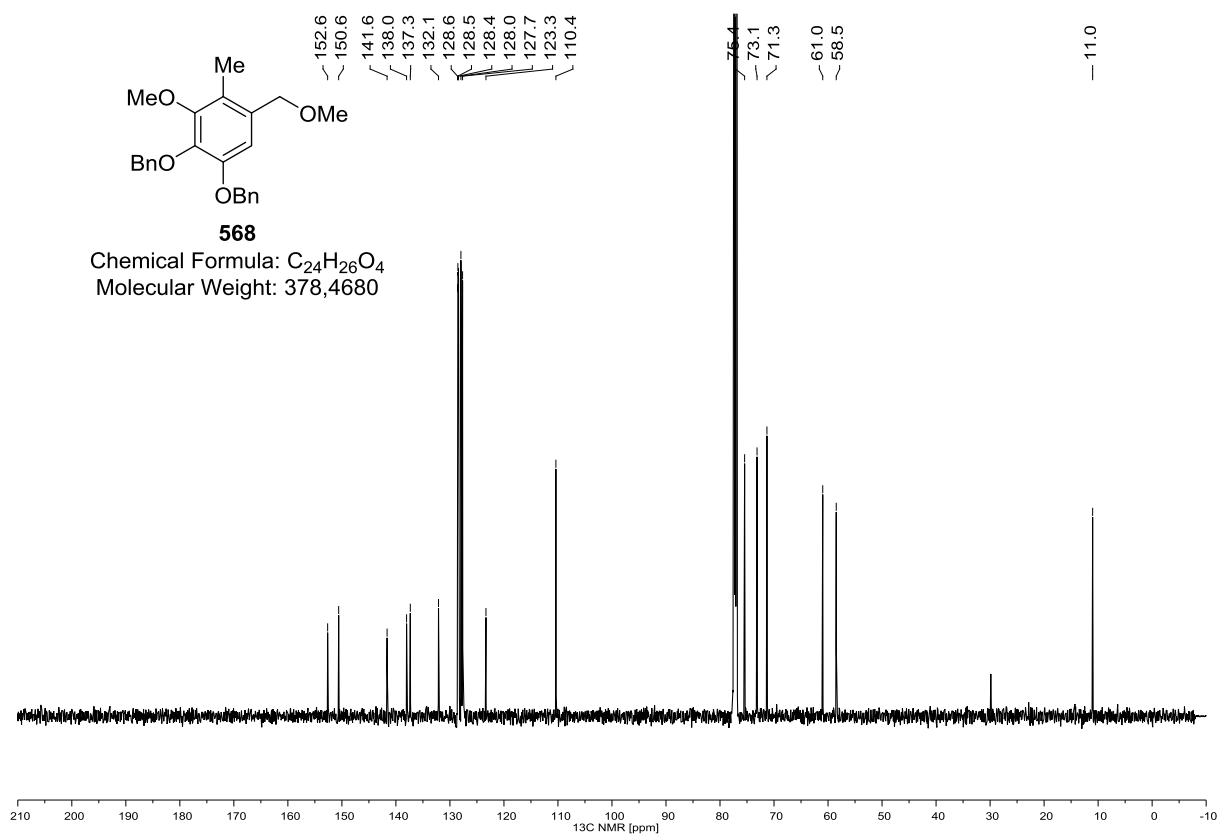
260 (^1H NMR, 400 MHz, CDCl_3)**260 (^{13}C NMR, 100 MHz, CDCl_3)**

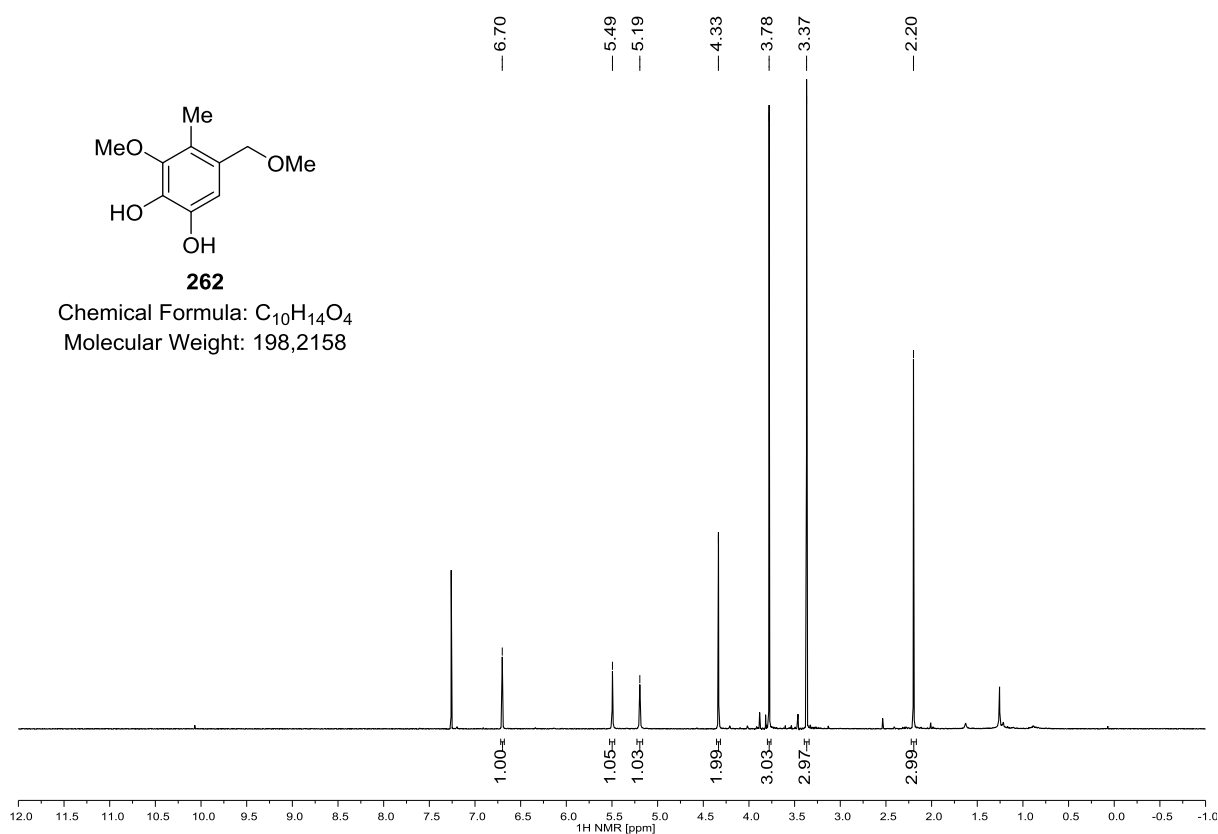
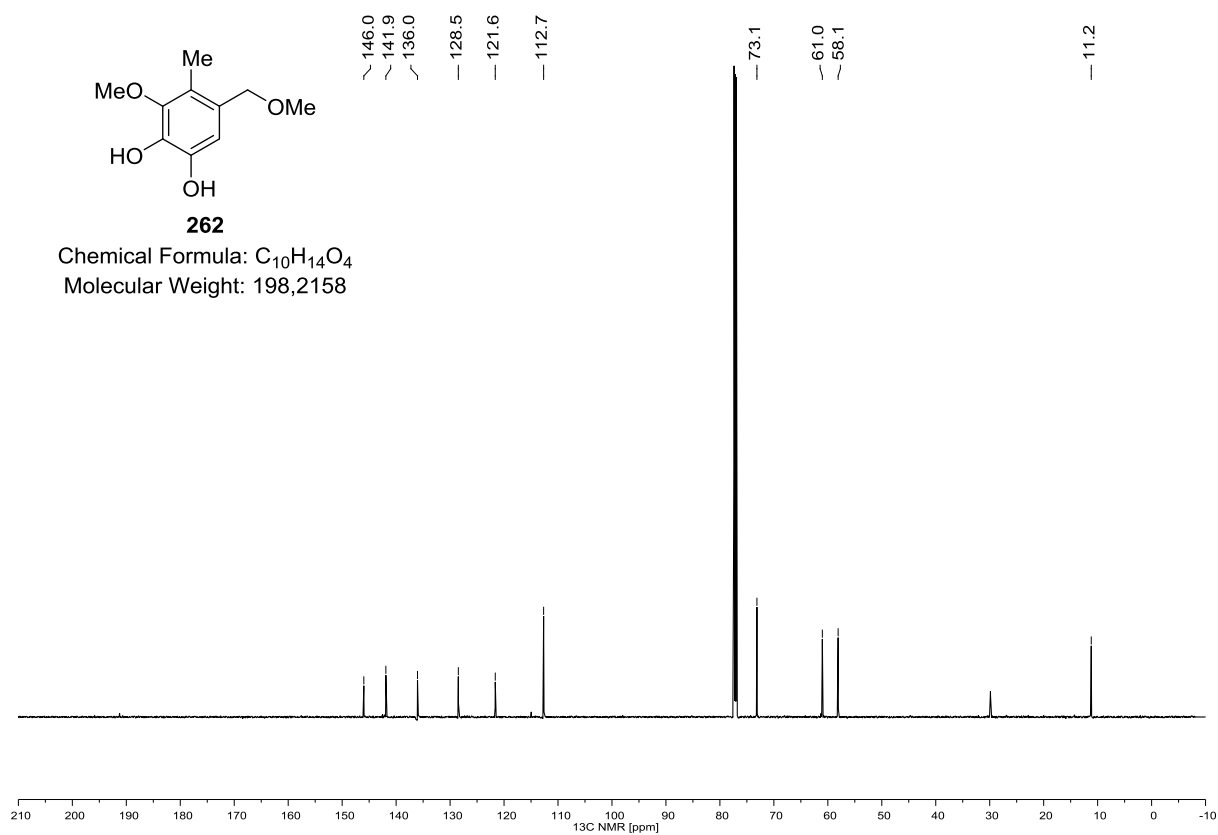
171 (^1H NMR, 400 MHz, $(\text{D}_3\text{C})_2\text{CO}$)**171 (^{13}C NMR, 100 MHz, $(\text{D}_3\text{C})_2\text{CO}$)**

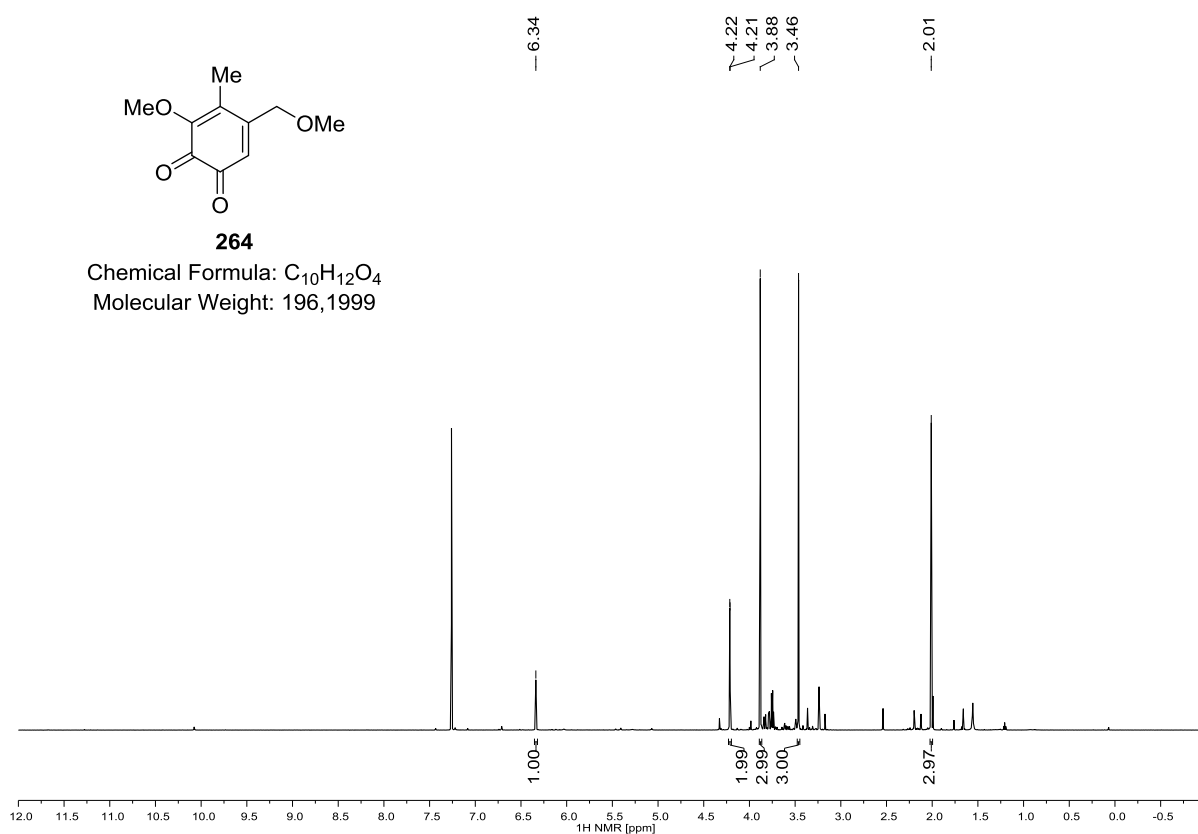
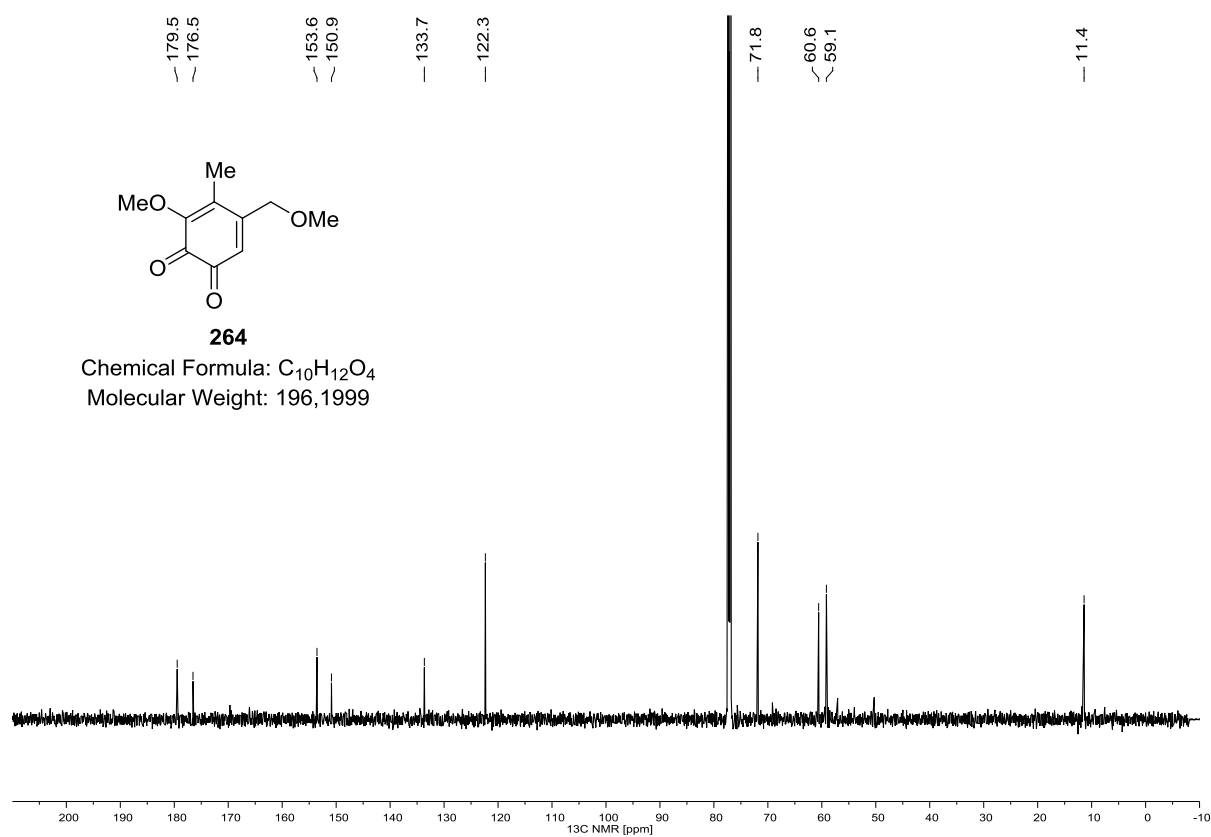
567 (^1H NMR, 400 MHz, CDCl_3)**567 (^{13}C NMR, 100 MHz, CDCl_3)**

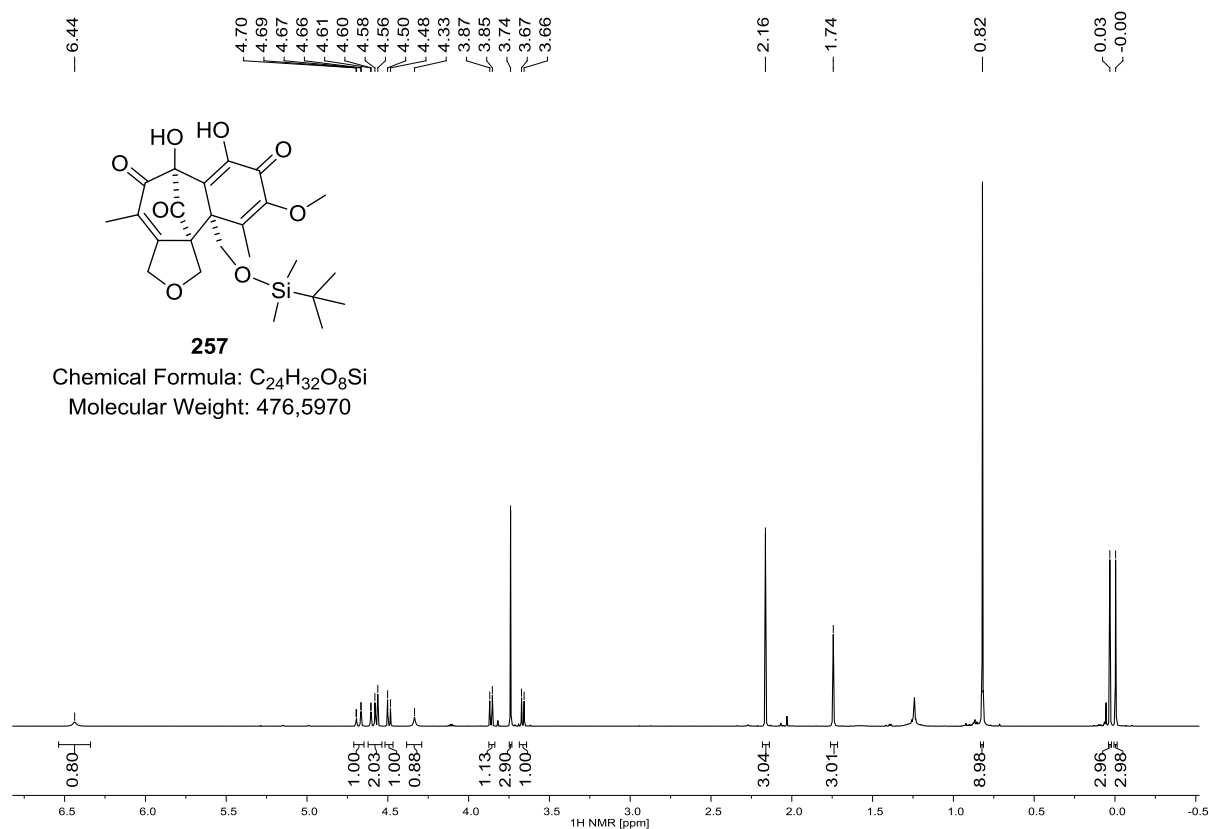
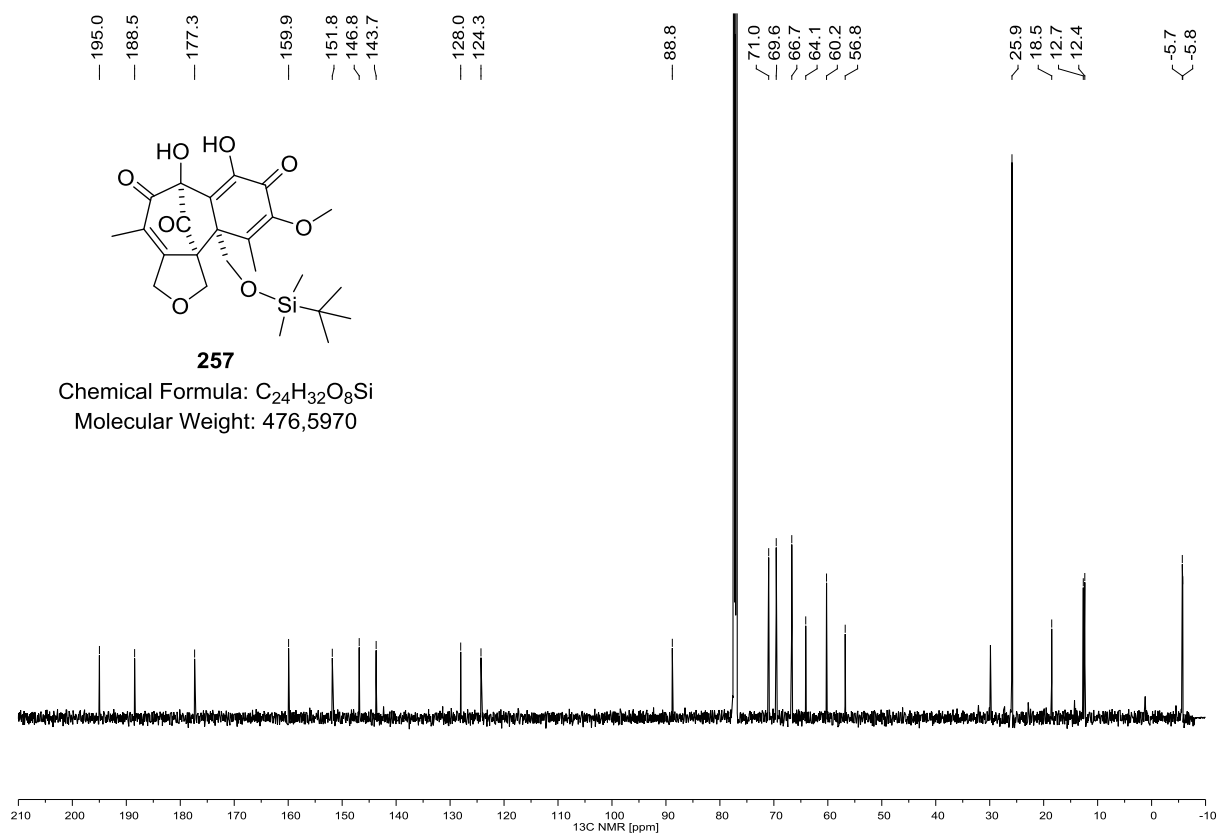
261 (^1H NMR, 400 MHz, THF-d^8)**261 (^{13}C NMR, 100 MHz, THF-d^8)**

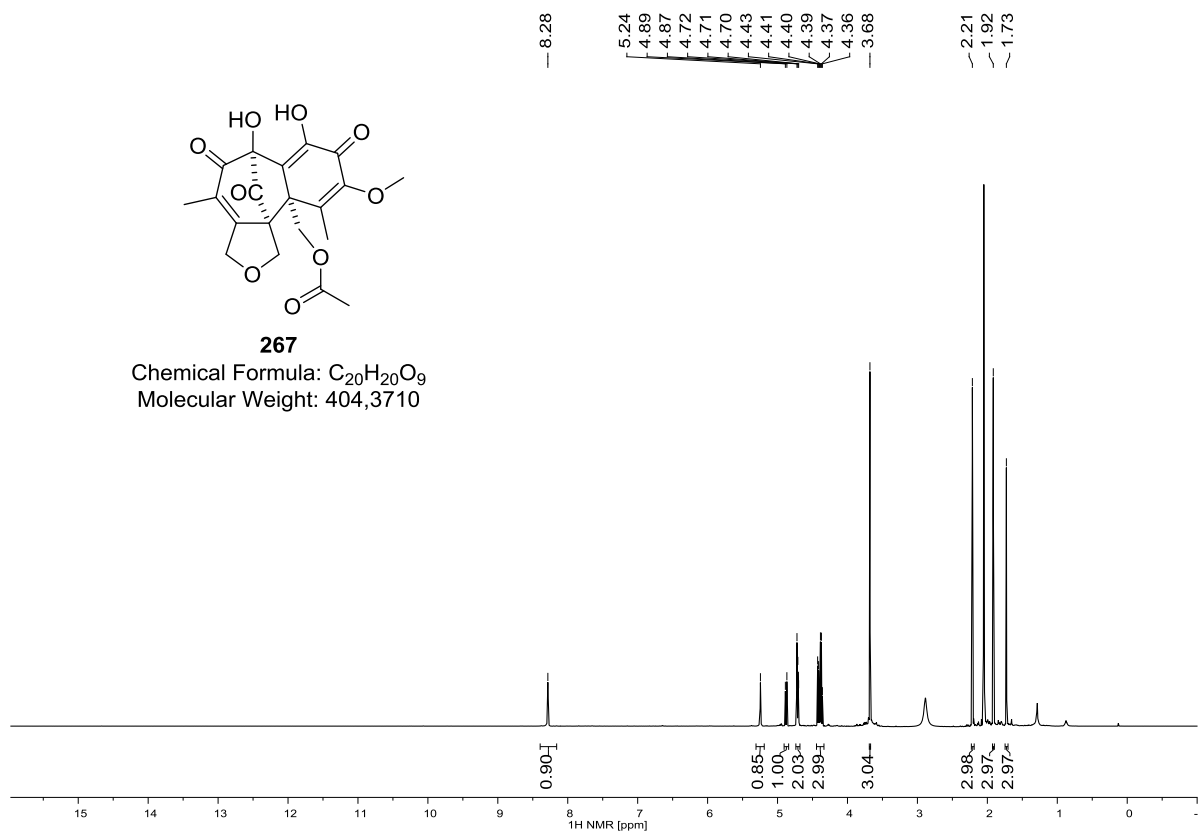
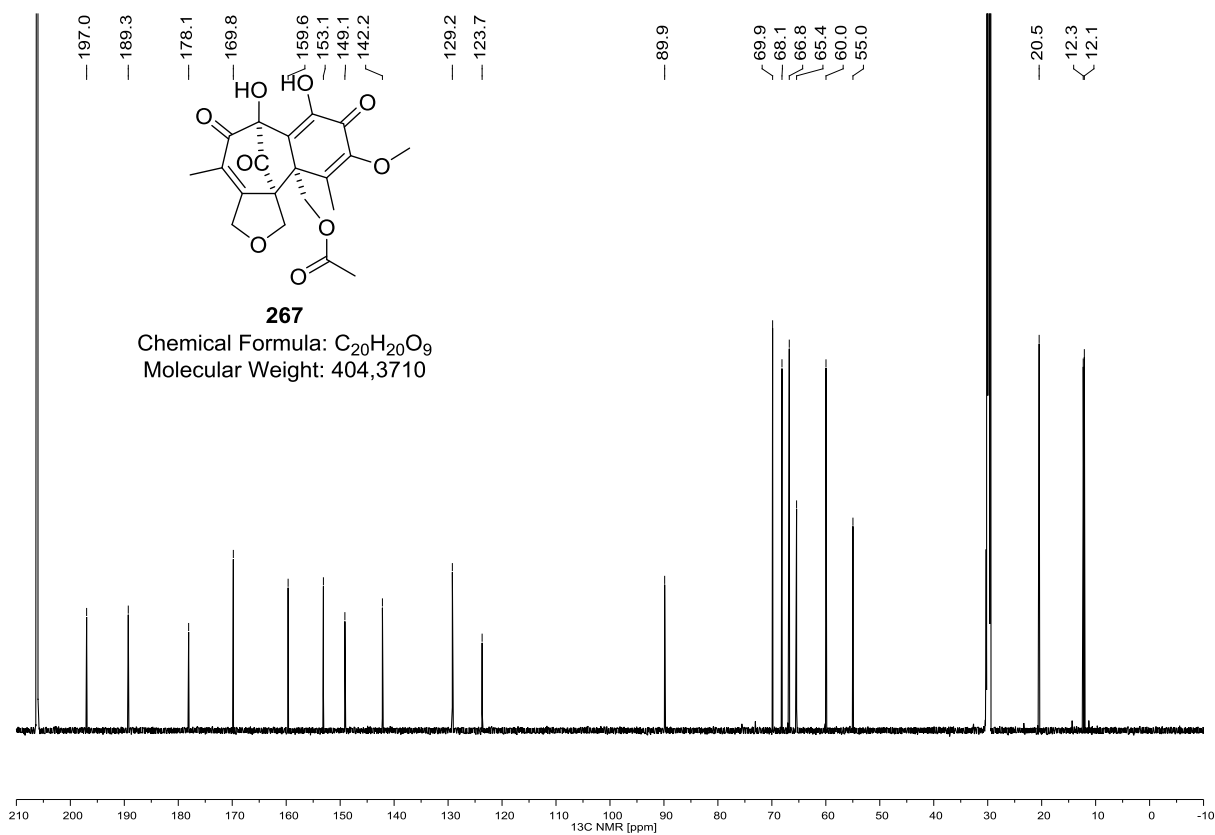
263 (^1H NMR, 600 MHz, CDCl_3)**263 (^{13}C NMR, 150 MHz, CDCl_3)**

568 (^1H NMR, 600 MHz, CDCl_3)**568 (^{13}C NMR, 150 MHz, CDCl_3)**

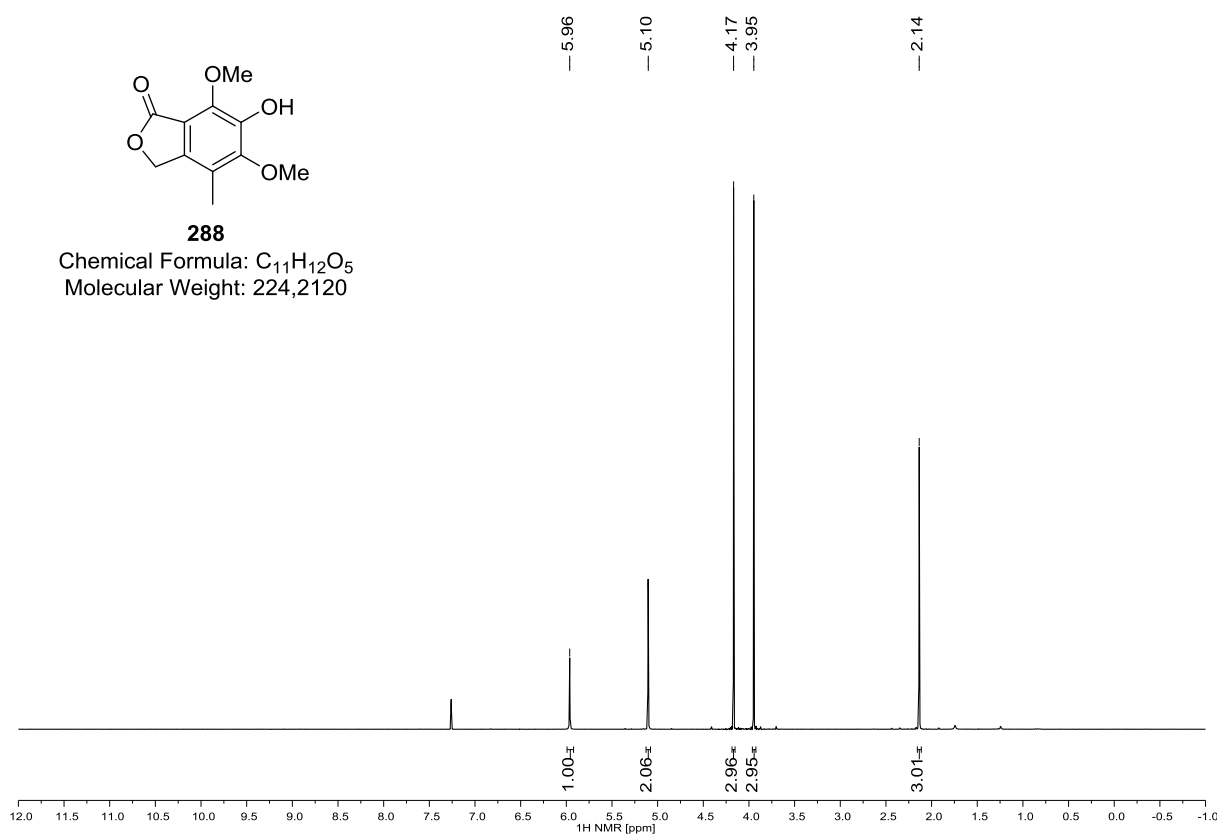
262 (^1H NMR, 300 MHz, CDCl_3)**262 (^{13}C NMR, 75 MHz, CDCl_3)**

264 (^1H NMR, 600 MHz, CDCl_3)**264 (^{13}C NMR, 150 MHz, CDCl_3)**

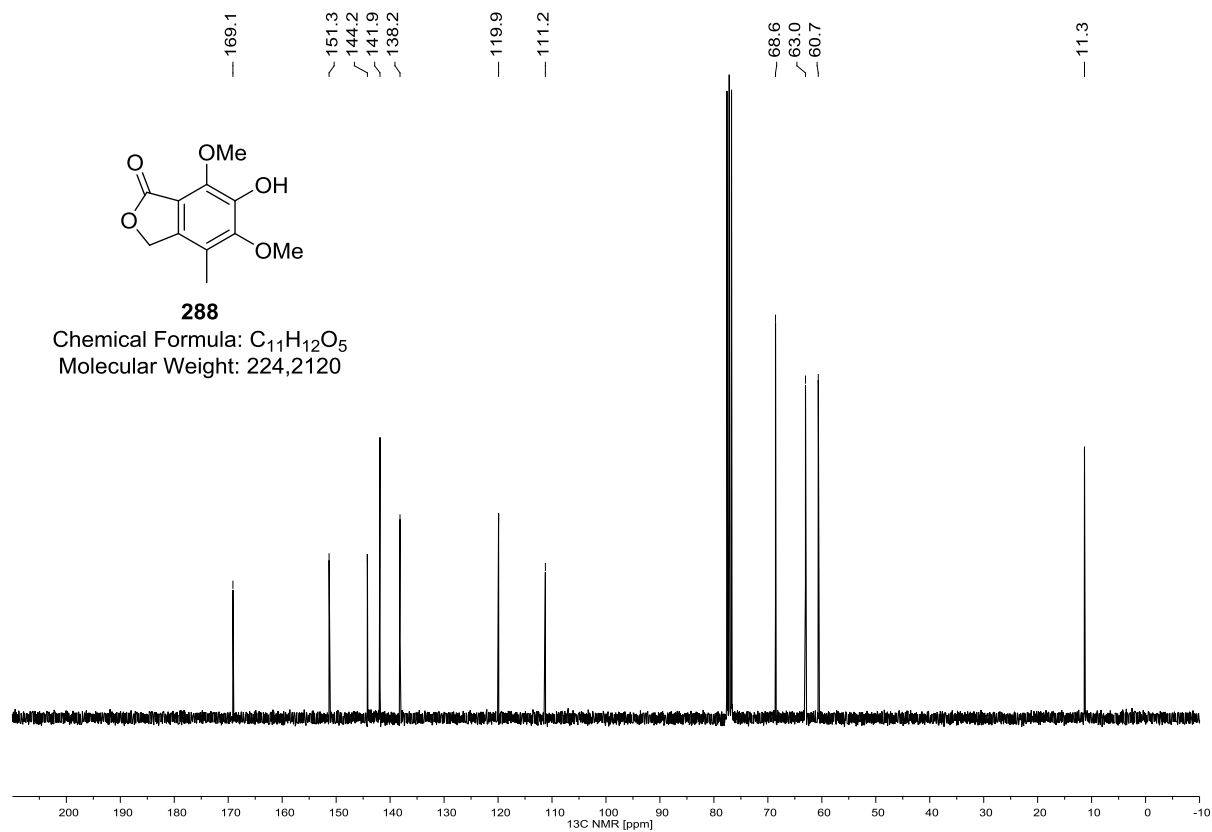
257 (¹H NMR, 600 MHz, CDCl₃)**257 (¹³C NMR, 150 MHz, CDCl₃)**

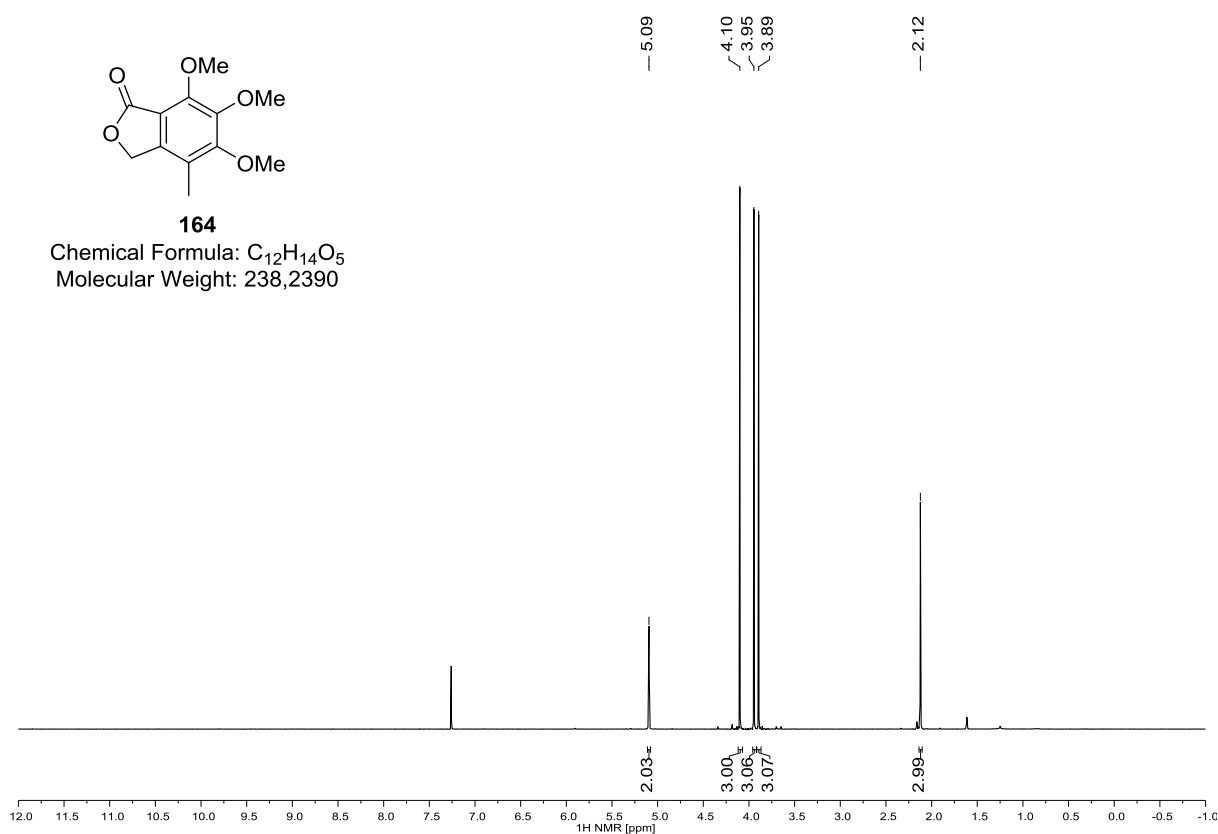
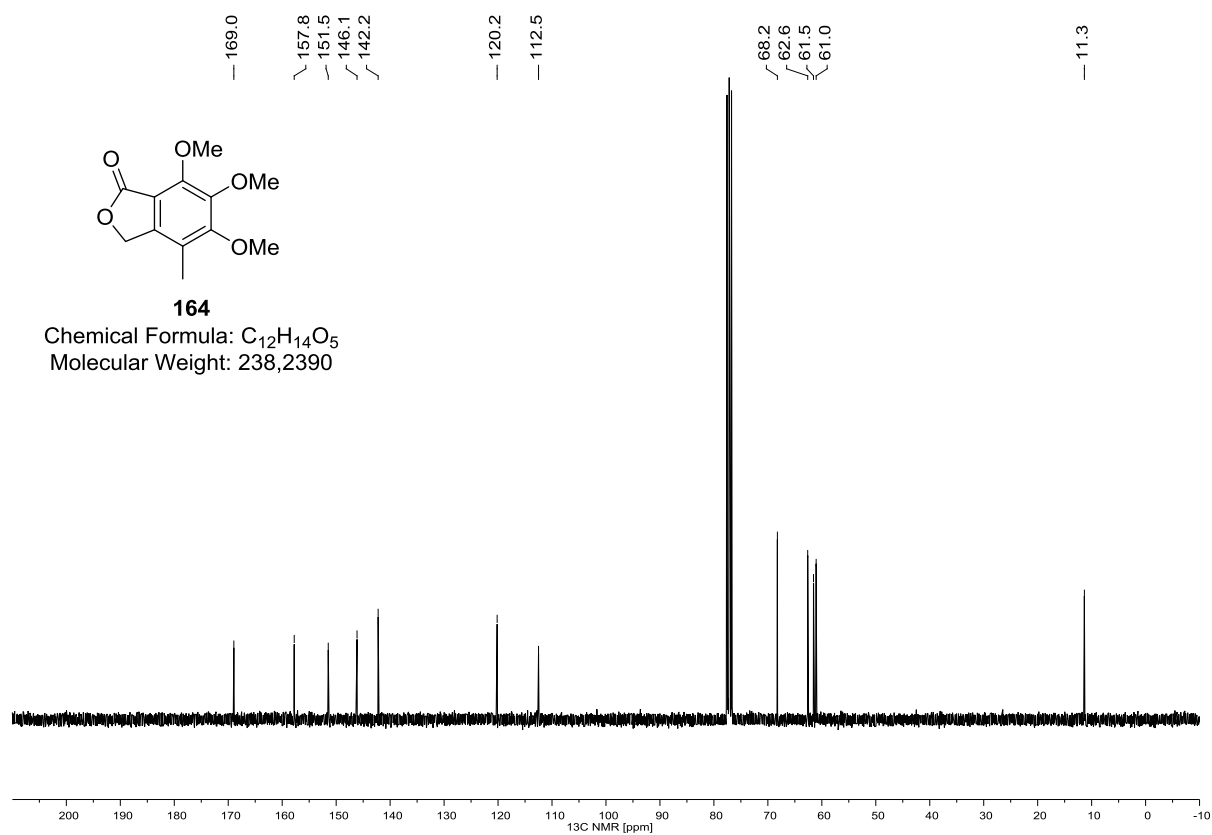
267 (^1H NMR, 800 MHz, $(\text{D}_3\text{C})_2\text{CO}$)**267 (^1H NMR, 200 MHz, $(\text{D}_3\text{C})_2\text{CO}$)**

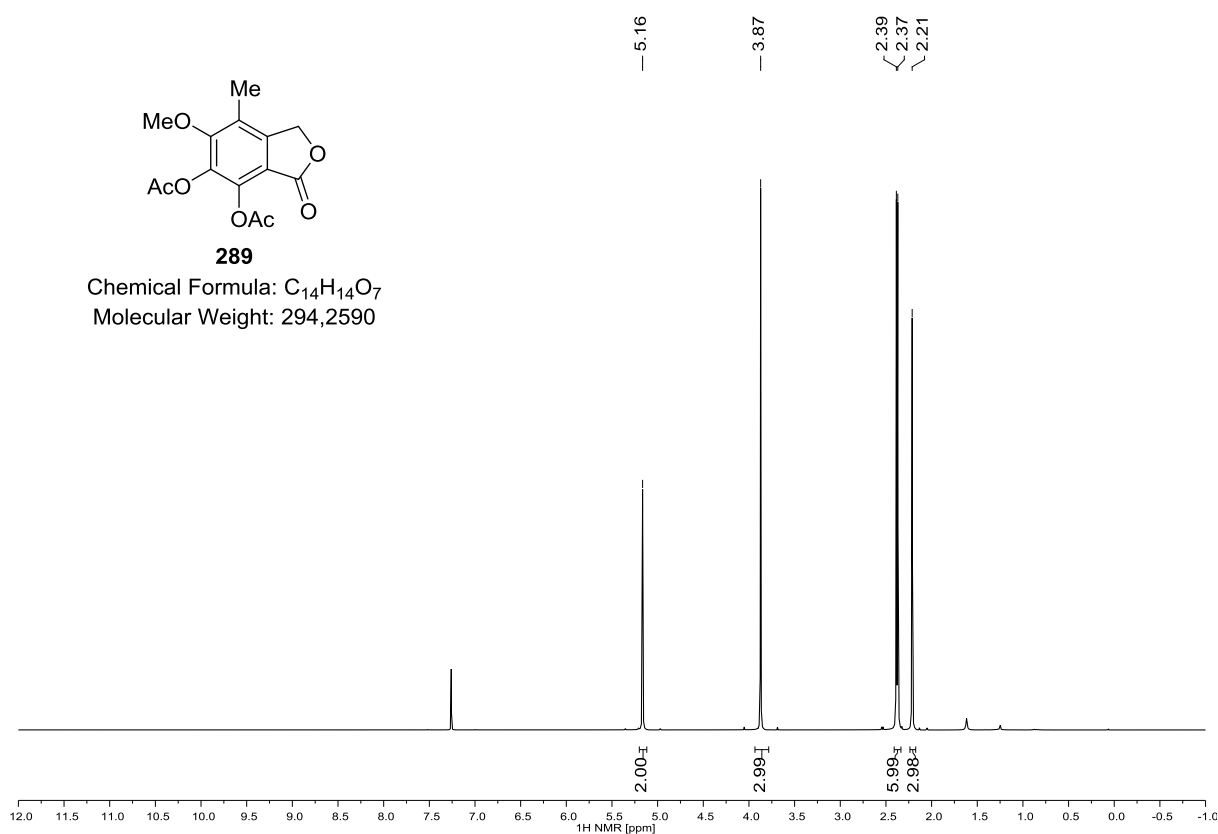
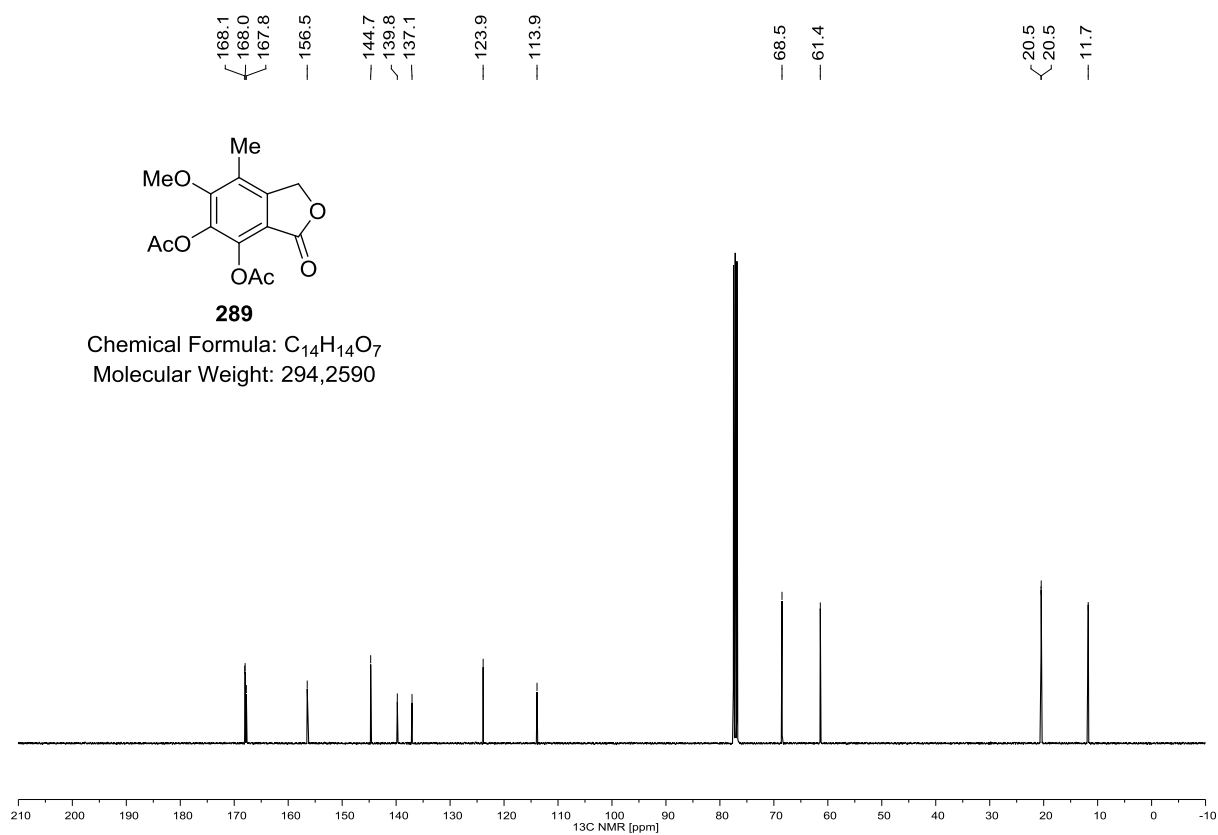
288
Chemical Formula: C₁₁H₁₂O₅
Molecular Weight: 224,2120

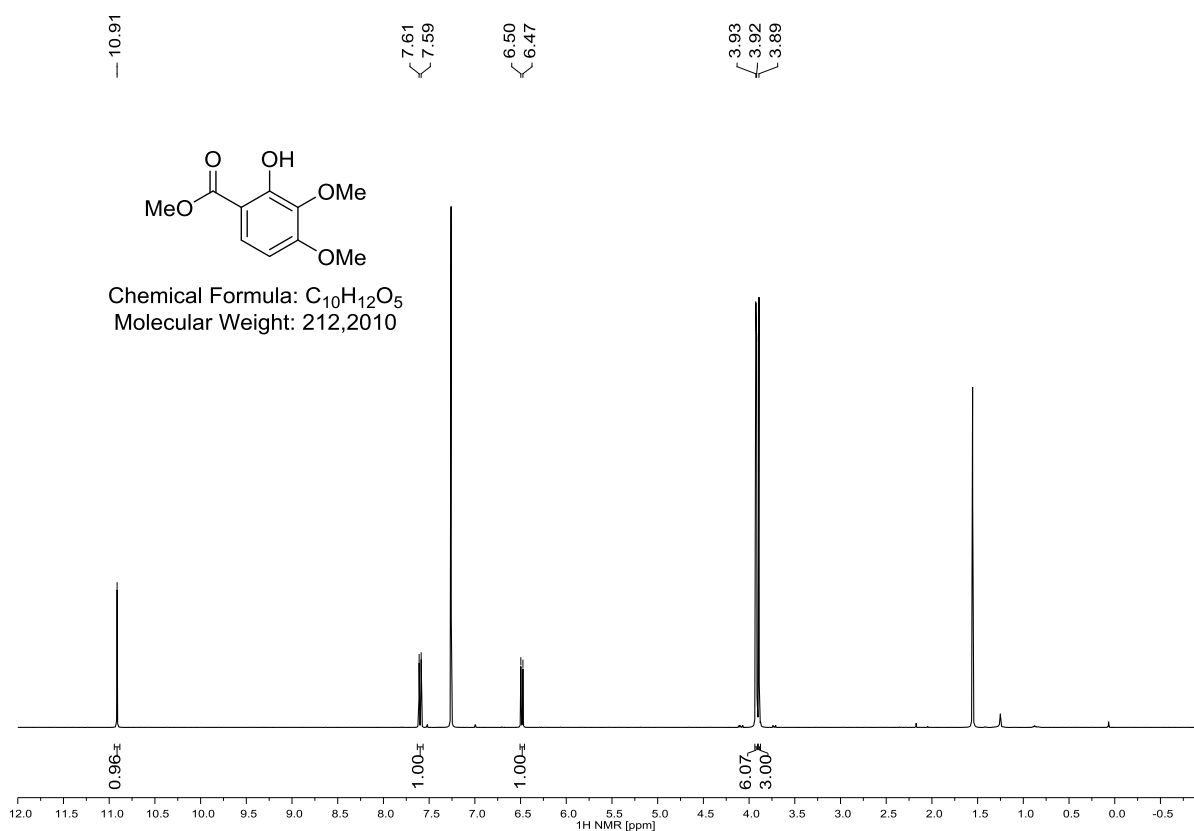
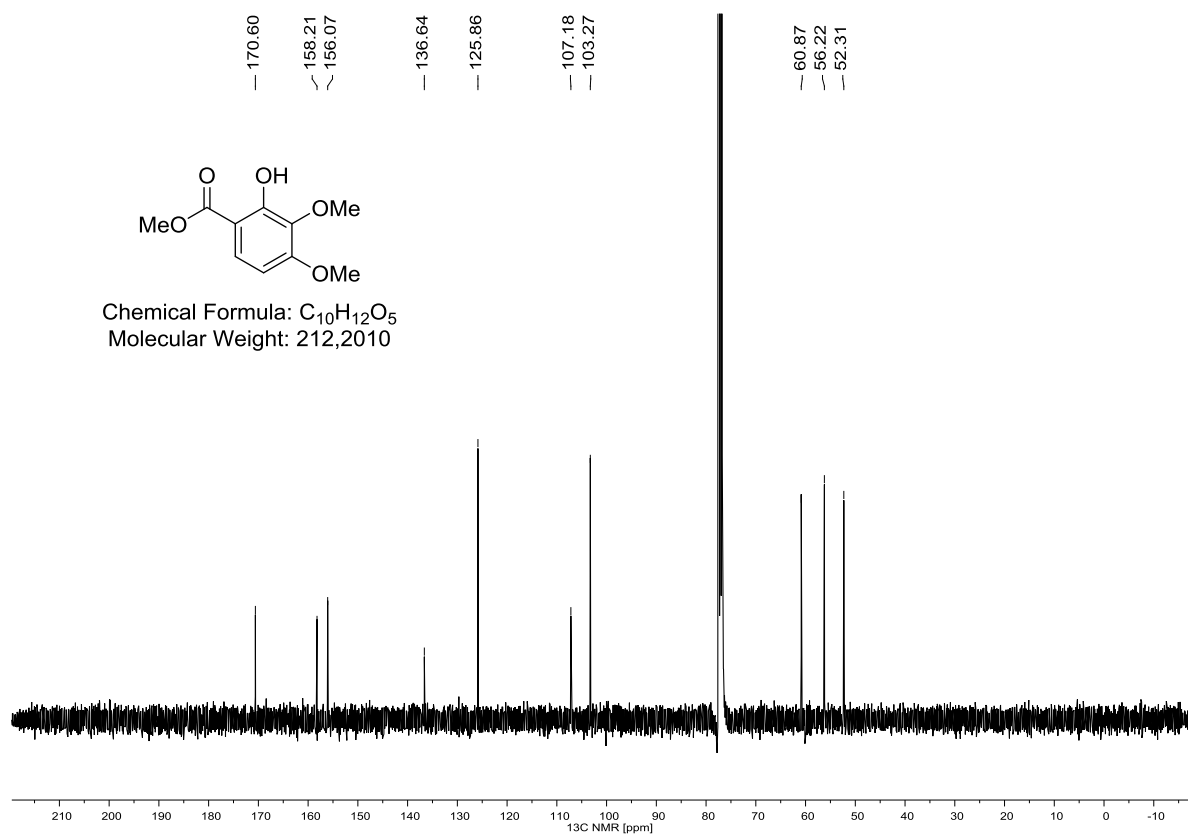


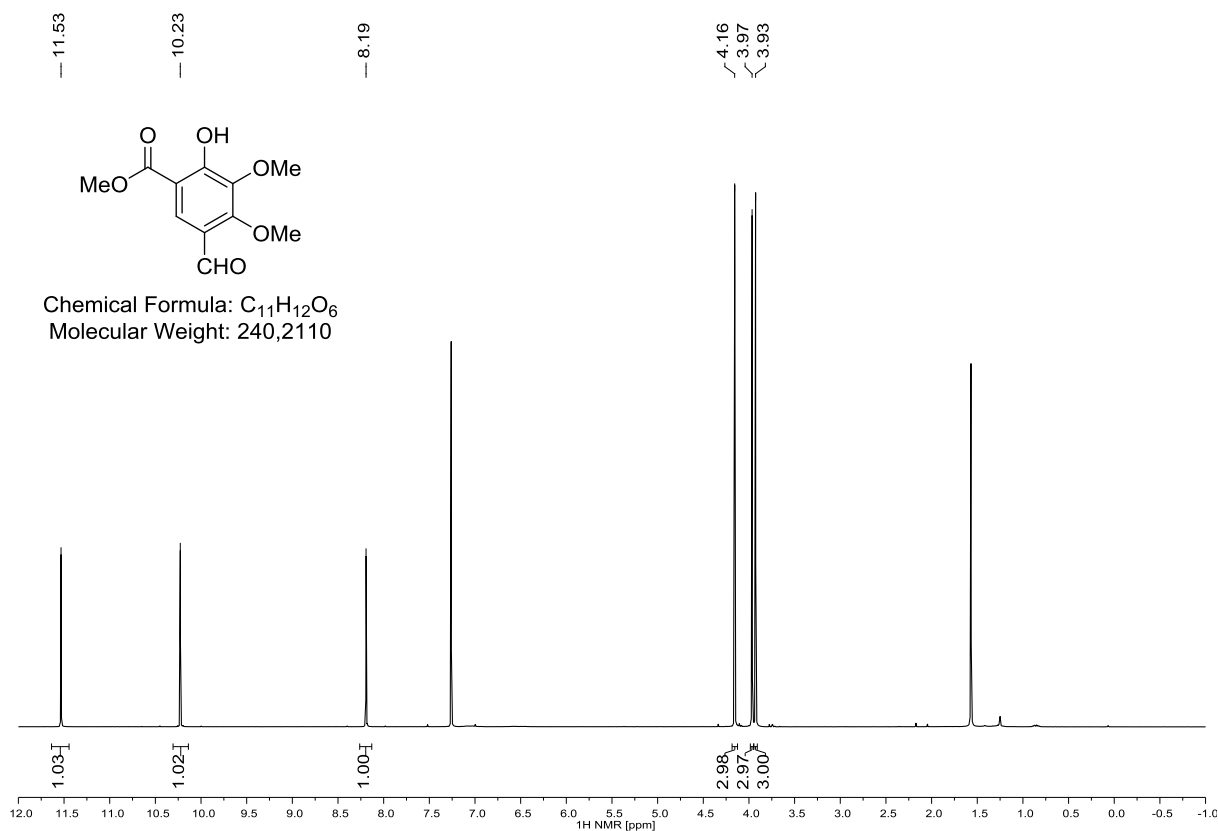
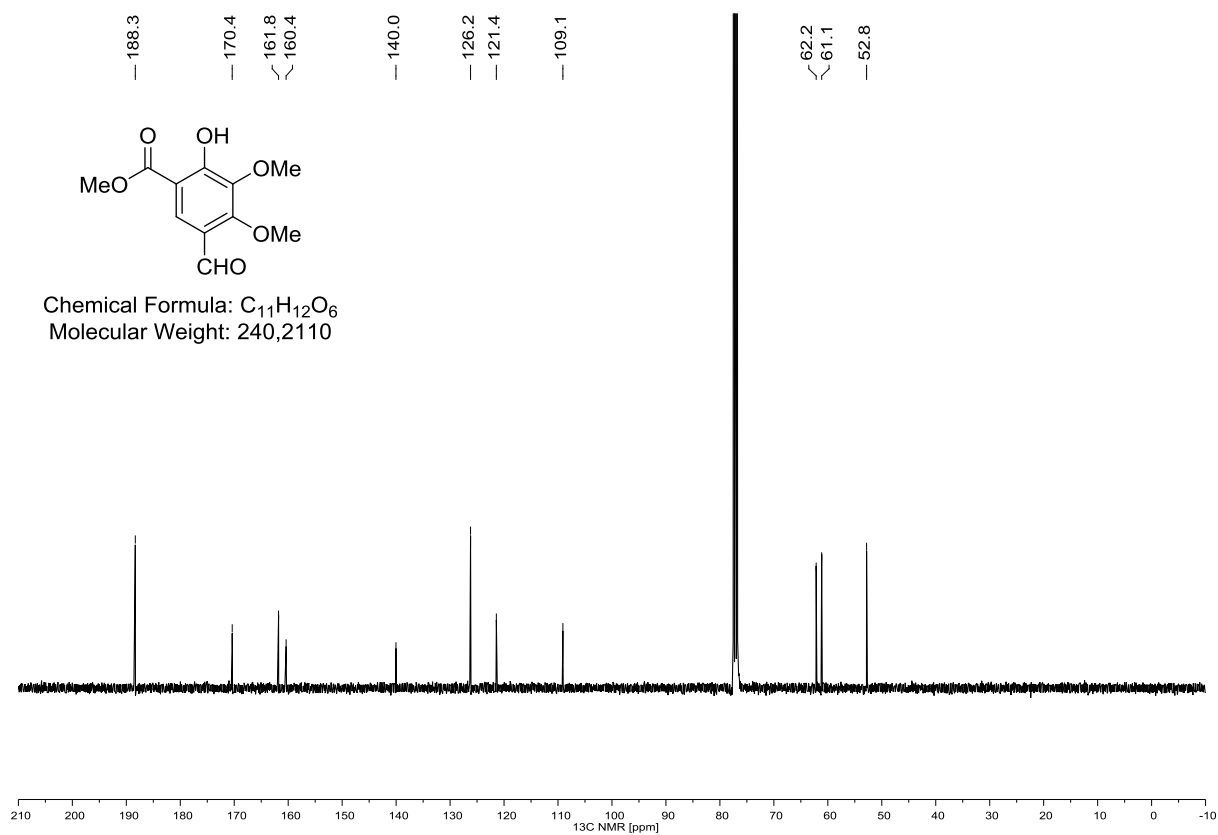
288
Chemical Formula: C₁₁H₁₂O₅
Molecular Weight: 224,2120

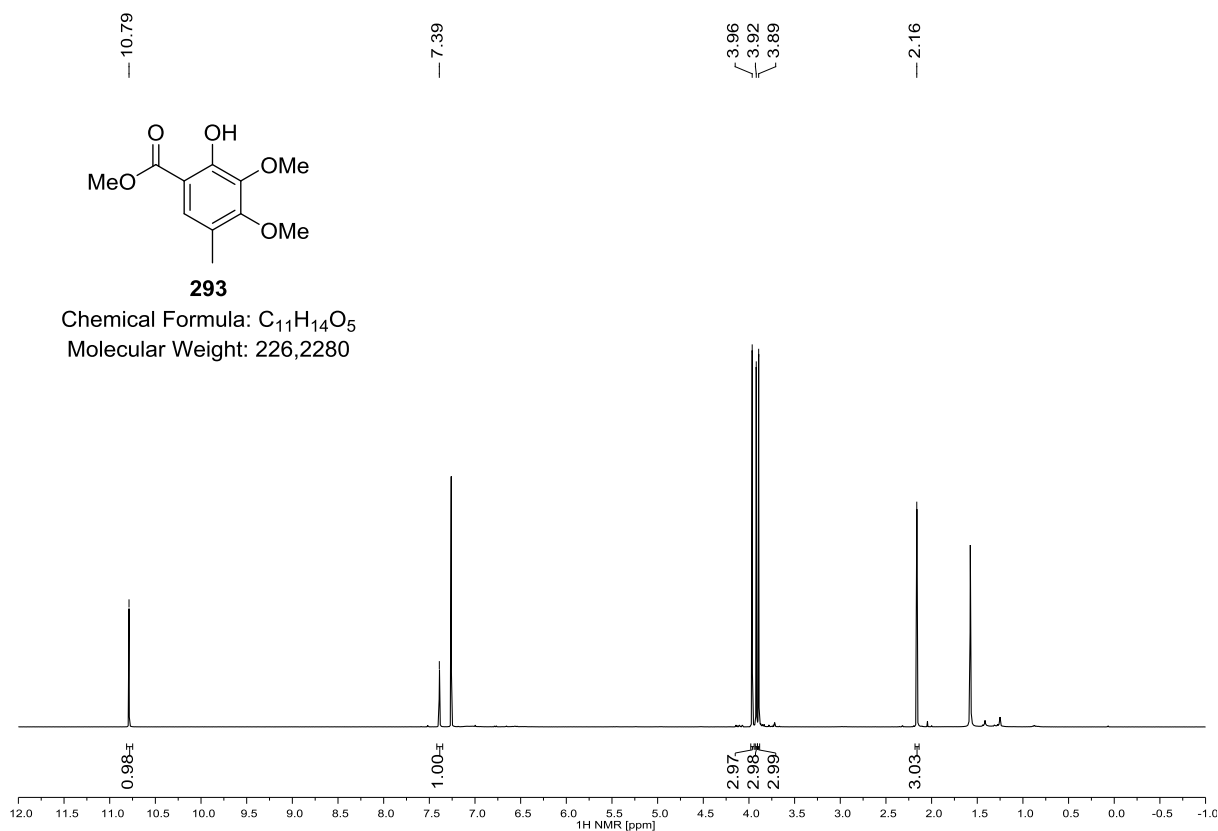
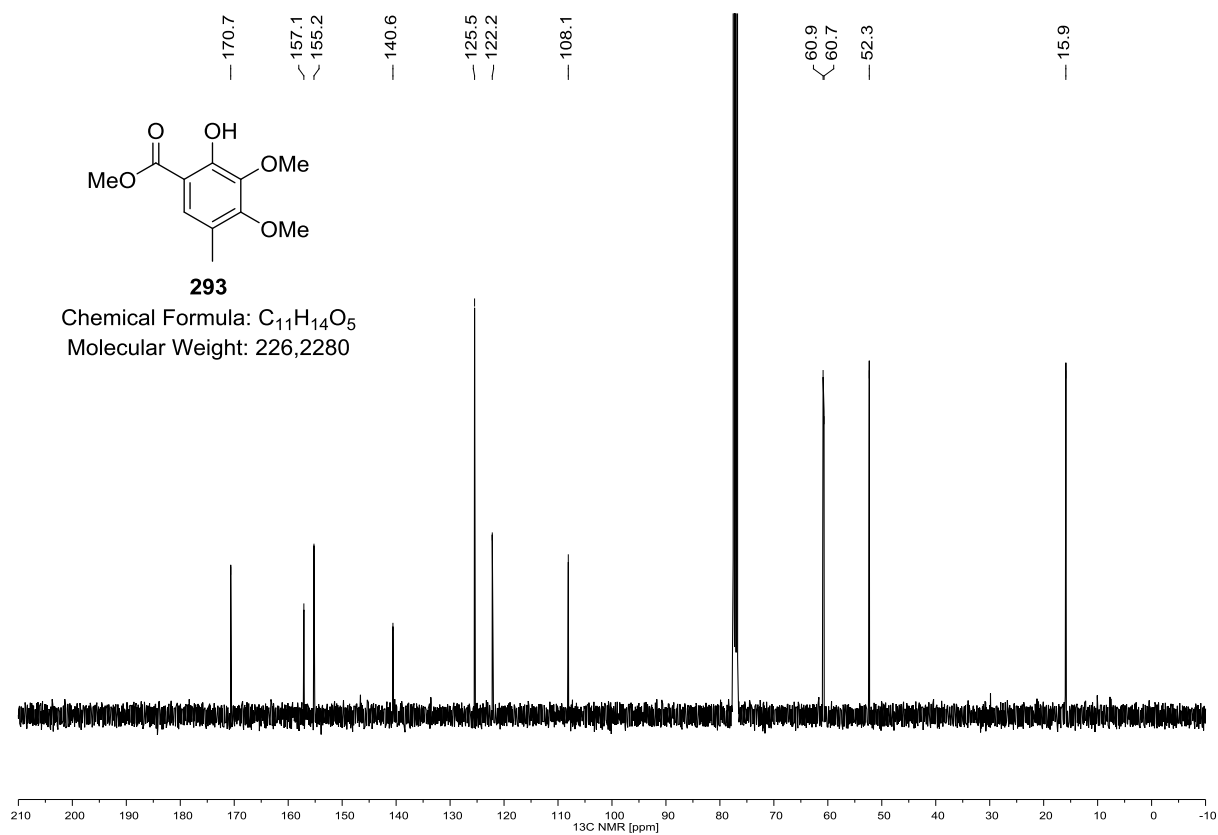


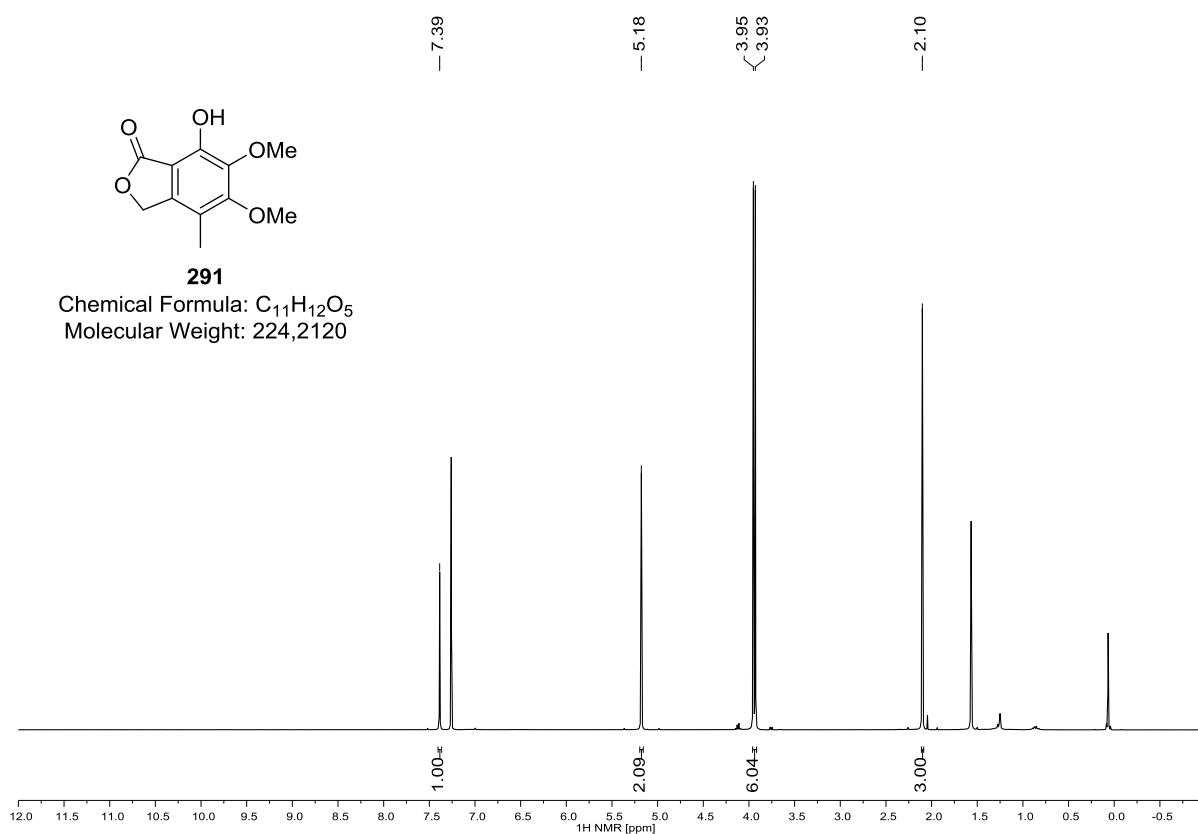
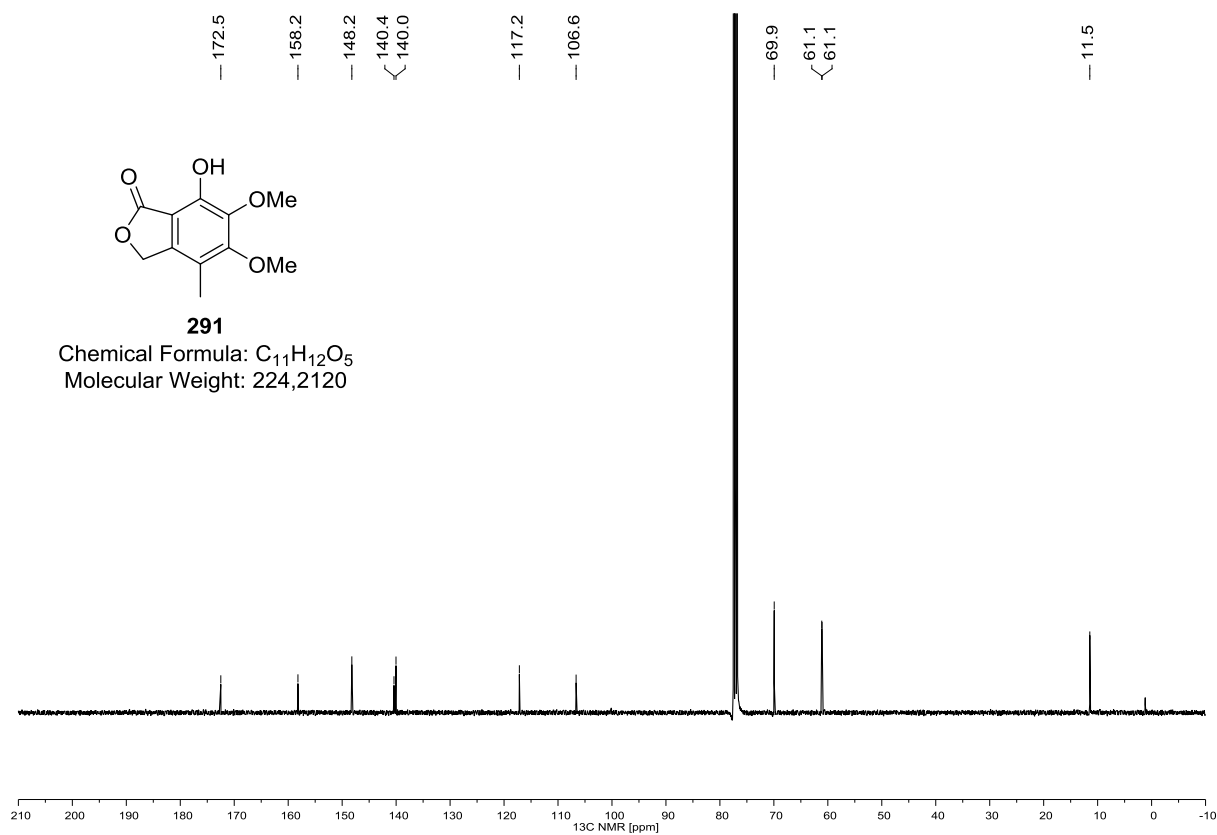
164 (^1H NMR, 300 MHz, CDCl_3)**164** (^{13}C NMR, 75 MHz, CDCl_3)

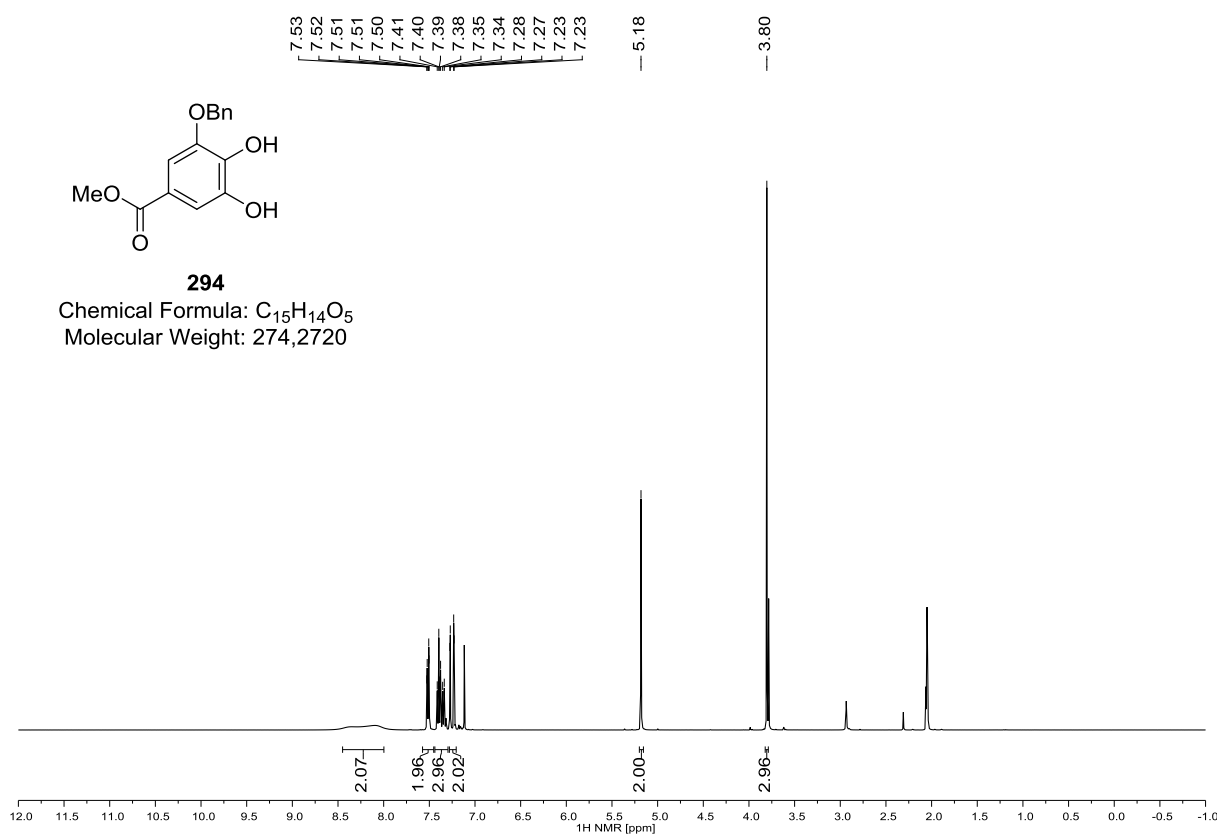
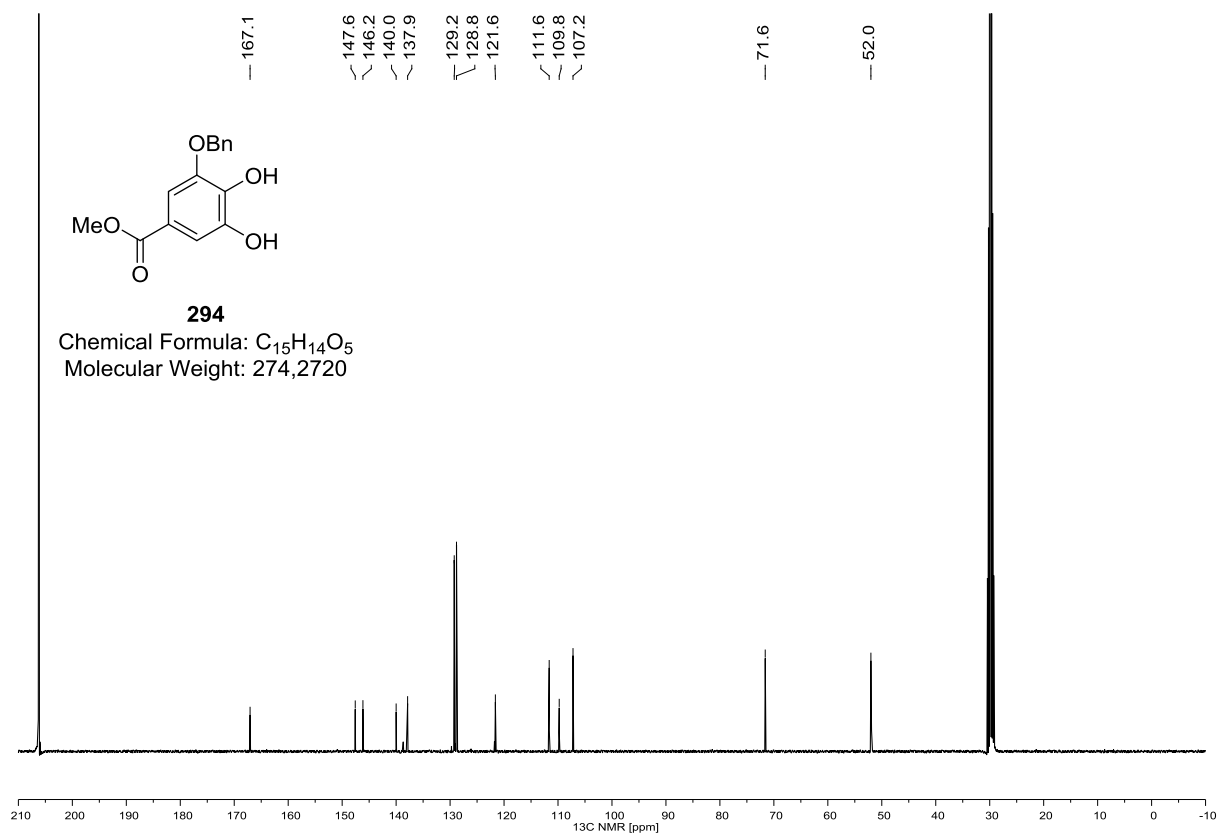
289 (^1H NMR, 400 MHz, CDCl_3)**289 (^{13}C NMR, 100 MHz, CDCl_3)**

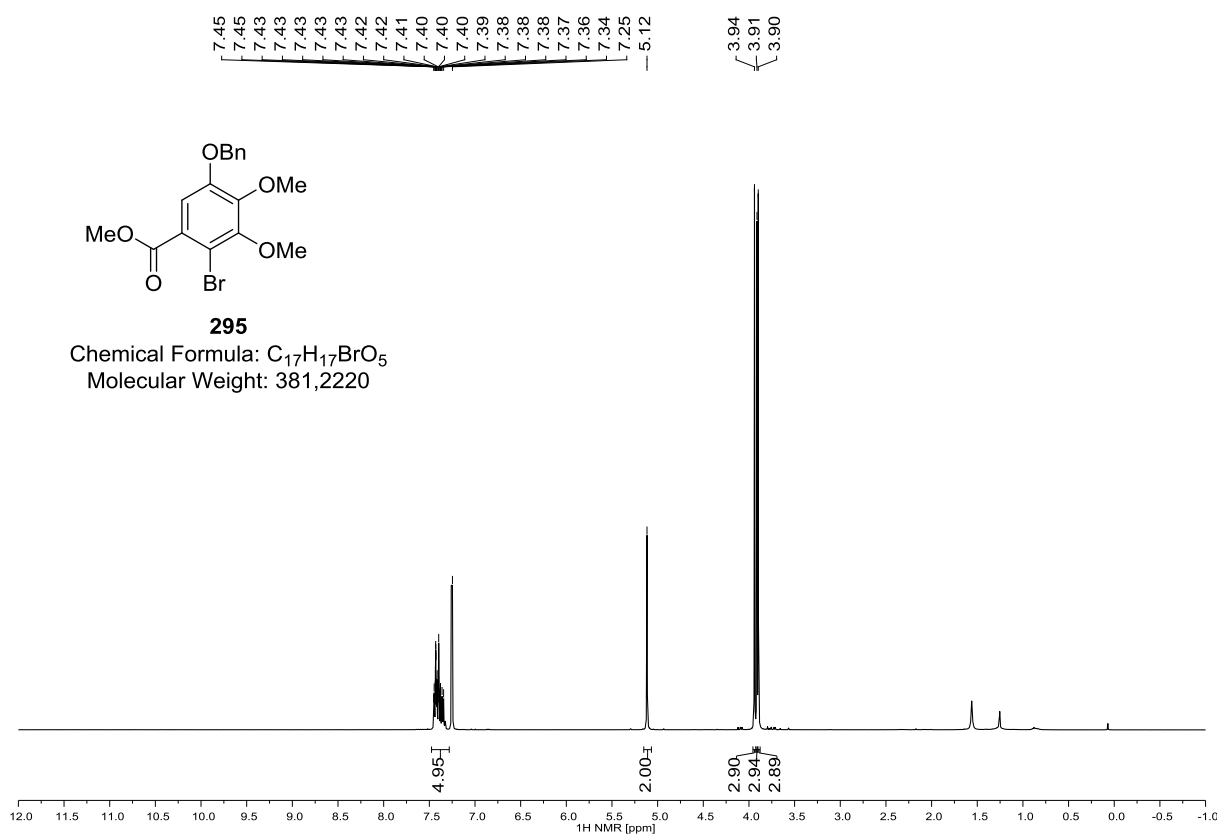
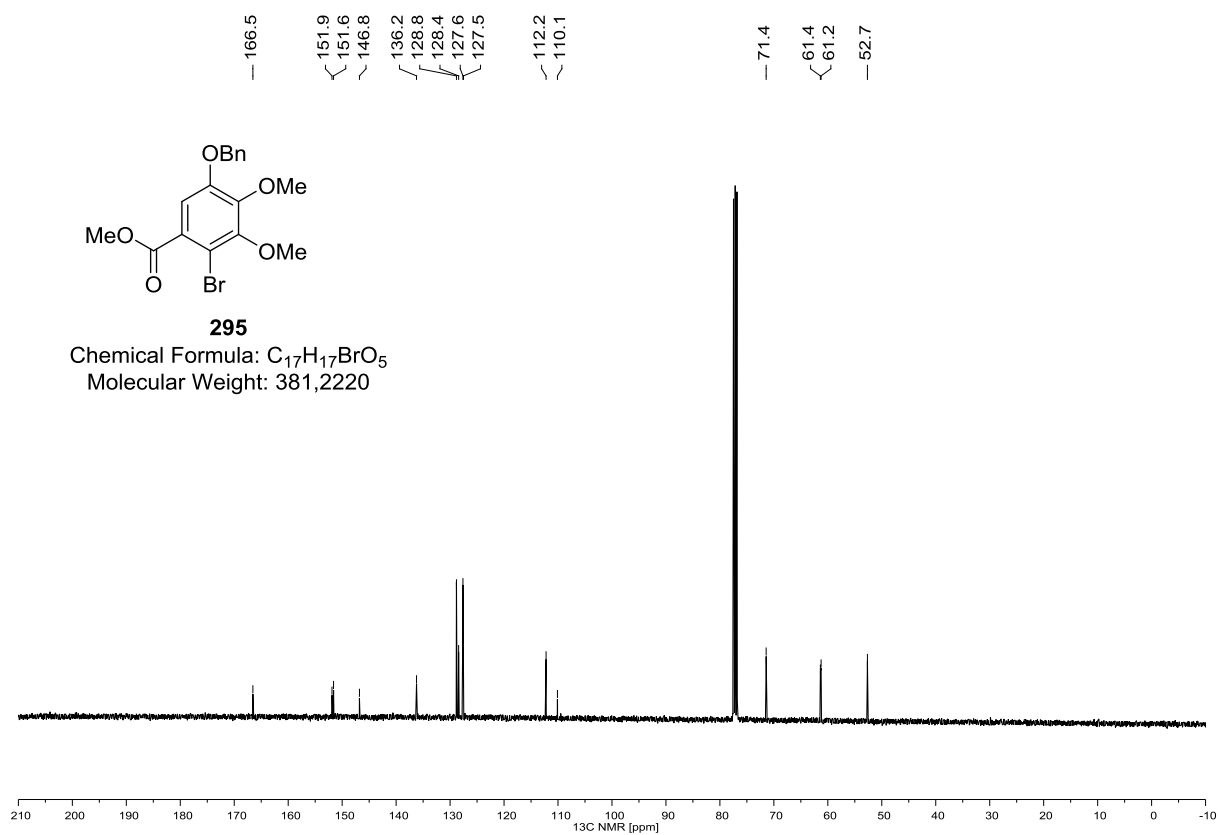
^1H NMR, 400 MHz, CDCl_3  **^{13}C NMR, 100 MHz, CDCl_3** 

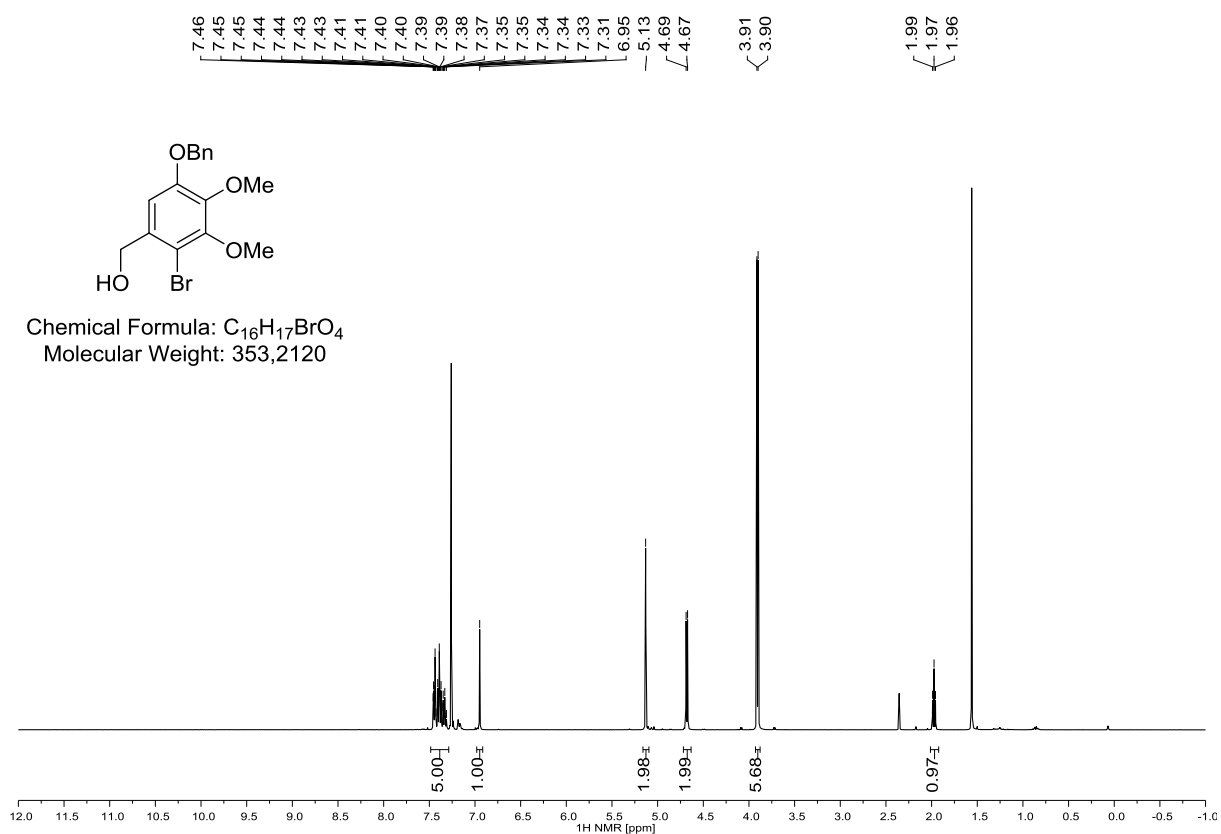
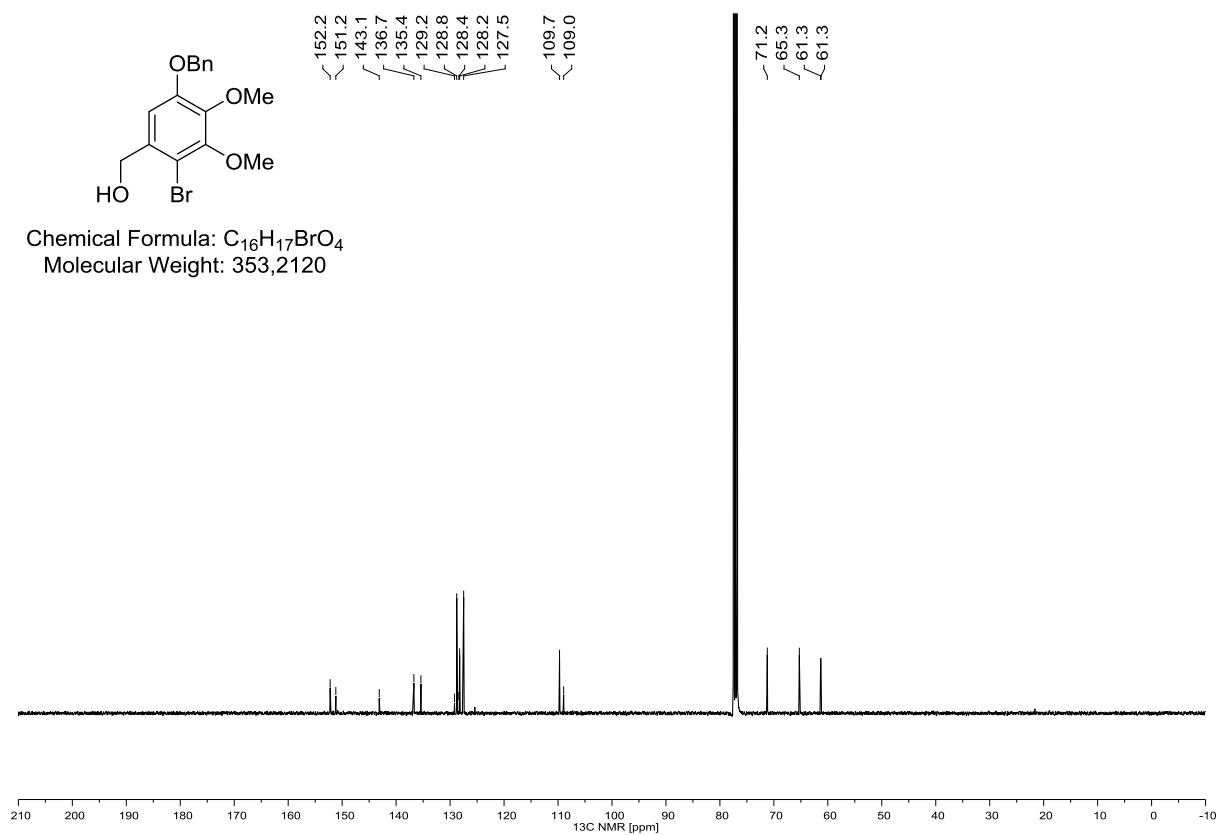
^1H NMR, 400 MHz, CDCl_3  **^{13}C NMR, 100 MHz, CDCl_3** 

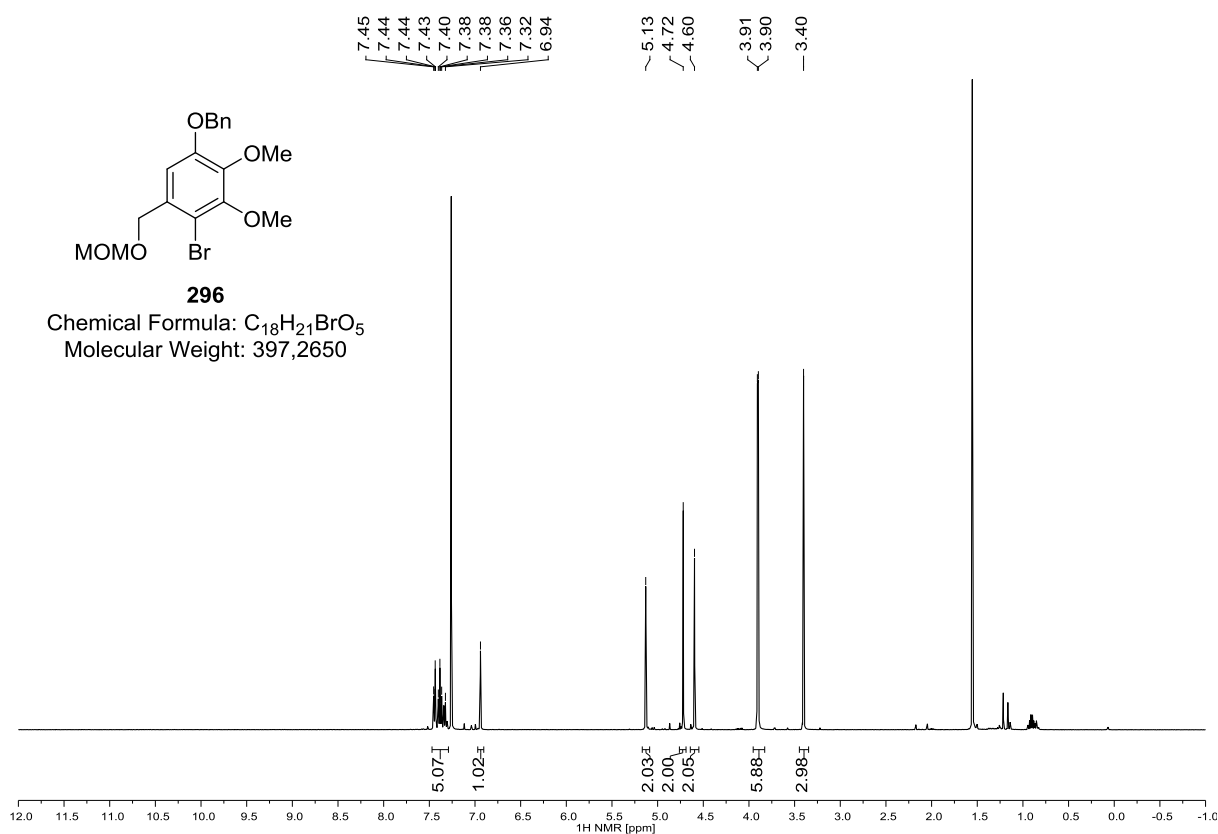
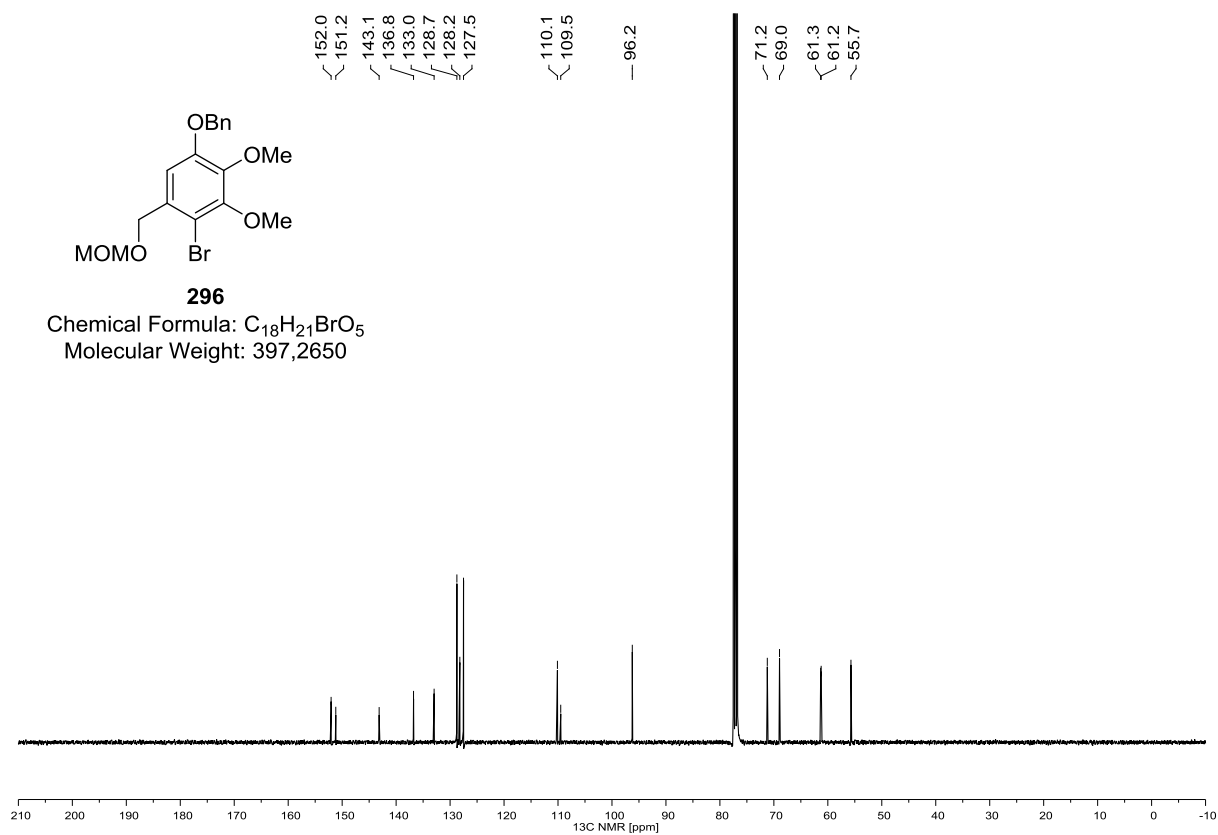
293 (^1H NMR, 400 MHz, CDCl_3)**293 (^{13}C NMR, 100 MHz, CDCl_3)**

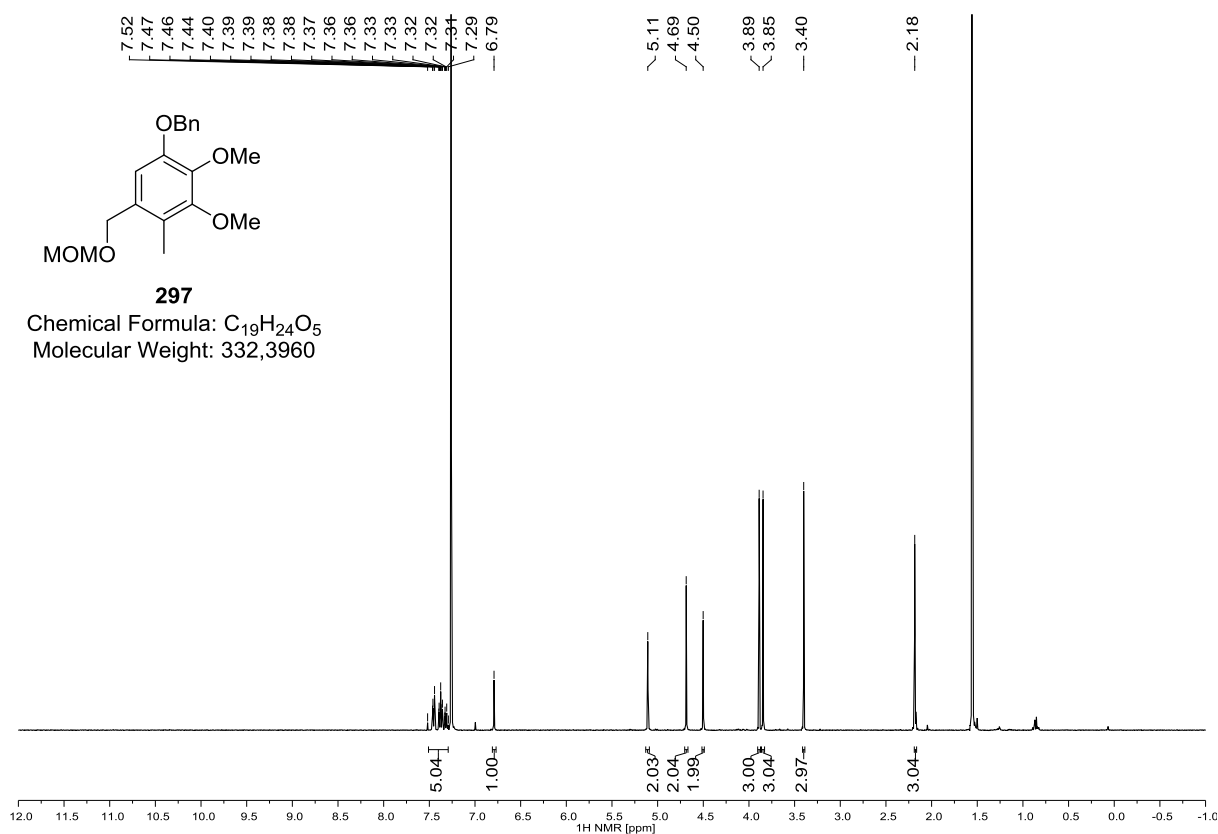
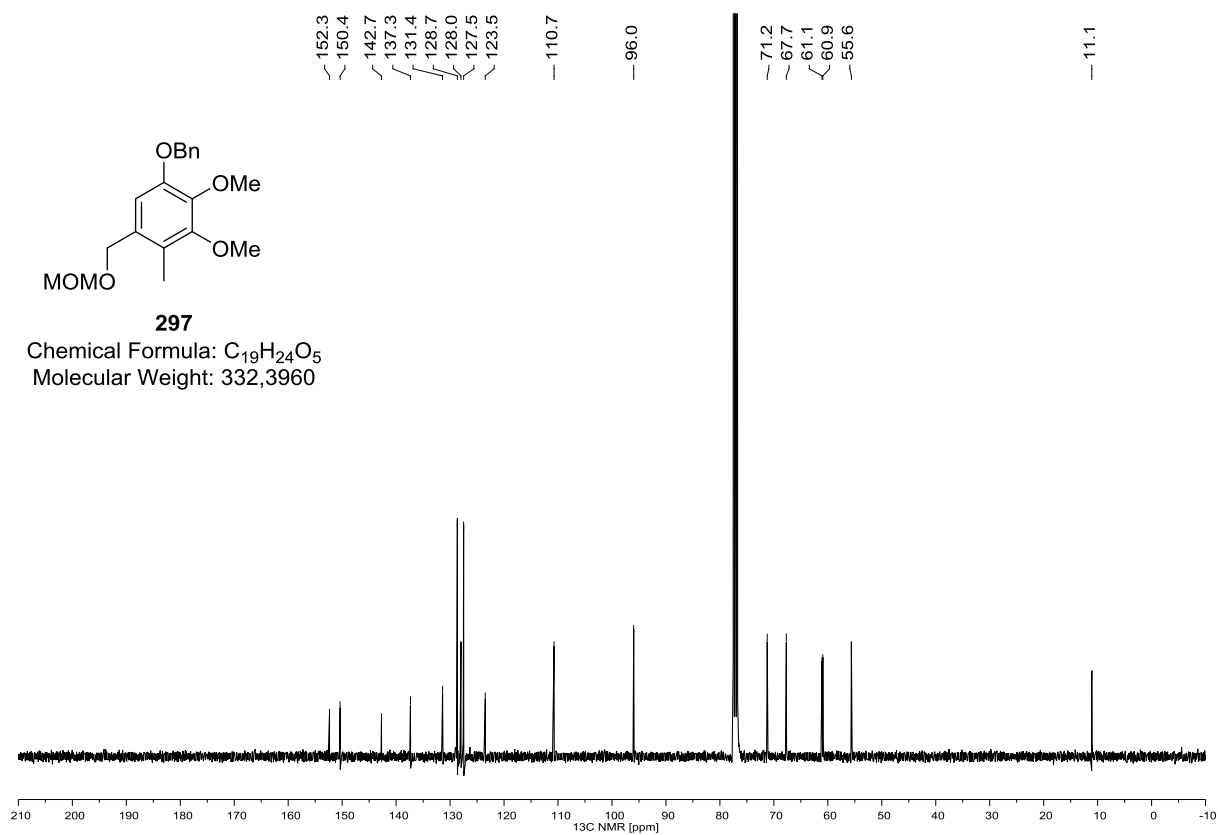
291 (^1H NMR, 400 MHz, CDCl_3)**291 (^{13}C NMR, 100 MHz, CDCl_3)**

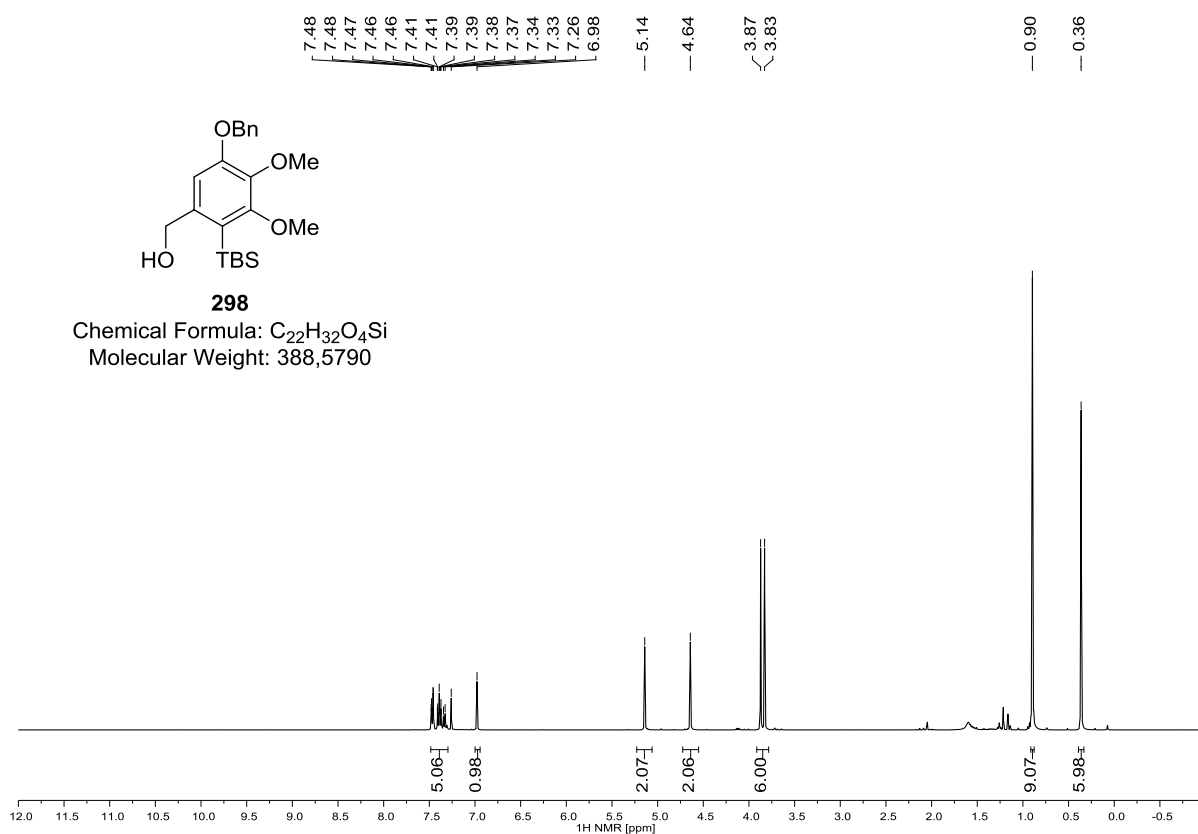
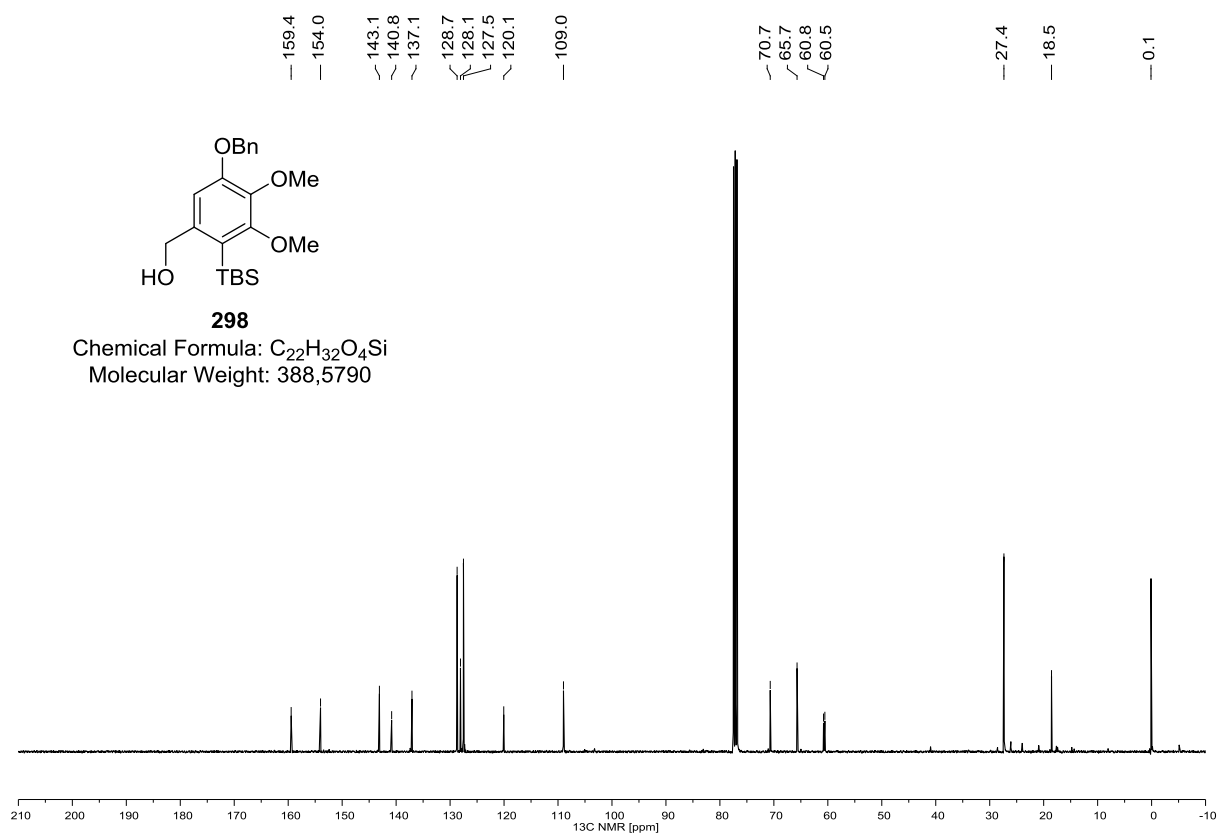
294 (^1H NMR, 400 MHz, $(\text{D}_3\text{C})_2\text{CO}$)**294 (^{13}C NMR, 100 MHz, $(\text{D}_3\text{C})_2\text{CO}$)**

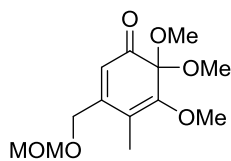
295 (^1H NMR, 400 MHz, CDCl_3)**295 (^{13}C NMR, 100 MHz, CDCl_3)**

^1H NMR, 400 MHz, CDCl_3  **^{13}C NMR, 100 MHz, CDCl_3** 

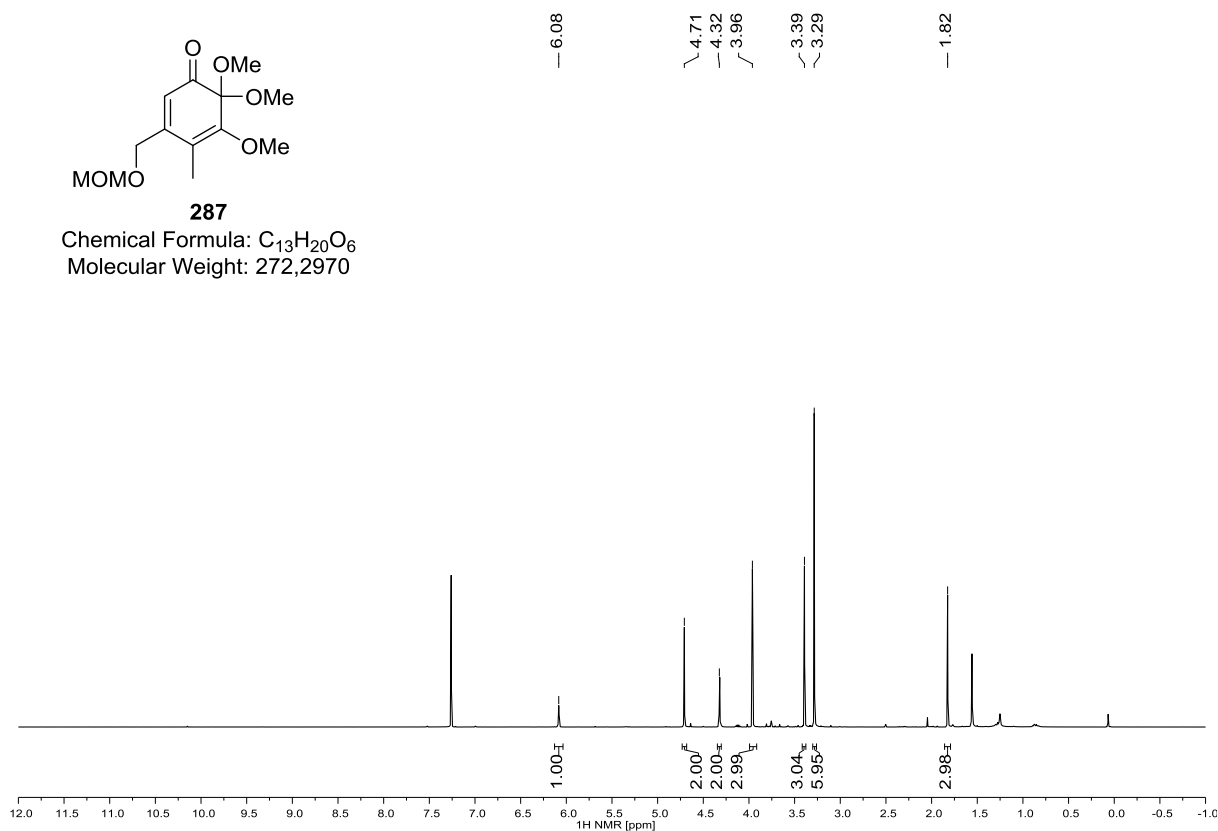
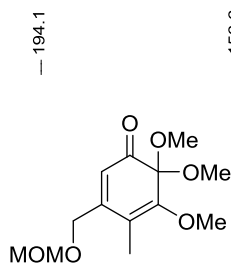
296 (^1H NMR, 400 MHz, CDCl_3)**296 (^{13}C NMR, 100 MHz, CDCl_3)**

297 (^1H NMR, 400 MHz, CDCl_3)**297 (^{13}C NMR, 100 MHz, CDCl_3)**

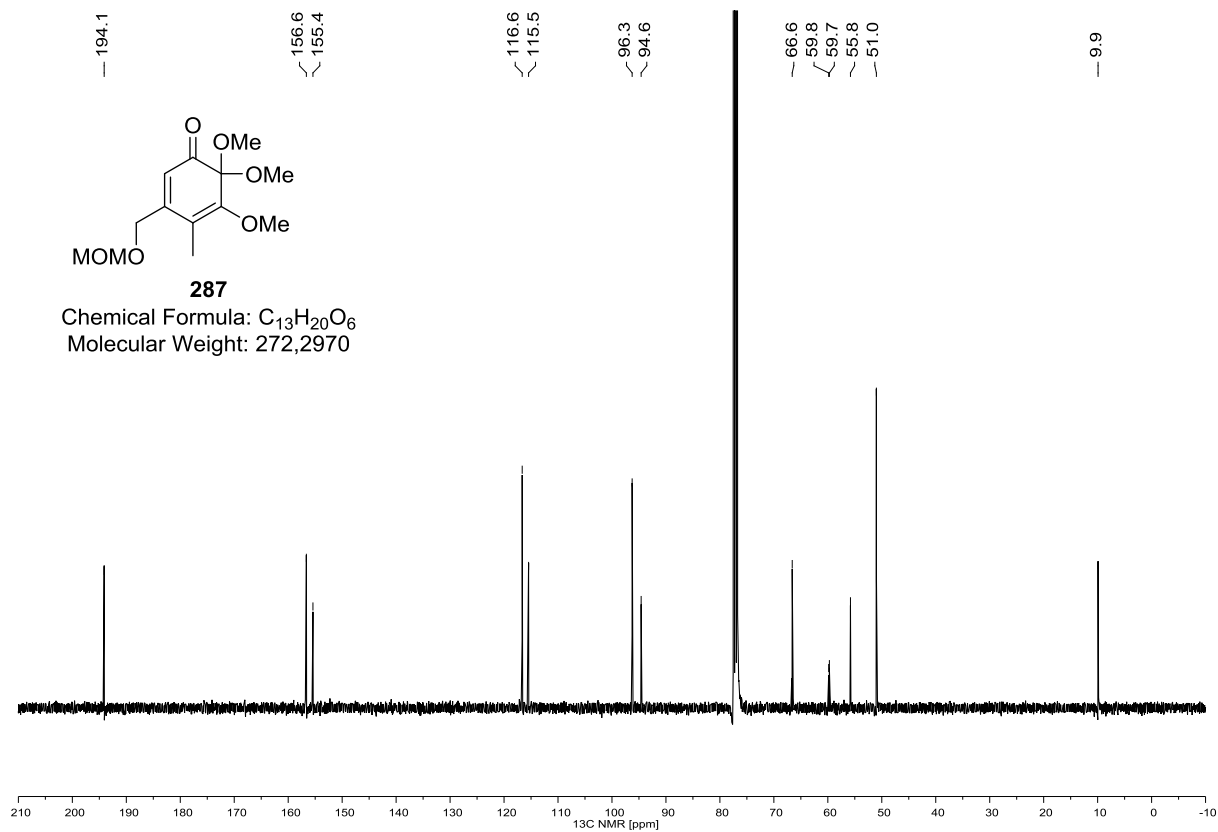
298 (¹H NMR, 400 MHz, CDCl₃)**298 (¹³C NMR, 100 MHz, CDCl₃)**

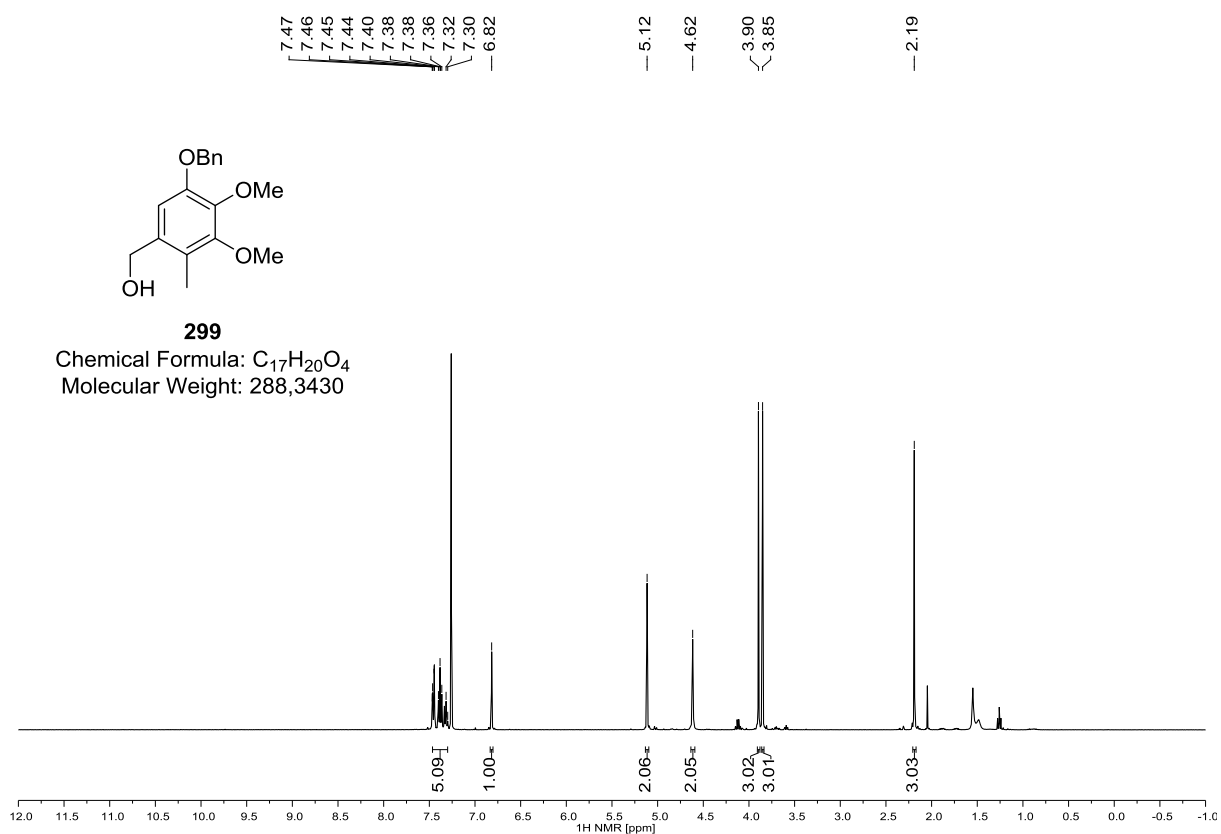
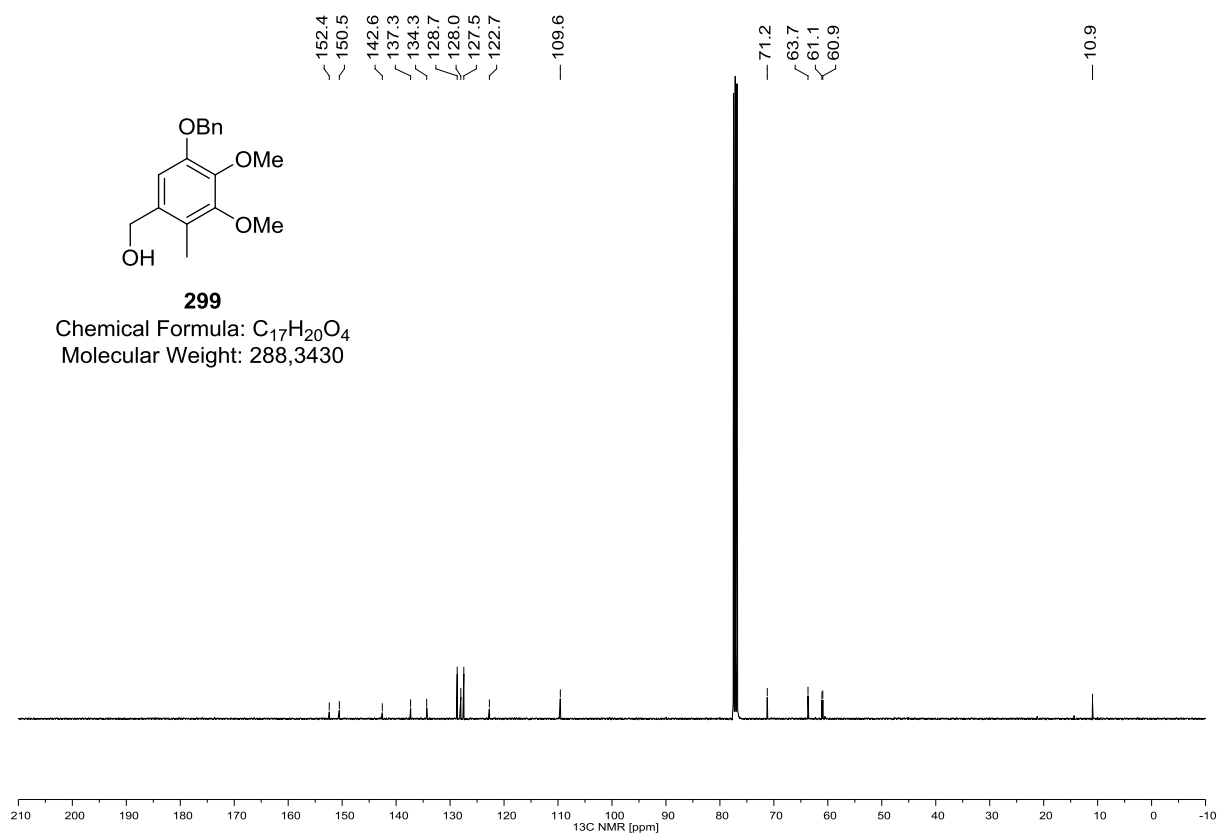
287 (^1H NMR, 400 MHz, CDCl_3)**287**

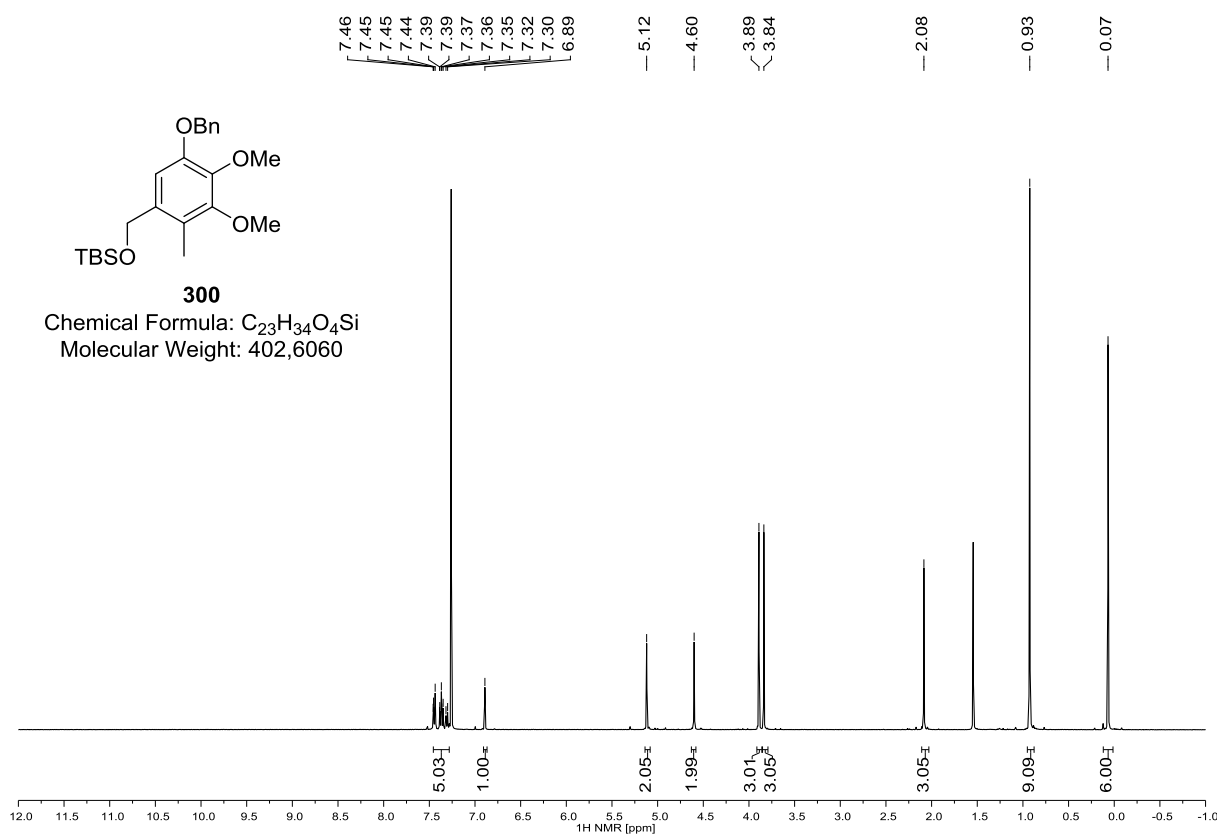
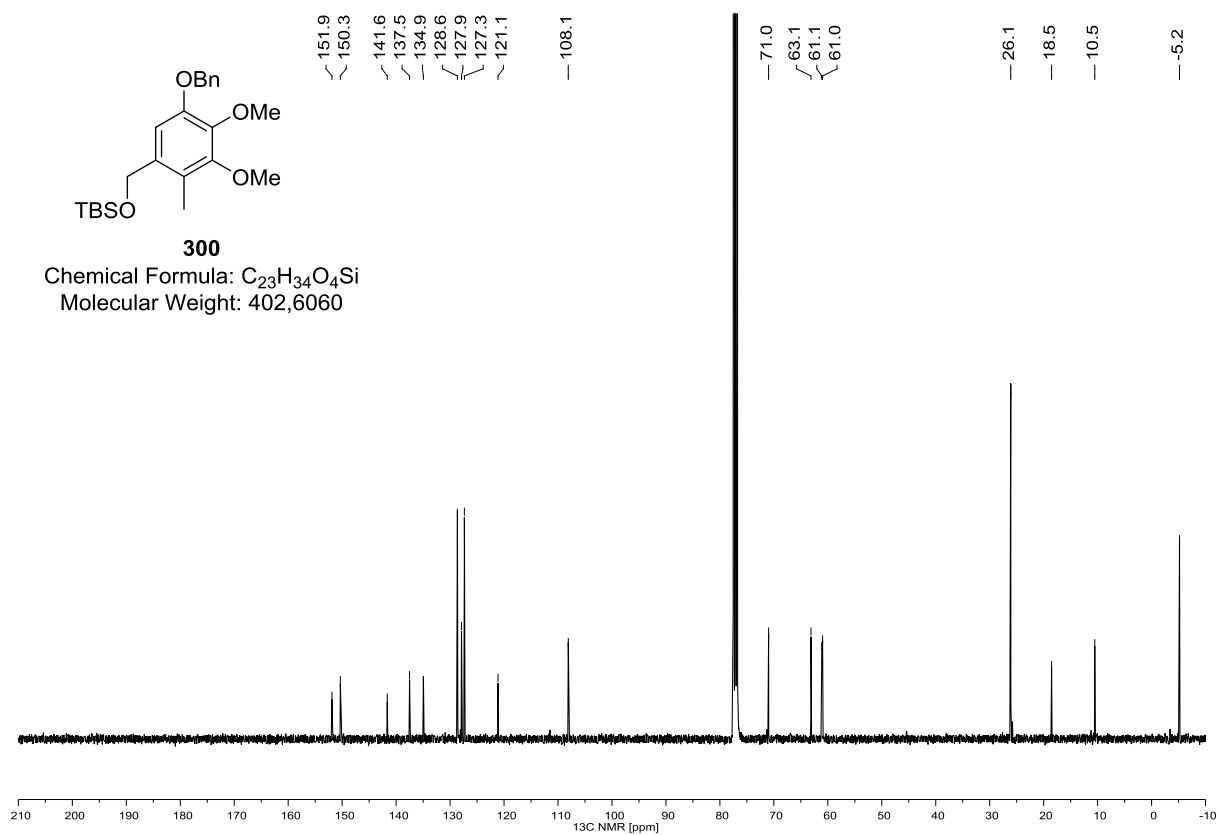
Chemical Formula: $\text{C}_{13}\text{H}_{20}\text{O}_6$
Molecular Weight: 272,2970

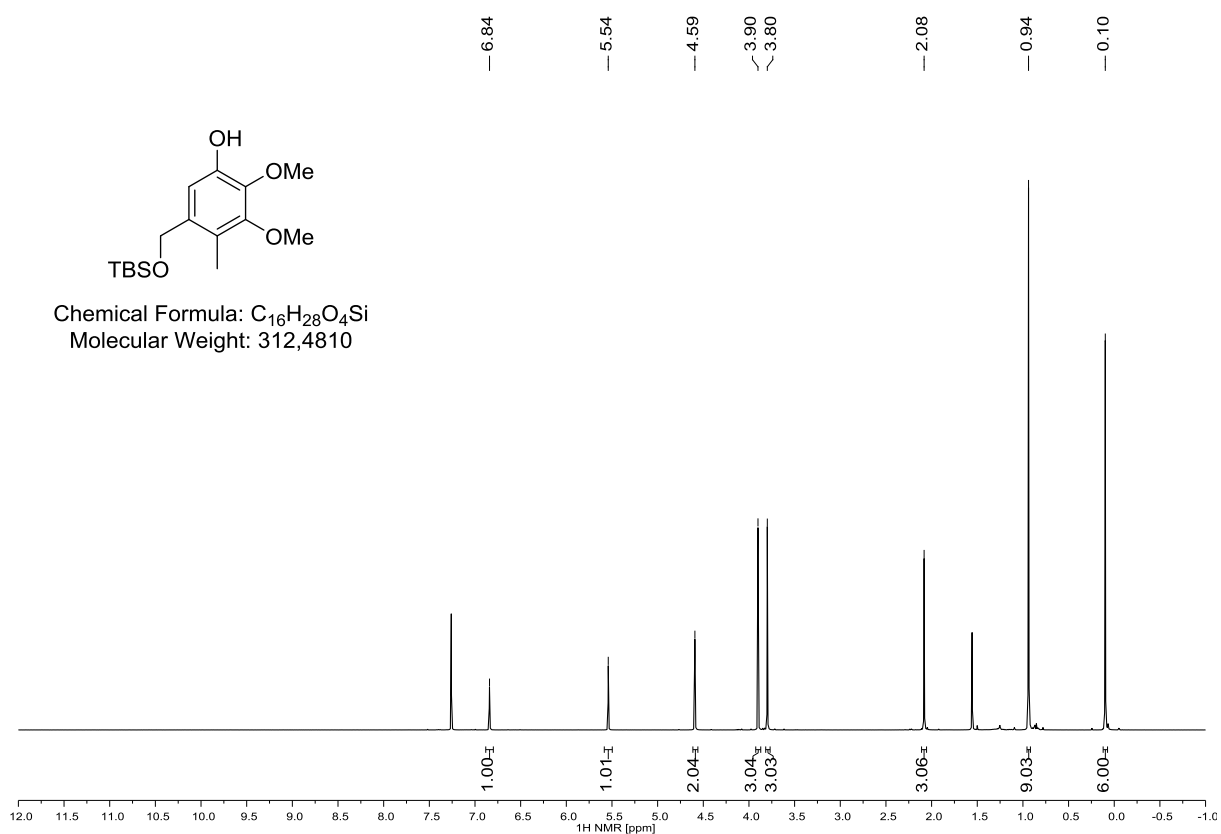
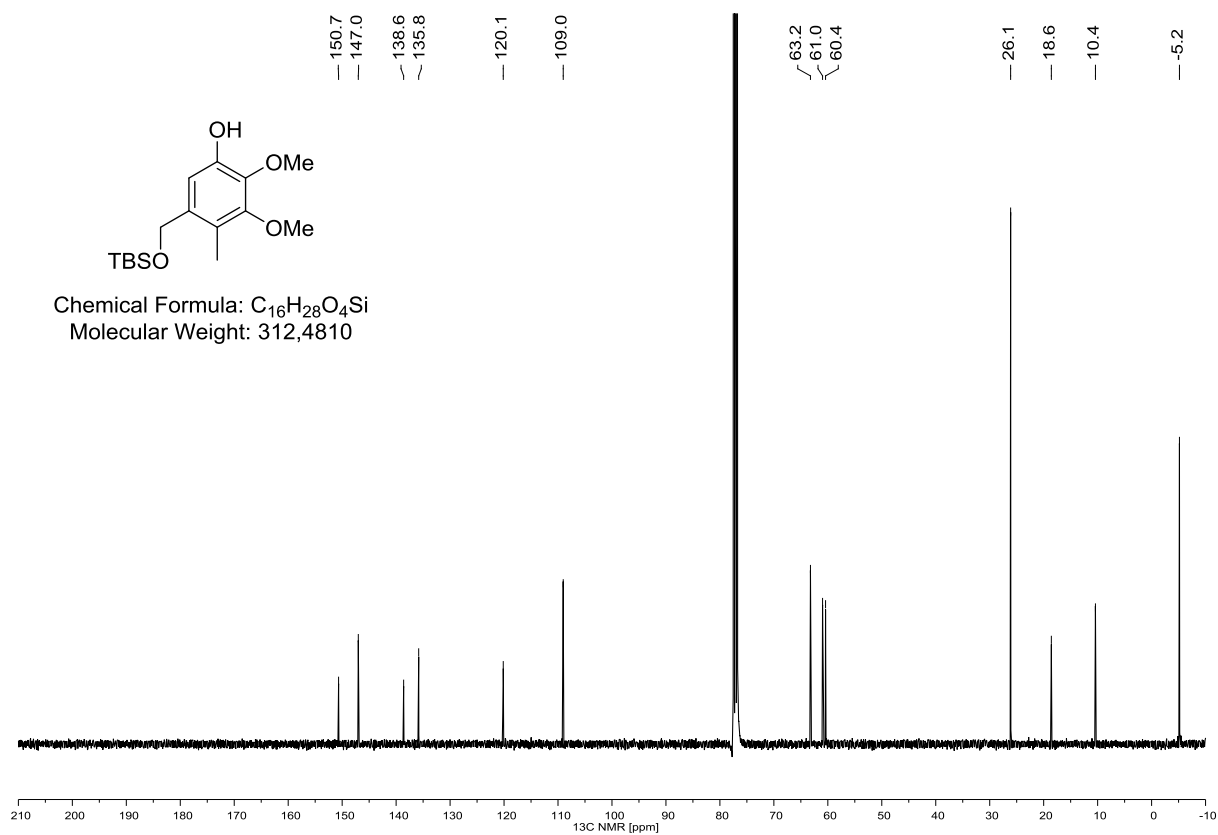
**287 (^{13}C NMR, 100 MHz, CDCl_3)****287**

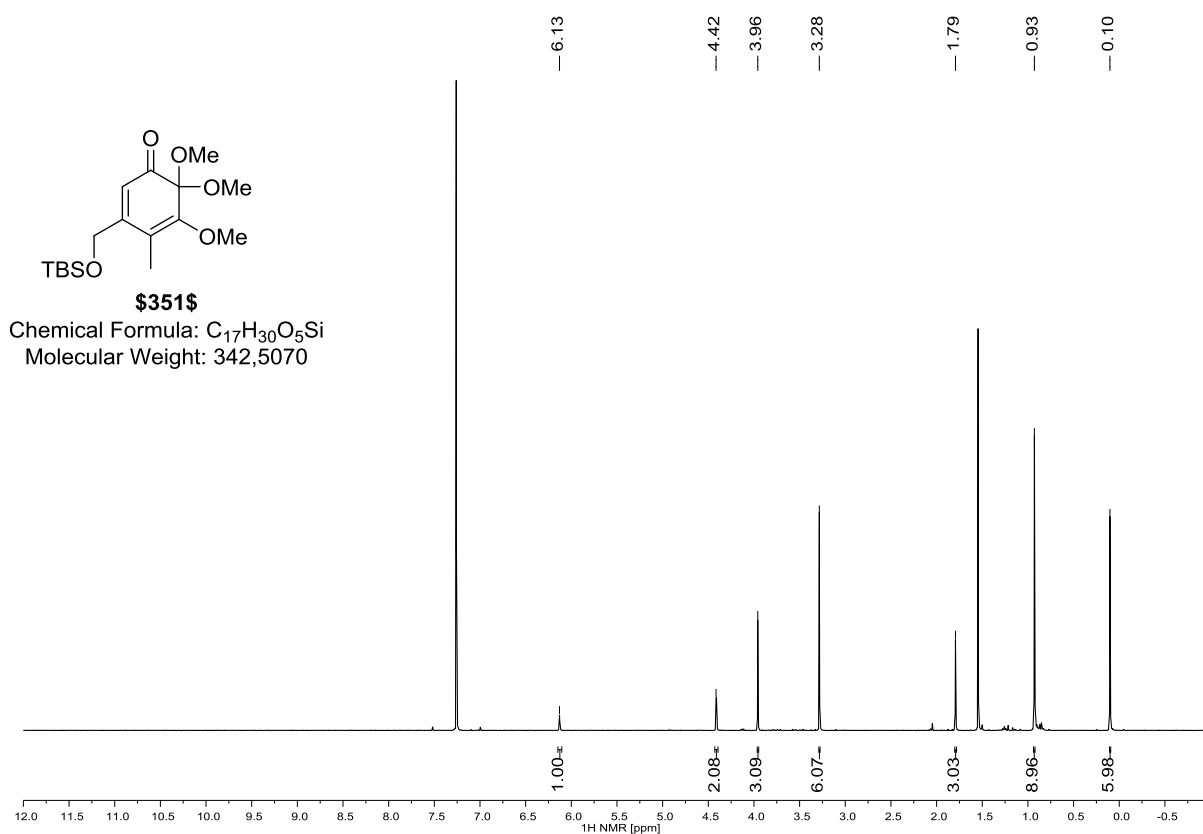
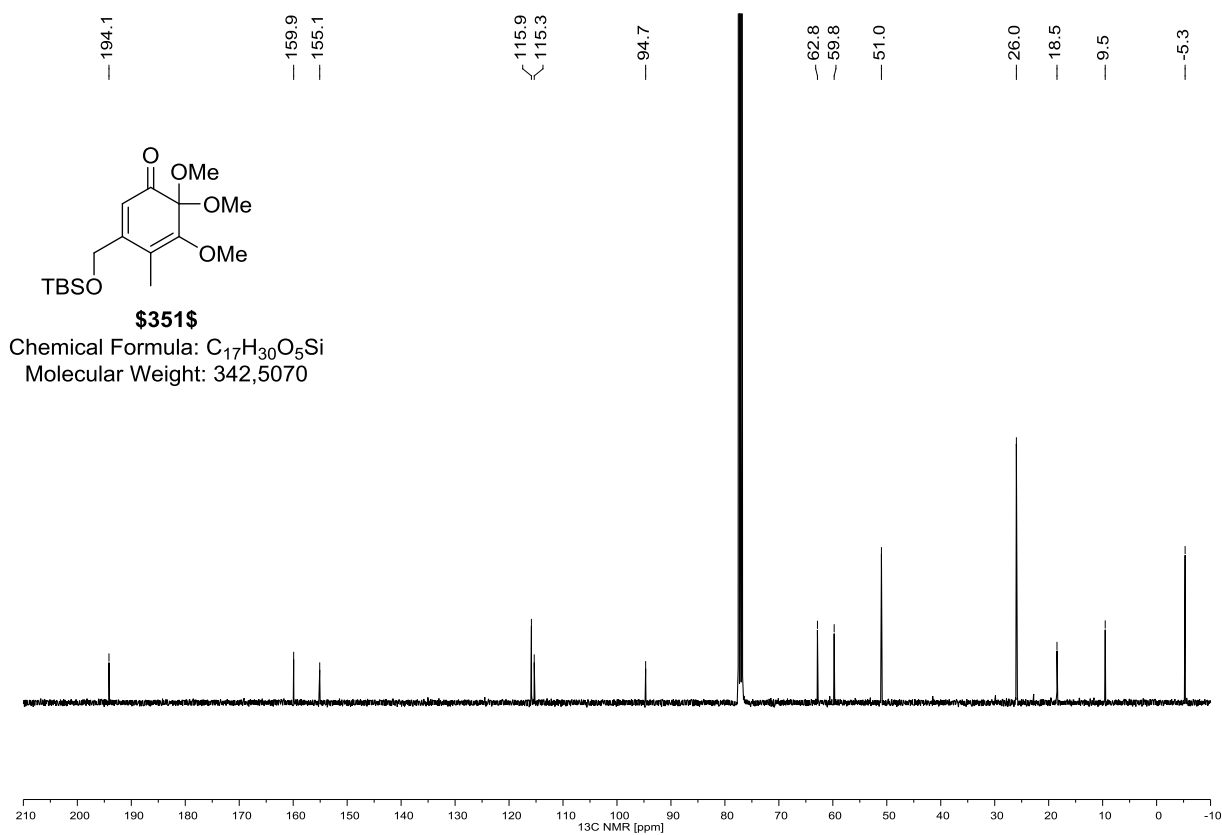
Chemical Formula: $\text{C}_{13}\text{H}_{20}\text{O}_6$
Molecular Weight: 272,2970

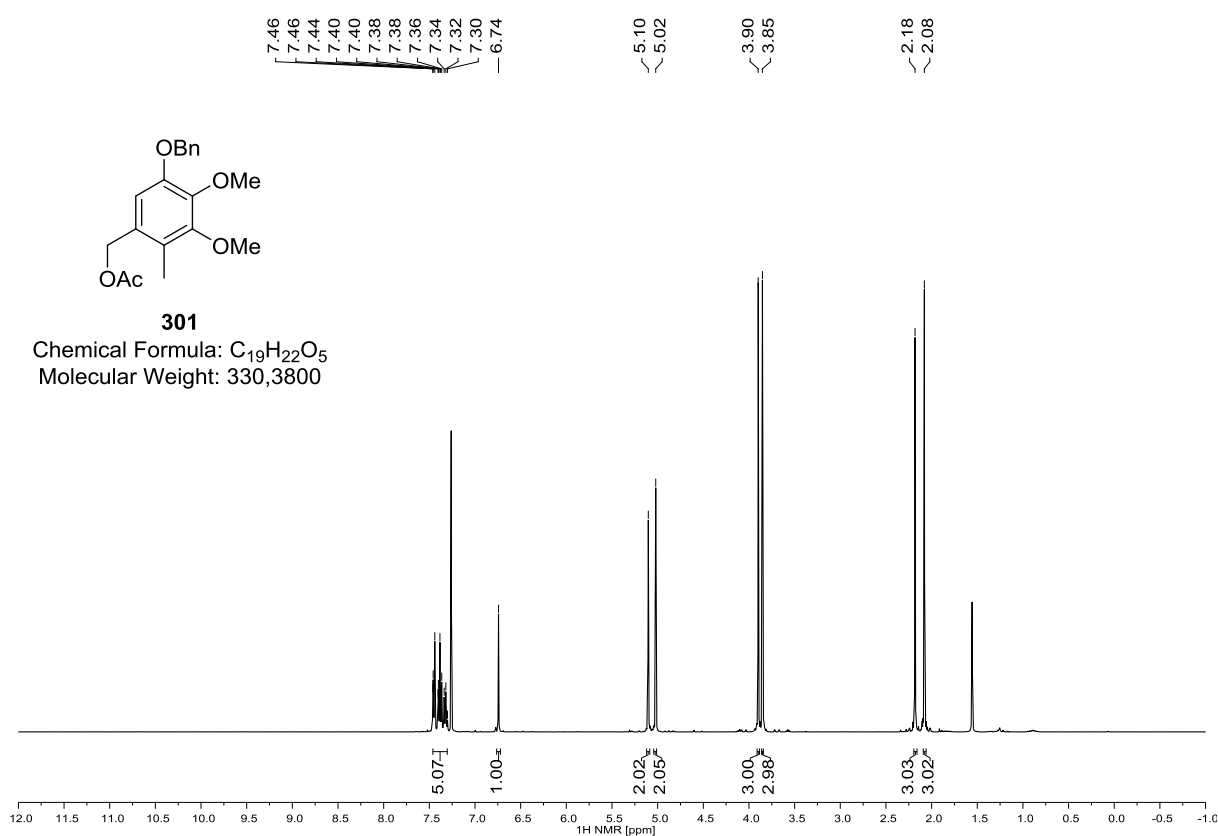
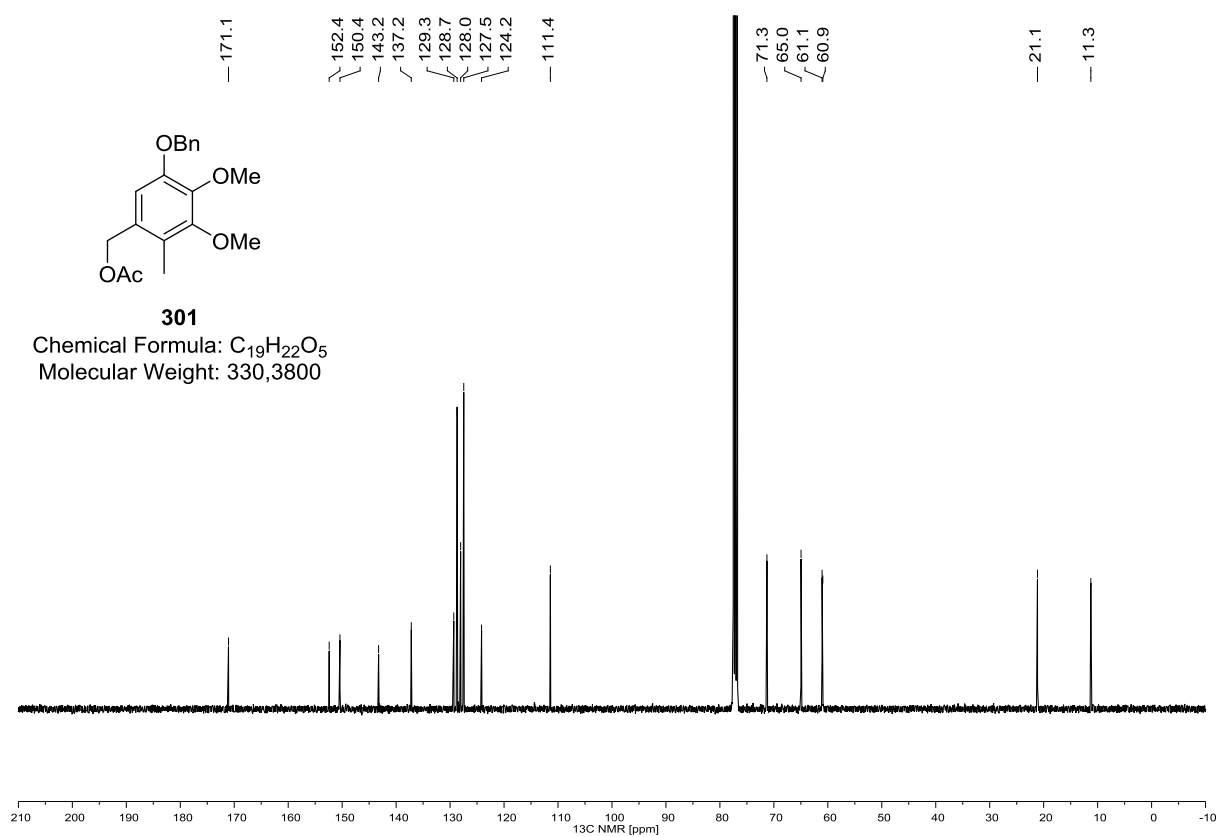


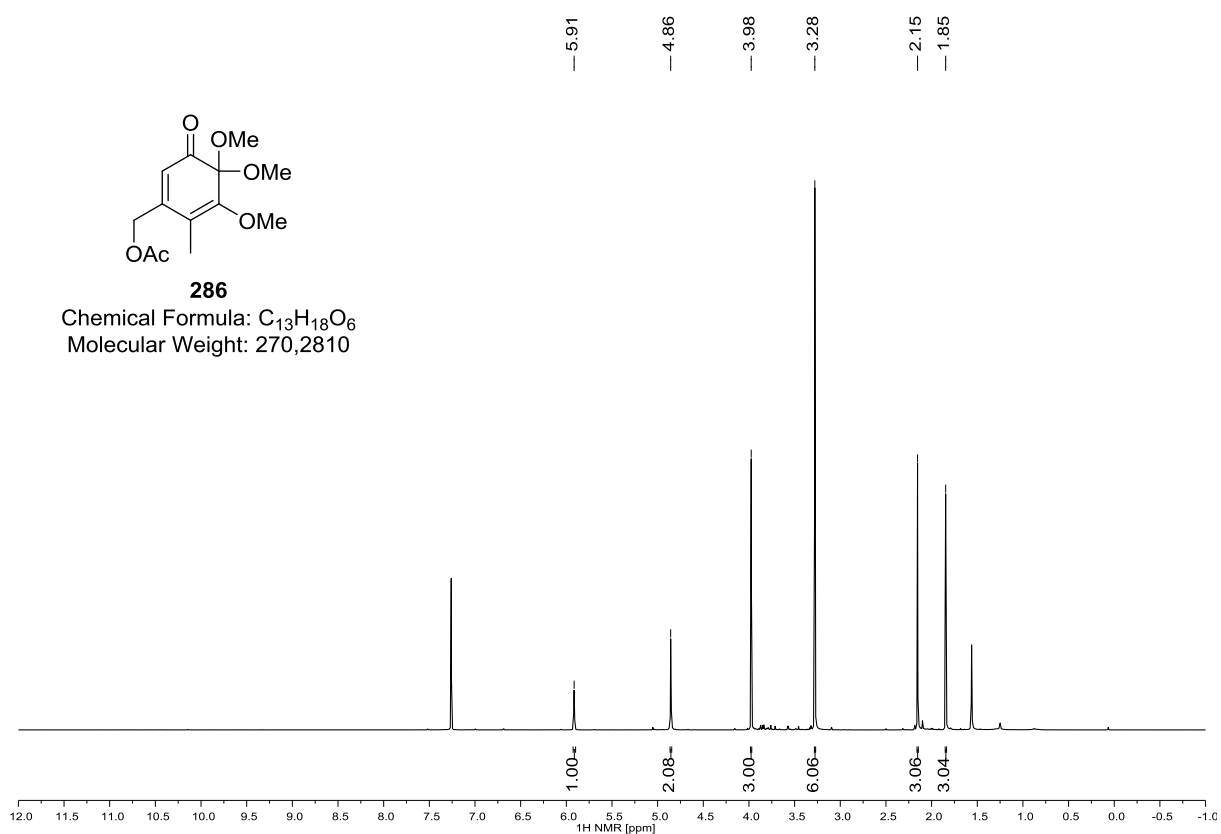
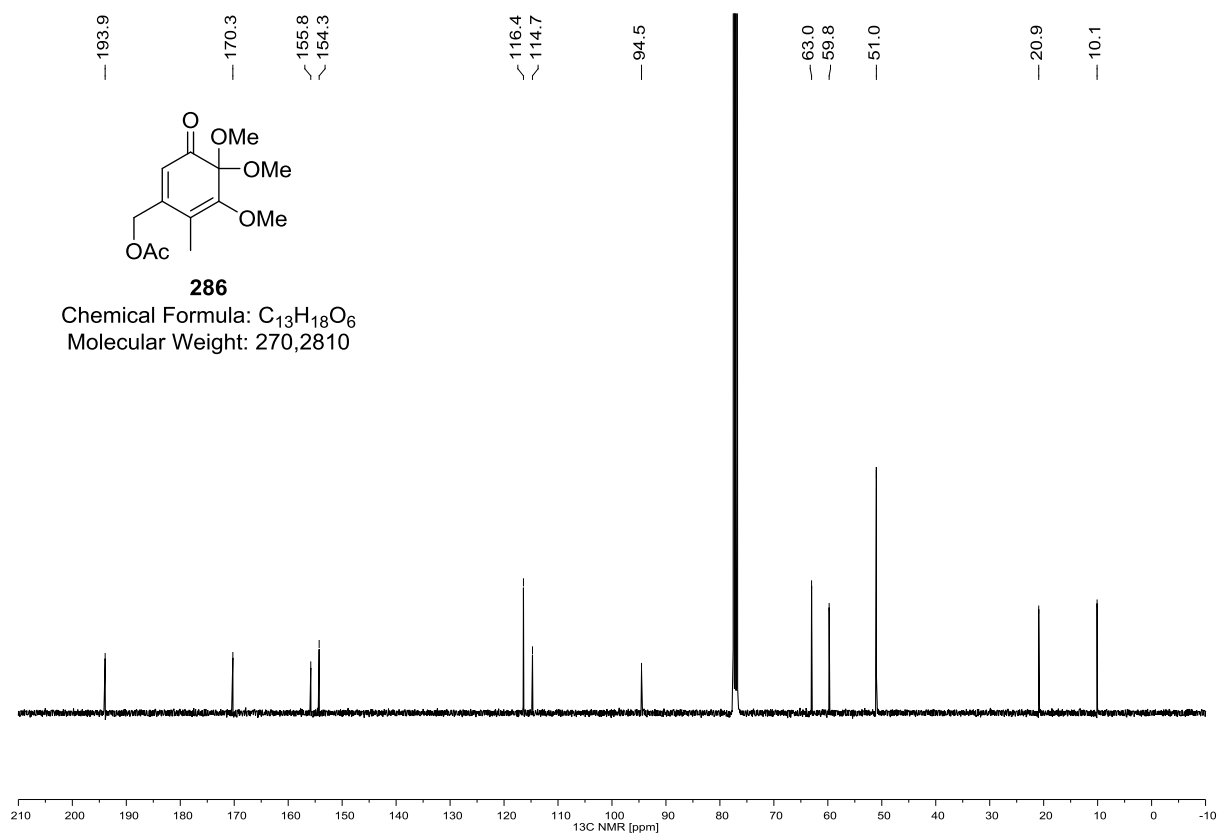
299 (¹H NMR, 400 MHz, CDCl₃)**299 (¹³C NMR, 100 MHz, CDCl₃)**

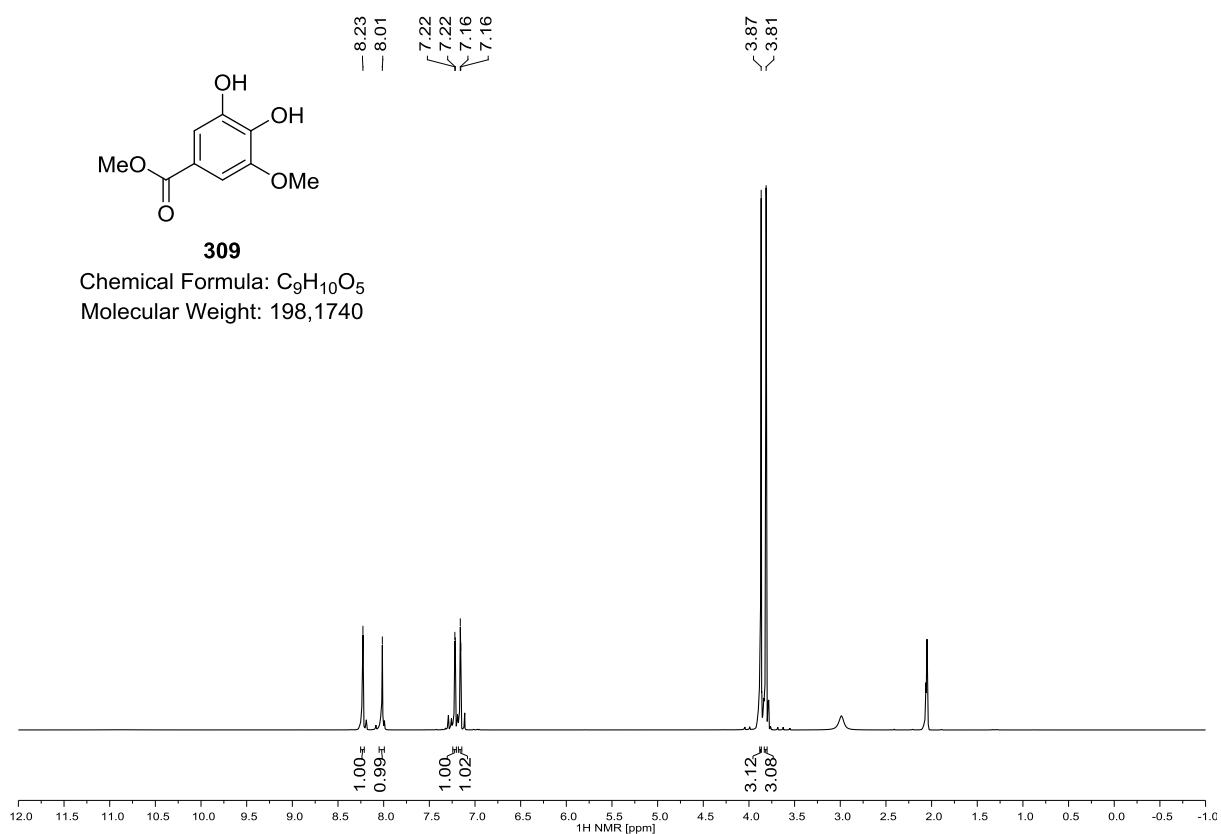
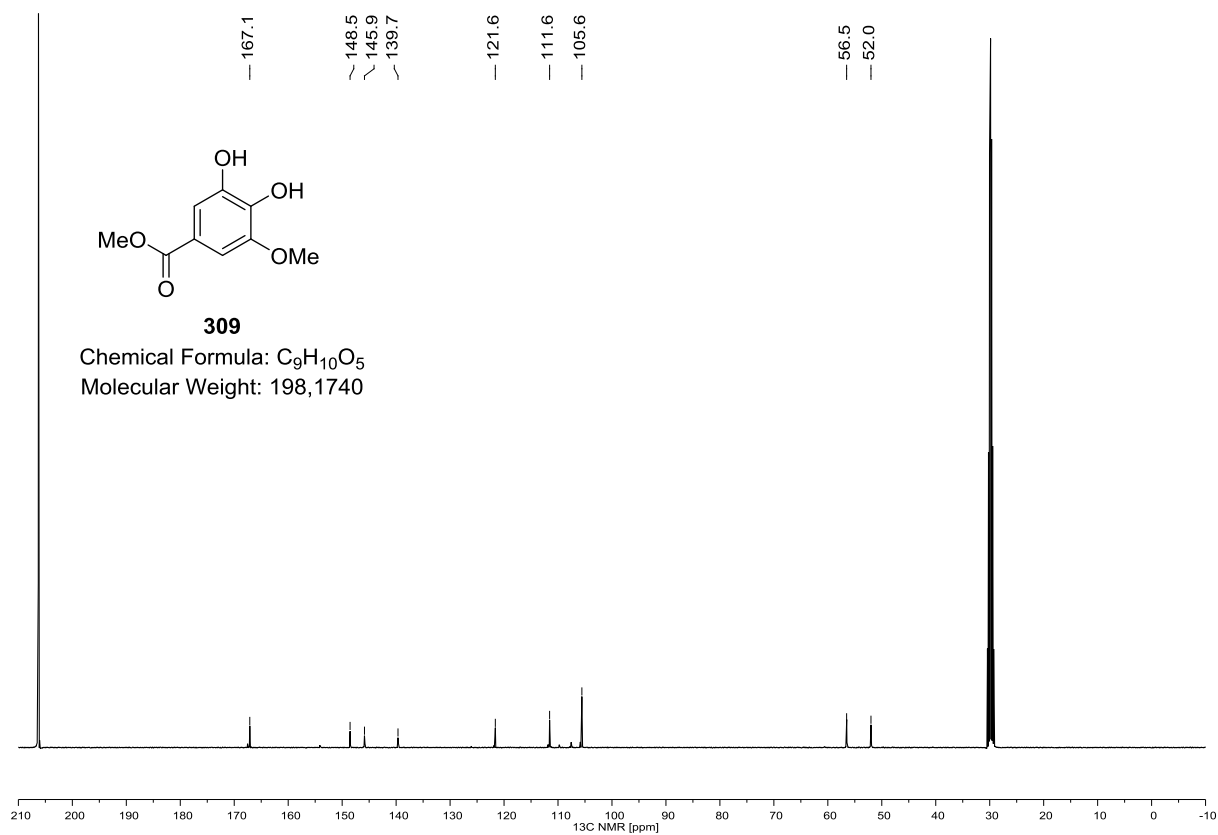
300 (¹H NMR, 400 MHz, CDCl₃)**300 (¹³C NMR, 100 MHz, CDCl₃)**

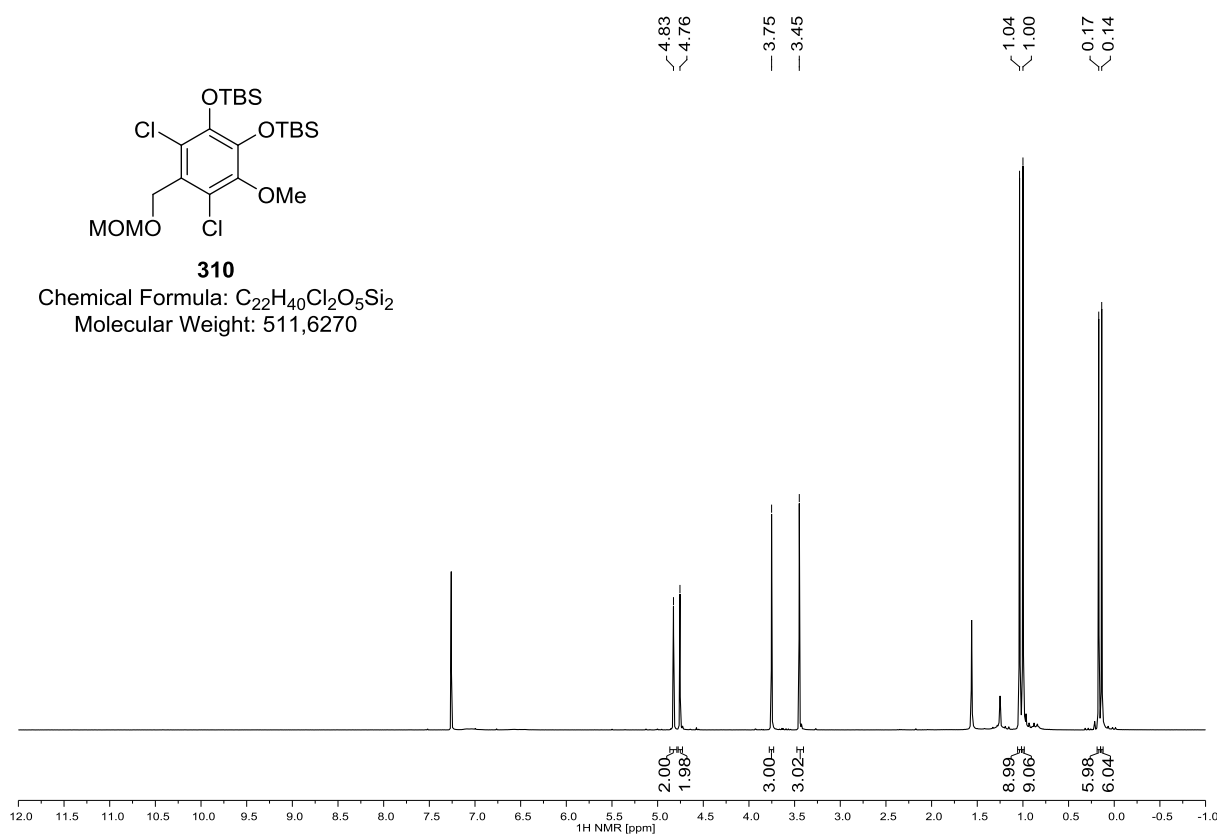
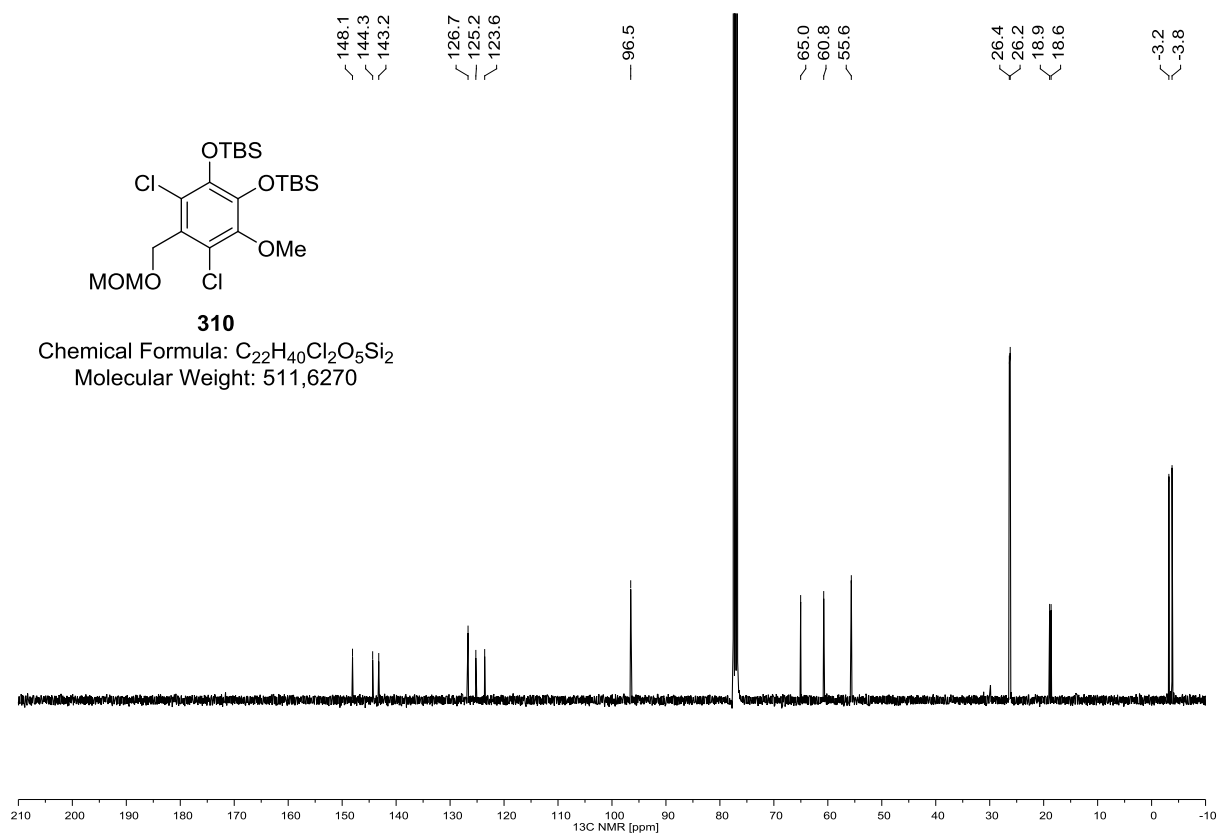
^1H NMR, 400 MHz, CDCl_3  **^{13}C NMR, 100 MHz, CDCl_3** 

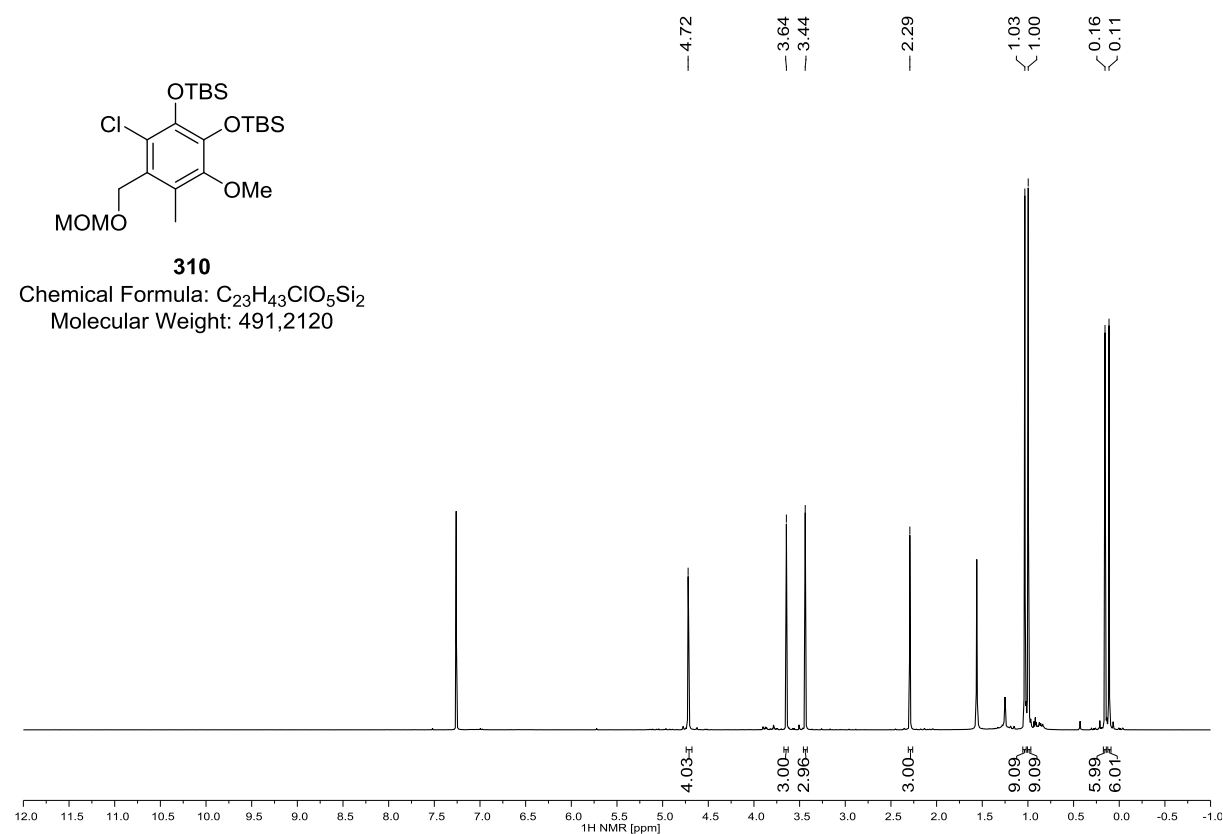
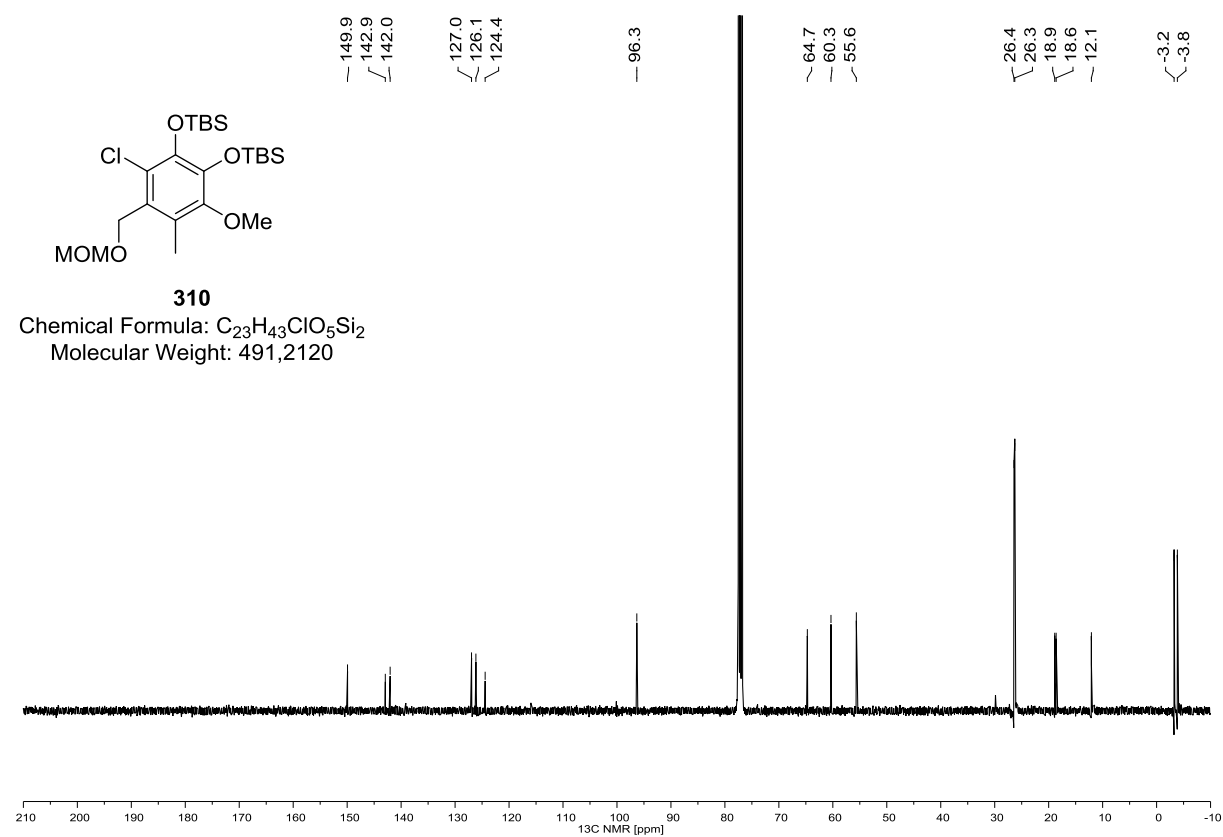
285 (^1H NMR, 400 MHz, CDCl_3)285 (^{13}C NMR, 100 MHz, CDCl_3)

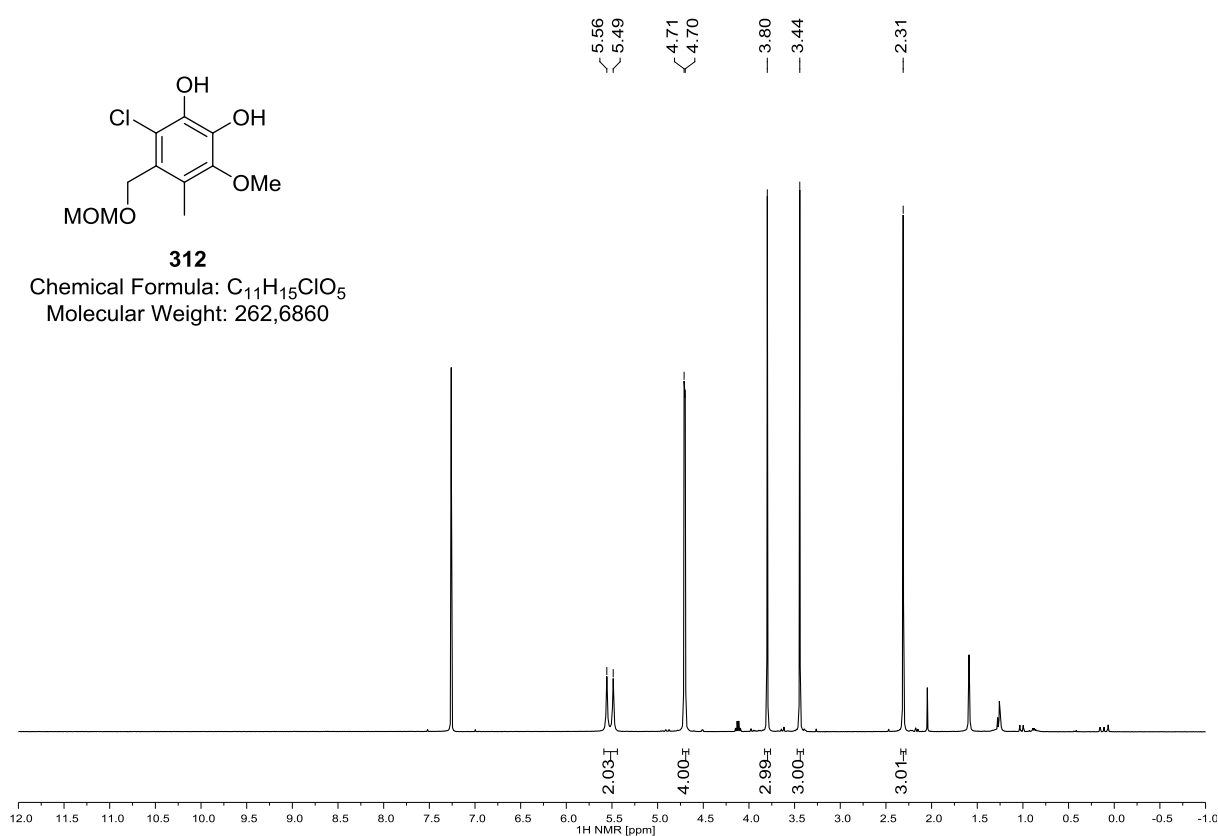
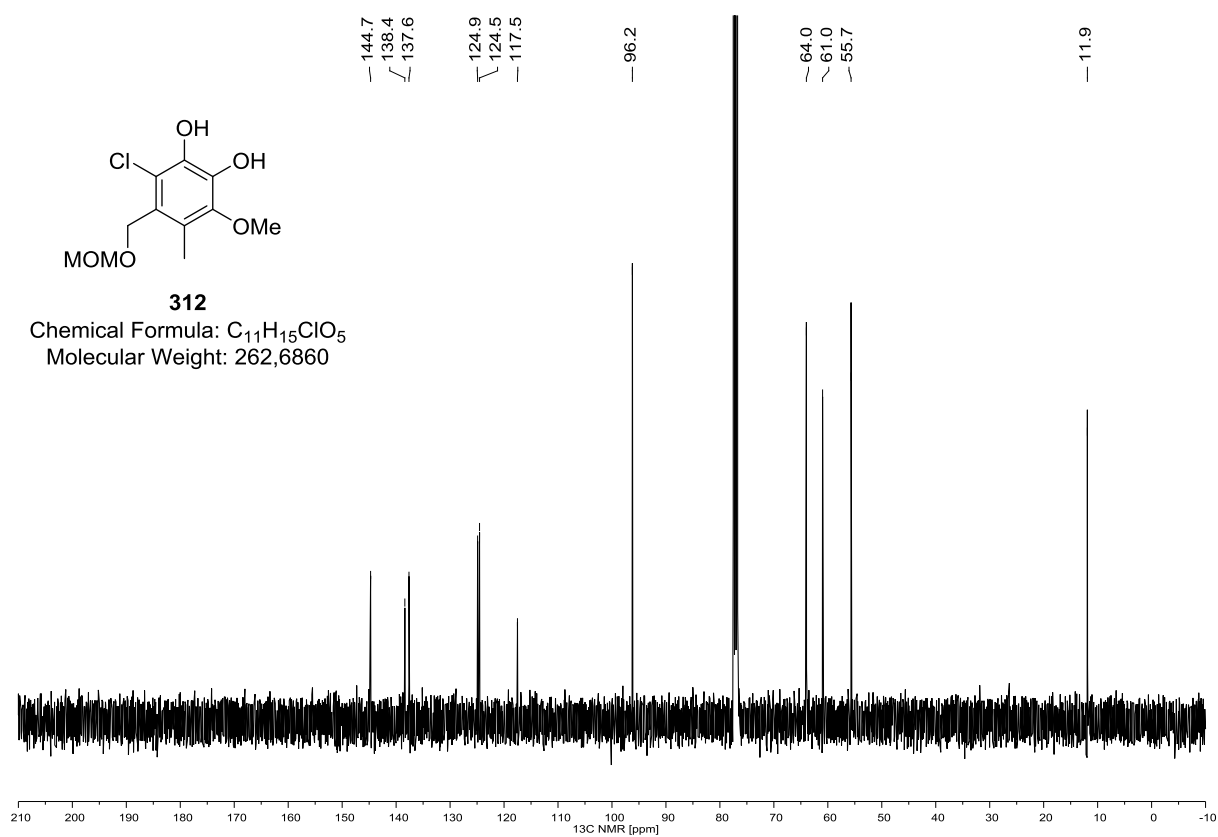
301 (^1H NMR, 400 MHz, CDCl_3)**301 (^{13}C NMR, 100 MHz, CDCl_3)**

286 (^1H NMR, 400 MHz, CDCl_3)**286 (^{13}C NMR, 100 MHz, CDCl_3)**

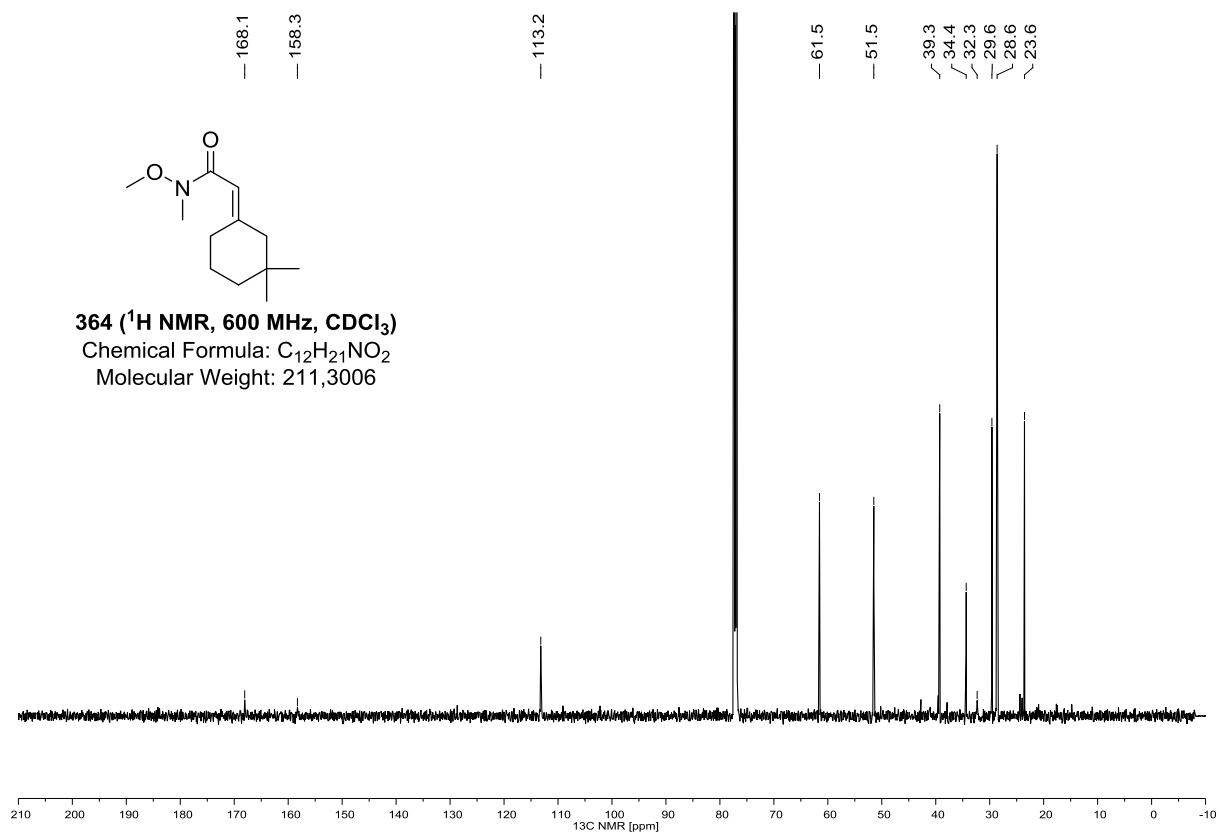
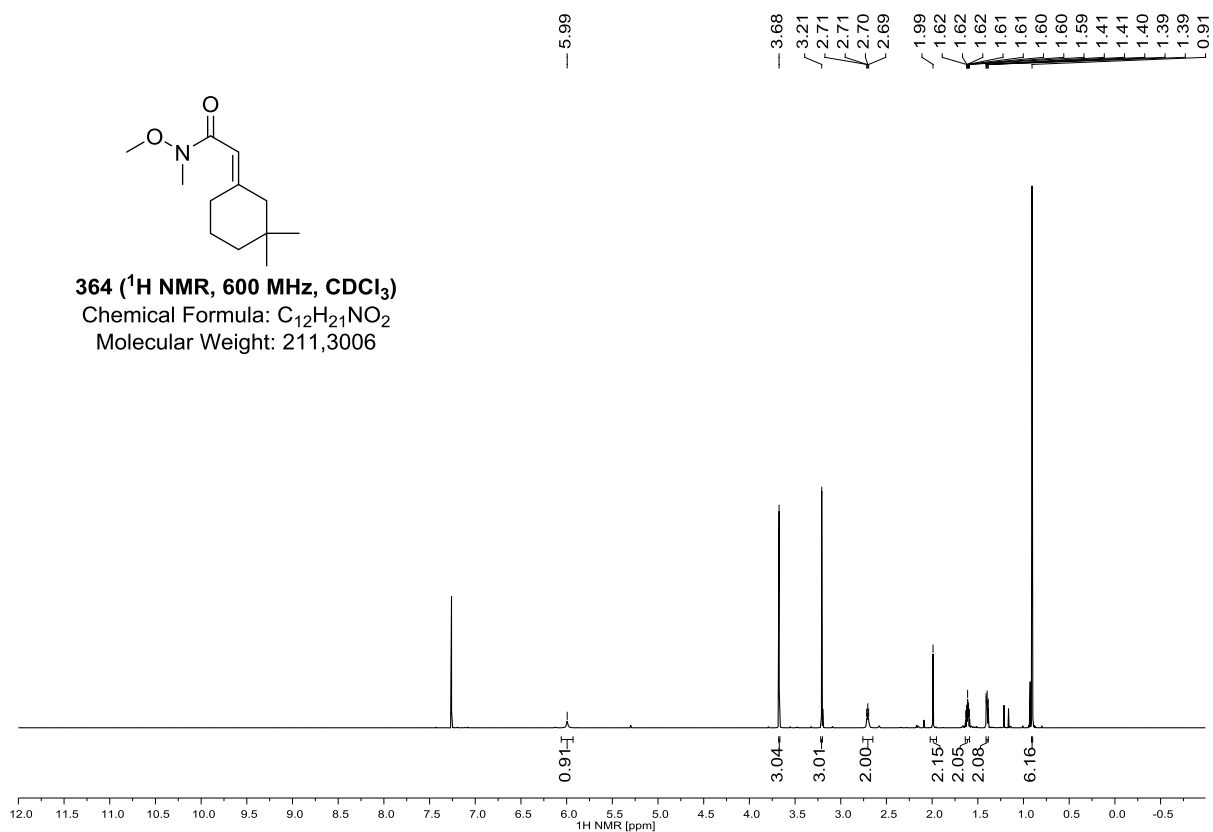
309 (^1H NMR, 400 MHz, $(\text{D}_3\text{C})_2\text{CO}$)**309 (^{13}C NMR, 100 MHz, $(\text{D}_3\text{C})_2\text{CO}$)**

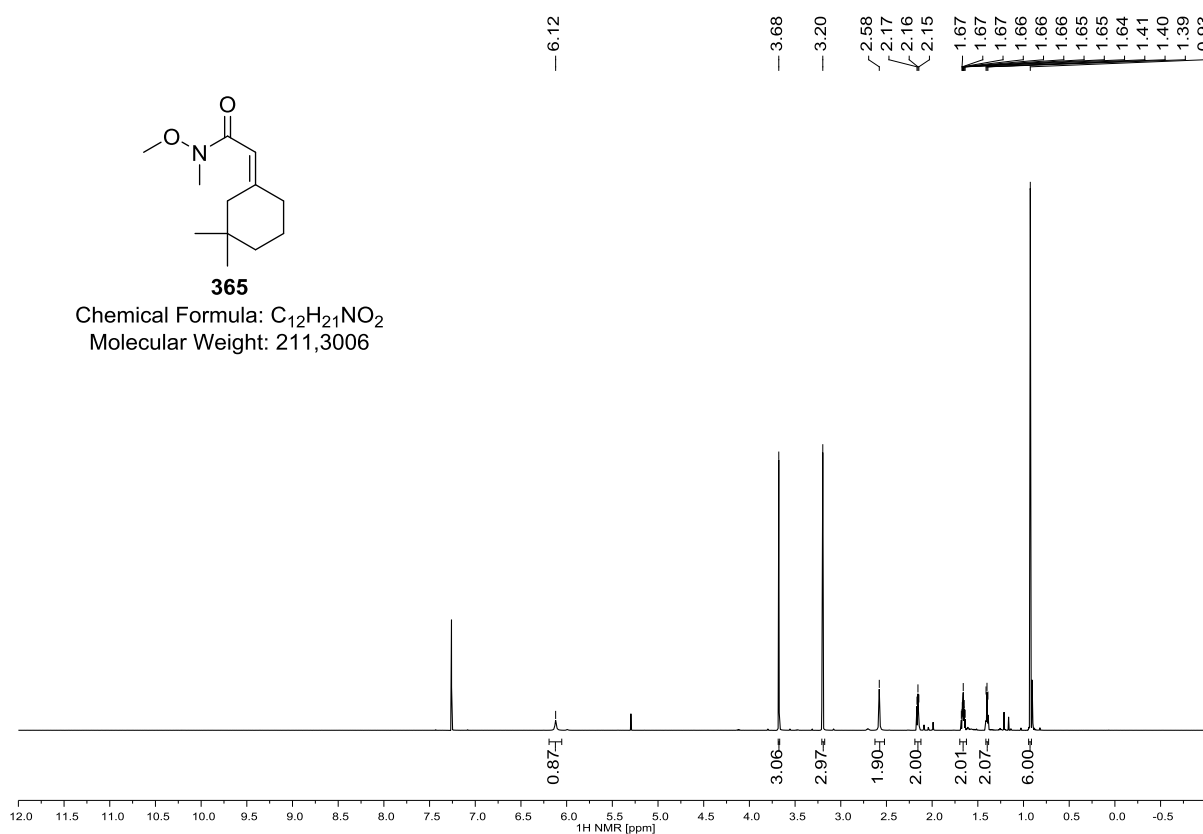
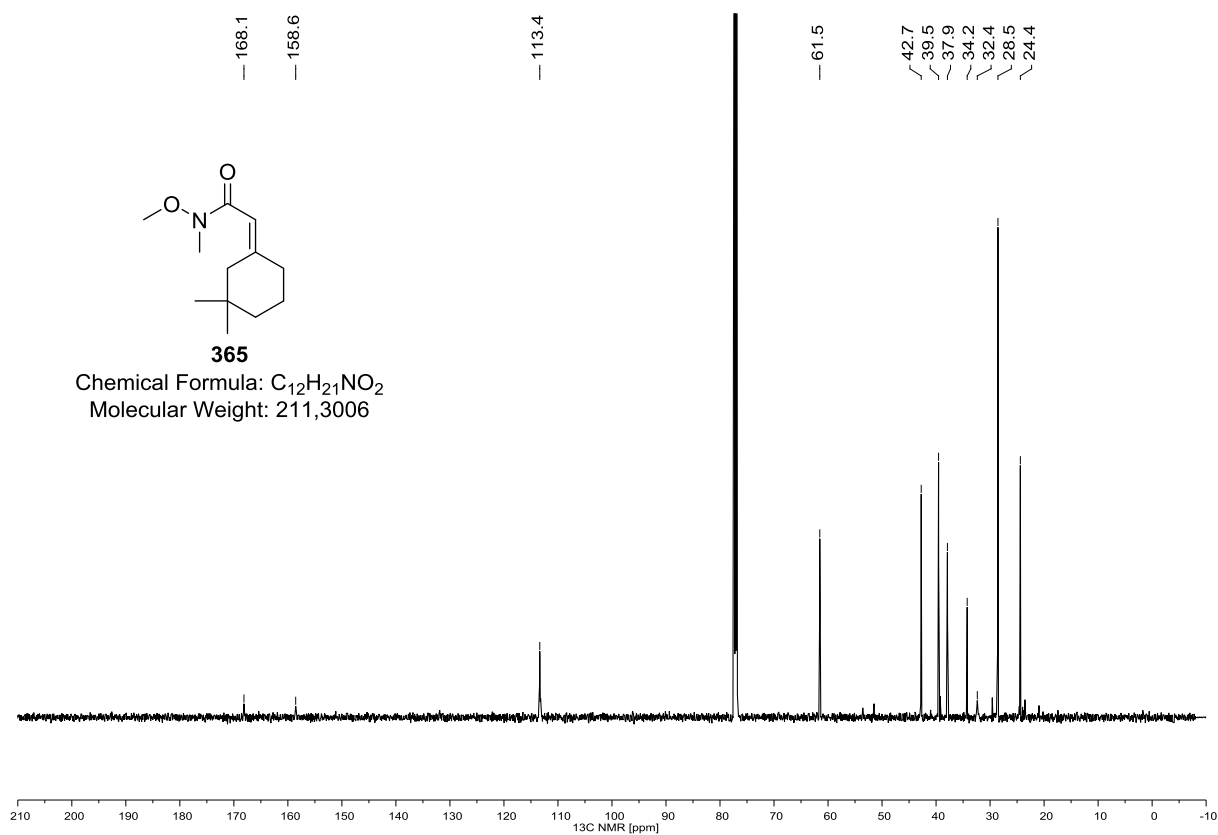
310 (^1H NMR, 400 MHz, CDCl_3)**310 (^1H NMR, 400 MHz, CDCl_3)**

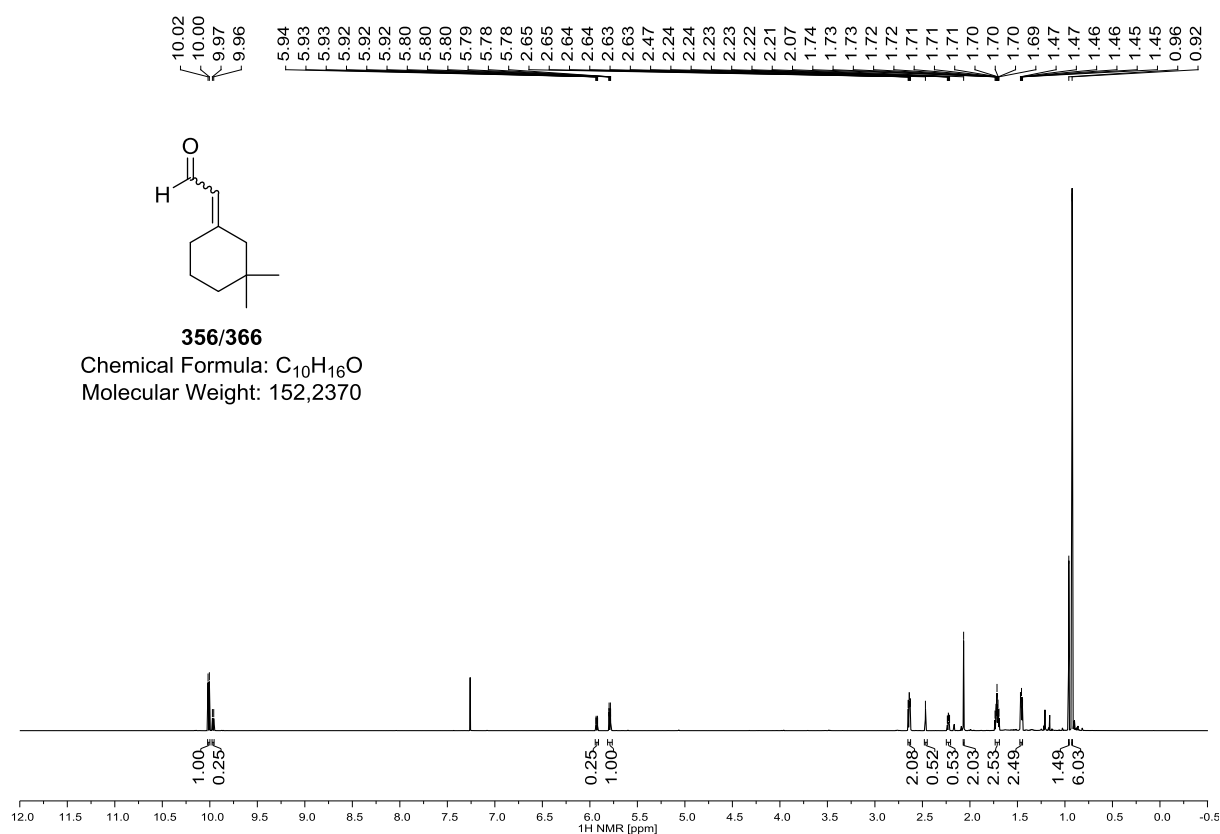
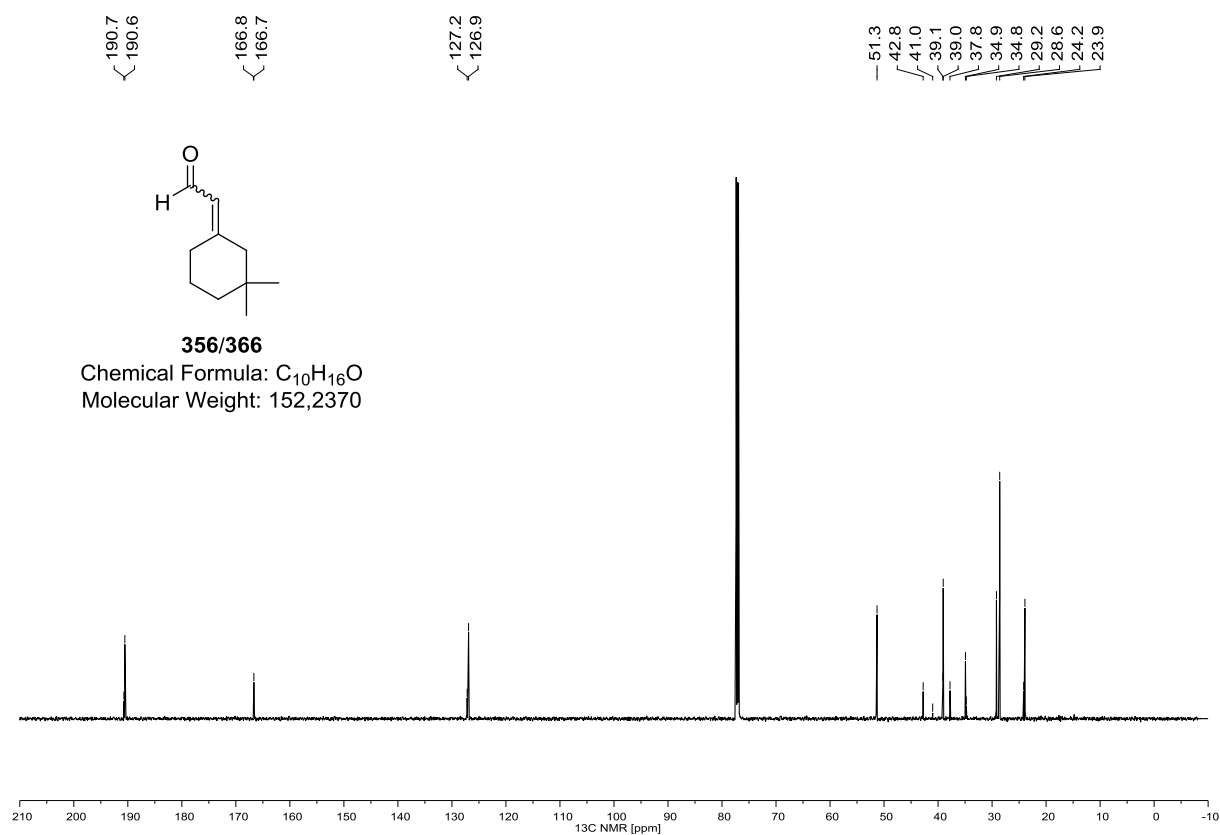
311 (^1H NMR, 400 MHz, CDCl_3)311 (^{13}C NMR, 100 MHz, CDCl_3)

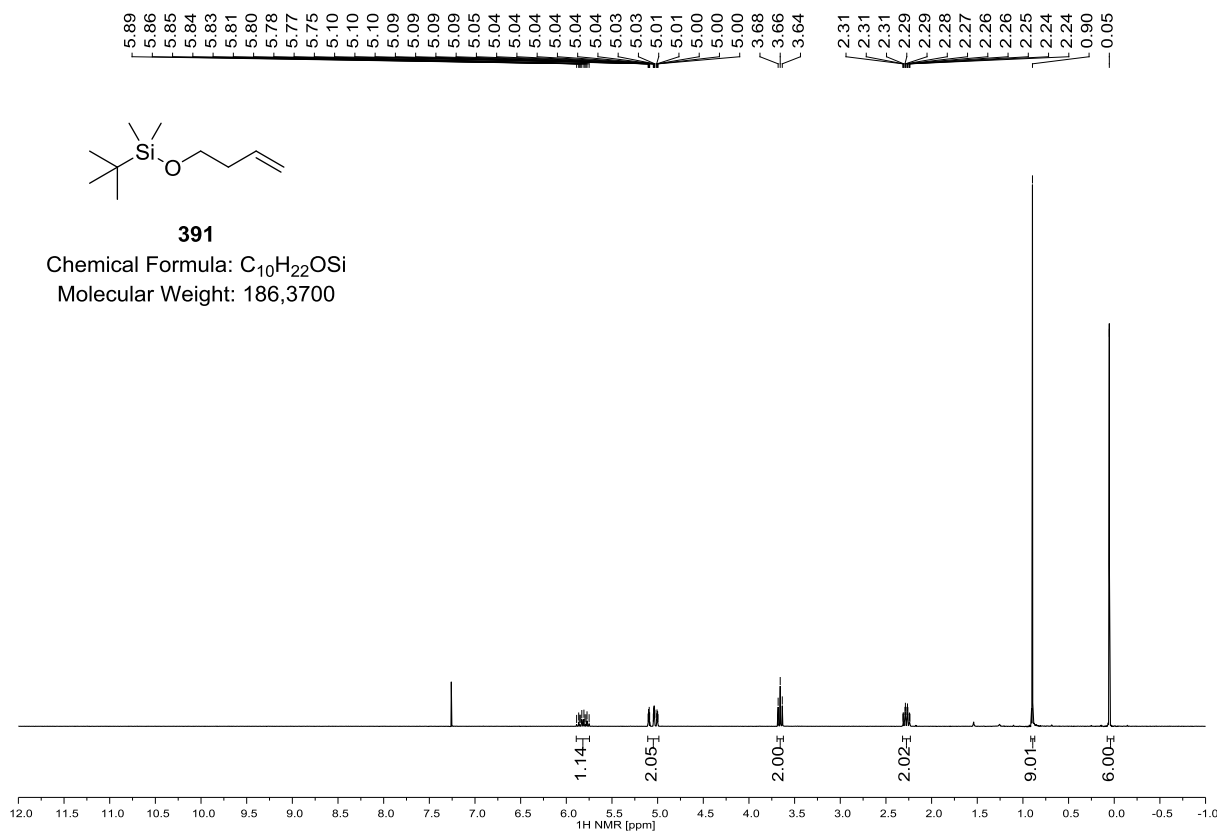
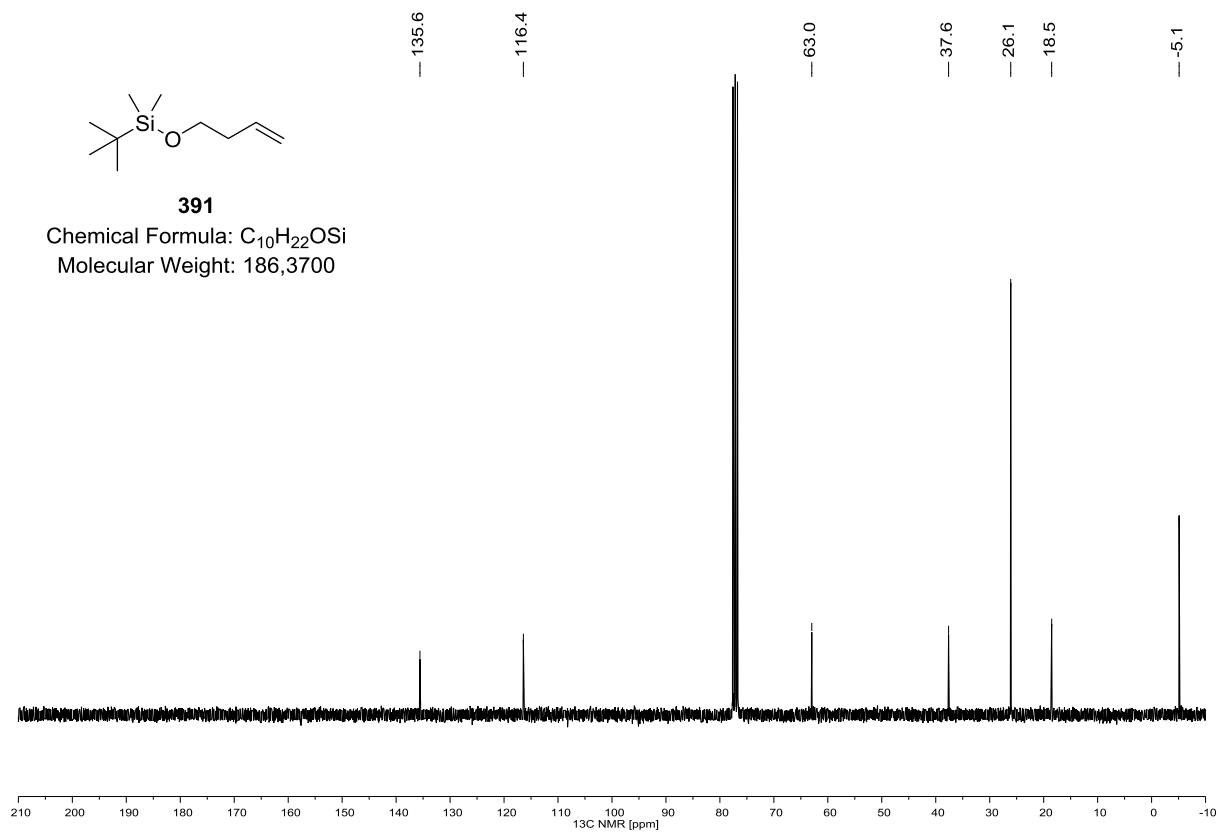
312 (^1H NMR, 400 MHz, CDCl_3)**312 (^{13}C NMR, 100 MHz, CDCl_3)**

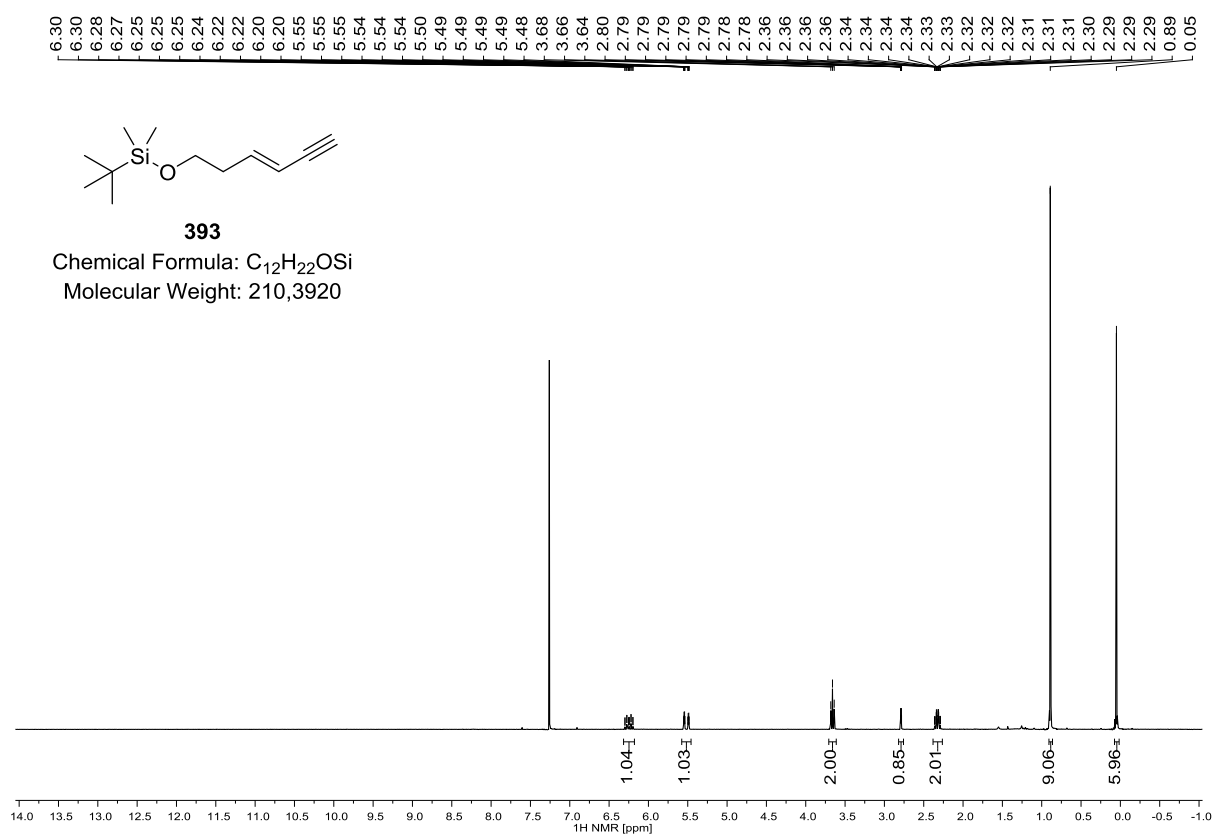
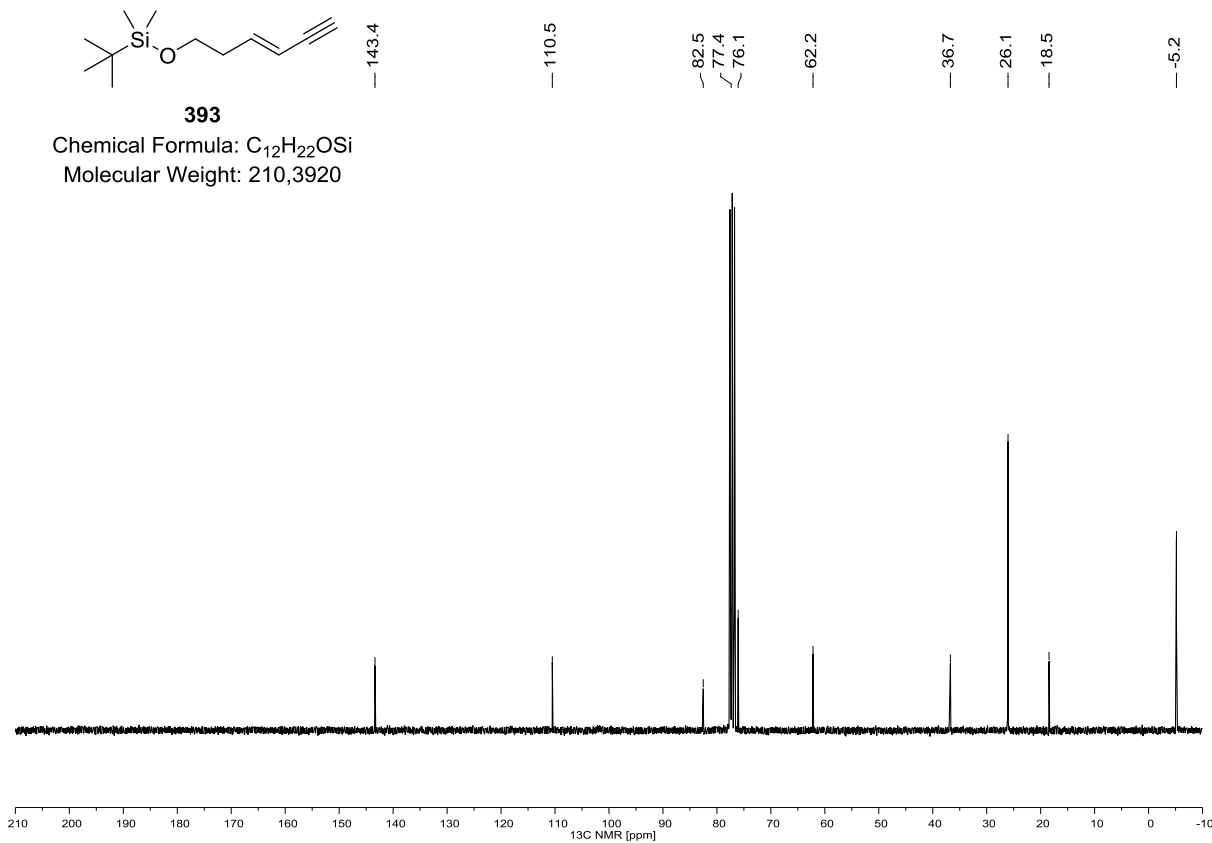
7.2 PART II: Total Synthesis of Gracilin Natural Products

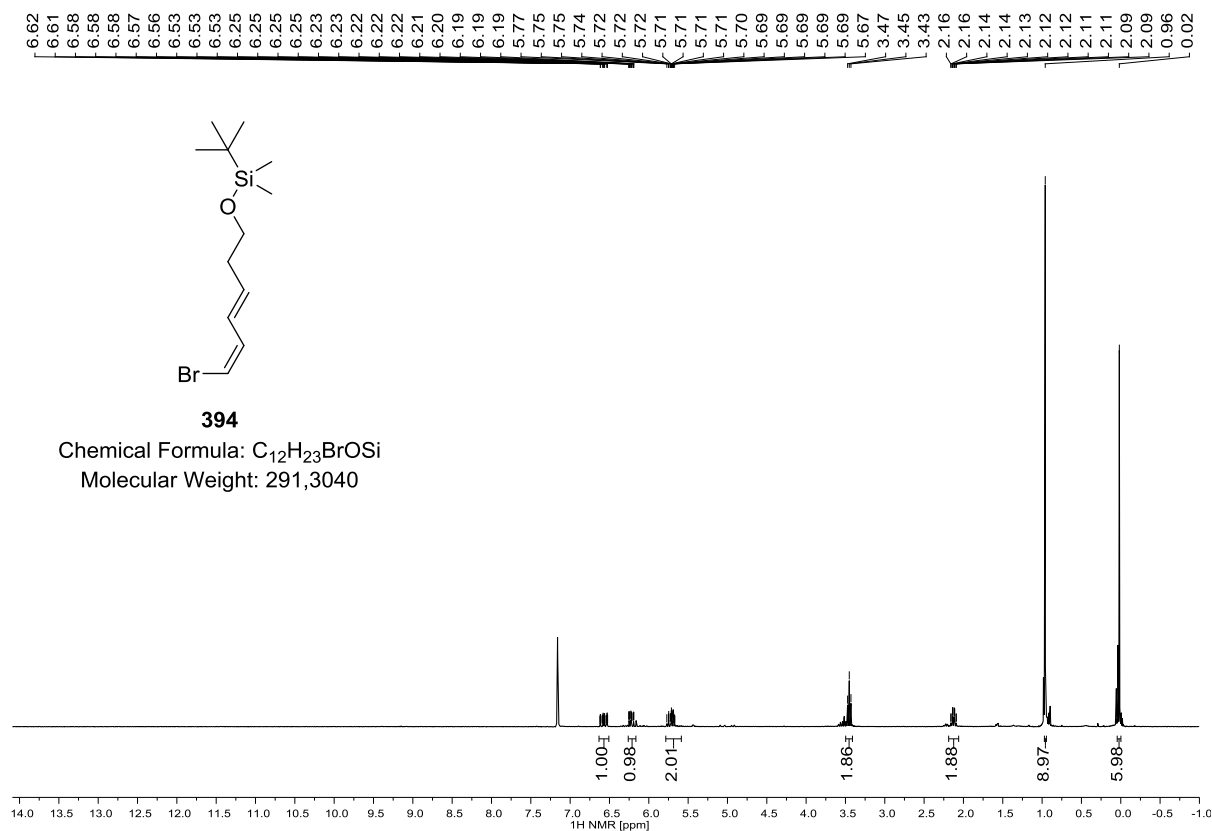
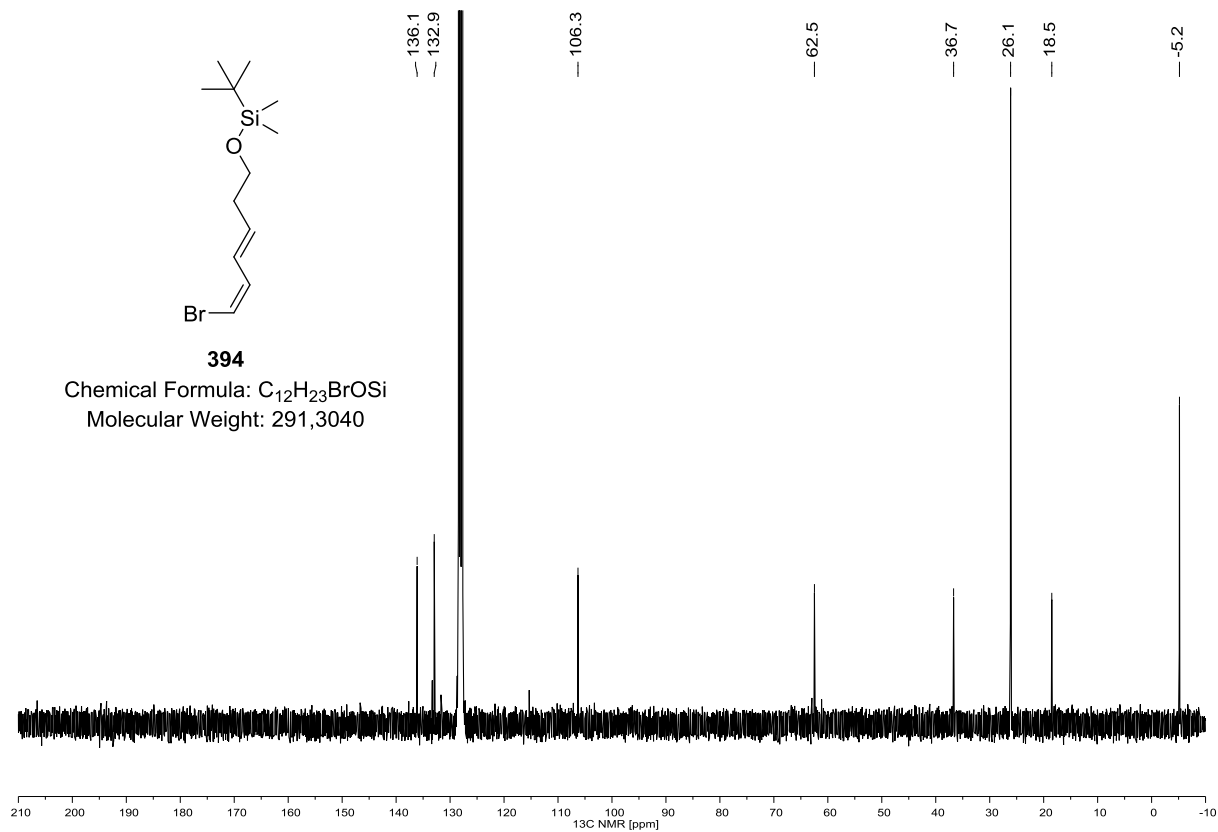


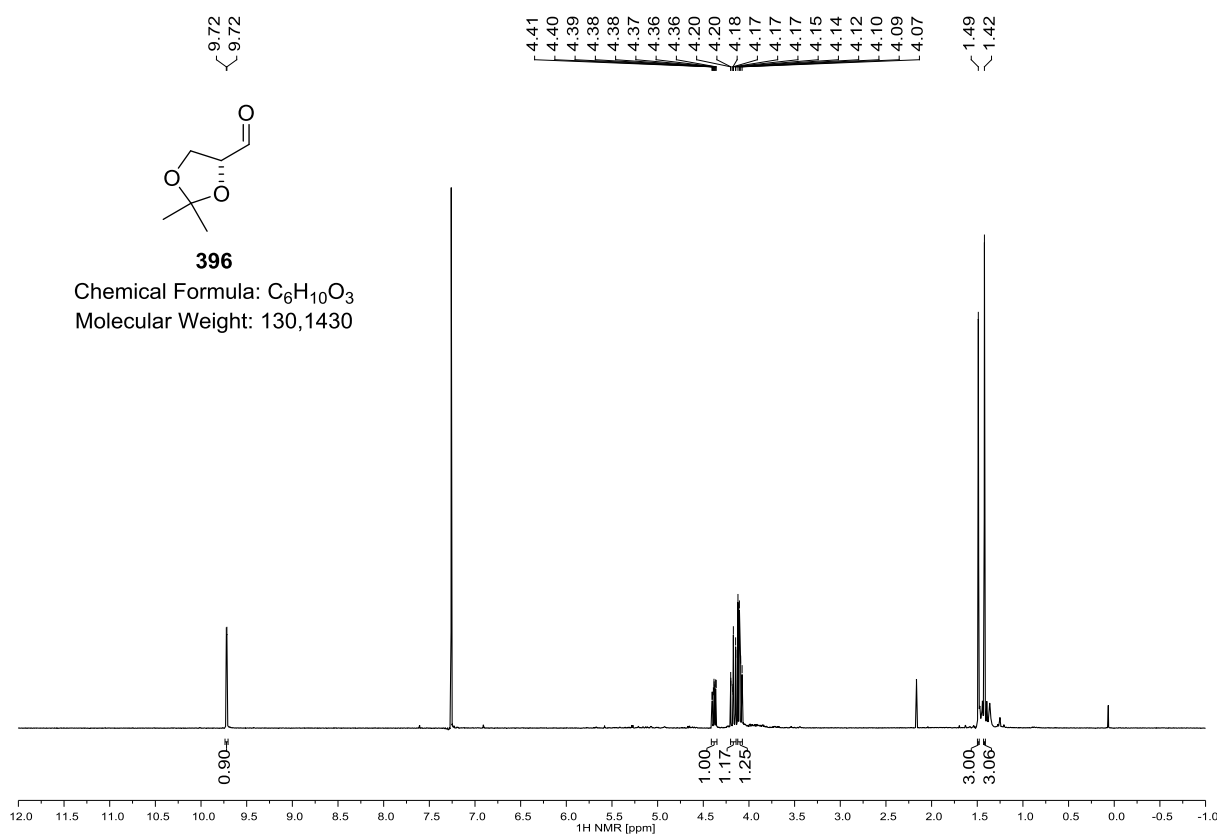
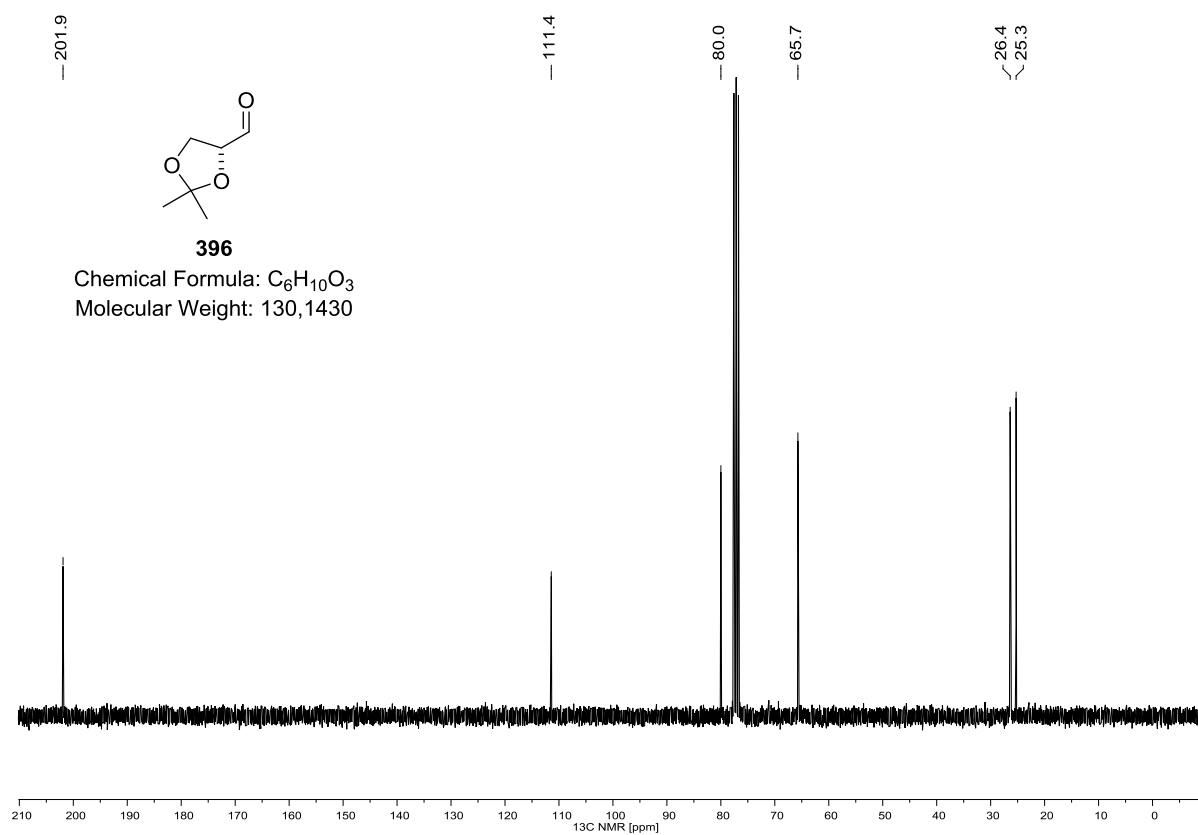
365 (^1H NMR, 600 MHz, CDCl_3)**365 (^{13}C NMR, 150 MHz, CDCl_3)**

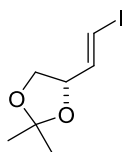
356/366 (^1H NMR, 600 MHz, CDCl_3)**356/366 (^{13}C NMR, 150 MHz, CDCl_3)**

391 (^1H NMR, 300 MHz, CDCl_3)**391 (^{13}C NMR, 75 MHz, CDCl_3)**

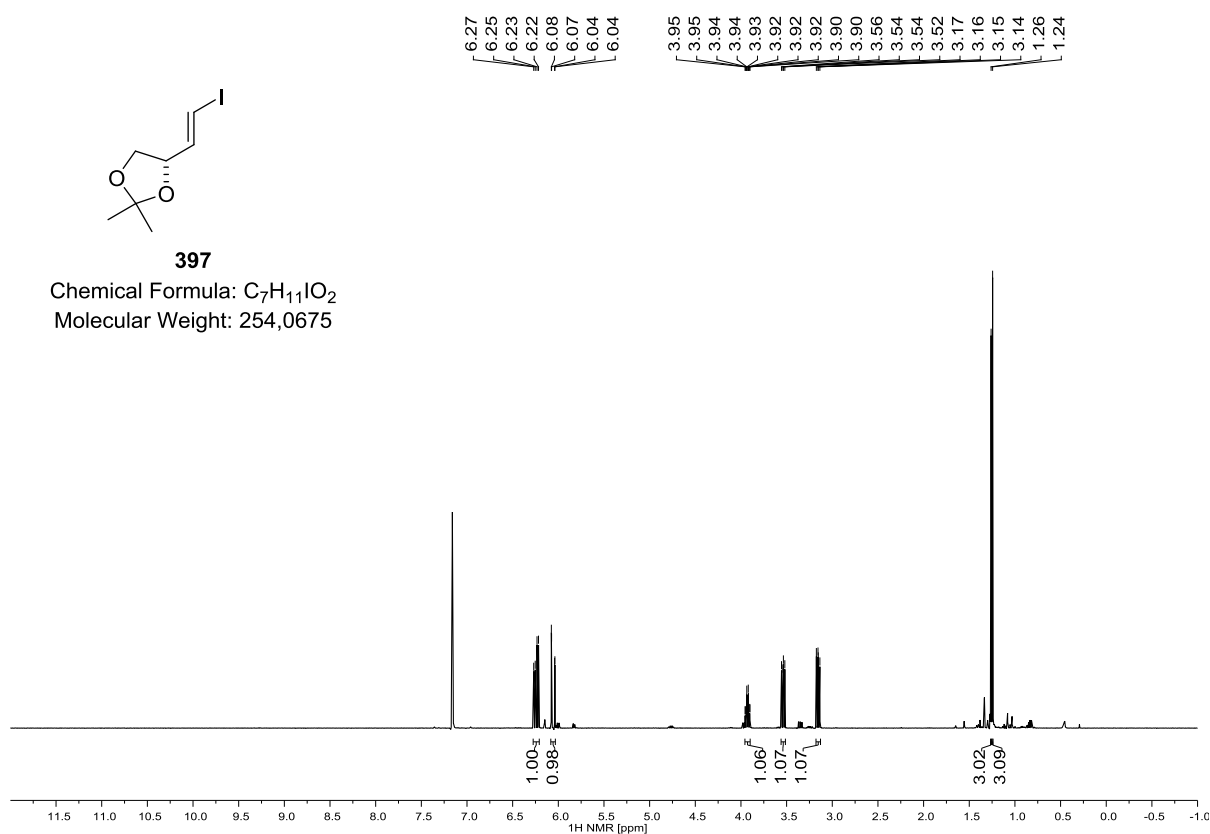
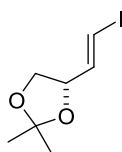
393 (^1H NMR, 300 MHz, CDCl_3)**393 (^{13}C NMR, 75 MHz, CDCl_3)**

394 (^1H NMR, 300 MHz, C_6D_6)**394 (^{13}C NMR, 75 MHz, C_6D_6)**

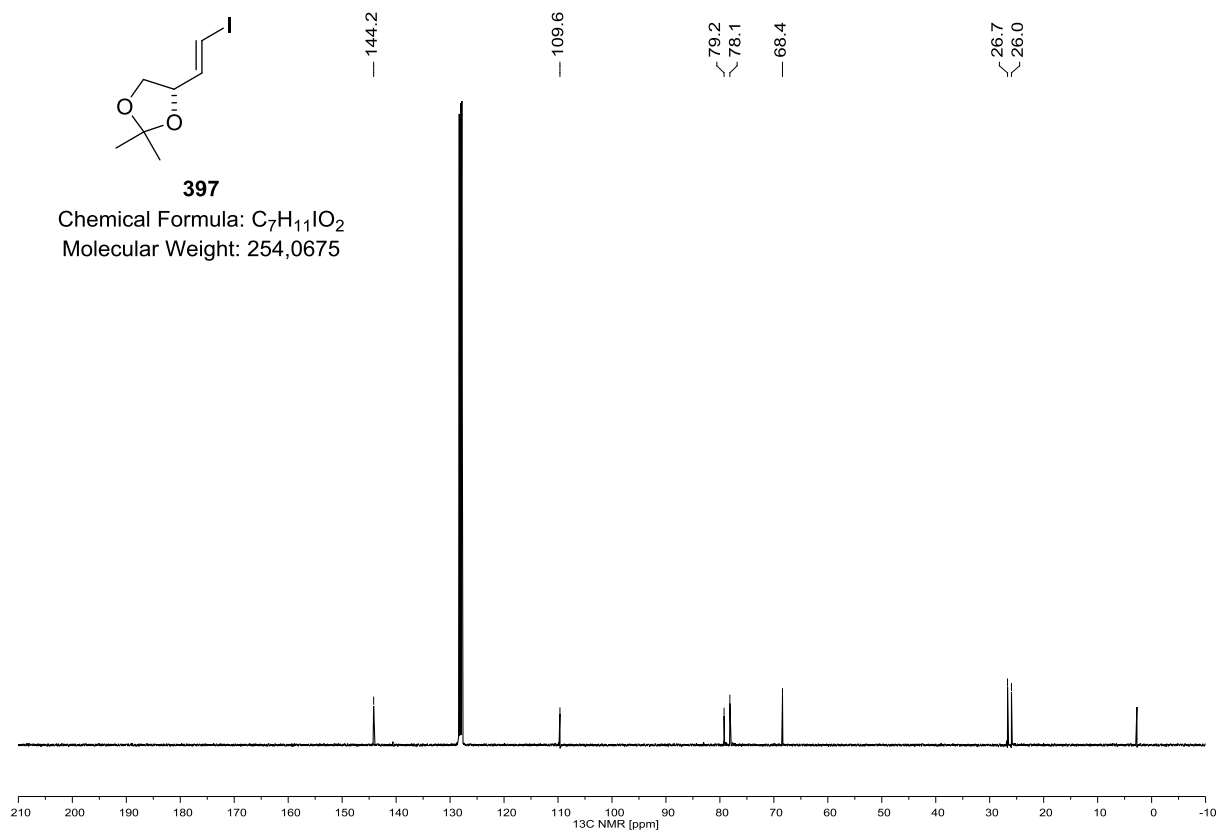
396 (^1H NMR, 300 MHz, CDCl_3)**396 (^{13}C NMR, 75 MHz, CDCl_3)**

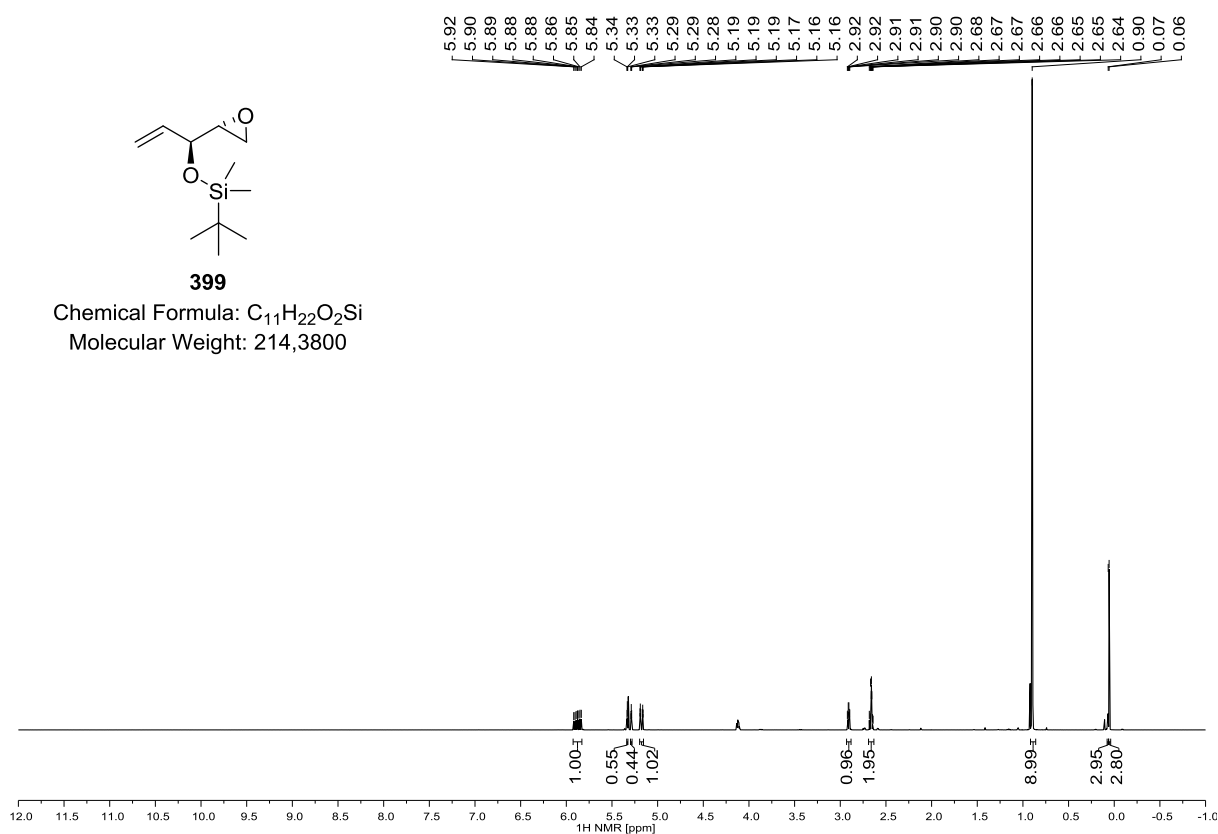
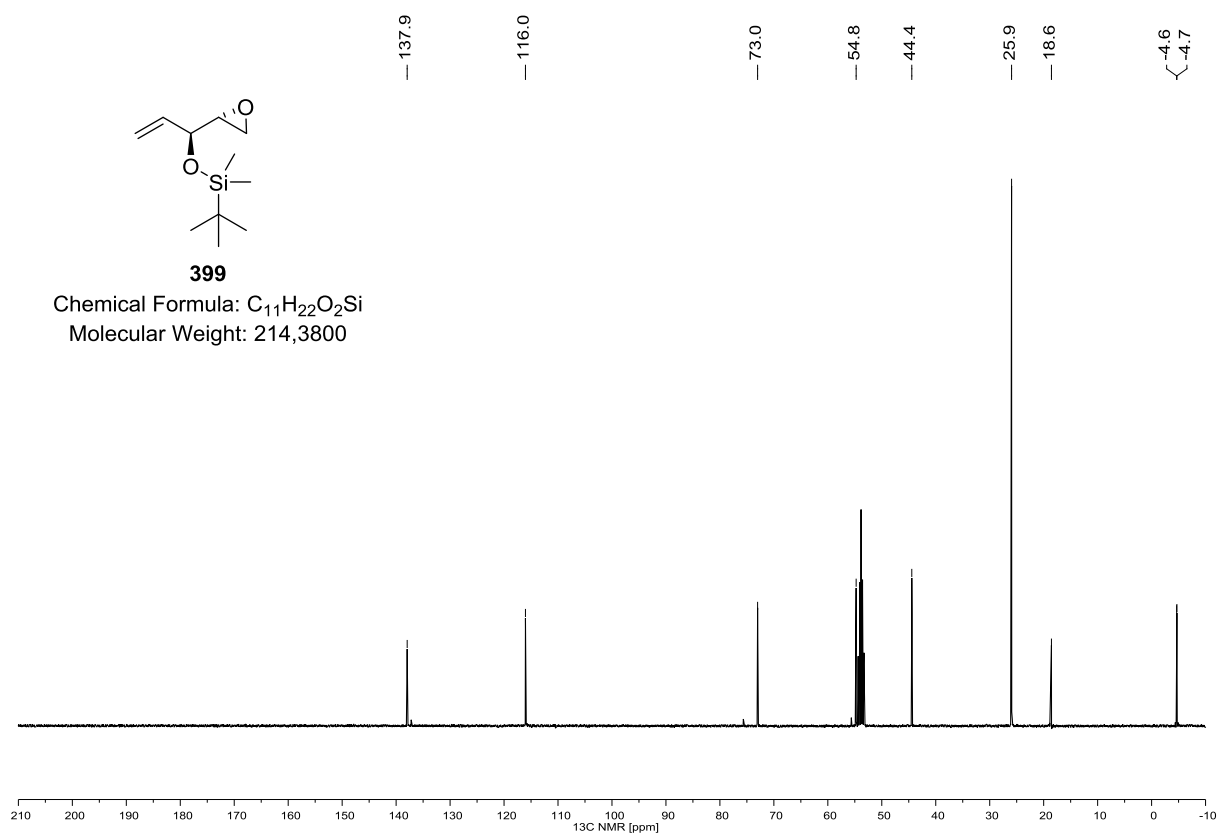
397 (^1H NMR, 400 MHz, C_6D_6)**397**Chemical Formula: $\text{C}_7\text{H}_{11}\text{IO}_2$

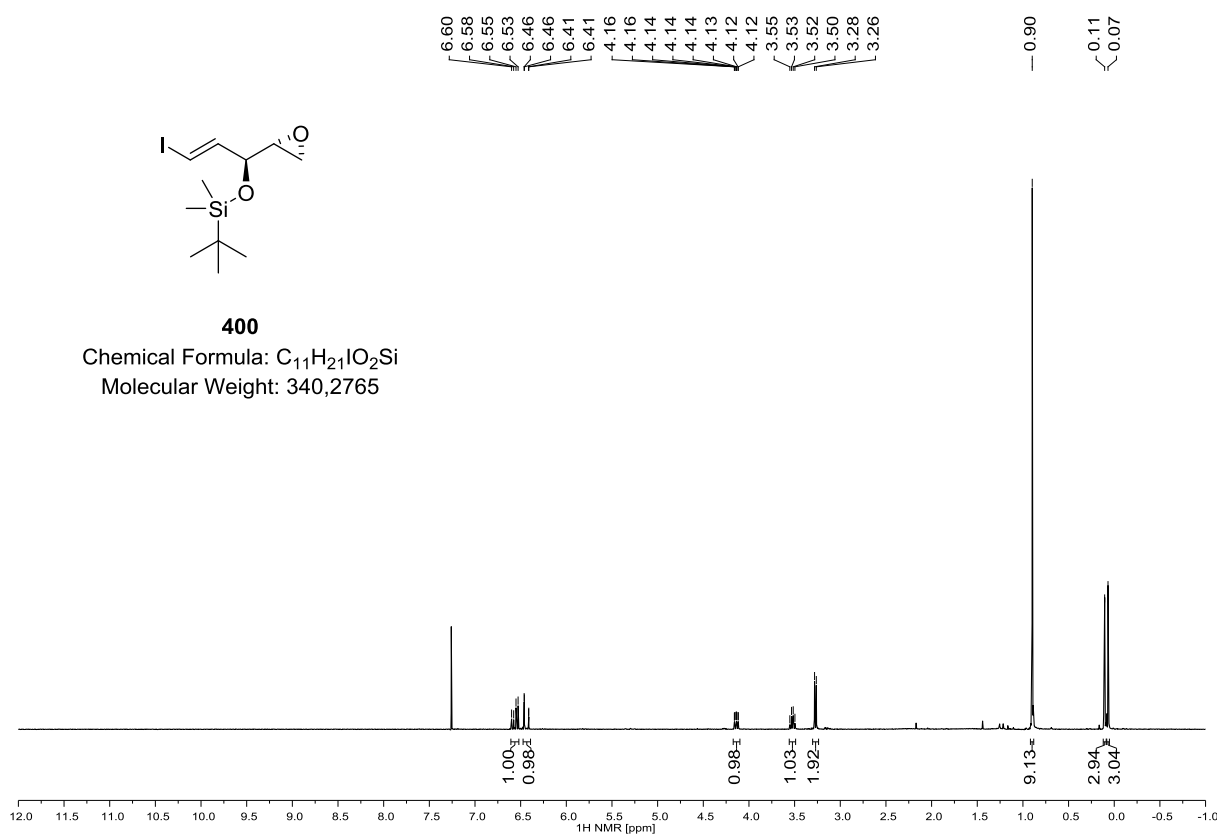
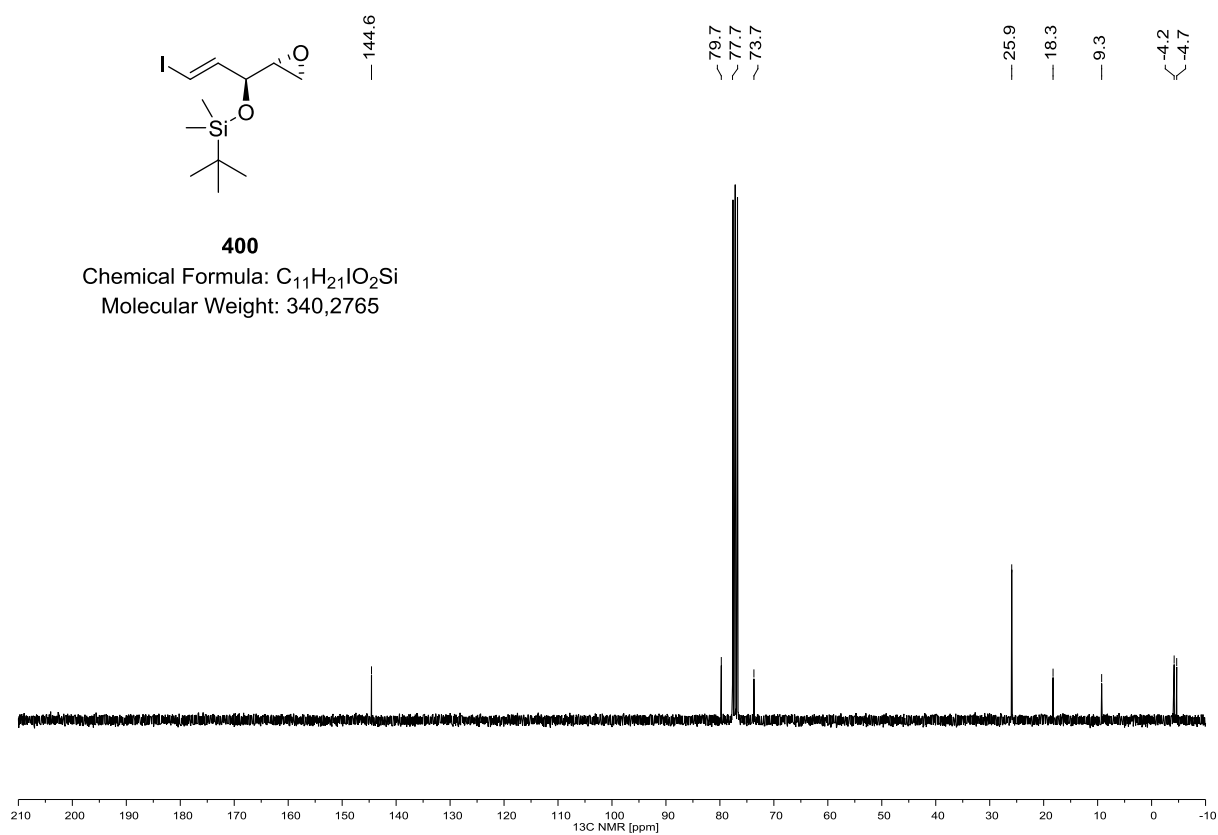
Molecular Weight: 254,0675

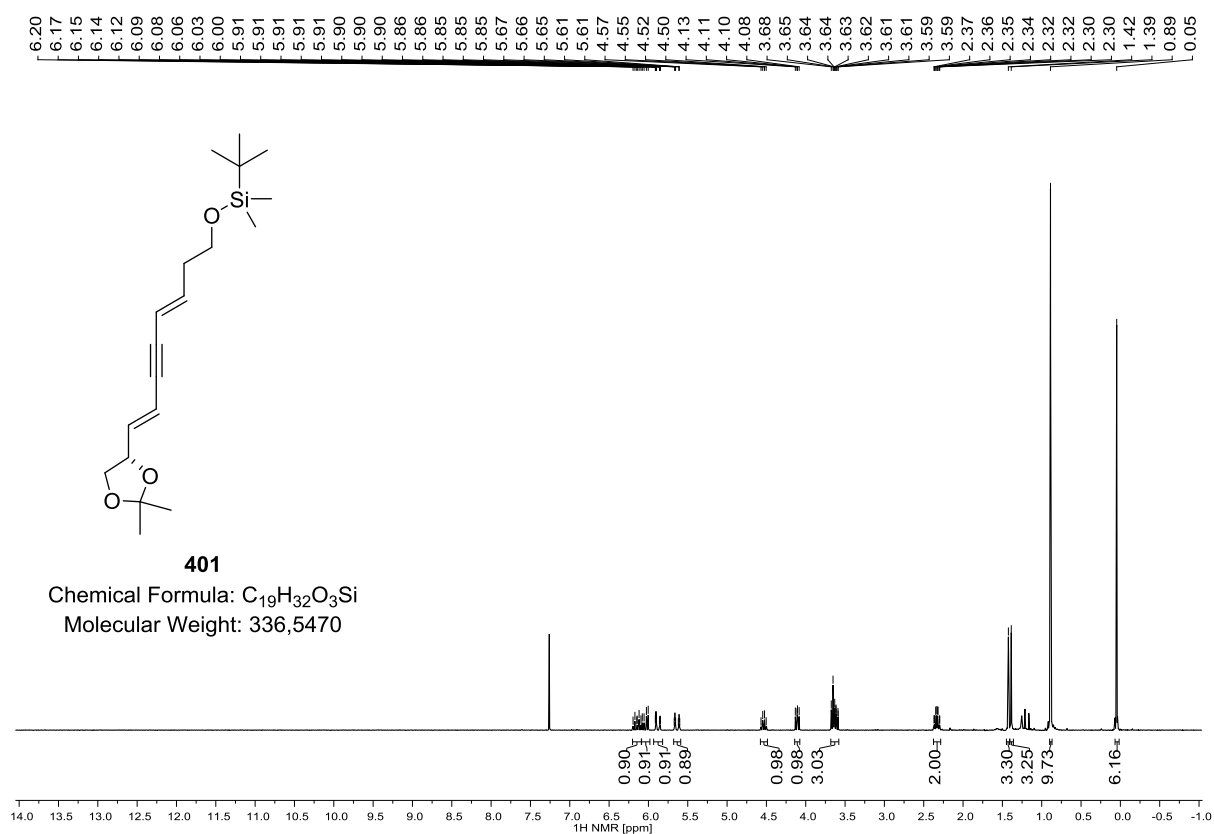
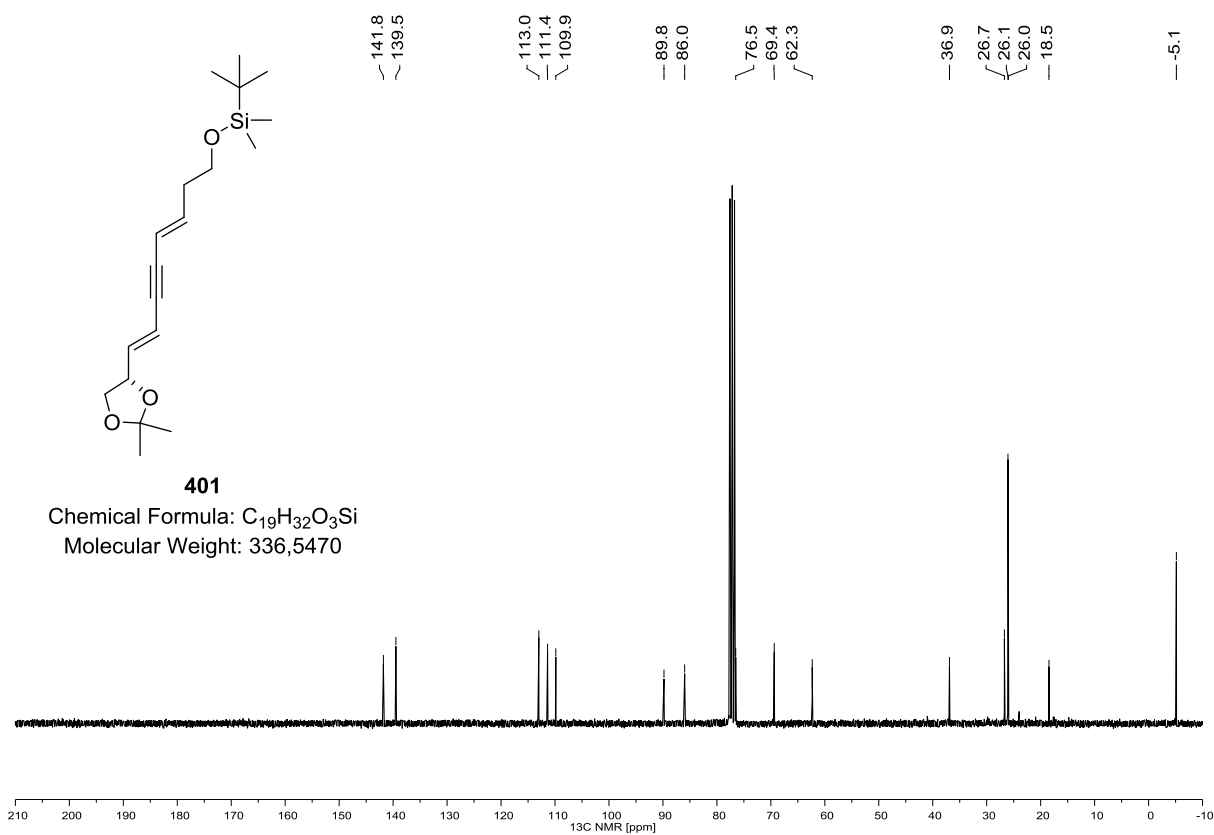
**397 (^{13}C NMR, 100 MHz, C_6D_6)****397**Chemical Formula: $\text{C}_7\text{H}_{11}\text{IO}_2$

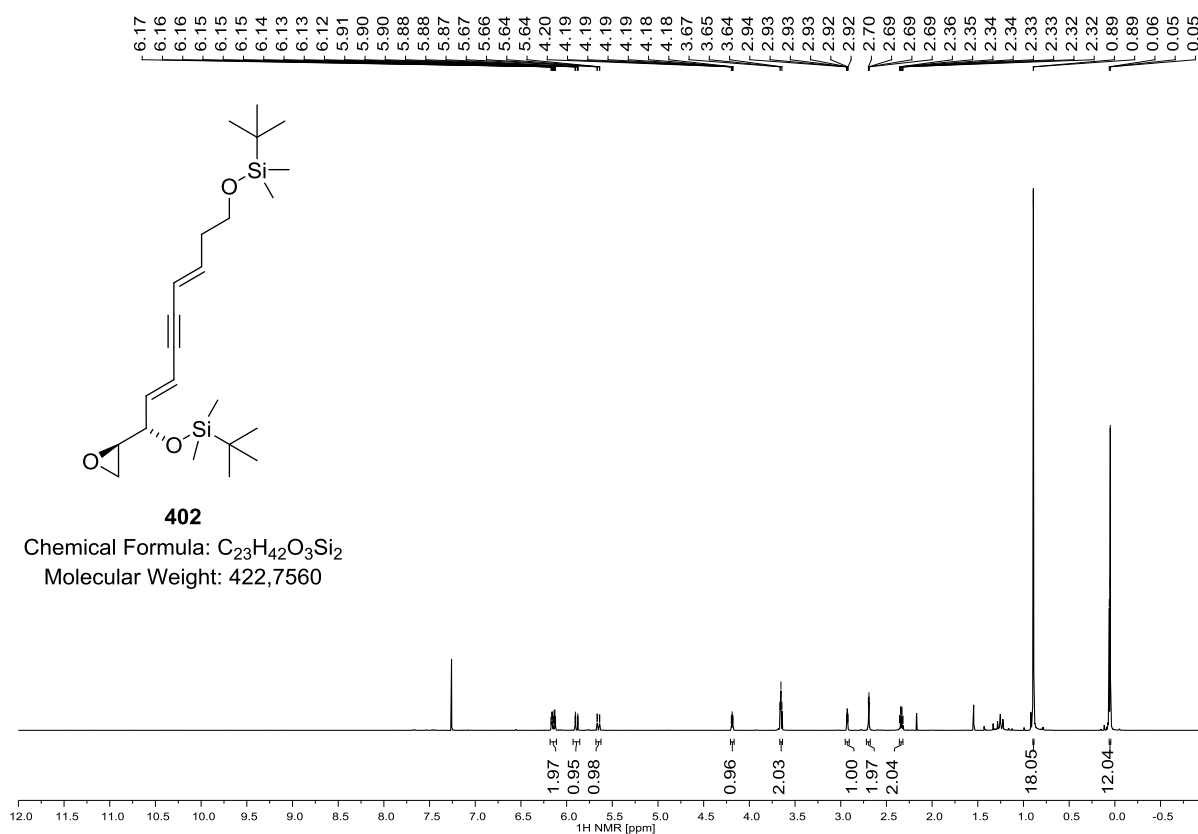
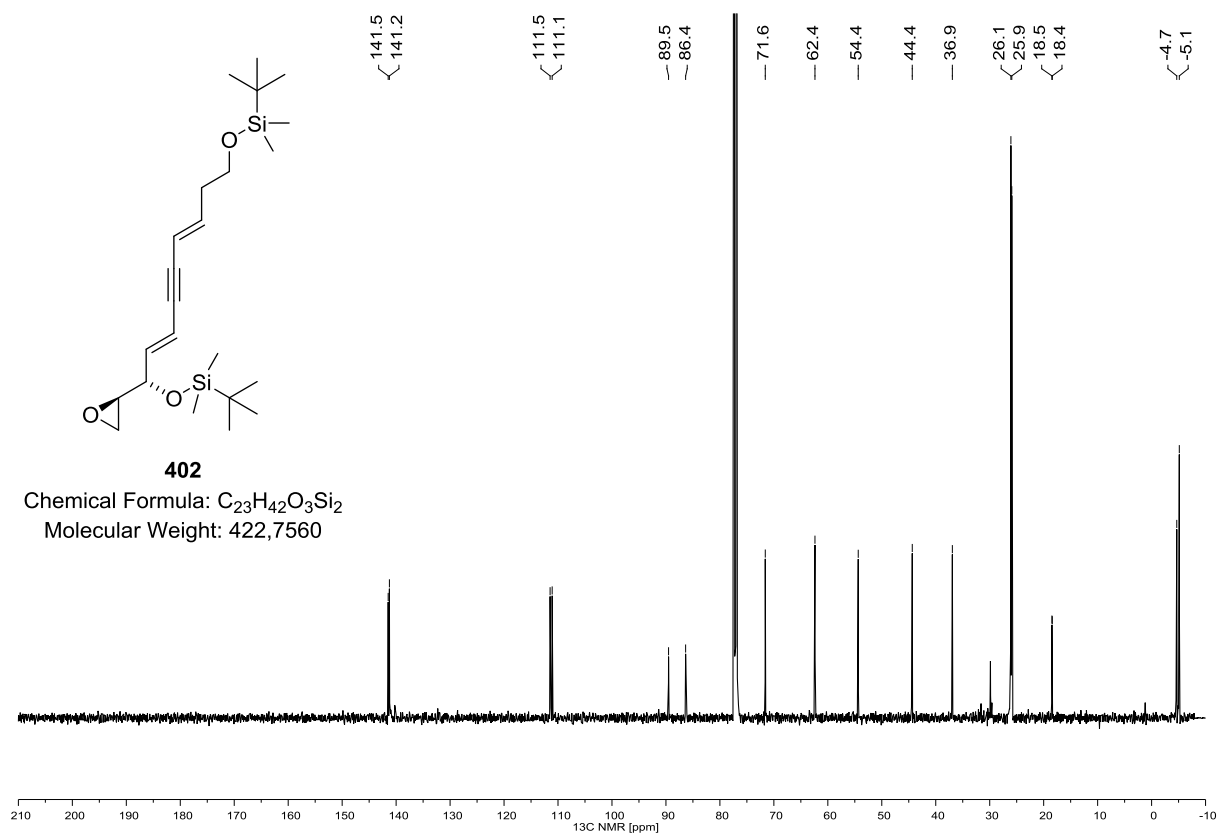
Molecular Weight: 254,0675

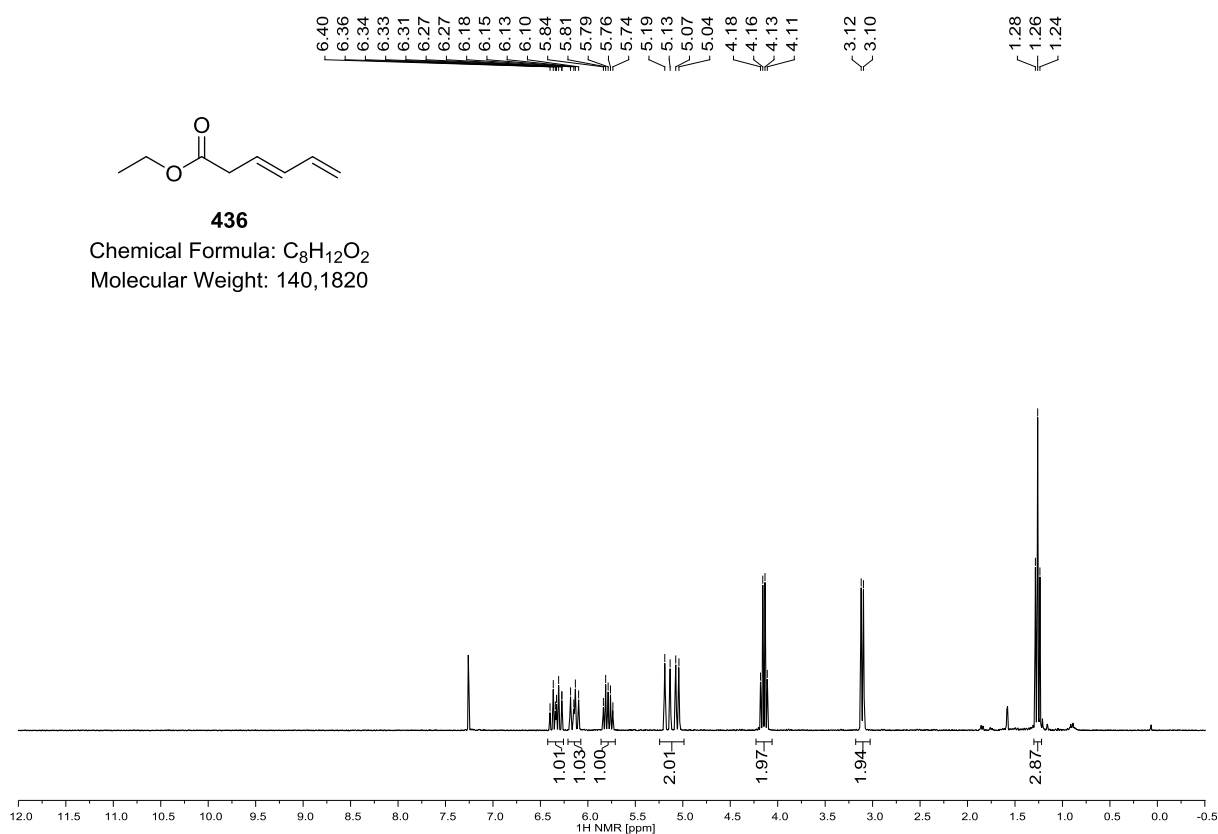
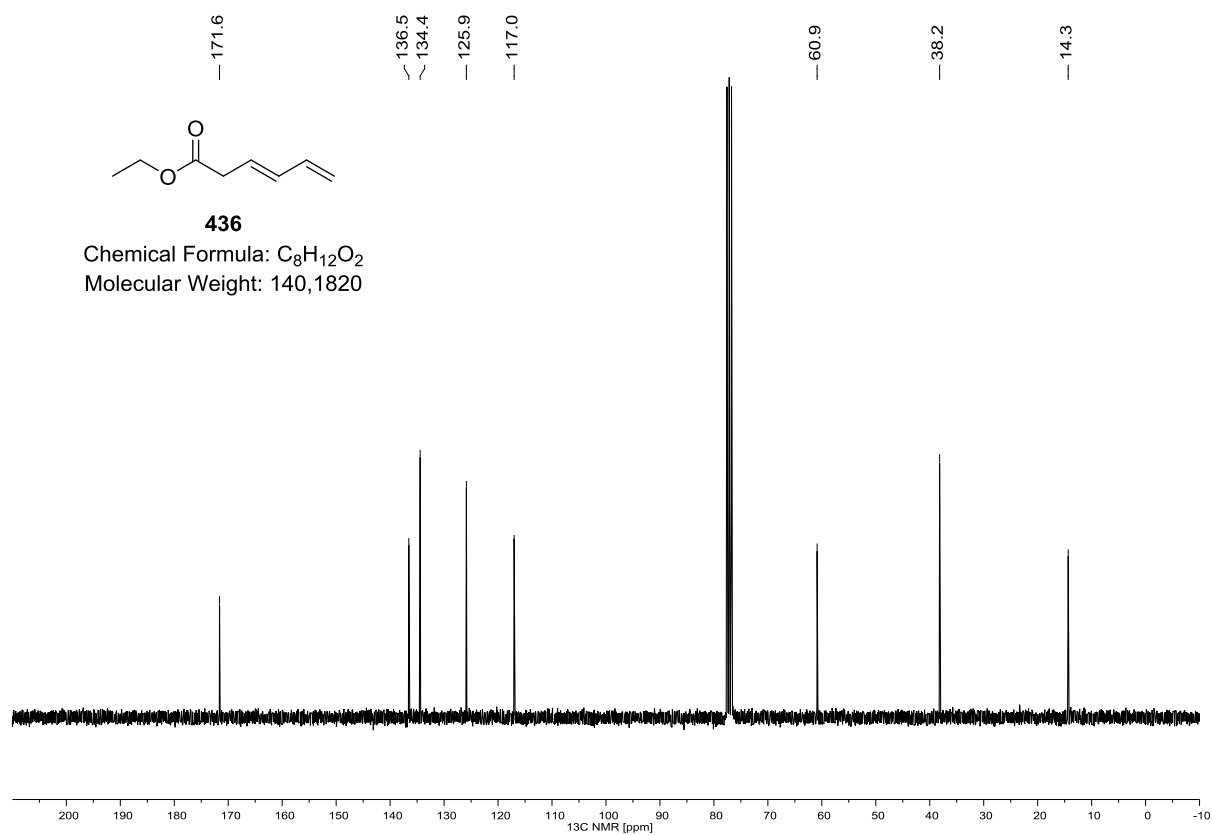


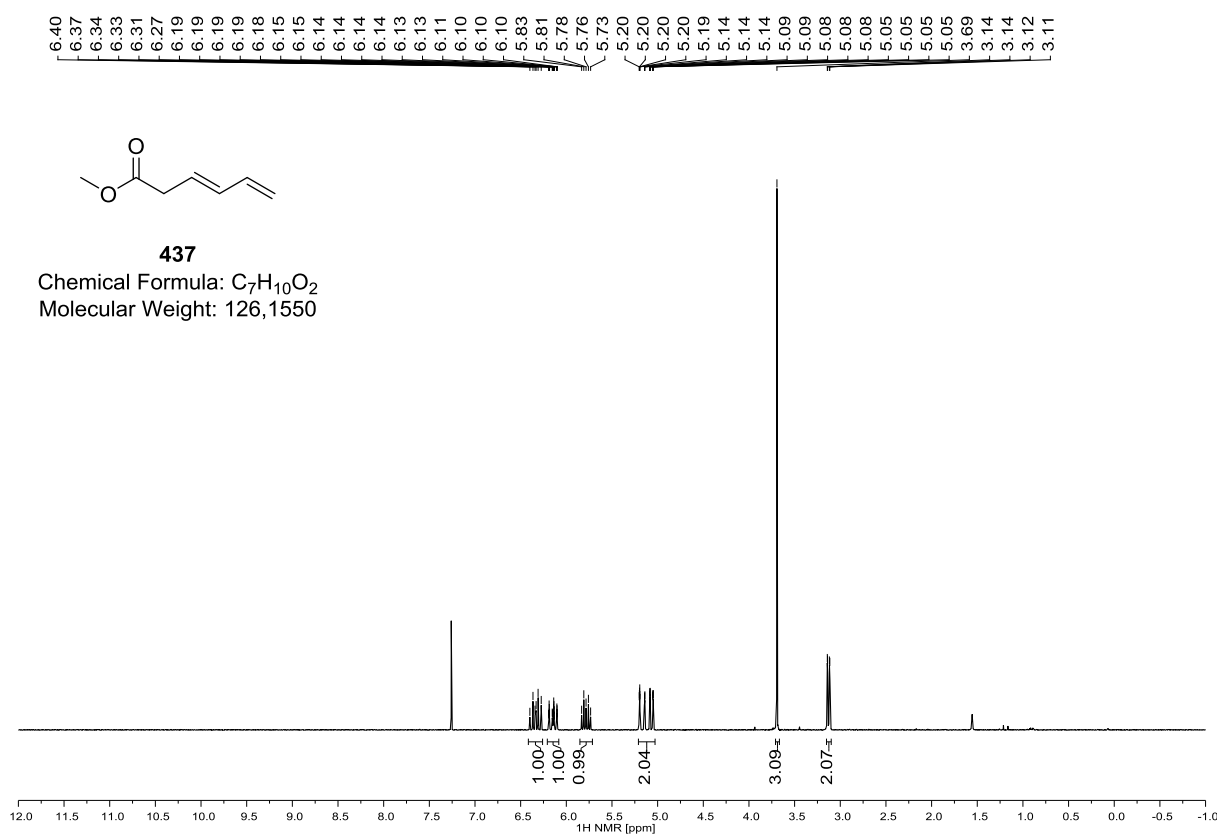
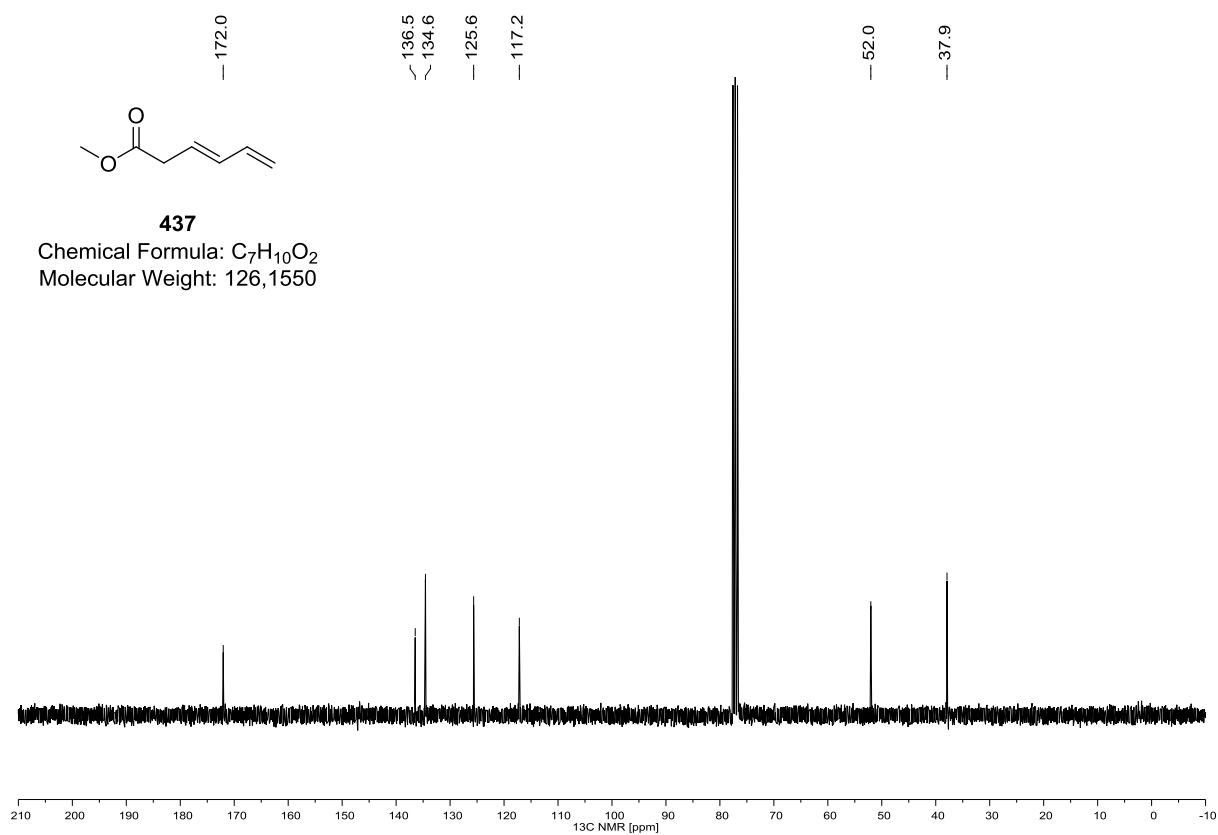
399 (^1H NMR, 400 MHz, CD_2Cl_2)**399 (^{13}C NMR, 100 MHz, CD_2Cl_2)**

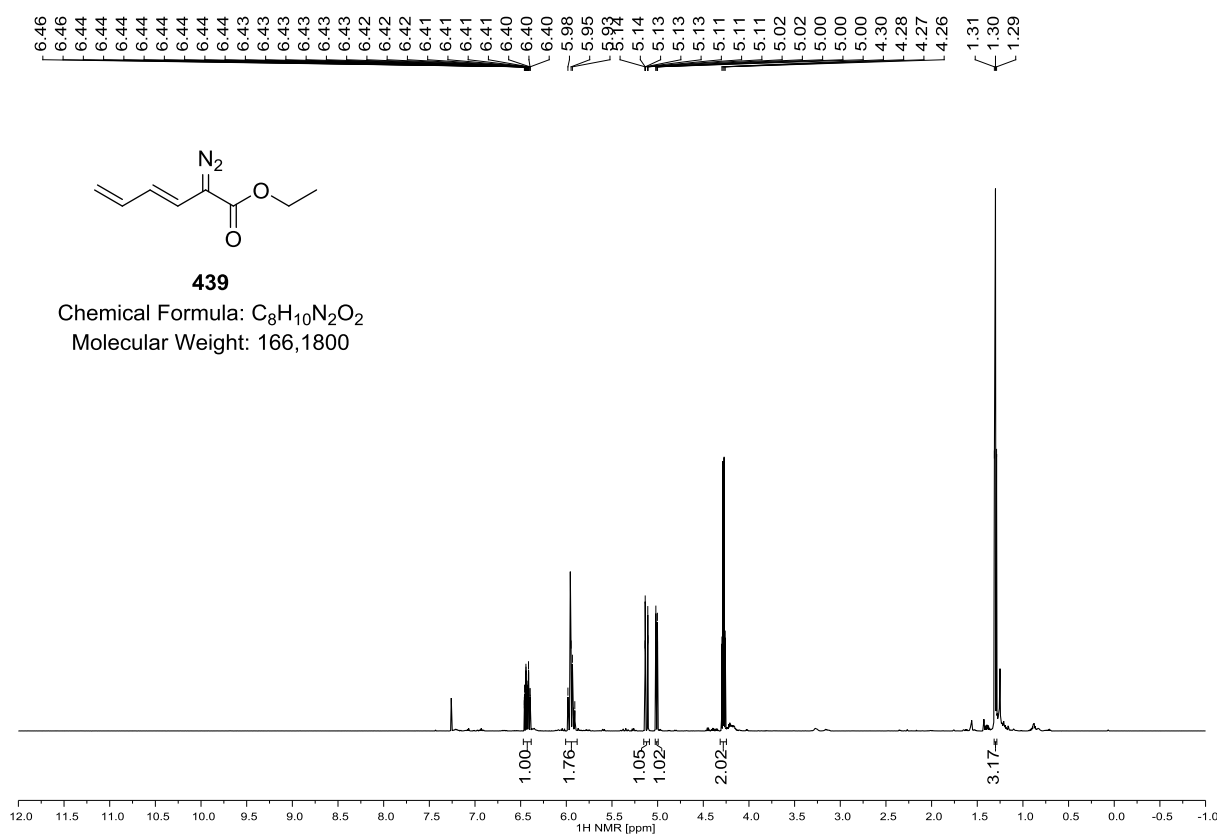
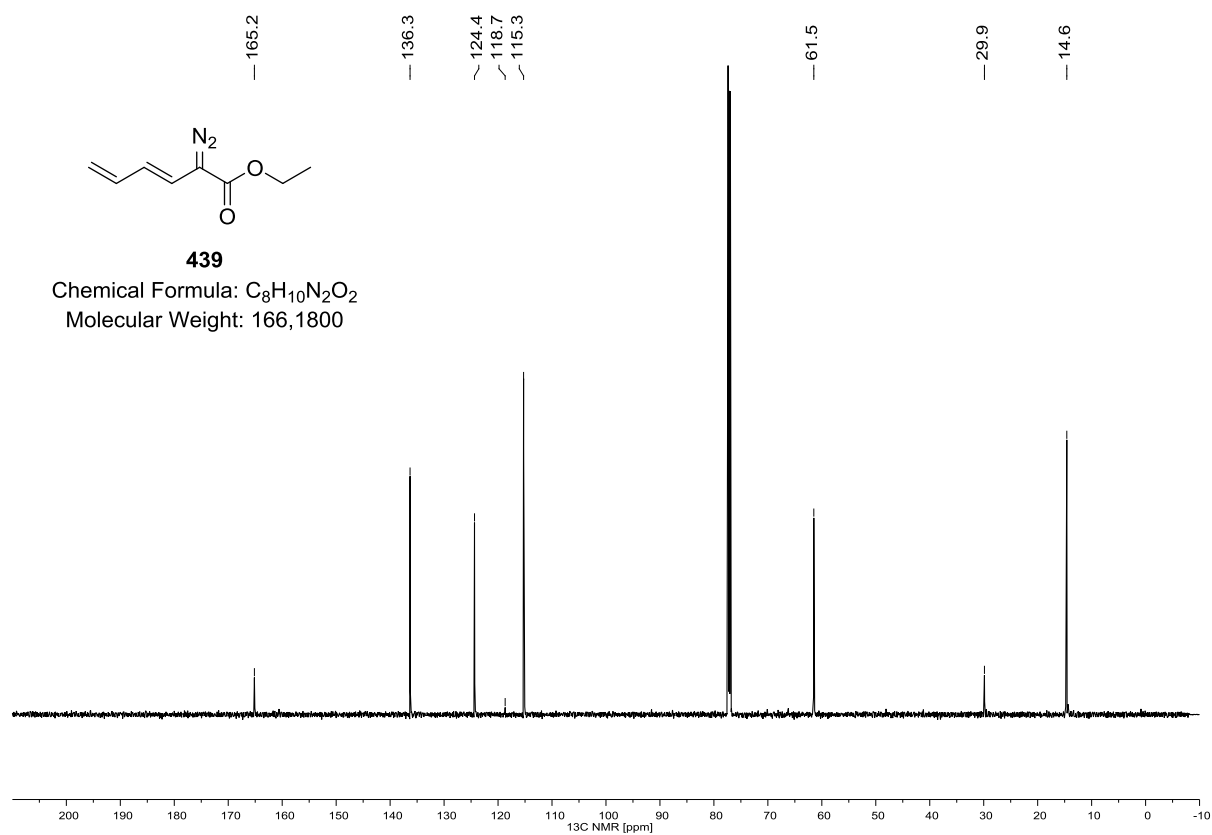
400 (¹H NMR, 300 MHz, CDCl₃)**400 (¹³C NMR, 75 MHz, CDCl₃)**

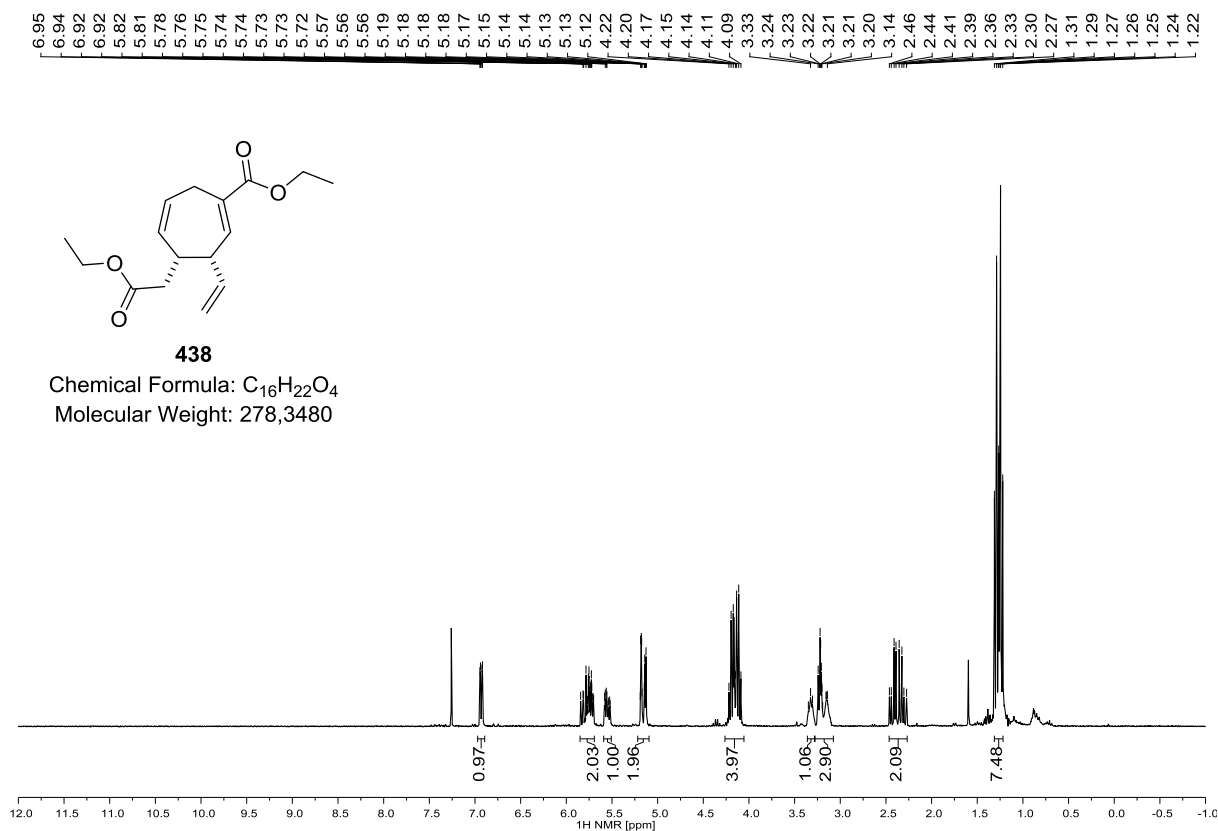
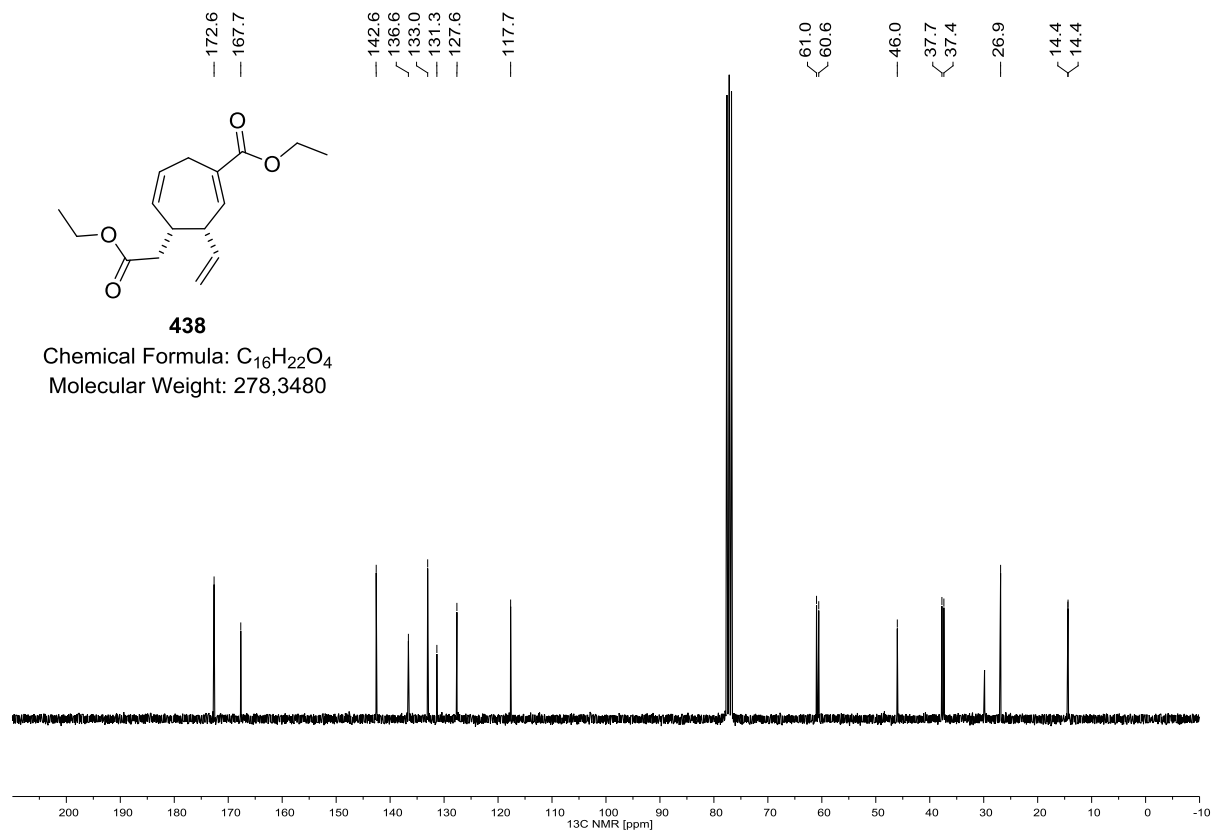
401 (^1H NMR, 300 MHz, CDCl_3)**401 (^{13}C NMR, 75 MHz, CDCl_3)**

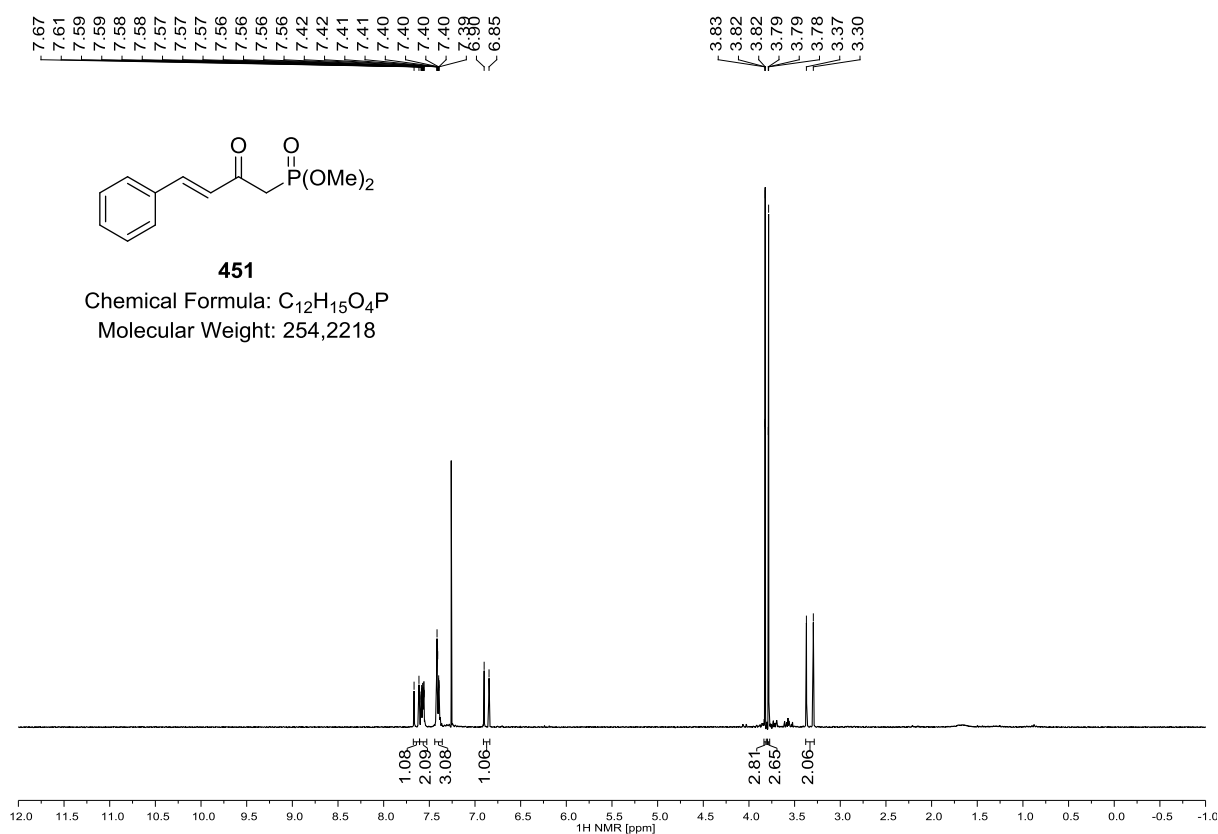
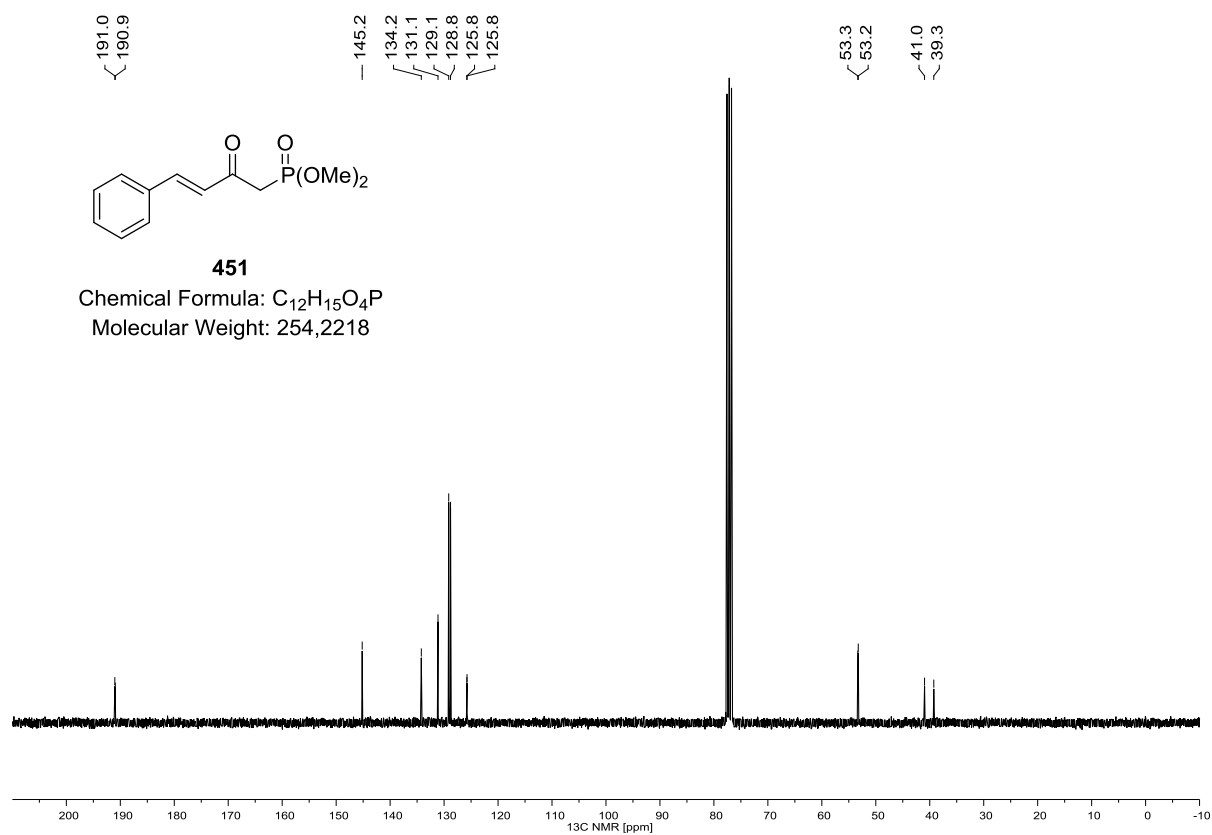
402 (^1H NMR, 600 MHz, CDCl_3)**402 (^{13}C NMR, 150 MHz, CDCl_3)**

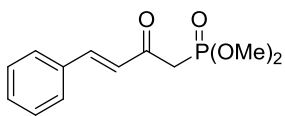
436 (^1H NMR, 300 MHz, CDCl_3)**436 (^{13}C NMR, 75 MHz, CDCl_3)**

437 (^1H NMR, 300 MHz, CDCl_3)**437 (^{13}C NMR, 75 MHz, CDCl_3)**

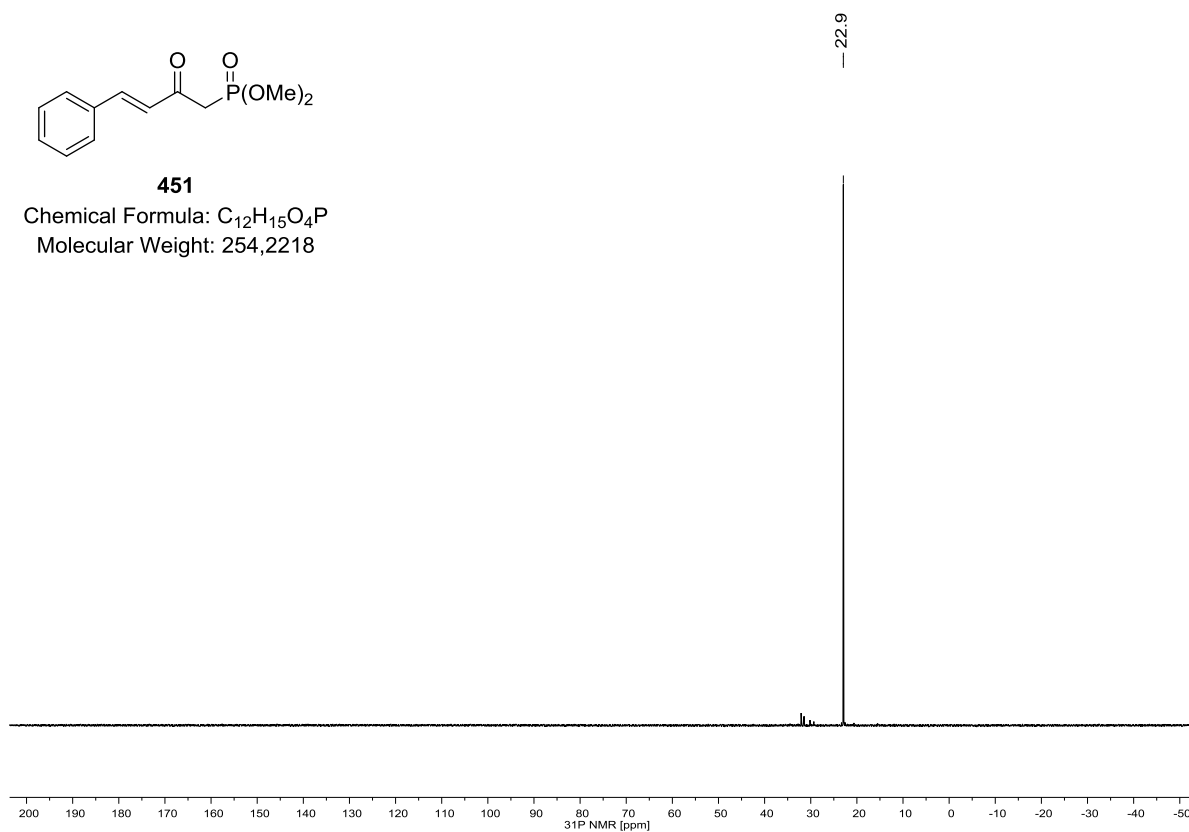
439 (^1H NMR, 600 MHz, CDCl_3)**439 (^{13}C NMR, 150 MHz, CDCl_3)**

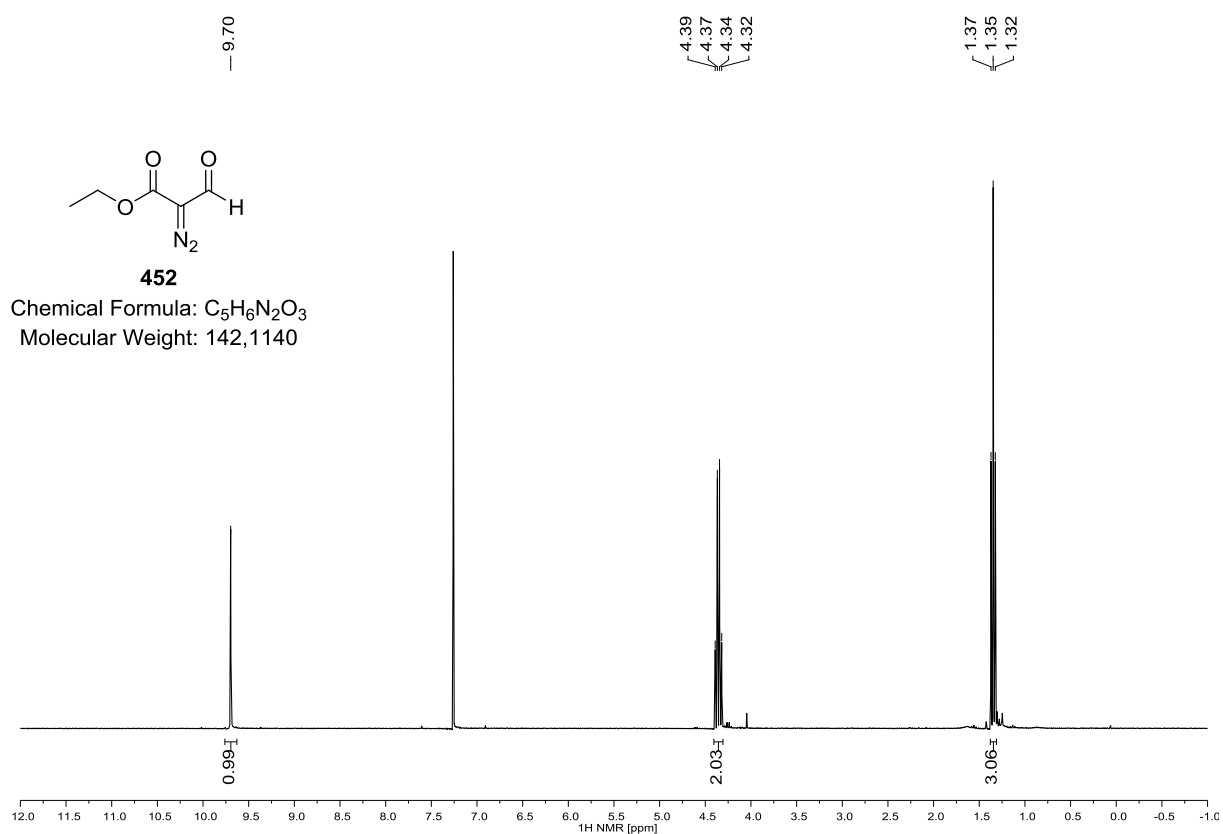
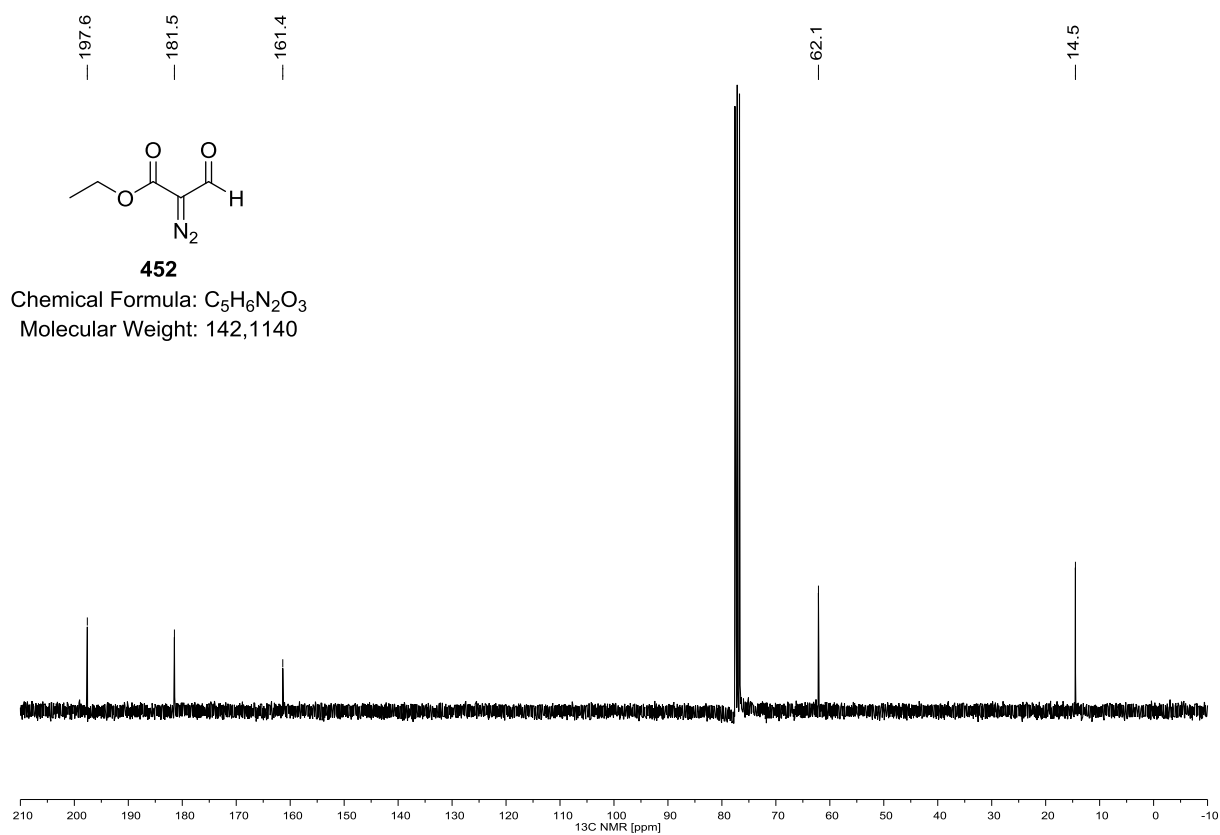
438 (^1H NMR, 300 MHz, CDCl_3)**438 (^{13}C NMR, 75 MHz, CDCl_3)**

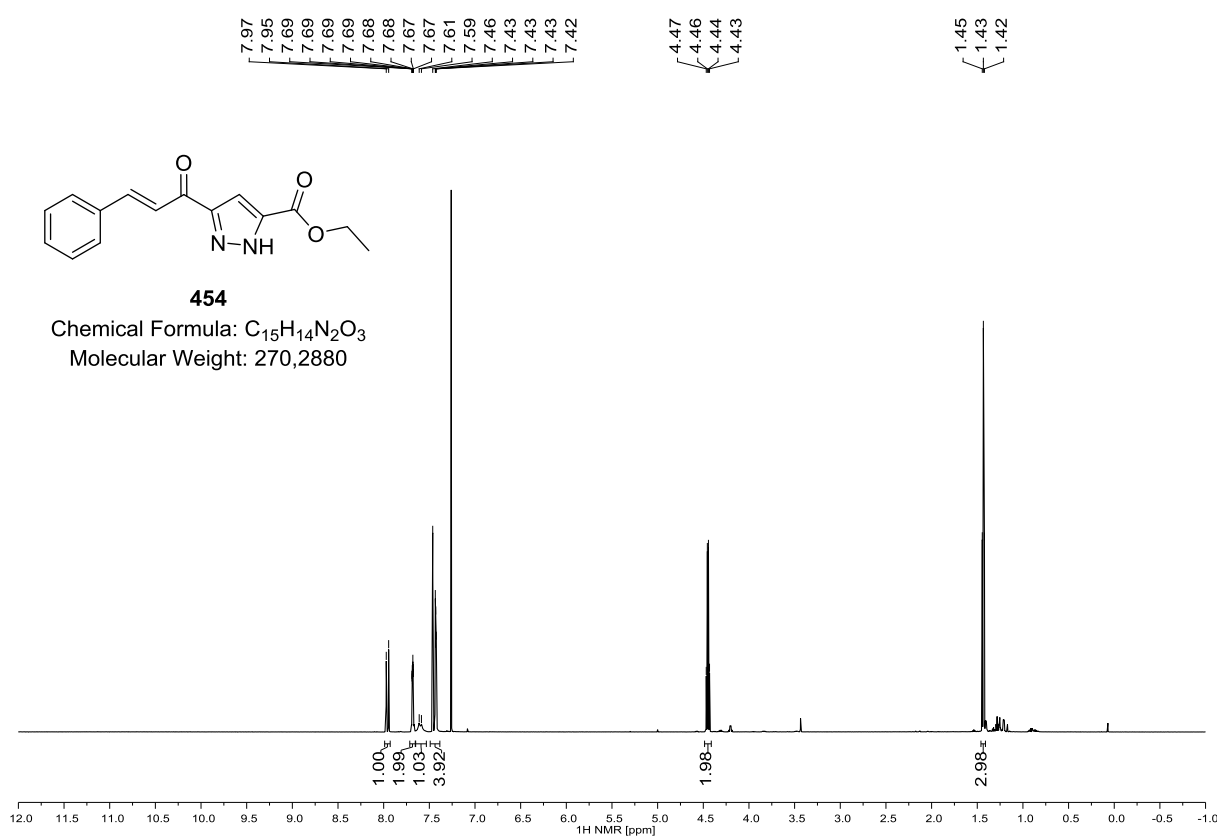
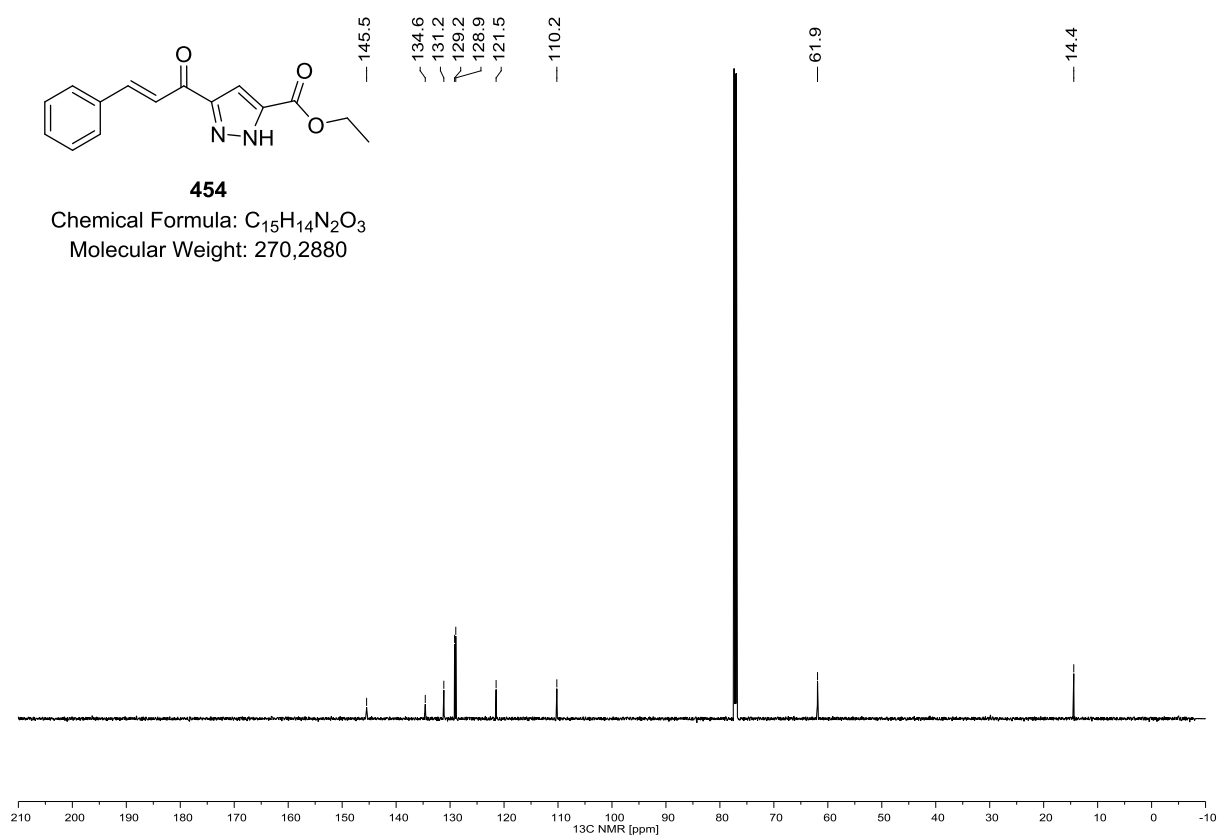
451 (^1H NMR, 300 MHz, CDCl_3)**451 (^{13}C NMR, 75 MHz, CDCl_3)**

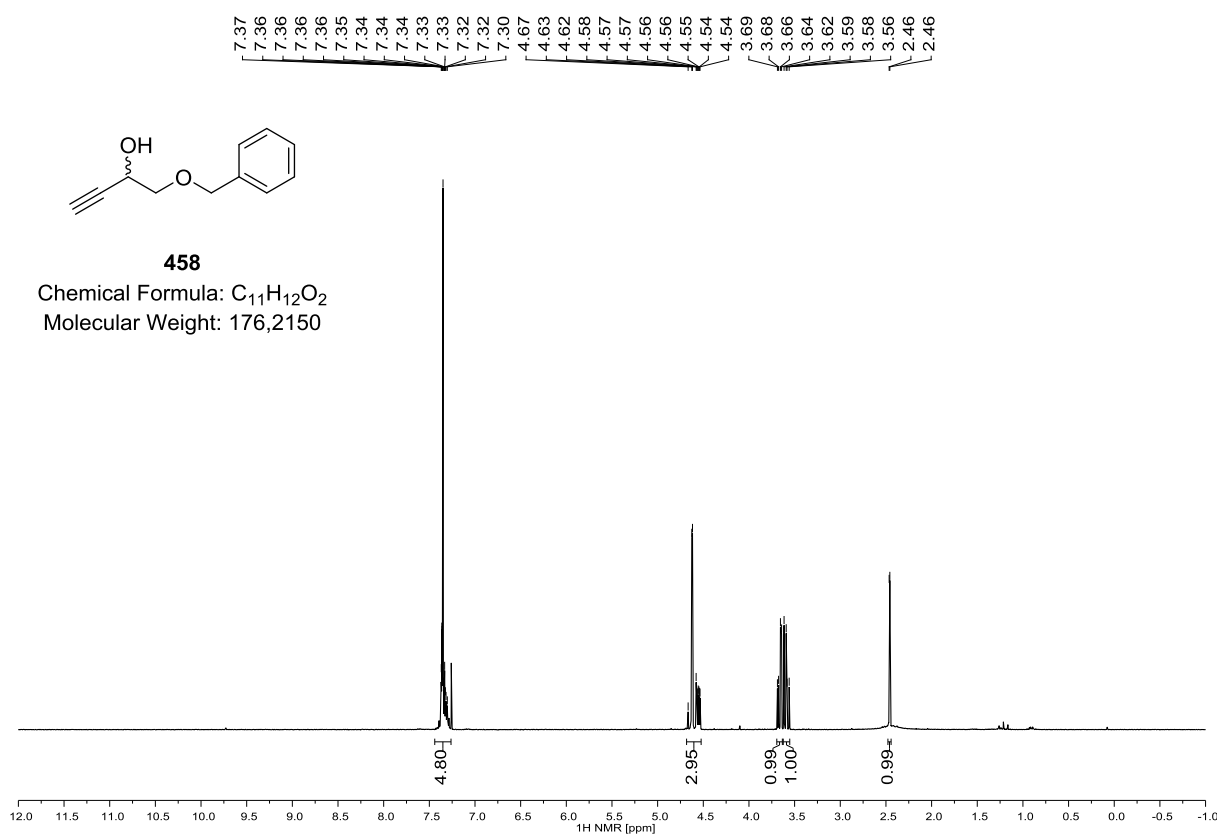
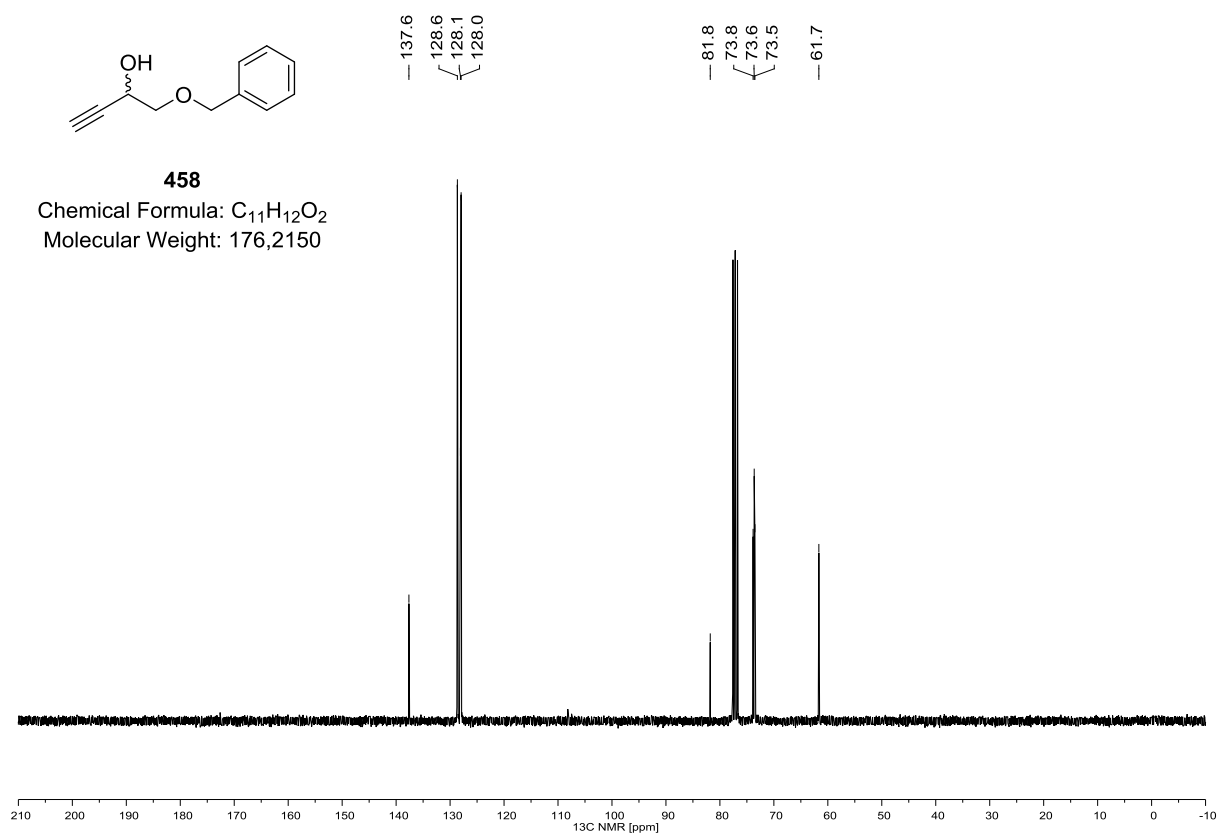
451 (^{31}C NMR, 162 MHz, CDCl_3)**451**Chemical Formula: $\text{C}_{12}\text{H}_{15}\text{O}_4\text{P}$

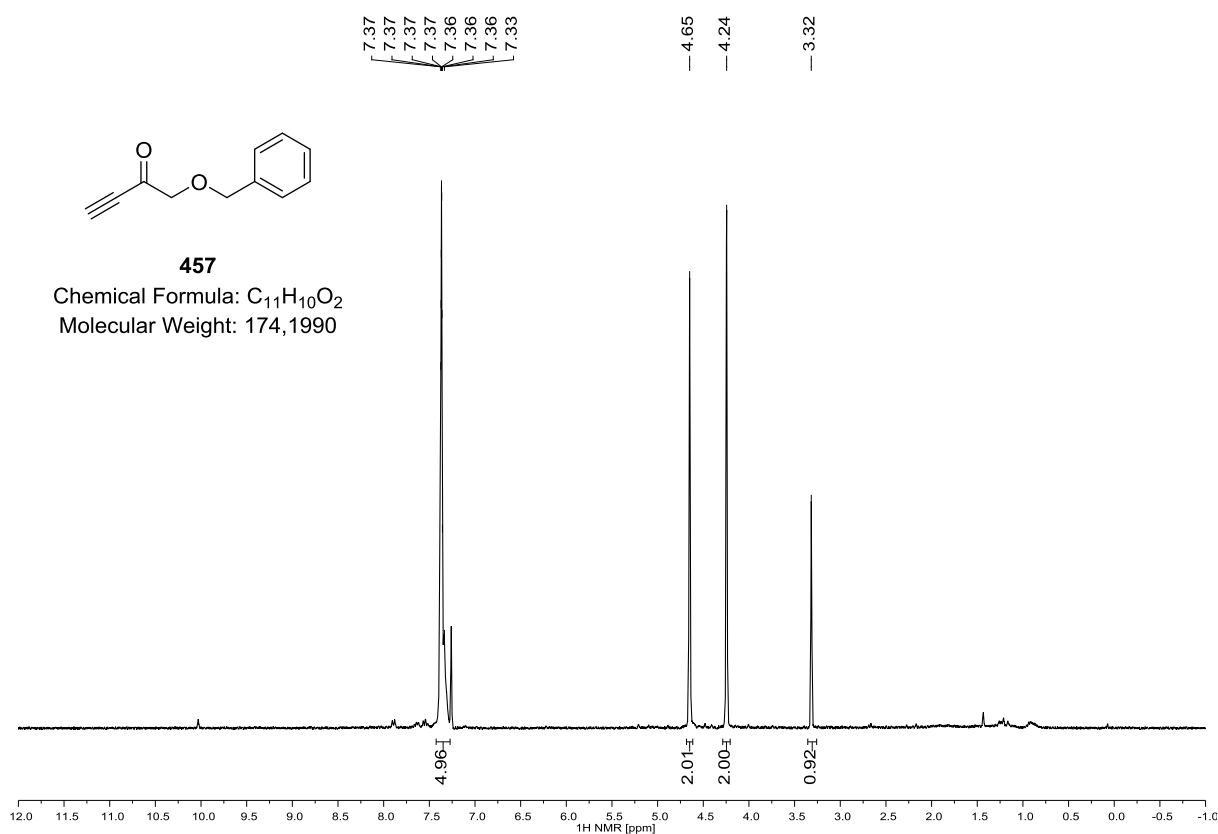
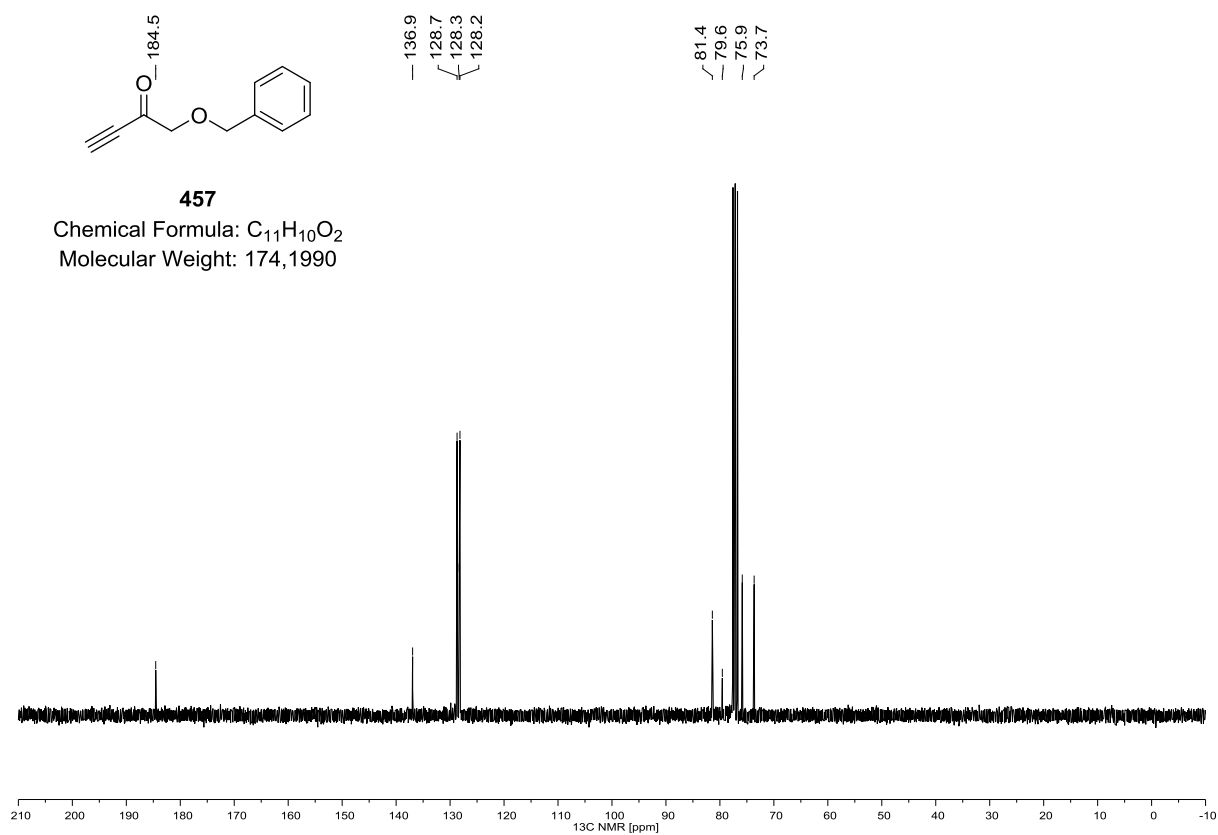
Molecular Weight: 254,2218

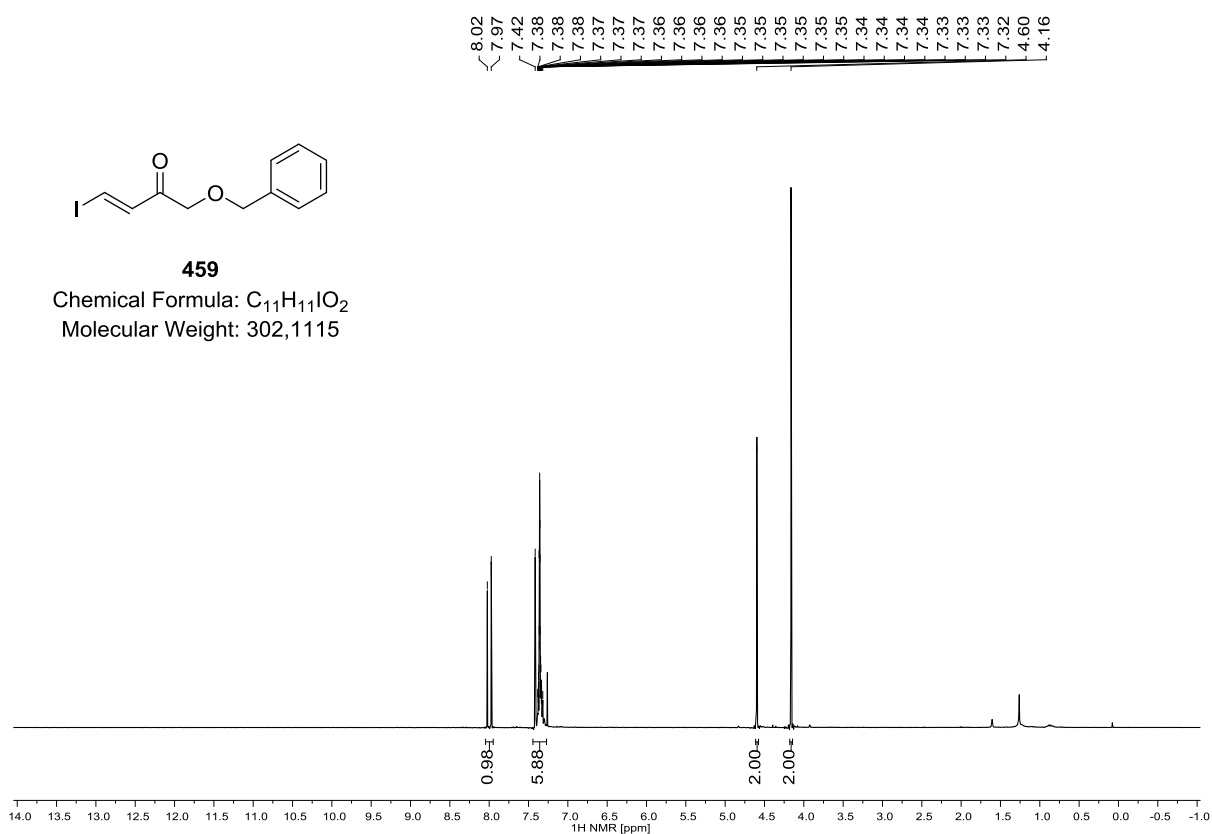
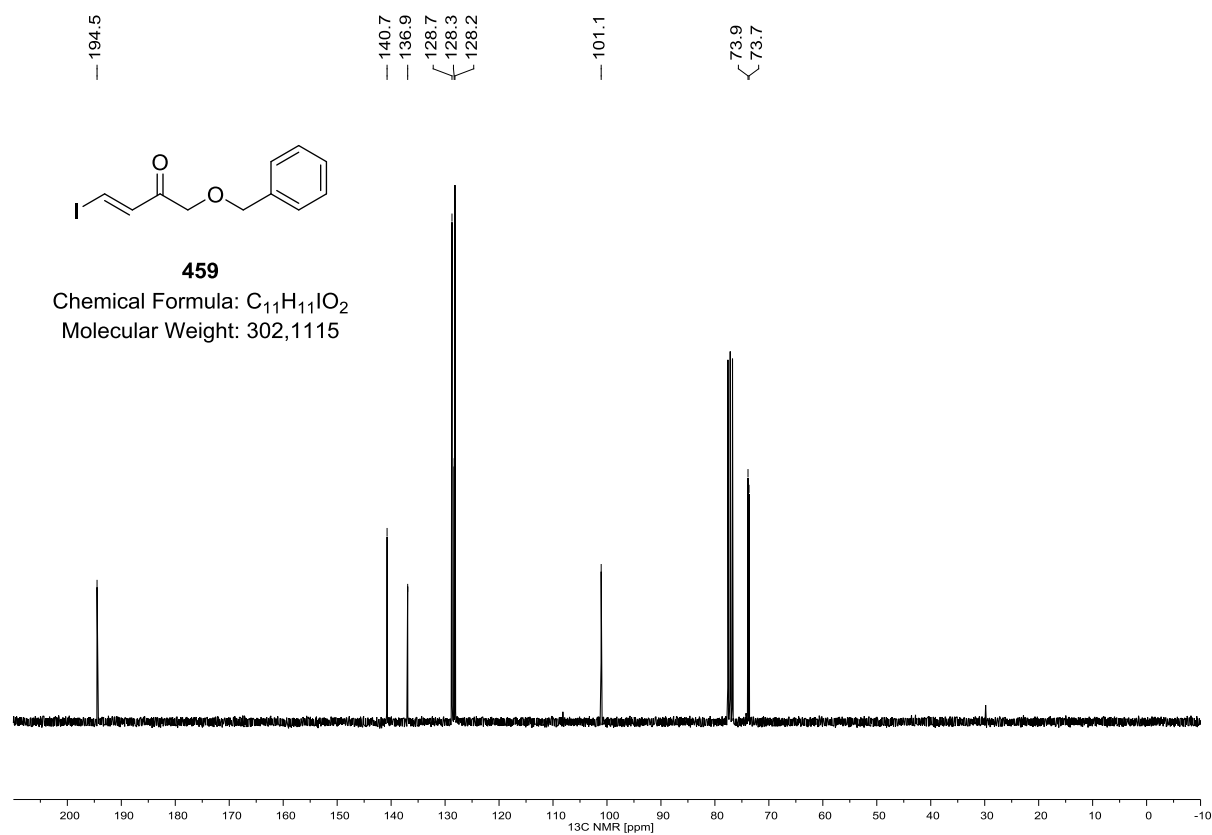


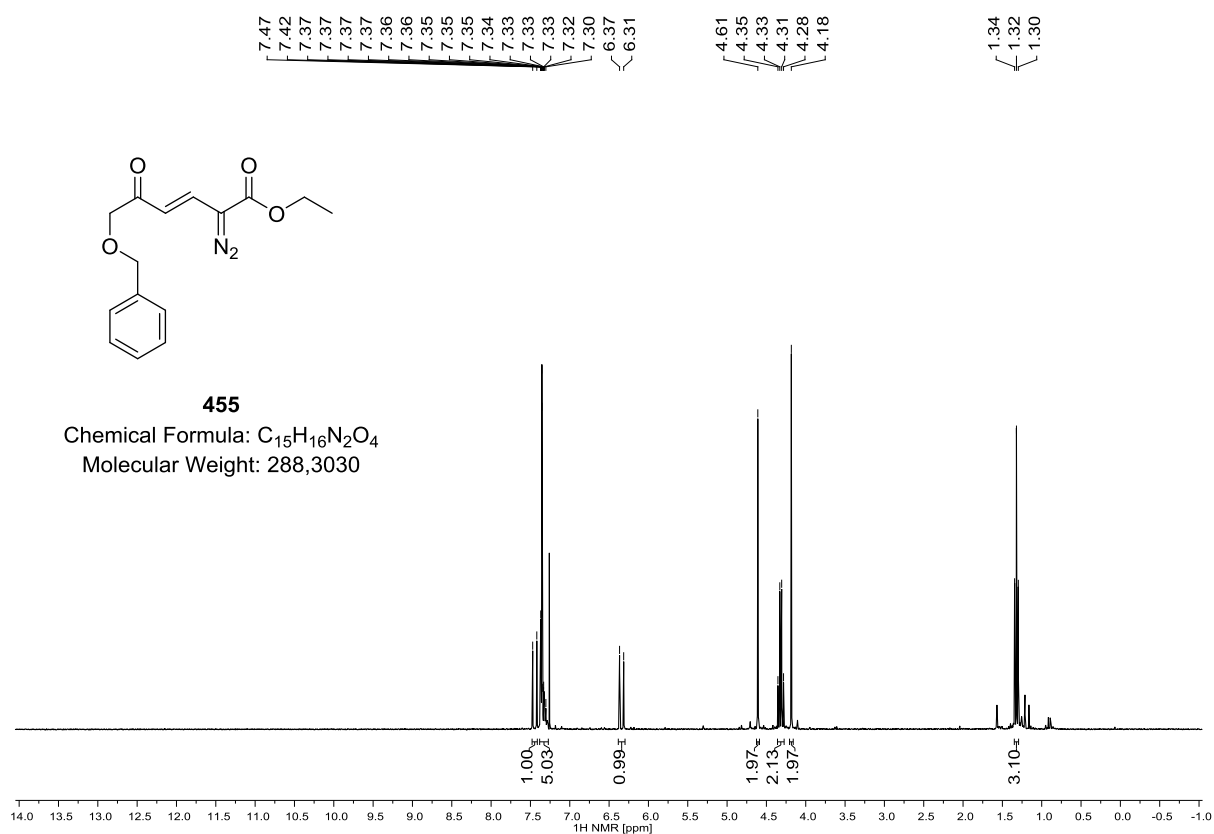
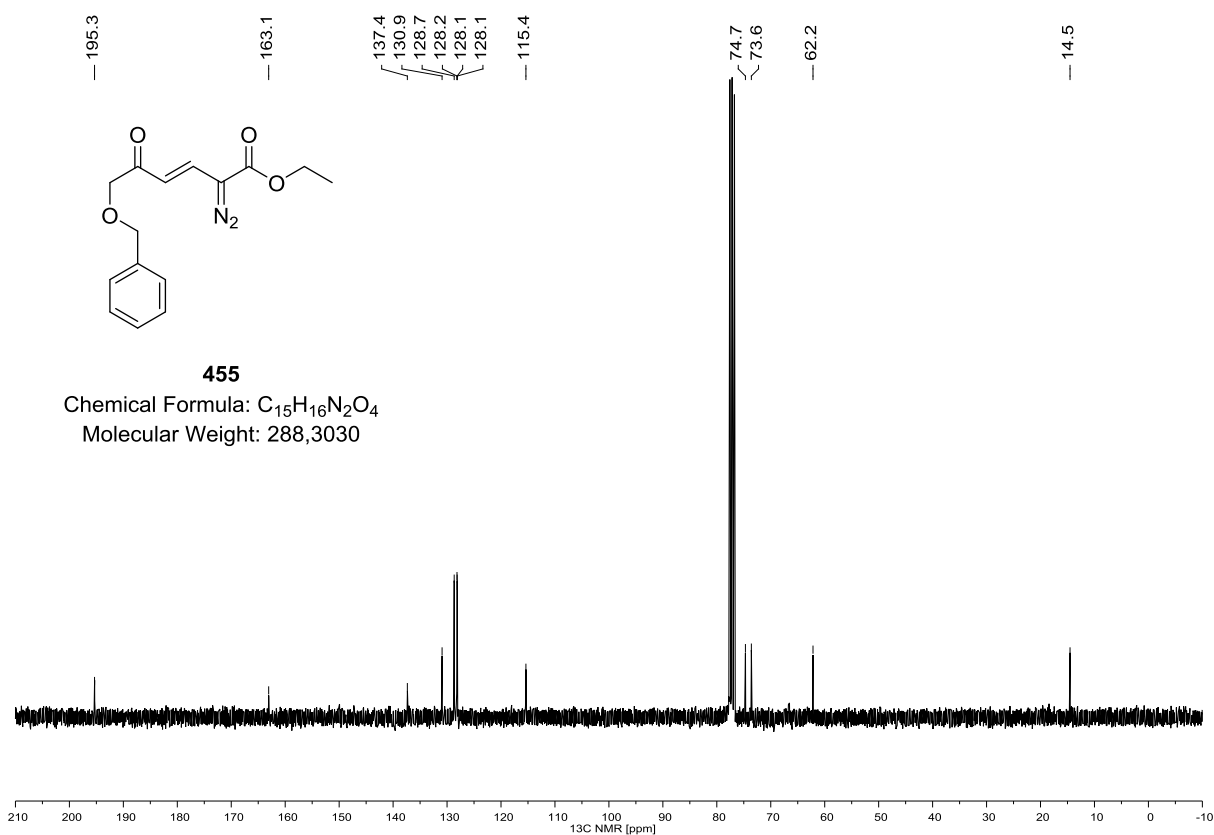
452 (^1H NMR, 300 MHz, CDCl_3)**452 (^{13}C NMR, 75 MHz, CDCl_3)**

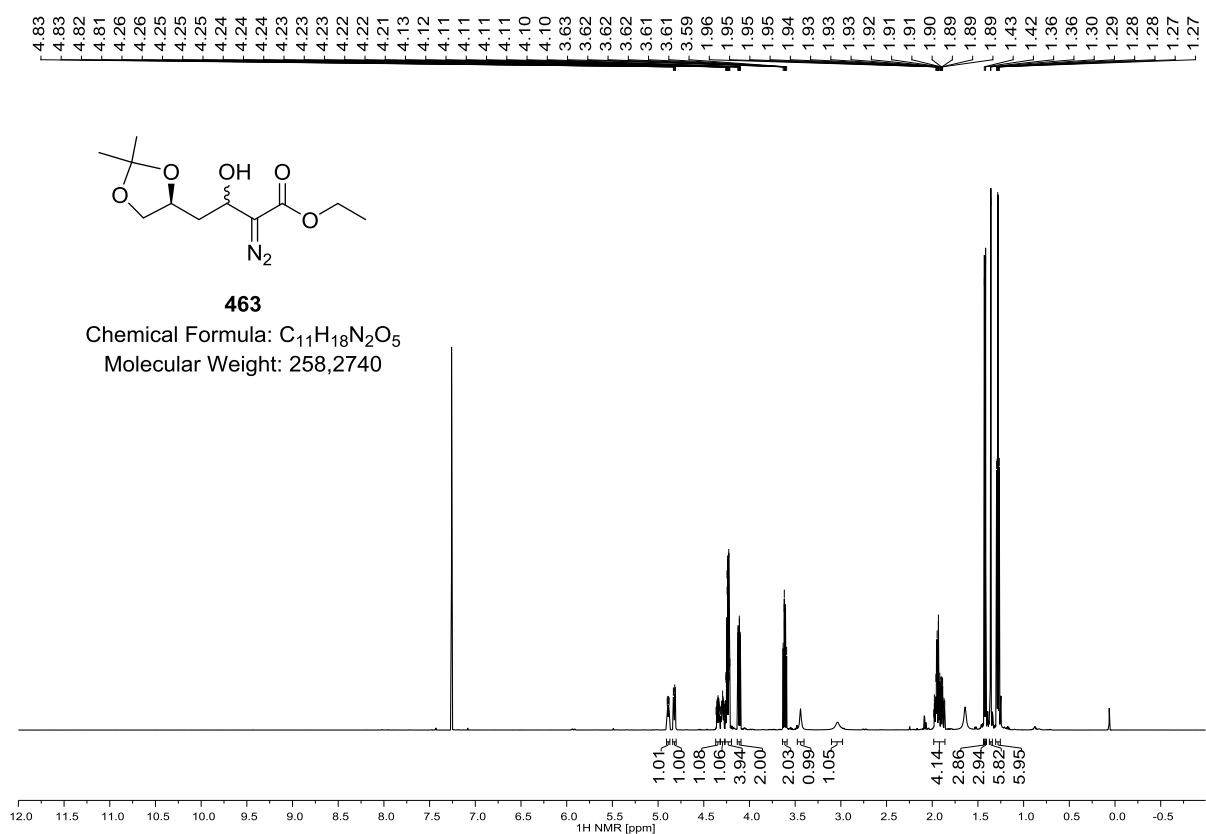
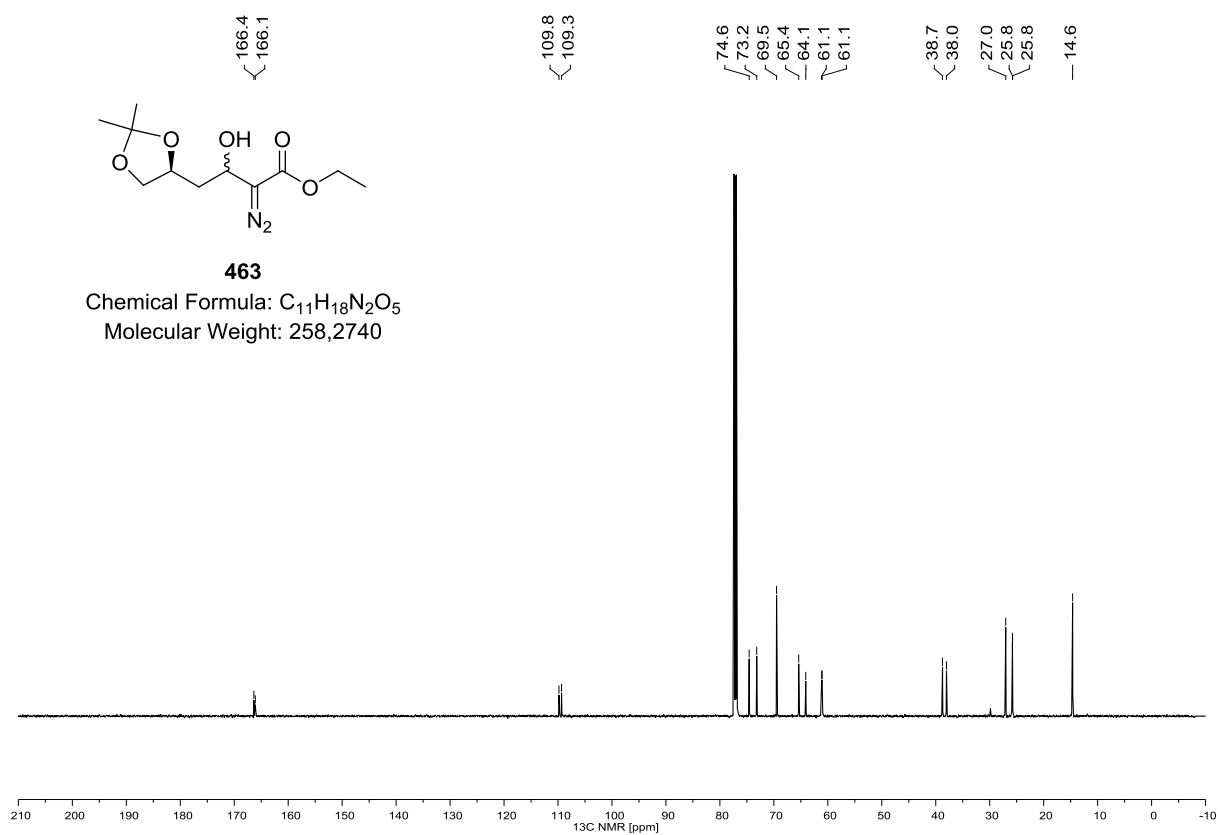
454 (^1H NMR, 600 MHz, CDCl_3)**454 (^{13}C NMR, 150 MHz, CDCl_3)**

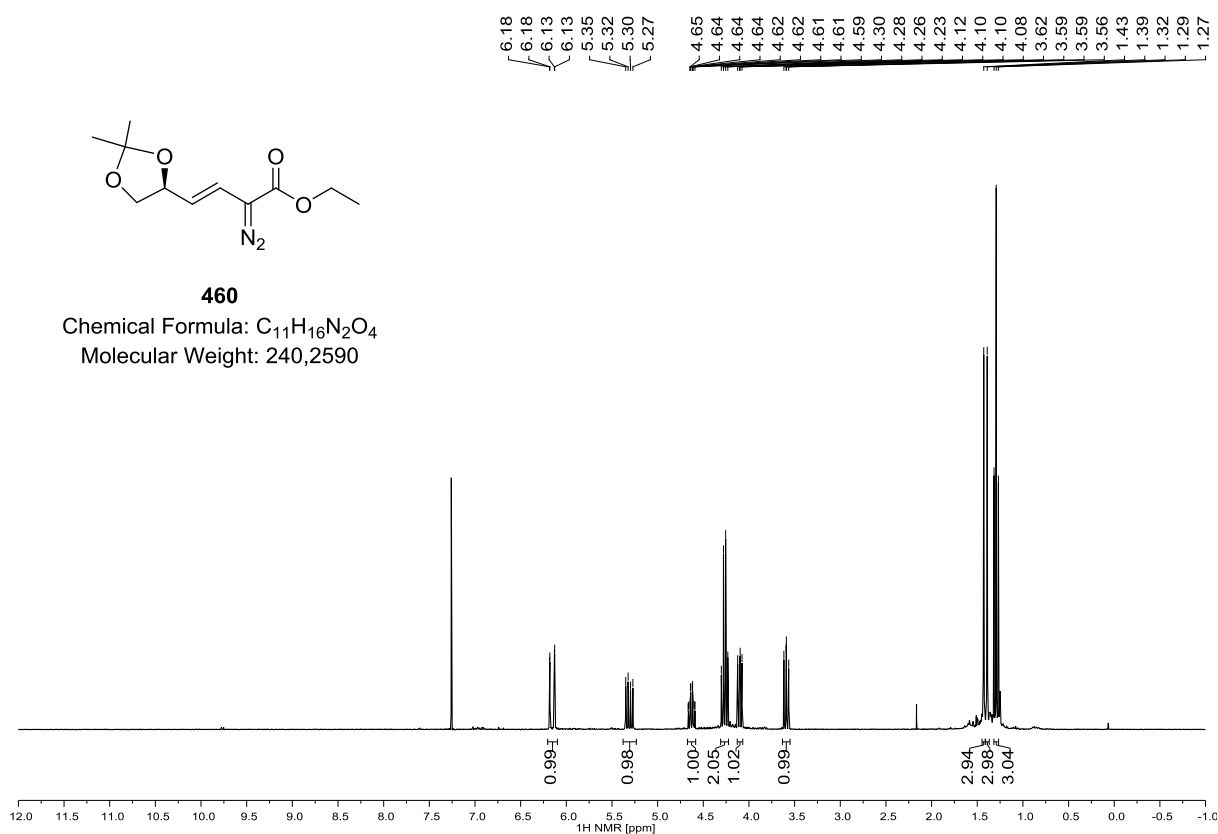
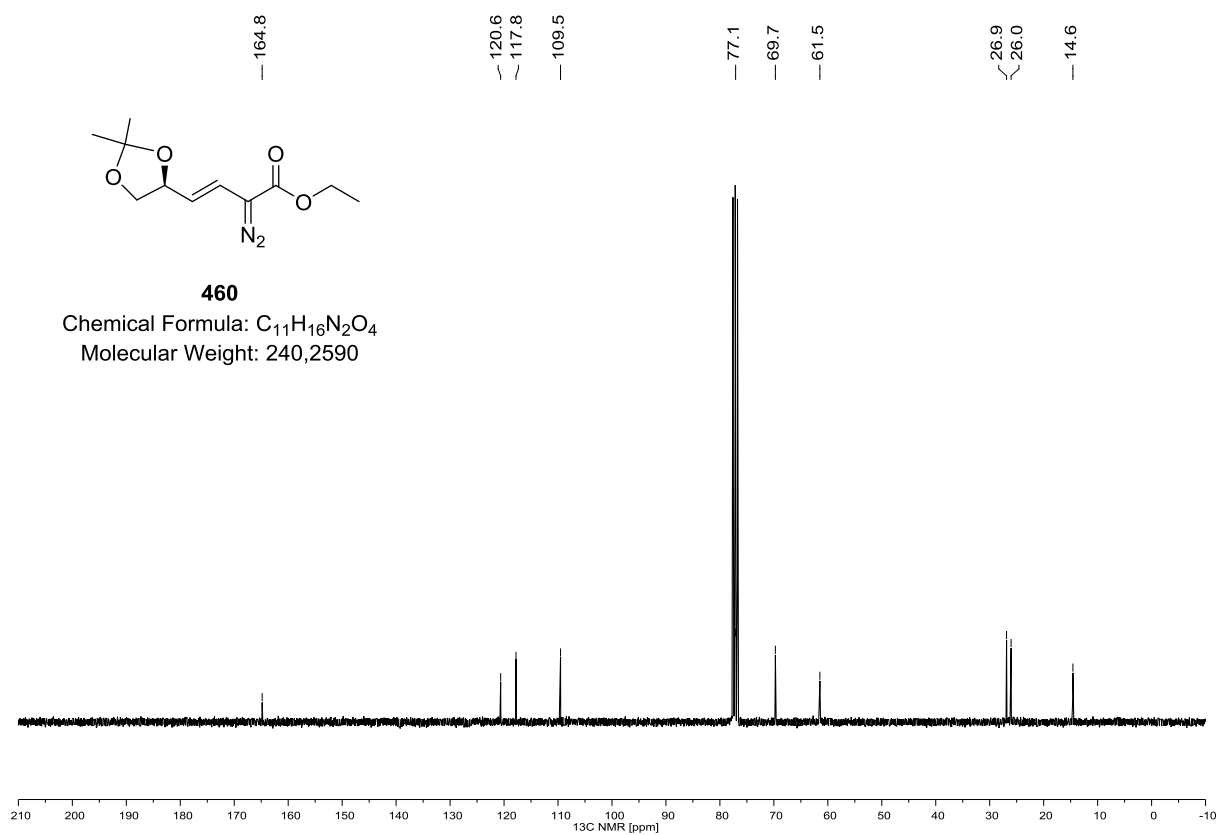
458 (^1H NMR, 300 MHz, CDCl_3)**458 (^{13}C NMR, 75 MHz, CDCl_3)**

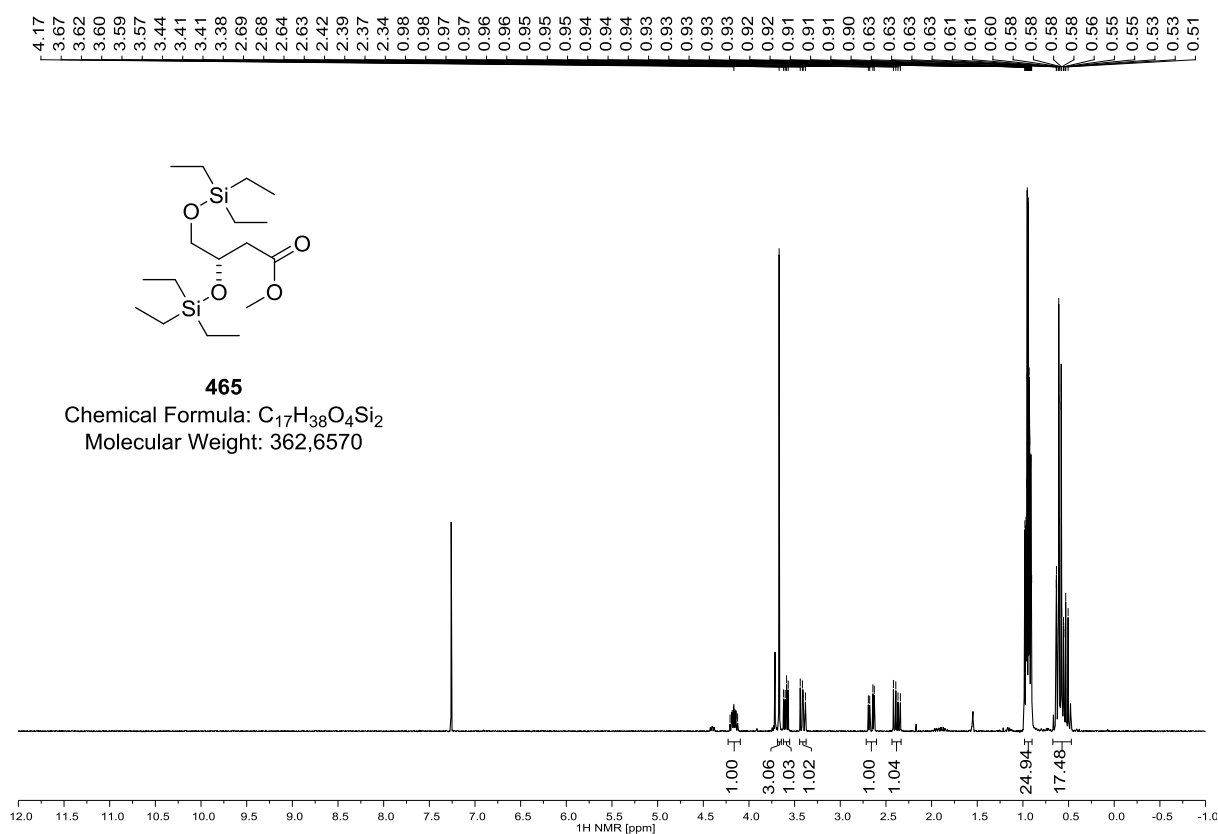
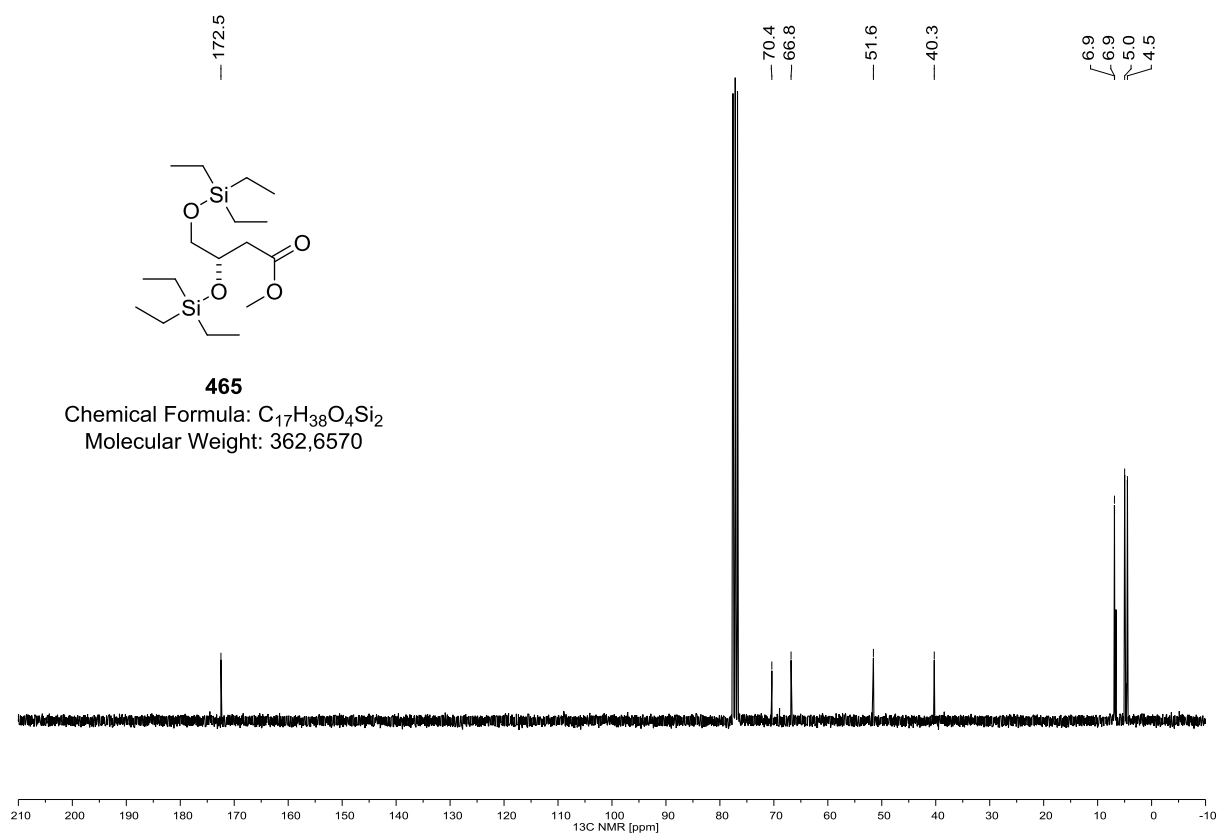
457 (^1H NMR, 300 MHz, CDCl_3)**457 (^{13}C NMR, 75 MHz, CDCl_3)**

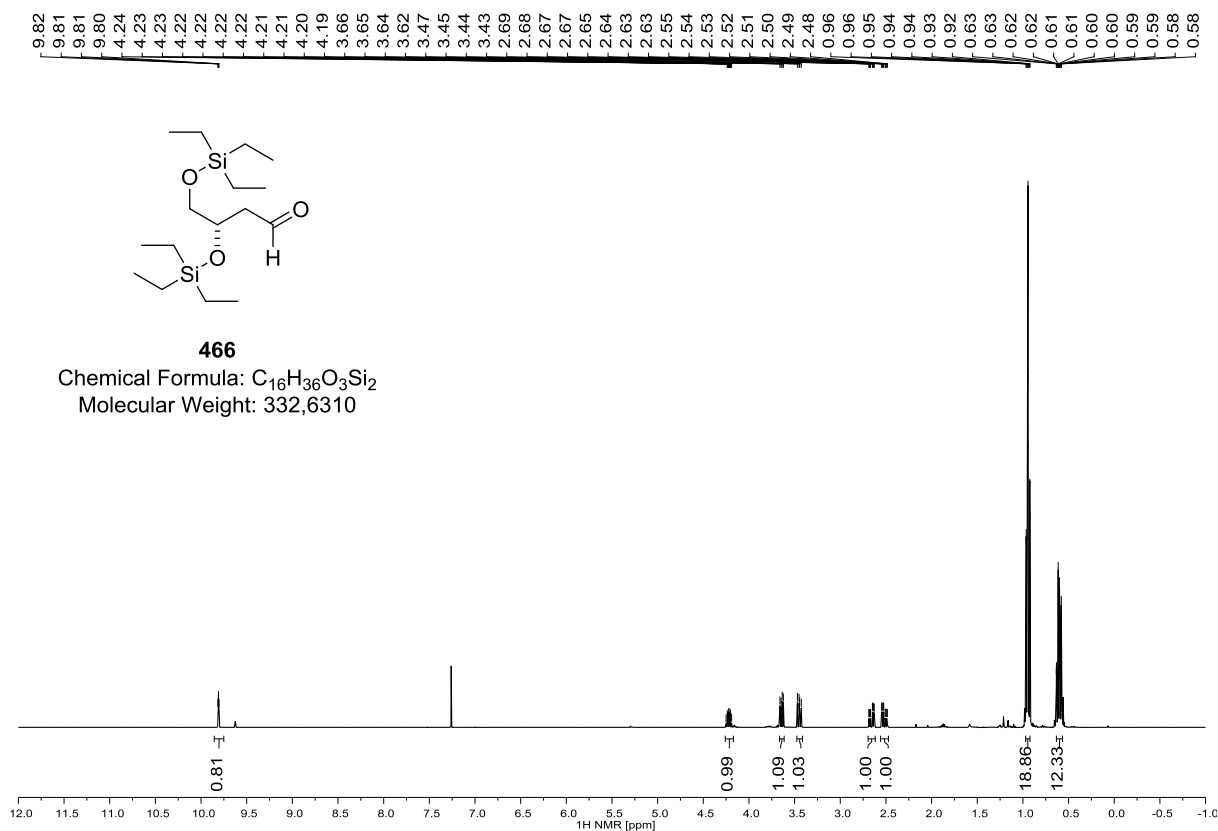
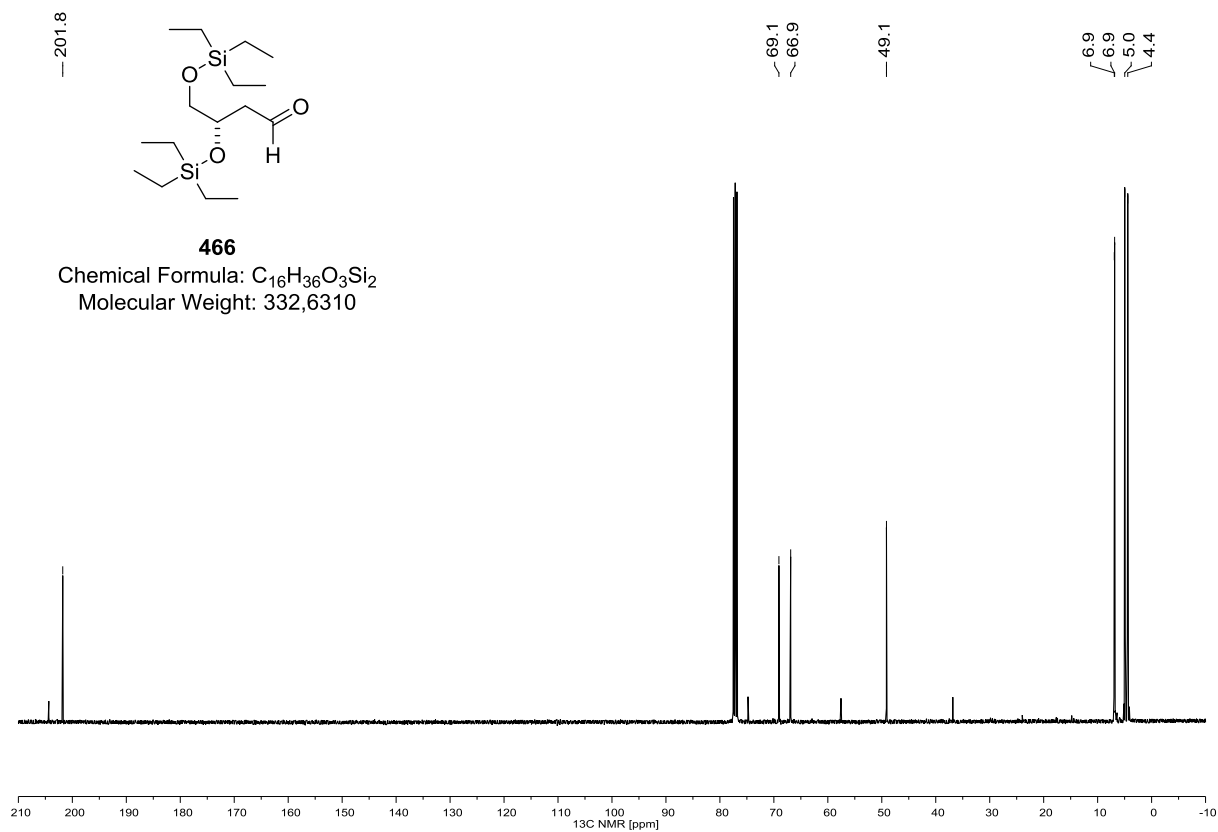
459 (^1H NMR, 300 MHz, CDCl_3)**459 (^{13}C NMR, 75 MHz, CDCl_3)**

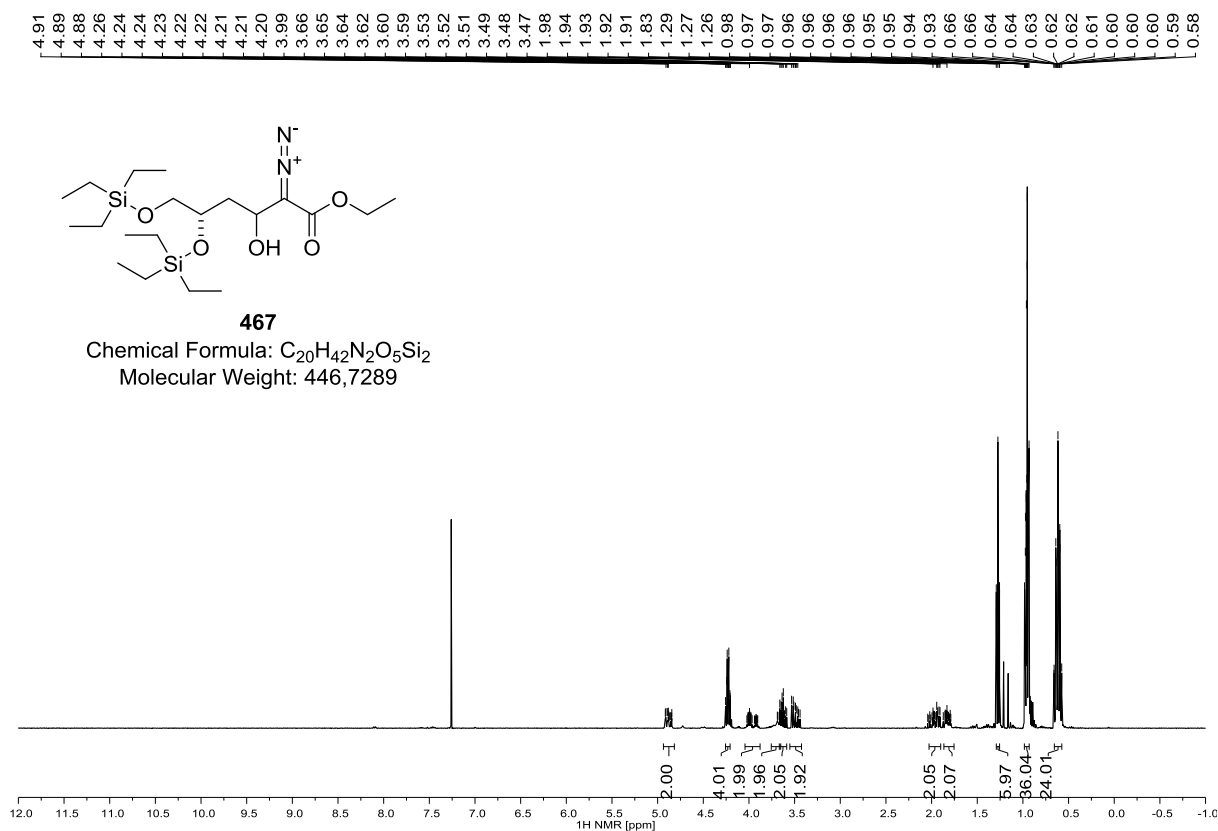
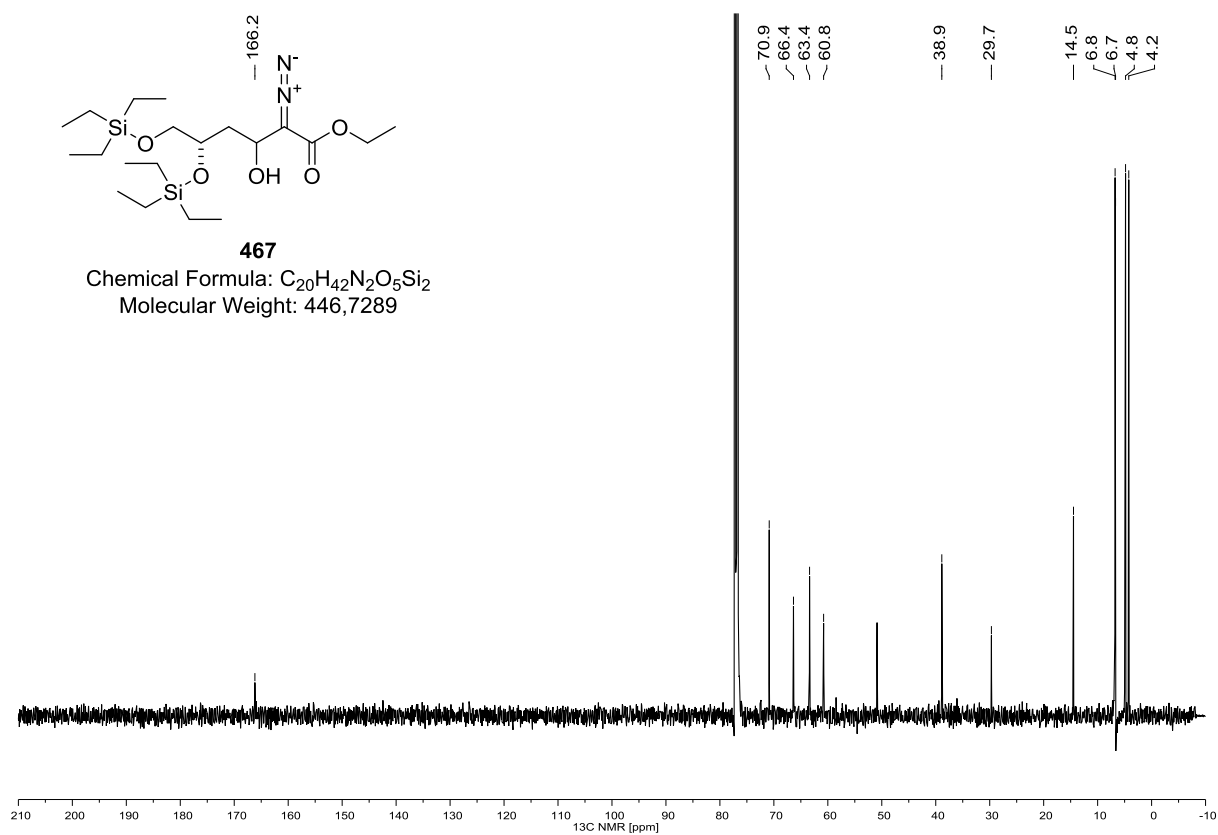
455 (^1H NMR, 300 MHz, CDCl_3)**455 (^{13}C NMR, 75 MHz, CDCl_3)**

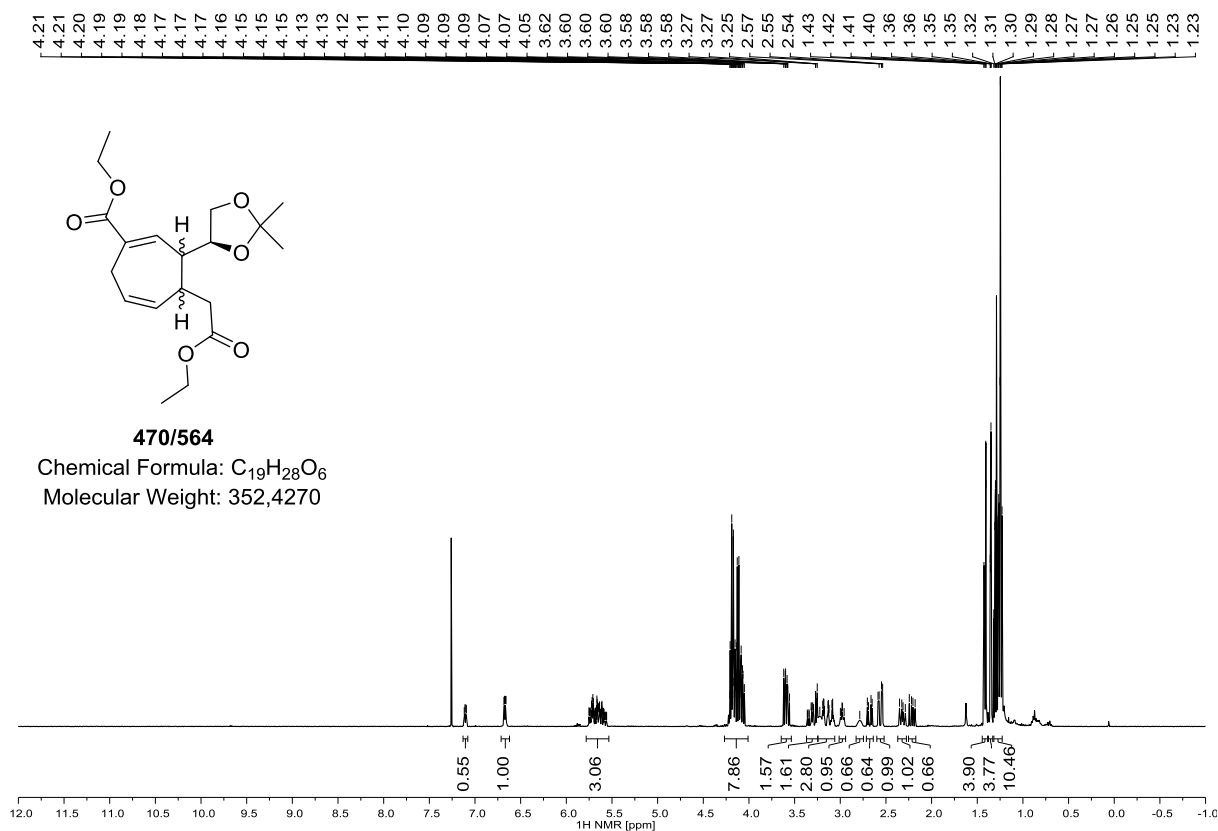
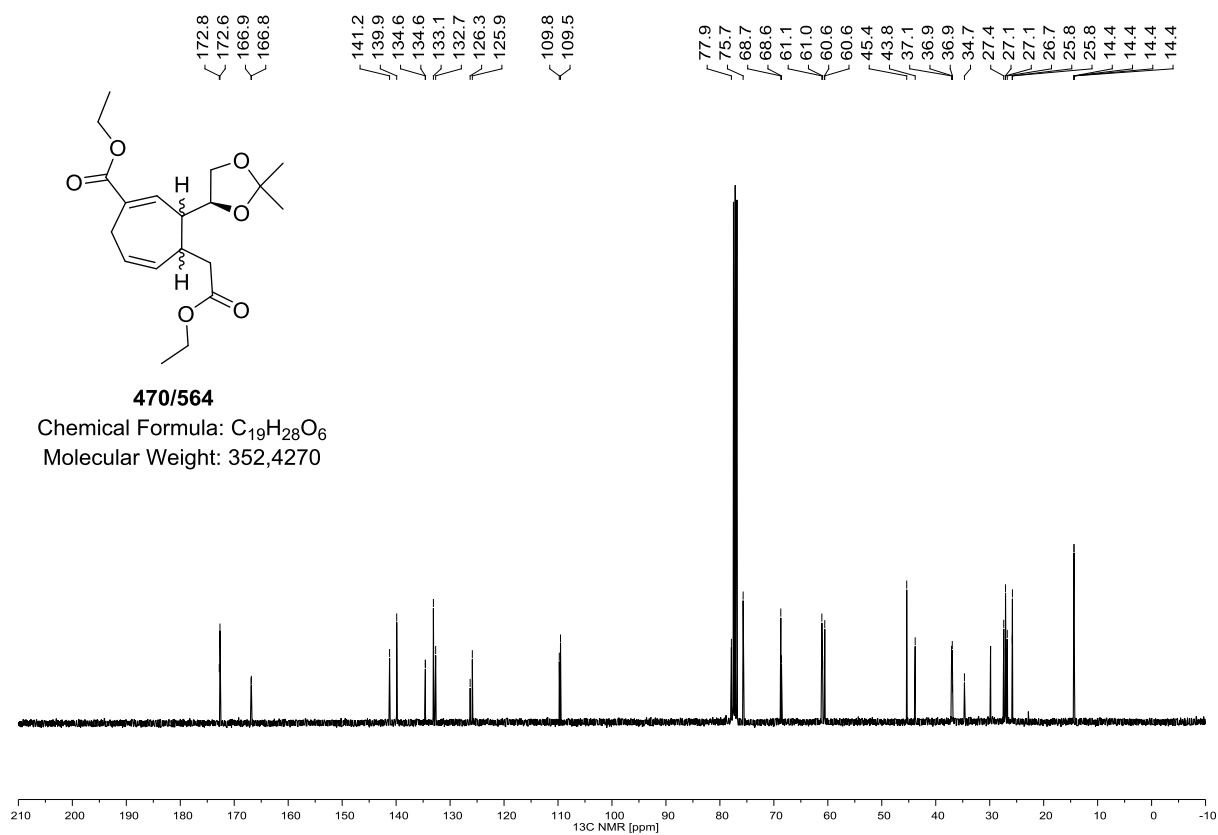
463 (^1H NMR, 600 MHz, CDCl_3)**463 (^{13}C NMR, 150 MHz, CDCl_3)**

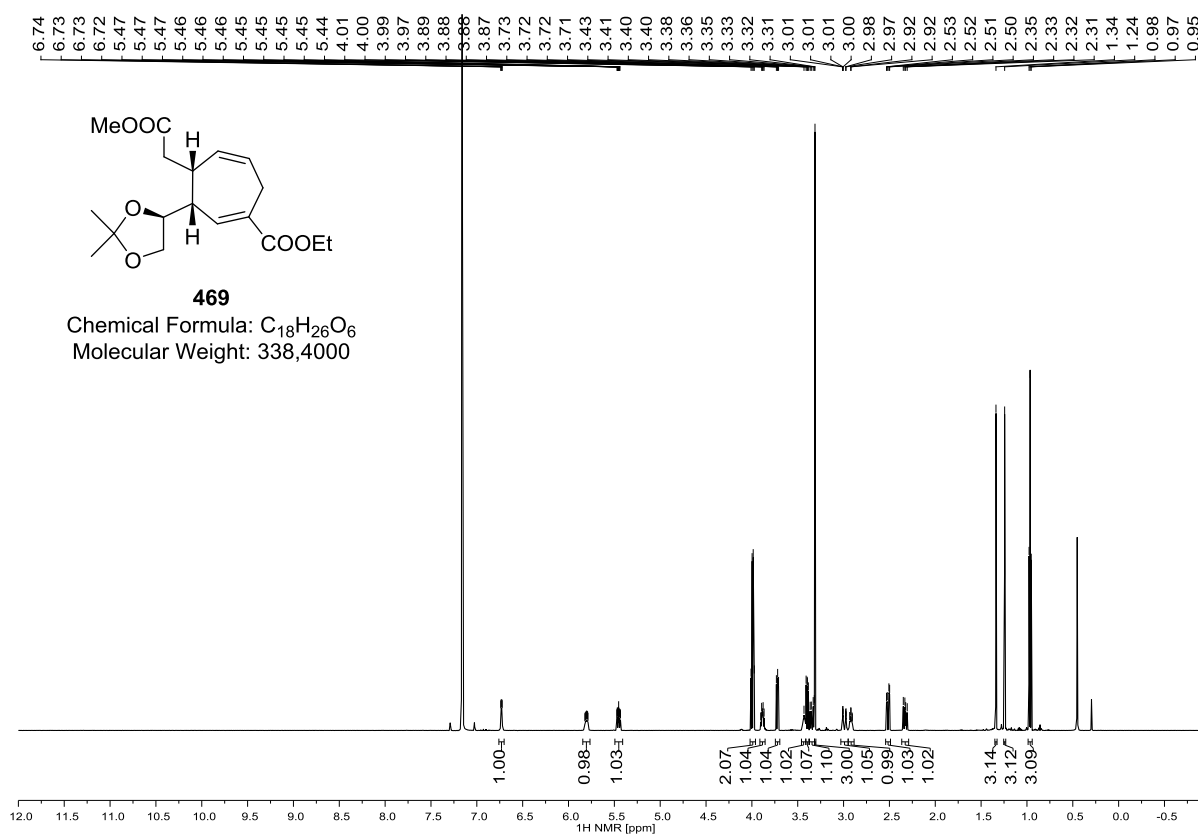
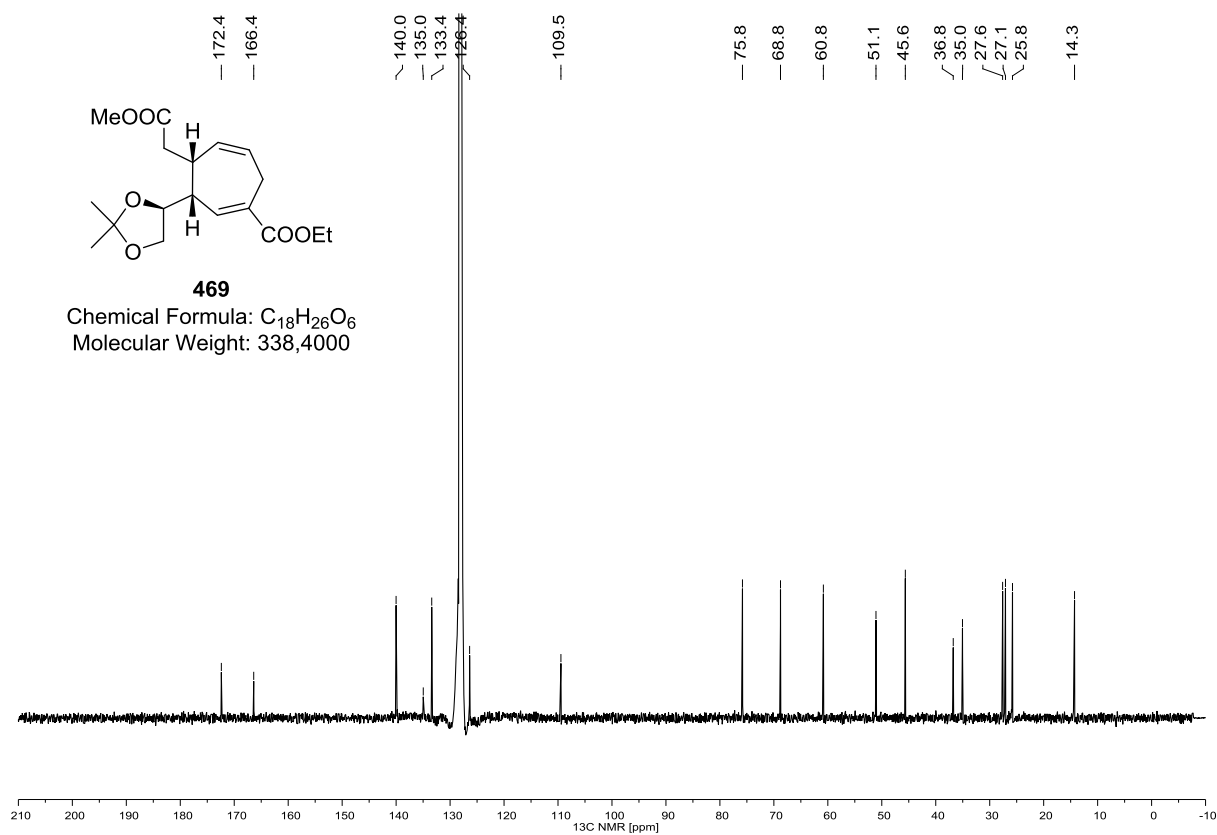
460 (^1H NMR, 300 MHz, CDCl_3)**460 (^{13}C NMR, 75 MHz, CDCl_3)**

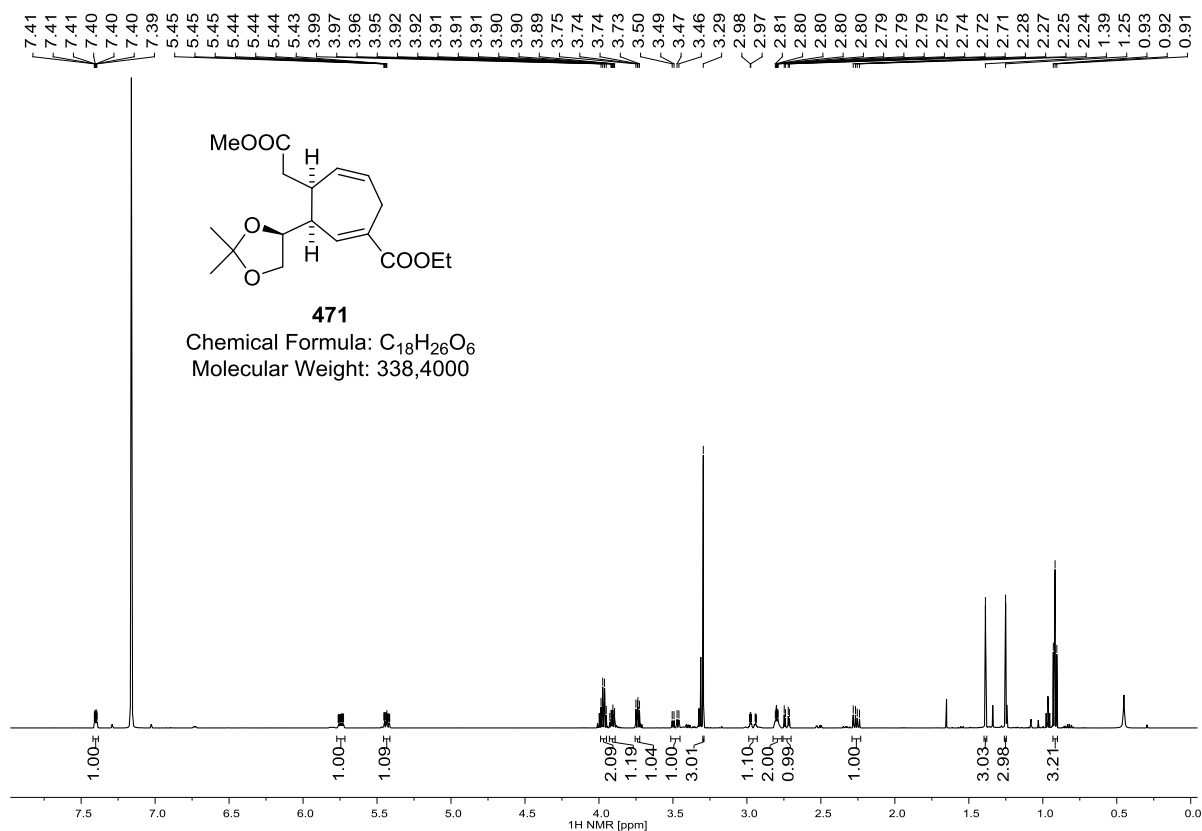
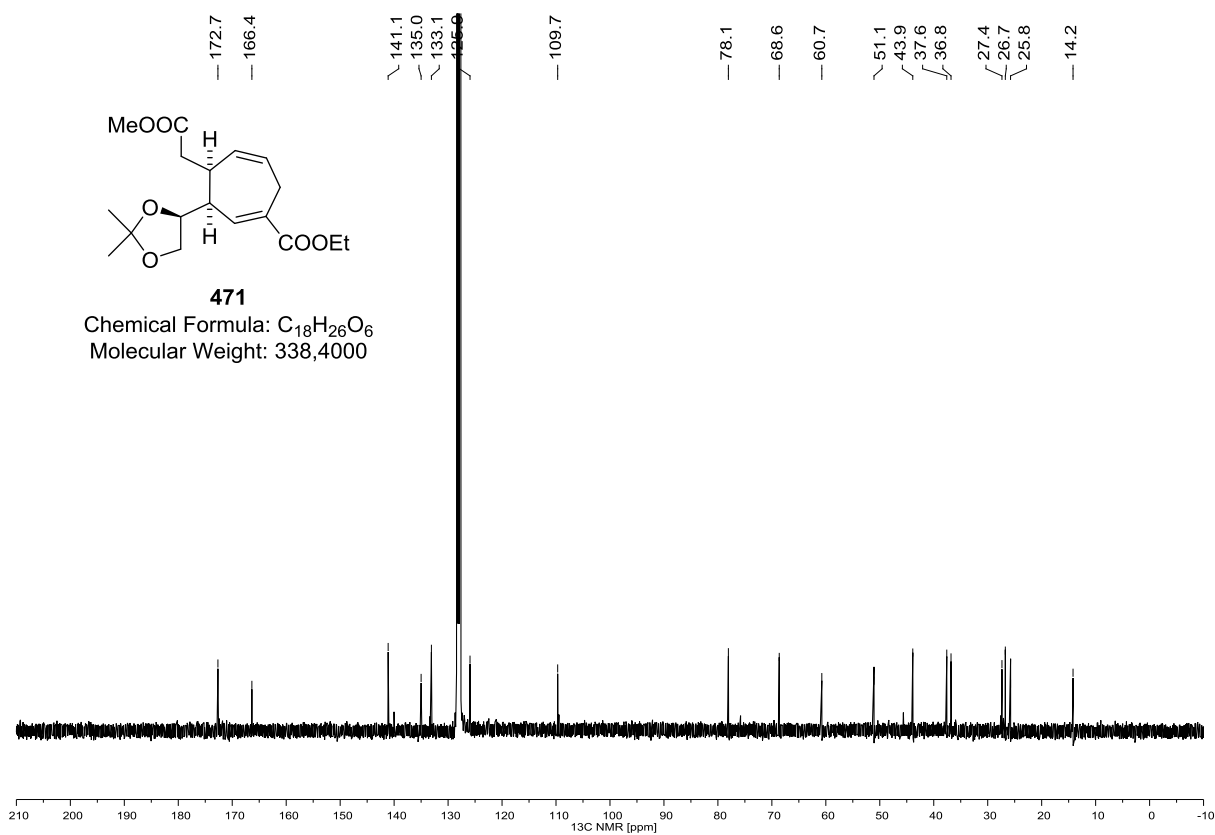
465 (^1H NMR, 300 MHz, CDCl_3)**465 (^{13}C NMR, 75 MHz, CDCl_3)**

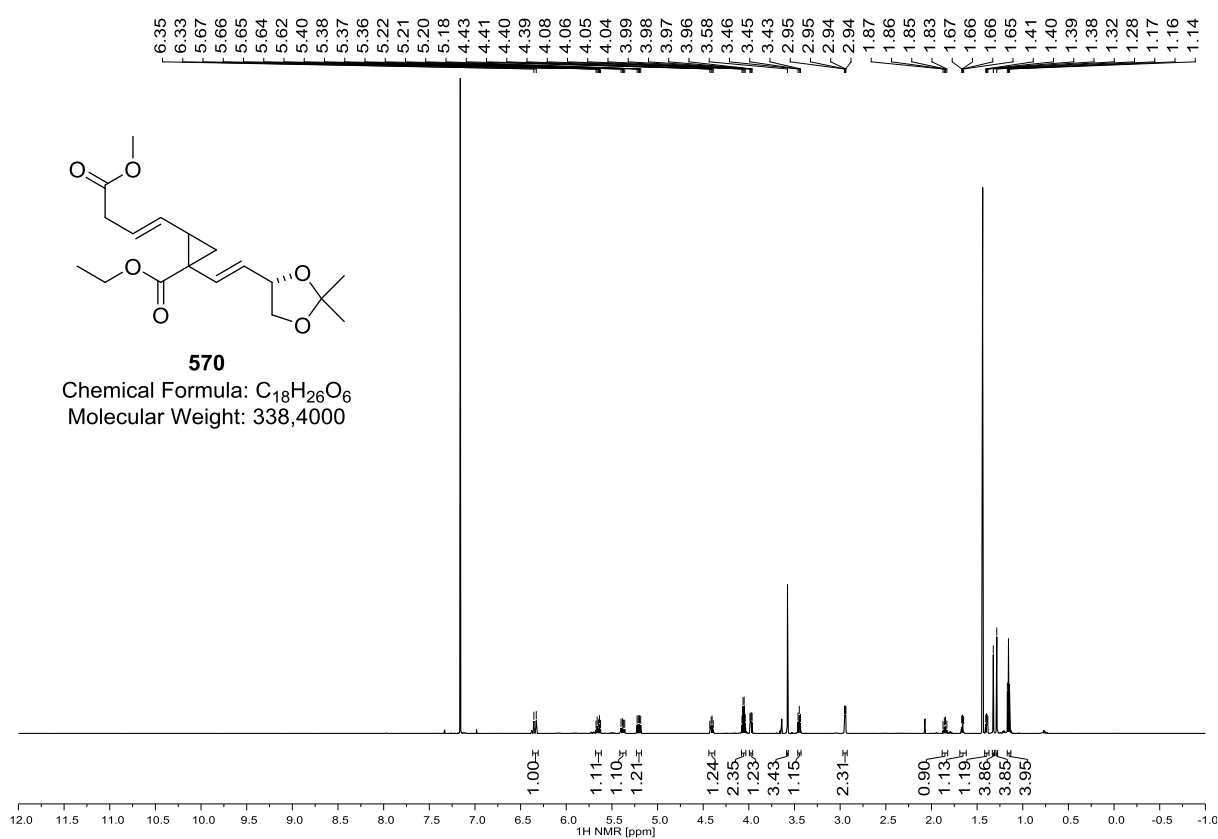
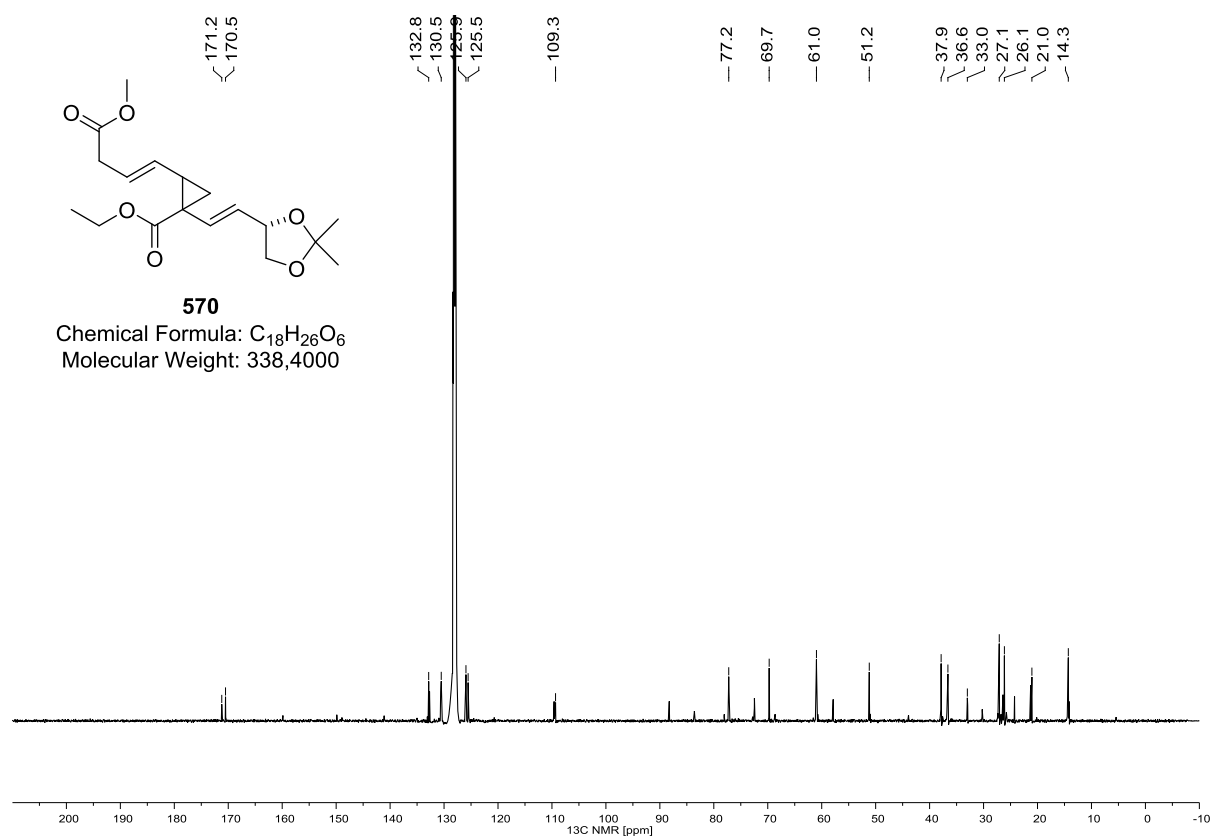
466 (^1H NMR, 400 MHz, CDCl_3)**466 (^{13}C NMR, 100 MHz, CDCl_3)**

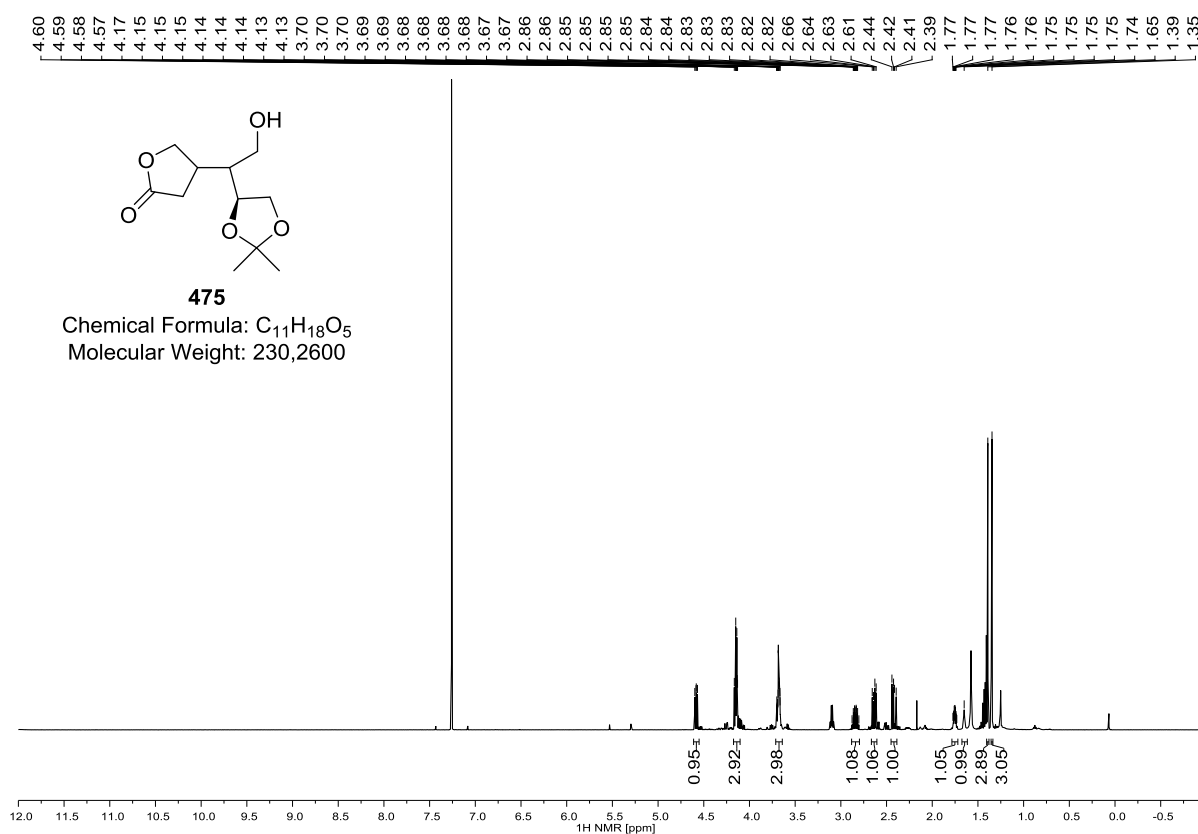
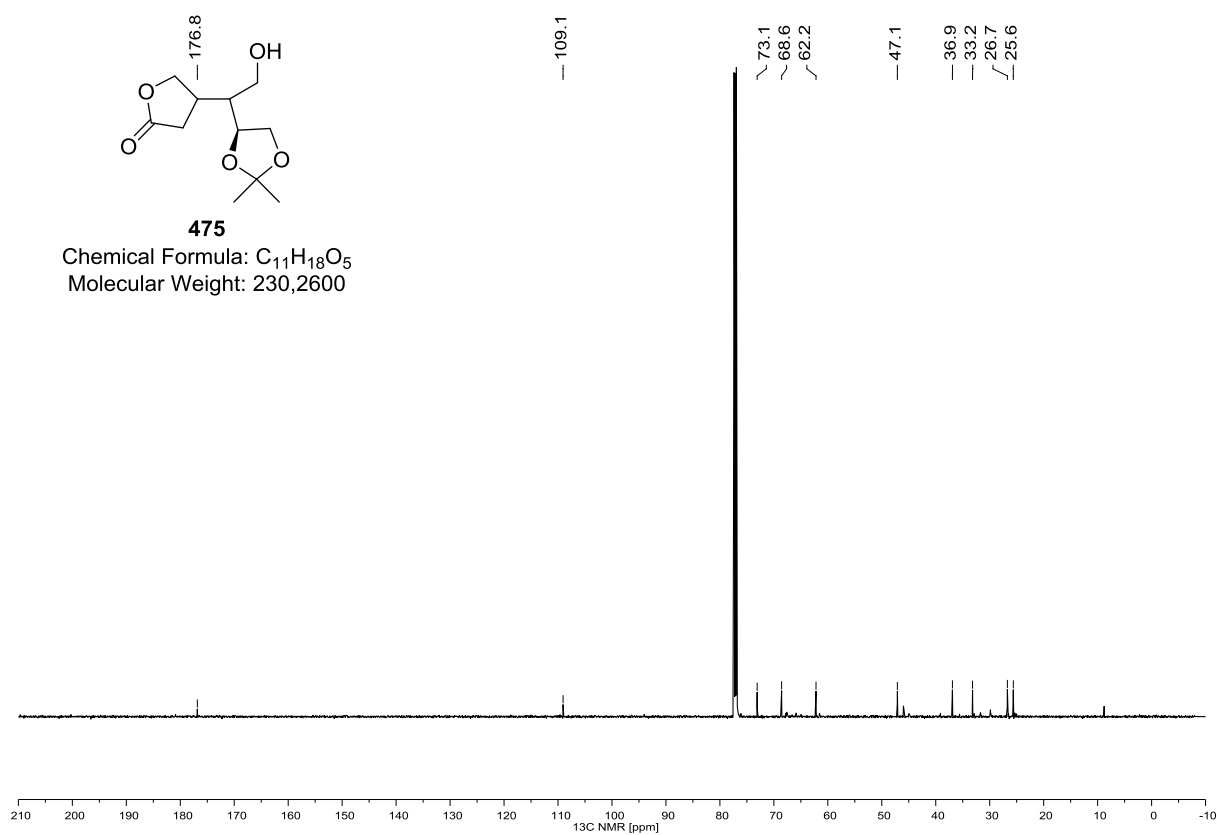
467 (^1H NMR, 600 MHz, CDCl_3)**467 (^{13}C NMR, 150 MHz, CDCl_3)**

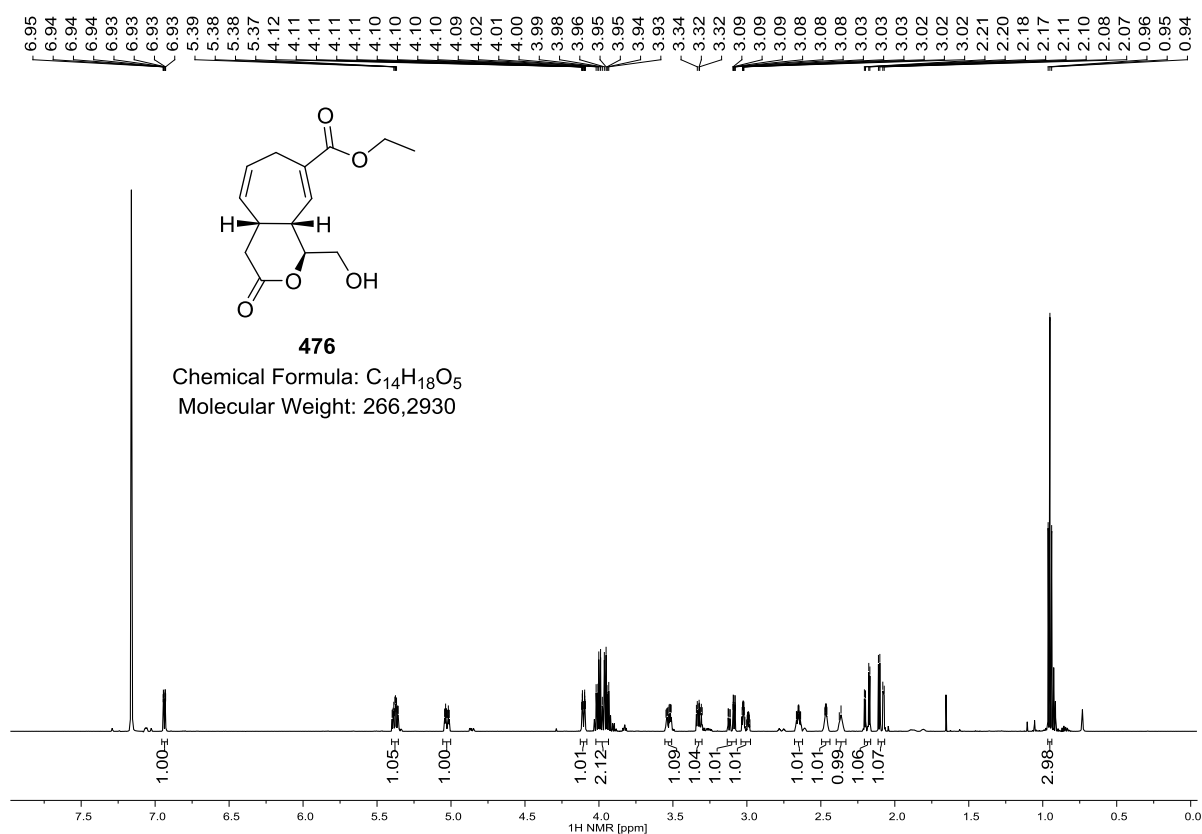
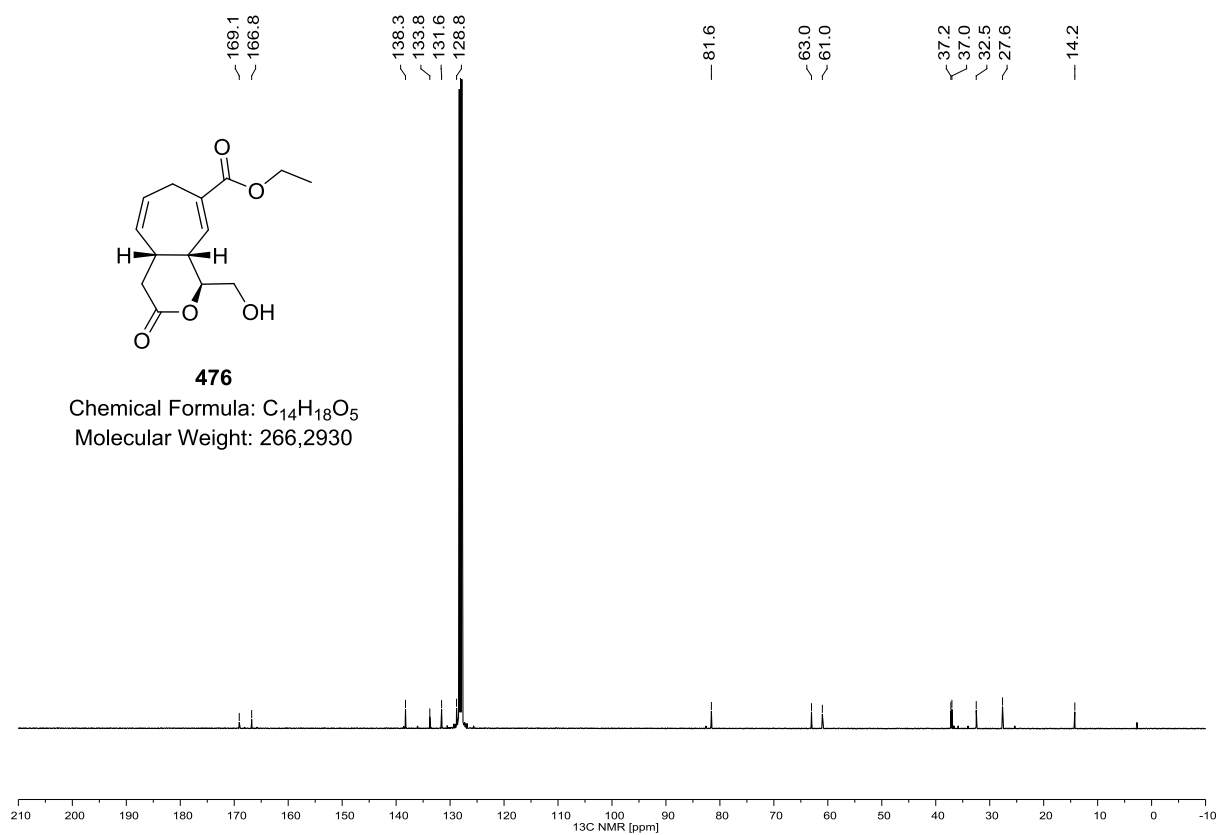
470/564 (^1H NMR, 400 MHz, CDCl_3)**470/564 (^{13}C NMR, 100 MHz, CDCl_3)**

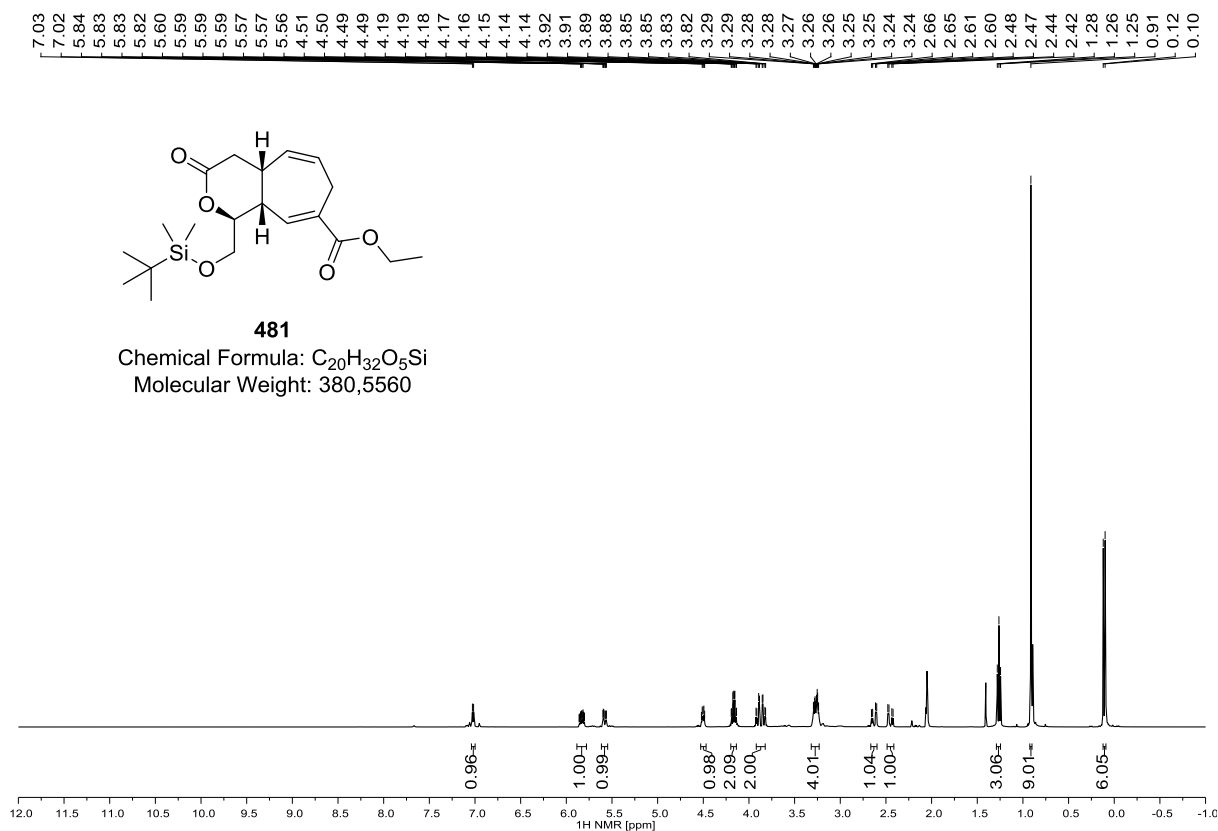
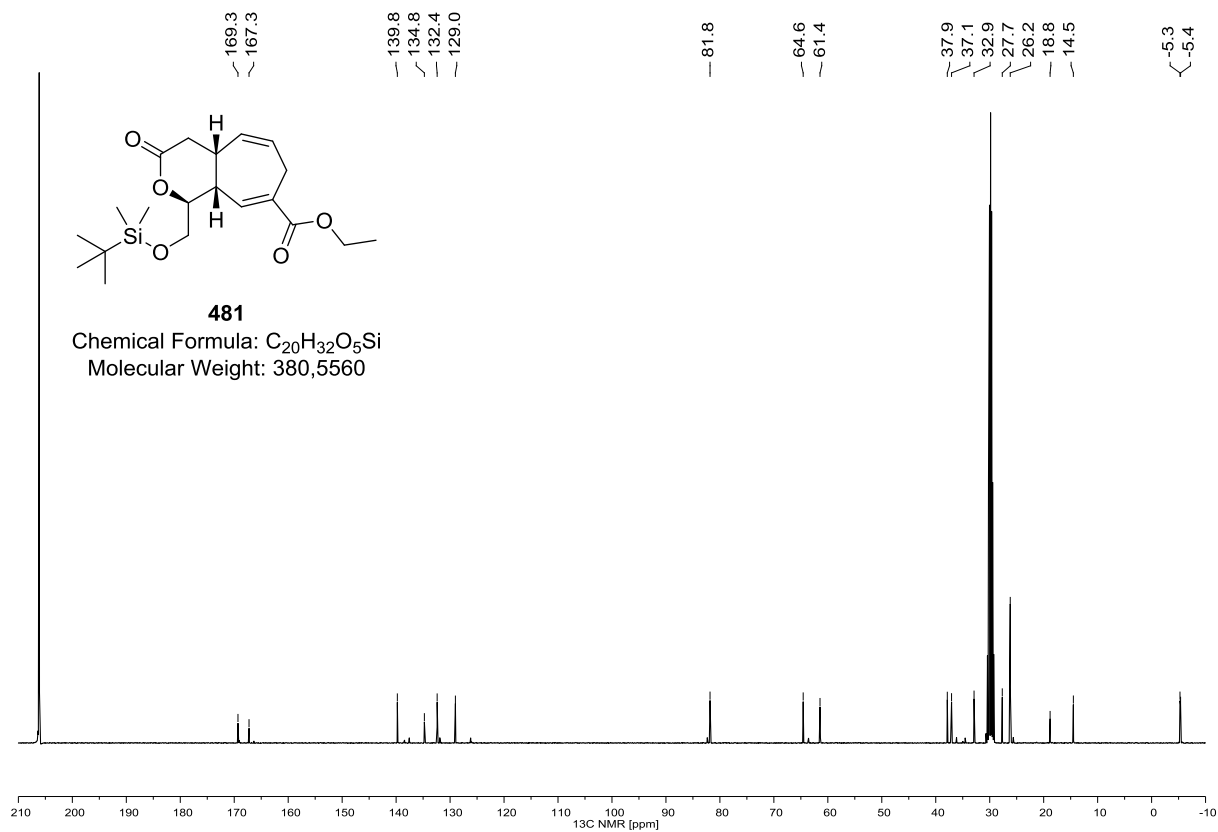
469 (^1H NMR, 600 MHz, C_6D_6)**469 (^{13}C NMR, 150 MHz, C_6D_6)**

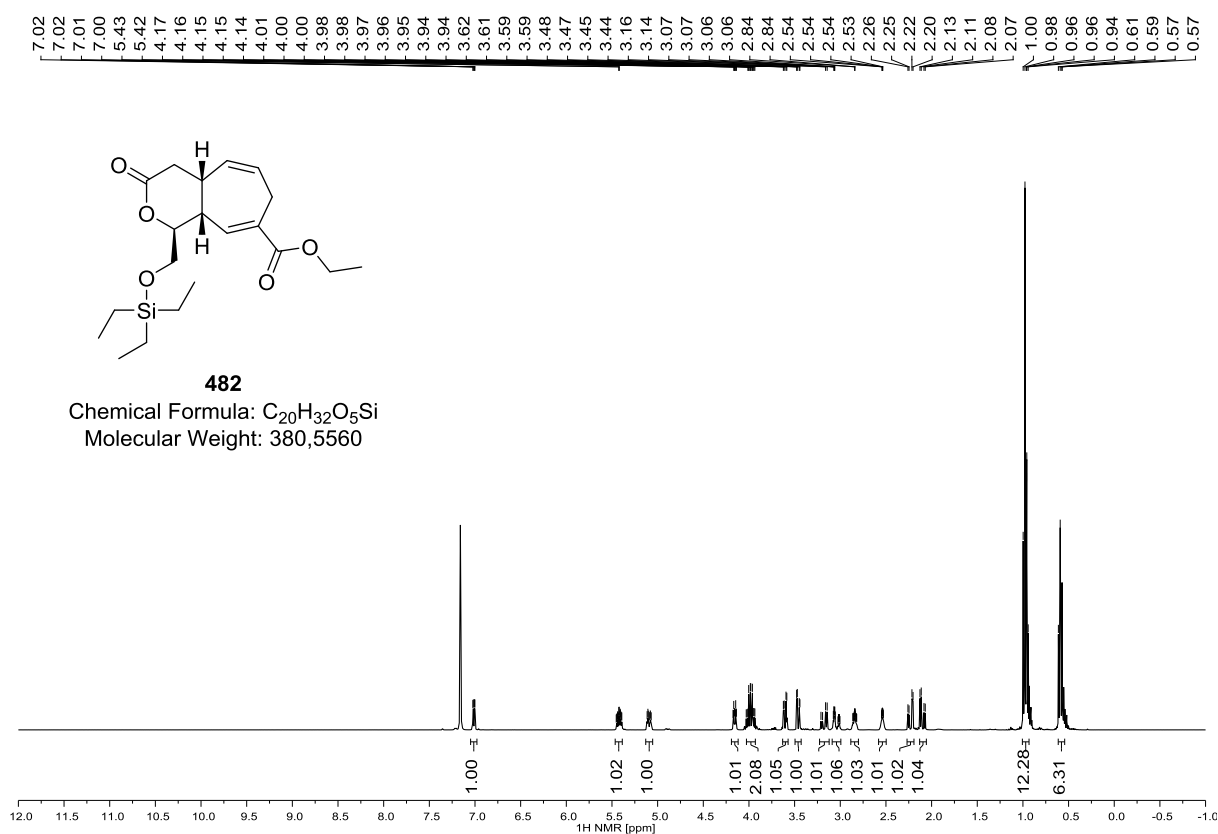
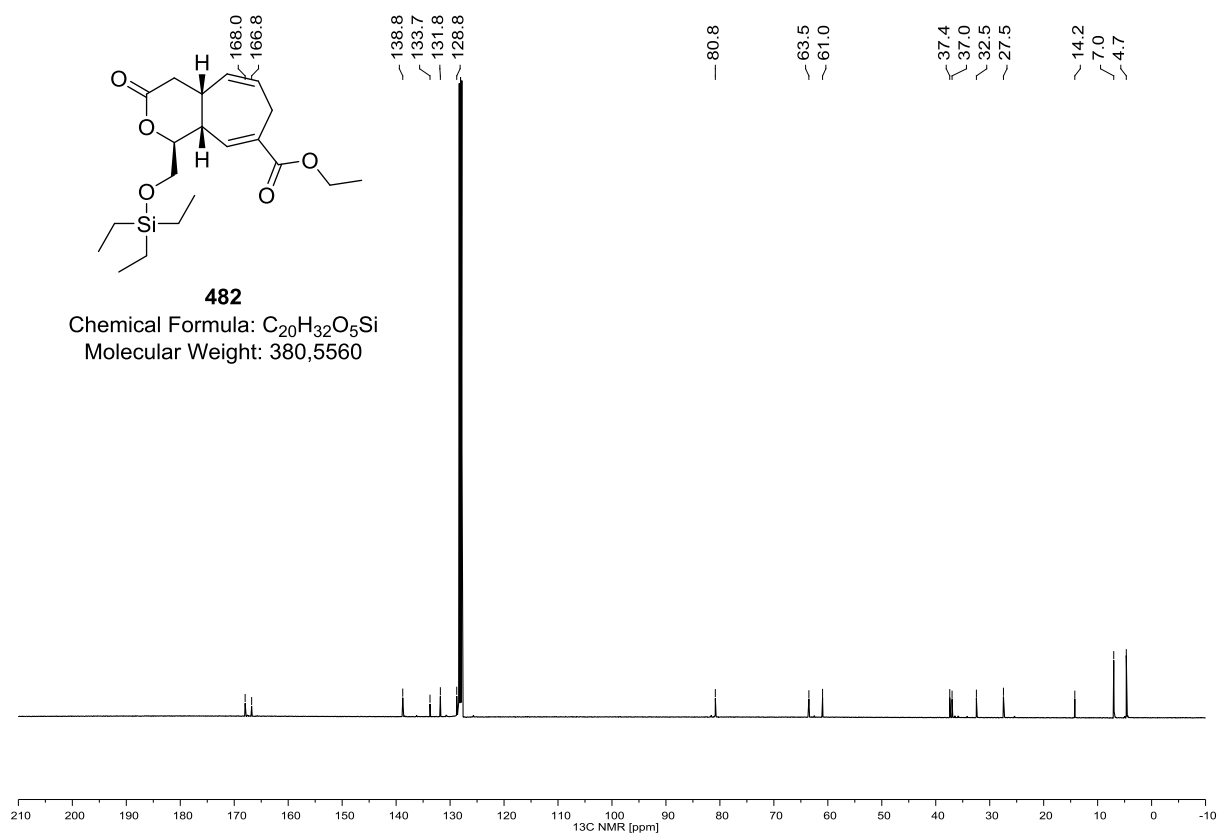
471 (^1H NMR, 600 MHz, C_6D_6)**471 (^{13}C NMR, 150 MHz, C_6D_6)**

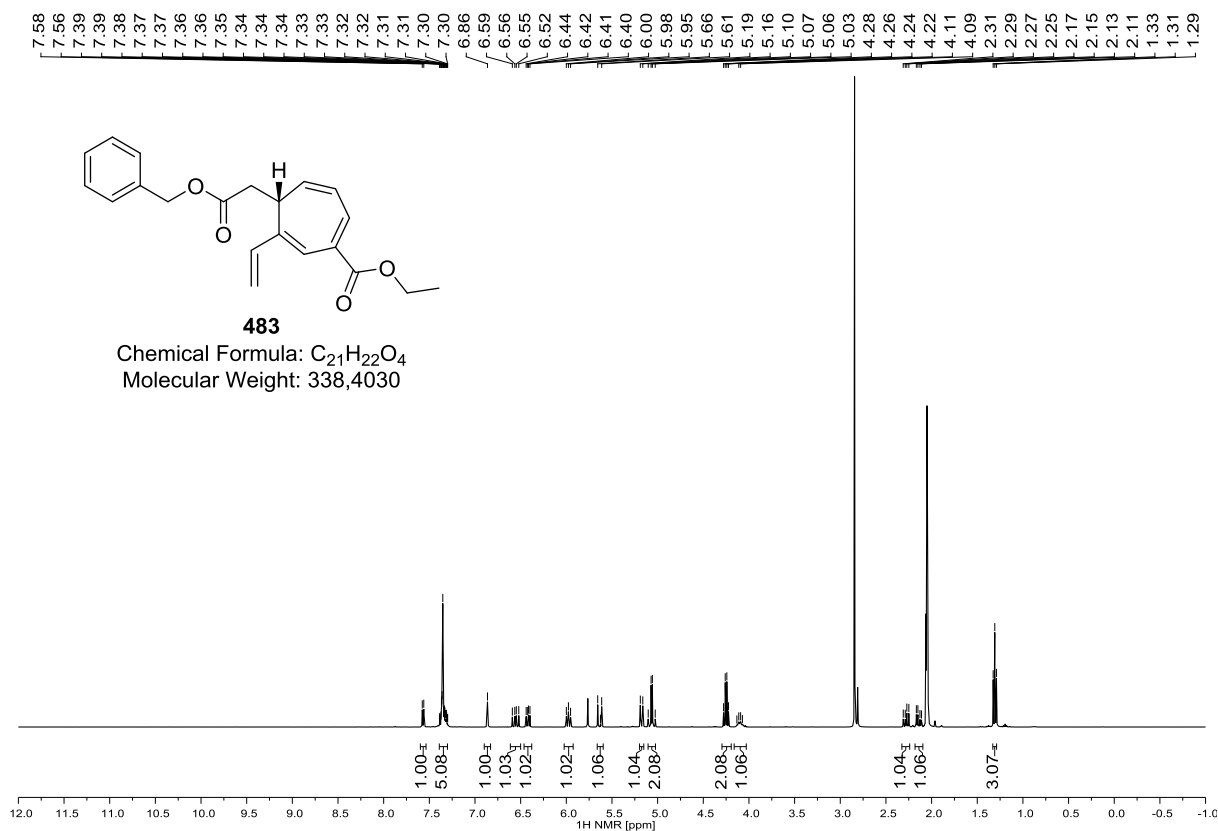
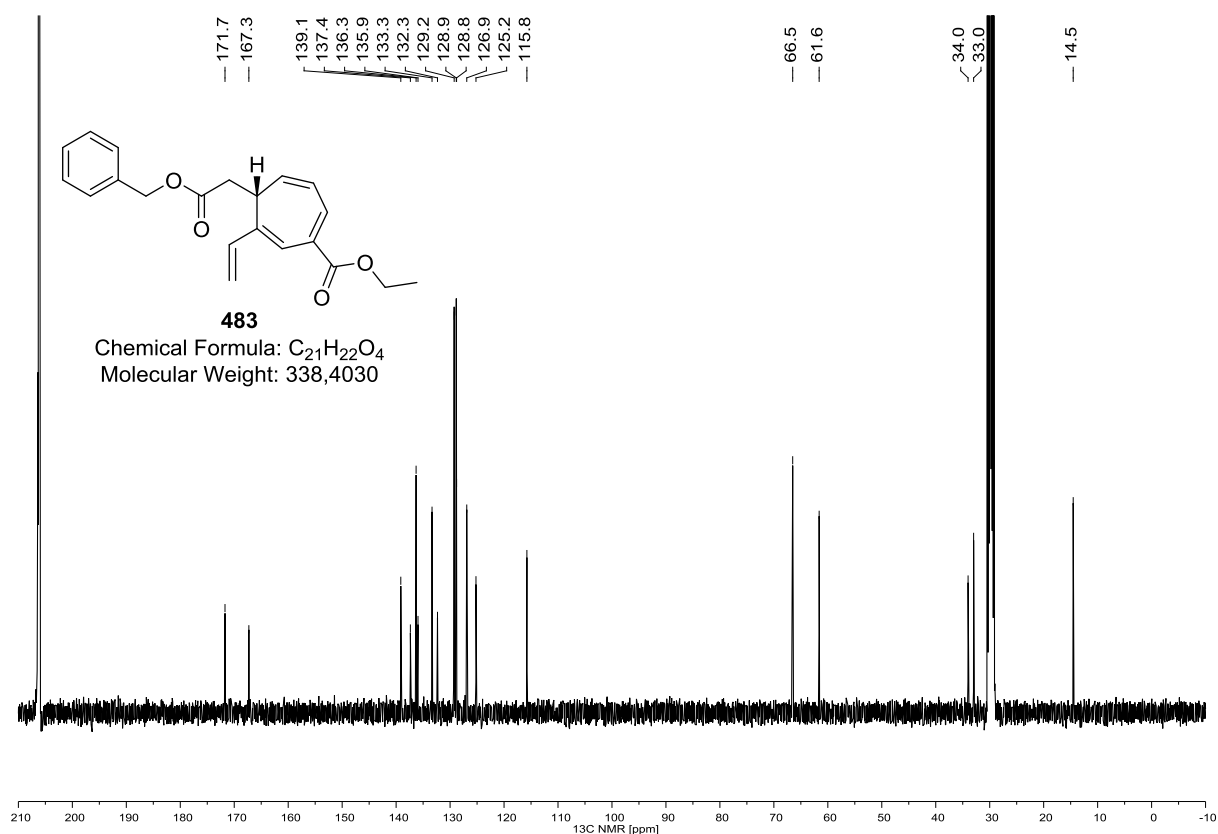
570 (^1H NMR, 600 MHz, C_6D_6)570 (^{13}C NMR, 150 MHz, C_6D_6)

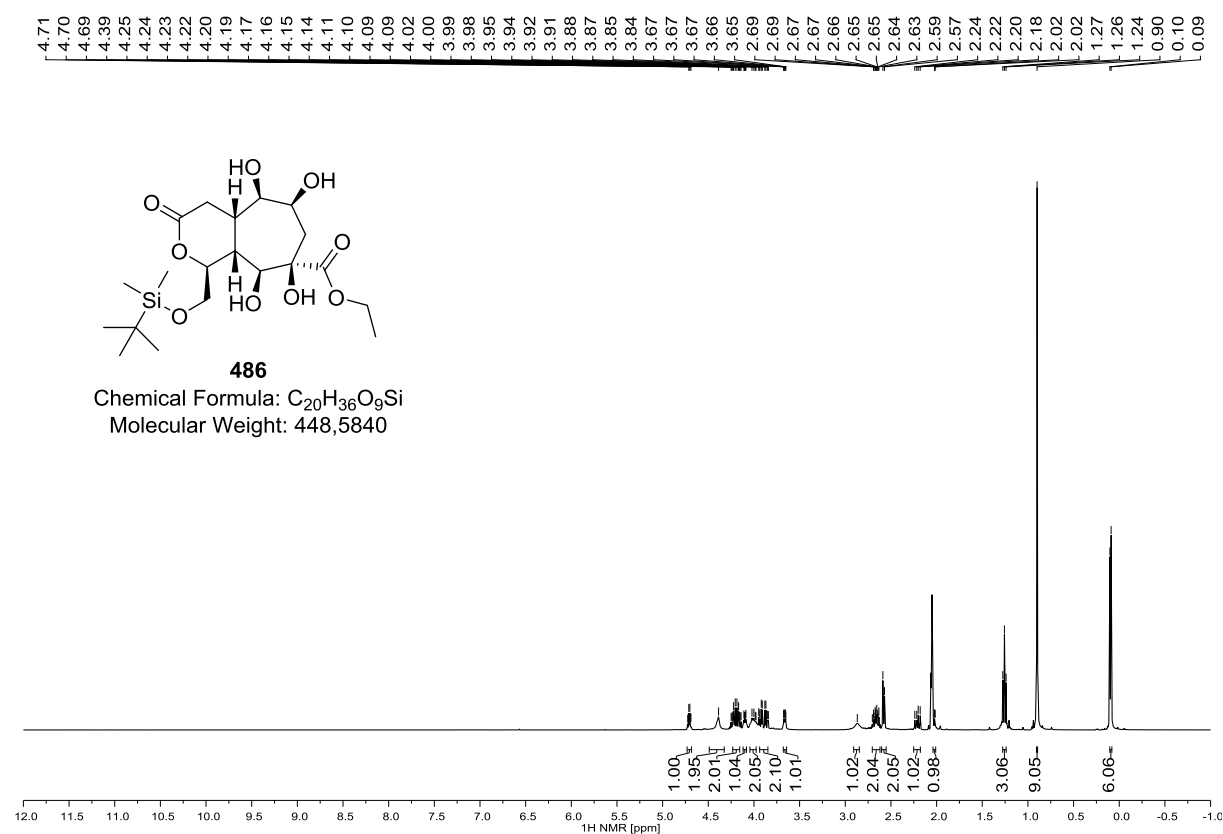
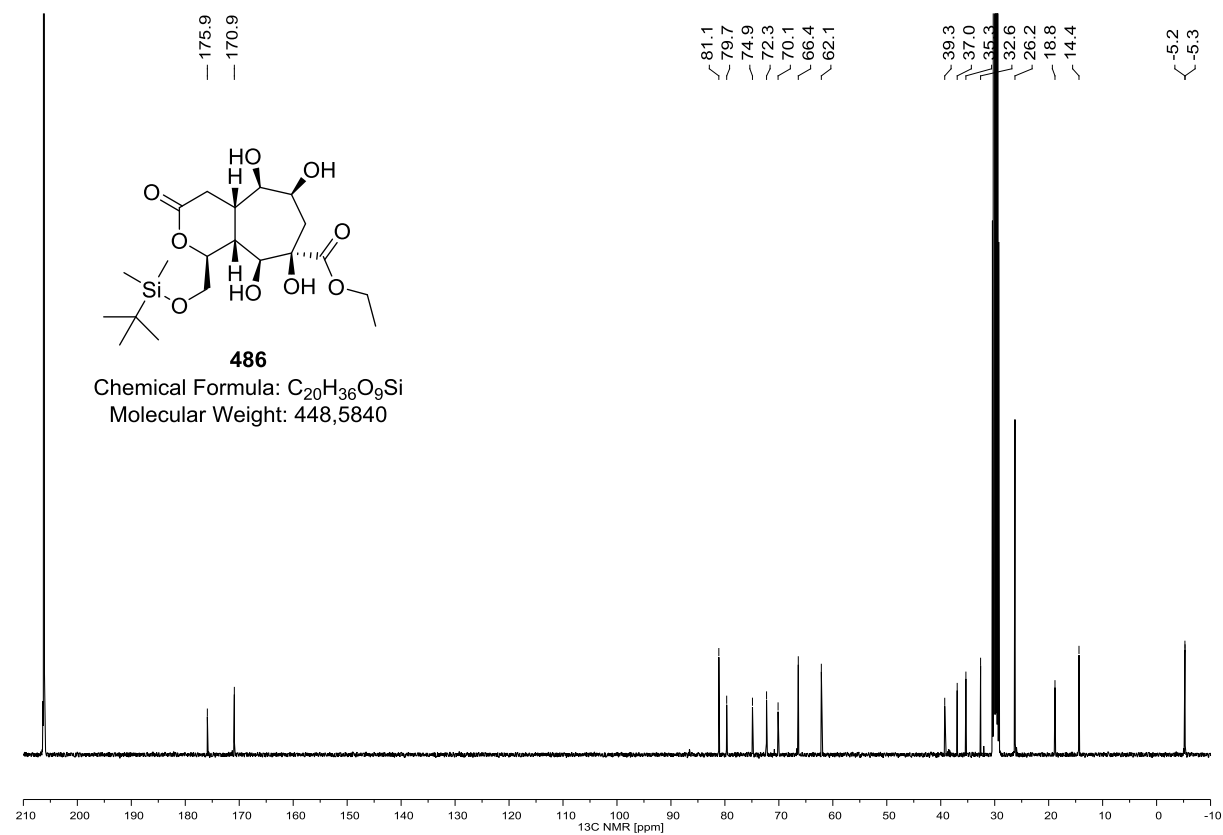
475 (^1H NMR, 600 MHz, CDCl_3)**475 (^{13}C NMR, 150 MHz, CDCl_3)**

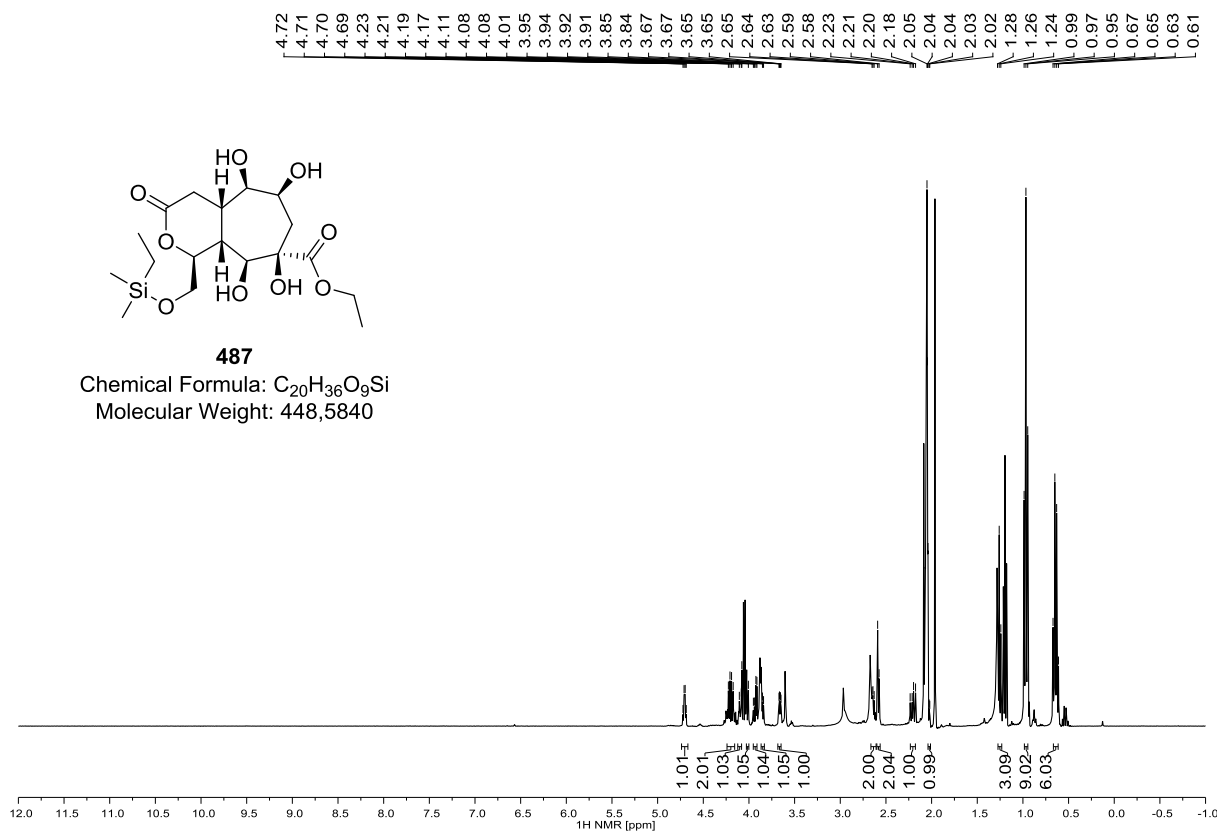
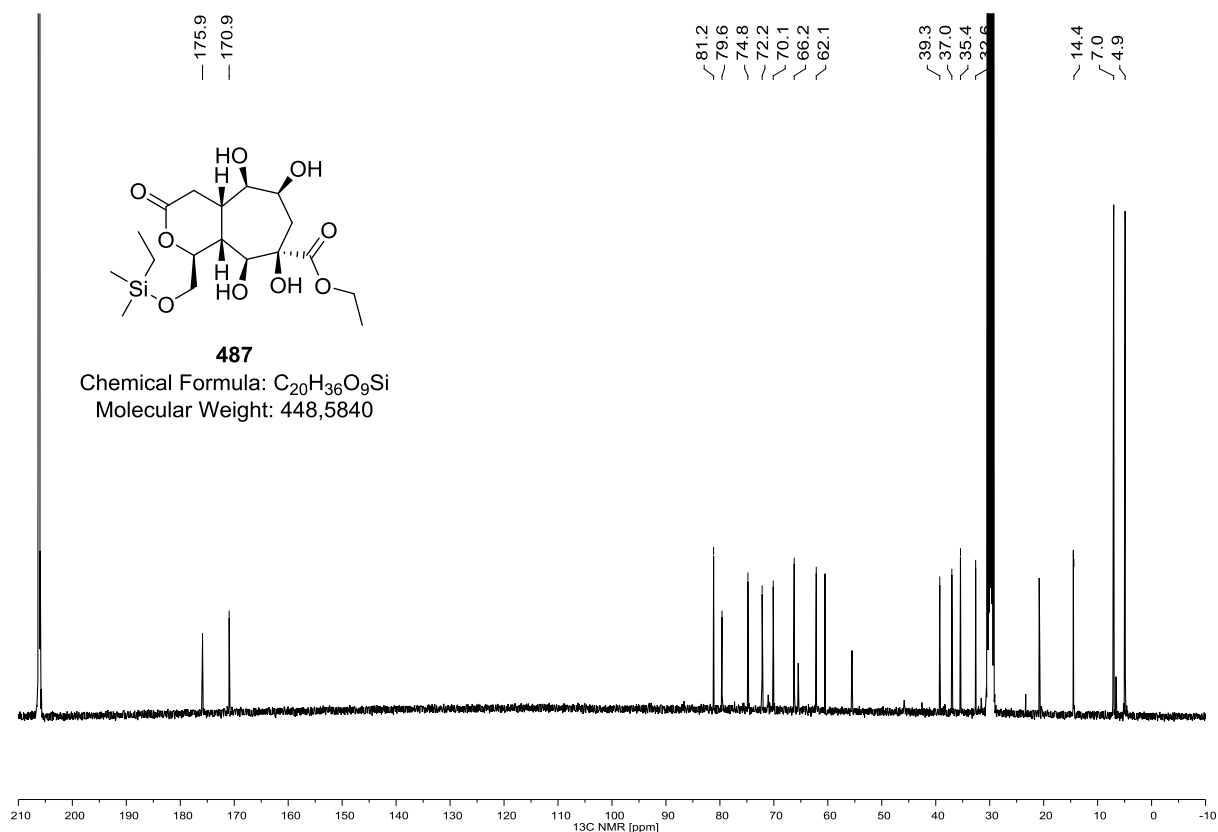
476 (^1H NMR, 600 MHz, C_6D_6)**476 (^{13}C NMR, 150 MHz, C_6D_6)**

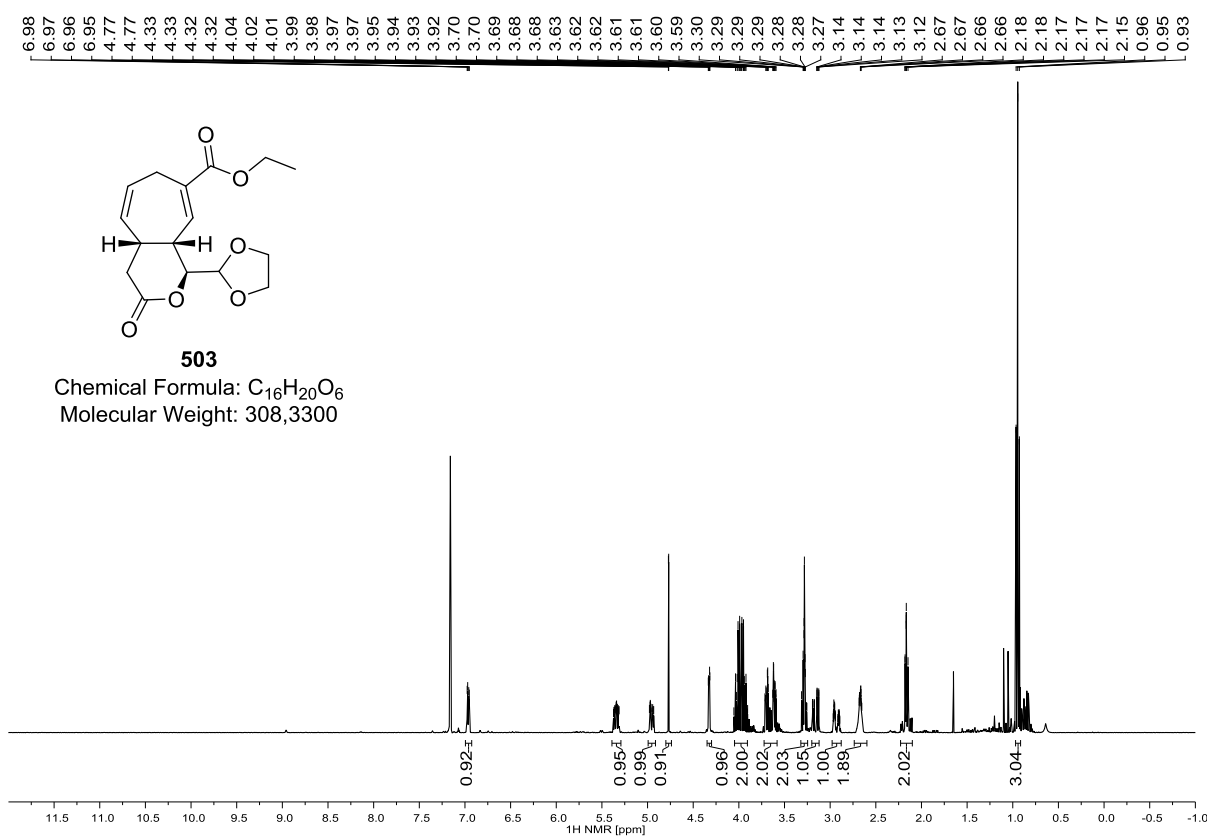
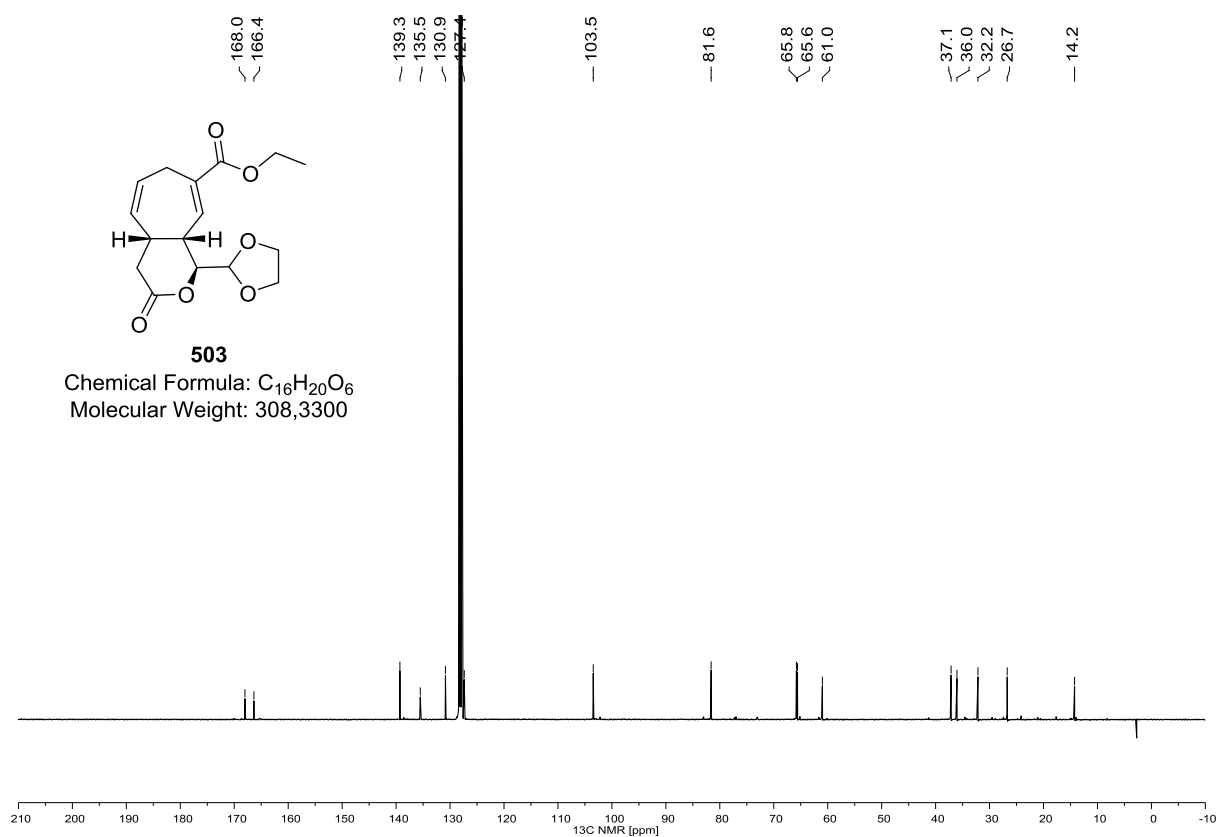
481 (^1H NMR, 400 MHz, $(\text{D}_3\text{C})_2\text{CO}$)**481 (^{13}C NMR, 100 MHz, $(\text{D}_3\text{C})_2\text{CO}$)**

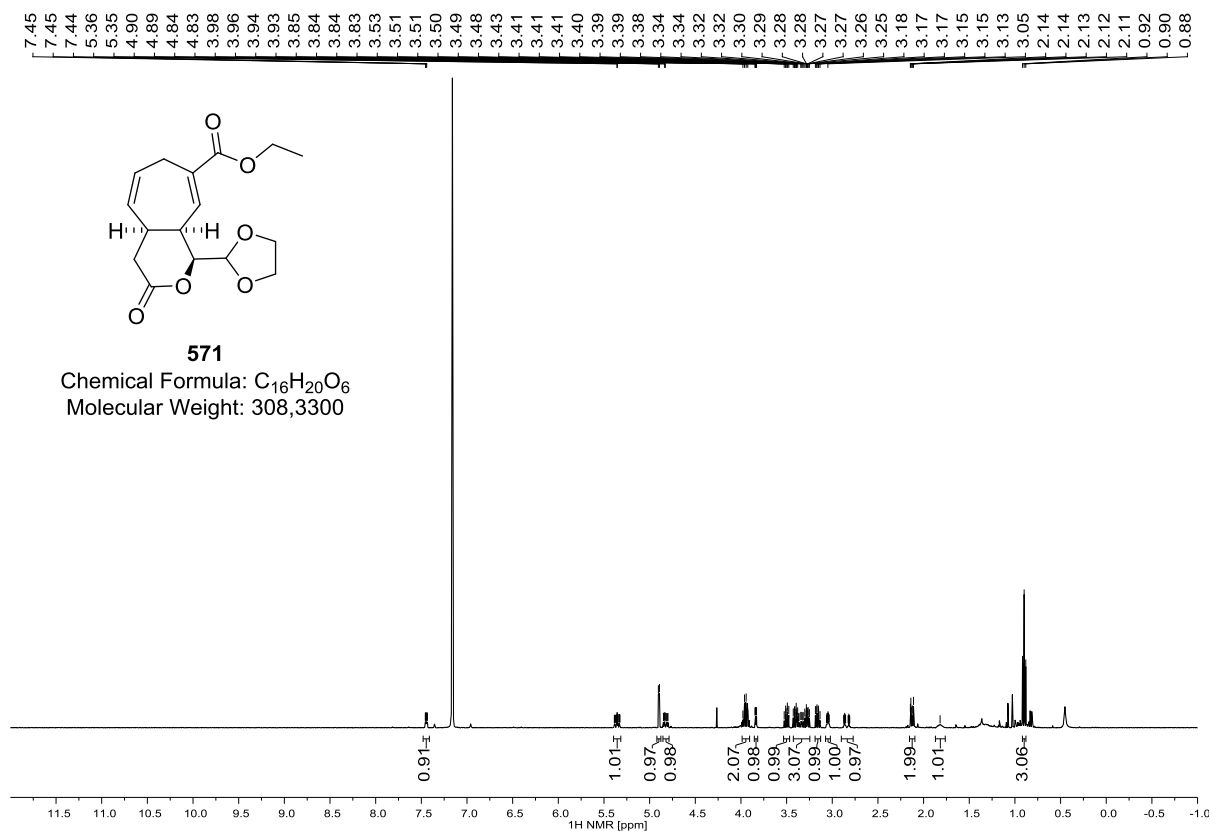
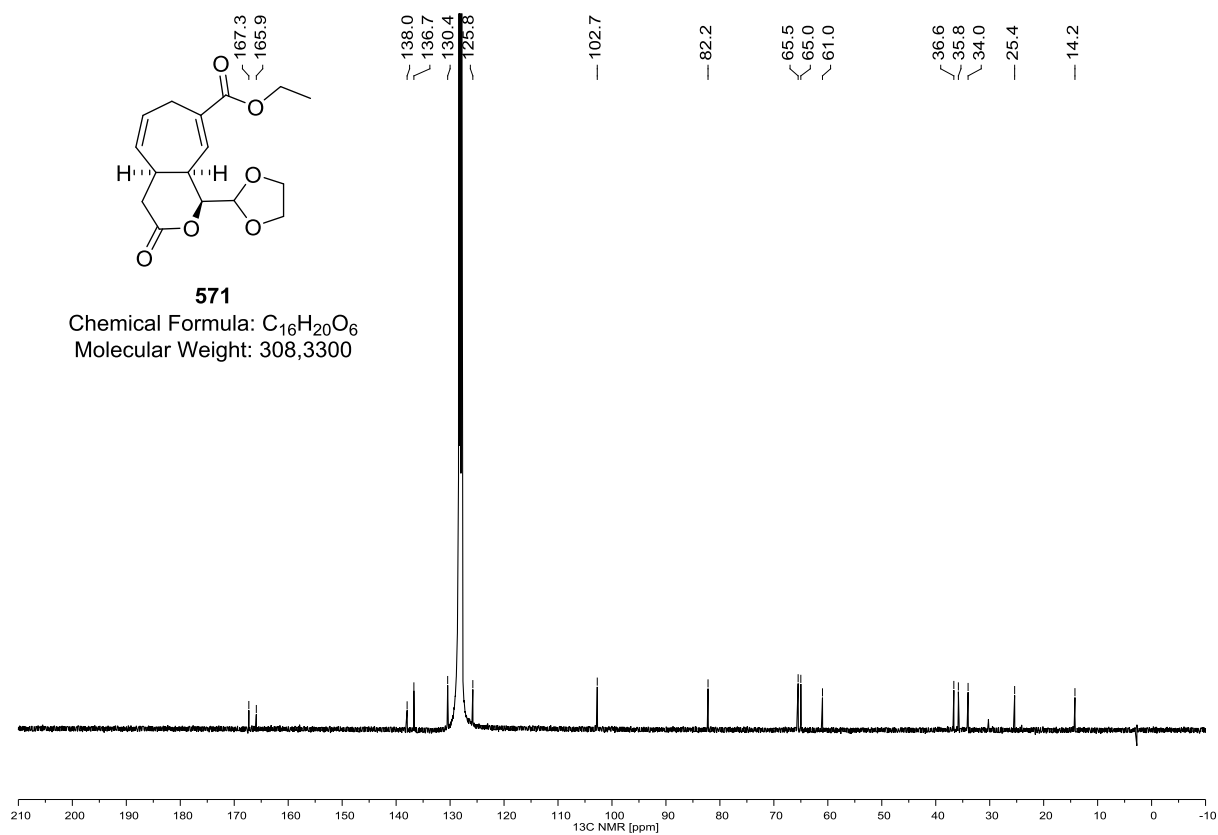
482 (^1H NMR, 400 MHz, C_6D_6)**482 (^{13}C NMR, 100 MHz, C_6D_6)**

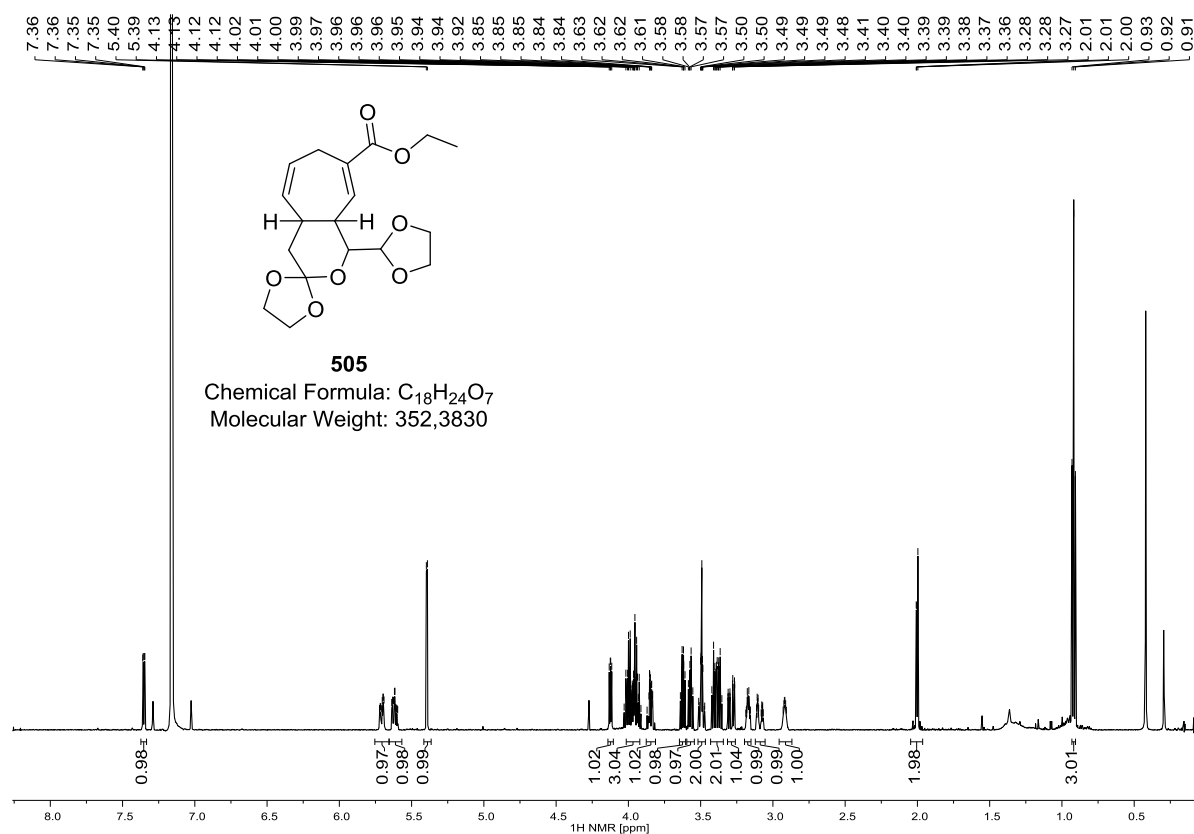
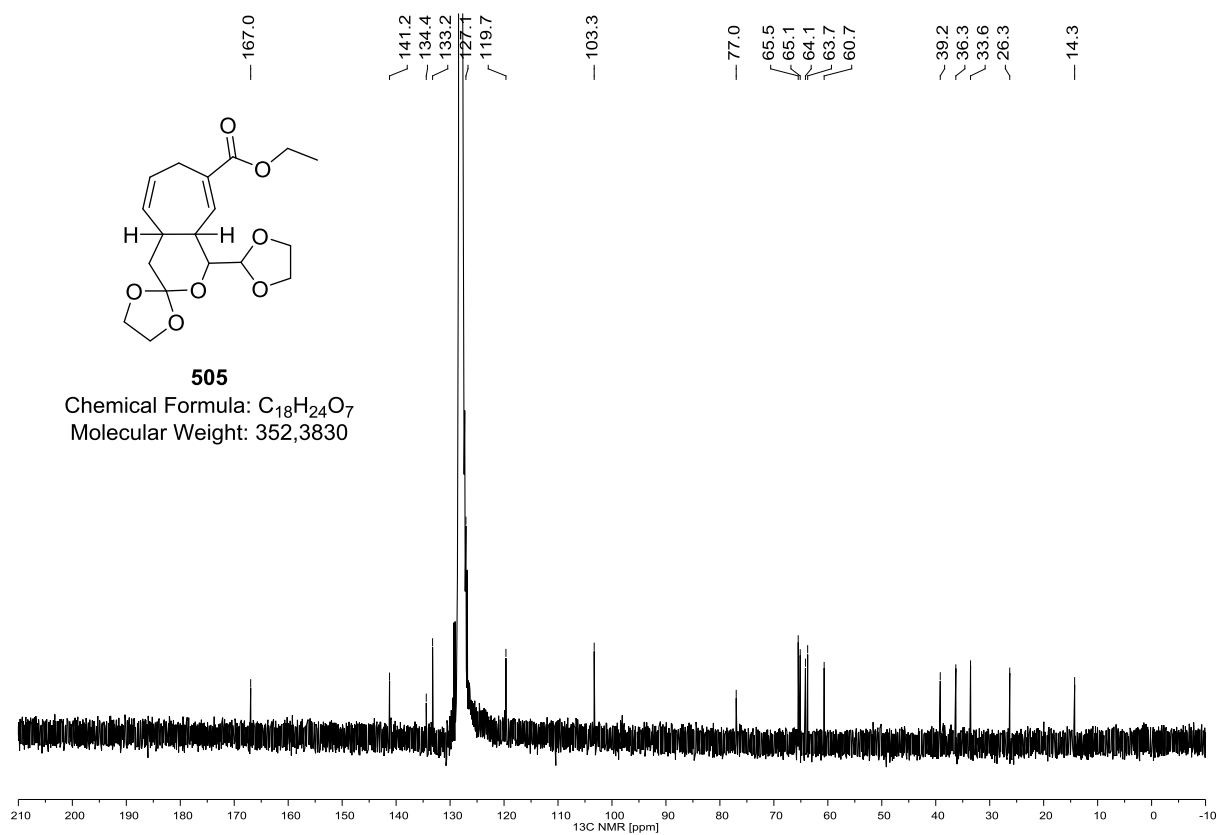
483 (^1H NMR, 400 MHz, $(\text{D}_3\text{C})_2\text{CO}$)**483 (^{13}C NMR, 100 MHz, $(\text{D}_3\text{C})_2\text{CO}$)**

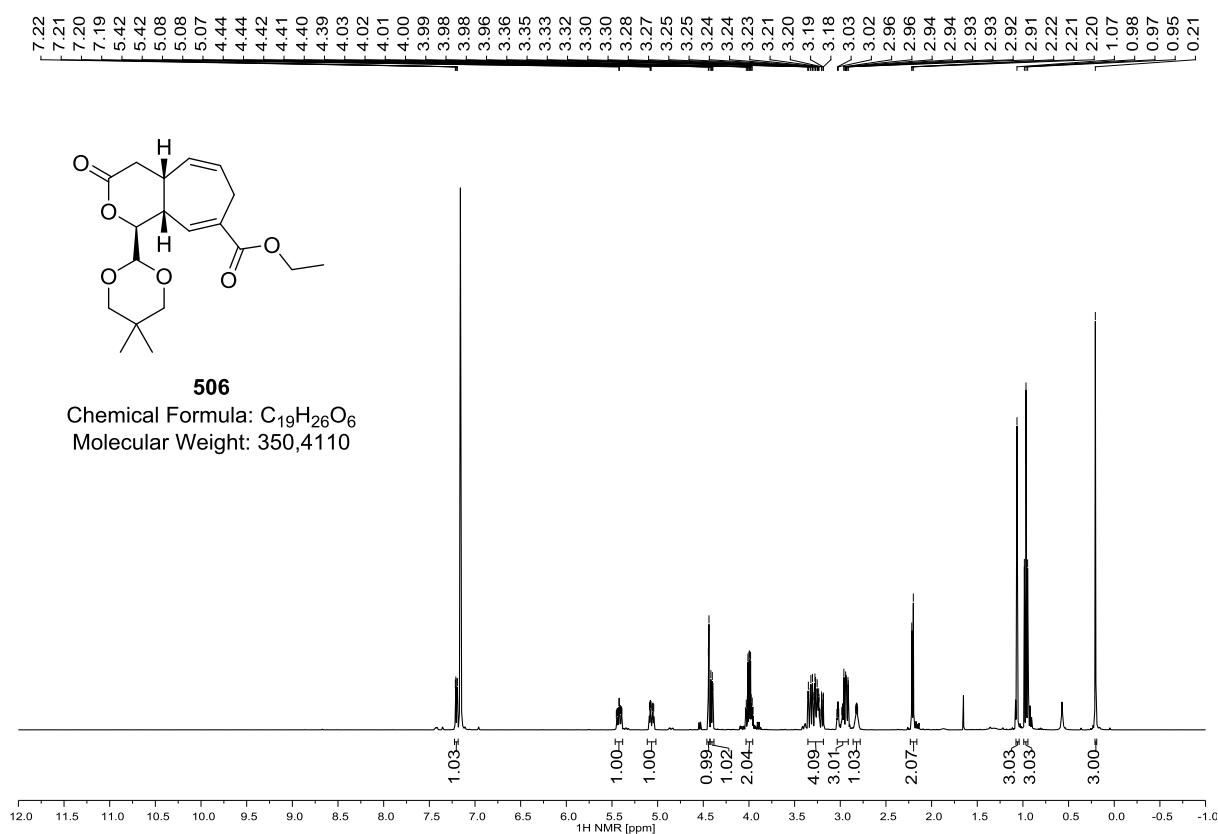
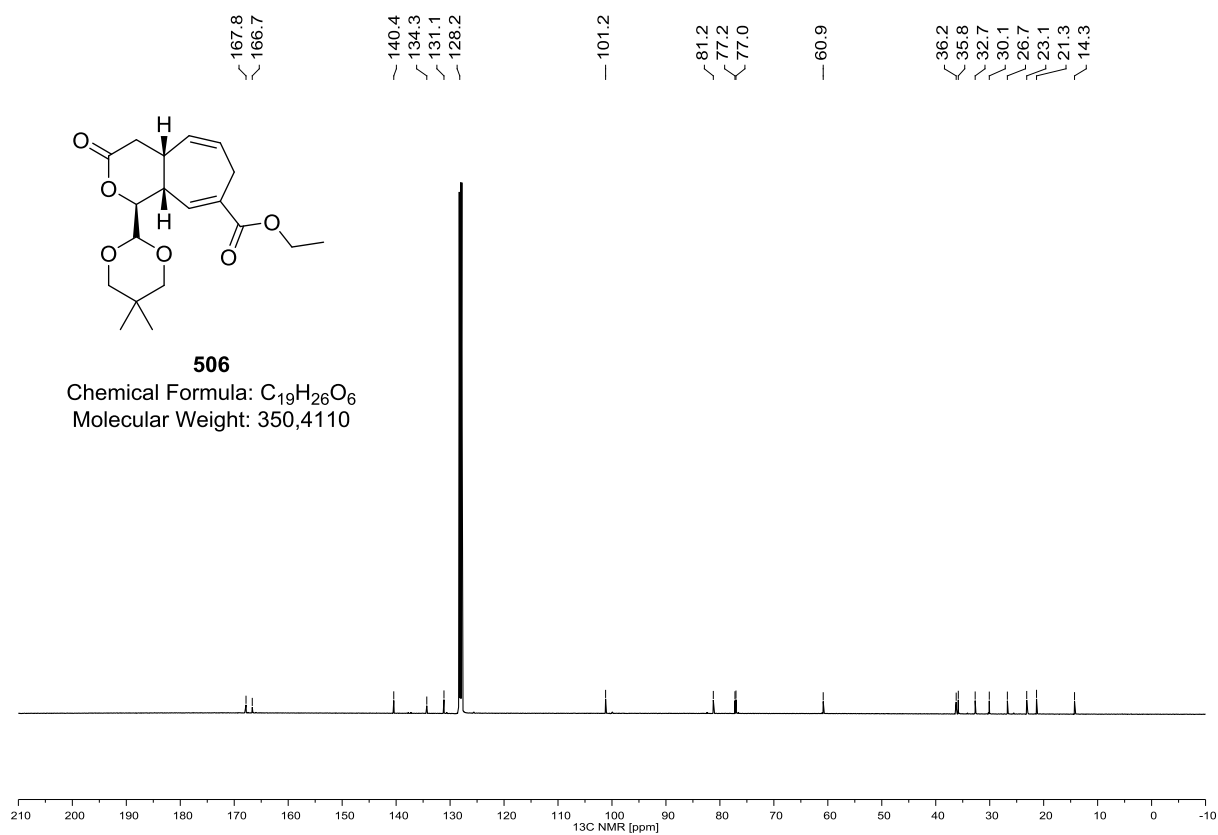
486 (^1H NMR, 400 MHz, $(\text{D}_3\text{C})_2\text{CO}$)

486 (^{13}C NMR, 100 MHz, $(\text{D}_3\text{C})_2\text{CO}$)


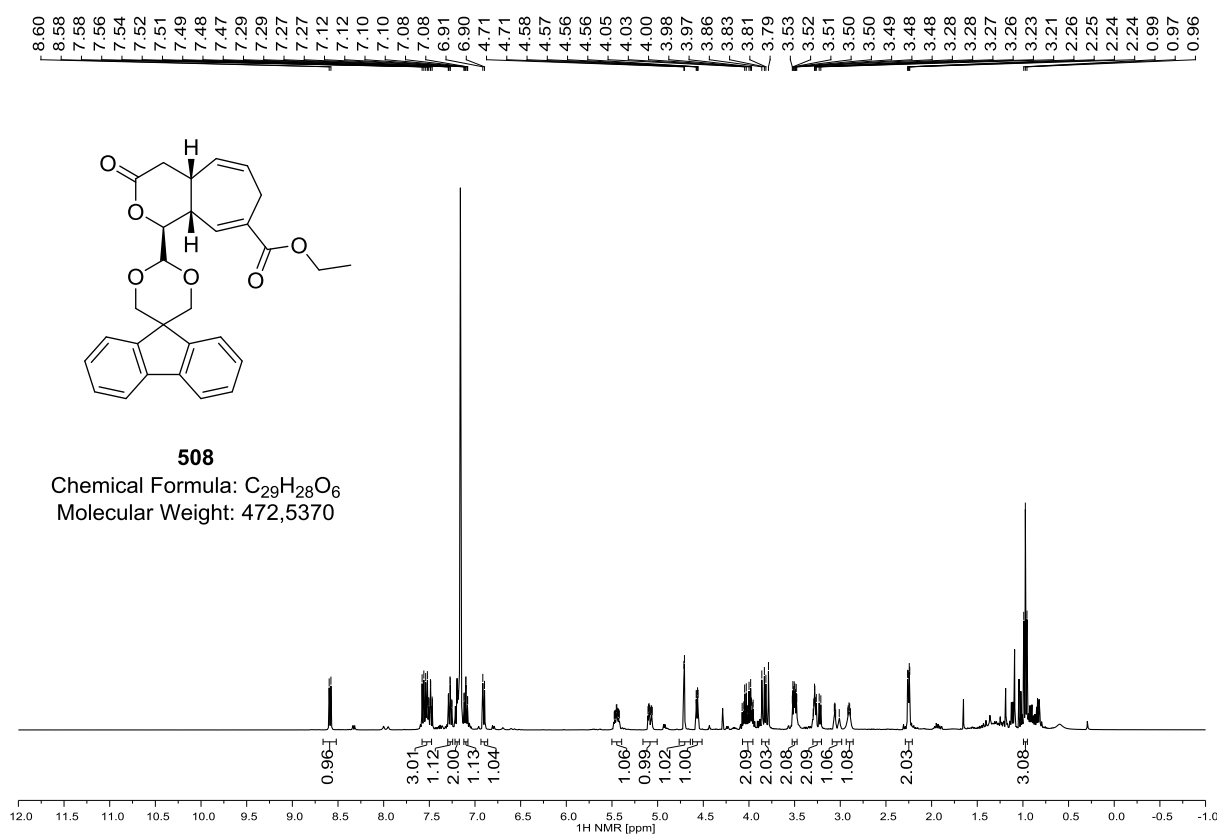
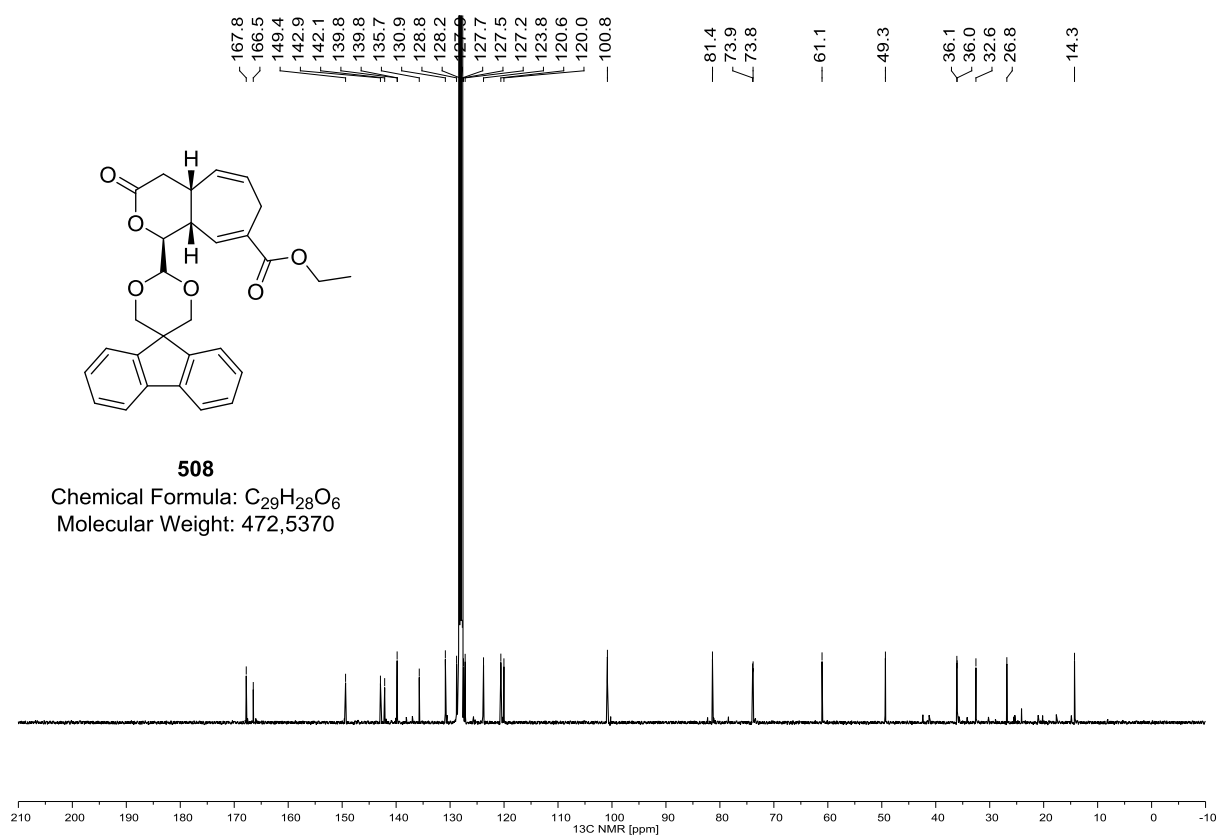
487 (^1H NMR, 400 MHz, $(\text{D}_3\text{C})_2\text{CO}$)**487 (^{13}C NMR, 100 MHz, $(\text{D}_3\text{C})_2\text{CO}$)**

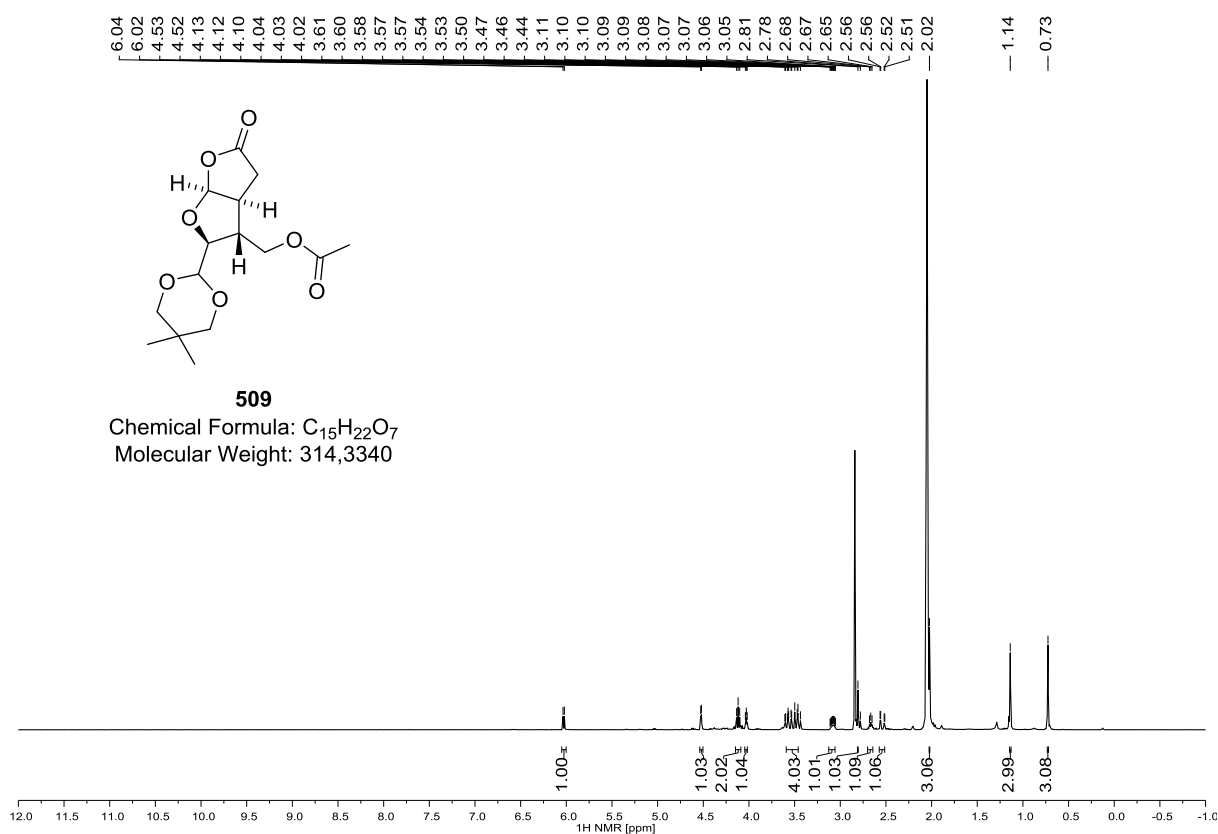
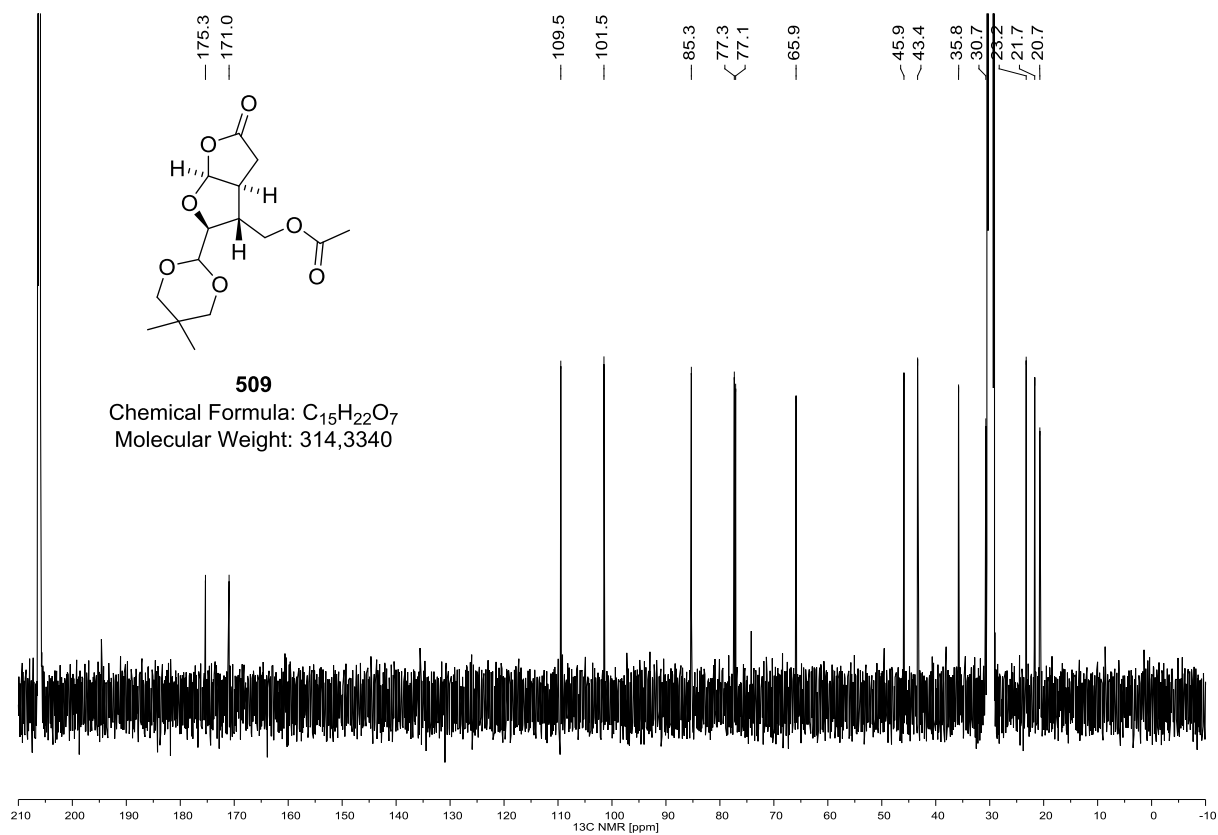
503 (^1H NMR, 400 MHz, C_6D_6)**503 (^{13}C NMR, 100 MHz, C_6D_6)**

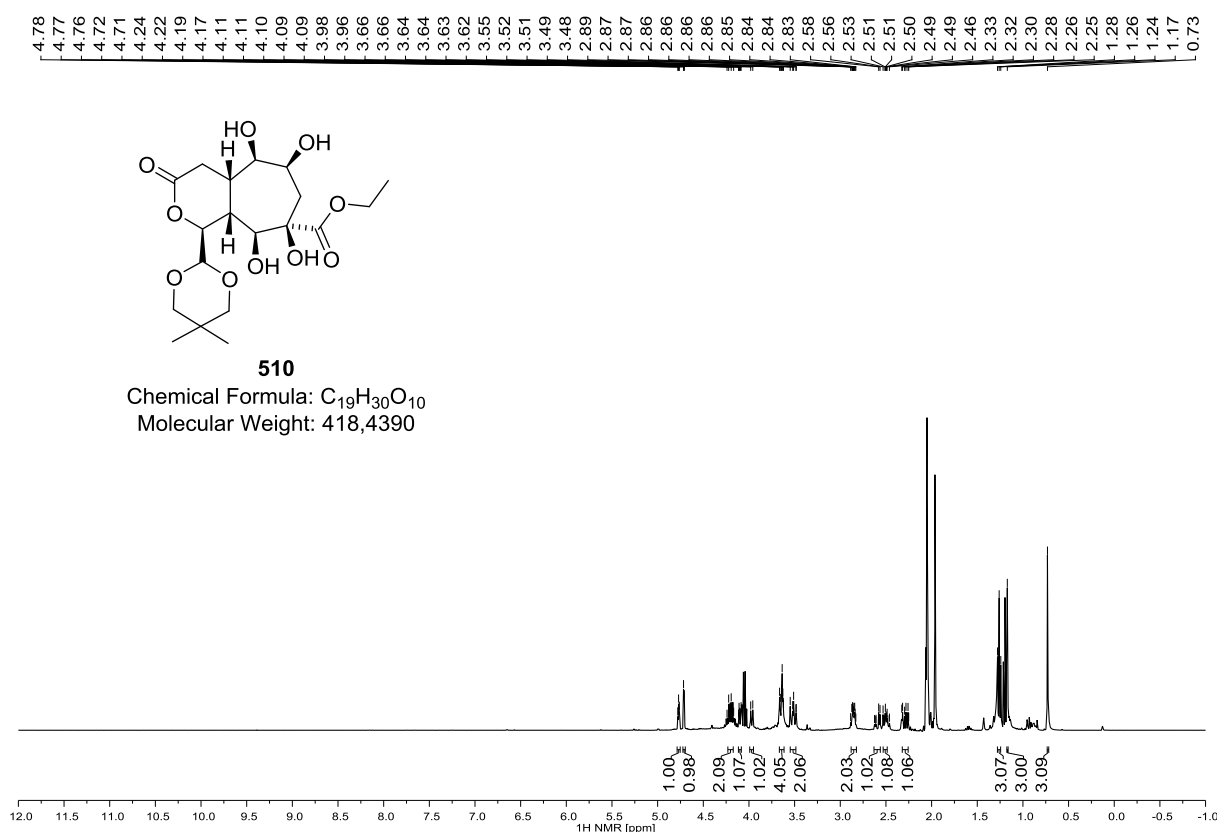
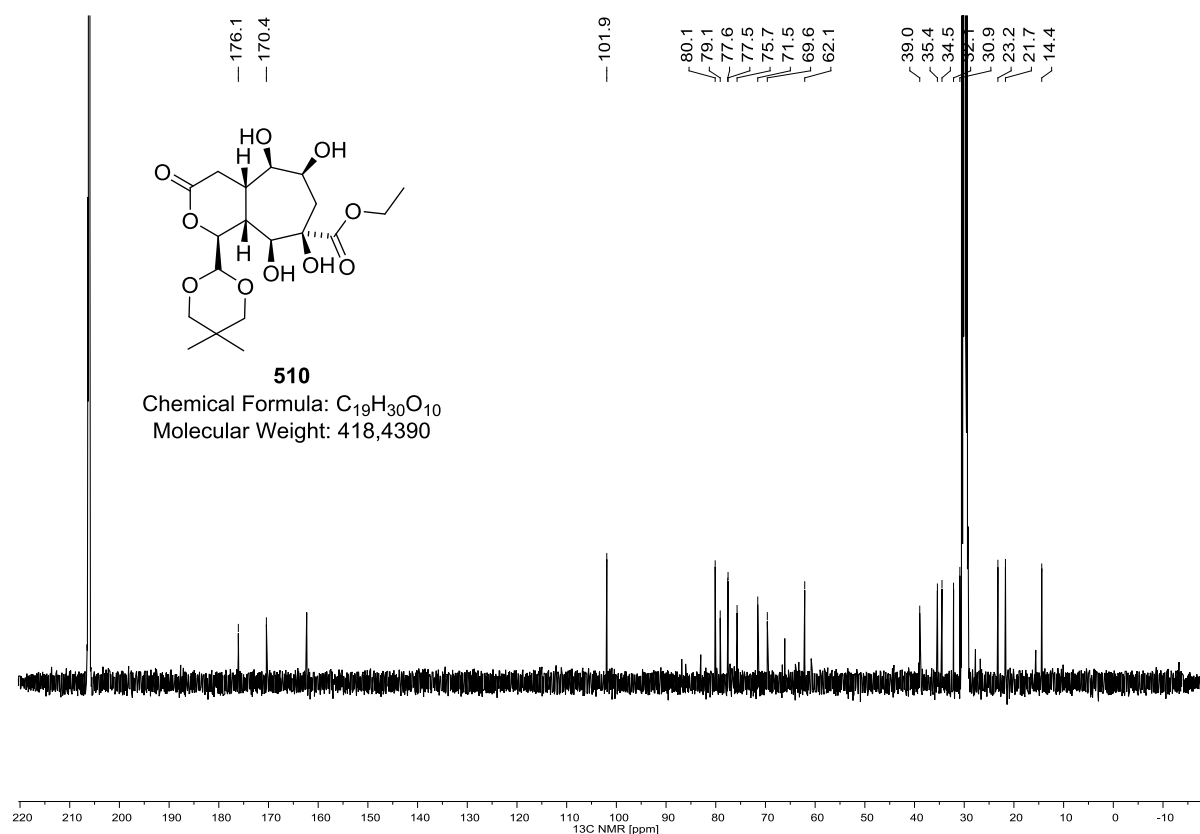
571 (^1H NMR, 400 MHz, C_6D_6)**571 (^{13}C NMR, 100 MHz, C_6D_6)**

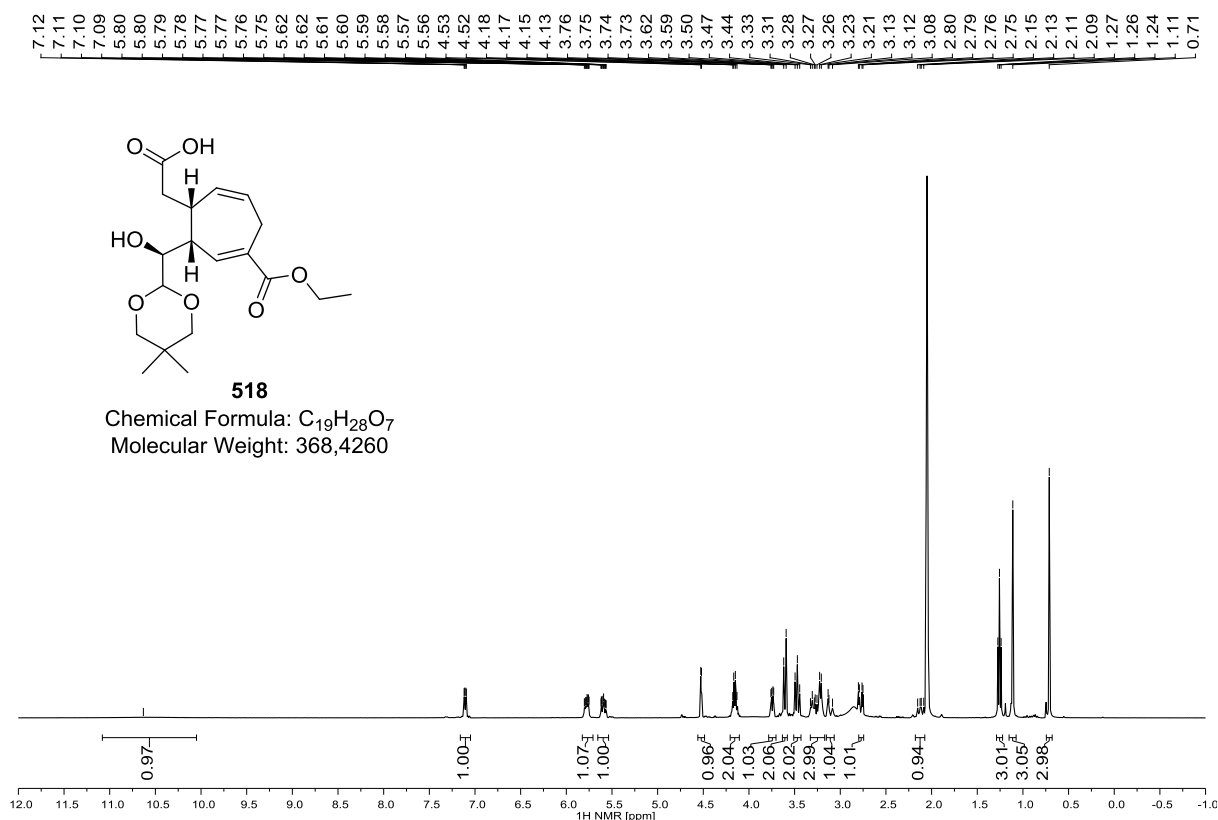
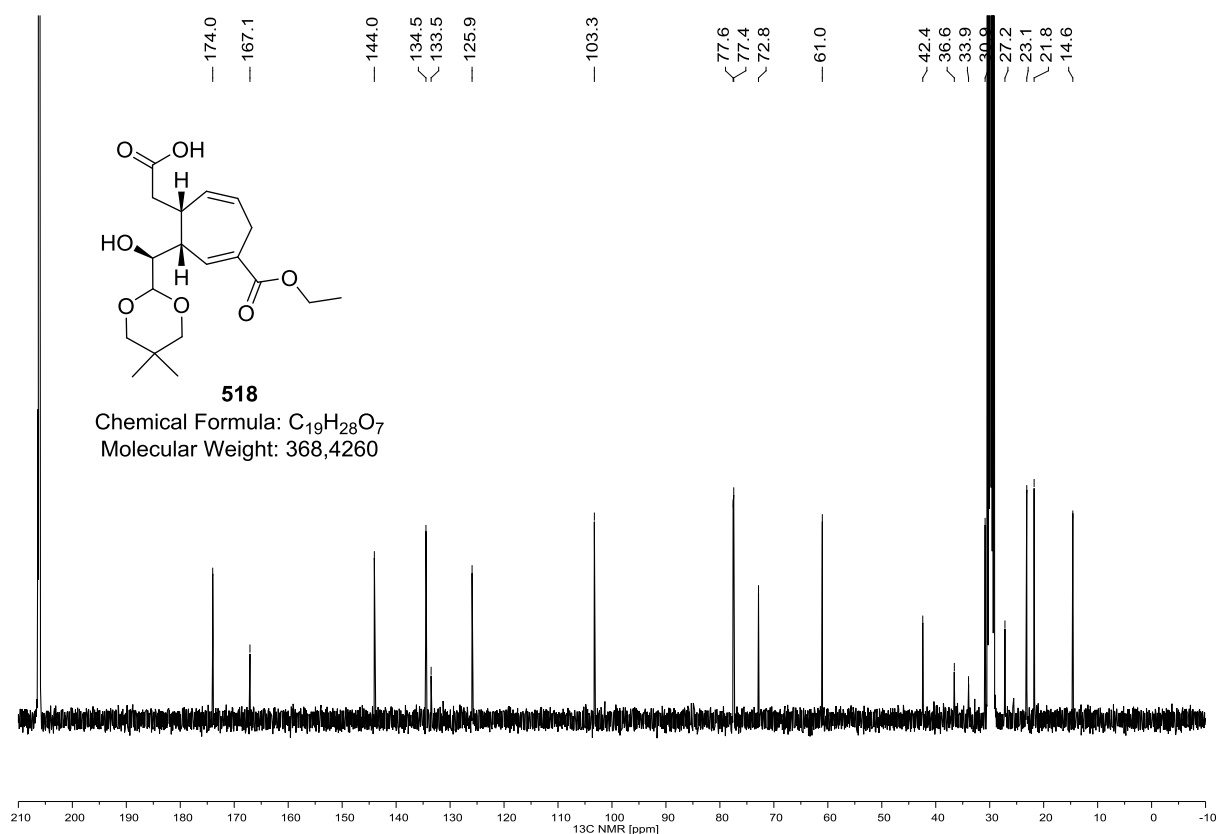
505 (^1H NMR, 400 MHz, C_6D_6)505 (^{13}C NMR, 100 MHz, C_6D_6)

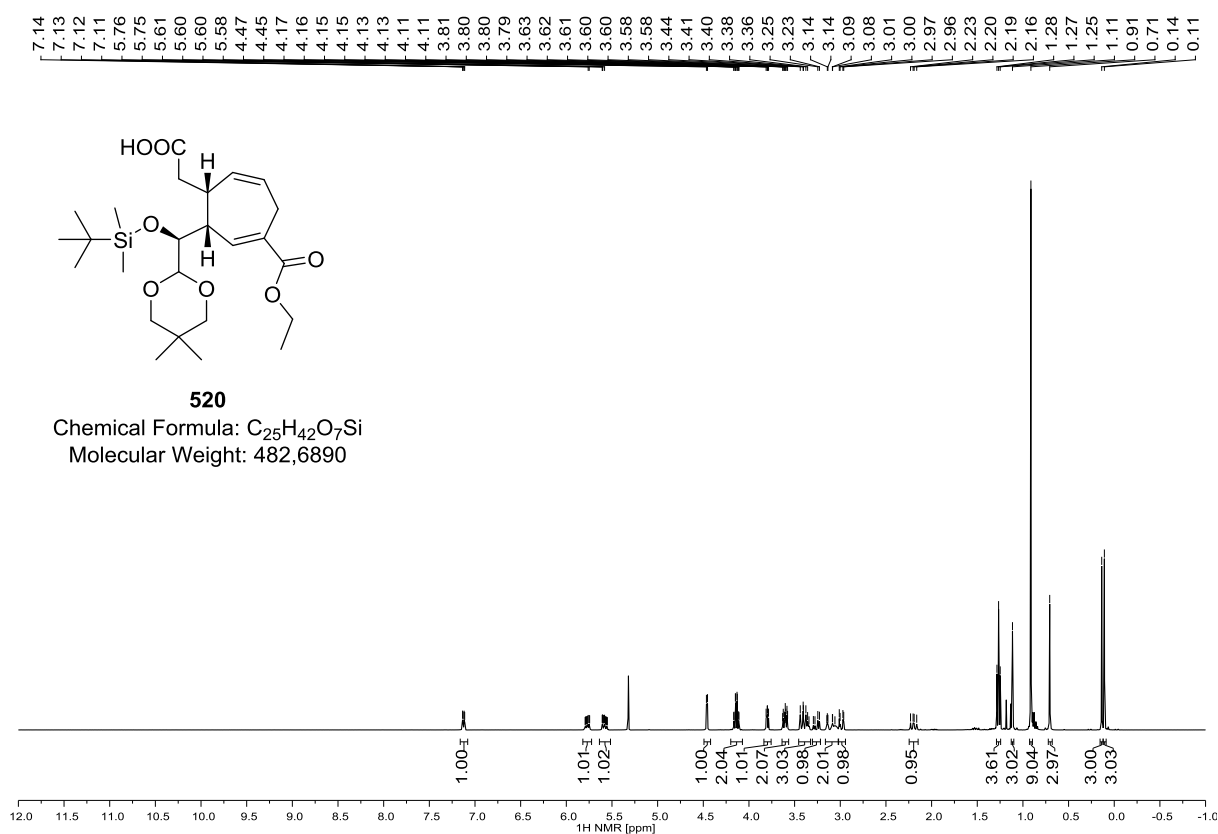
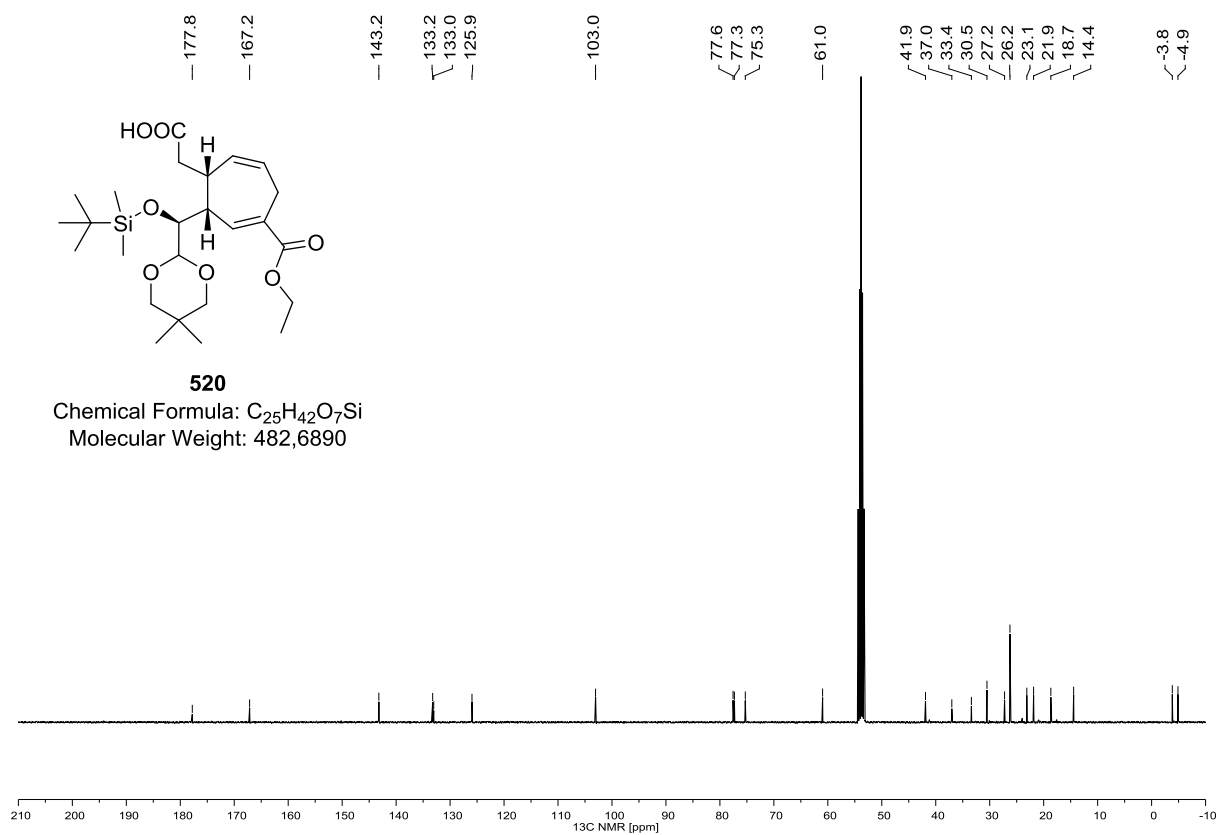
506 (^1H NMR, 400 MHz, C_6D_6)**506 (^{13}C NMR, 100 MHz, C_6D_6)**

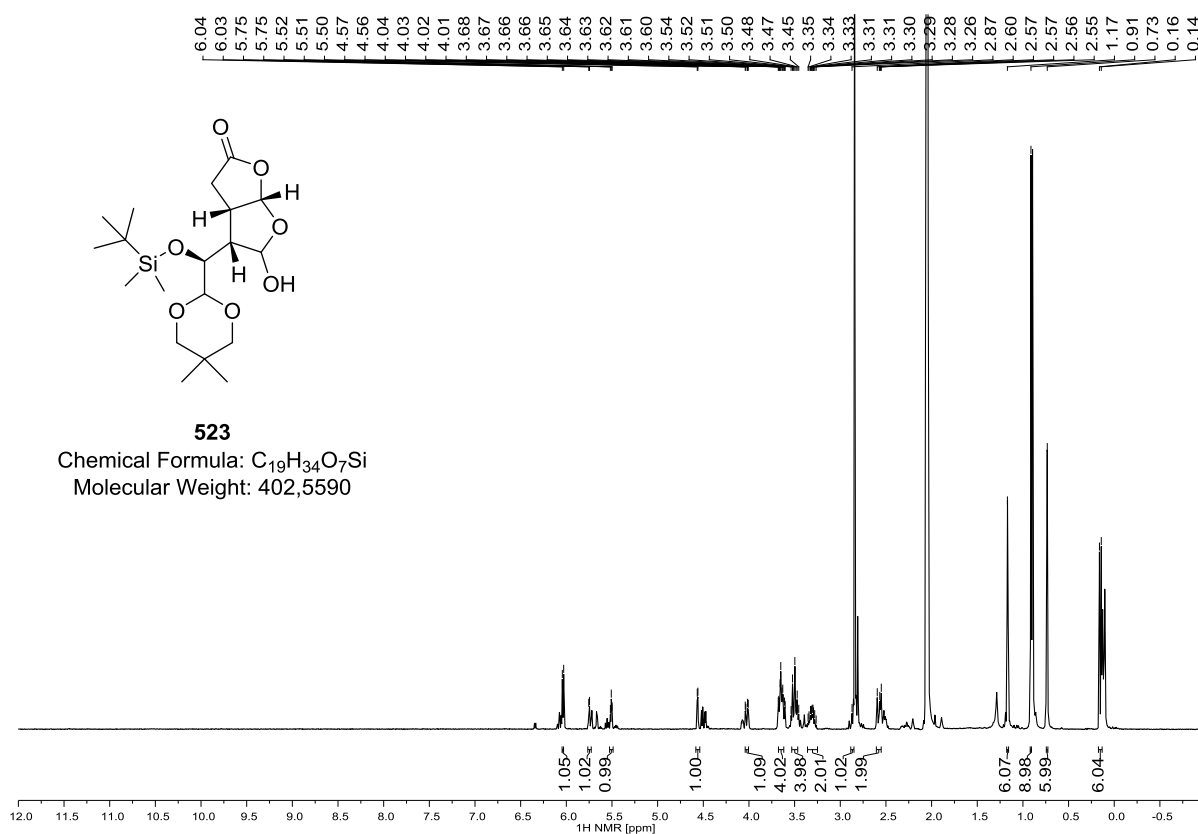
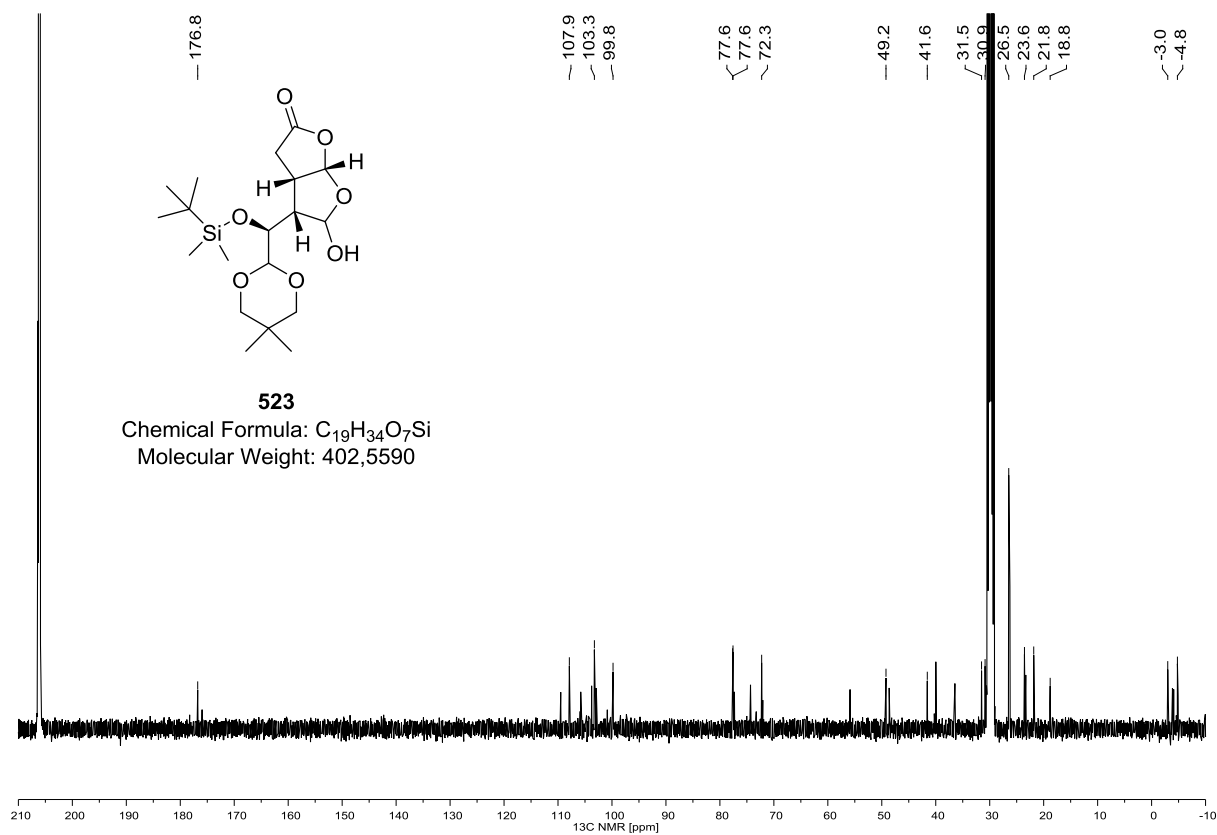
508 (^1H NMR, 400 MHz, C_6D_6)**508 (^{13}C NMR, 100 MHz, C_6D_6)**

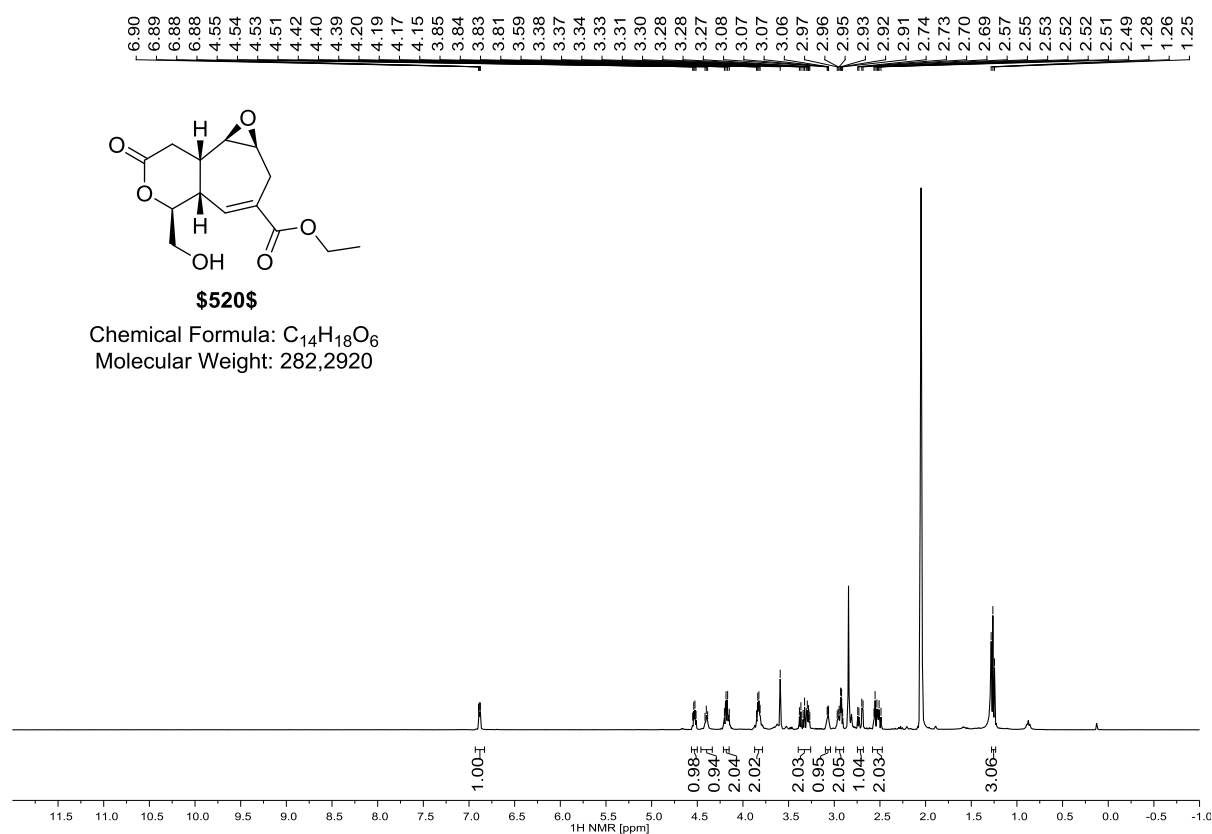
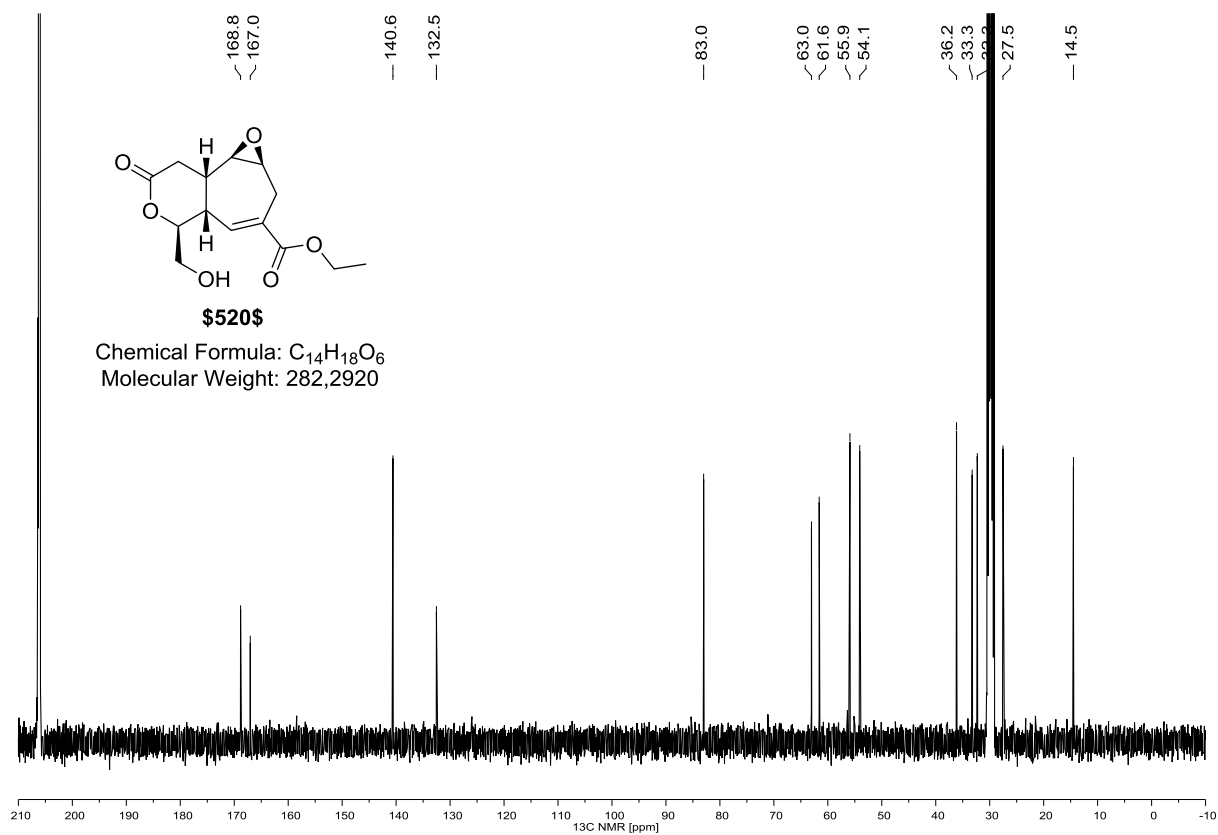
509 (^1H NMR, 400 MHz, $(\text{D}_3\text{C})_2\text{CO}$)**509 (^{13}C NMR, 100 MHz, $(\text{D}_3\text{C})_2\text{CO}$)**

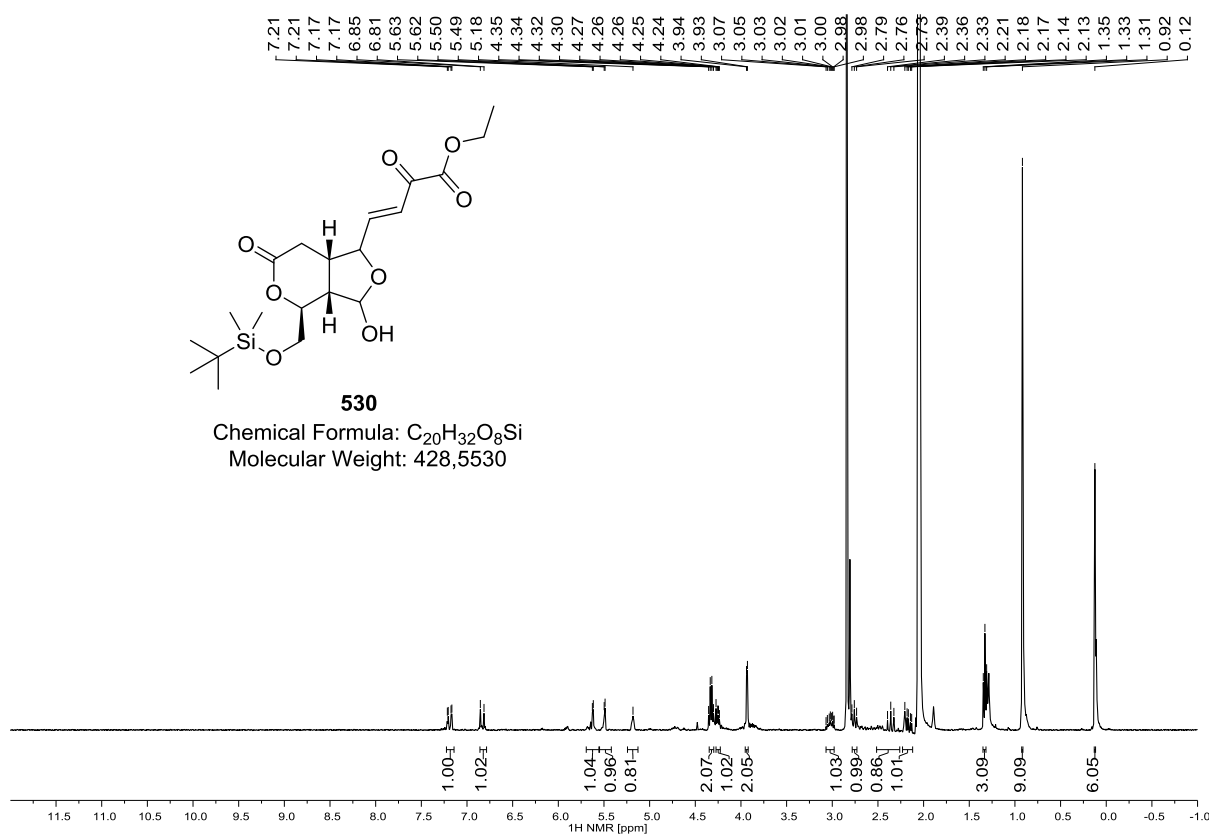
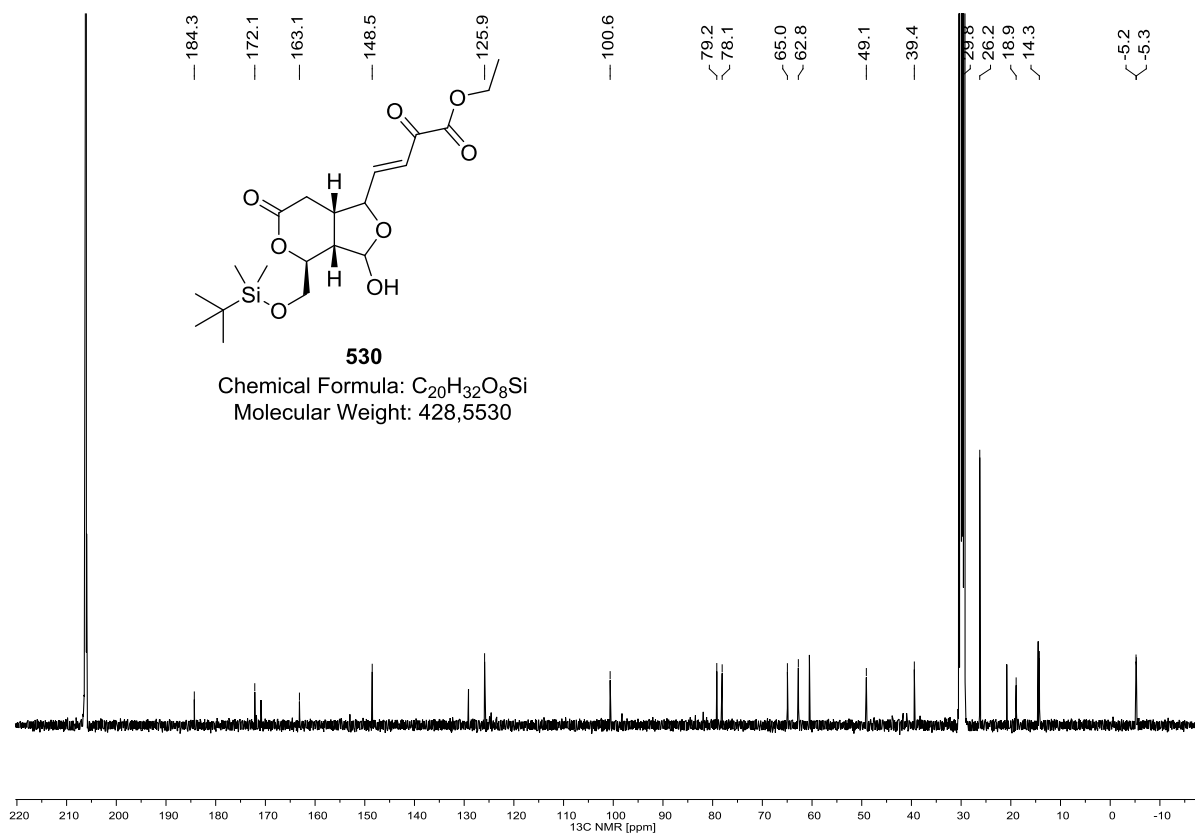
510 (^1H NMR, 400 MHz, $(\text{D}_3\text{C})_2\text{CO}$)**510 (^{13}C NMR, 100 MHz, $(\text{D}_3\text{C})_2\text{CO}$)**

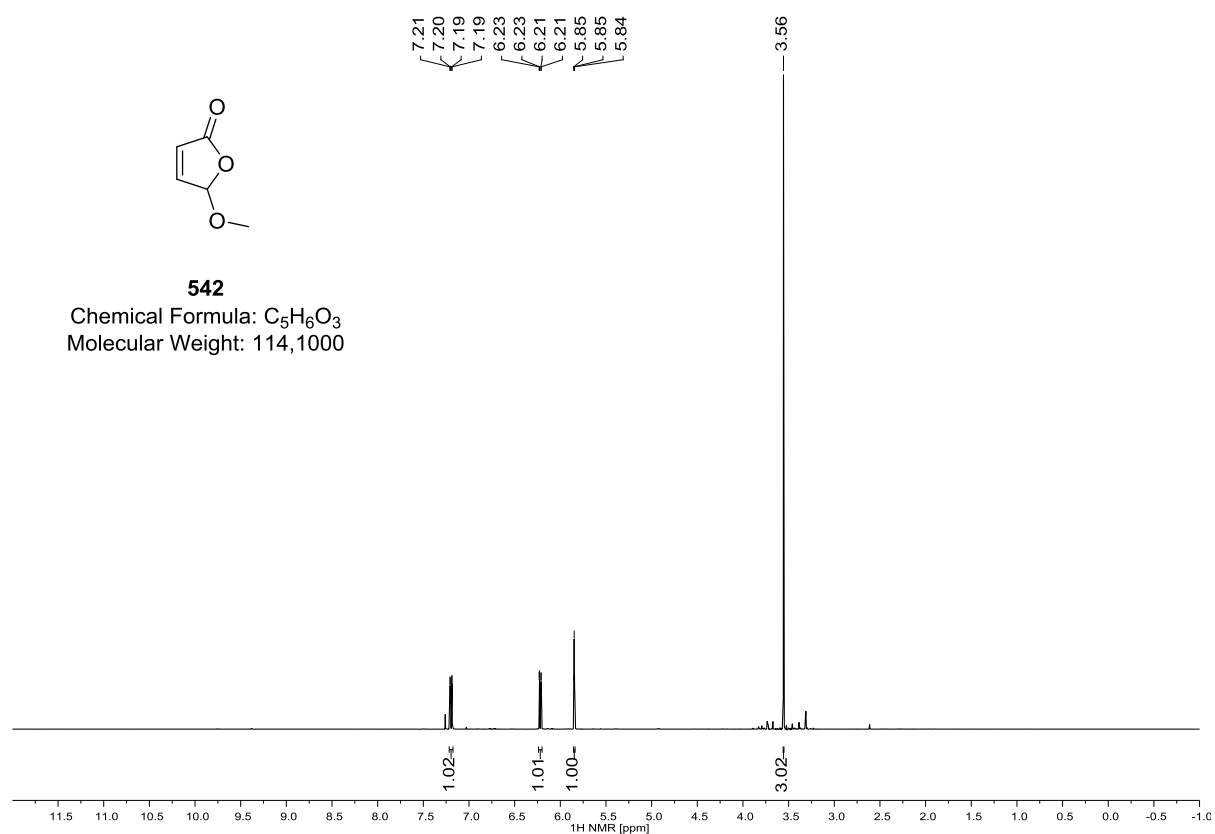
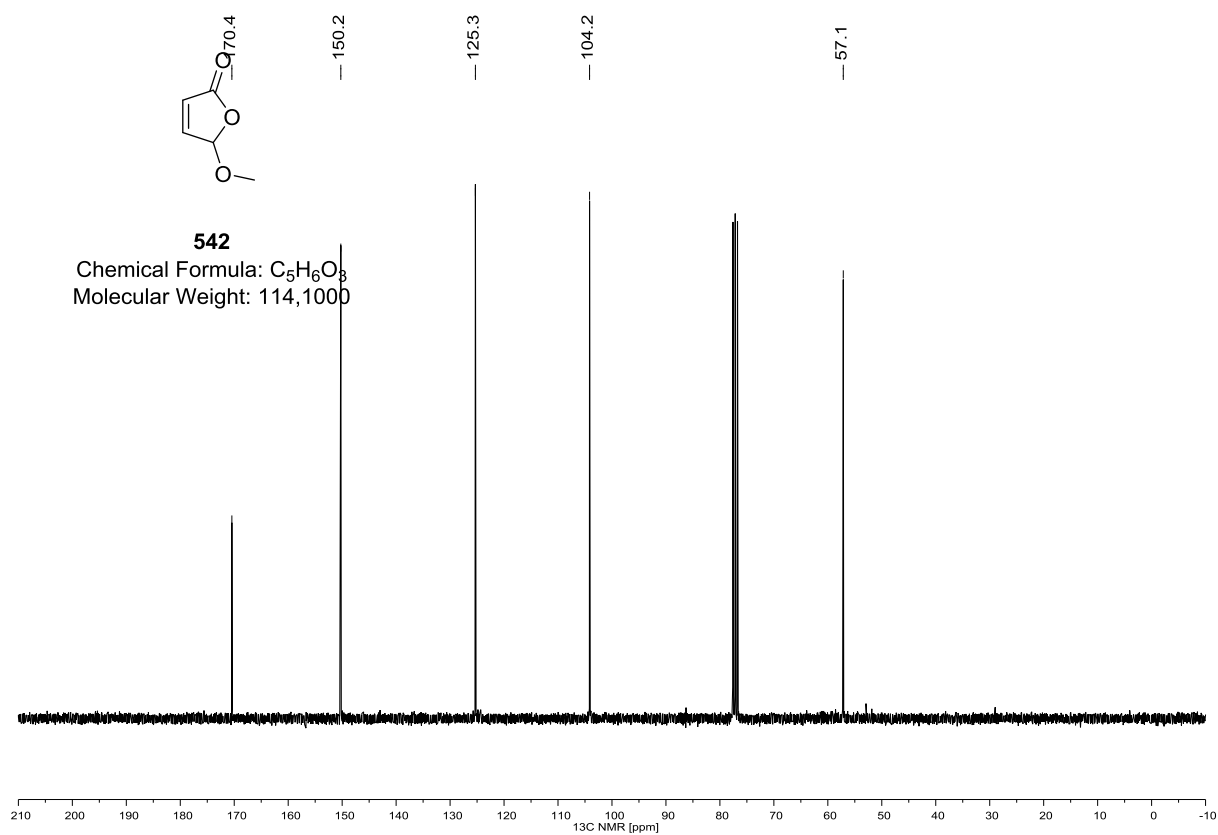
518 (^1H NMR, 400 MHz, $(\text{D}_3\text{C})_2\text{CO}$)**518 (^{13}C NMR, 100 MHz, $(\text{D}_3\text{C})_2\text{CO}$)**

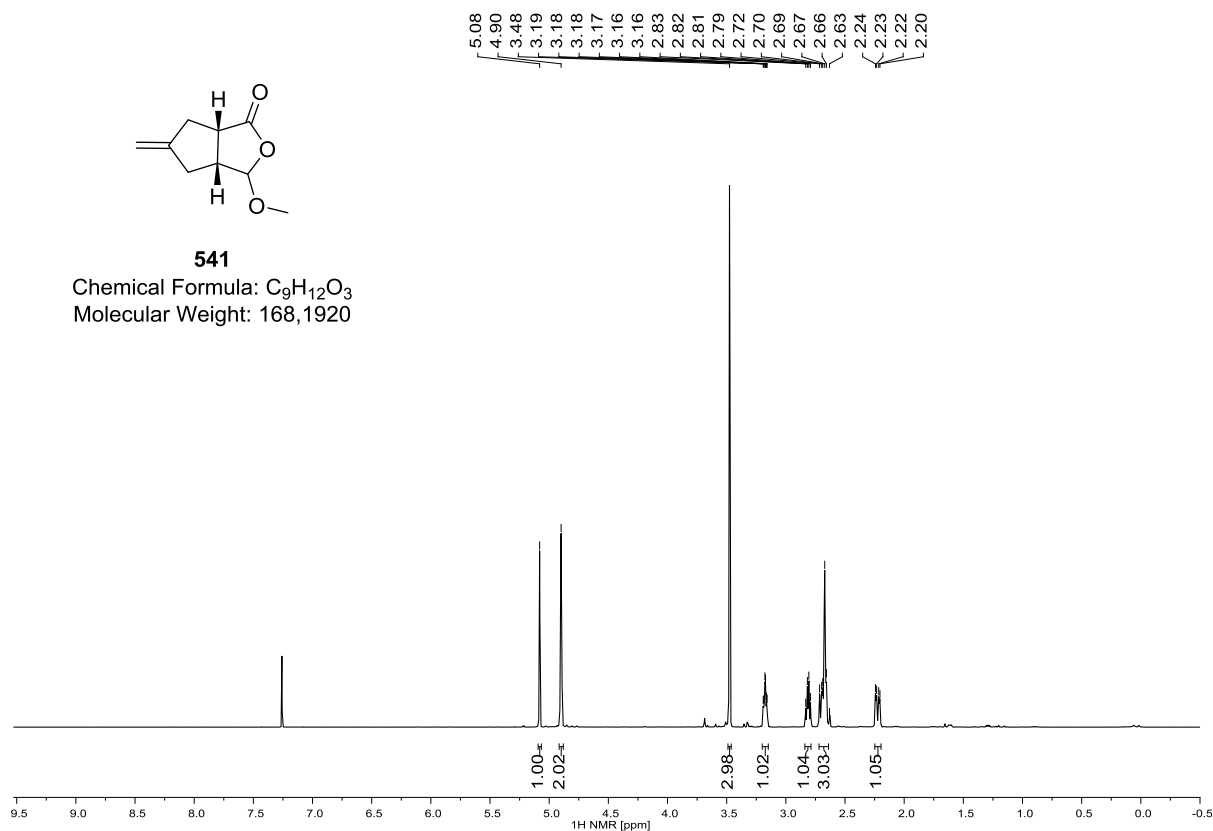
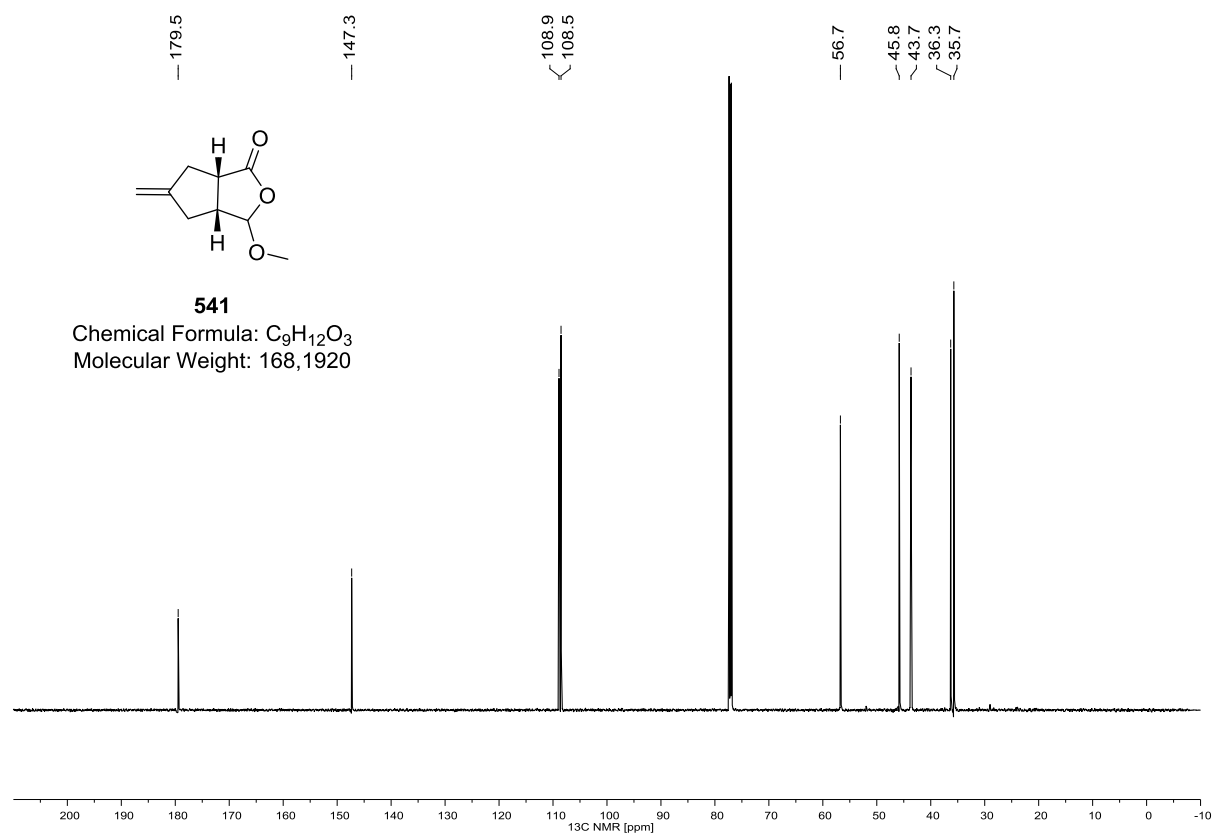
520 (^1H NMR, 400 MHz, CD_2Cl_2)

520 (^{13}C NMR, 100 MHz, CD_2Cl_2)


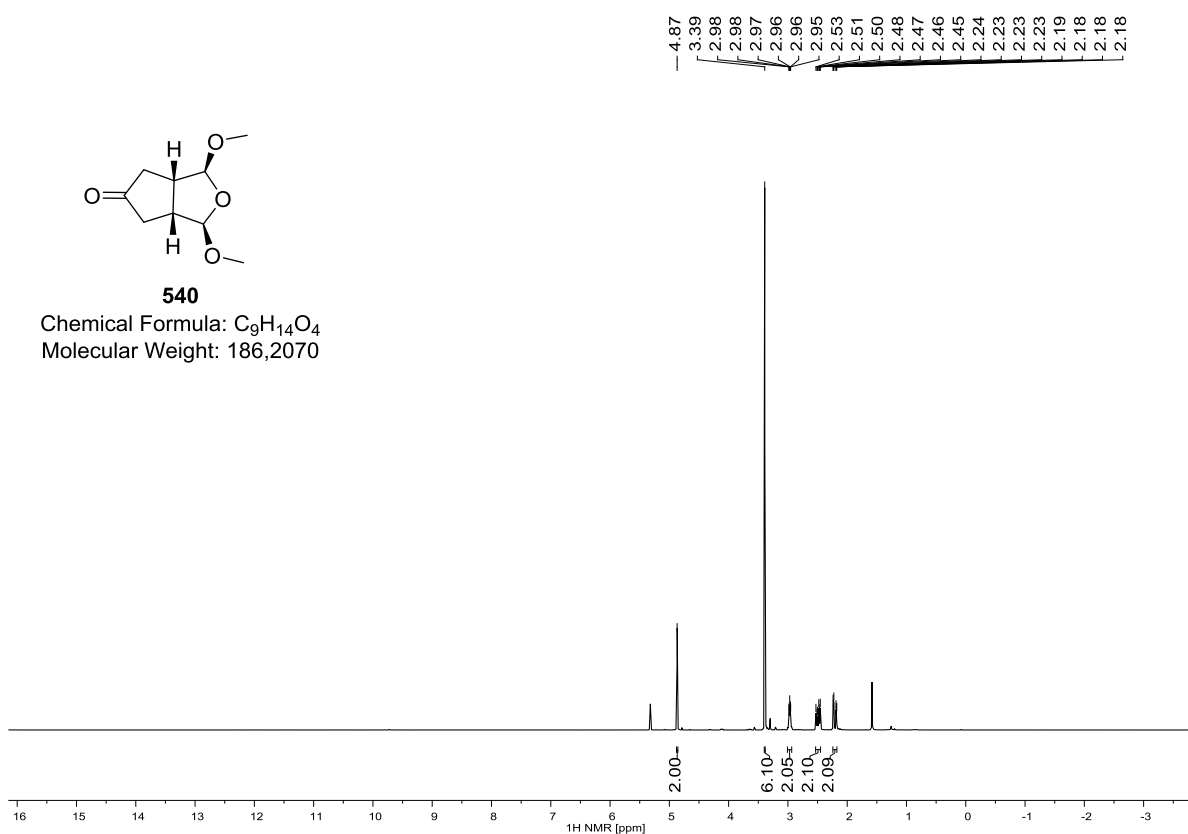
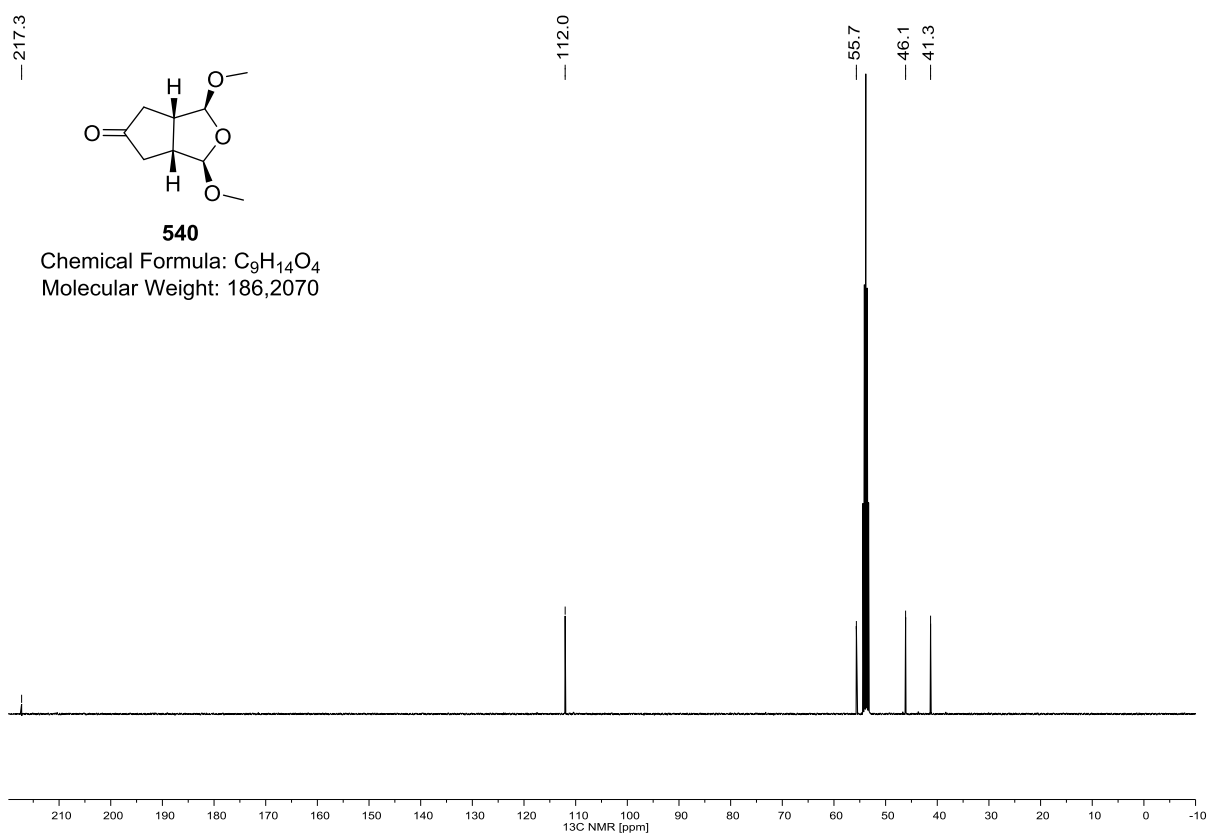
523 (^1H NMR, 400 MHz, $(\text{D}_3\text{C})_2\text{CO}$)**523 (^{13}C NMR, 100 MHz, $(\text{D}_3\text{C})_2\text{CO}$)**

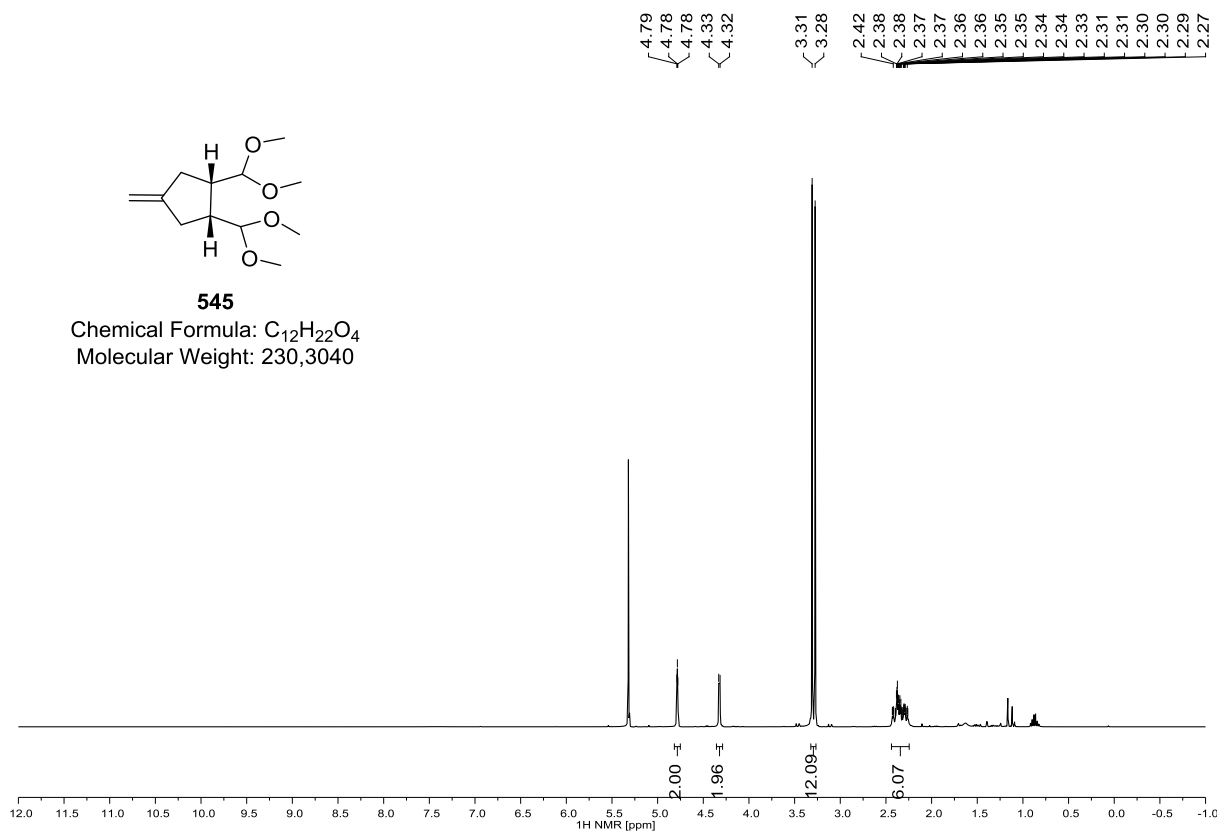
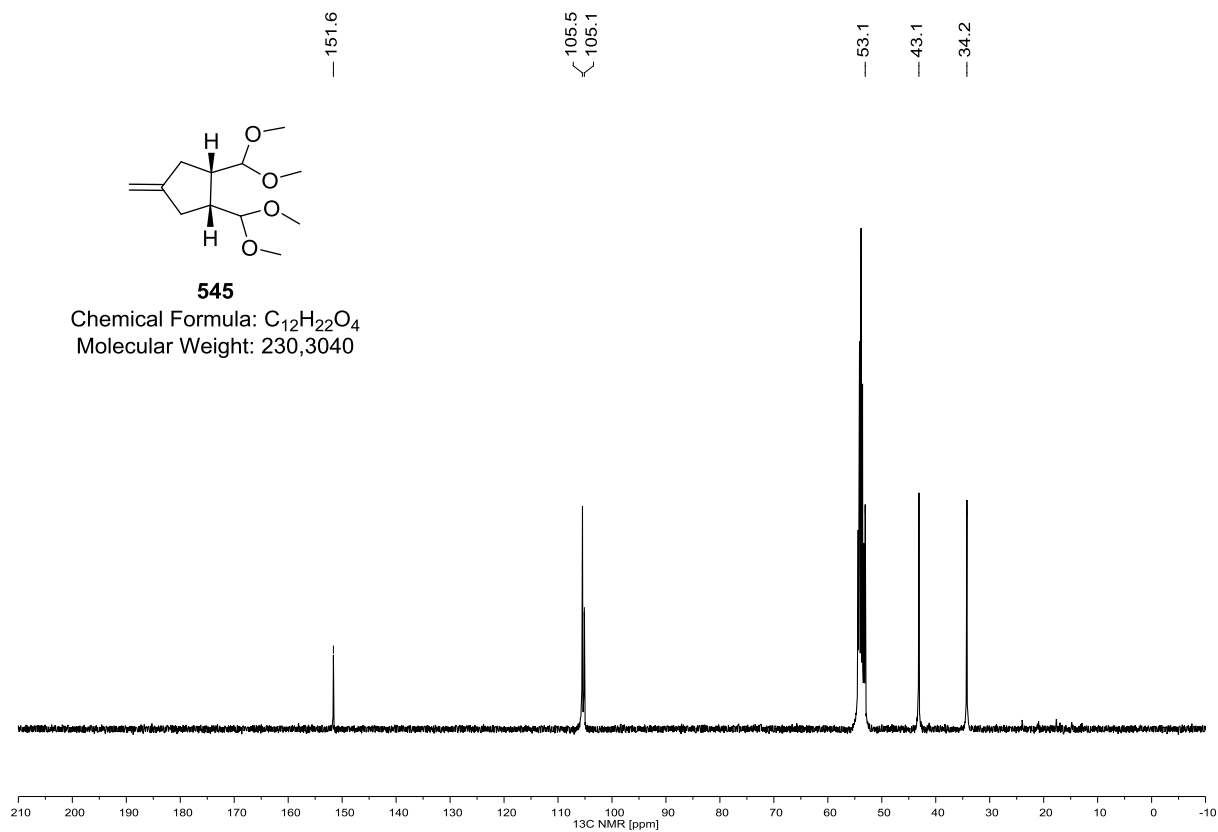
526 (^1H NMR, 400 MHz, $(\text{D}_3\text{C})_2\text{CO}$)526 (^{13}C NMR, 100 MHz, $(\text{D}_3\text{C})_2\text{CO}$)

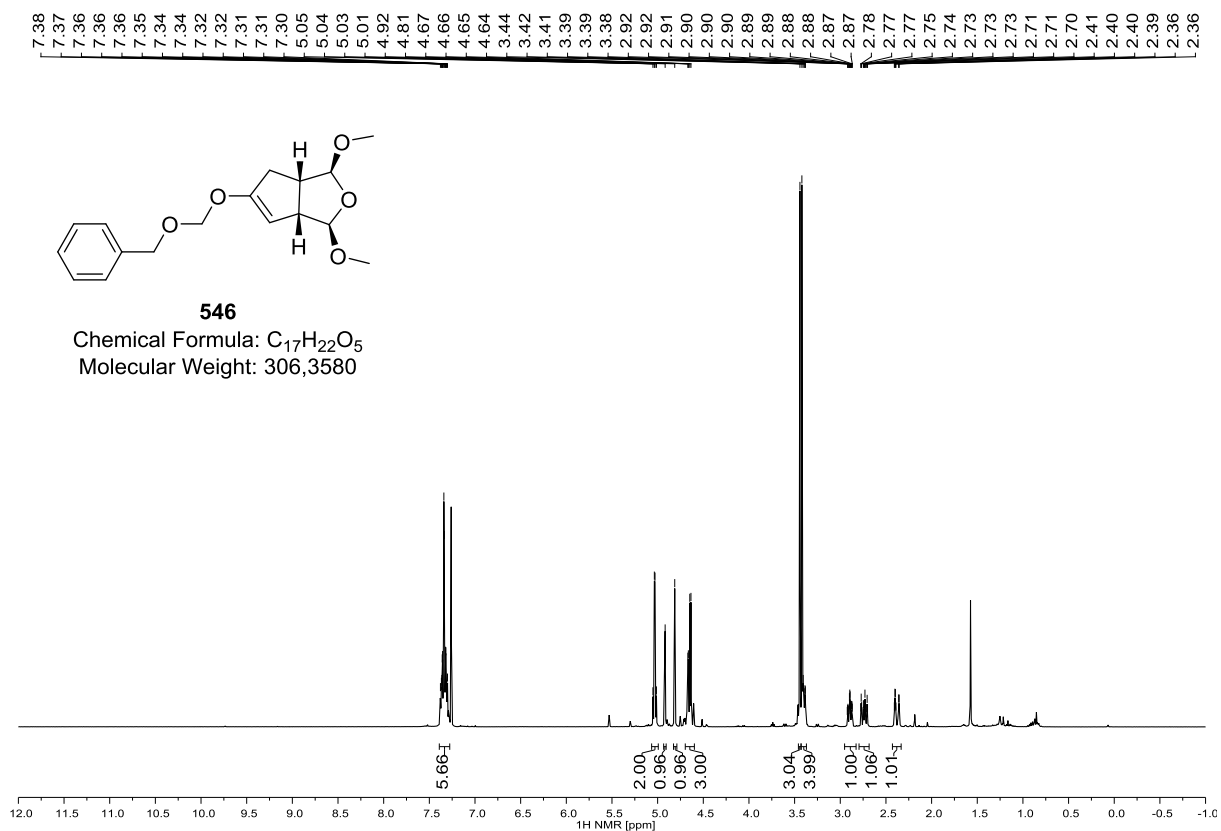
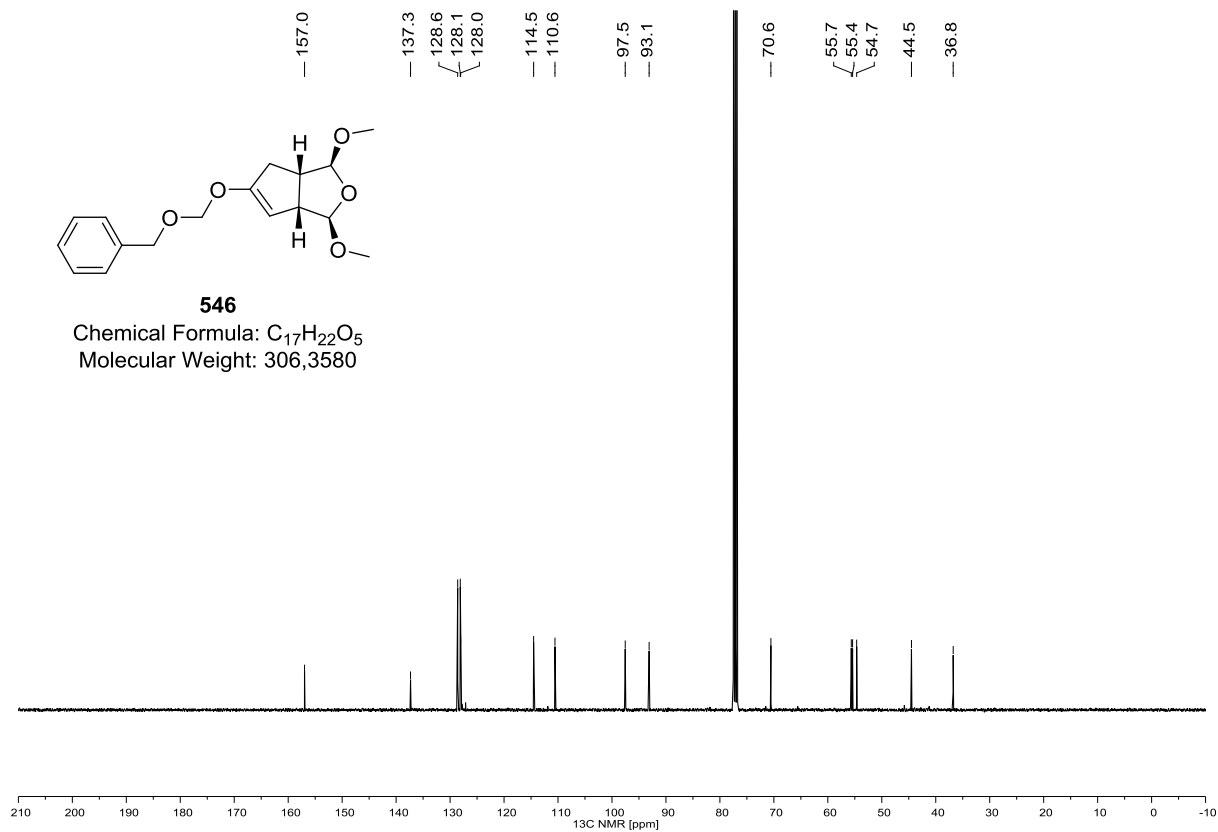
530 (^1H NMR, 400 MHz, $(\text{D}_3\text{C})_2\text{CO}$)**530 (^{13}C NMR, 100 MHz, $(\text{D}_3\text{C})_2\text{CO}$)**

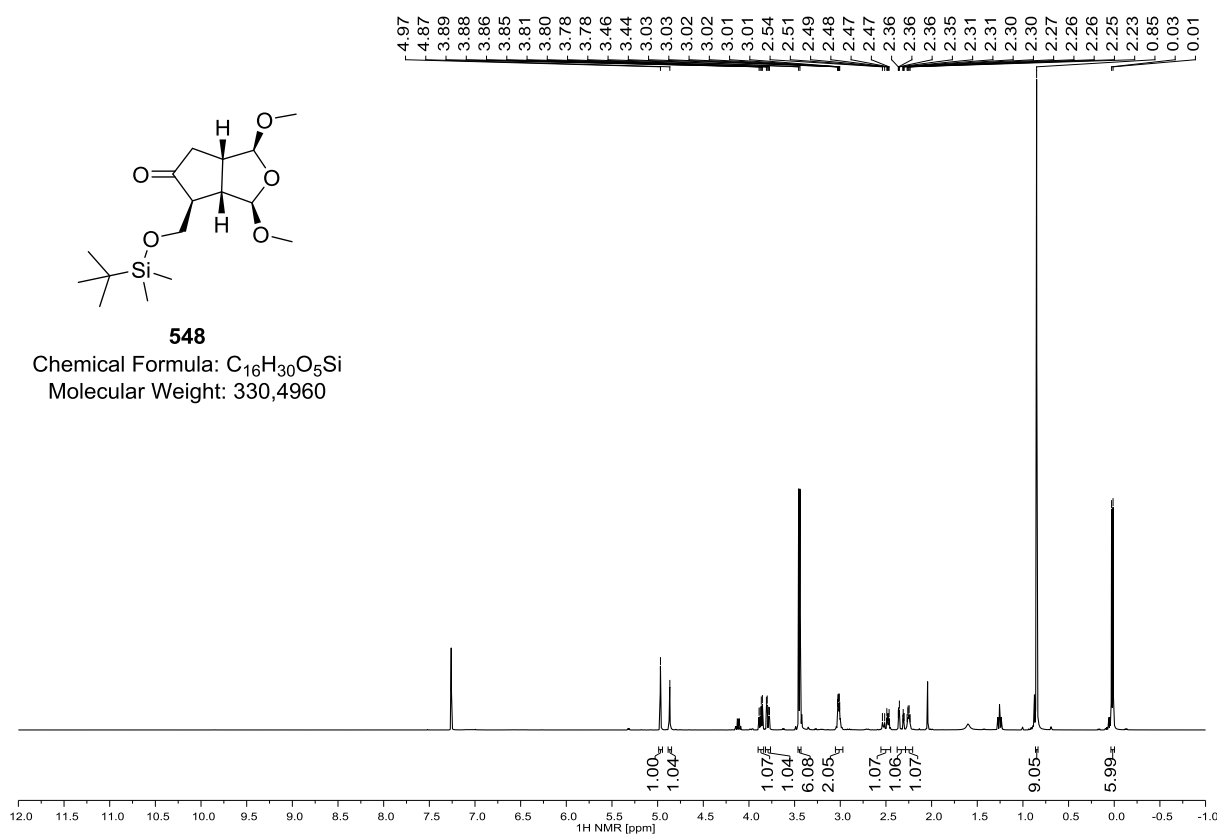
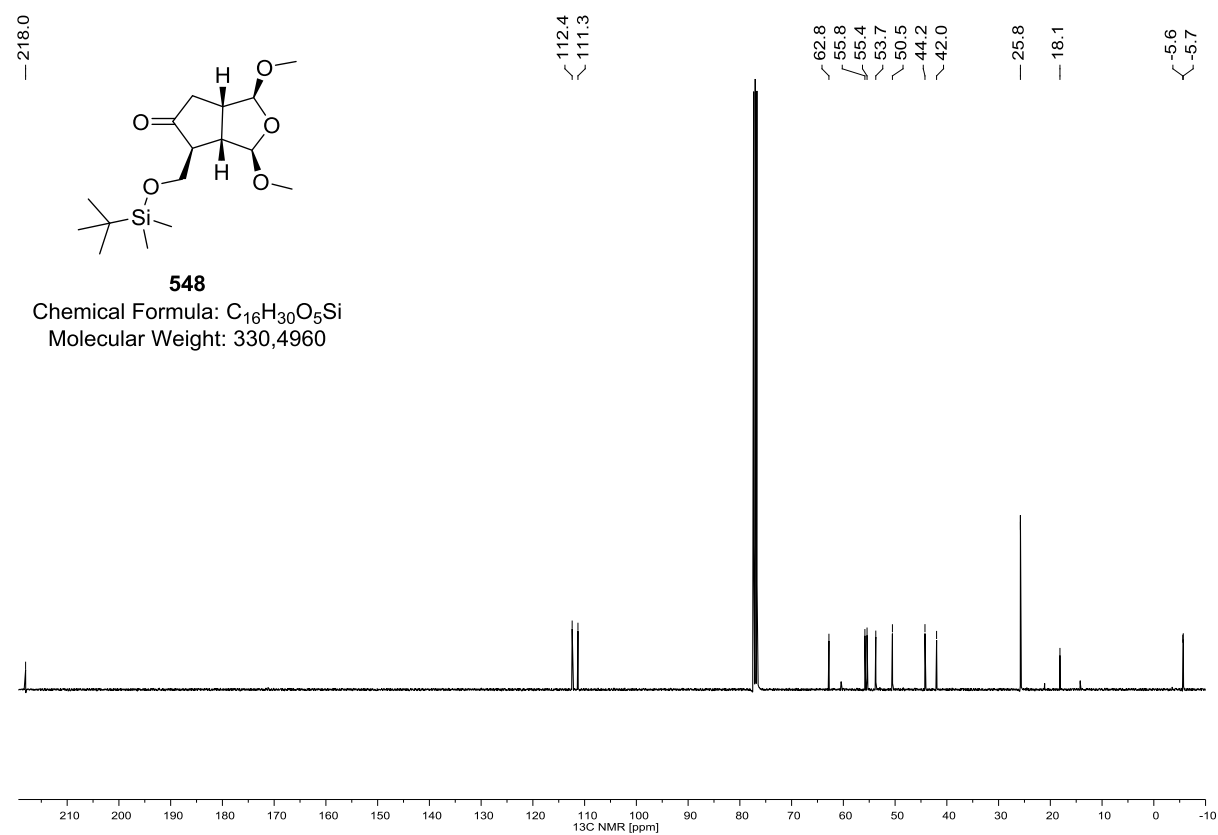
542 (^1H NMR, 400 MHz, CDCl_3)**542 (^{13}C NMR, 100 MHz, CDCl_3)**

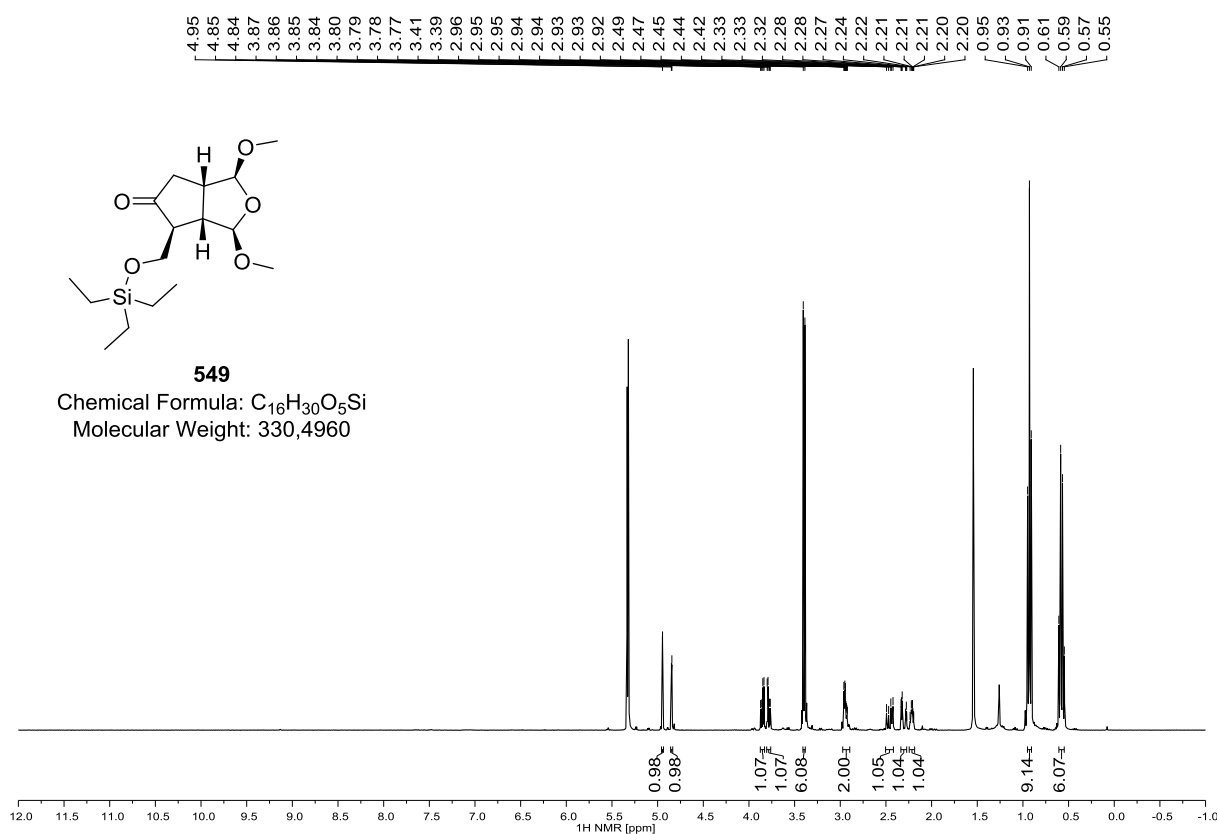
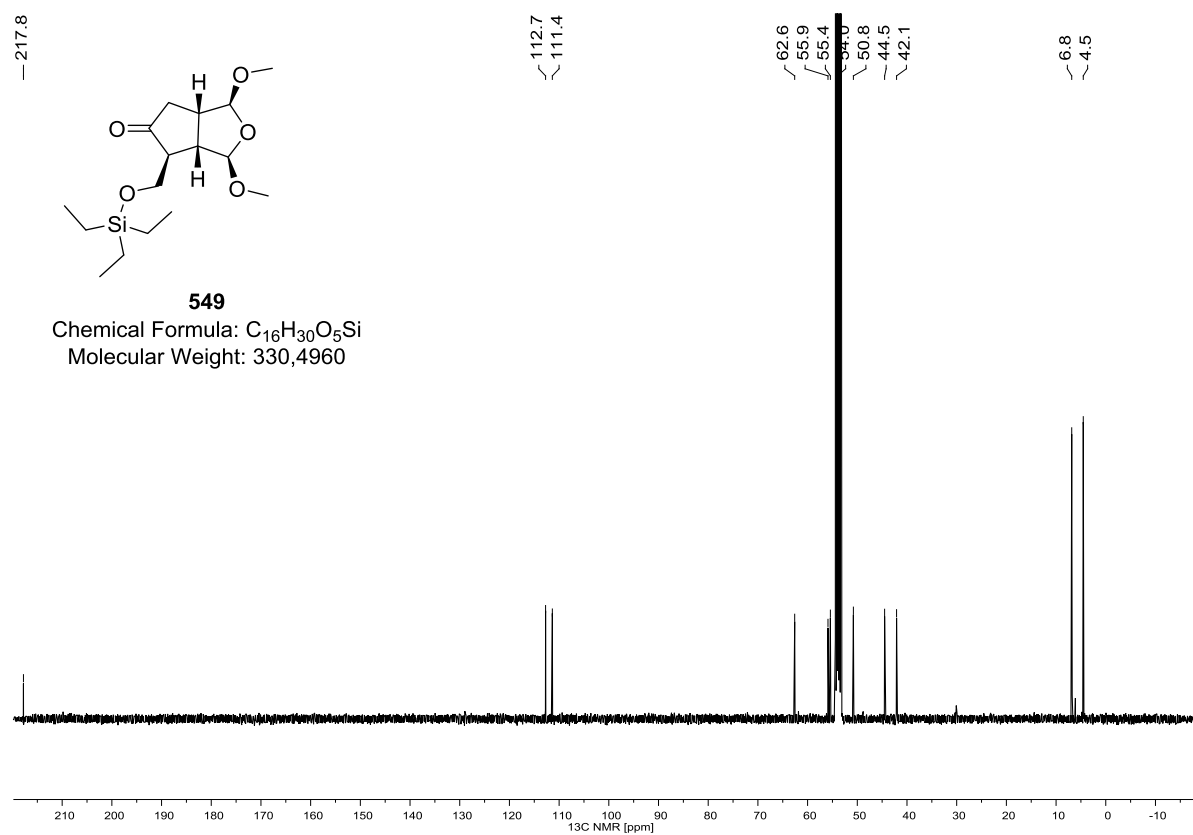
541 (^1H NMR, 400 MHz, CDCl_3)**541 (^{13}C NMR, 100 MHz, CDCl_3)**

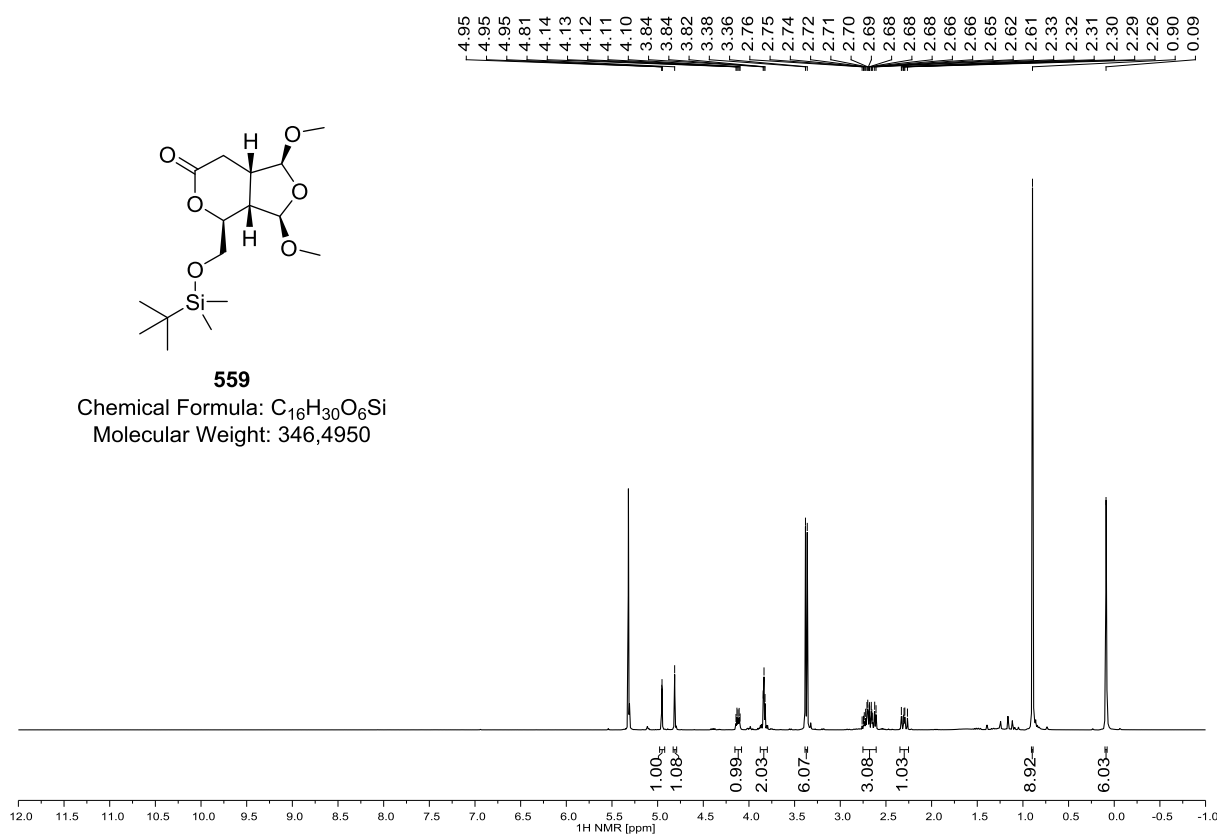
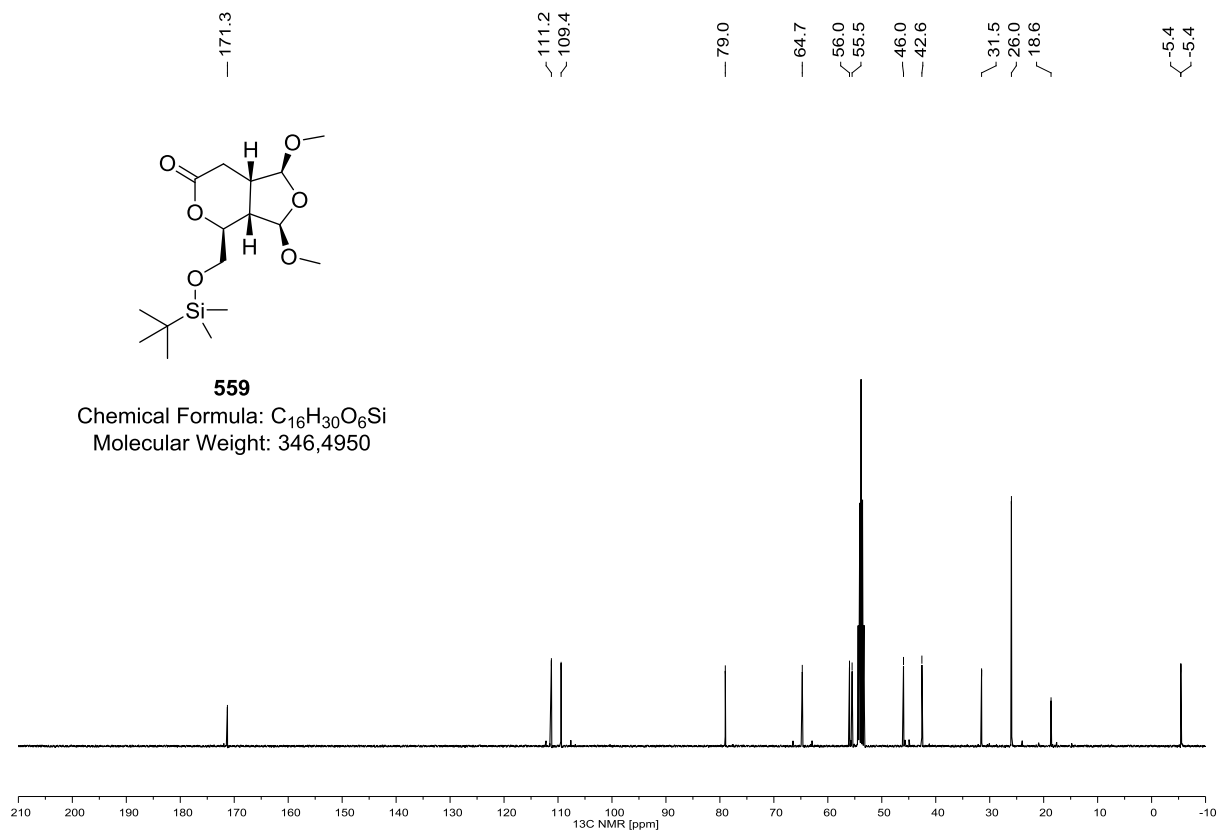
545 (^1H NMR, 400 MHz, CD_2Cl_2)545 (^{13}C NMR, 100 MHz, CD_2Cl_2)

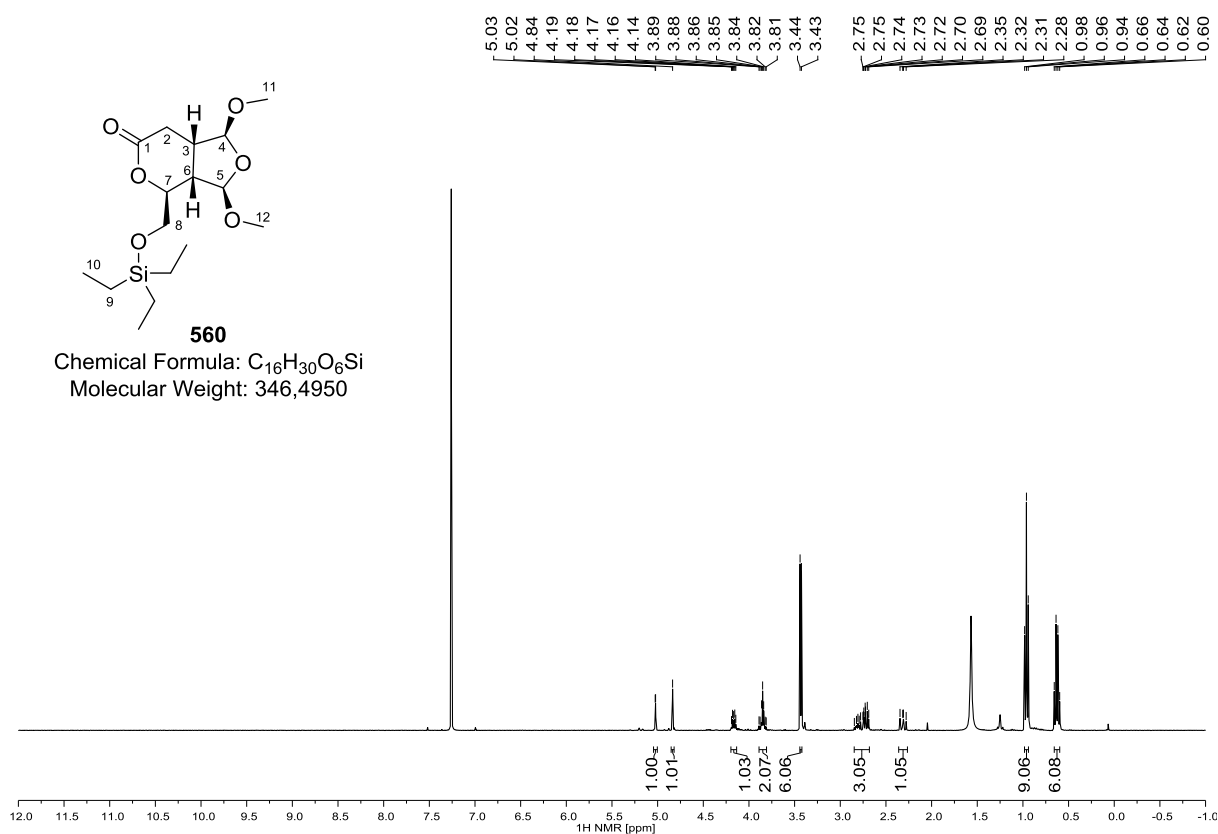
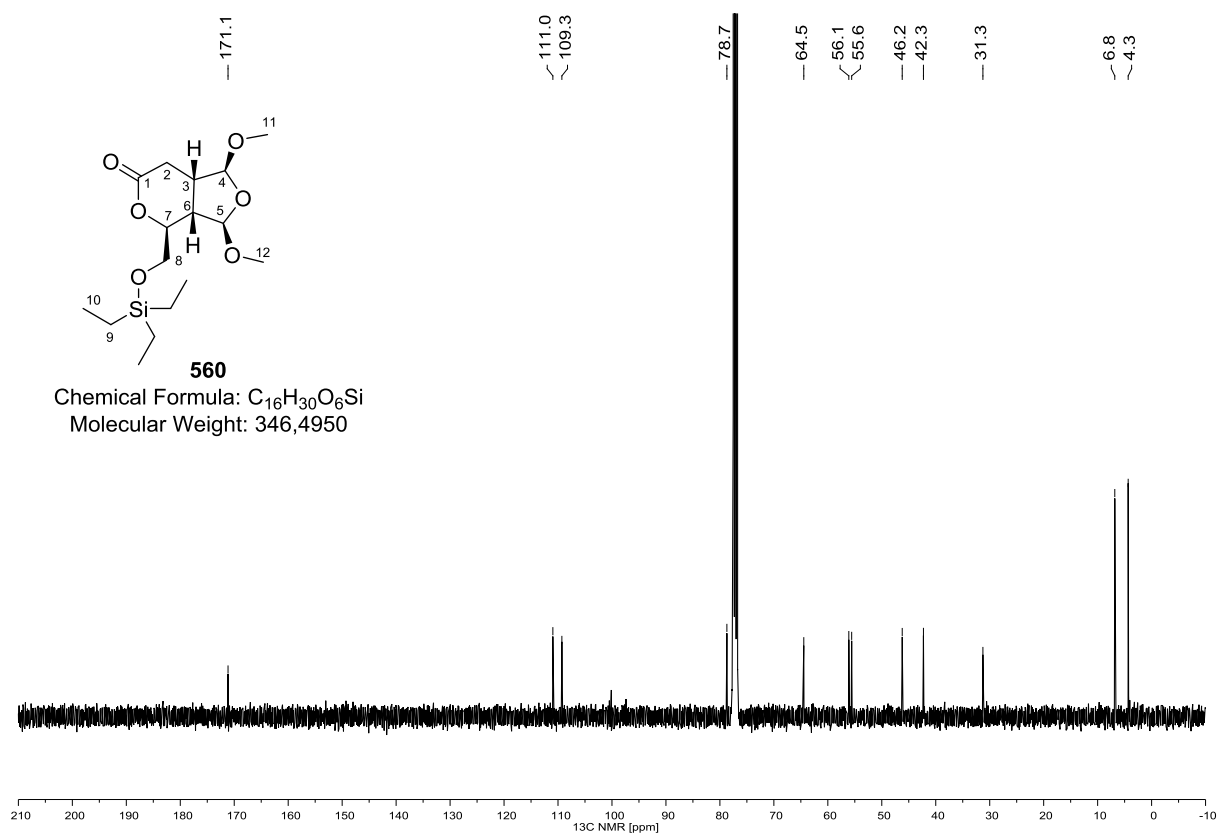
545 (^1H NMR, 400 MHz, CD_2Cl_2)**545 (^{13}C NMR, 100 MHz, CD_2Cl_2)**

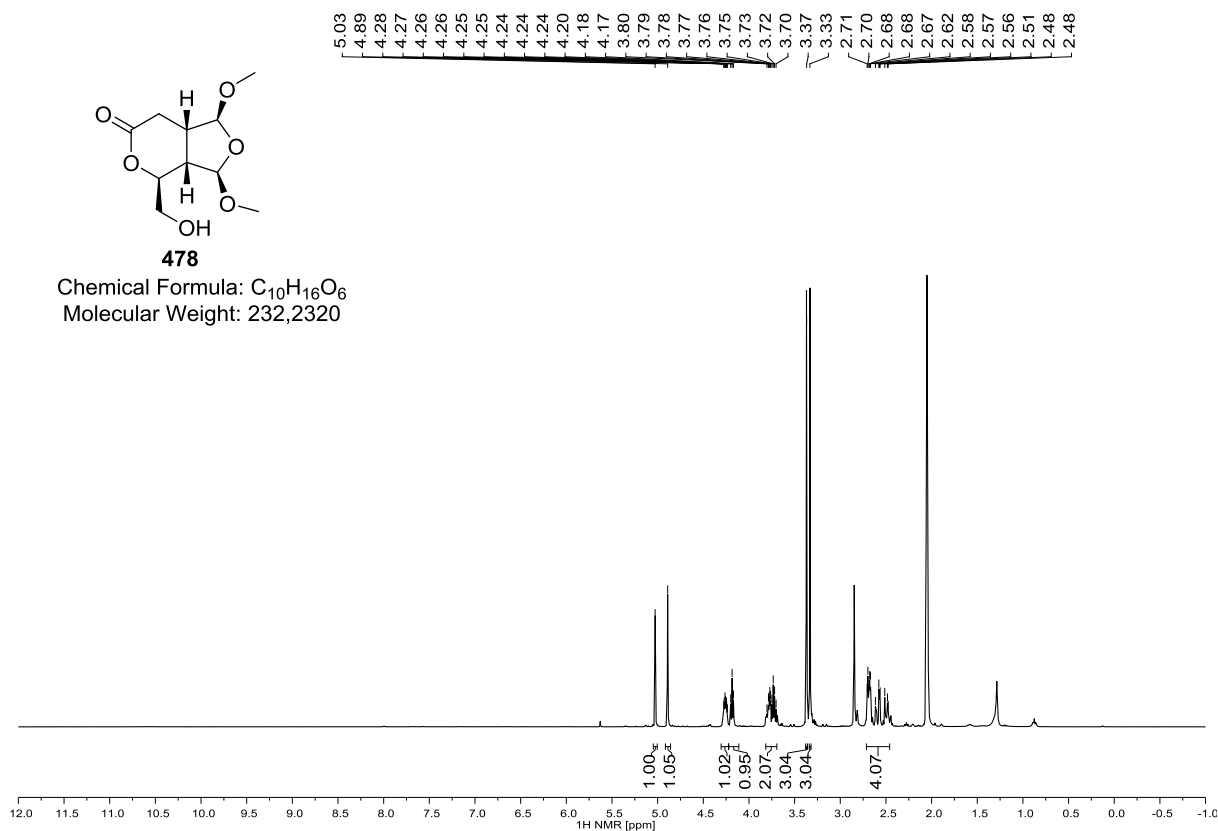
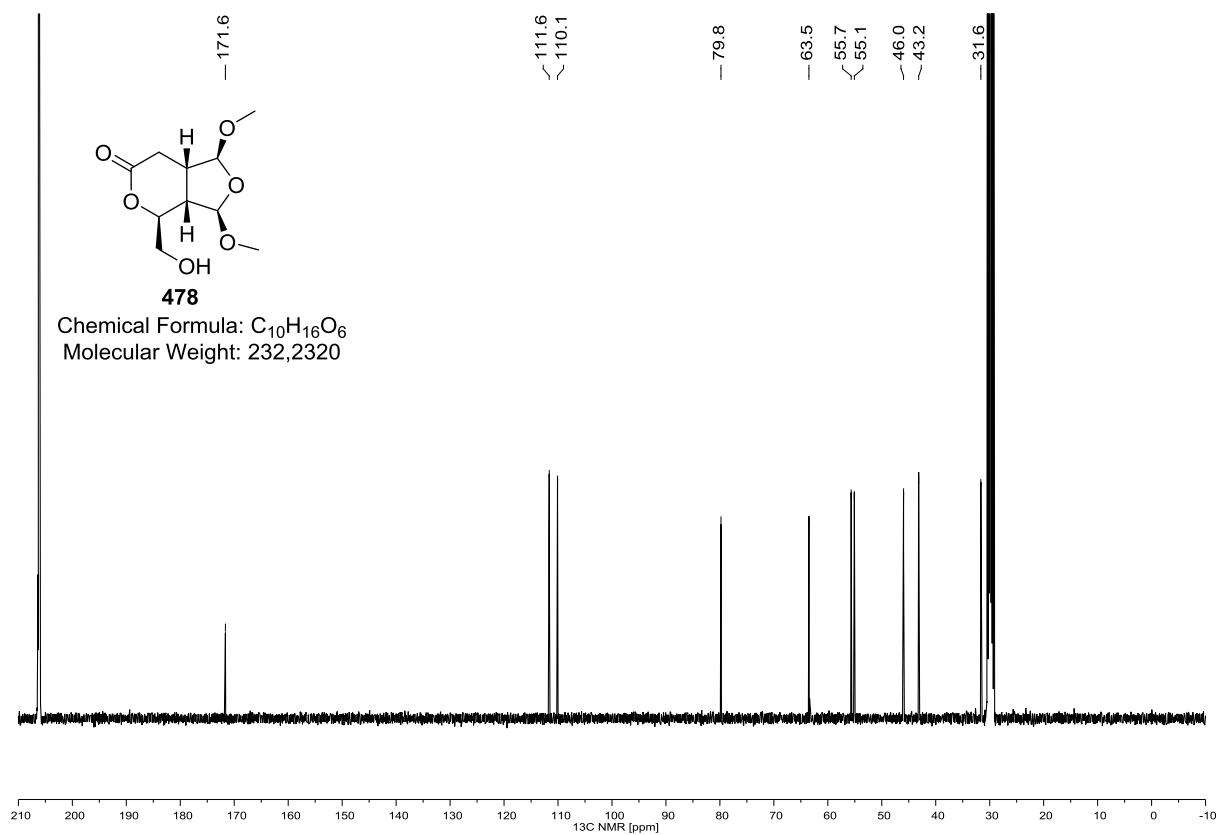
546 (^1H NMR, 400 MHz, CDCl_3)**546 (^{13}C NMR, 100 MHz, CDCl_3)**

548 (^1H NMR, 400 MHz, CDCl_3)**548 (^{13}C NMR, 100 MHz, CDCl_3)**

549 (^1H NMR, 400 MHz, CD_2Cl_2)549 (^{13}C NMR, 100 MHz, CD_2Cl_2)

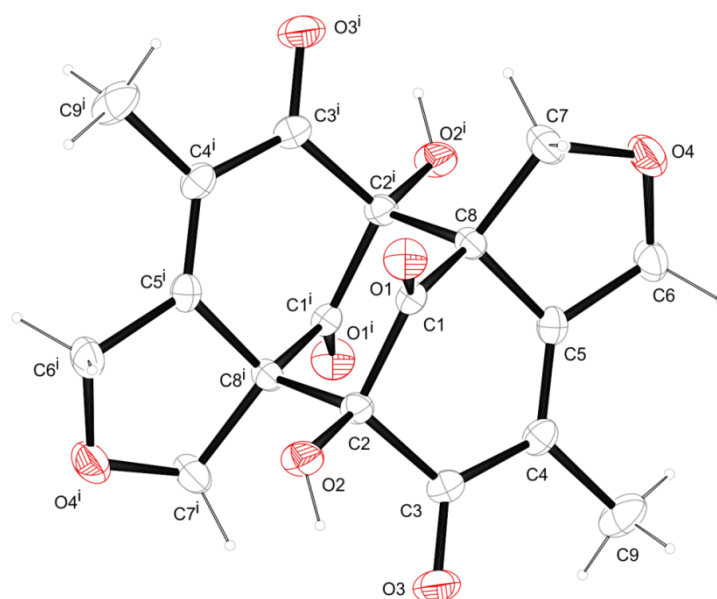
559 (^1H NMR, 400 MHz, CDCl_3)**559 (^{13}C NMR, 100 MHz, CDCl_3)**

560 (^1H NMR, 400 MHz, CDCl_3)**560 (^{13}C NMR, 100 MHz, CDCl_3)**

478 (^1H NMR, 400 MHz, $(\text{D}_3\text{C})_2\text{CO}$)**478 (^{13}C NMR, 100 MHz, $(\text{D}_3\text{C})_2\text{CO}$)**

8. CRYSTALLOGRAPHIC DATA

8.1 Dibefurin (CCDC 1022042)



Crystallographic data.

net formula	$\text{C}_{18}\text{H}_{16}\text{O}_8$
$M_r/\text{g mol}^{-1}$	360.315
crystal size/mm	$0.172 \times 0.156 \times 0.151$
T/K	173(2)
radiation	'Mo $\text{K}\alpha$
diffractometer	'Bruker D8Quest'
crystal system	monoclinic
space group	$P2_1/c$
$a/\text{\AA}$	8.0238(4)
$b/\text{\AA}$	12.6344(5)
$c/\text{\AA}$	8.0807(4)
$\alpha/^\circ$	90
$\beta/^\circ$	114.8884(12)
$\gamma/^\circ$	90
$V/\text{\AA}^3$	743.11(6)
Z	2
calc. density/ g cm^{-3}	1.61033(13)
μ/mm^{-1}	0.128
absorption correction	multi-scan
transmission factor range	0.7024–0.7457
refls. measured	17973
R_{int}	0.0349
mean $\sigma(I)/I$	0.0183
θ range	2.80–28.37
observed refls.	1650

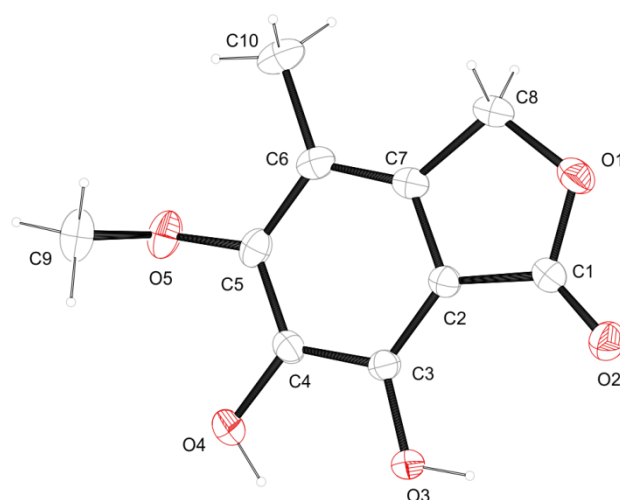
<i>x</i> , <i>y</i> (weighting scheme)	0.0741, 0.3582
hydrogen refinement	mixed
refls in refinement	1856
parameters	123
restraints	0
$R(F_{\text{obs}})$	0.0472
$R_w(F^2)$	0.1313
<i>S</i>	1.094
shift/error _{max}	0.001
max electron density/e Å ⁻³	0.395
min electron density/e Å ⁻³	-0.291

C-bound H: constr, O-bound H: refall.

Symmetry code in figure: *i* = -*x*, 1-*y*, -*z*.

Number	Label	Charge	SybylType	Xfrac + ESD	Yfrac + ESD	Zfrac + ESD	Symm. op.
1	C1	0	C.2	-0.088878	0.601752	-0.010777	<i>x</i> , <i>y</i> , <i>z</i>
2	C2	0	C.3	0.017903	0.551291	0.176382	<i>x</i> , <i>y</i> , <i>z</i>
3	C3	0	C.2	0.221569	0.585516	0.25295	<i>x</i> , <i>y</i> , <i>z</i>
4	C4	0	C.2	0.304989	0.605358	0.124759	<i>x</i> , <i>y</i> , <i>z</i>
5	C5	0	C.2	0.197289	0.604076	-0.054758	<i>x</i> , <i>y</i> , <i>z</i>
6	C6	0	C.3	0.247342	0.63901	-0.204988	<i>x</i> , <i>y</i> , <i>z</i>
7	H6A	0	H	0.32933	0.701479	-0.166719	<i>x</i> , <i>y</i> , <i>z</i>
8	H6B	0	H	0.310751	0.581414	-0.238803	<i>x</i> , <i>y</i> , <i>z</i>
9	C7	0	C.3	-0.078206	0.636239	-0.31956	<i>x</i> , <i>y</i> , <i>z</i>
10	H7A	0	H	-0.165419	0.592427	-0.420396	<i>x</i> , <i>y</i> , <i>z</i>
11	H7B	0	H	-0.14324	0.700402	-0.307831	<i>x</i> , <i>y</i> , <i>z</i>
12	C8	0	C.3	-0.003532	0.573476	-0.14098	<i>x</i> , <i>y</i> , <i>z</i>
13	C9	0	C.3	0.505326	0.634377	0.20387	<i>x</i> , <i>y</i> , <i>z</i>
14	H9A	0	H	0.551109	0.62816	0.109368	<i>x</i> , <i>y</i> , <i>z</i>
15	H9B	0	H	0.574566	0.586481	0.304988	<i>x</i> , <i>y</i> , <i>z</i>
16	H9C	0	H	0.520838	0.707396	0.248803	<i>x</i> , <i>y</i> , <i>z</i>
17	O1	0	O.2	-0.225219	0.653884	-0.050672	<i>x</i> , <i>y</i> , <i>z</i>
18	O2	0	O.3	-0.059771	0.576468	0.295694	<i>x</i> , <i>y</i> , <i>z</i>
19	H2	0	H	0.024744	0.594393	0.392921	<i>x</i> , <i>y</i> , <i>z</i>
20	O3	0	O.2	0.302562	0.599267	0.416591	<i>x</i> , <i>y</i> , <i>z</i>
21	O4	0	O.3	0.077047	0.665188	-0.3557	<i>x</i> , <i>y</i> , <i>z</i>
22	C1	0	C.2	0.088878	0.398248	0.010777	- <i>x</i> ,1- <i>y</i> , <i>-z</i>

23	C2	0	C.3	-0.017903	0.448709	-0.176382	-x,1-y,-z
24	C3	0	C.2	-0.221569	0.414484	-0.25295	-x,1-y,-z
25	C4	0	C.2	-0.304989	0.394642	-0.124759	-x,1-y,-z
26	C5	0	C.2	-0.197289	0.395924	0.054758	-x,1-y,-z
27	C6	0	C.3	-0.247342	0.36099	0.204988	-x,1-y,-z
28	H6A	0	H	-0.32933	0.298521	0.166719	-x,1-y,-z
29	H6B	0	H	-0.310751	0.418586	0.238803	-x,1-y,-z
30	C7	0	C.3	0.078206	0.363761	0.31956	-x,1-y,-z
31	H7A	0	H	0.165419	0.407573	0.420396	-x,1-y,-z
32	H7B	0	H	0.14324	0.299598	0.307831	-x,1-y,-z
33	C8	0	C.3	0.003532	0.426524	0.14098	-x,1-y,-z
34	C9	0	C.3	-0.505326	0.365623	-0.20387	-x,1-y,-z
35	H9A	0	H	-0.551109	0.37184	-0.109368	-x,1-y,-z
36	H9B	0	H	-0.574566	0.413519	-0.304988	-x,1-y,-z
37	H9C	0	H	-0.520838	0.292604	-0.248803	-x,1-y,-z
38	O1	0	O.2	0.225219	0.346116	0.050672	-x,1-y,-z
39	O2	0	O.3	0.059771	0.423532	-0.295694	-x,1-y,-z
40	H2	0	H	-0.024744	0.405607	-0.392921	-x,1-y,-z
41	O3	0	O.2	-0.302562	0.400733	-0.416591	-x,1-y,-z
42	O4	0	O.3	-0.077047	0.334812	0.3557	-x,1-y,-z

8.2 6,7-dihydroxy-5-methoxy-4-methylisobenzofuran-1(3*H*)-one (196)

Crystallographic data.

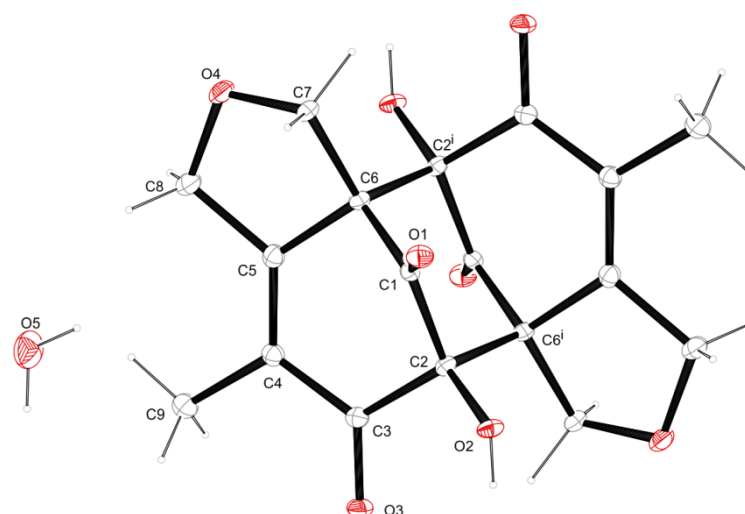
net formula	$\text{C}_{10}\text{H}_{10}\text{O}_5$
$M_r/\text{g mol}^{-1}$	210.183
crystal size/mm	$0.156 \times 0.135 \times 0.108$
T/K	173(2)
radiation	'Mo $\text{K}\alpha$
diffractometer	'Bruker D8Venture'
crystal system	monoclinic
space group	$P2_1/c$
$a/\text{\AA}$	8.0259(8)
$b/\text{\AA}$	9.7086(9)
$c/\text{\AA}$	12.0339(12)
$\alpha/^\circ$	90
$\beta/^\circ$	98.220(3)
$\gamma/^\circ$	90
$V/\text{\AA}^3$	928.05(16)
Z	4
calc. density/ g cm^{-3}	1.5043(3)
μ/mm^{-1}	0.122
absorption correction	multi-scan
transmission factor range	0.9192–0.9590
refls. measured	19139
R_{int}	0.0345
mean $\sigma(I)/I$	0.0199
θ range	3.31–27.60
observed refls.	1745
x, y (weighting scheme)	0.0576, 0.5086
hydrogen refinement	mixed
refls in refinement	2121
parameters	146
restraints	0
$R(F_{\text{obs}})$	0.0403

$R_w(F^2)$	0.1140
S	1.038
shift/error _{max}	0.001
max electron density/e Å ⁻³	0.327
min electron density/e Å ⁻³	-0.287

C-bound H: constr, O-bound H: refall.

Number	Label	Charge	SybylType	Xfrac + ESD	Yfrac + ESD	Zfrac + ESD	Symm. op.
1	C1	0	C.2	0.215156	0.732944	0.579573	x,y,z
2	C2	0	C.2	0.267061	0.590099	0.565092	x,y,z
3	C3	0	C.2	0.37401	0.505105	0.635301	x,y,z
4	C4	0	C.2	0.407082	0.374702	0.594784	x,y,z
5	C5	0	C.2	0.334343	0.331669	0.487877	x,y,z
6	C6	0	C.2	0.224211	0.416617	0.417352	x,y,z
7	C7	0	C.2	0.19412	0.545653	0.459038	x,y,z
8	C8	0	C.3	0.089584	0.661294	0.40459	x,y,z
9	H8A	0	H	0.129039	0.689222	0.333639	x,y,z
10	H8B	0	H	-0.030283	0.634046	0.388228	x,y,z
11	C9	0	C.3	0.293416	0.090022	0.482103	x,y,z
12	H9A	0	H	0.315088	0.080718	0.563988	x,y,z
13	H9B	0	H	0.332031	0.006922	0.447217	x,y,z
14	H9C	0	H	0.172399	0.102134	0.458104	x,y,z
15	C10	0	C.3	0.147309	0.37151	0.301717	x,y,z
16	H10A	0	H	0.025066	0.363226	0.298791	x,y,z
17	H10B	0	H	0.194314	0.282123	0.284551	x,y,z
18	H10C	0	H	0.172453	0.4398	0.246486	x,y,z
19	O1	0	O.3	0.11172	0.772264	0.485834	x,y,z
20	O2	0	O.2	0.248279	0.810869	0.65788	x,y,z
21	O3	0	O.3	0.454304	0.534852	0.739376	x,y,z
22	H3	0	H	0.442546	0.618589	0.760822	x,y,z
23	O4	0	O.3	0.518945	0.290054	0.658656	x,y,z
24	H4	0	H	0.565892	0.333069	0.715303	x,y,z
25	O5	0	O.3	0.382199	0.207398	0.448482	x,y,z

8.3 Dibefurin mixed with isomer 184 (CCDC 1022043)



Crystallographic data.

net formula	$C_{18}H_{18.30}O_{9.15}$
$M_r/g\ mol^{-1}$	381.032
crystal size/mm	$0.170 \times 0.040 \times 0.030$
T/K	100(2)
radiation	'Mo $K\alpha$
diffractometer	'Bruker D8Venture'
crystal system	monoclinic
space group	$P2_1/n$
$a/\text{\AA}$	10.1773(8)
$b/\text{\AA}$	6.1835(5)
$c/\text{\AA}$	12.7105(10)
$\alpha/^\circ$	90
$\beta/^\circ$	90.823(2)
$\gamma/^\circ$	90
$V/\text{\AA}^3$	799.81(11)
Z	2
calc. density/ $g\ cm^{-3}$	1.5822(2)
μ/mm^{-1}	0.129
absorption correction	multi-scan
transmission factor range	0.9373–0.9985
refls. measured	18459
R_{int}	0.0541
mean $\sigma(I)/I$	0.0275
θ range	3.21–26.39
observed refls.	1331
x, y (weighting scheme)	0.0566, 0.5971
hydrogen refinement	mixed
refls in refinement	1638
parameters	150
restraints	2
$R(F_{obs})$	0.0448

$R_w(F^2)$	0.1149
S	1.061
shift/error _{max}	0.001
max electron density/e Å ⁻³	0.361
min electron density/e Å ⁻³	-0.218

C-bound H: constr, O-bound H: refall.

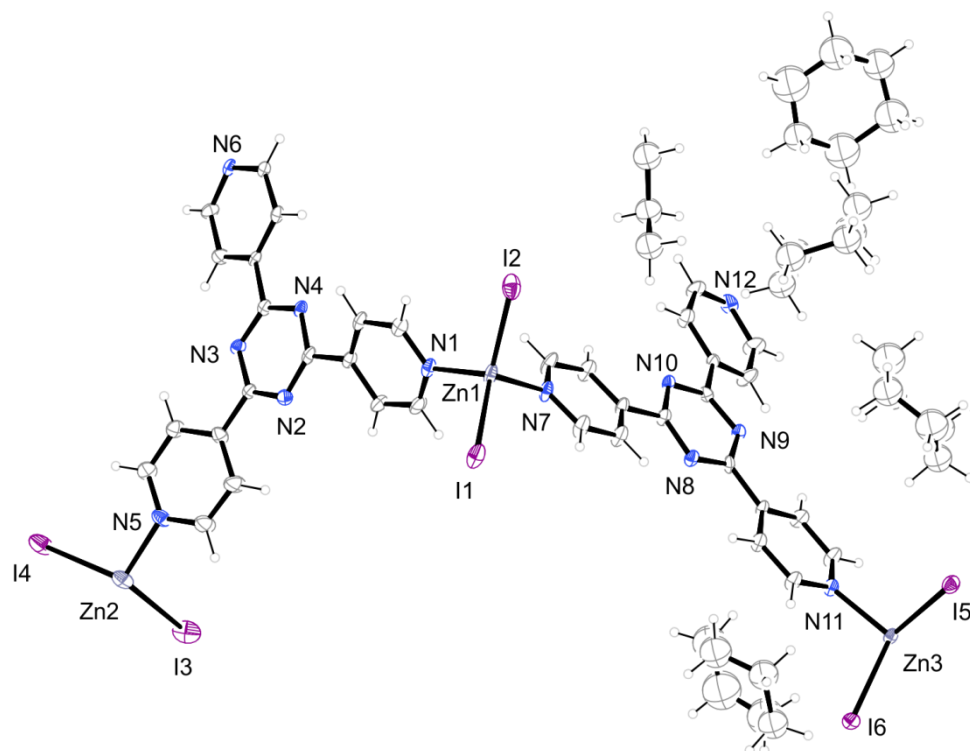
Disorder handled by split model, sof ratio 0.9/0.1, figure shows main part only.

Symmetry code i = 1-x, 2-y, 1-z.

Number	Label	Charge	SybylType	Xfrac + ESD	Yfrac + ESD	Zfrac + ESD	Symm. op.
1	C1	0	C.2	0.530054	0.781392	0.535798	x,y,z
2	C2	0	C.3	0.55426	0.84182	0.421802	x,y,z
3	H2	0	H	0.660694	0.715882	0.322973	x,y,z
4	C3	0	C.2	0.42751	0.803389	0.355054	x,y,z
5	C4	0	C.3	0.299734	0.817525	0.407721	x,y,z
6	C5	0	C.3	0.296256	0.856437	0.511674	x,y,z
7	C6	0	C.3	0.415317	0.905691	0.580621	x,y,z
8	C7	0	C.3	0.371734	0.82996	0.689578	x,y,z
9	H7A	0	H	0.39542	0.676436	0.701197	x,y,z
10	H7B	0	H	0.413405	0.918664	0.745657	x,y,z
11	C8	0	C.3	0.181766	0.832328	0.583871	x,y,z
12	H8A	0	H	0.114605	0.944092	0.568296	x,y,z
13	H8B	0	H	0.140938	0.688033	0.575013	x,y,z
14	C9	0	C.3	0.178264	0.768519	0.343963	x,y,z
15	H9A	0	H	0.102068	0.765264	0.390211	x,y,z
16	H9B	0	H	0.187873	0.627561	0.309678	x,y,z
17	H9C	0	H	0.165457	0.880701	0.290327	x,y,z
18	O4	0	O.3	0.232202	0.857416	0.688755	x,y,z
19	C91	0	C.3	0.178264	0.768519	0.343963	x,y,z
20	H9D	0	H	0.174347	0.616118	0.320257	x,y,z
21	H9E	0	H	0.166564	0.867154	0.283196	x,y,z
22	O41	0	O.3	0.078452	0.818679	0.436889	x,y,z
23	C81	0	C.3	0.150815	0.870562	0.533067	x,y,z
24	H8D	0	H	0.12725	0.767607	0.589383	x,y,z
25	H8E	0	H	0.128144	101.833	0.556669	x,y,z
26	C71	0	C.3	0.371734	0.82996	0.689578	x,y,z

27	H7C	0	H	0.387134	0.674129	0.696497	x,y,z
28	H7D	0	H	0.277937	0.860294	0.697856	x,y,z
29	H7E	0	H	0.42228	0.907062	0.744012	x,y,z
30	O1	0	O.2	0.5942	0.650819	0.583935	x,y,z
31	O2	0	O.3	0.659196	0.722344	0.384993	x,y,z
32	O3	0	O.2	0.439076	0.758674	0.262355	x,y,z
33	C1	0	C.2	0.469946	121.861	0.464202	1-x,2-y,1-z
34	C2	0	C.3	0.44574	115.818	0.578198	1-x,2-y,1-z
35	H2	0	H	0.339306	128.412	0.677027	1-x,2-y,1-z
36	C3	0	C.2	0.57249	119.661	0.644946	1-x,2-y,1-z
37	C4	0	C.3	0.700266	118.248	0.592279	1-x,2-y,1-z
38	C5	0	C.3	0.703744	114.356	0.488326	1-x,2-y,1-z
39	C6	0	C.3	0.584683	109.431	0.419379	1-x,2-y,1-z
40	C7	0	C.3	0.628266	117.004	0.310422	1-x,2-y,1-z
41	H7A	0	H	0.60458	132.356	0.298803	1-x,2-y,1-z
42	H7B	0	H	0.586595	108.134	0.254343	1-x,2-y,1-z
43	C8	0	C.3	0.818234	116.767	0.416129	1-x,2-y,1-z
44	H8A	0	H	0.885395	105.591	0.431704	1-x,2-y,1-z
45	H8B	0	H	0.859062	131.197	0.424987	1-x,2-y,1-z
46	C9	0	C.3	0.821736	123.148	0.656037	1-x,2-y,1-z
47	H9A	0	H	0.897932	123.474	0.609789	1-x,2-y,1-z
48	H9B	0	H	0.812127	137.244	0.690322	1-x,2-y,1-z
49	H9C	0	H	0.834543	11.193	0.709673	1-x,2-y,1-z
50	O4	0	O.3	0.767798	114.258	0.311245	1-x,2-y,1-z
51	C91	0	C.3	0.821736	123.148	0.656037	1-x,2-y,1-z
52	H9D	0	H	0.825653	138.388	0.679743	1-x,2-y,1-z
53	H9E	0	H	0.833436	113.285	0.716804	1-x,2-y,1-z
54	O41	0	O.3	0.921548	118.132	0.563111	1-x,2-y,1-z
55	C81	0	C.3	0.849185	112.944	0.466933	1-x,2-y,1-z
56	H8D	0	H	0.87275	123.239	0.410617	1-x,2-y,1-z
57	H8E	0	H	0.871856	0.98167	0.443331	1-x,2-y,1-z
58	C71	0	C.3	0.628266	117.004	0.310422	1-x,2-y,1-z
59	H7C	0	H	0.612866	132.587	0.303503	1-x,2-y,1-z
60	H7D	0	H	0.722063	113.971	0.302144	1-x,2-y,1-z

61	H7E	0	H	0.57772	109.294	0.255988	1-x,2-y,1-z
62	O1	0	O.2	0.4058	134.918	0.416065	1-x,2-y,1-z
63	O2	0	O.3	0.340804	127.766	0.615007	1-x,2-y,1-z
64	O3	0	O.2	0.560924	124.133	0.737645	1-x,2-y,1-z
65	O5	0	O.3	0.108078	0.315873	0.479134	x,y,z
66	H51	0	H	0.179861	0.32682	0.510143	x,y,z
67	H52	0	H	0.103727	0.305472	0.413936	x,y,z

8.4 $(\text{Zn}_3\text{C}_{36}\text{H}_{24}\text{I}_6\text{N}_{12} \cdot \text{C}_6\text{H}_{12})_n$ 

Crystallographic data.

net formula	$\text{C}_{63}\text{H}_{78}\text{I}_6\text{N}_{12}\text{Zn}_3$
$M_r/\text{g mol}^{-1}$	1960.97
crystal size/mm	$0.080 \times 0.060 \times 0.010$
T/K	100(2)
radiation	'Mo K α
diffractometer	'Bruker D8Venture'
crystal system	monoclinic
space group	$C2/c$
$a/\text{\AA}$	34.566(2)
$b/\text{\AA}$	15.0883(10)
$c/\text{\AA}$	29.304(2)
$\alpha/^\circ$	90
$\beta/^\circ$	100.4193(18)
$\gamma/^\circ$	90
$V/\text{\AA}^3$	15031.4(17)
Z	8
calc. density/ g cm^{-3}	1.73307(20)
μ/mm^{-1}	3.458

absorption correction	multi-scan
transmission factor range	0.7424–0.8620
refls. measured	127561
R_{int}	0.0454
mean $\sigma(I)/I$	0.0480
θ range	2.95–25.19
observed refls.	9715
x, y (weighting scheme)	0.0801, 500.8572
hydrogen refinement	constr
refls in refinement	13400
parameters	622
restraints	0
$R(F_{\text{obs}})$	0.0721
$R_w(F^2)$	0.1932
S	1.054
shift/error _{max}	0.001
max electron density/e \AA^{-3}	4.766
min electron density/e \AA^{-3}	–2.400

Cyclohexane refined isotropically. Large voids in the structure...

Number	Label	Charge	SybylType	Xfrac + ESD	Yfrac + ESD	Zfrac + ESD	Symm. op.
1	C1	0	C.2	0.424841	0.998091	0.420221	x,y,z
2	H1	0	H	0.411187	102.822	0.393658	x,y,z
3	C2	0	C.2	0.455682	0.945317	0.414972	x,y,z
4	H2	0	H	0.463617	0.9394	0.385731	x,y,z
5	C3	0	C.2	0.475343	0.89999	0.454155	x,y,z
6	C4	0	C.2	0.463299	0.911203	0.495017	x,y,z
7	H4	0	H	0.47588	0.880306	0.521884	x,y,z
8	C5	0	C.2	0.432145	0.968706	0.49738	x,y,z
9	H5	0	H	0.424502	0.978807	0.526495	x,y,z
10	C6	0	C.2	0.5077	0.837845	0.449216	x,y,z
11	C7	0	C.2	0.557822	0.798189	0.414976	x,y,z
12	C8	0	C.2	0.539885	0.710072	0.469598	x,y,z
13	C9	0	C.2	0.584376	0.815558	0.382532	x,y,z

14	C10	0	C.2	0.576349	0.879437	0.348504	x,y,z
15	H10	0	H	0.552561	0.912352	0.344916	x,y,z
16	C11	0	C.2	0.602879	0.895233	0.319854	x,y,z
17	H11	0	H	0.597345	0.940546	0.297101	x,y,z
18	C12	0	C.2	0.644447	0.788445	0.356158	x,y,z
19	H12	0	H	0.6687	0.75734	0.359664	x,y,z
20	C13	0	C.2	0.619112	0.768835	0.38595	x,y,z
21	H13	0	H	0.625459	0.723621	0.40863	x,y,z
22	C14	0	C.2	0.544309	0.625329	0.495935	x,y,z
23	C15	0	C.2	0.571893	0.563057	0.486823	x,y,z
24	H15	0	H	0.586507	0.572664	0.462755	x,y,z
25	C16	0	C.2	0.577273	0.488926	0.513046	x,y,z
26	H16	0	H	0.595599	0.446183	0.506249	x,y,z
27	C17	0	C.2	0.523309	0.606869	0.529661	x,y,z
28	H17	0	H	0.503547	0.64666	0.535721	x,y,z
29	C18	0	C.2	0.530913	0.529549	0.555189	x,y,z
30	H18	0	H	0.51606	0.516926	0.5787	x,y,z
31	C19	0	C.2	0.320756	0.942367	0.410121	x,y,z
32	H19	0	H	0.338039	0.908796	0.432521	x,y,z
33	C20	0	C.2	0.293258	0.898384	0.378171	x,y,z
34	H20	0	H	0.291628	0.835563	0.378903	x,y,z
35	C21	0	C.2	0.26863	0.944877	0.345809	x,y,z
36	C22	0	C.2	0.271598	103.723	0.346383	x,y,z
37	H22	0	H	0.254557	107.219	0.324415	x,y,z
38	C23	0	C.2	0.29918	107.574	0.378796	x,y,z
39	H23	0	H	0.301137	113.854	0.379003	x,y,z
40	C24	0	C.2	0.238509	0.900655	0.309839	x,y,z
41	C25	0	C.2	0.192435	0.909139	0.24567	x,y,z
42	C26	0	C.2	0.206059	0.77851	0.282296	x,y,z
43	C27	0	C.2	0.170116	0.95965	0.206562	x,y,z
44	C28	0	C.2	0.143265	0.917715	0.173017	x,y,z
45	H28	0	H	0.140731	0.855027	0.173195	x,y,z
46	C29	0	C.2	0.120361	0.966937	0.139564	x,y,z
47	H29	0	H	0.101747	0.937019	0.116956	x,y,z

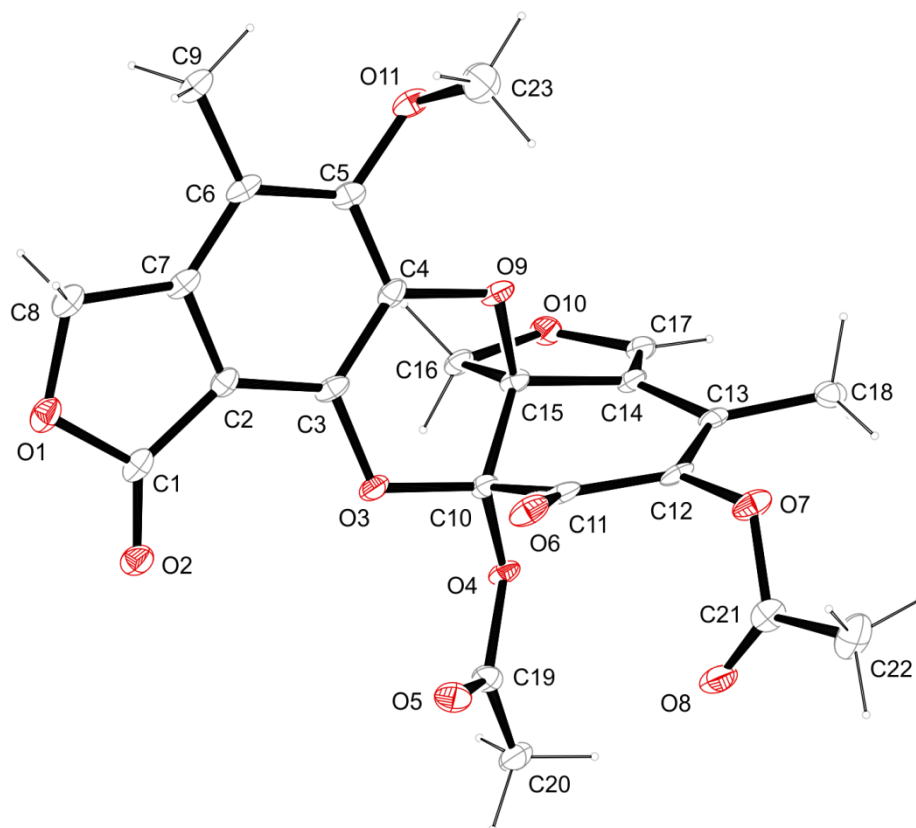
48	C30	0	C.2	0.173957	105.027	0.202418	x,y,z
49	H30	0	H	0.193026	108.161	0.223841	x,y,z
50	C31	0	C.2	0.150052	109.521	0.167112	x,y,z
51	H31	0	H	0.153238	115.739	0.164289	x,y,z
52	C32	0	C.2	0.199703	0.680159	0.282615	x,y,z
53	C33	0	C.2	0.175726	0.642214	0.244781	x,y,z
54	H33	0	H	0.164065	0.677184	0.218975	x,y,z
55	C34	0	C.2	0.169297	0.552871	0.245611	x,y,z
56	H34	0	H	0.151831	0.527421	0.220236	x,y,z
57	C35	0	C.2	0.217616	0.625943	0.317885	x,y,z
58	H35	0	H	0.23536	0.649585	0.343557	x,y,z
59	C36	0	C.2	0.209216	0.53572	0.315199	x,y,z
60	H36	0	H	0.220802	0.498575	0.340132	x,y,z
61	N1	0	N.2	0.412836	100.982	0.459885	x,y,z
62	N2	0	N.2	0.529778	0.857221	0.4183	x,y,z
63	N3	0	N.2	0.563735	0.72259	0.439614	x,y,z
64	N4	0	N.2	0.511107	0.766581	0.477122	x,y,z
65	N5	0	N.2	0.63668	0.848491	0.322875	x,y,z
66	N6	0	N.2	0.55846	0.4724	0.547703	x,y,z
67	N7	0	N.2	0.323916	102.998	0.410664	x,y,z
68	N8	0	N.2	0.219913	0.950805	0.275618	x,y,z
69	N9	0	N.2	0.183855	0.82237	0.247998	x,y,z
70	N10	0	N.2	0.233327	0.813242	0.314834	x,y,z
71	N11	0	N.2	0.122725	105.375	0.137001	x,y,z
72	N12	0	N.2	0.185789	0.499524	0.279409	x,y,z
73	ZN1	0	Zn	0.364019	108.954	0.462091	x,y,z
74	ZN2	0	Zn	0.67214	0.865221	0.274433	x,y,z
75	ZN3	0	Zn	0.079741	112.884	0.09416	x,y,z
76	I1	0	I	0.379902	123.917	0.430036	x,y,z
77	I2	0	I	0.340216	105.342	0.536355	x,y,z
78	I3	0	I	0.628303	0.843569	0.195438	x,y,z
79	I4	0	I	0.73338	0.774825	0.303515	x,y,z
80	I5	0	I	0.027691	116.047	0.142347	x,y,z
81	I6	0	I	0.116057	123.844	0.052042	x,y,z

82	N6	0	N.3	0.05846	10.276	0.047703	-1/2+x,1.5-y,-1/2+z
83	N12	0	N.3	0.685789	0.999524	0.279409	1/2+x,1/2+y,z
84	ZN2	0	Zn	0.17214	0.365221	0.274433	-1/2+x,-1/2+y,z
85	ZN3	0	Zn	0.579741	0.371158	0.59416	1/2+x,1.5-y,1/2+z
86	C37	0	C.3	0.219963	0.948289	0.06644	x,y,z
87	H37A	0	H	0.218591	0.943936	0.099819	x,y,z
88	H37B	0	H	0.24251	0.986716	0.063146	x,y,z
89	C38	0	C.3	0.184455	0.985371	0.041573	x,y,z
90	H38A	0	H	0.181634	104.622	0.053173	x,y,z
91	H38B	0	H	0.162057	0.950008	0.048399	x,y,z
92	C39	0	C.3	0.181791	0.989338	-0.010823	x,y,z
93	H39A	0	H	0.155393	101.089	-0.025417	x,y,z
94	H39B	0	H	0.201516	103.189	-0.018343	x,y,z
95	C40	0	C.3	0.18887	0.899974	-0.030321	x,y,z
96	H40A	0	H	0.165156	0.862871	-0.03096	x,y,z
97	H40B	0	H	0.192858	0.907411	-0.062716	x,y,z
98	C41	0	C.3	0.220975	0.856302	-0.005384	x,y,z
99	H41A	0	H	0.244865	0.884969	-0.012754	x,y,z
100	H41B	0	H	0.22052	0.794933	-0.017423	x,y,z
101	C42	0	C.3	0.225907	0.850632	0.045777	x,y,z
102	H42A	0	H	0.252506	0.828085	0.058827	x,y,z
103	H42B	0	H	0.206306	0.809106	0.054522	x,y,z
104	C43	0	C.3	0.137879	0.748495	0.366812	x,y,z
105	H43A	0	H	0.124946	0.779246	0.338256	x,y,z
106	H43B	0	H	0.166663	0.751854	0.368131	x,y,z
107	C44	0	C.3	0.125879	0.655939	0.364328	x,y,z
108	H44A	0	H	0.142613	0.623038	0.389749	x,y,z
109	H44B	0	H	0.13059	0.630789	0.334612	x,y,z
110	C45	0	C.3	0.082827	0.641332	0.367824	x,y,z
111	H45A	0	H	0.077904	0.57744	0.371922	x,y,z
112	H45B	0	H	0.06564	0.661537	0.338947	x,y,z
113	C46	0	C.3	0.07345	0.693914	0.409536	x,y,z
114	H46A	0	H	0.045059	0.68803	0.41036	x,y,z
115	H46B	0	H	0.088274	0.667842	0.438493	x,y,z

116	C47	0	C.3	0.0829	0.784243	0.408053	x,y,z
117	H47A	0	H	0.075432	0.815023	0.43501	x,y,z
118	H47B	0	H	0.067876	0.811153	0.37944	x,y,z
119	C48	0	C.3	0.127471	0.796122	0.408936	x,y,z
120	H48A	0	H	0.133964	0.859901	0.40783	x,y,z
121	H48B	0	H	0.142693	0.770718	0.437842	x,y,z
122	C49	0	C.3	0.066033	0.769623	0.234104	x,y,z
123	H49A	0	H	0.063564	0.790367	0.2655	x,y,z
124	H49B	0	H	0.091929	0.789355	0.227983	x,y,z
125	C50	0	C.3	0.064415	0.665195	0.232984	x,y,z
126	H50A	0	H	0.087059	0.640227	0.254726	x,y,z
127	H50B	0	H	0.039862	0.644007	0.242272	x,y,z
128	C51	0	C.3	0.065765	0.637599	0.185736	x,y,z
129	H51A	0	H	0.06556	0.572042	0.184306	x,y,z
130	H51B	0	H	0.09074	0.658338	0.177359	x,y,z
131	C52	0	C.3	0.031352	0.673398	0.150211	x,y,z
132	H52A	0	H	0.00605	0.652411	0.157579	x,y,z
133	H52B	0	H	0.033384	0.65286	0.118645	x,y,z
134	C53	0	C.3	0.033651	0.776697	0.152865	x,y,z
135	H53A	0	H	0.057614	0.796643	0.141759	x,y,z
136	H53B	0	H	0.010623	0.801941	0.131868	x,y,z
137	C54	0	C.3	0.034506	0.810803	0.199502	x,y,z
138	H54A	0	H	0.008756	0.799504	0.208677	x,y,z
139	H54B	0	H	0.038605	0.875739	0.199467	x,y,z
140	C55	0	C.3	0.093414	0.045172	0.261089	x,y,z
141	H55A	0	H	0.101424	-0.012626	0.249784	x,y,z
142	H55B	0	H	0.0895	0.087244	0.234731	x,y,z
143	C56	0	C.3	0.052219	0.033482	0.280407	x,y,z
144	H56A	0	H	0.041583	0.092586	0.286074	x,y,z
145	H56B	0	H	0.032689	0.002904	0.256744	x,y,z
146	C57	0	C.3	0.058262	-0.015544	0.321548	x,y,z
147	H57A	0	H	0.065638	-0.076919	0.314786	x,y,z
148	H57B	0	H	0.033328	-0.018222	0.333629	x,y,z
149	C58	0	C.3	0.088987	0.022099	0.357254	x,y,z

150	H58A	0	H	0.092886	-0.0165	0.385028	x,y,z
151	H58B	0	H	0.08057	0.081189	0.366429	x,y,z
152	C59	0	C.3	0.127229	0.030792	0.339822	x,y,z
153	H59A	0	H	0.146739	0.059259	0.364336	x,y,z
154	H59B	0	H	0.137031	-0.029409	0.334755	x,y,z
155	C60	0	C.3	0.125336	0.079194	0.298958	x,y,z
156	H60A	0	H	0.150973	0.075501	0.288516	x,y,z
157	H60B	0	H	0.120249	0.142268	0.305071	x,y,z
158	C61	0	C.3	0.235375	0.785039	0.454879	x,y,z
159	H61A	0	H	0.209974	0.810327	0.45963	x,y,z
160	H61B	0	H	0.238339	0.797857	0.422558	x,y,z
161	C62	0	C.3	0.234808	0.693722	0.461257	x,y,z
162	H62A	0	H	0.259372	0.667686	0.454265	x,y,z
163	H62B	0	H	0.212436	0.667873	0.439439	x,y,z
164	C63	0	C.3	0.230896	0.670052	0.511518	x,y,z
165	H63A	0	H	0.205223	0.690877	0.517844	x,y,z
166	H63B	0	H	0.232269	0.604983	0.515852	x,y,z
167	C61	0	C.3	0.264625	0.714961	0.545121	1/2-x,1.5-y,1-z
168	H61A	0	H	0.290026	0.689673	0.54037	1/2-x,1.5-y,1-z
169	H61B	0	H	0.261661	0.702143	0.577442	1/2-x,1.5-y,1-z
170	C62	0	C.3	0.265192	0.806278	0.538743	1/2-x,1.5-y,1-z
171	H62A	0	H	0.240628	0.832314	0.545735	1/2-x,1.5-y,1-z
172	H62B	0	H	0.287564	0.832127	0.560561	1/2-x,1.5-y,1-z
173	C63	0	C.3	0.269104	0.829948	0.488482	1/2-x,1.5-y,1-z
174	H63A	0	H	0.294777	0.809123	0.482156	1/2-x,1.5-y,1-z
175	H63B	0	H	0.267731	0.895017	0.484148	1/2-x,1.5-y,1-z

8.5 *rac*-(6*aR*,12*aR*)-5-methoxy-4,10-dimethyl-1,12-dioxo-1,3-dihydro-7*H*-[1,4]dioxino[2,3-*d*:3,2-*d'*:6,5-*e'*]trienobenzofuran-11,12*a*(12*H*)-diyl diacetate (240) (CCDC 1022044)



Crystallographic data.

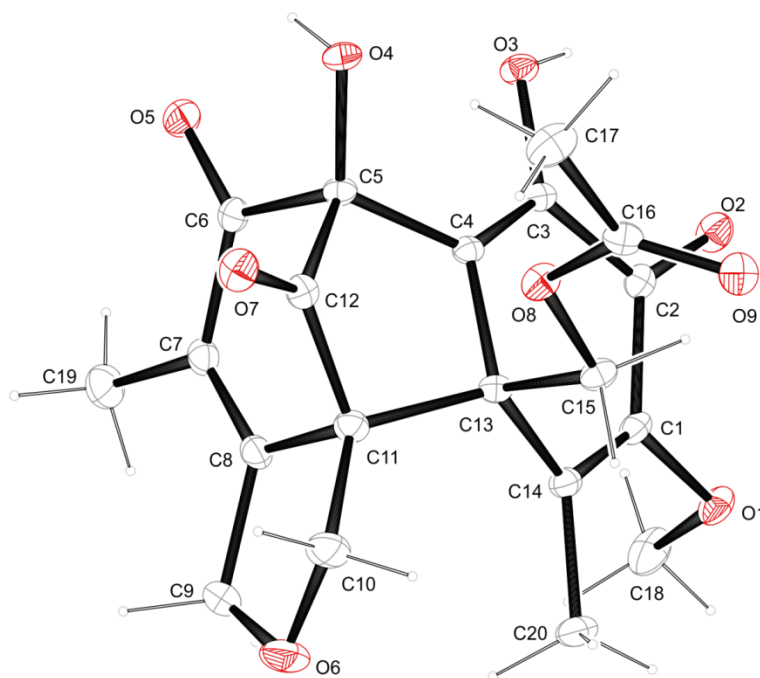
net formula	C ₂₃ H ₂₀ O ₁₁
<i>M_r</i> /g mol ⁻¹	472.398
crystal size/mm	0.100 × 0.050 × 0.040
<i>T</i> /K	100(2)
radiation	'Mo Kα
diffractometer	'Bruker D8Venture'
crystal system	monoclinic
space group	<i>P</i> 2 ₁ / <i>n</i>
<i>a</i> /Å	14.330(2)
<i>b</i> /Å	8.4955(13)
<i>c</i> /Å	16.966(3)
<i>α</i> /°	90
<i>β</i> /°	93.780(5)
<i>γ</i> /°	90
<i>V</i> /Å ³	2060.9(5)
<i>Z</i>	4
calc. density/g cm ⁻³	1.5225(4)
μ/mm ⁻¹	0.123
absorption correction	multi-scan
transmission factor range	0.8102–0.9579
refls. measured	21166

R_{int}	0.1429
mean $\sigma(I)/I$	0.0895
θ range	3.00–25.05
observed refls.	2334
x, y (weighting scheme)	0.0553, 8.5329
hydrogen refinement	constr
refls in refinement	3651
parameters	312
restraints	0
$R(F_{\text{obs}})$	0.0899
$R_w(F^2)$	0.2099
S	1.135
shift/error _{max}	0.001
max electron density/e \AA^{-3}	0.442
min electron density/e \AA^{-3}	−0.297

Number	Label	Charge	SybylType	Xfrac + ESD	Yfrac + ESD	Zfrac + ESD	Symm. op.
1	C1	0	C.2	−0.044602	0.811774	0.477745	x,y,z
2	C2	0	C.2	0.033512	0.73486	0.524538	x,y,z
3	C3	0	C.2	0.129782	0.748695	0.521062	x,y,z
4	C4	0	C.2	0.186468	0.67186	0.578189	x,y,z
5	C5	0	C.2	0.148524	0.572868	0.633731	x,y,z
6	C6	0	C.2	0.052338	0.548711	0.634746	x,y,z
7	C7	0	C.2	−0.002497	0.637186	0.580797	x,y,z
8	C8	0	C.3	−0.105729	0.64776	0.571081	x,y,z
9	H8A	0	H	−0.133186	0.543534	0.55748	x,y,z
10	H8B	0	H	−0.131465	0.685237	0.620464	x,y,z
11	C9	0	C.3	0.008934	0.438115	0.691403	x,y,z
12	H9A	0	H	−0.02726	0.35742	0.661579	x,y,z
13	H9B	0	H	−0.032493	0.497389	0.724261	x,y,z
14	H9C	0	H	0.05834	0.387637	0.725201	x,y,z
15	C10	0	C.3	0.263025	0.840397	0.462071	x,y,z
16	C11	0	C.2	0.303242	0.698119	0.419062	x,y,z
17	C12	0	C.2	0.404969	0.680396	0.428519	x,y,z
18	C13	0	C.2	0.460165	0.743198	0.489292	x,y,z
19	C14	0	C.2	0.413266	0.83961	0.545749	x,y,z
20	C15	0	C.3	0.309499	0.837639	0.546762	x,y,z
21	C16	0	C.3	0.290951	0.981221	0.599249	x,y,z
22	H16A	0	H	0.262707	106.829	0.567056	x,y,z

23	H16B	0	H	0.24804	0.952717	0.640372	x,y,z
24	C17	0	C.2	0.447464	0.945685	0.598589	x,y,z
25	H17	0	H	0.512672	0.961828	0.609283	x,y,z
26	C18	0	C.3	0.562635	0.715714	0.499773	x,y,z
27	H18A	0	H	0.59493	0.816621	0.508104	x,y,z
28	H18B	0	H	0.584166	0.664772	0.452428	x,y,z
29	H18C	0	H	0.576394	0.647622	0.5457	x,y,z
30	C19	0	C.2	0.261064	101.346	0.349049	x,y,z
31	C20	0	C.3	0.298901	116.022	0.321862	x,y,z
32	H20A	0	H	0.269378	118.622	0.269742	x,y,z
33	H20B	0	H	0.366565	114.949	0.318168	x,y,z
34	H20C	0	H	0.286382	124.432	0.359264	x,y,z
35	C21	0	C.2	0.44947	0.631807	0.299256	x,y,z
36	C22	0	C.3	0.498593	0.516833	0.251553	x,y,z
37	H22A	0	H	0.503018	0.558187	0.198006	x,y,z
38	H22B	0	H	0.463778	0.417473	0.249102	x,y,z
39	H22C	0	H	0.561589	0.498519	0.275886	x,y,z
40	C23	0	C.3	0.245553	0.355411	0.668218	x,y,z
41	H23A	0	H	0.286653	0.314075	0.711838	x,y,z
42	H23B	0	H	0.281397	0.369317	0.621476	x,y,z
43	H23C	0	H	0.194253	0.281195	0.656075	x,y,z
44	O1	0	O.3	-0.126526	0.759239	0.507344	x,y,z
45	O2	0	O.2	-0.046473	0.903464	0.423591	x,y,z
46	O3	0	O.3	0.16515	0.841389	0.462826	x,y,z
47	O4	0	O.3	0.290864	0.98376	0.427654	x,y,z
48	O5	0	O.2	0.209969	0.922422	0.311289	x,y,z
49	O6	0	O.2	0.25321	0.604581	0.381691	x,y,z
50	O7	0	O.3	0.446316	0.578549	0.376116	x,y,z
51	O8	0	O.2	0.416626	0.755992	0.279466	x,y,z
52	O9	0	O.3	0.283217	0.690403	0.581328	x,y,z
53	O10	0	O.3	0.382647	102.771	0.635415	x,y,z
54	O11	0	O.3	0.20809	0.503903	0.69052	x,y,z

8.6 *rac*-(((6*S*,10*aS*,10*bR*)-6,7-dihydroxy-9-methoxy-4,10-dimethyl-5,8,11-trioxo-3,5,6,8-tetrahydro-1*H*,10*aH*-6,10*b*-methanobenzo[3,4]cyclohepta[1,2-*c*]furan-10*a*-yl)methyl acetate (267)



Crystallographic data.

net formula	$C_{20}H_{20}O_9$
$M_r/g\ mol^{-1}$	404.36
crystal size/mm	$0.100 \times 0.090 \times 0.080$
T/K	100(2)
radiation	MoK α
diffractometer	'Bruker D8Venture'
crystal system	monoclinic
space group	'P 21/n'
$a/\text{\AA}$	12.4719(4)
$b/\text{\AA}$	10.4198(3)
$c/\text{\AA}$	14.7987(5)
$\alpha/^\circ$	90
$\beta/^\circ$	109.9144(10)
$\gamma/^\circ$	90
$V/\text{\AA}^3$	1808.16(10)
Z	4
calc. density/ $g\ cm^{-3}$	1.485

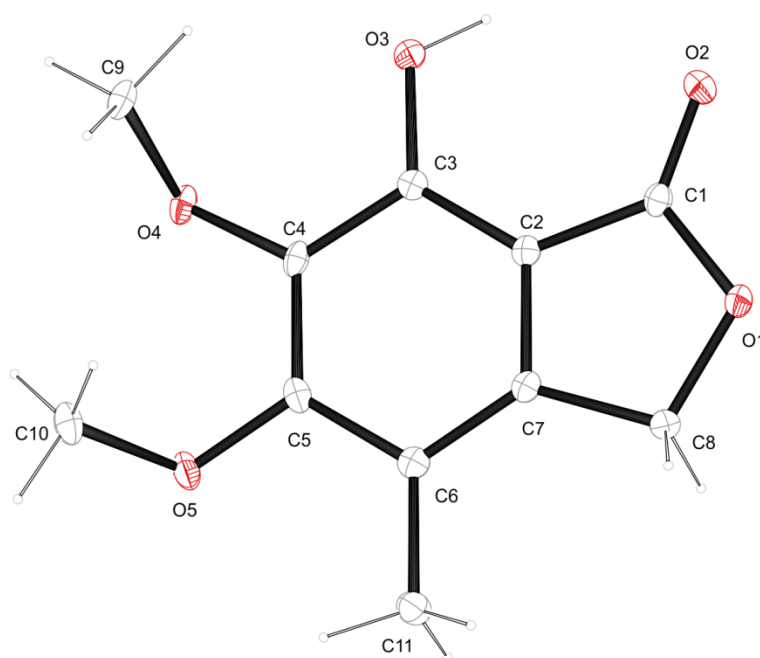
μ/mm^{-1}	0.118
absorption correction	multi-scan
transmission factor range	0.9259–0.9585
refls. measured	43959
R_{int}	0.0356
mean $\sigma(I)/I$	0.0172
θ range	2.442–26.43
observed refls.	3097
x, y (weighting scheme)	0.0453, 1.1557
hydrogen refinement	mixed
refls in refinement	3711
parameters	274
restraints	0
$R(F_{\text{obs}})$	0.0379
$R_w(F^2)$	0.1001
S	1.045
shift/error _{max}	0.001
max electron density/e \AA^{-3}	0.304
min electron density/e \AA^{-3}	−0.279

C-H: constr, O-H: refall.

Number	Label	Charge	SybylType	Xfrac + ESD	Yfrac + ESD	Zfrac + ESD	Symm. op.
1	C1	0	C.2	0.15802	0.48743	0.493802	x,y,z
2	C2	0	C.2	0.153128	0.494621	0.392519	x,y,z
3	C3	0	C.2	0.210428	0.38984	0.358674	x,y,z
4	C4	0	C.2	0.246097	0.285861	0.412974	x,y,z
5	C5	0	C.3	0.33136	0.188454	0.402608	x,y,z
6	C6	0	C.2	0.447135	0.261039	0.438561	x,y,z
7	C7	0	C.2	0.487265	0.298146	0.540839	x,y,z
8	C8	0	C.2	0.429617	0.254467	0.595986	x,y,z
9	C9	0	C.3	0.465468	0.263791	0.702898	x,y,z
10	H9A	0	H	0.544734	0.232795	0.733012	x,y,z
11	H9B	0	H	0.461505	0.35391	0.722715	x,y,z
12	C10	0	C.3	0.325027	0.104354	0.652495	x,y,z

13	H10A	0	H	0.246784	0.090534	0.653204	x,y,z
14	H10B	0	H	0.362879	0.01994	0.656799	x,y,z
15	C11	0	C.3	0.321749	0.174398	0.561068	x,y,z
16	C12	0	C.2	0.339183	0.090944	0.481755	x,y,z
17	C13	0	C.3	0.217459	0.261356	0.502784	x,y,z
18	C14	0	C.2	0.191456	0.382277	0.548677	x,y,z
19	C15	0	C.3	0.104398	0.185198	0.473909	x,y,z
20	H15A	0	H	0.085229	0.162839	0.531627	x,y,z
21	H15B	0	H	0.041332	0.236958	0.430312	x,y,z
22	C16	0	C.2	0.027344	0.000281	0.381469	x,y,z
23	C17	0	C.3	0.055898	-0.116356	0.336216	x,y,z
24	H17A	0	H	-0.005507	-0.133853	0.275389	x,y,z
25	H17B	0	H	0.064602	-0.189773	0.379526	x,y,z
26	H17C	0	H	0.127403	-0.102248	0.323932	x,y,z
27	C18	0	C.3	0.204724	0.68852	0.569008	x,y,z
28	H18A	0	H	0.234582	0.721004	0.520111	x,y,z
29	H18B	0	H	0.266765	0.64914	0.621456	x,y,z
30	H18C	0	H	0.171999	0.759661	0.594311	x,y,z
31	C19	0	C.3	0.596101	0.372678	0.579197	x,y,z
32	H19A	0	H	0.607762	0.422259	0.527035	x,y,z
33	H19B	0	H	0.660022	0.313294	0.606015	x,y,z
34	H19C	0	H	0.591737	0.431252	0.62964	x,y,z
35	C20	0	C.3	0.183155	0.377959	0.647956	x,y,z
36	H20A	0	H	0.137586	0.45075	0.656202	x,y,z
37	H20B	0	H	0.259812	0.382767	0.696123	x,y,z
38	H20C	0	H	0.146673	0.297555	0.65605	x,y,z
39	O1	0	O.3	0.118077	0.594447	0.526755	x,y,z
40	O2	0	O.2	0.111882	0.586354	0.340765	x,y,z
41	O3	0	O.3	0.231081	0.405477	0.275456	x,y,z
42	H3	0	H	0.208852	0.478367	0.252091	x,y,z
43	O4	0	O.3	0.312335	0.137191	0.311612	x,y,z
44	H4	0	H	0.364803	0.170056	0.294332	x,y,z
45	O5	0	O.2	0.496971	0.281989	0.382747	x,y,z
46	O6	0	O.3	0.388741	0.185582	0.731374	x,y,z

47	O7	0	O.2	0.363312	-0.020623	0.483597	x,y,z
48	O8	0	O.3	0.121217	0.070796	0.426127	x,y,z
49	O9	0	O.2	-0.065754	0.031069	0.380747	x,y,z

8.7 7-hydroxy-5,6-dimethoxy-4-methylisobenzofuran-1(3*H*)-one (291)

Crystallographic data.

net formula	$C_{11}H_{12}O_5$
$M_r/g\ mol^{-1}$	224.21
crystal size/mm	$0.140 \times 0.060 \times 0.040$
T/K	100(2)
radiation	MoK α
diffractometer	'Bruker D8Venture'
crystal system	monoclinic
space group	'P 21/c'
$a/\text{\AA}$	9.7456(6)
$b/\text{\AA}$	14.7151(10)
$c/\text{\AA}$	7.3781(5)
$\alpha/^\circ$	90
$\beta/^\circ$	110.408(2)
$\gamma/^\circ$	90
$V/\text{\AA}^3$	991.66(11)
Z	4
calc. density/ $g\ cm^{-3}$	1.502
μ/mm^{-1}	0.120
absorption correction	multi-scan
transmission factor range	0.9005–0.9585

refls. measured	18453
R_{int}	0.0559
mean $\sigma(I)/I$	0.0317
θ range	3.255–26.39
observed refls.	1500
x , y (weighting scheme)	0.0570, 0.5092
hydrogen refinement	mixed
refls in refinement	2032
parameters	152
restraints	0
$R(F_{\text{obs}})$	0.0442
$R_w(F^2)$	0.1163
S	1.029
shift/error _{max}	0.001
max electron density/e \AA^{-3}	0.306
min electron density/e \AA^{-3}	−0.277

C-H: constr, O-H: refall.

Number	Label	Charge	SybylType	Xfrac + ESD	Yfrac + ESD	Zfrac + ESD	Symm. op.
1	C1	0	C.2	−0.030692	0.331801	−0.033259	x,y,z
2	C2	0	C.2	0.104002	0.297449	0.105844	x,y,z
3	C3	0	C.2	0.22461	0.344875	0.226239	x,y,z
4	H3	0	H	0.152746	0.461128	0.163804	x,y,z
5	C4	0	C.2	0.343218	0.293502	0.343344	x,y,z
6	C5	0	C.2	0.337471	0.198079	0.335329	x,y,z
7	C6	0	C.2	0.213118	0.150281	0.218101	x,y,z
8	C7	0	C.2	0.098458	0.202925	0.105058	x,y,z
9	C8	0	C.3	−0.048201	0.175763	−0.035602	x,y,z
10	H8A	0	H	−0.037105	0.135764	−0.137505	x,y,z
11	H8B	0	H	−0.105913	0.143326	0.03117	x,y,z
12	C9	0	C.3	0.549804	0.393119	0.413967	x,y,z
13	H9A	0	H	0.601504	0.356641	0.346933	x,y,z
14	H9B	0	H	0.621208	0.424239	0.524162	x,y,z
15	H9C	0	H	0.488177	0.438226	0.32452	x,y,z
16	C10	0	C.3	0.595012	0.165691	0.449784	x,y,z
17	H10A	0	H	0.65079	0.109052	0.464801	x,y,z
18	H10B	0	H	0.644674	0.206618	0.557513	x,y,z
19	H10C	0	H	0.588185	0.194848	0.32752	x,y,z
20	C11	0	C.3	0.207287	0.048566	0.214804	x,y,z
21	H11A	0	H	0.159533	0.027575	0.081475	x,y,z
22	H11B	0	H	0.15151	0.027425	0.294455	x,y,z
23	H11C	0	H	0.307001	0.024141	0.266323	x,y,z
24	O1	0	O.3	−0.1187	0.260419	−0.117886	x,y,z
25	O2	0	O.2	−0.069432	0.409708	−0.078254	x,y,z

26	O3	0	O.3	0.231044	0.436635	0.242175	x,y,z
27	O4	0	O.3	0.459476	0.334716	0.481973	x,y,z
28	O5	0	O.3	0.449961	0.145917	0.449079	x,y,z

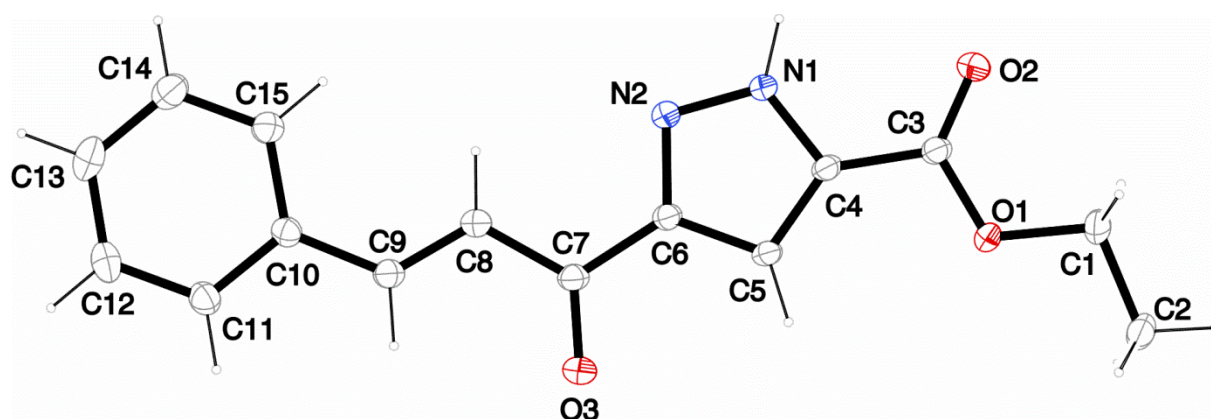
8.8 ethyl 3-cinnamoyl-1*H*-pyrazole-5-carboxylate (454)

Table 1.

1. Crystallographic data.

	1
net formula	$\text{C}_{15}\text{H}_{14}\text{N}_2\text{O}_3$
$M_r/\text{g mol}^{-1}$	270.283
crystal size/mm	$0.48 \times 0.22 \times 0.15$
T/K	173(2)
radiation	MoK α
diffractometer	'Oxford XCalibur'
crystal system	triclinic
space group	$P1\bar{1}21$
$a/\text{\AA}$	6.9637(10)
$b/\text{\AA}$	8.9276(11)
$c/\text{\AA}$	11.1074(11)
$\alpha/^\circ$	89.958(9)
$\beta/^\circ$	89.797(10)
$\gamma/^\circ$	78.677(11)
$V/\text{\AA}^3$	677.09(14)
Z	2
calc. density/ g cm^{-3}	1.3257(3)
μ/mm^{-1}	0.094
absorption correction	'multi-scan'
transmission factor range	0.95513–1.00000
refls. measured	3940
R_{int}	0.0291
mean $\sigma(I)/I$	0.0524

θ range	4.35–28.80
observed refls.	2349
x, y (weighting scheme)	0.0399, 0.1197
hydrogen refinement	mixed
refls in refinement	2951
parameters	186
restraints	0
$R(F_{\text{obs}})$	0.0462
$R_w(F^2)$	0.1179
S	1.073
shift/error _{max}	0.001
max electron density/e \AA^{-3}	0.173
min electron density/e \AA^{-3}	−0.192

C-bound H: constr, N-bound H: refall.

Number	Label	Charge	SybylType	Xfrac + ESD	Yfrac + ESD	Zfrac + ESD	Symm. op.
1	O1	0	O.3	0.664924	0.309287	0.356097	x,y,z
2	O2	0	O.2	0.834319	0.110279	0.251051	x,y,z
3	O3	0	O.2	−0.078205	0.424565	0.128975	x,y,z
4	N1	0	N.3	0.504733	0.114326	0.107097	x,y,z
5	H1	0	H	0.60344	0.033906	0.082127	x,y,z
6	N2	0	N.2	0.332494	0.136301	0.050858	x,y,z
7	C1	0	C.3	0.837013	0.308823	0.430349	x,y,z
8	H1A	0	H	0.943909	0.33655	0.381416	x,y,z
9	H1B	0	H	0.883877	0.206122	0.465224	x,y,z
10	C2	0	C.3	0.777048	0.424015	0.52852	x,y,z
11	H2A	0	H	0.73441	0.525513	0.492903	x,y,z
12	H2B	0	H	0.888571	0.425072	0.581861	x,y,z
13	H2C	0	H	0.668993	0.396705	0.574922	x,y,z
14	C3	0	C.2	0.687741	0.204929	0.268862	x,y,z
15	C4	0	C.2	0.509351	0.2163	0.196718	x,y,z
16	C5	0	C.2	0.328496	0.311814	0.198433	x,y,z
17	H5	0	H	0.284816	0.396045	0.250536	x,y,z
18	C6	0	C.2	0.222496	0.257567	0.106283	x,y,z

19	C7	0	C.2	0.01803	0.318936	0.070662	x,y,z
20	C8	0	C.2	-0.061114	0.24968	-0.033493	x,y,z
21	H8	0	H	0.018	0.165482	-0.073535	x,y,z
22	C9	0	C.2	-0.242268	0.303481	-0.072402	x,y,z
23	H9	0	H	-0.314507	0.388406	-0.029645	x,y,z
24	C10	0	C.2	-0.343202	0.247535	-0.172966	x,y,z
25	C11	0	C.2	-0.539702	0.311916	-0.192918	x,y,z
26	H11	0	H	-0.603401	0.393174	-0.143036	x,y,z
27	C12	0	C.2	-0.643311	0.258824	-0.284654	x,y,z
28	H12	0	H	-0.777429	0.302894	-0.297027	x,y,z
29	C13	0	C.2	-0.550658	0.141726	-0.35783	x,y,z
30	H13	0	H	-0.621016	0.105006	-0.420796	x,y,z
31	C14	0	C.2	-0.354426	0.077401	-0.339519	x,y,z
32	H14	0	H	-0.290739	-0.002757	-0.390409	x,y,z
33	C15	0	C.2	-0.252001	0.129421	-0.247904	x,y,z
34	H15	0	H	-0.118132	0.084457	-0.235675	x,y,z

8.9 ethyl (3*S*,4*S*)-3-((*S*)-2,2-dimethyl-1,3-dioxolan-4-yl)-4-(2-methoxy-2-oxoethyl)cyclohepta-1,5-diene-1-carboxylate (471)

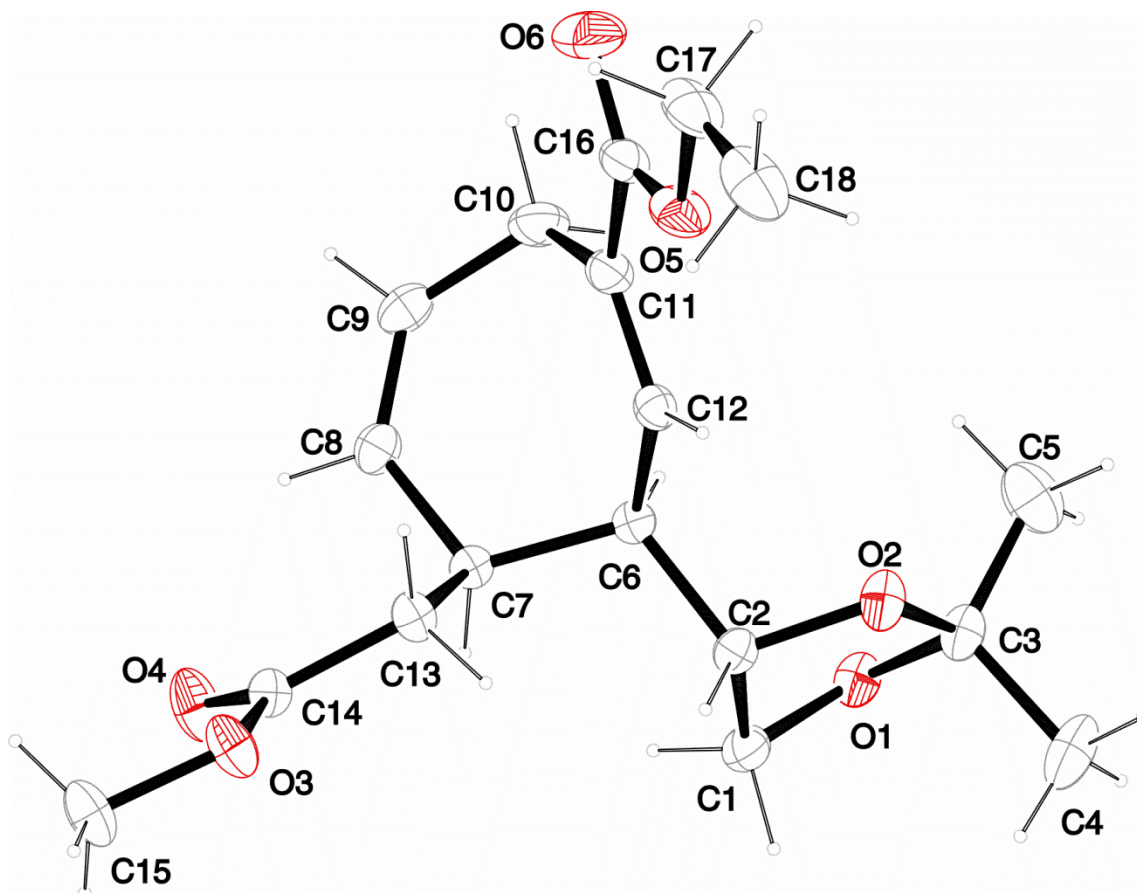


Table 1.

1. Crystallographic data.

	1
net formula	$C_{18}H_{26}O_6$
$M_r/g\ mol^{-1}$	338.395
crystal size/mm	$0.475 \times 0.126 \times 0.119$
T/K	200(2)
radiation	'Mo $K\alpha$
diffractometer	'Bruker D8Quest'
crystal system	orthorhombic
space group	$P2_12_12_1$
$a/\text{\AA}$	5.9270(2)
$b/\text{\AA}$	14.8998(5)
$c/\text{\AA}$	20.0765(8)

$\alpha/^\circ$	90
$\beta/^\circ$	90
$\gamma/^\circ$	90
$V/\text{\AA}^3$	1772.98(11)
Z	4
calc. density/ g cm^{-3}	1.26776(8)
μ/mm^{-1}	0.094
absorption correction	multi-scan
transmission factor range	0.6788–0.7456
refls. measured	14983
R_{int}	0.0328
mean $\sigma(I)/I$	0.0313
θ range	2.45–27.54
observed refls.	3352
x, y (weighting scheme)	0.0384, 0.2101
hydrogen refinement	constr
Flack parameter	−0.1(8)
refls in refinement	4064
parameters	221
restraints	0
$R(F_{\text{obs}})$	0.0366
$R_w(F^2)$	0.0848
S	1.032
shift/error _{max}	0.001
max electron density/ e \AA^{-3}	0.189
min electron density/ e \AA^{-3}	−0.164

Correct structure derived from synthesis.

1711 Friedel pairs measured.

Number	Label	Charge	SybylType	Xfrac + ESD	Yfrac + ESD	Zfrac + ESD	Symm. op.
1	O1	0	O.3	0.990331	0.318484	0.681435	x,y,z
2	O2	0	O.3	0.675045	0.280794	0.623601	x,y,z
3	O3	0	O.3	0.01844	0.207842	0.875351	x,y,z
4	O4	0	O.2	0.354396	0.174242	0.917544	x,y,z
5	O5	0	O.3	0.215119	0.012309	0.594403	x,y,z

6	O6	0	O.2	0.412237	-0.110893	0.621182	x,y,z
7	C1	0	C.3	0.805501	0.331079	0.725468	x,y,z
8	H1A	0	H	0.760559	0.395001	0.727713	x,y,z
9	H1B	0	H	0.841717	0.30952	0.77087	x,y,z
10	C2	0	C.3	0.621854	0.274131	0.693441	x,y,z
11	H2	0	H	0.469618	0.300286	0.702623	x,y,z
12	C3	0	C.3	0.896727	0.317584	0.616315	x,y,z
13	C4	0	C.3	0.877175	0.412012	0.588457	x,y,z
14	H4A	0	H	0.778301	0.447816	0.617174	x,y,z
15	H4B	0	H	0.813539	0.409477	0.543443	x,y,z
16	H4C	0	H	102.707	0.439684	0.586775	x,y,z
17	C5	0	C.3	103.859	0.257428	0.573749	x,y,z
18	H5A	0	H	119.428	0.279564	0.573242	x,y,z
19	H5B	0	H	0.978785	0.256957	0.528242	x,y,z
20	H5C	0	H	103.559	0.196381	0.591894	x,y,z
21	C6	0	C.3	0.630289	0.175986	0.715191	x,y,z
22	H6	0	H	0.790897	0.15596	0.711739	x,y,z
23	C7	0	C.3	0.555833	0.16234	0.788719	x,y,z
24	H7	0	H	0.635229	0.20888	0.815896	x,y,z
25	C8	0	C.2	0.627288	0.071989	0.81527	x,y,z
26	H8	0	H	0.626316	0.066654	0.862422	x,y,z
27	C9	0	C.2	0.691054	-0.000876	0.782754	x,y,z
28	H9	0	H	0.732983	-0.050381	0.809884	x,y,z
29	C10	0	C.3	0.706611	-0.016486	0.708853	x,y,z
30	H10A	0	H	0.855205	0.005269	0.693152	x,y,z
31	H10B	0	H	0.70041	-0.081912	0.700454	x,y,z
32	C11	0	C.2	0.525377	0.028266	0.668299	x,y,z
33	C12	0	C.2	0.493368	0.116538	0.670388	x,y,z
34	H12	0	H	0.380904	0.142658	0.642803	x,y,z
35	C13	0	C.3	0.301446	0.177342	0.798132	x,y,z
36	H13A	0	H	0.256471	0.232597	0.774181	x,y,z
37	H13B	0	H	0.218531	0.126426	0.778018	x,y,z
38	C14	0	C.2	0.234452	0.185858	0.870182	x,y,z
39	C15	0	C.3	-0.071075	0.211727	0.942464	x,y,z

40	H15A	0	H	-0.058669	0.15245	0.963297	x,y,z
41	H15B	0	H	-0.229966	0.229805	0.940918	x,y,z
42	H15C	0	H	0.014878	0.255552	0.96856	x,y,z
43	C16	0	C.2	0.381241	-0.030851	0.626091	x,y,z
44	C17	0	C.3	0.065206	-0.042939	0.55443	x,y,z
45	H17A	0	H	-0.008467	-0.088654	0.582846	x,y,z
46	H17B	0	H	0.152297	-0.074316	0.519383	x,y,z
47	C18	0	C.3	-0.10788	0.015689	0.523511	x,y,z
48	H18A	0	H	-0.19047	0.047791	0.558449	x,y,z
49	H18B	0	H	-0.213347	-0.021095	0.497665	x,y,z
50	H18C	0	H	-0.034163	0.059099	0.493996	x,y,z

8.10 ethyl (1*S*,4*aR*,9*aR*)-1-(hydroxymethyl)-3-oxo-1,3,4,4*a*,7,9*a*-hexahydrocyclohepta[*c*]pyran-8-carboxylate (476)

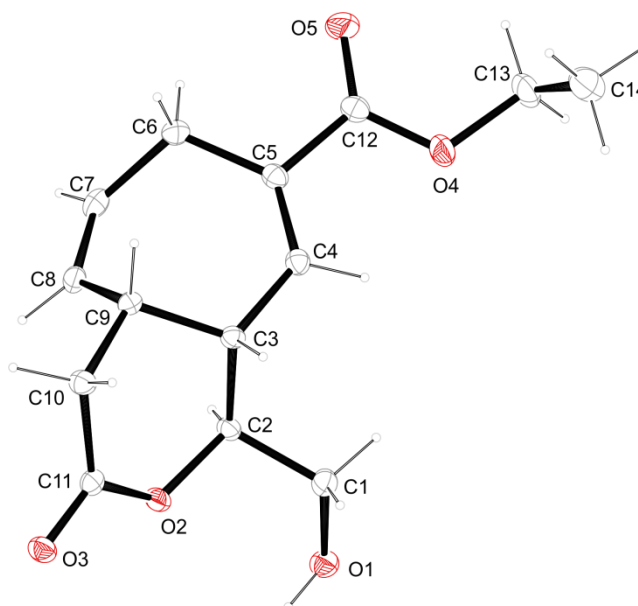


Table 1.

1. Crystallographic data.

	1
net formula	$\text{C}_{14}\text{H}_{18}\text{O}_5$
$M_r/\text{g mol}^{-1}$	266.290
crystal size/mm	$0.133 \times 0.074 \times 0.059$
T/K	100(2)
radiation	'Mo $\text{K}\alpha$
diffractometer	'Bruker D8Venture'
crystal system	orthorhombic
space group	$P2_12_12_1$
$a/\text{\AA}$	5.0950(2)
$b/\text{\AA}$	14.2661(5)
$c/\text{\AA}$	17.6871(7)
$\alpha/^\circ$	90
$\beta/^\circ$	90
$\gamma/^\circ$	90
$V/\text{\AA}^3$	1285.60(8)
Z	4
calc. density/ g cm^{-3}	1.37583(9)
μ/mm^{-1}	0.104

absorption correction	multi-scan
transmission factor range	0.9510–0.9705
refls. measured	40180
R_{int}	0.0360
mean $\sigma(I)/I$	0.0161
θ range	3.08–27.59
observed refls.	2777
x, y (weighting scheme)	0.0369, 0.4087
hydrogen refinement	mixed
Flack parameter	0.1(7)
refls in refinement	2960
parameters	176
restraints	0
$R(F_{\text{obs}})$	0.0300
$R_w(F^2)$	0.0756
S	1.060
shift/error _{max}	0.001
max electron density/e \AA^{-3}	0.292
min electron density/e \AA^{-3}	−0.228

C-bound H: constr, O-bound H: refall.

Flack-Test meaningless, no anomalous scatterer, correct structure derived from synthesis.

Number	Label	Charge	SybylType	Xfrac + ESD	Yfrac + ESD	Zfrac + ESD	Symm. op.
1	O1	0	O.3	0.089191	0.48513	0.46373	x,y,z
2	H1	0	H	0.041149	0.430505	0.451609	x,y,z
3	C1	0	C.3	0.349227	0.479957	0.492006	x,y,z
4	H1A	0	H	0.42062	0.544252	0.496557	x,y,z
5	H1B	0	H	0.45943	0.445551	0.455195	x,y,z
6	O2	0	O.3	0.26903	0.336512	0.555806	x,y,z
7	C2	0	C.3	0.368374	0.431805	0.568251	x,y,z
8	H2	0	H	0.249399	0.464605	0.604612	x,y,z
9	O3	0	O.2	0.292369	0.184136	0.56116	x,y,z
10	C3	0	C.3	0.648687	0.432884	0.600363	x,y,z
11	H3	0	H	0.7682	0.411739	0.558885	x,y,z
12	O4	0	O.3	0.890732	0.709346	0.627405	x,y,z

13	C4	0	C.2	0.73026	0.531068	0.621172	x,y,z
14	H4	0	H	0.754451	0.572573	0.579752	x,y,z
15	O5	0	O.2	0.968741	0.698573	0.751116	x,y,z
16	C5	0	C.2	0.773473	0.568235	0.689233	x,y,z
17	C6	0	C.3	0.738136	0.523246	0.766207	x,y,z
18	H6A	0	H	0.902798	0.490361	0.779608	x,y,z
19	H6B	0	H	0.711216	0.573578	0.803952	x,y,z
20	C8	0	C.2	0.484303	0.381191	0.727867	x,y,z
21	H8	0	H	0.340291	0.340138	0.736081	x,y,z
22	C7	0	C.2	0.514108	0.454541	0.7727	x,y,z
23	H7	0	H	0.387228	0.464581	0.811216	x,y,z
24	C11	0	C.2	0.387549	0.25855	0.579938	x,y,z
25	C12	0	C.2	0.889395	0.664587	0.693694	x,y,z
26	C10	0	C.3	0.629035	0.264638	0.628587	x,y,z
27	H10A	0	H	0.784246	0.248763	0.597442	x,y,z
28	H10B	0	H	0.615871	0.217322	0.669356	x,y,z
29	C9	0	C.3	0.67165	0.360771	0.66421	x,y,z
30	H9	0	H	0.854522	0.363249	0.684644	x,y,z
31	C13	0	C.3	101.442	0.80103	0.623679	x,y,z
32	H13A	0	H	106.534	0.821629	0.675078	x,y,z
33	H13B	0	H	0.889373	0.847391	0.60277	x,y,z
34	C14	0	C.3	125.292	0.795443	0.574222	x,y,z
35	H14A	0	H	138.013	0.752075	0.596659	x,y,z
36	H14B	0	H	133.219	0.857781	0.569705	x,y,z
37	H14C	0	H	120.231	0.772821	0.523977	x,y,z

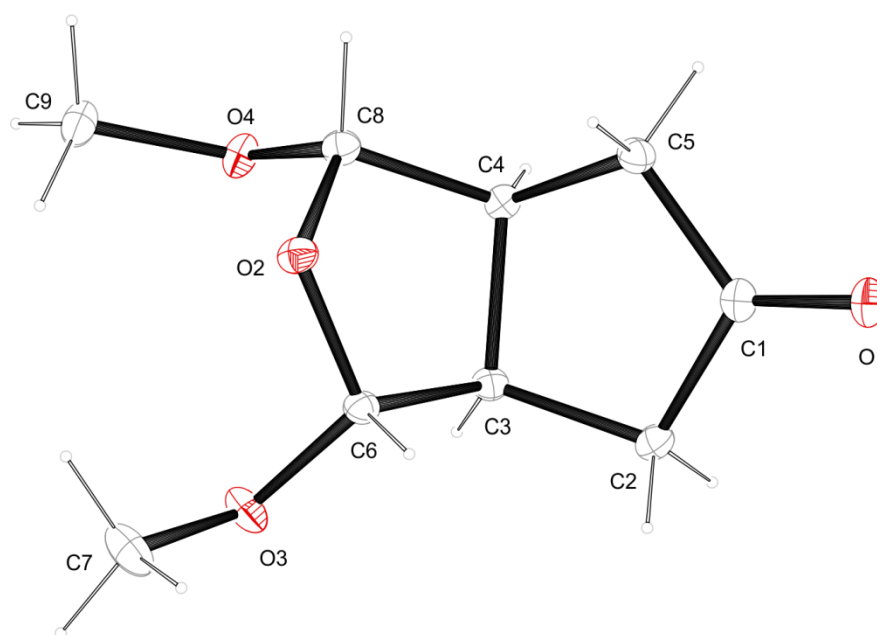
8.11 *rac*-(1*R*,3*S*,3*aS*,6*aR*)-1,3-dimethoxytetrahydro-1*H*-cyclopenta[*c*]furan-5(3*H*)-one (540)


Table 1.

1. Crystallographic data.

	1
net formula	C ₉ H ₁₄ O ₄
$M_r/\text{g mol}^{-1}$	186.20
crystal size/mm	0.150 × 0.050 × 0.030
T/K	100(2)
radiation	MoK α
diffractometer	'Bruker D8Venture'
crystal system	monoclinic
space group	'P 21/c'
$a/\text{\AA}$	9.0759(7)
$b/\text{\AA}$	11.1481(10)
$c/\text{\AA}$	9.3195(8)
$\alpha/^\circ$	90
$\beta/^\circ$	104.767(2)
$\gamma/^\circ$	90
$V/\text{\AA}^3$	911.79(13)
Z	4
calc. density/g cm ⁻³	1.356
μ/mm^{-1}	0.106
absorption correction	multi-scan

transmission factor range	0.8913–0.9585
refls. measured	10487
R_{int}	0.0515
mean $\sigma(I)/I$	0.0398
θ range	2.954–26.43
observed refls.	1377
x, y (weighting scheme)	0.0340, 0.5210
hydrogen refinement	constr
refls in refinement	1861
parameters	120
restraints	0
$R(F_{\text{obs}})$	0.0408
$R_w(F^2)$	0.0930
S	1.033
shift/error _{max}	0.001
max electron density/e \AA^{-3}	0.258
min electron density/e \AA^{-3}	−0.220

Number	Label	Charge	SybylType	Xfrac + ESD	Yfrac + ESD	Zfrac + ESD	Symm. op.
1	C1	0	C.2	0.391194	0.619451	0.015702	x,y,z
2	C2	0	C.3	0.237896	0.557186	−0.018629	x,y,z
3	H2A	0	H	0.244916	0.476559	−0.060919	x,y,z
4	H2B	0	H	0.160765	0.60459	−0.090628	x,y,z
5	C3	0	C.3	0.195085	0.547402	0.129707	x,y,z
6	H3	0	H	0.0839	0.563339	0.115811	x,y,z
7	C4	0	C.3	0.291527	0.643123	0.232738	x,y,z
8	H4	0	H	0.234717	0.720371	0.229269	x,y,z
9	C5	0	C.3	0.434001	0.658432	0.176245	x,y,z
10	H5A	0	H	0.467405	0.743254	0.184628	x,y,z
11	H5B	0	H	0.51804	0.608181	0.234631	x,y,z
12	C6	0	C.3	0.240603	0.429861	0.21411	x,y,z
13	H6	0	H	0.297706	0.378191	0.158988	x,y,z
14	C7	0	C.3	0.140132	0.253997	0.292276	x,y,z
15	H7A	0	H	0.044137	0.211425	0.28555	x,y,z
16	H7B	0	H	0.195618	0.262429	0.396746	x,y,z

17	H7C	0	H	0.202289	0.208468	0.2394	x,y,z
18	C8	0	C.3	0.320538	0.584485	0.383823	x,y,z
19	H8	0	H	0.415697	0.61685	0.451992	x,y,z
20	C9	0	C.3	0.198722	0.546854	0.575325	x,y,z
21	H9A	0	H	0.111722	0.571242	0.612845	x,y,z
22	H9B	0	H	0.29372	0.566833	0.648741	x,y,z
23	H9C	0	H	0.194363	0.460152	0.557386	x,y,z
24	O1	0	O.2	0.467222	0.635591	-0.072093	x,y,z
25	O2	0	O.3	0.337087	0.460277	0.355995	x,y,z
26	O3	0	O.3	0.108541	0.370262	0.226798	x,y,z
27	O4	0	O.3	0.193417	0.608557	0.439787	x,y,z

8.12 *rac*-(1*S*,3*R*,3*aS*,4*S*,7*aS*)-4-(hydroxymethyl)-1,3-dimethoxytetrahydro-3*H*-furo[3,4-*c*]pyran-6(1*H*)-one (478)

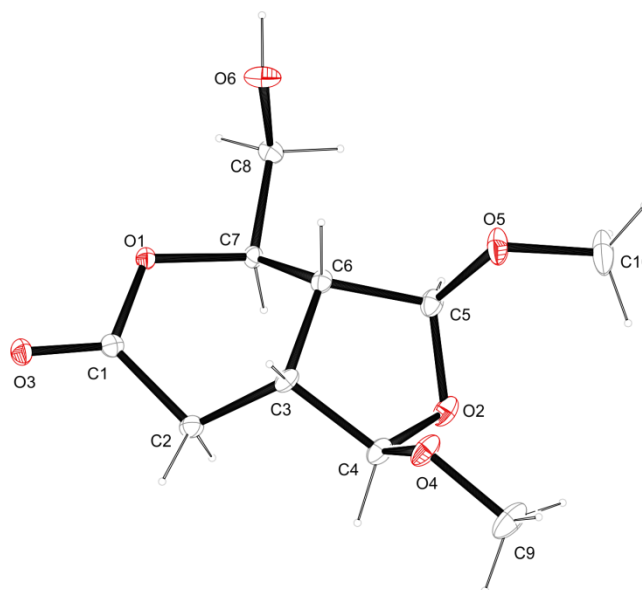


Table 1.

1. Crystallographic data.

	1
net formula	$\text{C}_{10}\text{H}_{16}\text{O}_6$
$M_r/\text{g mol}^{-1}$	232.23
crystal size/mm	$0.140 \times 0.030 \times 0.020$
T/K	100(2)
radiation	$\text{MoK}\alpha$
diffractometer	'Bruker D8Venture'
crystal system	orthorhombic
space group	'P b c n'
$a/\text{\AA}$	29.0686(13)
$b/\text{\AA}$	5.3102(3)
$c/\text{\AA}$	14.1305(7)
$\alpha/^\circ$	90
$\beta/^\circ$	90
$\gamma/^\circ$	90
$V/\text{\AA}^3$	2181.19(19)
Z	8
calc. density/ g cm^{-3}	1.414
μ/mm^{-1}	0.117
absorption correction	multi-scan

transmission factor range	0.8915–0.9580
refls. measured	19646
R_{int}	0.0393
mean $\sigma(I)/I$	0.0240
θ range	2.967–25.38
observed refls.	1595
x, y (weighting scheme)	0.0282, 1.7957
hydrogen refinement	mixed
refls in refinement	1993
parameters	151
restraints	0
$R(F_{\text{obs}})$	0.0374
$R_w(F^2)$	0.0857
S	1.057
shift/error _{max}	0.001
max electron density/e \AA^{-3}	0.212
min electron density/e \AA^{-3}	−0.221

C-H: constr, O-H: refall.

Number	Label	Charge	SybylType	Xfrac + ESD	Yfrac + ESD	Zfrac + ESD	Symm. op.
1	O1	0	O.3	0.291031	0.629851	0.535441	x,y,z
2	O2	0	O.3	0.389321	125.052	0.500355	x,y,z
3	O3	0	O.2	0.283118	0.413807	0.404626	x,y,z
4	O4	0	O.3	0.447071	100.356	0.430511	x,y,z
5	O5	0	O.3	0.417579	110.074	0.646658	x,y,z
6	O6	0	O.3	0.31671	0.654483	0.726642	x,y,z
7	H6	0	H	0.303798	0.635549	0.783756	x,y,z
8	C1	0	C.2	0.299897	0.595213	0.443793	x,y,z
9	C2	0	C.3	0.330878	0.785453	0.398566	x,y,z
10	H2A	0	H	0.314115	0.946359	0.390625	x,y,z
11	H2B	0	H	0.340244	0.725381	0.335102	x,y,z
12	C3	0	C.3	0.373818	0.8287	0.459776	x,y,z
13	H3	0	H	0.394513	0.678765	0.455184	x,y,z
14	C4	0	C.3	0.400289	106.445	0.431349	x,y,z

15	H4	0	H	0.390342	1.122	0.367149	x,y,z
16	C5	0	C.3	0.379	113.364	0.588293	x,y,z
17	H5	0	H	0.354966	123.297	0.622508	x,y,z
18	C6	0	C.3	0.360415	0.8723	0.56419	x,y,z
19	H6A	0	H	0.375674	0.74321	0.605051	x,y,z
20	C7	0	C.3	0.308627	0.860942	0.578173	x,y,z
21	H7	0	H	0.294114	100.924	0.546379	x,y,z
22	C8	0	C.3	0.293834	0.854242	0.680045	x,y,z
23	H8A	0	H	0.301481	101.608	0.711066	x,y,z
24	H8B	0	H	0.260134	0.829365	0.683924	x,y,z
25	C9	0	C.3	0.475373	120.556	0.397675	x,y,z
26	H9A	0	H	0.466449	125.051	0.332964	x,y,z
27	H9B	0	H	0.507675	115.277	0.398423	x,y,z
28	H9C	0	H	0.4714	135.192	0.439126	x,y,z
29	C10	0	C.3	0.435513	13.334	0.681564	x,y,z
30	H10A	0	H	0.448174	143.129	0.628855	x,y,z
31	H10B	0	H	0.459866	12.992	0.727769	x,y,z
32	H10C	0	H	0.410799	142.928	0.712008	x,y,z

9. REFERENCES

- [1] R. Hoffmann, R. B. Woodward, *J. Am. Chem. Soc.* **1965**, *87*, 2046–2048.
- [2] R. B. Woodward, R. Hoffmann, *J. Am. Chem. Soc.* **1965**, *87*, 395–397.
- [3] R. B. Woodward, R. Hoffmann, *J. Am. Chem. Soc.* **1965**, *87*, 2511–2513.
- [4] A. J. Humphrey, D. O'Hagan, *Nat. Prod. Rep.* **2001**, *18*, 494–502.
- [5] A. Baeyer, A. Emmerling, *Ber. dtsch. chem. Ges.* **1870**, *3*, 514–517.
- [6] A. Ladenburg, *Ber. dtsch. chem. Ges.* **1886**, *19*, 439–441.
- [7] R. Willstätter, W. Müller, *Ber. dtsch. chem. Ges.* **1898**, *31*, 2655–2669.
- [8] R. Willstätter, A. Bode, *Liebigs Ann. Chem.* **1903**, *326*, 42–78.
- [9] P. Rabe, K. Kindler, *Ber. dtsch. chem. Ges.* **1918**, *51*, 466–467.
- [10] R. B. Woodward, W. E. Doering, *J. Am. Chem. Soc.* **1944**, *66*, 849.
- [11] R. B. Woodward, W. E. Doering, *J. Am. Chem. Soc.* **1945**, *67*, 860–874.
- [12] R. B. Woodward, *Pure Appl. Chem.* **1973**, *33*, 145–177.
- [13] R. W. Armstrong, J.-M. Beau, S. H. Cheon, W. J. Christ, H. Fujioka, W.-H. Ham, L. D. Hawkins, H. Jin, S. H. Kang, Y. Kishi, M. J. Martinelli, W. W. McWhorter, M. Mizuno, M. Nakata, A. E. Stutz, F. X. Talamas, M. Taniguchi, J. A. Tino, K. Ueda, J. Uenishi, J. B. White, M. Yonaga, *J. Am. Chem. Soc.* **1989**, *111*, 7530–7533.
- [14] E. M. Suh, Y. Kishi, *J. Am. Chem. Soc.* **1994**, *116*, 11205–11206.
- [15] E. J. Corey, J. A. Katzenellenbogen, N. W. Gilman, S. A. Roman, B. W. Erickson, *J. Am. Chem. Soc.* **1968**, *90*, 5618–5620.
- [16] Y. Kishi, T. Fukuyama, M. Aratani, F. Nakatsubo, T. Goto, S. Inoue, H. Tanino, S. Sugiura, H. Kakoi, *J. Am. Chem. Soc.* **1972**, *94*, 9219–9221.
- [17] R. B. Woodward, E. Logusch, K. P. Nambiar, K. Sakan, D. E. Ward, B.-W. Au-Yeung, P. Balaram, L. J. Browne, P. J. Card, C. H. Chen, R. B. Chênevert, A. Fliri, K. Frobel, H.-J. Gais, G. Garratt, K. Hayakawa, W. Heggie, D. P. Hesson, D. Hoppe, I. Hoppe, J. A. Hyatt, D. Ikeda, P. A. Jacobi, K. S. Kim, Y. Kobuke, K. Kojima, K. Krowicki, V. J. Lee, T. Leutert, S. Malchenko, J. Martens, R. S. Matthews, B. S. Ong, J. B. Press, T. V. Rajan Babu, G. Rousseau, M. Sauter, M. Suzuki, K. Tatsuta, L. M. Tolbert, A. Truesdale, I. Uchida, Y. Ueda, T. Uyehara, A. T. Vasella, W. C. Vladuchick, A. Wade, R. M. Williams, H. N.-C. Wong, *J. Am. Chem. Soc.* **1981**, *103*, 3215–3217.
- [18] B. M. Trost, *Science* **1991**, *254*, 1471–1477.
- [19] B. M. Trost, N. Cramer, H. Bernsmann, *J. Am. Chem. Soc.* **2007**, *129*, 3086–3087.
- [20] M. Reiter, S. Torssell, S. Lee, D. W. C. MacMillan, *Chem. Sci.* **2010**, *1*, 37–42.
- [21] N. S. Rajapaksa, M. A. McGowan, M. Rienzo, E. N. Jacobsen, *Org. Lett.* **2013**, *15*, 706–709.
- [22] M. G. Charest, C. D. Lerner, J. D. Brubaker, D. R. Siegel, A. G. Myers, *Science* **2005**, *308*, 395–398.
- [23] M. J. Yu, W. Zheng, B. M. Seletsky, *Nat. Prod. Rep.* **2013**, *30*, 1158–1164.
- [24] K. C. Nicolaou, S. A. Snyder, *Angew. Chem. Int. Ed.* **2005**, *44*, 1012–1044.
- [25] C. L. Chandler, B. List, *J. Am. Chem. Soc.* **2008**, *130*, 6737–6739.
- [26] J. M. Holland, M. Lewis, A. Nelson, *Angew. Chem. Int. Ed.* **2001**, *40*, 4082–4084.
- [27] J. A. Enquist, Jr., B. M. Stoltz, *Nature* **2008**, *453*, 1228–1231.
- [28] O. L. Chapman, M. R. Engel, J. P. Springer, J. C. Clardy, *J. Am. Chem. Soc.* **1971**, *93*, 6696–6698.
- [29] Z. Xiong, E. J. Corey, *J. Am. Chem. Soc.* **2000**, *122*, 9328–9329.
- [30] M. Ichikawa, M. Takahashi, S. Aoyagi, C. Kibayashi, *J. Am. Chem. Soc.* **2004**, *126*, 16553–16558.
- [31] M. C. de la Torre, M. A. Sierra, *Angew. Chem. Int. Ed.* **2004**, *43*, 160–181.
- [32] R. Robinson, *J. Chem. Soc. Trans.* **1917**, *111*, 762–768.
- [33] W. S. Johnson, M. B. Gravestock, B. E. McCarry, *J. Am. Chem. Soc.* **1971**, *93*, 4332–4334.
- [34] C. H. Heathcock, *Proc. Natl. Acad. Sci. U. S. A.* **1996**, *93*, 14323–7.
- [35] D. A. Vosburg, C. D. Vanderwal, E. J. Sorensen, *J. Am. Chem. Soc.* **2002**, *124*, 4552–4553.
- [36] A. Eschenmoser, *Angew. Chem. Int. Ed.* **1988**, *27*, 5–39.
- [37] C. F. Bender, F. K. Yoshimoto, C. L. Paradise, J. K. De Brabander, *J. Am. Chem. Soc.* **2009**, *131*, 11350–11352.
- [38] K. C. Nicolaou, D. J. Edmonds, P. G. Bulger, *Angew. Chem. Int. Ed.* **2006**, *45*, 7134–7186.
- [39] A. S. Lee, B. B. Liau, M. D. Shair, *J. Am. Chem. Soc.* **2014**, *136*, 13442–13452.
- [40] M. Müller, B. Kusebauch, G. Liang, C. M. Beaudry, D. Trauner, C. Hertweck, *Angew. Chem. Int. Ed.* **2006**, *45*, 7835–7838.
- [41] E. J. Sorensen, *Bioorg. Med. Chem.* **2003**, *11*, 3225–3228.
- [42] C. M. Beaudry, J. P. Malerich, D. Trauner, *Chem. Rev.* **2005**, *105*, 4757–4778.
- [43] A. Skiredj, M. A. Benididir, D. Joseph, K. Leblanc, G. Bernadat, L. Evanno, E. Poupon, *Angew. Chem. Int. Ed.* **2014**, *53*, 6419–6424.

- [44] Y. Ding, J. R. de Wet, J. Cavalcoli, S. Li, T. J. Greshock, K. A. Miller, J. M. Finefield, J. D. Sunderhaus, T. J. McAfoos, S. Tsukamoto, R. M. Williams, D. H. Sherman, *J. Am. Chem. Soc.* **2010**, *132*, 12733–12740.
- [45] A. Hager, D. Mazunin, P. Mayer, D. Trauner, *Org. Lett.* **2011**, *13*, 1386–1389.
- [46] J. Sperry, J. J. P. Seijberg, F. M. Stiemke, M. A. Brimble, *Org. Biomol. Chem.* **2009**, *7*, 2599–2603.
- [47] W. M. Bandaranayake, J. E. Banfield, D. S. C. Black, *J. Chem. Soc. Chem. Commun.* **1980**, 902–903.
- [48] K. C. Nicolaou, N. A. Petasis, R. E. Zipkin, J. Uenishi, *J. Am. Chem. Soc.* **1982**, *104*, 5555–5557.
- [49] K. C. Nicolaou, N. A. Petasis, J. Uenishi, R. E. Zipkin, *J. Am. Chem. Soc.* **1982**, *104*, 5557–5558.
- [50] K. C. Nicolaou, R. E. Zipkin, N. A. Petasis, *J. Am. Chem. Soc.* **1982**, *104*, 5558–5560.
- [51] K. C. Nicolaou, N. A. Petasis, R. E. Zipkin, *J. Am. Chem. Soc.* **1982**, *104*, 5560–5562.
- [52] L. Pouységu, D. Deffieux, S. Quideau, *Tetrahedron* **2010**, *66*, 2235–2261.
- [53] S. P. Roche, J. A. Porco, Jr., *Angew. Chem. Int. Ed.* **2011**, *50*, 4068–4093.
- [54] L. N. Mander, *Synlett* **1991**, 134–144.
- [55] A. R. Pape, K. P. Kaliappan, E. P. Kündig, *Chem. Rev.* **2000**, *100*, 2917–2940.
- [56] Q. Ding, Y. Ye, R. Fan, *Synthesis* **2013**, 1–16.
- [57] M. Tissot, R. J. Phipps, C. Lucas, R. M. Leon, R. D. M. Pace, T. Ngouansavanh, M. J. Gaunt, *Angew. Chem.* **2014**, *53*, 13498–13501.
- [58] D. H. R. Barton, G. W. Kirby, W. Steglich, G. M. Thomas, *Proc. Chem. Soc.* **1963**, 203–204.
- [59] M. A. Schwartz, I. S. Mami, *J. Am. Chem. Soc.* **1975**, *97*, 1239–1240.
- [60] P. Magnus, N. Sane, B. P. Fauber, V. Lynch, *J. Am. Chem. Soc.* **2009**, *131*, 16045–16047.
- [61] D. F. Taber, T. D. Neubert, A. L. Rheingold, *J. Am. Chem. Soc.* **2002**, *124*, 12416–12417.
- [62] P. N. Carlsen, T. J. Mann, A. H. Hoveyda, A. J. Frontier, *Angew. Chem. Int. Ed.* **2014**, *53*, 9334–9338.
- [63] M. O. Ratnikov, L. E. Farkas, E. C. McLaughlin, G. Chiou, H. Choi, S. H. El-Khalafy, M. P. Doyle, *J. Org. Chem.* **2011**, *76*, 2585–2593.
- [64] E. M. Simmons, A. R. Hardin, X. Guo, R. Sarpong, *Angew. Chem. Int. Ed.* **2008**, *47*, 6650–6653.
- [65] L. Liu, Y. Gao, C. Che, N. Wu, D. Z. Wang, C.-C. Li, Z. Yang, *Chem. Commun.* **2009**, 662–664.
- [66] J. L. Frie, C. S. Jeffrey, E. J. Sorensen, *Org. Lett.* **2009**, *11*, 5394–5397.
- [67] A. N. Flyer, C. Si, A. G. Myers, *Nat. Chem.* **2010**, *2*, 886–892.
- [68] K. C. Nicolaou, D. J. Edmonds, A. Li, G. S. Tria, *Angew. Chem. Int. Ed.* **2007**, *46*, 3942–3945.
- [69] W. Steglich, H.-T. Huppertz, B. Steffan, *Angew. Chem. Int. Ed.* **1985**, *97*, 716–717.
- [70] J. Gagnepain, F. Castet, S. Quideau, *Angew. Chem. Int. Ed.* **2007**, *46*, 1533–1535.
- [71] T. Suzuki, A. Sasaki, N. Egashira, S. Kobayashi, *Angew. Chem. Int. Ed.* **2011**, *50*, 9177–9179.
- [72] Y. Nishiyama, Y. Han-ya, S. Yokoshima, T. Fukuyama, *J. Am. Chem. Soc.* **2014**, *136*, 6598–6601.
- [73] V. Varghese, T. Hudlicky, *Angew. Chem. Int. Ed.* **2014**, *53*, 4355–4358.
- [74] S. A. Snyder, F. Kontes, *J. Am. Chem. Soc.* **2009**, *131*, 1745–1752.
- [75] R. A. Bélanger, D. Berney, H. Borschber, R. Brousseau, A. Doutheau, J. Durand, H. Katayama, R. Lapalme, D. Leturc, C. Liao, F. MacLachlan, R. Saintonge, J. Maffrand, F. Marazza, R. Martino, C. Moreau, L. Saint-Laurent, P. Soucy, L. Ruest, P. Deslongchamps, *Can. J. Chem.* **1979**, *57*, 3348–3354.
- [76] K. C. Nicolaou, J. Wang, Y. Tang, L. Botta, *J. Am. Chem. Soc.* **2010**, *132*, 11350–11363.
- [77] X. Bao, Y.-X. Cao, W.-D. Chu, H. Qu, J.-Y. Du, X.-H. Zhao, X.-Y. Ma, C.-T. Wang, C.-A. Fan, *Angew. Chem. Int. Ed.* **2013**, *52*, 14167–14172.
- [78] J.-P. Lumb, K. C. Choong, D. Trauner, *J. Am. Chem. Soc.* **2008**, *130*, 9230–9231.
- [79] R. H. Thomson, *Naturally Occurring Quinones IV. Recent Advances*, Springer, London, **1997**.
- [80] C. C. Nawrat, C. J. Moody, *Angew. Chem. Int. Ed.* **2014**, *53*, 2056–2077.
- [81] K. C. Nicolaou, Y. H. Lim, C. D. Papageorgiou, J. L. Piper, *Angew. Chem. Int. Ed.* **2005**, *44*, 7917–7921.
- [82] C. Li, R. P. Johnson, J. A. Porco, *J. Am. Chem. Soc.* **2003**, *125*, 5095–5106.
- [83] R. Meier, S. Strych, D. Trauner, *Org. Lett.* **2014**, *16*, 2634–2637.
- [84] H. P. Pepper, J. H. George, *Angew. Chem. Int. Ed.* **2013**, *52*, 12170–12173.
- [85] I. P. Singh, J. Sidana, S. B. Bharate, W. J. Foley, *Nat. Prod. Rep.* **2010**, *27*, 393–416.
- [86] M. Lohrie, W. Knoche, *J. Am. Chem. Soc.* **1993**, *115*, 919–924.
- [87] P. Lu, Z. Gu, A. Zakarian, *J. Am. Chem. Soc.* **2013**, *135*, 14552–14555.
- [88] P. Lu, A. Mailyan, Z. Gu, D. M. Guptill, H. Wang, H. M. L. Davies, A. Zakarian, *J. Am. Chem. Soc.* **2014**, *136*, 17738–17749.
- [89] K. C. Nicolaou, K. B. Simonsen, G. Vassilikogiannakis, P. S. Baran, V. P. Vidali, E. N. Pitsinos, E. A. Couladouros, *Angew. Chem. Int. Ed.* **1999**, *38*, 3555–3559.
- [90] I. Uchida, T. Ando, N. Fukami, K. Yoshida, M. Hashimoto, T. Tada, S. Koda, Y. Morimoto, *J. Org. Chem.* **1987**, *52*, 5292–5293.
- [91] T. J. Maimone, J. Shi, S. Ashida, P. S. Baran, *J. Am. Chem. Soc.* **2009**, *131*, 17066–17067.
- [92] Q. Yang, J. T. Njardarson, C. Draghici, F. Li, *Angew. Chem. Int. Ed.* **2013**, *52*, 8648–8651.
- [93] F. Li, S. S. Tartakoff, S. L. Castle, *J. Am. Chem. Soc.* **2009**, *131*, 6674–6675.
- [94] M. Nakamura, A. Hirai, M. Sogi, E. Nakamura, *J. Am. Chem. Soc.* **1998**, *120*, 5846–5847.

- [95] A. Girard, *Ber. dtsh. chem. Ges.* **1869**, 2, 554–563.
- [96] A. G. Perkin, A. B. Steven, *J. Chem. Soc. Trans.* **1903**, 192–201.
- [97] H. F. Dean, M. Nierenstein, *Ber. dtsh. chem. Ges.* **1913**, 46, 3868–3879.
- [98] R. Willstätter, H. Heiss, *Liebigs Ann.* **1923**, 433, 17–33.
- [99] J. A. Barltrop, J. S. Nicholson, *J. Chem. Soc.* **1948**, 116–120.
- [100] M. J. S. Dewar, *Nature* **1945**, 155, 50–51.
- [101] M. J. S. Dewar, *Nature* **1945**, 155, 141–142.
- [102] R. D. Haworth, B. P. Moore, P. L. Pauson, *J. Chem. Soc.* **1948**, 1045–1051.
- [103] R. D. Haworth, B. P. Moore, P. L. Pauson, *J. Chem. Soc.* **1949**, 3271–3278.
- [104] D. Caunt, W. D. Crow, R. D. Haworth, C. A. Vodoz, *J. Chem. Soc.* **1950**, 1631–1635.
- [105] J. D. Dunitz, *Nature* **1952**, 169, 1087–1088.
- [106] A. Critchlow, R. D. Haworth, P. L. Pauson, *J. Chem. Soc.* **1951**, 1318–1325.
- [107] J.-C. Salfeld, *Angew. Chem.* **1957**, 69, 723–724.
- [108] L. Horner, W. Dürckheimer, *Z. Naturforsch. B* **1959**, 14, 744–746.
- [109] L. Horner, K. H. Weber, W. Dürckheimer, *Chem. Ber.* **1961**, 64, 2881–2887.
- [110] J.-C. Salfeld, E. Baume, *Chem. Ber.* **1964**, 97, 307–311.
- [111] W. Dürckheimer, E. F. Paulus, *Angew. Chem. Int. Ed.* **1985**, 24, 224–225.
- [112] E. Yanase, K. Sawaki, S. Nakatsuka, *Synlett* **2005**, 2661–2663.
- [113] Y. Matsuo, T. Tanaka, I. Kouno, *Tetrahedron Lett.* **2009**, 50, 1348–1351.
- [114] T.-W. Wu, L.-H. Zeng, J. Wu, K.-P. Fung, R. D. Weisel, A. Hempel, N. Camerman, *Biochem. Pharm.* **1996**, 52, 1073–1080.
- [115] R. Bentley, *Nat. Prod. Rep.* **2008**, 25, 118–138.
- [116] P. L. Pauson, *Chem. Rev.* **1955**.
- [117] Y. Takino, A. Ferreti, V. Flanagan, M. Gianturco, M. Vogel, *Tetrahedron Lett.* **1965**, 6, 4019–4025.
- [118] Y. Matsuo, Y. Yamada, T. Tanaka, I. Kouno, *Phytochemistry* **2008**, 69, 3054–3061.
- [119] Y. Kawabe, Y. Aihara, Y. Hirose, A. Sakurada, A. Yoshida, M. Inai, T. Asakawa, Y. Hamashima, T. Kan, *Synlett* **2013**, 479–482.
- [120] D. Klostermeyer, L. Knops, T. Sindlinger, K. Polborn, W. Steglich, *Eur. J. Org. Chem.* **2000**, 603–609.
- [121] L. Kerschensteiner, F. Löbermann, W. Steglich, D. Trauner, *Tetrahedron* **2011**, 67, 1536–1539.
- [122] H. Ren, S. Grady, D. Gamenara, H. Heinzen, P. Moyna, S. L. Croft, H. Kendrick, V. Yardley, G. Moyna, *Bioorg. Med. Chem. Lett.* **2001**, 11, 1851–1854.
- [123] H. Ren, S. Grady, M. Banghart, J. S. Moulthrop, H. Kendrick, V. Yardley, S. L. Croft, G. Moyna, *Eur. J. Med. Chem.* **2003**, 38, 949–957.
- [124] K. Cheng, X. Wang, S. Zhang, H. Yin, *Angew. Chem. Int. Ed.* **2012**, 51, 12246–12249.
- [125] T. Graening, H.-G. Schmalz, *Angew. Chem. Int. Ed.* **2004**, 43, 3230–3256.
- [126] A. G. Perkin, A. B. Steven, *J. Chem. Soc., Trans.* **1906**, 802–808.
- [127] L. Horner, W. Dürckheimer, *Z. Naturforsch. B* **1959**, 14, 742–743.
- [128] J.-C. Salfeld, *Chem. Ber.* **1960**, 93, 737–745.
- [129] H.-J. Teuber, P. Heinrich, M. Dietrich, *Liebigs Ann. Chem.* **1966**, 696, 64–71.
- [130] H.-J. Teuber, M. Dietrich, *Chem. Ber.* **1967**, 100, 2908–2917.
- [131] H.-J. Teuber, G. Steinmetz, *Chem. Ber.* **1965**, 98, 666–684.
- [132] J. Cecelsky, *Monatsh. für Chemie* **1899**, 20, 779–791.
- [133] H. Erdtman, G. Moussa, M. Nilsson, *Acta Chem. Scand.* **1969**, 23, 2515–2518.
- [134] J. A. Beisler, J. V. Silverton, A. Penttilä, D. H. S. Horn, H. M. Fales, *J. Am. Chem. Soc.* **1971**, 93, 4850–4855.
- [135] W. Flaig, T. Ploetz, H. Biergans, *Liebigs Ann.* **1955**, 597, 196–213.
- [136] A. Critchlow, E. Haslam, R. D. Haworth, P. B. Tinker, N. M. Waldron, *Tetrahedron* **1967**, 23, 2829–2847.
- [137] V. V. Tkachev, S. M. Aldoshin, G. V. Shilov, V. N. Komissarov, Y. A. Sayapin, M. S. Korobov, G. S. Borodkin, V. I. Minkin, *Russ. Chem. Bull. Int. Ed.* **2007**, 56, 276–280.
- [138] L. C. de Lima Fávaro, F. L. de Melo, C. I. Aguilar-Vildoso, W. L. Araújo, *PLoS One* **2011**, 6, e14828.
- [139] L. C. de Lima Fávaro, F. L. de Souza Sebastianes, W. L. Araújo, *PLoS One* **2012**, 7, e36826.
- [140] J.-M. Wang, G.-Z. Ding, L. Fang, J.-G. Dai, S.-S. Yu, Y.-H. Wang, X.-G. Chen, S.-G. Ma, J. Qu, S. Xu, D. Du, *J. Nat. Prod.* **2010**, 73, 1240–1249.
- [141] P. J. L. Bell, P. Karuso, *J. Am. Chem. Soc.* **2003**, 125, 9304–9305.
- [142] P. C. Bamford, G. L. F. Norris, G. Ward, *Trans. Br. Mycol. Soc.* **1961**, 44, 354–356.
- [143] G. Petterson, *Acta Chem. Scand.* **1965**, 19, 1724–1732.
- [144] Y. Ishikawa, T. Ito, K. H. Lee, *J. Jpn. Oil Chem. Soc.* **1996**, 45, 1321–1326.
- [145] N. H. Lee, J. B. Gloer, D. T. Wicklow, *Bull. Korean Chem. Soc.* **2007**, 28, 877–879.
- [146] A. Abdel-Lateff, K. M. Fisch, A. D. Wright, G. M. König, *Planta Med.* **2003**, 69, 831–834.
- [147] H. V. Kemami Wangun, K. Ishida, C. Hertweck, *Eur. J. Org. Chem.* **2008**, 3781–3784.
- [148] F. M. Talontsi, B. Dittrich, A. Schöffler, H. Sun, H. Laatsch, *Eur. J. Org. Chem.* **2013**, 3174–3180.

- [149] M. El Amrani, D. Lai, A. Debbab, A. H. Aly, K. Siems, C. Seidel, M. Schnekenburger, A. Gaigneaux, M. Diederich, D. Feger, W. Lin, P. Proksch, *J. Nat. Prod.* **2014**, 77, 49–56.
- [150] G. M. Brill, U. Premachandran, J. P. Karwowski, R. Henry, D. K. Cwik, L. M. Traphagen, P. E. Humphrey, M. Jackson, J. J. Clement, N. S. Burres, S. Kadam, R. H. Chen, J. B. McAlpine, *J. Antibiot. (Tokyo)* **1996**, 49, 124–128.
- [151] F. Rusnak, P. Mertz, *Physiol. Rev.* **2000**, 80, 1483–1521.
- [152] K. A. Jørgensen, P. B. Koefoed-Nielsen, N. Karamperis, *Scand. J. Immunol.* **2003**, 57, 93–98.
- [153] M. Sieber, R. Baumgrass, *Cell Commun. Signal.* **2009**, 7, 25–43.
- [154] M. Krauze-Baranowska, *Acta Pol. Pharm.* **2002**, 59, 403–410.
- [155] R. D. Hartley, W. H. Morrison III, F. Balza, G. H. N. Towers, *Phytochemistry* **1990**, 29, 3699–3703.
- [156] A. I. Hamed, I. Springuel, N. A. El-Emary, H. Mitome, Y. Yamada, *Phytochemistry* **1997**, 45, 1257–1261.
- [157] R. B. Filho, M. P. de Souza, M. E. O. Mattos, *Phytochemistry* **1981**, 20, 345–346.
- [158] W. R. Gutekunst, P. S. Baran, *J. Am. Chem. Soc.* **2011**, 133, 19076–19079.
- [159] F. D. da Silva Araújo, L. C. de Lima Fávoro, W. L. Araújo, F. L. de Oliveira, R. Aparicio, A. J. Marsaioli, *Eur. J. Org. Chem.* **2012**, 5225–5230.
- [160] M. K. Ilg, Master Thesis, *Toward the Biomimetic Total Synthesis of Epicolactone*, Ludwig Maximilian University of Munich, **2013**.
- [161] B. M. Trost, G. T. Rivers, J. M. Gold, *J. Org. Chem.* **1980**, 45, 1835–1838.
- [162] F. E. King, T. J. King, *J. Chem. Soc.* **1942**, 726–727.
- [163] H. N. Simpson, *J. Phys. Chem.* **1965**, 69, 1707–1710.
- [164] H. H. Eldaroti, S. A. Gadir, M. S. Refat, A. M. A. Adam, *J. Pharm. Anal.* **2014**, 4, 81–95.
- [165] D. A. Khobragade, S. G. Mahamulkar, L. Pospíšil, I. Cisařová, L. Rulíšek, U. Jahn, *Chem. Eur. J.* **2012**, 18, 12267–12277.
- [166] P. Garge, R. Chikate, S. Padhye, J. Savariault, P. de Loth, J.-P. Tuchagues, *Inorg. Chem.* **1990**, 29, 3315–3320.
- [167] J. M. Leal, B. Garcia, P. L. Domingo, *Coord. Chem. Rev.* **1998**, 173, 79–131.
- [168] R. Gao, Z. Yuan, Z. Zhao, X. Gao, *Bioelectrochem. Bioenerg.* **1998**, 45, 41–45.
- [169] B. S. Thyagarajan, *Chem. Rev.* **1958**, 58, 439–460.
- [170] A. I. Scott, *Quart. Rev. Chem. Soc.* **1965**, 1–35.
- [171] N. S. Burres, U. Premachandran, S. Hoselton, D. Cwik, J. E. Hochlowski, Q. Ye, G. N. Sunga, J. P. Karwowski, M. Jackson, D. N. Whittern, J. B. McAlpine, *J. Antibiot. (Tokyo)* **1995**, 48, 380–386.
- [172] J. B. Baell, G. A. Holloway, *J. Med. Chem.* **2010**, 53, 2719–2740.
- [173] H. Skvara, M. Dawid, E. Kleyn, B. Wolff, J. G. Meingassner, H. Knight, T. Dumortier, T. Kopp, N. Fallahi, G. Stary, C. Burkhart, O. Grenet, J. Wagner, Y. Hijazi, R. E. Morris, C. Mcgeown, C. Rordorf, C. E. M. Griffiths, G. Stingl, T. Jung, *J. Clin. Invest.* **2008**, 118, 3151–3159.
- [174] P. R. Wenner, F. Di Padova, P. A. Keown, *J. Immunol. Methods* **1997**, 201, 125–135.
- [175] A. M. Eliassen, R. P. Thedford, K. R. Claussen, C. Yuan, D. Siegel, *Org. Lett.* **2014**, 16, 3628–3631.
- [176] M. Makosza, K. Sienkiewicz, *J. Org. Chem.* **1998**, 63, 4199–4208.
- [177] R. S. Varma, K. P. Naicker, *Org. Lett.* **1999**, 1, 189–192.
- [178] J. Xu, X. Wang, C. Shao, D. Su, G. Cheng, Y. Hu, *Org. Lett.* **2010**, 12, 1964–1967.
- [179] J. D. Sunderhaus, H. Lam, G. B. Dudley, *Org. Lett.* **2003**, 5, 4571–4573.
- [180] K. W. Anderson, T. Ikawa, R. E. Tundel, S. L. Buchwald, *J. Am. Chem. Soc.* **2006**, 128, 10694–10695.
- [181] Y.-H. Zhang, J.-Q. Yu, *J. Am. Chem. Soc.* **2009**, 131, 14654–14655.
- [182] A. Axelrod, A. M. Eliassen, M. R. Chin, K. Zlotkowski, D. Siegel, *Angew. Chem. Int. Ed.* **2013**, 52, 3421–3424.
- [183] L. A. Paquette, M. R. Sivik, *Synth. Commun.* **1991**, 21, 467–479.
- [184] A. Pelter, R. I. H. Al-Bayati, M. T. Ayoub, W. Lewis, P. Pardasani, R. Hansel, *J. Chem. Soc., Perkin Trans. 1* **1987**, 717–742.
- [185] A. Pelter, R. Al-Bayati, W. Lewis, *Tetrahedron Lett.* **1982**, 23, 353–356.
- [186] J. Málek, *Organic Reactions: Reduction by Metal Alkoxyaluminum Hydrides. Part II. Carboxylic Acids and Derivatives, Nitrogen Compounds, and Sulfur Compounds*, John Wiley & Sons, Inc., Hoboken, NJ, USA, **1988**.
- [187] J. W. Patterson, *Tetrahedron* **1993**, 49, 4789–4798.
- [188] P. H. Nelson, S. F. Carr, B. H. Devens, E. M. Eugui, F. Franco, C. Gonzalez, R. C. Hawley, D. G. Loughhead, D. J. Milan, E. Papp, J. W. Patterson, S. Rouhafza, E. B. Sjogren, D. B. Smith, R. A. Stephenson, F. X. Talamas, A. M. Waltos, R. J. Weikert, J. C. Wu, *J. Med. Chem.* **1996**, 39, 4181–4196.
- [189] T. Okabayashi, A. Iida, K. Takai, Y. Nawate, T. Misaki, Y. Tanabe, *J. Org. Chem.* **2007**, 72, 8142–8145.
- [190] I. Iqbal, M. Imran, P. Langer, *Synthesis* **2009**, 2430–2434.
- [191] M. Watanabe, M. Tsukazaki, Y. Hamada, M. Iwao, S. Furukawa, *Chem. Pharm. Bull.* **1989**, 37, 2948–2951.
- [192] S. A. P. Quintiliano, L. F. Silva, Jr., *Tetrahedron Lett.* **2012**, 53, 3808–3810.

- [193] C. K. Lau, P. C. Bélanger, J. Scheigetz, C. Dufresne, H. W. R. Williams, A. L. Maycock, Y. Guindon, T. Bath, A. L. Dallob, D. Denis, A. W. Ford-Hutchinson, P. H. Gale, S. L. Hopple, L. G. Letts, S. Luell, C. S. McFarlane, E. MacIntyre, R. Meurer, D. K. Miller, H. Piechuta, D. Riendeau, J. Rokach, C. Rouzert, *J. Med. Chem.* **1989**, *32*, 1190–1197.
- [194] A. Yanagisawa, M. Taga, T. Atsumi, K. Nishimura, K. Ando, T. Taguchi, H. Tsumuki, I. Chujo, S. Mohri, *Org. Process Res. Dev.* **2011**, *15*, 376–381.
- [195] S. P. Cook, S. J. Danishefsky, *Org. Lett.* **2006**, *8*, 5693–5695.
- [196] W. K. Anderson, T. L. Boehm, G. M. Makara, R. T. Swann, *J. Med. Chem.* **1996**, *39*, 46–55.
- [197] M. Bielitz, J. Pietruszka, *Chem. Eur. J.* **2013**, *19*, 8300–8308.
- [198] T. M. Cresp, J. A. Elix, S. Kurokawa, M. V. Sargent, *Aust. J. Chem.* **1972**, *25*, 2167–2184.
- [199] M. Node, M. Ozeki, L. Planas, M. Nakano, H. Takita, D. Mori, S. Tamatani, T. Kajimoto, *J. Org. Chem.* **2010**, *75*, 190–196.
- [200] F. J. Fañanás, A. Mendoza, T. Arto, B. Temelli, F. Rodríguez, *Angew. Chem. Int. Ed.* **2012**, *51*, 4930–4933.
- [201] G. Solladié, N. Gehrold, J. Maignan, *Eur. J. Org. Chem.* **1999**, 2309–2314.
- [202] A. Ciogli, A. Dalla Cort, F. Gasparrini, L. Lunazzi, L. Mandolini, A. Mazzanti, C. Pasquini, M. Pierini, L. Schiaffino, F. Yafteh Mihan, *J. Org. Chem.* **2008**, *73*, 6108–6118.
- [203] Y. Xu, Y. Wei, *Synth. Commun.* **2010**, *40*, 3423–3429.
- [204] G. R. Lopes, D. C. G. A. Pinto, A. M. S. Silva, *R. Soc. Chem. Adv.* **2014**, *4*, 37244–37265.
- [205] S.-Y. Seo, V. K. Sharma, N. Sharma, *J. Agric. Food Chem.* **2003**, *51*, 2837–2853.
- [206] Y. Inokuma, S. Yoshioka, J. Ariyoshi, T. Arai, Y. Hitora, K. Takada, S. Matsunaga, K. Rissanen, M. Fujita, *Nature* **2013**, *495*, 461–466.
- [207] Y. Inokuma, S. Yoshioka, J. Ariyoshi, T. Arai, M. Fujita, *Nat. Protoc.* **2014**, *9*, 246–252.
- [208] O. Shiota, H. Morita, K. Takeya, H. Itokawa, *Tetrahedron* **1995**, *51*, 1107–1120.
- [209] A. G. González, N. L. Alvarenga, A. Estévez-Braun, A. G. Ravelo, I. L. Bazzocchi, L. Moujir, *Tetrahedron* **1996**, *52*, 9597–9608.
- [210] A. G. González, N. L. Alvarenga, I. L. Bazzocchi, A. G. Ravelo, L. Moujir, *J. Nat. Prod.* **1999**, *62*, 1185–1187.
- [211] N. E. Jacobsen, E. M. K. Wijeratne, J. Corsino, M. Furlan, V. D. S. Bolzani, A. A. L. Gunatilaka, *Bioorg. Med. Chem.* **2008**, *16*, 1884–1889.
- [212] Y. Aoyagi, Y. Takahashi, Y. Satake, H. Fukaya, K. Takeya, R. Aiyama, T. Matsuzaki, S. Hashimoto, T. Shiina, T. Kurihara, *Tetrahedron Lett.* **2005**, *46*, 7885–7887.
- [213] M. Node, S. Kodama, Y. Hamashima, T. Katoh, K. Nishide, T. Kajimoto, *Chem. Pharm. Bull.* **2006**, *54*, 1662–1679.
- [214] A. Nudelman, J. Herzig, H. E. Gottlieb, E. Keinan, J. Sterling, *Carbohydr. Res.* **1987**, *162*, 145–152.
- [215] P. A. Grieco, H. L. Sham, J. Inanaga, H. Kim, P. A. Tuthill, *J. Chem. Soc., Chem. Commun.* **1984**, 1345–1347.
- [216] T. Kawabata, P. A. Grieco, H.-L. Sham, H. Kim, J. Y. Jaw, S. Tu, *J. Org. Chem.* **1987**, *52*, 3346–3354.
- [217] D. Trauner, PhD Thesis, *Formal Total Synthesis of (–)-Morphine*, University of Vienna, **1997**.
- [218] L. M. Salonen, M. Ellermann, F. Diederich, *Angew. Chem. Int. Ed.* **2011**, *50*, 4808–4842.
- [219] J.-L. Brayer, D. Calvo, F. Ottello, *Monofunctionalization of Phenolic Hydroxy onto a Polyphenol*, **1993**, US5,198,571.
- [220] B. J. E. Baldwin, *J. Chem. Soc., Chem. Commun.* **1976**, 734–736.
- [221] G. Mehta, R. Vidya, *J. Org. Chem.* **2000**, *65*, 3497–3502.
- [222] L. A. Paquette, M. J. Wyvratt, O. Schallner, D. F. Schneider, W. J. Begley, R. M. Blankenship, *J. Am. Chem. Soc.* **1976**, *98*, 6744–6745.
- [223] L. A. Paquette, R. J. Ternansky, D. W. Balogh, G. Kentgen, *J. Am. Chem. Soc.* **1983**, *105*, 5446–5450.
- [224] T. Guney, G. A. Kraus, *Org. Lett.* **2013**, *15*, 613–615.
- [225] R. A. Keyzers, P. T. Northcote, M. T. Davies-Coleman, *Nat. Prod. Rep.* **2006**, *23*, 321–334.
- [226] L. Mayol, V. Piccialli, D. Sica, *Tetrahedron Lett.* **1985**, *26*, 1357–1360.
- [227] L. Mayol, V. Piccialli, D. Sica, *Tetrahedron Lett.* **1985**, *26*, 1253–1256.
- [228] L. Mayol, V. Piccialli, D. Sica, *J. Nat. Prod.* **1986**, *49*, 823–828.
- [229] L. Mayol, V. Piccialli, D. Sica, *Tetrahedron* **1986**, *42*, 5369–5376.
- [230] A. Rueda, A. Losada, R. Fernández, C. Cabañas, L. F. García-Fernández, F. Reyes, C. Cuevas, *Lett. Drug Des. Discov.* **2006**, *3*, 753–760.
- [231] M. E. Rateb, W. E. Houssen, M. Schumacher, W. T. A. Harrison, M. Diederich, R. Ebel, M. Jaspars, *J. Nat. Prod.* **2009**, *72*, 1471–1476.
- [232] M. Tischler, R. J. Andersen, M. I. Choudhary, J. Clardy, *J. Org. Chem.* **1991**, *56*, 42–47.
- [233] M. Leirós, J. A. Sánchez, E. Alonso, M. E. Rateb, W. E. Houssen, R. Ebel, M. Jaspars, A. Alfonso, L. M. Botana, *Mar. Drugs* **2014**, *12*, 700–718.
- [234] S. Gandhi, A. Y. Abramov, *Oxid. Med. Cell. Longev.* **2012**, 428010.

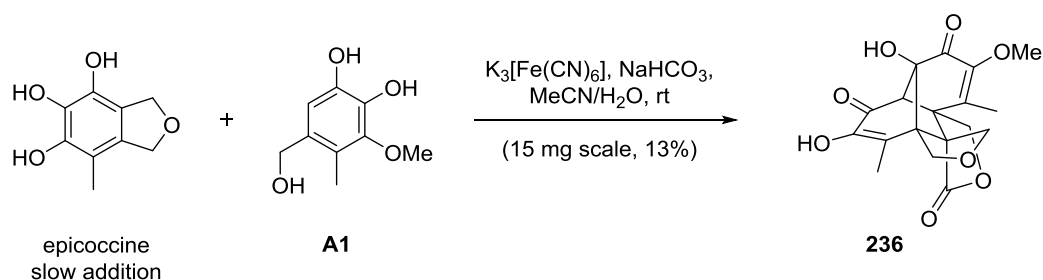
- [235] A. Melo, L. Monteiro, R. M. F. Lima, D. M. de Oliveira, M. D. de Cerqueira, R. S. El-Bachá, *Oxid. Med. Cell. Longev.* **2011**, 467180.
- [236] E. J. Corey, M. A. Letavic, *J. Am. Chem. Soc.* **1995**, *117*, 9616–9617.
- [237] E. J. Corey, M. A. Letavic, *J. Am. Chem. Soc.* **1995**, *117*, 12017.
- [238] E. J. Corey, *Angew. Chem. Int. Ed.* **2002**, *41*, 1650–1667.
- [239] N. L. Harvey, J. Krysiak, S. Chamni, S. W. Cho, S. a Sieber, D. Romo, *Chem. Eur. J.* **2015**, *21*, 1425–1428.
- [240] C. M. Rasik, M. K. Brown, *Angew. Chem. Int. Ed.* **2014**, *53*, 14522–14526.
- [241] B. M. Trost, M. L. Crawley, *J. Am. Chem. Soc.* **2002**, *124*, 9328–9329.
- [242] H. W. Sünemann, A. de Meijere, *Angew. Chem. Int. Ed.* **2004**, *43*, 895–897.
- [243] E. J. Corey, J. Streith, *J. Am. Chem. Soc.* **1964**, *86*, 950–951.
- [244] V. A. Bakulev, *Russ. Chem. Rev.* **1995**, *64*, 99–124.
- [245] S. Brandänge, H. Leijonmarck, *Chem. Commun.* **2004**, 292–293.
- [246] T.-Q. Yu, Y. Fu, L. Liu, Q.-X. Guo, *J. Org. Chem.* **2006**, *71*, 6157–6164.
- [247] H. Venkataraman, J. K. Cha, *J. Org. Chem.* **1989**, *54*, 2505–2506.
- [248] M. E. Jung, S.-J. Min, *Tetrahedron* **2007**, *63*, 3682–3701.
- [249] R. Hayashi, M. C. Walton, R. P. Hsung, J. H. Schwab, X. Yu, *Org. Lett.* **2010**, *12*, 5768–5771.
- [250] R. Hayashi, Z.-X. Ma, R. P. Hsung, *Org. Lett.* **2012**, *14*, 252–255.
- [251] L. M. Bishop, J. E. Barbarow, R. G. Bergman, D. Trauner, *Angew. Chem. Int. Ed.* **2008**, *47*, 8100–8103.
- [252] C. W. Spangler, S. Ibrahim, D. C. Bookbinder, S. Ahmad, *J. Chem. Soc., Perkin Trans. II* **1979**, 717–719.
- [253] P. Sharma, D. J. Ritson, J. Burnley, J. E. Moses, *Chem. Commun.* **2011**, 47, 10605–10607.
- [254] K. Prantz, J. Mulzer, *Chem. Eur. J.* **2010**, *16*, 485–506.
- [255] C. H. Sugisaki, Y. Ruland, M. Baltas, *Eur. J. Org. Chem.* **2003**, 672–688.
- [256] C. L. Benson, F. G. West, *Org. Lett.* **2007**, *9*, 2545–2548.
- [257] W. Boland, N. Schroer, C. Sieler, M. Feigel, *Helv. Chim. Acta* **1987**, *70*, 1025–1040.
- [258] H. M. L. Davies, J. R. Denton, *Chem. Soc. Rev.* **2009**, *38*, 3061–3071.
- [259] Y. Lian, L. C. Miller, S. Born, R. Sarpong, H. M. L. Davies, *J. Am. Chem. Soc.* **2010**, *132*, 12422–12425.
- [260] A. S. Kende, T. L. Smalley, H. Huang, N. York, R. V May, Y. Ye, *J. Am. Chem. Soc.* **1999**, *121*, 7431–7432.
- [261] K. M. Brummond, S. Mao, S. N. Shinde, P. J. Johnston, B. W. Day, *J. Comb. Chem.* **2009**, *11*, 486–494.
- [262] L. C. Miller, J. M. Ndungu, R. Sarpong, *Angew. Chem. Int. Ed.* **2009**, *48*, 2398–2402.
- [263] H. M. L. Davies, N. J. S. Hubby, *Tetrahedron Lett.* **1992**, *33*, 6935–6938.
- [264] H. M. L. Davies, G. Ahmed, M. R. Churchill, *J. Am. Chem. Soc.* **1996**, *118*, 10774–10782.
- [265] J. Xu, E. J. E. Caro-Diaz, E. A. Theodorakis, *Org. Lett.* **2010**, *12*, 3708–3711.
- [266] J. Xu, E. J. E. Caro-Diaz, A. Batova, S. D. E. Sullivan, E. A. Theodorakis, *Chem. Asian J.* **2012**, *7*, 1052–1060.
- [267] M. P. Doyle, D. C. Forbes, *Chem. Rev.* **1998**, *98*, 911–935.
- [268] H. M. L. Davies, J. R. Manning, *Nature* **2008**, *451*, 417–424.
- [269] D. Gillingham, N. Fei, *Chem. Soc. Rev.* **2013**, *42*, 4918–4931.
- [270] A. Padwa, S. F. Hornbuckle, *Chem. Rev.* **1991**, *91*, 263–309.
- [271] Q. Xiao, Y. Zhang, J. Wang, *Acc. Chem. Res.* **2013**, *46*, 236–247.
- [272] W. Kirmse, *Eur. J. Org. Chem.* **2002**, 2193–2256.
- [273] J. Podlech, D. Seebach, *Angew. Chem. Int. Ed.* **1995**, *34*, 471–472.
- [274] W. Li, J. Wang, X. Hu, K. Shen, W. Wang, Y. Chu, L. Lin, X. Liu, X. Feng, *J. Am. Chem. Soc.* **2010**, *132*, 8532–8533.
- [275] T. Ye, M. A. McKervey, *Chem. Rev.* **1994**, *94*, 1091–1160.
- [276] M. Guillaume, Z. Janousek, H. G. Viehe, *Synthesis* **1995**, 920–921.
- [277] Y. Wang, S. Zhu, *Org. Lett.* **2003**, *5*, 745–748.
- [278] J. Linder, T. P. Garner, H. E. L. Williams, M. S. Searle, C. J. Moody, *J. Am. Chem. Soc.* **2011**, *133*, 1044–1051.
- [279] N. Jiang, J. Wang, *Tetrahedron Lett.* **2002**, *43*, 1285–1287.
- [280] C. Peng, J. Cheng, J. Wang, *J. Am. Chem. Soc.* **2007**, *129*, 8708–8709.
- [281] M. Regitz, *Synthesis* **1972**, 351–373.
- [282] T. Horneff, S. Chuprakov, N. Chernyak, V. Gevorgyan, V. V Fokin, *J. Am. Chem. Soc.* **2008**, *130*, 14972–14974.
- [283] P. Yates, *J. Am. Chem. Soc.* **1952**, *74*, 5376–5381.
- [284] J. L. Maxwell, K. C. Brown, D. W. Bartley, T. Kodadek, *Science* **1992**, *256*, 1544–1547.
- [285] M. C. Pirrung, H. Liu, A. T. Morehead, Jr., *J. Am. Chem. Soc.* **2002**, *124*, 1014–1023.
- [286] Z. Qu, W. Shi, J. Wang, *J. Org. Chem.* **2001**, *66*, 8139–8144.
- [287] F. M. Wong, J. Wang, A. C. Hengge, W. Wu, *Org. Lett.* **2007**, *9*, 1663–1665.

- [288] H. M. L. Davies, P. R. Bruzinski, D. H. Lake, N. Kong, M. J. Fall, *J. Am. Chem. Soc.* **1996**, *118*, 6897–6907.
- [289] M. C. Pirrung, A. T. Morehead, *J. Am. Chem. Soc.* **1994**, *116*, 8991–9000.
- [290] K. P. Kornecki, J. F. Briones, V. Boyarskikh, F. Fullilove, J. Autschbach, K. E. Schrote, K. M. Lancaster, H. M. L. Davies, J. F. Berry, *Science* **2013**, *342*, 351–354.
- [291] H. M. L. Davies, D. G. Stafford, B. D. Doan, J. H. Houser, *J. Am. Chem. Soc.* **1998**, *120*, 3326–3331.
- [292] M. P. Doyle, *Chem. Rev.* **1986**, *86*, 919–939.
- [293] E. M. McGarrigle, D. G. Gilheany, *Chem. Rev.* **2005**, *105*, 1563–1602.
- [294] M. P. Doyle, *Recl. Trav. Chim. Pays-Bas* **1991**, *110*, 305–316.
- [295] J. Hansen, H. M. L. Davies, *Coord. Chem. Rev.* **2008**, *252*, 545–555.
- [296] R. P. Lutz, *Chem. Rev.* **1984**, *84*, 205–247.
- [297] S. Krüger, T. Gaich, *Beilstein J. Org. Chem.* **2014**, *10*, 163–193.
- [298] M. Kimura, A. Ezoe, M. Mori, Y. Tamaru, *J. Am. Chem. Soc.* **2005**, *127*, 201–209.
- [299] C. A. Miller, R. A. Batey, *Org. Lett.* **2004**, *6*, 699–702.
- [300] G. Vidari, A. Dapiaggi, G. Zanoni, L. Garlaschelli, *Tetrahedron Lett.* **1993**, *34*, 6485–6488.
- [301] D. Xu, G. A. Crispino, K. B. Sharpless, *J. Am. Chem. Soc.* **1992**, *114*, 7570–7571.
- [302] H. C. Kolb, M. S. VanNieuwenhze, K. B. Sharpless, *Chem. Rev.* **1994**, *94*, 2483–2547.
- [303] D. P. Provencal, C. Gardelli, J. A. Lafontaine, J. W. Leahy, *Tetrahedron Lett.* **1995**, *36*, 6033–6036.
- [304] S. J. Danishefsky, D. M. Armistead, F. E. Wincott, H. G. Selnick, R. Hungate, *J. Am. Chem. Soc.* **1987**, *109*, 8117–8119.
- [305] M. B. Andrus, S. D. Lepore, J. A. Sclafani, *Tetrahedron Lett.* **1997**, *38*, 4043–4046.
- [306] P. Wipf, Y. Kim, D. M. Goldstein, *J. Am. Chem. Soc.* **1995**, *117*, 11106–11112.
- [307] S. V. Ley, A. Armstrong, D. Díez-Martín, M. J. Ford, P. Grice, J. G. Knight, H. C. Kolb, A. Madin, C. A. Marby, S. Mukherjee, A. N. Shaw, A. M. Z. Slawin, S. Vile, A. D. White, D. J. Williams, M. Woods, *J. Chem. Soc., Perkin Trans. 1* **1991**, 667–692.
- [308] M. H. Junttila, O. O. E. Hormi, *J. Org. Chem.* **2009**, *74*, 3038–3047.
- [309] G. A. Crispino, K. S. Jeong, H. C. Kolb, Z. M. Wang, D. Xu, K. B. Sharpless, *J. Org. Chem.* **1993**, *58*, 3785–3786.
- [310] K. H. Jensen, M. S. Sigman, *Org. Biomol. Chem.* **2008**, *6*, 4083–4088.
- [311] Y. Li, D. Song, V. M. Dong, *J. Am. Chem. Soc.* **2008**, *130*, 2962–2964.
- [312] W. Zhong, S. Liu, J. Yang, X. Meng, Z. Li, *Org. Lett.* **2012**, *14*, 3336–3339.
- [313] J. R. Coombs, F. Haeffner, L. T. Kliman, J. P. Morken, *J. Am. Chem. Soc.* **2013**, *135*, 11222–11231.
- [314] S. Lee, S. Kim, *Org. Lett.* **2008**, *10*, 4255–4258.
- [315] J. L. Brewbaker, H. Hart, *J. Am. Chem. Soc.* **1969**, *91*, 711–715.
- [316] M. C. Bagley, K. E. Bashford, C. L. Hesketh, C. J. Moody, *J. Am. Chem. Soc.* **2000**, *122*, 3301–3313.
- [317] M. J. Niphakis, B. J. Turunen, G. I. Georg, *J. Org. Chem.* **2010**, *75*, 6793–6805.
- [318] M. J. Lilly, N. A. Miller, A. J. Edwards, A. C. Willis, P. Turner, M. N. Paddon-Row, M. S. Sherburn, *Chem. Eur. J.* **2005**, *11*, 2525–2536.
- [319] R. Varala, R. Enugala, S. Nuvula, S. R. Adapa, *Tetrahedron Lett.* **2006**, *47*, 877–880.
- [320] D. Yang, G. C. Micalizio, *J. Am. Chem. Soc.* **2012**, *134*, 15237–15240.
- [321] E. E. Wyatt, S. Fergus, W. R. J. D. Galloway, A. Bender, D. J. Fox, A. T. Plowright, A. S. Jessiman, M. Welch, D. R. Spring, *Chem. Commun.* **2006**, 3296–3298.
- [322] F. Sarabia, S. Chammaa, F. J. López Herrera, *Tetrahedron* **2001**, *57*, 10271–10279.
- [323] P. R. Krishna, Y. L. Prapurna, M. Alivelu, *Eur. J. Org. Chem.* **2011**, 5089–5095.
- [324] V. V. Pagar, A. M. Jadhav, R.-S. Liu, *J. Am. Chem. Soc.* **2011**, *133*, 20728–20731.
- [325] A. J. Ndakala, M. Hashemzadeh, R. C. So, A. R. Howell, *Org. Lett.* **2002**, *4*, 1719–1722.
- [326] A. Aponick, C.-Y. Li, J. A. Palmes, *Org. Lett.* **2009**, *11*, 121–124.
- [327] R. E. Moore, J. A. Pettus, J. Mistysyn, *J. Org. Chem.* **1974**, *39*, 2201–2207.
- [328] N. Maulide, J.-C. VanHerck, A. Gautier, I. E. Markó, *Acc. Chem. Res.* **2007**, *40*, 381–392.
- [329] B. H. Lipshutz, D. F. Harvey, *Synth. Commun.* **1982**, *12*, 267–277.
- [330] S. E. Sen, S. L. Roach, J. K. Boggs, G. J. Ewing, J. Magrath, *J. Org. Chem.* **1997**, *62*, 6684–6686.
- [331] J. B. Arterburn, M. C. Perry, *Org. Lett.* **1999**, *1*, 769–771.
- [332] A. B. Smith, III, M. Fukui, H. A. Vaccaro, J. R. Empfield, *J. Am. Chem. Soc.* **1991**, *113*, 2071–2092.
- [333] M. S. Newman, R. J. Harper, Jr., *J. Am. Chem. Soc.* **1958**, *80*, 6350–6355.
- [334] B. M. Trost, M. K. Mao, J. M. Balkovec, P. Buhlmyer, *J. Am. Chem. Soc.* **1986**, *108*, 4965–4973.
- [335] P. Deslongchamps, P. Atlani, D. Fréhel, A. Malaval, C. Moreau, *Can. J. Chem.* **1974**, *52*, 3651–3664.
- [336] K. C. Nicolaou, V. A. Adsool, C. R. H. Hale, *Org. Lett.* **2010**, *12*, 1552–1555.
- [337] S. Dong, L. A. Paquette, *J. Org. Chem.* **2005**, *70*, 1580–1596.
- [338] G. A. Olah, B. G. Balaram Gupta, S. C. Narang, R. Malhotra, *J. Org. Chem.* **1979**, *44*, 4272–4275.
- [339] G.-J. ten Brink, I. W. C. E. Arends, R. A. Sheldon, *Chem. Rev.* **2004**, *104*, 4105–4123.
- [340] M. Lerm, H.-J. Gais, K. Cheng, C. Vermeeren, *J. Am. Chem. Soc.* **2003**, *125*, 9653–9667.
- [341] V. Lutz, N. Park, C. Rothe, C. Krüger, A. Baro, S. Laschat, *Eur. J. Org. Chem.* **2013**, 761–771.

- [342] V. Lutz, F. Mannchen, M. Krebs, N. Park, C. Krüger, A. Raja, F. Sasse, A. Baro, S. Laschat, *Bioorg. Med. Chem.* **2014**, *22*, 3252–3261.
- [343] S. Chandrasekhar, C. Sridhar, P. Srihari, *Tetrahedron Asymmetry* **2012**, *23*, 388–394.
- [344] B. M. Trost, F. D. Toste, *J. Am. Chem. Soc.* **2003**, *125*, 3090–3100.
- [345] K. C. Nicolaou, L. Shi, M. Lu, M. R. Pattanayak, A. A. Shah, H. A. Ioannidou, M. Lamani, *Angew. Chem. Int. Ed.* **2014**, *53*, 10970–10974.
- [346] A. Chen, J. Xu, W. Chiang, C. L. L. Chai, *Tetrahedron* **2010**, *66*, 1489–1495.
- [347] J. Casas, H. Sundén, A. Córdova, *Tetrahedron Lett.* **2004**, *45*, 6117–6119.
- [348] O. Piva, S. Comesse, *Eur. J. Org. Chem.* **2000**, 2417–2424.
- [349] M. T. Gieseler, M. Kalesse, *Org. Lett.* **2011**, *13*, 2430–2432.
- [350] K. J. Quinn, L. Islamaj, S. M. Couvertier, K. E. Shanley, B. L. Mackinson, *Eur. J. Org. Chem.* **2010**, 5943–5945.
- [351] R. D. Connell, M. Tebbe, A. R. Gangloff, P. Helquist, *Tetrahedron* **1993**, *49*, 5445–5459.

ADDENDUM

As a part of this thesis, the biosynthetic hypothesis presented in 2.2.1 General Biosynthetic Proposal was recently supported by the successful synthesis of epicolactone. According to the guidelines for oxidative pyrogallol dimerizations detailed in 2.1.3.4 Conceptualization of Substrate-Dependent Reactivity Trends, a selectively protected phenol methyl ether **A1** was employed (Scheme 187). Oxidation of this compound under conditions similar to the oxidative dimerization of epicoccine to dibefurin, followed by slow addition of epicoccine afforded *O*-Me-protected epicolactone **236** in an isolated yield of 13% on *m* = 15 mg scale.



Scheme 187. Successful oxidative dimerization of epicoccine with benzyl alcohol **A1**.

Further analysis of the reaction mixture showed the presence of two major byproducts **A2** and **A3** of this dimerization reaction as judged by NMR and MS (Figure 51). Regioisomer **A2** was hereby formed next to the desired product in a ratio *r* (**236:A2**)= 1.8:1 and conveniently separable by extraction into slightly basic medium.

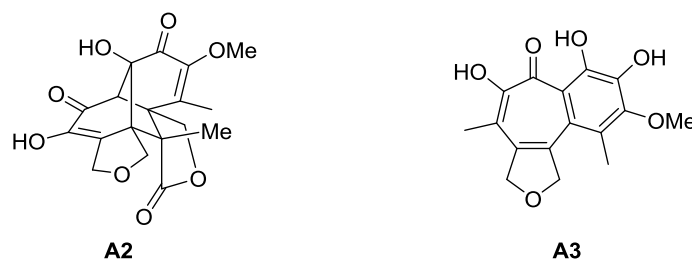
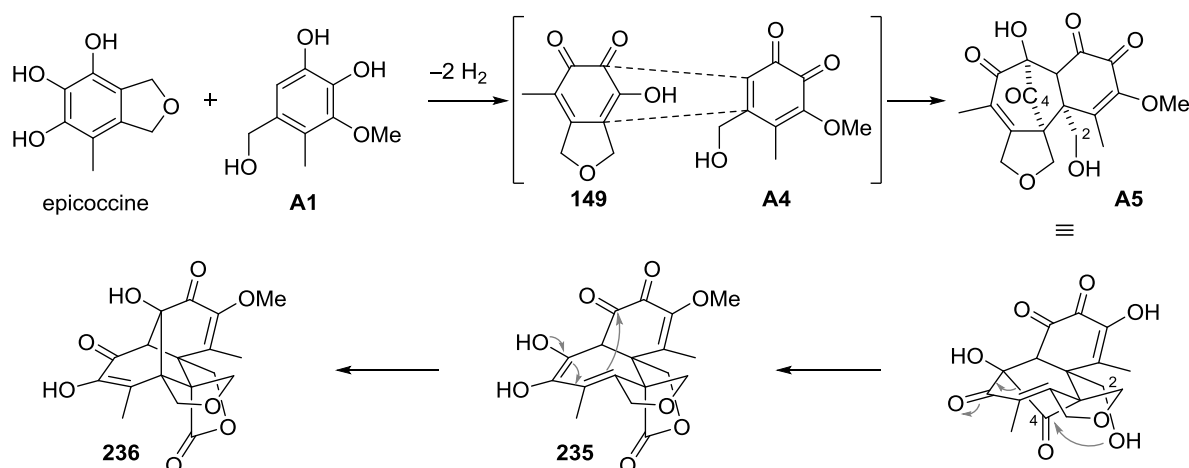


Figure 51. Byproducts of oxidative dimerization of epicoccine and benzyl alcohol **A1**.

The formation of a structurally similar isomer alongside the desired product was also previously observed in the dibefurin synthesis (see 2.3.2.2 Oxidation of Epicoccine and Dibefurin Formation). Since the oxidative heterodimerization of epicoccine with another pyrogallol derivative is likely to occur in Nature, this result could have important implications. Potentially, isomer **A2** also constitutes a natural product that has thus far eluded isolation.

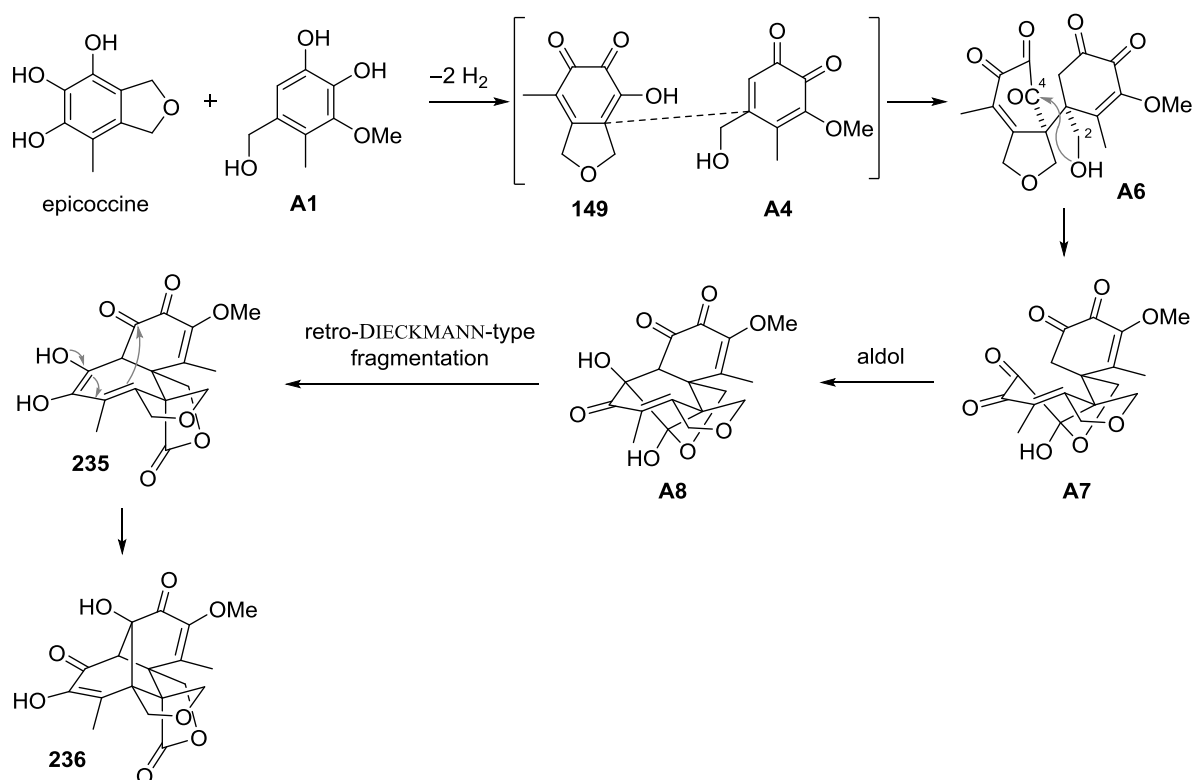
Mechanistically, it seems unlikely that the oxidative dimerization cascade proceeds through an intermediate such as **152** due to the side reactions observed in this thesis (see 2.2.1 General Biosynthetic Proposal and 2.3.4.5.4 Final Studies Toward the Synthesis of Epicolactone). It is possible that after oxidation, quinone **149** and benzyl alcohol **A4** first dimerize to intermediate **A5**, a protected

version of diketone **151**, in which the tautomerization to the enol tautomer of type **152**, a two-step intermolecular process, would be slower than the intramolecular attack of C2O onto C4 (Scheme 188). Without the enol tautomerization, the high driving force for rearomatization would not exist and the cascade could proceed to Me-protected epicolactone **236** via intermediate **235**. Employing protected versions of alcohol **A1** such as catechols **170**, **261** or **262** was therefore misleading since the C2O attack on C4 was impossible, eventually leading to the isolation of the thermodynamically more stable enol tautomer of type **152** that is prone to rearomatization.



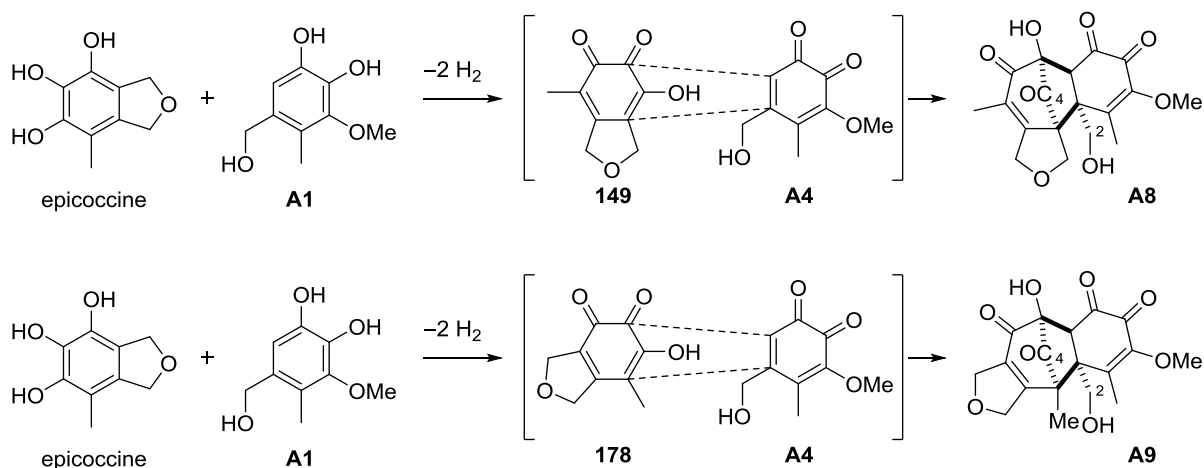
Scheme 188. Potential mechanism of oxidative dimerization to avoid intermediates such as **152** (1).

As an alternative to this mechanistic proposal, epicoccine and benzyl alcohol **A1** could first dimerize by MICHAEL-type addition of enol **149** to enone **A4** to give intermediate **A6**. A bond between C2O and C4 could then be forged prior to the previously postulated aldol reaction to yield lactol **A7** (Scheme 189). This process would prevent the formation of intermediates such as **152**. In analogy to the original biosynthetic proposal, hemiacetal **A7** could undergo aldol addition to yield lactol **A8** that would furnish the previously suggested intermediate **235** upon retro-DIECKMANN-type fragmentation. Final vinylogous aldol reaction would afford Me-protected epicolactone **236**.



Scheme 189. Potential mechanism of oxidative dimerization to avoid intermediates such as **152** (2).

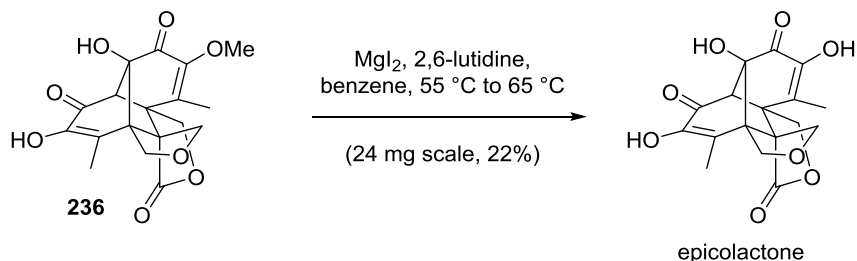
The formation of isomer **A2** can be rationalized by a different regioselectivity of the initial dimerization (Scheme 190). Instead of quinone **149**, its tautomer **178** could dimerize to yield diketone **A9** that would furnish isomer **A2** by an analogous cascade process.



Scheme 190. Rationale for the formation of isomer **A2**.

The aromatic benzotropolone **A3** can form because water has to be employed as a cosolvent due to the otherwise insoluble oxidant potassium ferricyanide. In principle, this product could arise from lactone hydrolysis of *e.g.* intermediate **235**. Upon oxidation of the ene diol unit, the resulting product would be prone to decarboxylation and cleavage of formaldehyde to yield the aromatic benzotropolone core.

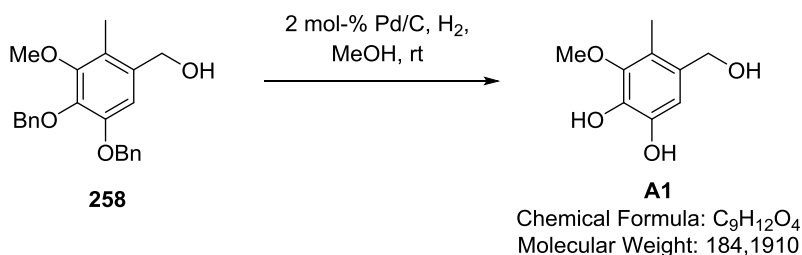
It was found that pentacycle **236** can be demethylated to furnish the natural product epicolactone by using MgI_2 with 2,6-lutidine as a scavenger for MeI at slightly increased temperature (Scheme 191). The final deprotection conditions as well as the purification protocol will require further optimization.



Scheme 191. Successful epicolactone synthesis.

In summary, a complex biosynthetic hypothesis was validated by the successful biomimetic synthesis of epicolactone. The oxidative dimerization cascade enables the formation of four adjacent tetrasubstituted carbon atoms, three of which are quaternary, with the correct diastereoselectivity from simple aromatic pyrogallol derivatives.

5-(hydroxymethyl)-3-methoxy-4-methylbenzene-1,2-diol (**A1**)

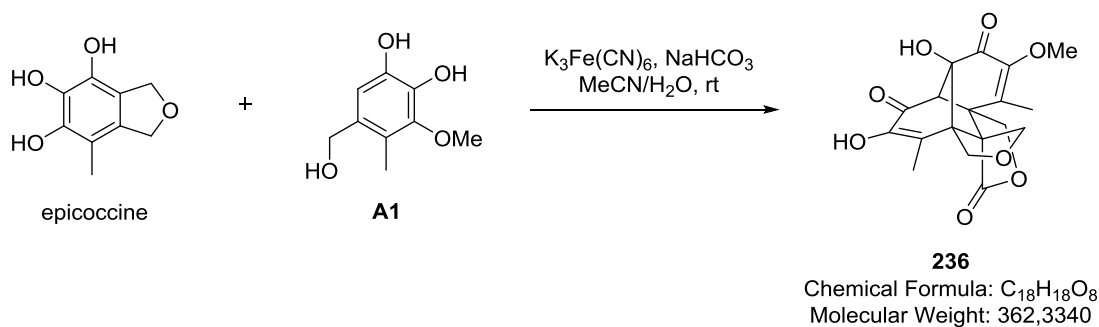


Benzyl alcohol **258** (500 mg, 1.37 mmol) was dissolved in MeOH (7.0 ml) and palladium on activated charcoal (10 wt-%, 30 mg, 0.027 mmol, 0.02 eq.) was added. The reaction vessel was evacuated and filled with hydrogen gas for three times and the reaction mixture was stirred under hydrogen gas atmosphere for 13.5 h at rt. The reaction mixture was filtered and the organic phase was concentrated under reduced pressure to afford the title compound as a colorless solid (237 mg, 94%). The product could be used in the subsequent steps without further purification.

TLC	$R_f = 0.61$ (100% EtOAc).
m.p.:	159–160 °C (decomposition).
^1H NMR	(400 MHz, $(\text{D}_3\text{C})_2\text{CO}$): δ 7.55 (s, 1H), 7.41 (s, 1H), 6.69 (s, 1H), 4.47 (d, $J = 5.8$ Hz, 2H), 3.83 (t, $J = 5.8$ Hz, 1H), 3.71 (s, 3H), 2.12 (s, 3H) ppm.
^{13}C NMR	(100 MHz, $(\text{D}_3\text{C})_2\text{CO}$): δ 147.3, 144.1, 137.6, 132.0, 120.4, 111.6, 63.0, 60.3, 10.8 ppm.
HRMS	((-)-ESI, m/z): calc. $[\text{M}-\text{H}]^-$: 183.0657; found: 183.0663 $[\text{M}-\text{H}]^-$.

IR $\tilde{\nu}$ = 3344 (br, w), 3202 (br, m), 2993 (w), 2936 (w), 2903 (w), 2832 (vw), 1619 (w), 1518 (w), 1489 (w), 1461 (m), 1431 (m), 1408 (w), 1379 (w), 1306 (s), 1260 (m), 1235 (s), 1216 (s), 1184 (m), 1093 (vs), 998 (s), 960 (s), 942 (vs), 879 (s), 864 (s), 832 (m), 759 (m), 713 (s), 692 (s), 642 (m), 620 (s), 579 (s), 563 (s) cm^{-1} .

Epicolactone methyl ether **236**



Benzyl alcohol **A1** (15 mg, 0.082 mmol, 1.0 eq.) was dissolved in MeCN (0.5 ml) and potassium ferricyanide (133 mg, 0.496 mmol, 6.0 eq.) and NaHCO_3 (41 mg, 0.496 mmol, 6.0 eq.) dissolved in water (2.0 ml) were added dropwise. Subsequently, epicoccine (15 mg, 0.082 mmol) in MeCN/ H_2O (9:1, 0.5 ml) was added via a syringe pump over 2.5 h. After stirring for 0.5 h, pH 5 phosphate buffer ($c = 1 \text{ M}$, 5 ml) was added and the aqueous phase extracted with EtOAc (4x10 ml). The combined organic phase was extracted with sat. aq. NaHCO_3 solution (2x50 ml), dried over Na_2SO_4 and concentrated under reduced pressure. The crude product was purified by preparative TLC (5% MeOH/ CH_2Cl_2) to afford the title compound as a colorless oil (4 mg, 13%).

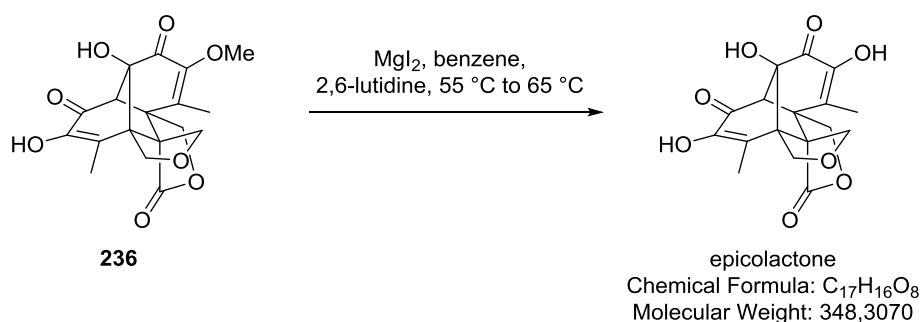
TLC R_f = 0.49 (5% MeOH/ CH_2Cl_2).

^1H NMR (800 MHz, DMSO- d_6): δ 8.51 (s, 1H), 6.00 (s, 1H), 4.53 (d, $J = 9.7 \text{ Hz}$, 1H), 4.17 (d, $J = 9.7 \text{ Hz}$, 1H), 3.91 (d, $J = 9.7 \text{ Hz}$, 1H), 3.76 (d, $J = 10.8 \text{ Hz}$, 1H), 3.66 (d, $J = 9.7 \text{ Hz}$, 1H), 3.57 (d, $J = 10.8 \text{ Hz}$, 1H), 3.57 (s, 3H), 3.15 (s, 1H), 2.05 (s, 3H), 1.79 (s, 3H) ppm.

^{13}C NMR (200 MHz, DMSO- d_6): δ 192.7, 189.9, 175.6, 149.2, 146.7, 144.3, 127.3, 91.0, 72.9, 70.1, 68.0, 67.9, 67.1, 66.5, 59.2, 49.8, 14.3, 13.6 ppm.

HRMS (EI, m/z): calc. $[\text{M}^+]$: 362.1002; found: 362.0998 $[\text{M}^+]$.

IR $\tilde{\nu}$ = 3423 (br, w), 2986 (vw), 2936 (vw), 2876 (vw), 1770 (s), 1729 (m), 1671 (vs), 1638 (s), 1475 (w), 1446 (w), 1392 (m), 1374 (m), 1356 (m), 1321 (w), 1289 (w), 1242 (s), 1218 (s), 1175 (s), 1145 (m), 1101 (s), 1081 (s), 1044 (vs), 1020 (m), 1003 (w), 982 (m), 967 (w), 952 (w), 933 (m), 885 (vw), 858 (vw), 803 (w), 789 (w), 744 (vw), 717 (w), 689 (w), 625 (vw) cm^{-1} .

Epicolactone

Me-epicolactone **236** (24 mg, 0.065 mmol) was suspended in benzene (1.5 ml) and MgI_2 (90 mg, 0.23 mmol, 5.0 eq.) was added. The suspension was heated to 55 °C and the reaction was monitored by LC/MS. After 2 h, 2,6-lutidine (11 μl , 11 mg, 0.098 mmol, 1.5 eq.) was added. After further 6 h, more MgI_2 (20 mg, 0.072 mmol, 1.1 eq.) was introduced. After further 11 h, more MgI_2 (20 mg, 0.072 mmol, 1.1 eq.) and 2,6-lutidine (10 μl , 10 mg, 0.093 mmol, 1.4 eq.) were added. The reaction mixture was stirred for 2 h before the temperature was increased to 65 °C. After further stirring for 28 h, pH 5 phosphate buffer ($c = 1\text{ M}$, 5 ml) and sat. aq. $\text{Na}_2\text{S}_2\text{O}_3$ solution (5 ml) were added and the reaction mixture was extracted with EtOAc (4x10 ml). The combined organic phases were dried over Na_2SO_4 and concentrated under reduced pressure. The crude product was purified by preparative TLC (5% $\text{MeOH}/\text{CH}_2\text{Cl}_2$) to afford the natural product as a colorless solid (5 mg, 22%).

TLC $R_f = 0.37$ (5% $\text{MeOH}/\text{CH}_2\text{Cl}_2$).

^1H NMR (800 MHz, DMSO-d_6): δ 8.61 (s, 1H), 8.49 (s, 1H), 6.06 (s, 1H), 4.51 (d, $J = 9.6\text{ Hz}$, 1H), 4.16 (d, $J = 9.6\text{ Hz}$, 1H), 3.91 (d, $J = 9.6\text{ Hz}$, 1H), 3.70 (d, $J = 10.5\text{ Hz}$, 1H), 3.65 (d, $J = 9.6\text{ Hz}$, 1H), 3.53 (d, $J = 10.5\text{ Hz}$, 1H), 3.06 (s, 1H), 1.97 (s, 3H), 1.79 (s, 3H) ppm.

^{13}C NMR (200 MHz, DMSO-d_6): δ 192.7, 190.0, 175.9, 146.6, 145.8, 128.6, 127.3, 90.8, 73.0, 71.2, 68.3, 67.6, 67.1, 66.6, 50.1, 14.3, 12.9 ppm.

HRMS (EI, m/z): calc. $[\text{M}^+]$: 348.0845; found: 348.0829 $[\text{M}^+]$.

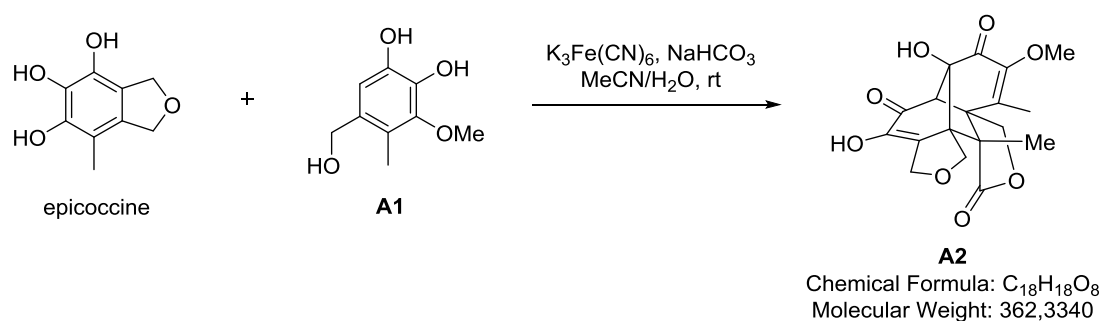
IR $\tilde{\nu} = 3410$ (br, w), 2982 (vw), 2923 (w), 2852 (vw), 1769 (m), 1728 (m), 1670 (s), 1638 (s), 1473 (vw), 1445 (w), 1392 (m), 1375 (m), 1354 (s), 1241 (vs), 1218 (s), 1177 (s), 1143 (m), 1100 (s), 1076 (s), 1042 (vs), 1000 (m), 962 (w), 933 (m), 900 (w), 857 (w), 802 (w), 787 (w), 755 (w), 716 (w), 689 (w) cm^{-1} .

¹H NMR (DMSO-d₆):

chemical shift δ/ppm (natural sample) ^[159]	chemical shift δ/ppm (synthetic sample)	Δδ/ppm
8.61 (s, 1H)	8.61 (s, 1H)	0.00
8.50 (s, 1H)	8.49 (s, 1H)	-0.01
6.07 (s, 1H)	6.06 (s, 1H)	-0.01
4.51 (d, <i>J</i> = 9.6 Hz, 1H)	4.51 (d, <i>J</i> = 9.6 Hz, 1H)	0.00
4.16 (d, <i>J</i> = 9.6 Hz, 1H)	4.16 (d, <i>J</i> = 9.6 Hz, 1H)	0.00
3.90 (d, <i>J</i> = 9.8 Hz, 1H)	3.91 (d, <i>J</i> = 9.6 Hz, 1H)	+0.01
3.70 (d, <i>J</i> = 10.4 Hz, 1H)	3.70 (d, <i>J</i> = 10.5 Hz, 1H)	0.00
3.65 (d, <i>J</i> = 9.8 Hz, 1H)	3.65 (d, <i>J</i> = 9.6 Hz, 1H)	0.00
3.53 (d, <i>J</i> = 10.4 Hz, 1H)	3.53 (d, <i>J</i> = 10.5 Hz, 1H)	0.00
3.06 (s, 1H)	3.06 (s, 1H)	0.00
1.96 (s, 3H)	1.97 (s, 3H)	+0.01
1.79 (s, 3H)	1.79 (s, 3H)	0.00

¹³C NMR (DMSO-d₆):

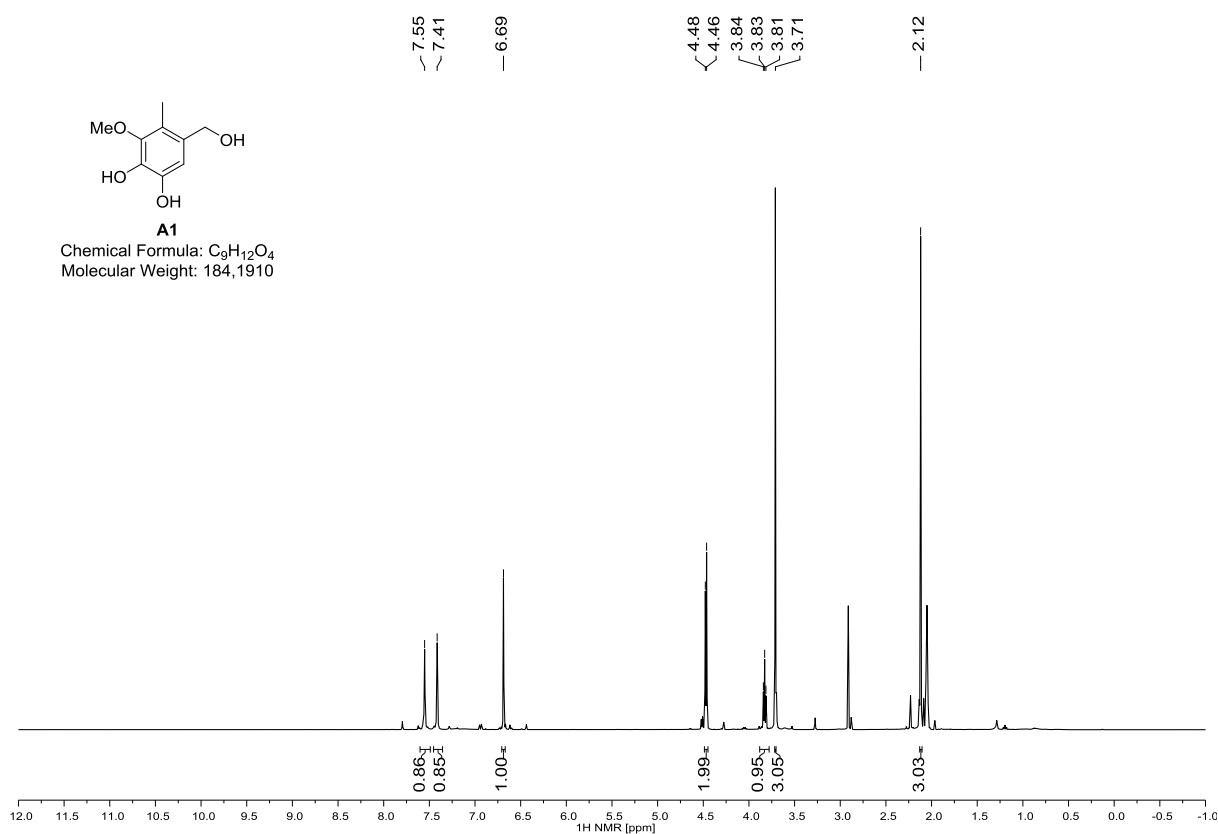
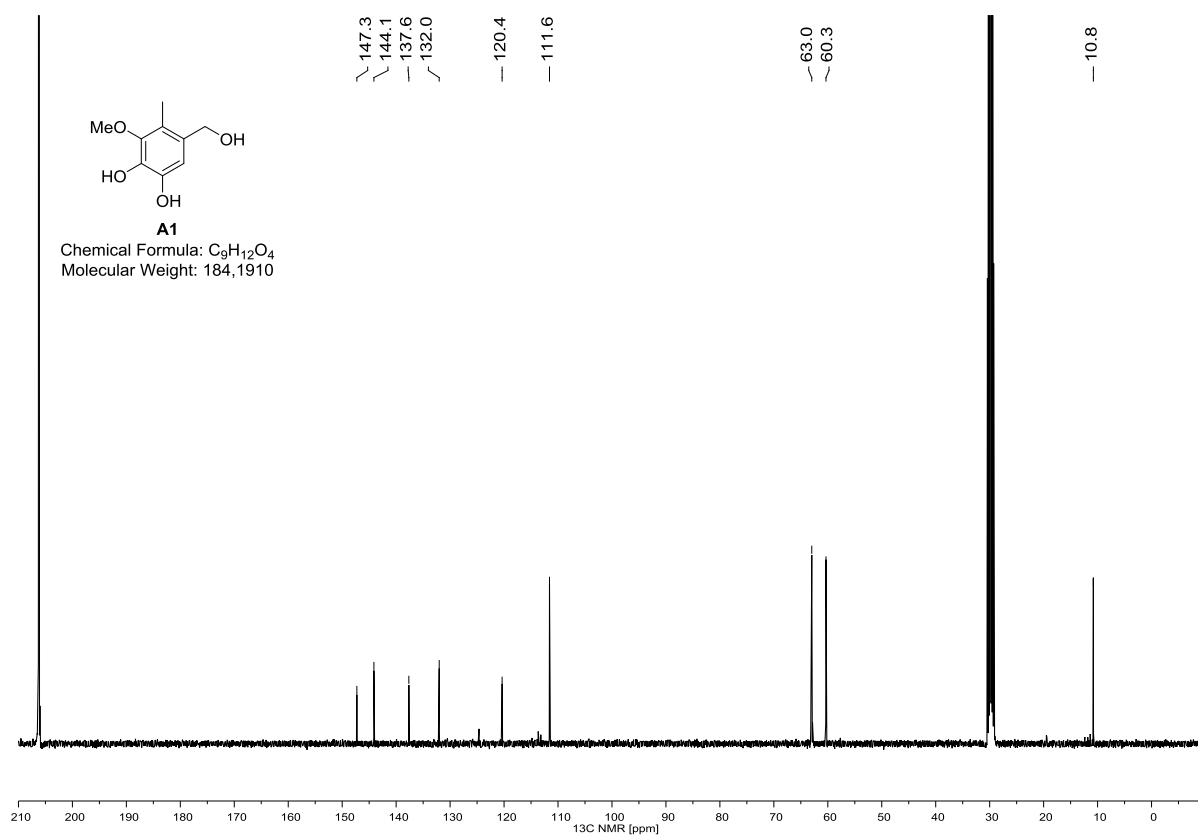
chemical shift δ/ppm (natural sample) ^[159]	chemical shift δ/ppm (synthetic sample)	Δδ/ppm
192.8	192.7	-0.1
190.1	190.0	-0.1
176.0	175.9	-0.1
146.6	146.6	0.0
145.9	145.8	-0.1
128.7	128.6	-0.1
127.5	127.3	-0.2
90.9	90.8	-0.1
73.0	73.0	0.0
71.3	71.2	-0.1
68.3	68.3	0.0
67.7	67.6	-0.1
67.2	67.1	-0.1
66.6	66.6	0.0
50.1	50.1	0.0
14.4	14.3	-0.1
13.0	12.9	-0.1

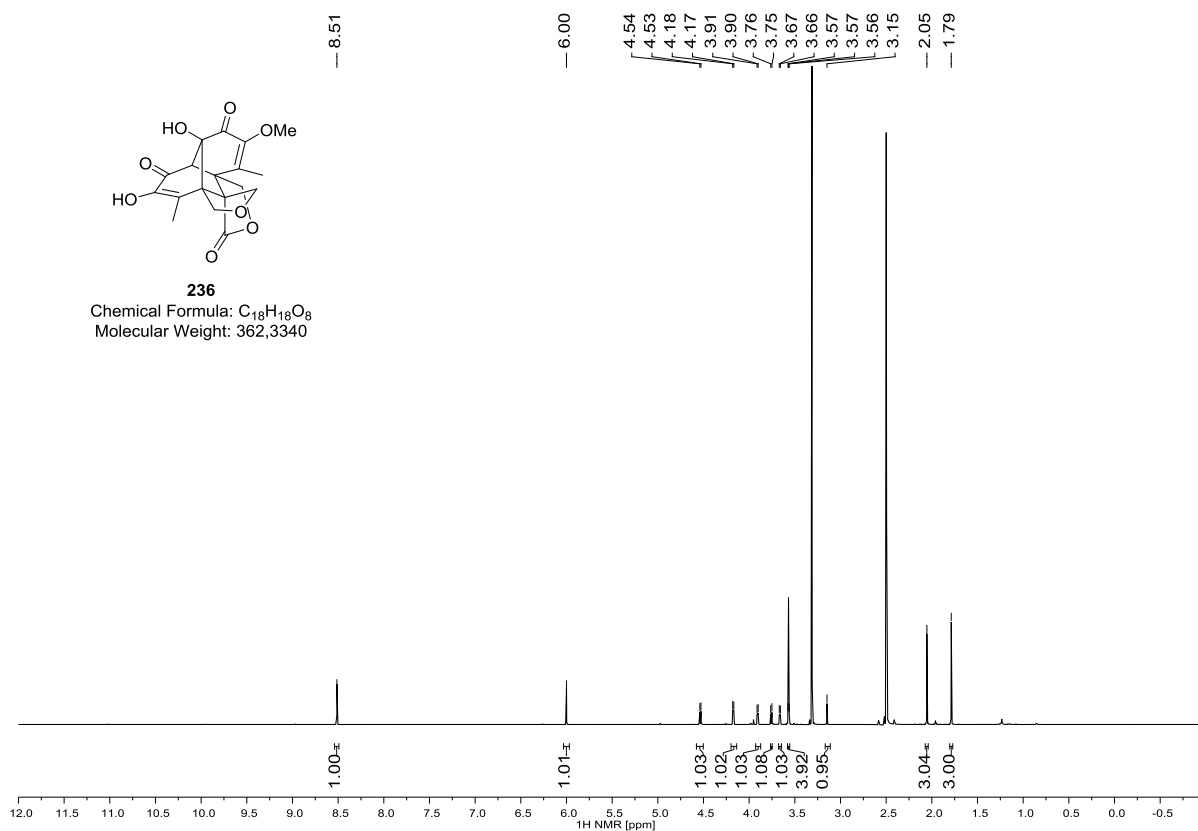
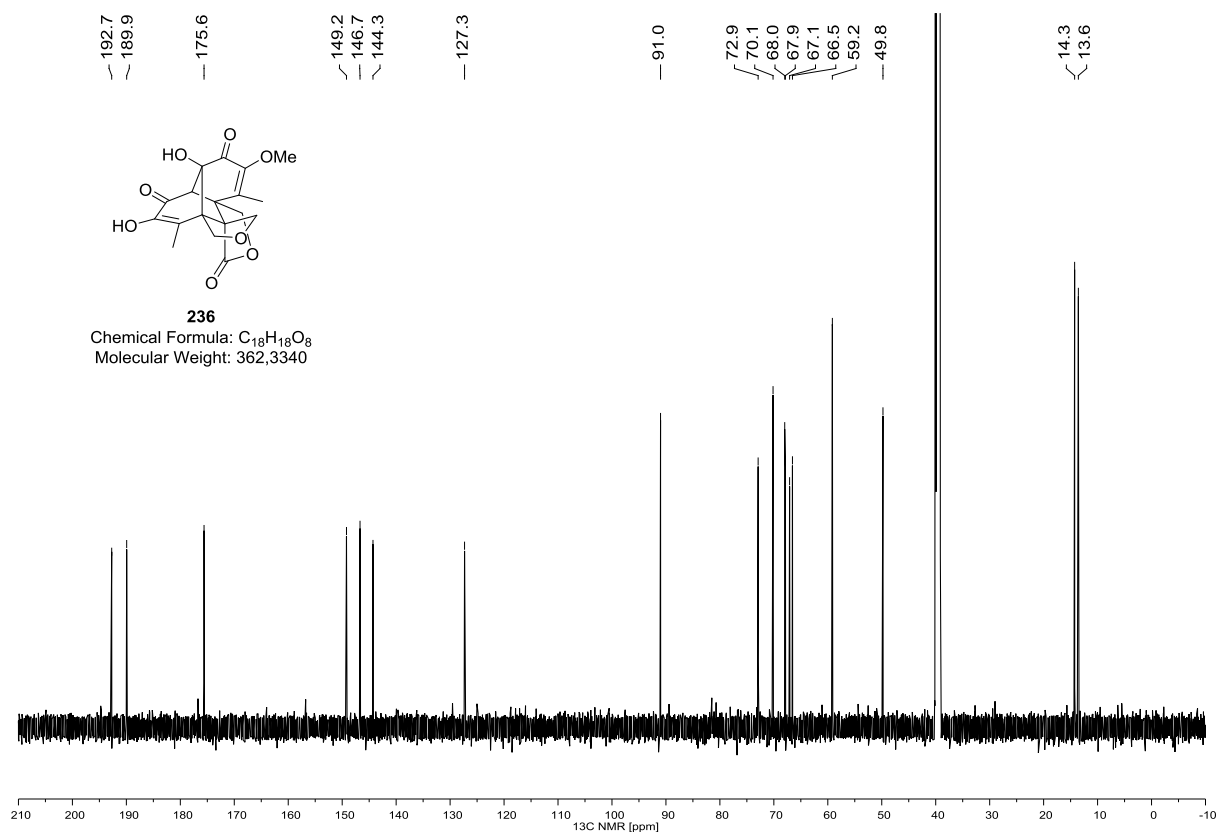
Regioisomer A2

Benzyl alcohol **A1** (30 mg, 0.16 mmol, 1.0 eq.) was dissolved in MeCN (1.0 ml) and potassium ferricyanide (266 mg, 0.991 mmol, 6.0 eq.) and NaHCO₃ (82 mg, 0.991 mmol, 6.0 eq.) dissolved in water (4.0 ml) were added dropwise. Subsequently, epicoccine (30 mg, 0.16 mmol) in MeCN/H₂O (4:1, 1.0 ml) was added via a syringe pump over 2 h. After stirring for 1 h, pH 5 phosphate buffer (*c* = 1 M, 10 ml) was added and the aqueous phase extracted with EtOAc (5x15 ml). The combined organic phase was extracted with sat. aq. NaHCO₃ solution (2x50 ml) and the combined aqueous phase acidified with conc. aq. HCl solution. The aqueous phase was extracted with EtOAc (3x100 ml) and the combined organic phase dried over Na₂SO₄ and concentrated under reduced pressure. The crude product was purified by preparative TLC (5% MeOH/CH₂Cl₂) to afford the title compound as a colorless solid (9 mg, 15%).

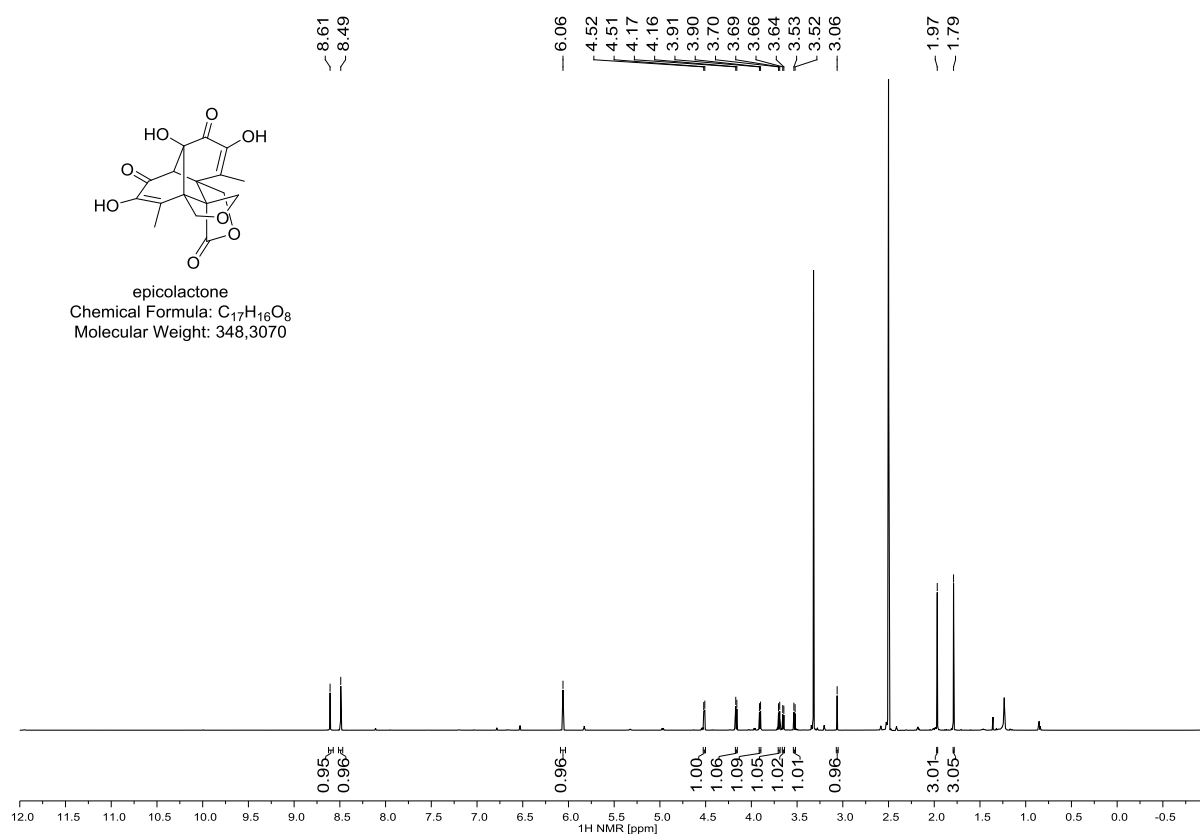
This dimerization trial was conducted on larger scale and resulted in a better yield, which could represent a general feature of this cascade process.

TLC	R _f = 0.40 (5% MeOH/CH ₂ Cl ₂).
m.p.:	204–207 °C (decomposition)
¹H NMR	(400 MHz, DMSO-<i>d</i>₆): δ 9.00 (s, 1H), 6.29 (s, 1H), 4.64 (d, <i>J</i> = 10.2 Hz, 1H), 4.38 (d, <i>J</i> = 16.1 Hz, 1H), 4.27 (d, <i>J</i> = 16.1 Hz, 1H), 4.22 (d, <i>J</i> = 10.2 Hz, 1H), 3.85 (d, <i>J</i> = 10.1 Hz, 1H), 3.75 (d, <i>J</i> = 10.1 Hz, 1H), 3.58 (s, 3H), 3.17 (s, 1H), 2.04 (s, 3H), 1.08 (s, 3H) ppm.
¹³C NMR	(100 MHz, DMSO-<i>d</i>₆): δ 193.7, 190.8, 176.3, 149.9, 149.0, 140.3, 136.8, 88.5, 68.1, 67.8, 66.3, 65.6, 59.8, 59.6, 59.5, 51.2, 17.4, 14.4 ppm.
HRMS	(EI, <i>m/z</i>): calc. [<i>M</i> ⁺]: 362.1002; found: 362.0984 [<i>M</i> ⁺].
IR	$\tilde{\nu}$ = 3388 (w), 2991 (vw), 2929 (w), 2848 (vw), 1760 (m), 1695 (w), 1666 (vs), 1611 (w), 1483 (vw), 1449 (w), 1376 (m), 1324 (w), 1273 (w), 1229 (w), 1211 (w), 1180 (w), 1157 (w), 1143 (w), 1086 (s), 1042 (m), 1024 (m), 1014 (m), 976 (w), 915 (vw), 902 (vw), 857 (vw), 821 (vw), 744 (vw), 626 (vw) cm ⁻¹ .

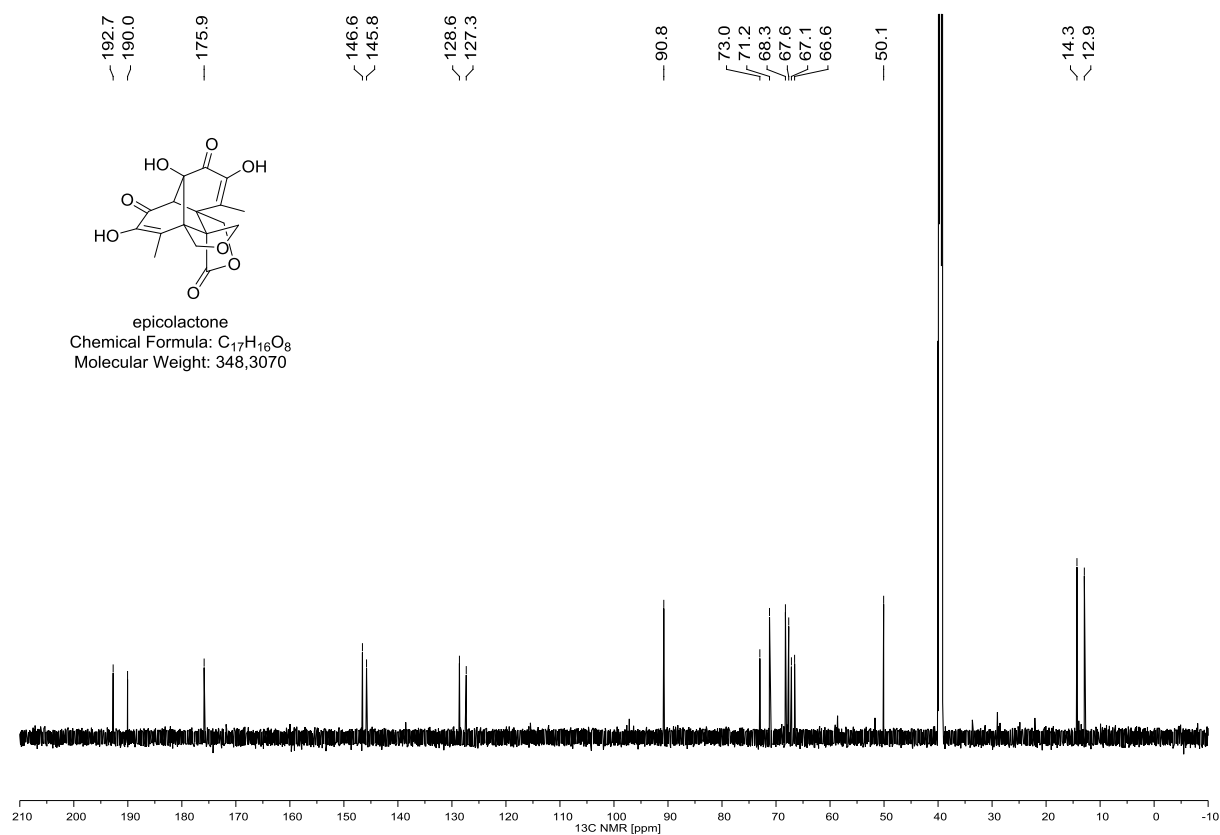
A1 (^1H NMR, 400 MHz, $(\text{D}_3\text{C})_2\text{CO}$)**A1 (^{13}C NMR, 100 MHz, $(\text{D}_3\text{C})_2\text{CO}$)**

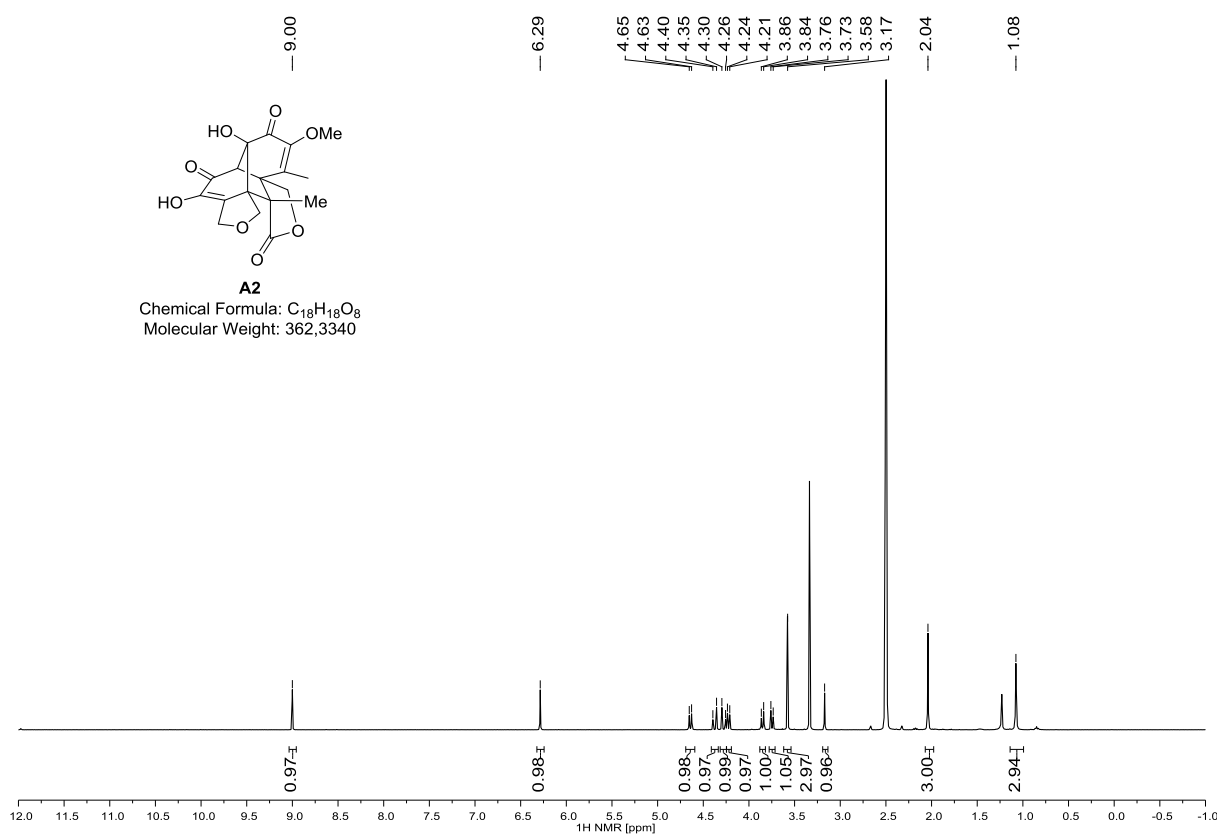
236 (^1H NMR, 800 MHz, DMSO- d_6)**236 (^{13}C NMR, 200 MHz, DMSO- d_6)**

Epicolactone (¹H NMR, 800 MHz, DMSO-d₆)



Epicolactone (¹³C NMR, 200 MHz, DMSO-d₆)



A2 (¹H NMR, 400 MHz, DMSO-d₆)**A2 (¹³C NMR, 100 MHz, DMSO-d₆)**